THE UNIVERSITY OF CHICAGO

DEVELOPMENT OF TRANSITION METAL MEDIATED CASCADES AND THEIR APPLICATION TOWARDS THE SYNTHESIS OF RETIGERANIC ACID A

A DISSERTATION SUBMITTED TO

THE FACULTY OF THE DIVISION OF THE PHYSICAL SCIENCES

IN CANDIDACY FOR THE DEGREE OF

DOCTOR OF PHILOSOPHY

DEPARTMENT OF CHEMISTRY

BY

JONATHAN HARVEY KEIM

CHICAGO, ILLINOIS

MARCH 2022

"*I leave Sisyphus at the foot of the mountain. One always finds one's burden again. But Sisyphus teaches the higher fidelity that negates the gods and raises rocks. He too concludes that all is well. This universe henceforth without a master seems to him neither sterile nor futile. Each atom of that stone, each mineral flake of that night-filled mountain, in itself, forms a world. The struggle itself toward the heights is enough to fill a man's heart. One must imagine Sisyphus happy.*"

– Albert Camus

TABLE OF CONTENTS

LIST OF SCHEMES

LIST OF FIGURES

LIST OF TABLES

List of Abbreviations

Ac	acetyl
acac	acetylacetonate
BHT	butylated hydroxy toluene
Boc	tert-butyloxycarbonyl
COD	1,5-cyclooctadiene
Cy	cyclohexyl
Cyp	cyclopentyl
DABCO	1,4-diazabicyclo[2.2.2]octane
DBN	1,5-diazabicyclo(4.3.0)non-5-ene
DBU	1,8-diazabicyclo(5.4.0)undec-7-ene

DCE	1,2-dichloroethane
DHA	9,10-dihydroanthracene
DIPEA	N,N-diisopropylethylamine
DMAP	4-dimethylaminopyridine
DME	1,2-dimethoxyethane
DMF	dimethylformamide
DMP	Dess-Martin periodinane
DMSO	dimethylsulfoxide
DQ	duroquinone
dr	diastereomeric ratio
E_a	energy of activation
EDC	1-ethyl-3-(3-dimethylaminopropyl)carbodiimide
EDG	electron donating groups
ee	enantiomeric excess
Et	ethyl
EWG	electron withdrawing group
^{F}stb	4,4′-bis(trifluoromethyl)-*trans*-stilbene
HAT	hydrogen atom transfer

HFIP	1,1,1,3,3,3-hexafluoro-2-propanol
HMPA	hexamethylphosphoramide
*i*Pr	isopropyl
KHMDS	potassium hexamethyldisilazide
LDA	lithium diisopropyl amide
LiHMDS	lithium hexamethyldisilazide
LTBA	$LiAlH(OtBu)_3$
*m*CPBA	*meta*-chloroperbenzoic acid
Me	methyl
MeTBD	7-methyl-1,5,7-triazabicyclo[4.4.0]dec-5-ene
Ms	mesyl
NaHMDS	sodium hexamethyldisilazide
*n*Bu	*n*-butyl
Nf	nonaflate
NMI	N-methyl imidazole
NMO	N-methyl morpholine oxide
Ph	phenyl
Piv	pivlate

PMHS	polymethylhydrosiloxane
PMP	1,2,2,6,6-pentamethylpiperidine
R_f	retention factor
rr	regioisomeric ratio
TBAF	tetrabutylammonium fluoride
TBAT	tetrabutylammonium difluorotriphenylsilicate
TBC	4-*tert*-catechol
TBD	1,5,7-triazabicyclo[4.4.0]dec-5-ene
TBS	*tert*-butyldimethylsilyl
*t*Bu	*tert*-butyl
TDAE	tetrakis(dimethylamino)ethylene
TEMPO	(2,2,6,6-tetramethylpiperidin-1-yl)oxyl
TES	triethylsilyl
Tf	triflate
TMS	trimethylsilyl
TMTU	tetramethylthiourea
Ts	tosyl
μW	microwave heating

))) sonication

Acknowledgments

If it takes a village to raise a child then it takes a small city for someone to get a PhD. At least, that was the case for me. I began the journey to this point just over 11 years ago as a chemistry major at Baylor University, but I could not have foreseen even a fraction of the twists and turns my life would take in ever higher and higher education. Throughout the many ups and downs, I have had the tremendous fortune to be surrounded by incredibly supportive and helpful people who have made it possible for me to not only earn my doctorate, but also, and more importantly, grow and mature as a human being. As I alluded, there are too many people who have helped me in one way or another over the years to thank them all individually, but I have listed below some of the most important people I have had the pleasure to know.

I would like to begin by thanking my advisor, Prof. Scott Snyder, who has proven to be an exceptional mentor time and time again over the course of my graduate career. Before even joining his group, You asked if I wanted to follow him as he moved from Scripps Florida to the University of Chicago, which was not a place I'd ever imagined myself ending up. Sight unseen I decided to take you up on the offer. As much as I was looking forward to living in sunny south Florida, it was definitely the right choice. You have been so incredibly kind, understanding, and patient throughout the many struggles of my time in your lab. When I felt I didn't have what it took to make it through early on, you bolstered my courage to press on. When my total synthesis hit a major roadblock, you gave me the freedom to go out and find my way through the wilds of the Nickel Heck even when I wasn't sure of where I was going. I learned from you how to think

intelligently about not only solving problems, but also how to choose and frame those problems. You gave me so many opportunities, from serving as group manager to mentoring and teaching junior students. Your door was always open whenever I needed guidance or to talk through an issue or problem. I honestly doubt whether I would have been able to get a PhD with almost any other advisor. I will always be grateful that you asked me to follow you and will look back fondly upon my time in your lab.

Next, I would like to thank the members of the Snyder lab who I have had the pleasure to work with over the years. Our group has had some of the most exemplary chemists I have ever known whose knowledge and creativity has been an inspiration, guide, and resource throughout my time in the group. I would not be the chemist I am today if not for the daily assistance of my colleagues who were always happy to discuss chemistry and help tackle the problems du jour. I have greatly enjoyed the countless hours spent discussing and learning about one another's chemistry and amusing one another with various hijinks, shenanigans, and general horseplay. In particular, I would like to thank Dr. Charles Cole, Dr. Dipendu Das, Dr. Lilia Fuentes, Dr. Jeremy Boilevin, Russell Kielawa, Philipp Gemmel, Dr. Cooper Taylor, Prof. Hyung-Ming Chi, and Dr. Vladislav Lisynak for their friendship, support, and sympathetic ears to the continuous Dia del Juanathon marathons that is my life. I would also like to thank Dr. Christoph Lentsch, Dr. Jennifer Pitzen, Prof. Hyung-Min Chi, Prof. Ming Yang, and Prof. Pengfei Hu for their mentorship early on in my time in the lab. I would also like to thank Dr. Charles Cole, Russell Kielawa, and Phillipp Gemmel for their help editing this thesis. Additionally, I would like to thank Dr. Tessa Lynch-Colameta for her assistance in the hunt for gainful employment.

I would also like to thank Prof. Guangbin Dong and Prof. John Anderson both for serving on my committee, and also for the many helpful conversations over the years that helped me to navigate my forays into organometallic chemistry.

Much of my work has been part of collaborations with other researchers whose contributions have been invaluable to these projects. First and foremost, I would like to thank Dr. Dipendu Das for being an exceptional collaborator whose work ethic, drive, and seemingly unflappable demeanor truly made it a joy to work with him. If ever I have a future collaborator who is half as helpful as Dipendu, I will count myself incredibly lucky. I would also like to thank Joseph Schneider from the Anderson lab at University of Chicago who has been an immense help with his contribution of DFT calculations for the intermolecular Ni Heck project. In addition, I would also like to thank Andrew Cummins and Will Guy for their assistance with the base mediated Nickel Heck and our studies toward retigeranic acid A respectively. It was a pleasure to work with and mentor both of you and I learned so much from you both.

I would also like to thank a bevy of unofficial collaborators in the department who have provided me with expertise, equipment, or a laugh when one was need. From the Rawal group, I'd like to thank Dr. Ferdinand Taenzler, Dr. Mike Rombola, Dr. Pavel Elkin, and Kyle Cassaidy for being incredibly welcoming and supportive to the point I was even made an (unofficial) honorary member of the Rawal lab. Whenever I needed a reagent, a off the wall idea, a truly esoteric piece of glassware, or to just waste a few hours you all were happy to assist and for that I am truly grateful. From the Dong lab, I would like to thank Dr. Brent Billet, Shinyoung Choi, and Dr. Alex Rago who provided assistance and equipment whenever I needed it. In particular, I would like to thank Brent, who was an amazing resource and help in keeping my sanity whenever chemistry was misbehaving. From the Anderson lab, I would to thank Dr. Andrew McNeece who

was my go to source for all things metals and inorganic chemistry. Also, his occasional incursions into organic synthesis provided excellent teaching opportunities as well as being a source of great hilarity.

I would be remiss to not thank the many members of my cohort who were some of my first and longest friends in Chicago. In particular I would like to thank Huw Rees and Dr. Laura Watkins. Huw, you were an amazing roommate and friend for five years and I couldn't ask for more. You were always able to push me to be better and to try new things especially the stand up comedy classes we took. Those shows and the open mics are some of my favorite memories from my time in Chicago and I wouldn't have them without you. Laura, you're a wonderful person and a true friend who has been there with me through thick and thin. I'll miss our walk and talks around campus, which were immensely helpful to me over the years. More broadly, I'd like to thank Dave, Natalie, Ben, Airi, Sara, Youjin, Ryan, Ferdinand, Piyush, Matt, and many more for being friends throughout the trenches of graduate school.

A researcher is only as good as his support staff and I have had the luck to have excellent staff to work with. I'd like to thank Verenice Noyola for her assistance and guidance through the early days of my time at Chicago. I would especially like to thank Laura Luburich and Mike Reedy for keeping Searle standing and functioning despite all our of best efforts. I would like to thank Dr. Antoni Jukiewicz, Dr. Josh Kurutz, Dr. Jin Qin, Dr. Alex Fliatov, Dr. Andrew Mcneece, Dr. Kate Jesse for maintaining all of the facilities and making it possible for the synthetic chemists to do their work as efficiently and effectively as possible. Further, I would like to thank Dr. Vera Dragisch and Melinda Moore for their assistance over the years on handling the various trials and tribulations of student life. I would especially like to thank Dr. Valerie Keller who was a truly excellent supervisor when I was a teaching assistant. You always had time to chat and lend a

sympathetic ear to a beleaguered student and provide them with the motivation and resolve to push forward. I would also like to thank Dr. Britni Ratliff for the opportunity to work as part of the CliC-O program, which was one of the most enjoyable experiences in my graduate career. Further, I would like to thank the TA's I worked with, Alessandra Leong, Eric Cormack, and Murrie Affini, who were a pleasure to lead and provided me with endless opportunities to grow as a mentor and a teacher.

The path that led me to first pursuing and then earning a PhD was a long one and my love of chemistry has been fostered by many different teachers and mentors along the way. I would like to thank Frank Cardulla for producing an amazing series of lectures on introductory chemistry that made chemistry make sense to me. From then on I knew I wanted to do chemistry because nothing else was quite as beautiful and understandable. At Baylor, I would like to thank Prof. Patrick Farmer for the opportunity to work in his lab and Dr. Carrie Poe who was my first mentor and provided me with an invaluable education in the realities of research. I would especially like to thank Prof. Rizalia Klausmeyer who kindled my love of organic chemistry. Your enthusiastic support was critical in my success at Baylor and set the stage for everything I've accomplished since. I'd also like to thank Prof. Pennington for his rigorous introductory chemistry where upon informing him that a few of us had technically answered an exam question correctly that "you have won the moral victory, but not the points victory." At Harvey Mudd, I would like to thank Prof. David Vosburg for graciously taking me into his lab and giving me my first taste of synthetic chemistry. You were a great help then and an even greater help as a resource and advisor throughout graduate school. I'd also like to thank Dr. Nick Chiappini for his friendship and for answering every random question I ever had about chemistry. At the University of Nottingham, I would like to thank Prof. Christopher Moody for allowing me to work in his lab and for being an

excellent partner for playing pool against the rest of the lab. I'd also like to thank Dr. Chris Blunt for his mentorship as well as Hannah, Martyn, Eve, Emma, Hiroki, and the rest of lab for their help in starting as a researcher and learning how to be proper British as well.

I would also like to thank those who have helped me out in so very many ways over the years as my dear friends: Adam, Julius, Kyle, Chuck, Brandon, Nick, Tucker, Megan, Devyn, Brett, Dylan, Steve, Luke, Harry, Gio, Nico, Georgie, Taylor, the Tim's, Dino, Abz, Robbie, Shaddy, Eric, Todd, Sara, Liam, Sam, Kelcie, Manuel, Pete, Max, Zach, Yuka, Rock, Eric, Chad, Sierra, Melissa, Stephanie, Bob, Ray, Mark, Henry, Jean, Chase, Maurice, Alyssa, Josh, Darryl, Sarah, Mike, Tayo, Calvin, Michal, Christine, Mike, Sascha, Gurameen, Margie, Scotty, Joe, Dylan, Matt, Jessie, Kathleen, Josh, Sivan, and many more. I couldn't and wouldn't be where I am today without each and everyone of you. You have all played roles, some major and some minor, but all essential for me to be at this point and for that I thank you all.

Finally, I would like to thank my family. Mom and Dad, you raised me with a love of knowledge, learning, and science that set the stage for everything I've accomplished here. You instilled a desire to be the best that I could be at whatever I did even if it was just digging ditches. You taught me the importance of being kind and helpful to all those around you and I've tried my best to emulate that spirit for better or worse. I'd like to thank my siblings Ben, Miriam, Kate, and Paul for all the help they've given me over the years whether it be advice, an introduction, editing, or whatever else I may need, you all have always had my back and been there for me when I needed it. I would like to thank all my grandparents, George and Sandy Keim, Weber and Joanne Shows, and Harvey and Joanne Hall. I especially want to thank my Grandma Hall, who recently passed away. You were a truly wonderful woman whose only worry was to be of service to those

around you. I am so grateful that I was your grandson and grew up having such a loving and caring person in my life. I love you all dearly and I hope that I've made you all proud.

Abstract

Development of Transition Metal Mediated Heck Cascades

And Their Application Towards the Synthesis of Retigeranic Acid A

Jonathan Harvey Keim

Cascade reactions are among the most powerful and elegant tools available to chemists allowing for the quick and efficient construction of complex molecules form simple starting materials. This class of reactions has shown its worth time and time again in the arena of natural product synthesis, which has and continues to serve as the proving ground for chemical methods. Over the last century, a vast number of challenging targets have succumbed to syntheses enabled by both biomimetic and rationally designed cascades. However, despite the plethora of work done, much still remains to be done with even the most well studied methodologies still have largely unexplored areas. This dissertation herein reports the study of transition metal mediated cascades particularly Mizoroki-Heck cascades for the construction of complex polycyclic frameworks.

Chapter 1 describes the inspiration for the initial work towards the total synthesis of the pentacyclic sesterterpene retigeranic acid A as part of our group's interest in the synthesis of unfunctionalized terpenes via Pd-Mediated Heck cascade. The lessons learned over the course of our initial attempts with the cascade ultimately proved to be the impetus that led us to begin our studies on Ni mediated Heck cascades, of which only a handful of examples have been reported in contrast to the veritable ocean of Pd literature.

Chapter 2 begins with a brief introduction into the unique properties of Ni in the context of the Heck reaction and a overview of the state of the Ni Heck reaction. Next, we report our development of mild base-mediated conditions for aryl and vinyl triflates. Our conditions have proved quite general and give comparable, and in some cases superior, yields and selectivities to the corresponding Pd reaction. We are able to access a wide variety of spirocyclic and fused ring systems and applications with systems taken from the total synthesis literature are discussed.

Chapter 3 focuses on an intriguing intermolecular variant of the Heck reaction in which Ni exhibits divergent reactivity to Pd leading to the formation of 1,2-dihydronapthalenes. Following our initial discovery of the novel selectivity using our base mediated conditions, we chose instead to focus on the development of racemic and enantioselective conditions using a reducing metal mediated approach, which allowed us to access a wide variety of 1,2-dihydronapthlenes in good yield and *ee*. The application of this new strategy in the total syntheses of furomollugin and norcardione B as well a discussion of the origin of the observed [6-*endo*-trig] selectivity are also found within this chapter.

Chapter 4 concludes the dissertation by returning to our studies towards retigeranic acid A now via a new Pd-enolate in the hopes of overcoming the β-hydride elimination and [3-*exo*-trig] pathways that hampered our original approach. Following the synthesis of enoate and enone based

cascades substrates, we found the formation of the vinyl cyclopropane motif via the [3-*exo*-trig] pathway was unavoidable leading us to investigate both radical and Rh catalyzed [3+2] cyclizations in order to access the target. Future work towards retigeranic acid A is also discussed.

Chapter 1

Initial Studies Toward Retigeranic Acid A Via a Heck-Cascade Approach

1.1 Introduction

Terpenes comprise one of the largest classes of natural products and possess some of the most intriguing and synthetically challenging structures known to chemists. Sesterterpenes are among the more complicated and synthetically enticing members of the class with selected examples shown in Figure 1.1. These C_{25} terpenes and the related sesterterpenoids comprise a very small fraction of the overall terpene field and are relatively rare in nature, with approximately 1000 compounds having been isolated.[1,2] This rarity is reportedly due to the relatively low occurrence of sesterterpene synthases in nature, an enzyme required to effect the necessary transformations of the geranylfarnesyl pyrophosphate precursor.

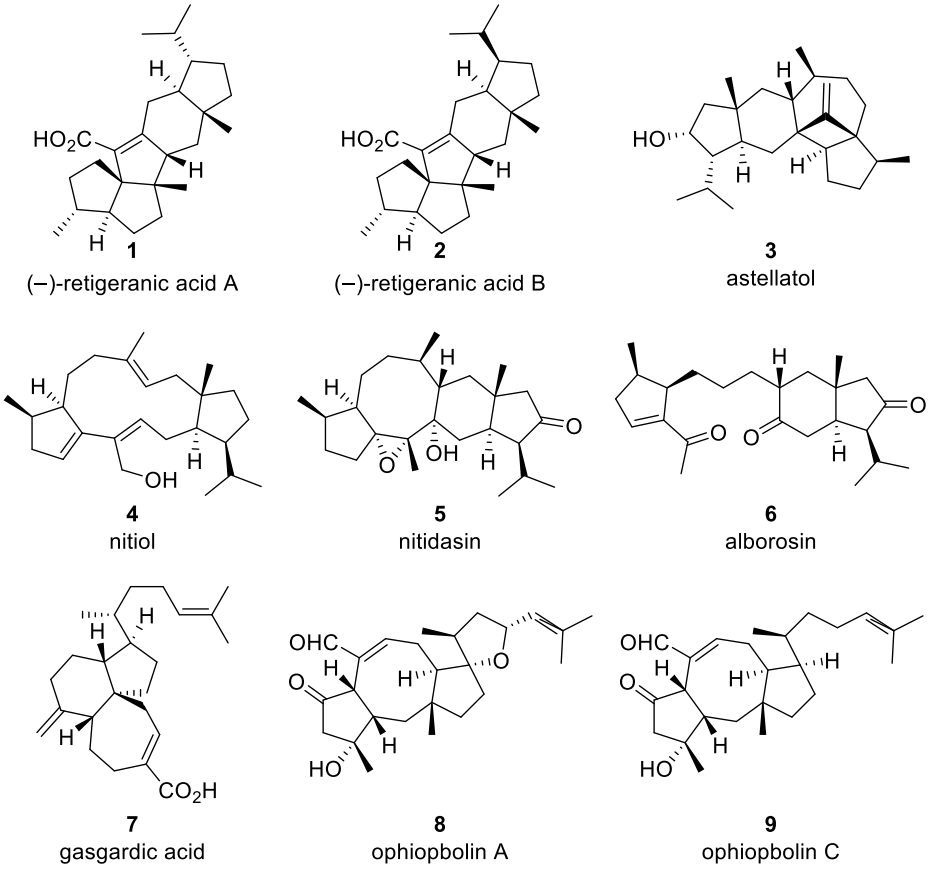

Figure 1.1 Sesterterpene and sesterterpenoid natural products.

One sesterterpene that has elicited considerable effort from the synthetic community over the last 40 years is (–)-retigeranic acid A **1**. Initially isolated from a lichen found in the eastern Himalayas as a mixture with its epimer (–)-retigeranic acid B **2**, the structure and absolute configuration of **1** was confirmed by X-ray crystallography, which in turn revealed a variety of challenging and distinguishing features. Most striking is the unique pentacyclic core comprised of a *trans*-hydrindane (AB rings) and an angular triquinane (CDE rings) motif. Notably, **1** has almost no functionalization, with only an α,β-unsaturated carboxylic acid present throughout the saturated hydrocarbon. However, while lacking functional groups, the structure is densely populated with 8 stereocenters as well as 3 all-carbon quaternary centers, 2 of which are vicinal. Despite its lack of reported biological activity, such structural features make **1** a formidable and enticing challenge to synthetic chemists even to this day.

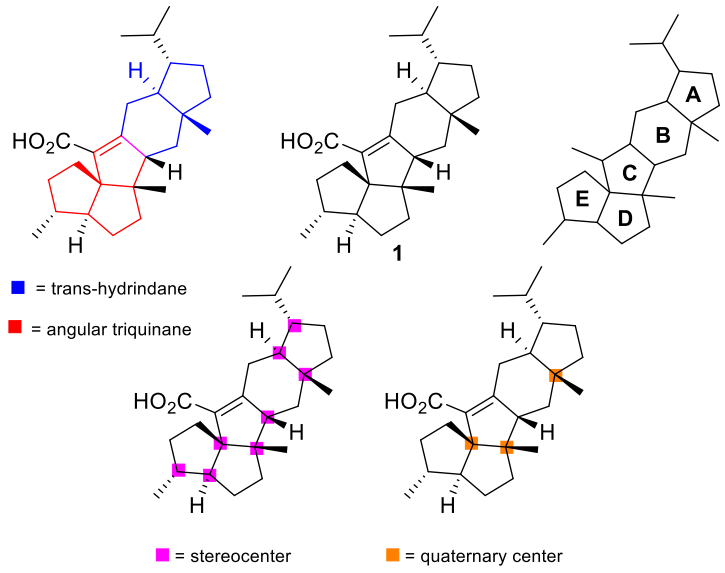

Figure 1.2 Structural features of **1**.

1.2 Recent Studies Toward the Synthesis of Retigeranic Acid A

As mentioned earlier, significant effort has been devoted to the synthesis of **1** with 4 previously reported total syntheses[3–6] and numerous studies toward. As many of these approaches

have been covered previously in reviews[7] and book chapters[8] they will not be discussed in detail at present. Nonetheless, a brief summary of the key transformations in the various total syntheses is presented in Figure 1.3. Recently the Yang group has made two separate reports on their efforts to access **1** using the Pauson-Khand reaction (PKR).[9,10] This section will begin by discussing the recent synthetic studies covered by the Yang group and conclude with a general overview of the previous strategies used to synthesize **1**.

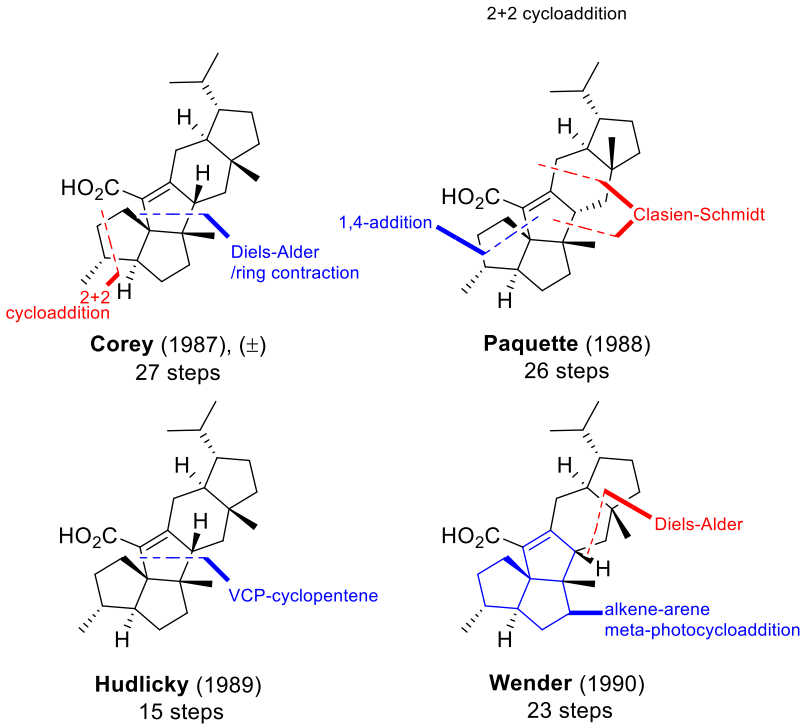

Figure 1.3 Summary of key transformations in the reported total syntheses of **1**.

The Yang group's initial report set out to synthesize the ABCD rings of **1**. Beginning with ketoester **10**, which was converted to enone **11** in 52% yield by addition to the *in situ* formed iminium and subsequent elimination. Next, **11** was reacted with Waser's reagent to give enyne **13,** which was then subjected to $LiAlH_4$ and TBS protection of the resulting primary alcohol to give **14**. The Yang group then utilized a Rh-catalyzed [3+2] cycloaddition[11] developed in their lab as a means to generate vicinal all-carbon quaternary centers. Under these conditions aldehyde **15**

was accessed in 91% as a single diastereomer. Subsequent DIBAL-H reduction, TBS protection, and allylic oxidation gave enone **16**, which then underwent 1,2-addition with methallylmagnesium chloride to afford tertiary alcohol **17.** Chromium-mediated oxidative rearrangement then gave

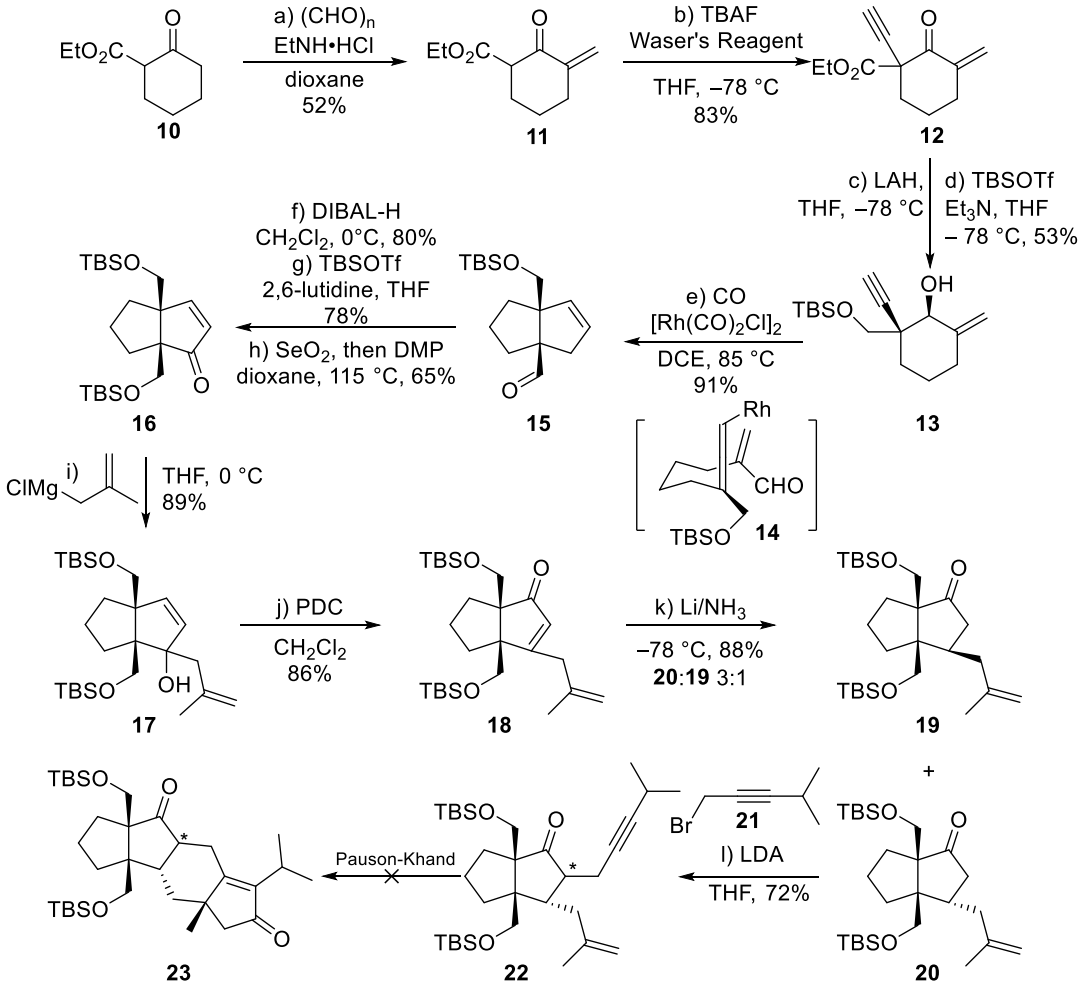

Scheme 1.1 Yang's initial Rh [3+2] approach.

gave enone **18**, which was reduced under Birch conditions yielding a 3:1 mixture of diastereomers favoring the desired ketone, **20**. Following enolate alkylation with propargyl bromide **21** the enyne moiety required for the PKR had been accessed as an inseparable mixture of diastereomers. Unfortunately, enyne **22** could not be converted to the desired cyclization product **23** under a variety of conditions, reportedly due to an unfavorable orientation of the alkyne, which prevented

Co coordination. Thus, they opted for a more rigid framework with the desired conformation locked into place. **20** underwent an aldol reaction to give propargyl alcohol **24.** This was then converted to enyne **25** via a mesylation/elimination procedure. Pleasingly, when **25** was subjected

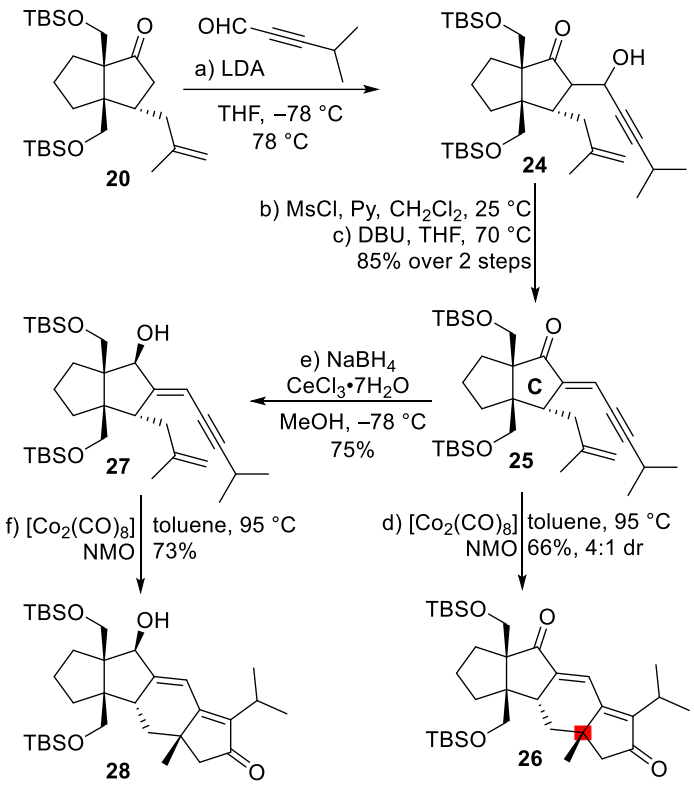

Scheme 1.2 Yang's completion of the ABCD core of **1.**

to PKR conditions the desired tetracycle **26** was accessed in a 66% yield with a 4:1 dr at the carbon highlighted in red, favoring the desired stereochemistry. DFT calculations indicated that introducing a sp^3 carbon into the C ring could destabilize the transition state of the undesired diastereomer, thereby improving selectivity. This hypothesis proved correct, with alcohol **27** giving the desired tetracycle **28** in 73% yield as a single diastereomer. While **28** could not be advanced to the natural product, they were able to install all the quaternary centers within the target as well as several stereocenters.

Following their previous studies, the Yang group recently published a report on further efforts to access **1** in which they were able to access the full ABCDE ring framework of the target. To begin, **29**, obtained in 5 steps from the Hajos-Parish ketone, underwent a hydrazone formation and fragmentation procedure that gave ketone **30** in 86% yield. Wittig olefination then gave enyne

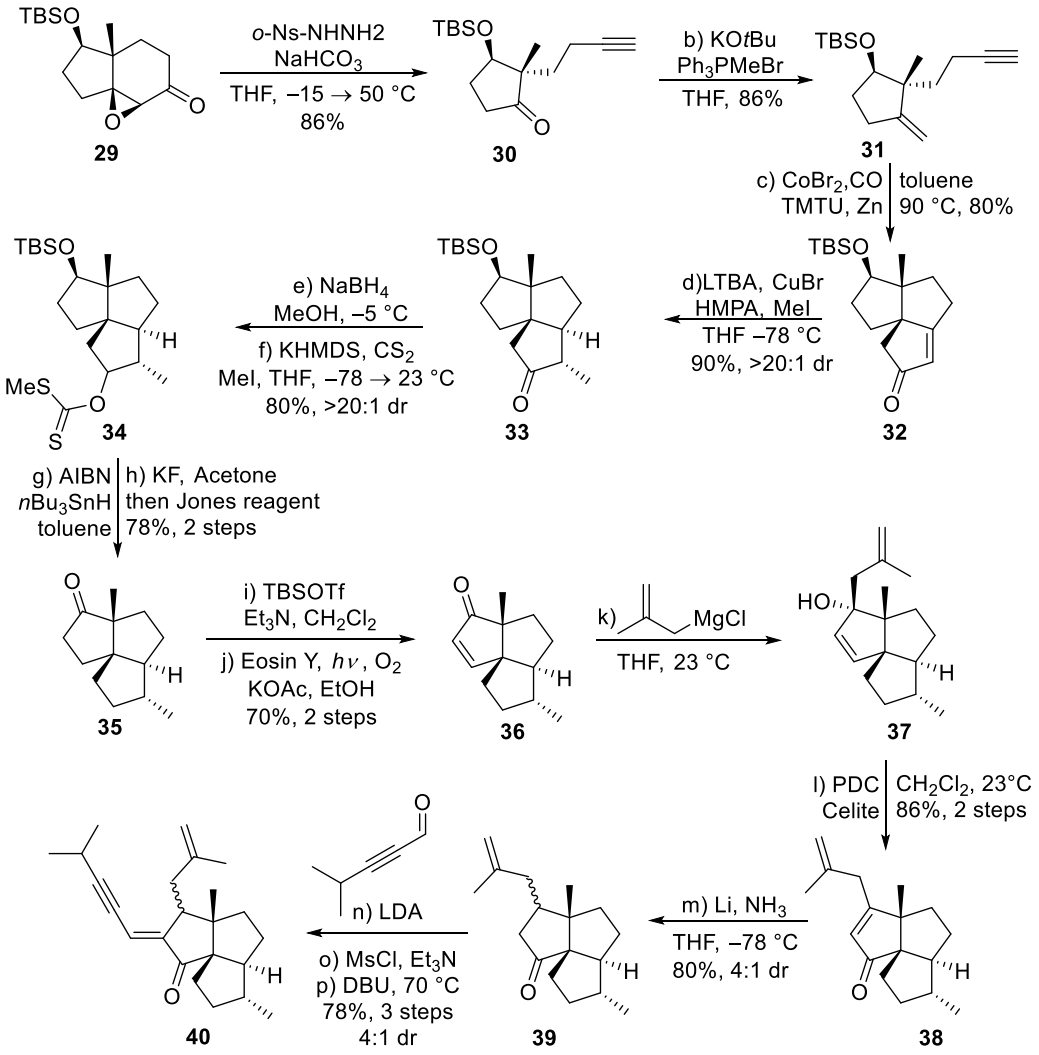

Scheme 1.3 Yang's Pauson-Khand approach to triquinane core of **1**.

31 in 86% yield. The first PKR of the route produced the desired angular triquinane **32** as a single diastereomer in 90% yield. Of particular note is the substitution of $CoBr_2$ and tetramethylthiourea (TMTU) for the more costly $Co_2(CO)_8$ and hydroscopic NMO. Conjugate reduction with

$LiAlH(OtBu)_3$ (LTBA) and trapping of the resultant enolate with MeI gave ketone **33**. A series of oxidation state manipulations then afforded enone **36**. The Yang group then utilized the same strategy from their previous synthesis to install the required enyne motif giving triquinane **40** as a 4:1 mixture of inseparable diastereomers. Luche reduction of **40** gave alcohol **41** in a 70% yield,

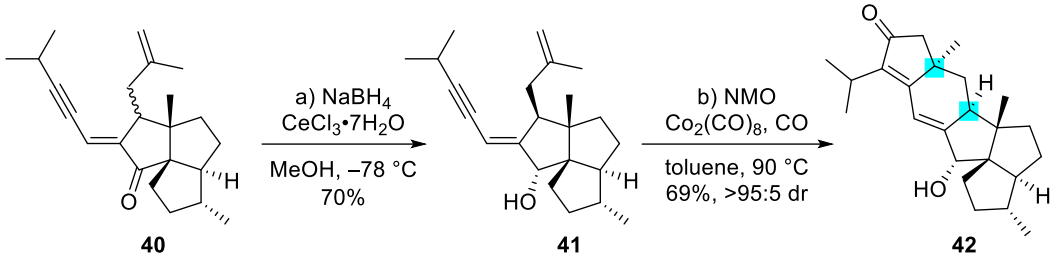

Scheme 1.4 Pauson-Khand reaction of **41** displaying undesired diastereoselectivity.

but the stereochemical identity of the isomer could not be ascertained until the following PKR revealed tetracycle **42** to possess the undesired configuration at the two highlighted carbons. As such, they set out to access the precursor with the appropriate stereochemistry.

To start, enone **38** was epoxidized with *m*CPBA and the resultant epoxide **43** was opened via a γ-deprotonation to give dienone **44.** Hydrogenation and tosylation yielded ketone **45**,

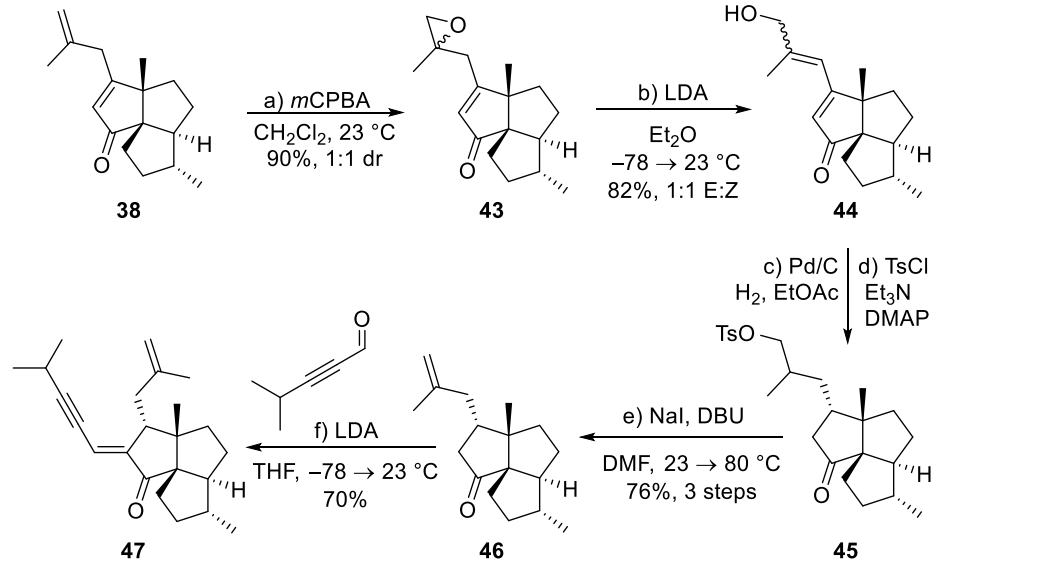

Scheme 1.5 Preparation of Pauson-Khand substrate **47** with correct stereochemistry.

pleasingly with the desired stereochemistry at the β-position. Reintroduction of the 1,1-disubstituted olefin followed by LDA-mediated aldol condensation yielded enyne **47**. The PKR of **47** using $Co_2(CO)_8$ and NMO completed the synthesis of the ABCDE ring framework of **1** giving the desired diastereomer **48** in 45% and the epimer **49** in 23% yield. Attempts to utilize

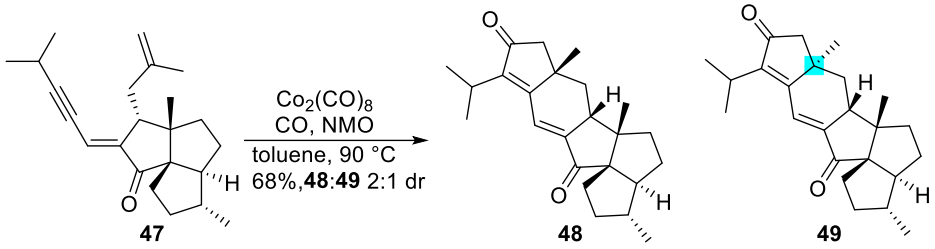

Scheme 1.6 Pauson-Khand reaction of **47** and establishment of the carbon framework of **1**.

catalytic conditions with $CoBr_2$ and TMTU gave only a combined 37% yield in a 2.4:1 dr favoring **48**. At this stage, the remaining hurdles were the installation of the carboxylic acid and the final two stereocenters on the AB ring system. While the previous report succeeded in installing the quaternary carbons and many important stereocenters, this approach allows for the construction of the entire polycyclic frame. Despite the fact that neither approach afforded the target of interest, they each provide important synthetic insight for future work.

As we reviewed the work of the Yang group, other studies toward, and especially the completed total syntheses, we looked for a common thread amongst them that might inspire a new approach to the target. We found that a while a wide variety of chemistry and strategies had been employed, shown in Figure 1.4, all of the currently reported syntheses fall into one of two approaches. Regardless of using a linear or convergent route, the ABCDE core of **1** is formed by building either the *trans*-hydrindane (AB) or angular triquinane (CDE) first and then constructing the remaining rings off the respective motifs. As such, we were curious whether there was a way

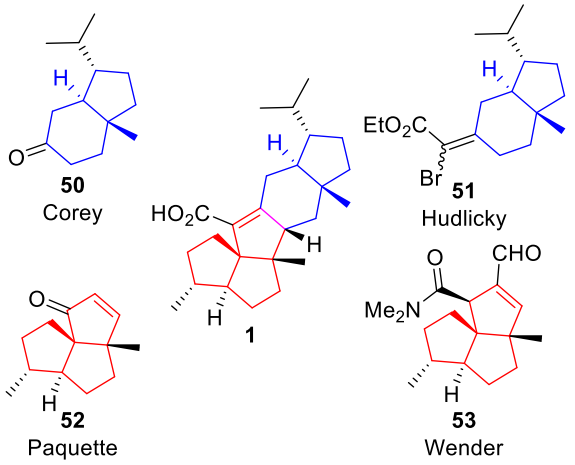

Figure 1.4 Key intermediates from the previous total syntheses.

in which both motifs could be formed in a single step. Our first indication of how this may be accomplished was the identification of a 1,3-*trans* motif in the D ring.

1.3 1,3-Trans Inspired Cascade Approach

The so-called 1,3-*trans* motif was identified as part of the Snyder group's synthesis of presilphiperfolan-8-ol **54**, when Dr. Pengfei Hu noted that this relationship is found not only

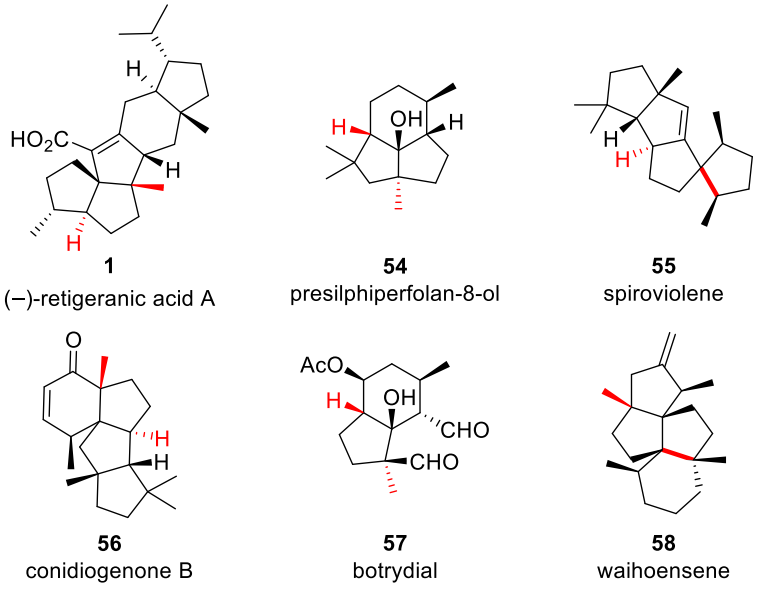

Figure 1.5 Natural products with the 1,3-trans relationship.

amongst **54** and its relatives, but also many different families of natural products.[12] The examples in Figure 1.5, all contain this motif, with the relevant substituents denoted in red. Upon noting this commonality, he sought a solution to quickly and diastereoselectively establish the

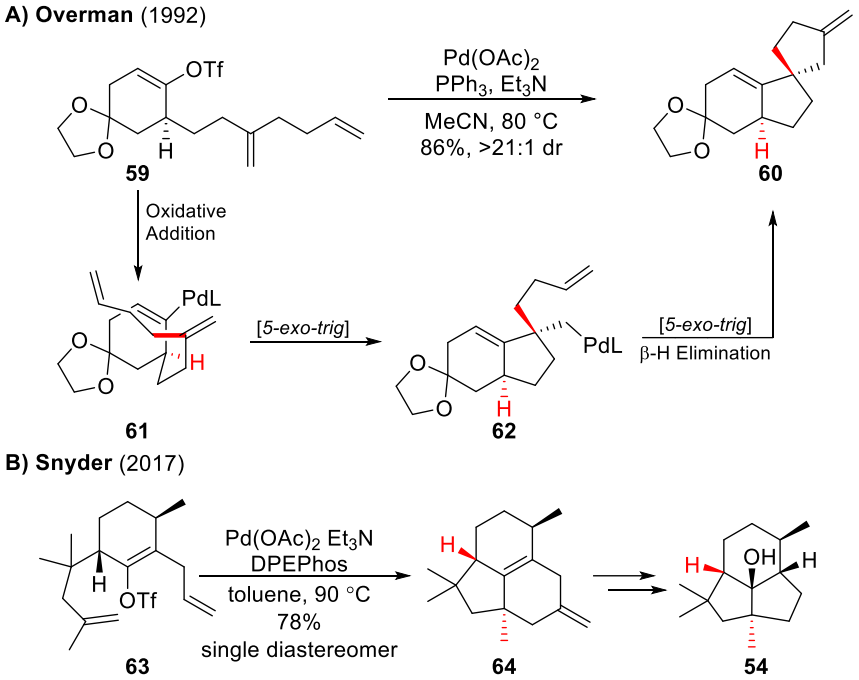

Scheme 1.7 A) Overman's seminal work on Heck cascade and rationale for the formation of the 1,3-trans relationship **B)** Our synthesis of **54** using a Heck cascade to establish the 1,3-trans relationship.

relationship, thereby affording a potential general strategy to access numerous natural products. One answer was found in the Overman group's work on Pd-mediated intramolecular Heck cascades, wherein they reported highly diastereoselective cyclizations of vinyl triflates to form spirocycles such as diene **60**.[13] Dr. Hu noted that during the reaction a 1,3-*trans* relationship was established. This high diastereoselectivity arises due to the geometric constraints of the 4-membered transition state of the migratory insertion step, as well as the proximity of a chiral center, which force the intermediate to adopt a conformation like **61** for the [5-*exo*-trig] cyclization to occur. With this precedent in mind, Dr. Hu developed a route to **54** via a Heck cascade using the (+)-pulegone derived vinyl triflate **64**. Upon identification of appropriate conditions, **63** was

converted into tricycle **64** in 78% yield, as a single diastereomer with the desired 1,3-*trans* motif. With this core in hand, Dr. Hu was able to achieve the first total synthesis of **54**.

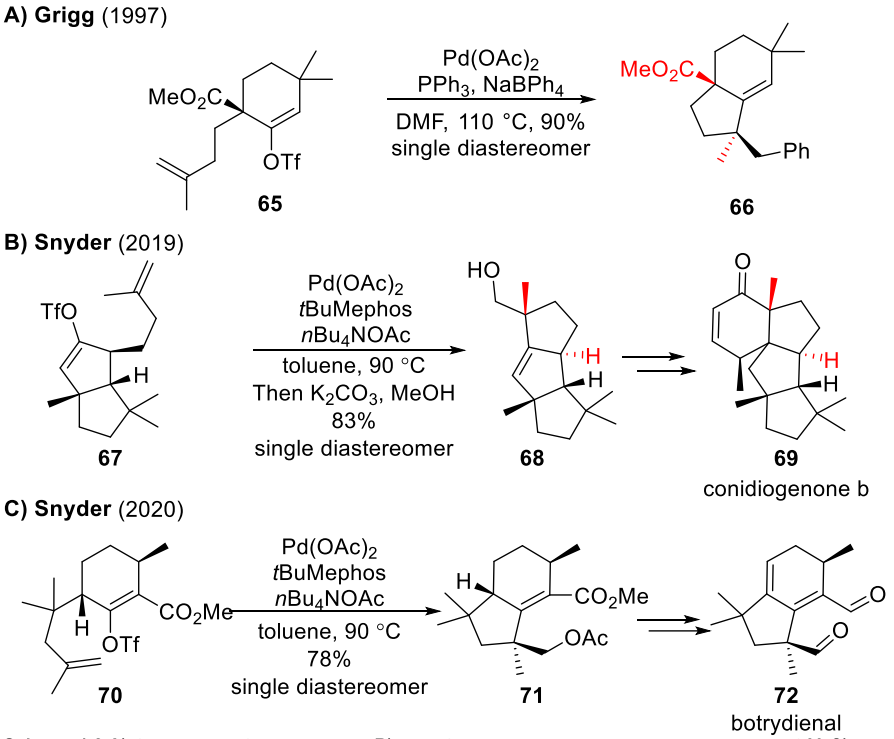

Scheme 1.8 A) Grigg's Heck-Suzuki cascade **B)** Heck functionalization cascade in our synthesis of **69 C)** Heck functionalization cascade in our synthesis of **72.**

Another source of inspiration for the 1,3-*trans* approach was the work of the Grigg group, who reported on highly diastereoselective Heck-functionalization cascades, which could give bicycles such as ester **66** as single diastereomers.[14] For our group's work on the conidiogenone family, we developed a related, but novel, cascade, which allowed for the use of oxygen nucleophiles to displace the Pd species following the migratory insertion step.[15] Using vinyl triflate **67**, we were able to effectively access alcohol **68** in an 83% yield allowing us to synthesize conidiogenone B **69** and several other family members. In further studies of this cascade the synthesis of botrydienal **72** was also accomplished.[16]

Returning to our target of interest **1**, upon identification of the 1,3-*trans* motif in the D ring, and based on our previous efforts, we believed that this could be introduced via a similar Heck cyclization. Furthermore, given the arrangement of the fused tricycle, we wondered if the Heck reaction could be extended to form not only the D ring, but also the B & C rings in a single step. Retrosynthetically such a cascade could be initiated from vinyl triflate **73**, as shown in Scheme 1.9. In a forward sense, we propose that the cascade could proceed via oxidative addition of Pd

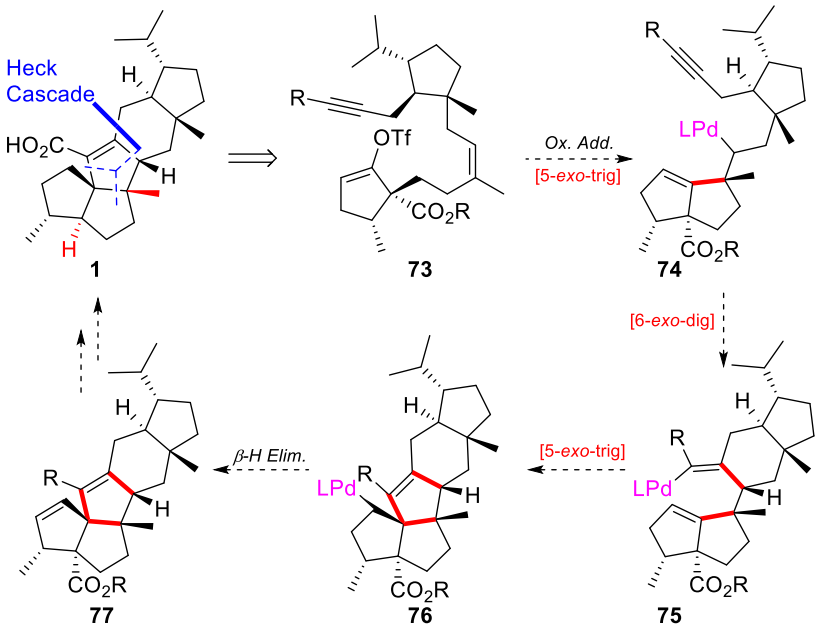

Scheme 1.9 Mechanism for proposed 1,3-trans inspired Heck cascade.

into the vinyl triflate, followed by a [5-*exo*-trig] cyclization to arrive at tricycle **74**. Next, **74** could undergo a subsequent [6-*exo*-dig] cyclization onto the pendant alkyne to give tetracycle **75**. Then a second [5-*exo*-trig] cyclization and finally β-hydride elimination would produce pentacycle **77** with the completed ABCDE framework. Further transformations would allow access to **1**.

1.4 Potential Competing Pathways

While plausible, the proposed cascade was likely to be a particularly challenging one. This is due in large part to the nature of intermediate **74**, which has the potential to undergo competitive

pathways that would interrupt the intended cascade. The first and initially more concerning pathway is that of β-hydride elimination to give a product such as olefin **75**. The second pathway we foresaw was a potential competitive migratory insertion where the Pd could insert into the trisubstituted olefin (highlighted in green) in a [3-*exo*-trig] fashion, which, following β-hydride elimination, would yield vinyl cyclopropane **76**.

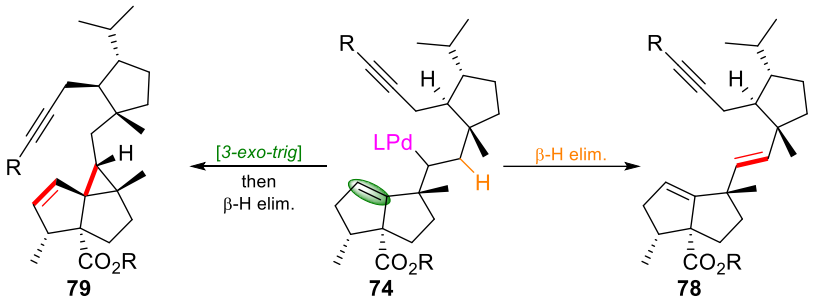

Scheme 1.10 Potential competing pathways for the desired [6-*exo*-dig] in the proposed Heck cascade.

At the outset, the β-hydride elimination pathway was the larger concern as Heck cascades generally proceed via intermediates that cannot undergo β-hydride elimination, such as vinylic or neopentylic Pd species. This is due to the relative ease of β-hydride elimination compared to migratory insertion for Pd. In fact, this has been exploited by the de Meijere group to access

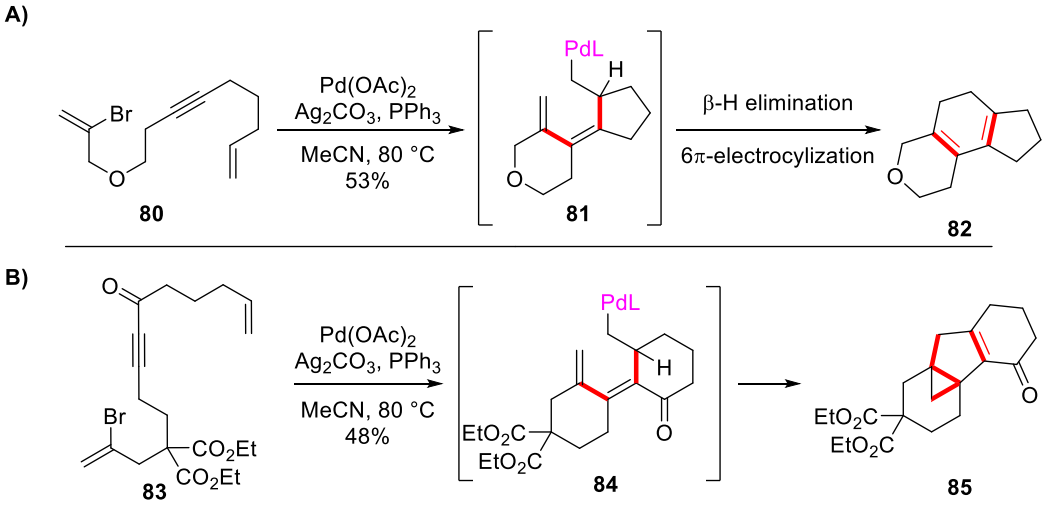

Scheme 1.11 Competition between pathways where **A)** β-H elimination prevails or **B)** migratory insertion prevails. Red coloring indicates where Pd formed C-C bonds.

substituted dienes like **82**, as shown in Scheme 1.11.[17] Here, the cascade proceeds first via a [6-*exo*-dig] and subsequent [5-*exo*-trig] cyclization to arrive at **81**. The alkyl Pd intermediate then undergoes β-hydride elimination, followed by 6π-electrocyclization to arrive at **82**, which could be oxidized to give an arene product. While rare, examples of Heck cascades wherein migratory insertion outcompetes β-hydride elimination are known.[18] In another example from the de Meijere group, a very closely related cascade produces intermediate **84**. This species was initially designed to undergo β-hydride elimination–6π electrocyclization sequence like **81**, but instead proceeded via a [5-*exo*-trig] cyclization followed by a [3-*exo*-trig] and β-hydride elimination to arrive at tetracycle **85** as the sole product of the reaction. Given the similarities of the cascades, it is not immediately evident as to why the selectivity should shift so dramatically. As such, it is not surprising that cascades of this type are generally found serendipitously rather than by rational design.

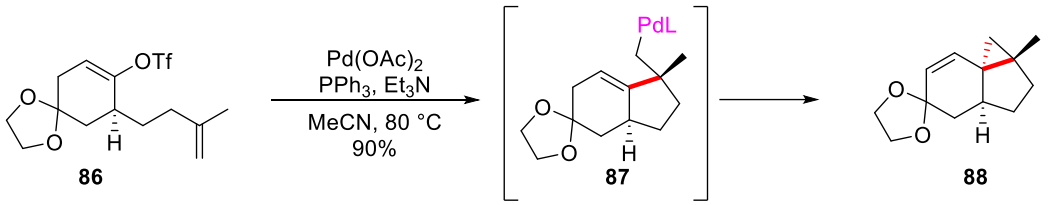

Scheme 1.12 [3-*exo*-trig] example from Overman.

For the second competing pathway, [3-*exo*-trig] cyclization, it was unclear as to how prevalent it would be with our substrate. [3-*exo*-trig] cyclizations are relatively uncommon in Heck cyclizations, but some examples are known as shown above from the Overman group.[13,19] It is intriguing to note that intermediate **87** is almost identical to **62**, and yet no product arising from the [3-*exo*-trig] pathway was observed in that case. The higher temperature required for the formation of **88** would suggest that the [3-*exo*-trig] pathway is a higher energy pathway. A further reason why the [3-*exo*-trig] pathway is usually not observed is that it appears to be readily

reversible. Negishi reported an intriguing cyclization that appeared to proceed via [6-*endo*-trig] cyclization, but with apparent inversion of the olefin stereochemistry to give diene **90**.[20] They instead proposed a cascade that proceeds via an initial [5-*exo*-trig]/[3-*exo*-trig] sequence to arrive at cyclopropane **92**, which, rather than undergoing β-hydride elimination, performs a C-C bond rotation so that the Pd is now aligned with the other C-C bond of the cyclopropane. Retro-[3-*exo*-trig] cyclization gives cyclohexene **94** and β-hydride elimination then yields **90**. If the [3-*exo*-trig] cyclization is truly a reversible process, then other pathways within our own proposed sequence

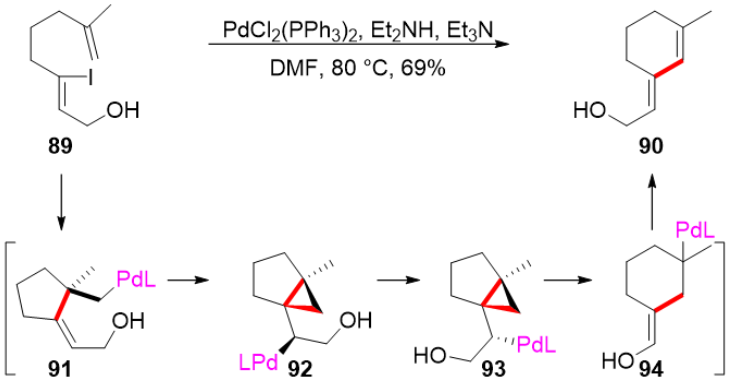

Scheme 1.13 Apparent stereoinvertive [6-*endo*-trig] via a proposed cyclopropyl intermediate.

could outcompete cyclopropane formation. However, as with β-hydride elimination, it appears to be quite challenging to predict which pathway is preferred when other migratory insertions can out compete the [3-*exo*-trig] cyclization. As shown in Scheme 1.14, even in closely related cascades wildly different product distributions are observed. From vinyl bromide **95**, tetracycle **97** is formed as the major product with ether **98**, while an almost 1:1 ratio of tetracycle **101** and tricycle **102** is observed in the case of diester **99**.[17] In the Negishi example from Scheme 1.14, a [6-*exo*-trig] pathway is slightly more favorable than the [3-*exo*-trig] competitor, which offers hope that with possible substrate control or under the appropriate conditions our desired [6-*exo*-dig] cyclization may be the predominant pathway.

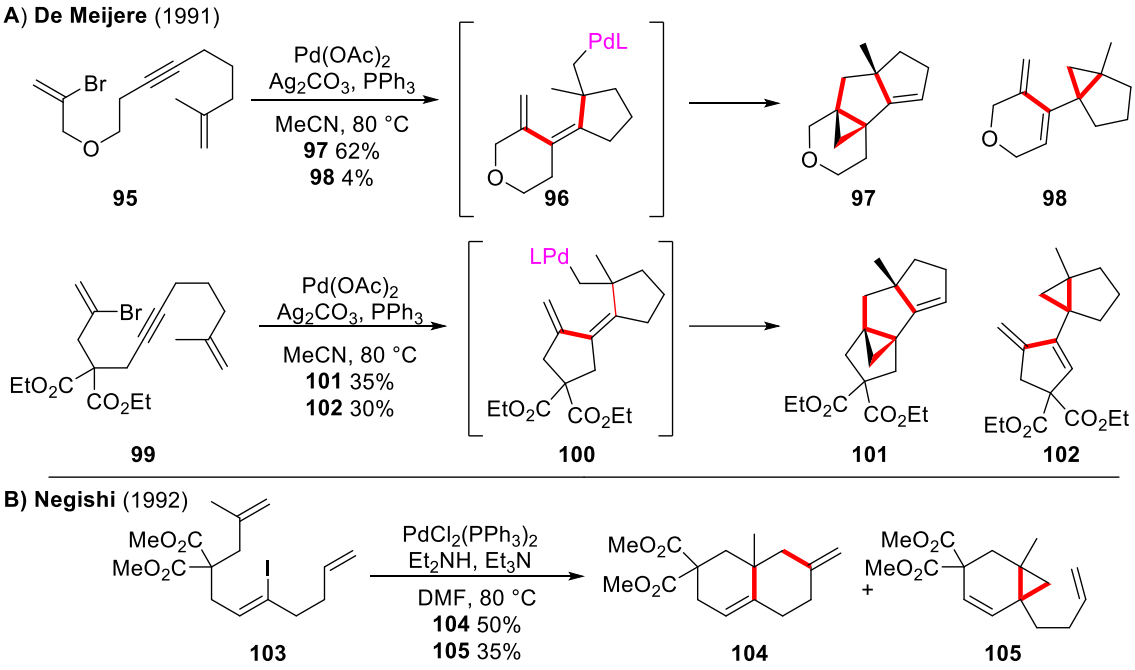

Scheme 1.14 Examples of [3-*exo*-trig] competing with other cyclization modes from **A)** de Meijere and **B)** Negishi.

Intramolecular Heck cascades are quite complex with a subtle interplay of factors controlling the balancing act of competing pathways. With this in mind, we viewed our proposed cascade as an opportunity to develop a deeper understanding of that balancing act and use that understanding to further what is known and what is possible with the Heck reaction.

1.5 Retrosynthesis of Cascade precursor

With our proposed cascade in hand, we then pursued access to the required precursor, vinyl triflate **73**. Retrosynthetically, our first step was to cut the trisubstituted olefin, which could be formed via a Julia-Kocienski olefination between sulfone **95** and diketone **97**. This was expected to be a challenging step due to the stereospecific requirements of our substrate, and precedented difficulties associated with tri-substituted olefin formation. Further, the multiple acidic sites on **97** could protonate the sulfone preventing any olefination event from occurring. The sulfone moiety could be introduced using Baran's reductive olefin coupling method using a 1,1-disubstituted

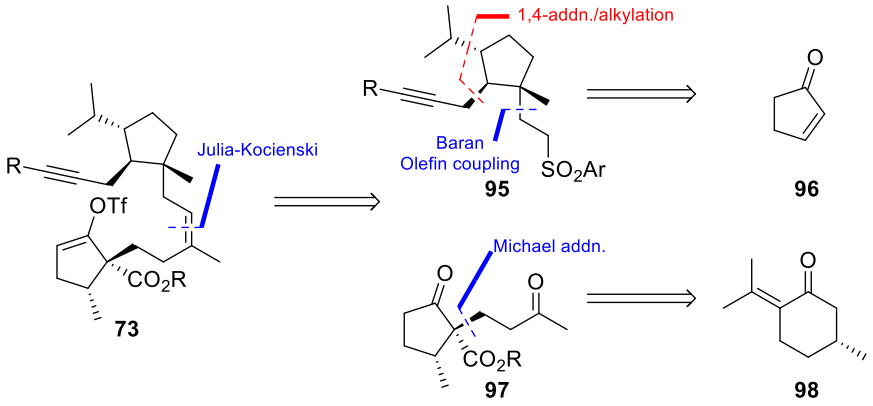

Figure 1.6 Retrosynthesis of Heck cascade precursor **73**.

olefin as the donor and a vinyl sulfone as the acceptor.[21] Next the isopropyl and propargyl groups could be introduced via vicinal difunctionalization of commercially available cyclopentenone **96**. On the other hand, diketone **97** could be accessed via a chiral pool synthesis starting from (+)-pulegone **98**.[22,23]

1.6 Accessing Racemic Cascade Precursors

To begin our campaign toward retigeranic acid A **1**, we first sought a route to access the Heck cascade precursors utilizing more readily accessible racemic starting materials. We appreciated that the proposed Julia-Kociesnki olefination between a racemic sulfone and diketone would result in a mixture of eight stereoisomers, which may render the subsequent transformations challenging to interpret. However, a successful Julia-Kocienski olefination would at least establish a route to the carbon skeleton of the cascade precursors providing a beachhead for further forays. As such, we set out to access an appropriate sulfone coupling partner.

Starting from cyclopentenone **96**, we attempted a variety of conditions for a tandem vicinal difunctionalization using an isopropyl organocuprate and a TMS-protected propargyl bromide. However, while we observed complete conversion of **96** to the 1,4-addition product, the following alkylation step proceeded poorly and only trace ketone **99** was ever observed. As such, we instead

used a two-step method[24,25] wherein the conjugate addition product was trapped as a silyl enol ether **100** in quantitative yield. **100** was then converted into a lithium enolate with MeLi and alkylated with propargyl iodide **102** in the presence of DMPU to give **99** in good yield over two

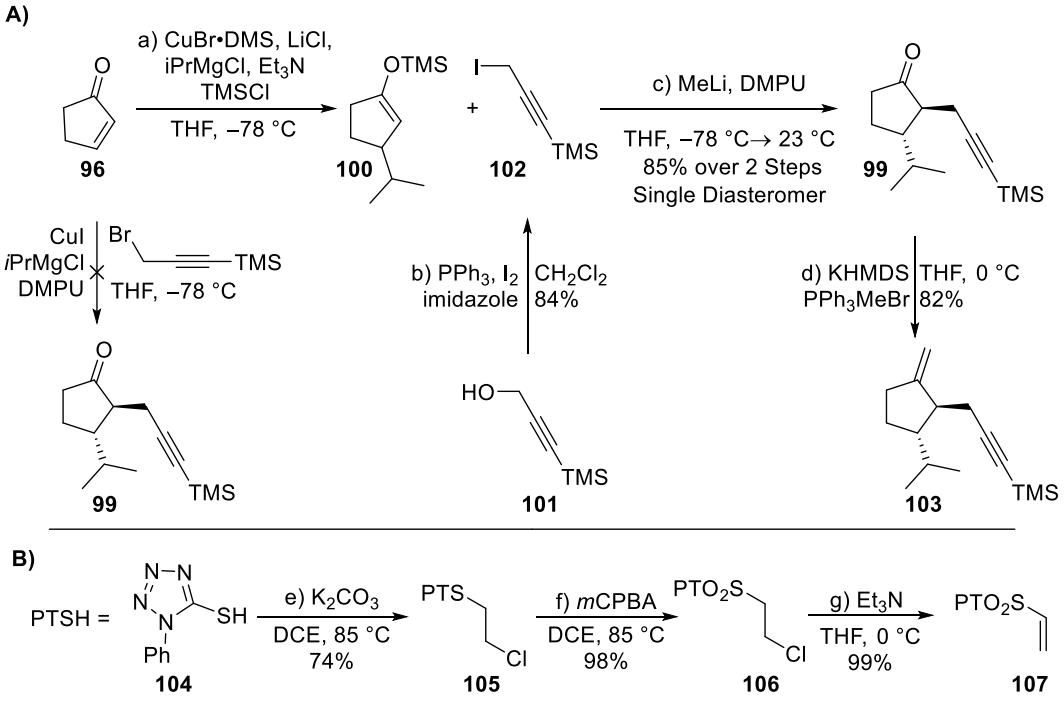

Scheme 1.15. Synthesis of **A)** Julia-Kocienski precursor **103** and **B)** vinyl sulphone for reductive olefin coupling: a) CuBr•DMS (2.15 equiv.), LiCl (2.15 equiv.), *i*PrMgCl (2.3 equiv.), TMSCl (1.5 equiv.), Et_3N (1.5 equiv.), THF (0.4 M), –78 °C, 1.5 hr; b) PPh_3 (1.5 equiv.), I_2 (1.5 equiv.), imidazole (1.5 equiv.), CH_2Cl_2 (0.5 M), 0 °C, 1 hr, 84%; c) MeLi (1.1 equiv.), DMPU (14.1 equiv.), THF (0.08 M), –40 °C, 1 hr, then **102** (1.5 equiv), –78 °C → 23 °C, 12 hr, 85% over 2 steps; d) PPh_3MeBr (2.2 equiv.), KHMDS (2.0 equiv.), THF (0.4 M), 0 °C, 2 hr, 82%; e) K_2CO_3 (2.0 equiv.), DCE (0.1 M), 85 °C, 74%; f) *m*CPBA (5.0 equiv.), DCE (0.1 M), 85 °C, 3 hr, 98%; g) Et_3N (1.0 equiv.), THF(0.2 M), 0 °C, 30 min, 99%.

steps as a single diastereomer. We assumed that the obtained compound was the *trans*-isomer based on literature comparisons.[24,25] Next, **99** was converted into cyclopentene **103** via a Wittig olefination using Ph_3PMeBr and KHMDS. Despite the simplicity of **99**, the choice of base proved to be crucial with *n*-BuLi leading to decomposition, LDA and LiHMDS suffering from poor conversion, and KO*t*Bu proceeding with desilylation of the alkyne. We then turned our attention to the synthesis of vinyl sulfone **107** via modified literature reported alkylation/oxidation/elimination sequence.[26] In our hands, the literature procedure for the final elimination step led to poor yields of impure **107** that would quickly degrade upon attempts to

purify using the reported column chromatography conditions or recrystallization. By reducing the reaction temperature to 0 ˚C and using exactly 1.0 equivalent of Et_3N, the formation of side products was effectively inhibited. Further, it was found that the Et_3N•HCl byproducts could be precipitated through the addition of Et_2O allowing **107** to be purified by filtration.

With both **103** and **107** in hand, we turned our attention to the reductive olefin coupling.[21,27] Initially, it was unclear if the π-bonds of the alkyne would be innocent in the reaction[28] and as vinyl sulfones are known to be challenging substrates,[21] we first attempted the

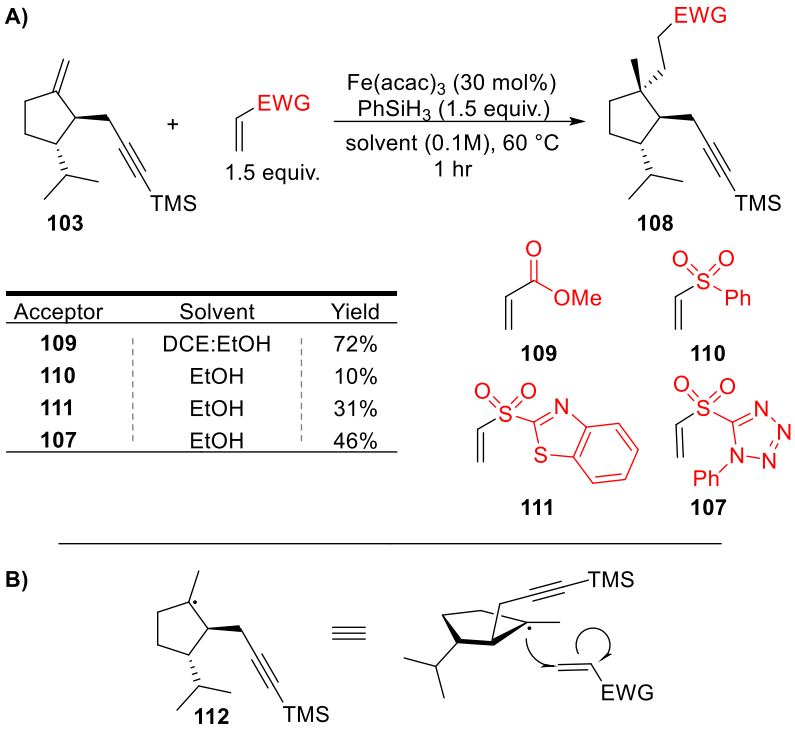

Acceptor	Solvent	Yield
109	DCE:EtOH	72%
110	EtOH	10%
111	EtOH	31%
107	EtOH	46%

Scheme 1.16 A) Reductive olefin coupling of **103** and radical acceptors **B)** Proposed rational for observed diastereoselectivity.

coupling with methyl acrylate **109**. Pleasingly, the reaction proceeded smoothly giving the desired product in a 72% yield as a single diastereomer. Moving to phenyl vinyl sulfone **110**, no product formation was observed even with Baran's optimized conditions. With the benzothiazole sulfone **111**[29] and phenyltetrazole sulfone **107** modest yields of the respective Julia-Kocienski precursors

were isolated as single diastereomers. The high diastereoselectivity likely arises from the propargyl group blocking the top face of the cyclopentane forcing the radical acceptors to approach from the bottom face as shown in Scheme 1.16. Reproducibility issues in the synthesis of **111** and its lower yields in the reductive olefin coupling led us to move forward with **107**. Attempts to increase the yield of the coupling ultimately proved unfruitful.

The next task was to access a suitable diketone model system **115**. We first attempted to synthesize the diketone via a Mukiyama-Michael with methyl vinyl ketone **114**, but only desilylation to form cyclopentanone **116** or **114** polymerization were observed with a variety of Lewis acids.[30–33] Using the Stork-Jung vinyl silane **117** we were able to access **115**, but the procedure required several steps and was too low yielding to be feasible.[34,35] Pleasingly, through an HFIP promoted conjugate addition, **115** was synthesized in 77% yield.[36]

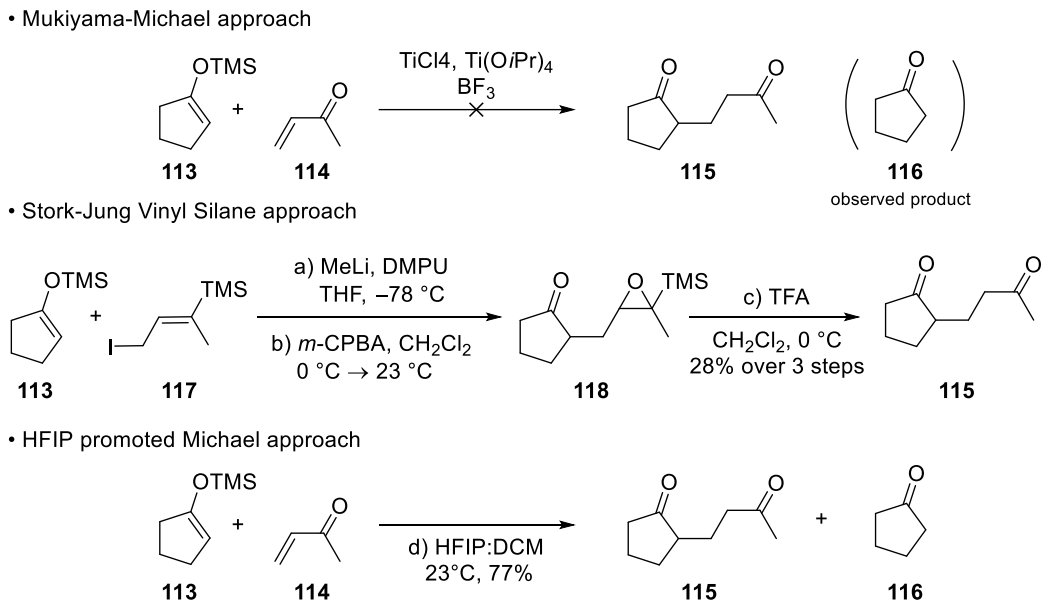

Scheme 1.17 Synthesis of Diketone **115**: a) MeLi (1.1 equiv.), DMPU (14.1 equiv.), **114** (1.5 equiv.), THF (0.1M), –78 °C → 23 °C, 12 hr, 64%; *m*-CPBA (1.15 equiv.), CH_2Cl_2 (0.5 M), 0 °C → 23 °C, 2 hr; c) TFA (1.4 equiv.), CH_2Cl_2 (0.7 M), 0 °C, 43% over 2 steps; d) **113** (2.0 equiv.), **114** (1.0 equiv.), HFIP:CH_2Cl_2 (4:1, 0.33 M), 23 °C, 77%.

We then began our investigations of the Julia-Kocienski olefination. In our initial base screening, only LiHMDS gave any of the desired ketone **120** and even then, only in a 7% yield

and 1:1 *E*/*Z* ratio. Using excess sulfone increased the yield to 25%, but conversion remained low with both starting materials recovered in almost quantitative yield brsm, suggesting the self-condensation of **119** was not the issue.[37] The poor conversion combined with the observed rapid disappearance of the bright-yellow sulfone anion upon addition of **115** led us to suspect that the sulfone anion was acting as a base rather than a nucleophile, deprotonating **115**. The Saskai group encountered a similar issue in their synthesis of gambieric acid A, which incorporated a similar

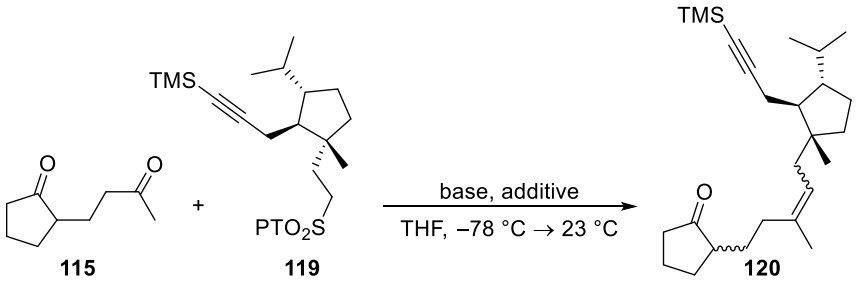

115 **119** **120**

Base (equiv.)	**115** equiv.	**119** equiv.	Additive (equiv.)	Yield	Z:E
KHMDS (1.0)	1.5	1.0	-	0%	-
LDA (1.0)	1.5	1.0	-	0%	-
LiHMDS (1.0)	1.5	1.0	-	7%	1:1
LiHMDS (1.0)	1.0	1.5	-	25%	1:1
LiHMDS (1.0)	1.0	1.5[b]	$CeCl_3$ (1.6)[a]	30%	2:1
LiHMDS (1.0)	1.0	1.5[b]	$CeCl_3$ (2.0)[a]	35%	2:1
LiHMDS (1.0)	1.0	1.5[b]	$CeCl_3$ (5.0)[a]	37%	2:1
LiHMDS (1.0)	1.0	1.5[b]	$CeCl_3$ (2.0)[c]	65%	2:1

Table 1.1 Screening of Julia-Kocienski olefination conditions: [a]$CeCl_3$ dried by heating at 150 °C under vacuum for 1 hr [b]Azeotropically dried with benzene three times [c]Commercial anhydrous $CeCl_3$ stored in glovebox.

Julia-Kocienski olefination of a methyl ketone.[38,39] They found that through the use of anhydrous $CeCl_3$ the yields could be increased dramatically, and the reaction now favored their desired *E* isomer in a 2:1 ratio. $CeCl_3$ is well known[40] to promote 1,2-additions to carbonyls, especially easily enolizable ones, either by acting as a highly-oxophilic Lewis acid[41] or through the formation of highly nucleophilic organocerium compounds[42] that exhibit markedly lower basicity compared to their organolithium and organomagnesium equivalents. In our first attempt using 1.6 equivalents of $CeCl_3$, we now observed a 30% yield and by increasing the equivalents to 2.0, a

35% yield was achieved. Further increasing of the $CeCl_3$ equivalents had little effect. We were concerned that the $CeCl_3$ used in the reaction, which was stored outside the glovebox, was either still hydrated to some degree despite heating it under vacuum or that the drying process was causing decomposition[40] of the $CeCl_3$. As such, we purchased anhydrous $CeCl_3$ and pleasingly the yield increased to 65% in a 1:2 *E*/*Z* ratio indicating that the quality of the $CeCl_3$ had indeed been at fault. It is intriguing to note that while the observed ratio of olefin isomers in our reaction and that of the Saskai group were the same, the favored isomer was different.

With effective conditions for the Julia-Kocienski in hand, we next attempted to complete the synthesis of the racemic cascade precursor through the introduction of a vinyl triflate and the conversion of the TMS-protected alkyne into the corresponding ynoate. Our first approach was to directly convert **120** into ynoate **121** through deprotection of the TMS-capped alkyne with CsF and trapping of the resultant anion with an electrophile. Both methyl chloroformate and CO_2/MeI provided **121**, but in similarly poor yields. We then attempted a two-step process where the TMS was cleaved almost quantitatively under basic conditions and the free alkyne was then carbonylated under Pd catalyzed conditions. Unfortunately, these carbonylation conditions gave **121** in lower overall yields than the CsF conditions. With the small amount of **121** formed, we attempted to convert **121** into vinyl triflate **122**, however, the ynoate proved unstable under the reaction conditions and only decomposition was observed. As such, we changed the strategy to instead form the vinyl triflate first and then deprotect the alkyne and introduce the ynoate. Vinyl triflate formation proceeded smoothly with complete regiocontrol. The subsequent desilylation reaction proved challenging as will be discussed further below, but ultimately, we were able to find successful conditions to access **123**.[43] Base mediated carbonylation proceeded in modest yield to give **122** with on small amounts of **121** observed arising from vinyl triflate hydrolysis.

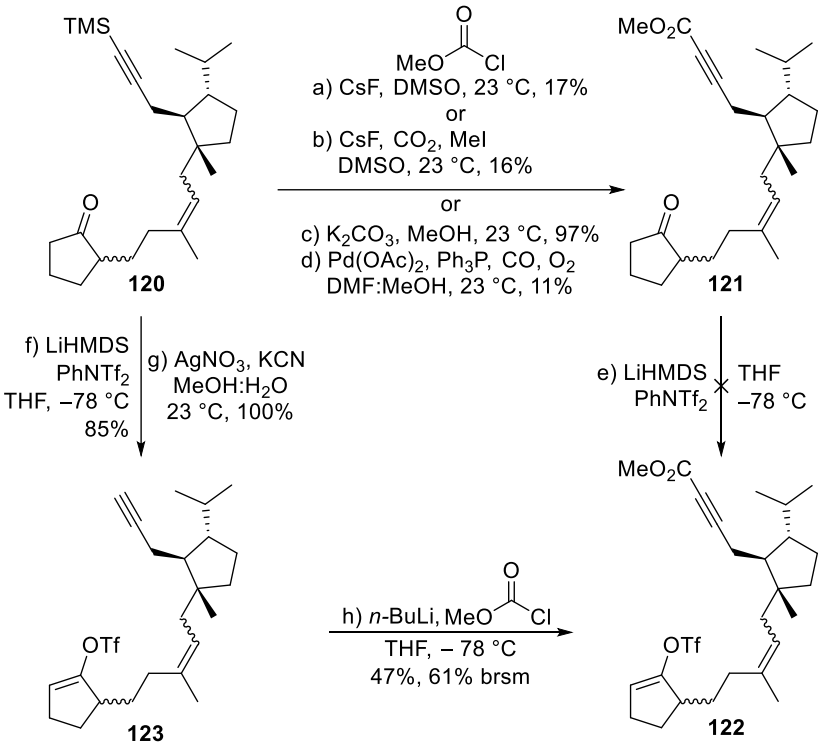

Scheme 1.18 Synthesis of model cascade substrates: a) CsF (2.0 equiv.), methyl chloroformate (2.0 equiv), DMF (0.2 M), 23 °C, 14 hr, 17%; b) CsF (2.0 equiv.), CO_2, MeI (1.2 equiv.), DMSO (0.5 M), 23 °C, 4 hr, 16%; c) K_2CO_3 (5.0 equiv.), MeOH (0.5 M), 23 °C, 12 hr, 97%; d) $Pd(OAc)_2$ (30 mol%), Ph_3P (60 mol%), CO, O_2, MeOH (0.2 M), DMF (0.1 M), 23 °C, 24 hr, 11%; e) LiHMDS (2.5 equiv.), $PhNTf_2$ (2.0 eq), THF (0.1 M), –78 °C → 23 °C, 4 hr; f) LiHMDS (1.5 equiv), $PhNTf_2$ (1.1 equiv.), THF (0.1 M), –78 °C → 23 °C, 5 hr, 85%; g) $AgNO_3$ (2.7 quiv.), KCN (10.0 equiv.), MeOH (22 M), H_2O (0.25 M), 23 °C, 30 min, 100%; h) *n*-BuLi (1.5 equiv.), methyl chloroformate (5.0 equiv.), THF (0.1 M), – 78 °C, 4 hr, 47%, 61% brsm.

As mentioned above, the conversion of **124** to **123** proved non-trivial due to the hydrolytic instability of the vinyl triflate moiety. K_2CO_3 in methanol proceeded with complete hydrolysis of the vinyl triflate giving ketone **125** in quantitative yield. TBAF proved more effective giving **125** and **123** in a 1:1 ratio, with hydrolysis presumably due to the hydroxide content in the reagent. We thought moving to more acidic fluoride conditions would prevent hydrolysis and indeed, HF•Py did not hydrolyze the triflate, nor did it cleave the TMS group. As such, we attempted to buffer the TBAF with KH_2PO_4 or AcOH, which did prevent hydrolysis, but the conversion was incomplete even after extended reaction times of 24 hours or more. Further, the relatively small R_f difference between **124** and **123** meant that any reaction with incomplete conversion was

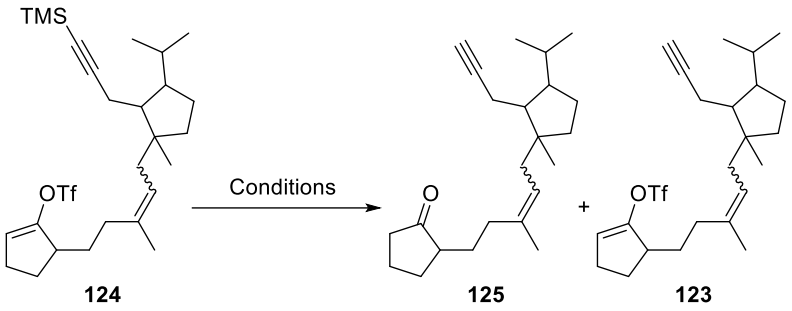

Conditions	**125** Yield	**123** yield
K_2CO_3, MeOH, 23°C	100%	0%
TBAF, THF, 23 °C	47%	48%
HF•Py, THF, 23 °C	0%	0%
TBAF•$3H_2O$, KH_2PO_4, THF, 23 °C	0%	66%
TBAF, AcOH, THF, 23 °C	0%	20%
$AgNO_3$, KCN, MeOH:H_2O, 23°C	0%	100%

Table 1.2 Screening conditions for the removal of the TMS group in the presence of a viny triflate.

exceedingly difficult to purify. Pleasingly, we found very mild Ag promoted conditions that quickly and efficiently effected the desilylation with no detected hydrolysis.[43] The deprotection is suggested to proceed via Ag complexation to the alkyne providing sufficient activation for nucleophilic displacement via CN^-, yielding TMSCN and a Ag-acetylide species that is subsequently quenched.

With this material in hand, we made our first attempts toward the desired Heck cascade. Unsurprisingly, the mixture of diastereomers led the reactions of both **124** and **122** to be too complex for interpretation. However, we were able to at least observe complete consumption of the starting material as evidenced by the lack of ^{19}F NMR signals in the crude reaction mixture.

1.7 Accessing Enantiopure Cascade Precursors

With a practical route to the cascade precursors established, our focus turned to accessing enantioenriched Julia-Kocienski coupling partners. For the diketone portion we opted to employ a similar strategy to the Paquette[4] and Hudlicky[5] syntheses, using a chiral pool approach starting from (+)-pulegone. Using literature reported procedures,[22,23] (+)-pulegone first underwent a

dibromination reaction, and subsequent base mediated Favorskii rearrangement yielding crude ester **126**. Ketone containing impurities were converted into water soluble semicarbazones by refluxing the crude mixture with semicarbazide•HCl and NaOAc. Next, **126** was subjected to ozonolysis with a reductive workup to yield ketoester **128** in 75% yield from **98**. Diketone **130**

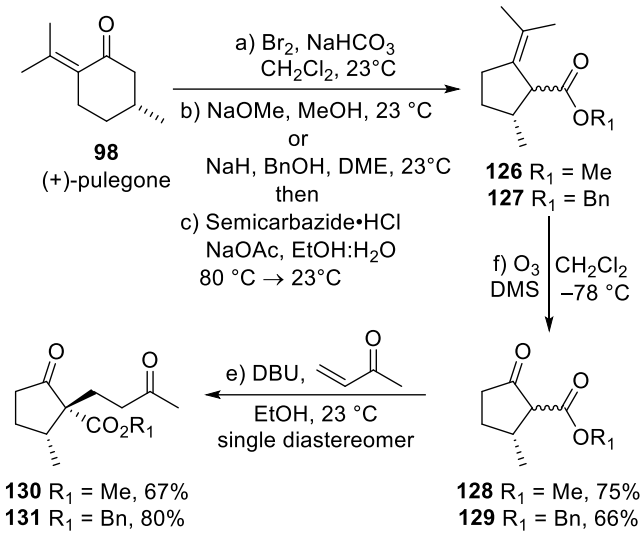

Scheme 1.19 Chiral pool synthesis of diketones **130** and **131**: a) Br_2 (1.02 equiv.), $NaHCO_3$ (0.5 equiv.), CH_2Cl_2 (1.0 M), 23 °C, 30 min; b) NaOMe (2.2 equiv.), MeOH (2.0 M), 23 °C, 12 hr; NaH (5 equiv.), BnOH (6 equiv.), DME (2.0 M), 23 °C, 12 hr; c) NaOAc (0.50 equiv.), semicarbazide•HCl (0.50 equiv.), EtOH (1.0 M), H_2O (1.0 M), 80°C for 1 hr then 23 °C, 12 hr; d) O_3, DMS (1.2 equiv.), CH_2Cl_2 (0.4 M), –78 °C, 4 hr,**128** 75%, **129** 66%; e) DBU (25 mol%), MVK (1.2 equiv.), EtOH (0.1 M), 23 °C, 15 min, **130** 67%, 50% from (+)-pulegone, **131** 80%, **131** 53% from **98**.

was then synthesized using a DBU catalyzed conjugate addition with MVK in an overall 50% yield from (+)-pulegone. The corresponding benzyl ester **131** was made via the same route in an overall 53% yield, using benzyl alcohol and NaH in the Favorskii rearrangement instead.

For the sulfone, several potential routes were available to access the required ketone precursor in an enantioenriched fashion, the most obvious of which would be to render the vicinal difunctionalization enantioselective. Considerable effort[44–48] has gone into the development of

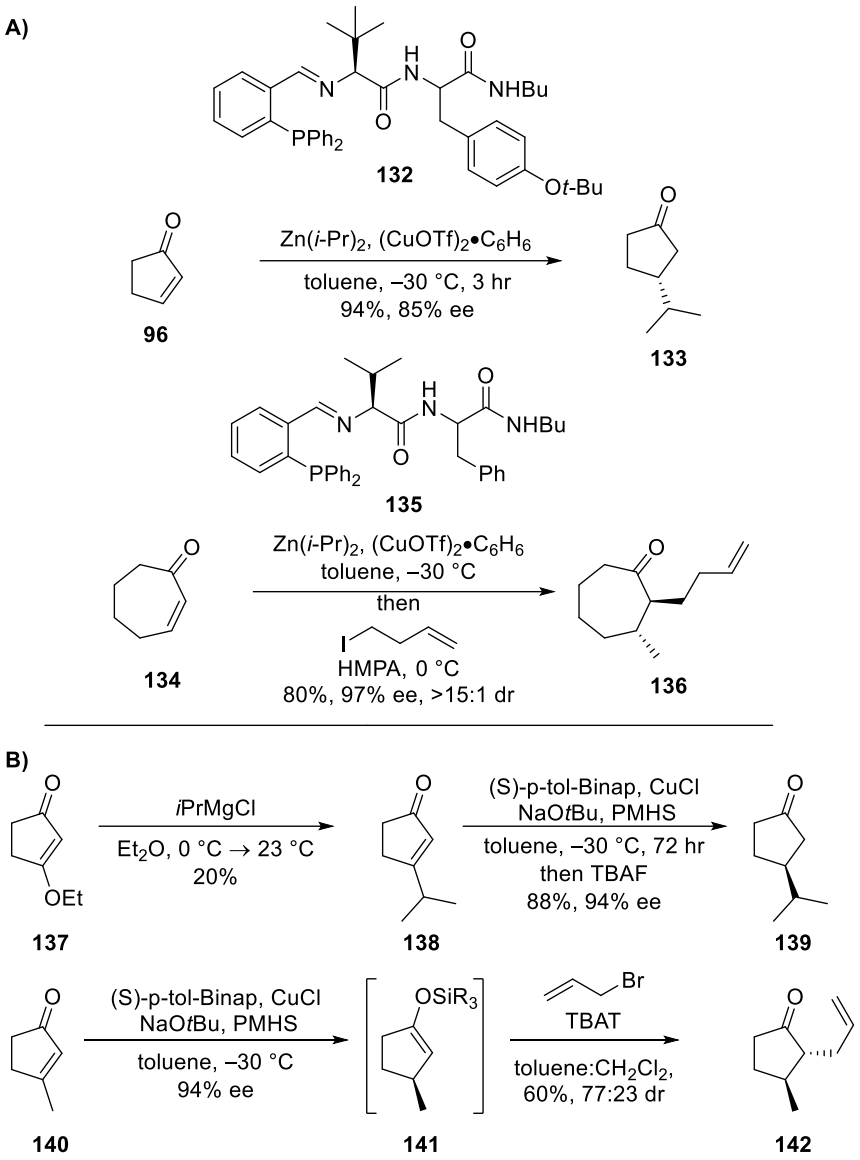

Scheme 1.20 Enantioselective appoaches to ketone **99** via **A)** Cu-catalyzed conjugate addition of organozincates and **B)** Cu-catalyzed conjugate reduction.

transition-metal catalyzed enantioselective conjugate additions and a wide variety of solutions for numerous systems are known. Simple cyclopentenone **96** remains a challenging substrate due to its high inherent reactivity and flat structure making enantioinduction particularly difficult. The most effective example to date is a report from the Hoveyda group which utilized a modular peptide-based phosphine ligand and Cu(OTf)•C_6H_6 system with organozinc reagents, which gave cyclopentanone **133** containing the requisite isopropyl group in a 94% yield and 85% ee as shown

in Scheme 1.20.[44] Further, a separate example demonstrated that the zinc enolate could be alkylated with 4-iodobutene in the presence of HMPA, giving cycloheptanone **136** in an 80% yield and 97% *ee* with a 15:1 dr. **136** was then elaborated into the natural product clavularin B. An alternative approach to the addition of a carbon nucleophile would be a conjugate reduction. The Buchwald group reported a highly effective asymmetric Cu–H system using readily available poly(methylhydrosiloxane) (PMHS) as the reducing agent that gave a variety of β-alkyl substituted cyclopentanones with *ee* ranging between 92-99%.[49] Cyclopentenone **139** was accessed in an 88% yield and 94% *ee*, albeit with 90% conversion after 72 h. The Buchwald group also found that the intermediate silyl enol ethers could be converted to enolates by tetrabutylammonium difluorotriphenylsilicate (TBAT), which serves as an anhydrous fluoride anion source. These enolates could be readily alkylated with activated electrophiles such as allyl bromide in a one-pot reduction/alkylation cascade.[50]

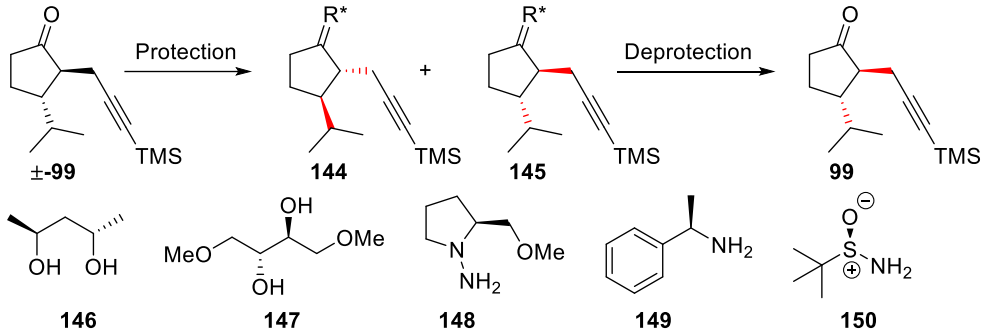

Scheme 1.21 Chiral resolution of ketone **99** via chiral auxillaries.

Another potential tack is chiral resolution of **99**. A common strategy, as shown in Scheme 1.21, to affect such a separation without the use of preparatory chiral HPLC is to employ a chiral auxiliary. The resulting diastereomers are then separable via chromatography, recrystallization, or some other physical method. This strategy is more commonly used for the resolution of chiral

amines, carboxylic acids, and alcohols, but examples with ketones are known. Some potential auxiliaries are the diols 1**46** and **147**,[51] the proline derived hydrazine **148**, 1-phenylethylamine

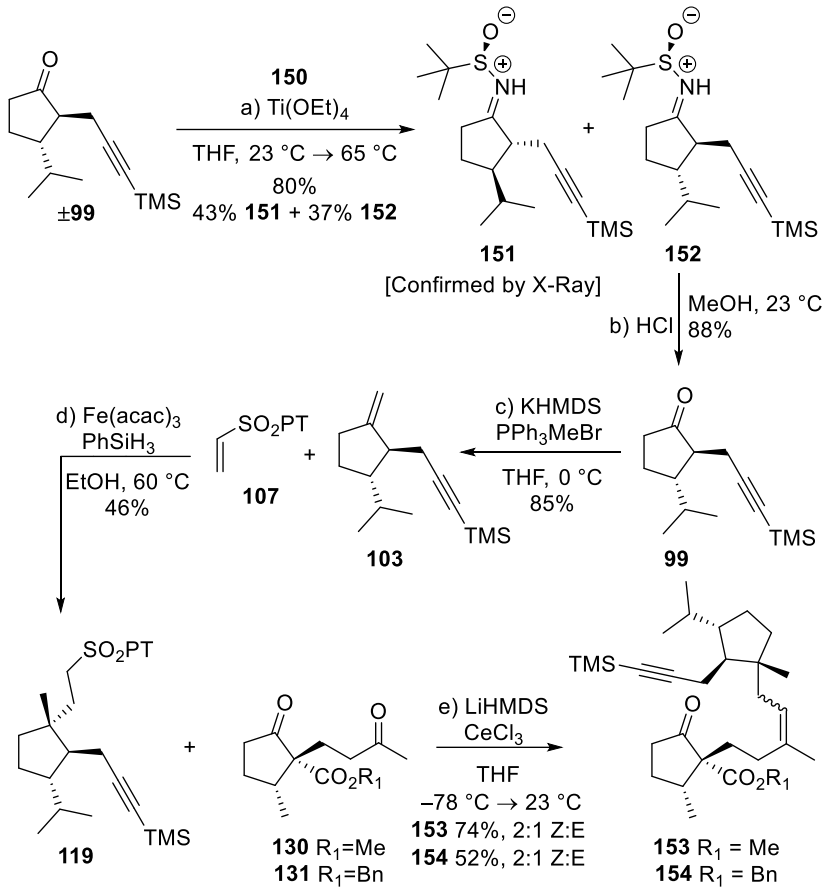

Scheme 1.22 Using chiral resolution to access Julia-Kocienski products: a) (*R*)-tBu-sulfinamide (1.0 equiv.), $Ti(OEt)_4$ (3.0 equiv.), THF (0.6 M), 65 °C, 12 hr; b) HCl (100 equiv., 3 M), MeOH (0.02 M), 23 °C, 40 min, 88%; c) PPh_3MeBr (2.2 equiv.), KHMDS (2.0 equiv.), THF (0.4 M), 0 ° C, 2 hr, 85%; d) **107** (1.5 equiv.), $Fe(acac)_3$ (30 mol%), $PhSiH_3$ (1.5 equiv.), EtOH (0.2 M), 60 ° C, 30 min, 46%; e) LiHMDS (1.5 equiv.) **119** (1.5 equiv.), $CeCl_3$ (2.0 equiv.), THF (0.1 M), –78 ° C → 23 °C, 12 hr, **153** 74% 2:1 Z:E; **154** 52%, 2:1 Z:E.

149,[52] or Ellman's auxiliary **150**.[53] At first glance the enantioselective methods are more appealing both from an elegance and synthetic efficiency perspective. However, the chiral resolution approach appeared more attractive due to the ease of implementation and expected rate of success.

As shown in Scheme 1.23, condensing Ellman's auxiliary **150** onto racemic **99** gave the resultant diastereomeric sulfinimines **151** and **152** that pleasingly proved easily separable by

column chromatography. In addition, **151** was highly crystalline allowing us to unambiguously identify the stereochemistry via X-ray crystallography. From there **152** was hydrolyzed under acidic conditions to yield enantiopure **99** in a 65% yield over two steps. Next, Wittig olefination and reductive olefin coupling gave sulfone **119** setting the stage for the Julia-Kocienski coupling. Both ketoester **130** and **131** proved competent giving the respective olefins **153** and **154** in 74%

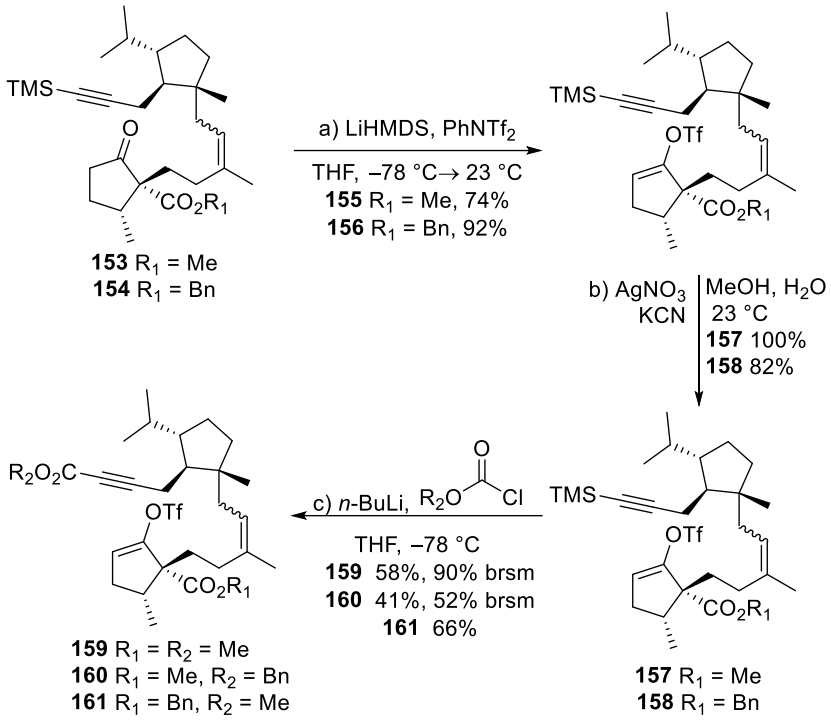

Scheme 1.23 Synthesis of cascade precursors: a) LiHMDS (1.5 equiv.), $PhNTf_2$ (1.1 equiv.), THF (0.1 M), -78 °C, 12 hr, **155** 74%, **156** 92%; b) $AgNO_3$ (2.7 equiv.), KCN (10.0 equiv.), MeOH (22 M), H_2O (0.25 M), 23 °C, 30 min, **157** 100%, **158** 82%; c) n-BuLi (1.5 equiv.), methyl or benzyl chloroformate (5.0 equiv.), THF (0.1 M), - 78 °C, 4 hr, **159** 58%, 90% brsm, **160** 41%, 52% brsm, **161** 66%.

and 52% yield, both with a 1:2 *E*/*Z* ratio. On larger scale, we observed that the olefin isomers of **153** were potentially separable by column chromatography. After extensive screening of eluent systems, a ternary mixture with a gravity column (silica gel, toluene:CH_2Cl_2:Et_2O 38:1:1) gave effective separation of the isomers allowing for identification by NOESY correlation, proving that the *Z* isomer is in fact favored and providing a clear route to entering the Heck cascade with a

single isomer. From here, the established procedure of triflation, desilylation, and base mediated carbonylation yielded the desired cascade precursors.

1.8 Initial Attempts with the Heck Cascade

We began our study of the cascade with **153** using our previously reported conditions from the presilphiperfolan-8-ol synthesis.[12] With DPEPhos, we observed a 2.5:1 ratio between two products, the first being initially identified as the desired **162** due to what were believed to be the characteristic cyclopentene peaks. The second was assigned as olefin **163** arising from the β-hydride elimination pathway due to the two strongly coupled doublets in the olefin region (J = 15.9 Hz, *trans*-olefin coupling). Subsequent failed attempts to elaborate what was believed to be **162** led us to examine the ^{1}H and ^{13}C NMR spectra more closely. Upon reconsideration, it was found that alkyne signals were still present in the ^{13}C NMR indicating that rather than the desired

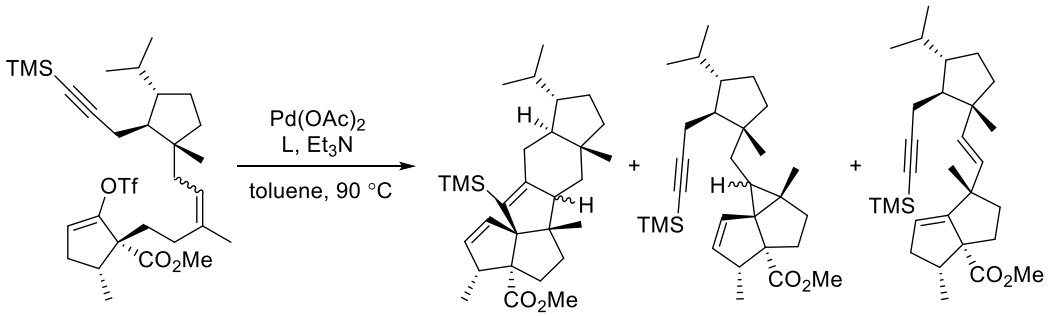

153
2:1 Z:E

162 **163** **164**

Ligand	Yield	**162** :	**163** :	**164**
DPEphos	54%[a]	0	2.5	1.0
PPh_3	85%[b]	0	2.0	1.0
dppe	70%[b]	0	1.0	1.0
Xantphos	71%[b]	0	1.0	2.0
S-BINAP	60%[b]	0	13	1.0
R-BINAP	84%[b]	0	13	1.0

Table 1.3 Ligand effects on the Heck Cascade of **153**: [a] Isolated yield [b] Determined by ^{1}H NMR using 1,3,5-trimethoxybenzene as an internal standard; $Pd(OAc)_2$ (10 mol%),Bidentate L (20 mol%) or monodentate (40 mol%), Et_3N (3.0 equiv.), toluene (0.1 M), 90 °C, 12 hr.

[6-*exo*-dig] cyclization occurring, the [3-*exo*-trig] pathway was operative, instead resulting in vinyl cyclopropane **164**. We next attempted a ligand screen in the hope that one may provide better

selectivity for our desired pathway or inhibit one of the undesired pathways. Unfortunately, after examining a variety of monodentate and bidentate phosphine ligands only formation of **163** and **164** was ever observed, generally with poor selectivity between the two pathways. *R*- and *S*-BINAP proved the exceptions with both giving **163** as the major product in a 13:1 ratio. We hypothesized that the TMS alkyne was simply not reactive enough, either due to steric or electronic factors, for our desired [6-*exo*-dig] pathway to occur. As such, the ynoate cascade substrates became the next target of our focus.

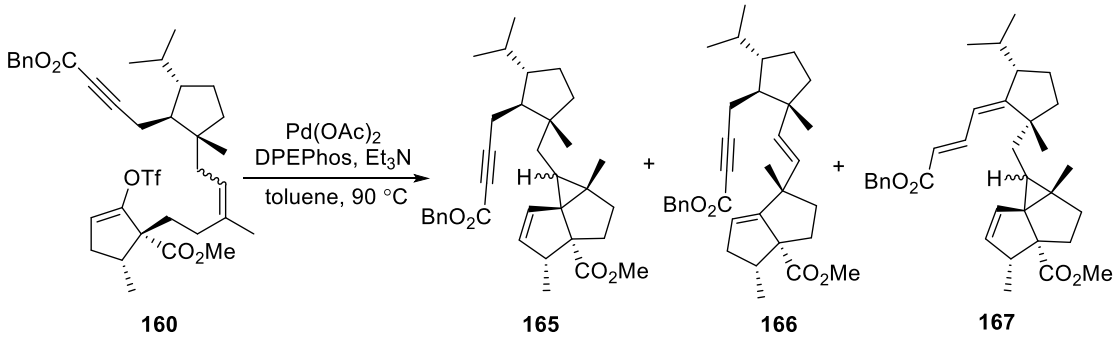

160 **165** **166** **167**

Scheme 1.24 Heck cascade attempts with ynoate **160**: $Pd(OAc)_2$ (10 mol%), DPEPhos (20 mol%), Et_3N (3 equiv.), toluene (0.1 M), 90 °C, 12 hr.

The ynoate moiety did prove to be considerably more reactive leading to complex reaction mixtures. Purification by preparative TLC gave products that were tentatively identified as vinyl cyclopropane **165**, olefin **166**, and dienoate **167**, which is presumably formed via a phosphine catalyzed isomerization of the ynoate.[54,55] The benzyl ester of the ynoate complicated identification due to overlap of the benzyl peaks with other olefin signals. To simplify the data interpretation, ynoate **159** was examined next. Using DPEPhos as ligand, the reaction mixture was very complex, and we were only able to tentatively identify dienoates **168** and **169**. Switching to *R*-BINAP yielded a cleaner reaction, but the reaction was selective for the vinyl cyclopropane **170**, similar to what was observed with **153**. Even then, the yield for **170** was only 33%. *S*-BINAP similarly favored the [3-*exo*-trig] pathway, but now the major isolated product was enoate **172**,

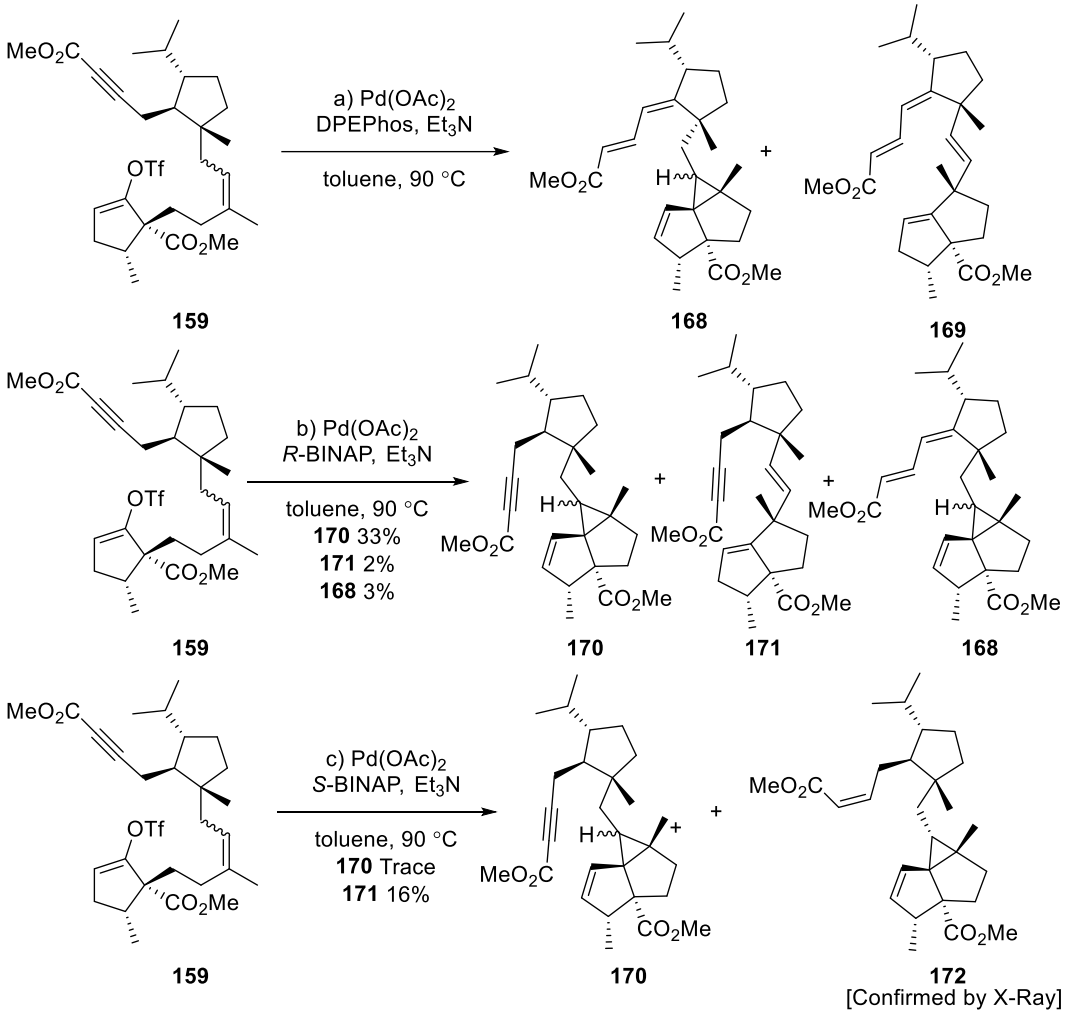

Scheme 1.25 Heck cascade attempts with ynoate **159**: a) $Pd(OAc)_2$ (10 mol%), DPEPhos (20 mol%), Et_3N (3 equiv.), toluene (0.1 M), 90 °C, 12 hr; b) $Pd(OAc)_2$ (10 mol%), R-BINAP (20 mol%), Et_3N (3 equiv.), toluene (0.1 M), 90 °C, 12 hr, **170** 33%, **171** 2%, **168** 3%; c) $Pd(OAc)_2$ (10 mol%), S-BINAP (20 mol%), Et_3N (3 equiv.), toluene (0.1 M), 90 °C, 12 hr **171** 16%.

which could potentially arise from Pd–H insertion in to the ynoate and reductive elimination with a hydride abstracted from a triethylamine donor. Pleasingly, **172** proved to be crystalline and the absolute configuration of the product was determined from the X-ray crystal structure. The structure, shown in the experimental section below, conclusively proved the formation of the vinyl cyclopropane moiety and the establishment of the 1,3-*trans* relationship during the initial [5-*exo*-trig] cyclization. However, it was clear that under the originally devised Pd-mediated conditions, the undesired reaction pathways would be unavoidable.

1.9 Nickel Heck Approach

At this point in our efforts to move forward, we turned to the literature for inspiration on how best to proceed. A computational study by the Gomez-Bengoa group on the E_a of intramolecular migratory insertions of Ni, Pd, and Pt came to our attention.[56] On the simple model system, shown in Scheme 1.26, they found that the E_a for the [3-*exo*-trig] pathway was surprisingly low at only 2.5 kcal/mol. This was somewhat surprising considering the additional ring strain introduced and the higher temperatures required in the Overman example.[13] For comparison, the [6-*exo*-trig] pathway was found to be almost 20 kcal/mol higher. While these E_a are not representative of our system, we began to suspect that at least the relative differences were similar based on our observed results. As such, our problem seemed inescapable as long as the reaction was mediated by Pd.

As we considered our next direction, one potential solution was the substitution of Ni for Pd in the cascade. Ni is reported[56–59] to undergo migratory insertion more readily than Pd. The Gomez-Bengoa study found that in all examined instances, Ni had consistently lower E_a barriers, which would imply that our apparently challenging [6-*exo*-dig] cyclization may now be more accessible. However, this decreased barrier also applies to the [3-*exo*-trig] pathway, which on the above model system was found to have an almost negligible E_a of only 0.5 kcal/mol. However, the report also remarks on the disparity between the apparent ease of the [3-*exo*-trig] pathway and the paucity of known examples given the breadth of the Heck literature.[17,19,20,60–62] The calculated $\Delta G^{\ddagger}$ for the cyclopropane formation showed that the reaction was endergonic by ~2 kcal/mol and thus reversible. They proposed that unless the [3-*exo*-trig] pathway is coupled with a subsequent exergonic terminating step such as β-hydride elimination, there may simply be no cyclopropane product observed as another more thermodynamically favorable path takes over. As such, the [3-

A)

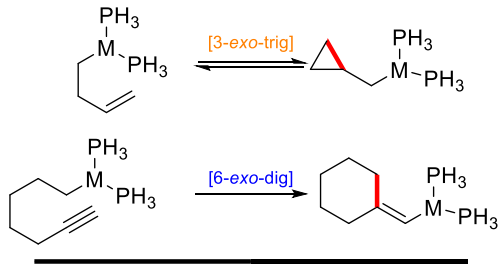

M	[3-*exo*-trig]*	[6-*exo*-dig]*	β-H Elim.*
Pd	2.5	21.2	8
Ni	0.5	9.6	15

*E_a (kcal/mol)

B)

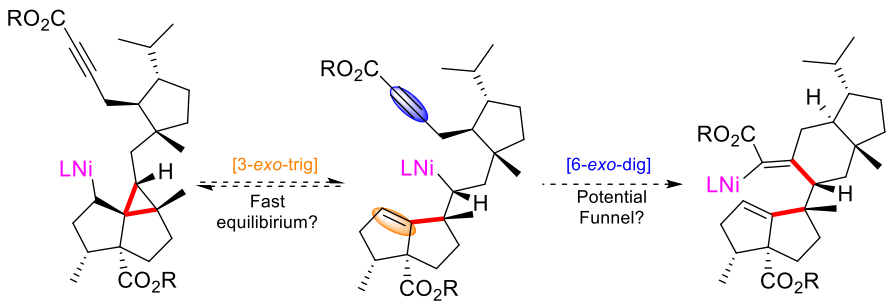

Scheme 1.26 A) Calculated E_a for intramolecular migratory insertions and β-hydride elimination for Pd and Ni, **B)** Proposed Heck cascade.

exo-trig] pathway may exist as an equilibrium between the cyclized and linear forms until a subsequent step such as migratory insertion or β-hydride elimination can occur. And as Ni undergoes β-hydride elimination less readily than Pd,[57] any such equilibrium may be long lived enough for our now more readily accessible [6-*exo*-dig] cyclization to occur. With this hypothesis in mind, we set out to find conditions for a Ni-mediated Heck cascade.

1.10 Conclusion

This chapter presents our initial efforts toward the total synthesis of retigeranic acid A **1** via a Heck cascade. In the process, we have developed scalable and effective routes allowing us to access enantiopure cascade precursors **153** and **159** in 8 and 10 steps respectively from commercially available materials. In the course of our studies, we utilized a chiral resolution with Ellman's auxillary **150**, accomplished a challenging intermolecular Julia-Kocienski olefination

with a $CeCl_3$, and overcame the sensitive vinyl triflate to access the ynoate precursors. Upon attempting our cascade, we found that with the Pd-mediated system, the [3-*exo*-trig] and β-hydride elimination pathways outcompeted our desired [6-*exo*-dig] pathway, rendering our initial approach unfeasible. From these results, we have identified the potential for a new strategy utilizing the less commonly studied Ni-Heck reaction.

1.11 References

[1] H. J. Shirley, M. L. Jamieson, M. A. Brimble, C. D. Bray, *Nat. Prod. Rep.* **2018**, *35*, 210–219.

[2] H. Chai, R. Yin, Y. Liu, H. Meng, X. Zhou, G. Zhou, X. Bi, X. Yang, T. Zhu, W. Zhu, Z. Deng, K. Hong, *Sci. Reports 2016 61* **2016**, *6*, 1–11.

[3] E. J. Corey, M. C. Desai, T. A. Engler, *J. Am. Chem. Soc.* **1985**, *107*, 4339–4341.

[4] L. A. Paquette, J. Wright, G. J. Drtina, R. A. Roberts, *J. Org. Chem.* **1987**, *52*, 2960–2962.

[5] T. Hudlicky, L. Radesca-Kwart, L. Li, T. Bryant, *Tetrahedron Lett.* **1988**, *29*, 3283–3286.

[6] P. A. Wender, S. K. Singh, *Tetrahedron Lett.* **1990**, *31*, 2517–2520.

[7] D. T. Hog, R. Webster, D. Trauner, *Nat. Prod. Rep.* **2012**, *29*, 752–779.

[8] D. R. Adams, T. Hudlický, in *Total Synth. Nat. Prod.*, Springer Berlin Heidelberg, Berlin, Heidelberg, **2012**, pp. 235–258.

[9] J. Zhang, X. Wang, S. Li, D. Li, S. Liu, Y. Lan, J. Gong, Z. Yang, *Chem. – A Eur. J.* **2015**, *21*, 12596–12600.

[10] X. Wang, D. Li, J. Zhang, J. Gong, J. Fu, Z. Yang, *Org. Lett.* **2021**, *23*, 5092–5097.

[11] R. Long, J. Huang, W. Shao, S. Liu, Y. Lan, J. Gong, Z. Yang, *Nat. Commun. 2014 51* **2014**, *5*, 1–10.

[12] P. Hu, S. A. Snyder, *J. Am. Chem. Soc.* **2017**, *139*, 5007–5010.

[13] L. E. Overman, M. M. Abelman, D. J. Kucera, V. D. Tran, D. J. Ricca, *Pure Appl. Chem.* **1992**, *64*, 1813–1819.

[14] B. Burns, R. Grigg, V. Santhakumar, V. Sridharan, P. Stevenson, T. Worakun, *Tetrahedron* **1992**, *48*, 7297–7320.

[15] P. Hu, H. M. Chi, K. C. DeBacker, X. Gong, J. H. Keim, I. T. Hsu, S. A. Snyder, *Nature* **2019**, *569*, 703–707.

[16] H. Yi, P. Hu, S. A. Snyder, *Angew. Chemie Int. Ed.* **2020**, *59*, 2674–2678.

[17] F. E. Meyer, P. J. Parsons, A. De Meijere, *J. Org. Chem.* **1991**, *56*, 6487–6488.

[18] S. Schweizer, Z.-Z. Song, F. E. Meyer, P. J. Parsons, A. de Meijere, *Angew. Chemie Int. Ed.* **1999**, *38*, 1452–1454.

[19] R. Grigg, U. Sakee, V. Sridharan, S. Sukirthalingam, R. Thangavelauthum, *Tetrahedron* **2006**, *62*, 9523–9532.

[20] Z. Owczarczyk, F. Lamaty, E. J. Vawter, E. Negishi, *J. Am. Chem. Soc.* **1992**, *114*, 10091–10092.

[21] J. C. Lo, D. Kim, C.-M. Pan, J. T. Edwards, Y. Yabe, J. Gui, T. Qin, S. Gutiérrez, J. Giacoboni, M. W. Smith, P. L. Holland, P. S. Baran, *J. Am. Chem. Soc.* **2017**, *139*, 2484–

2503.

[22] J. W. Lane, K. L. Spencer, S. R. Shakya, N. C. Kallan, P. J. Stengel, T. Remarchuk, *Org. Process Res. Dev.* **2014**, *18*, 1641–1651.

[23] D. A. Siler, J. D. Mighion, E. J. Sorensen, *Angew. Chemie Int. Ed.* **2014**, *53*, 5332–5335.

[24] G. De Bo, I. E. Markó, *European J. Org. Chem.* **2011**, *2011*, 1859–1869.

[25] J. Robertson, R. J. D. Hatley, D. J. Watkin, *J. Chem. Soc. Perkin Trans. 1* **2000**, 3389–3396.

[26] E. Rodrigo, S. Morales, S. Duce, J. L. G. Ruano, M. B. Cid, V. K. Aggarwal, L. S. Ding, Y. C. Chen, D. R. Birhade, M. P. Shinde, *Chem. Commun.* **2011**, *47*, 11267.

[27] J. C. Lo, Y. Yabe, P. S. Baran, *J. Am. Chem. Soc.* **2014**, *136*, 1304–1307.

[28] M. D. Greenhalgh, A. S. Jones, S. P. Thomas, *ChemCatChem* **2015**, *7*, 190–222.

[29] R. Melngaile, A. Sperga, K. K. Baldridge, J. Veliks, *Org. Lett.* **2019**, *21*, 7174–7178.

[30] P. Duhamel, G. Dujardin, L. Hennequin, J.-M. Poirier, Y. Ohizumi, Y. Hirata, *J. Chem. Soc. Perkin Trans. 1* **1992**, *59*, 387.

[31] P. Duhamel, L. Hennequin, N. Poirier, J. M. Poirier, *Tetrahedron Lett.* **1985**, *26*, 6201–6204.

[32] K. Kakiuchi, M. Ue, H. Tsukahara, T. Shimizu, T. Miyao, Y. Tobe, Y. Odaira, M. Yasuda, K. Shima, *J. Am. Chem. Soc.* **2002**, *111*, 3707–3712.

[33] J. M. Poirier, L. Hennequin, *Tetrahedron* **1989**, *45*, 4191–4202.

[34] G. Stork, M. E. Jung, *J. Am. Chem. Soc.* **2002**, *96*, 3682–3684.

[35] J. A. Singletary, H. Lam, G. B. Dudley, *J. Org. Chem.* **2004**, *70*, 739–741.

[36] M. O. Ratnikov, V. V. Tumanov, W. A. Smit, *Angew. Chemie Int. Ed.* **2008**, *47*, 9739–9742.

[37] J. Pospíšil, *Tetrahedron Lett.* **2011**, *52*, 2348–2352.

[38] K. Tsubone, K. Hashizume, H. Fuwa, M. Sasaki, *Tetrahedron Lett.* **2011**, *52*, 548–551.

[39] H. Fuwa, K. Ishigai, K. Hashizume, M. Sasaki, *J. Am. Chem. Soc.* **2012**, *134*, 11984–11987.

[40] G. Bartoli, E. Marcantoni, M. Marcolini, L. Sambri, *Chem. Rev.* **2010**, *110*, 6104–6143.

[41] G. Bartoli, M. Bosco, R. Dalpozzo, E. Marcantoni, L. Sambri, *Chem. - A Eur. J.* **1997**, *3*, 1941–1950.

[42] D. C. Johnson II, T. S. Widlanski, *J. Org. Chem.* **2003**, *68*, 5300–5309.

[43] H. M. Schmidt, J. F. Arens, *Recl. des Trav. Chim. des Pays-Bas* **1967**, *86*, 1138–1142.

[44] S. J. Degrado, H. Mizutani, A. H. Hoveyda, *J. Am. Chem. Soc* **2001**, *123*, 755–756.

[45] H. Pellissier, *Adv. Synth. Catal.* **2015**, *357*, 2745–2780.

[46] A. Alexakis, J. E. Bäckvall, N. Krause, O. Pàmies, M. Diéguez, *Chem. Rev.* **2008**, *108*, 2796–2823.

[47] S. R. Harutyunyan, T. den Hartog, K. Geurts, A. J. Minnaard, B. L. Feringa, *Chem. Rev.* **2008**, *108*, 2824–2852.

[48] D. Vargová, I. Némethová, K. Plevová, R. Šebesta, *ACS Catal.* **2019**, *9*, 3104–3143.

[49] Y. Moritani, D. H. Appella, V. Jurkauskas, S. L. Buchwald, *J. Am. Chem. Soc.* **2000**, *122*, 6797–6798.

[50] J. Yun, S. L. Buchwald, *Org. Lett.* **2001**, *3*, 1129–1131.

[51] H. Fujioka, Y. Kita, *Stud. Nat. Prod. Chem.* **1994**, *14*, 469–516.

[52] M. Wosińska-Hrydczuk, J. Skarżewski, *Mol. 2020, Vol. 25, Page 4907* **2020**, *25*, 4907.

[53] M. T. Robak, M. A. Herbage, J. A. Ellman, *Chem. Rev.* **2010**, *110*, 3600–3740.

[54] B. M. Trost, U. Kazmaier, *J. Am. Chem. Soc.* **2002**, *114*, 7933–7935.

[55] S. D. Rychnovsky, J. Kim, *J. Org. Chem.* **2002**, *59*, 2659–2660.

[56] B. Fiser, J. M. Cuerva, E. Gómez-Bengoa, *Organometallics* **2018**, *37*, 390–395.

[57] Bo-Lin Lin, Lei Liu, Yao Fu, Shi-Wei Luo, Qian Chen, Q.-X. Guo, *Organometallics* **2004**, *23*, 2114.

[58] V. P. Ananikov, *ACS Catal.* **2015**, *5*, 1964–1971.

[59] S. Z. Tasker, E. A. Standley, T. F. Jamison, *Nature* **2014**, *509*, 299–309.

[60] Y. Zhang, E. Negishi, *J. Am. Chem. Soc.* **1989**, *111*, 3454–3456.

[61] H. Henniges, F. E. Meyer, U. Schick, F. Funke, P. J. Parsons, A. De Meijere, *Tetrahedron* **1996**, *52*, 11545–11578.

[62] A. de Meijere, P. von Zezschwitz, S. Bräse, *Acc. Chem. Res.* **2005**, *38*, 413–422.

1.12 Experimental Section

General Information All reactions were carried out under an argon atmosphere with dry solvents under anhydrous conditions, unless otherwise noted. Dry tetrahydrofuran (THF), toluene, diethyl ether (Et_2O) dichloromethane (CH_2Cl_2), and acetonitrile (CH_3CN) were obtained by passing commercially available pre-dried, oxygen-free formulations through activated alumina columns. Yields refer to chromatographically and spectroscopically (^1H and ^{13}C NMR) homogeneous materials, unless otherwise stated. Reagents were purchased at the highest commercial quality and used without further purification, unless otherwise stated. Reactions were magnetically stirred and monitored by thin-layer chromatography (TLC) carried out on 0.25 mm E. Merck silica gel plates (60F-254) using UV light as visualizing agent, and an ethanolic solution of phosphomolybdic acid and cerium sulfate or a solution of $KMnO_4$ in aq. $NaHCO_3$ and heat as developing agents. SiliCycle silica gel (60, academic grade, particle size 0.040–0.063 mm) was used for flash column chromatography. Preparative thin-layer chromatography separations were carried out on 0.50 mm E. Merck silica gel plates (60F-254). NMR spectra were recorded on Bruker 500 MHz instruments and calibrated using residual undeuterated solvent as an internal reference. The following abbreviations were used to explain the multiplicities: s = singlet, d = doublet, t = triplet, q = quartet, br = broad, app = apparent.

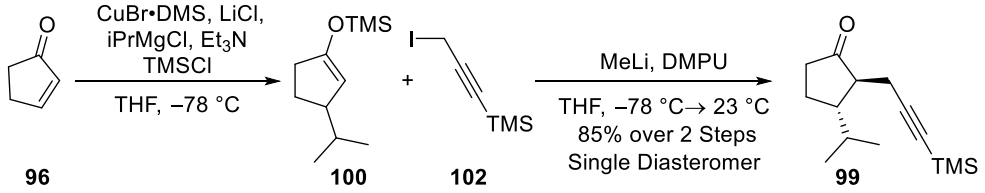

Ketone 99 To a flame dried flask was added LiCl (6.67 g, 157 mmol, 2.15 equiv.) and CuBr•DMS (41.7 g, 157 mmol, 2.15 equiv.). The flask was evacuated, heated with a heat gun for several minutes [**Warning**: Gas evolution can lead to material bumping violently], flushed with N_2, and allowed to cool to 23 ˚C and this drying procedure was repeated 3 times. THF (182 mL, 0.4 M) was added, and the resultant orange suspension was stirred at 23 ˚C for 10 minutes then the mixture

was cooled to –78 ˚C. Next, *i*PrMgCl (84 mL, 2.0 M in THF, 2.3 equiv.) was added to give a dark black suspension that was stirred for 15 minutes at the same temperature. TMSCl (13.8 mL, 109.5 mmol, 1.5 equiv.) and cyclopentenone **96** (6.11 mL, 73 mmol, 1 equiv.) were added sequentially to no visible change and the reaction was stirred at –78 ˚C until full consumption of the starting material was indicated by TLC (silica gel, hexanes:EtOAc 1:9) (usually 1 hr). Then, Et_3N (15.3 mL, 109.5 mmol, 1.5 equiv.) was added and the reaction was removed from the cooling bath and allowed to warm to 23 ˚C. Celite and pentane (100 mL) were then added, and the black mixture was stirred vigorously for 15 minutes then filtered to give a white suspension that was washed with $NaHCO_3$ (2 x 150 mL). The organic layer was then dried with $MgSO_4$, filtered, and most of the solvent was removed to give crude silyl enol ether **100** as a light-yellow oil that was taken forward without further purification.

Crude silyl **100** was added to a flame dried flask fitted with an addition funnel under N_2 followed by THF (605 ml) and the light-yellow solution was cooled to –40 ˚C. Freshly titrated MeLi (50 mL, 1.6 M Et_2O) was added, and the yellow solution was stirred at – 40 ˚C for 1 hr. The reaction was then cooled to –78 ˚C and DMPU (125 mL, 80.3 mmol, 14.1 equiv.) was added. Next, propargyl iodide **102** (26.2 g, 109 mmol, 1.5 equiv.) and THF (307 mL) were added to the addition funnel and the mixture was added dropwise over 30 min. The reaction was then allowed to slowly warm to 23 ˚C overnight. The reaction was quenched with NH_4Cl (300 mL), the layers were separated, and the aqueous layer was extracted with Et_2O (3 x 200 mL). The combined organic layers were dried with $MgSO_4$, filtered, and concentrated. The resultant residue was purified via flash column chromatography (silica gel, hexanes/Et_2O, 19:1) to yield ketone **99** as a light yellow oil (14.6 g, 85%) **99**: R_f = 0.21 (silica gel, hexanes/Et_2O, 19:1); ^1H NMR (500 MHz,

$CDCl_3$) δ 2.61 – 2.53 (m, 2H), 2.44 – 2.31 (m, 1H), 2.13 – 1.90 (m, 5H), 1.58 – 1.45 (m, 2H), 1.02 (d, *J* = 6.9 Hz, 3H), 0.93 (d, *J* = 6.8 Hz, 3H), 0.12 (s, 9H).

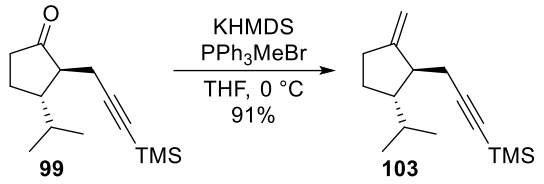

99 **103**

Cyclopentene 103 To a flame dried flask under N_2 was added PPh_3MeBr (16.8 g, 47.1 mmol, 2.2 equiv.) and THF (30 mL) to give a white suspension that was cooled to 0 ˚C. Then, KHMDS (43 mL, 1.0 M THF, 2.0 equiv.) was added to give a bright yellow suspension that was stirred at the same temperature for 30 min. Next, ketone **99** (5.06 g, 21.0 mmol, 1.0 equiv.) was added as a solution in THF (20 mL) and the reaction was stirred at 0 ˚C until full consumption of starting material was confirmed by TLC (silica gel, hexanes:Et_2O, 19:1). The now red suspension was quenched with saturated NH_4Cl (20 mL) and diluted with DI H_2O (10 mL) and Et_2O (20 mL). The layers were separated, and the aqueous layer was extracted with Et_2O (3 x 20 mL), and the combined organic layers were dried with $MgSO_4$, filtered, and concentrated. The resultant residue was purified via flash column chromatography (silica gel, hexanes) to yield cyclopentene **103** as a colorless oil (4.47 g, 91% yield) **103**: R_f = 0.43 (silica gel, hexanes); ^{1}H NMR (500 MHz, $CDCl_3$) δ 4.94 – 4.88 (m, 2H), 2.42 – 2.24 (m, 5H), 1.79 – 1.60 (m, 3H), 1.34 (dq, *J* = 12.1, 8.8 Hz, 1H), 0.94 (d, *J* = 6.6 Hz, 3H), 0.86 (d, *J* = 6.6 Hz, 3H), 0.14 (s, 8H).

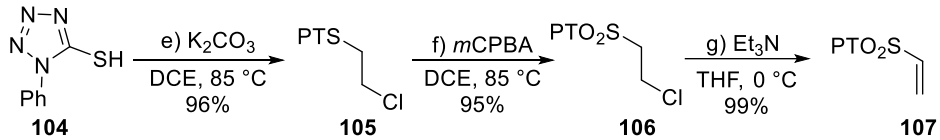

104 **105** **106** **107**

Thioether 105 To a flask fitted with a reflux condenser was added K_2CO_3 (20.7 g, 150 mmol, 2.5 equiv.), 1-Phenyl-1H-tetrazole-5-thiol (10.7 g, 60 mmol, 1 equiv.), and DCE (250 mL) to give a

white suspension that was then heated to reflux for 12 hr or until full consumption of starting material was confirmed by TLC (hexanes:EtOAc, 4:1). The reaction was diluted with DI H_2O (250 mL) and the layers were separated. The aqueous layer was extracted with CH_2Cl_2 (2 x 150 mL), and the combined organic layers were washed with DI H_2O (200 mL), brine (200 mL), dried with $MgSO_4$, and concentrated to give thioether **105** as a yellow solid (14.0 g, 96%) that was taken forward without further purification. **105**: R_f = 0.52; ^{1}H NMR (500 MHz, $CDCl_3$) δ 7.58 (d, *J* = 3.5 Hz, 5H), 3.96 (t, *J* = 6.8 Hz, 2H), 3.73 (t, *J* = 6.8 Hz, 2H).

Sulphone 106 To a flask fitted with a reflux condenser was added *m*CPBA (50.0 g, 290 mmol, 5.0 equiv.), thioether **105** (14.0 g, 58.0 mmol, 1.0 equiv.), and DCE (580 mL) and the yellow solution was heated to reflux for 4 hr or until full consumption of the starting material was confirmed by TLC (hexanes:EtOAc, 7:3). The reaction was cooled to 23 ˚C to give a white suspension that was filtered, and the filtrate was added to a separatory funnel then washed with saturated $NaHSO_3$ (200 mL), $NaHCO_3$ (2 x 250 mL), brine (200 mL). The organic layer was then dried with $MgSO_4$ and concentrated to give sulphone **106** as a light-yellow solid (14.91 g, 95%) that was taken forward without further purification. **106** R_f = 0.25 (silica gel, hexanes:EtOAc, 3:1); ^{1}H NMR (500 MHz, $CDCl_3$) δ 7.70 – 7.58 (m, 5H), 7.26 (d, *J* = 2.1 Hz, 1H), 4.17 (t, *J* = 7.5 Hz, 2H), 4.04 (dt, *J* = 7.6, 3.6 Hz, 2H).

Vinyl Sulphone 107 To a flame dried flask under N_2 was added THF (73 mL) and sulphone **107** (4.00 g, 14.58 mmol, 1.0 equiv.) to give a light-yellow solution that was cooled to 0˚C. Then Et_3N 2.03 mL, 14.58 mm, 1.0 equiv.) was added dropwise over 5 min to give a yellow-white suspension that was stirred at the same temperature for 30 min (Note: **106** and **107** have identical R_f values so TLC cannot indicate the stage of the reaction). Then Et_2O (73 mL) was added, and the suspension was stirred at 0 ˚C for 10 min then filtered and concentrated to give vinyl sulphone **107** as a light-

yellow solid (3.44 g, 99%). **107** R_f = 0.25 (silica gel, hexanes:EtOAc, 3:1); ^{1}H NMR (500 MHz, $CDCl_3$) δ 7.73 – 7.60 (m, 5H), 7.14 (dd, *J* = 16.5, 9.9 Hz, 1H), 6.68 (dd, *J* = 16.5, 1.2 Hz, 1H), 6.50 (dd, *J* = 9.9, 1.2 Hz, 1H).

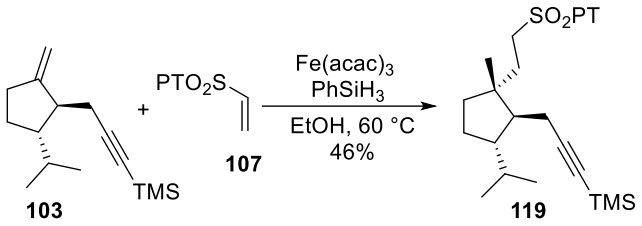

Sulphone 119 To a flask was added EtOH (52 mL), $Fe(acac)_3$ (1.10 g, 3.12 mmol, 30 mol%), cyclopentene **103** (2.44 g, 10.4 mmol, 1.0 equiv.), and vinyl sulphone **107** (3.51 g, 15.6 mmol, 1.5 equiv.) to give a red suspension. Then $PhSiH_3$ (1.92 mL, 15.6 mmol, 1.5 equiv.) was added and the mixture was immediately placed in a preheated oil bath at 60 ˚C and the reaction was stirred at that temperature until complete consumption of starting material was indicated by TLC (silica gel, hexanes). Then the reaction was cooled to 23 ˚C and diluted with brine (40 mL) and extracted with Et_2O (3 x 40 mL). The combined organic layers were washed with brine (40 mL), dried with $MgSO_4$, and concentrated. The resultant residue was purified first by a short silica plug (hexanes:EtOAc 9:1) to remove inorganic salts followed by flash column chromatography (silica gel, hexanes:Et_2O 9:1) to give sulphone **119** as a colorless oil that become a gummy white solid (2.26 g, 46%). **119**: R_f = 0.24 (silica gel, hexanes:Et_2O 9:1); ^{1}H NMR (500 MHz, $CDCl_3$) δ 7.74 – 7.67 (m, 2H), 7.67 – 7.55 (m, 3H), 3.76 (pd, *J* = 14.3, 4.5 Hz, 2H), 2.30 – 2.13 (m, 3H), 1.93 – 1.77 (m, 2H), 1.69 – 1.58 (m, 2H), 1.56 – 1.34 (m, 5H), 0.98 (s, 3H), 0.91 (d, *J* = 6.9 Hz, 3H), 0.82 (d, *J* = 6.8 Hz, 3H), 0.10 (s, 8H).

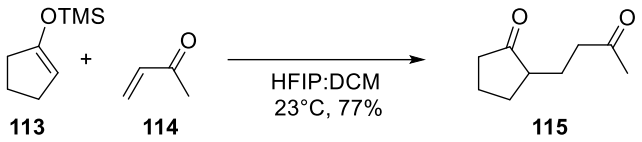

Diketone 115[2] To a dry flask under nitrogen was added HFIP (2.4 mL), CH_2Cl_2 (0.6 mL), freshly distilled methyl vinyl ketone **114** (0.08 mL, 1 mmol, 1.0 equiv.), and silyl enol ether **113** (312 mg, 2.0 mmol, 2.0 equiv.) were added sequentially at 23 ˚C to give a clear colorless solution that was stirred for 20 min. The solvent was then evaporated, and the resultant residue was purified by flash column chromatography (silica gel, hexanes:EtOAc 3:1) to give diketone **115** as a colorless oil (120 mg, 77%). **115**: R_f = 0.25; ^{1}H NMR (500 MHz, $CDCl_3$) δ 2.64 – 2.49 (m, 2H), 2.34 – 2.24 (m, 1H), 2.24 – 1.87 (m, 8H), 1.80 – 1.74 (m, 1H), 1.68 – 1.60 (m, 1H), 1.51 (dtd, *J* = 12.4, 10.5, 6.6 Hz, 1H).

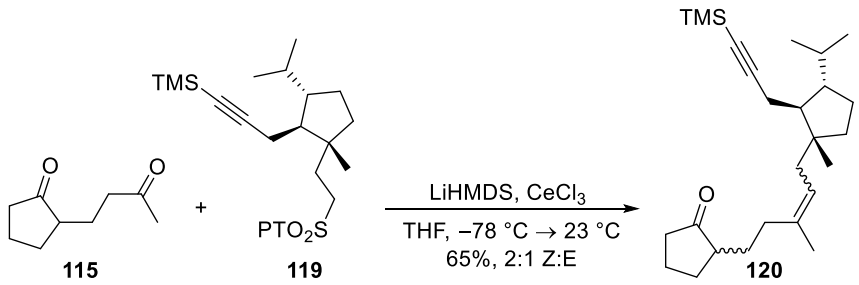

Ketone 120 To a dry flask with a stir bar in the glovebox was added $CeCl_3$ (1.33 g, 5.4 mmol, 2.0 equiv.) then the flask was sealed with a septum, removed from the glovebox, fitted with a N_2 balloon, and placed in an ice bath. THF (16.2 mL) was added dropwise to give a grey-white suspension that was removed from the ice bath and sonicated for 2 hr.

To a dry flask was added sulphone **119** (1.93 g, 4.08 mmol, 1.5 equiv.) as a solution in anhydrous benzene. **119** was then azeotropically dried (3 x 5 mL benzene) and then dissolved in

THF (8.1 mL) and cooled to – 78 ˚C. LiHMDS (4.1 mL, 1.0 M THF, 1.5 equiv.) was added to give a bright orange solution that was then stirred at the same temperature for 1 hr.

The flask with the $CeCl_3$ suspension was removed from the sonicator and diketone **115** (419 mg, 2.7 mmol, 1.0 equiv.) was added as a solution in THF (2.7 mL) and stirred at 23 ˚C for 30 min. The suspension was then cooled to – 78˚C. The orange solution of sulphone anion was then added to the $CeCl_3$ suspension via a cannula to yield a yellow suspension that was allowed to slowly warm to 23 ˚C overnight. The now reddish-brown suspension was quenched with NH_4Cl (15 mL) and diluted with DI H_2O (10 mL) and Et_2O (10 mL) and the layers were separated. The aqueous layer was extracted with Et_2O (3 x 15 mL) then the combined organic layers were dried with $MgSO_4$ and concentrated. The resultant residue was then purified via flash column chromatography (silica gel, hexanes:Et_2O 24:1) to give ketone **120** as a colorless oil (700 mg, 65%, 2:1 Z:E). **120**: R_f = 0.68 (silica gel, hexanes:EtOAc 17:3); ^{1}H NMR (500 MHz, $CDCl_3$) δ 5.24 – 5.20 (m, 1H), 2.35 – 1.73 (m, 15H), 1.70 (s, 2H), 1.60 (s, 1H), 1.54 – 1.5 (m, 3H), 1.44 – 1.23 (m, 7H), 0.91 – 0.88 (m, 4H), 0.82 (s, 6H), 0.13 (s, 8H).

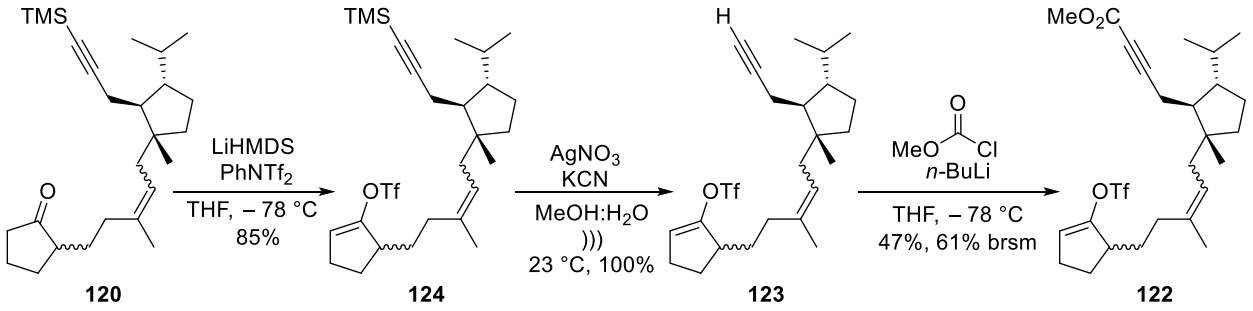

Viny Triflate 124 To a dry flask was added ketone **120** (400 mg, 1.0 mmol, 1.0 equiv.), which was dried azeotropically dried (3 x 5 mL benzene) then dissolved in THF (6 mL) and cooled to – 78 ˚C. LiHMDS (1.5 mL, 1.0 M THF, 1.5 equiv.) was added to give a light-yellow solution that was then warmed to 0 ˚C and stirred for 2 hr. The reaction was then cooled to –78 ˚C and then

$PhNTf_2$ (409 mg, 1.1 mmol, 1.1 equiv.) was added as a solution in THF (4 mL). Upon completion of addition, the reaction was warmed to 0 ˚C and stirred at that temperature until complete consumption of starting material was confirmed by TLC (silica gel, hexanes:Et_2O 19:1). The reaction was quenched with saturated $NaHCO_3$ (5 mL), diluted with DI H_2O (5 mL) and hexanes (5 mL), and the layers were separated. The aqueous layer was extracted with hexanes (3 x 10 mL) and the combined organic layers were washed with saturated $NaHCO_3$ (3 x 10 mL), dried with $MgSO_4$, filtered, and concentrated. The resultant residue was purified by flash column chromatography (silica gel, hexanes:Et_2O 99:1) to give vinyl triflate **124** as a colorless oil (452 mg, 85%). **124**: R_f = 0.18; ^{1}H NMR (500 MHz, $CDCl_3$) δ 5.63 (dq, *J* = 4.8, 2.4 Hz, 1H), 5.23 (t, *J* = 7.6 Hz, 1H), 2.81 – 2.78 (m, 1H), 2.40 – 2.36 (m, 2H), 2.28 – 2.09 (m, 5H), 2.09 – 1.83 (m, 5H), 1.72 – 1.59 (m, 6H), 1.59 – 1.48 (m, 5H), 1.40 – 1.32 (m, 3H), 1.31 – 1.18 (m, 3H), 0.90 (d, *J* = 6.9 Hz, 3H), 0.86 – 0.78 (m, 7H), 0.13 (s, 9H).

Alkyne 123 To a flask was added vinyl triflate **124** (280 mg, 0.526 mmol, 1.0 equiv.) as a solution in MeOH (2.6 mL) to give a colorless solution that was sonicated at 23 ˚C. $AgNO_3$ (241 mg, 1.42 mmol, 2.7 equiv.) was added as a solution in MeOH:H_2O (3 mL, 3:1) and the reaction became a grey-brown suspension that sonicated for 20 min. Then KCN (342 mg, 5.26 mmol, 10.0 equiv.) was added as a solution in H_2O (0.53 mL) and a gummy grey solid formed. The reaction was sonicated for 20 min or until full consumption of starting material was indicated by TLC (silica gel, hexanes:Et_2O 99:1). The reaction was then diluted with DI H_2O (4 mL) and hexanes (5 mL), and the layers were separated. The aqueous layer was extracted with hexanes (3 x 10 mL) and the combined organic layers were dried with $MgSO_4$, filtered, and concentrated. The resultant residue was then purified via flash column chromatography (silica gel, hexanes:Et_2O 99:1) to give alkyne **123** as a colorless oil (241 mg, 100%). **123**: R_f = 0.20; ^{1}H NMR (500 MHz, $CDCl_3$) δ 5.63 (s, 1H),

5.24 (s, 1H), 2.79 (s, 1H), 2.40 – 2.35 (m, 2H), 2.23 (s, 1H), 2.22 – 2.15 (m, 3H), 2.10 – 2.06 (m, 2H), 1.93 (s, 1H), 1.82 (s, 1H), 1.71 (s, 2H), 1.61 (s, 2H), 1.41 – 1.28 (m, 6H), 0.94 – 0.89 (m, 3H), 0.87 (s, 3H), 0.82 (d, J = 6.7 Hz, 3H).

Ynoate 122 To a dry flask was added alkyne **123** (80.9 mg, 0.176 mmol, 1.0 equiv.). which was dried azeotropically (3 x 2 mL benzene) then dissolved in THF (1.8 mL) and the colorless solution was cooled to –78 ˚C. Then, *n*-BuLi (0.17 mL, 1.6 M hexanes, 1.5 equiv.) was added to give a yellow solution that was stirred at the same temperature for 1 hr. Next, methyl chloroformate (0,07 mL, 0.88 mmol, 5 equiv.) was added and the reaction was stirred at the same temperature for 2 hr. The reaction was then quenched with saturated $NaHCO_3$ (3 mL), diluted with Et_2O (3 mL), and the layers were separated. The aqueous layer was extracted with Et_2O (3 x 5 mL), washed with brine, dried with $MgSO_4$, filtered and concentrated. The resultant residue was purified via flash column chromatography (silica gel, hexanes:Et_2O 99:1 to 19:1) to give and alkyne **123** (19 mg) and ynoate **122** as a colorless oil (43 mg, 47%, 61% brsm). **122**: R_f = 0.28 (silica gel, hexanes:Et_2O 19:1); ^{1}H NMR (500 MHz, $CDCl_3$) δ 5.63 (s, 1H), 5.21 (s, 1H), 3.74 (s, 3H), 2.87 – 2.66 (m, 0H), 2.39 – 2.34 (m, 2H), 2.32 (t, J = 5.1 Hz, 3H), 2.26 – 2.12 (m, 3H), 2.12 – 1.85 (m, 1H), 1.78 (s, 1H), 1.70 (s, 2H), 1.60 (s, 3H), 1.48 – 1.23 (m, 1H), 0.94 – 0.89 (m, 3H), 0.86 (s, 3H), 0.82 (dd, J = 6.7, 2.3 Hz, 3H).

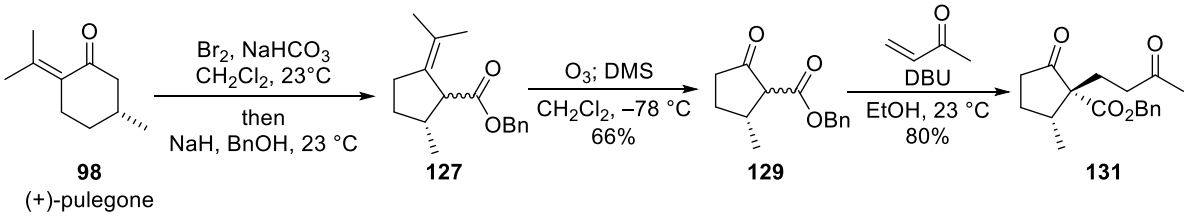

Ketoester 129 To a flask was added (+)-pulegone **98** (8.14 mL, 50 mmol, 1 equiv.), $NaHCO_3$ (2.1 g, 25 mmol, 0.5 equiv.), and CH_2Cl_2 (30 mL) to give a white suspension that was cooled to – 10

˚C. Br_2 (2.61 mL, 51 mmol, 1.02 equiv.) was added dropwise to yield a dark brown suspension that was stirred for 30 min at 23 ˚C. To a separate flask NaH (4.4 g, 110 mmol, 2.2 equiv.) and DME (50 mL) were added to give a grey suspension that was cooled to 0 ˚C. BnOH (12.95 mL, 125 mmol, 2.5 equiv.) was added dropwise and then the reaction was warmed to 23 ˚C and stirred for 15 min to give a yellow-white suspension. Next, the bromination reaction was filtered and slowly added to the benzyl alcohol solution. The tan suspension was stirred at 23 ˚C for 12 hr. The reaction was then quenched with HCl (150 mL, 1 M) and diluted with Et_2O (100 mL) then the layers were separated. The aqueous layer was extracted with Et_2O (3 x 150 mL), and the combined organic layers were washed with brine (150 mL), dried with $MgSO_4$, and concentrated to give an orange oil.

The orange oil was then added to a flask and dissolved in EtOH:H_2O (500 mL, 1:1). NaOAc (3.69 g, 45 mmol, 0.9 equiv.) and semicarbazide•HCl (3.75 g, 50 mmol, 1.0 equiv.) were added and the orange solution was heated to reflux for 1 hr then cooled to 23 ˚C and stirred for 12 hr. The mixture was then diluted with Et_2O (100 mL) and DI H_2O (50 mL) then the layers were separated. The aqueous layer was extracted with Et_2O (4 x 150 mL), and the combined organic layers were washed with brine (200 mL), dried with $MgSO_4$, and concentrated to give crude ester **127** an orange oil.

127 was then dissolved in CH_2Cl_2 (100 mL), and the orange solution was cooled to –78 ˚C. O_3 was then sparged through the reaction until full consumption of starting material was confirmed by TLC (silica gel, hexanes:EtOAc 9:1). Next, N_2 was sparged through the reaction to remove O_3 then DMS (4.4 mL, 60 mmol, 1.2 equiv.) was added and the reaction was allowed to warm to 23 ˚C and stir for 2 hrs. The reaction was then concentrated, and resultant residue was purified by flash column chromatography (silica gel, hexanes:EtOAc 9:1) to yield ketoester **129** as a colorless oil that quickly became rose-colored upon exposure to air (7.36 g, 66% over). **129**: R_f = 0.41 (silica

gel, hexanes:EtOAc 17:3); ^{1}H NMR (500 MHz, $CDCl_3$) δ 7.40 – 7.29 (m, 5H), 5.20 (s, 2H), 2.83 (d, *J* = 11.5 Hz, 1H), 2.62 (tt, *J* = 11.3, 6.4 Hz, 1H), 2.48 – 2.25 (m, 2H), 2.20 (dddd, *J* = 12.7, 8.5, 6.2, 2.0 Hz, 1H), 1.56 – 1.39 (m, 1H), 1.18 (d, *J* = 6.5 Hz, 3H).

Diketone 131 Adapting a literature procedure,[4] ketoester **129** (5.83 g, 25 mmol, 1 equiv.) was added to a dried flask under N_2 as a solution in EtOH (250 mL) at 23 ˚C. Next, freshly distilled methyl vinyl ketone **114** (2.45 mL, 30 mmol, 1.2 equiv.) and DBU (0.93 mL, 6.25 mmol, 0.25 equiv.) were added sequentially and the clear colorless solution was stirred for 15 min or until full consumption of the starting material was confirmed by TLC (silica gel, hexanes:EtOAc 4:1). The light-yellow reaction was then concentrated, and the resultant residue was purified by flash column chromatography (silica gel, hexanes:EtOAc 4:1) to give diketone **129** as a colorless oil (6.05 g, 80%). **129**: R_f = 0.26 (silica gel, hexanes:EtOAc 4:1); ^{1}H NMR (500 MHz, $CDCl_3$) δ 7.44 – 7.28 (m, 5H), 5.19 (d, *J* = 12.3 Hz, 1H), 5.08 (d, *J* = 12.3 Hz, 1H), 2.85 (ddd, *J* = 17.9, 10.4, 5.1 Hz, 1H), 2.56 – 2.41 (m, 2H), 2.31 – 2.20 (m, 1H), 2.20 – 2.12 (m, 3H), 2.11 (s, 3H), 2.08 – 1.96 (m, 2H), 1.86 (ddd, *J* = 14.5, 10.5, 5.0 Hz, 1H), 1.69 (dtd, *J* = 12.7, 11.2, 8.6 Hz, 1H), 0.97 (d, *J* = 6.9 Hz, 3H).

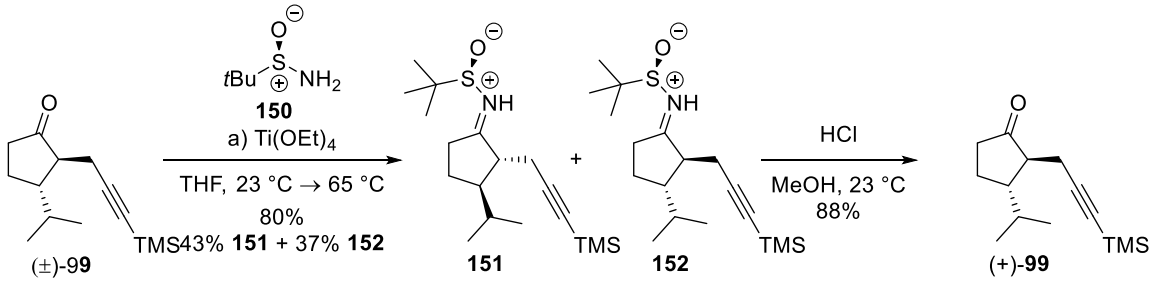

Sulfinimine 151 and **152** To a dry flask was added racemic ketone (±)-**99** (13.6 g, 57.6 mmol, 1 equiv.) and THF (96 mL) to give a colorless solution. Then $Ti(OEt)_4$ (36.2 mL, 173 mmol, 3 equiv.) was added at 23 ˚C and stirred for 5 min to give a yellow solution. (R)-2-methyl-2-

propanesulfinamide **150** (7.68 g, 53.4, 1.1 equiv.) was added and the reaction was then heated to 65 ˚C overnight or until full consumption of starting material was confirmed by TLC (silica gel, hexanes:EtOAc 9:1). The reaction was then cooled to 23 ˚C and quenched with EtOAc (250 mL) then poured into a flask with brine (300 mL). The resultant mixture was then filtered through celite, and the layers were separated. The organic layer was washed with brine (2 x 100 mL) and then the combined aqueous layers were extracted with EtOAc (150 mL). The combined organic layers were dried with $MgSO_4$ and concentrated. The resultant residue was purified by flash column chromatography (silica gel, hexanes:EtOAc 19:1 to 9:1 to 17:3) to give sulfinimine **151** as orange crystals (8.70 g, 43%) and **152** as an orange oil (7.13 g, 37%). **151**: R_f = 0.25 (silica gel, hexane:EtOAc 9:1); ^{1}H NMR (500 MHz, $CDCl_3$) δ 3.13 – 2.89 (m, 1H), 2.72 – 2.53 (m, 3H), 2.43 – 2.21 (m, 1H), 1.98 – 1.86 (m, 3H), 1.44 (q, *J* = 12.8 Hz, 1H), 1.27 (s, 9H), 1.01 (dd, *J* = 6.5, 2.9 Hz, 3H), 0.89 (dd, *J* = 6.1, 3.1 Hz, 3H), 0.12 (s, 9H).

152: R_f = 0.13 (silica gel, hexanes:EtOAc 9:1); ^{1}H NMR (500 MHz, $CDCl_3$) δ 3.16 – 3.07 (m, 1H), 2.79 – 2.71 (m, 1H), 2.55 (dt, *J* = 17.4, 3.3 Hz, 1H), 2.46 – 2.40 (m, 1H), 2.32 – 2.21 (m, 1H), 1.97 (q, *J* = 7.2 Hz, 2H), 1.88 (q, *J* = 6.6 Hz, 1H), 1.50 (t, *J* = 10.5 Hz, 1H), 1.25 (d, *J* = 2.6 Hz, 9H), 1.03 – 0.97 (m, 3H), 0.90 (d, *J* = 2.4 Hz, 4H), 0.11 (d, *J* = 2.6 Hz, 9H).

(+)-Ketone 99 To a flask was added sulfinimine **152** (7.13 g, 21.0 mmol, 1.0 equiv.) followed by MeOH (1 L) and HCl (700 mL, 3M, 100 equiv.) and the light-yellow solution was stirred at 23 ˚C until full consumption of starting material was confirmed by TLC (silica gel, hexanes:EtOAc 17:3). The reaction was then concentrated to half volume and extracted with CH_2Cl_2 (3 x 250 mL). The combined organic layers were dried with $MgSO_4$ and concentrated. The resultant residue was purified by flash column chromatography (silica gel, hexanes:Et_2O 19:1) to give (+)-ketone **99** as a colorless oil (4.14 g, 88%). Spectral data was identical to that reported above.

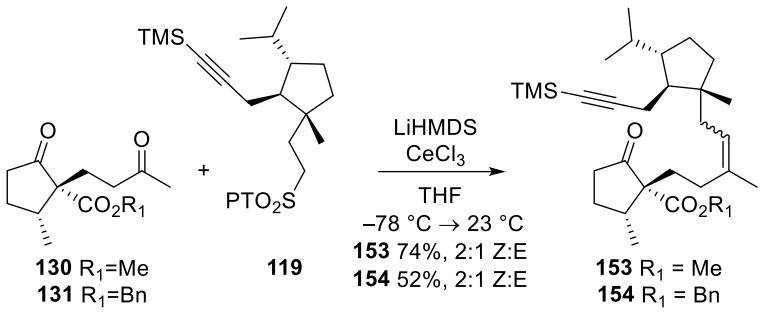

Ketone 153 Using the same procedure as ketone **120**, sulphone **119** (4.99 g, 10.6 mmol, 1.5 equiv.) and diketone **130** (1.69 g, 7.04 mmol, 1.0 equiv.) were reacted and the resultant residue was purified by flash column chromatography (silica gel, hexanes:toluene 7:3 to 0:1) to give ketone **153** as a colorless oil (2.53 g, 74%, 2:1 Z:E). The olefin isomers could be separated using gravity column chromatography (silica gel, toluene:Et_2O:CH_2Cl_2 38:1:1) to give Z-**153** and E-**153**. Z-**153**: R_f = 0.73 (silica gel, toluene:Et_2O:CH_2Cl_2 38:1:1); ^{1}H NMR (500 MHz, $CDCl_3$) δ 5.20 (t, *J* = 7.5 Hz, 1H), 3.68 (s, 3H), 2.54 (dd, *J* = 18.5, 8.3 Hz, 1H), 2.36 – 2.00 (m, 8H), 1.89 (d, *J* = 268.7 Hz, 3H), 1.84 – 1.68 (m, 4H), 1.71 (s, 3H), 1.58 – 1.48 (m, 2H), 1.42 – 1.25 (m, 3H), 1.06 (d, *J* = 6.9 Hz, 3H), 0.90 (d, *J* = 6.9 Hz, 3H), 0.84 – 0.78 (m, 6H), 0.12 (s, 9H).

E-**153**: R_f = 0.71 (silica gel, toluene:Et_2O:CH_2Cl_2 38:1:1); ^{1}H NMR (500 MHz, $CDCl_3$) δ 5.22 (t, *J* = 7.7 Hz, 1H), 3.67 (s, 3H), 2.53 (dd, *J* = 18.5, 8.5 Hz, 1H), 2.36 – 1.67 (m, 14H), 1.62 (s, 3H), 1.58 – 1.45 (m, 2H), 1.42 – 1.23 (m, 3H), 1.04 (d, *J* = 6.8 Hz, 3H), 0.89 (d, *J* = 6.8 Hz, 3H), 0.82 (s, 3H), 0.80 (d, *J* = 6.7 Hz, 3H), 0.12 (s, 9H).

Ketone 154 Using the same procedure as ketone **120**, sulphone **119** (250 mg, 0.529 mmol, 1.5 equiv.) and diketone **131** (106.6 mg, 0.357 mmol, 1.0 equiv.) were reacted and the resultant residue was purified by flash column chromatography (silica gel, hexanes:EtOAc 19:1) to give ketone **154** as a colorless oil (100 mg, 52%, 2:1 Z:E). **154**: R_f = 0.18 (silica gel, hexanes:EtOAc 19:1); ^{1}H NMR (500 MHz, $CDCl_3$) δ 7.40 – 7.28 (m, 5H), 5.26 – 5.15 (m, 2H), 5.07 (d, *J* = 12.3 Hz, 1H),

2.57 – 2.46 (m, 1H), 2.36 – 1.72 (m, 13H), 1.70 (s, 2H), 1.61 – 1.58 (m, 1H), 1.58 – 1.47 (m, 2H), 1.42 – 1.23 (m, 4H), 1.03 – 0.93 (m, 3H), 0.93 – 0.87 (m, 3H), 0.85 – 0.78 (m, 6H), 0.13 (s, 3H), 0.12 (s, 6H).

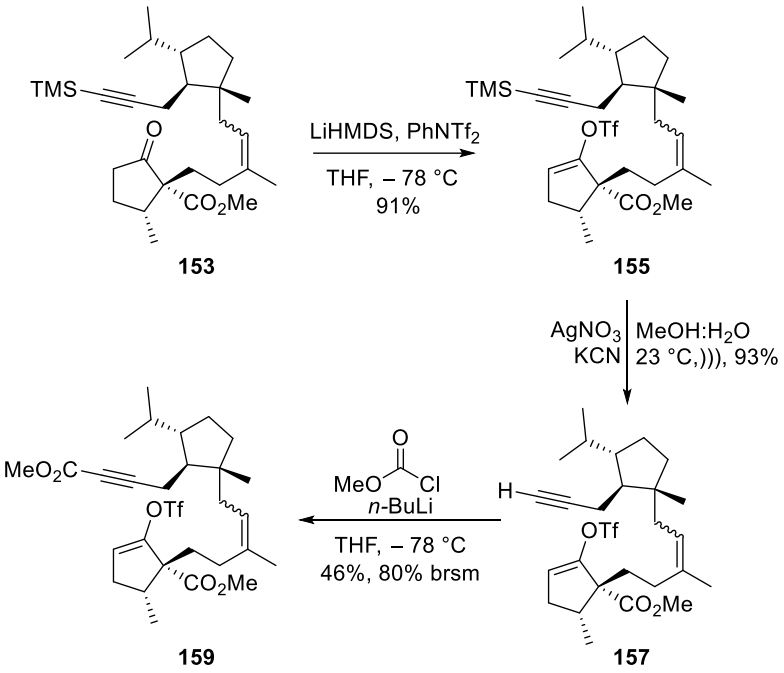

Vinyl Triflate 153 Using the same procedure as vinyl triflate **124**, Ketone **153** (391 mg, 0.829 mmol, 1.0 equiv.) was reacted and the resultant residue was purified by flash column chromatography (silica gel, hexanes:Et_2O 49:1) to give vinyl triflate **155** as a colorless oil (454 mg, 91%). **155** R_f = 0.21 (silica gel, hexanes:Et_2O 49:1), ^1H NMR (400 MHz, $CDCl_3$) δ 5.86 – 5.79 (m, 1H), 5.27 – 5.19 (m, 1H), 3.73 (s, 2H), 3.72 (s, 1H), 2.63 – 2.41 (m, 2H), 2.28 – 2.06 (m, 4H), 1.98 – 1.77 (m, 5H), 1.72 (s, 2H), 1.63 (s, 1H), 1.42 – 1.26 (m, 2H), 1.03 (d, *J* = 5.6 Hz, 2H), 1.01 (d, *J* = 5.6 Hz, 1H), 0.90 (d, *J* = 6.9 Hz, 3H), 0.83 (s, 3H), 0.81 (d, *J* = 6.8 Hz, 3H), 0.13 (s, 3H), 0.12 (s, 6H); ^{19}F NMR (376 MHz, $CDCl_3$) δ -74.03 (d, *J* = 16.3 Hz).

***Z*-155** ^1H NMR (500 MHz, $CDCl_3$) δ 5.83 (t, *J* = 2.6 Hz, 1H), 5.23 (t, *J* = 7.5 Hz, 1H), 3.73 (s, 3H), 2.57 (ddd, *J* = 15.6, 8.1, 2.9 Hz, 1H), 2.47 (h, *J* = 7.2 Hz, 1H), 2.24 (dd, *J* = 17.2, 6.3 Hz,

1H), 2.20 – 2.07 (m, 4H), 1.94 – 1.82 (m, 4H), 1.82 – 1.78 (m, 1H), 1.72 (s, 3H), 1.75 – 1.67 (m, 1H), 1.53 – 1.48 (m, 1H), 1.44 – 1.32 (m, 2H), 1.03 (d, *J* = 7.0 Hz, 3H), 0.90 (d, *J* = 6.9 Hz, 3H), 0.83 (s, 3H), 0.81 (d, *J* = 6.8 Hz, 3H), 0.12 (s, 9H).

Alkyne 157 Using the same procedure as alkyne **123**, vinyl triflate **155** (454 mg, 0.751 mmol, 1.0 equiv.) was reacted and the resultant residue was purified by flash column chromatography (silica gel, hexanes:Et_2O 49:1) to give alkyne **157** as a colorless oil (373 mg, 93%). **157**: R_f = 0.24 (silica gel, hexanes:Et_2O 49:1); ^{1}H NMR (500 MHz, $CDCl_3$) δ 5.85 – 5.80 (m, 1H), 5.29 – 5.19 (m, 1H), 3.72 (s, 2H), 3.72 (s, 1H), 2.61 – 2.42 (m, 2H), 2.27 – 2.08 (m, 5H), 1.97 – 1.86 (m, 3H), 1.88 – 1.75 (m, 2H), 1.72 (s, 2H), 1.63 (s, 1H), 1.55 – 1.48 (m, 1H), 1.45 – 1.26 (m, 2H), 1.03 (d, *J* = 5.5 Hz, 2H), 1.01 (d, *J* = 5.4 Hz, 1H), 0.91 (d, *J* = 6.8 Hz, 3H), 0.86 (s, 3H), 0.81 (d, *J* = 6.7 Hz, 3H).

***Z*-157** ^{1}H NMR (500 MHz, $CDCl_3$) δ 5.83 (t, *J* = 2.6 Hz, 1H), 5.22 (t, *J* = 7.4 Hz, 1H), 3.72 (s, 3H), 2.57 (ddd, *J* = 15.5, 8.1, 2.9 Hz, 1H), 2.47 (h, *J* = 7.3 Hz, 1H), 2.25 – 2.09 (m, 5H), 1.95 – 1.75 (m, 6H), 1.72 (s, 3H), 1.69 – 1.48 (m, 10H), 1.43 – 1.29 (m, 3H), 1.02 (d, *J* = 6.9 Hz, 3H), 0.91 (d, *J* = 6.8 Hz, 3H), 0.86 (s, 3H), 0.81 (d, *J* = 6.7 Hz, 3H).

Ynoate 159 Using the same procedure as ynoate **122**, alkyne **157** (373 mg, 0.70 mmol, 1.0 equiv.) was reacted and the resultant residue was purified by flash column chromatography (silica gel, hexanes:Et_2O 9:1) to give ynoate **159** as a colorless oil (190 mg, 46%, 80% brsm) and recovered alkyne **157** (160 mg). **159**: R_f = 0.21 (silica gel, hexanes:Et_2O 9:1); ^{1}H NMR (500 MHz, $CDCl_3$) δ 5.86 – 5.80 (m, 1H), 5.26 – 5.17 (m, 1H), 3.75 (s, 1H), 3.74 (s, 2H), 3.72 (s, 2H), 3.72 (s, 1H), 2.56 (dddd, *J* = 16.1, 8.2, 5.4, 3.0 Hz, 1H), 2.46 (qd, *J* = 7.2, 5.5 Hz, 1H), 2.40 – 2.05 (m, 3H), 1.95 – 1.85 (m, 1H), 1.87 – 1.73 (m, 1H), 1.72 (d, *J* = 1.4 Hz, 2H), 1.62 (d, *J* = 1.3 Hz, 1H), 1.59 (d, *J* = 6.4 Hz, 1H), 1.45 – 1.23 (m, 3H), 1.02 (d, *J* = 4.3 Hz, 2H), 1.01 (d, *J* = 4.3 Hz, 1H), 0.91 (d, *J* = 6.8 Hz, 2H), 0.86 (s, 1H), 0.82 (d, *J* = 6.7 Hz, 3H).

***Z*-159** ^{1}H NMR (500 MHz, $CDCl_3$) δ 5.83 (t, *J* = 2.7 Hz, 1H), 5.21 (t, *J* = 7.5 Hz, 1H), 3.74 (s, 3H), 3.72 (s, 3H), 2.57 (ddd, *J* = 15.6, 8.1, 3.0 Hz, 1H), 2.47 (h, *J* = 7.0 Hz, 1H), 2.36 (dd, *J* = 17.6, 6.7 Hz, 1H), 2.27 (dd, *J* = 17.6, 5.9 Hz, 1H), 2.19 – 2.07 (m, 3H), 1.95 – 1.85 (m, 2H), 1.80 (s, 3H), 1.74 – 1.71 (m, 3H), 1.71 – 1.65 (m, 1H), 1.64 – 1.57 (m, 2H), 1.46 – 1.30 (m, 3H), 1.02 (d, *J* = 7.1 Hz, 3H), 0.91 (d, *J* = 6.8 Hz, 3H), 0.86 (s, 3H), 0.82 (d, *J* = 6.7 Hz, 3H).

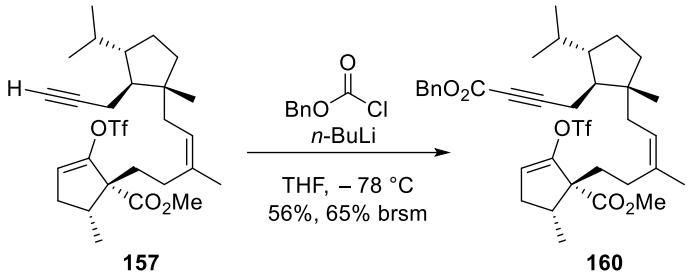

157 **160**

Ynoate 160 Using the same procedure as ynoate **122**, alkyne **157** (53 mg, 0.5 mmol, 1.0 equiv.) was reacted and the resultant residue was purified by flash column chromatography (silica gel, hexanes:Et_2O 23:2) to give ynoate **160** as a light-yellow oil (37 mg, 56%, 65% brsm, 2:1 Z:E) and alkyne **157** (8 mg). **160**: R_f = 0.23 (silica gel, hexanes:Et_2O 9:1); ^{1}H NMR (500 MHz, $CDCl_3$) δ 7.41 – 7.29 (m, 5H), 5.81 (t, *J* = 2.8 Hz, 1H), 5.25 – 5.13 (m, 3H), 3.72 (s, 3H), 2.60 – 2.50 (m, 1H), 2.50 – 2.40 (m, 1H), 2.39 – 2.18 (m, 3H), 2.18 – 2.04 (m, 3H), 1.95 – 1.74 (m, 5H), 1.71 (s, 2H), 1.68 – 1.50 (m, 4H), 1.46 – 1.27 (m, 4H), 1.01 (d, *J* = 7.0 Hz, 3H), 0.90 (d, *J* = 6.8 Hz, 4H), 0.86 (s, 2H), 0.85 (s, 1H), 0.81 (d, *J* = 6.8 Hz, 2H).

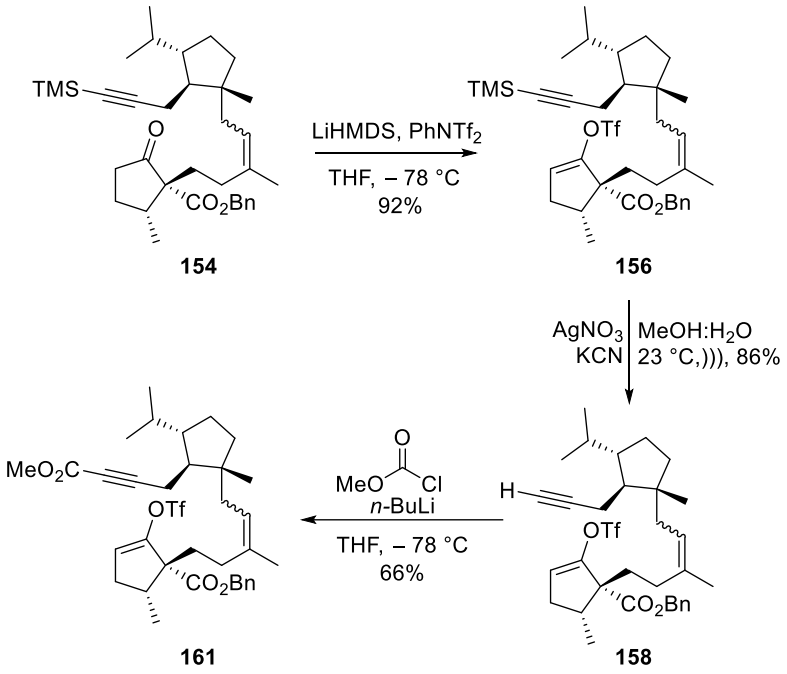

Vinyl Triflate 156 Using the same procedure as vinyl triflate **124**, Ketone **154** (100 mg, 0.182 mmol, 1.0 equiv.) was reacted and the resultant residue was purified by flash column chromatography (silica gel, hexanes:Et_2O 24:1) to give vinyl triflate **156** as a colorless oil (114 mg, 92%). **156** R_f = 0.53 (silica gel, hexanes:EtOAc 19:1), ^{1}H NMR (500 MHz, $CDCl_3$) δ 7.37 – 7.28 (m, 5H), 5.83 (dt, *J* = 4.7, 2.5 Hz, 1H), 5.25 – 5.19 (m, 2H), 5.10 (d, *J* = 12.2 Hz, 1H), 2.63 – 2.38 (m, 2H), 2.29 – 2.17 (m, 2H), 2.17 – 2.05 (m, 3H), 1.96 – 1.78 (m, 6H), 1.71 (s, 2H), 1.71 (s, 3H), 1.61 (s, 1H), 1.57 – 1.48 (m, 3H), 1.43 (d, *J* = 2.7 Hz, 1H), 1.40 – 1.34 (m, 1H), 0.99 – 0.94 (m, 3H), 0.91 – 0.87 (m, 6H), 0.84 – 0.79 (m, 3H), 0.12 (d, *J* = 4.0 Hz, 9H).

Alkyne 158 Using the same procedure as alkyne **123**, vinyl triflate **156** (114 mg, 0.167 mmol, 1.0 equiv.) was reacted and the resultant residue was purified by flash column chromatography (silica gel, hexanes:Et_2O 49:1) to give alkyne **158** as a colorless oil (87.6 mg, 82%). **158**: R_f = 0.57 (silica gel, hexanes:EtOAc 19:1); ^{1}H NMR (500 MHz, $CDCl_3$) δ 7.40 – 7.28 (m, 5H), 5.85 – 5.80 (m, 1H), 5.27 – 5.19 (m, 2H), 5.10 (d, *J* = 12.2 Hz, 1H), 2.57 – 2.42 (m, 1H), 2.29 – 2.05 (m, 4H), 1.96

– 1.76 (m, 3H), 1.72 – 1.69 (m, 2H), 1.68 – 1.62 (m, 0H), 1.61 (d, *J* = 1.4 Hz, 1H), 1.59 – 1.47 (m, 1H), 1.45 – 1.24 (m, 4H), 0.95 (d, *J* = 6.9 Hz, 3H), 0.90 (d, *J* = 6.8 Hz, 3H), 0.85 (s, 1H), 0.81 (d, *J* = 6.7 Hz, 3H).

Ynoate 161 Using the same procedure as ynoate **122**, alkyne **158** (87.6 mg, 0.144 mmol, 1.0 equiv.) was reacted and the resultant residue was purified by flash column chromatography (silica gel, hexanes:Et_2O 9:1) to give ynoate **161** as a colorless oil (63.8 mg, 66%). **161**: R_f = 0.53 (silica gel, hexanes:Et_2O 9:1); ^1H NMR (500 MHz, $CDCl_3$) δ 7.43 – 7.27 (m, 5H), 5.83 (dt, *J* = 4.9, 2.5 Hz, 1H), 5.27 – 5.15 (m, 2H), 5.09 (d, *J* = 12.2 Hz, 1H), 3.74 (s, 1H), 3.73 (s, 2H), 2.58 – 2.42 (m, 2H), 2.39 – 2.01 (m, 6H), 1.95 – 1.74 (m, 6H), 1.71 (s, 2H), 1.63 – 1.55 (m, 4H), 1.41 – 1.28 (m, 3H), 0.95 (d, *J* = 6.9 Hz, 3H), 0.91 (d, *J* = 6.8 Hz, 3H), 0.85 (s, 3H), 0.81 (d, *J* = 6.7 Hz, 3H).

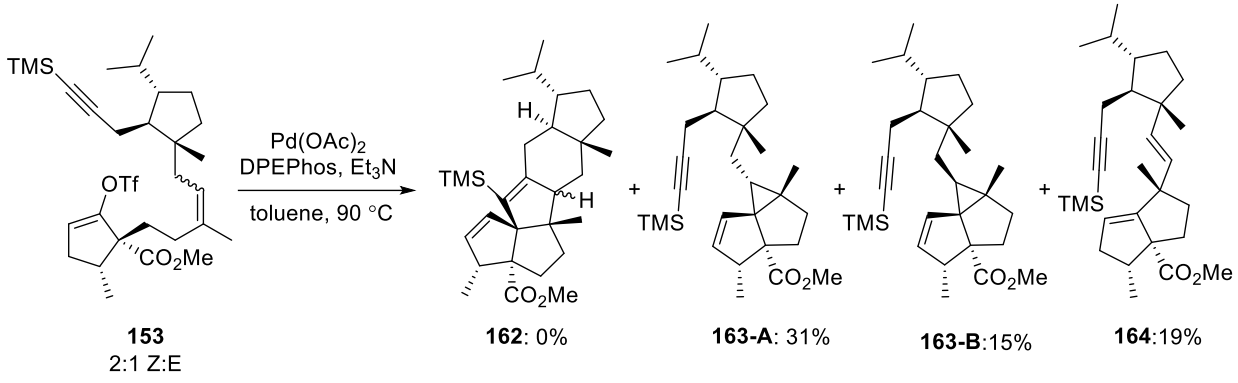

153 2:1 Z:E | **162**: 0% | **163-A**: 31% | **163-B**:15% | **164**:19%

Cascade reaction of vinyl triflate 153 To a dry vial under Ar was added $Pd(OAc)_2$ (1.2 mg, 0.005 mmol, 10 mol%), DPEPhos (5.4 mg, 0.01 mmol, 20 mol%), Et_3N (0.02 mL, 0.15 mmol, 3.0 equiv.) and toluene (0.3 mL) to give a reddish-brown suspension that was sparged for 15 min with Ar. Then vinyl triflate **153** (30.6 mg, 0.05 mmol, 1.0 equiv.) was added as a solution in degassed toluene (0.2 mL) and the mixture was sparged for a further 5 min, sealed with a Teflon lined cap, and heated to 90 ˚C for 12 hr. The reaction was then cooled to 23 ˚C, diluted with Et_2O (2 mL), filtered through a celite plug, and concentrated. The resultant residue was purified via preparatory

TLC (silica gel, hexanes:Et_2O 24:1) to give vinyl cyclopropane **163-A** as a colorless oil (7.0 mg, 31%, vinyl cyclopropane **163-B** as a colorless oil (3.4 mg, 15%), and diene **164** (4.3 mg, 19%). **163-A**: R_f = 0.14 (silica gel, hexanes:Et_2O 49:1); ^{1}H NMR (500 MHz, $CDCl_3$) δ 5.51 (dd, *J* = 5.8, 1.7 Hz, 1H), 5.47 (dd, *J* = 5.7, 2.8 Hz, 1H), 3.63 (s, 3H), 2.99 – 2.80 (m, 1H), 2.25 (dd, *J* = 17.2, 4.9 Hz, 1H), 2.07 (dd, *J* = 17.2, 7.8 Hz, 1H), 2.03 – 1.89 (m, 4H), 1.81 – 1.72 (m, 1H), 1.63 – 1.50 (m, 1H), 1.48 – 1.38 (m, 2H), 1.38 – 1.27 (m, 2H), 1.06 (s, 3H), 0.99 (d, *J* = 7.4 Hz, 3H), 0.92 (d, *J* = 6.9 Hz, 4H), 0.85 (s, 3H), 0.83 (d, *J* = 6.7 Hz, 3H), 0.13 (s, 9H); ^{13}C NMR (126 MHz, $CDCl_3$) δ 176.23, 133.56, 132.37, 108.01, 85.23, 67.05, 52.19, 51.01, 50.99, 50.84, 47.97, 44.74, 38.20, 34.98, 33.85, 33.79, 32.95, 30.99, 29.80, 23.69, 22.61, 21.96, 21.87, 21.23, 17.03, 15.02.

163-B: R_f = 0.24 (silica gel, hexanes:Et_2O 49:1); ^{1}H NMR (500 MHz, $CDCl_3$) δ 5.55 (dd, *J* = 5.8, 1.7 Hz, 1H), 5.52 (dd, *J* = 5.9, 2.6 Hz, 1H), 3.63 (s, 3H), 2.91 – 2.78 (m, 1H), 2.23 (dd, *J* = 17.2, 7.0 Hz, 1H), 2.17 (dd, *J* = 17.2, 6.4 Hz, 1H), 2.12 – 2.00 (m, 1H), 1.94 – 1.73 (m, 5H), 1.70 – 1.61 (m, 1H), 1.59 – 1.50 (m, 1H), 1.48 – 1.39 (m, 2H), 1.38 – 1.23 (m, 4H), 1.03 (d, *J* = 7.3 Hz, 3H), 0.97 (s, 3H), 0.90 (d, *J* = 6.9 Hz, 3H), 0.84 (s, 3H), 0.83 – 0.80 (m, 3H), 0.13 (s, 9H); ^{13}C NMR (126 MHz, $CDCl_3$) δ 175.79, 134.22, 128.43, 108.09, 85.12, 69.14, 52.74, 50.90, 50.33, 50.10, 49.02, 44.86, 38.66, 38.57, 37.36, 33.55, 32.71, 29.73, 29.53, 23.44, 22.48, 20.81, 20.01, 17.07, 15.67, 15.27, 0.21.

164: R_f = 0.31 (silica gel, hexanes:Et_2O 49:1); ^{1}H NMR (500 MHz, $CDCl_3$) δ 5.55 – 5.51 (m, 1H), 5.33 (d, *J* = 15.8 Hz, 1H), 5.24 (d, *J* = 15.8 Hz, 1H), 3.64 (s, 3H), 2.62 – 2.39 (m, 3H), 2.38 – 2.27 (m, 1H), 2.20 (dd, *J* = 17.1, 4.7 Hz, 1H), 2.11 – 1.82 (m, 5H), 1.61 (ddd, *J* = 13.5, 8.8, 5.5 Hz, 2H), 1.50 (td, *J* = 8.7, 4.6 Hz, 1H), 1.36 (tdt, *J* = 17.6, 12.2, 6.4 Hz, 5H), 1.16 (s, 3H), 0.96 (d, *J* = 7.0 Hz, 3H), 0.90 (d, *J* = 6.8 Hz, 3H), 0.84 – 0.80 (m, 6H), 0.12 (s, 9H); ^{13}C NMR (126 MHz,

$CDCl_3$) δ 175.15, 159.60, 136.48, 133.14, 122.94, 107.99, 85.21, 68.17, 51.32, 50.00, 49.13, 48.98, 47.07, 43.93, 42.25, 39.65, 31.65, 29.53, 27.34, 23.30, 22.51, 19.96, 19.27, 16.71, 15.01.

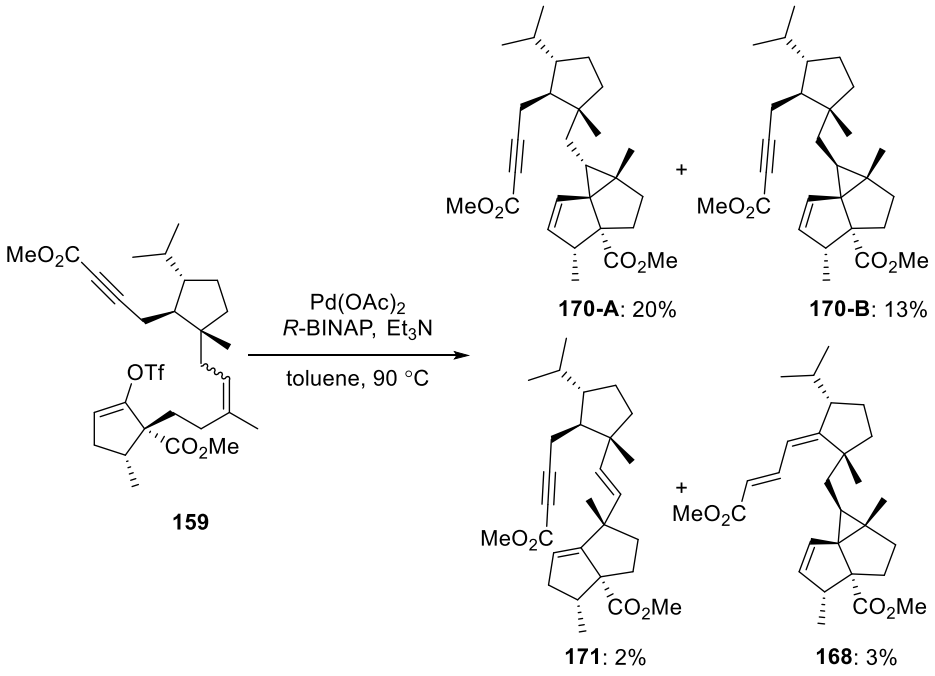

Cascade reaction of ynoate 159 To a dry vial under Ar was added $Pd(OAc)_2$ (1.1 mg, 0.0051 mmol, 20 mol%), R-BINAP (6.3 mg, 0.0102 mmol, 40 mol%), Et_3N (0.01 mL, 0.076 mmol, 3.0 equiv.) and toluene (0.15 mL) to give a reddish-brown suspension that was sparged for 10 min with Ar. Then, ynoate **159** (15.0 mg, 0.0254 mmol, 1.0 equiv.) was added as a solution in degassed toluene (0.1 mL) and the mixture was sparged for a further 5 min, sealed with a Teflon lined cap, and heated to 90 ˚C for 12 hr. The reaction was then cooled to 23 ˚C, diluted with Et_2O (1 mL), filtered through a celite plug, and concentrated. The resultant residue was purified via preparatory TLC (silica gel, hexanes:Et_2O 23:2) to give vinyl cyclopropane **170-A** as a colorless oil (2.2 mg, 20%), vinyl cyclopropane **170-B** as a colorless oil (1.5 mg, 13%), and diene **171** and dienoate **168** as a 1:1.25 mixture (0.3 mg, 5%). **170-A**: R_f = 0.23 (silica gel, hexanes:Et_2O 9:1); ^1H NMR (500 MHz, $CDCl_3$) δ 5.51 (dd, *J* = 5.9, 1.7 Hz, 1H), 5.47 (dd, *J* = 5.8, 2.7 Hz, 1H), 3.75 (s,

3H), 3.62 (s, 3H), 2.97 – 2.87 (m, 1H), 2.34 (dd, *J* = 17.6, 6.4 Hz, 1H), 2.25 (dd, *J* = 17.5, 6.1 Hz, 1H), 2.02 – 1.85 (m, 4H), 1.85 – 1.75 (m, 1H), 1.75 – 1.64 (m, 1H), 1.64 – 1.58 (m, 1H), 1.53 – 1.27 (m, 5H), 1.05 (s, 3H), 0.99 (d, *J* = 7.4 Hz, 3H), 0.93 (d, *J* = 6.9 Hz, 3H), 0.91 (s, 3H), 0.83 (d, *J* = 6.7 Hz, 3H).

170-B: R_f = 0.32 (silica gel, hexane:Et_2O 9:1); ^1H NMR (500 MHz, $CDCl_3$) δ 5.55 (dd, *J* = 5.8, 1.5 Hz, 1H), 5.53 (dd, *J* = 5.9, 2.4 Hz, 1H), 3.74 (s, 3H), 3.63 (s, 3H), 2.89 – 2.80 (m, 1H), 2.32 (d, *J* = 2.2 Hz, 1H), 2.31 (d, *J* = 1.3 Hz, 1H), 2.10 – 1.99 (m, 1H), 1.94 – 1.71 (m, 7H), 1.71 – 1.57 (m, 1H), 1.55 – 1.43 (m, 4H), 1.41 – 1.27 (m, 5H), 1.25 (s, 2H), 1.03 (d, *J* = 7.4 Hz, 3H), 0.97 (s, 3H), 0.94 – 0.86 (m, 8H), 0.82 (d, *J* = 6.7 Hz, 4H).

171 & **168**: R_f = 0.43 (silica gel, hexanes:Et_2O 9:1); ^1H NMR (500 MHz, $CDCl_3$) δ 6.31 (dt, *J* = 11.3, 7.4 Hz, 1H), 5.75 (d, *J* = 11.6 Hz, 1H), 5.58 – 5.53 (m, 2H), 5.51 (dd, *J* = 5.8, 2.7 Hz, 1H), 5.34 (d, *J* = 15.9 Hz, 1H), 5.26 (d, *J* = 15.8 Hz, 1H), 3.74 (s, 3H), 3.71 (s, 3H), 3.64 (s, 3H), 3.62 (s, 3H), 2.89 – 2.73 (m, 2H), 2.67 – 2.54 (m, 2H), 2.52 (dd, *J* = 7.2, 3.3 Hz, 1H), 2.47 – 2.39 (m, 1H), 2.37 – 2.25 (m, 2H), 2.22 – 2.13 (m, 1H), 2.09 – 1.99 (m, 2H), 1.97 – 1.76 (m, 6H), 1.74 – 1.59 (m, 7H), 1.53 (d, *J* = 7.8 Hz, 4H), 1.44 – 1.29 (m, 13H), 1.15 (s, 3H), 1.03 (d, *J* = 7.3 Hz, 3H), 0.96 (d, *J* = 7.0 Hz, 3H), 0.93 (s, 3H), 0.91 (d, *J* = 6.8 Hz, 3H), 0.88 – 0.86 (m, 6H), 0.85 – 0.82 (m, 6H), 0.80 – 0.75 (m, 6H).

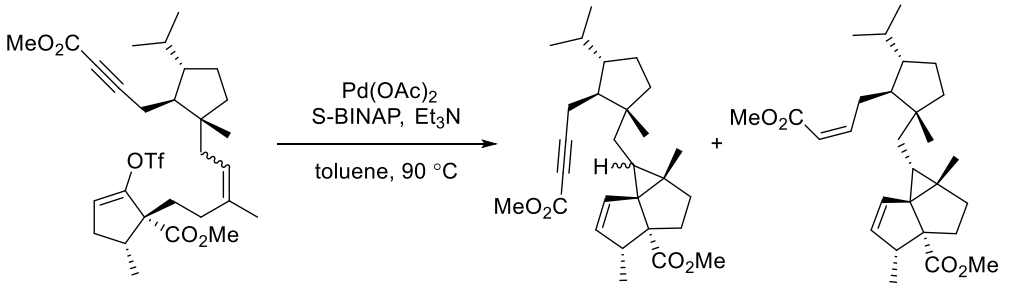

158 **170**: Trace **172**: 16% [Confirmed by X-Ray]

Cascade reaction of ynoate 158 To a dry vial under Ar was added $Pd(OAc)_2$ (6.7 mg, 0.030 mmol, 20 mol%), S-BINAP (37.4 mg, 0.060 mmol, 40 mol%), Et_3N (0.06 mL, 0.45 mmol, 3.0 equiv.) and toluene (1.0 mL) to give a reddish-brown suspension that was sparged for 10 min with Ar. Then, ynoate **158** (88.5 mg, 0.15 mmol, 1.0 equiv.) was added as a solution in degassed toluene (0.50 mL) and the mixture was sparged for a further 5 min, sealed with a Teflon lined cap, and heated to 90 ˚C for 12 hr. The reaction was then cooled to 23 ˚C, diluted with Et_2O (3 mL), filtered through a celite plug, and concentrated. The resultant residue was purified first via preparatory TLC (silica gel, hexanes:Et_2O 9:1) and then second with preparatory TLC (silica gel, CH_2Cl_2) to give enoate **172** as a colorless solid (10.9 mg, 16%), X-Ray quality crystals were obtained via slow evaporation from pentane. **172**: R_f = 0.25 (silica gel, hexanes:Et_2O 9:1); ^1H NMR (500 MHz, $CDCl_3$) δ 6.25 (dt, *J* = 11.5, 7.4 Hz, 1H), 5.73 (dd, *J* = 11.6, 2.2 Hz, 1H), 5.50 (dd, *J* = 5.8, 1.6 Hz, 1H), 5.46 (dd, *J* = 5.9, 2.7 Hz, 1H), 3.70 (s, 3H), 3.62 (s, 3H), 2.95 – 2.87 (m, 1H), 2.78 – 2.60 (m, 2H), 2.04 – 1.84 (m, 4H), 1.68 (qd, *J* = 6.7, 3.7 Hz, 2H), 1.61 – 1.47 (m, 4H), 1.44 – 1.27 (m, 5H), 1.25 (s, 1H), 1.12 (dd, *J* = 10.4, 2.5 Hz, 1H), 1.03 (s, 3H), 0.98 (d, *J* = 7.5 Hz, 3H), 0.87 (d, *J* = 6.3 Hz, 6H), 0.79 (d, *J* = 6.3 Hz, 3H); ^{13}C NMR (126 MHz, $CDCl_3$) δ 176.31, 167.07, 151.92, 133.55, 132.31, 118.89, 66.93, 52.39, 51.38, 51.11, 51.05, 51.00, 50.41, 45.19, 38.65, 35.80, 33.95, 33.82, 33.01, 31.14, 30.75, 29.72, 23.13, 22.74, 21.79, 21.08, 16.82, 15.03.

1.13 X-Ray Crystallographic Data

General information: The diffraction data were measured at 100 K on a Bruker D8 VENTURE diffractometer equipped with a microfocus Mo-target X-ray tube (λ = 0.71073 Å) and PHOTON 100 CMOS detector. Data were collected using ω scans to survey a hemisphere of reciprocal space. Data reduction and integration were performed with the Bruker APEX4 software package (Bruker

AXS, version 2021.4-0, 2021). Data were scaled and corrected for absorption effects using the multi-scan procedure as implemented in SADABS (Bruker AXS, version 2014/5, Krause, Herbst-Irmer, Sheldrick & Stalke, *J. Appl. Cryst.* **2015**, *48*, 3-10). The structure was solved by SHELXT (Version 2018/2: Sheldrick, G. M. *Acta Crystallogr*. **2015**, ***A71***, 3-8) and refined by a full-matrix least-squares procedure using OLEX2 (O. V. Dolomanov, L. J. Bourhis, R. J. Gildea, J. A. K. Howard and H. Puschmann. J. Appl. Crystallogr. **2009**, *42*, 339-341) (XL refinement program version 2018/3, Sheldrick, G. M. Acta Crystallogr. **2015**, *C71*, 3-8). Crystallographic data and details of the data collection and structure refinement are listed in Table 1.

Specific details for structure refinement: All atoms were refined with anisotropic thermal parameters. All hydrogen atoms were included in idealized positions for structure factor calculations. All structures are drawn with thermal ellipsoids at 50% probability.

Figure 1.7 ORTEP representation of **151**

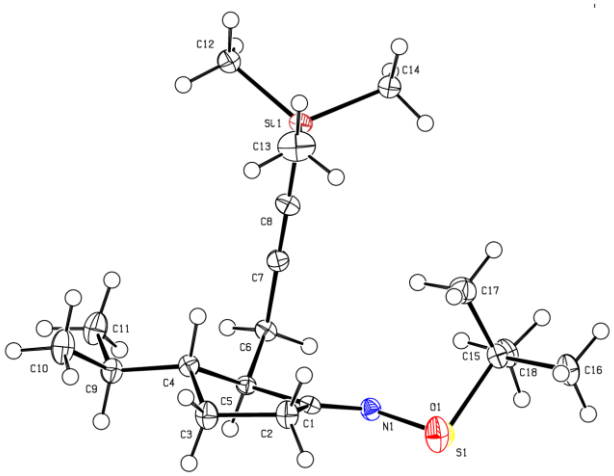

Crystal data and structure refinement for JonKeim.

Identification code	JonKeim
Empirical formula	$C_{18}H_{33}NOSSi$
Formula weight	339.60
Temperature/K	100(2)

Figure 1.7 cont.

Crystal system	orthorhombic
Space group	$P2_12_12_1$
a/Å	10.6630(7)
b/Å	10.8155(8)
c/Å	17.9360(13)
α/°	90
β/°	90
γ/°	90
Volume/Å^3	2068.5(3)
Z	4
ρ_{calc}g/cm^3	1.091
μ/mm^{-1}	0.217
F(000)	744.0
Crystal size/mm^3	0.15 × 0.1 × 0.1
Radiation	MoKα (λ = 0.71073)
2Θ range for data collection/°	4.398 to 66.306
Index ranges	$-16 \leq h \leq 15$, $-16 \leq k \leq 16$, $-22 \leq l \leq 27$
Reflections collected	24669
Independent reflections	7734 [R_{int} = 0.0420, R_{sigma} = 0.0549]
Data/restraints/parameters	7734/0/207
Goodness-of-fit on F^2	1.034
Final R indexes [I>=2σ (I)]	R_1 = 0.0412, wR_2 = 0.0831
Final R indexes [all data]	R_1 = 0.0645, wR_2 = 0.0908
Largest diff. peak/hole / e Å^{-3}	0.44/-0.20
Flack parameter	0.02(3)

Figure 1.8 ORTEP representation of **172**

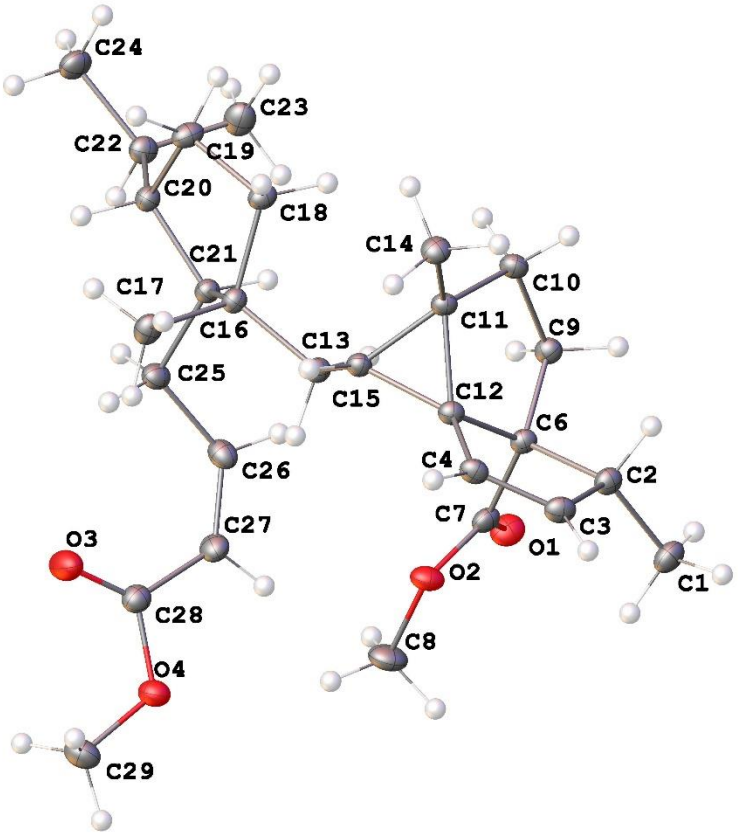

Crystal data and structure refinement for Cu_0676_keim.

Identification code	Cu_0676_keim
Empirical formula	$C_{28}H_{42}O_4$
Formula weight	442.61
Temperature/K	100(2)
Crystal system	monoclinic
Space group	$P2_1$
a/Å	13.1173(3)
b/Å	6.4240(2)
c/Å	15.0152(4)
α/°	90
β/°	94.4300(10)
γ/°	90
Volume/Å^3	1261.48(6)
Z	2
ρ_{calc}g/cm^3	1.165
μ/mm^{-1}	0.596
F(000)	484.0
Crystal size/mm^3	0.22 × 0.07 × 0.04

Figure 1.8 cont.

Radiation	CuKα (λ = 1.54178)
2Θ range for data collection/°	5.904 to 149.202
Index ranges	$-16 \leq h \leq 16$, $-6 \leq k \leq 7$, $-18 \leq l \leq 18$
Reflections collected	27118
Independent reflections	4754 [R_{int} = 0.0445, R_{sigma} = 0.0303]
Data/restraints/parameters	4754/1/296
Goodness-of-fit on F^2	1.018
Final R indexes [I>=2σ (I)]	R_1 = 0.0329, wR_2 = 0.0804
Final R indexes [all data]	R_1 = 0.0359, wR_2 = 0.0822
Largest diff. peak/hole / e $Å^{-3}$	0.27/-0.14
Flack parameter	0.00(8)
Hooft parameter	0.01(8)

$R_{int} = \Sigma \mid F_o^2 - \langle F_o^2 \rangle \mid / \Sigma \mid F_o^2 \mid$

$R1 = \Sigma \mid \mid F_o \mid - \mid F_c \mid \mid / \Sigma \mid F_o \mid$

$wR2 = [\Sigma [w (F_o^2 - F_c^2)^2] / \Sigma [w (F_o^2)^2]]^{1/2}$

$\text{Goodness-of-fit} = [\Sigma [w (F_o^2 - F_c^2)^2] / (n-p)^{1/2}$

n: number of independent reflections; p: number of refined parameters

1.14 ^{1}H and ^{13}C NMR Spectra

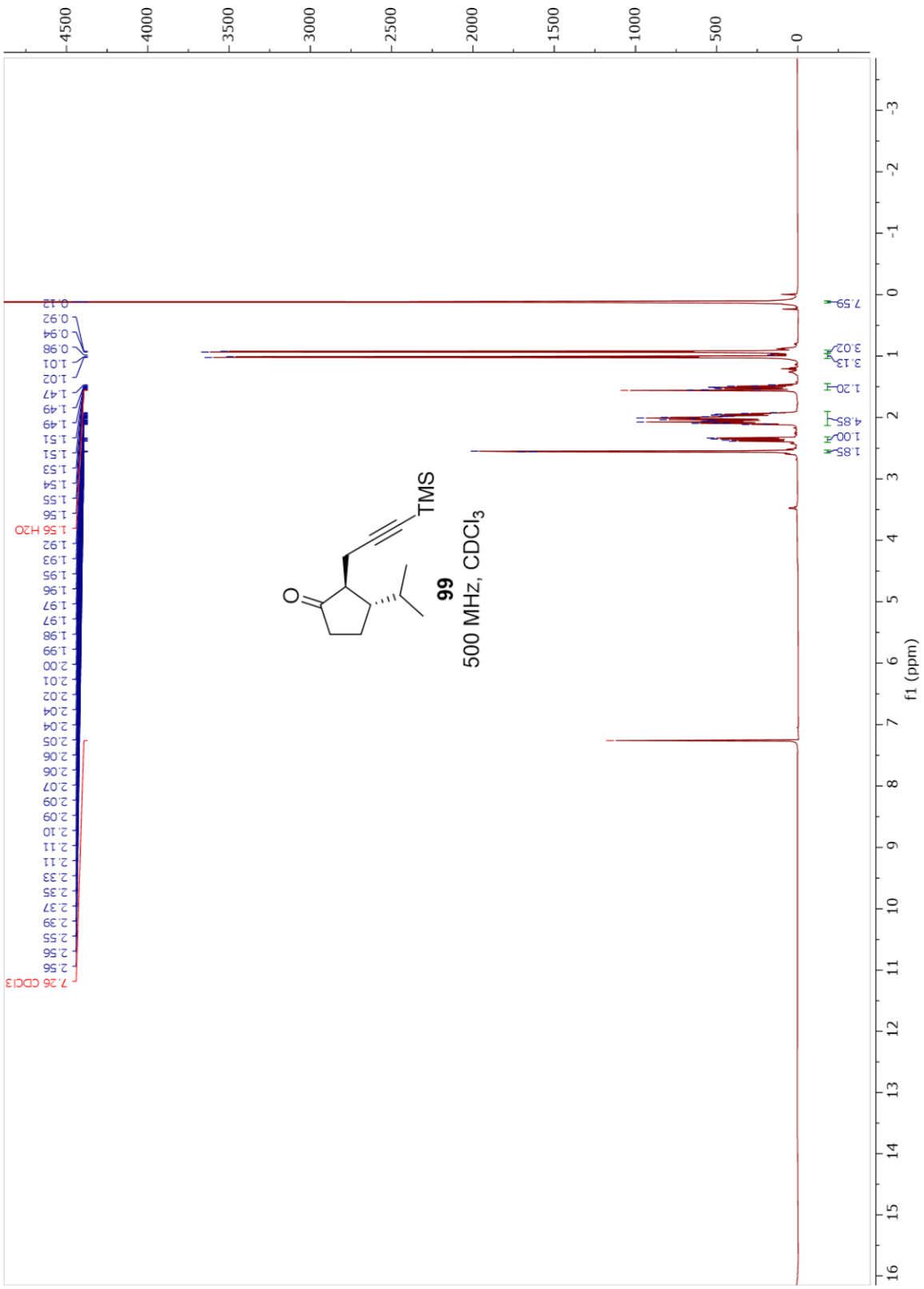

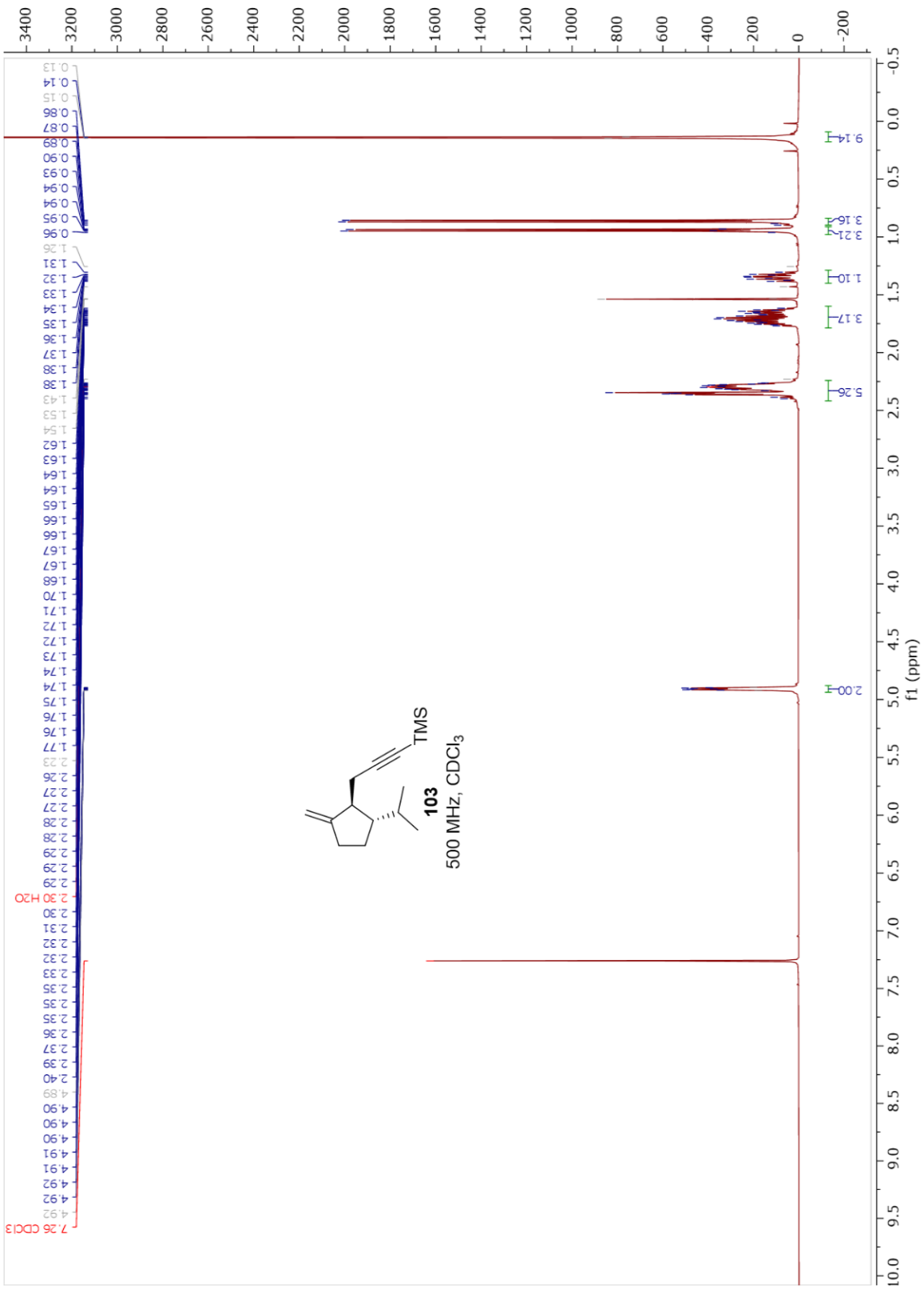
TMS
103
500 MHz, CDCl3
f1 (ppm)

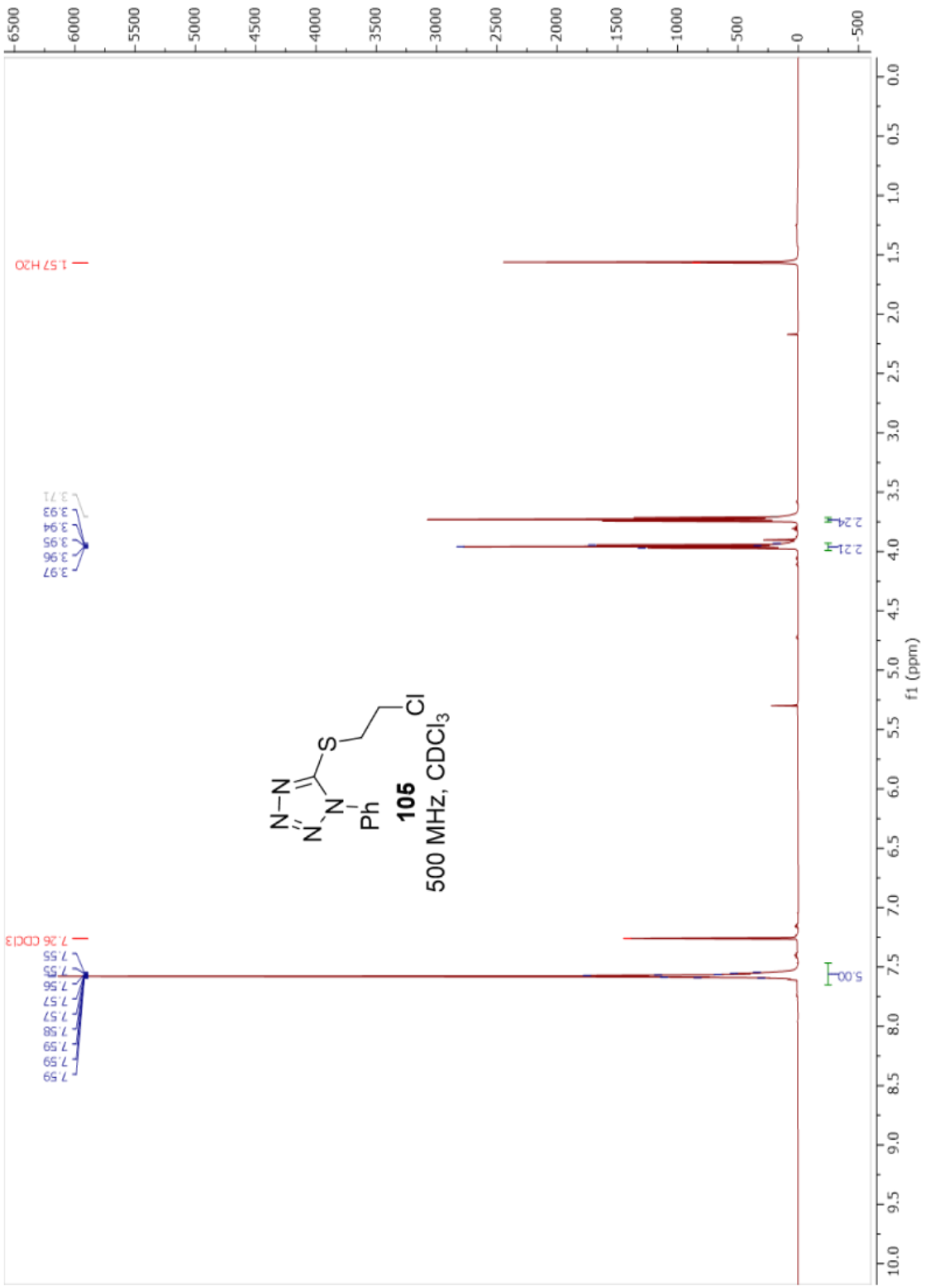
105
500 MHz, CDCl3
f1 (ppm)

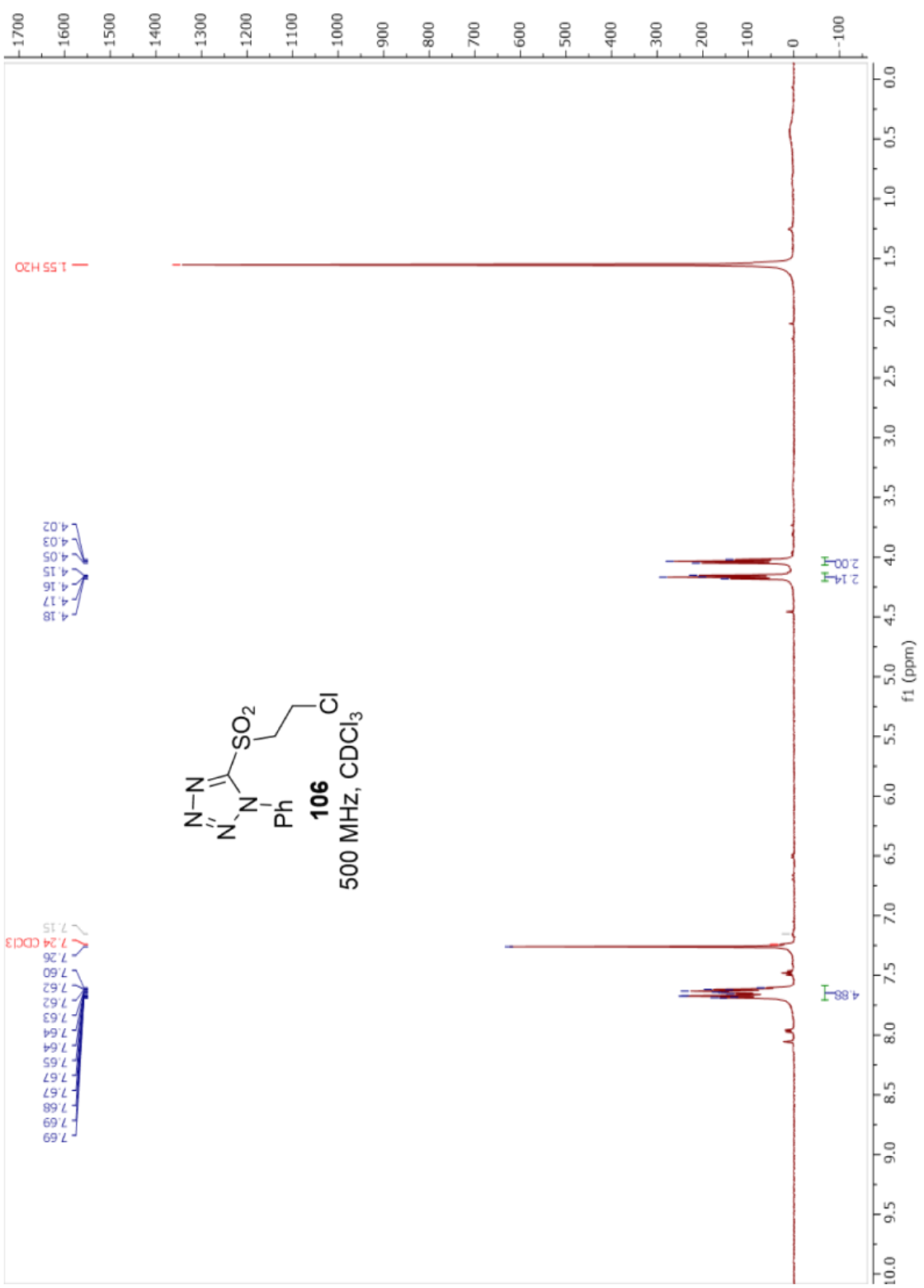
106
500 MHz, CDCl3
Ph
SO2
Cl
1.55 H2O
7.24 CDCl3
f1 (ppm)

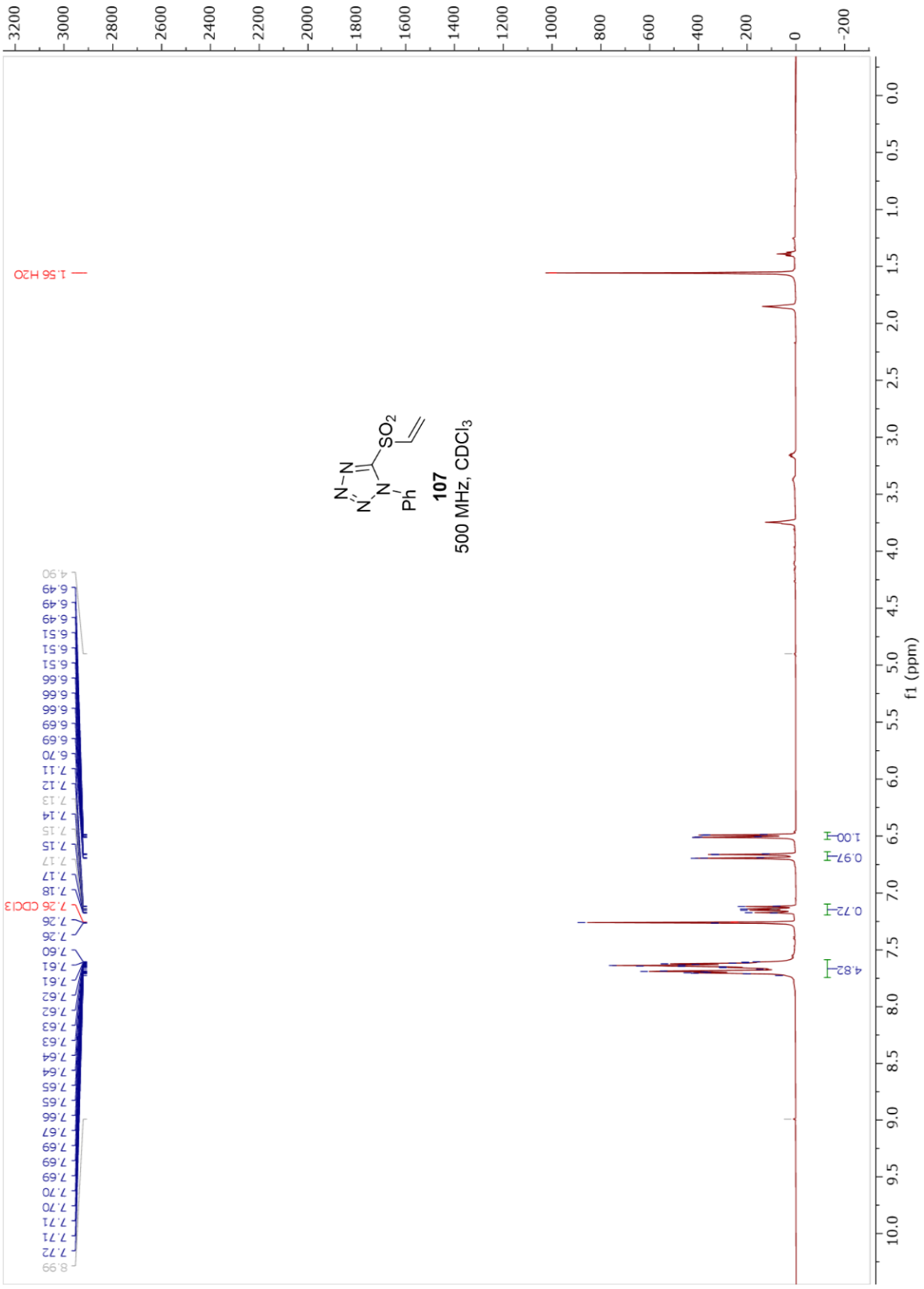
107
500 MHz, CDCl3
Ph
SO2
1.56 H2O
7.26 CDCl3
4.82
0.72
0.97
1.00
f1 (ppm)

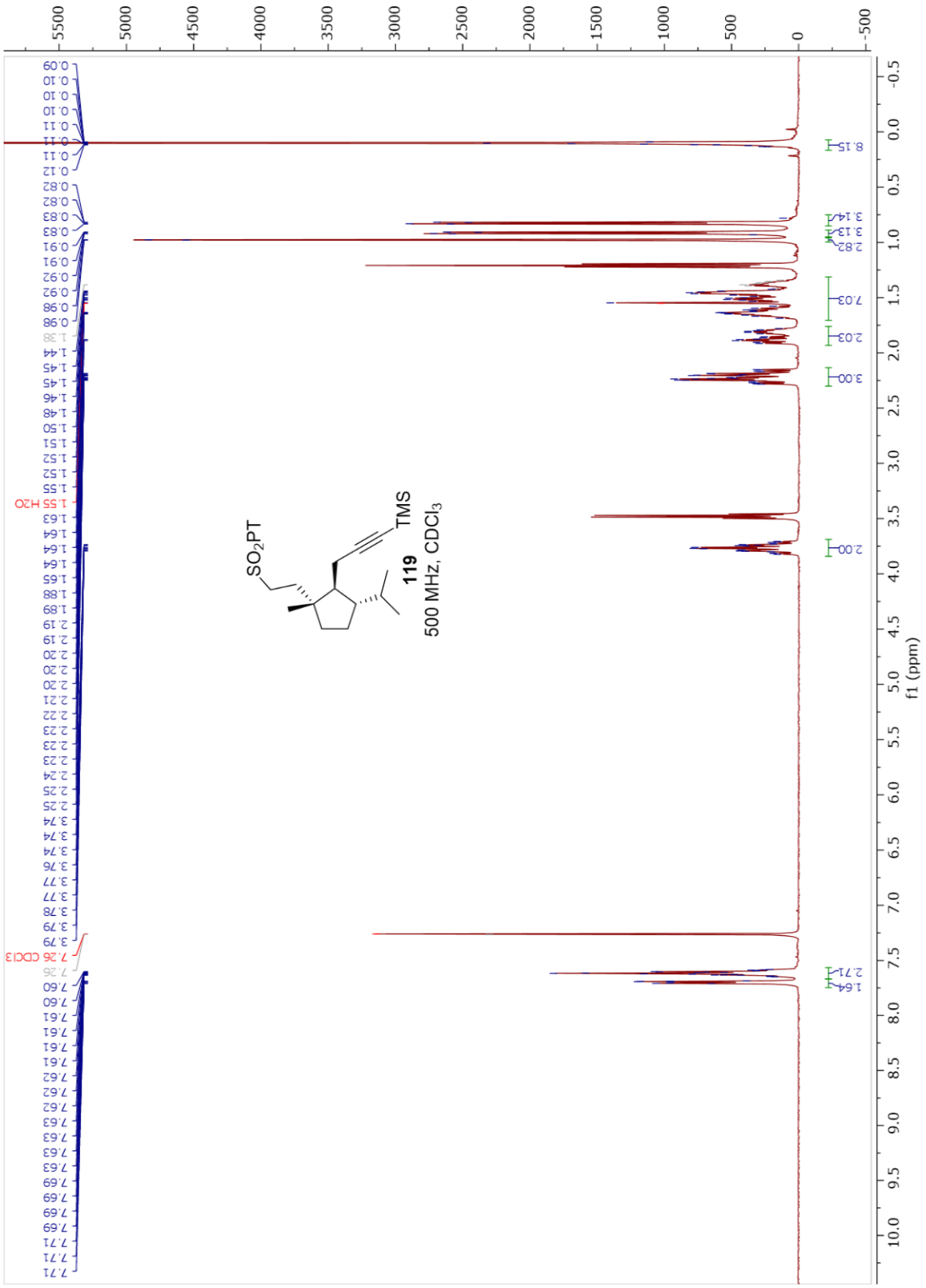
SO2PT
TMS
119
500 MHz, CDCl3
f1 (ppm)
H2O
CDCl3

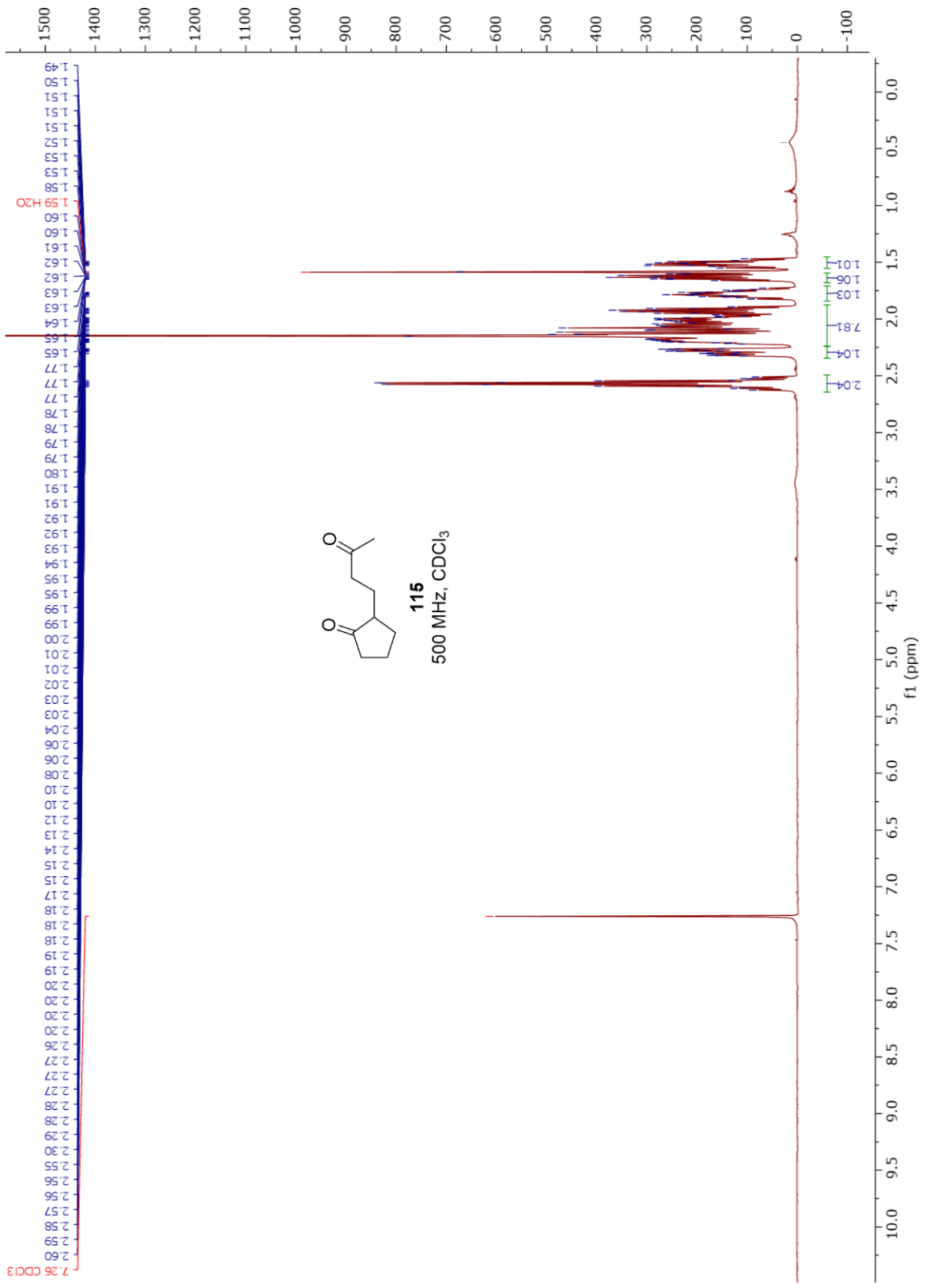
115
500 MHz, CDCl3
f1 (ppm)

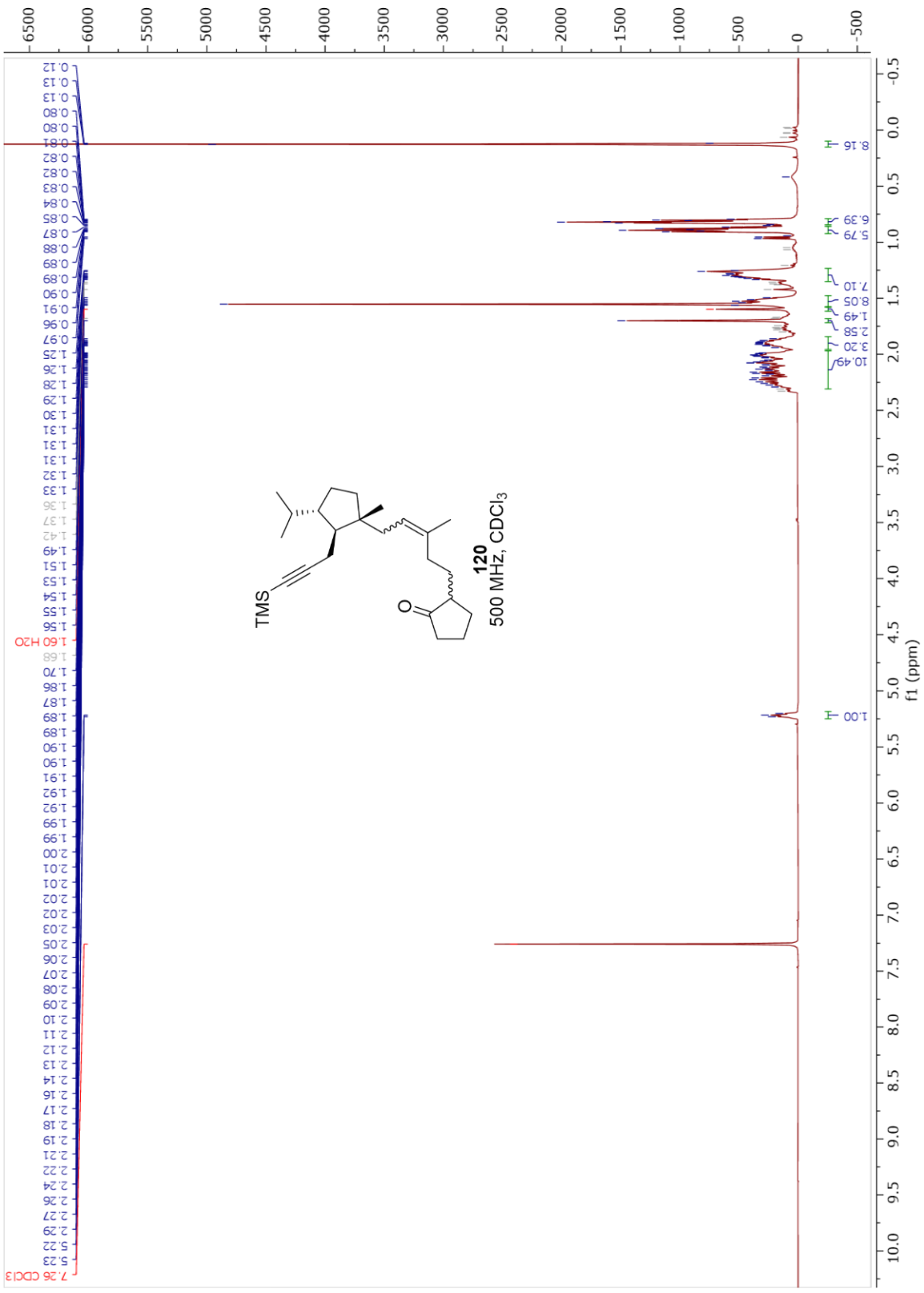
TMS
O
120
500 MHz, CDCl3
f1 (ppm)
8.16
6.39
5.79
7.10
8.05
1.49
2.58
3.20
10.49
1.00
7.26 CDCl3
1.60 H2O

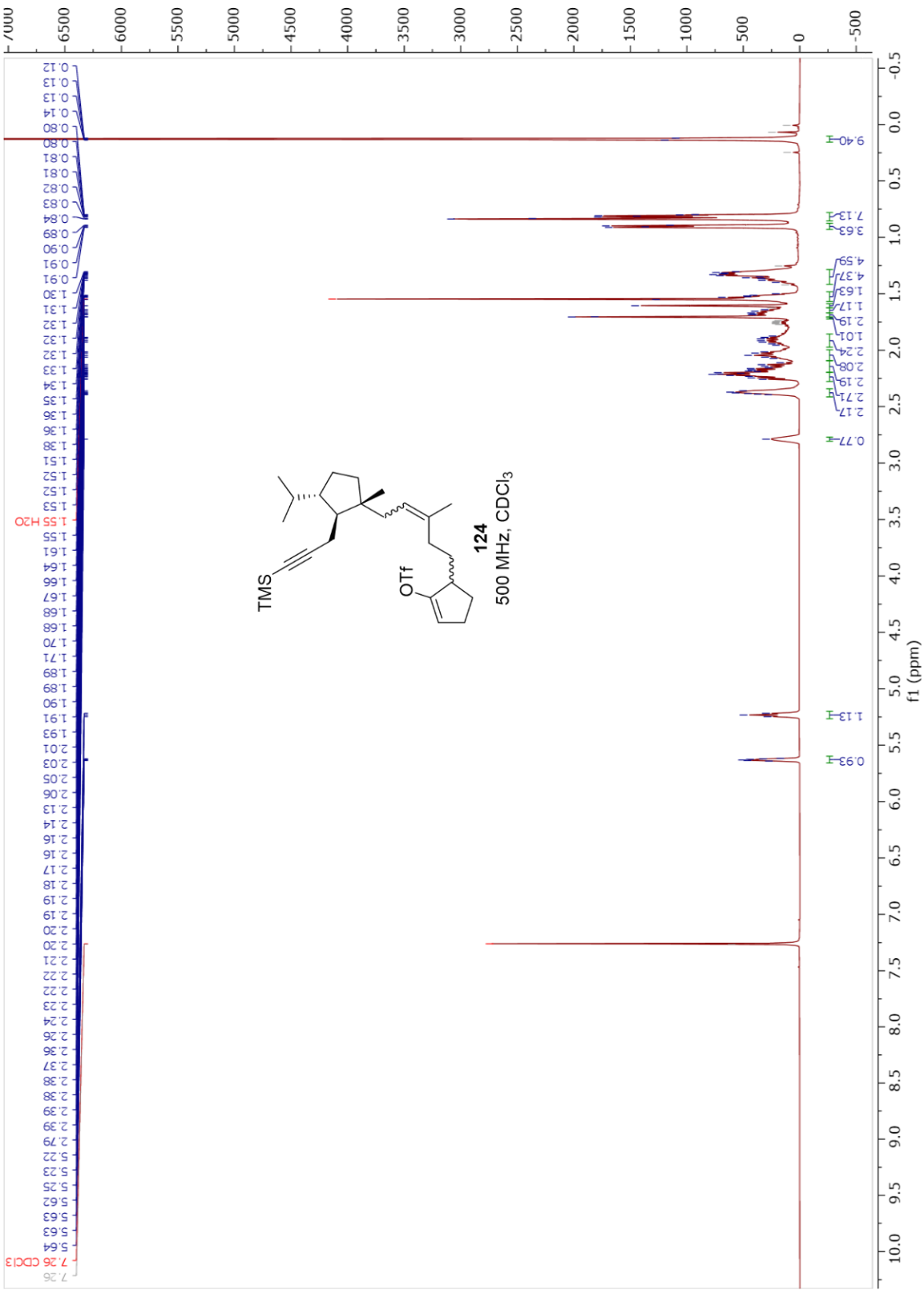
TMS
OTf
124
500 MHz, CDCl3
f1 (ppm)

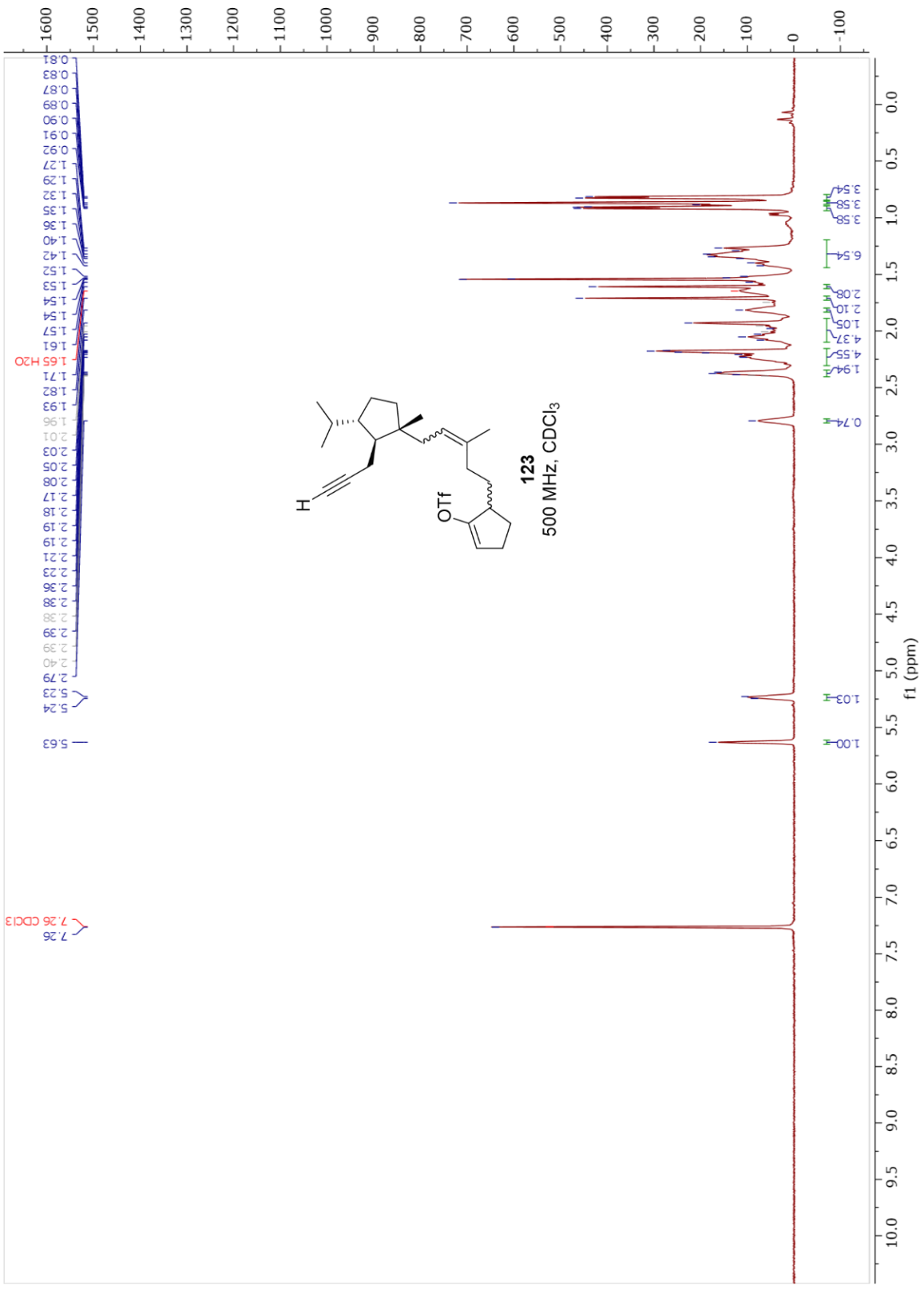
123
500 MHz, CDCl3
H
OTf
f1 (ppm)
7.26 CDCl3
1.65 H2O

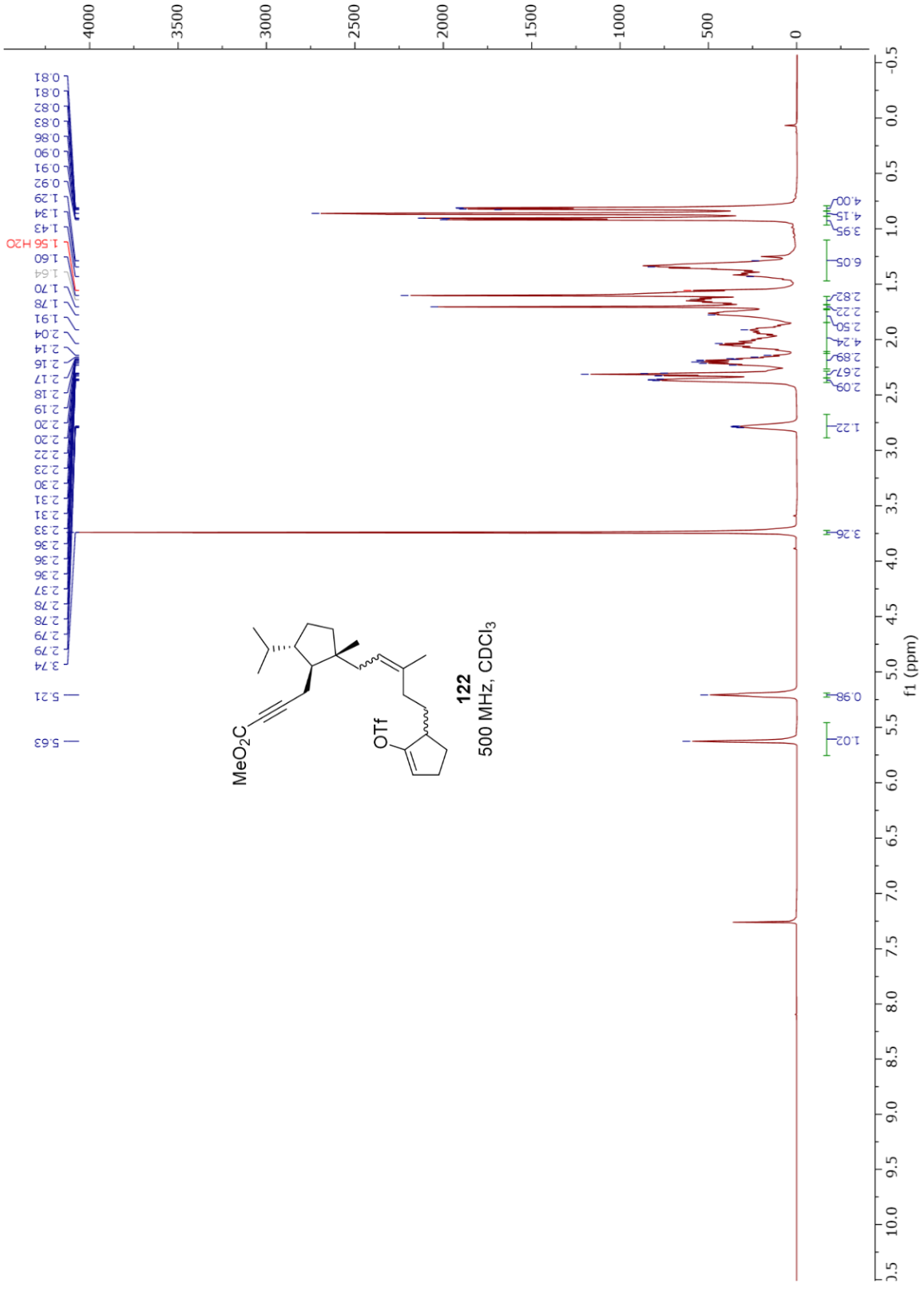
122
500 MHz, CDCl3
MeO2C
OTf
f1 (ppm)
1.56 H2O

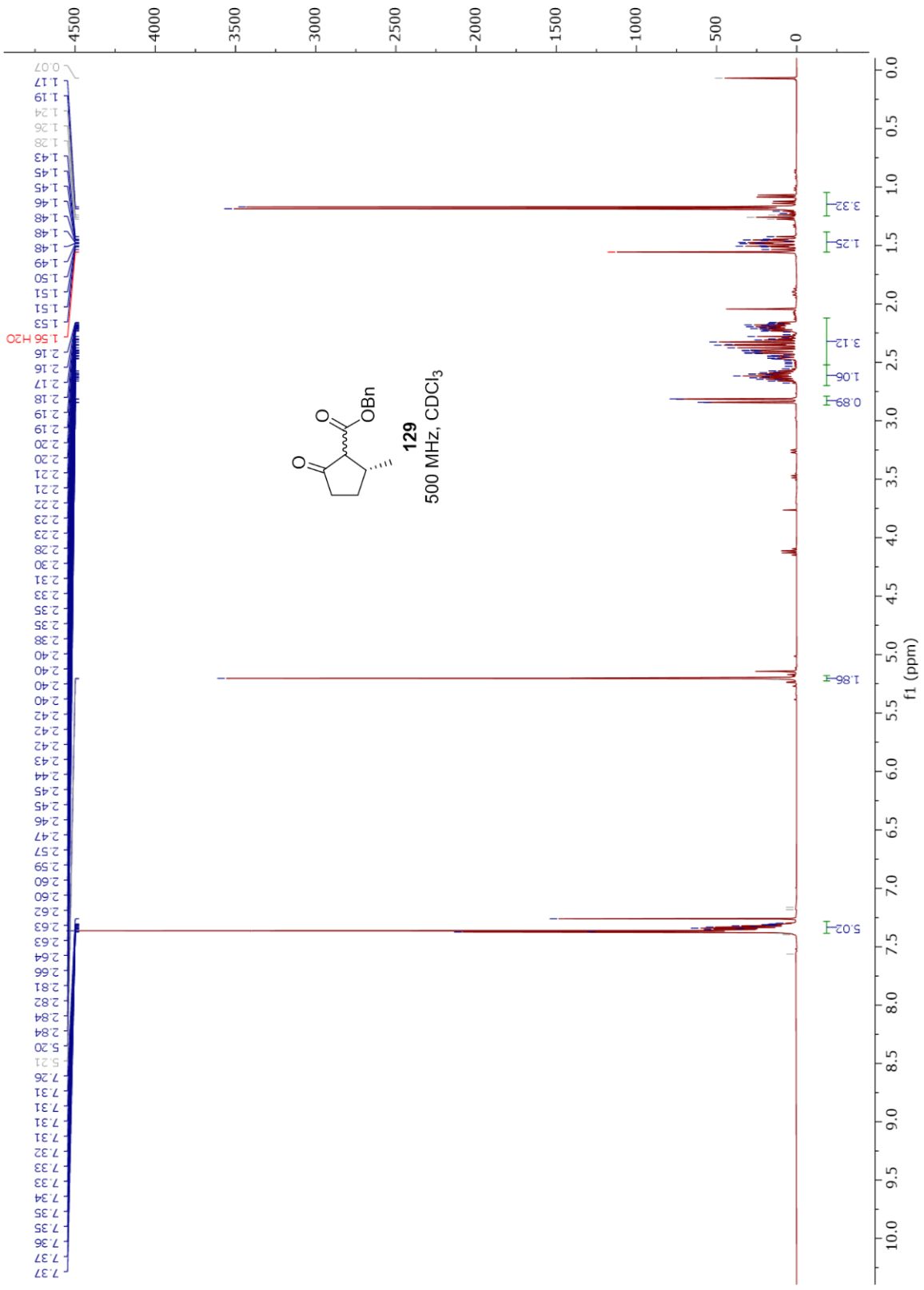
OBn
O
O
129
500 MHz, CDCl3
H2O
5.02
1.86
3.32
1.25
3.12
1.06
0.89
f1 (ppm)

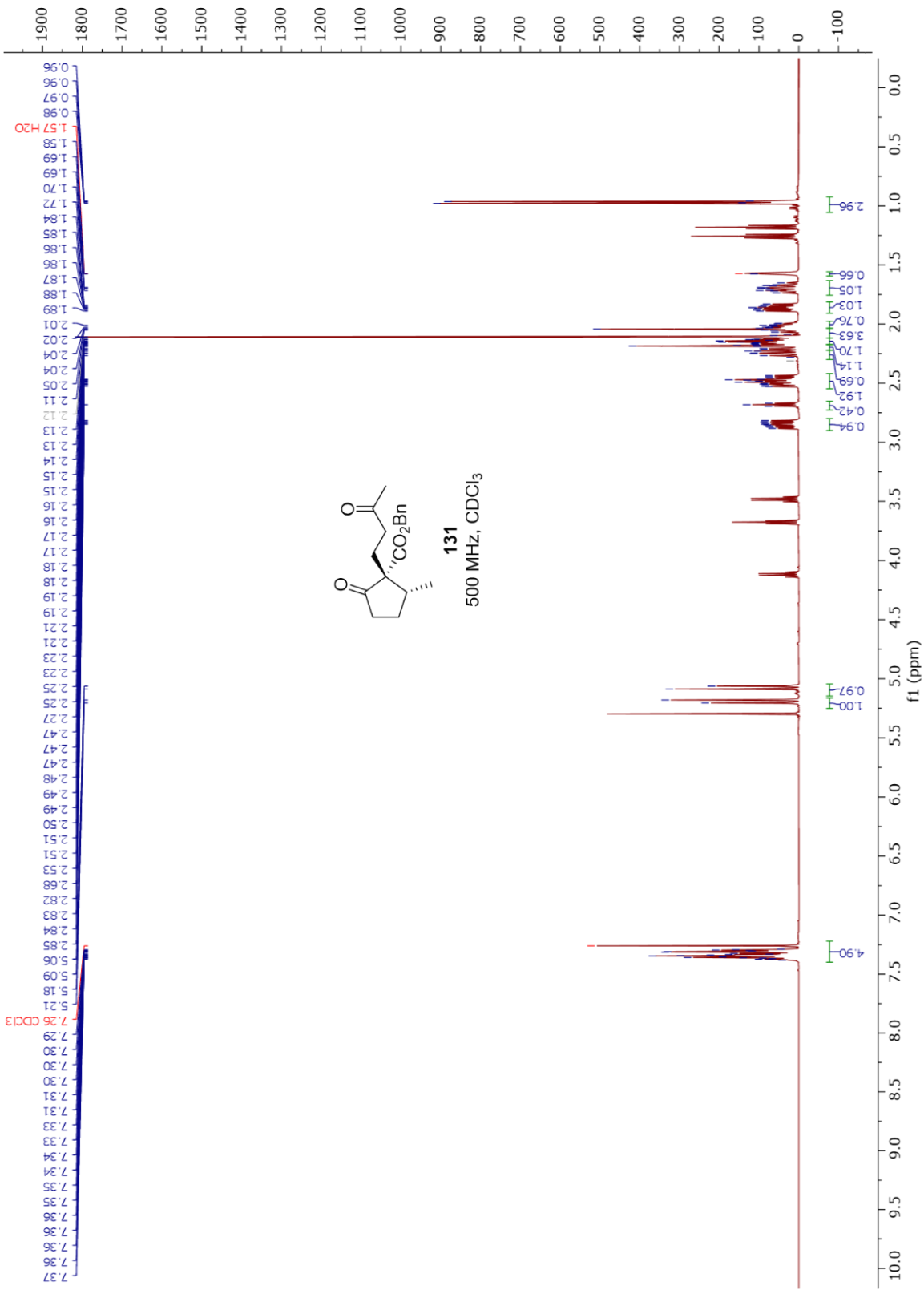
131
500 MHz, CDCl3
CO2Bn
f1 (ppm)

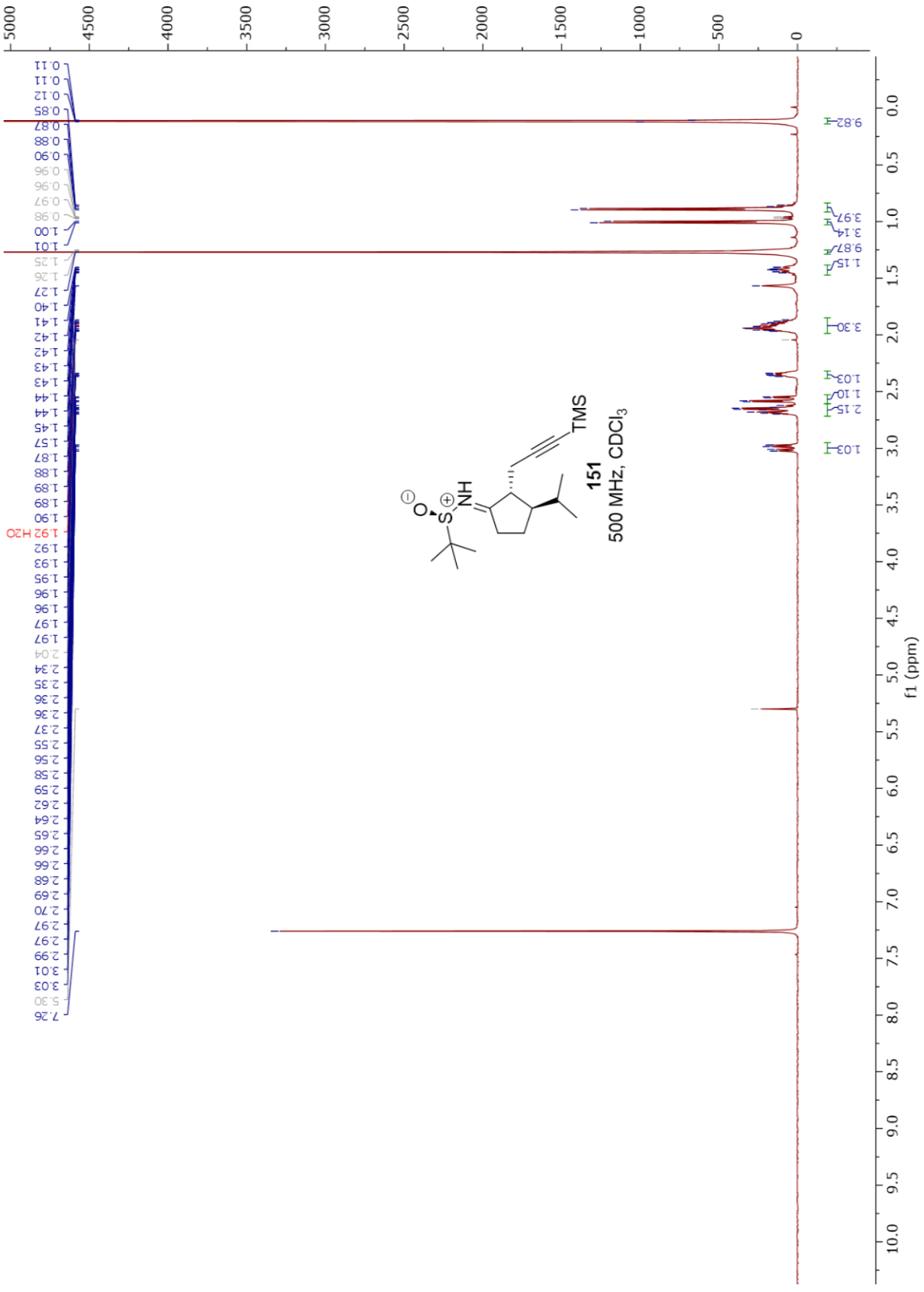
TMS
151
500 MHz, CDCl3
f1 (ppm)

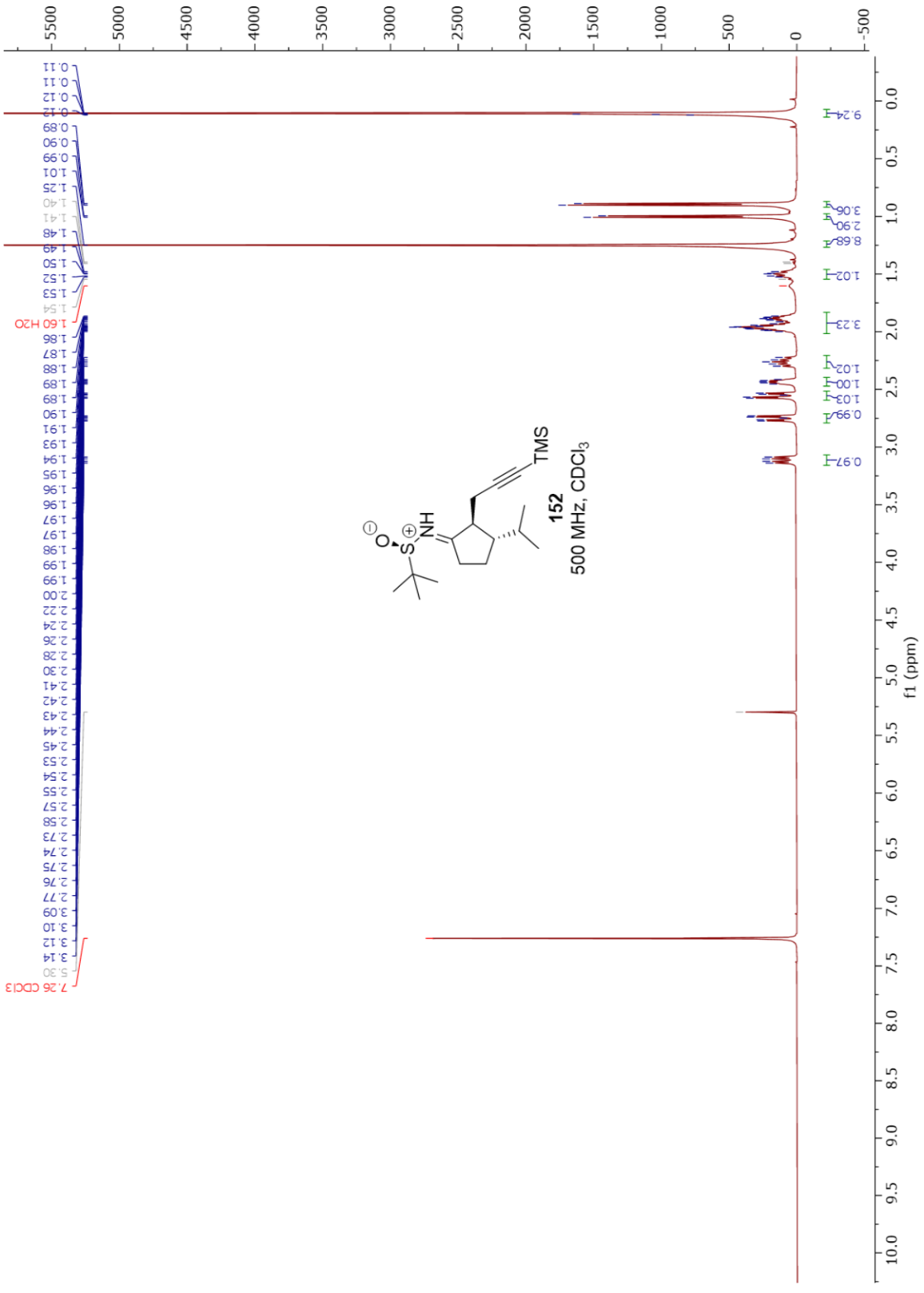
TMS
152
500 MHz, CDCl3
f1 (ppm)
1.60 H2O
7.26 CDCl3

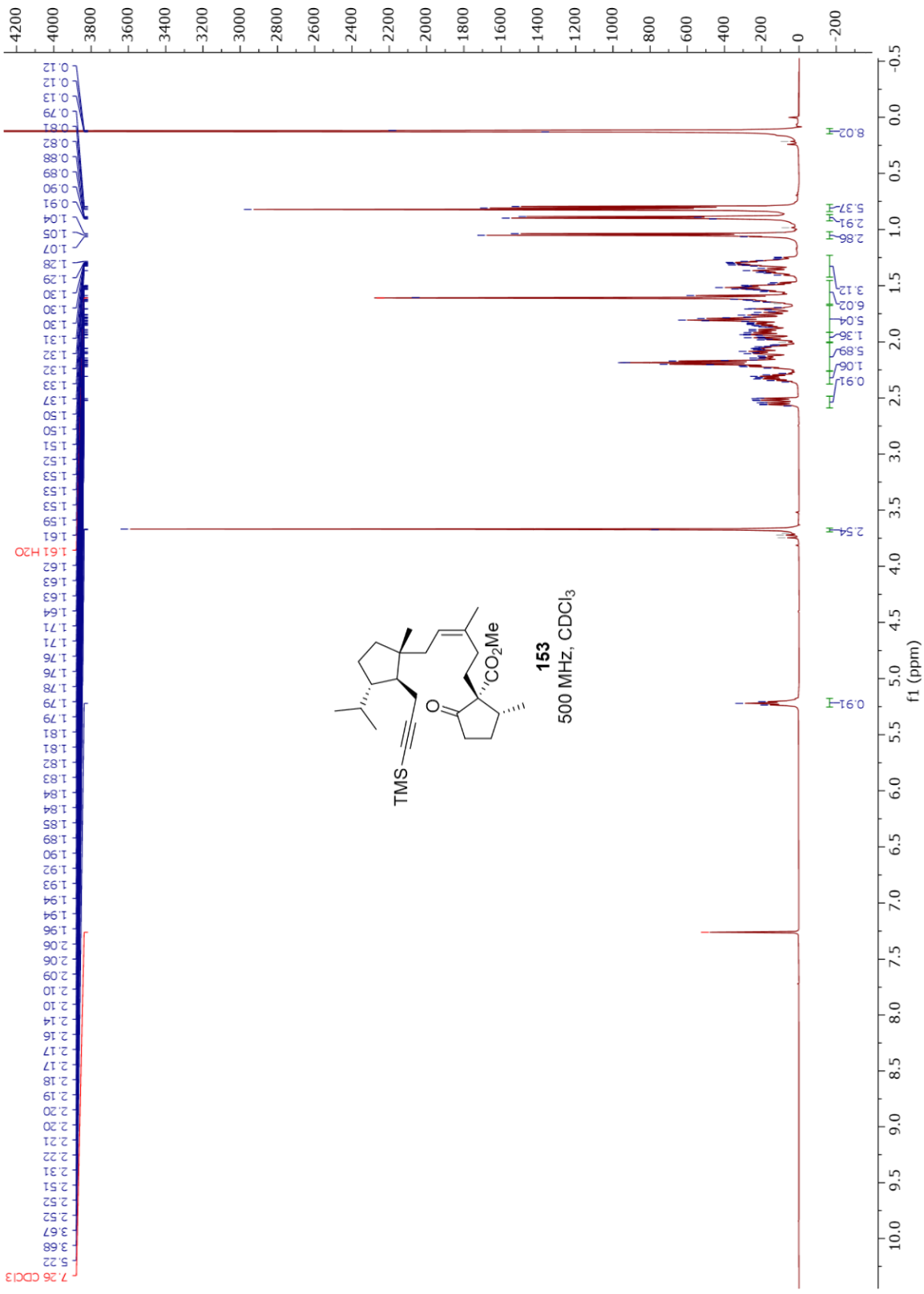
TMS
O
CO2Me
153
500 MHz, CDCl3
f1 (ppm)

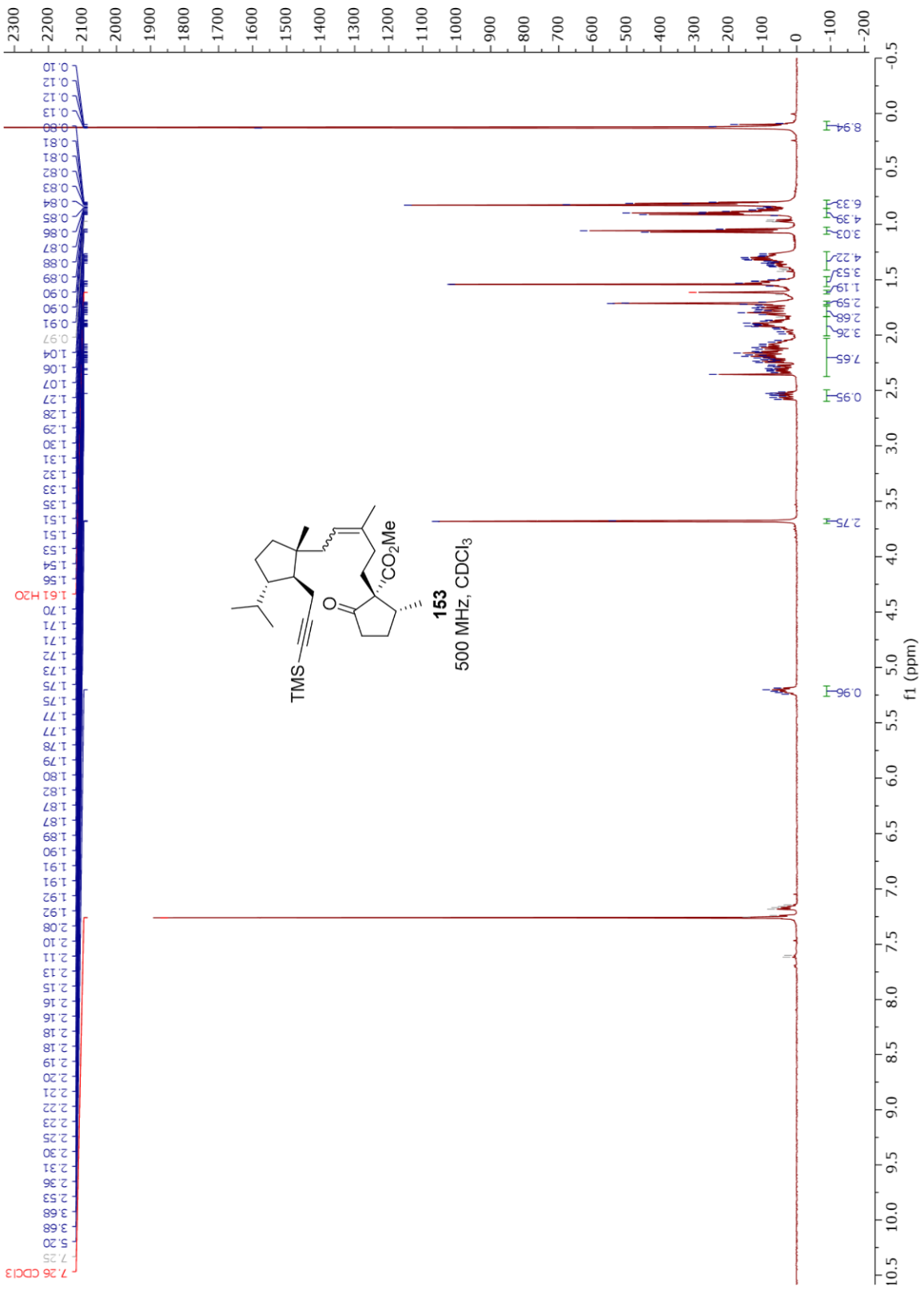
TMS
O
CO2Me
153
500 MHz, CDCl3
f1 (ppm)

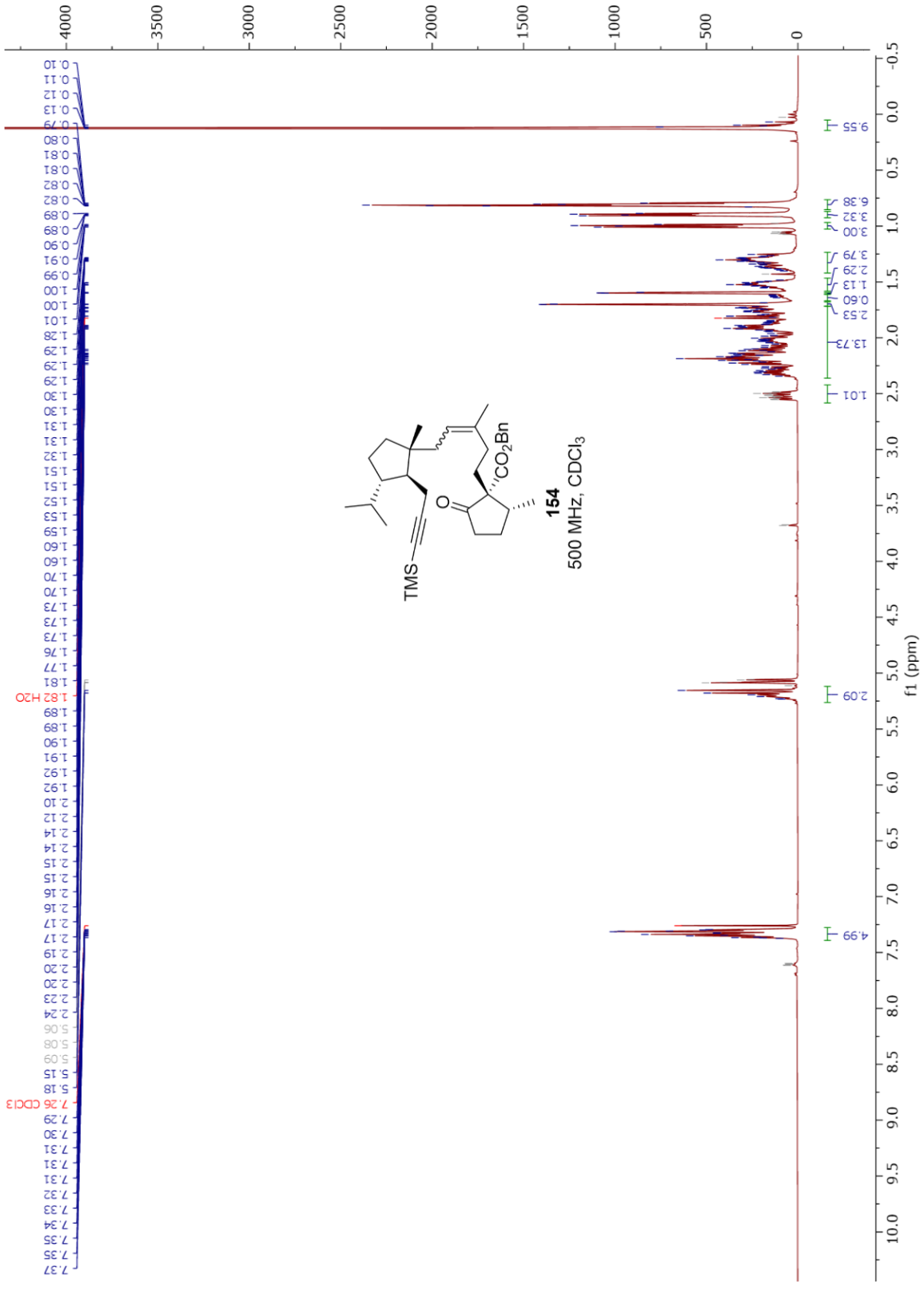
TMS
CO2Bn
O
154
500 MHz, CDCl3
f1 (ppm)
1.82 H2O
7.26 CDCl3

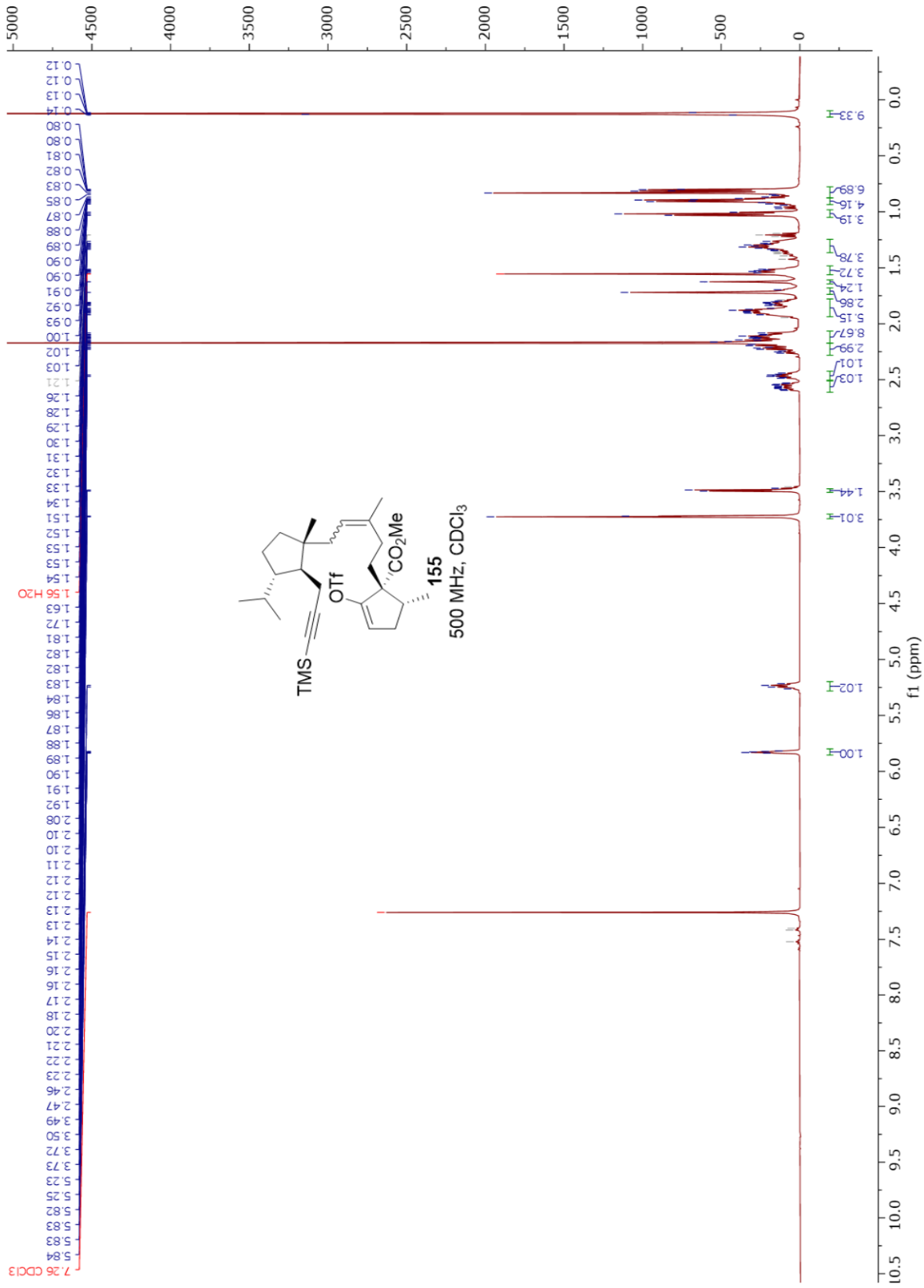
TMS
OTf
CO2Me
155
500 MHz, CDCl3
f1 (ppm)

4500
4000
3500
3000
2500
2000
1500
1000
500
0
-74.01
-74.06
TMS
OTf
CO2Me
155
480 MHz, CDCl3
-5
-10
-15
-20
-25
-30
-35
-40
-45
-50
-55
-60
-65
-70
-75
-80
-85
-90
-95
f1 (ppm)

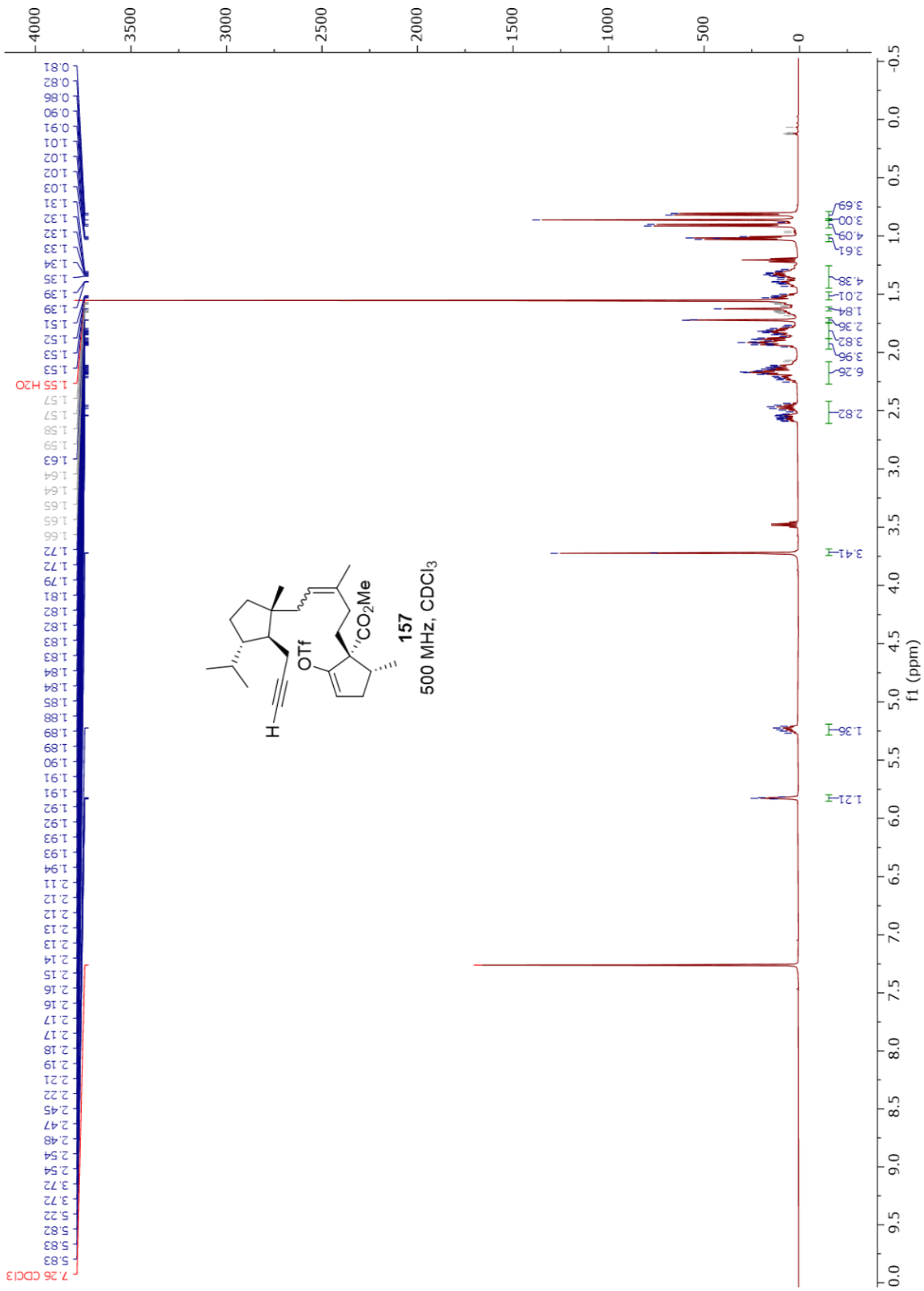
OTf
CO2Me
H
157
500 MHz, CDCl3
f1 (ppm)

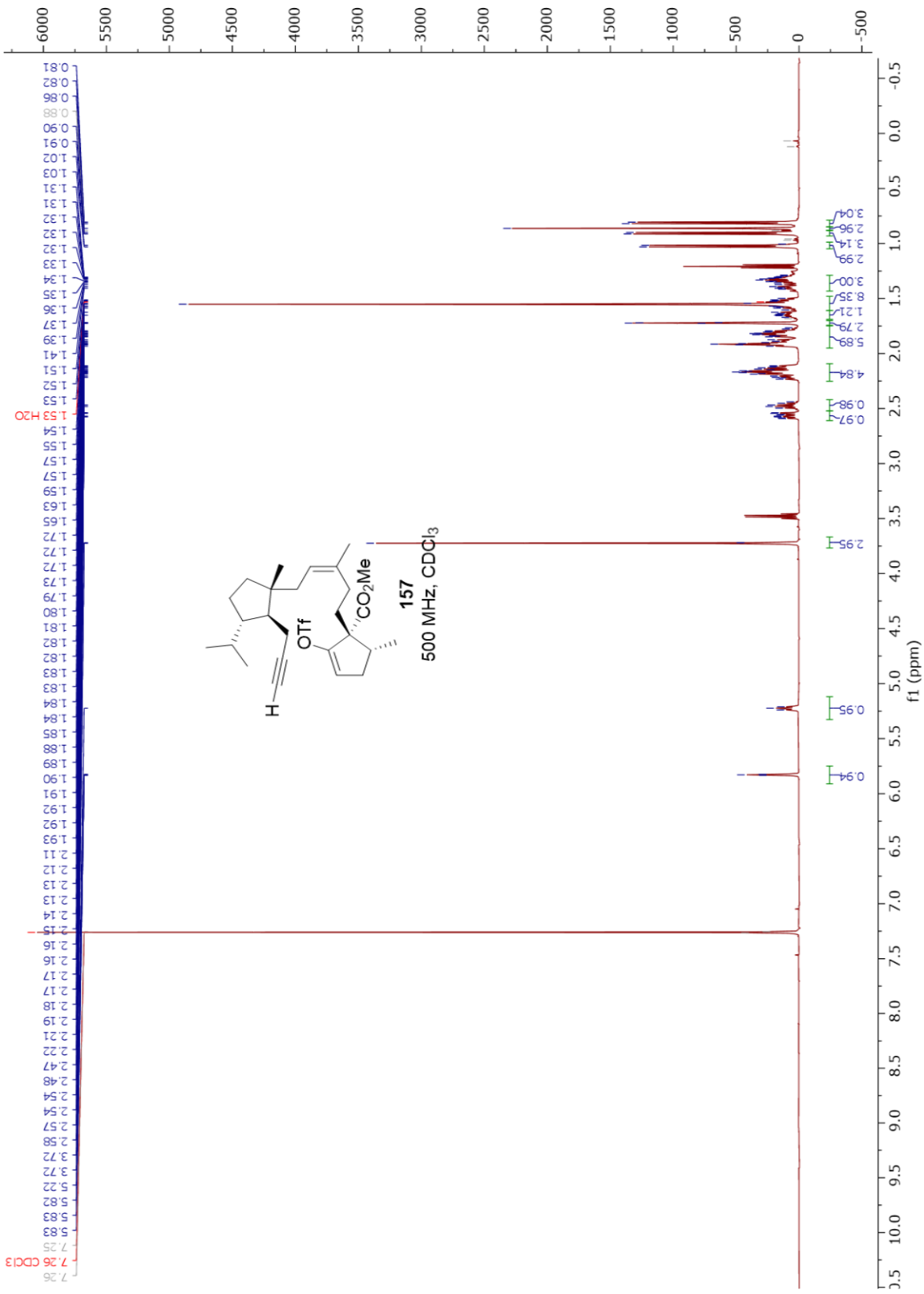
157
500 MHz, CDCl3
OTf
CO2Me
H
f1 (ppm)
7.26 CDCl3
1.53 H2O

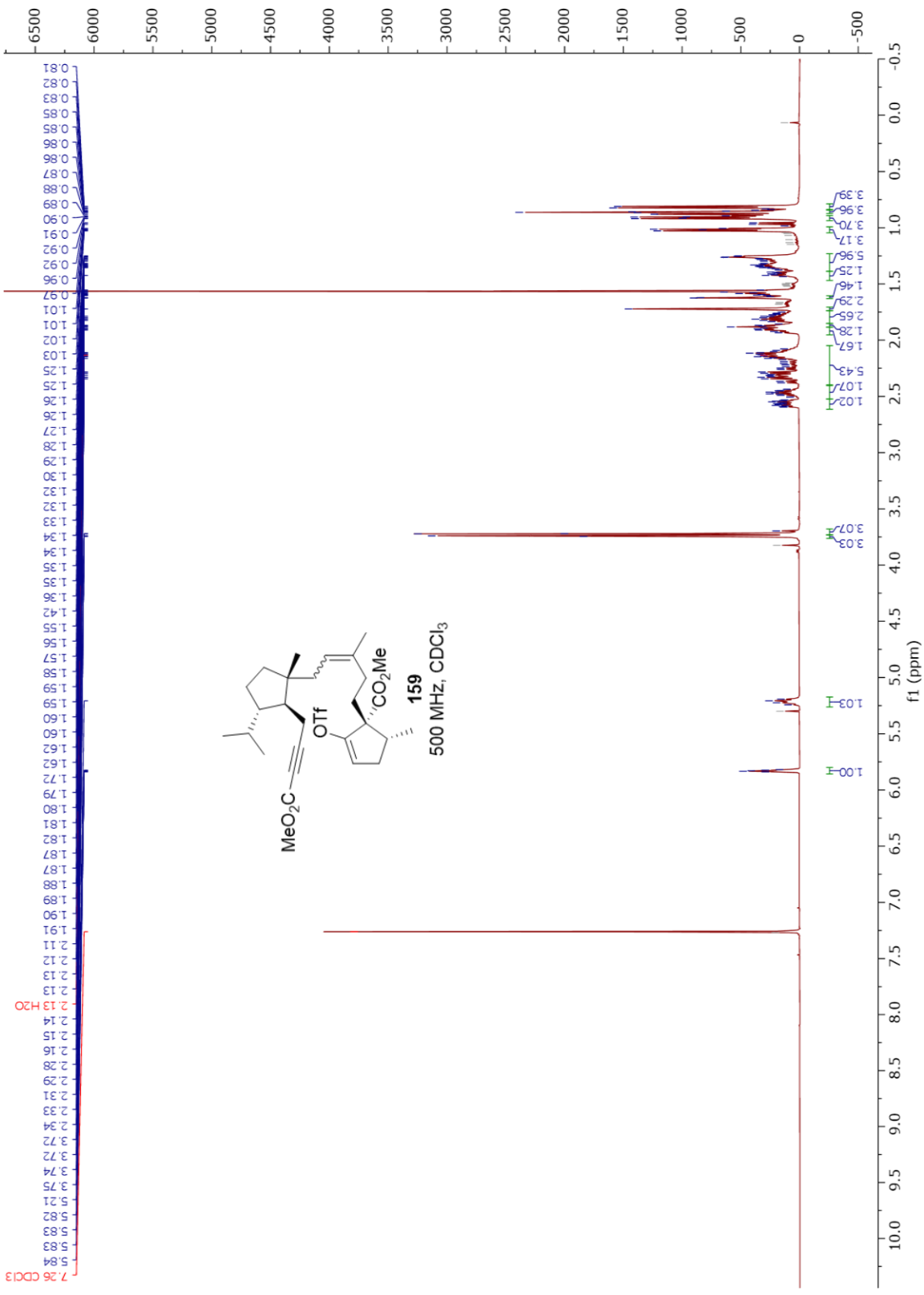
MeO2C
OTf
CO2Me
159
500 MHz, CDCl3
f1 (ppm)

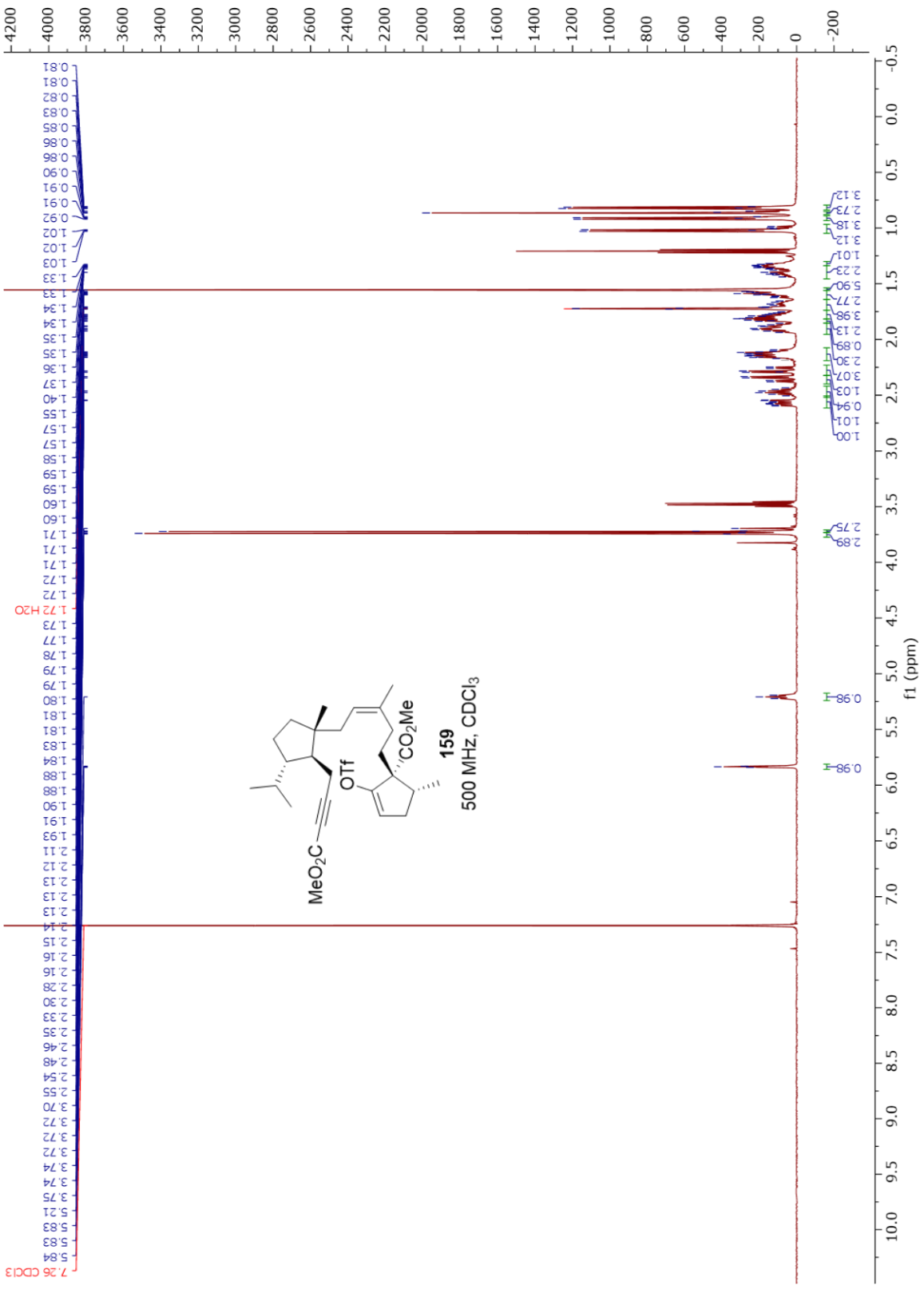
MeO2C
OTf
CO2Me
159
500 MHz, CDCl3
f1 (ppm)

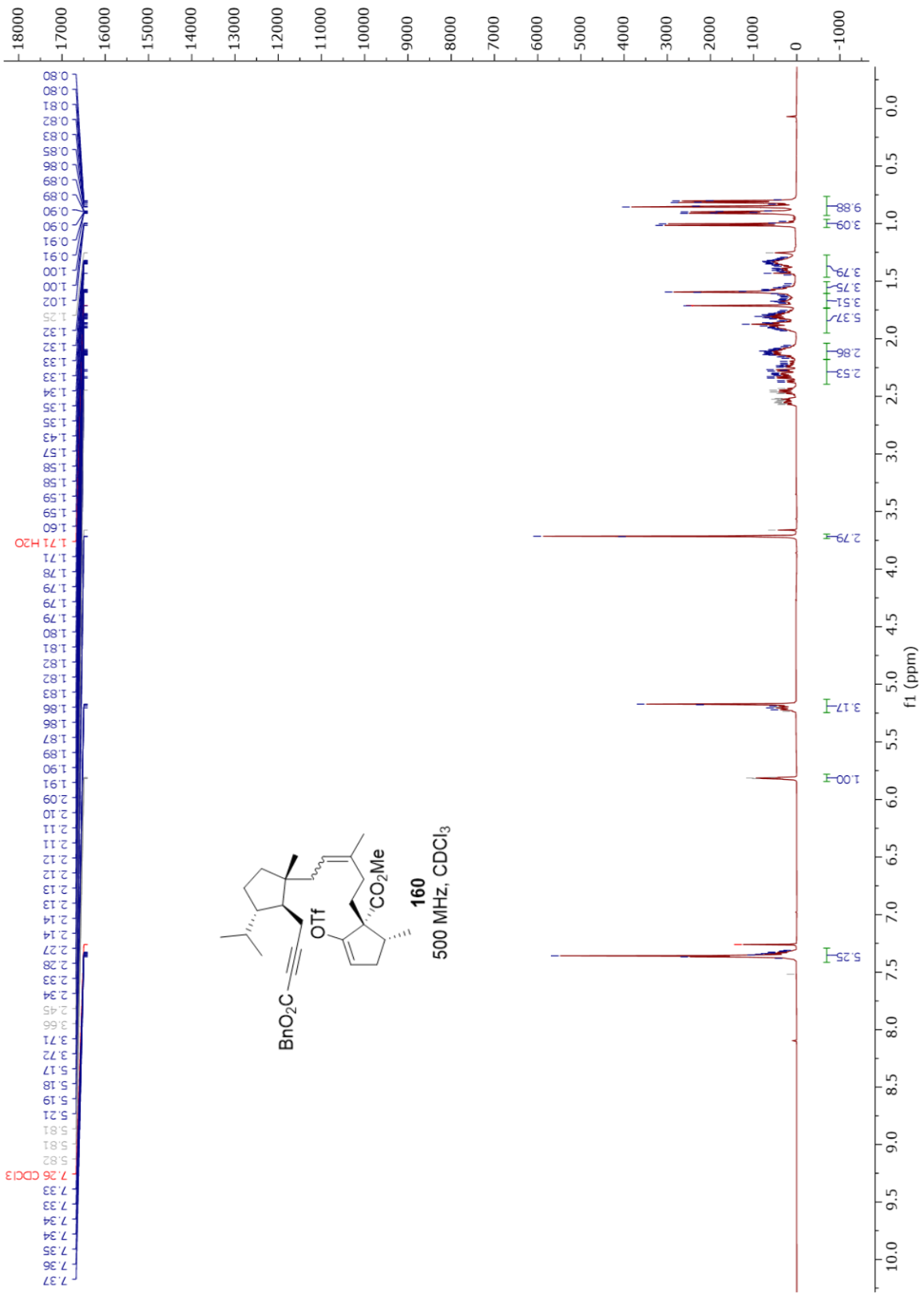
BnO2C
OTf
CO2Me
160
500 MHz, CDCl3
f1 (ppm)
H2O
CDCl3

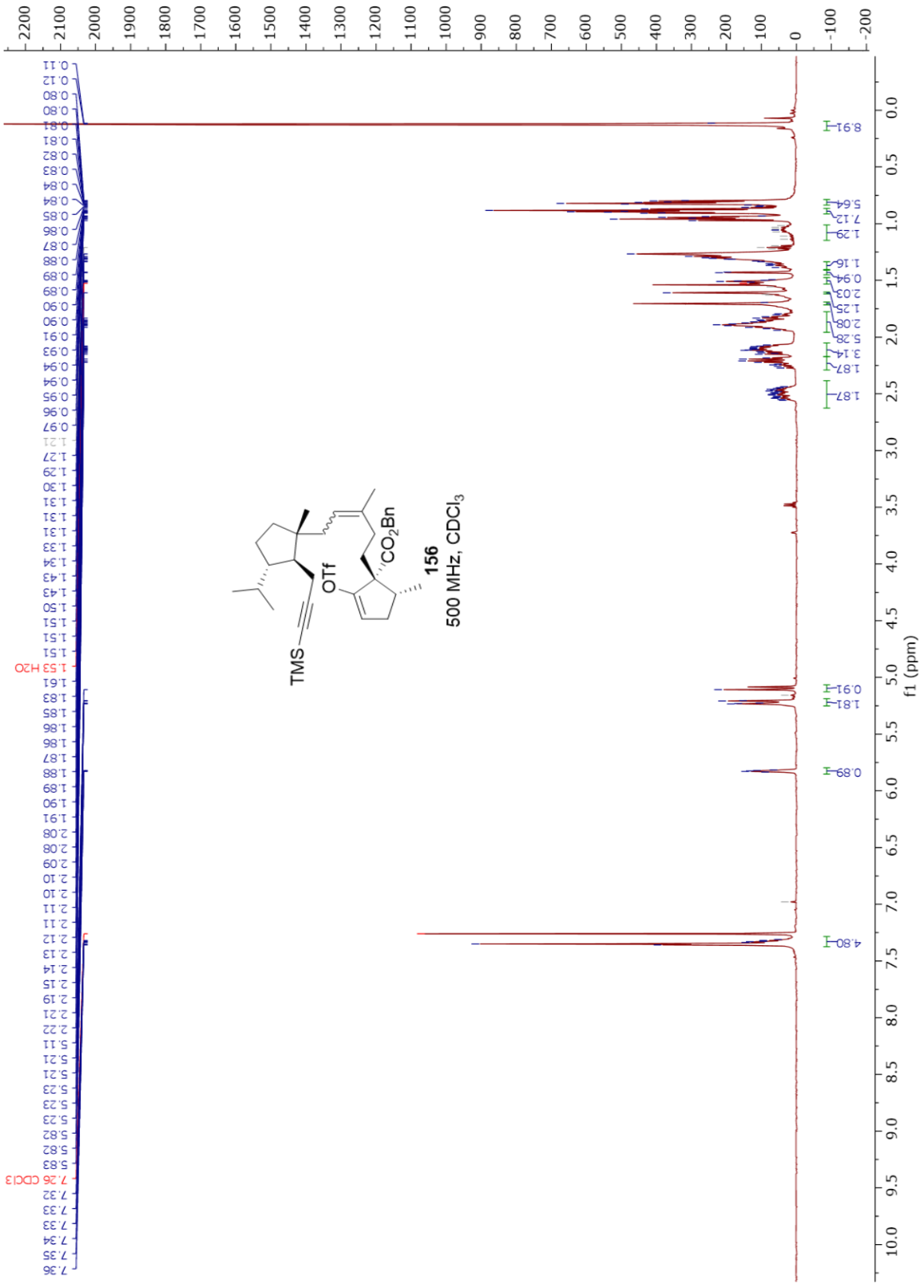
TMS
OTf
CO2Bn
156
500 MHz, CDCl3
f1 (ppm)
CDCl3
H2O

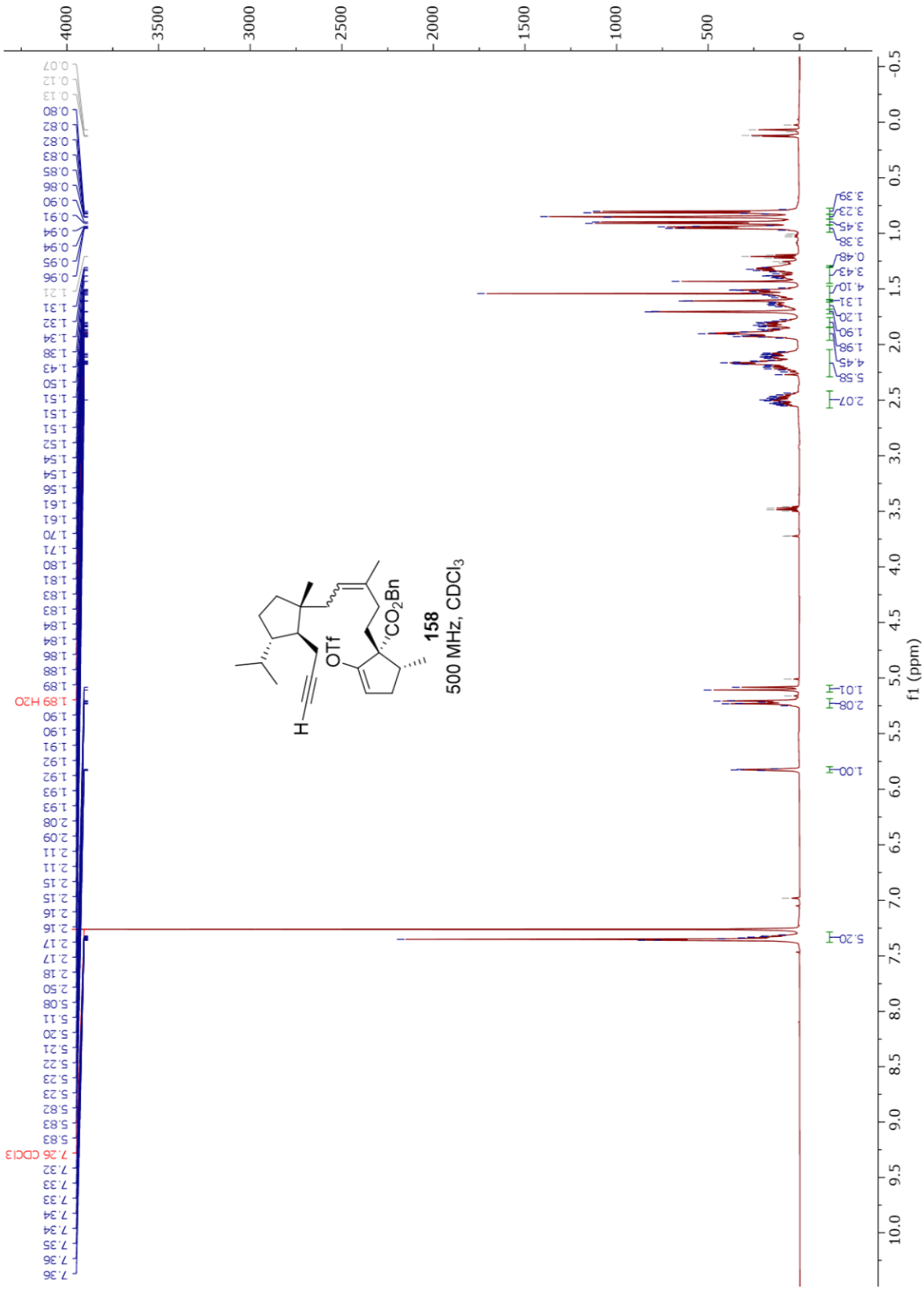
158
500 MHz, CDCl3
OTf
CO2Bn
H
H2O
CDCl3
f1 (ppm)

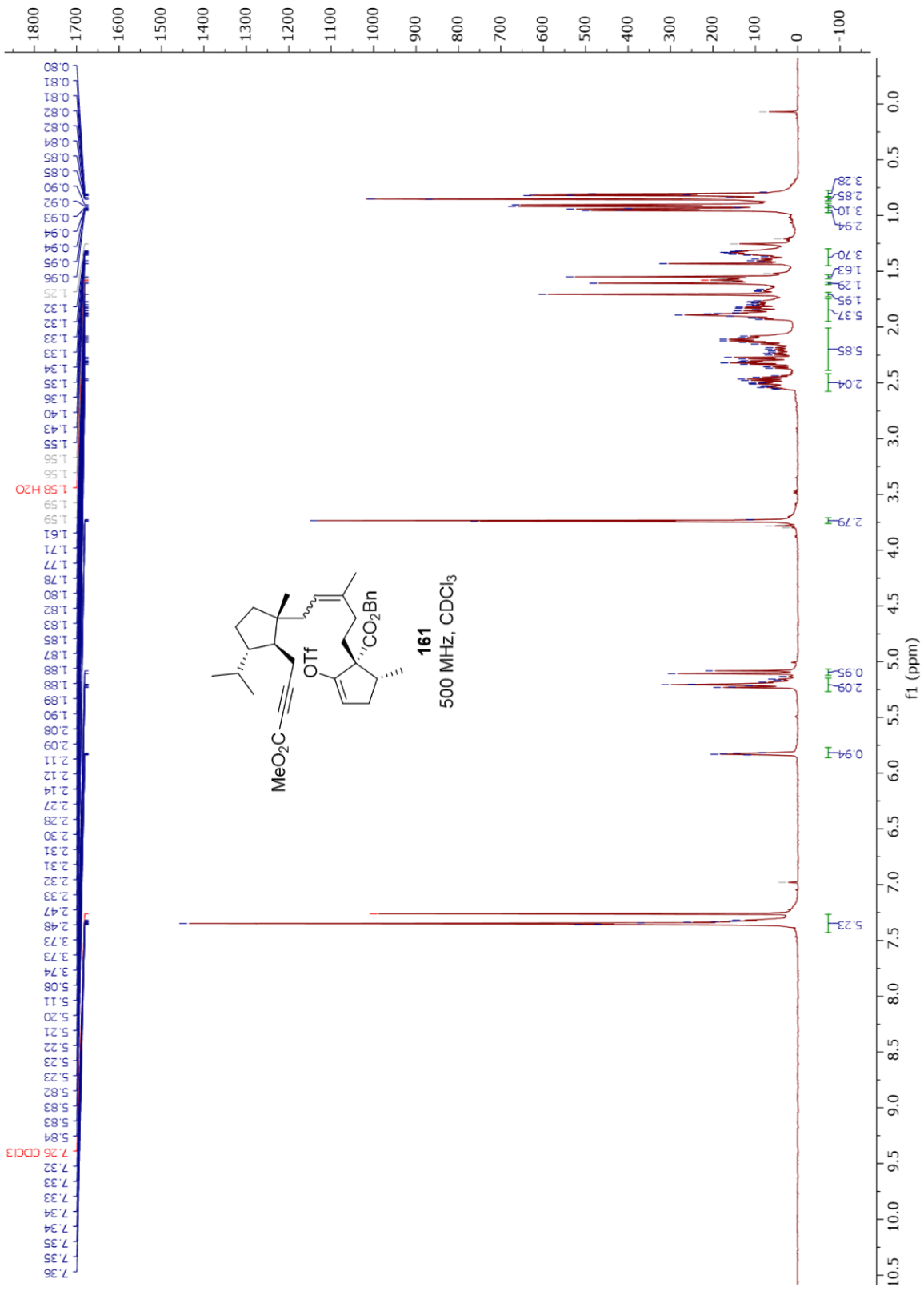
MeO2C
OTf
CO2Bn
161
500 MHz, CDCl3
f1 (ppm)

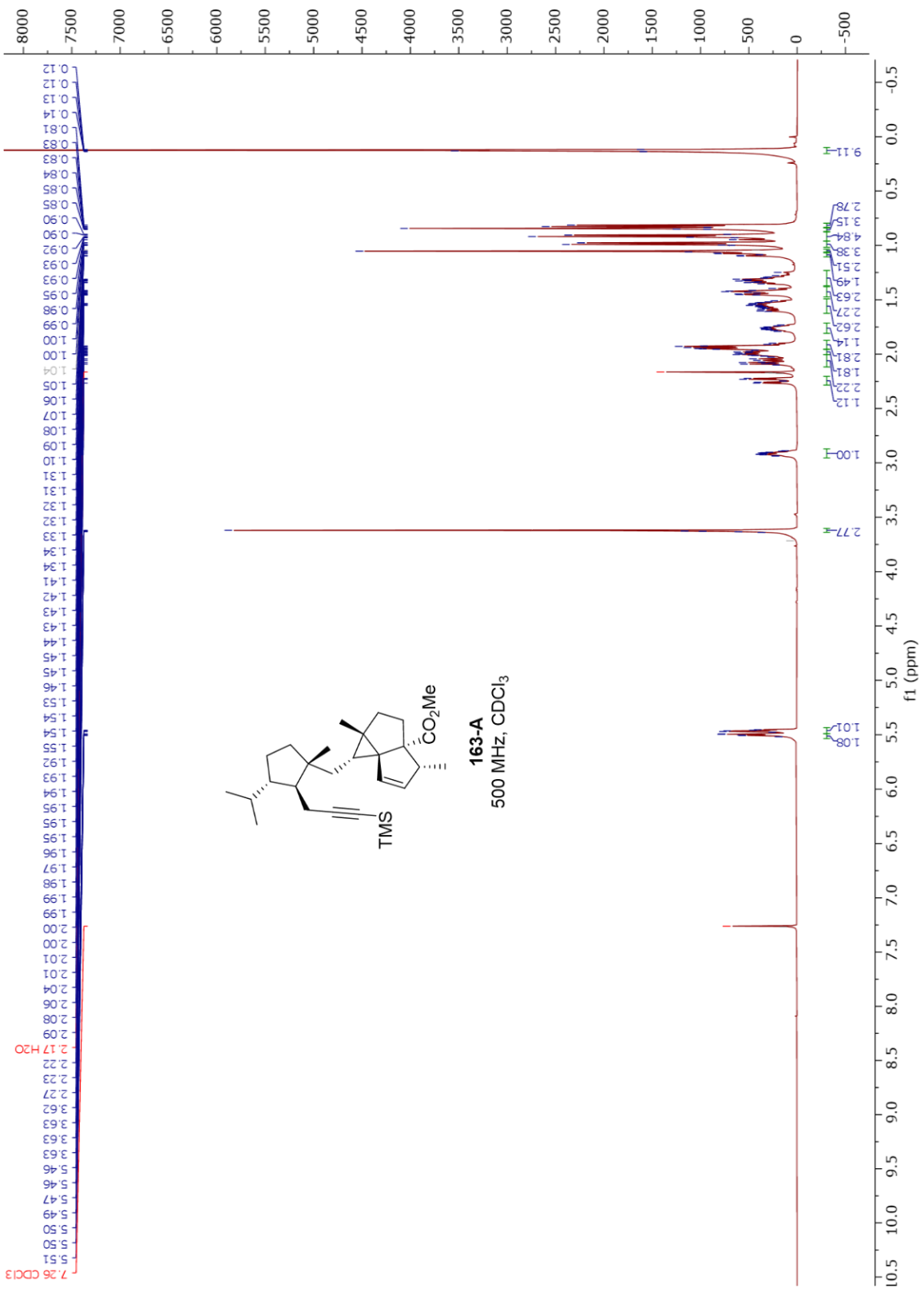
TMS
CO2Me
163-A
500 MHz, CDCl3
f1 (ppm)

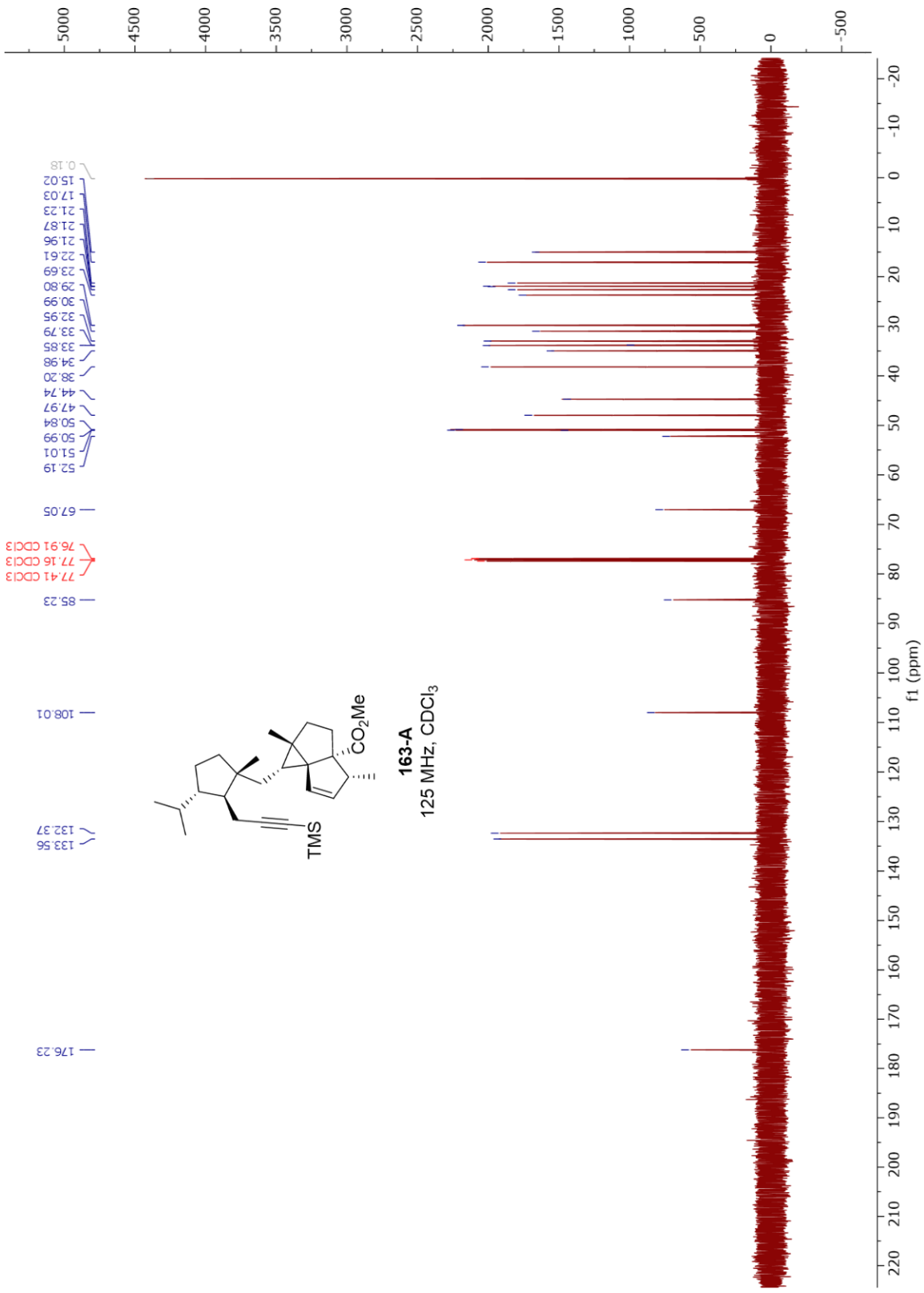
163-A
125 MHz, CDCl3
TMS
CO2Me
f1 (ppm)

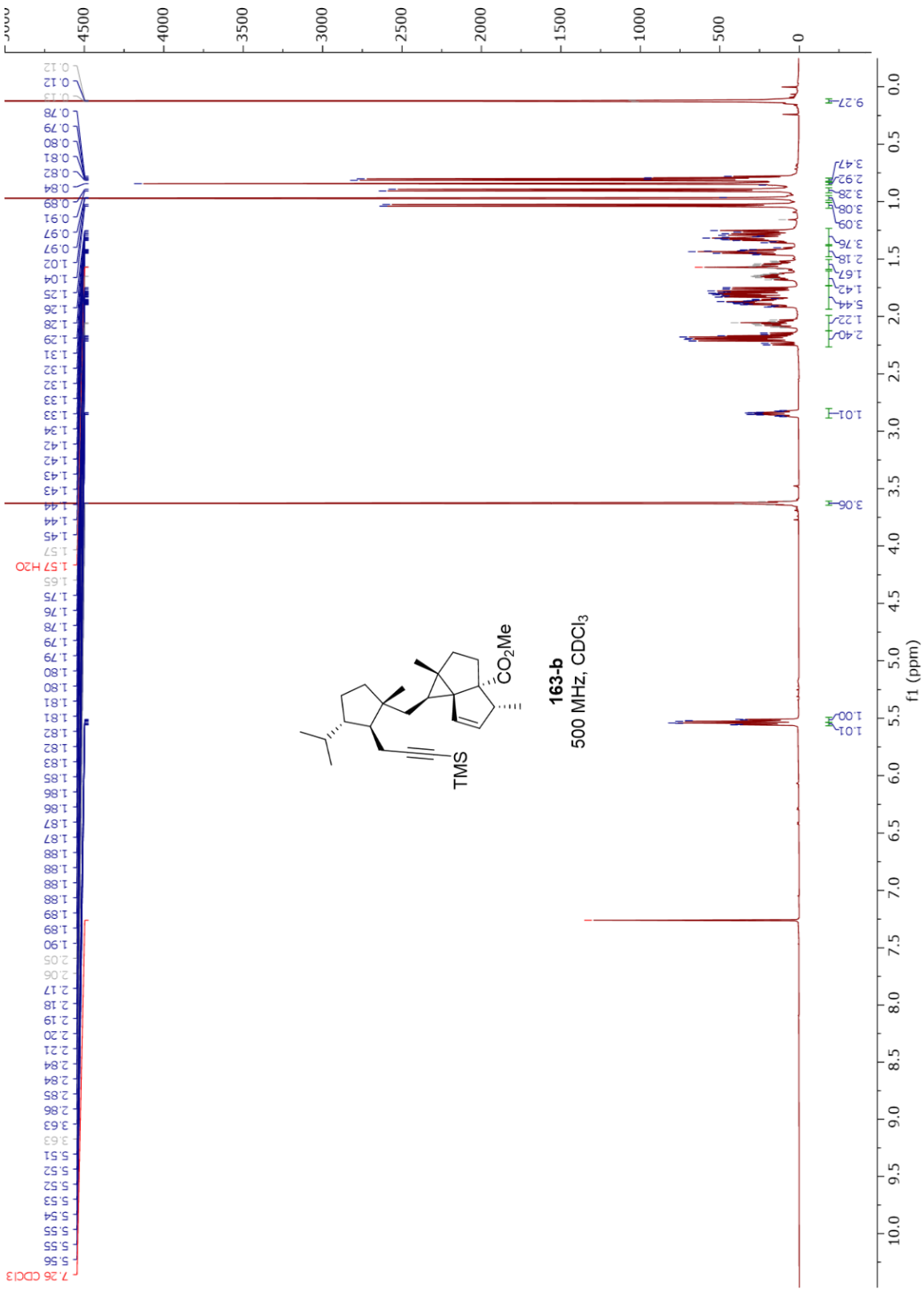
163-b
500 MHz, CDCl3
TMS
CO2Me
f1 (ppm)
7.26 CDCl3
1.57 H2O

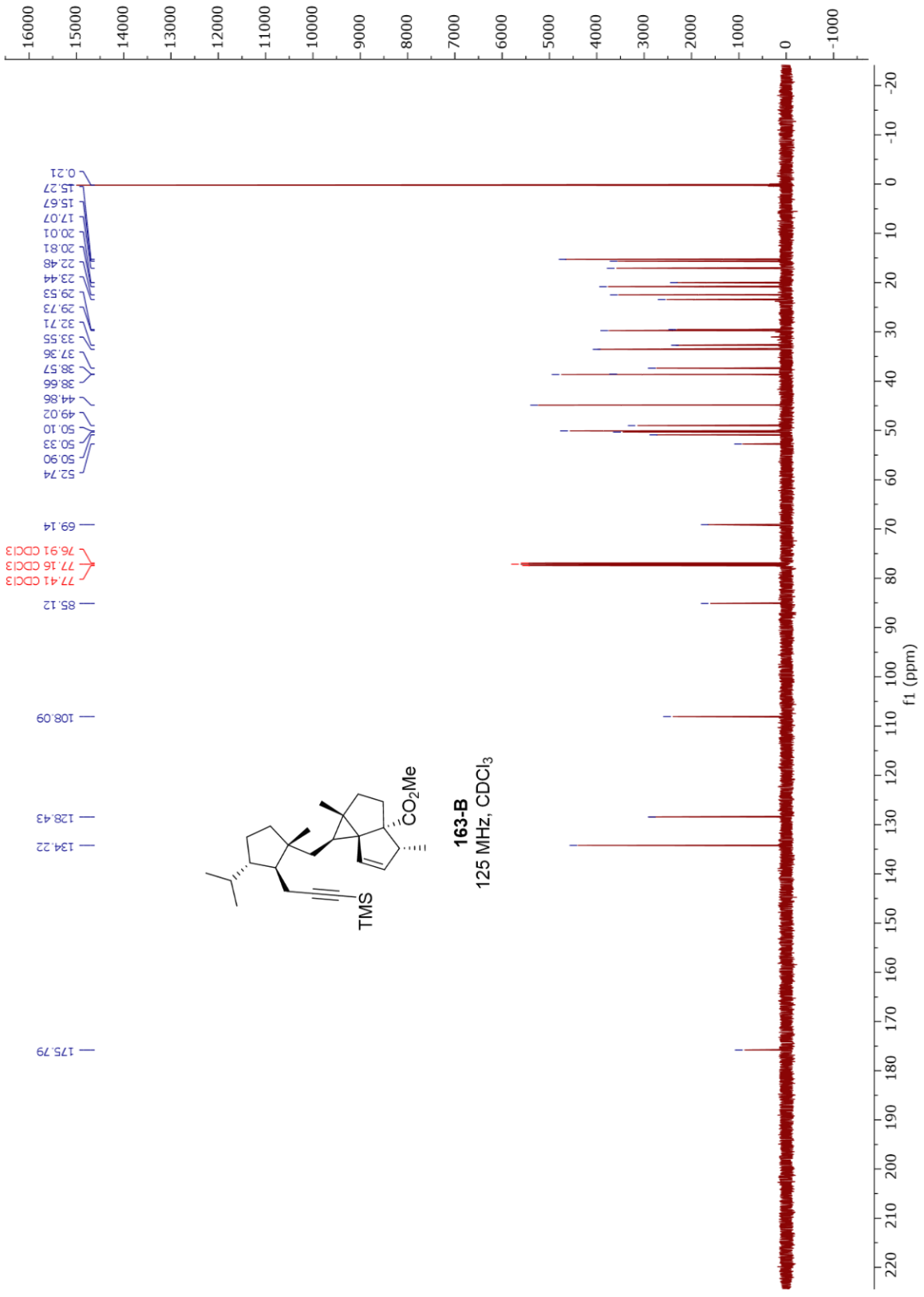
0.21
15.27
15.67
17.07
20.01
20.81
22.48
23.44
29.53
29.73
32.71
33.55
37.36
38.57
38.66
44.86
49.02
50.10
50.33
50.90
52.74
69.14
76.91 CDCl3
77.16 CDCl3
77.41 CDCl3
85.12
108.09
128.43
134.22
175.79
TMS
CO2Me
163-B
125 MHz, CDCl3
f1 (ppm)

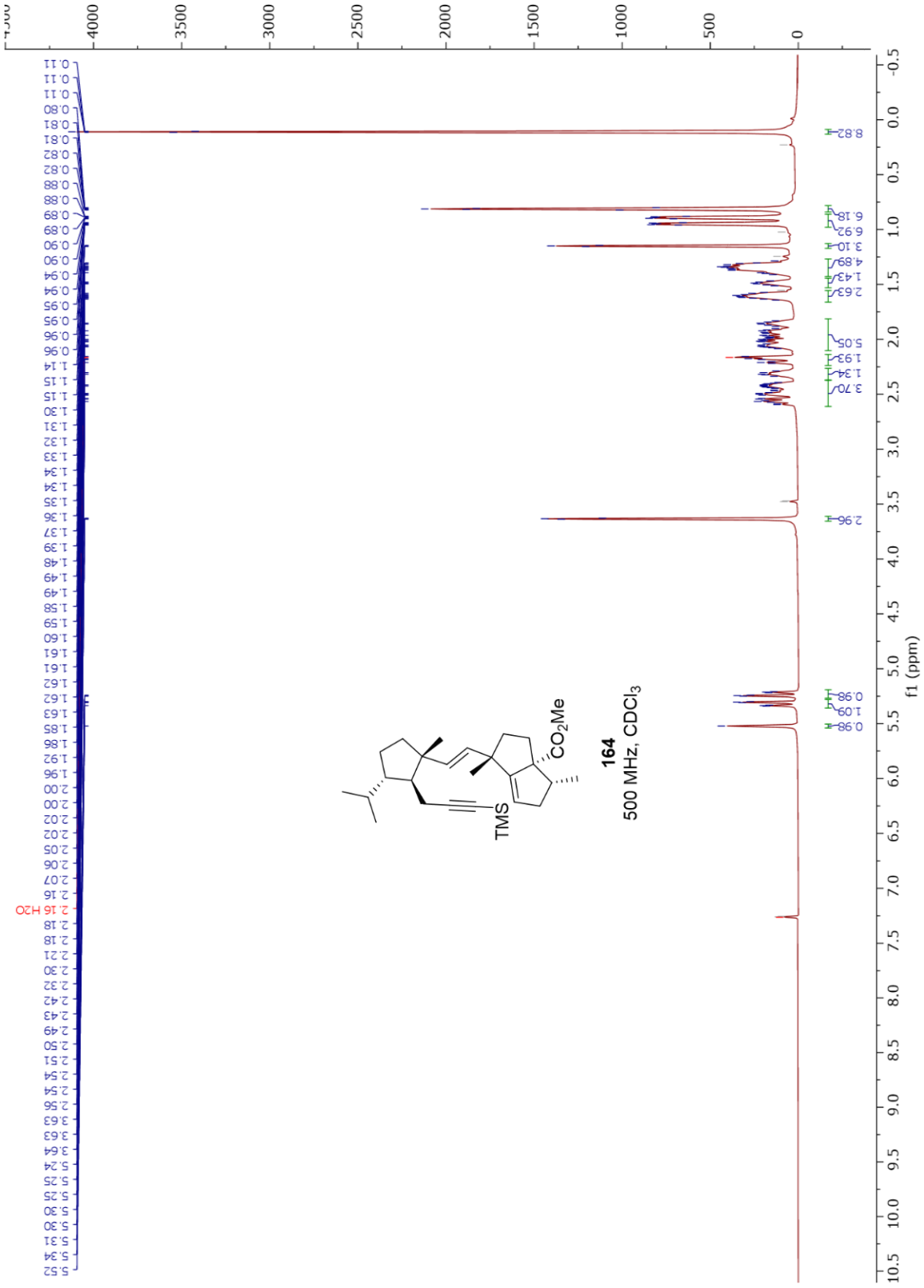
TMS
CO2Me
164
500 MHz, CDCl3
f1 (ppm)
H2O

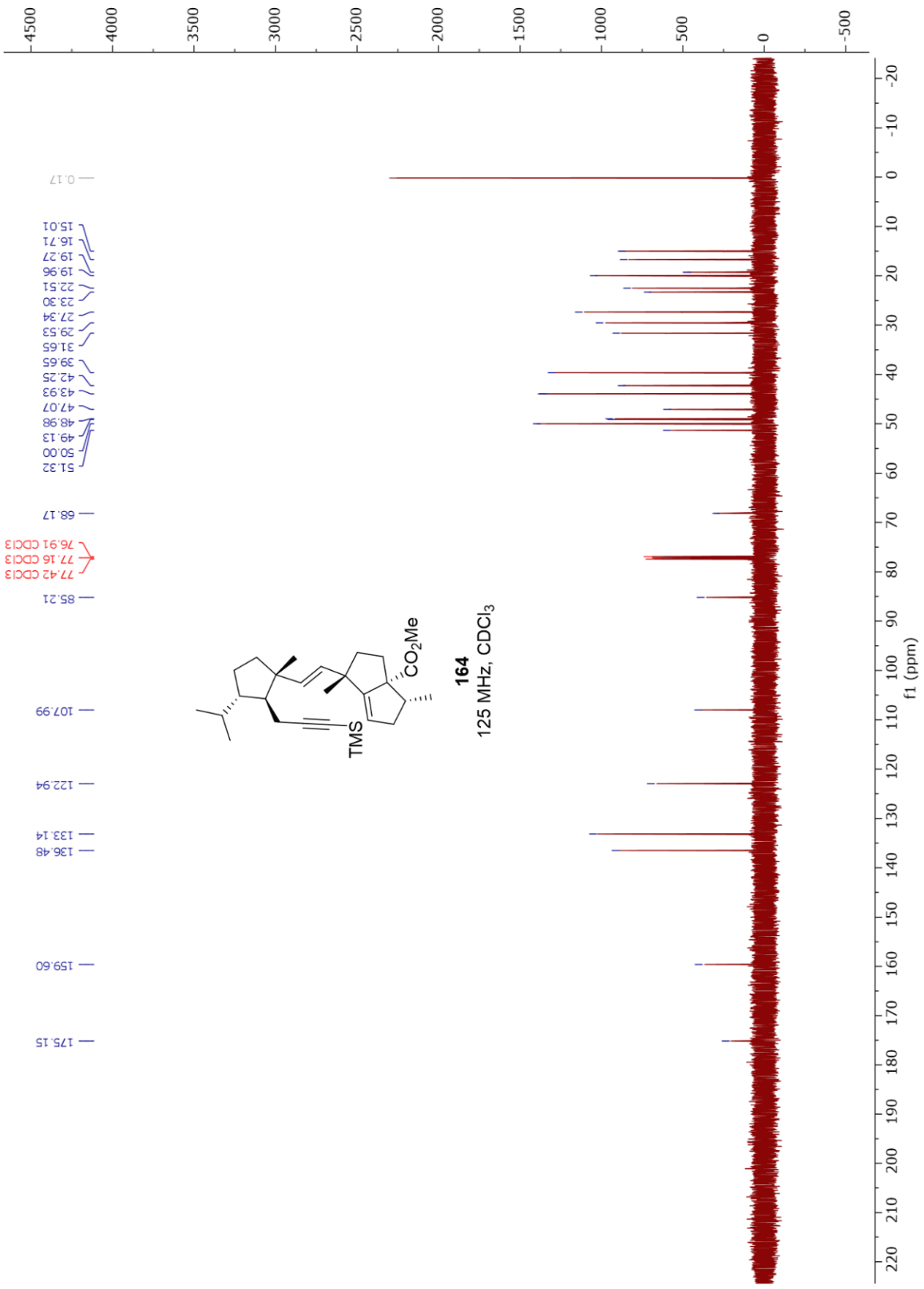
TMS
CO2Me
164
125 MHz, CDCl3
f1 (ppm)

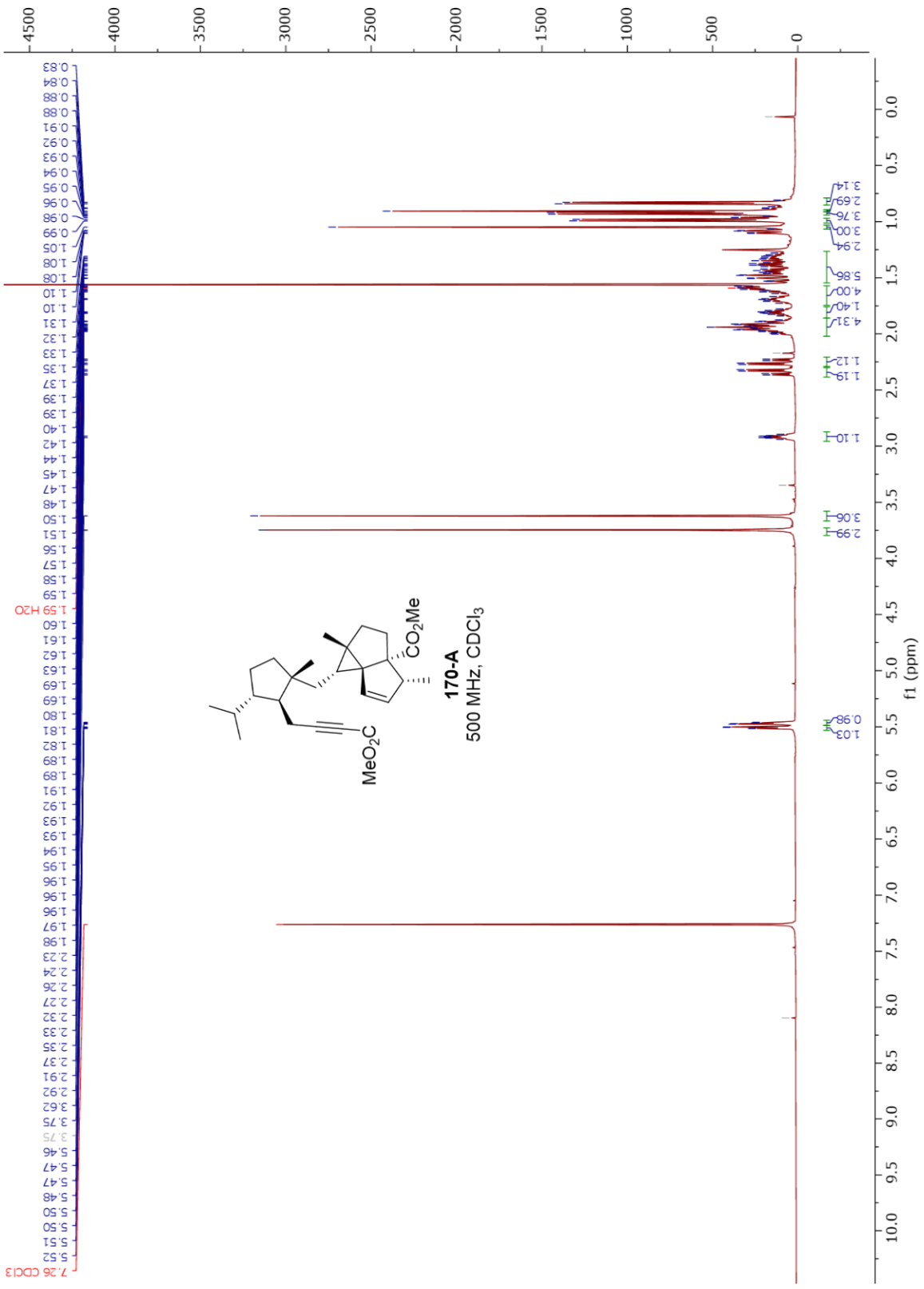
170-A
500 MHz, CDCl3
CO2Me
MeO2C
f1 (ppm)

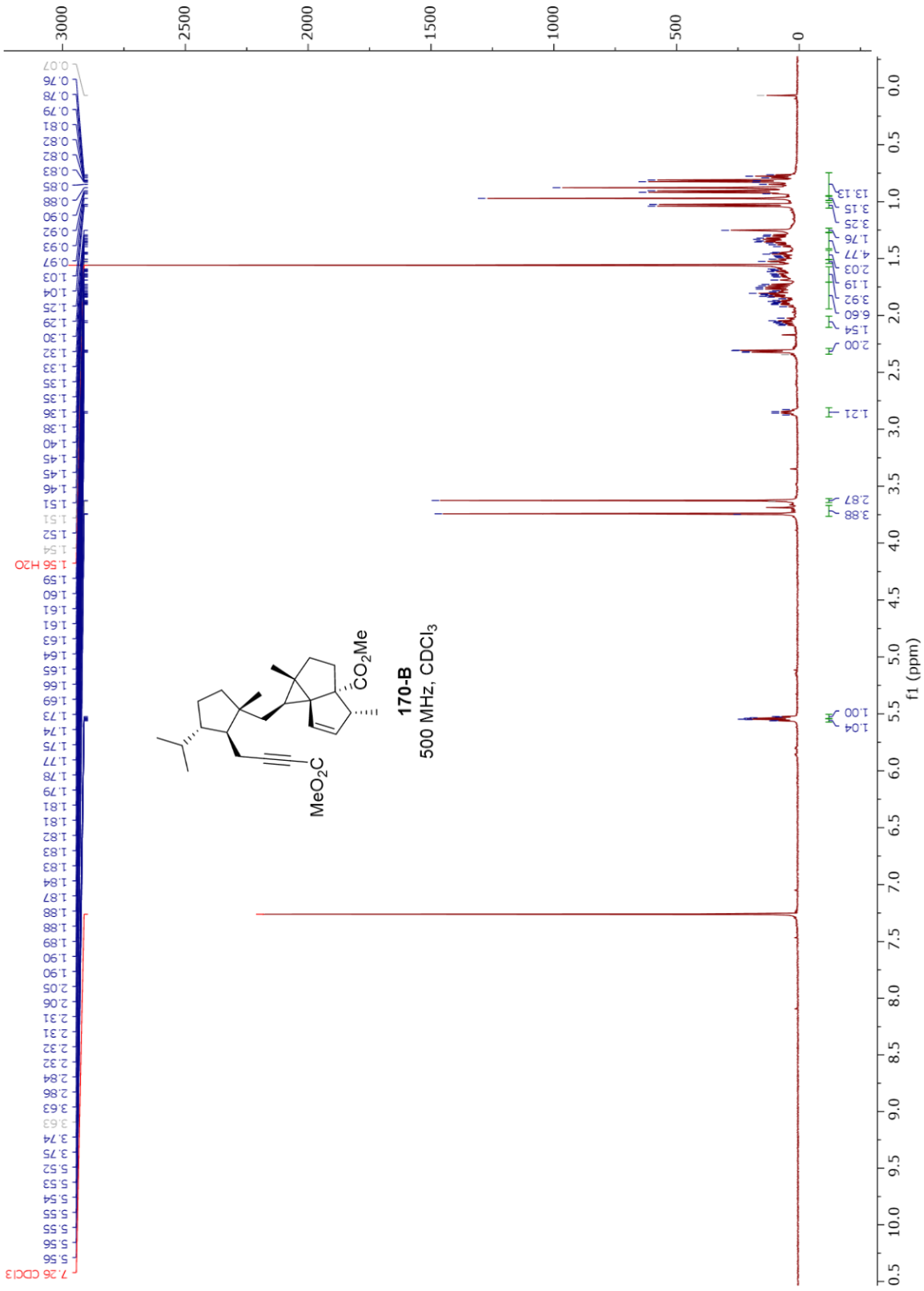
170-B
500 MHz, CDCl3
CO2Me
MeO2C
f1 (ppm)

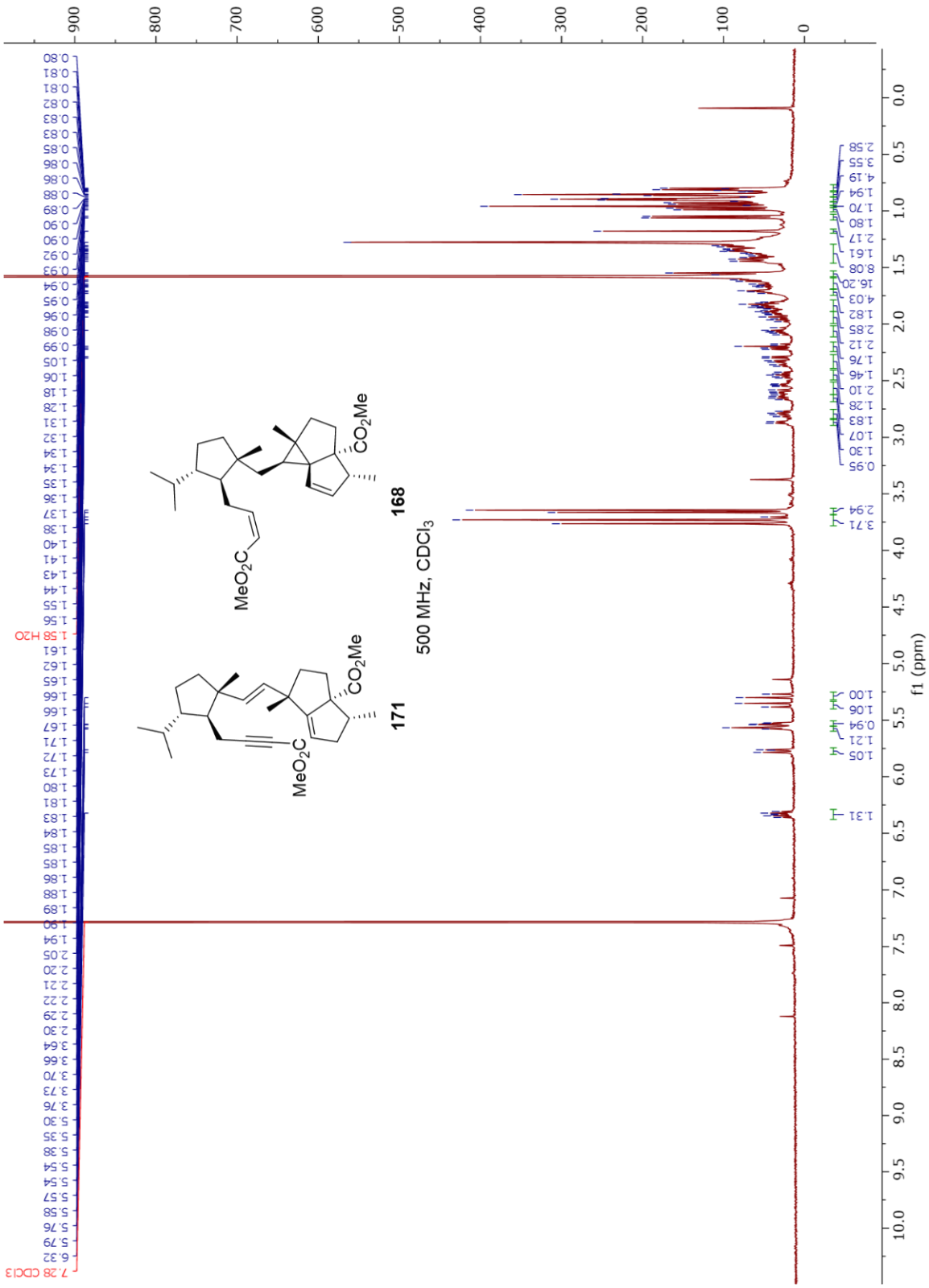
168
171
500 MHz, CDCl3
MeO2C
CO2Me
f1 (ppm)

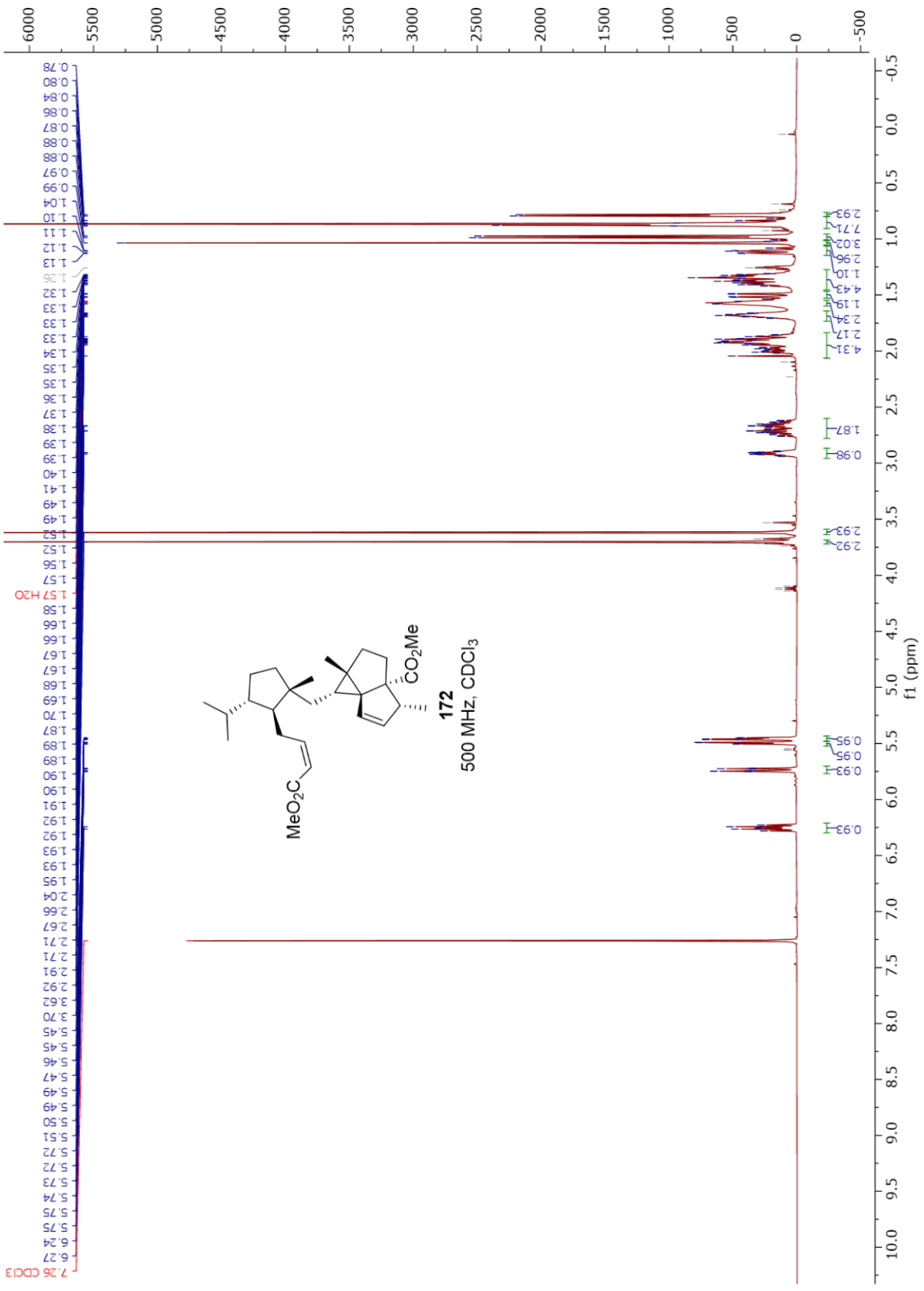
CO2Me
MeO2C
172
500 MHz, CDCl3
f1 (ppm)

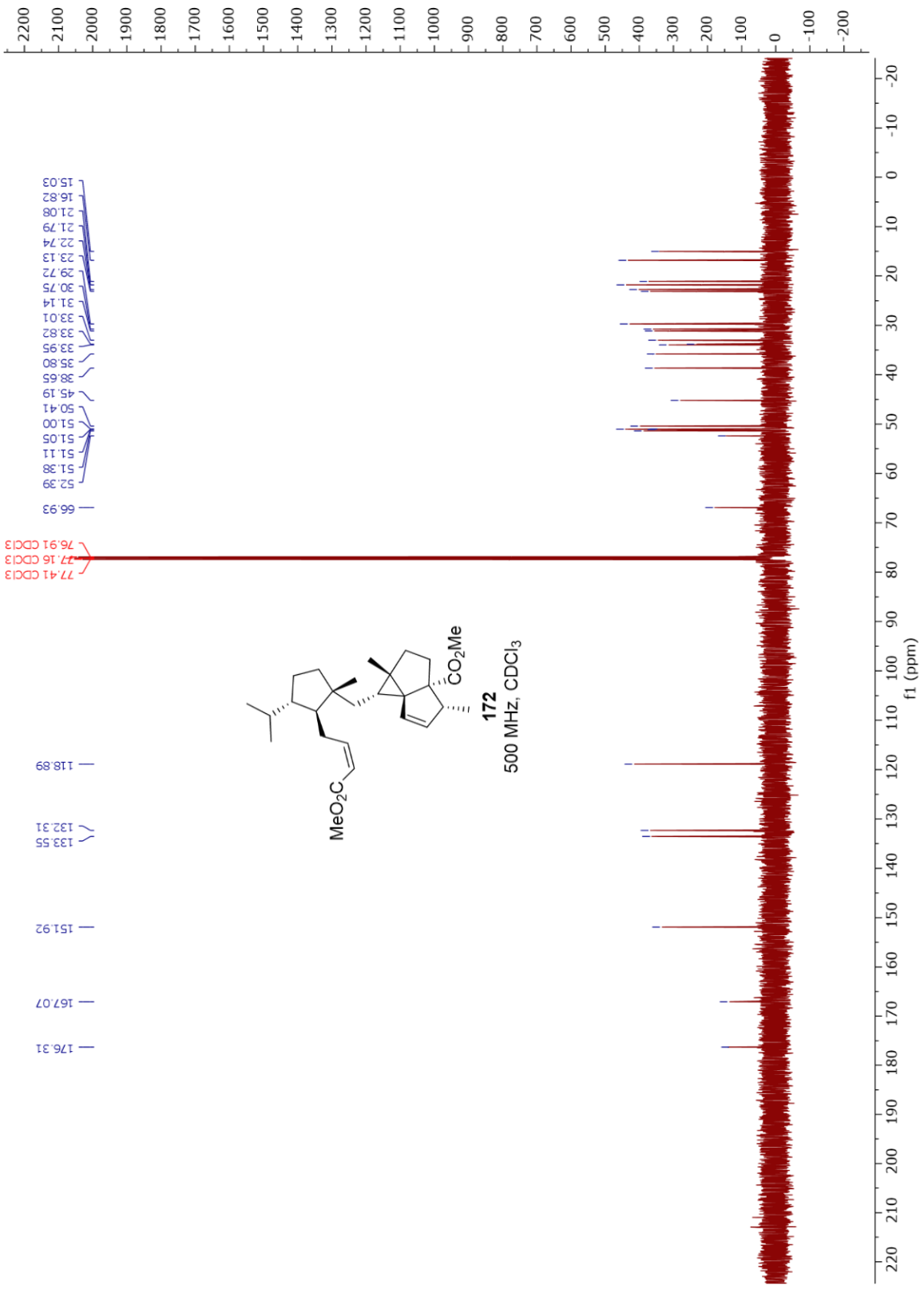
MeO2C
CO2Me
172
500 MHz, CDCl3
f1 (ppm)

Chapter 2

Development of General Conditions for Intramolecular Nickel Heck Cascades

2.1 Introduction to Ni Catalysis

While used extensively in catalysis throughout the last century, Ni has never quite received the same acclaim of its group 10 congener Pd from the synthetic community. Fittingly taking its name from an antagonistic imp, its reputation is one of impressive, but often unpredictable and uncontrolled reactivity.[1,2] Ni catalysis, however, has experienced a renaissance over the last two decades leading to a new appreciation and deeper understanding of how to tame the purportedly unruly metal.[3–5] This interest was largely driven by the pressing need for a cheaper and sustainable alternative to Pd. Comprising a significant fraction of the Earth's crust, Ni is indeed considerably more abundant, but its unique chemical properties make it more than just a cheap

	Ni	Pd
% of Earth's crust	1.8%	0.00000063%
$/Mol	$1.4/mol	$850/mol
Atomic Radii	0.124 nm	0.139 nm
Electronegativity	1.91	2.2
Lewis Acidity	Harder	Softer
Oxidation States	-1, 0, +1, +2,+3, +4	0, +1, +2, +3, +4

Table 2.1 General overview of Ni and Pd.

substitute for Pd. Ni provides novel reactivity profiles and distinct challenges for the synthetic chemist. For example, one of the most notable differences is Ni's ability to easily adopt the Ni^{I} and Ni^{III} oxidation states, which are not commonly invoked in Pd catalysis. Thus, while Pd generally proceeds via 2 e^- (Pd^0/Pd^{II} or Pd^{II}/Pd^{IV}) cycles, Ni catalysis exhibits a wide variety of cycles, potentially including radical pathways.[6] This mechanistic promiscuity allows for reactivity that would be otherwise inaccessible with Pd, such as Weix's sp^2-sp^3 cross-electrophile couplings which reportedly proceeds via a Ni^{II}/Ni^{I}/ Ni^{III}/Ni^{I} cycle.[7] On the other hand, Ni is also able to undergo comproportionation and disproportionation, which can lead to off-cycle species that can undergo undesired reactivity or act as catalyst sinks which stall the reaction.[2] Further, the prevalence of paramagnetic Ni^{I} species can render reactions challenging to monitor by NMR

adding an extra layer of complexity when trying to determine mechanism. One area in particular in which the synthetic community has only recently begun to truly exploit the benefits—and address the challenges—of Ni catalysis is the Heck reaction. Despite being known for decades,[8] the Ni-Heck reaction has remained largely underdeveloped.[4] As such, great opportunities to utilize the properties of Ni in the Heck reaction remain untapped, in part due to how Ni's properties play out in the different elementary steps of the reaction's mechanism.

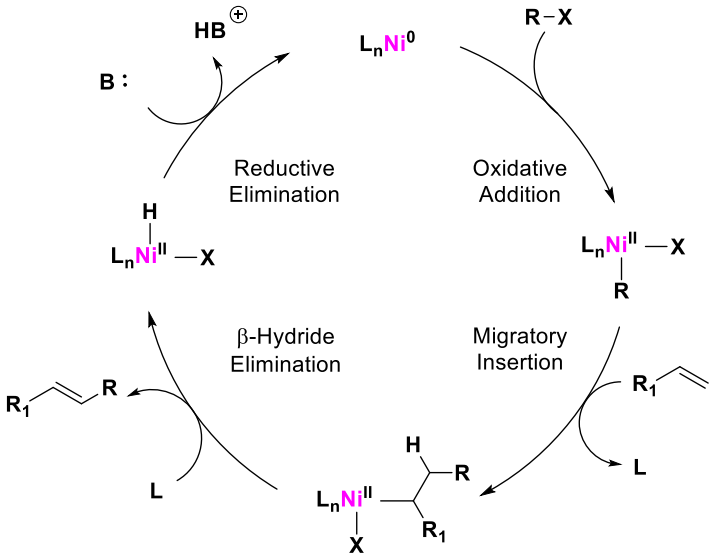

Figure 2.1 Generalized mechanism of the base mediated Ni-Heck Reaction

Section 2.2 Oxidative Addition

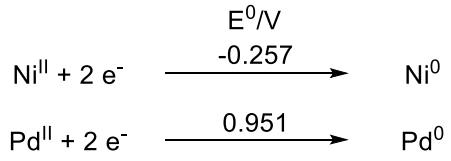

Scheme 2.1 Reduction potentials of Ni and Pd.

At the outset of the Heck reaction, Ni truly excels when compared to Pd due in large part to it being more electropositive than its congener. This implies that Ni^0 more readily donates electron density, which is evidenced by its considerably lower reduction potential.[6] The first step for oxidative addition in the Heck reaction requires coordination of the aryl- or vinyl-X partner to

the M^0 complex. Due to substantial back bonding from the Ni^0,[9] π-systems form bonds that in some cases can be 20 kcal/mol stronger with Ni^0 than with Pd^0 complexes.[2] Further, Tolman found that the K_{eq} for ethylene binding in $(PPh_3)_2Ni^0$ is 10^4 larger than $(PPh_3)_2Pd^0$.[10] Following binding, the metal species must then undergo the usually (but not always) $2e^-$ oxidative addition. Computational studies have shown that Ni^0 species undergo oxidative addition much more readily than Pd^0 with energy differences between the two species ranging from 2-4 kcal/mol.[9] In practical terms, Pd applications are often limited to OTf, I, Br, and in some cases Cl, but Ni is able to utilize

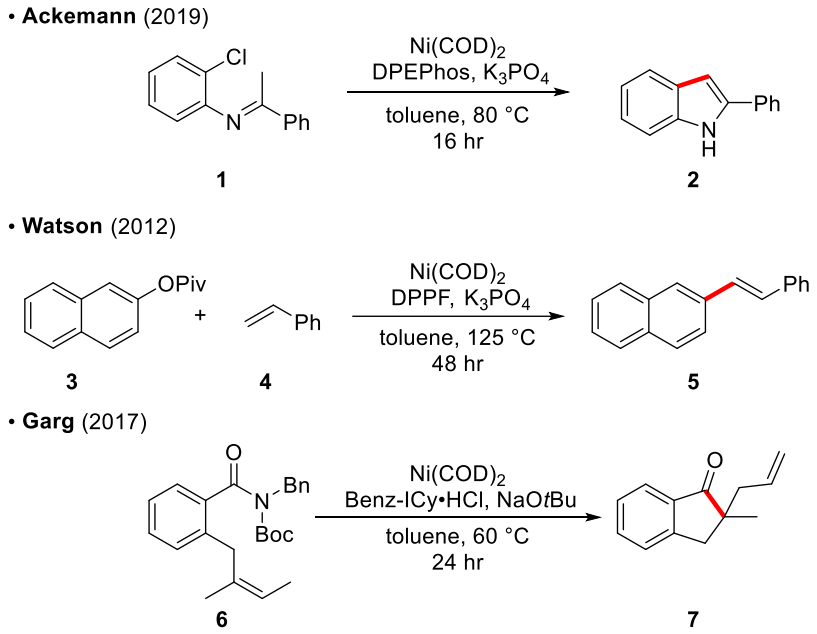

Scheme 2.2 Representative examples of traditionally unreactive coupling partners in the Ni Heck.

traditionally unreactive partners such as ethers, carbonates, mesylates, carbamates, sulfonamides, nitriles, alcohols, and even some fluorides.[1] Three representative examples are shown in scheme 2.2. Of particular note is the Garg example which utilizes Boc-protected aryl amides as the coupling partner at remarkably mild temperatures for such an unreactive bond.

2.3 Migratory Insertion

Moving on to migratory insertion, Ni once again proves to be more reactive than Pd. This is borne out in the olefin polymerization literature, where diimine Ni complexes have been shown to have an approximate 4-5 kcal/mol lower E_a for the rate limiting migratory insertion step leading to turnover numbers 10^4 larger than the Pd equivalent.[11,12] One study conducted by the Brookhart group investigated the mechanism of chain walking for Ni and Pd catalysts, and demonstrated that alkyl Pd complexes could bind ethylene readily and were stable at –78 ˚C, but the alkyl Ni complexes upon exposure to ethylene underwent multiple migratory insertions even at –130 ˚C. Computational studies have also found similar trends for migratory insertions.[9,13] Furthermore,

	trig[a]				dig[a]			
Ni	3-*exo*	0.5	34.6	4-*endo*	3-*exo*	1.0	58.4	4-*endo*
	4-*exo*	16.7	17.5	5-*endo*	4-*exo*	9.7	32.5	5-*endo*
	5-*exo*	9.3	8.2	6-*endo*	5-*exo*	9.2	12.6	6-*endo*
	6-*exo*	9.8	16.1	7-*endo*	6-*exo*	9.6	8.4	7-*endo*
Pd	3-*exo*	2.6	44.3	4-*endo*	3-*exo*	3.6	62.9	4-*endo*
	4-*exo*	22.6	26.7	5-*endo*	4-*exo*	18	40.1	5-*endo*
	5-*exo*	11.9	16.1	6-*endo*	5-*exo*	13.2	25.9	6-*endo*
	6-*exo*	15.6	18.4	7-*endo*	6-*exo*	21.2	24.2	7-*endo*

Table 2.2 Calculated E_a for intramolecular migratory insertions for Ni and Pd.
[a] All calues in kcal/mol.

in all examples examined, Ni had a consistently lower E_a for intramolecular cyclizations with both alkenes and alkynes. From that study, one particularly interesting result was the finding that while Pd favors [5-*exo*-trig] cyclizations over the [6-*endo*-trig] pathway by roughly 4 kcal/mol; however, Ni has no such preference with only an approximate 1 kcal/mol difference favoring [6-*exo*-trig] cyclization. This suggests that it may be possible for Ni to undergo either pathway, with potentially tunable selectivity based on ligand choice. In fact, the Cramer group has reported just such a case. In a Ni-mediated cycloisomerization of pyridone **8**, they found that with bulky electron rich phosphine ligands the [5-*exo*-trig] is favored while NHC ligands favored the [6-*endo*-trig]

pathway. Given the predominance of the [5-*exo*-trig] cyclization in the Pd-Heck literature, this controllable selectivity suggest an enticing possibility of divergent reactivity with Ni.

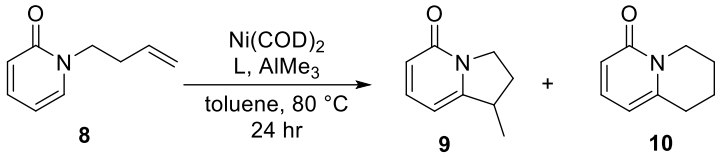

L	Yield	**9**:**10**
PCy_3	70%	>95:5
IMes	70%	>5:95

Scheme 2.3 Ligand controlled regiodivergent Heck-type cycloisomerizations.

Section 2.4 β-Hydride Elimination

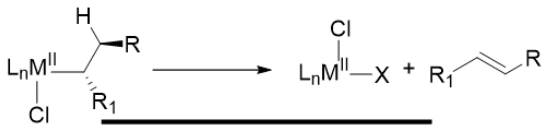

M	$E_{a\text{-}\beta H}$	$E_{a\text{-}\beta H}$	$\Delta G_{\beta H}$
Ni	8.7	14.7	12.7
Pd	10.8	8.5	4.0

Table 2.3 Calculated E_a and ΔG for β-hydride elimination with Ni and Pd: All values in kcal/mol.

As Ni excels at migratory insertion, it follows that the corresponding reverse reaction, β-elimination, would be challenging. This is indeed confirmed by both computational[9,14] and experimental[11] studies showing the E_a is approximately 4-5 kcal/mol higher for Ni than for Pd. Once again turning to the polymerization literature, it has been noted that cationic diimine Ni complexes can produce polyethylene that is far less branched than Pd complexes as a result of relatively slow β-hydride elimination.[11,12] As shown in Scheme 2.4, following initial migratory insertion into ethylene the β-agostic complex **12** is formed. Now if β-hydride elimination is fast, as with Pd, then hydrido complex **15** is formed and following subsequent reinsertion, the more thermodynamically stable β-agostic complex **16** is accessed. From there ethylene complexation, migratory insertion, and further β-hydride elimination and chain walking leads to highly branched polymers (about 70 methyls/1000 carbons). Conversely, if β-hydride elimination is slow

compared to ethylene complexation and migratory insertion, as has been demonstrated with Ni, then chain growth can occur without β-hydride elimination and chain walking generating polymers with almost negligible branching. It should be noted that, as with the Cramer example in the

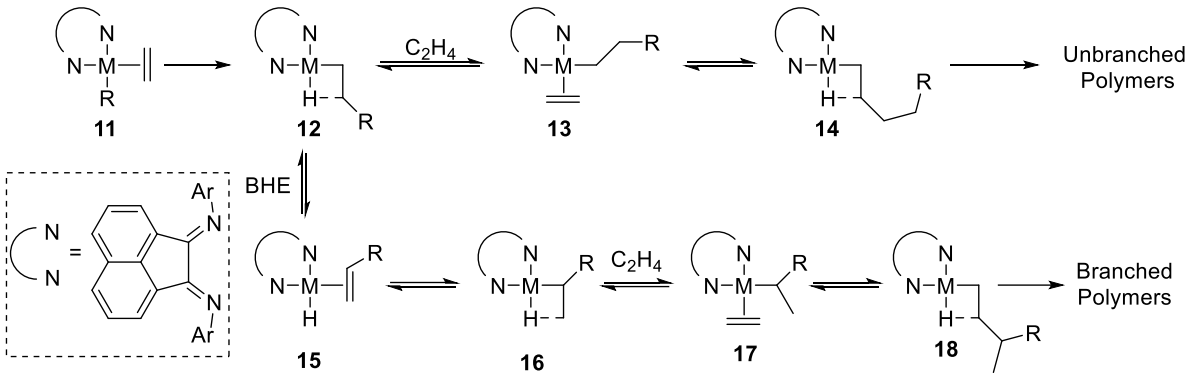

Scheme 2.4 Effect of β-hydride elimination on the formation of branched and unbranched polyethylene polymers.

previous section, Ni's preference for β-hydride elimination can be strongly influenced by the reaction conditions with high temperatures or low pressures of ethylene leading to highly branched polymers. This variable β-hydride elimination has also been noted in the Ni-Heck literature. In several early examples of the Ni-Heck, there were reports of the formation of both Heck-type substitution products as well as saturated addition products.[15–17] For example, the Ronchi group observed the selective formation of the saturated product **22** with their conditions, while the

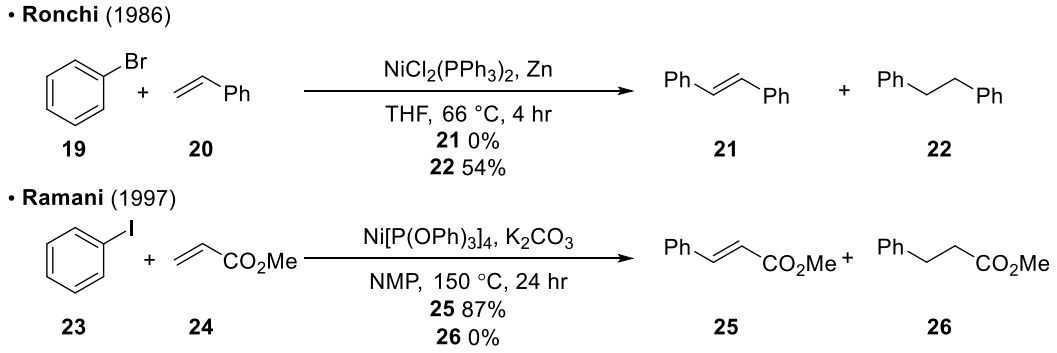

Scheme 2.5 Formation of substituted or saturated products.

Ramani group reported selectivity for the Heck product methyl cinnamate **25**. While this ability to fine tune the β-hydride elimination has been used extensively in the cross coupling literature[1] it has yet to be used to great effect in the context of the Heck reaction.

Section 2.5 Reductive Elimination

The final step of the reaction is the reductive elimination of HX from the Ni^{II} species to regenerate the Ni^0 and start the cycle over again. As it is the microscopic reverse of oxidative addition, it is no surprise that Ni struggles with reductive elimination with a ΔG of 14.4 kcal/mol to Pd's -4.4 kcal/mol.[9] This is somewhat surprising giving the prevalence of Ni in the cross coupling literature, but it should be noted that those reactions proceed via a migratory reductive elimination rather than deprotonation. And in fact, when looking at C-C bond formation, Ni has a

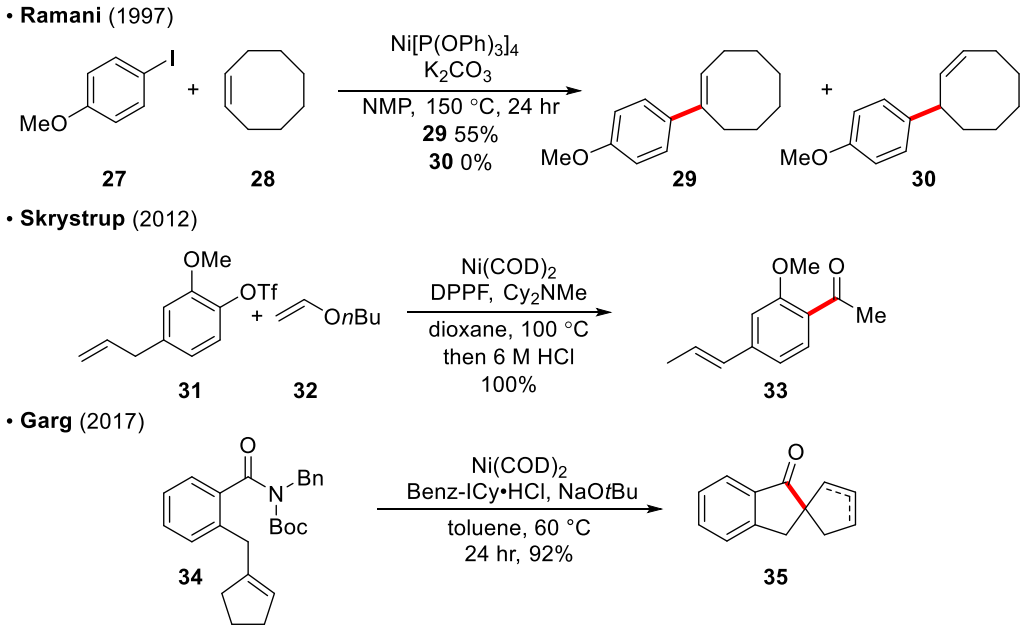

Scheme 2.6 Examples of Ni-H mediated isomerization.

lower E_a for reductive elimination due to the relatively weak Ni-C bonds.[2] The reticence of Ni-H to undergo deprotonation comes as a result of its greater electropositivity, which makes it a significantly weaker acid than Pd-H.[18] Practically, what this entails is that while Pd-H's are

readily deprotonated by amines, carbonates, or acetates,[8] Ni-H species often require strong organometallic bases[19] or forcing conditions[17] with long reaction times in order to facilitate catalyst regeneration. The slow deprotonation leads to a long-lived Ni-H species that can undergo reinsertion to an olefin leading to alkene isomerization. And indeed, this has been noted in the Ni-Heck literature. As shown in Scheme 2.7 examples from the Ramani,[17] Skrystrup,[20] and Garg[21] groups all exhibit olefin isomerization arising from the Ni-H species. In order to address this issue, two major approaches have been developed in order to help promote reductive elimination. The first and most commonly used method is to utilize a stoichiometric reductant, usually Mn or Zn, to effectively promote catalyst regeneration.[16,22,23] While reducing metals are the most common, organic reductants such as tetrakis(dimethylamino)ethylene (TDAE)[24] or electrochemical

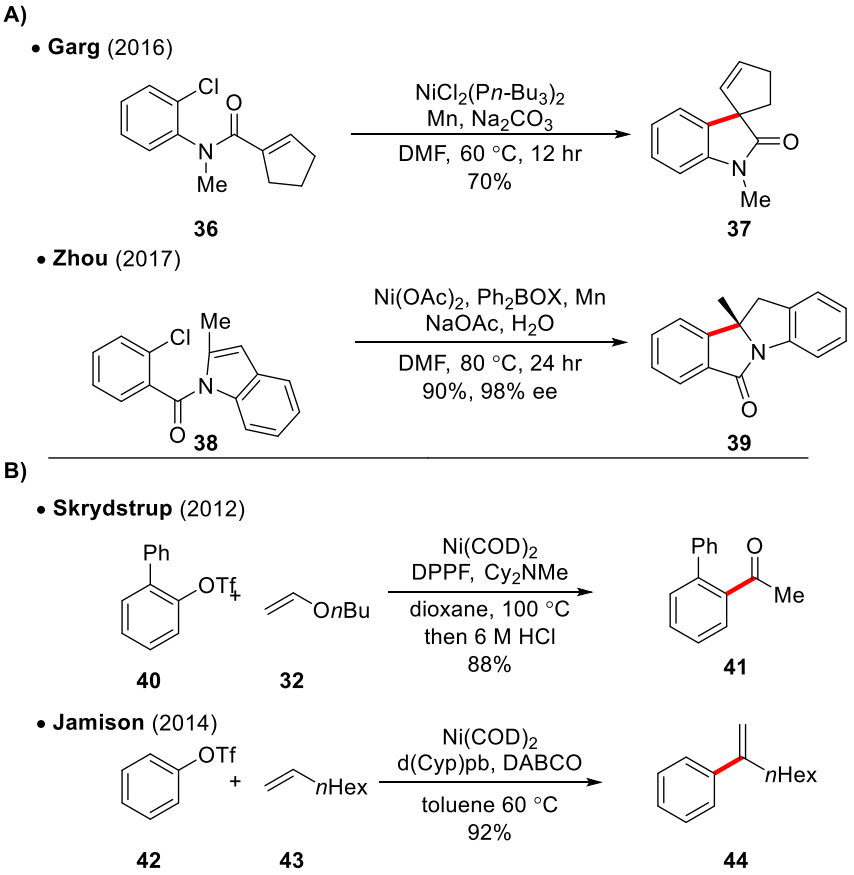

Scheme 2.7 Representative examples of **A)** reducing metal approach and **B)** cationic-Heck approach.

methods[25] have also been reported. The second approach is to access the cationic-Heck pathway through the use of triflate coupling partners. As triflate is a non-coordinating anion, the Ni complex will be cationic, which will make the Ni-H species more electron poor and thus acidic enough for more traditional amine bases to be used.[20,26] While both of these approaches are able to effectively promote the reductive elimination, isomerization has still been observed in both cases.[16,20] This often leads to either the use of bulky ligands[26] to prevent reinsertion, or limits the substrate scope to cases where reinsertion is challenging. As such, the Ni-H issue must be addressed on a case-to-case basis. Another strategy of note completely negates the issue of Ni-H isomerization by avoiding the formation of the Ni-H species. Following the initial Heck reaction, the alkyl-Pd species undergoes a cross coupling reaction which proceeds via a migratory reductive elimination, which as discussed earlier is quite favorable for Ni, thus side stepping β-hydride elimination and Ni-H formation.[27–31] However, as our efforts are focused on the classical Heck mechanism, this strategy will not be discussed further.

2.6 Ni Heck Cascades

While Pd-Heck cascades have been studied thoroughly,[8,32–34] the corresponding Ni cascades have been largely ignored. To the best of our knowledge, only a handful of examples exist in the literature and all of those are intermolecular, rather than intramolecular, cascades. The first examples we were able to find came from the Cheng group with some representative examples shown in Scheme 2.8.[35–37] In their initial publication, they report on the cyclization of aryl iodide **45** with 3 equivalents of a symmetrical dialkyl acetylene **46** to yield unsymmetrical biaryl **48**. This reaction is particularly interesting as it proceeds via an uncommon β-carbon elimination rather than the usual β-hydride elimination. Analysis of the head space of the reaction with **45** revealed the presence of ethylene suggesting that β-hydride elimination occurs following the β-carbon

elimination allowing the reaction to proceed. This is further supported by the observation that 2-butyne, which would yield a Ni-Me species incapable of β-hydride elimination, did not give a biaryl, rather undergoing a [5-*exo*-trig] cyclization and subsequent β-hydride elimination to yield a cyclopentadiene. Their next report focused on β-iodoketone **49** and its reaction with **46** to give

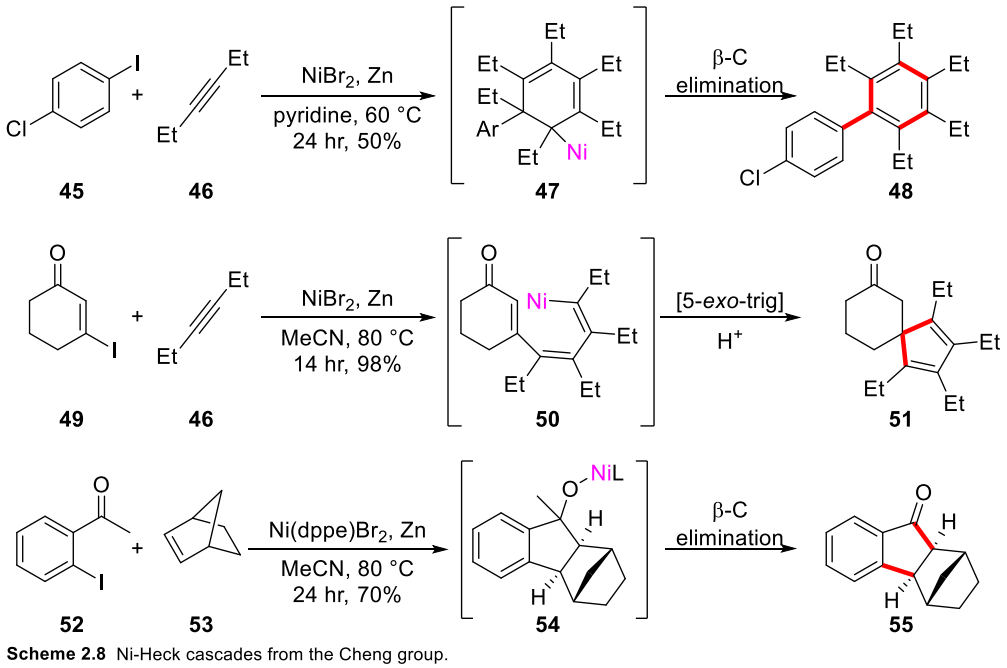

Scheme 2.8 Ni-Heck cascades from the Cheng group.

cyclopentadiene **52**. It is interesting to note that in this case, only 2 equivalents of **50** were incorporated due to the competition of the intramolecular [5-*exo*-trig] cyclization. In a more recent study, they reported a Larock annulation of 2-iodoacetophenone **53** and norbornene **54** that once again proceeded via a β-carbon elimination. However, unlike the first example, substrates such as **53** that led to alkyl Ni-I species unable to undergo β-hydride elimination were still reactive. Presumably, two Me-Ni-I species could exchange ligands to form $NiMe_2$, which could extrude ethane to regenerate the Ni^0, and NiI_2, which could be reduced by the Zn.

The Kong group reported an intra-intermolecular Ni-Heck cascade, which is particularly notable for the use of difluoroolefins.[38] The initial intramolecular Heck cyclization of amide **56**

is unremarkable, but following the [5-*exo*-trig] cyclization the resultant alkyl Ni species then undergoes an intermolecular Heck reaction with the unusual difluorostyrene **57** to give intermediate **58**. The reaction then proceeds with a very uncommon β-F elimination to yield the monofluorinated product **59**. The reaction would give mixtures of *E*/*Z* isomers, but it was found

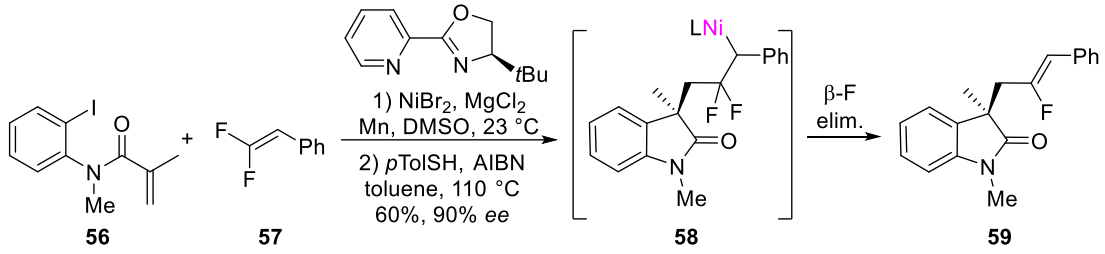

Scheme 2.9 Kong's intermolecular Ni Heck cascade of difluorostyrenes.

that using radical conditions the mixture could be cleanly converted into the less hindered *E* isomer. While it is remarkable to note that the reaction proceeded with **57**, it is even more remarkable that the presence of at least one fluoride is apparently necessary for the success of the reaction as styrene or other dihalogenated styrenes failed to give any product, which may suggest that β-F elimination proceeds more easily than β-hydride elimination, β-carbon elimination, or other β-halogen eliminations.

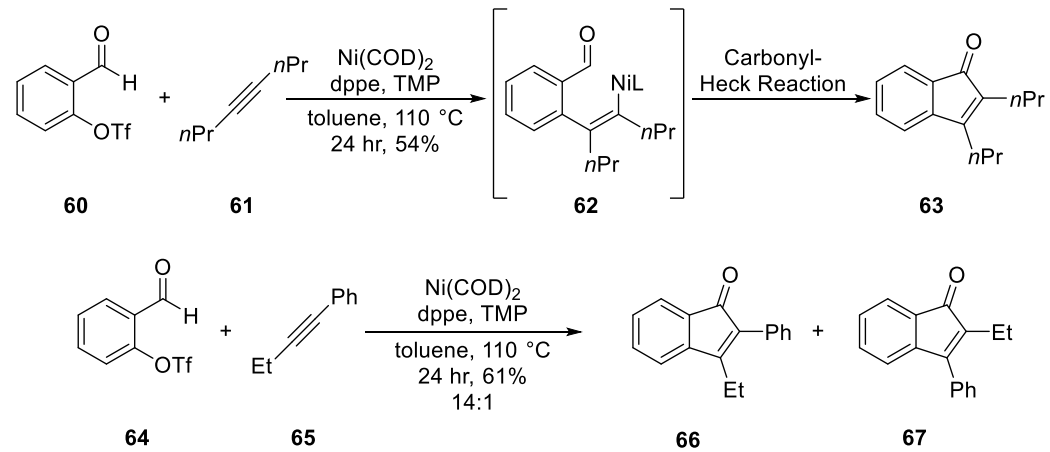

Scheme 2.10 Larock annulation of symmertical and unsymmetrical alkynes.

Next, the Rong group reported a Larock annulation of aryl triflate **60** and acetylene **61** to give indanone **63**.[39] The cascade is mainly of note for the fact that it utilizes the cationic- Heck approach rather than the reducing metal conditions that most groups favor. Also, unsymmetrical alkynes such as **65** were able to be used in the reaction—though for high selectivity either an electronic or steric bias was required.

Finally, the most recent report from the Kong group describes a very intriguing Heck type cascade that proceeds via a so-called hydrogen auto transfer strategy. At first glance, the reaction appears to be almost identical to the Larock annulation of the Rong group, but for the fact this

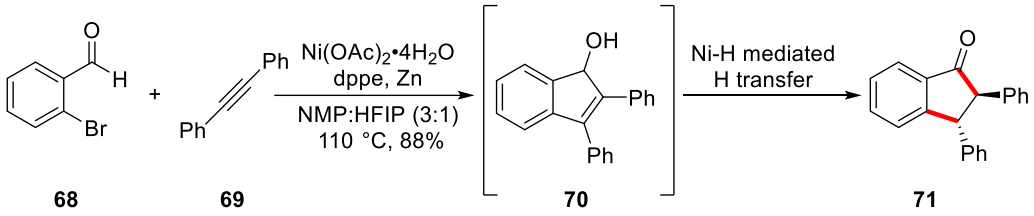

Scheme 2.11 Ni-Larock annulation using a H-autotransfer strategy.

reaction yields indanone **71** rather than an indenone. They propose that the reaction proceeds via a Larock annulation, followed by reinsertion of the Ni-H species into the enone then a final protonation. They provide support for their proposal by way of the observation that after 12 hours of reaction time, indenol **70** was isolated in a 31% yield and upon resubjection of **70** to the reaction conditions, clean conversion to **71** was observed indicating that **70** is a key intermediate in the reaction. Further deuterium labelling studies indicate that the benzylic-H of **70** is the source of the hydride. While the indanone synthesis was distinct enough to be of note, the Kong group then extended the reaction by utilizing 1,6-enyne **72** to conduct a spirocyclization to give indanone **73** in excellent yield. They propose the reaction proceeds via a similar Larock annulation to give indenone **74**. However, instead of reinserting into the enone, the Ni-H inserts into the 1,1-disubstituted olefin to yield the alkyl Ni species **75**, which then undergoes a [5-*exo*-trig] cyclization

and subsequent protonation to arrive at **73**. The high selectivity of reinsertion of the Ni-H into the 1,1-disubstituted olefin in a Markovnikov fashion to yield **76** is somewhat surprising, as the Ni complex should have a strong preference for the less hindered carbon. One could make the argument that the product of anti-Markovnikov addition may be unable to cyclize, but Ni can readily undergo [6-*exo*-trig] cyclizations so this is unlikely to be the reason. What is likely

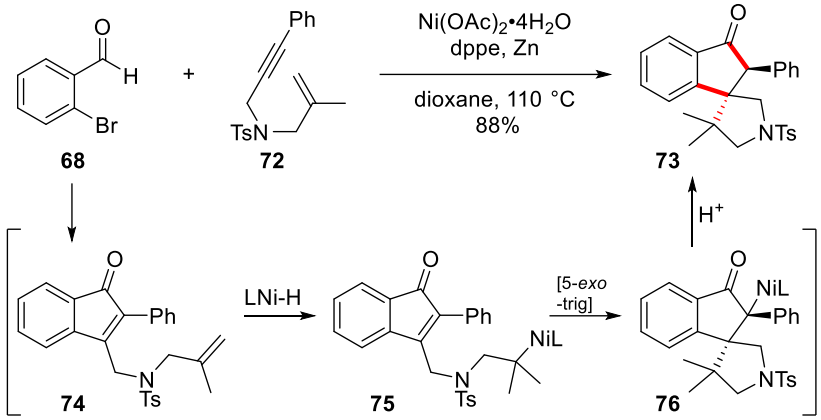

Scheme 2.12 Spirocyclization of enynes mediated by Ni-H.

occurring is the NTs moiety is acting as a directing group that guides the Ni-H reinsertion allowing for the less favorable Markovnikov addition to occur. This supposition is supported by the fact that all successful examples of this cascade contain the NTs moiety. Attempts to use either C or O linkers in the 1,6-enyne only gave indenol products similar to **74**. Further, attempts to use a 1,7-enyne with the 1,1-disubstituted olefin one carbon further away from the NTs similarly gave an indenol product. The Kong groups work is an incredibly impressive cascade as it manages to jump back and forth between inter- and intramolecular pathways while maintaining high regio- and chemoselectivity.

2.7 Project Goals and Direction

A large part of the challenge and opportunity of Ni catalysis is that, unlike Pd with its consistent and well-defined preferences, Ni often lies in the borderlands of the potential energy

surface, able to easily shift between different reactivities. While this promiscuity has given Ni a reputation befitting its devilish name, it is possible for Ni to be properly corralled with the appropriate choice of ligand and reaction conditions. With this is mind we set out to try to develop our own cascade conditions. Our stated goal for the project was to develop general conditions for intramolecular Ni-Heck cascades of aryl and vinyl triflates. The first choice we had to make was

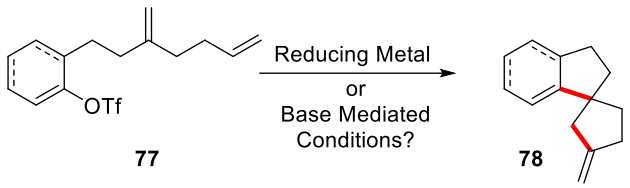

Scheme 2.13 General intramolecular Ni-Heck cascade of aryl and vinyl triflates.

whether we would focus on reducing metal or base-mediated conditions. The reducing metal conditions were by far more well developed and more thoroughly applied than the base-mediated counterparts. However, when we started this project, the examples of an aryl triflate with reducing metal conditions often resulted in poor yields.[22,40] Since then a report[41] of the successful application of sulfonates and reducing metal conditions has been published; however, at the time we were working under the assumption that the reducing metal conditions were ideal for halide partners and the base-mediated conditions were appropriate for triflates. As the ultimate goal was to apply this in the synthesis of retigeranic acid A, via a vinyl triflate, we opted to pursue the base-mediated conditions.

2.8 Initial Screening with Monocyclization

As Ni-catalysis was a new area of research for our group, we first sought to gain experience with a simple monocyclization to familiarize ourselves to the idiosyncrasies of Ni before attempting the more complex cascade reactions. The easily prepared aryl triflate **79** was selected as a model compound. For our first condition set, we decided to start with the Skyrdstrup[20]

conditions rather than Jamison's[26] as it was suspected the bulky d(Cyp)pb ligand would find the intramolecular cyclizations challenging. Pleasingly, with our first attempts we were able to access indane **80** in a 51% yield. A brief screening of ligands showed DPEPhos to be the best of those investigated giving **80** as the sole product of the reaction. The related Xantphos exhibited similarly high reactivity but proceeded with the formation of several inseparable side products. In the solvent

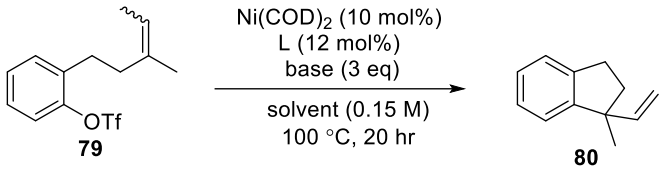

Entry	Ligand	Yield[a]
1	DPPF	51%
2	dppe	0%
3	dppp	0%
4	BINAP	60%
5	DPEPhos	75%
6	Xantphos	79%[b]
7	Segphos	48%[b]

Entry	Solvent	Yield[a]
1	1,4-dioxane	75%
2	THF	0%
3	DME	85%
4	toluene	33%
5	DMF	80%

Entry	Base	Yield[a]
1	Cy_2NMe	75%
2	Et_3N	65%
3	DIPEA	54%
4	PMP	42%
5	pyridine	26%
6	Proton Sponge	59%
7	K_2CO_3	43%
8	KOAc	17%

Table 2.4 Condition screening for monocyclization of triflate **79**. [a]isolated yields [b] contained inseparable impurities. Conditions for ligand screen: NiCOD(10 mol%), L (12 mol%), Cy_2NMe (3 equiv), dioxane (0.15 M), 100 °C, 20 hr; solvent screen: NiCOD(10 mol%), DPEPhos (12 mol%), Cy_2NMe (3 equiv), solvent (0.15 M), 100 °C, 20 hr; base screen:NiCOD(10 mol%), DPEPhos (12 mol%), base (3 equiv), dioxane (0.15 M), 100 °C, 20 hr.

screen, DME provided the highest yield, but for practical reason we decided to move forward using dioxane. The poor performance of THF compared to the other ethereal solvents was quite puzzling, but later results suggest that the quality of the THF, which had been degassed by sparging with $Ar_{(g)}$ rather than via freeze-pump-thaw, was at fault rather than THF itself being unsuitable for the reaction. The base screening showed Cy_2NMe to be the optimal base, but suggested that amine bases in general are competent at effecting the requisite reductive elimination to regenerate the Ni(0) species. In fact, even a weak base such as K_2CO_3 was able to deprotonate the Ni-H species to some degree giving **80** in a modest 43% yield. With these results in hand, we felt more confident in our ability to investigate the cascade reactions.

And lo! Like Sisyphus before us, the gods saw fit to smite us for our hubris. Unfortunately, our optimized monocyclization conditions with triflate **82** were highly ineffective giving the desired spirocycle **83** in only a 15% yield. The ^{1}H and ^{19}F NMR spectra indicated that **82** was only a minor component of a complex mixture of isomerized products **84**, starting materials **85**,

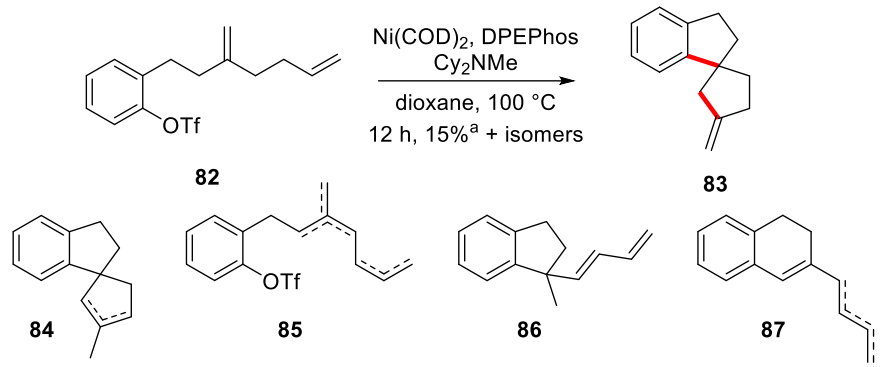

Scheme 2.14 Initial cascade attempt using optimized conditions from monocyclization. [a]GC yield using dodecane as an internal standard

or cyclized products arising from **85**. Given the prevalence of olefin isomerization, the Ni-H species was the obvious culprit for these issues. Upon further consideration, it becomes clear that in the model monocyclization, Ni-H isomerization would not have a stark impact because **80** cannot be isomerized and **79** contains a trisubstituted olefin, which is substantially harder for Ni-H to insert into compared to the 1,1-disubstituted and terminal olefins of **82**. Suitably humbled, we began our optimizations in earnest.

2.9 Base Screening

As the Ni-H mediated isomerization issue proved as problematic as we had expected, our focus was on how best to promote the recalcitrant reductive elimination. Working on the assumption that the reductive elimination was base mediated, the first variable we chose to examine was the choice of base. As shown in Table 2.5 (full details in experimental section), traditional bases for the Pd-Heck reaction such as K_2CO_3, KOAc, and Et_3N proved completely

ineffective at suppressing isomerization. This could be due to the Ni-H's lower acidity[9,18] compared to Pd or the increased steric demand arising from the shorter Ni-P bonds.[1,43] The former could explain the poor performance of the weaker bases such as K_2CO_3. However, the fact that most of the amine bases were effective in the monocyclization would suggest that they are basic

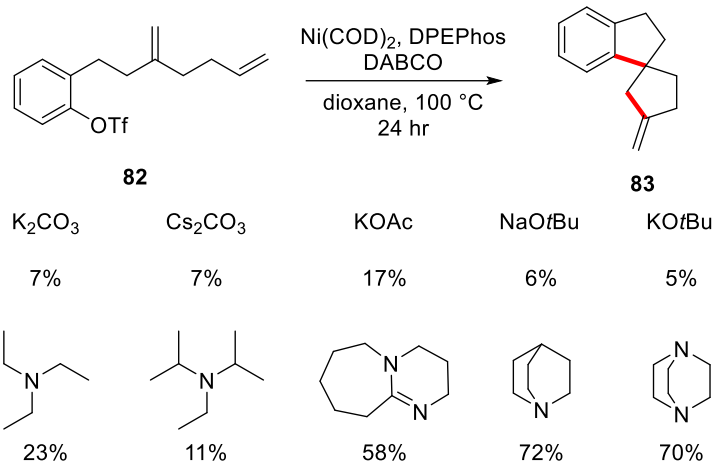

Table 2.5 Base screening intramolecular Ni-Heck cascade conditions.Yields determined by GC using dodecane as an internal standard. $Ni(COD)_2$ (10 mol%), DPEPhos (12 mol%), base (3 equiv.), dioxane (0.15 M), 100 °C, 24 hr.

enough to deprotonate the Ni-H, but that they do so at a slow enough rate that the Ni-H is sufficiently long lived to reinsert and isomerize olefins. As such, we opted to use the unhindered base DABCO, which has been shown previously by Jamison[26] to inhibit Ni-H mediated isomerization of 1,1-disubstituted olefins. Pleasingly, DABCO proved to be highly effective, yielding **83** in a 70% yield with almost no detectable isomerization products present in the ^1H NMR spectra. Given that Et_3N has a similar pK_a values,[44,45] DABCO's efficacy likely arises from the easily accessible lone pair affecting a more kinetically favorable deprotonation and subsequently shortening the life-span of the Ni-H species.

It should be noted, however, that in our first attempts to use DABCO essentially no conversion was observed. The key proved to be purifying the DABCO via sublimation. We found that commercial DABCO was competent in the reaction if stored in a dry glove box upon opening,

but sublimed DABCO provided the highest and most consistent yields. Because DABCO is known to form hydrates[46] and given the reaction requires strictly anhydrous conditions, it is reasonable to assume the water content of the unpurified DABCO was at fault for the lack of conversion.

2.10 Ligand Screening

With our optimal base identified, we moved forward to ligand screening. The reaction proved more tolerant of variation of the ligand than base, with several phosphine ligands proving competent. In the course of our screening, we noted a trend of increased yield, conversion, and purity going from dppe to dppp to dppb. Curious to see if the pattern held, we explored the rest of

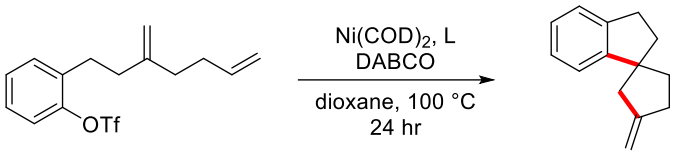

82 **83**

L	Bite ∠	Yield[a]	L	Bite ∠	Yield[a]
dppm	72°	20%	dppbz	83°	40%
dppe	85°	28%	binap	92°	54%
dppp	91°	45%	dppf	95°	57%
dppb	98°	56%	diop	97°	53%
dpppe	-	70%	dpephos	102°	70%
dpphex	-	60%	xantphos	107°	33%

Table 2.6 Ligand screening and the effect of ligand bite angle. [a]Yield determined by GC using dodecane as an internal standard. $Ni(COD)_2$ (10 mol%), L (12 mol%), DABCO (3 equiv.), dioxane (0.15 M), 100 °C, 24 hr.

this family of ligands using dppm, dpppe, and dpphex. The trend held up to dpppe, which proved to be the optimal ligand both in this series and overall, before the yield begins to drop off with dpphex. While DPEphos gave similar yields, dpppe gave product of similar purity as to what is observed with Pd with almost no isomerization products observed in the GC or ^{1}H NMR. The observed trend correlates well with the increasing bite angle of the bidentate ligands as shown in Table 2.6. Larger bite angle ligands are reported[47,48] to promote RE, but the exact rationale for why is understandably highly variable and dependent on the nature of the metal and type of

reaction in question. For example, larger bite angles force other substituents bound to the metal closer together.[47] This closer proximity can promote the reductive elimination in order to relieve strain or by leading the complex to adopt a structure closer to the transition state for a migratory-type reductive elimination.[49] However, that particular pathway is more relevant to cross-couplings than the assumed base-mediated reductive elimination of our system. A more applicable proposal is that larger bite angles destabilize the square planar Ni^{II} intermediates and in turn stabilize the tetrahedral Ni^{0} species.[48,50] Another possibility is that the deprotonation proceeds via a dissociative pathway with loss of one of the phosphines to yield a more reactive 3-center complex, which again proceeds more easily with larger bite angles ligand. The trend is most obvious in the dppm-dpphex series due to their similar structural features, but generally holds for the other bidentate phosphine ligands investigated as shown in Table 2.6 (full details in SI). The bite angle is however only predictive of a general trend and structural differences such as increased rigidity (dppe vs dppbz or dpephos vs xantphos) can lead to substantial differences in reactivity. Taken together, these results seem to suggest that the optimal range of ligand bite angle to prevent Ni-H isomerization is ~100-105˚. However, there is the important caveat that the particular requirements of any given Ni-Heck cascade could easily lead to this range changing in order to accommodate the balancing act of the different portions of the mechanism as well as off-cycle reactivity.

2.11 Solvent Screening

Solvent screening proved much less complex than the previous variables. Similarly to the monocyclization studies, ethereal solvents consistently performed well with DME once again proving the best. It is unclear the exact role the ethereal solvents are playing, with the most obvious being their ability to coordinate to and thus potentially stabilize or destabilize unspecified

intermediates in the cascade. Given that hypothesis, it is interesting to note that MeCN, a common solvent in the Pd-Heck, is completely incompetent in the reaction with poor yield and high rates of isomerization. Nitriles are known to coordinate to Ni complexes[51] and even promote reactivity by generating more active precatalysts,[52] but in this particular application even the addition of 1 equivalent of PhCN proved deleterious in most cases (Table S7).

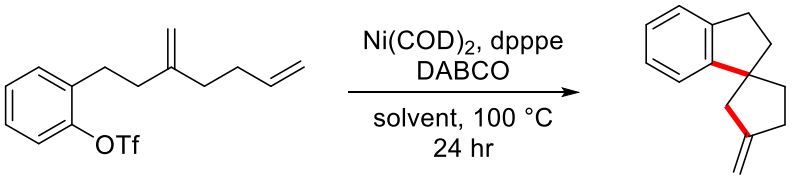

82 **83**

Entry	Solvent	Yield[a]
1	dioxane	70%
2	THF	69%
3	DME	76%
4	diglyme	73%
5	toluene	53%
6	MeCN	6%
7	DMF	21%

Table 2.7 Solvent screening. [a]Yield determined by GC using dodecane as an internal standard. $Ni(COD)_2$ (10 mol%), L (12 mol%), DABCO (3 equiv.), dioxane (0.15 M), 100 ° C, 24 hr.

2.12 Temperature Screening

We next tested the effect of the reaction temperature. The cascade proceeded smoothly at temperatures in the 23-100 ˚C range with 2-9% variation in yield. Increasing the temperature beyond 120 ˚C proceeded with not only a moderate 13% drop in yield, but also with increased amounts of observed isomerization. Surprisingly, the cascade even proceeded at 0 ˚C, though a prolonged 48 hr reaction time was required to ensure complete conversion. This result is noteworthy in part because Heck reactions run below 23 ˚C are quite rare.[8] Even more remarkable

is the fact that the suppression of Ni-H isomerization and Ni^0 regeneration proceed so smoothly despite its usual recalcitrance.

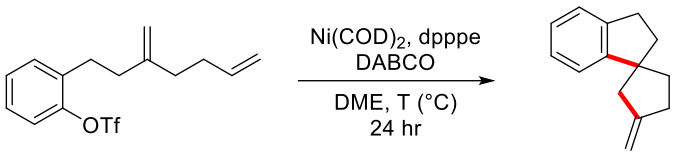

82 **83**

Entry	T (°C)	Conversion[a]	Yield[a]
1	0	100%	68%[b]
2	23	100%	74%
3	40	100%	68%
4	60	100%	68%
5	80	100%	67%
6	100	100%	76%
7	120	100%	63%

Table 2.8 Temperature screening. [a]Yield determined by GC using dodecane as an internal standard.[b]Reaction run for 48 hr $Ni(COD)_2$ (10 mol%), dpppe (12 mol%), DABCO (3 equiv.), DME (0.15 M), T (°C), 24 hr.

2.13 Catalyst Screening

While the screening of the catalyst source is usually a key component of the optimization of transition metal catalyzed reactions because our conditions require a Ni^0 source for initiation to occur, our options for Ni sources were relatively limited. Traditionally, $Ni(COD)_2$ is the Ni^0 source of choice[5] as it often exhibits the highest reactivity of the handful of Ni^0 sources readily available, as was the case in this study. As $Ni(COD)_2$ is air, moisture, and temperature sensitive, much Ni^0 catalysis has long been confined to the glovebox. In more recent years, however, considerable effort has been put into generating a bevy of new bench-stable Ni^0 precatalysts.[53–55] Many of these are Ni^{II} species that undergo a reduction to Ni^0 via thermal or chemical activation, which can add complications to an already sensitive reaction. For example, both the Jamison[56] and Doyle[55] precatalysts contain a chloride ligand, which means that activation via the thermal method would likely render our cationic pathway non-feasible due to the presence of an X type

ligand. Further, as a result of the reduction mechanism, the maximum theoretical yield of Ni^0 is 50% of the Ni^{II}. The Jamison group addressed this by utilizing an intramolecular Heck reaction to generate a Ni-H species that is subsequently deprotonated, but the synthesis of these precatalysts begins to become somewhat tedious.[54] This is especially true considering each ligand trial requires the synthesis of a different precatalyst. Recently though, both the Cornella group[57] and the Engle group[58] reported novel bench-stable Ni^0 sources, $Ni(^{F}stb)_3$ and Ni(COD)(DQ) respectively. We were very excited by these reports as it meant our Ni^0 catalysis may no longer

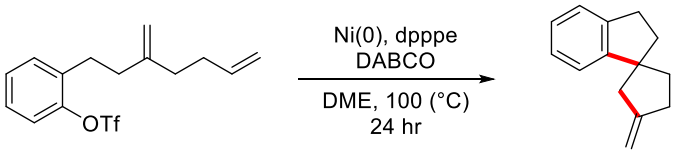

82 **83**

Entry	Ni Source	Conversion[a]	Yield[a]
1	$Ni(COD)_2$	100%	76%
2	$Ni(PPh_3)_4$	100%	70%
3	$Ni(^{F}stb)_3$	100%	63%
4	$Ni(^{F}stb)_3$	91%	47%[b]
5	Ni(COD)(DQ)	100%	64%
6	Ni(COD)(DQ)	0%	0%[b]

Table 2.9 Ni source screening. [a]Yield determined by GC using dodecane as an internal standard.[b]Reaction setup outside the glovebox Ni(0) (10 mol%), dpppe (12 mol%), DABCO (3 equiv.), DME (0.15 M), 100 °C, 24 hr.

require a glovebox. Both $Ni(^{F}stb)_3$ and Ni(COD)(DQ) proved to be comparably competent in the reaction, albeit giving slightly lower yields than $Ni(COD)_2$. Excitingly, $Ni(^{F}stb)_3$ gave a 47% yield when run using standard Schlenk techniques, showing the feasibility of work outside the glovebox. However, Ni(COD)(DQ) gave no reaction whatsoever, despite numerous attempts with increasingly stringent technique. In every attempt, the reaction started as a dark-red solution, visually identical to the reaction setup in the glovebox; however, after an hour of heating, the reaction was completely clear and colorless indicating the Ni^0 species was no longer present. Even upon extended heating, no reaction was observed. Given the comparable reactivity in the

glovebox, we suspect the issue arises from the different spectator ligands, which in the Ni(COD)(DQ) case apparently leads to a substantially more sensitive (dpppe)Ni^0 species.

2.14 Leaving Group Screening

The final variable to consider was the identity of the leaving group on the aryl ring. Both aryl chloride **88** and bromide **89** in the presence of TESOTf,[26] which acts as a halide scavenger, gave **83** in moderate yields, but of similar purity to what was observed with **82**. The efficacy of the aryl chloride is a good example of how Ni excels at oxidative addition.[1] It should be noted

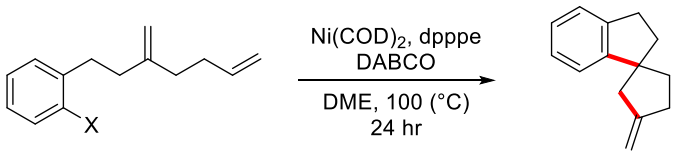

83

Compound	X	TESOTf (equiv.)	Yield[a]
82	OTf	0	76%
88	Cl	2	54%
89	Br	2	49%
90	I	2	12%
91	OTs	0	30%
92	OMs	0	20%
93	ONf	0	76%

Table 2.10 Leaving group screening. [a]Yield determined by GC using dodecane as an internal standard. $Ni(COD)_2$ (10 mol%), dppe (12 mol%), DABCO (3 equiv.), DME (0.15 M), 100 (°C), 24 hr.

that attempts to utilize aryl halides in the absence of a halide scavenger yielded little to no conversion and no product formation, indicating the importance of the cationic pathway to our conditions. However, attempts to use less active partners such as aryl ethers or pivalates proved unsuccessful, which is not entirely surprising as these partners generally require higher temperatures.[59] For sulfonates, only the nonaflate gave comparable yield to the triflate with mesylates and tosylates performing poorly.

2.15 Comparison to Literature Conditions

With our optimized conditions in hand, we wanted to see how they would fare compared to both the Pd-Heck[60,61] as well as literature reported conditions[20,22,26,59,62,63] for the Ni-Heck reaction. Pleasingly, our Ni conditions compare favorably to Overman's Pd conditions, giving **83** in comparable yield and purity. Furthermore, our conditions compared even more favorably to

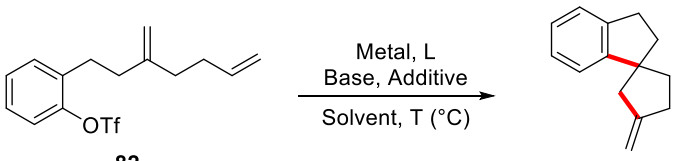

82 **83**

Entry	Metal	Ligand	Base	Additive	Solvent	T (°C)	Conversion[a]	Yield
1	$Ni(COD)_2$	dpppe	DABCO	-	DME	23	100%	76%[b]
2	$Pd(OAc)_2$	PPh_3	Ag_2CO_3	-	MeCN	23	100%	80%[b,c]
3	$Ni(COD)_2$	Triphos	TMP	-	toluene	110	52%	13%[a]
4	$Ni(COD)_2$	DPPF	K_3PO_4	-	toluene	125	69%	7%[a]
5	$Ni(COD)_2$	DPPF	Cy_2NMe	-	dioxane	100	63%	9%[a]
6	$Ni(COD)_2$	d(Cyp)pb	DABCO	-	toluene	60	16%	11%[a]
7	$Ni(COD)_2$	DPEPhos	KO*t*Bu	-	toluene	80	100%	4%[a]
8	$NiCl_2(PnBu_3)_2$	-	Na_2CO_3	Mn	DMF	60	28%	7%[a]

Table 2.11 Comparison of our conditions to literature reported Pd- and Ni-Heck conditions. [a]determined by GC using dodecane as an internal standard [b]isolated yields [c]ArI was used instead of ArOTf.

literature reported base-mediated Ni-Heck conditions (Table 2.11 Entry 3-7). In all cases the yields of the previously reported conditions were below 15%, and all except for Jamison's conditions (entry 6) exhibited high degrees of isomerization. Reducing metal conditions[22] also proved completely ineffective with the triflate **82** with poor yield and conversion. These results and the results of our optimization efforts illustrate both the power of our conditions as well as the sensitivity and challenge of Ni-Heck cascades.

2.16 Testing the Limit of Olefin Isomerization Suppression

To further probe how effective our conditions were at preventing Ni-H isomerization, we utilized an allyl containing substrate **94** based on the isomerization of a similar substrate observed

by the Skrydstrup group.[20] **94** is a particularly challenging substrate upon which to suppress olefin isomerization as the Ni-H should be readily able to insert into the unhindered terminal olefin. The availability of this reactive site, coupled with the significant thermodynamic drive for the formation of the conjugated disubstituted styrene, account for the ready isomerization of the olefin.

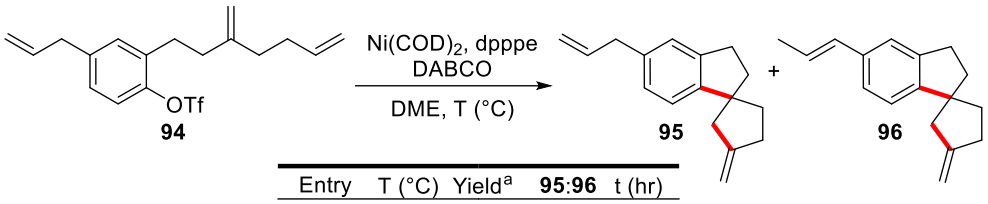

Entry	T (°C)	Yield[a]	**95**:**96**	t (hr)
1	100	93%	>1:20	4
2	23	97%	6:1	24
3	0	96%	20:1	48

Table 2.12 Testing our conditions ability to suppress Ni-H mediated isomerization:[a] isolated yields; $Ni(COD)_2$ (10 mol%), dpppe (12 mol%), DABCO (3 equiv.), DME (0.15 M).

We ran our first experiment at 100 ˚C to mimic the conditions of the Skrydstrup case, and while the cyclization was highly efficient, so was the isomerization giving the styrene **96** in a >20:1 ratio. Pleasingly, running the reaction at 23 ˚C maintained the yield, and now gave allyl **95** as the major product in a 6:1 ratio. Further reducing the reaction temperature to 0 ˚C almost completely suppressed the isomerization, albeit with a prolonged reaction time. It is intriguing to note that our conditions can readily suppress the isomerization of the 1,1-disubstituted olefin in **96** even at 100 ˚C, but **95**'s allyl group is so sensitive to the Ni-H that even 23 ˚C is insufficient to completely suppress it. The complete reversal of selectivity caused by the tuning of one variable deftly demonstrates the complexity of these cascades and the difficulty of balancing the competing pathways.

2.17 Cascade Scalability

As a final test of the robustness of our conditions, we wanted to see how the cascade of **82** would perform at larger scales. Pleasingly, at a 10 mmol scale the reaction provided the best yield

for the cascade observed so far at an excellent 87%, with identical purity to that observed at the 0.1 mmol scale.

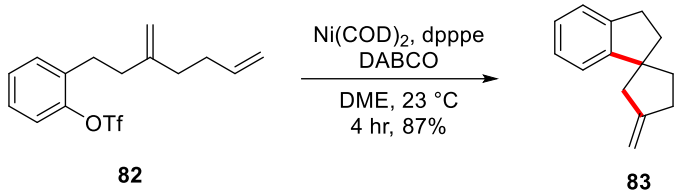

Scheme 2.15 Scale up of optimized intramolecular Ni-Heck cascade. $Ni(COD)_2$ (10 mol%), dpppe (12 mol%), DABCO (3 equiv.), DME (0.15 M), 23 °C, 4 hr, 87%.

2.18 Mechanistic Probing

As mentioned previously, mechanisms in Ni catalysis can be notoriously difficult to discern due to Ni's ability to undergo a variety of $1e^-$ pathways. However, we suspected that the reaction was likely proceeding via a Ni^0/Ni^{II} cycle similar to that invoked for the classical Pd-Heck. Our screening attempts indicate that the catalyst regeneration likely proceeds via deprotonation given the importance of the choice of base and the fact that X^- type ligands, which would force the

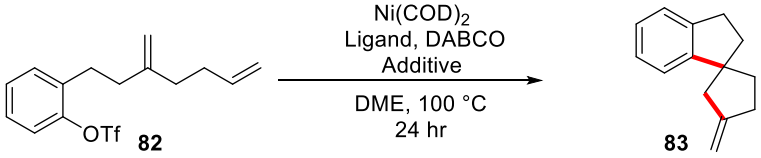

Entry	Ligand	Additive	Equiv.	Conversion[a]	Yield[a]
1	DPEphos	nBu$_4$NOAc	0.2	42%	4%
2	dpppe	TEMPO	1	10%	0%
3	dpppe	Galvinoxyl	1	3%	0%
4	dpppe	BHT	1	100%	76%
5	dpppe	DHA	1	100%	68%
6	dpppe	DPE	1	100%	65%

Table 2.13 Probing the Ni-Heck cascade mechanism: [a]determined by GC using dodecane as an internal standard; $Ni(COD)_2$ (10 mol%), L (12 mol%), additive (0.2-1.0 equiv.), DME (0.15 M), 100 °C, 24 hr.

reaction to proceed via the neutral mechanism, lead to substantially more isomerization occurring. However, the cyclizations could be occurring via a radical pathway due to Ni-C homolytic cleavage, which is known to occur readily.[2] As such, we wanted to test for the presence of any

radical intermediates or character in the reaction. We conduct our standard cascade in the presence of a variety of radical traps namely TEMPO, galvinoxyl free radical, butylated hydroxy toluene (BHT), 9,10-dihydroanthracene (DHA), and 1,1-diphenylethylene (DPE). Both TEMPO and galvinoxyl completely shut down the reaction, with no product formation observed and almost no conversion of starting material. However, no TEMPO adducts were detected on TLC, NMR, or MS suggesting that a C centered radical was not trapped in the reaction. Instead, we propose that the electron rich Ni^0 species either formed a complex with the TEMPO[64] and galvinoxyl or underwent a $1e^-$ pathway to yield an unreactive Ni^I species. Additionally, the $H^\bullet$ donors BHT and DHA had no effect on the reaction and the radical acceptor DPE behaved similarly. These collective finding seem to suggest that the reaction does not proceed via radical intermediates, or at least long-lived radical intermediates. While this agrees with our proposed Ni^0/Ni^{II} cycle, more in depth studies are required to conclusively prove the exact mechanism.

2.19 Aryl Triflate Substrate Scope

Next, our attention turned to examine the substrate scope of the Ni-Heck cascade. Many of the substrates we chose are pulled from or inspired by the Pd-Heck literature. Beyond easing the design portion of the project, this cohort was chosen to see how Ni performs in a variety of different cascade variants with readily available benchmarks for comparison. Further, in the event that Ni's distinct chemical properties might lead to complementary reactivity to the Pd-Heck, the comparisons would allow us to quickly identify and pursue those directions.

To start, the range of ring sizes that could be easily accessed was explored. We were able to access the 5,6-spirocycle **98** in good yield, albeit slightly lower than that reported by Overman. Attempts to extend the scope and access 5,7-spirocycle **100** were unsuccessful as competing

pathways such as a [6-*endo*-trig] cyclization leading to dihydronapthalene **101** and complex product mixtures. While disappointing, this result provides another concise illustration of how

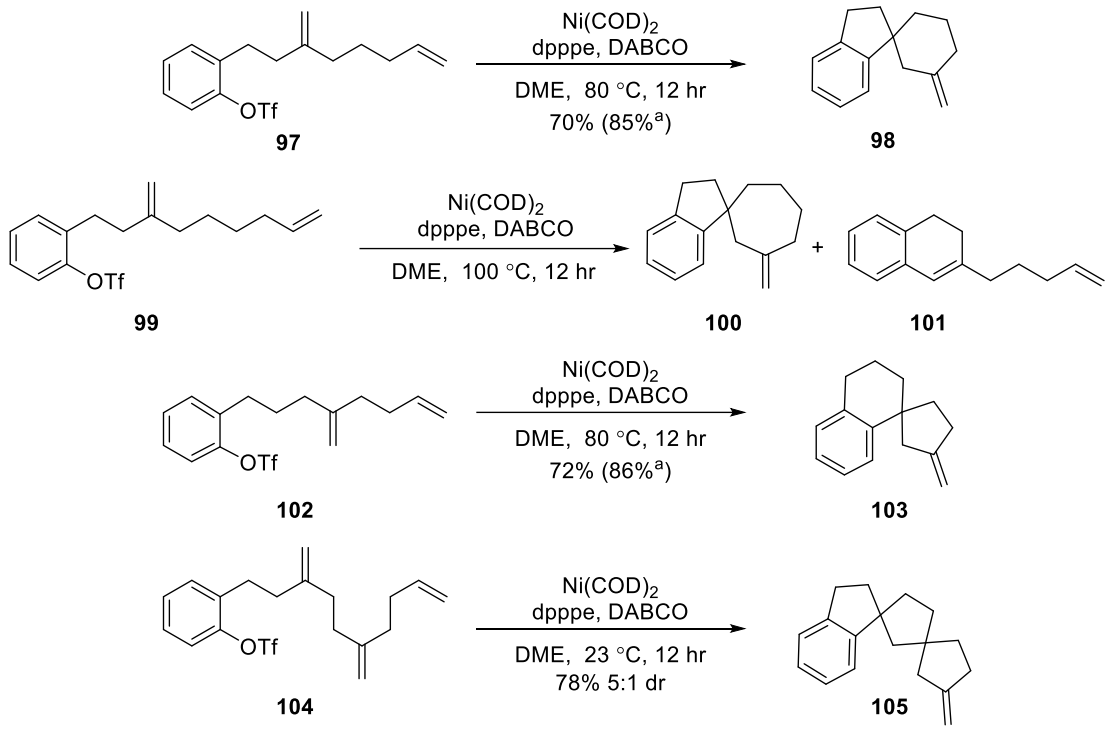

Scheme 2.16 Scope of spirocyclic ring formation from ArOTf: (XX%) are from corresponding literature examples; [a]ArI used instead of ArOTf; $Ni(COD)_2$ (10 mol%), dpppe (12 mol%), DABCO (3 equiv.), DME (0.15 M).

these cascade intermediates exist in an equilibrium. Even if one pathway in the initial step is energetically preferable a sufficiently unfavorable downstream barrier can lead to reversal of observed selectivity at the earlier step. Pleasingly, we were able to access the 6,5-spirocycle **103** in good yield. Attempts to access 6,6 and higher spirocycles yielded similar complex mixtures to what was observed with **99**. The cascade could be extended to a tricyclization to give 5,5,5-spirocycle **105** in 78% yield and a 5:1 dr. The dr is notable as tricyclizations with Pd proceed with a 1:1 dr.[60]

Beyond spirocycles, fused ring systems are also products of interest. When triflate **106** was utilized we accessed a 3:1 mixture of diene **107** and tricycle **108**, which shows a modest increase in selectivity compared to the Pd example[61,65] which gave **107** and **108** in a 1.5:1 ratio.

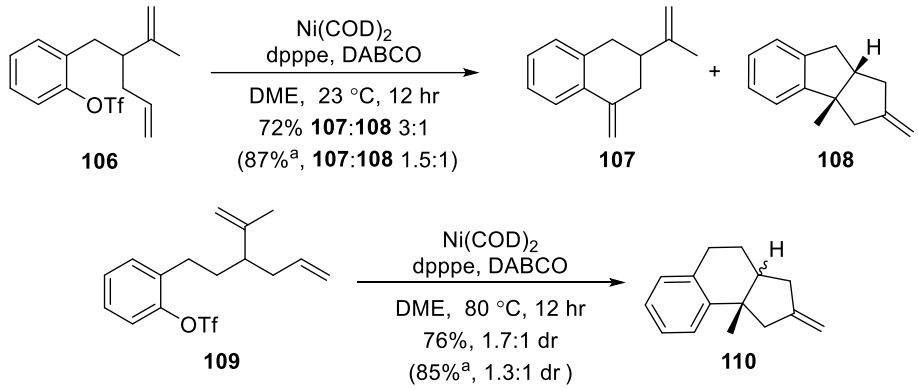

Scheme 2.17 Scope of fused ring formation. (XX%) are from corresponding literature examples. [a]ArI used instead of ArOTf.

We attributed the stronger preference for **197** to the increased steric discrimination of the Ni species[1,43] relative to Pd, which leads the less demanding monosubstituted olefin to be the favored coupling partner. By using the related triflate **109** the homologation prevented any 7-membered ring formation from occurring and the desired 6,5-fused product **110** was formed in a good 76% yield in a 1.7:1 dr.[66]

2.20 Vinyl Triflate Scope

Vinyl triflate **111** proved to be an excellent substrate giving the desired 5,5-spirocycle 112 in a 90% yield in >20:1 d.r., a marked improvement in yield from analogous Pd results.[60] Triflate **113** which arises from a 1,3-diketone was also an effective substrate giving the desired spirocycle **114** in good yield with only a trace amount of a dienone arising from an initial 6-endo-trig cyclization as was observed with Pd.[60] Cycloheptanone derived vinyl triflate **115** gave the desired vinyl cyclopropane **116** in a moderate yield, but without any alkene isomerization observed. The lack of isomerization is especially notable as in the literature report with Pd,[67] the product was

isolated as a 1:1 mixture of **116** and alkene isomers **117**. Even though a triflate was already being used, a full equivalent of the highly toxic $TlNO_3$, usually used as a halide scavenger, was required to suppress Pd-H isomerization, which highlights the challenge isomerization poses even for Pd.

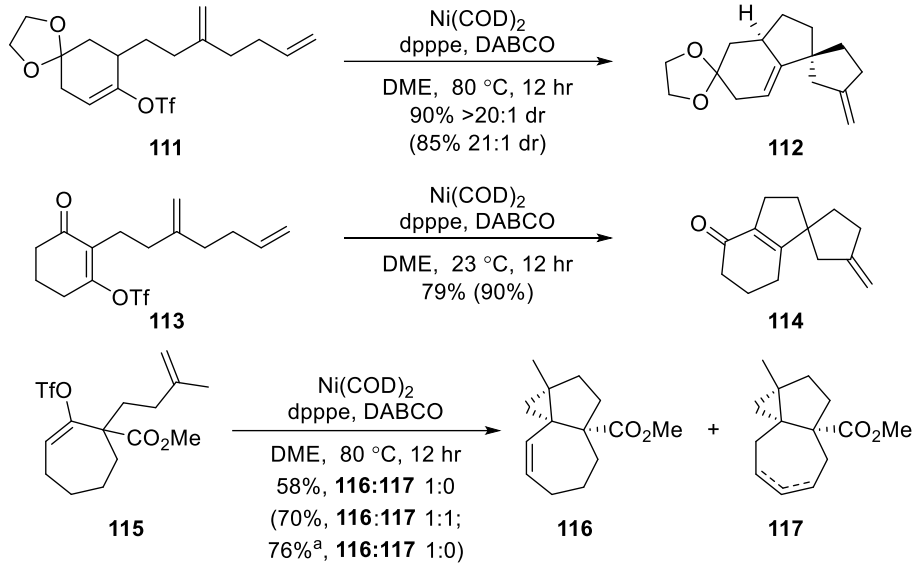

Scheme 2.18 Scope of vinyl triflate substrates. (XX%) are from corresponding literature examples.[a]1 equiv. of $Tl(NO_3)_3$ used.

2.21 Applications in Total Synthesis

Having shown the efficacy of our conditions in a variety of Heck cascades, we wondered how Ni would fare on more challenging substrates from the natural product literature. Our first substrate was from the Keay group's synthesis of (+)-xestoquinone, where they used triflate

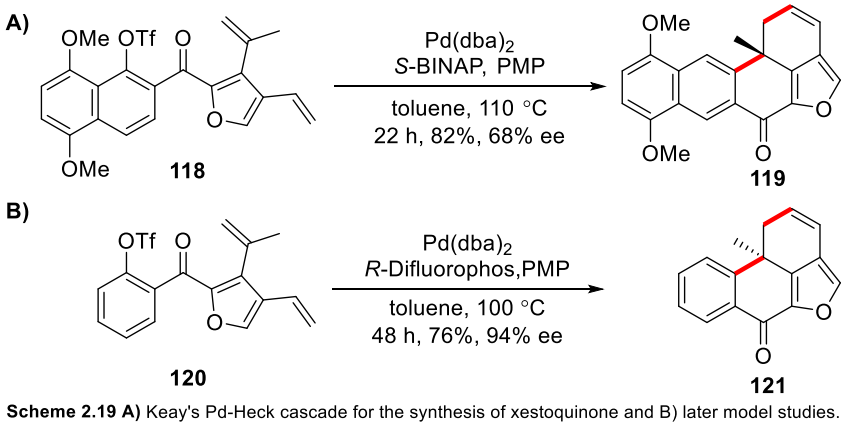

Scheme 2.19 A) Keay's Pd-Heck cascade for the synthesis of xestoquinone and B) later model studies.

120 as a model system for their key step.[68,69] Our standard conditions suffered from poor conversion and gave a low yield of **121,** as well as reduction and dimerization products. A brief screening of conditions (full details in experimental) led us to adapt our conditions to emulate those Keay reported[69] previously which effectively suppressed the competing pathways. The key changes being running the reaction under μW conditions, which drastically shortened reaction times, and at low concentrations (0.05 M) to favor intramolecular pathways and avoid biphenyl

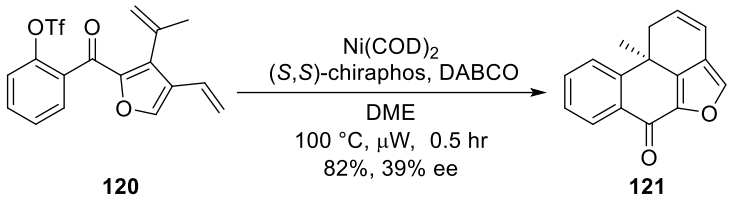

Scheme 2.20 Optimized conditions for Ni-Heck cascade of Keay's model system. $Ni(COD)_2$ (10 mol%, (S,S)-chiraphos (12 mol%), DABCO (3 equiv.) DME (0.05 M), 100 ° C, μW, 0.5 hr, 82%, 39% ee.

formation. In order to render the reaction enantioselective, we screened a variety of chiral bidentate phosphine ligands (full details in experimental) and were able to access the desired tetracycle **121** in an 82% yield with 39% *ee* using (*S*,*S*)-chiraphos. While the *ee* was only modest, it should be noted that this is a particularly challenging cascade to render enantioselective with the Keay group publishing numerous studies on the subject.

Our next target is indenone **124** from the Sarpong group's synthesis of pauciflorol F.[70] While the reaction is not technically a Heck cascade, rather a Larock annulation, it proceeds by the overall same mechanism. Further, the Kong group's recent report has a related Ni-cascade that yields indanones **126** and **127** via a hydrogen borrowing mechanism, which would provide our first Ni comparison. The Larock annulation of triflate **128** and alkyne **123** proceeded cleanly under our standard conditions, giving **124** and **125** in a combined modest 46%, but in a 3:1 rr favoring the desired **124**. DPEPhos proved to be a superior ligand to dpppe giving the desired indenone **124**

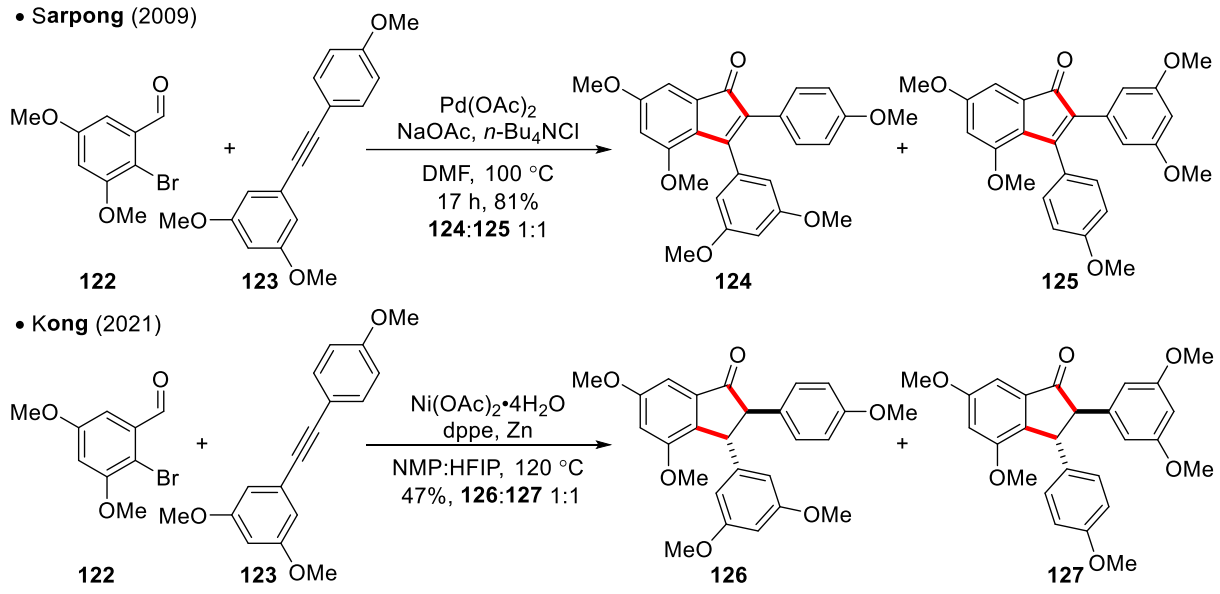

Scheme 2.21 Previous Heck cascade syntheses of pauciflorol **F.**

in an improved 78% yield and a comparable 2.9:1 rr. The rr is a considerable improvement to the 1:1 ratio reported by both Sarpong[70] and the Kong group.[38] As the Kong group also used Ni, we suspect the improvement is not arising from the use of Ni, but rather the triflate. The cationic pathway is well known to improve regioselectivity in the Pd-Heck reaction of electron rich olefins and is likely playing a similar role in this instance.[8,71] The efficacy of the reaction is also of note based on Ni's previously reported[26] reticence to react with sterically encumbered aryl sulfonates.

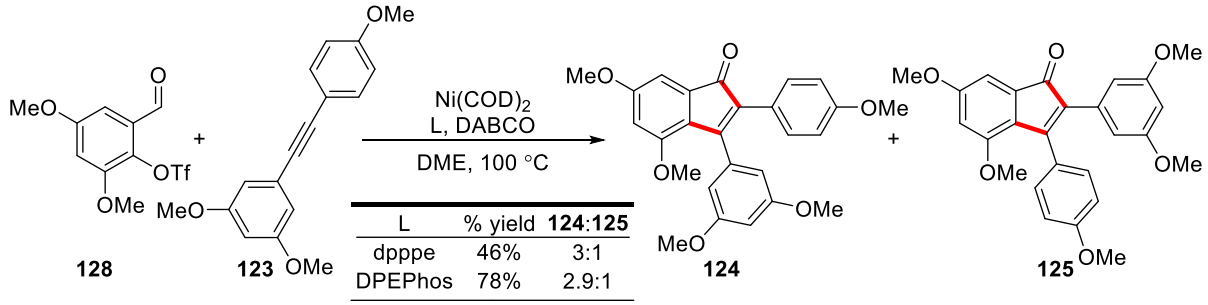

Scheme 2.22 Synthesis of **124** using our condtiions:**128** (1 equiv.), **123** (2 equiv.), $Ni(COD)_2$ (10 mol%), L (12 mol%), DABCO (3 equiv.), DME (0.15 M), 100 °C, 12 hr, 78%, **124**:**125** 2.9:1.

Moving onto vinyl triflate substrates, we decided to attempt the cascade from our group's synthesis of presilphiperfolanol.[72] Unfortunately, triflate **129** gave none of the desired tricycle

130 instead giving a mixture in which triene **131** was the major component. Screening of several phosphine ligands gave no improvement. The exact issue preventing the cascade from succeeding

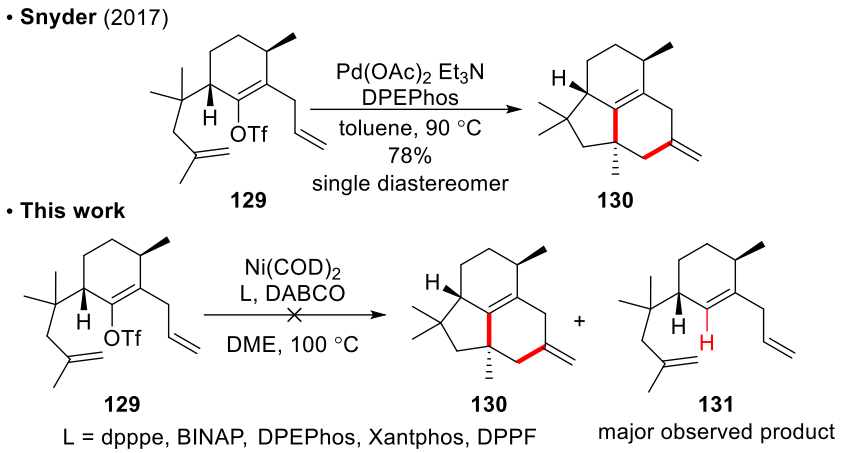

Scheme 2.23 Attempted Ni-Heck cascade of **131**: $Ni(COD)_2$ (10 mol%), L (12 mol%), DABCO (3 equiv.), DME (0.15 M), 100 °C, 12 hr.

remains unclear to us. Oxidative addition was evidently proceeding smoothly given the lack of signals in the ^{19}F NMR of the crude material. As such either one of the subsequent migratory insertion steps or the terminating β-hydride elimination is too challenging for Ni to accomplish. Further attempts to achieve the cascade were unsuccessful and it remains a limitation of the method.

To conclude our studies, we returned to our retigeranic acid A cascade. As the reader will recall, our hypothesis had been that Ni's ability to undergo migratory insertion more facilely and its slower β-hydride elimination might allow us to finally achieve our desired [*6-exo-dig*] cyclization. In our first attempt with the TMS-alkyne **132** and our standard conditions, we were somewhat surprised to observe no reaction whatsoever with only unreacted starting material being observed. After double checking the quality of our reagents, we resubjected **132** to the reaction and observed the same result. Attempting the reaction with a bevy of phosphine ligands, higher temperatures, or with the ynoate substrate **133** yielded no changes. The apparent inability of the

Ni species to undergo oxidative addition into is particularly striking given that the cascade with **115** proceeds smoothy. Even though **129** did not undergo the cascade, the oxidative addition was successful on a substrate that is arguably as or even more hindered than **132** and **133**.

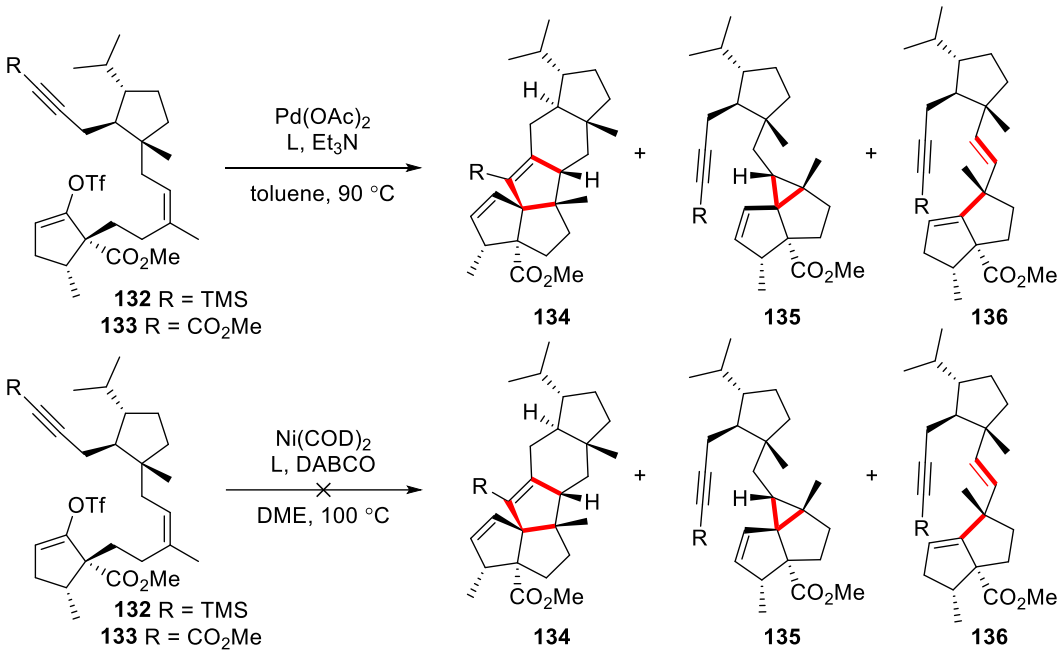

Scheme 2.24 Attempted Ni-Heck cascade towards retigeranic acid A

2.22 Conclusion

This chapter presents our group's more recent contribution to the Heck literature and our first foray into Ni catalysis. By successfully identifying the key issue for base-mediated Ni-Heck cascades as Ni's reluctance to undergo reductive elimination, we were able to develop a set of general conditions for both aryl and vinyl triflates that promote reductive elimination and thus effectively suppress Ni-H mediated isomerization. With these conditions, we were able to show the Ni can perform a wide variety of different Heck cascades often in comparable and in some cases superior yields or selectivities to Pd. The challenges posed by **129**, **132**, and **133** show that significant work remains in order to expand the scope of the Ni-Heck to match its cousin's advanced state of development. Further, these studies set the stage for our subsequent work with

Ni where we made some of the most intriguing and exciting discoveries of my graduate career as will be discussed in the next chapter.

2.23 References

[1] S. Z. Tasker, E. A. Standley, T. F. Jamison, *Nature* **2014**, *509*, 299–309.

[2] V. P. Ananikov, *ACS Catal.* **2015**, *5*, 1964–1971.

[3] H. Pellissier, *Adv. Synth. Catal.* **2015**, *357*, 2745–2780.

[4] S. Bhakta, T. Ghosh, *Adv. Synth. Catal.* **2020**, *362*, 5257–5274.

[5] A. L. Clevenger, R. M. Stolley, J. Aderibigbe, J. Louie, *Chem. Rev.* **2020**, *120*, 6124–6196.

[6] J. Diccianni, Q. Lin, T. Diao, *Acc. Chem. Res.* **2020**, *53*, 906–919.

[7] D. J. Weix, *Acc. Chem. Res.* **2015**, *48*, 1767–1775.

[8] I. P. Beletskaya, A. V. Cheprakov, *Chem. Rev.* **2000**, *100*, 3009–3066.

[9] Bo-Lin Lin, Lei Liu, Yao Fu, Shi-Wei Luo, Qian Chen, Q.-X. Guo, *Organometallics* **2004**, *23*, 2114.

[10] C. A. Tolman, W. C. Seidel, D. H. Gerlach, *J. Am. Chem. Soc.* **2002**, *94*, 2669–2676.

[11] M. D. Leatherman, S. A. Svejda, L. K. Johnson, M. Brookhart, *J. Am. Chem. Soc.* **2003**, *125*, 3068–3081.

[12] L. K. Johnson, C. M. Killian, M. Brookhart, *J. Am. Chem. Soc.* **2002**, *117*, 6414–6415.

[13] B. Fiser, J. M. Cuerva, E. Gómez-Bengoa, *Organometallics* **2018**, *37*, 390–395.

[14] D. G. Musaev, K. Morokuma, *Top. Catal. 1999 71* **1999**, *7*, 107–123.

[15] G. P. Boldrini, D. Savoia, E. Tagliavini, C. Trombini, A. U. Ronchi, *J. Organomet. Chem.*

1986, *301*, C62–C64.

[16] S. A. Lebedev, V. S. Lopatina, E. S. Petrov, I. P. Beletskaya, *J. Organomet. Chem.* **1988**, *344*, 253–259.

[17] S. Iyer, C. Ramesh, A. Ramani, *Tetrahedron Lett.* **1997**, *38*, 8533–8536.

[18] R. H. Morris, *J. Am. Chem. Soc.* **2014**, *136*, 1948–1959.

[19] L. E. Hanna, E. R. Jarvo, *Angew. Chemie Int. Ed.* **2015**, *54*, 15618–15620.

[20] T. M. Gøgsig, J. Kleimark, S. O. Nilsson Lill, S. Korsager, A. T. Lindhardt, P.-O. Norrby, T. Skrydstrup, *J. Am. Chem. Soc.* **2012**, *134*, 443–452.

[21] J. M. Medina, J. Moreno, S. Racine, S. Du, N. K. Garg, *Angew. Chemie Int. Ed.* **2017**, *56*, 6567–6571.

[22] J.-N. Desrosiers, L. Hie, S. Biswas, O. V. Zatolochnaya, S. Rodriguez, H. Lee, N. Grinberg, N. Haddad, N. K. Yee, N. K. Garg, C. H. Senanayake, *Angew. Chemie Int. Ed.* **2016**, *55*, 11921–11924.

[23] X. Qin, M. W. Y. Lee, J. S. Zhou, *Angew. Chemie Int. Ed.* **2017**, *56*, 12723–12726.

[24] A. García-Domínguez, Z. Li, C. Nevado, *J. Am. Chem. Soc.* **2017**, *139*, 6835–6838.

[25] B. R. Walker, C. S. Sevov, *ACS Catal.* **2019**, *9*, 7197–7203.

[26] S. Z. Tasker, A. C. Gutierrez, T. F. Jamison, *Angew. Chemie Int. Ed.* **2014**, *53*, 1858–1861.

[27] Q. Lin, T. Diao, *J. Am. Chem. Soc* **2019**, *141*, 25.

[28] S. KC, R. K. Dhungana, N. Khanal, R. Giri, *Angew. Chemie* **2020**, *132*, 8124–8128.

[29] Y. Jin, C. Wang, *Angew. Chemie Int. Ed.* **2019**, *58*, 6722–6726.

[30] Y. Li, K. Wang, Y. Ping, Y. Wang, W. Kong, *Org. Lett.* **2018**, *20*, 921–924.

[31] K. Wang, Z. Ding, Z. Zhou, W. Kong, *J. Am. Chem. Soc.* **2018**, *140*, 12364–12368.

[32] A. de Meijere, P. von Zezschwitz, S. Bräse, *Acc. Chem. Res.* **2005**, *38*, 413–422.

[33] T. Vlaar, E. Ruijter, R. V. A. Orru, *Adv. Synth. Catal.* **2011**, *353*, 809–841.

[34] A. B. Dounay, L. E. Overman, *Chem. Rev.* **2003**, *103*, 2945–2963.

[35] K.-C. Kong, C.-H. Cheng, *J. Chem. Soc. Chem. Commun.* **1991**, 423–424.

[36] K. C. Kong, C. H. Cheng, *Organometallics* **2002**, *11*, 1972–1975.

[37] P. Shukla, C. H. Cheng, **2006**, DOI 10.1021/OL061051P.

[38] T. Ma, Y. Chen, Y. Li, Y. Ping, W. Kong, *ACS Catal.* **2019**, *9*, 9127–9133.

[39] F. Liu, Y. Li, X. Wang, Q. Qiang, Z. Yan, Y. Zhang, Z.-Q. Rong, *Org. Chem. Front.* **2021**, *8*, 3847–3852.

[40] J.-N. Desrosiers, J. Wen, S. Tcyrulnikov, S. Biswas, B. Qu, L. Hie, D. Kurouski, L. Wu, N. Grinberg, N. Haddad, C. A. Busacca, N. K. Yee, J. J. Song, N. K. Garg, X. Zhang, M. C. Kozlowski, C. H. Senanayake, *Org. Lett.* **2017**, *19*, 3338–3341.

[41] J. S. Zhou, X. Huang, S. Teng, Y. R. Chi, *Chem. Commun.* **2021**, *57*, 3933–3936.

[42] **N.d.**

[43] V. P. Ananikov, *ACS Catal.* **2015**, *5*, 1964–1971.

[44] I. M. Kolthoff, M. K. Chantooni, S. Bhowmik, *J. Am. Chem. Soc.* **1968**, *90*, 23–28.

[45] R. L. Benoit, D. Lefebvre, M. Fréchette, *Can. J. Chem.* **1987**, *65*, 996–1001.

[46] U. V. Mallavadhani, *Encycl. Reagents Org. Synth.* **2001**, DOI 10.1002/047084289X.RD010M.

[47] P. Dierkes, P. W. N. M. van Leeuwen, *J. Chem. Soc. Dalt. Trans.* **1999**, 1519–1530.

[48] M. N. Birkholz, Z. Freixa, P. Van Leeuwen, *Chem. Soc. Rev.* **2009**, *38*, 1099–1118.

[49] † Erik Zuidema, †,‡ and Piet W. N. M. van Leeuwen, ‡,§ Carles Bo*, *Organometallics* **2005**, *24*, 3703–3710.

[50] S. Otsuka, *J. Organomet. Chem.* **1980**, *200*, 191–205.

[51] A. L. Clevenger, R. M. Stolley, N. D. Staudaher, N. Al, A. L. Rheingold, R. T. Vanderlinden, J. Louie, *Organometallics* **2018**, *37*, 3259–3268.

[52] S. Ge, R. A. Green, J. F. Hartwig, *J. Am. Chem. Soc.* **2014**, *136*, 1617–1627.

[53] N. Hazari, P. R. Melvin, M. M. Beromi, *Nat. Rev. Chem. 2017 13* **2017**, *1*, 1–16.

[54] J. M. Weber, A. R. Longstreet, T. F. Jamison, *Organometallics* **2018**, *37*, 2716–2722.

[55] J. D. Shields, E. E. Gray, A. G. Doyle, *Org. Lett.* **2015**, *17*, 2166–2169.

[56] E. A. Standley, S. J. Smith, P. Müller, T. F. Jamison, *Organometallics* **2014**, *33*, 2012–2018.

[57] L. Nattmann, R. Saeb, N. Nöthling, J. Cornella, *Nat. Catal.* **2020**, *3*, 6–13.

[58] V. T. Tran, Z. Q. Li, O. Apolinar, J. Derosa, M. V. Joannou, S. R. Wisniewski, M. D. Eastgate, K. M. Engle, *Angew. Chemie - Int. Ed.* **2020**, *59*, 7409–7413.

[59] A. R. Ehle, Q. Zhou, M. P. Watson, *Org. Lett.* **2012**, *14*, 1202–1205.

[60] L. E. Overman, M. M. Abelman, D. J. Kucera, V. D. Tran, D. J. Ricca, *Pure Appl. Chem.* **1992**, *64*, 1813–1819.

[61] M. M. Abelman, L. E. Overman, *J. Am. Chem. Soc.* **1988**, *110*, 2328–2329.

[62] J. K. Vandavasi, X. Y. Hua, H. Ben Halima, S. G. Newman, *Angew. Chemie - Int. Ed.* **2017**, *56*, 15441–15445.

[63] H. Long, K. Xu, S. Chen, J. Lin, D. Wu, B. Wu, X. Tian, L. Ackermann, *Org. Lett.* **2019**, *21*, 3053–3056.

[64] D. Isrow, B. Captain, *Inorg. Chem.* **2011**, *50*, 5864–5866.

[65] A. Ali, G. B. Gill, G. Pattenden, G. A. Roan, T. S. Kam, *J. Chem. Soc. - Perkin Trans. 1* **1996**, 1081–1093.

[66] A. Ali, G. B. Gill, G. Pattenden, G. A. Roan, T.-S. Kam, *J. Chem. Soc. Perkin Trans. 1* **1996**, 1081.

[67] R. Grigg, U. Sakee, V. Sridharan, S. Sukirthalingam, R. Thangavelauthum, *Tetrahedron* **2006**, *62*, 9523–9532.

[68] S. P. Maddaford, N. G. Andersen, W. A. Cristofoli, B. A. Keay, *J. Am. Chem. Soc.* **1996**, *118*, 10766–10773.

[69] D. Lucciola, B. Keay, *Synlett* **2011**, *2011*, 1618–1622.

[70] J. L. Jeffrey, R. Sarpong, *Org. Lett.* **2009**, *11*, 5450–5453.

[71] J. Ruan, J. Xiao, *Acc. Chem. Res.* **2011**, *44*, 614–626.

[72] P. Hu, S. A. Snyder, *J. Am. Chem. Soc.* **2017**, *139*, 5007–5010.

2.24 Experimental Section

General Information All reactions outside of the glovebox were carried out under a nitrogen atmosphere with dry solvents under anhydrous conditions using standard Schlenk technique, unless otherwise noted. All glove box reactions were carried out under a nitrogen atmosphere with dry solvents degassed by freeze-pump-thaw and stored in sealed Schlenk flasks over 4 Å molecular sieves. Dry tetrahydrofuran (THF), toluene, diethyl ether (Et_2O) dichloromethane (CH_2Cl_2), and acetonitrile (CH_3CN) were obtained by passing commercially available pre-dried, oxygen-free formulations through activated alumina columns. Dry dimethoxyethane (DME) and 1,4-dioxane were prepared by distillation from Na/benzophenone. Reagents were purchased at the highest commercial quality and used without further purification, unless otherwise stated. 1,4-diazabicyclo[2.2.2]octane (DABCO), quinuclidine, urotropine, imidazole, triazabicyclodecene (TBD), and 7-Methyl-1,5,7-triazabicyclo[4.4.0]dec-5-ene (MeTBD) were purified via sublimation. 1,8-diazobicyclo[5.4.0]undec-7-ene (DBU), Et_3N, and *i*-Pr_2NEt were distilled from CaH_2. $Ni(COD)_2$ and 1,5-bis(diphenylphosphine)pentane (dpppe) were purchased from Strem. Yields refer to chromatographically and spectroscopically (^1H and ^{13}C NMR) homogeneous materials, unless otherwise stated. Reactions were magnetically stirred and monitored by thin-layer chromatography (TLC) carried out on 0.25 mm E. Merck silica gel plates (60F-254) using UV light as visualizing agent, and an ethanolic solution of phosphomolybdic acid and cerium sulfate or a solution of $KMnO_4$ in aq. $NaHCO_3$ and heat as developing agents. SiliCycle silica gel (60, academic grade, particle size 0.040–0.063 mm) was used for flash column chromatography. Preparative thin-layer chromatography separations were carried out on 0.50 mm E. Merck silica gel plates (60F-254). NMR spectra were recorded on Bruker 500 MHz or 400 MHz instruments and calibrated using residual undeuterated solvent as an internal reference. The following

abbreviations were used to explain the multiplicities: s = singlet, d = doublet, t = triplet, q = quartet, br = broad, app = apparent. IR spectra were recorded on a Perkin-Elmer 1000 series FT-IR spectrometer. High-resolution mass spectra (HRMS) were recorded on Agilent 6244 Tof-MS using ESI (Electrospray Ionization). All *ee* measurements were determined by HPLC on Daicel Chiralcel or Chiralpak columns.

Synthesis of Triflate 82

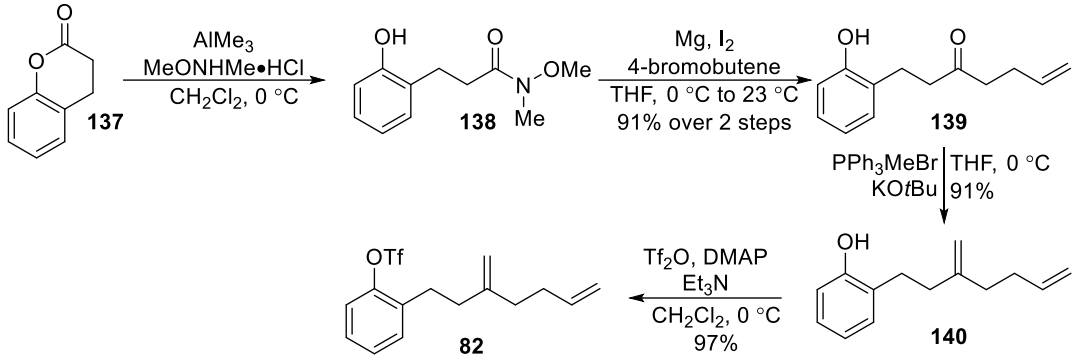

General Procedure A: Weinreb amide 138

To a flask was added MeONHMe•HCl (9.75 g, 100 mmol, 2.5 equiv.) followed by CH_2Cl_2 (80 mL) and the resultant suspension was cooled to 0 °C. An exit needle was placed in the septa and then $AlMe_3$ (50.0 mL, 2.0 M in hexanes, 2.5 equiv.) was added dropwise over the course of 10 min (Warning: substantial gas evolution was observed!). Once the addition was complete, the exit needle was removed, and the now colorless solution was stirred at 0 °C for 1 h. Dihydrocoumarin **137** (5.06 mL, 40.0 mmol, 1.0 equiv.) was then added dropwise over the course of 5 min and the resultant colorless solution was stirred at 0 °C until full conversion was observed via TLC (silica gel, hexanes/EtOAc, 1.5:1). The reaction contents were then quenched carefully by the addition of saturated aqueous $NaHCO_3$ (100 mL) and diluted with deionized H_2O (100 mL). The resultant layers were separated, and the aqueous layer was extracted with CH_2Cl_2 (3 × 150

mL). The combined organic layers were then dried (Na_2SO_4), filtered, and concentrated to yield Weinreb amide **138** as a colorless oil that was taken forward without any further purification.

General Procedure B: Ketone 139

To a 3-neck flask fitted with a reflux condenser was added Mg turnings (5.44 g, 224 mmol, 5.6 equiv.) that were then activated by the addition of a single crystal of I_2. THF (160 mL) was added followed by 4-bromobutene (16.2 mL, 160 mmol, 4.0 equiv.) to yield a grey-brown solution of the Grignard reagent that was stirred for 1 h at 23 °C. To a separate flask was added crude Weinreb amide **138** and THF (40 mL) to give a colorless solution that was cooled to 0 °C. The solution of Grignard reagent was then transferred via cannula into the solution of **138** and the resultant brown solution was allowed to warm slowly to 23 °C overnight. The reaction was then quenched by the addition of saturated aqueous NH_4Cl (150 mL) and diluted with Et_2O (100 mL). The resultant layers were separated, and the aqueous layer was extracted with Et_2O (3 × 100 mL). The combined organic layers were then dried ($MgSO_4$), filtered, and concentrated. The resultant residue was purified via flash column chromatography (silica gel, hexanes/EtOAc, 9:1) to yield ketone **139** (7.40 g, 91% yield) as a colorless oil which existed as a 4:1 mixture of the ketone and hemiketal forms based on NMR analysis. **139**: R_f = 0.22 (silica gel, hexanes/EtOAc, 6:1); IR (film) ν_{max} 3391 (bs), 3076, 2931, 1699, 1641 cm^{-1}; ^1H NMR (400 MHz, $CDCl_3$) δ 7.60 (t, *J* = 1.2 Hz, 1 H), 7.16–6.99 (m, 2.4 H), 6.92–6.78 (m, 2.4 H), 5.92 (ddt, *J* = 16.8, 10.2, 6.6 Hz, 0.2 H), 5.75 (ddt, *J* = 16.8, 10.2, 6.5 Hz, 1 H), 5.17–5.08 (m, 0.2 H), 5.07–4.90 (m, 2.2 H), 3.10–2.96 (m, 0.2 H), 2.94–2.78 (m, 4 H), 2.70 (ddd, *J* = 16.6, 5.7, 3.0 Hz, 0.50 H), 2.52 (t, *J* = 7.4 Hz, 2 H), 2.32 (dqt, *J* = 8.8, 7.4, 1.5 Hz, 2.40 H), 2.05 (ddd, *J* = 13.3, 6.1, 2.9 Hz, 0.20 H), 2.01–1.91 (m, 0.40 H), 1.89–1.78 (m, 0.2 H); ^{13}C NMR (101 MHz, $CDCl_3$) δ 213.23, 154.46, 152.61, 138.38, 136.68, 130.59, 129.30, 128.08, 127.73, 127.41, 121.98, 120.80, 120.76, 117.54, 117.15, 115.69, 115.29,

97.69, 77.36, 44.55, 41.73, 40.46, 29.87, 27.80, 27.75, 23.26, 21.43; HRMS (ESI) calcd for $C_{13}H_6O_2$ $[M]^+$ 204.1150, found 204.1146.

General Procedure C: Phenol 140

To a flask at 23 °C was added methyl triphenylphosphonium bromide (28.5 g, 79.9 mmol, 2.2 equiv.) followed by THF (50 mL) and the resulting white suspension was cooled to 0 °C. KO*t*Bu (8.15 g, 72.6 mmol, 2.0 equiv.) was then added portionwise over the course of 5 min to yield a bright yellow suspension that was stirred for 30 min at 0 °C. Next, a solution of ketone **139** (7.40 g, 36.3 mmol, 1.0 equiv.) in THF (22 mL) was added in one portion to give a orange-red suspension that was stirred at 0 °C for 1 h until full conversion was observed by TLC (silica gel, hexanes/EtOAc, 9:1). The reaction contents were then quenched by the addition of saturated aqueous NH_4Cl (100 mL) and diluted with Et_2O (50 mL). The layers were then separated and the aqueous layer was extracted with Et_2O (3 × 100 mL). The combined organic layers were dried ($MgSO_4$), filtered, and concentrated. The resultant residue was then purified via flash column chromatography (silica gel, hexanes/EtOAc, 20:1) to give phenol **140** (6.70 g, 91% yield) as a colorless oil. **140**: R_f = 0.18 (silica gel, hexanes/EtOAc, 20:1); IR (film) ν_{max} 3446, 3076, 3033, 2977, 2930, 2856, 1641, 1609 cm^{-1}; ^1H NMR (400 MHz, $CDCl_3$) δ 7.17–7.05 (m, 2 H), 6.89 (td, *J* = 7.5, 1.2 Hz, 1 H), 6.76 (dd, *J* = 8.0, 1.2 Hz, 1 H), 5.85 (ddt, *J* = 16.8, 10.2, 6.2 Hz, 1 H), 5.05 (dq, *J* = 17.1, 1.6 Hz, 1 H), 4.98 (ddt, *J* = 10.1, 2.2, 1.2 Hz, 1 H), 4.82 (dd, *J* = 11.1, 1.6 Hz, 2 H), 4.74 (s, 1 H), 2.81–2.70 (m, 2 H), 2.34 (ddd, *J* = 9.4, 5.9, 1.3 Hz, 2 H), 2.30–2.13 (m, 4 H); ^{13}C NMR (101 MHz, $CDCl_3$) δ 153.52, 149.13, 138.61, 130.28, 128.32, 127.34, 121.02, 115.40, 114.71, 109.68, 36.19, 35.77, 32.14, 28.84; HRMS (ESI) calcd for $C_{14}H_{19}O$ $[M+H]^+$ 203.1430, found 203.1424.

General Procedure D: Triflate 82

Phenol **140** (3.03 g, 15.0 mmol, 1.0 equiv.) was taken up into a syringe then transferred to a flask with CH_2Cl_2 (20 mL + 10 mL wash, 30 mL total) followed by 4-DMAP (0.366 g, 1.50 mmol, 0.1 equiv.) and Et_3N (4.20 mL, 30.0 mmol, 2.0 equiv.) at 23 °C. The resultant colorless solution was cooled to 0 °C and then Tf_2O (3.80 mL, 22.5 mmol, 1.5 equiv.) was added dropwise over the course of 5 min, yielding a dark red solution. Upon consumption of the starting material as determined by TLC (silica gel, hexanes/EtOAc, 9:1), the reaction was diluted with deionized H_2O (50 mL) then the layers were separated. The aqueous layer was extracted with CH_2Cl_2 (3 × 50 mL) then the combined organic layers were dried ($MgSO_4$), filtered, and concentrated. The resultant residue was purified via flash column chromatography (silica gel, hexanes) to give triflate **82** (4.86 g, 97% yield) as a colorless oil. **82**: R_f = 0.28 (silica gel, hexanes); IR (film) ν_{max} 3079, 2933, 2890, 1644 cm^{-1}; ^1H NMR (400 MHz, $CDCl_3$) δ 7.37–7.22 (m, 4 H), 5.83 (ddt, *J* = 16.8, 10.2, 6.3 Hz, 1 H), 5.04 (dq, *J* = 17.1, 1.6 Hz, 1 H), 4.97 (ddt, *J* = 10.1, 2.2, 1.2 Hz, 1 H), 4.79 (dd, *J* = 6.3, 1.5 Hz, 2 H), 2.90–2.81 (m, 2 H), 2.38–2.29 (m, 2 H), 2.28–2.11 (m, 4 H); ^{13}C NMR (101 MHz, $CDCl_3$) δ 148.15, 147.73, 138.39, 134.92, 131.34, 128.49, 127.99, 123.52, 121.46, 120.34, 117.16, 114.82, 113.98, 110.40, 77.36, 36.34, 35.44, 32.12, 28.75.; ^{19}F NMR (376 MHz, $CDCl_3$) δ -73.94.; HRMS (ESI) calcd for $C_{15}H_{18}F_3O_3S$ $[M+H]^+$ 335.0923, found 335.0917.

Synthesis of Tosylate 91

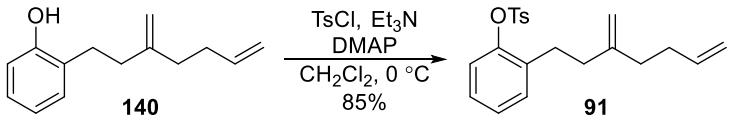

Phenol **140** (0.101 g, 0.500 mmol, 1.0 equiv.) was taken up into a syringe then transferred to a flask with CH_2Cl_2 (1.5 mL + 1 mL wash, 2.5 mL total) followed by 4-DMAP (6.1 mg, 0.050

mmol, 0.1 equiv.) and Et_3N (0.140 mL, 1.00 mmol, 2.0 equiv.) at 23 °C. The colorless solution was cooled to 0 °C then *p*-TsCl (0.142 g, 0.750 mmol, 1.5 equiv.) was added to give a colorless solution that was allowed to stir at 0 °C. Upon consumption of starting material as determined by TLC (silica gel, hexanes/EtOAc, 9:1; typically 1 hr), the reaction contents were diluted with deionized H_2O (5 mL) and the layers were separated. The aqueous layer was then extracted with CH_2Cl_2 (3 × 5 mL) then the combined organic layers were dried ($MgSO_4$), filtered, and concentrated. The resultant residue was purified via flash column chromatography (silica gel, hexanes:Et_2O, 9:1) to give tosylate **91** (0.151 g, 85% yield) as a colorless oil. **91**: R_f = 0.19 (silica gel, hexanes:Et_2O, 9:1); IR (film) ν_{max} 3076, 2977, 2926, 1652, 1598 cm^{-1}; ^1H NMR (400 MHz, $CDCl_3$) δ 7.80–7.72 (m, 2 H), 7.36–7.28 (m, 2 H), 7.22–7.10 (m, 3 H), 7.11–7.03 (m, 1 H), 5.81 (ddt, *J* = 16.8, 10.2, 6.5 Hz, 1 H), 5.08–5.00 (m, 1 H), 4.97 (ddt, *J* = 10.1, 2.2, 1.2 Hz, 1 H), 4.73 (d, *J* = 1.6 Hz, 1 H), 4.69–4.64 (m, 1 H), 2.60–2.51 (m, 2 H), 2.46 (s, 3 H), 2.24–2.13 (m, 4 H), 2.08 (dd, *J* = 9.1, 5.9 Hz, 2 H); ^{13}C NMR (101 MHz, $CDCl_3$) δ 148.32, 148.15, 145.44, 138.53, 135.43, 133.44, 130.60, 129.97, 128.50, 127.25, 127.16, 122.47, 114.73, 109.75, 77.36, 36.23, 35.54, 32.10, 28.48, 21.87; HRMS (ESI) calcd for $C_{21}H_{24}O_3SNa$ $[M+Na]^+$ 379.1338, found 379.1332.

Synthesis of Mesylate 92

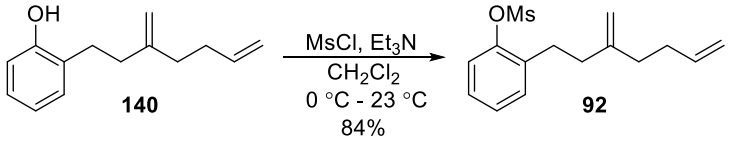

Phenol **140** (0.101 g, 0.500 mmol, 1.0 equiv.) was taken up into a syringe then transferred to a flask with CH_2Cl_2 (1.5 mL + 1.0 mL, 2.5 mL total) followed by Et_3N (0.140 mL, 1.00 mmol, 2.0 equiv.) at 23 °C. The colorless solution was cooled to 0 °C and MsCl (0.060 mL, 0.750 mmol,

1.5 equiv.) was added, yielding a colorless solution that was then allowed to slowly warm to 23 °C with stirring overnight. Upon consumption of the starting material as determined by TLC (silica gel, hexanes/EtOAc, 9:1), the reaction was diluted with deionized H_2O (5 mL) and then the layers were separated. The aqueous layer was extracted with CH_2Cl_2 (3 × 5 mL) and the combined organic layers were dried ($MgSO_4$), filtered, and concentrated. The resultant residue was purified via flash column chromatography (silica gel, hexanes:Et_2O, 9:1) to give mesylate **92** (0.117 g, 84% yield) as a pale yellow oil. **92**: R_f = 0.24 (silica gel, hexanes:Et_2O, 9:1); IR (film) ν_{max} 3076, 3031, 2977, 2936, 1642 cm^{-1}; ^1H NMR (400 MHz, $CDCl_3$) δ 7.36–7.20 (m, 5 H), 5.83 (ddt, *J* = 16.8, 10.2, 6.3 Hz, 1 H), 5.04 (dq, *J* = 17.0, 1.6 Hz, 1 H), 4.97 (ddt, *J* = 10.2, 2.2, 1.2 Hz, 1 H), 4.82–4.76 (m, 2 H), 3.21 (s, 3 H), 2.89–2.80 (m, 2 H), 2.38–2.29 (m, 2 H), 2.29–2.12 (m, 4 H); ^{13}C NMR (101 MHz, $CDCl_3$) δ 148.26, 147.56, 138.47, 135.21, 130.96, 127.58, 127.45, 122.15, 114.81, 110.04, 38.45, 36.47, 35.58, 32.12, 28.87; HRMS (ESI) calcd for $C_{15}H_{21}O_3S$ $[M+H]^+$ 281.1206, found 281.1204.

Synthesis of Nonaflate 93

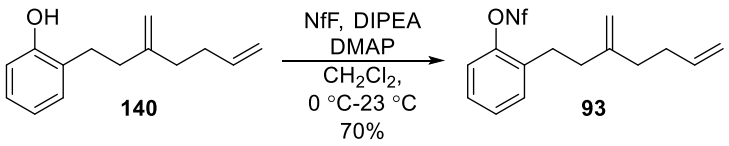

Phenol **140** (0.101 g, 0.500 mmol, 1.0 equiv.) was taken up into a syringe then transferred to a flask with CH_2Cl_2 (0.5 mL + 0.5 mL wash, 1 mL total) followed by 4-DMAP (3.0 mg, 0.025 mmol, 0.05 equiv.) and *i*-Pr_2NEt (0.11 mL, 0.6 mmol, 1.2 equiv.) at 23 °C. The resultant colorless solution was then cooled to 0 °C and nonafluorobutanesulfonyl fluoride (0.100 mL, 0.550 mmol, 1.1 equiv.) was added to give a light pink solution that was slowly allowed to warm to 23 °C overnight with stirring. Upon consumption of starting material as determined by TLC (silica gel,

hexanes/EtOAc, 9:1), the reaction was diluted with deionized H_2O (5 mL) and then the layers were separated. The aqueous layer was extracted with CH_2Cl_2 (3 × 5 mL) and the combined organic layers were dried ($MgSO_4$), filtered, and concentrated. The resultant residue was purified via flash column chromatography (silica gel, hexanes) to give nonaflate **93** (0.170 g, 70% yield) as a colorless oil. **93**: R_f = 0.32 (silica gel, hexanes); IR (film) ν_{max} 3080, 2981, 2934, 1644 cm^{-1}; ^1H NMR (400 MHz, $CDCl_3$) δ 7.37–7.26 (m, 4 H), 5.83 (ddt, *J* = 16.8, 10.2, 6.3 Hz, 1 H), 5.04 (dq, *J* = 17.1, 1.6 Hz, 1 H), 4.97 (ddt, *J* = 10.2, 2.2, 1.2 Hz, 1 H), 4.79 (dd, *J* = 5.8, 1.5 Hz, 2 H), 2.91–2.82 (m, 2 H), 2.34 (dd, *J* = 9.7, 6.7 Hz, 2 H), 2.28–2.11 (m, 4 H); ^{13}C NMR (101 MHz, $CDCl_3$) δ 148.26, 147.73, 138.39, 135.03, 131.36, 128.51, 128.02, 121.53, 114.80, 110.38, 36.35, 35.44, 32.11, 28.84; ^{19}F NMR (376 MHz, $CDCl_3$) δ –80.60, –109.75 to –109.88 (m), –120.74 to –120.85 (m), –125.71 to –125.85 (m); HRMS (ESI) calcd for $C_{18}H_{18}F_9O_3S$ $[M+H]^+$ 485.0827, found 485.0825.

Synthesis of Pivaloate 141

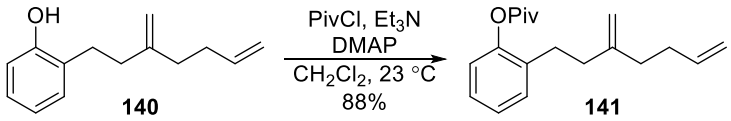

Phenol **140** (0.101 g, 0.500 mmol, 1.0 equiv.) was taken up into a syringe then transferred to a flask with CH_2Cl_2 (1.5 mL + 1.0 mL, 2.5 mL total) followed by 4-DMAP (12.2 mg, 0.100 mmol, 0.2 equiv.) and Et_3N (0.140 mL, 1.00 mmol, 2 equiv.) at 23 °C. Then PivCl (0.120 mL, 1.00 mmol, 2.0 equiv.) was added to give a colorless solution that was stirred at 23 °C. Upon consumption of the starting material as determined by TLC (silica gel, hexanes/EtOAc, 9:1; typically 2 h), the reaction was diluted with deionized H_2O (5 mL) and then the layers were separated. The aqueous layer was extracted with CH_2Cl_2 (3 × 5 mL) and then the combined organic

layers were dried ($MgSO_4$), filtered, and concentrated. The resultant residue was purified via flash column chromatography (silica gel, hexanes:Et_2O, 49:1) to give pivaloate **142** (0.126 g, 88% yield) as a colorless oil. **142**: R_f = 0.24 (silica gel, hexanes:Et_2O, 49:1); IR (film) ν_{max} 3078, 2976, 2933, 1750, 1643 cm^{-1}; ^1H NMR (400 MHz, $CDCl_3$) δ 7.25–7.12 (m, 3 H), 6.97 (dd, *J* = 7.8, 1.5 Hz, 1 H), 5.82 (ddt, *J* = 16.8, 10.2, 6.3 Hz, 1 H), 5.02 (dq, *J* = 17.1, 1.7 Hz, 1 H), 4.96 (ddt, *J* = 10.2, 2.2, 1.2 Hz, 1 H), 4.80–4.75 (m, 2 H), 2.69–2.60 (m, 2 H), 2.30–2.09 (m, 6 H), 1.37 (s, 9 H), 1.27 (s, 2 H); ^{13}C NMR (126 MHz, $CDCl_3$) δ 177.17, 149.29, 148.53, 138.46, 134.12, 130.26, 127.19, 126.03, 122.32, 114.76, 109.56, 39.33, 36.59, 35.81, 32.17, 28.80, 27.38, 26.67; HRMS (ESI) calcd for $C_{19}H_{26}ONa$ $[M+Na]^+$ 309.1825, found 309.1820.

Synthesis of Anisole 142

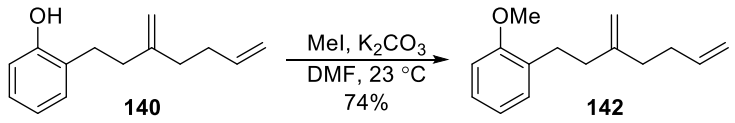

Phenol **140** (0.101 g, 0.500 mmol, 1.0 equiv.) was taken up into a syringe then transferred to a flask with DMF (0.5 mL + 0.5 mL wash, 1 mL total) followed by K_2CO_3 (0.207 g, 1.50 mmol, 3.0 equiv.) at 23 °C. Then MeI (0.040 mL, 0.550 mmol, 1.1 equiv.) was added, yielding a colorless solution that was then allowed to stir at 23 °C. Upon consumption of starting material as determined by TLC (silica gel, hexanes/EtOAc, 9:1; typically 12 h), the reaction contents were diluted with deionized H_2O (5 mL) and Et_2O (10 mL) and then the layers were separated. The aqueous layer was extracted with Et_2O (3 × 5 mL) and the combined organic layers were washed with deionized H_2O (10 mL), dried ($MgSO_4$), filtered, and concentrated. The resultant residue was purified via flash column chromatography (silica gel, hexanes) to give anisole **142** (0.151 g, 85% yield) as a colorless oil. **142**: R_f = 0.27 (silica gel, hexanes); IR (film) ν_{max} 3076, 2932, 2834, 1642,

1601 cm^{-1}; ^1H NMR (400 MHz, $CDCl_3$) δ 7.23–7.11 (m, 2 H), 6.93–6.81 (m, 2 H), 5.85 (ddt, *J* = 16.8, 10.3, 6.2 Hz, 1 H), 5.09–4.90 (m, 2 H), 4.89–4.74 (m, 2 H), 3.83 (s, 3 H), 2.79–2.71 (m, 2 H), 2.33–2.13 (m, 6 H); ^{13}C NMR (101 MHz, $CDCl_3$) δ 157.56, 149.36, 138.77, 130.78, 129.81, 127.15, 120.49, 114.58, 110.34, 109.28, 55.36, 36.33, 35.73, 32.18, 31.08, 29.01; HRMS (ESI) calcd for $C_{15}H_{21}O$ $[M+H]^+$ 217.1587, found 217.1597.

Synthesis of Carbonate 143

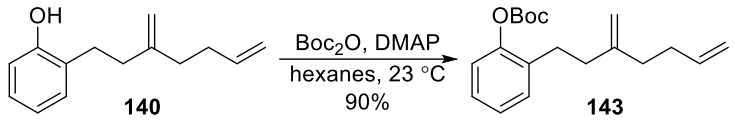

Phenol **140** (0.101 g, 0.500 mmol, 1.0 equiv.) was taken up into a syringe then transferred to a flask with hexanes (0.40 mL + 0.31 mL wash, 0.71 mL total) followed by 4-DMAP (3.0 mg, 0.050 mmol, 0.05 equiv.) at 23 °C. Then Boc_2O (0.130 g, 0.600 mmol, 1.2 equiv.) was added, yielding a colorless solution that was allowed to stir at 23 °C. Upon consumption of starting material as determined by TLC (silica gel, hexanes/EtOAc, 9:1; typically 30 min), the reaction contents were diluted with deionized H_2O (5 mL) and then the layers were separated. The aqueous layer was extracted with hexanes (3 × 5 mL) and the combined organic layers were dried ($MgSO_4$), filtered, and concentrated. The resultant residue was purified via flash column chromatography (silica gel, hexanes/Et_2O, 49:1) to give carbonate **143** (0.136 g, 90% yield) as a colorless oil. **143**: R_f = 0.19 (silica gel, hexanes/Et_2O, 49:1); IR (film) ν_{max} 3077, 2980, 2933, 1758 cm^{-1}; ^1H NMR (400 MHz, $CDCl_3$) δ 7.26–7.13 (m, 3 H), 7.09 (dd, *J* = 7.8, 1.6 Hz, 1 H), 5.83 (ddt, *J* = 16.8, 10.2, 6.3 Hz, 1 H), 5.09–4.93 (m, 2 H), 4.81–4.75 (m, 2 H), 2.75–2.66 (m, 2 H), 2.33–2.18 (m, 4 H), 2.18–2.11 (m, 2 H), 1.55 (s, 9 H); ^{13}C NMR (101 MHz, $CDCl_3$) δ 152.25, 149.38, 148.60, 138.53,

134.19, 130.29, 127.26, 126.24, 122.25, 114.75, 109.79, 83.46, 36.51, 35.63, 32.15, 28.94, 27.84; HRMS (ESI), calcd for $C_{19}H_{26}O_3$ $[M]^+$ 302.1882, no molecular ion was detected.

Synthesis of Triflate 97

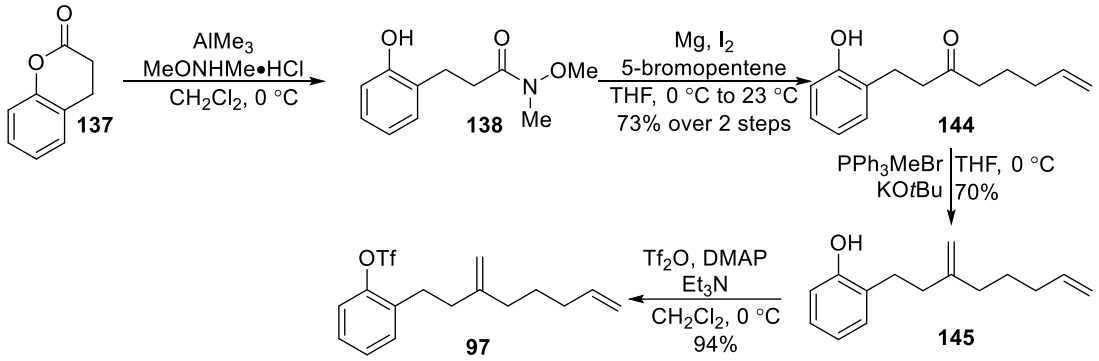

Ketone 144. Following general procedure A, **137** (0.840 mL, 6.00 mmol, 1.0 equiv.) was converted into crude Weinreb amide **138**. The reaction was worked up as usual and was taken forward without purification. Following general procedure B, crude Weinreb amide **138** was reacted with the Grignard reagent from 5-bromopentene to give ketone **144**. The reaction was worked up as usual and then purified by flash column chromatography (silica gel, hexanes/EtOAc, 9:1) to yield ketone **144** (0.956 g, 73% yield over 2 steps) as a colorless oil that existed in a 5:1 ratio of the ketone and hemiketal forms based on NMR analysis. **144**: R_f = 0.22 (silica gel, hexanes/EtOAc, 9:1); IR (film) ν_{max} 3373 (bs), 3076, 3038, 2976, 2932, 1700 cm^{-1}; ^1H NMR (500 MHz, $CDCl_3$) δ 7.68 (s, 1 H), 7.14–7.06 (m, 2.4 H), 7.04 (dd, *J* = 7.5, 1.7 Hz, 2.4 H), 6.91–6.77 (m, 2.4 H), 5.84 (ddt, *J* = 16.9, 10.2, 6.6 Hz, 0.2 H), 5.71 (ddt, *J* = 17.0, 10.2, 6.7 Hz, 1 H), 5.09–4.87 (m, 2.4 H), 3.02 (ddd, *J* = 17.5, 12.4, 6.0 Hz, 0.2 H), 2.91–2.77 (m, 4 H), 2.69 (ddd, *J* = 16.3, 5.8, 2.9 Hz, 0.2 H), 2.49–2.38 (m, 2.2 H), 2.14 (q, *J* = 7.1 Hz, 0.4 H), 2.07–1.95 (m, 2.4 H), 1.89–1.78 (m, 0.6 H), 1.71–1.59 (m, 2.4 H); ^{13}C NMR (101 MHz, $CDCl_3$) δ 213.22, 154.45, 152.60, 139.03, 138.38, 136.68, 130.58, 129.29, 128.07, 127.72, 127.40, 121.98, 120.79, 120.75, 117.50,

117.15, 115.67, 115.27, 114.60, 97.69, 77.36, 44.52, 41.72, 40.99, 40.45, 29.86, 28.46, 27.79, 27.75, 23.28, 21.43; HRMS (ESI) calcd for $C_{14}H_{17}O$ $[(M+H)-H_2O]^+$ 201.1274, found 201.1264.

Phenol 145. Following general procedure C, ketone **144** (0.956 g, 4.38 mmol, 1.0 equiv.) was converted into phenol **145**. The reaction was worked up as usual and then purified via flash column chromatography (silica gel, hexanes/EtOAc, 20:1) to give phenol **145** (0.671 g, 70% yield) as a colorless oil. **145**: R_f = 0.18 (silica gel, hexanes/EtOAc, 20:1); IR (film) ν_{max} 3446 (bs), 3075, 2977, 2931, 2859, 1700, 1642 cm^{-1}; ^1H NMR (400 MHz, $CDCl_3$) δ 7.16–7.04 (m, 2 H), 6.87 (td, *J* = 7.4, 1.2 Hz, 1 H), 6.75 (dd, *J* = 8.0, 1.2 Hz, 1 H), 5.82 (ddt, *J* = 16.9, 10.2, 6.7 Hz, 1 H), 5.07–4.97 (m, 1 H), 4.97–4.92 (m, 1 H), 4.80 (dd, *J* = 9.4, 1.7 Hz, 2 H), 4.68 (s, 1 H), 2.79– 2.71 (m, 2 H), 2.36–2.27 (m, 2 H), 2.16–2.01 (m, 4 H), 1.56 (tt, *J* = 9.0, 6.8 Hz, 2 H); ^{13}C NMR (101 MHz, $CDCl_3$) δ 153.52, 149.66, 138.92, 130.28, 128.35, 127.33, 121.02, 115.41, 114.69, 109.53, 36.12, 35.88, 33.57, 28.89, 27.13; HRMS (ESI) calcd for $C_{15}H_{21}O$ $[M+H]^+$ 217.1587, found 217.1582.

Triflate 97. Following general procedure D, phenol **146** (0.432 g, 2.00 mmol, 1.0 equiv.) was converted into triflate **97**. The reaction was worked up as usual and purified via flash column chromatography (silica gel, hexanes) to give triflate **97** (0.654 g, 94% yield) as a colorless oil. **97**: R_f = 0.28 (silica gel, hexanes); IR (film) ν_{max} 3078, 2979, 2934, 1645 cm^{-1}; ^1H NMR (400 MHz, $CDCl_3$) δ 7.37–7.21 (m, 4 H), 5.82 (ddt, *J* = 16.9, 10.2, 6.6 Hz, 1 H), 5.07–4.98 (m, 1 H), 4.98–4.92 (m, 1 H), 4.78 (dd, *J* = 7.8, 1.6 Hz, 2 H), 2.89–2.76 (m, 2 H), 2.33 (ddd, *J* = 9.2, 5.9, 1.2 Hz, 2 H), 2.12–2.02 (m, 4 H), 1.55 (p, *J* = 7.6 Hz, 2 H); ^{13}C NMR (126 MHz, $CDCl_3$) δ 148.22, 148.14, 138.81, 134.97, 131.33, 128.47, 127.97, 121.46, 114.76, 110.22, 36.25, 35.53, 33.53, 28.77, 27.11; ^{19}F NMR (376 MHz, $CDCl_3$) δ –73.93; HRMS (ESI) calcd for $C_{16}H_{19}F_3O_3S$ $[M]^+$ 348.1007, no molecular ion was detected.

Synthesis of Triflate 102

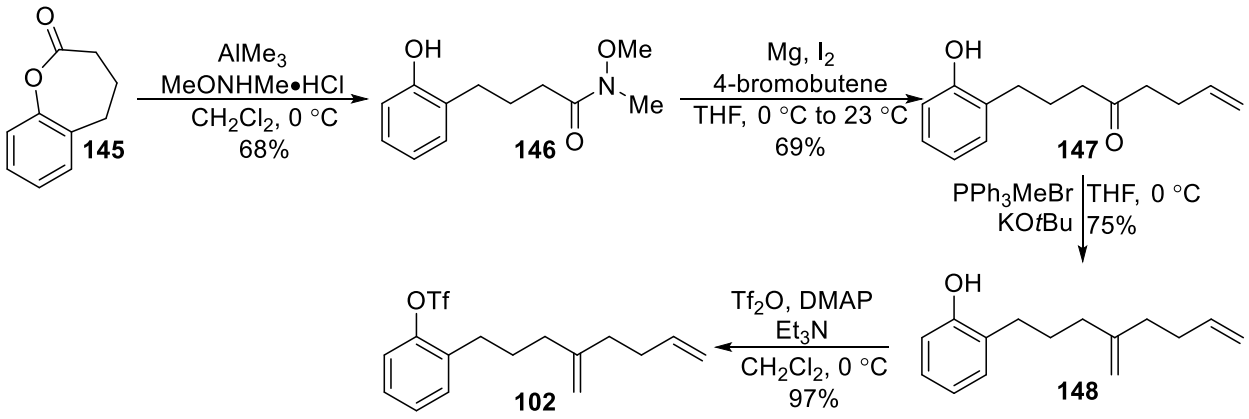

Weinreb amide 146 Following general procedure A, lactone **145** (6.48 g, 40.0 mmol, 1.0 equiv.) was converted to crude Weinreb amide **146**. The reaction was worked up as usual and the residue was purified by flash column chromatography (silica gel, hexanes/EtOAc, 1.5:1) to yield Weinreb amide **146** (5.96 g, 68% yield) as a colorless oil. **146**: R_f = 0.28 (silica gel, hexanes/EtOAc, 1.5:1); IR (film) ν_{max} 3289 (bs), 3054, 2970, 2940, 1635 cm^{-1}; ^1H NMR (400 MHz, $CDCl_3$) δ 8.30 (s, 1 H), 7.16–7.02 (m, 2 H), 6.91 (dd, *J* = 8.1, 1.3 Hz, 1 H), 6.80 (td, *J* = 7.4, 1.3 Hz, 1 H), 3.71 (s, 3 H), 3.25 (s, 3 H), 2.67–2.59 (m, 2 H), 2.53 (t, *J* = 6.0 Hz, 2 H), 1.93–1.81 (m, 2 H); ^{13}C NMR (101 MHz, $CDCl_3$) δ 175.17, 155.52, 129.84, 127.73, 127.17, 119.62, 116.59, 61.24, 32.22, 29.92, 29.85, 24.69; HRMS (ESI) calcd for $C_{15}H_{17}NO_2Na$ $[M+Na]^+$ 246.1101, found 246.1097.

Ketone 147 Following general procedure B, Weinreb amide **146** (2.23 g, 10.0 mmol, 1.0 equiv.) was reacted with the Grignard reagent from 4-bromobutene to give ketone **147**. The reaction was worked up as usual and then purified by flash column chromatography (silica gel, hexanes/EtOAc, 9:1) to yield ketone **147** (1.55 g, 68% yield) as a light-yellow oil. **147**: R_f = 0.24 (silica gel, hexanes/EtOAc, 9:1); IR (film) ν_{max} 3389 (bs), 3076, 2935, 1699, 1641, 1593 cm^{-1}; ^1H

NMR (400 MHz, $CDCl_3$) δ 7.12 (td, *J* = 7.7, 1.8 Hz, 2 H), 7.05 (dd, *J* = 7.5, 1.7 Hz, 2 H), 6.90–6.74 (m, 3 H), 5.81 (ddt, *J* = 16.8, 10.2, 6.5 Hz, 1 H), 5.09–4.99 (m, 2 H), 4.98 (q, *J* = 1.4 Hz, 1 H), 2.60–2.50 (m, 6 H), 2.42–2.31 (m, 2 H), 1.89–1.77 (m, 2 H); ^{13}C NMR (101 MHz, $CDCl_3$) δ 212.57, 154.73, 136.98, 130.09, 127.80, 127.28, 120.28, 116.14, 115.59, 42.01, 41.47, 29.71, 27.89, 23.81; HRMS (ESI) calcd for $C_{14}H_{19}O2$ $[M+H]^+$ 219.1380, found 219.1378.

Phenol 148 Following general procedure C, ketone **147** (1.50 g, 6.88 mmol, 1.0 equiv.) was converted into phenol **148**. The reaction was worked up as usual and then purified via flash column chromatography (silica gel, hexanes/EtOAc, 20:1) to give phenol **148** (1.11 g, 75% yield) as a colorless oil. **148**: R_f = 0.21 (silica gel, hexanes/EtOAc, 20:1); IR (film) ν_{max} 3446, 3075, 2932, 1641, 1591 cm^{-1}; ^1H NMR (400 MHz, $CDCl_3$) δ 7.16–7.05 (m, 2 H), 6.88 (td, *J* = 7.4, 1.2 Hz, 1 H), 6.76 (dd, *J* = 7.9, 1.2 Hz, 1 H), 5.83 (ddt, *J* = 16.8, 10.2, 6.3 Hz, 1 H), 5.03 (dq, *J* = 17.1, 1.7 Hz, 1 H), 4.96 (ddt, *J* = 10.2, 2.2, 1.2 Hz, 1 H), 4.82–4.75 (m, 2 H), 4.64 (s, 1 H), 2.66–2.57 (m, 2 H), 2.26–2.16 (m, 2 H), 2.16–2.07 (m, 4 H), 1.84–1.72 (m, 2 H); ^{13}C NMR (101 MHz, $CDCl_3$) δ 153.55, 149.02, 138.65, 130.37, 128.38, 127.27, 120.97, 115.37, 114.64, 109.50, 35.89, 35.49, 32.12, 29.64, 27.80; HRMS (ESI) calcd for $C_{15}H_{21}O_2$ $[M+H]^+$ 217.1587, found 217.1580.

Triflate 102 Following general procedure D, phenol **149** (0.432 g, 2.00 mmol, 1.0 equiv.) was converted into triflate **102**. The reaction was worked up as usual and purified via flash column chromatography (silica gel, hexanes) to give triflate **102** (0.675 g, 94% yield) as a colorless oil. **102**: R_f = 0.3 (silica gel, hexanes); IR (film) ν_{max} 3078, 2979, 2936, 1643 cm^{-1}; ^1H NMR (400 MHz, $CDCl_3$) δ 7.37–7.21 (m, 4 H), 5.82 (ddt, *J* = 16.9, 10.2, 6.3 Hz, 1 H), 5.02 (dq, *J* = 17.1, 1.6 Hz, 1 H), 4.96 (ddt, *J* = 10.3, 2.2, 1.2 Hz, 1 H), 4.77 (q, *J* = 1.7 Hz, 2 H), 2.76–2.67 (m, 2 H), 2.25–2.17 (m, 2 H), 2.17–2.05 (m, 4 H), 1.78 (tt, *J* = 9.2, 6.8 Hz, 2 H); ^{13}C NMR (126 MHz, $CDCl_3$) δ 148.35, 148.21, 138.55, 135.28, 131.34, 128.48, 127.89, 121.46, 120.02, 117.47, 114.70, 109.85,

35.85, 35.36, 32.10, 29.79, 28.07; ^{19}F NMR (376 MHz, $CDCl_3$) δ –73.95; HRMS (ESI) calcd for $C_{16}H_{19}F_3O_3S$ $[M]^+$ 348.1007, no molecular ion was detected.

Synthesis of Triflate 94

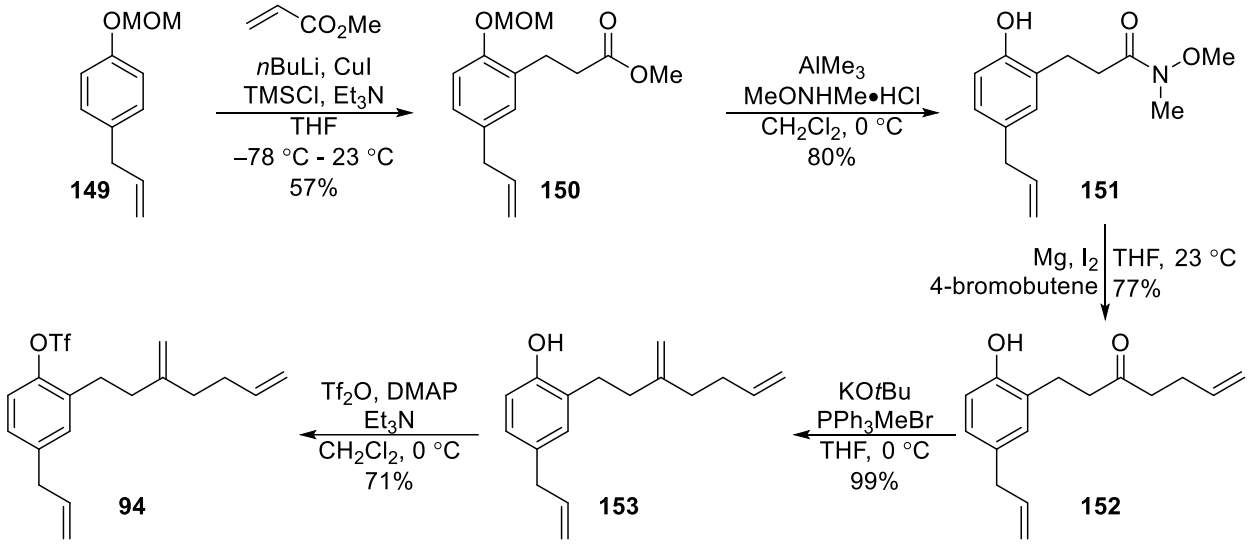

Ester 150 Using a literature procedure,[4] protected phenol **149**[5] (2.21 g, 12.4 mmol, 1.0 equiv.) was azeotropically dried with benzene three times and then dissolved in THF (12 mL) to give a colorless solution that was stirred at 23 °C. Then *n*BuLi (4.96 mL, 2.5 M in hexanes, 1.0 equiv.) was added dropwise to give a dark red solution that was stirred at 23 °C for 1 h. Separately, anhydrous CuI (2.36 g, 12.4 mmol, 1.0 equiv.) was then added to a flask followed by THF (13 mL) to give a grey suspension that was cooled to 0 °C. After 1 h, the red solution was added to the CuI suspension via cannula, affording a new dark green suspension that was stirred at 0 °C for 1 h. Upon completion, the suspension was then cooled to –78 °C and TMSCl (7.90 mL, 62.0 mmol, 5.0 equiv.), methyl acrylate (1.11 mL, 12.4 mmol, 1.0 equiv.), and Et_3N (1.72 mL, 12.4 mmol, 1.0 equiv.) were added sequentially. The resultant contents were then allowed to slowly warm to 23 °C and stirred for 48 h. Upon completion, the reaction contents were quenched with a mixture of saturated aqueous NH_4OH and NH_4Cl (50 mL, 1:9), diluted with Et_2O (20 mL), and

the layers were separated. The aqueous layer was extracted with Et_2O (3 × 25 mL) and the combined organic layers were washed with saturated aqueous NH_4OH until no blue color remained (~XX mL) and then were dried (Na_2SO_4), filtered, and concentrated. The resultant residue was purified via flash column chromatography (silica gel, hexanes/Et_2O, 9:1) to give ester **150** (1.87 g, 57% yield) as a colorless oil. **150**: R_f = 0.22 (silica gel, hexanes/Et_2O, 9:1); IR (film) ν_{max} 3446 (bs), 3076, 2997, 2951, 2904, 2847, 2827, 2789, 1737, 1608 cm^{-1}; ^1H NMR (500 MHz, $CDCl_3$) δ 7.00–6.95 (m, 3 H), 5.93 (ddt, *J* = 16.8, 10.0, 6.7 Hz, 1 H), 5.18 (s, 2 H), 5.08–5.02 (m, 2 H), 3.67 (s, 3 H), 3.47 (s, 3 H), 3.30 (dt, *J* = 6.7, 1.5 Hz, 2 H), 2.94 (dd, *J* = 8.8, 7.1 Hz, 2 H), 2.65–2.58 (m, 2 H); ^{13}C NMR (126 MHz, $CDCl_3$) δ 173.89, 153.66, 137.88, 133.35, 130.40, 129.54, 127.68, 115.67, 114.02, 94.55, 56.17, 51.69, 39.56, 34.44, 26.35; HRMS (ESI) calcd for $C_{15}H_{20}O_4$ $[M]^+$ 264.1362, no molecular ion was detected.

Weinreb amide 151 Following general procedure A, ester **150**[1] (1.87 g, 7.08 mmol, 1.0 equiv.) was converted into crude Weinreb amide **151**. The reaction was worked up as usual and the residue was purified by flash column chromatography (silica gel, hexanes/EtOAc, 4:1–2.5:1) to yield Weinreb amide **151** (1.61 g, 80% yield) as a colorless oil. **151**: R_f = 0.25 (silica gel, hexanes/EtOAc, 2.5:1); IR (film) ν_{max} 3242 (bs), 3077, 3055, 3005l 2976, 2938, 1771, 1637, 1500 cm^{-1}; ^1H NMR (400 MHz, $CDCl_3$) δ 8.79 (s, 1 H), 6.93 (dd, *J* = 8.2, 2.3 Hz, 1 H), 6.90–6.82 (m, 2 H), 5.94 (ddt, *J* = 16.8, 10.0, 6.7 Hz, 1 H), 5.13–4.99 (m, 2 H), 3.63 (s, 3 H), 3.29 (dd, *J* = 6.7, 1.5 Hz, 2 H), 3.18 (s, 3 H), 2.87 (td, *J* = 8.4, 4.9 Hz, 4 H); ^{13}C NMR (126 MHz, $CDCl_3$) δ 175.32, 153.48, 138.22, 131.86, 130.74, 128.21, 128.16, 118.07, 115.40, 61.18, 39.57, 33.99, 32.46, 23.94; HRMS (ESI) calcd for $C_{14}H_{18}NO_2$ $[(M+H)–H_2O]^+$ 232.1332, found 232.1328.

Ketone 152 Following general procedure B, Weinreb amide **151** (0.275 g, 1.10 mmol, 1.0 equiv.) was reacted with the Grignard reagent generated from 4-bromobutene to give ketone **152**.

The reaction was worked up as usual and then purified by flash column chromatography (silica gel, hexanes/EtOAc, 9:1) to yield ketone **152** (0.187 g, 77% yield) as a colorless oil that existed in a 3:1 ratio of the ketone and hemiketal forms based on NMR analysis. **152**: R_f = 0.22 (silica gel, hexanes/EtOAc, 9:1); IR (film) ν_{max} 3335 (bs), 3078, 2980, 2927, 1701, 1639 cm^{-1}; ^1H NMR (400 MHz, $CDCl_3$) δ 7.46 (d, *J* = 1.1 Hz, 1 H), 6.92 (dt, *J* = 6.9, 2.5 Hz, 1 H), 6.87–6.78 (m, 2 H), 6.02–5.84 (m, 2 H), 5.75 (ddt, *J* = 16.8, 10.2, 6.5 Hz, 1 H), 5.17–4.91 (m, 5 H), 3.33–3.24 (m, 2 H), 2.91–2.77 (m, 4 H), 2.72–2.54 (m, 1 H), 2.51 (t, *J* = 7.4 Hz, 2 H), 2.39–2.25 (m, 2 H), 1.99–1.87 (m, 1 H); ^{13}C NMR (126 MHz, $CDCl_3$) δ 213.22, 152.77, 150.92, 138.42, 138.08, 136.71, 132.30, 132.24, 130.59, 129.24, 128.19, 127.62, 117.62, 117.10, 115.71, 115.52, 115.31, 97.67, 77.36, 44.70, 40.49, 39.61, 39.54, 29.93, 27.82, 23.23, 21.47; HRMS (ESI) calcd for $C_{16}H_{19}O$ $[M+H]^+$ 227.1430, found 227.1430.

Phenol 153 Following general procedure C, ketone **152** (90.0 mg, 0.370 mmol, 1.0 equiv.) was converted into phenol **153**. The reaction was worked up as usual and then purified via flash column chromatography (silica gel, hexanes/EtOAc, 20:1) to give phenol **153** (89.0 mg, 99% yield) as a colorless oil. **153**: R_f = 0.18 (silica gel, hexanes/EtOAc, 20:1); IR (film) ν_{max} 3446, 3077, 3003, 297, 2926, 2853, 1640, 1611, 1506 cm^{-1}; ^1H NMR (400 MHz, $CDCl_3$) δ 6.97–6.86 (m, 2 H), 6.69 (d, *J* = 8.0 Hz, 1 H), 6.02–5.77 (m, 2 H), 5.11–5.01 (m, 3 H), 4.97 (ddt, *J* = 10.1, 2.1, 1.2 Hz,1 H), 4.81 (dd, *J* = 12.3, 1.7 Hz, 2 H), 4.56 (d, *J* = 1.8 Hz,1 H), 3.31 (dd, *J* = 6.7, 1.5 Hz, 2 H), 2.77–2.69 (m, 2 H), 2.32 (dd, *J* = 9.7, 6.6 Hz, 2 H), 2.28–2.13 (m, 4 H); ^{13}C NMR (101 MHz, $CDCl_3$) δ 151.83, 149.19, 138.63, 138.10, 132.47, 130.45, 128.25, 127.29, 115.51, 115.39, 114.71, 109.65, 39.57, 36.31, 35.78, 32.15, 28.98; HRMS (ESI) calcd for $C_{17}H_{23}O$ $[M+H]^+$ 243.1743, found 243.1744.

Triflate 94 Following general procedure D, phenol **154** (89.0 mg, 0.368 mmol, 1.0 equiv.) was converted into triflate **94**. The reaction was worked up as usual and purified via flash column chromatography (silica gel, hexanes) to give triflate **94** (97.8 mg, 71% yield) as a colorless oil. **94**: R_f = 0.21 (silica gel, hexanes); IR (film) ν_{max} 3080, 2980, 2928, 2853, 1642, 1611 cm^{-1}; ^1H NMR (500 MHz, $CDCl_3$) δ 7.21–7.06 (m, 2 H), 6.00–5.78 (m, 1 H), 5.15–5.07 (m, 1 H), 5.07–4.95 (m, 1 H), 4.80 (dd, *J* = 5.2, 1.4 Hz, 1 H), 3.39 (dd, *J* = 6.7, 1.6 Hz, 1 H), 2.87–2.79 (m, 1 H), 2.36–2.27 (m, 1 H), 2.27–2.12 (m, 2 H); ^{13}C NMR (101 MHz, $CDCl_3$) δ 147.80, 146.47, 140.59, 138.41, 136.57, 134.72, 131.37, 128.04, 121.32, 120.34, 117.16, 116.79, 114.80, 110.35, 39.62, 36.42, 35.43, 32.12, 28.83; ^{19}F NMR (376 MHz, $CDCl_3$) δ –73.93; HRMS (ESI) calcd for $C_{18}H_{22}O_3S$ $[M+H]^+$ 375.1236, found 375.1232.

Synthesis of Triflate 104

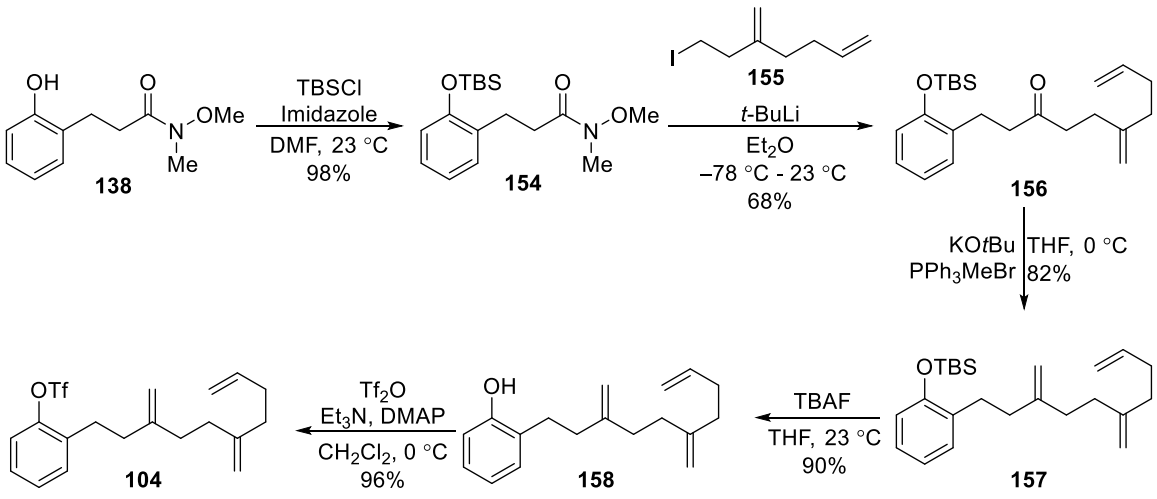

Silyl Ether 154. Weinreb amide **138** (0.627 g, 3.00 mmol, 1 equiv.) was added to a flask followed by DMF (3 mL), imidazole (408 mg, 6.00 mmol, 2 equiv.), and TBSCl (678 mg, 4.50 eq, 1.5 equiv.) at 23 °C. The resulting colorless solution was stirred at 23 °C. Upon completion of the reaction as indicated by TLC (silica gel, hexanes/EtOAc 1.5:1; typically 4 hr), the reaction contents

were quenched with saturated aqueous NH_4Cl (5 mL), diluted with EtOAc (5 mL), and the layers were separated. The aqueous layer was then extracted with EtOAc (3 × 10 mL) and the combined organic layers were washed with brine (15 mL), dried (Na_2SO_4), filtered, and concentrated. The resultant residue was purified via flash column chromatography (silica gel, hexanes/EtOAc, 6:1) to give silyl ether **154** (0.860 g, 89% yield) as a colorless oil. **154**: R_f = 0.19 (silica gel, hexanes/EtOAc, 6:1); IR (film) ν_{max} 2956, 2931, 2897, 2858, 1670, 1599, 1582 cm^{-1}; ^1H NMR (400 MHz, $CDCl_3$) δ 7.18 (dd, *J* = 7.5, 1.8 Hz, 1 H), 7.08 (ddd, *J* = 8.0, 7.4, 1.8 Hz, 1 H), 6.88 (td, *J* = 7.4, 1.2 Hz, 1 H), 6.79 (dd, *J* = 8.1, 1.2 Hz, 1 H), 3.58 (s, 3 H), 3.16 (s, 3 H), 2.92 (dd, *J* = 8.9, 6.8 Hz, 2 H), 2.72 (t, *J* = 7.9 Hz, 2 H), 1.01 (s, 9 H), 0.24 (s, 6 H); ^{13}C NMR (101 MHz, $CDCl_3$) δ 153.72, 132.46, 130.42, 126.96, 121.11, 118.53, 61.24, 31.62, 29.98, 25.95, 25.01, 18.38, –4.01; HRMS (ESI) calcd for $C_{17}H_{29}NO_3SiNa$ $[M+Na]^+$ 346.1809, found 346.1817.

Ketone 156 Following a literature procedure,[8] to a colorless solution of iodide **155**[7] (0.118 g, 0.500 mmol, 1.0 equiv.) in Et_2O (2 mL) at –78 °C was added *t*-BuLi (2.50 mL, 1.7 M in pentane, 2.0 equiv.) dropwise. Upon addition of the first drop a yellow color appeared, but disappeared over the course of the addition to give a clear colorless solution that was then stirred at –78 °C for 30 min. The cooling bath was then removed, and the reaction was stirred at 23 °C for 2 h. Upon warming the reaction contents became a white suspension and finally a yellow solution after the full 2 h of reaction time. The resultant yellow solution was then cooled to –78 °C and a solution of silyl ether **154** (0.161 g, 0.500 mmol, 1.0 equiv.) in Et_2O (0.5 mL) was added. The now colorless reaction was allowed to slowly warm to 23 °C overnight. Upon completion, the reaction contents were quenched with saturated aqueous NH_4Cl (5 mL), diluted with EtOAc (5 mL), and the layers were separated. The aqueous layer was then extracted with EtOAc (3 × 10 mL) and the combined organic layers were dried (Na_2SO_4), filtered, and concentrated. The resultant residue was purified

via flash column chromatography (silica gel, hexanes/EtOAc, 6:1) to give ketone **156** (0.126 g, 68% yield) as a colorless oil. **156**: R_f = 0.78 (silica gel, hexanes/EtOAc, 6:1); IR (film) ν_{max} 3076, 2955, 2930, 2897, 2858, 1716, 1642, 1599, 1582 cm^{-1}; ^1H NMR (500 MHz, $CDCl_3$) δ 7.12 (dd, *J* = 7.5, 1.8 Hz, 1 H), 7.08 (td, *J* = 7.7, 1.8 Hz, 1 H), 6.87 (td, *J* = 7.4, 1.2 Hz, 1 H), 6.78 (dd, *J* = 8.1, 1.2 Hz, 1 H), 5.80 (ddt, *J* = 16.9, 10.2, 6.5 Hz, 1 H), 5.02 (dq, *J* = 17.1, 1.7 Hz, 1 H), 4.96 (ddt, *J* = 10.2, 2.2, 1.3 Hz, 1 H), 4.74 (d, *J* = 1.4 Hz, 1 H), 4.68 (dd, *J* = 1.8, 1.0 Hz, 1 H), 2.86 (m, 2 H), 2.72 (m, 6.8 Hz, 2 H), 2.55–2.48 (m, 2 H), 2.31–2.24 (m, 2 H), 2.23–2.14 (m, 2 H), 2.12–2.05 (m, 2 H), 1.00 (s, 9 H), 0.24 (s, 6 H); ^{13}C NMR (126 MHz, $CDCl_3$) δ 209.88, 153.71, 147.86, 138.33, 131.66, 130.40, 127.32, 121.28, 118.54, 114.77, 109.46, 42.96, 41.20, 35.77, 32.05, 29.79, 25.90, 25.35, 18.33, –4.01; HRMS (ESI) calcd for $C_{23}H_{36}NaO_2Si$ $[M+Na]^+$ 395.2377, found 395.2375.

Triene 157. Following general procedure C, ketone **156** (0.129 g, 0.350 mmol, 1.0 equiv.) was converted into triene **157**. The reaction was worked up as usual and then purified via flash column chromatography (silica gel, hexanes) to give triene **157** (0.106 g, 82% yield) as a colorless oil. **157**: R_f = 0.14 (silica gel, hexanes); IR (film) ν_{max} 3077, 2930, 2858, 1643, 1599, 1582 cm^{-1}; ^1H NMR (500 MHz, $CDCl_3$) δ 7.14 (dd, *J* = 7.4, 1.8 Hz, 1 H), 7.07 (ddd, *J* = 8.1, 7.4, 1.8 Hz, 1 H), 6.88 (td, *J* = 7.4, 1.2 Hz, 1 H), 6.79 (dd, *J* = 8.1, 1.2 Hz, 1 H), 5.83 (ddt, *J* = 17.1, 12.7, 6.2 Hz, 1 H), 5.07–4.93 (m, 2 H), 4.82–4.73 (m, 4 H), 2.77–2.70 (m, 2 H), 2.33–2.26 (m, 2 H), 2.23–2.10 (m, 8 H), 1.02 (s, 9 H), 0.24 (s, 6 H); ^{13}C NMR (101 MHz, $CDCl_3$) δ 153.66, 149.61, 149.05, 138.63, 132.91, 130.16, 126.93, 121.15, 118.56, 114.65, 109.28, 109.03, 36.52, 35.64, 34.90, 34.64, 32.18, 29.31, 25.96, 18.39, –3.97; HRMS (ESI) calcd for $C_{24}H_{38}OSi$ $[M+H]^+$ 371.2765, found 371.2764.

Phenol 158. To a solution of triene **157** (0.106 g, 0.290 mmol, 1.0 equiv.) in THF (3 mL) at 23 °C was added TBAF (0.440 mL, 1.0 M in THF, 1.5 equiv.) and the resultant pale-yellow

reaction was stirred at 23 °C. Upon completion of the reaction as indicated by TLC (silica gel, hexanes/EtOAc 20:1; typically 30 min), the reaction contents were quenched with saturated aqueous NH_4Cl (5 mL), diluted with Et_2O (5 mL), and the layers were separated. The aqueous layer was then extracted with Et_2O (3 × 5 mL) and the combined organic layers were washed with brine (10 mL), dried (Na_2SO_4), filtered, and concentrated. The resultant residue was purified via flash column chromatography (silica gel, hexanes/EtOAc, 20:1) to give phenol **158** (67.0 mg, 90% yield) as a colorless oil. **158**: R_f = 0.25 (silica gel, hexanes/EtOAc, 20:1); IR (film) ν_{max} 3466, 3076, 2986, 2933,1644 cm^{-1}; ^1H NMR (400 MHz, $CDCl_3$) δ 7.17–7.05 (m, 2 H), 6.89 (td, *J* = 7.4, 1.2 Hz, 1 H), 6.76 (dd, *J* = 7.9, 1.2 Hz, 1 H), 5.84 (ddt, *J* = 16.8, 10.2, 6.3 Hz, 1 H), 5.09–5.01 (m, 1 H), 5.00–4.94 (m, 1 H), 4.86 –4.80 (m, 2 H), 4.79–4.73 (m, 3 H), 2.82–2.73 (m, 2 H), 2.40–2.31 (m, 2 H), 2.28–2.09 (m, 8 H); ^{13}C NMR (101 MHz, $CDCl_3$) δ 153.54, 149.58, 149.02, 138.64, 130.30, 128.32, 127.35, 121.02, 115.40, 114.67, 109.53, 109.39, 36.22, 35.56, 34.80, 34.54, 32.16, 28.94; HRMS (ESI) calcd for $C_{18}H_{25}O$ $[M+H]^+$ 257.1900, found 257.1901.

Triflate 104. Following general procedure D, phenol **158** (0.393 g, 1.53 mmol, 1.0 equiv.) was converted into triflate **104**. The reaction was worked up as usual and then purified via flash column chromatography (silica gel, hexanes) to give triflate **104** (0.570 g, 96% yield) as a colorless oil. **104**: R_f = 0.30 (silica gel, hexanes); IR (film) ν_{max} 3078, 2979, 2935, 2866, 1644 cm^{-1}; ^1H NMR (400 MHz, $CDCl_3$) δ 7.37–7.22 (m, 4 H), 5.83 (ddt, *J* = 16.8, 10.2, 6.3 Hz, 1 H), 5.08–4.99 (m, 1 H), 4.96 (ddt, *J* = 10.2, 2.2, 1.2 Hz, 1 H), 4.83–4.74 (m, 4 H), 2.90–2.82 (m, 2 H), 2.35 (td, *J* = 7.1, 3.2 Hz, 2 H), 2.26–2.08 (m, 8 H); ^{13}C NMR (101 MHz, $CDCl_3$) δ 148.82, 148.14, 138.60, 134.92, 131.34, 128.49, 128.01, 121.48, 114.67, 110.22, 109.47, 36.37, 35.56, 34.51, 34.44, 32.16, 28.81, 18.16, 12.16; ^{19}F NMR (376 MHz, $CDCl_3$) δ –73.91; HRMS (ESI) calcd for $C_{18}H_{22}O_3S$ $[M+H]^+$ 389.1393, found 389.1389.

Synthesis of Triflate 106

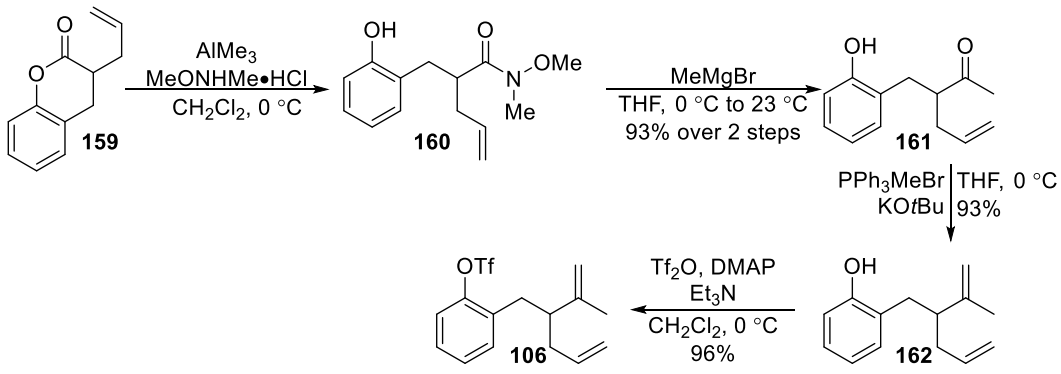

Ketone 161. Following general procedure A, lactone **159**[2] (1.13 g, 6.00 mmol, 1.0 equiv.) was converted to crude Weinreb amide **160**. The reaction was worked up as usual and was taken forward without purification. Following general procedure B, crude Weinreb amide **160** was reacted with MeMgBr to give ketone **161**. The reaction was worked up as usual and then purified by flash column chromatography (silica gel, hexanes/EtOAc, 9:1) to yield ketone **161** (1.13 g, 93% yield over 2 steps) as a colorless oil that existed in a 1.1:1 ratio of the ketone and hemiketal forms based on NMR analysis. **161**: R_f = 0.20 (silica gel, hexanes/EtOAc, 9:1); IR (film) ν_{max} 3380 (bs), 3076, 3039, 2998, 2978, 2933, 1697, 1640, 1609, 1586 cm^{-1}; ^1H NMR (400 MHz, $CDCl_3$) δ 7.18–7.01 (m, 2 H), 6.93–6.77 (m, 3 H), 5.98–5.71 (m, 1 H), 5.19–4.95 (m, 2 H), 3.14–2.91 (m, 1 H), 2.81–2.39 (m, 3 H), 2.37–2.24 (m, 0.5 H), 2.22–1.79 (m, 3 H), 1.65 (s, 1 H); ^{13}C NMR (101 MHz, $CDCl_3$) δ 214.24, 154.15, 152.50, 152.05, 136.50, 136.45, 134.81, 131.02, 129.66, 129.22, 128.03, 127.36, 126.21, 122.28, 120.89, 120.75, 120.66, 117.85, 116.93, 116.84, 116.81, 99.36, 98.64, 54.03, 39.98, 39.68, 36.54, 35.06, 34.04, 30.58, 29.89, 27.21, 27.00, 26.92, 24.48; HRMS (ESI) calcd for $C_{13}H_{17}O$ $[(M+H)-H_2O]^+$ 187.1117, found 187.1110.

Phenol 162. Following general procedure C, ketone **616** (0.817 g, 4.00 mmol, 1.0 equiv.) was converted into phenol **162**. The reaction was worked up as usual and then purified via flash

column chromatography (silica gel, hexanes/EtOAc, 20:1) to give phenol **162** (0.749 g, 93% yield) as a colorless oil. **162**: R_f = 0.17 (silica gel, hexanes/EtOAc, 20:1); IR (film) ν_{max} 3423 (bs), 3073, 3035, 2975, 2923, 2857, 1703, 1641, 1608, 1592 cm^{-1}; ^1H NMR (400 MHz, $CDCl_3$) δ 7.08 (m, 2 H), 6.85 (m, 1 H), 6.75 (dt, *J* = 7.4, 1.1 Hz, 1 H), 5.74 (ddt, *J* = 17.2, 10.2, 7.0 Hz, 1 H), 5.08–4.95 (m, 2 H), 4.80–4.70 (m, 2 H), 4.68 (dq, *J* = 1.6, 0.8 Hz, 1 H), 2.77–2.62 (m, 2 H), 2.49 (p, *J* = 7.2 Hz, 1 H), 2.27–2.12 (m, 2 H), 1.71–1.66 (m, 3 H); ^{13}C NMR (101 MHz, $CDCl_3$) δ 153.75, 147.87, 137.29, 131.26, 127.41, 127.03, 120.77, 115.89, 115.57, 111.74, 77.36, 47.28, 37.59, 34.52, 19.82; HRMS (ESI) calcd for $C_{14}H_{19}O$ $[M+H]^+$ 203.1430, found 203.1427.

Triflate 106. Following general procedure D, phenol **162** (0.404 g, 2.00 mmol, 1.0 equiv.) was converted into triflate **106**. The reaction was worked up as usual and purified via flash column chromatography (silica gel, hexanes) to give triflate **106** (0.641 mg, 96% yield) as a colorless oil. **106**: R_f = 0.27 (silica gel, hexanes); IR (film) ν_{max} 3076, 2926, 1645 cm^{-1}; ^1H NMR (400 MHz, $CDCl_3$) δ 7.33–7.20 (m, 4 H), 5.72 (ddt, *J* = 17.1, 10.2, 7.0 Hz, 1 H), 5.08–4.96 (m, 2 H), 4.71 (p, *J* = 1.5 Hz, 1 H), 4.57 (dt, *J* = 1.8, 0.9 Hz, 1 H), 2.84 (dd, *J* = 14.2, 6.4 Hz, 1 H), 2.72 (dd, *J* = 14.1, 8.8 Hz, 1 H), 2.49 (tt, *J* = 8.5, 6.4 Hz, 1 H), 2.26–2.09 (m, 2 H), 1.66 (dd, *J* = 1.5, 0.8 Hz, 3 H); ^{13}C NMR (126 MHz, $CDCl_3$) δ 148.42, 145.77, 136.60, 133.70, 132.11, 128.15, 128.00, 121.30, 120.00, 117.46, 116.22, 112.74, 47.58, 37.67, 34.10, 18.94; ^{19}F NMR (376 MHz, $CDCl_3$) δ –73.91; HRMS (ESI) calcd for $C_{15}H_{22}F_3O_3S$ $[M+H]^+$ 335.0923, found 335.0920.

Synthesis of Triflate 109

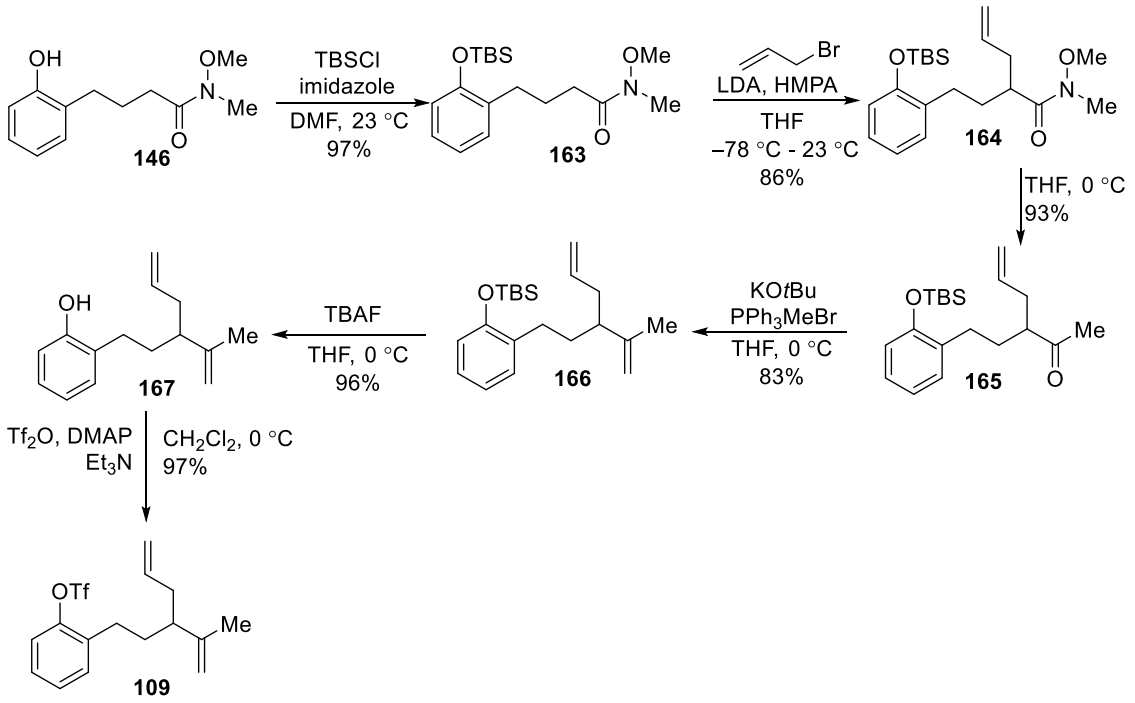

Silyl ether 163 To a solution of Weinreb amide **146** (3.35 g, 15.0 mmol, 1.0 equiv.) in DMF (15 mL) at 23 °C was added imidazole (2.04 g, 30.0 mmol, 2.0 equiv.) and TBSCl (3.39 g, 22.5 mmol, 1.5 equiv.). The resultant colorless solution was then stirred at 23 °C. Upon consumption of starting material as determined by TLC (silica gel, hexanes/EtOAc, 2:1; typically 1 h, the reaction contents were diluted with deionized H_2O (40 mL) and Et_2O (40 mL) and the layers were separated. The aqueous layer was extracted with Et_2O (3 × 20 mL). The combined organic layers were washed with deionized H_2O (3 × 20 mL), dried (Na_2SO_4), filtered, and concentrated. The resultant residue was purified via flash column chromatography (silica gel, hexanes/EtOAc, 6:1) to give silyl ether **163** (4.88 g, 97% yield) as a colorless oil. **163**: R_f = 0.30 (silica gel, hexanes/EtOAc, 6:1); IR (film) ν_{max} 2956, 2931, 2897, 2858, 1667, 1599, 1581 cm^{-1}; ^1H NMR (400 MHz, $CDCl_3$) δ 7.15 (dd, *J* = 7.5, 1.8 Hz, 1 H), 7.06 (td, *J* = 7.7, 1.8 Hz, 1 H), 6.87 (td, *J* = 7.4, 1.2 Hz, 1 H), 6.77 (dd, *J* = 8.0, 1.2 Hz, 1 H), 3.62 (s, 3 H), 3.16 (s, 3 H), 2.70–2.61

(m, 2 H), 2.43 (t, J = 7.7 Hz, 2 H), 1.99–1.87 (m, 2 H), 1.02 (s, 9 H), 0.23 (s, 6 H); ^{13}C NMR (101 MHz, $CDCl_3$) δ 153.72, 132.46, 130.42, 126.96, 121.11, 118.53, 61.24, 31.62, 29.98, 25.95, 25.01, 18.38, –4.01; HRMS (ESI) calcd for $C_{36}H_{63}N_2O_6Si_2$ $[2M+H]^+$ 675.4219, found 675.4225.

Silyl ether 164 To a solution of *i*-Pr_2NH (1.20 mL, 8.45 mmol, 1.2 equiv.) in THF (22 mL) at –10 °C was added *n*BuLi (6.11 mL, 1.28 M in Hexanes[3], 3 equiv.). The resultant pale-yellow solution was stirred at –10 °C for 30 min and then was cooled to –78 °C. Separately, silyl ether **163** (2.20 g, 6.52 mmol, 1.0 equiv.) was added to a flask and azeotropically dried with benzene three times before THF (10 mL) was added. The resultant solution of **163** was added dropwise to the premade LDA solution via a cannula over the course of 5 min and the resultant pale-yellow solution was stirred at –78 °C for 1 h. Next, allyl bromide (0.760 mL, 8.50 mmol, 1.3 equiv.) and anhydrous HMPA (2.80 mL, 15.7 mmol, 2.4 equiv.) were added sequentially at –78 °C and the cooling bath was removed. After either stirring overnight or upon consumption of starting material as determined by TLC (silica gel, hexanes/EtOAc, 6:1; typically 8 h), the reaction contents were quenched with saturated aqueous NH_4Cl (30 mL), diluted with Et_2O (10 mL), and the layers were separated. The aqueous layer was extracted with Et_2O (3 × 20 mL) and the combined organic extracts were dried (Na_2SO_4), filtered, and concentrated. The resultant residue was purified via flash column chromatography (silica gel, hexanes/EtOAc, 9:1) to give silyl ether **164** (2.14 g, 87% yield) as a colorless oil. **164**: R_f = 0.25 (silica gel, hexanes/EtOAc, 9:1); IR (film) ν_{max} 3075, 2957, 2930, 2858, 1643, 1599 cm^{-1}; ^{1}H NMR (500 MHz, $CDCl_3$) δ 7.13 (dd, J = 7.5, 1.8 Hz, 1 H), 7.05 (td, J = 7.6, 1.8 Hz, 1 H), 6.86 (td, J = 7.4, 1.2 Hz, 1 H), 6.76 (dd, J = 8.0, 1.2 Hz, 1 H), 5.75 (ddt, J = 17.1, 10.1, 7.0 Hz, 1 H), 5.05 (dq, J = 17.1, 1.6 Hz, 1 H), 4.98 (ddt, J = 10.2, 2.2, 1.1 Hz, 1 H), 3.59 (s, 3 H), 3.18 (s, 3 H), 2.95 (m, 1 H), 2.65 (ddd, J = 13.6, 10.1, 5.6 Hz, 1 H), 2.53 (ddd, J = 13.7, 10.3, 5.9 Hz, 1 H), 2.41 (dddt, J = 13.9, 8.2, 6.8, 1.3 Hz, 1 H), 2.28–

2.19 (m, 1 H), 1.98–1.86 (m, 1 H), 1.78 (ddt, *J* = 13.3, 10.8, 5.6 Hz, 1 H), 1.01 (s, 9 H), 0.22 (d, *J* = 3.9 Hz, 6 H); ^{13}C NMR (126 MHz, $CDCl_3$) δ 176.83, 153.62, 136.28, 132.49, 130.14, 126.89, 121.09, 118.48, 116.58, 61.42, 40.64, 36.76, 32.15, 28.22, 25.94, 18.37, –3.99, –4.06; HRMS (ESI) calcd for $C_{21}H_{35}NO_3SiNa$ $[M+Na]^+$ 400.2278, found 400.2271.

Ketone 165 Following general procedure B, silyl ether **164** (2.49 g, 6.60 mmol, 1.0 equiv.) was reacted with MeMgBr to give ketone **165**. The reaction was worked up as usual and then was purified by flash column chromatography (silica gel, hexanes/EtOAc, 20:1) to yield ketone **165** (2.03 g, 93% yield) as a colorless oil. **165**: R_f = 0.23 (silica gel, hexanes/EtOAc, 20:1); IR (film) ν_{max} 3075, 2958, 2929, 1700, 1643,1598 cm^{-1}; ^{1}H NMR (500 MHz, $CDCl_3$) δ 7.12–7.04 (m, 2 H), 6.88 (td, *J* = 7.4, 1.2 Hz, 1 H), 6.78 (dd, *J* = 8.0, 1.2 Hz, 1 H), 5.70 (ddt, *J* = 17.1, 10.2, 7.0 Hz, 1 H), 5.08–4.97 (m, 2 H), 2.63–2.49 (m, 3 H), 2.35 (dddt, *J* = 15.0, 8.2, 7.1, 1.3 Hz, 1 H), 2.23 (dddt, *J* = 14.2, 7.2, 5.9, 1.4 Hz, 1 H), 2.12 (s, 3 H), 1.96–1.85 (m, 1 H), 1.74 (dd, *J* = 4.8, 2.8 Hz, 1 H), 1.02 (s, 9 H), 0.23 (d, *J* = 1.3 Hz, 6 H); ^{13}C NMR (126 MHz, $CDCl_3$) δ 211.81, 153.65, 135.59, 132.15, 130.23, 127.13, 121.20, 118.61, 116.96, 52.46, 35.95, 31.28, 29.39, 28.38, 25.95, 18.39, –3.97, –3.99; HRMS (ESI) calcd for $C_{40}H_{63}O_3Si$ $[(2M+H)–H_2O]^+$ 647.4310, found 647.4305.

Diene 166 Following general procedure C, ketone **165** (1.98 g, 5.96 mmol, 1.0 equiv.) was converted into diene **166**. The reaction was worked up as usual and then purified via flash column chromatography (silica gel, hexanes) to give diene **166** (1.63 g, 83% yield) as a colorless oil. **166**: R_f = 0.17 (silica gel, hexanes); IR (film) ν_{max} 3073, 2956, 2929, 2858, 1643, 1599, 1582 cm^{-1}; ^{1}H NMR (400 MHz, $CDCl_3$) δ 7.11 (dd, *J* = 7.5, 1.8 Hz, 1 H), 7.05 (td, *J* = 7.7, 1.8 Hz, 1 H), 6.87 (td, *J* = 7.4, 1.2 Hz, 1 H), 6.77 (dd, *J* = 8.0, 1.2 Hz, 1 H), 5.72 (ddt, *J* = 16.9, 10.1, 6.7 Hz, 1 H), 5.04–4.91 (m, 2 H), 4.80 (dq, *J* = 2.9, 1.5 Hz, 1 H), 4.74 (d, *J* = 2.3 Hz, 1 H), 2.50 (qdd, *J* = 13.7, 10.5, 5.7 Hz, 2 H), 2.23–2.09 (m, 3 H), 1.77–1.63 (m, 4 H), 1.62–1.48 (m, 2 H), 1.01 (s, 9 H), 0.22 (s, 6

H); ^{13}C NMR (101 MHz, $CDCl_3$) δ 153.66, 147.15, 137.58, 133.40, 130.04, 126.69, 121.07, 118.57, 115.38, 111.96, 47.56, 38.38, 33.11, 28.57, 25.97, 18.59, 18.41, –3.96, –3.99; HRMS (ESI) calcd for $C_{21}H_{35}O_5Si$ $[M+H]^+$ 331.2452, found 331.2452.

Phenol 167. To a solution of diene **166** (0.825 g, 2.50 mmol, 1.0 equiv.) in THF (25 mL) at 0 °C was added TBAF (5.00 mL, 1.0 M in THF, 2.0 equiv.) and the resultant light-yellow reaction was allowed to stir at 0 °C. Upon consumption of starting material as determined by TLC (silica gel, hexanes; typically 20 min), the reaction contents were diluted with deionized H_2O (20 mL) and Et_2O (15 mL) and the layers were separated. The aqueous layer was extracted with Et_2O (3 × 15 mL) and the combined organic extracts were dried (Na_2SO_4), filtered, and concentrated. The resultant residue was purified via flash column chromatography (silica gel, hexanes/EtOAc, 20:1) to give silyl ether **167** (0.517 g, 96% yield) as a colorless oil. **167**: R_f = 0.42 (silica gel, hexanes/EtOAc, 9:1); IR (film) ν_{max} 3465 (bs), 3073, 2957, 2929, 2858, 1643 cm^{-1}; ^{1}H NMR (400 MHz, $CDCl_3$) δ 7.14–7.03 (m, 2 H), 6.86 (td, *J* = 7.4, 1.2 Hz, 1 H), 6.76 (dd, *J* = 7.9, 1.2 Hz, 1 H), 5.73 (ddt, *J* = 17.0, 10.1, 6.8 Hz, 1 H), 5.05–4.93 (m, 2 H), 4.86 (dq, *J* = 2.9, 1.5 Hz, 1 H), 4.78 (dd, *J* = 2.1, 0.9 Hz, 1 H), 4.66 (s, 1 H), 2.58 (ddd, *J* = 13.9, 10.1, 5.4 Hz, 1 H), 2.46 (ddd, *J* = 14.0, 10.1, 6.6 Hz, 1 H), 2.25–2.10 (m, 3 H), 1.78–1.57 (m, 6 H); ^{13}C NMR (126 MHz, $CDCl_3$) δ 153.56, 147.31, 137.40, 130.27, 128.51, 127.24, 120.96, 115.56, 115.42, 112.20, 46.99, 38.36, 32.86, 27.82, 18.71; HRMS (ESI) calcd for $C_{15}H_{21}O$ $[M+H]^+$ 217.1587, found 217.1586.

Triflate 109. Following general procedure D, phenol **16** (0.212 g, 1.00 mol, 1.0 equiv.) was converted to triflate **109**. The reaction was worked up as usual and purified via flash column chromatography (silica gel, hexanes/Et_2O, 99:1) to give triflate **109** (0.337 g, 97% yield) as a colorless oil. **109**: R_f = 0.15 (silica gel, hexanes); IR (film) ν_{max} 3075, 2977, 2928, 2875, 1644 cm^{-1}; ^{1}H NMR (500 MHz, $CDCl_3$) δ 7.33–7.21 (m, 4 H), 5.71 (ddt, *J* = 16.9, 10.1, 6.8 Hz, 1 H), 5.05–

4.97 (m, 2 H), 4.85 (p, *J* = 1.5 Hz, 1 H), 4.75 (d, *J* = 2.2 Hz, 1 H), 2.68 (ddd, *J* = 14.2, 10.9, 5.4 Hz, 1 H), 2.56 (ddd, *J* = 14.3, 10.8, 5.9 Hz, 1 H), 2.23–2.10 (m, 3 H), 1.76–1.56 (m, 5 H); ^{13}C NMR (126 MHz, $CDCl_3$) δ 148.18, 146.38, 137.09, 135.51, 131.37, 128.45, 127.80, 121.42, 115.75, 112.51, 47.25, 38.18, 33.01, 28.18, 18.45; ^{19}F NMR (376 MHz, $CDCl_3$) δ –73.91; HRMS (ESI) calcd for $C_{16}H_{20}F_3O_3S$ $[M+H]^+$ 349.1080, found 349.1079.

Synthesis of Triflate 111

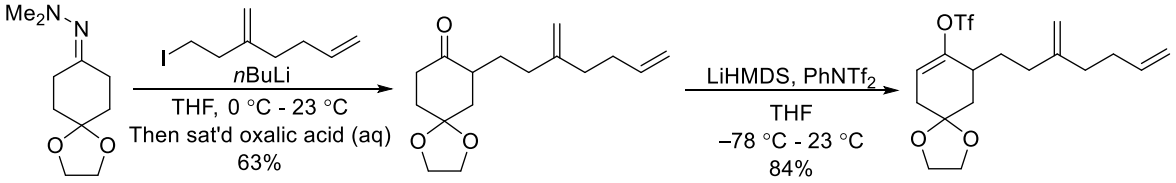

168 **169** **111**

Ketone 169. Using a literature procedure,[9] hydrazone **168** (0.198 g, 1.00 mmol, 1.0 equiv.) was dried azeotropically with benzene three times before being dissolved in THF (5 mL) and then cooled to 0 °C. Then, *n*-BuLi (0.750 mL, 1.6 M in hexanes, 1.2 equiv.) was added dropwise to give a yellow solution that was stirred at 0 °C for 2 h. A solution of iodide **155**[7] (0.283 g, 1.20 mmol, 1.2 equiv.) in THF (1.7 mL) was then added and the resultant yellow solution was allowed to warm to 23 °C overnight. Upon completion, the reaction contents were quenched with saturated aqueous NH_4Cl (5 mL), diluted with Et_2O (5 mL), and the layers were separated. The aqueous layer was extracted with Et_2O (3 × 5 mL) and the combined organic layers were concentrated directly. The resultant residue was dissolved in THF (4.1 mL) and then saturated aqueous oxalic acid (1.5 mL) was added at 23 °C and the reaction contents were stirred at 23 °C for 1 h. Upon consumption of starting material as determined by TLC (silica gel, CH_2Cl_2 /Et_2O, 1:1; typically 5 hr), the reaction contents were diluted with deionized H_2O (10 mL) and hexanes (10 mL) and the layers were separated. The aqueous layer was extracted with hexanes (3 × 5 mL) and then the

combined organic layers were dried (Na_2SO_4), filtered, and concentrated. The resultant residue was purified via flash column chromatography (silica gel, hexanes/EtOAc, 9:1→6:1) to give ketone **169** (0.168 g, 64% yield) as a light-yellow oil. **169**: R_f = 0.18 (silica gel, hexanes/EtOAc, 6:1); IR (film) ν_{max} 3050, 2983, 2933, 2890, 1715 cm^{-1}; ^1H NMR (400 MHz, $CDCl_3$) δ 5.81 (ddt, *J* = 16.8, 10.2, 6.4 Hz, 1 H), 5.02 (dq, *J* = 17.1, 1.7 Hz, 1 H), 4.95 (ddt, *J* = 10.1, 2.2, 1.2 Hz, 1 H), 4.74 (t, *J* = 1.1 Hz, 2 H), 4.11–3.97 (m, 4 H), 2.70–2.57 (m, 2 H), 2.37 (ddd, *J* = 14.2, 5.1, 3.3 Hz, 1 H), 2.24–1.90 (m, 10H), 1.71 (t, *J* = 13.1 Hz, 1 H), 1.36–1.23 (m, 1 H); ^{13}C NMR (101 MHz, $CDCl_3$) δ 211.63, 148.77, 138.59, 114.66, 109.66, 107.60, 64.89, 64.74, 45.97, 40.74, 38.43, 35.38, 34.83, 33.37, 32.11, 27.13; HRMS (ESI) calcd for $C_{16}H_{25}O_3$ $[M+H]^+$ 265.1798, found 265.1795.

Triflate 111. Ketone **169** (0.168 g, 0.640 mmol, 1.0 equiv.) was azeotropically dried with benzene three times before it was dissolved in THF (5 mL) and cooled to –78 °C. Then, LiHMDS (1.30 mL, 1.0 M in THF, 2.0 equiv.) was added and the yellow solution was stirred at –78 °C for 2 h. Then $PhNTf_2$ (0.456 g, 1.28 mmol, 1.2 equiv.) was added as a solution in THF (1.4 mL) and the reaction was allowed to warm to 23 °C overnight. Upon completion, the reaction contents were quenched with saturated aqueous $NaHCO_3$ (10 mL), diluted with hexanes (10 mL), and then the layers were separated. The aqueous layer was extracted with hexanes (3 × 10 mL) then the combined organic layers were washed with saturated aqueous $NaHCO_3$ (5 × 5 mL), dried ($MgSO_4$), filtered, and concentrated. The resultant residue was purified via flash column chromatography (silica gel, hexanes/EtOAc, 20:1→9:1) to give triflate **111** (0.195 g, 77% yield) as a yellow oil. **111**: R_f = 0.22 (silica gel, hexanes/EtOAc, 9:1); IR (film) ν_{max} 3078, 2933, 1683, 1645 cm^{-1}; ^1H NMR (400 MHz, $CDCl_3$) δ 5.82 (ddt, *J* = 16.8, 10.2, 6.3 Hz, 1 H), 5.68 (ddd, *J* = 5.1, 3.2, 1.9 Hz, 1 H), 5.03 (dq, *J* = 17.1, 1.7 Hz, 1 H), 4.96 (ddt, *J* = 10.2, 2.1, 1.2 Hz, 1 H), 4.79–4.74 (m, 2 H), 4.04–3.91 (m, 4 H), 2.83–2.69 (m, 1 H), 2.47 (dt, *J* = 17.7, 3.3 Hz, 1 H), 2.35 (ddt, *J* = 17.7, 5.0,

2.2 Hz, 1 H), 2.25–1.83 (m, 8 H), 1.71 (dd, J = 13.2, 9.0 Hz, 1 H), 1.68–1.55 (m, 1 H); ^{13}C NMR (101 MHz, $CDCl_3$) δ 151.19, 148.09, 138.42, 115.98, 114.78, 110.18, 106.61, 64.89, 64.75, 36.68, 36.63, 35.24, 34.63, 32.52, 32.08, 28.96; ^{19}F NMR (376 MHz, $CDCl_3$) δ –74.00; HRMS (ESI) calcd for $C_{17}H_{24}F_3O_5S$ $[M+H]^+$ 397.1291, found 396.1286.

Synthesis of Triflate 113

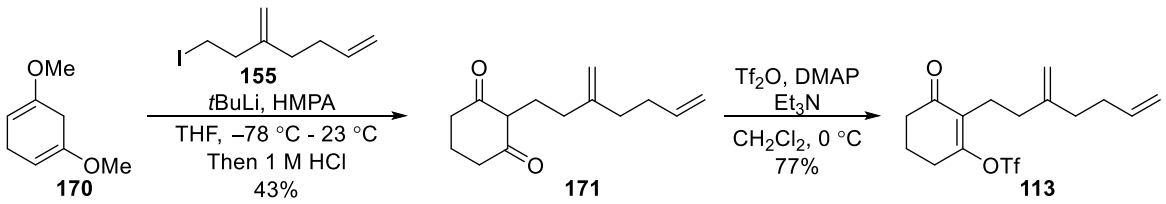

Diketone 171. Using a literature procedure,[6] a flask was charged with THF (4 mL) then cooled to –78 °C and *t*-BuLi (0.653 mL, 1.7 M in pentane, 1.11 equiv.) was added to give a bright yellow solution. A solution of dienol ether **170** (0.140 g, 1.00 mmol, 1.0 equiv.) in THF (1 mL) was then added with no visible change in reaction color and the resultant yellow solution was stirred at –78 °C for 1 h. HMPA (0.203 mL, 1.17 mmol, 1.17 equiv.) was then added, giving a dark red solution, followed by a solution of iodide **155**[7] (0.307 g, 1.30 mmol, 1.3 equiv.) in THF (1 mL). The resultant light yellow solution was then allowed to warm slowly to 23 °C overnight. The reaction was then quenched with saturated aqueous NH_4Cl (10 mL), diluted with Et_2O (5 mL), and the layers were separated. The aqueous layer was then extracted with Et_2O (3 × 5 mL) and the combined organic layers were washed with brine (10 mL) and concentrated. The resultant crude residue was added to a flask followed by a mixture of acetone and 1 M HCl (6 mL, 3:1) and the mixture was stirred at 23 °C. Upon completion as indicated by TLC (silica gel, hexanes/EtOAc 1.5:1; typically 1 h), the reaction contents were quenched with saturated aqueous $NaHCO_3$ (5 mL), diluted with Et_2O (5 mL), and the layers were separated. The aqueous layer was then extracted

with Et_2O (3 × 5 mL) and the combined organic layers were washed with brine (10 mL), dried (Na_2SO_4), filtered, and concentrated. The resultant residue was purified via flash column chromatography (silica gel, hexanes/Et_2O, 1.5:1) to give diketone **171** (0.136 g, 62% yield) as a colorless solid. **171**: R_f = 0.25 (silica gel, hexanes/Et_2O, 1.5:1); IR (film) ν_{max} 3079, 2990, 2946, 1720, 1712 cm^{-1}; ^1H NMR (500 MHz, $CDCl_3$) δ 6.68 (s, 1 H), 5.81 (ddq, *J* = 17.2, 10.3, 6.6 Hz, 1 H), 5.09–4.92 (m, 2 H), 4.84–4.65 (m, 2 H), 3.42 (t, *J* = 5.7 Hz, 0,3 H), 2.73–2.53 (m, 2 H), 2.41 (dd, *J* = 8.9, 6.6 Hz, 4 H), 2.31–1.70 (m, 10H); ^{13}C NMR (126 MHz, $CDCl_3$) δ 205.14, 149.74, 148.29, 138.78, 138.46, 116.05, 114.69, 114.46, 110.19, 109.15, 66.65, 39.97, 35.61, 35.18, 34.73, 33.49, 32.11, 31.99, 20.93, 20.71, 20.49, 18.29; HRMS (ESI) calcd for $C_{14}H_{21}O_2$ $[M+H]^+$ 221.1534, found 221.1534.

Triflate 113. Following general procedure D, diketone **171** (68.0 mg, 0.309 mmol, 1.0 equiv.) was converted into triflate **113**. The reaction was worked up as usual and then purified via flash column chromatography (silica gel, hexanes/EtOAc, 9:1) to give triflate **113** (84.0 mg, 77% yield) as a colorless oil that decomposed readily even when stored at –35 °C. **113**: R_f = 0.28 (silica gel, hexanes/EtOAc, 9:1); IR (film) ν_{max} 3079, 2936, 1690, 1660 cm^{-1} ^1H NMR (400 MHz, $CDCl_3$) δ 5.82 (ddt, *J* = 16.8, 10.2, 6.3 Hz, 1 H), 5.03 (dq, *J* = 17.1, 1.6 Hz, 1 H), 4.95 (ddt, *J* = 10.2, 2.2, 1.2 Hz, 1 H), 4.78–4.71 (m, 2 H), 2.76 (tt, *J* = 6.3, 1.2 Hz, 2 H), 2.52–2.43 (m, 4 H), 2.25–2.14 (m, 2 H), 2.14 (d, *J* = 4.8 Hz, 1 H), 2.14–2.05 (m, 4 H), 2.09–2.02 (m, 1 H); ^{13}C NMR (126 MHz, $CDCl_3$) δ 197.34, 162.13, 147.99, 138.49, 131.81, 119.67, 117.13, 114.70, 110.34, 37.00, 35.03, 34.56, 32.06, 28.86, 22.68, 20.77; ^{19}F NMR (376 MHz, $CDCl_3$) δ –74.31; HRMS (ESI) calcd for $C_{15}H_{18}F_3O_3S$ $[(M+H)–H_2O]^+$ 335.0929, found 335.0920.

Synthesis of Triflate 128

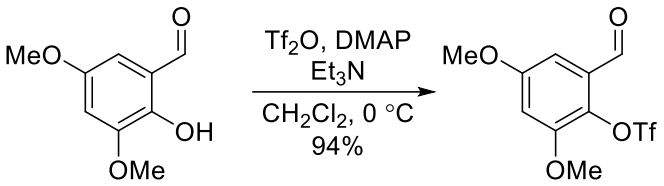

172 **128**

Triflate 128. Following general procedure D, phenol **172**[10] (0.533 g, 2.92 mmol, 1.0 equiv.) was converted into triflate **128**. The reaction was worked up as usual and then purified via flash column chromatography (silica gel, hexanes/EtOAc, 20:1→12:1) to give triflate **128** (0.862 g, 94% yield) as a colorless solid. **128**: R_f = 0.35 (silica gel, hexanes/EtOAc, 9:1); IR (film) ν_{max} 3054, 2986, 1700, 1595 cm^{-1}; ^1H NMR (400 MHz, $CDCl_3$) δ 10.22 (s, 1 H), 6.97 (d, *J* = 2.9 Hz, 1 H), 6.80 (d, *J* = 2.9 Hz, 1 H), 3.92 (s, 3 H), 3.87 (s, 3 H); ^{13}C NMR (101 MHz, $CDCl_3$) δ 186.55, 159.84, 152.77, 134.28, 129.97, 123.62, 120.43, 117.24, 114.06, 106.72, 102.43, 56.68, 56.17; ^{19}F NMR (376 MHz, $CDCl_3$) δ –72.70; HRMS (ESI) calcd for $C_{10}H_{10}F_3O_3S$ $[M+H]^+$ 315.1045, found 315.0144.

General procedure E: Conditions Screening for spirocycle 83

To a dry 2-dram vial in a glove-box was added ligand (0.012 mmol, 0.12 equiv.), base (0.300 mmol, 3.0 equiv.), and the Ni^0 source (0.010 mmol, 0.10 equiv.) followed by the reaction solvent (0.40 mL). The resultant mixture was stirred at 23 °C for 15 min. Then, triflate **82** (33.4 mg, 0.100 mmol, 1.0 equiv.) was added as a stock solution in the reaction solvent (0.18 mL, 185 mg/mL) and the vial was then sealed with a Teflon cap and heated at 100 °C for 24 h using a heating block. Upon completion, the contents were cooled to 23 °C, removed from the glove box, and diluted with Et_2O (0.5 mL) before being filtered through a silica plug with additional Et_2O

into a vial pre-charged with dodecane (~10 mg) as an internal standard. The final mixture was diluted to a volume of ~10 mL and the conversion and yield was then determined by GC analysis.

Table S1. Base Screening

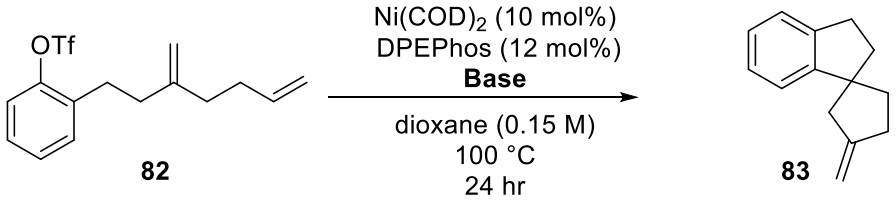

82 83

Entry	Base	Equiv.	Conversion[a]	Yield[a]
1	DABCO	3	100%	70%
2	DABCO	6	100%	74%
3	Quinuclidine	3	100%	70%
4	Quinuclidine	6	100%	73%
5	Cy_2NMe	3	100%	15%
6	Et_3N	3	100%	23%
7	DIPEA	3	>95%	11%
8	PMP	3	>95%	10%
9	urotropine	3	82%	9%
10	Proton Sponge	3	66%	7%
11	pyridine	3	69%	7%
12	imidazole	3	58%	8%
13	DBU	3	100%	58%
14	DBN	3	100%	39%
15	TBD	3	44%	0%
16	MeTBD	3	40%	19%
17	TMG	3	39%	16%
18	KOAc	5	54%	17%
19	K_2CO_3	5	81%	7%
20	Cs_2CO_3	5	80%	7%
21	NaO*t*Bu	5	100%	6%
22	KO*t*Bu	5	100%	5%

[a] Determined by GC using dodecane as an internal standard

Table S2. Ligand Screening

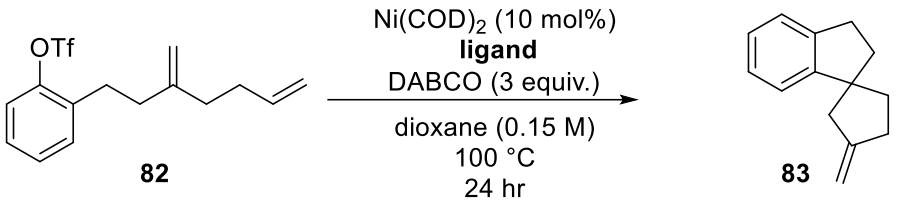

82 83

Entry	Ligand	mol%	Conversion[a]	Yield[a]
1	PPh_3	40	100%	56%
2	P(2-furyl)$_3$	40	80%	42%
3	$P(C_6F_5)_3$	40	22%	4%
4	P(3,5-CF_3-Ph)$_3$	40	65%	14%
5	PCy_3	40	82%	7%
6	P(OPh)$_3$	40	67%	34%
7	P(OEt)$_3$	40	10%	5%
8	$AsPh_3$	40	48%	12%
9	dppm	12	63%	20%
10	dppe	12	96%	28%
11	dppbz	12	100%	40%
12	dppp	12	100%	45%
13	dppb	12	100%	56%
14	dpppe	12	100%	70%
15	dpphex	12	100%	60%
16	DPEphos	12	100%	70%
17	Xantphos	12	100%	33%
18	BINAP	12	100%	54%
19	SEGPHOS	12	97%	40%
20	DPPF	12	100%	57%
21	DIOP	12	100%	53%
22	A	12	43%	13%
23	Triphos-1	12	100%	25%
24	Triphos-2	12	100%	12%
25	B	12	100%	64%
26	*i*PrPhox	12	91%	53%
27	CyJohnphos	12	76%	16%
28	Jackiephos	12	53%	13%
29	C	12	68%	12%
30	1,10-phenathroline	12	51%	18%

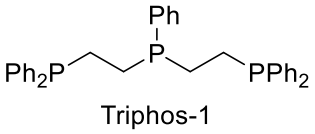

Triphos-1

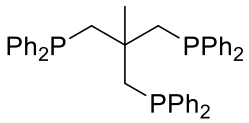

Triphos-2

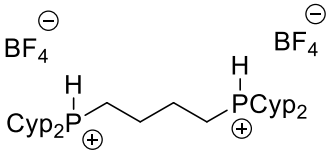

A

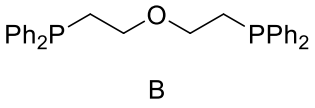

B

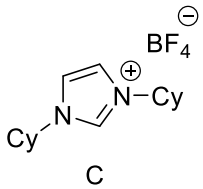

C

[a] Determined by GC using dodecane as an internal standard

Table S3. Solvent Screening

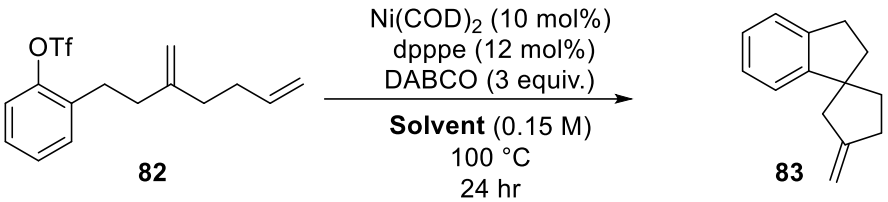

82 83

Entry	Solvent	Conversion[a]	Yield[a]
1	dioxane	100%	70%
2	THF	95%	69%
3	DME	100%	76%
4	diglyme	100%	73%
5	toluene	100%	53%
6	MeCN	100%	6%
7	DMF	100%	21%

[a] Determined by GC using dodecane as an internal standard

Table S4. Temperature Screening

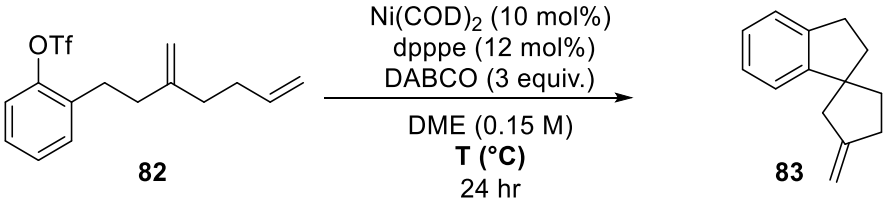

82 83

Entry	T (°C)	Conversion[a]	Yield[a]
1	0	100%	68%[b]
2	23	100%	74%
3	40	100%	68%
4	60	100%	68%
5	80	100%	67%
6	100	100%	76%
7	120	100%	63%

[a] Determined by GC using dodecane as an internal standard

[b] Reaction was run for 48 hr to ensure complete conversion

Table S5. Leaving Group Scope

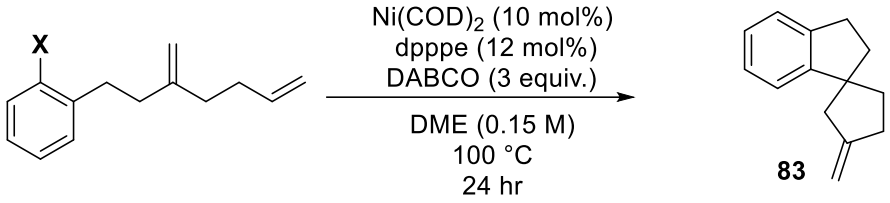

Compound	X	TESOTf (equiv.)	Yield[a]
82	OTf	**0**	76%[b]
88	Cl	**2**	54%[c]
89	Br	**2**	49%[c]
90	I	**2**	12%[c]
141	OPiv	**2**	0%[d]
142	OMe	**2**	0%[d]
143	OBoc	**2**	0%[d]
91	OTs	**0**	30%[c]
91	OTs	**2**	42%[c]
92	OMs	**0**	20%[c]
92	OMs	**2**	20%[c]
93	ONf	**0**	76%[b]
93	ONf	**2**	73%[b]

[a]Determined by GC using dodecane as an internal standard, [b] Complete conversion by TLC, [c] Incomplete conversion by TLC, [d] No conversion by TLC

Table S6. Nickel Source Screening

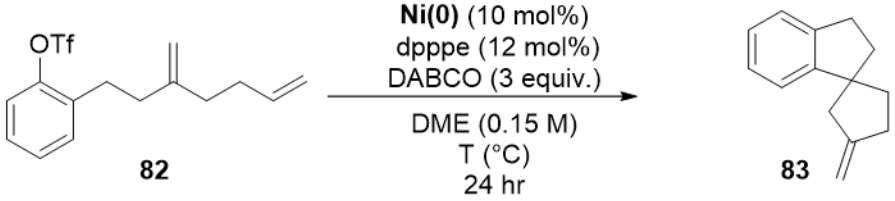

Entry	Ni Source	Conversion[a]	Yield[a]
1	$Ni(COD)_2$	100%	76%
2	$Ni(PPh_3)_4$	100%	70%
3	$Ni(^{F}stb)_3$	100%	63%
4	$Ni(^{F}stb)_3$	91%	47%[b]
5	Ni(COD)(DQ)	100%	64%
6	Ni(COD)(DQ)	0%	0%[b]

[a] Determined by GC using dodecane as an internal standard

[b] Reaction was setup outside of glovebox

Table S7. Additive Screening

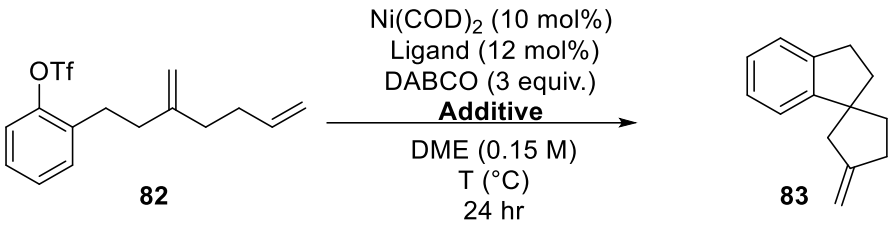

Entry	Ligand	Additive	Equiv.	Conversion[a]	Yield[a]
1	DPEphos	nBu$_4$NOAc	0.2	42%	4%
2	DPEphos	PhCN	1	100%	40%
3	dpppe	PhCN	1	100%	31%
4	BINAP	PhCN	1	100%	61%
5	Xantphos	PhCN	1	100%	46%
6	dpppe	TEMPO	1	10%	0%
7	dpppe	Galvinoxyl	1	3%	0%
8	dpppe	BHT	1	100%	76%
9	dpppe	DHA	1	100%	68%
10	dpppe	DPE	1	100%	65%

[a] Determined by GC using dodecane as an internal standard

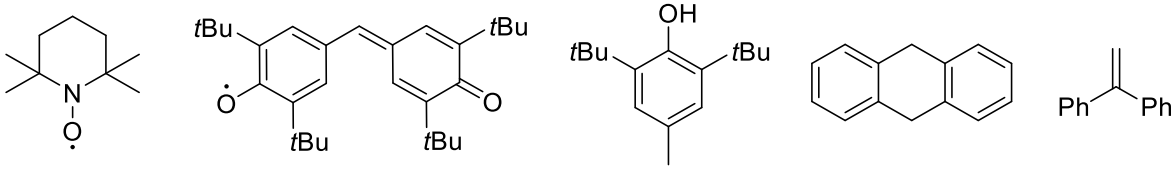

TEMPO Galvinoxyl Free Radical BHT DHA DPE

General Procedure F: Intramolecular Nickel Heck Cascade Conditions

To a dry flask in a glove-box was added dpppe (0.12 equiv.), DABCO (3.0 equiv.), and $Ni(COD)_2$ (0.1 equiv.) followed by DME (60% of total solvent) and the mixture was stirred at 23 °C for 15 min. Then, a solution of triflate (1.0 equiv.) in DME (40% of total solvent) was added and the flask was sealed and heated to the required temperature until starting material was fully consumed as shown by TLC analysis. The reaction contents were then cooled to 23 °C if heated, removed from the glove box, and diluted with Et_2O before filtered through a silica plug (using Et_2O as eluent). The filtrate was then concentrated and the residue was purified by flash column chromatography to give the desired product.

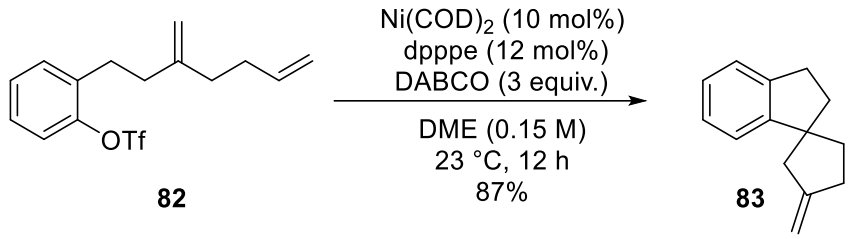

Spirocycle 83[11] Following general procedure F, triflate **82** (3.34 g, 10.0 mmol, 1.0 equiv.) was converted into spirocycle **83**. The reaction was worked up as usual and then purified via flash column chromatography (silica gel, pentanes) to give spirocycle **83** (1.61 g, 87% yield) as a colorless oil. **83**: R_f = 0.70 (silica gel, hexanes); IR (film) ν_{max} 3068, 3019, 2841, 2853, 1653 cm^{-1}; ^1H NMR (400 MHz, $CDCl_3$) δ 7.24–7.14 (m, 4 H), 4.96–4.93 (M, 2 H), 2.95–2.85 (m, 2 H), 2.60–2.41 (m, 4 H), 2.07–1.90 (m, 3 H), 1.83 (dddd, *J* = 12.4, 8.1, 4.2, 1.5 Hz, 1 H); ^{13}C NMR (101 MHz, $CDCl_3$) δ 152.18, 150.01, 143.82, 126.60, 126.52, 124.55, 122.30, 106.10, 55.10, 46.74, 39.18, 39.12, 31.75, 30.51; HRMS (ESI) calcd for $C_{14}H_{17}$ $[M+H]^+$ 185.1330, found 185.1325.

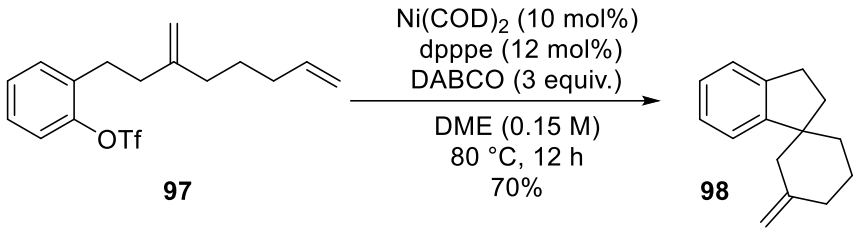

Spirocycle 98[11] Following general procedure F, triflate **97** (69.2 mg, 0.200 mmol, 1.0 equiv.) was converted into spirocycle **98**. The reaction was worked up as usual and then purified via flash column chromatography (silica gel, pentanes) to give spirocycle **98** (27.6 mg, 70% yield) as a colorless oil. **98**: R_f = 0.71 (silica gel, hexanes); IR (film) ν_{max} 3054, 2987, 2865, 1655 cm^{-1}; ^1H NMR (500 MHz, $CDCl_3$) δ 7.24–7.15 (m, 4 H), 4.76 (dt, *J* = 2.6, 1.6 Hz, 1 H), 4.64 (q, *J* = 1.9 Hz, 1 H), 2.94–2.80 (m, 2 H), 2.37–1.98 (m, 6 H), 1.80 (dddd, *J* = 13.7, 7.1, 3.1, 1.6 Hz, 3 H), 1.62 (dtd, *J* = 7.5, 3.6, 1.7 Hz, 1 H), 1.60–1.49 (m, 1 H); ^{13}C NMR (126 MHz, $CDCl_3$) δ 151.43, 147.73, 143.41, 126.71, 126.35, 124.75, 122.71, 108.87, 49.93, 46.27, 36.85, 35.82, 34.87, 29.94, 24.52.; HRMS (ESI) calcd for $C_{30}H_{37}$ $[2M+H]^+$ 397.2890, found 397.2896.

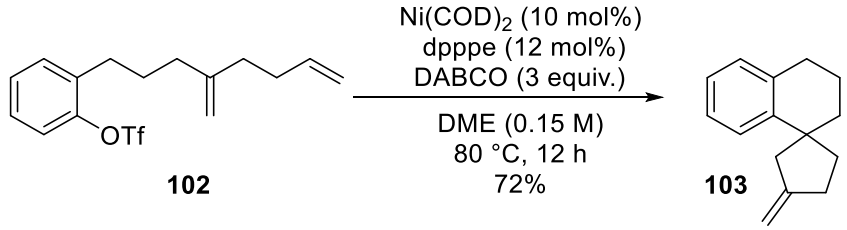

Spirocycle 103.[11] Following general procedure F, triflate **102** (34.8 mg, 0.100 mmol, 1.0 equiv.) was converted into spirocycle **103**. The reaction was worked up as usual and then purified via flash column chromatography (silica gel, pentanes) to give spirocycle **103** (14.2 mg, 72% yield) as a colorless oil with ~5% isomers present. An analytically pure sample was accessed using $AgNO_3$-impregnated silica gel. **103**: R_f = 0.70 (silica gel, hexanes); IR (film) ν_{max} 3051, 3017, 2935, 2863, 1683, 1599 cm^{-1}; ^1H NMR (500 MHz, $CDCl_3$) δ 7.35 (d, *J* = 7.9 Hz, 1 H), 7.16 (tdd,

J = 6.8, 2.1, 0.8 Hz, 1 H), 7.13–7.03 (m, 2 H), 4.93 (qd, *J* = 3.9, 1.9 Hz, 2 H), 2.80 (t, *J* = 6.3 Hz, 2 H), 2.69 (dd, *J* = 16.2, 2.6 Hz, 1 H), 2.61–2.41 (m, 3 H), 2.08 (dt, *J* = 12.9, 9.3 Hz, 1 H), 1.90–1.63 (m, 5 H); ^{13}C NMR (126 MHz, $CDCl_3$) δ 152.65, 144.27, 137.34, 129.11, 126.78, 126.08, 125.53, 106.01, 49.97, 45.51, 41.83, 35.76, 31.29, 30.72, 20.38; HRMS (ESI) calcd for $C_{30}H_{37}$ $[2M+H]^+$ 397.2890, found 397.2890.

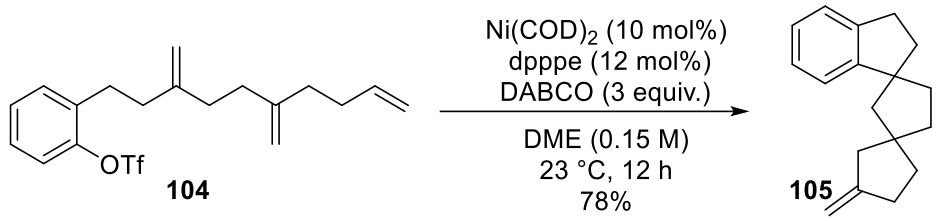

Spirocycle 105. Following general procedure F, triflate **104** (0.194 g, 0.500 mmol, 1.0 equiv.) was converted into spirocycle **105**. The reaction was worked up as usual and then purified via flash column chromatography (silica gel, pentanes) to give spirocycle **105** (0.186 g, 78%, dr = 5:1; major/minor diastereomer identity not determined) as a colorless oil with ~5% isomers present. An analytically pure sample was prepared using $AgNO_3$-impregnated silica gel. **105**: R_f = 0.75 (silica gel, hexanes); IR (film) ν_{max} 3053, 2942, 2859, 1709 cm^{-1}; ^{1}H NMR (500 MHz, $CDCl_3$) δ 7.25–7.06 (m, 4 H), 4.91–4.88 (m, 1 H), 4.86–4.83 (m, 1 H), 2.88 (t, *J* = 7.1 Hz, H), 2.46–2.31 (m, 4 H), 2.06 (td, *J* = 6.8, 4.4 Hz, 2 H), 1.96–1.65 (m, 2 H); ^{13}C NMR (126 MHz, $CDCl_3$) δ 152.80, 152.48, 152.13, 143.33, 126.61, 126.59, 126.23, 124.39, 122.18, 122.15, 105.66, 55.45, 55.40, 52.43, 52.30, 50.62, 50.59, 48.01, 47.89, 42.12, 41.96, 40.28, 40.25, 40.19, 38.72, 38.61, 31.81, 31.55, 30.81, 30.78; HRMS (ESI) calcd for $C_{18}H_{22}$ $[M]^{2+}$ 119.0856, found 119.0859.

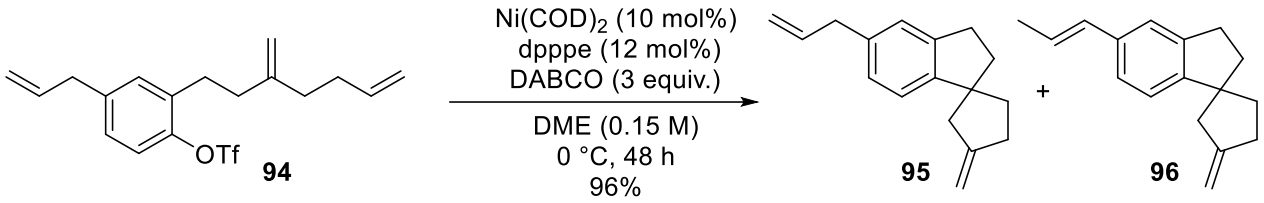

Spirocycle 95 and styrene 96. Following general procedure F, triflate **94** (74.4 mg, 0.200 mmol, 1.0 equiv.) was converted into spirocycle **95**. The reaction was worked up as usual and then purified via flash column chromatography (silica gel, pentanes) to give spirocycle **95** (42.9 mg, 96% yield, **95**:**96 =** 20:1) as a colorless oil. **95**: R_f = 0.71 (silica gel, hexanes); IR (film) ν_{max} 3054, 2983, 2945, 2859, 1608 cm^{-1}; ^1H NMR (400 MHz, $CDCl_3$) δ 7.15–6.89 (m, 3 H), 5.97 (ddt, *J* = 16.9, 10.0, 6.8 Hz, 1 H), 5.22–4.98 (m, 2 H), 4.95–4.89 (m, 2 H), 3.40–3.33 (m, 2 H), 2.95–2.78 (m, 2 H), 2.65–2.33 (m, 4 H), 2.05–1.75 (m, 4 H); ^{13}C NMR (101 MHz, $CDCl_3$) δ 152.26, 147.89, 144.20, 138.58, 137.97, 126.85, 124.71, 122.23, 115.69, 106.05, 54.80, 46.80, 40.32, 39.29, 39.23, 31.75, 30.44, 29.86; HRMS (ESI) calcd for $C_{17}H_{21}$ $[M+H]^+$ 225.1638, found 225.1637.

96: R_f = 0.72 (silica gel, hexanes); IR (film) ν_{max} 3071, 3051, 3006, 2928, 2855, 1653, 1637 cm^{-1}; ^1H NMR (500 MHz, $CDCl_3$) δ 7.22–7.02 (m, 4 H), 6.39 (dq, *J* = 15.8, 1.7 Hz, 1 H), 6.18 (dq, *J* = 15.8, 6.6 Hz, 1 H), 4.93 (h, *J* = 2.0 Hz, 2 H), 2.93–2.75 (m, 2 H), 2.59–2.39 (m, 2 H), 2.07–1.74 (m, 8 H); ^{13}C NMR (126 MHz, $CDCl_3$) δ 152.20, 148.80, 144.16, 136.75, 131.27, 124.84, 124.59, 122.27, 121.74, 106.08, 54.88, 46.72, 39.23, 39.17, 31.74, 30.41, 18.64; HRMS (ESI) $C_{17}H_{21}$ $[M+H]^+$ 225.1638, found 225.1630.

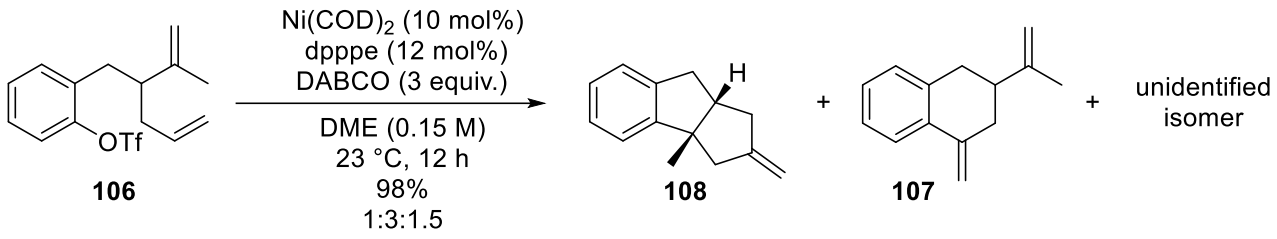

Tricycle 108 and diene 107.[11] Following general procedure F, triflate **106** (0.167 g, 0.500 mmol, 1.0 equiv.) was converted into tricycle **108** and diene **107**. The reaction was worked up as usual and then purified via flash column chromatography (silica gel, pentanes) to give tricycle **108**, diene **107**, and a unidentified isomer (0.092 g, 98% yield, **108**:**107**:isomer = 1:3:1.5) as a colorless oil. Analytically pure samples of **108** and **107** were prepared using Pattenden's procedure[12] and spectral data matched that previously reported. **108**: R_f = 0.65 (silica gel, hexanes); ^{1}H NMR (500 MHz, $CDCl_3$) δ 7.22–7.12 (m, 4 H), 4.76–4.70 (m, *J* = 1.8 Hz, 2 H), 3.17 (dd, *J* = 16.1, 7.8 Hz, 1 H), 2.71 –2.63 (m, 3 H), 2.57–2.41 (m, 2 H), 2.15–2.08 (m, 1 H), 1.33 (s, 3 H); ^{13}C NMR (126 MHz, $CDCl_3$) δ 152.55, 151.43, 142.17, 126.80, 126.64, 123.17, 105.45, 55.83, 46.98, 40.20, 37.73, 27.38.

107: R_f = 0.65 (silica gel, hexanes); ^{1}H NMR (500 MHz, $CDCl_3$) δ 7.70–7.63 (m, 1 H), 7.23–7.06 (m, 3 H), 5.53–5.50 (m, 1 H), 5.00–4.97 (m, 1 H), 4.85–4.78 (m, 2 H), 2.96–2.90 (m, 1 H), 2.85–2.75 (m, 1 H), 2.73–2.63 (m, 1 H), 2.53–2.41 (m, 2 H), 1.82 (s, 3 H); ^{13}C NMR (126 MHz, $CDCl_3$) δ 148.83, 143.37, 137.05, 134.27, 129.33, 127.90, 126.18, 124.15, 109.62, 108.55, 42.25, 38.42, 36.02, 20.84.

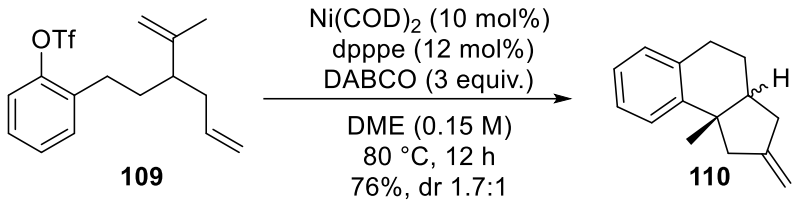

Tricycle 110.[11] Following general procedure F, triflate **109** (69.0 mg, 0.200 mmol, 1.0 equiv.) was converted into tricycle **110**. The reaction was worked up as usual and then purified via flash column chromatography (silica gel, pentanes) to give tricycle **110** (30.0 mg, 76%, dr = 1.7:1 based on ^{1}H NMR) as a colorless oil. Analytically pure samples of **110** were prepared via $AgNO_3$-impregnated silica gel. **110**: R_f = 0.63 (silica gel, hexanes); IR (film) ν_{max} 3067, 3015, 2929, 1683, 1660, 1598 cm^{-1}; ^{1}H NMR (400 MHz, $CDCl_3$) δ 7.30–7.22 (m, 2 H), 7.22–6.98 (m, 9 H), 5.05–5.01 (m, 1 H), 4.97 (m, 1 H), 4.89–4.81 (m, 3 H), 3.08–2.89 (m, 2 H), 2.83–2.59 (m, 8 H), 2.57–2.39 (m, 4 H), 2.30–2.08 (m, 3 H), 2.08–1.88 (m, 4 H), 1.88–1.69 (m, 3 H), 1.64–1.49 (m, 3 H), 1.32 (d, *J* = 1.2 Hz, 5 H), 0.99 (d, *J* = 1.0 Hz, 3 H); ^{13}C NMR (101 MHz, $CDCl_3$) δ 150.82, 150.72, 147.73, 144.66, 136.02, 135.84, 129.17, 128.80, 127.69, 126.27, 125.73, 125.50, 125.33, 125.11, 107.79, 106.30, 48.62, 45.96, 45.62, 44.98, 44.75, 44.19, 37.86, 35.29, 29.98, 29.13, 28.67, 26.82, 22.79, 22.16; HRMS (ESI) calcd for $C_{15}H_{19}$ $[M+H]^+$ 199.1481, found 199.1472.

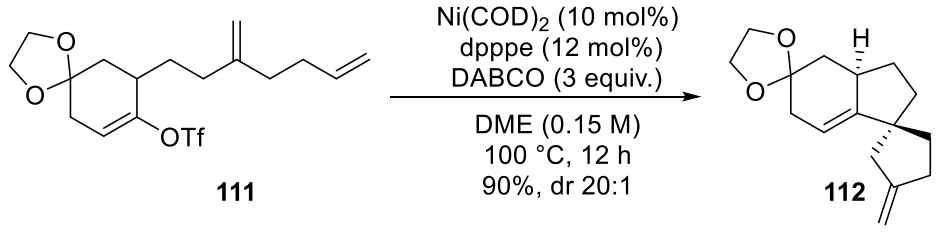

Spirocycle 112.[13] Following general procedure F, triflate **111** (0.119 g, 0.300 mmol, 1.0 equiv.) was converted into spirocycle **112**. The reaction was worked up as usual and then purified via flash column chromatography (silica gel, hexanes:EtOAc 19:1) to give spirocycle **112** (66.0

mg, 90%, dr = 20:1 based on ^{1}H NMR) as a colorless oil. **112**: R_f = 0.28 (silica gel, hexanes:EtOAc, 19:1); IR (film) ν_{max} 3054, 2984, 2948 cm^{-1}; ^{1}H NMR (400 MHz, $CDCl_3$) δ 5.33 (dt, *J* = 4.1, 3.0 Hz, 1 H), 4.82 (ddd, *J* = 6.8, 3.1, 1.9 Hz, 2 H), 4.08–3.87 (m, 4 H), 2.73–2.58 (m, 1 H), 2.50–2.15 (m, 6 H), 1.99 (ddd, *J* = 12.1, 5.0, 1.6 Hz, 1 H), 1.89 (dtd, *J* = 11.9, 6.8, 2.1 Hz, 1 H), 1.75–1.54 (m, 3 H), 1.52–1.32 (m, 2 H), 1.17 (qd, *J* = 11.4, 7.2 Hz, 1 H); ^{13}C NMR (101 MHz, $CDCl_3$) δ 152.54, 151.50, 112.62, 109.31, 105.59, 64.51, 64.47, 64.43, 51.53, 48.71, 40.84, 40.20, 38.80, 38.06, 36.35, 31.32, 30.78; HRMS (ESI) calcd for $C_{16}H_{23}O_2$ $[M+H]^+$ 247.1693, found 247.1687.

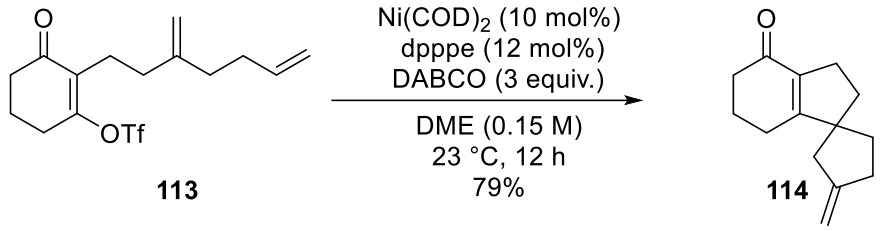

113 **114**

Spirocycle 114.[13] Following general procedure F, triflate **113** (71.0 mg, 0.200 mmol, 1.0 equiv.) was converted into spirocycle **114**. The reaction was worked up as usual and then purified via flash column chromatography (silica gel, hexanes:EtOAc 9:1) to give spirocycle **114** (32.0 mg, 79% yield) as a light yellow oil. **114**: R_f = 0.32 (silica gel, hexanes:EtOAc 9:1); IR (film) ν_{max} 3071, 2940, 2861, 1717, 1663, 1608 cm^{-1}; ^{1}H NMR (400 MHz, $CDCl_3$) δ 4.90 (p, *J* = 2.1 Hz, 2 H), 2.51–2.34 (m, 7 H), 2.26 (tt, *J* = 6.0, 2.4 Hz, 2 H), 2.22–2.13 (m, 1 H), 2.10–1.95 (m, 2 H), 1.87–1.73 (m, 3 H), 1.65–1.59 (m, 1 H); ^{13}C NMR (101 MHz, $CDCl_3$) δ 198.50, 169.22, 151.11, 137.16, 106.66, 58.98, 43.72, 37.98, 36.69, 36.31, 31.57, 26.75, 23.86, 23.04; HRMS (ESI) calcd for $C_{14}H_{19}O$ $[M+H]^+$ 203.1430, found 203.1432.

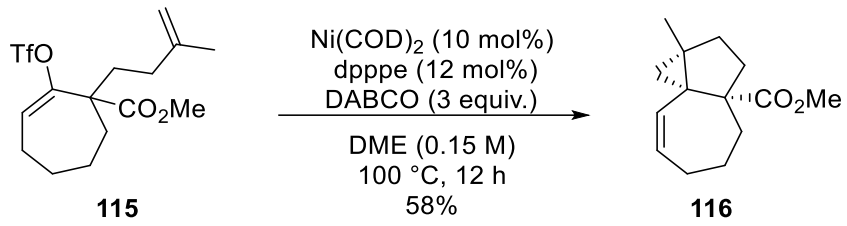

115 **116**

Cyclopropane 116[14] Following general procedure F, triflate **115** (88.0 mg, 0.250 mmol, 1.0 equiv.) was converted into tricycle **116**. The reaction was worked up as usual and then purified via flash column chromatography (silica gel, hexanes:Et_2O, 19:1) to give tricycle **116** (31.9 mg, 58% yield) as a light yellow oil. Spectral data matched that previously reported[14]. **116**: R_f = 0.24 (silica gel, hexanes:Et_2O, 19:1); ^{1}H NMR (500 MHz, $CDCl_3$) δ 5.69 (ddd, *J* = 12.0, 6.9, 3.2 Hz, 1 H), 5.08 (dd, *J* = 12.0, 2.8 Hz, 1 H), 3.67 (s, 3 H), 2.26–2.12 (m, 2 H), 2.06 (dddt, *J* = 17.2, 10.2, 4.3, 3.0 Hz, 1 H), 1.81–1.59 (m, 5 H), 1.52 (ddd, *J* = 13.5, 5.7, 3.4 Hz, 1 H), 1.47–1.36 (m, 1 H), 1.13 (s, 3 H), 1.00 (d, *J* = 5.2 Hz, 1 H), 0.42 (d, *J* = 5.2 Hz, 1 H); ^{13}C NMR (126 MHz, $CDCl_3$) δ 131.99, 130.55, 57.87, 51.66, 39.28, 35.01, 33.19, 32.92, 30.45, 25.13, 23.48, 19.64.

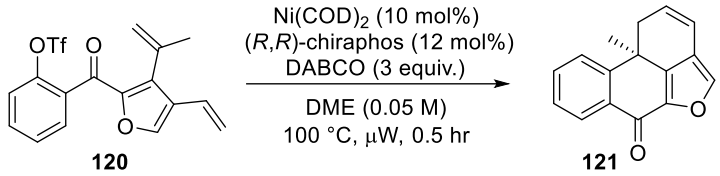

120 **121**

Tetracycle 121.[15] Using a modified procedure from Keay,[15] $Ni(COD)_2$ (3.7 mg, 0.013 mmol, 0.1 equiv.), (*R*,*R*)-chiraphos (11.6 mg, 0.027 mmol, 0.2 equiv.), and DABCO (0.171 g, 0.402 mmol, 3.0 equiv.) were added to a microwave vial followed by DME (4 mL). The resultant yellow solution was then stirred at 23 °C for 10 min. Next, a solution of triflate **120** (51.9 mg, 0.134 mmol, 1.0 equiv.) in DME (1.4 mL) was added and the vial was sealed and removed from the glovebox and placed in a microwave reactor and heated at 100 °C for 0.5 hr. Upon completion, the reaction contents were cooled to 23 °C, diluted with Et_2O (5 mL), and then filtered through a

silica plug, eluting with Et_2O. The filtrate was concentrated and the resulting residue was purified via flash column chromatography (silica gel, hexanes:EtOAc, 19:1→10:1) to give tetracycle **121** (26.0 mg, 82% yield) as a light yellow solid. Spectral data matched that previously reported[15]. **121**: R_f = 0.24 (silica gel, hexanes:Et_2O 19:1); ^{1}H NMR (500 MHz, $CDCl_3$) δ 8.37 (dd, *J* = 7.8, 1.5 Hz, 1 H), 7.64–7.54 (m, 2 H), 7.50 (dd, *J* = 7.8, 1.3 Hz, 1 H), 7.45 (td, *J* = 7.5, 1.3 Hz, 1 H), 6.61 (ddd, *J* = 9.6, 3.2, 0.8 Hz, 1 H), 6.06 (ddd, *J* = 9.8, 6.2, 2.2 Hz, 1 H), 2.94 (ddd, *J* = 16.6, 6.2, 0.9 Hz, 1 H), 2.53 (dt, *J* = 16.5, 2.8 Hz, 1 H), 1.47 (s, 3 H); ^{13}C NMR (126 MHz, $CDCl_3$) δ 172.72, 150.08, 144.39, 144.05, 141.52, 133.55, 132.34, 128.54, 128.18, 127.14, 125.25, 121.01, 117.83, 35.49, 34.77, 31.26. The enantiomeric excess was determined by chiral HPLC using a Daicel Chiralpak OD column (hexanes:*i*PrOH 9:1, flow rate of 1.0 mL/min, 254 nm) R_t = 11.5 min (*R*), R_t = 22.2 min (*S*): 39% ee.

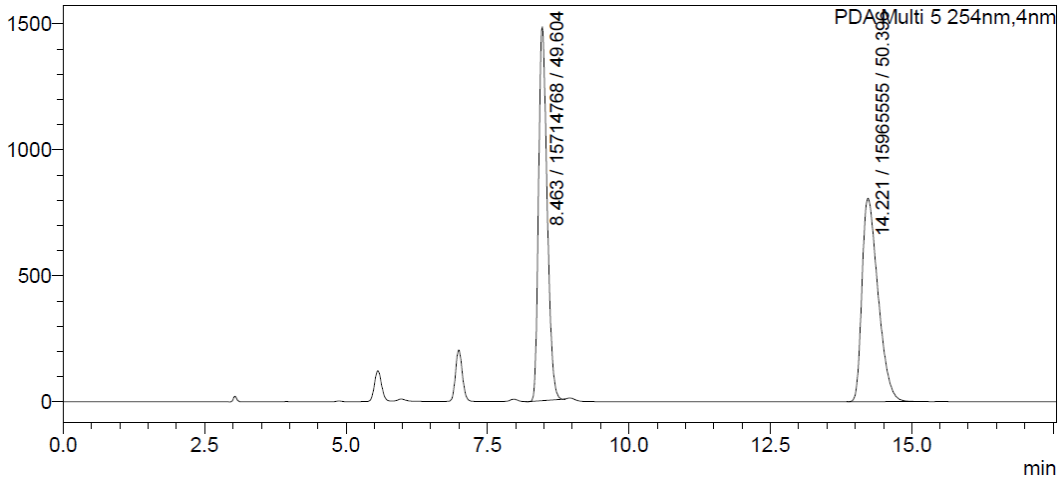

Peak#	Ret. Time	Area	Area%
1	8.463	15714768	49.604
2	14.221	15965555	50.396
Total		31680323	100.000

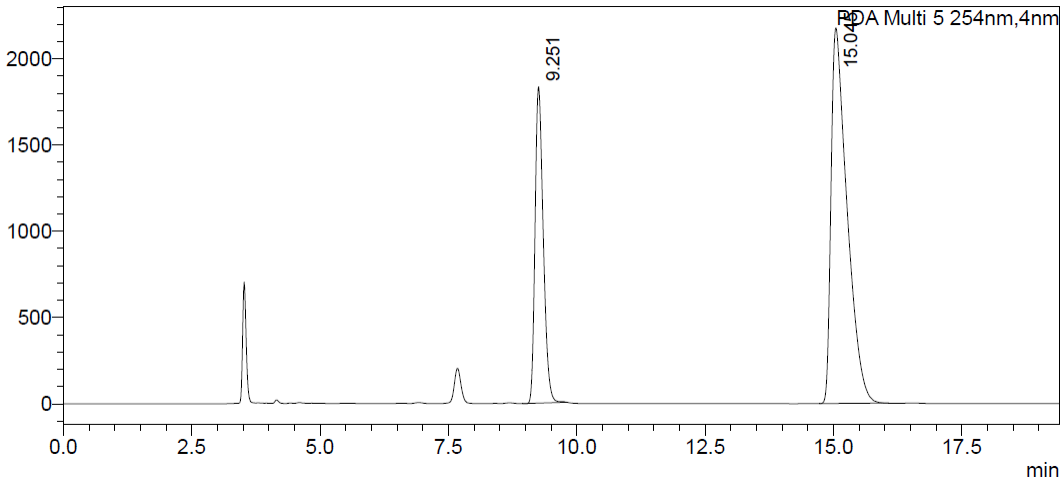

Peak#	Ret. Time	Area	Area%
1	9.251	20305726	30.127
2	15.045	47094091	69.873
Total		67399817	100.000

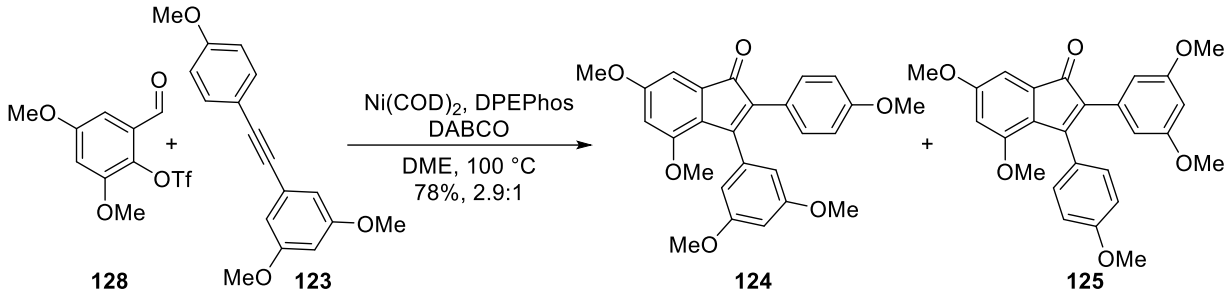

Indenone 124 and 125.[16] Following general procedure F except substituting DPEphos as ligand, triflate **122** (31.4 mg, 0.100 mmol, 1.0 equiv.) and alkyne **123** (53.6 mg, 0.200 mmol, 2.0 equiv.) were converted into indenone **124**. The reaction was worked up as usual and then purified via flash column chromatography (silica gel, hexanes:EtOAc 4:1→3:1) to give a mixture of indenones **124** and **125** (33.7 mg, 78%, **124**:**125** = 2.9:1) as a dark purple solid. Spectral data matched that previously reported[16]. **124 + 125**: R_f = 0.24 (silica gel, hexanes:EtOAc 3:1); ^{1}H NMR (400 MHz, $CDCl_3$) δ 7.33–7.27 (m, 1 H), 7.16–7.09 (m, 3.2 H), 6.88–6.82 (m, 3.2 H), 6.79–6.70 (m, 3.2 H), 6.49 (d, *J* = 2.3 Hz, 3.2 H), 6.43 (dq, *J* = 2.3, 1.1 Hz, 3.6 H), 6.31 (q, *J* = 1.5 Hz, 1 H), 3.86 (d, *J* = 1.9 Hz, 6.7 H), 3.82 (s, 1.4 H), 3.76 (s, 5.7 H), 3.70 (s, 8.9 H), 3.61 (d, *J* = 0.9 Hz, 8.9

H); ^{13}C NMR (126 MHz, $CDCl_3$) δ 196.75, 195.89, 162.93, 162.63, 160.31, 160.22, 158.99, 158.83, 156.74, 155.14, 154.83, 137.12, 134.20, 131.11, 130.61, 113.56, 113.06, 107.99, 106.69, 104.19, 103.98, 102.90, 102.75, 101.10, 100.23, 56.03, 55.88, 55.78, 55.48, 55.37, 55.29, 55.25.

2.25 NMR Spectra

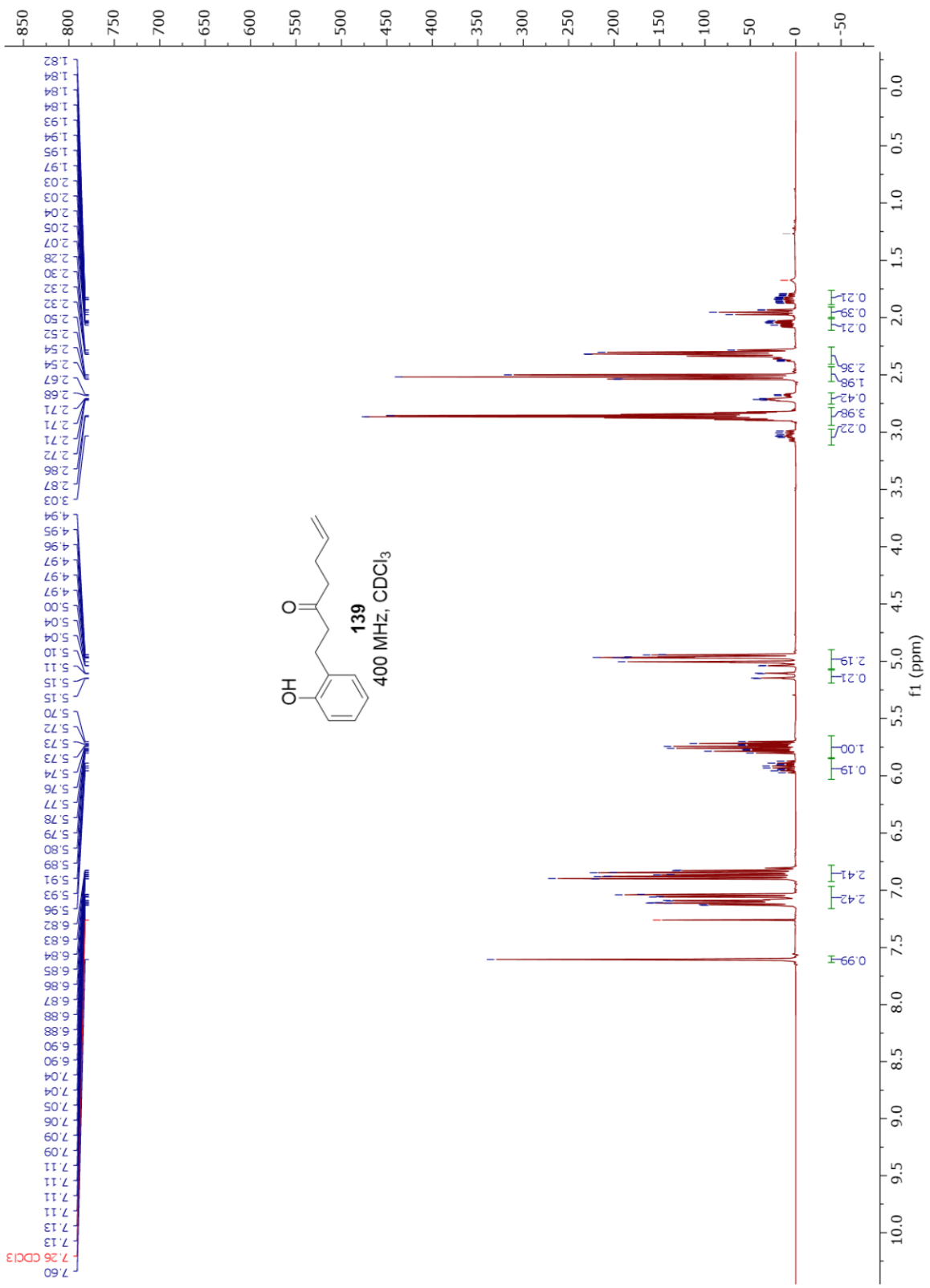

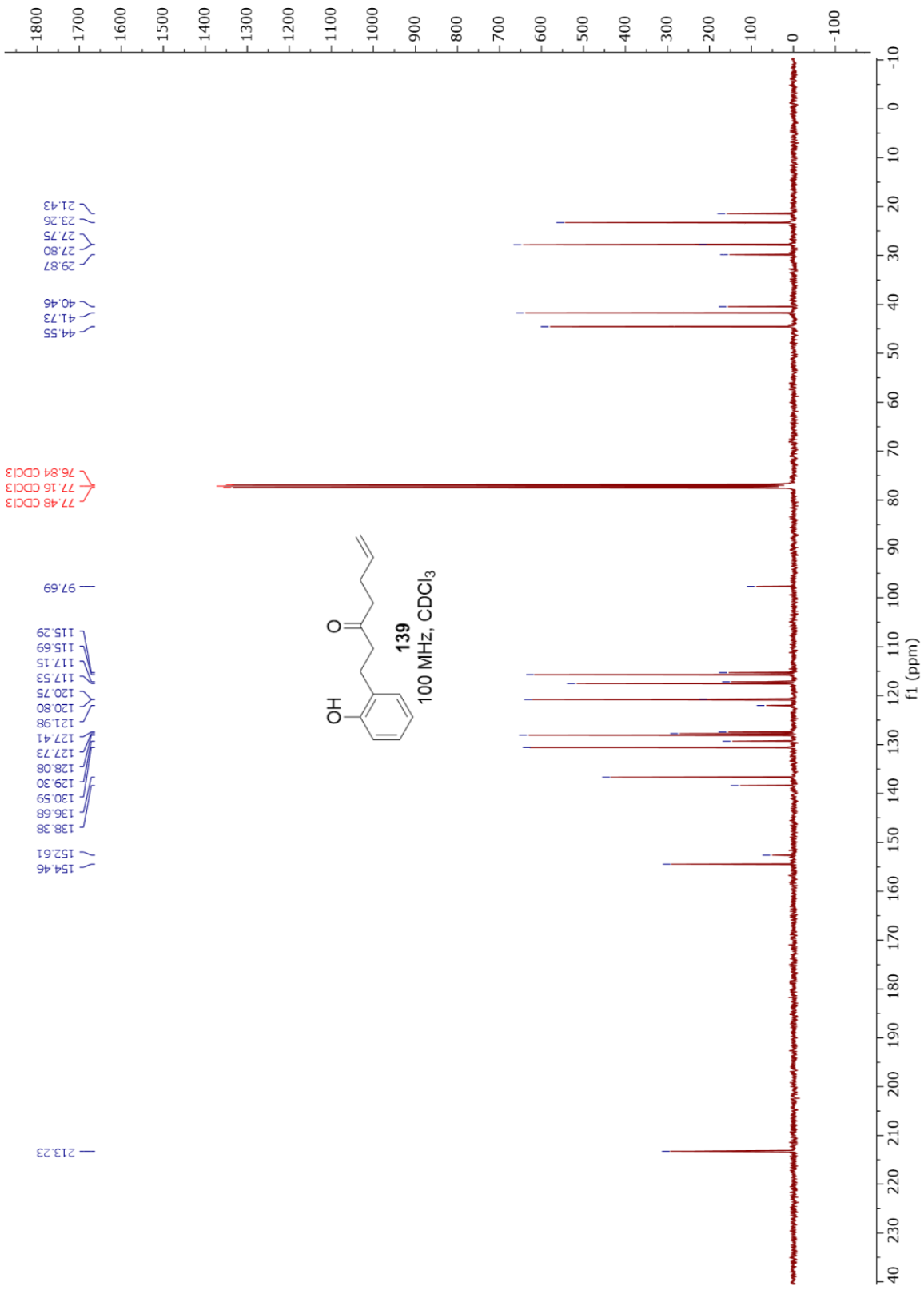
139
100 MHz, CDCl3
OH
O
f1 (ppm)
213.23
154.46
152.61
138.38
136.68
130.59
129.30
128.08
127.73
127.41
121.98
120.80
120.75
117.53
117.15
115.69
115.29
97.69
77.48 CDCl3
77.16 CDCl3
76.84 CDCl3
44.55
41.73
40.46
29.87
27.80
27.75
23.26
21.43

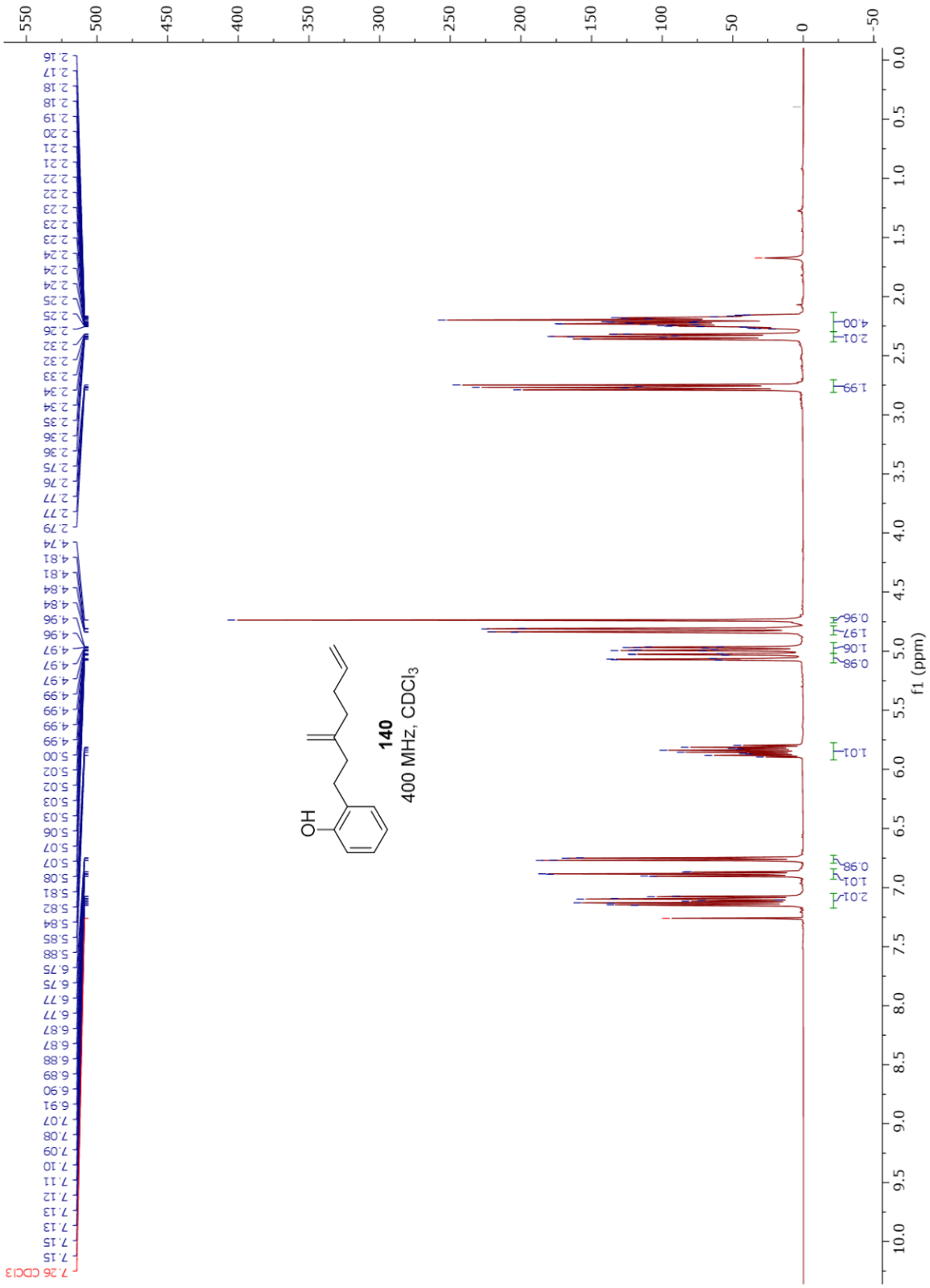
OH
140
400 MHz, CDCl3
f1 (ppm)

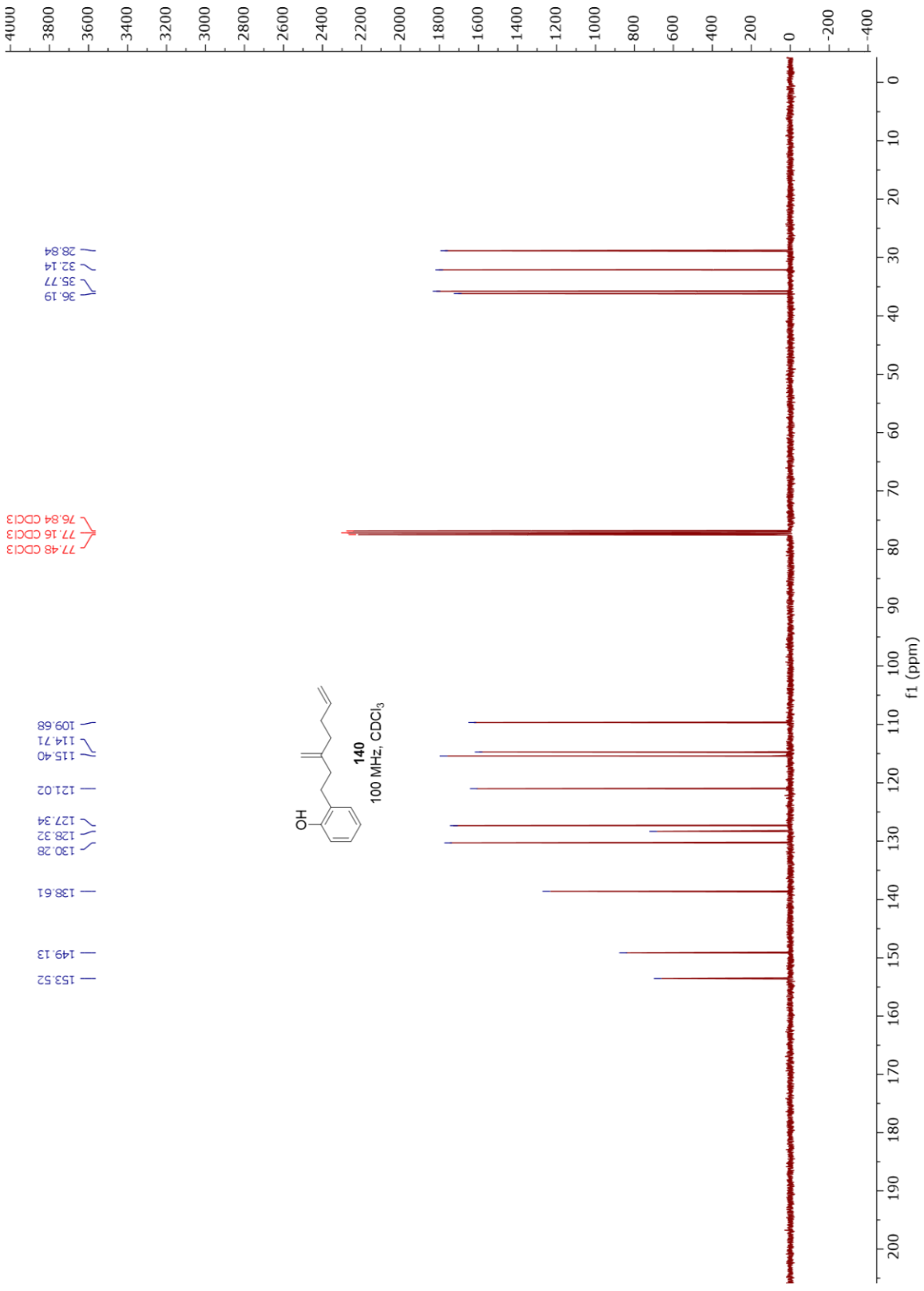
140
100 MHz, CDCl3
OH
f1 (ppm)
153.52
149.13
138.61
130.28
128.32
127.34
121.02
115.40
114.71
109.68
77.48 CDCl3
77.16 CDCl3
76.84 CDCl3
36.19
35.77
32.14
28.84

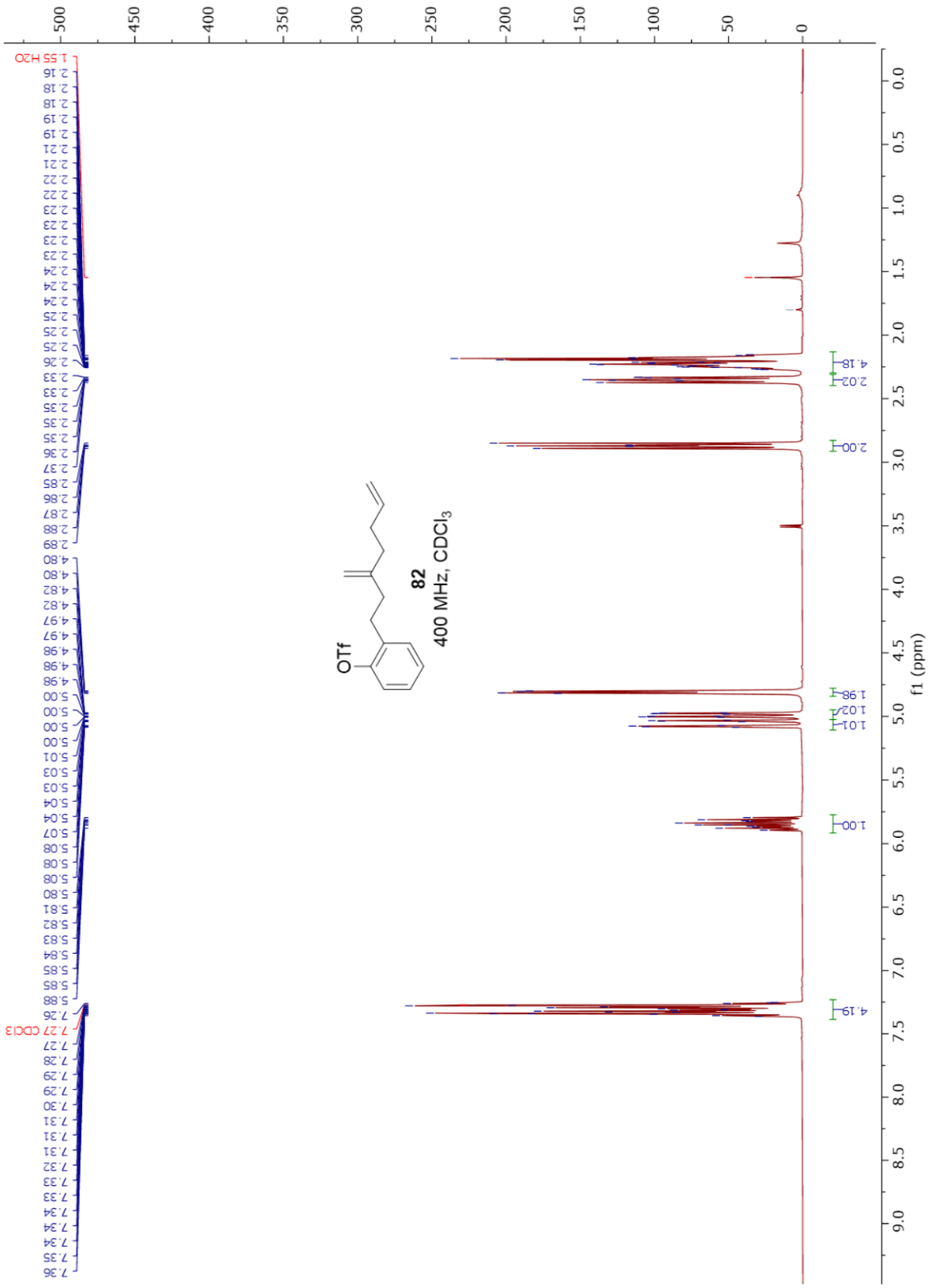
OTf
82
400 MHz, CDCl3
f1 (ppm)
1.55 H2O
7.27 CDCl3

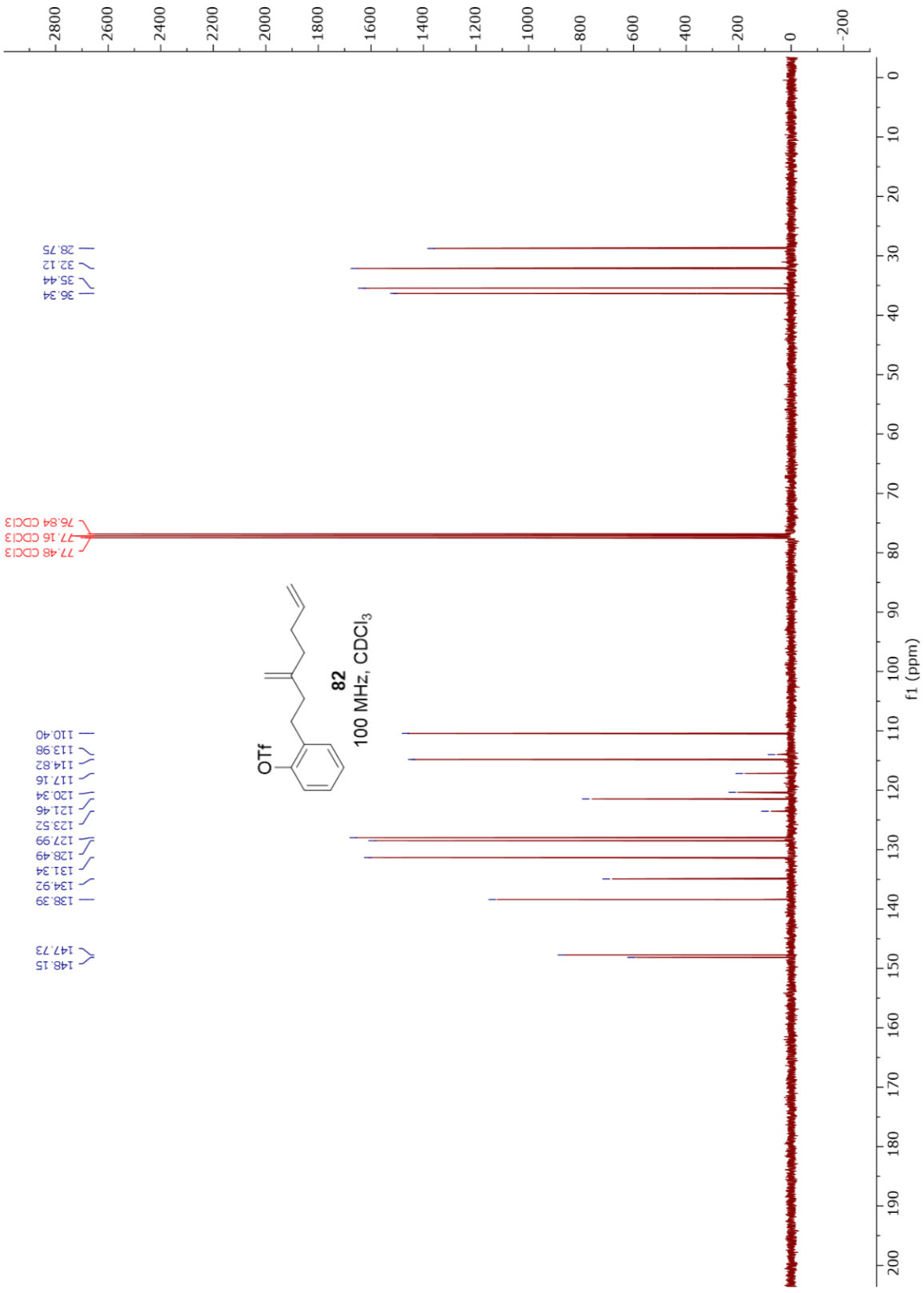
82
100 MHz, CDCl3
OTf
f1 (ppm)
77.48 CDCl3
77.16 CDCl3
76.84 CDCl3

OTf
82
376 MHz, CDCl3
-73.94
f1 (ppm)

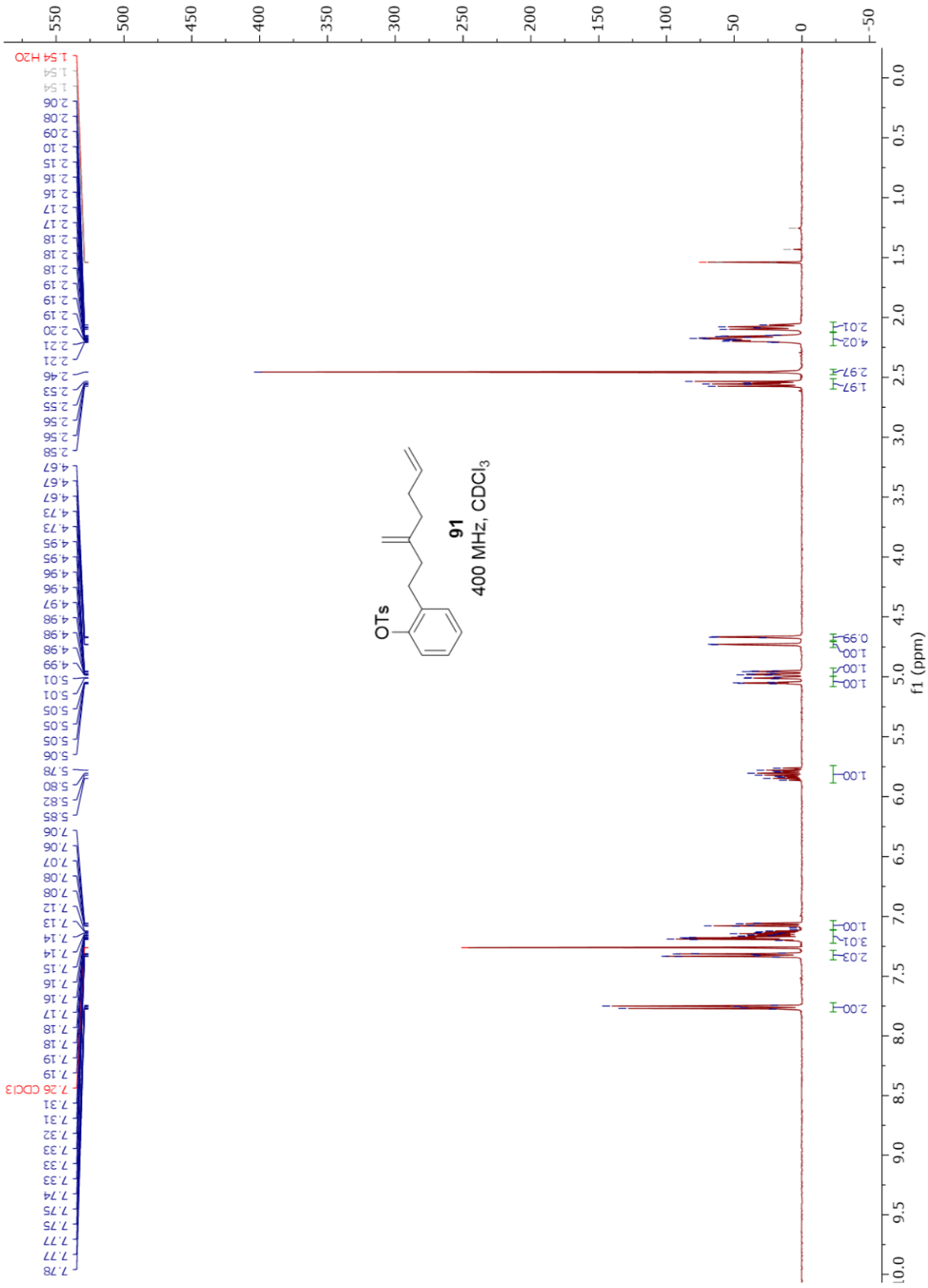
OTs
91
400 MHz, CDCl3
f1 (ppm)

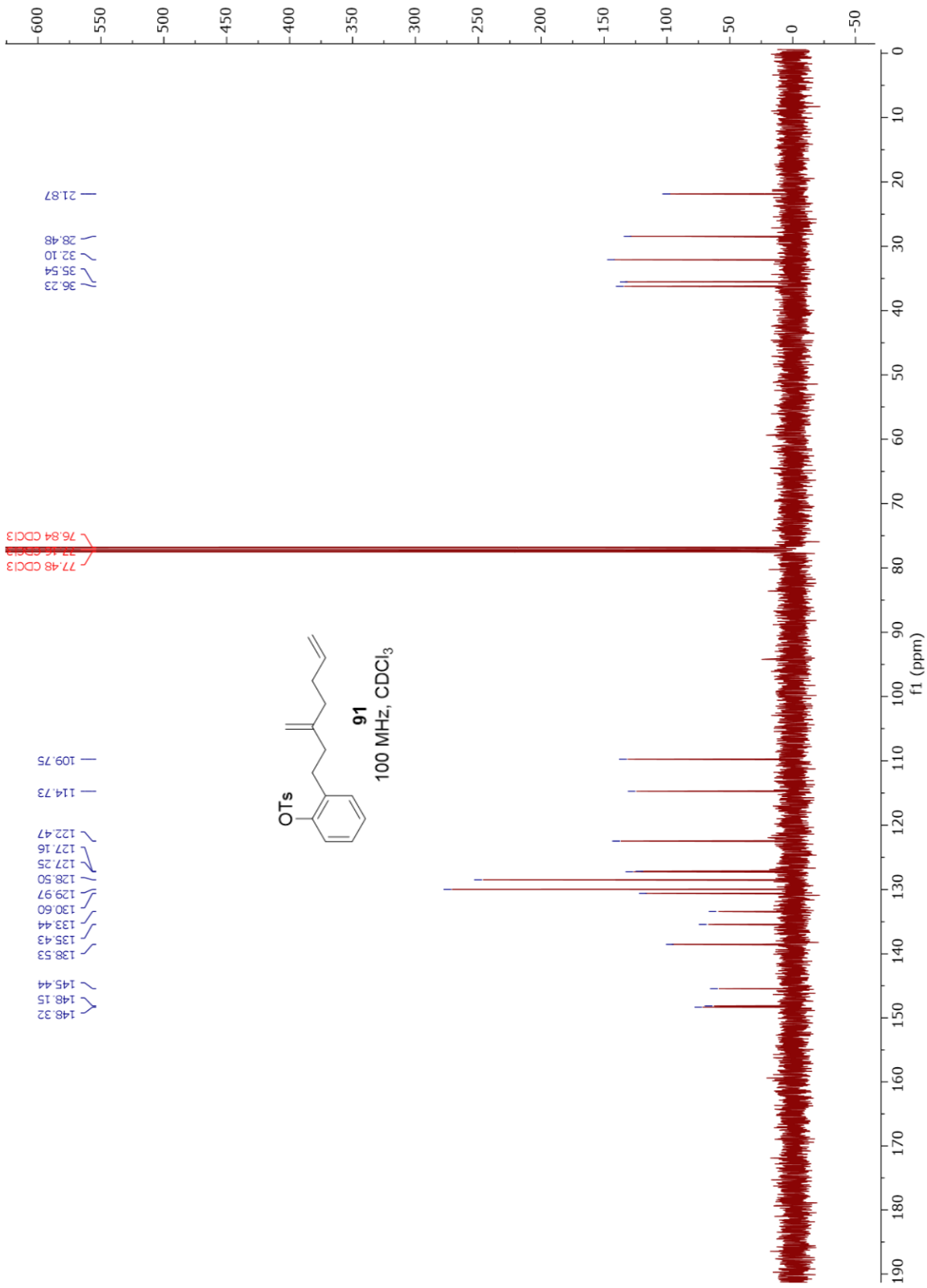
21.87
28.48
32.10
35.54
36.23
76.84 CDCl3
77.48 CDCl3
109.75
114.73
122.47
127.16
127.25
128.50
129.97
130.60
133.44
135.43
138.53
145.44
148.15
148.32
OTs
91
100 MHz, CDCl3
f1 (ppm)

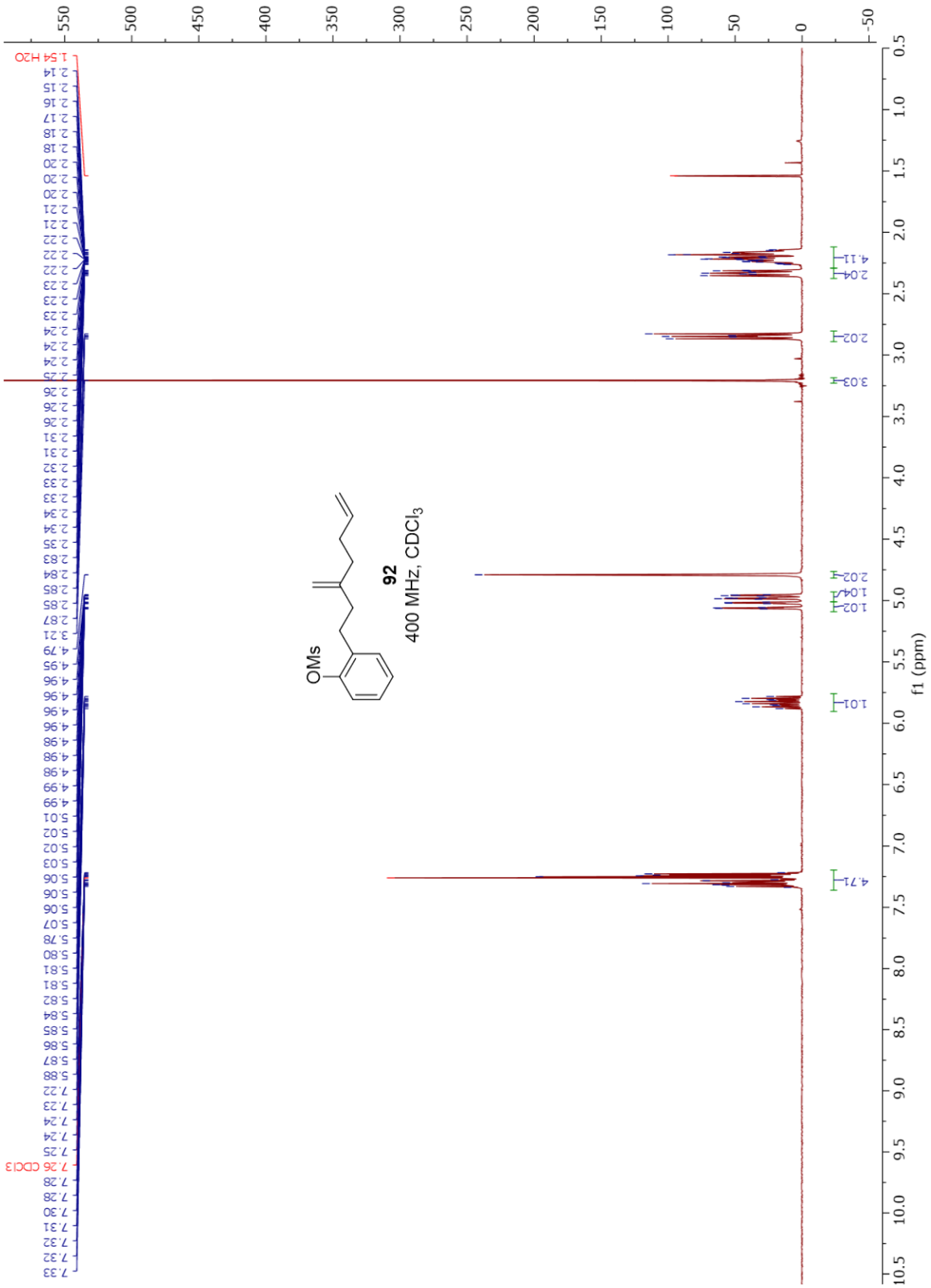
OMs
92
400 MHz, CDCl3
f1 (ppm)

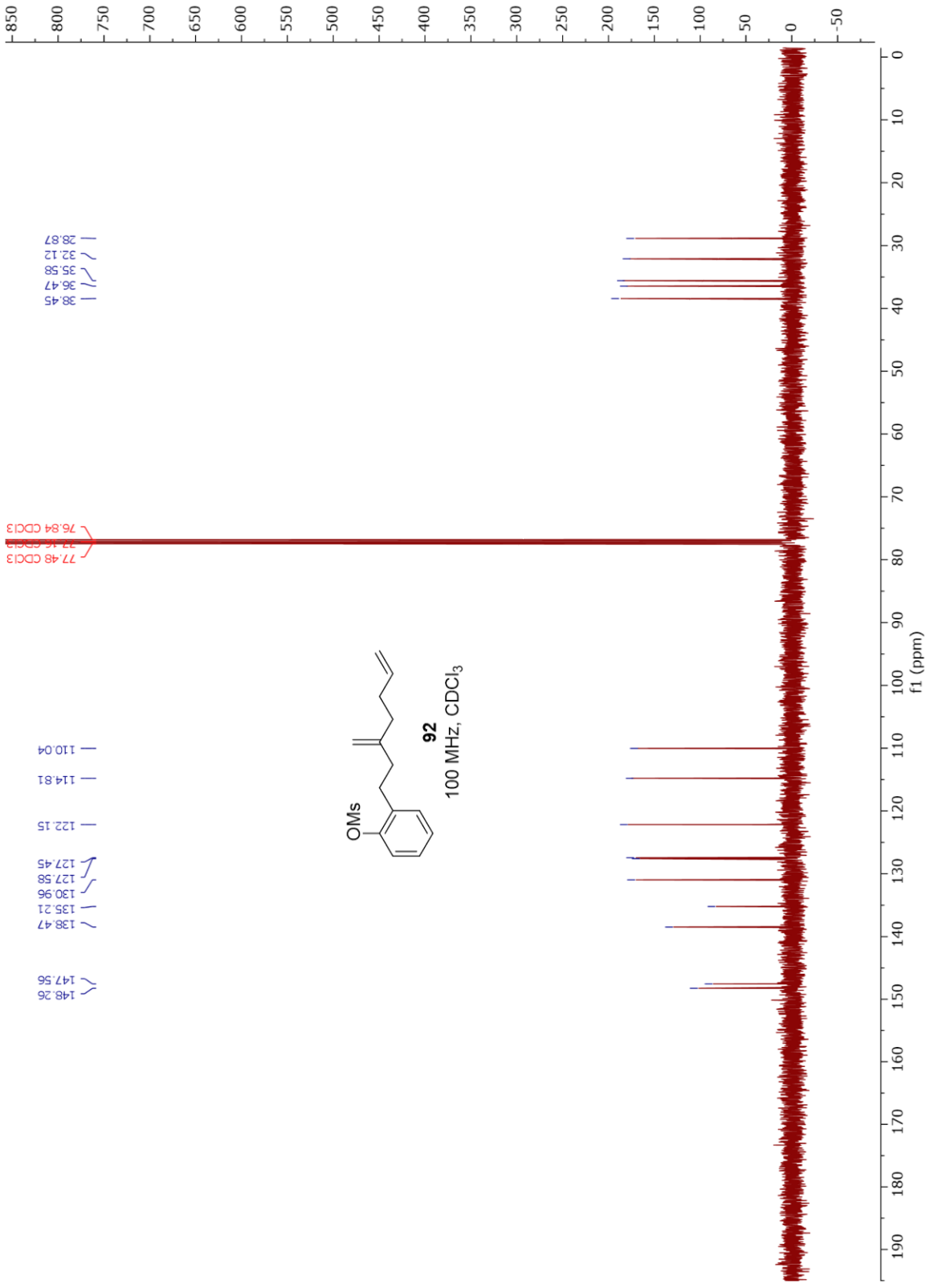
OMs
92
100 MHz, CDCl3
f1 (ppm)
77.48 CDCl3
76.84 CDCl3
148.26
147.56
138.47
135.21
130.96
127.58
127.45
122.15
114.81
110.04
38.45
36.47
35.58
32.12
28.87

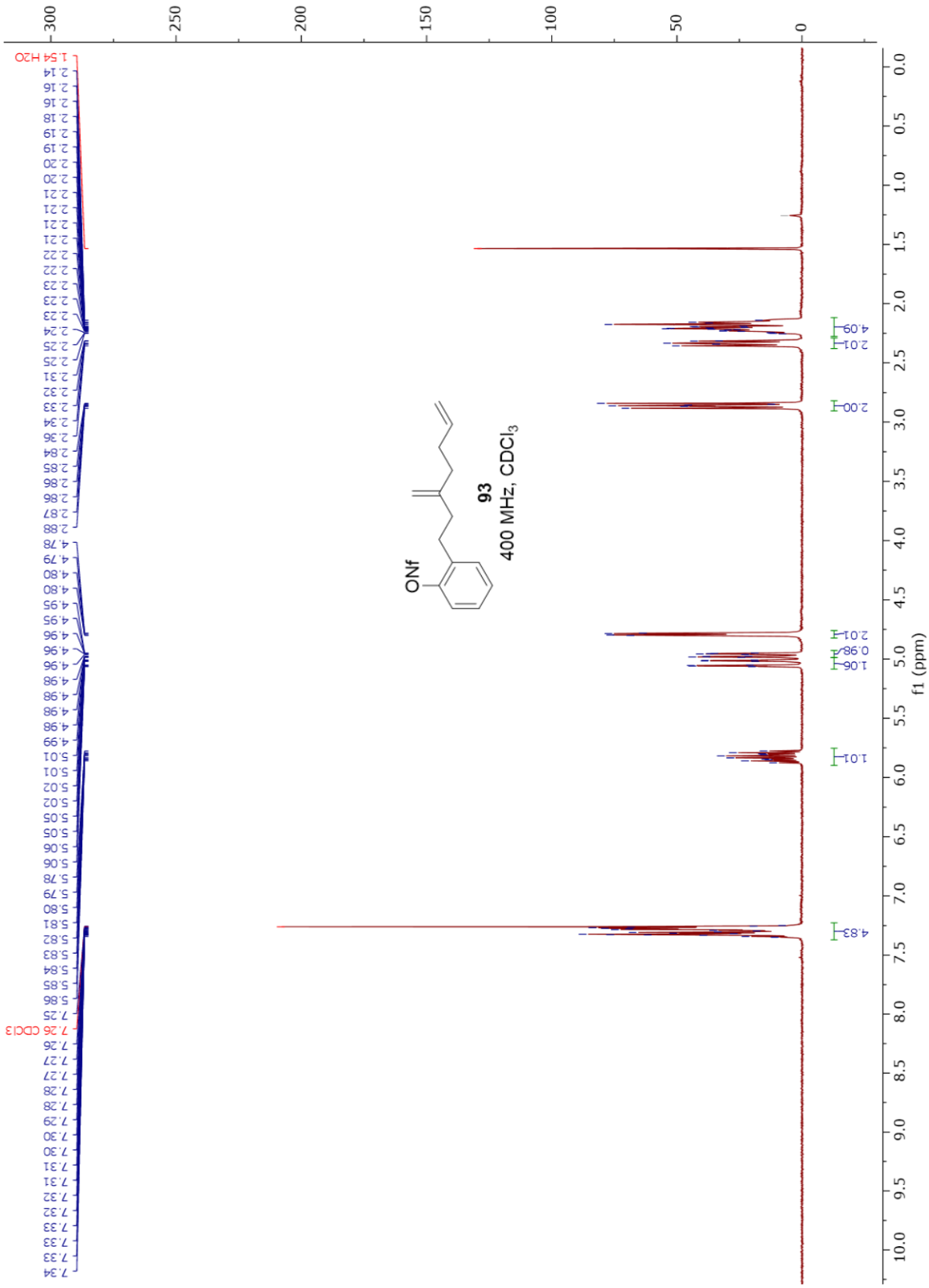
ONf
93
400 MHz, CDCl3
f1 (ppm)
4.83
1.01
1.06
0.98
2.01
2.00
2.01
4.09
7.26 CDCl3
1.54 H2O

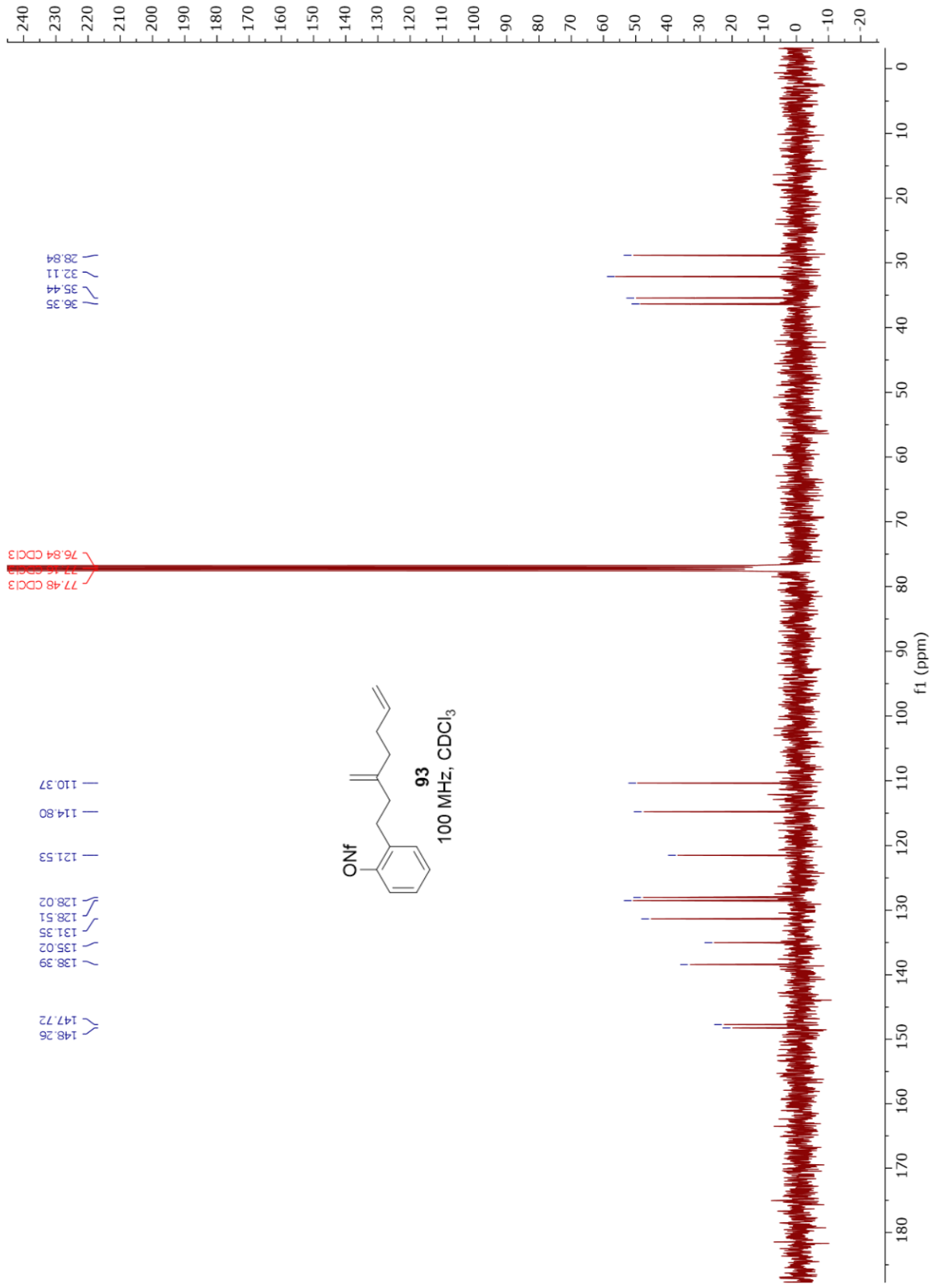
ONf
93
100 MHz, CDCl3
f1 (ppm)
77.48 CDCl3
76.84 CDCl3
148.26
147.72
138.39
135.02
131.35
128.51
128.02
121.53
114.80
110.37
36.35
35.44
32.11
28.84

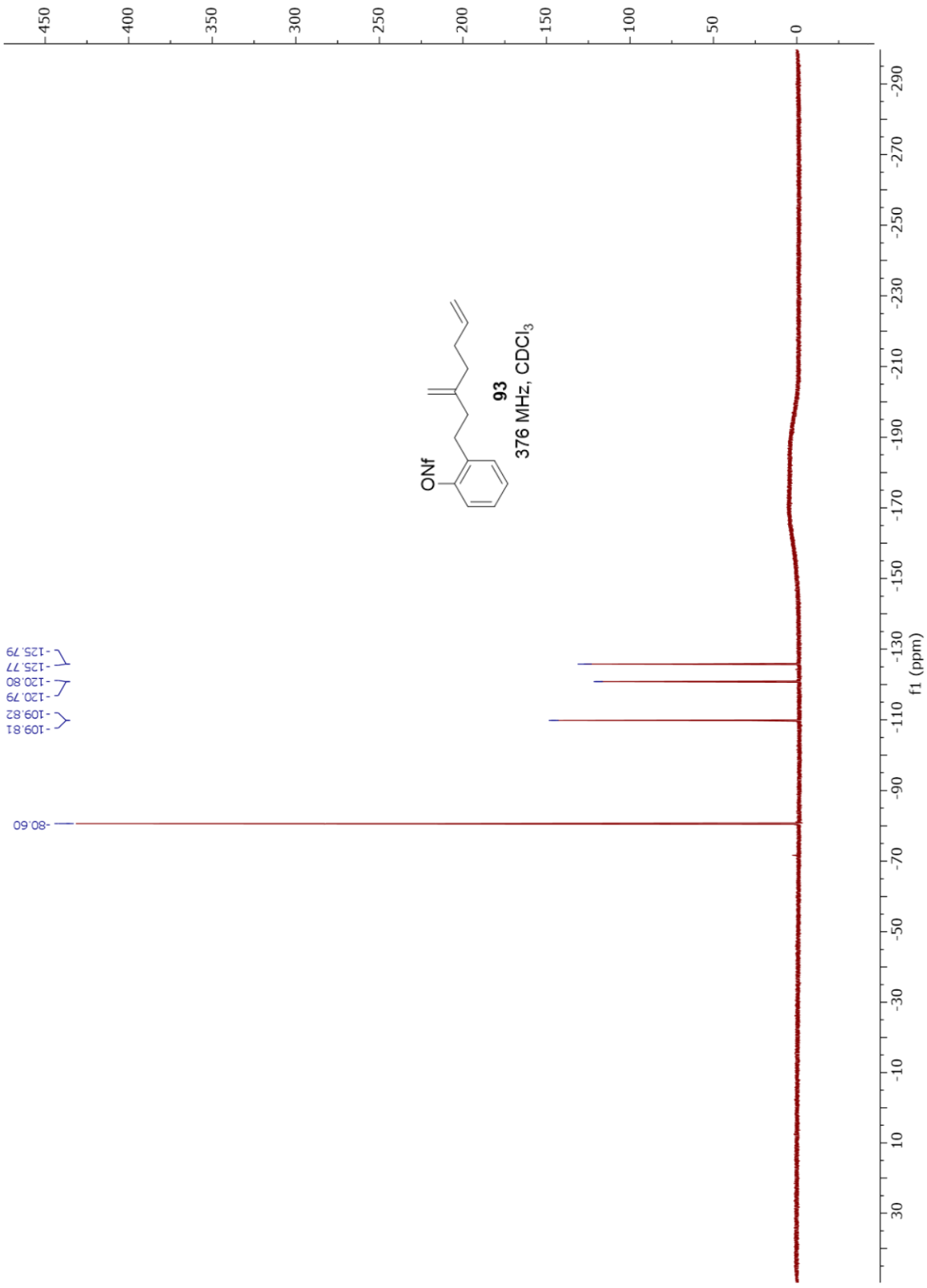
93
376 MHz, CDCl3
ONf
-80.60
-109.81
-109.82
-120.79
-120.80
-125.77
-125.79
f1 (ppm)

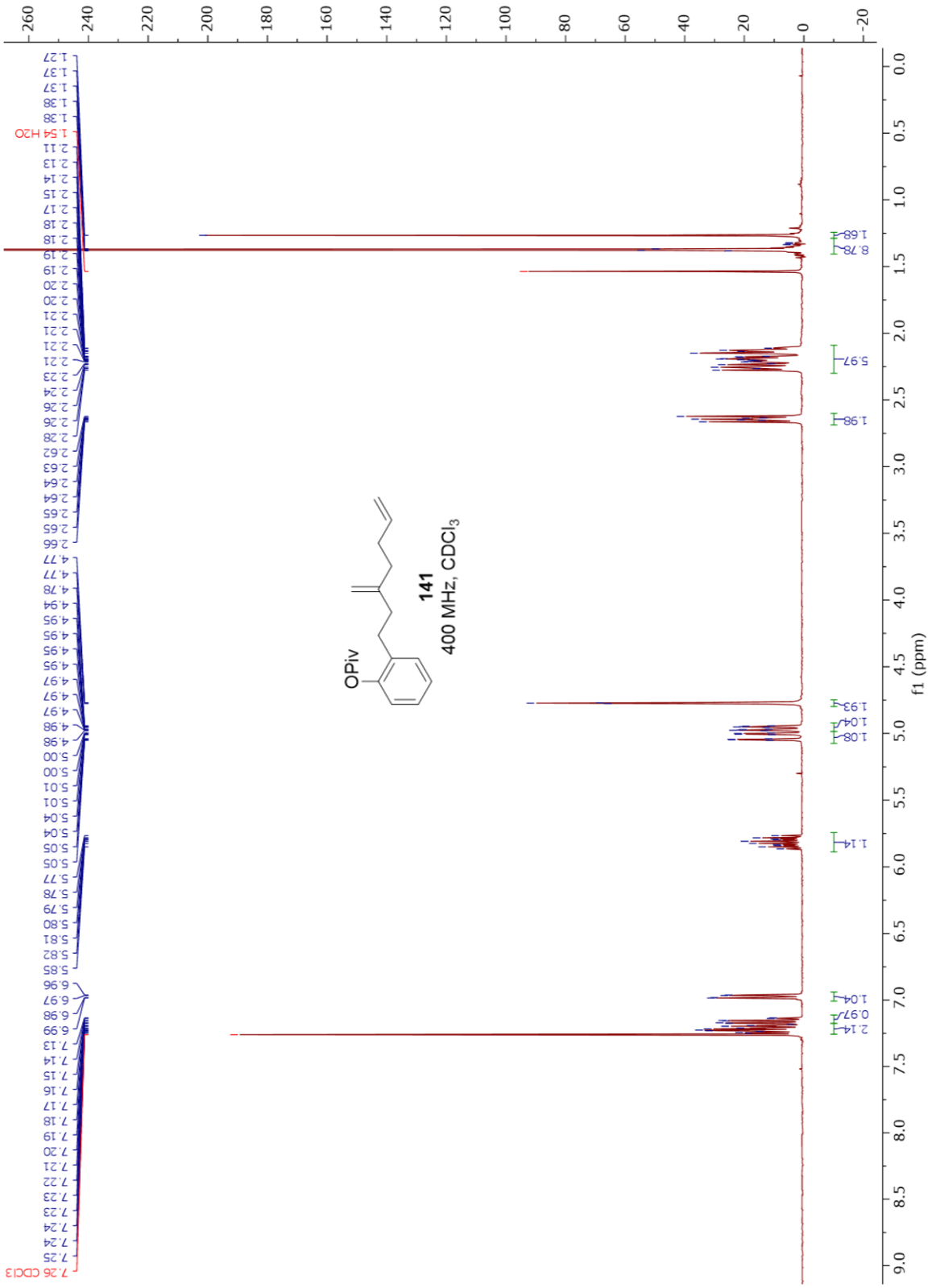
OPiv
141
400 MHz, CDCl3
f1 (ppm)

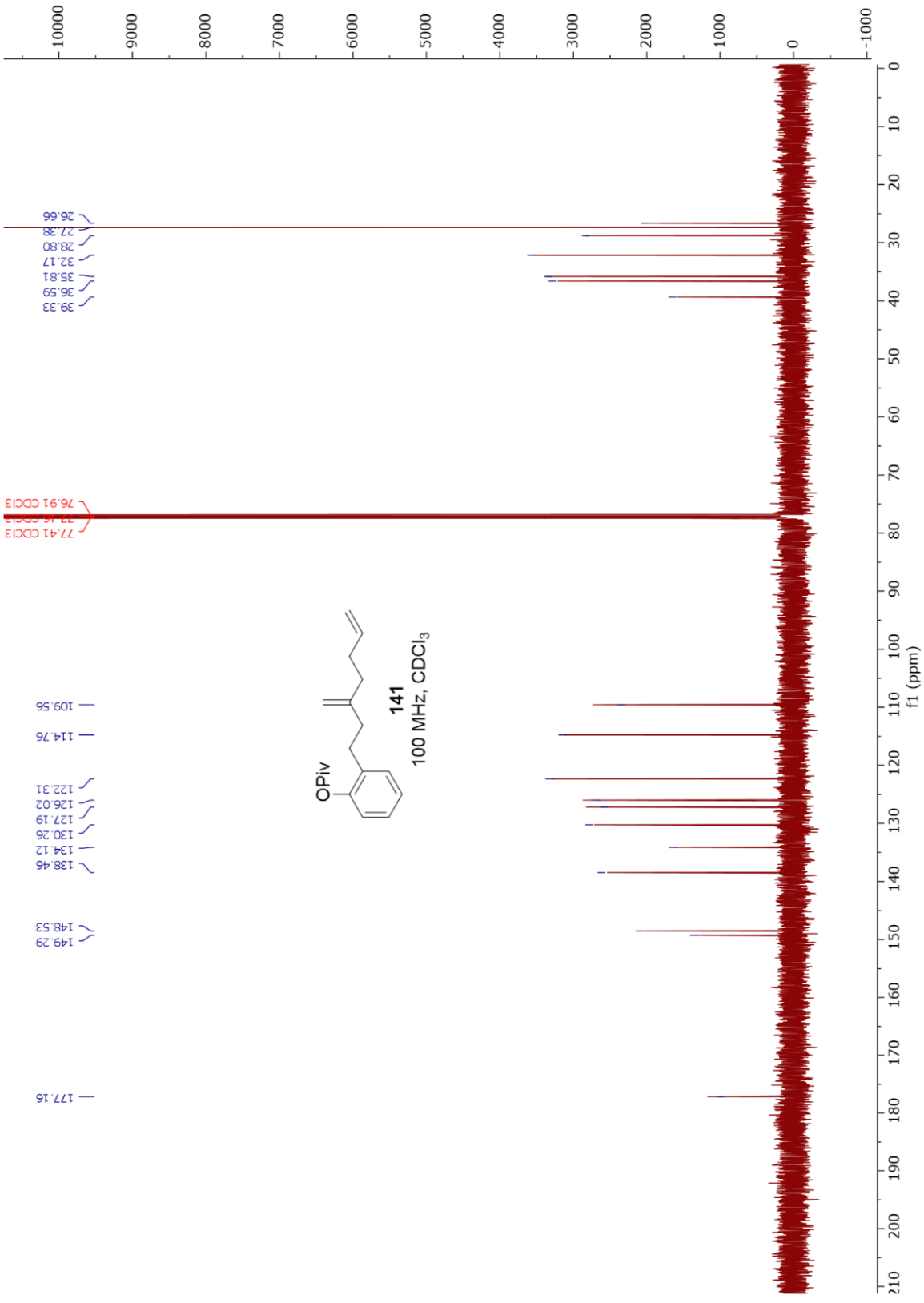
OPiv
141
100 MHz, CDCl3
f1 (ppm)
177.16
149.29
148.53
138.46
134.12
130.26
127.19
126.02
122.31
114.76
109.56
77.41 CDCl3
76.91 CDCl3
39.33
36.59
35.81
32.17
28.80
27.38
26.66

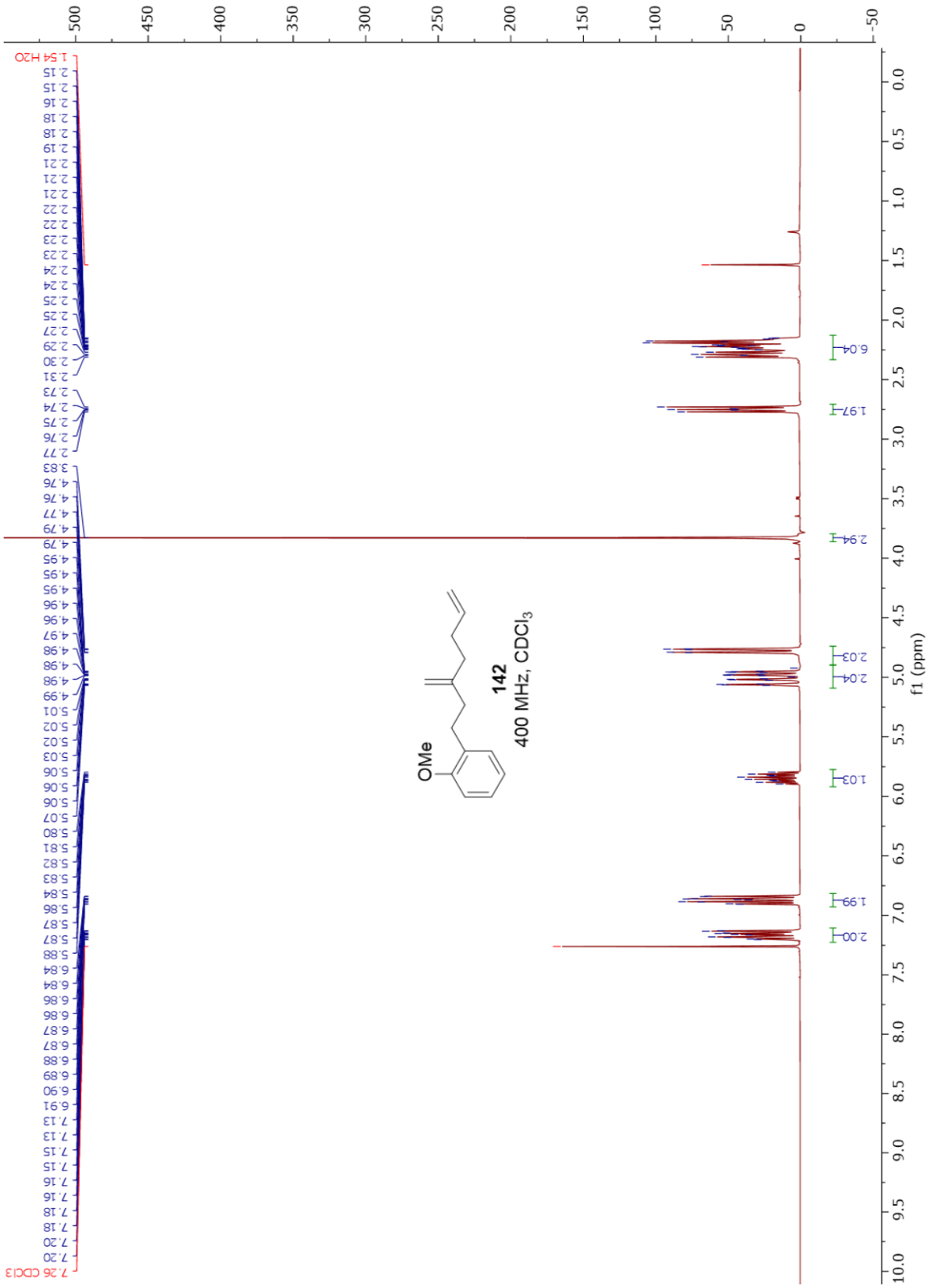
OMe
142
400 MHz, CDCl3
f1 (ppm)

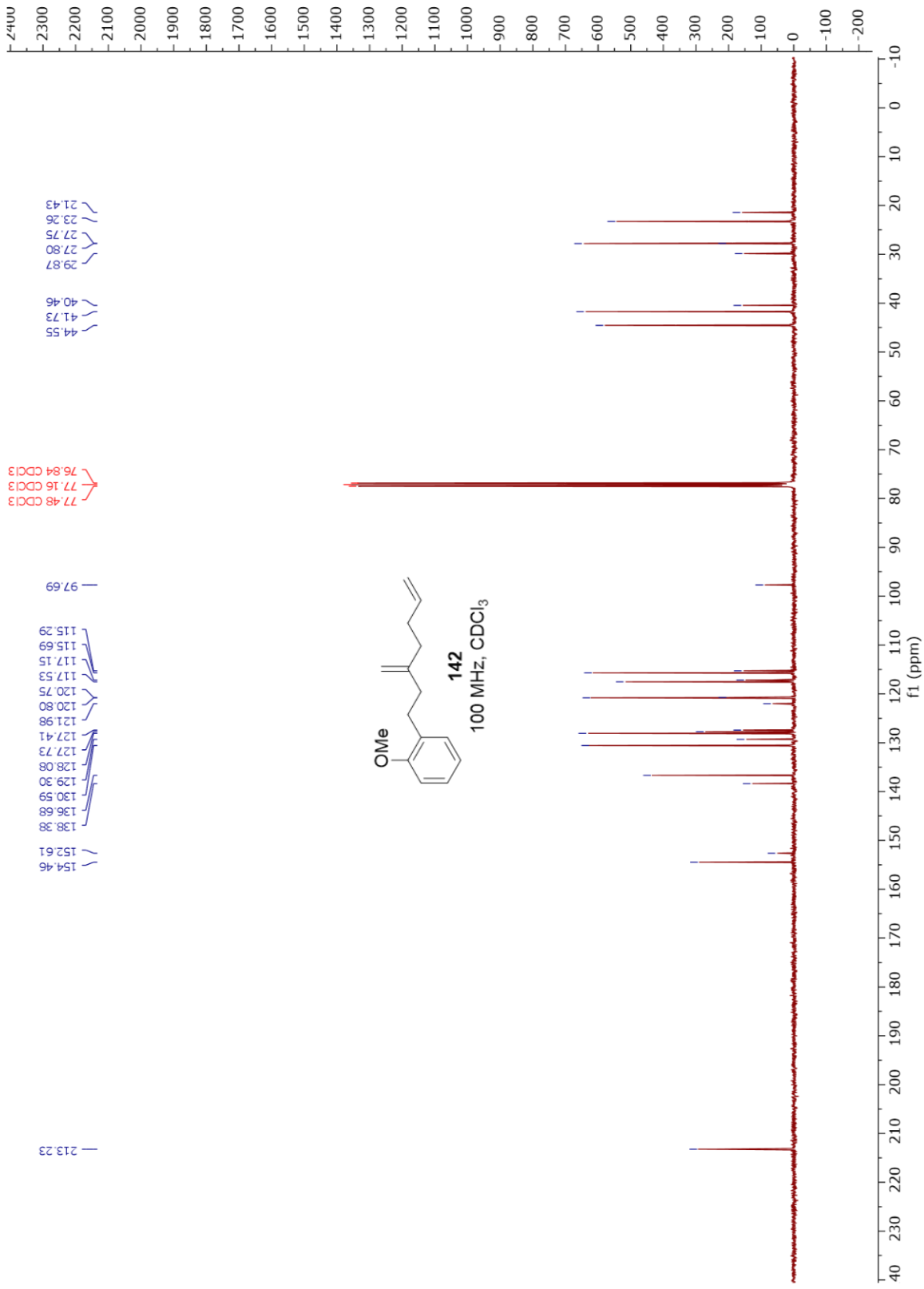
142
100 MHz, CDCl3
OMe
f1 (ppm)
213.23
154.46
152.61
138.38
136.68
130.59
129.30
128.08
127.73
127.41
121.98
120.80
120.75
117.53
117.15
115.69
115.29
97.69
77.48 CDCl3
77.16 CDCl3
76.84 CDCl3
44.55
41.73
40.46
29.87
27.80
27.75
23.26
21.43

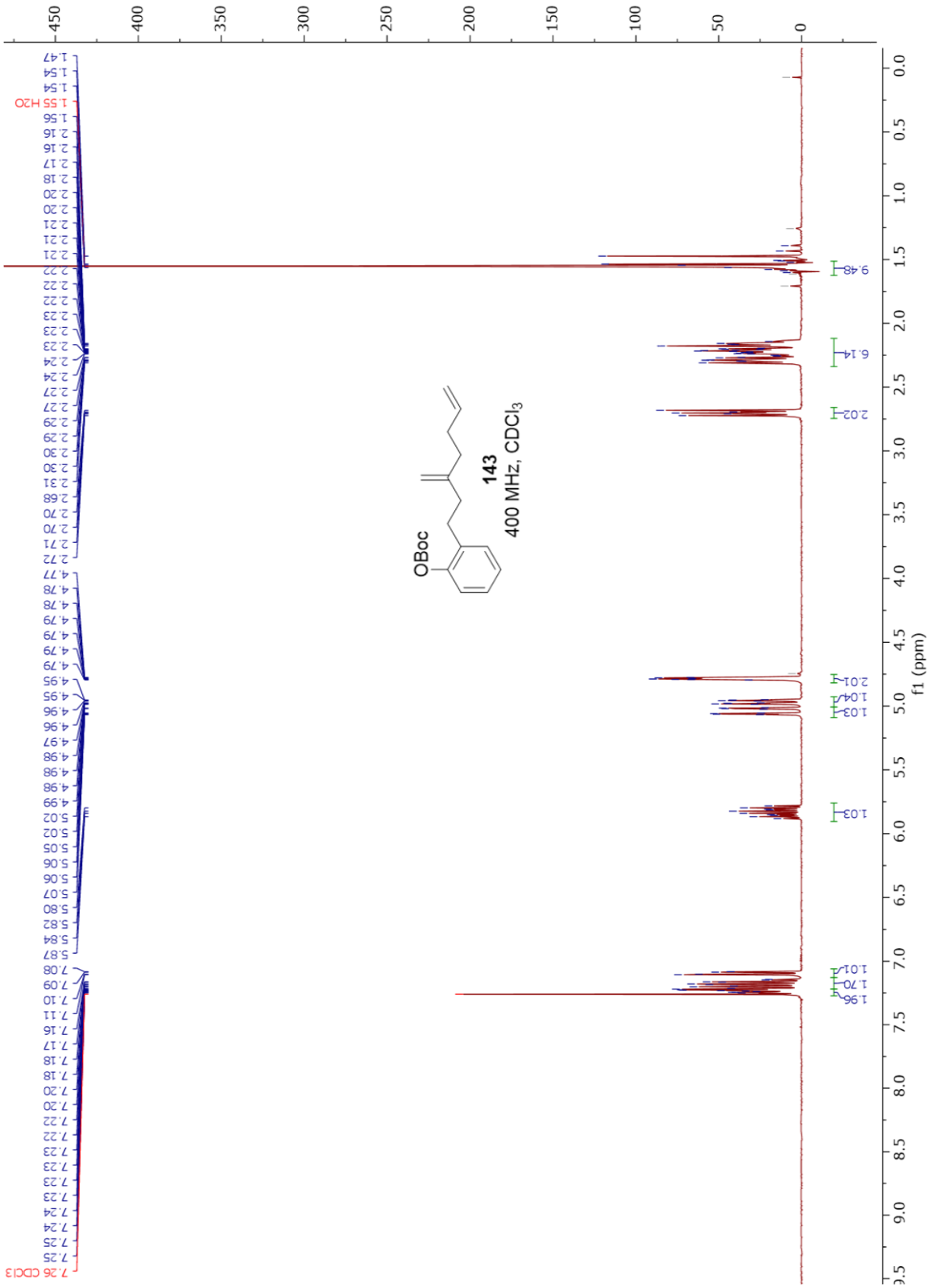
OBoc
143
400 MHz, CDCl3
f1 (ppm)

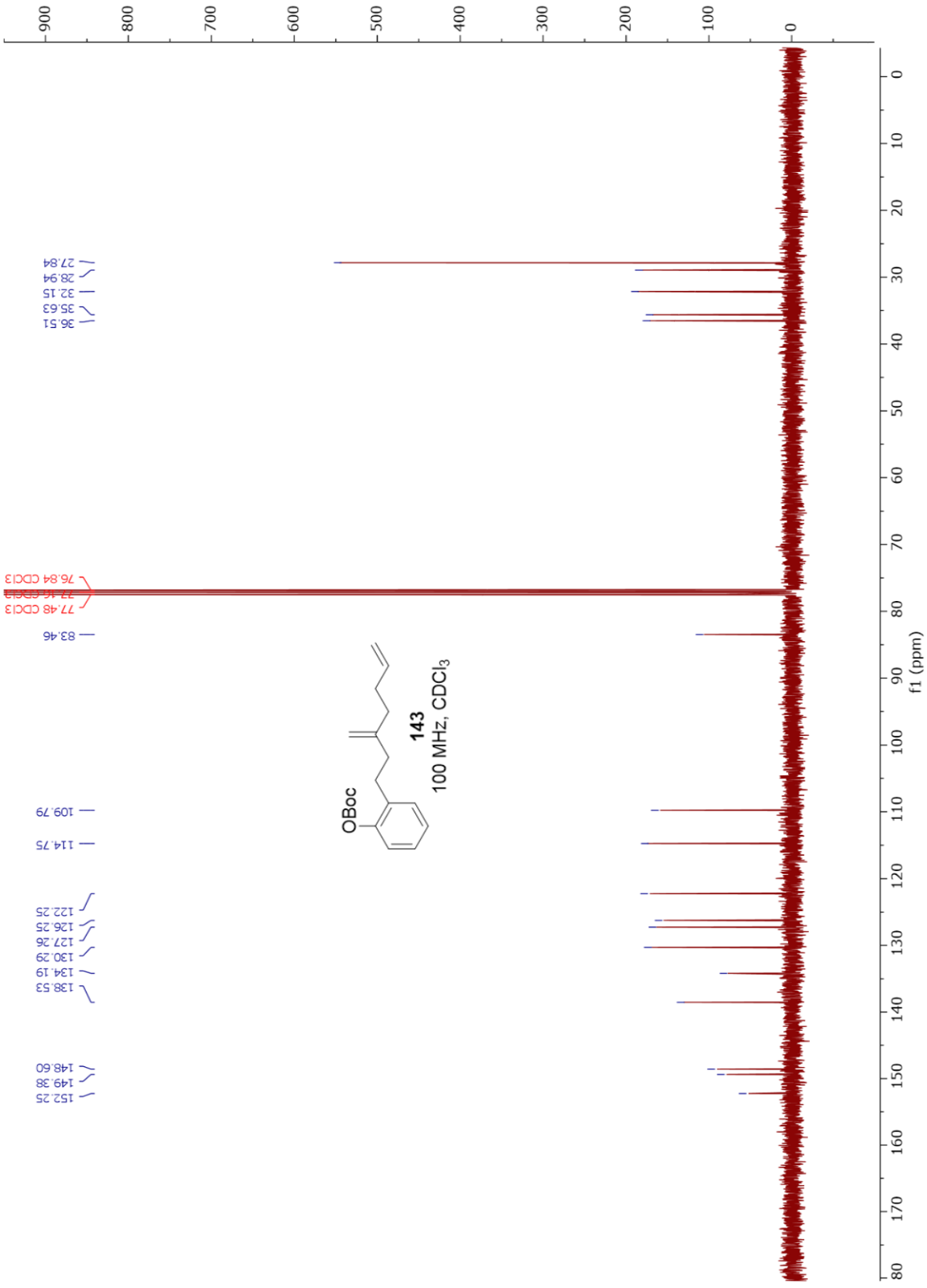
OBoc
143
100 MHz, CDCl3
f1 (ppm)
27.84
28.94
32.15
35.63
36.51
76.84 CDCl3
77.48 CDCl3
83.46
109.79
114.75
122.25
126.25
127.26
130.29
134.19
138.53
148.60
149.38
152.25

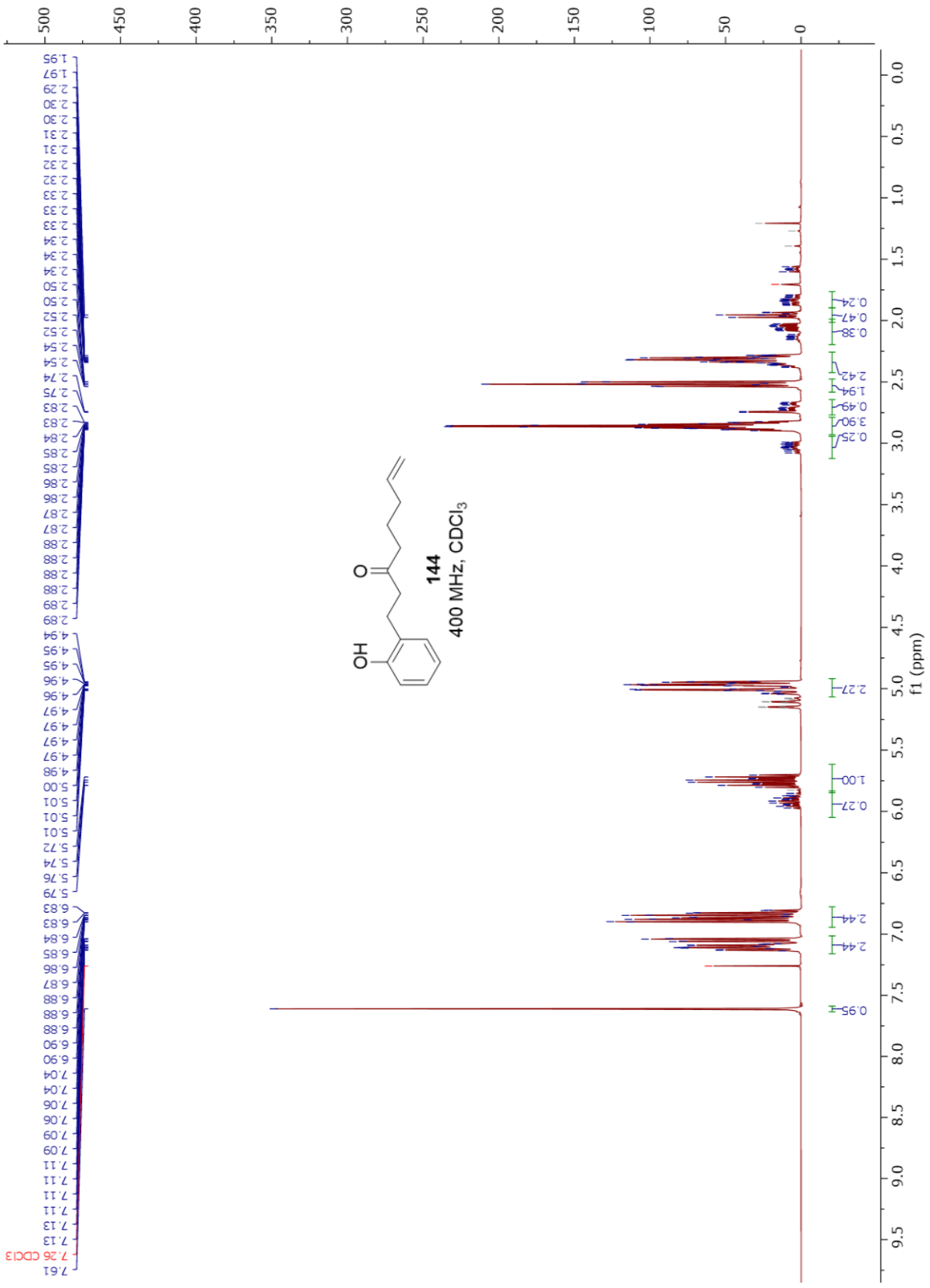
144
400 MHz, CDCl3
OH
O
f1 (ppm)

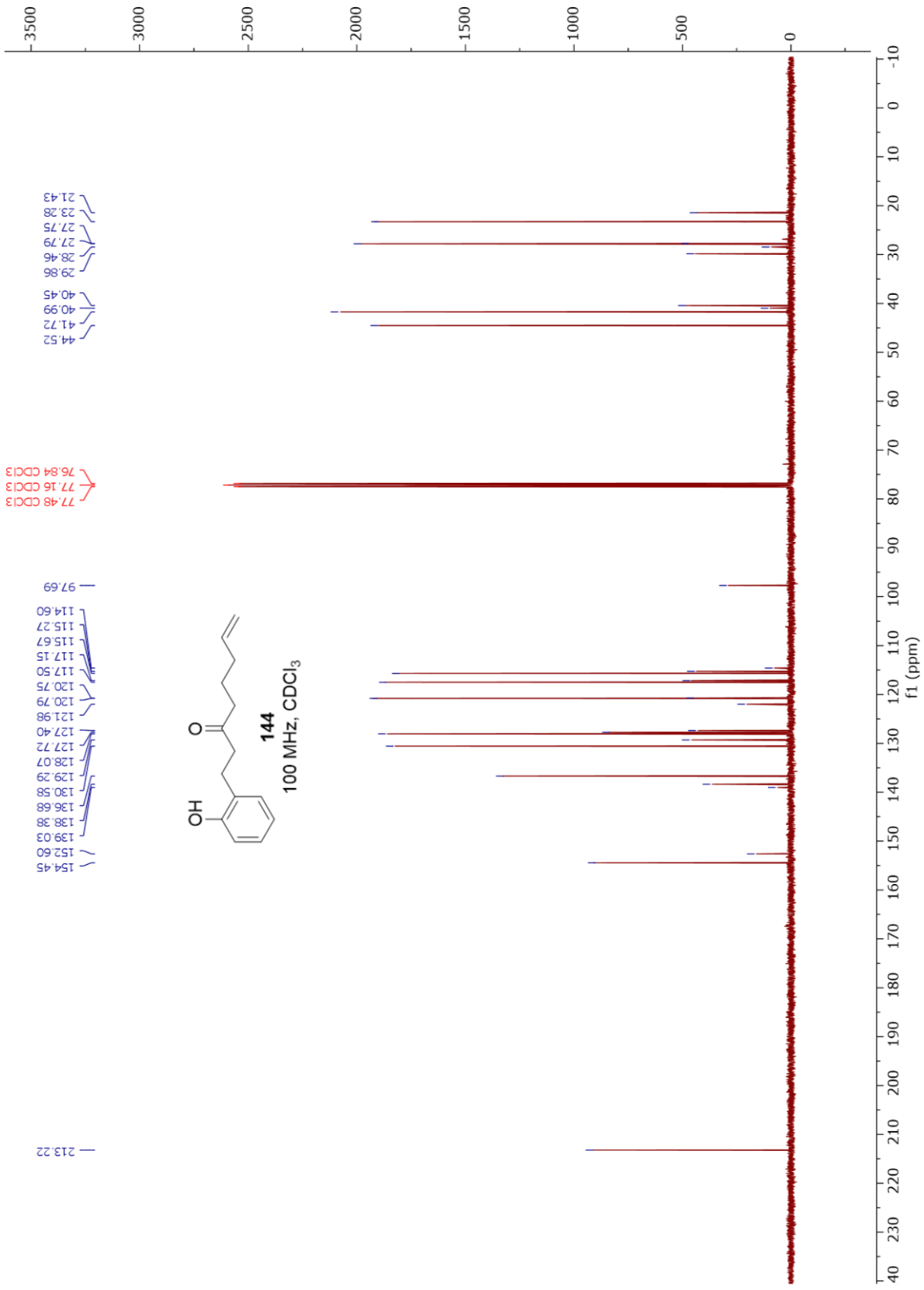
144
100 MHz, CDCl3
OH
O
21.43
23.28
27.75
27.79
28.46
29.86
40.45
40.99
41.72
44.52
76.84 CDCl3
77.16 CDCl3
77.48 CDCl3
97.69
114.60
115.27
115.67
117.15
117.50
120.75
120.79
121.98
127.40
127.72
128.07
129.29
130.58
136.68
138.38
139.03
152.60
154.45
213.22
f1 (ppm)

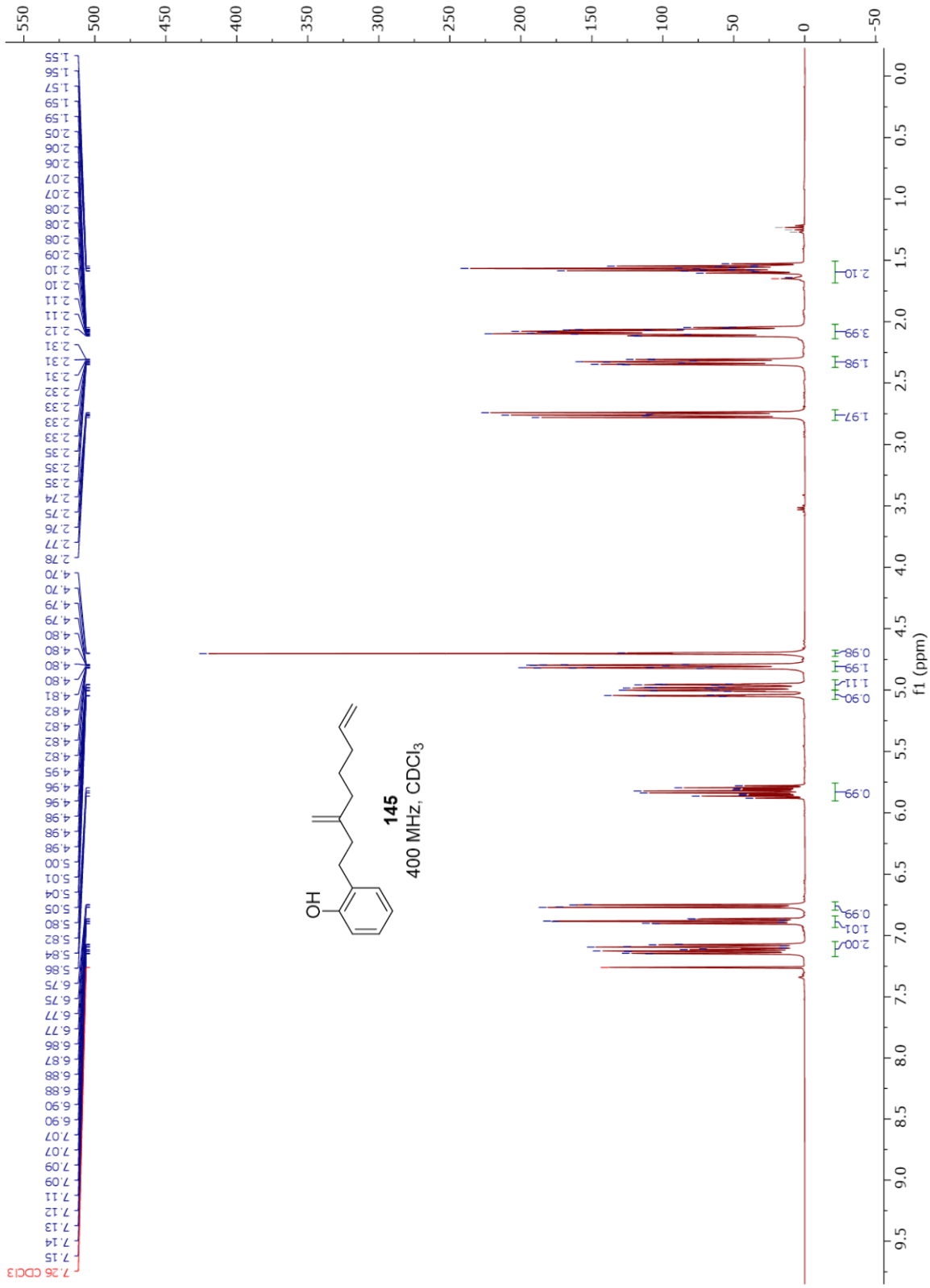
OH
145
400 MHz, CDCl3
f1 (ppm)

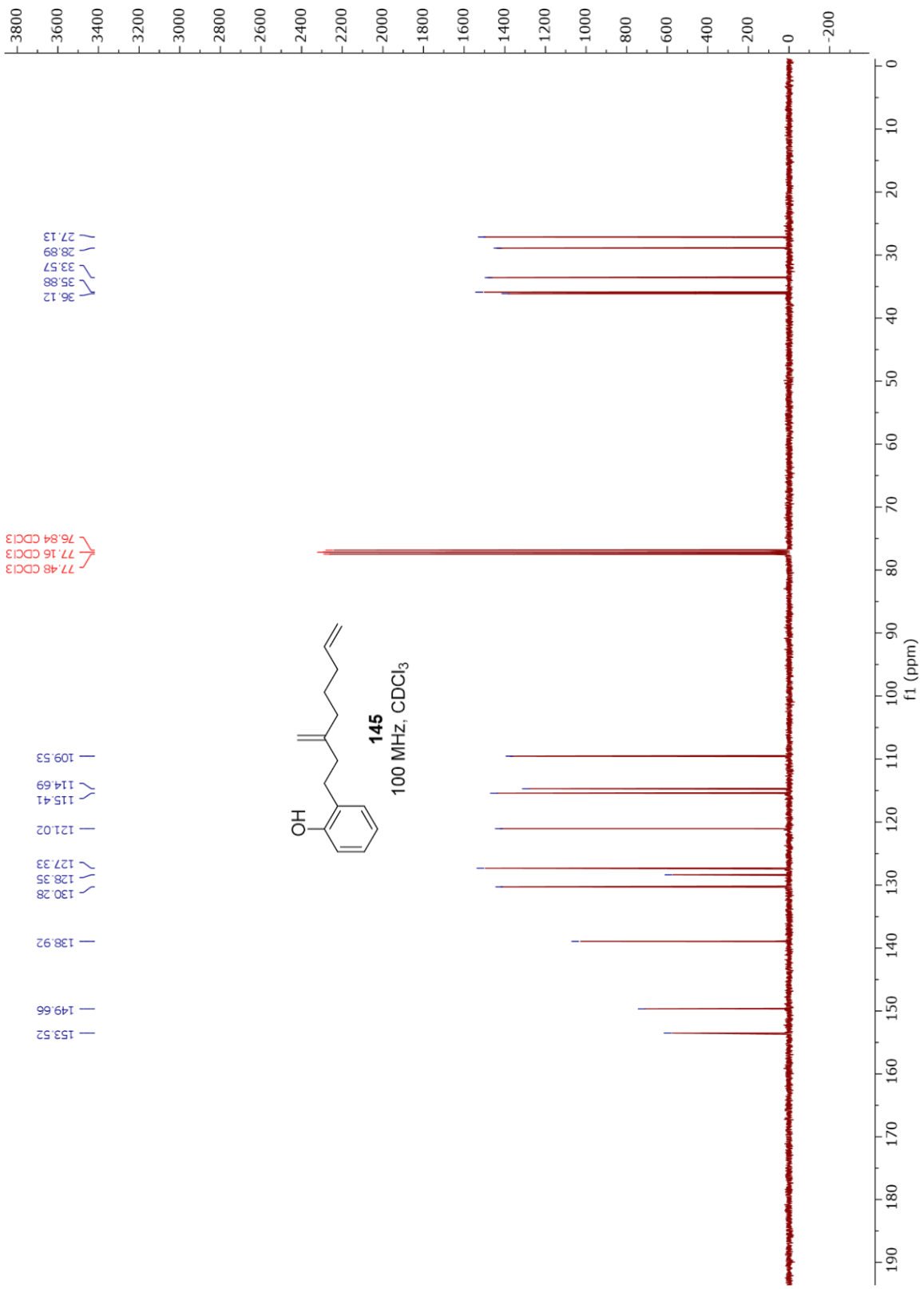
145
100 MHz, CDCl3
OH
f1 (ppm)
27.13
28.89
33.57
35.88
36.12
76.84 CDCl3
77.16 CDCl3
77.48 CDCl3
109.53
114.69
115.41
121.02
127.33
128.35
130.28
138.92
149.66
153.52

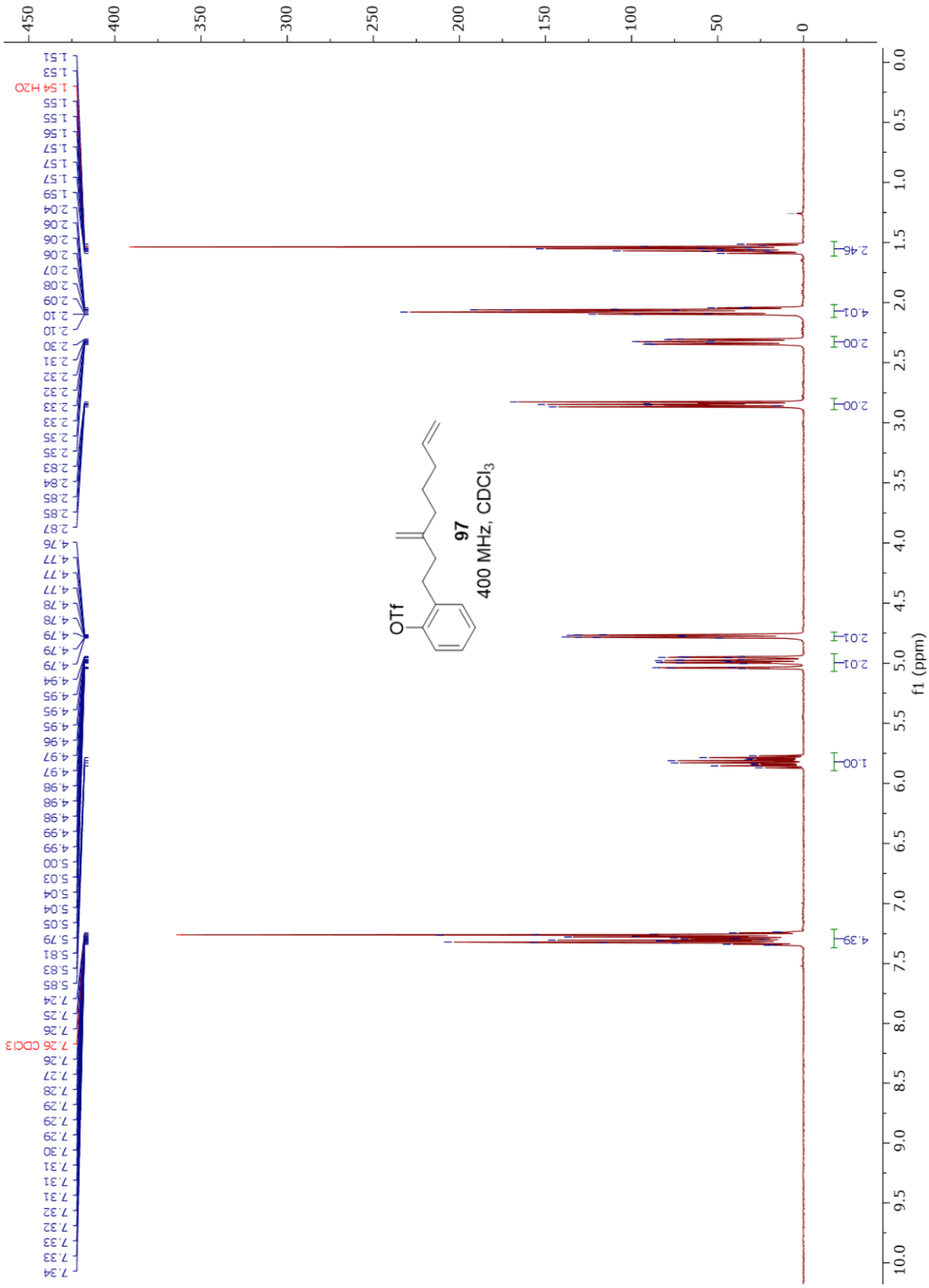
OTf
97
400 MHz, CDCl3
f1 (ppm)
1.54 H2O
7.26 CDCl3

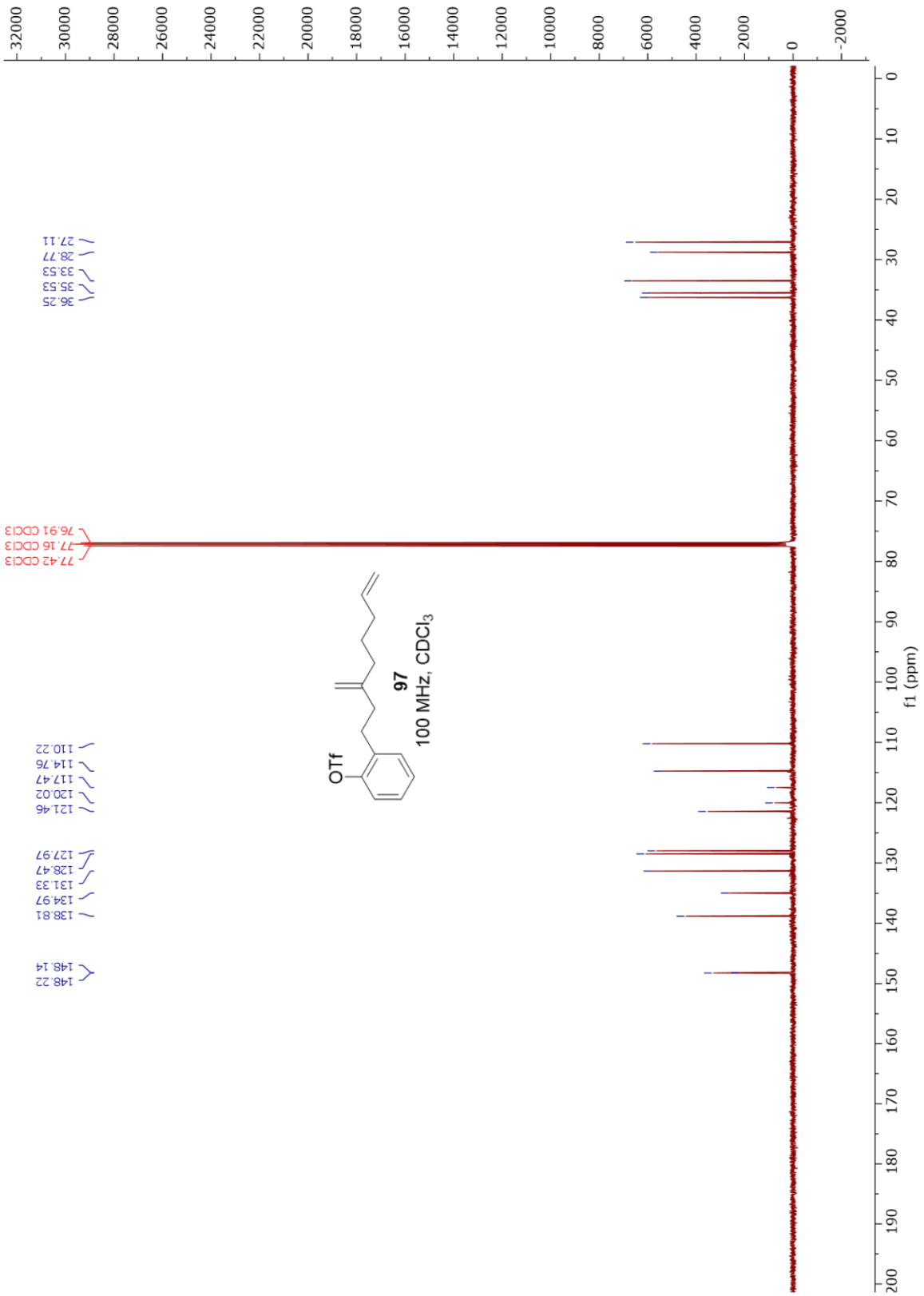
OTf
97
100 MHz, CDCl3
f1 (ppm)
77.42 CDCl3
77.16 CDCl3
76.91 CDCl3
148.22
148.14
138.81
134.97
131.33
128.47
127.97
121.46
120.02
117.47
114.76
110.22
36.25
35.53
33.53
28.77
27.11

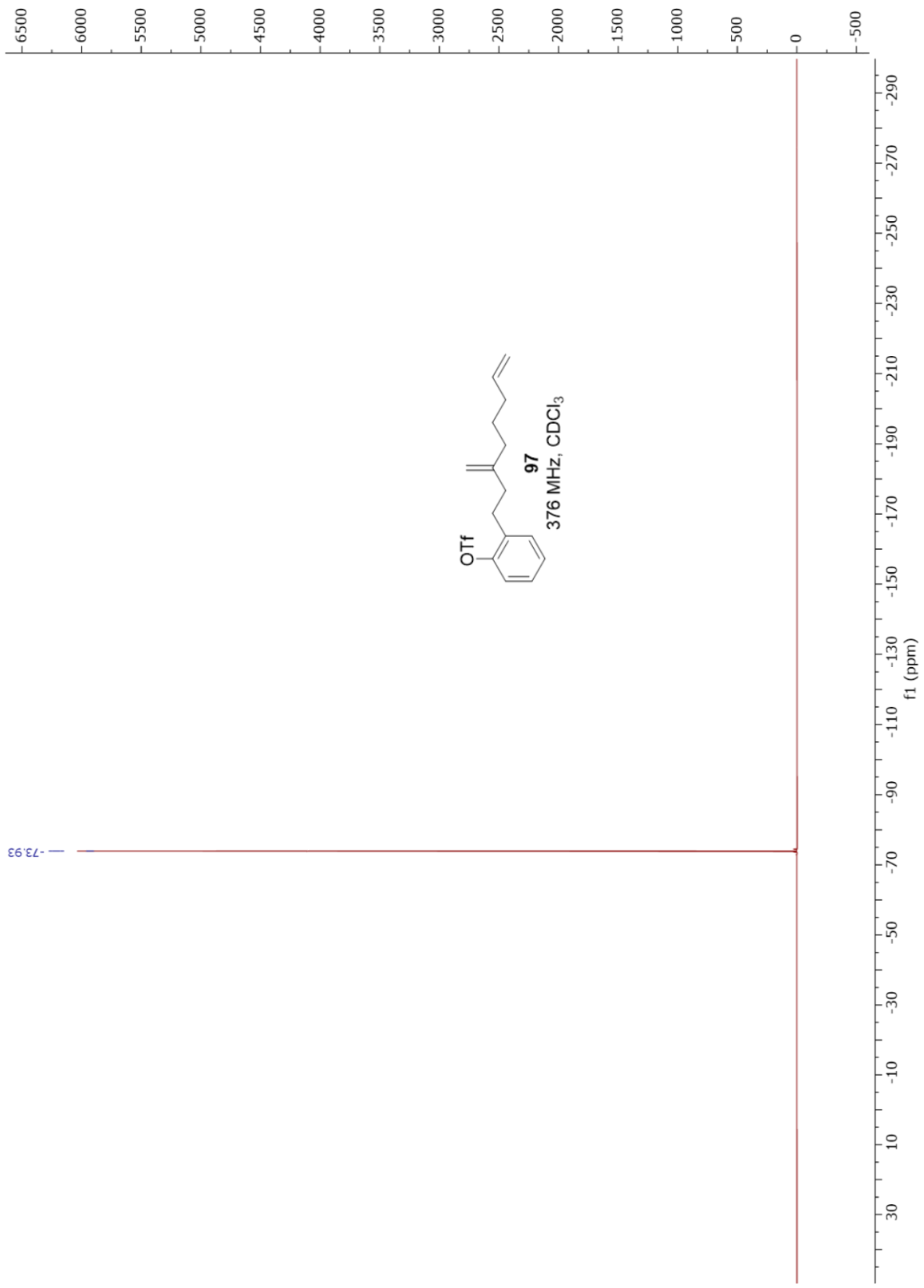
-73.93
OTf
97
376 MHz, $CDCl_3$
f1 (ppm)

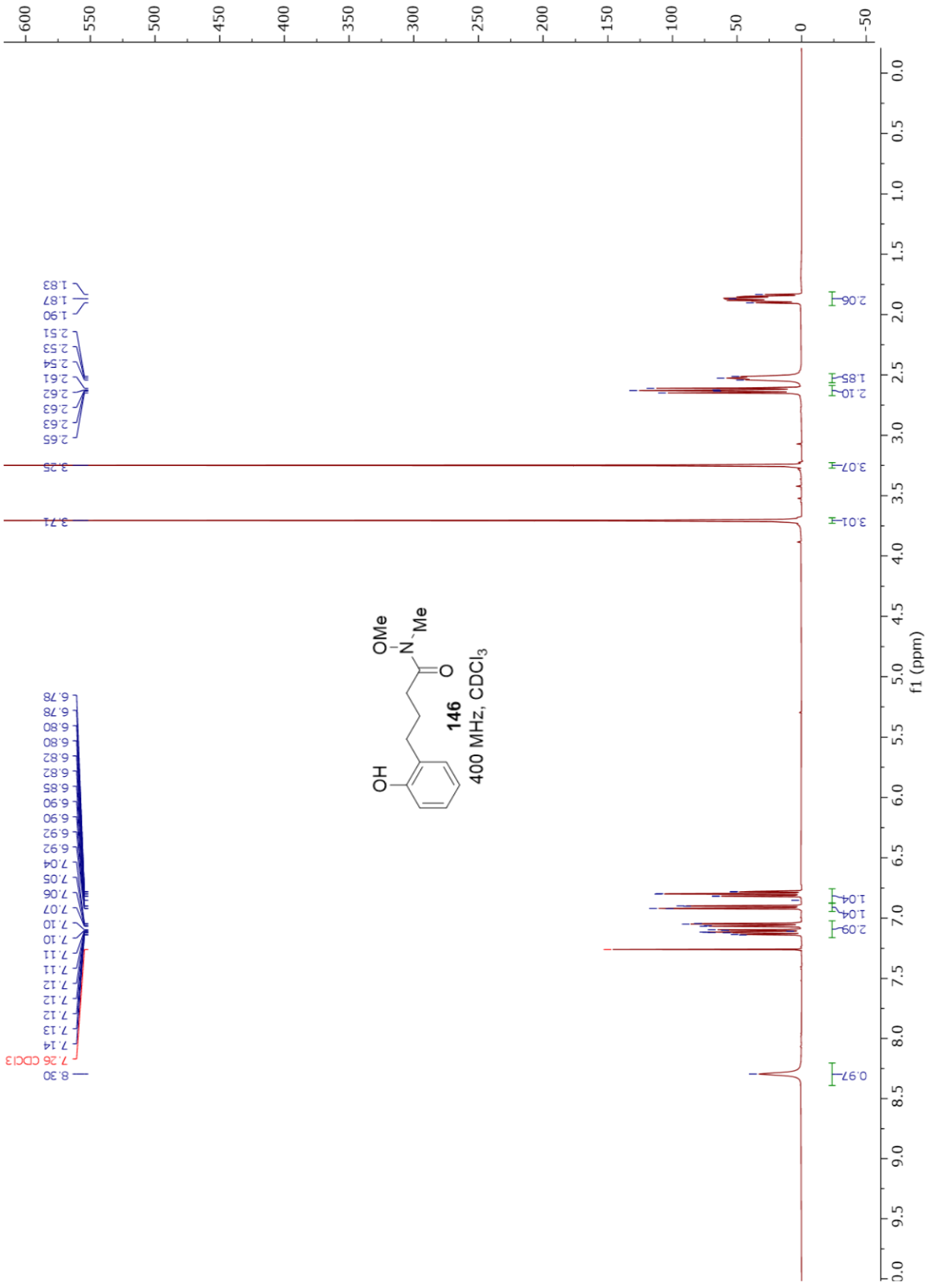
OMe
N
Me
O
OH
146
400 MHz, CDCl3
f1 (ppm)

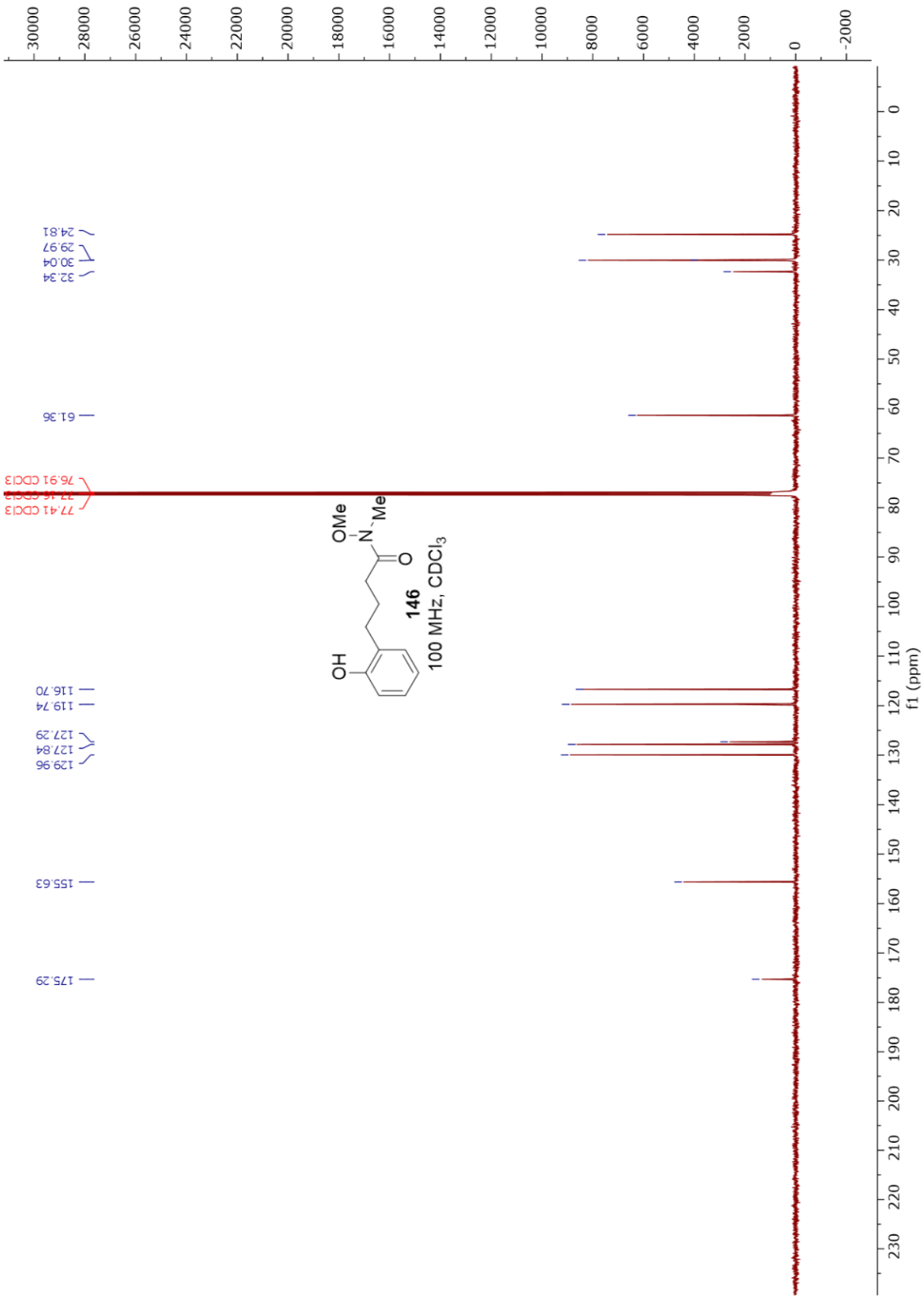
146
100 MHz, CDCl3
OMe
Me
N
O
OH
24.81
29.97
30.04
32.34
61.36
76.91 CDCl3
77.16 CDCl3
77.41 CDCl3
116.70
119.74
127.29
127.84
129.96
155.63
175.29
f1 (ppm)

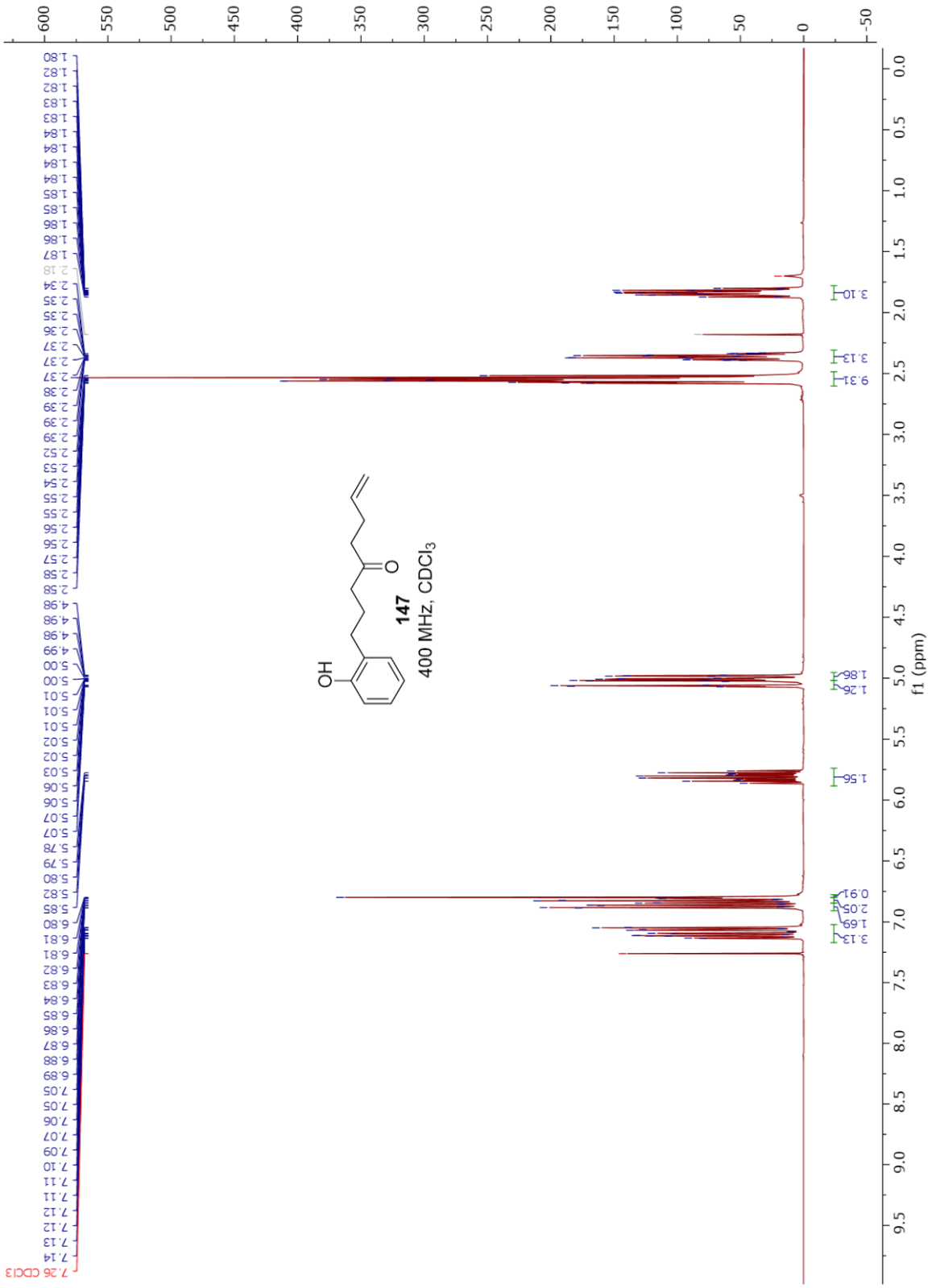
147
400 MHz, CDCl3
OH
O
f1 (ppm)

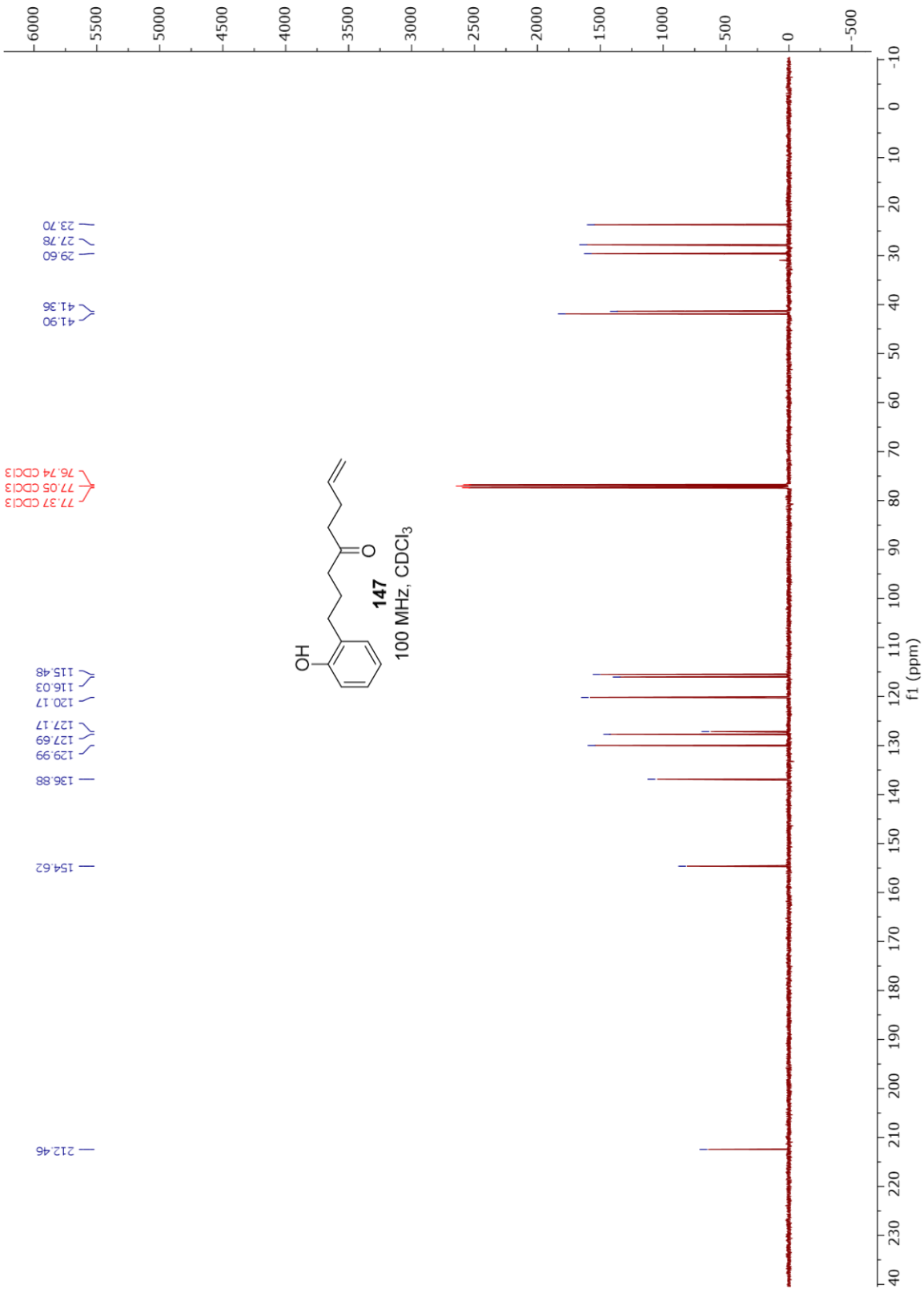
212.46
154.62
136.88
129.99
127.69
127.17
120.17
116.03
115.48
77.37 CDCl3
77.05 CDCl3
76.74 CDCl3
41.90
41.36
29.60
27.78
23.70
OH
O
147
100 MHz, CDCl3
f1 (ppm)

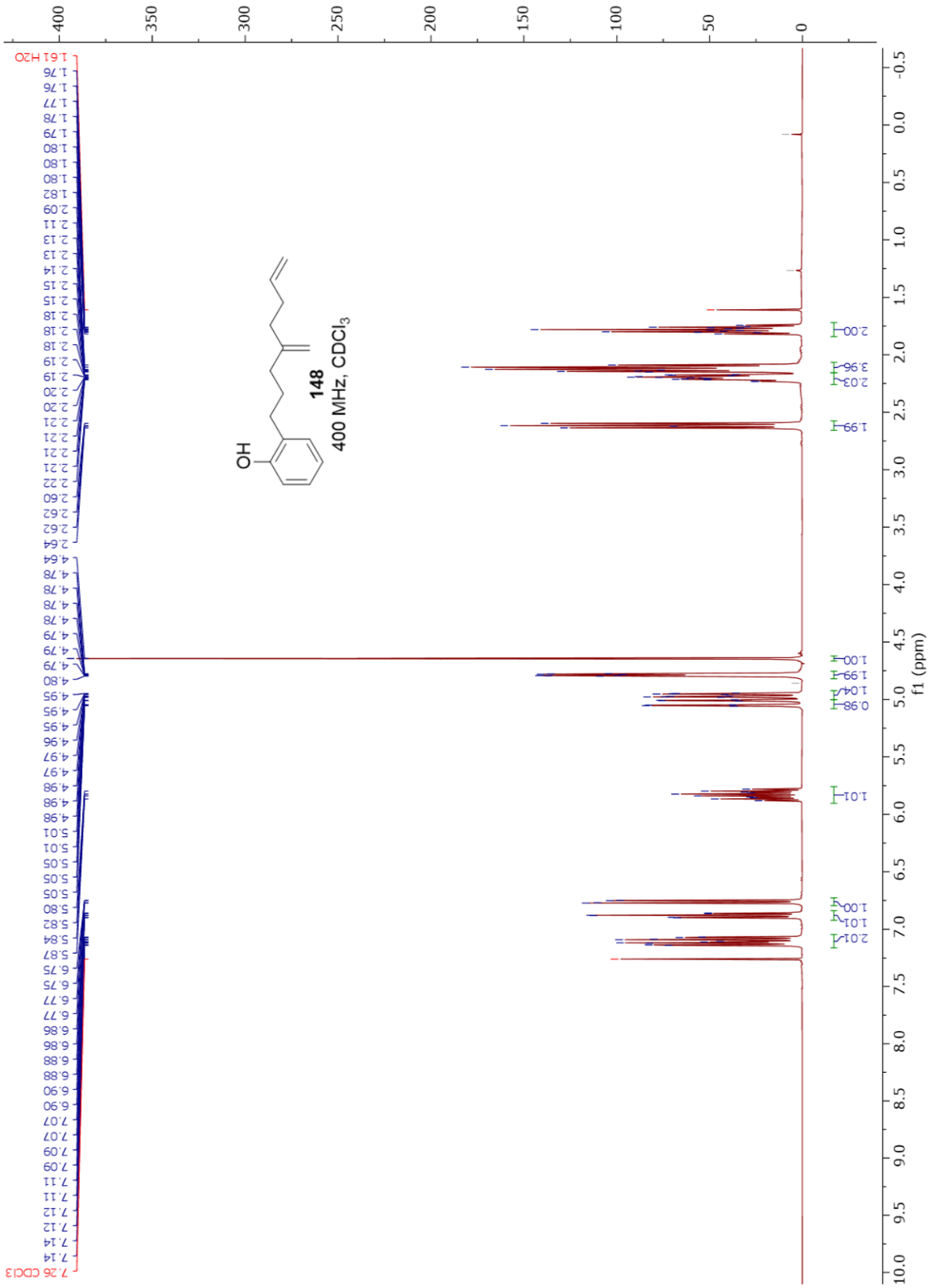
148
400 MHz, CDCl3
OH
f1 (ppm)

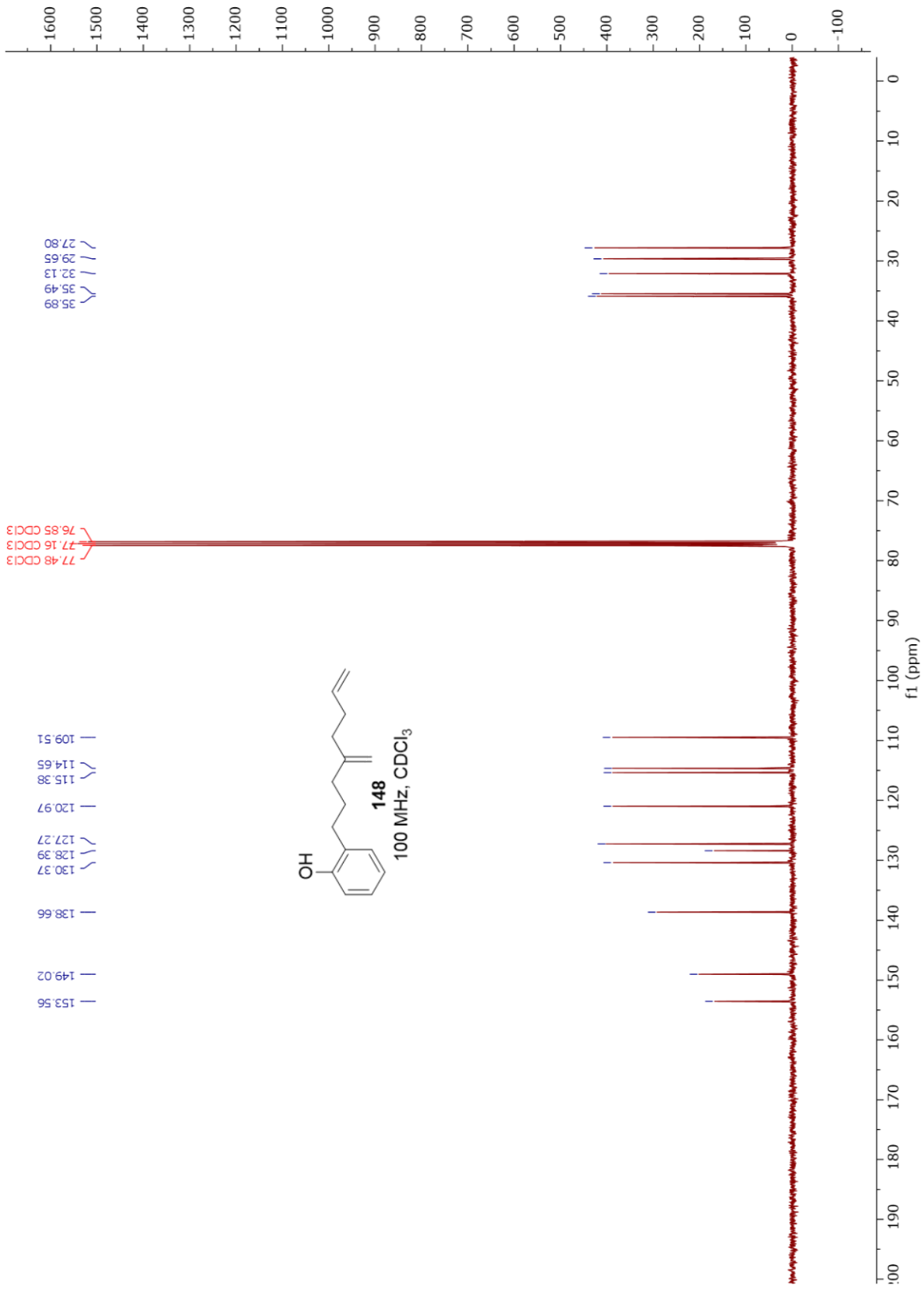
148
100 MHz, CDCl3
OH
153.56
149.02
138.66
130.37
128.39
127.27
120.97
115.38
114.65
109.51
77.48 CDCl3
77.16 CDCl3
76.85 CDCl3
35.89
35.49
32.13
29.65
27.80
f1 (ppm)

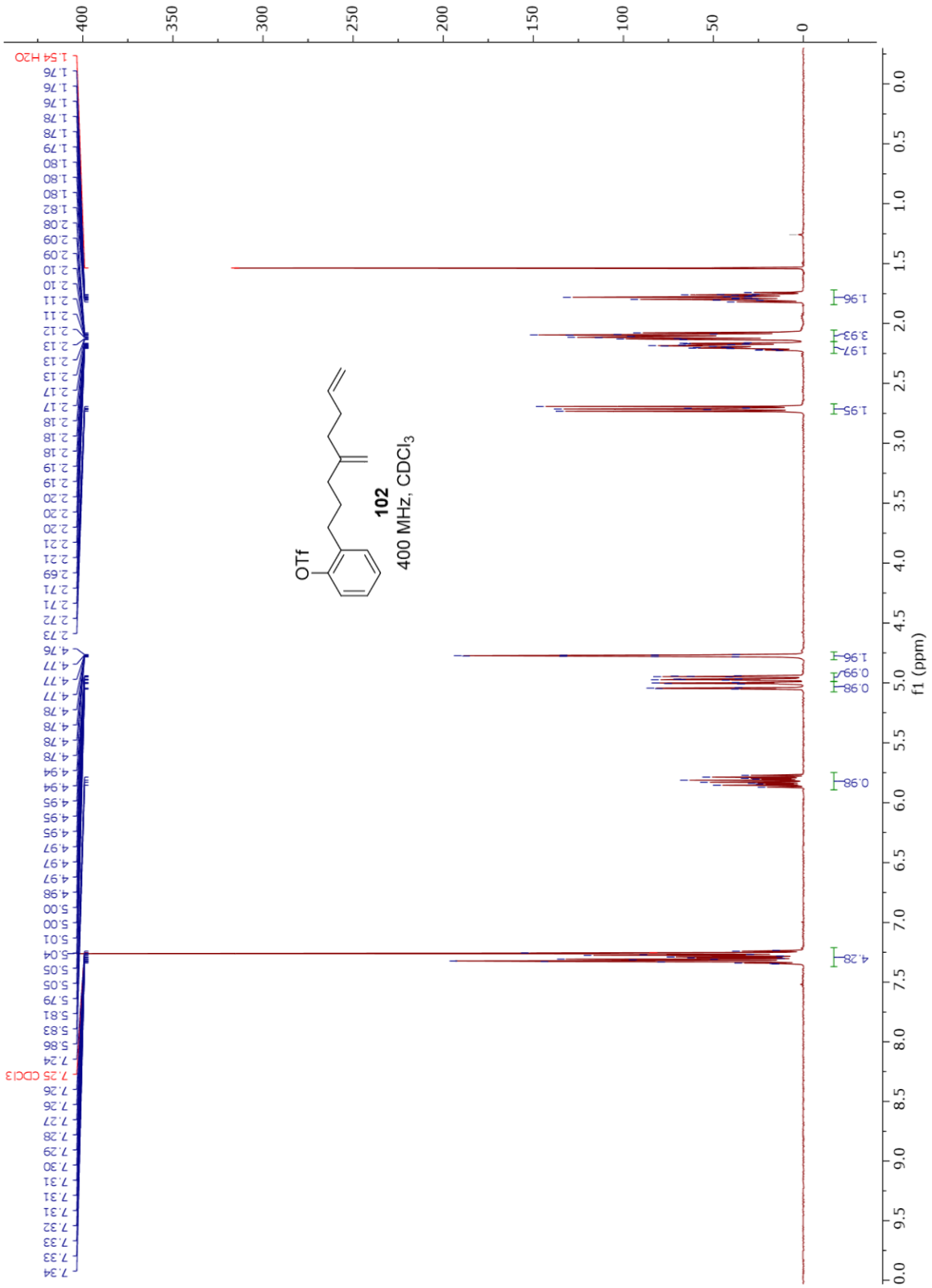
OTf
102
400 MHz, CDCl3
f1 (ppm)

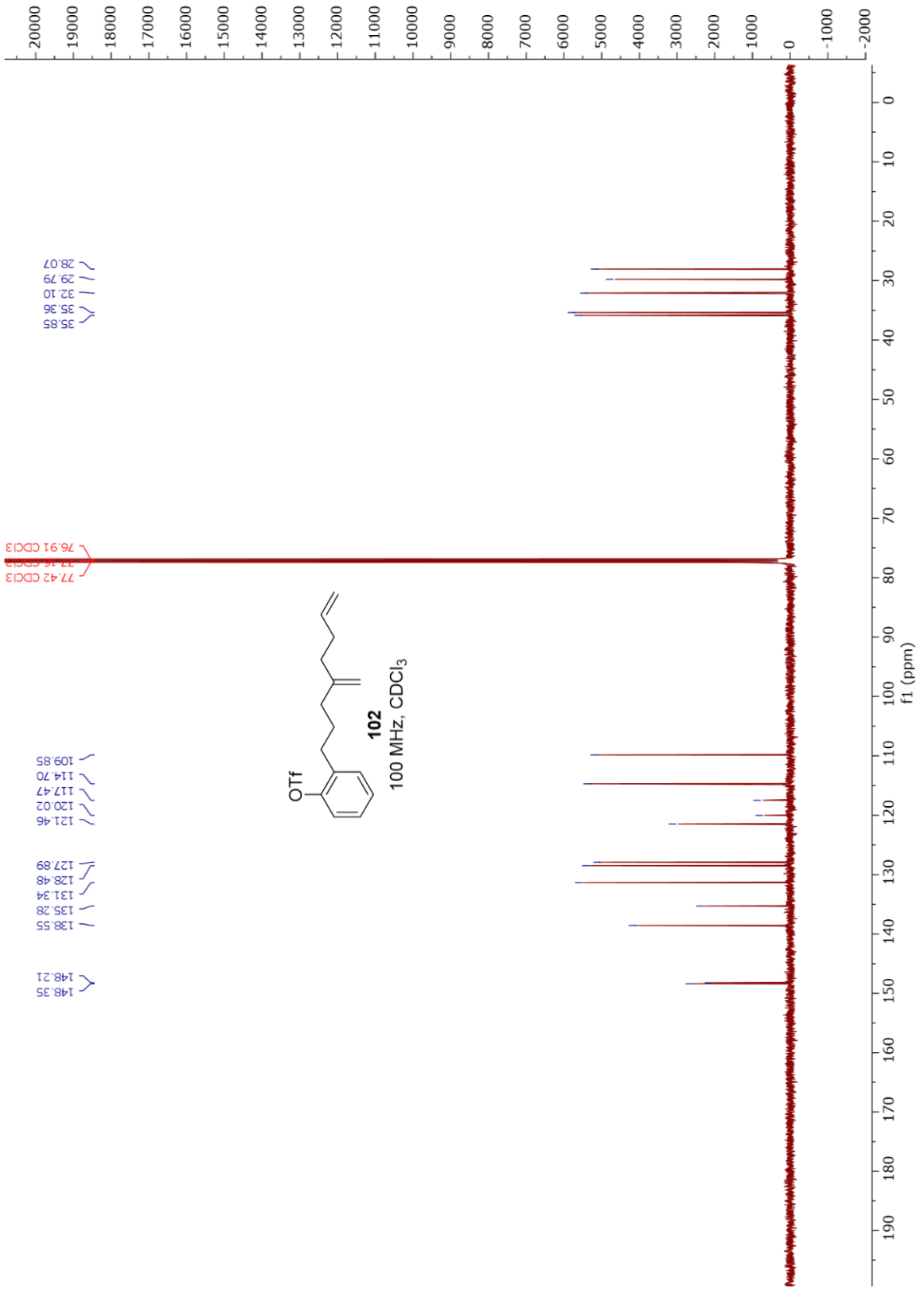
OTf
102
100 MHz, CDCl3
f1 (ppm)
77.42 CDCl3
76.91 CDCl3
148.35
148.21
138.55
135.28
131.34
128.48
127.89
121.46
120.02
117.47
114.70
109.85
35.85
35.36
32.10
29.79
28.07

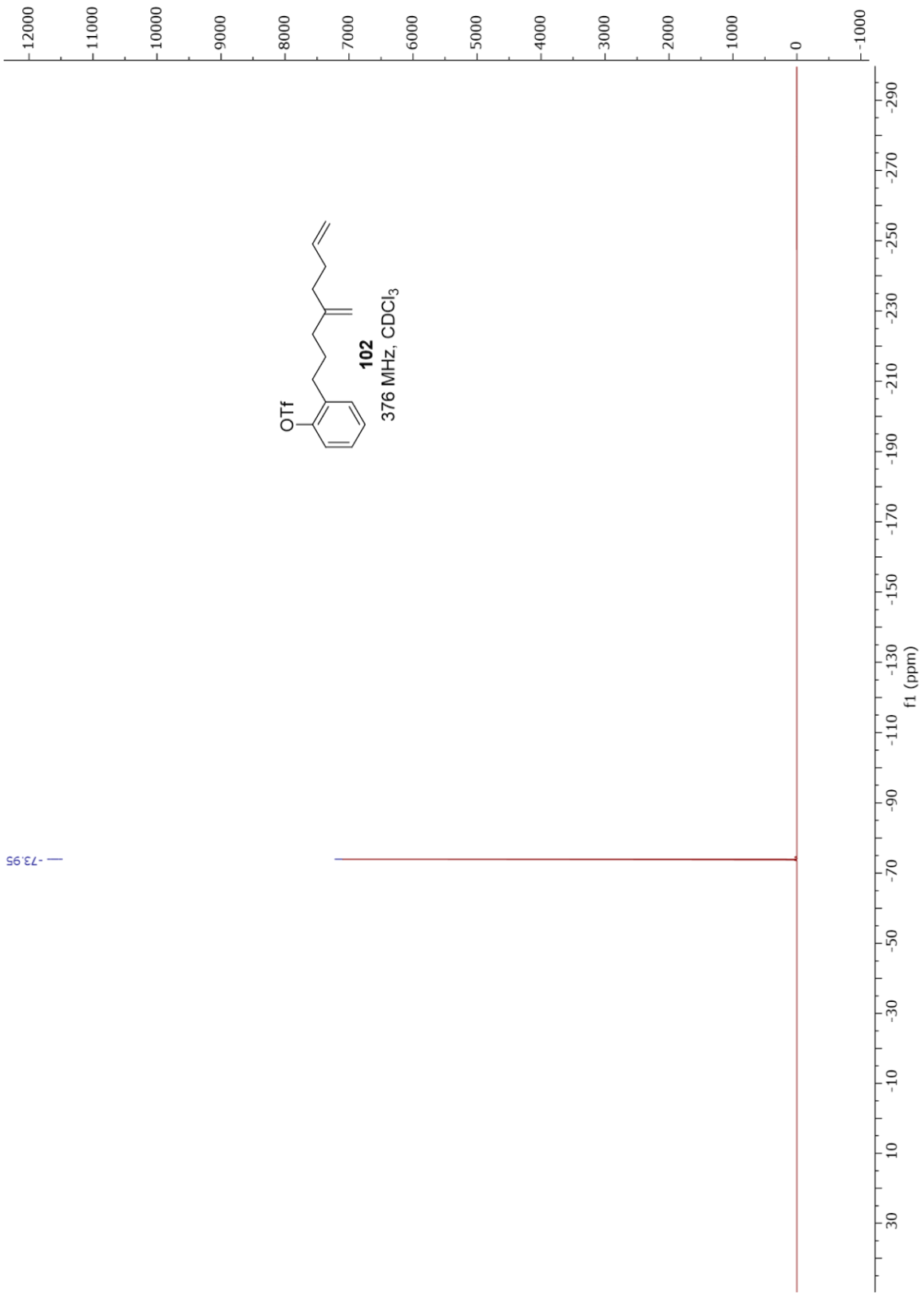
OTf
102
376 MHz, CDCl3
-73.95
f1 (ppm)

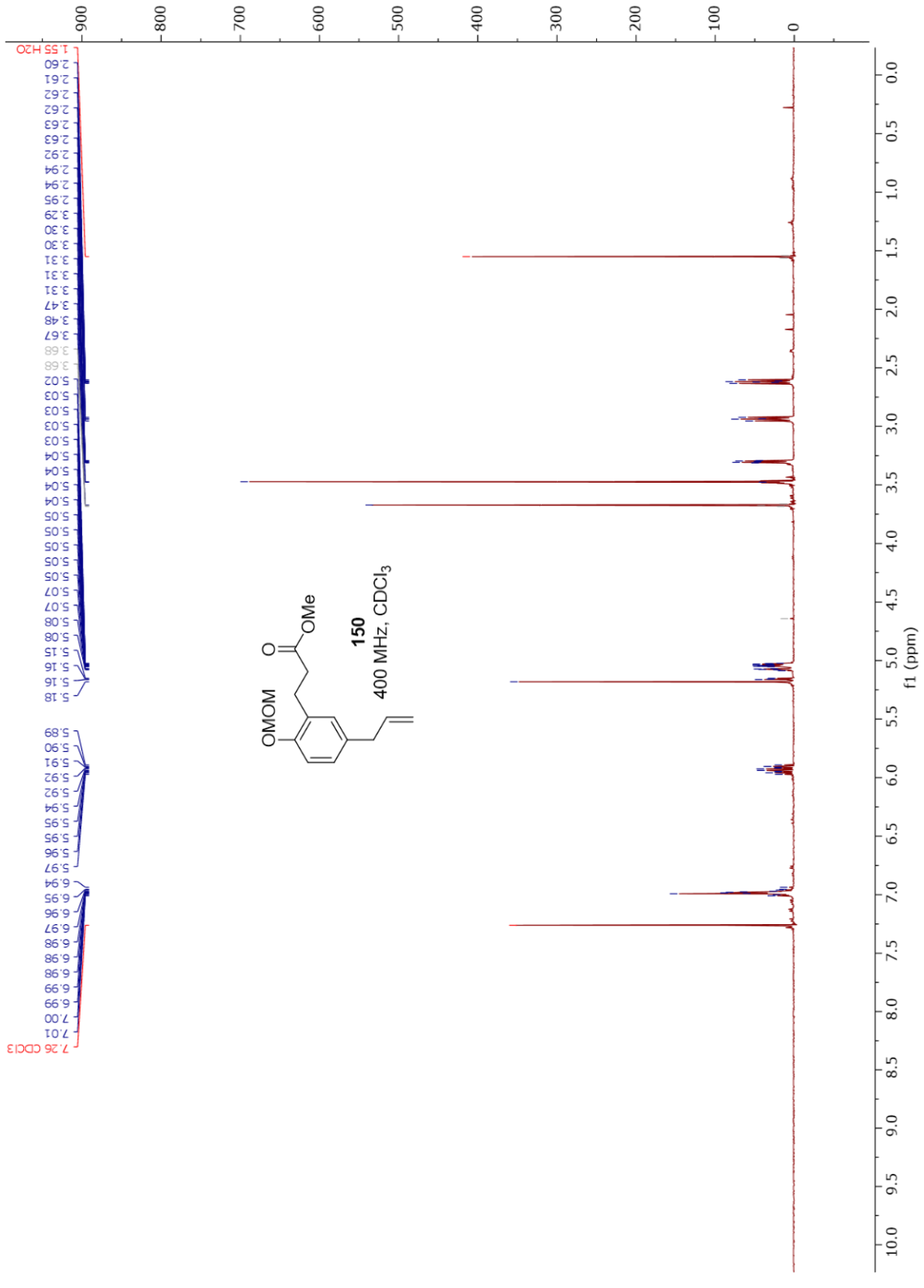
OMOM
O
OMe
150
400 MHz, CDCl3
f1 (ppm)

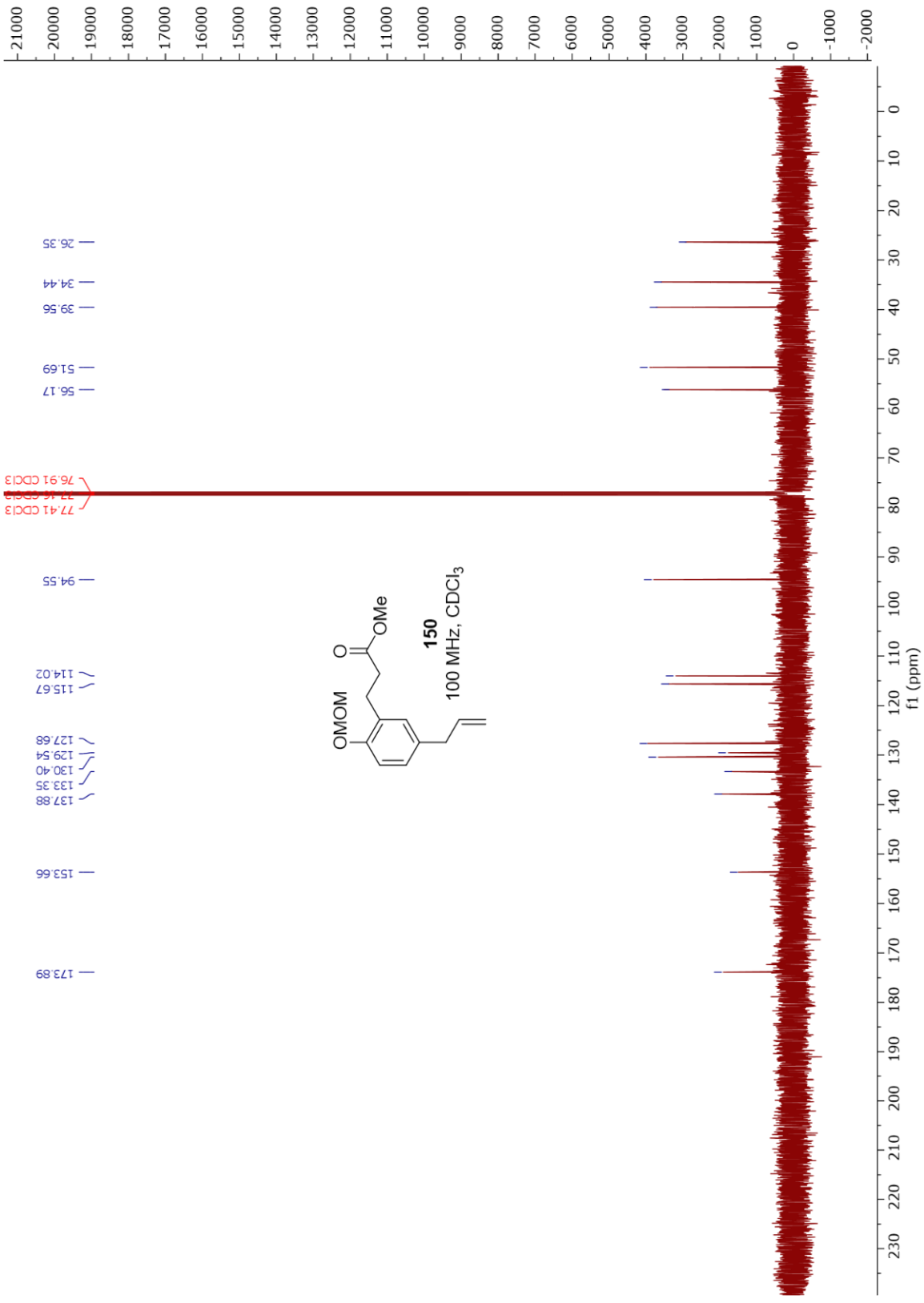
150
100 MHz, CDCl3
OMe
O
OMOM
26.35
34.44
39.56
51.69
56.17
76.91 CDCl3
77.16 CDCl3
77.41 CDCl3
94.55
114.02
115.67
127.68
129.54
130.40
133.35
137.88
153.66
173.89
f1 (ppm)

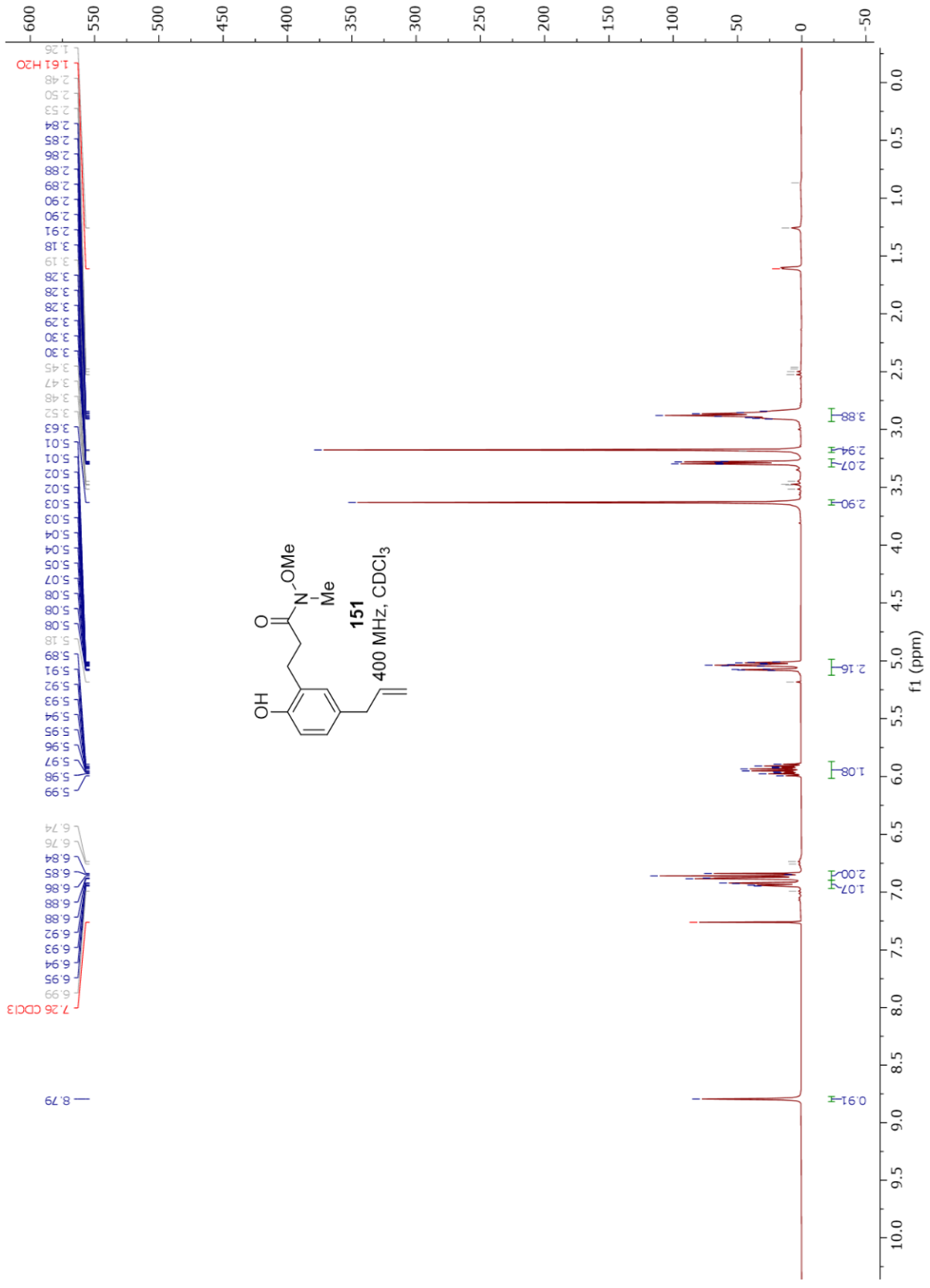
151
400 MHz, CDCl3
f1 (ppm)

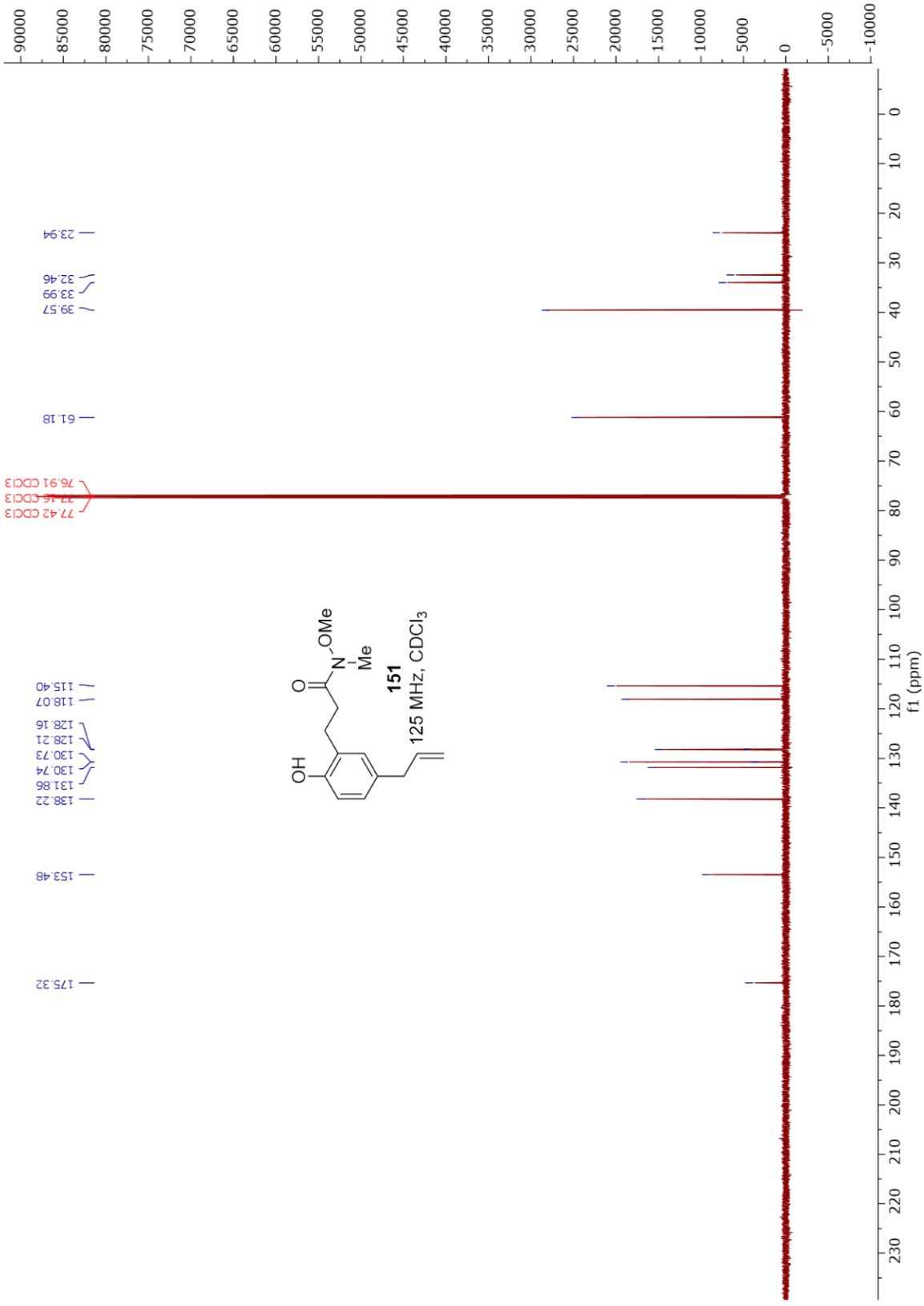
23.94
32.46
33.99
39.57
61.18
76.91 CDCl3
77.16 CDCl3
77.42 CDCl3
115.40
118.07
128.16
128.21
130.73
130.74
131.86
138.22
153.48
175.32
OH
O
N
OMe
Me
151
125 MHz, CDCl3
f1 (ppm)

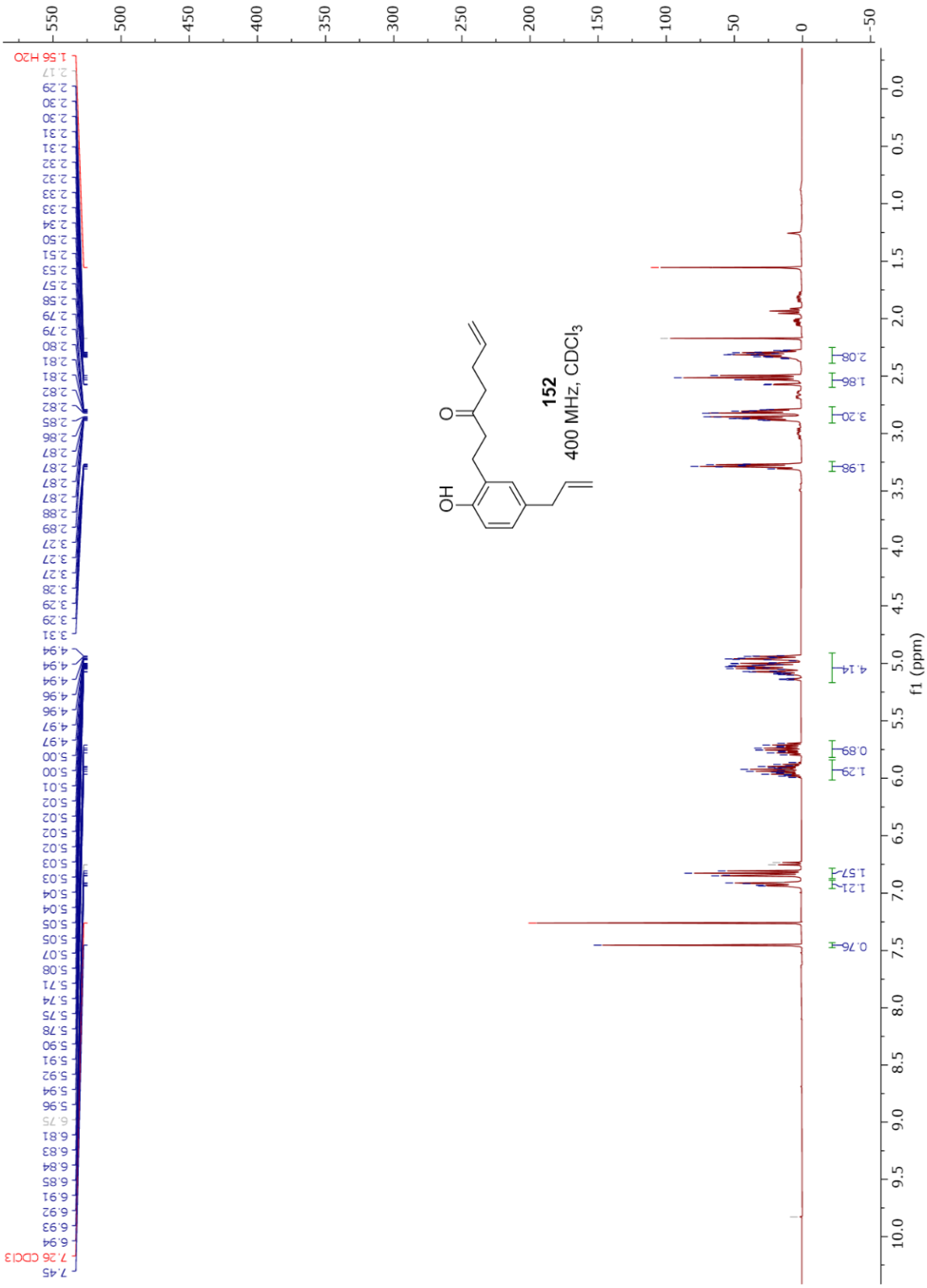
152
400 MHz, CDCl3
OH
O
f1 (ppm)
1.56 H2O
7.26 CDCl3
2.08
1.86
3.20
1.98
4.14
0.89
1.29
1.57
1.21
0.76

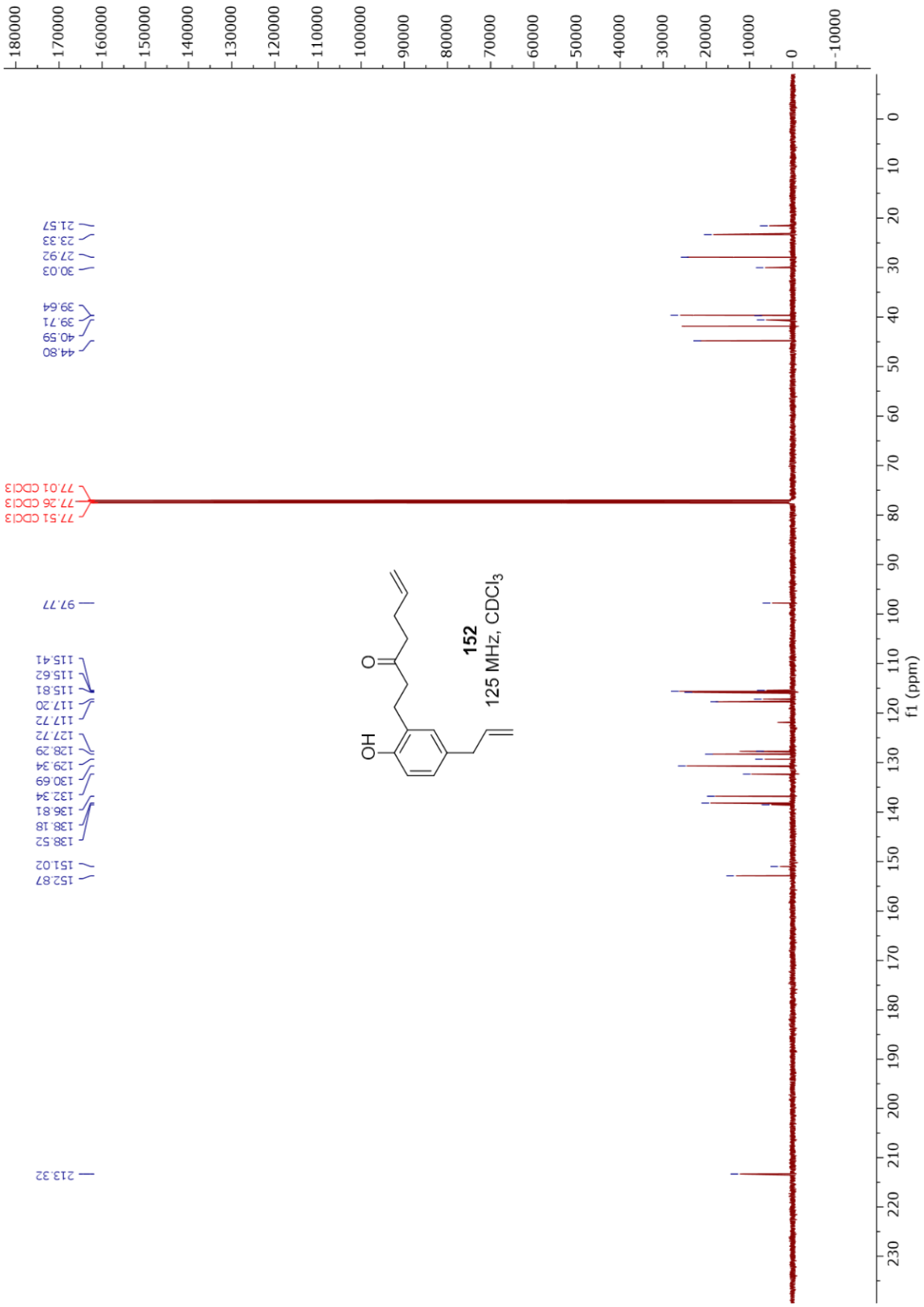
152
125 MHz, CDCl3
OH
O
f1 (ppm)
213.32
152.87
151.02
138.52
138.18
136.81
132.34
130.69
129.34
128.29
127.72
117.72
117.20
115.81
115.62
115.41
97.77
77.51 CDCl3
77.26 CDCl3
77.01 CDCl3
44.80
40.59
39.71
39.64
30.03
27.92
23.33
21.57

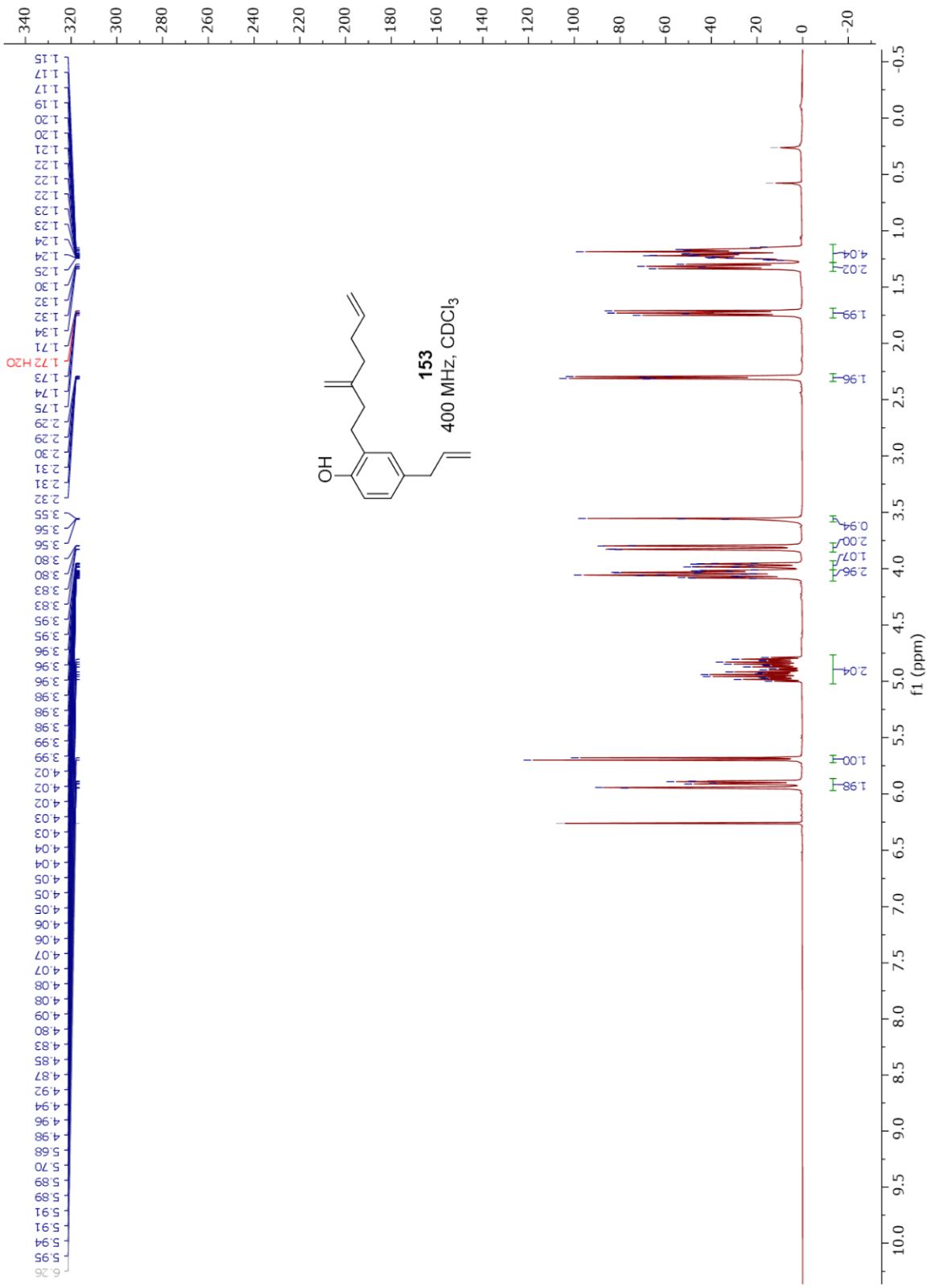
153
400 MHz, CDCl3
OH
f1 (ppm)
4.04
2.02
1.99
1.96
0.94
2.00
1.07
2.96
2.04
1.00
1.98
H2O

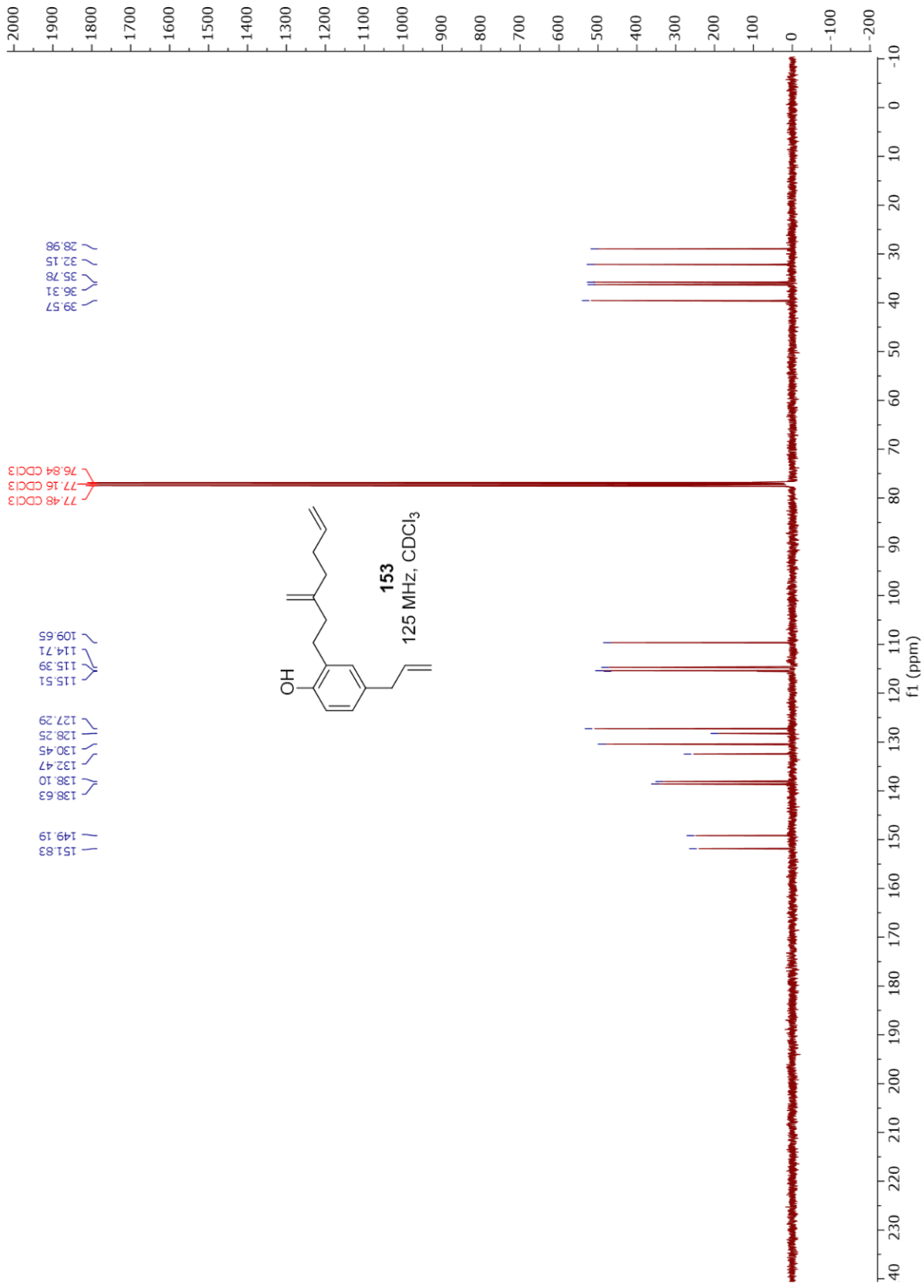
153
125 MHz, $CDCl_3$
OH
f1 (ppm)
77.48 CDCl3
77.16 CDCl3
76.84 CDCl3
151.83
149.19
138.63
138.10
132.47
130.45
128.25
127.29
115.51
115.39
114.71
109.65
39.57
36.31
35.78
32.15
28.98

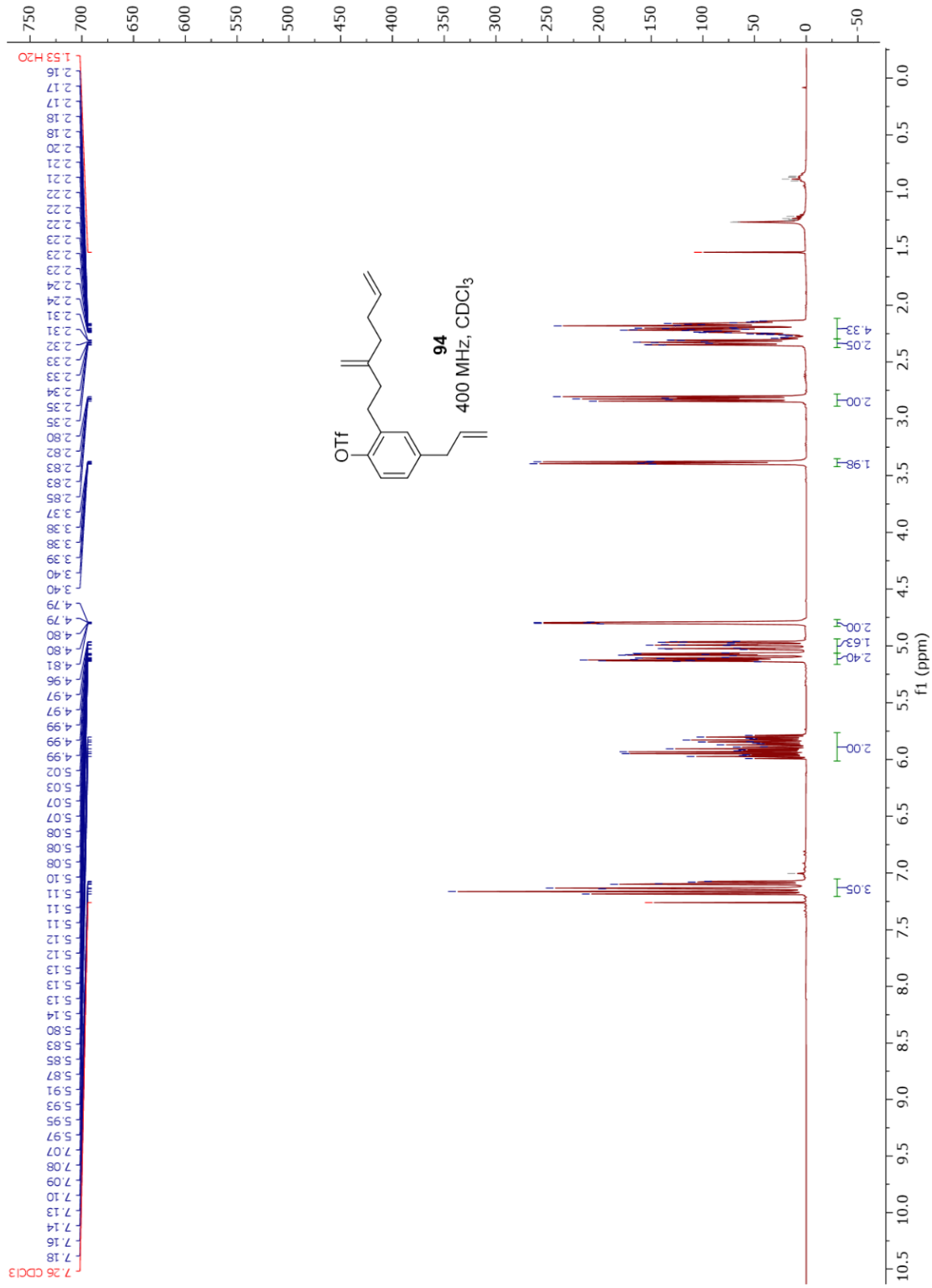
OTf
94
400 MHz, CDCl3
f1 (ppm)

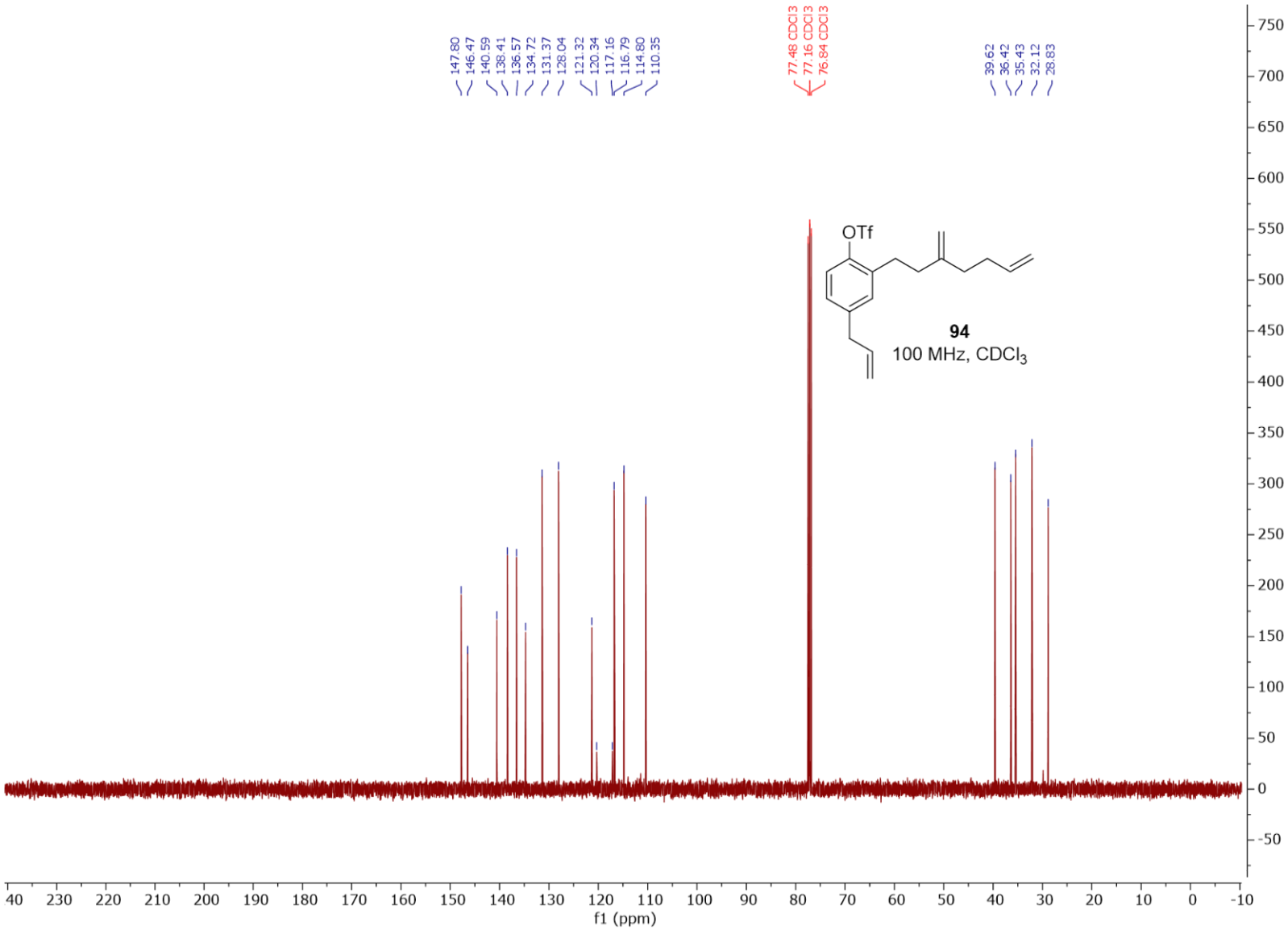
147.80
146.47
140.59
138.41
136.57
134.72
131.37
128.04
121.32
120.34
117.16
116.79
114.80
110.35
77.48 CDCl3
77.16 CDCl3
76.84 CDCl3
39.62
36.42
35.43
32.12
28.83
OTf
94
100 MHz, CDCl3
f1 (ppm)

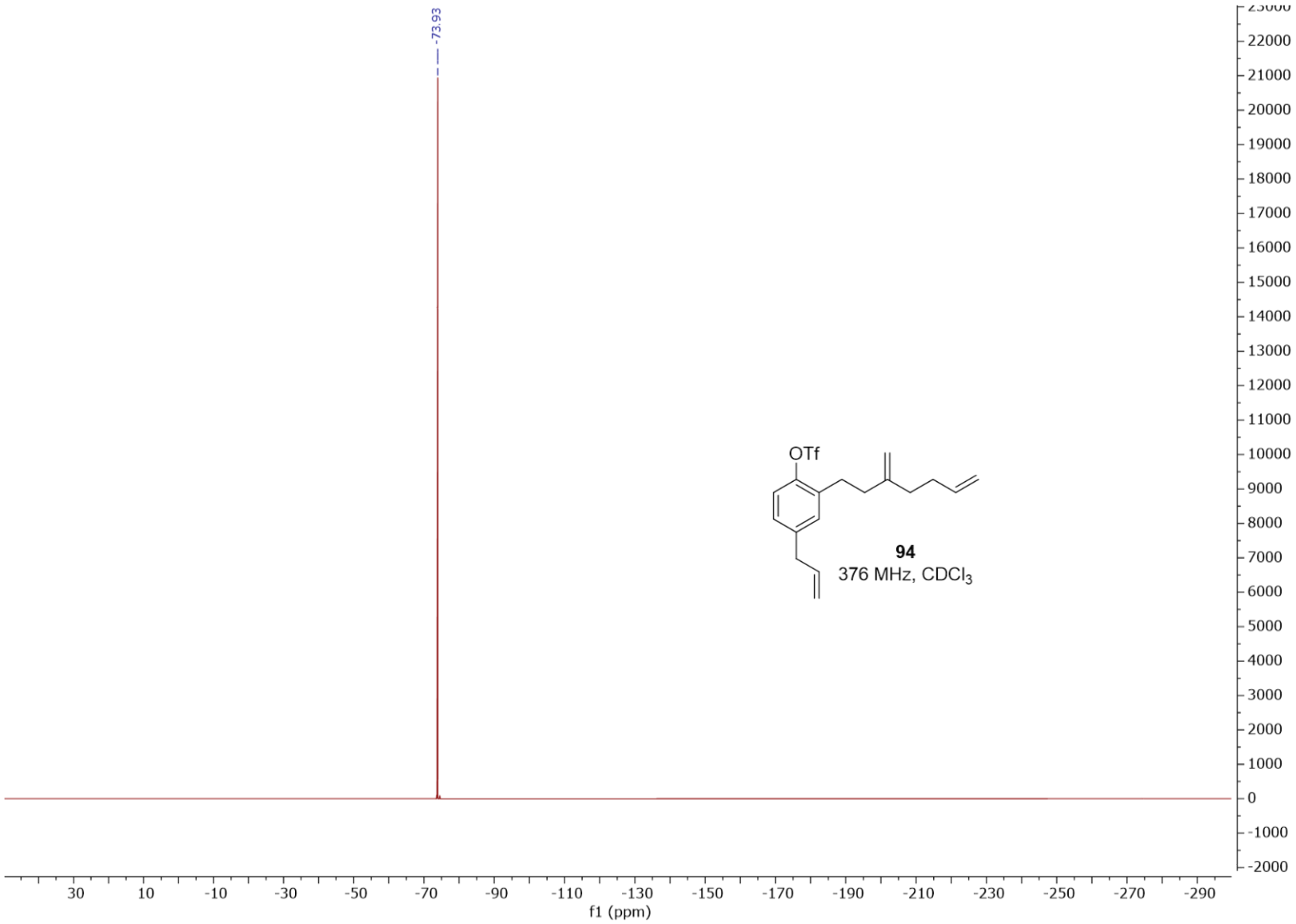
-73.93
OTf
94
376 MHz, CDCl3
f1 (ppm)

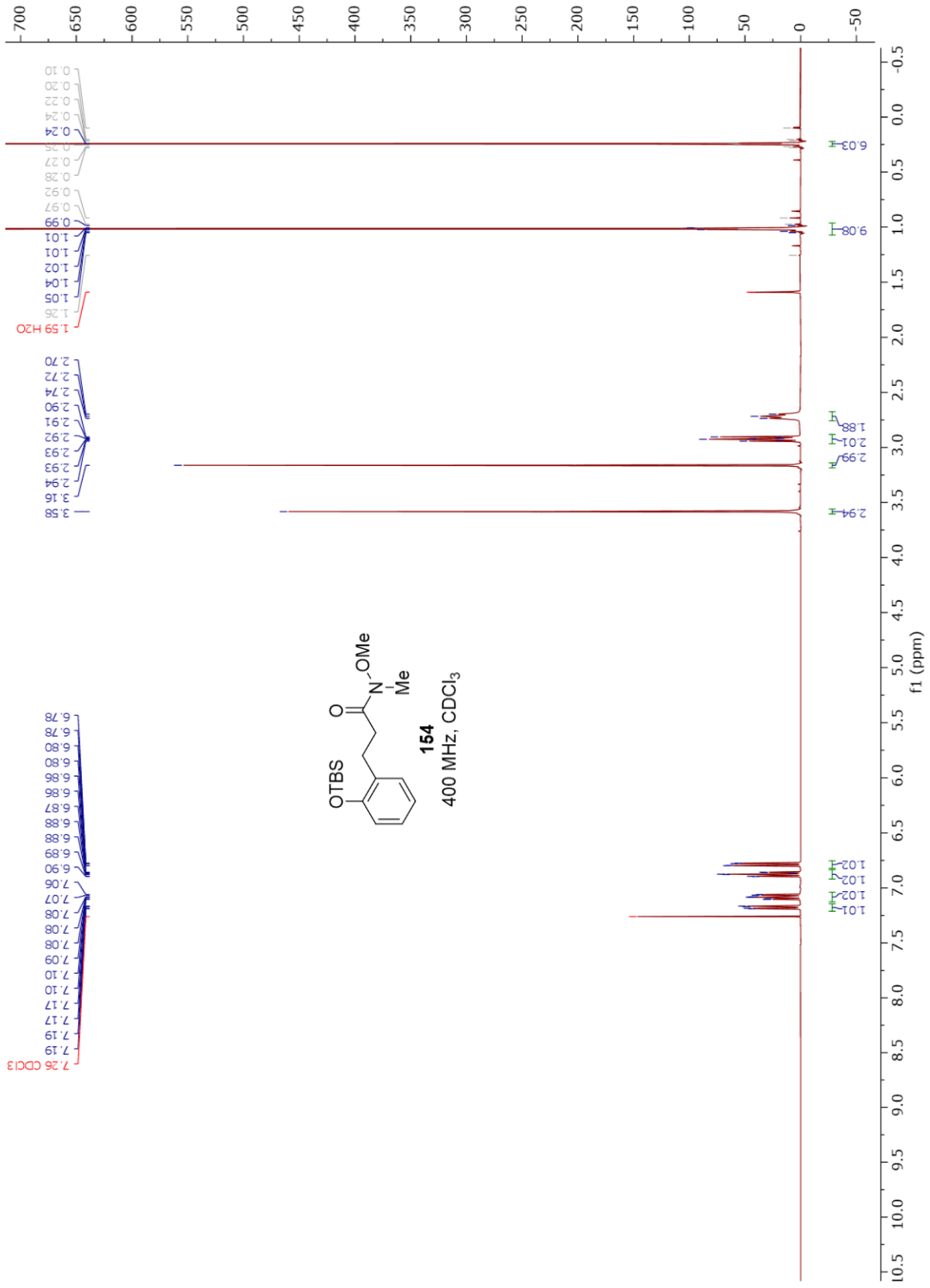
OTBS
O
N
OMe
Me
154
400 MHz, CDCl3
f1 (ppm)

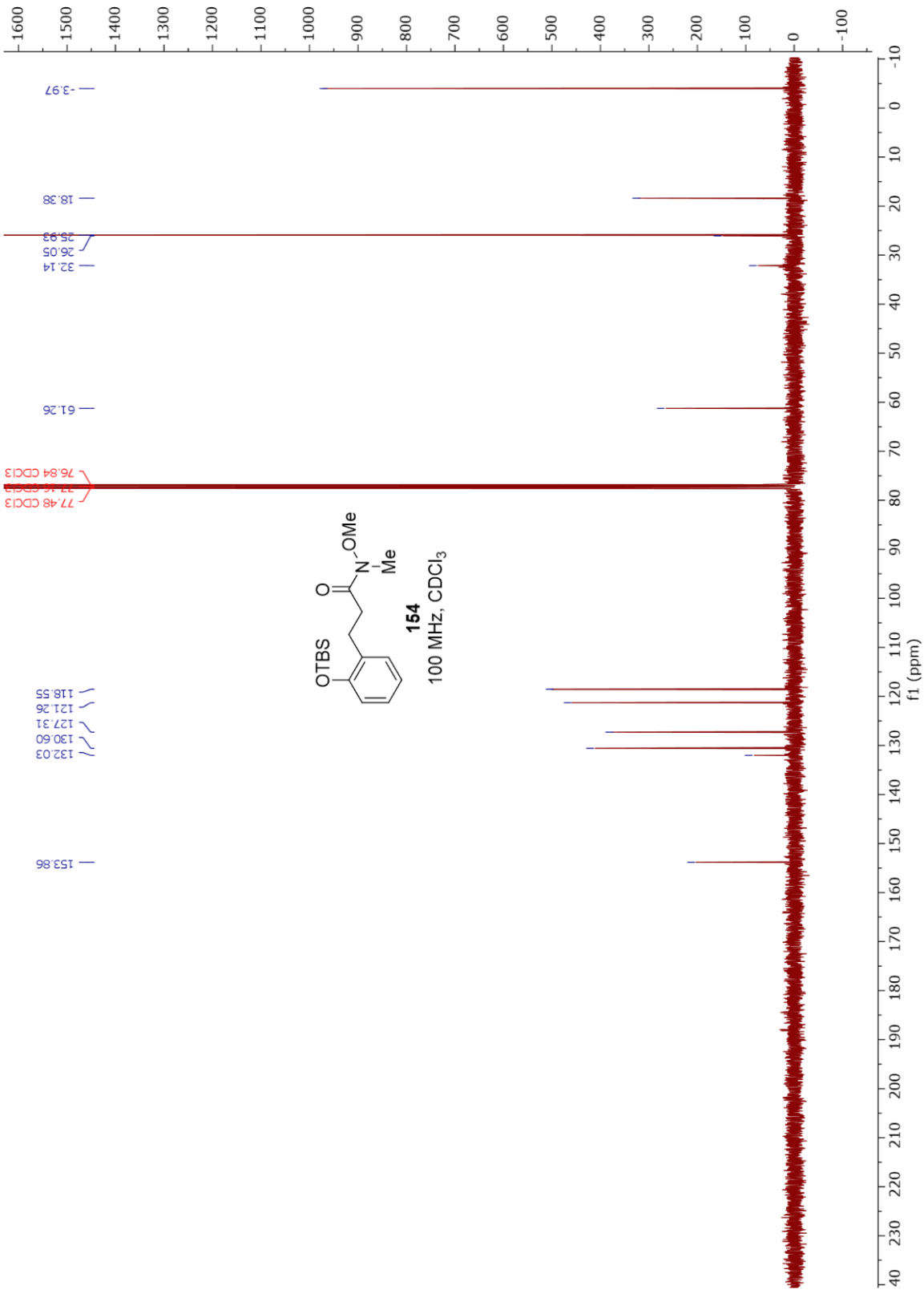
-3.97
18.38
25.93
26.05
32.14
61.26
76.84 CDCl3
77.16 CDCl3
77.48 CDCl3
118.55
121.26
127.31
130.60
132.03
153.86
OTBS
O
N
OMe
Me
154
100 MHz, CDCl3
f1 (ppm)

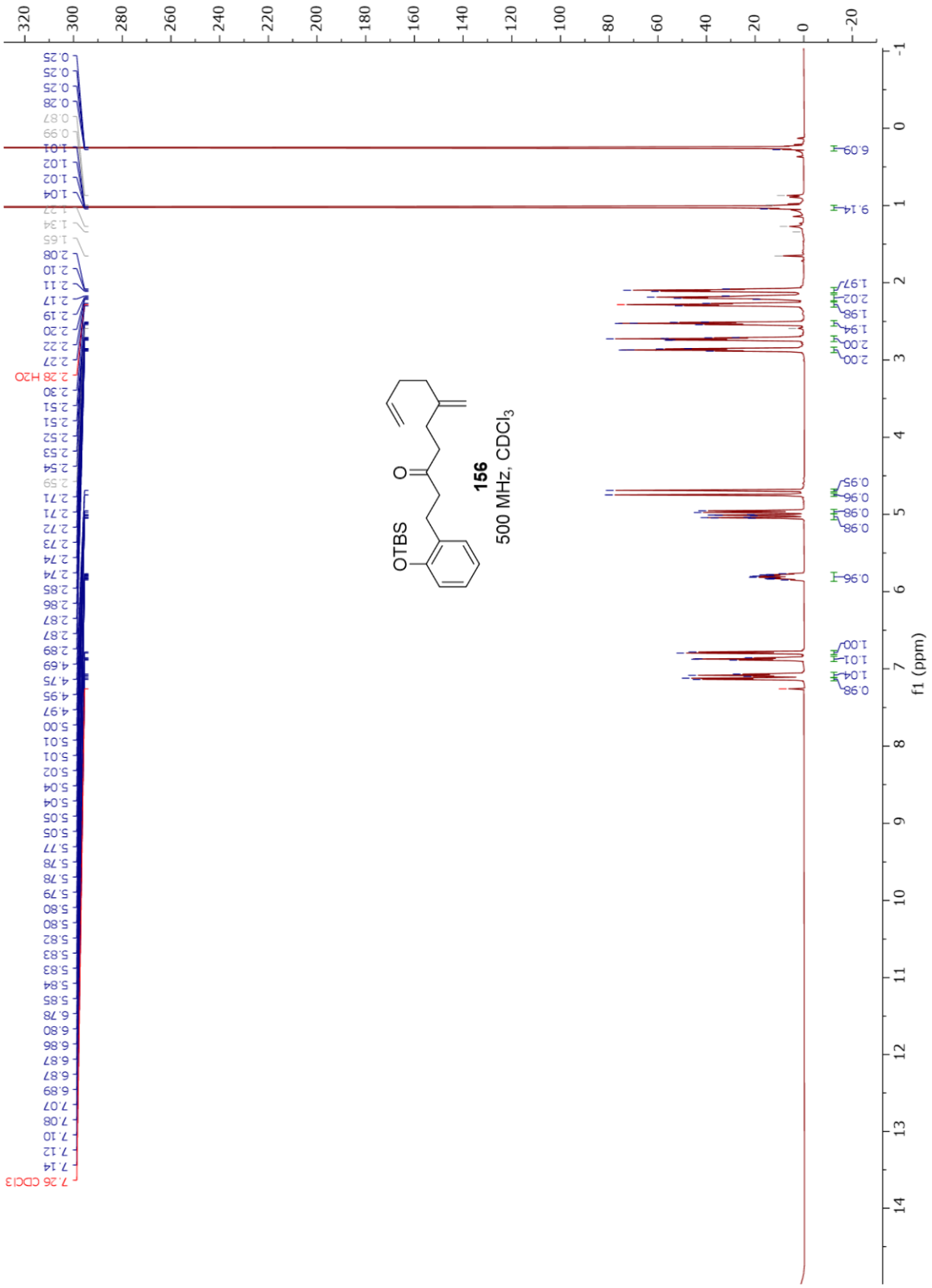
OTBS
O
156
500 MHz, CDCl3
f1 (ppm)

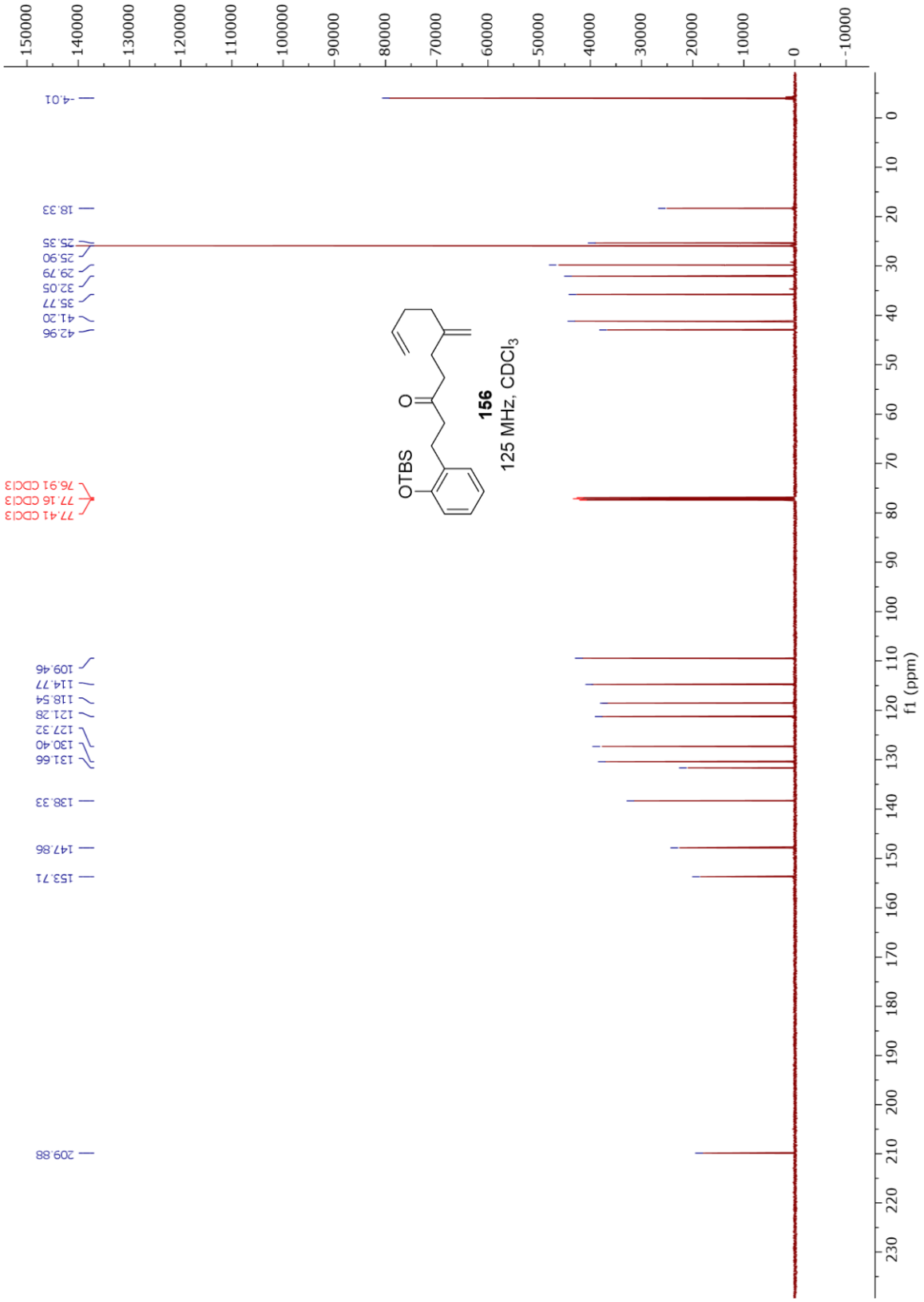
OTBS
O
156
125 MHz, CDCl3
-4.01
18.33
25.35
25.90
29.79
32.05
35.77
41.20
42.96
76.91 CDCl3
77.16 CDCl3
77.41 CDCl3
109.46
114.77
118.54
121.28
127.32
130.40
131.66
138.33
147.86
153.71
209.88
f1 (ppm)

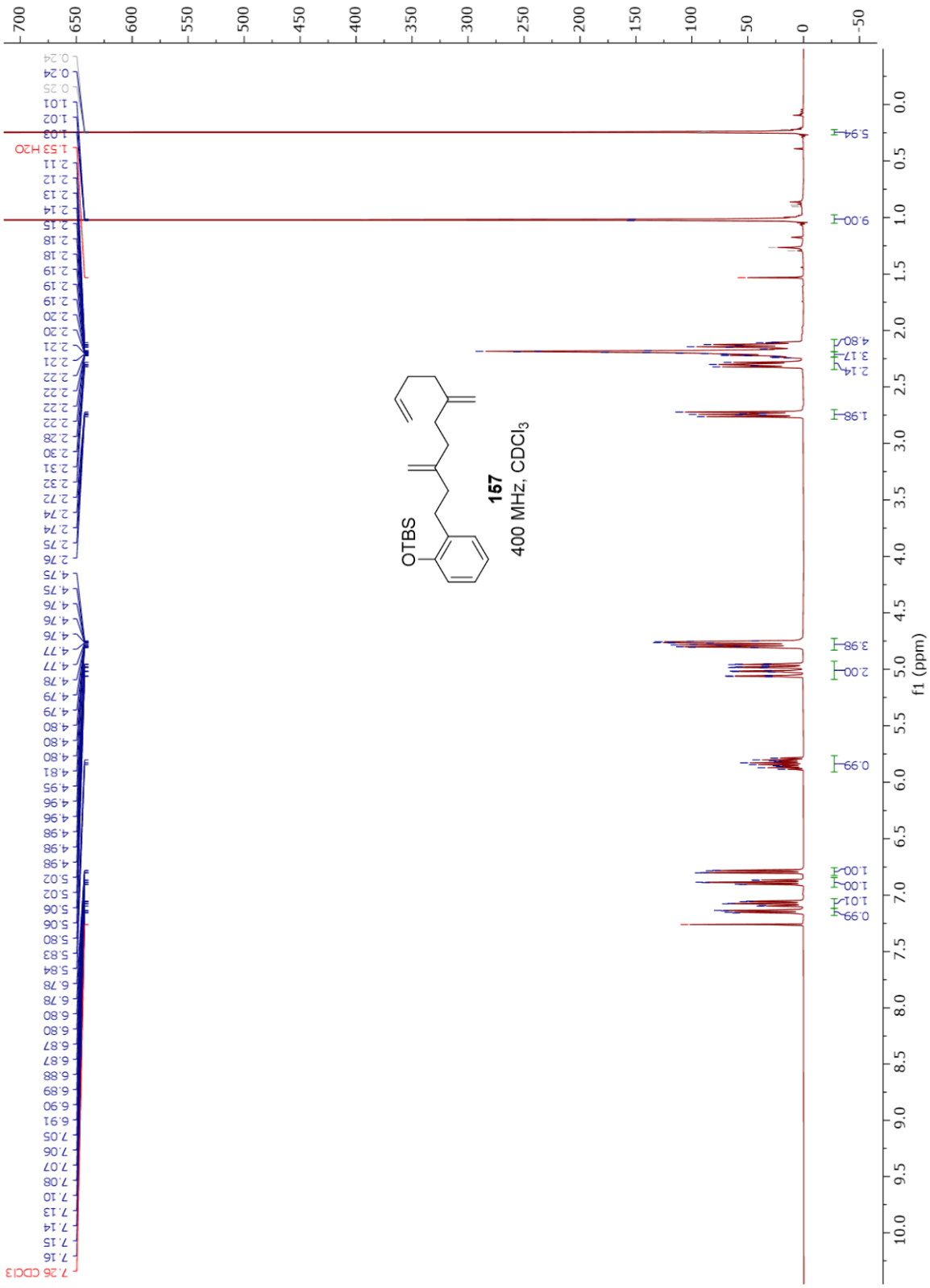
OTBS
157
400 MHz, CDCl3
f1 (ppm)

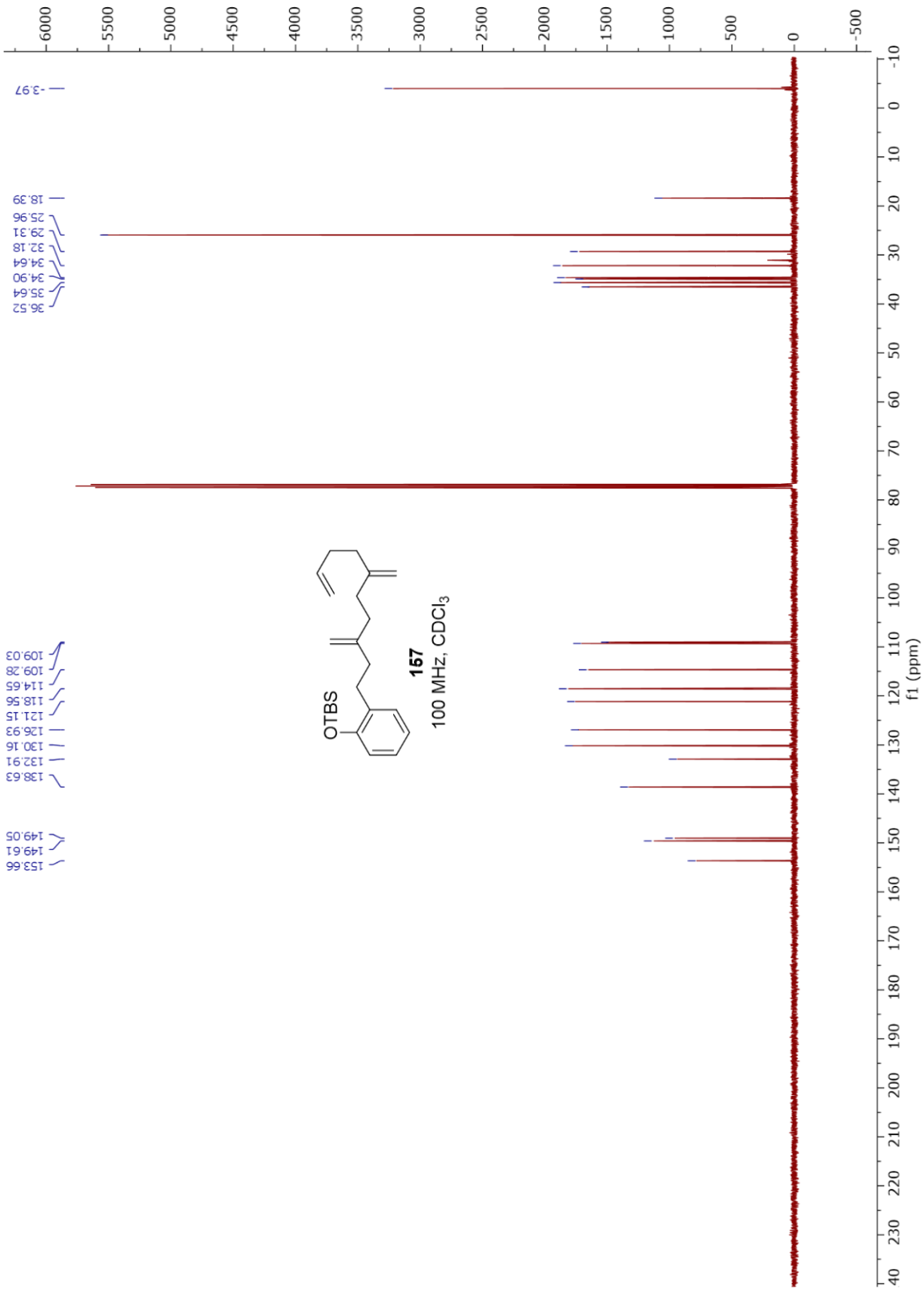
-3.97
18.39
25.96
29.31
32.18
34.64
34.90
35.64
36.52
109.03
109.28
114.65
118.56
121.15
126.93
130.16
132.91
138.63
149.05
149.61
153.66
OTBS
157
100 MHz, CDCl3
f1 (ppm)

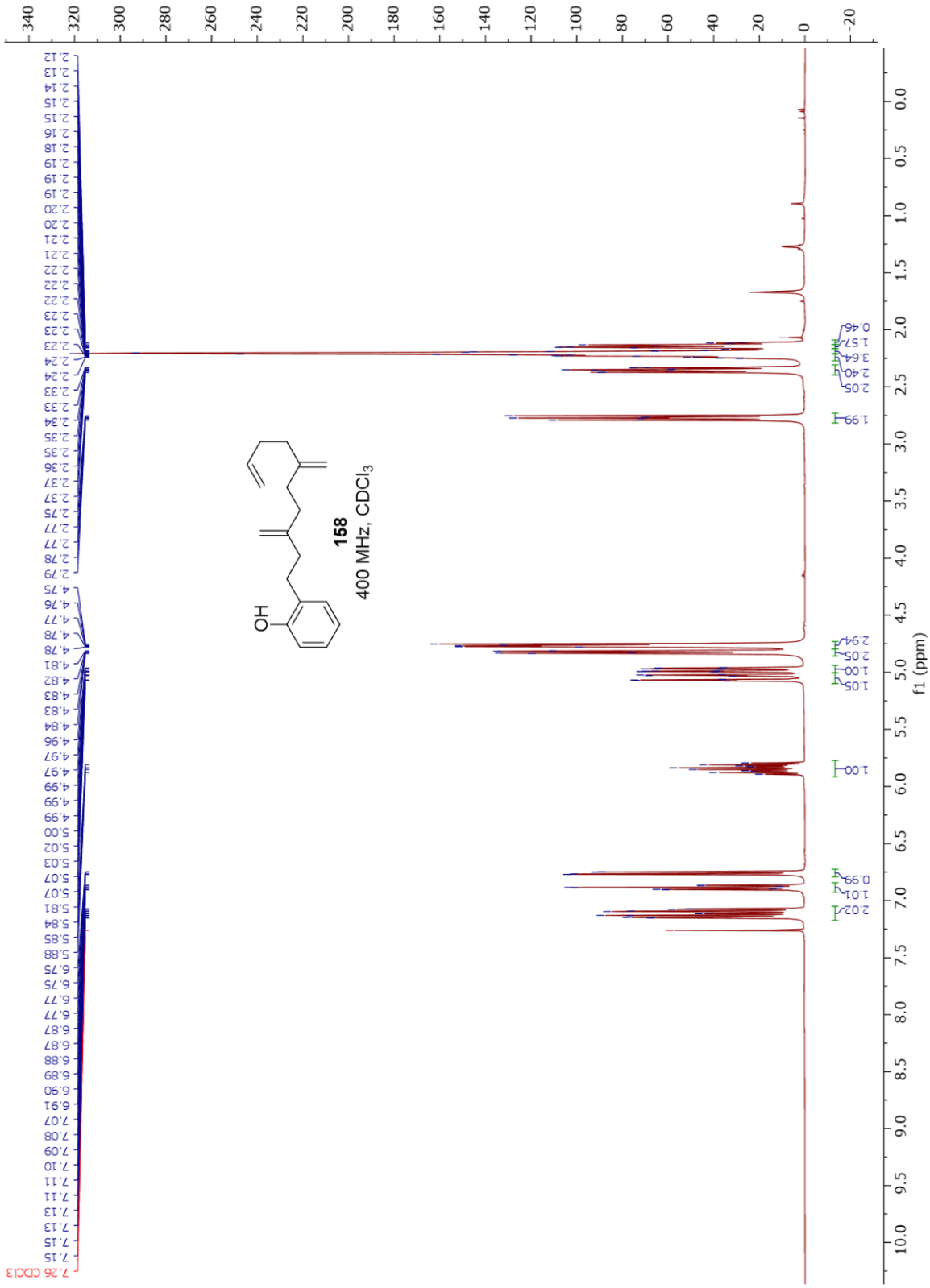
158
400 MHz, CDCl3
OH
f1 (ppm)

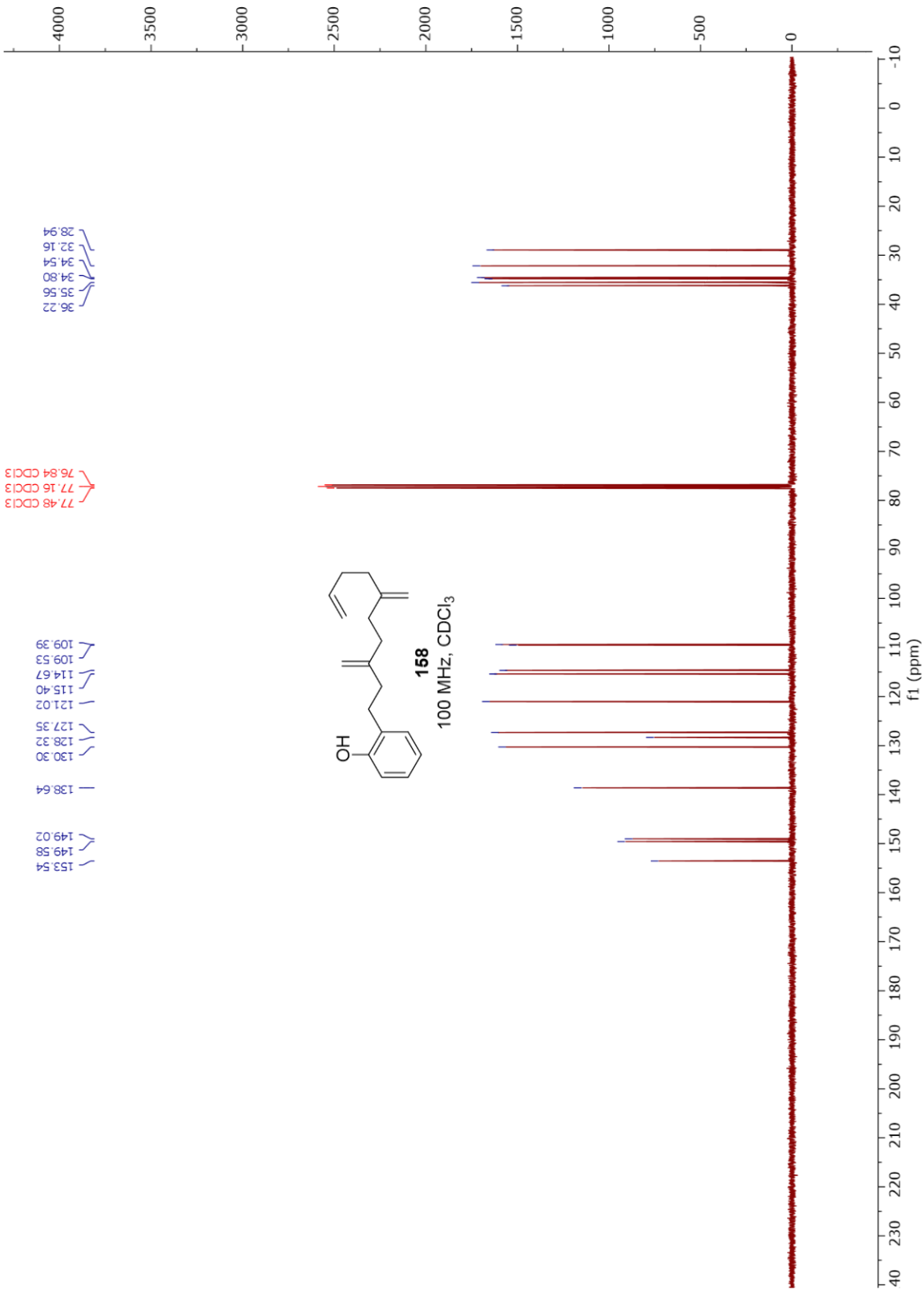
158
100 MHz, CDCl3
OH
f1 (ppm)
153.54
149.58
149.02
138.64
130.30
128.32
127.35
121.02
115.40
114.67
109.53
109.39
77.48 CDCl3
77.16 CDCl3
76.84 CDCl3
36.22
35.56
34.80
34.54
32.16
28.94

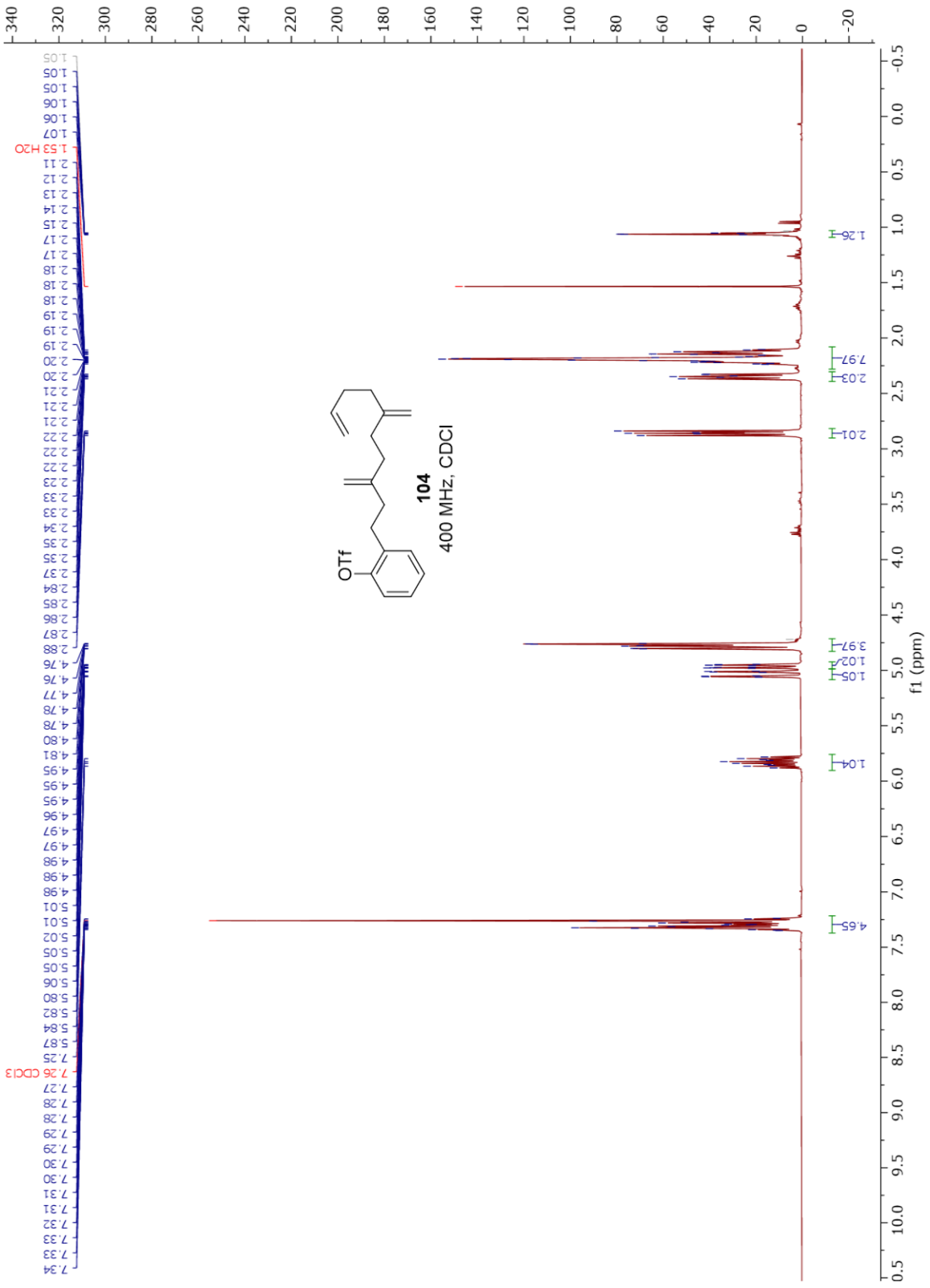
OTf
104
400 MHz, CDCl
f1 (ppm)
4.65
1.04
1.05
1.02
3.97
2.01
7.97
2.03
1.26
1.53 H2O
7.26 CDCl3

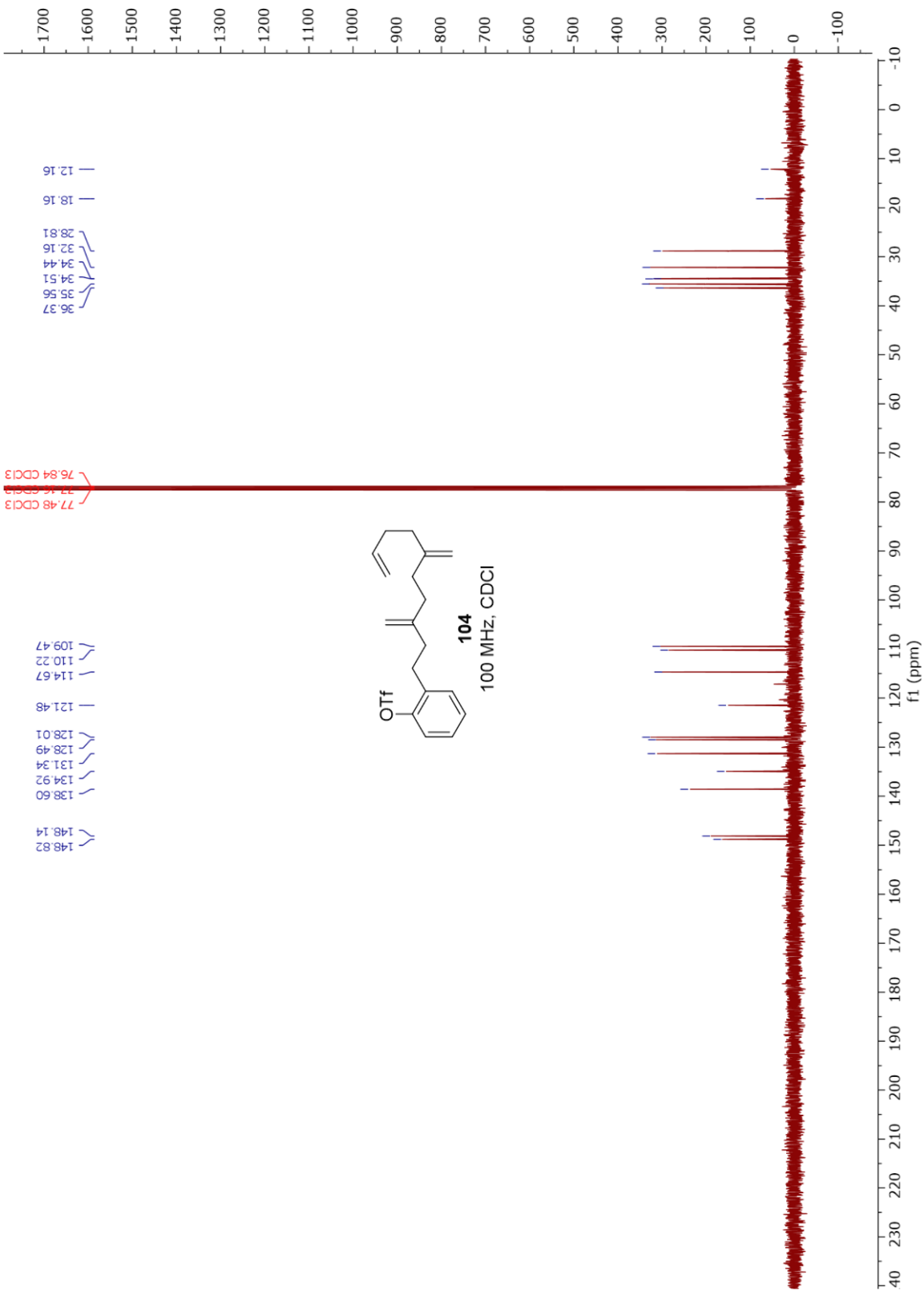
104
100 MHz, CDCl
OTf
f1 (ppm)
77.48 CDCl3
76.84 CDCl3
36.37
35.56
34.51
34.44
32.16
28.81
18.16
12.16
148.82
148.14
138.60
134.92
131.34
128.49
128.01
121.48
114.67
110.22
109.47

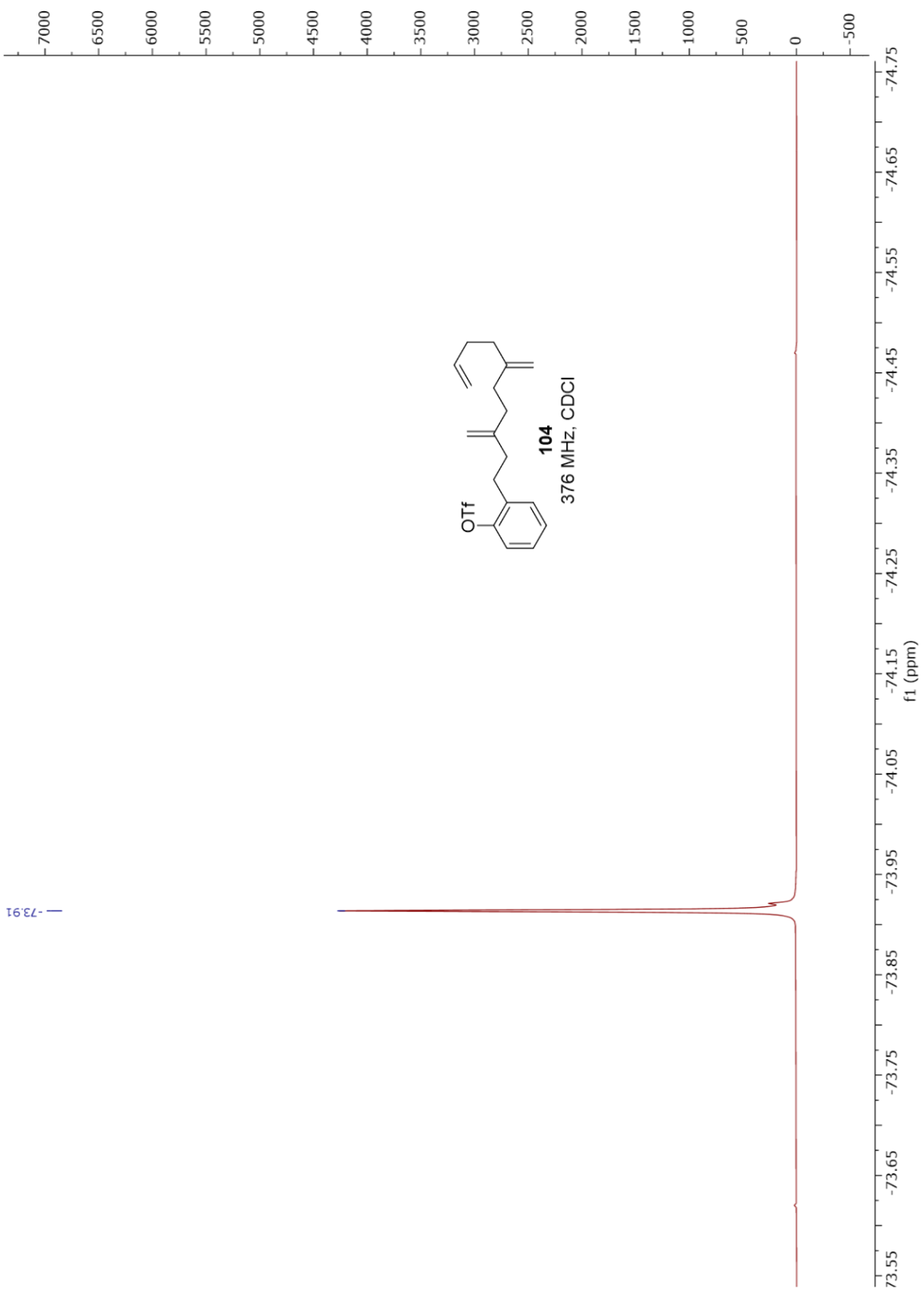
OTf
104
376 MHz, CDCl
-73.91
f1 (ppm)

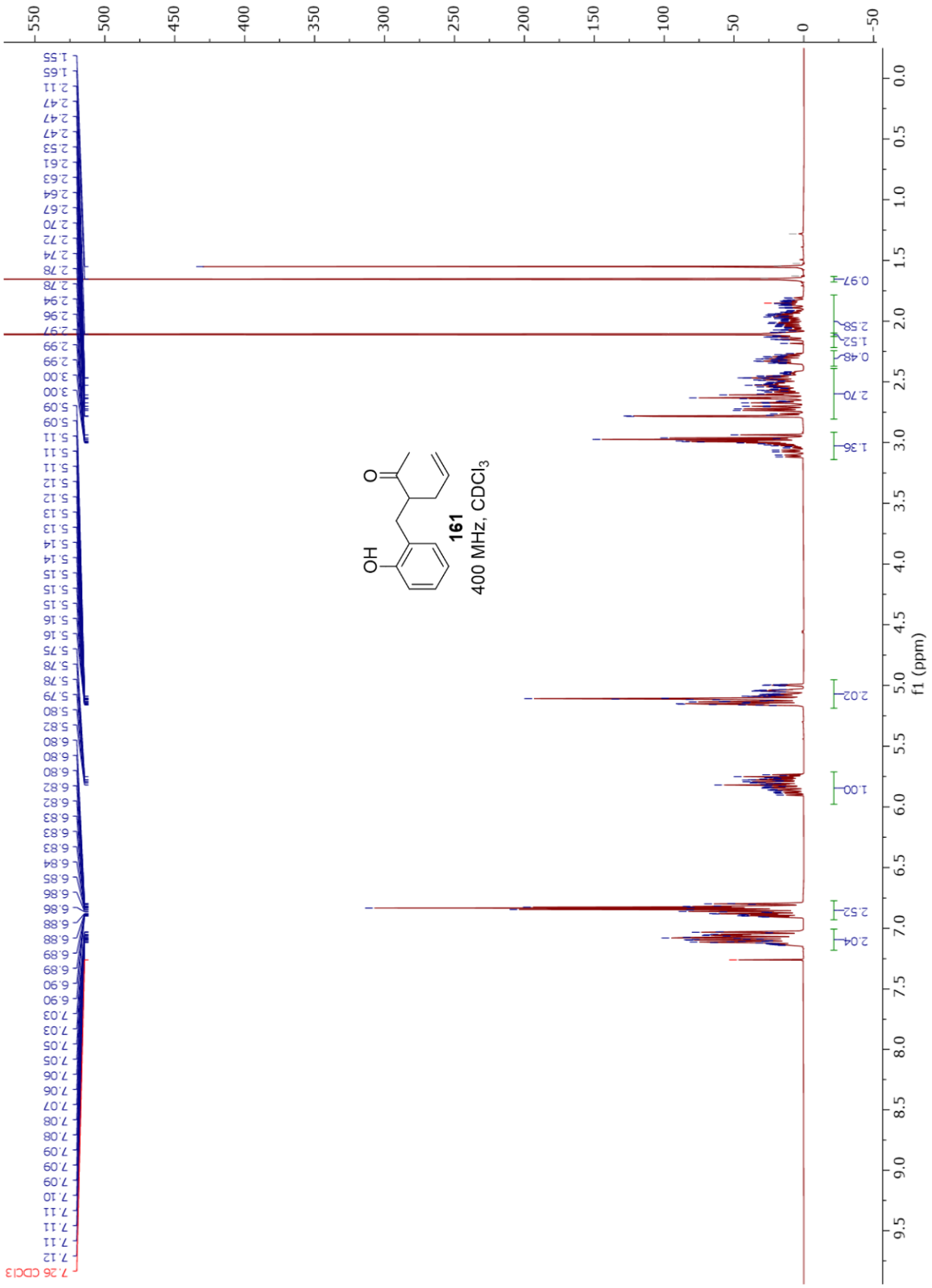
OH
O
161
400 MHz, CDCl3
f1 (ppm)

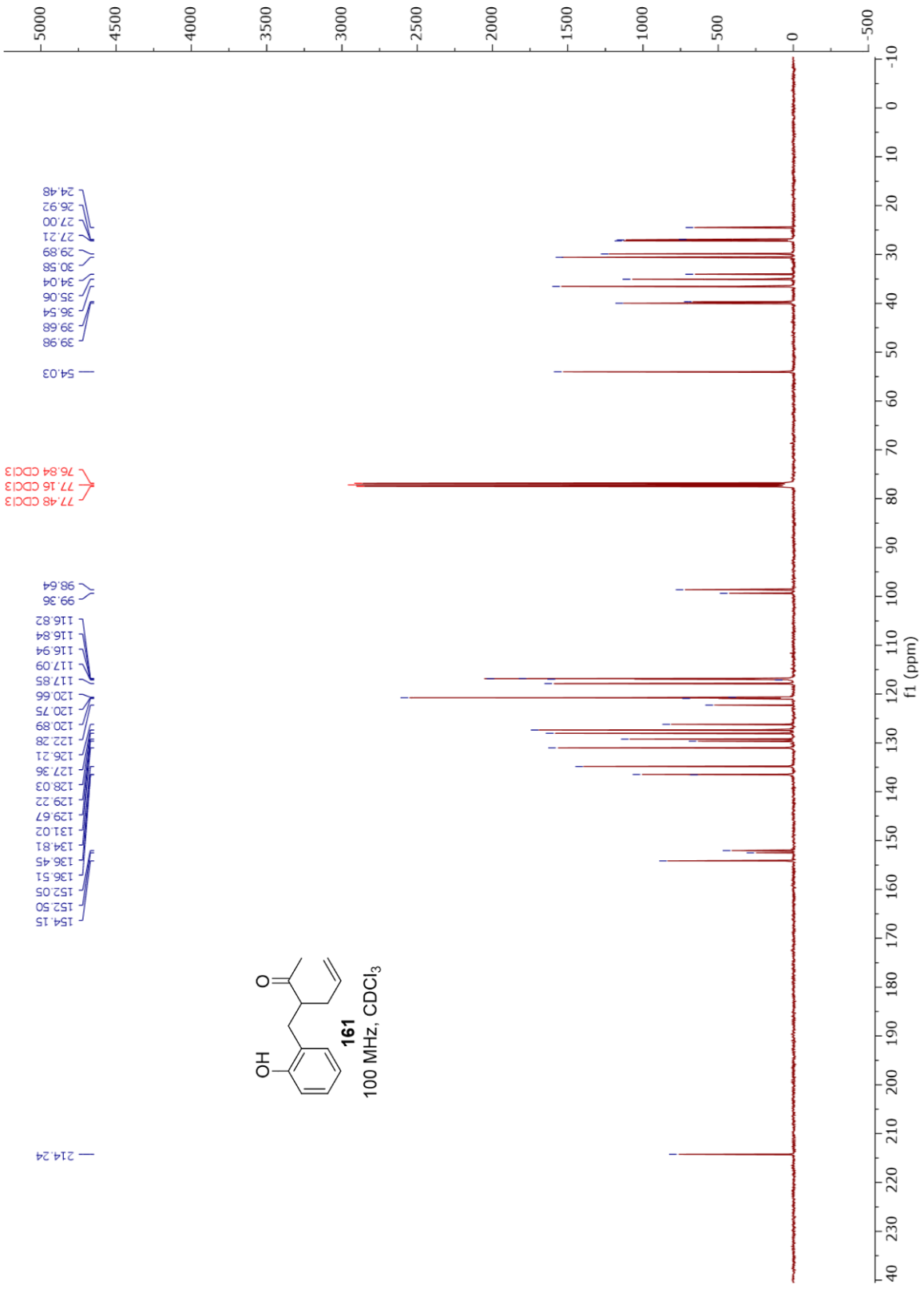
161
100 MHz, CDCl3
f1 (ppm)
214.24
154.15
152.50
152.05
136.51
136.45
134.81
131.02
129.67
129.22
128.03
127.36
126.21
122.28
120.89
120.75
120.66
117.85
117.09
116.94
116.84
116.82
99.36
98.64
77.48 CDCl3
77.16 CDCl3
76.84 CDCl3
54.03
39.98
39.68
36.54
35.06
34.04
30.58
29.89
27.21
27.00
26.92
24.48

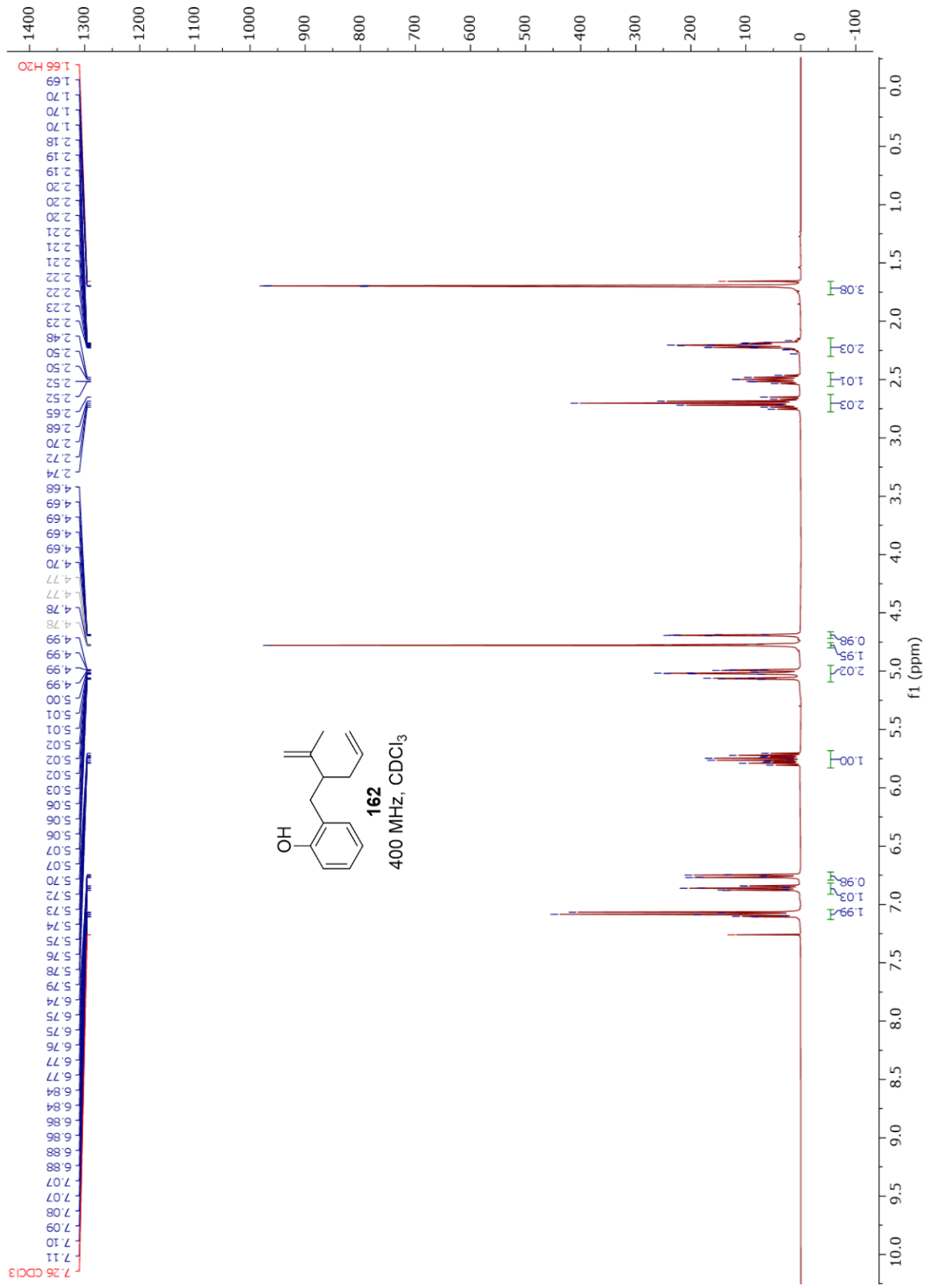
OH
162
400 MHz, CDCl3
f1 (ppm)

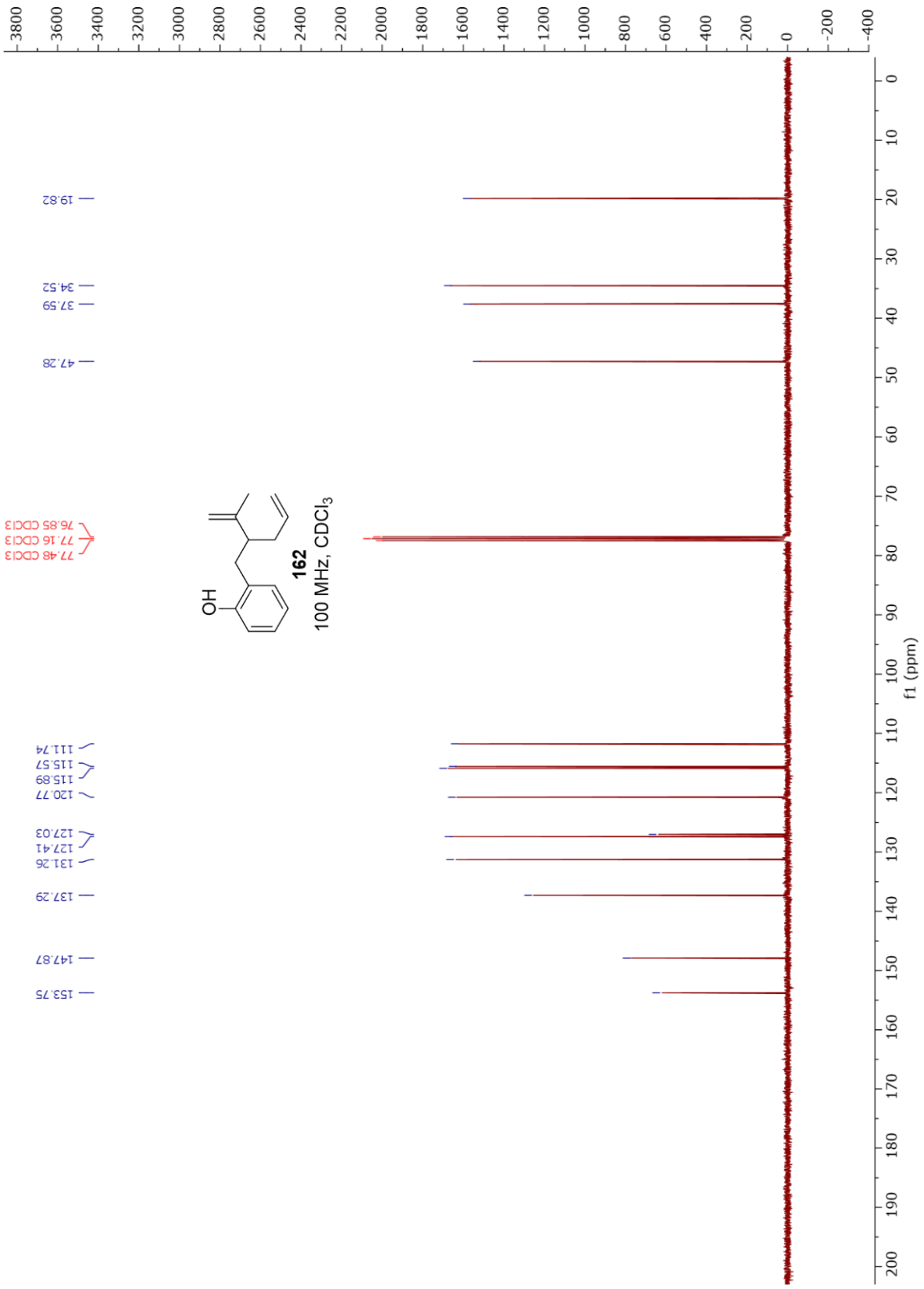
OH
162
100 MHz, CDCl3
19.82
34.52
37.59
47.28
76.85 CDCl3
77.16 CDCl3
77.48 CDCl3
111.74
115.57
115.89
120.77
127.03
127.41
131.26
137.29
147.87
153.75
f1 (ppm)

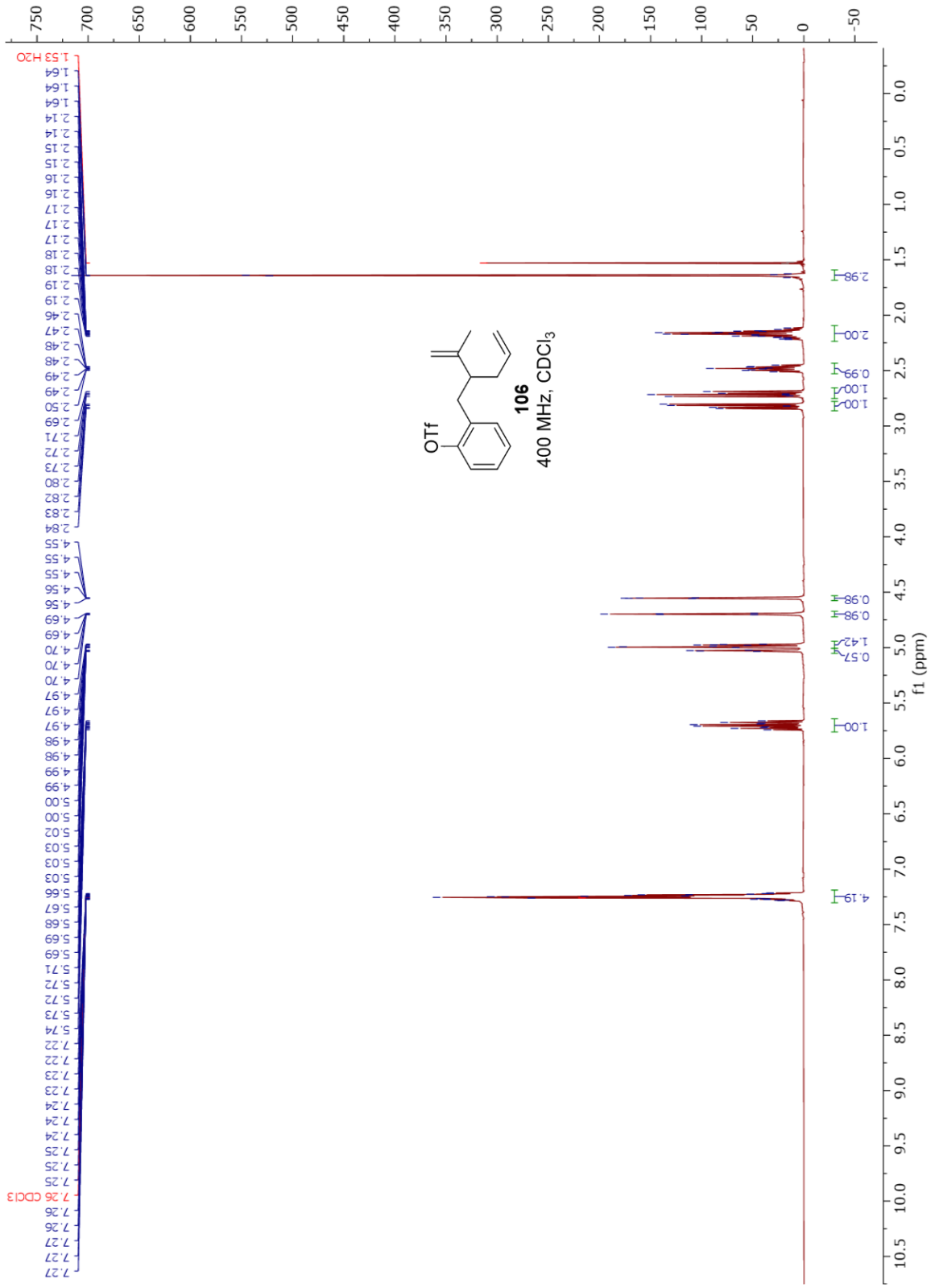
OTf
106
400 MHz, CDCl3
f1 (ppm)

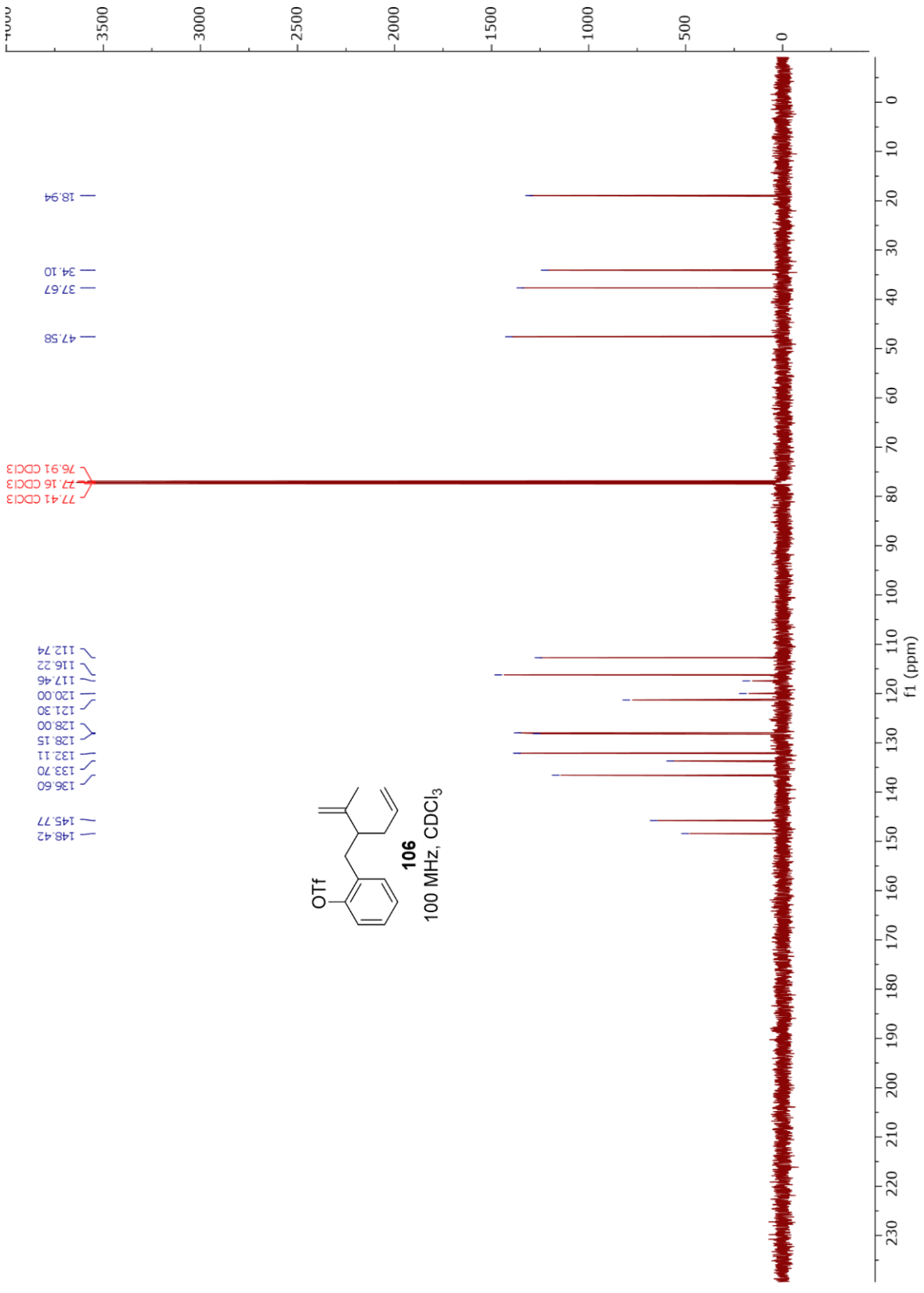
18.94
34.10
37.67
47.58
76.91 CDCl3
77.16 CDCl3
77.41 CDCl3
112.74
116.22
117.46
120.00
121.30
128.00
128.15
132.11
133.70
136.60
145.77
148.42
OTf
106
100 MHz, CDCl3
f1 (ppm)

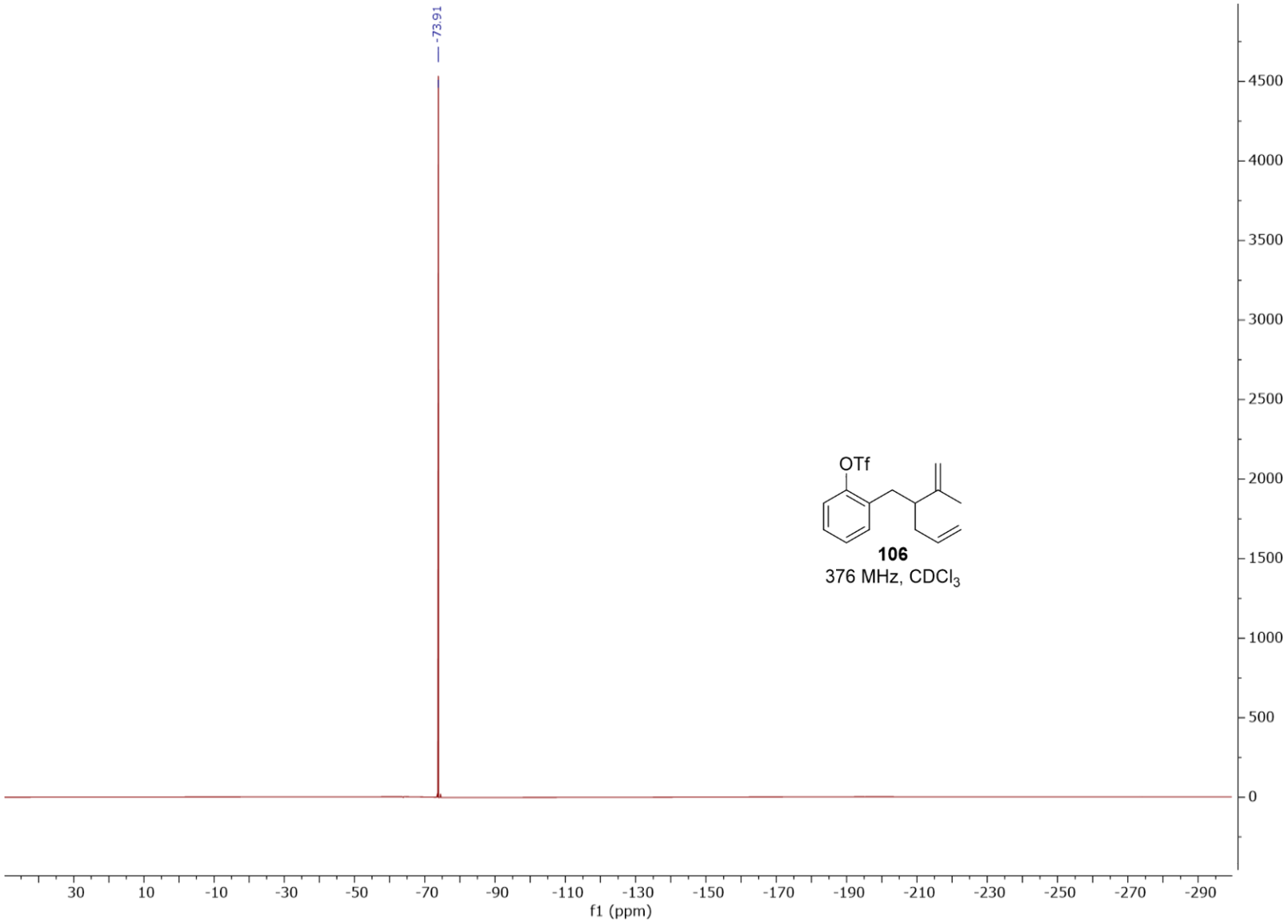
-73.91
OTf
106
376 MHz, CDCl3
4500
4000
3500
3000
2500
2000
1500
1000
500
0
30
10
-10
-30
-50
-70
-90
-110
-130
-150
-170
-190
-210
-230
-250
-270
-290
f1 (ppm)

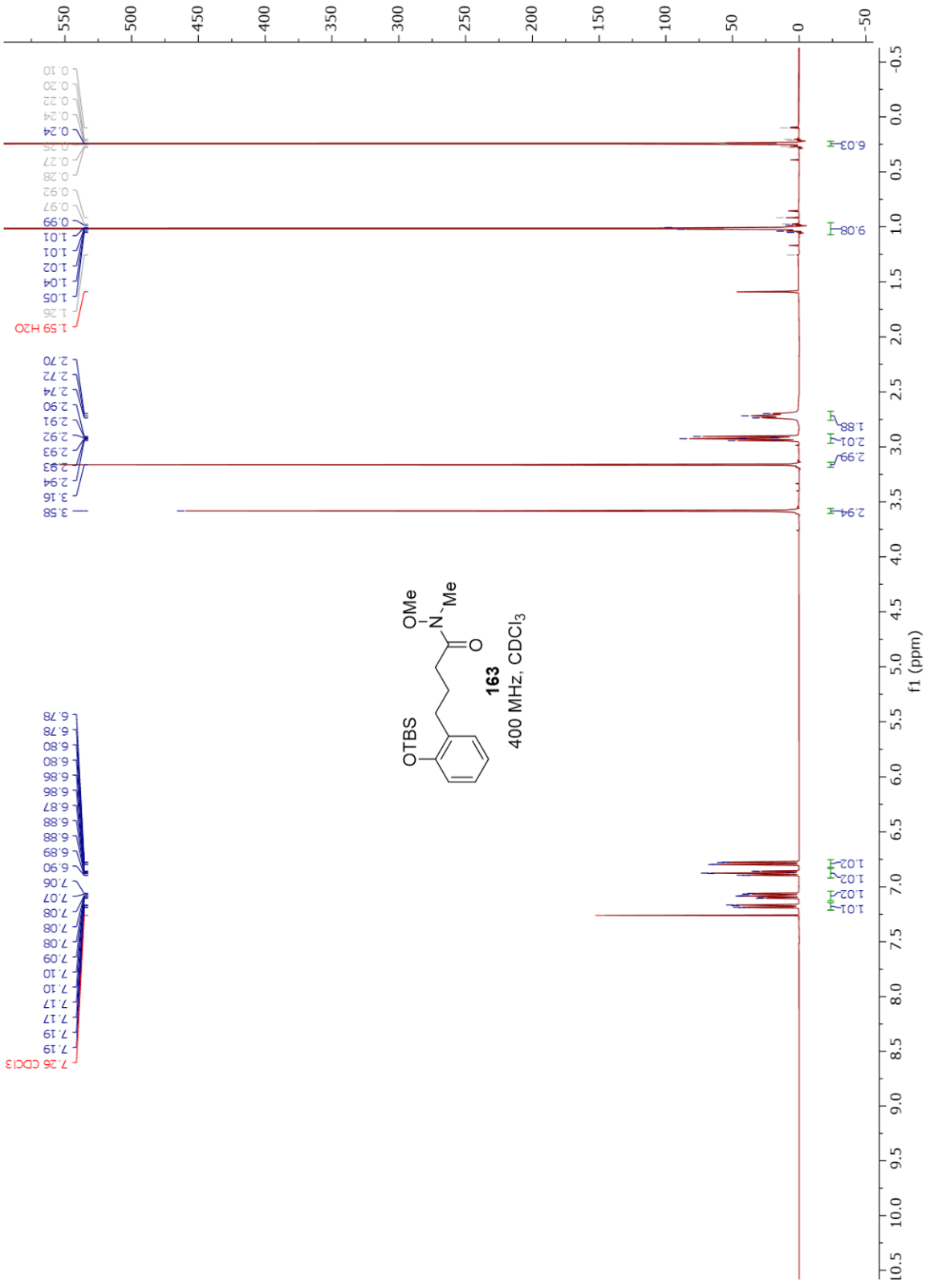
OMe
N
Me
O
OTBS
163
400 MHz, CDCl3
f1 (ppm)

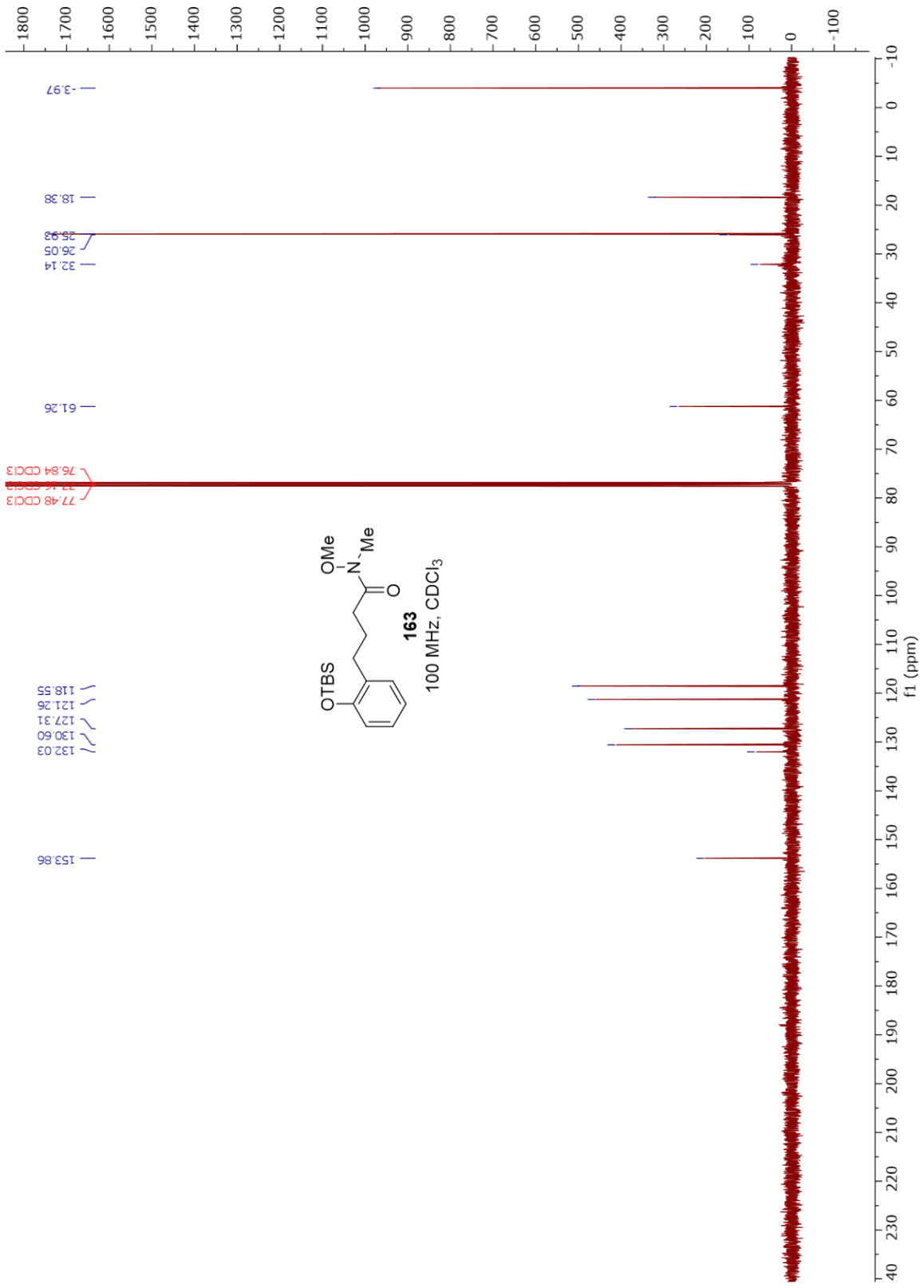
-3.97
18.38
25.93
26.05
32.14
61.26
76.84 CDCl3
77.16 CDCl3
77.48 CDCl3
118.55
121.26
127.31
130.60
132.03
153.86
OTBS
OMe
N
Me
O
163
100 MHz, CDCl3
f1 (ppm)

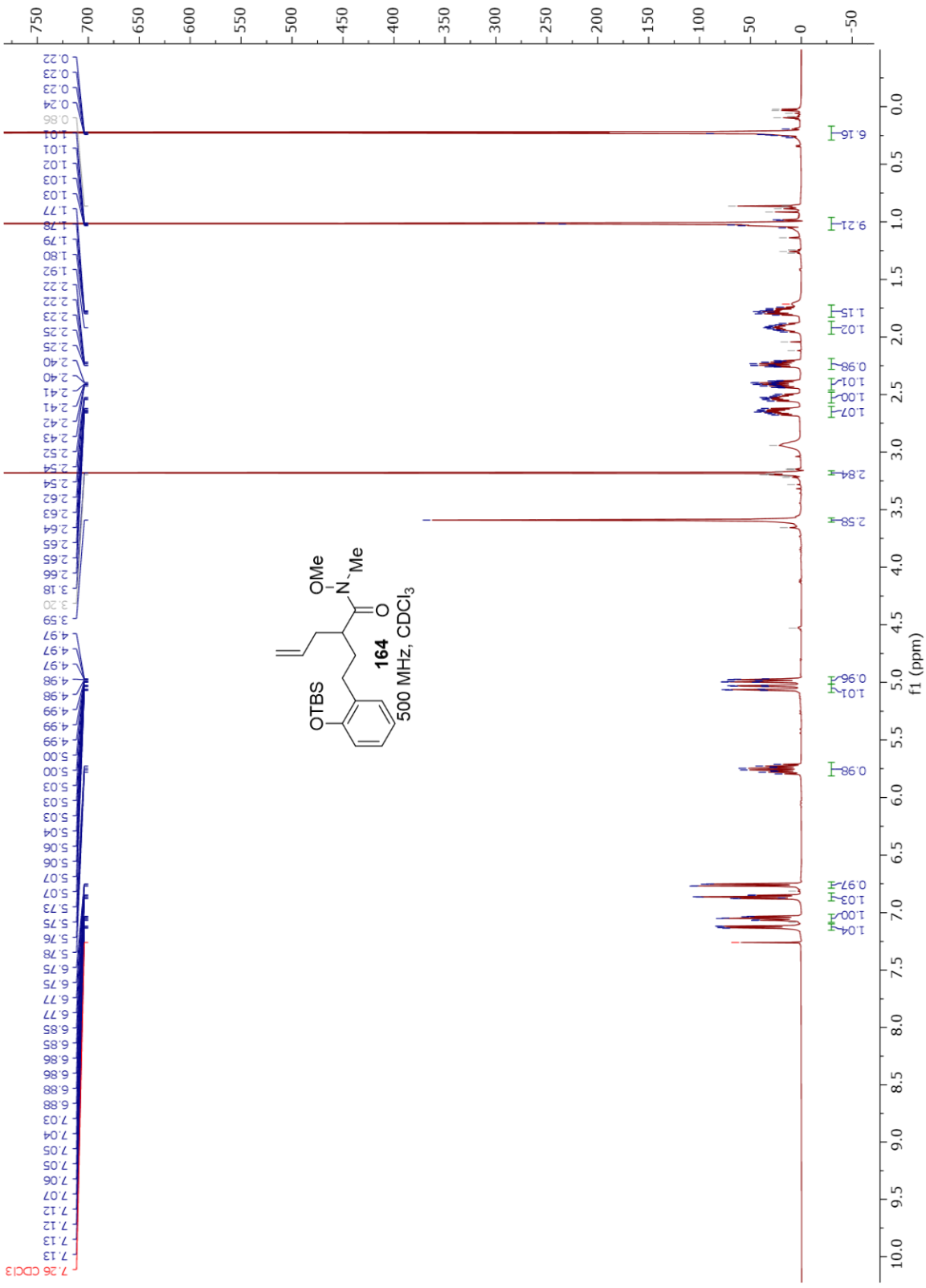
OMe
N
Me
O
OTBS
164
500 MHz, CDCl3
f1 (ppm)

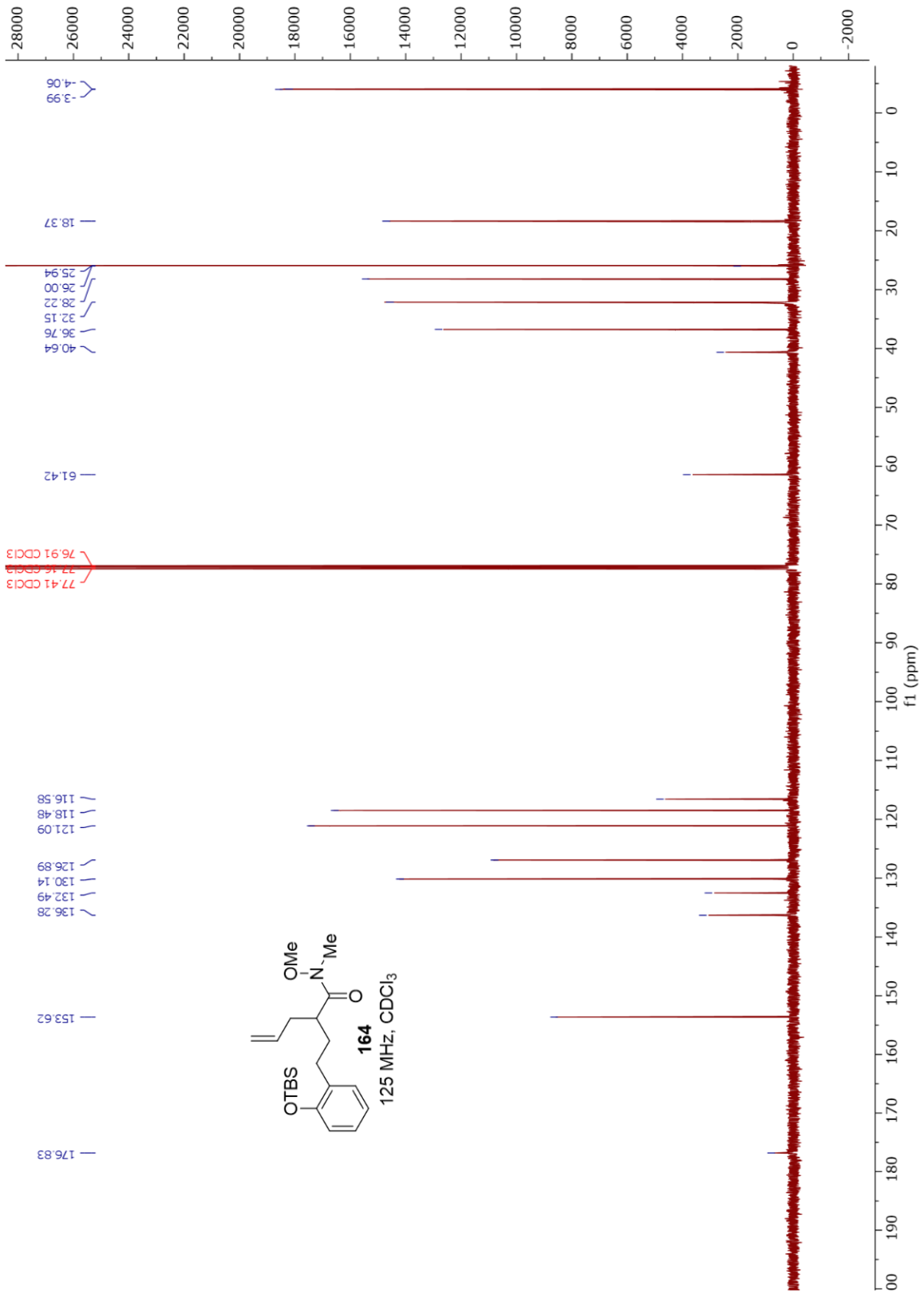
-4.06
-3.99
18.37
25.94
26.00
28.22
32.15
36.76
40.64
61.42
76.91 CDCl3
77.16 CDCl3
77.41 CDCl3
116.58
118.48
121.09
126.89
130.14
132.49
136.28
153.62
176.83
OMe
N
Me
O
OTBS
164
125 MHz, CDCl3
f1 (ppm)

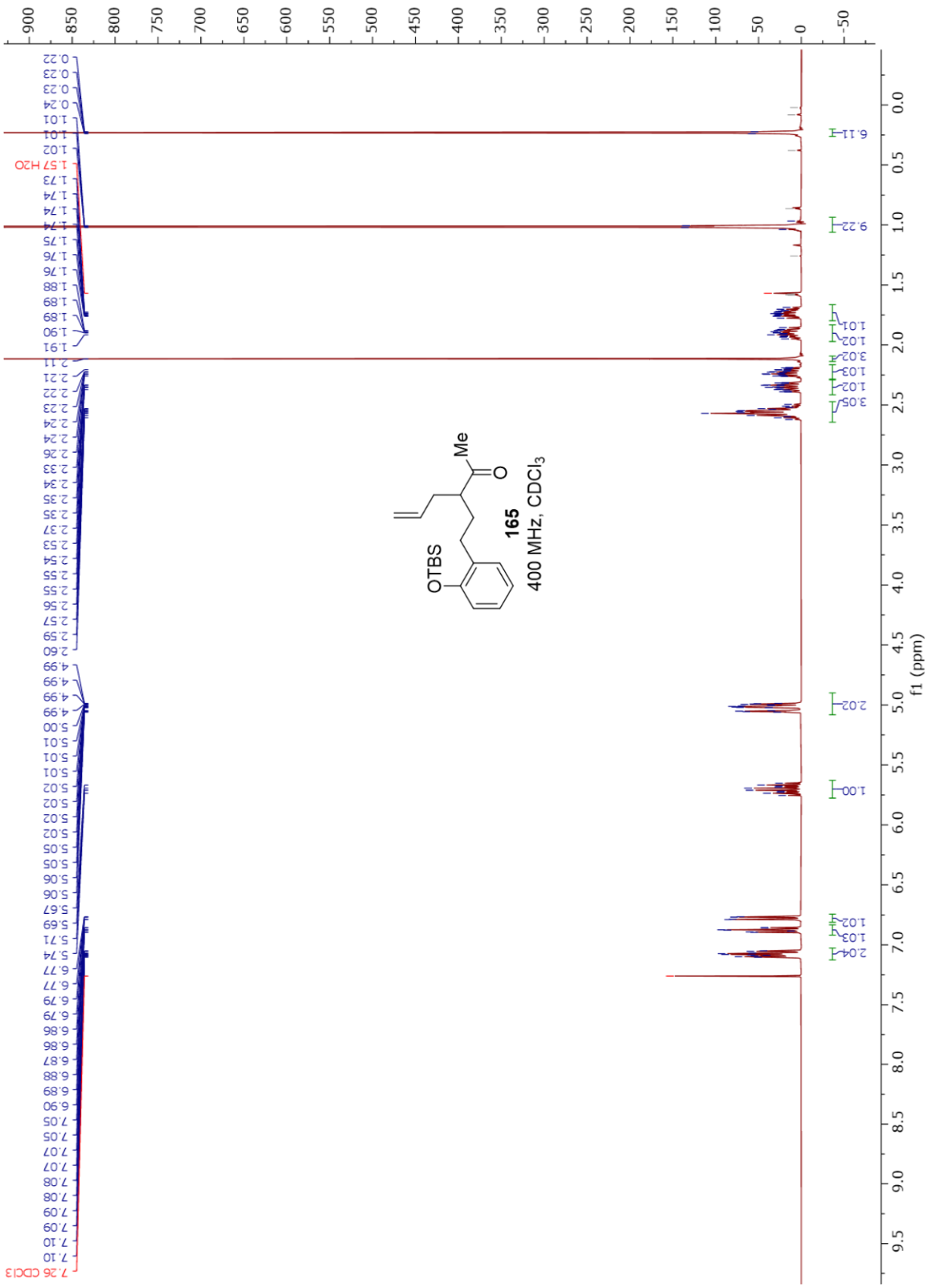
OTBS
Me
O
165
400 MHz, CDCl3
f1 (ppm)

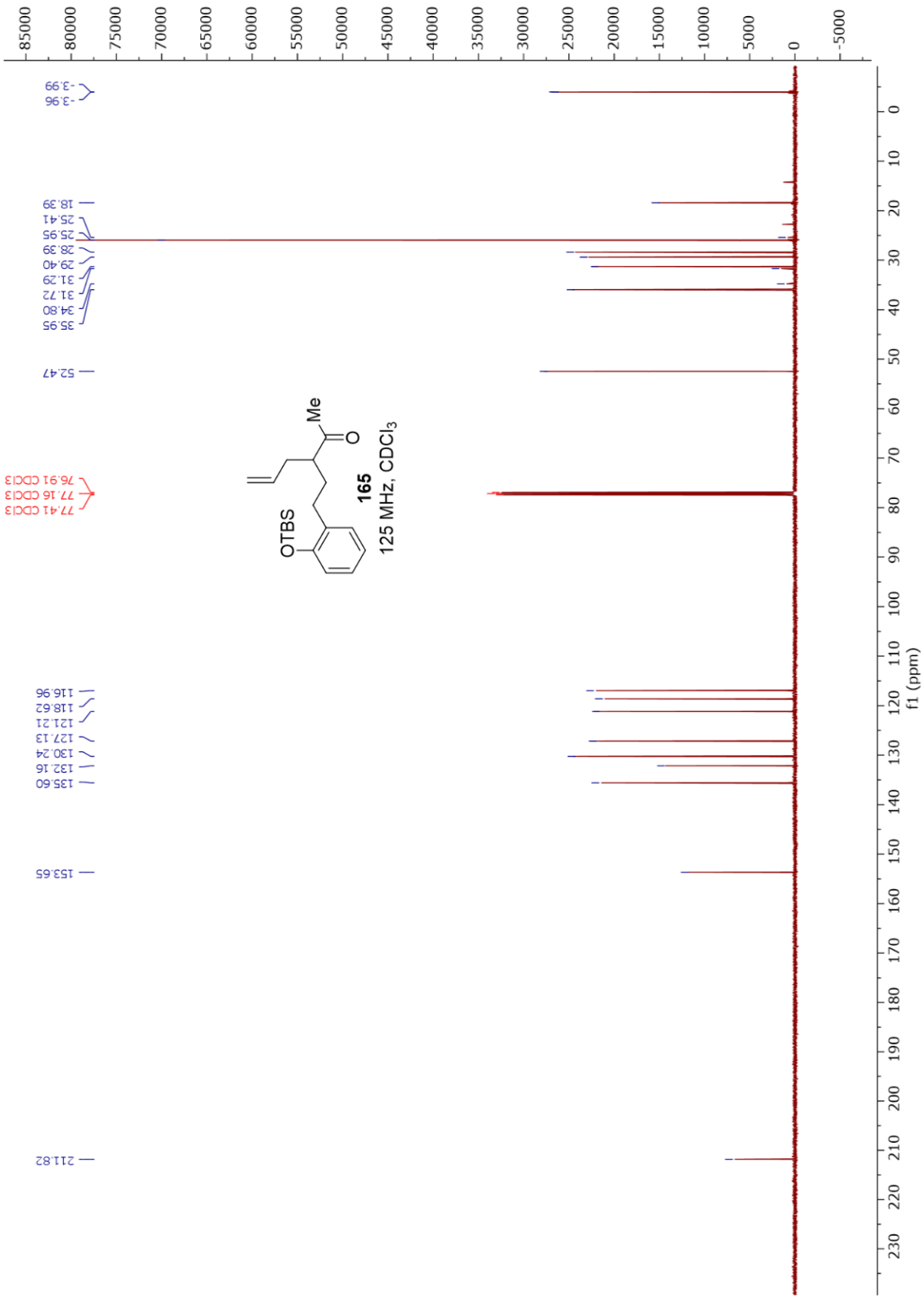
-3.96
-3.99
18.39
25.41
25.95
28.39
29.40
31.29
31.72
34.80
35.95
52.47
76.91 CDCl3
77.16 CDCl3
77.41 CDCl3
116.96
118.62
121.21
127.13
130.24
132.16
135.60
153.65
211.82
OTBS
Me
O
165
125 MHz, CDCl3
f1 (ppm)

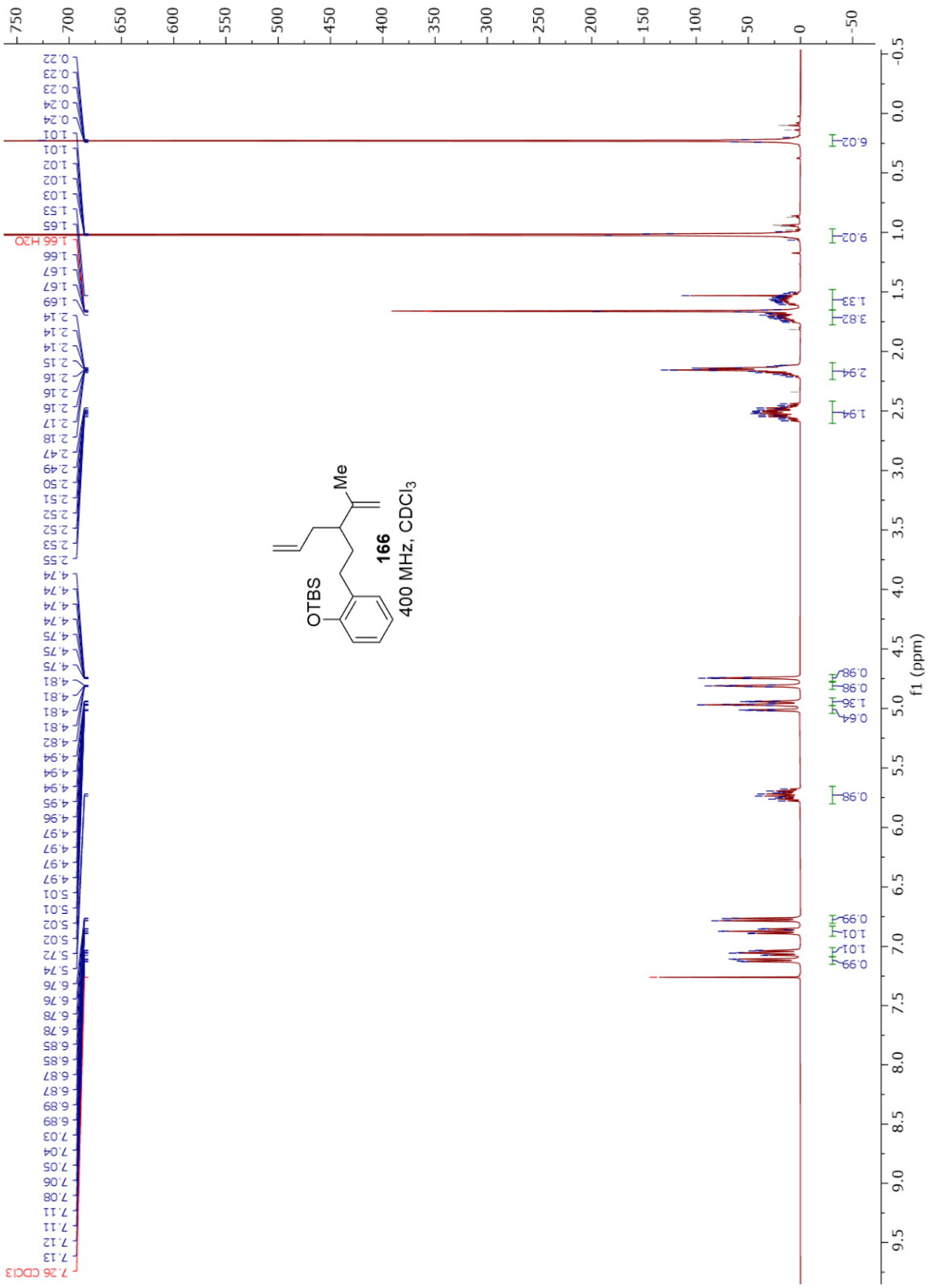
OTBS
Me
166
400 MHz, CDCl3
f1 (ppm)

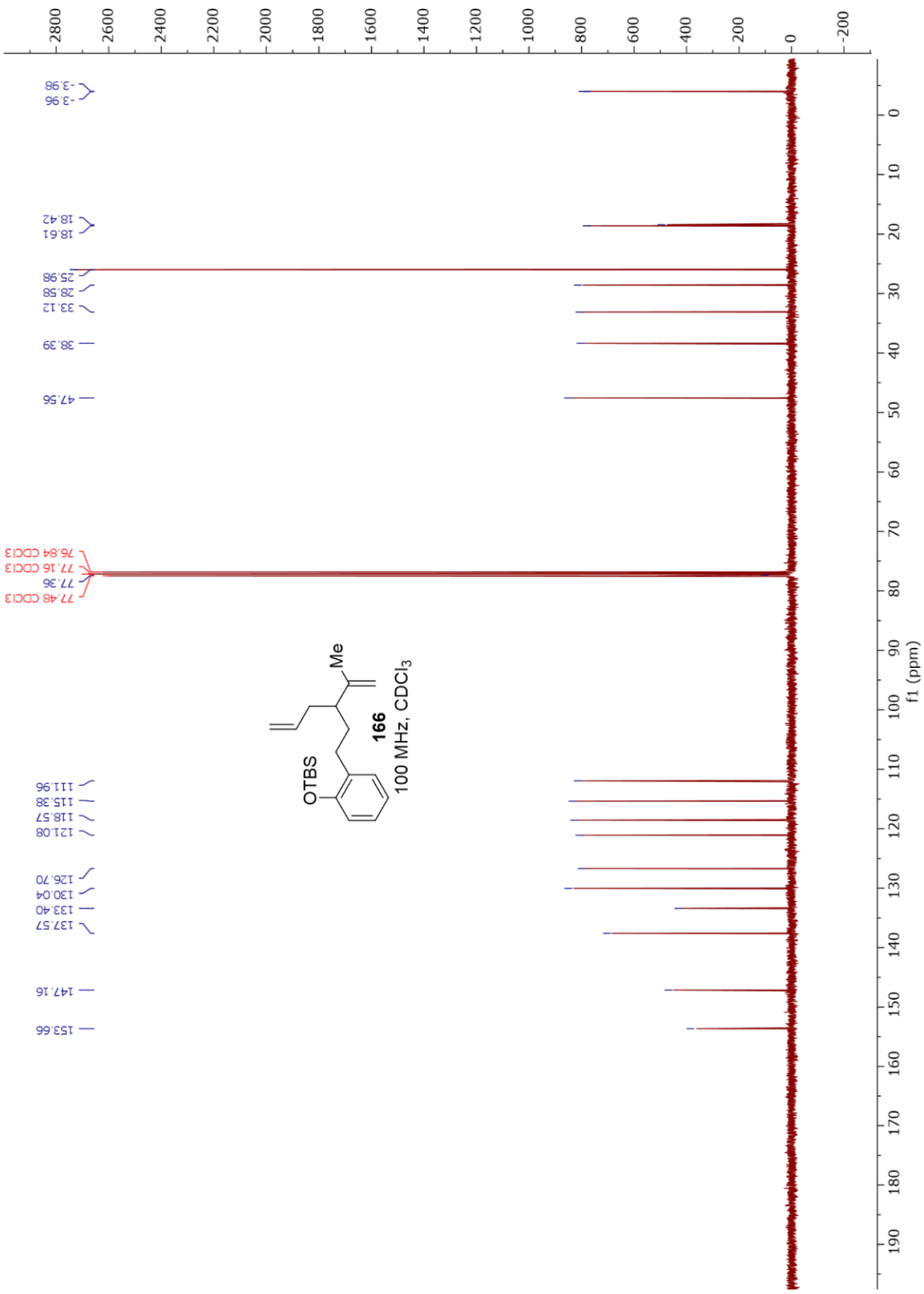
OTBS
Me
166
100 MHz, CDCl3
f1 (ppm)
-3.96
-3.98
18.42
18.61
25.98
28.58
33.12
38.39
47.56
76.84 CDCl3
77.16 CDCl3
77.36
77.48 CDCl3
111.96
115.38
118.57
121.08
126.70
130.04
133.40
137.57
147.16
153.66

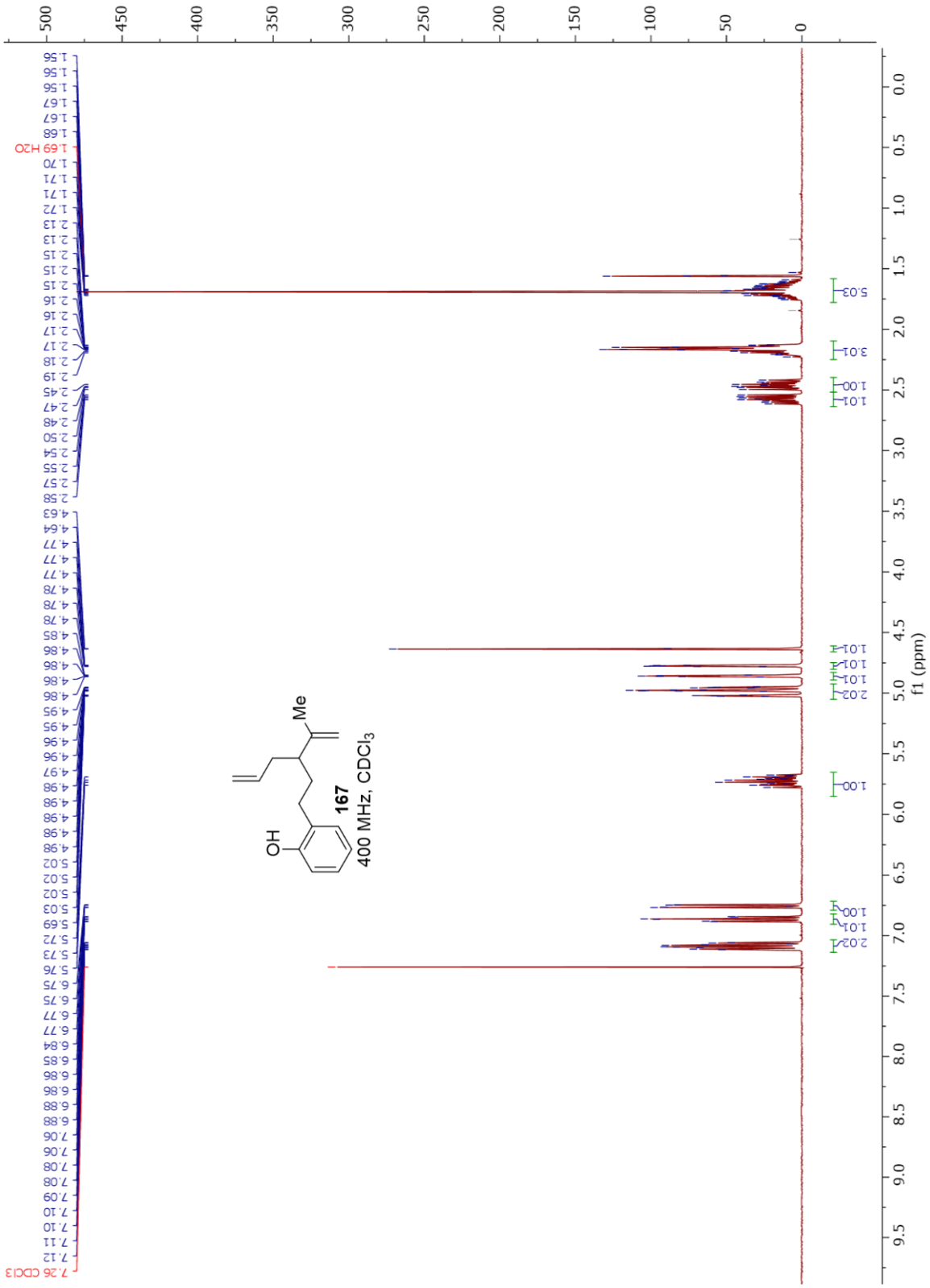
Me
OH
167
400 MHz, CDCl3
f1 (ppm)

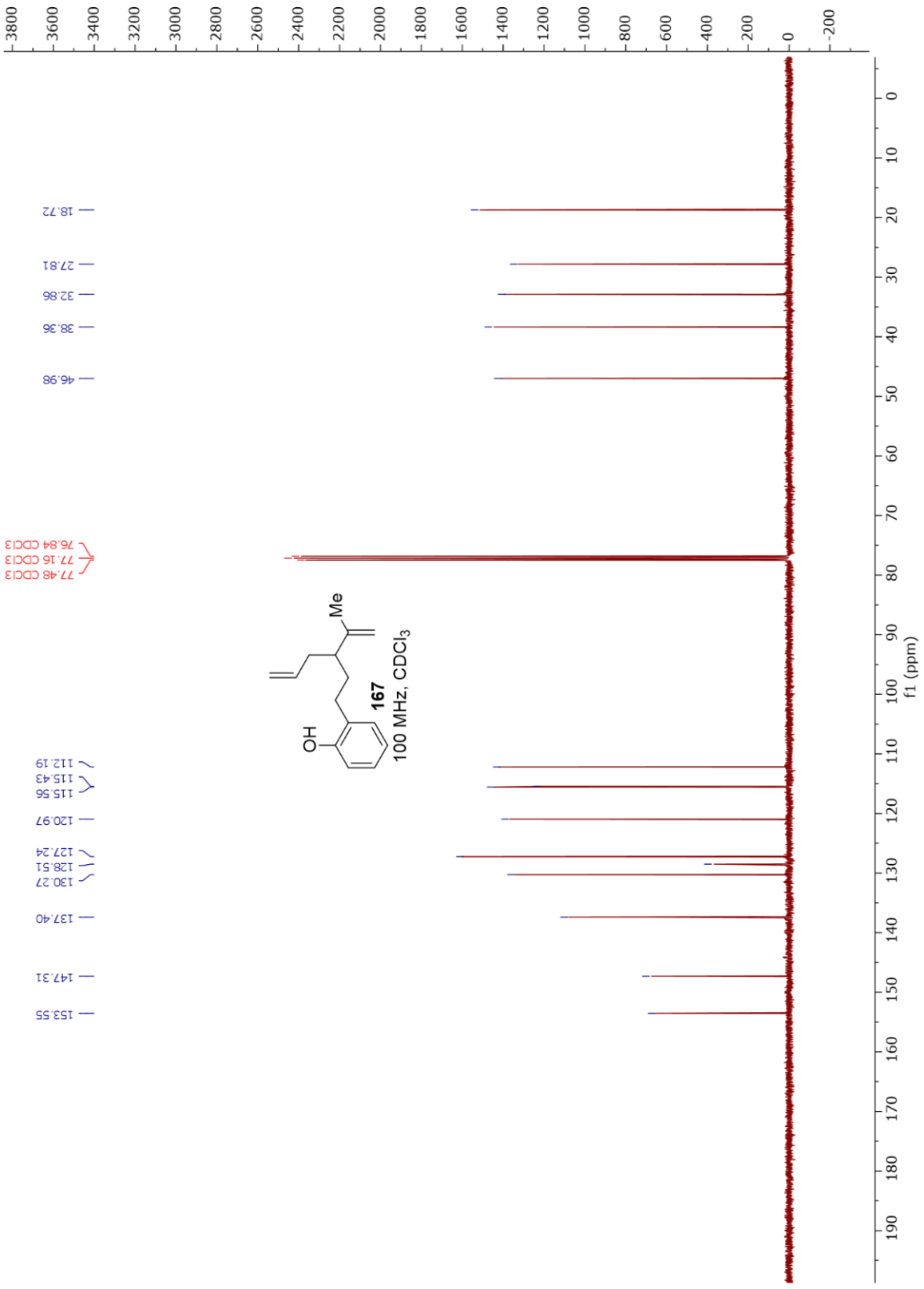
18.72
27.81
32.86
38.36
46.98
76.84 CDCl3
77.16 CDCl3
77.48 CDCl3
112.19
115.56
115.43
120.97
127.24
128.51
130.27
137.40
147.31
153.55
Me
OH
167
100 MHz, CDCl3
f1 (ppm)

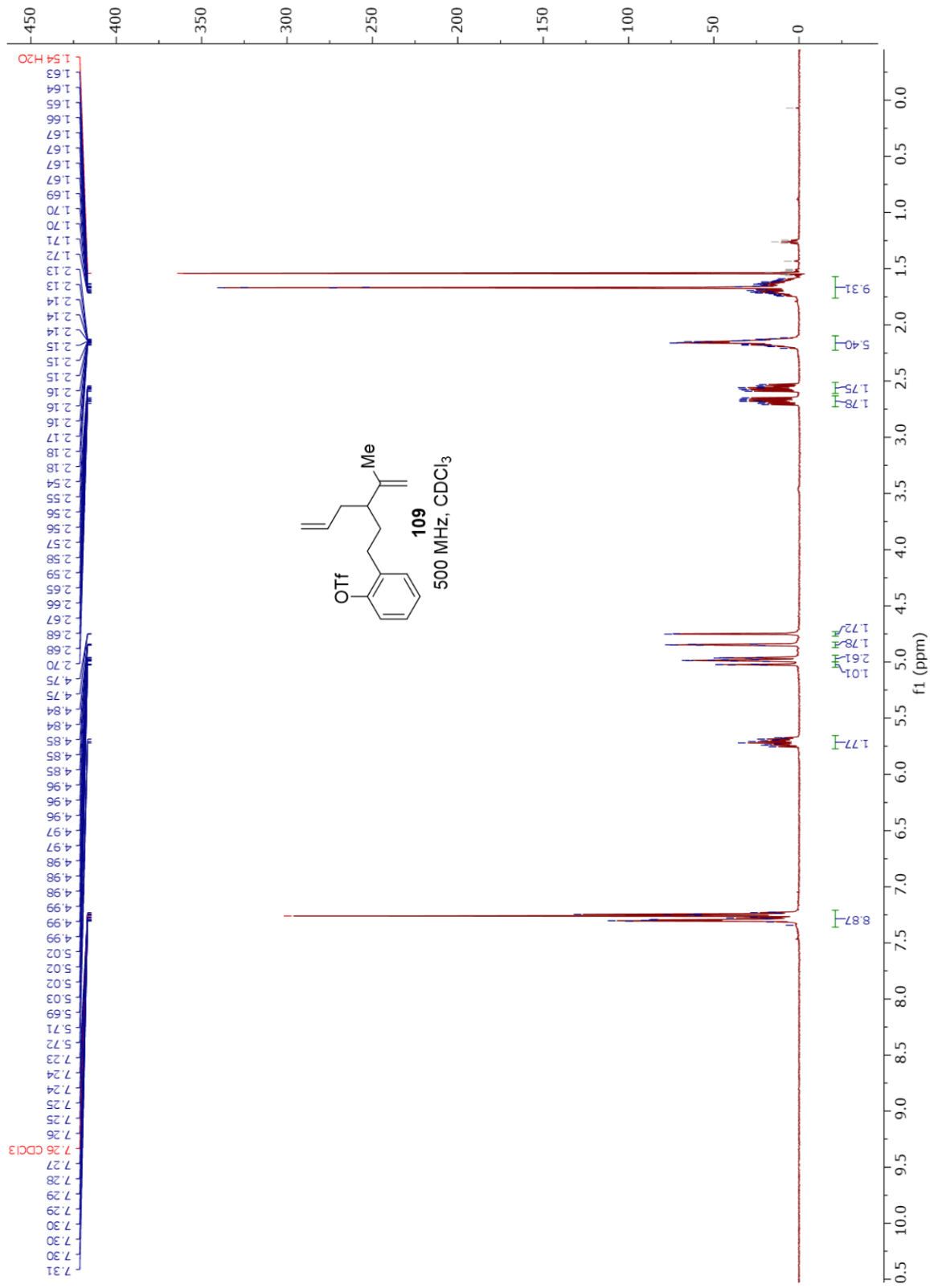
Me
OTf
109
500 MHz, CDCl3
f1 (ppm)

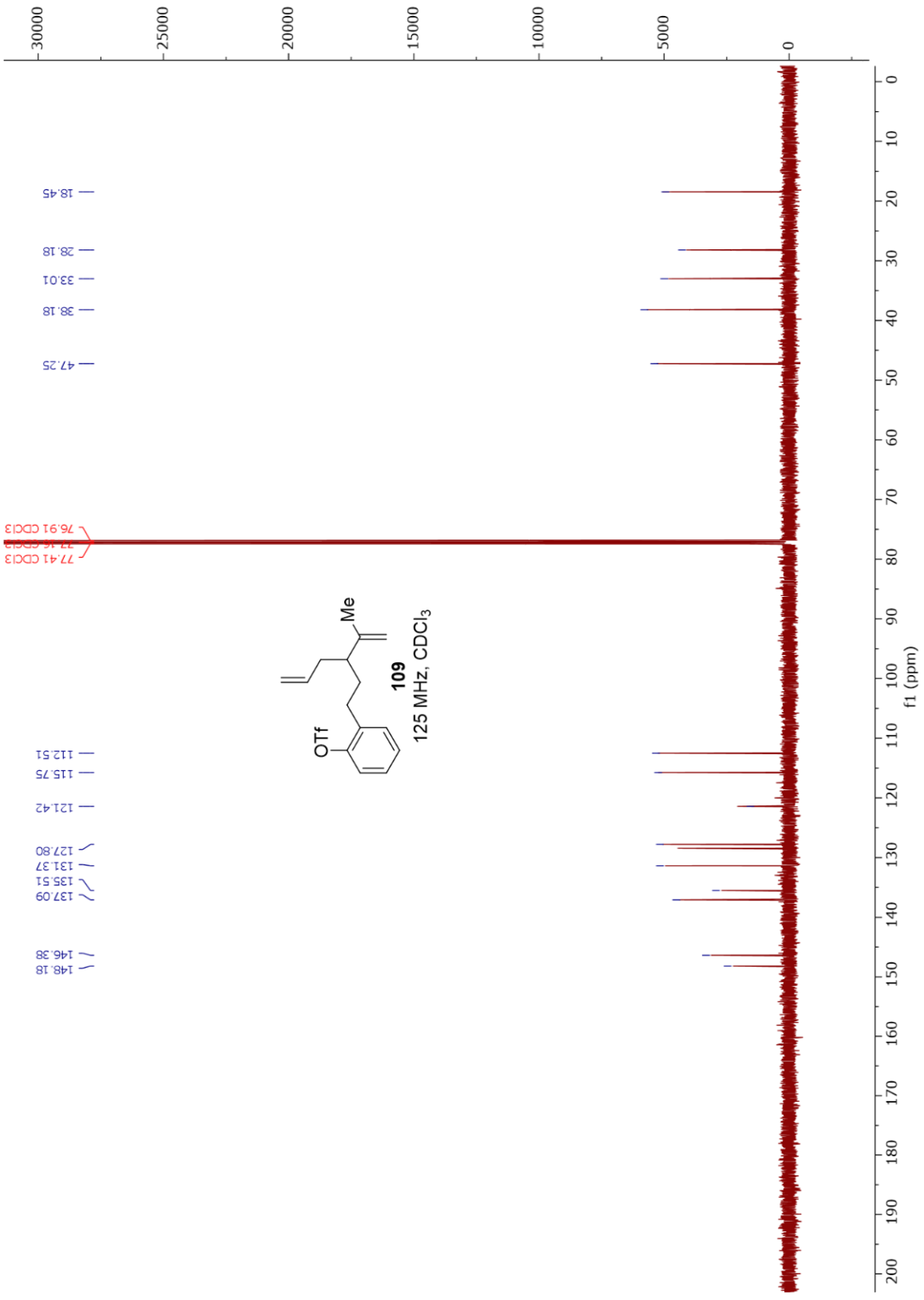
18.45
28.18
33.01
38.18
47.25
76.91 CDCl3
77.16 CDCl3
77.41 CDCl3
112.51
115.75
121.42
127.80
131.37
135.51
137.09
146.38
148.18
OTf
Me
109
125 MHz, CDCl3
f1 (ppm)


-73.91
OTf
Me
109
376 MHz, CDCl3
12000
11000
10000
9000
8000
7000
6000
5000
4000
3000
2000
1000
0
-1000
30
10
-10
-30
-50
-70
-90
-110
-130
-150
-170
-190
-210
-230
-250
-270
-290
f1 (ppm)

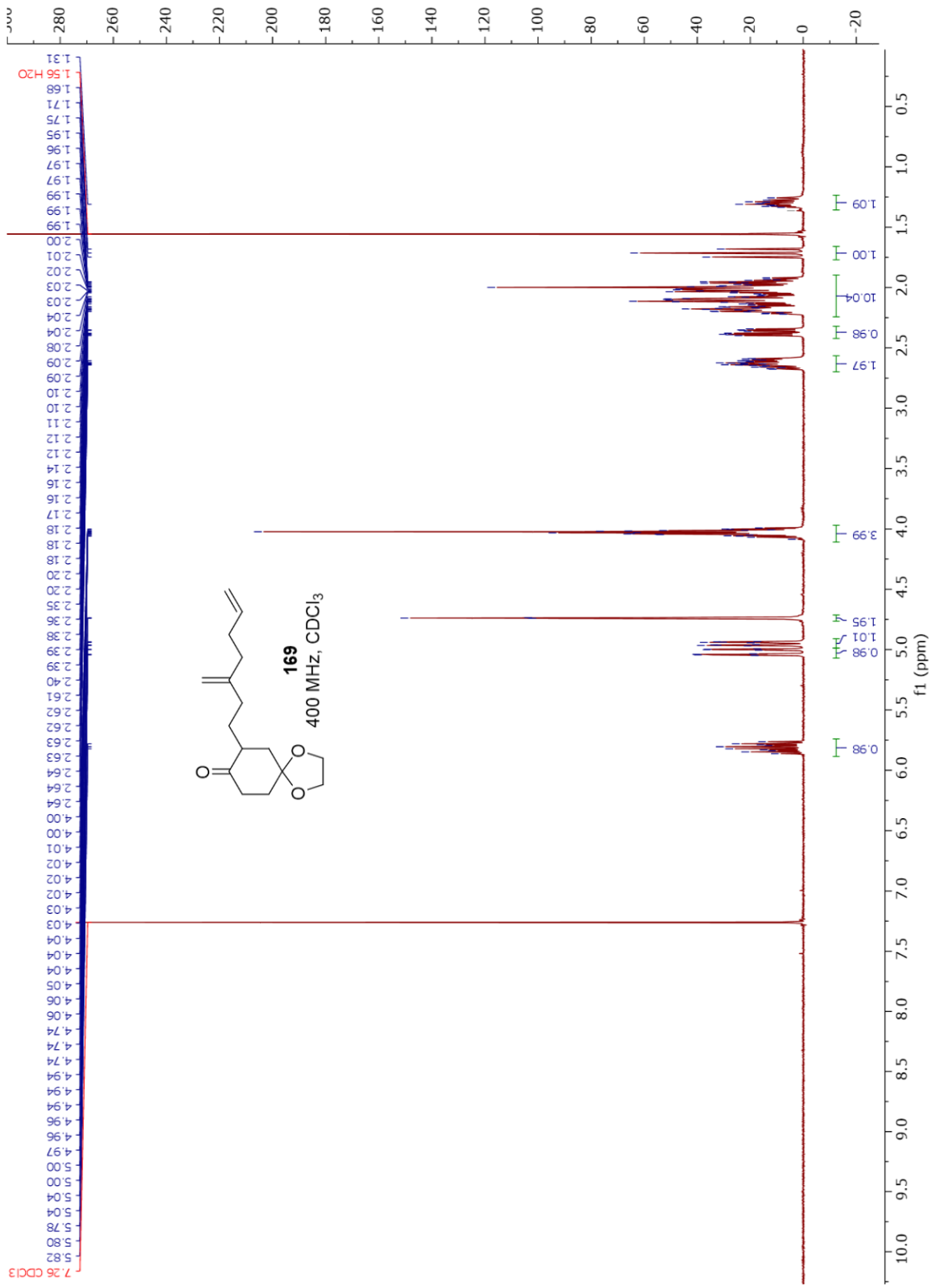
169
400 MHz, CDCl3
f1 (ppm)

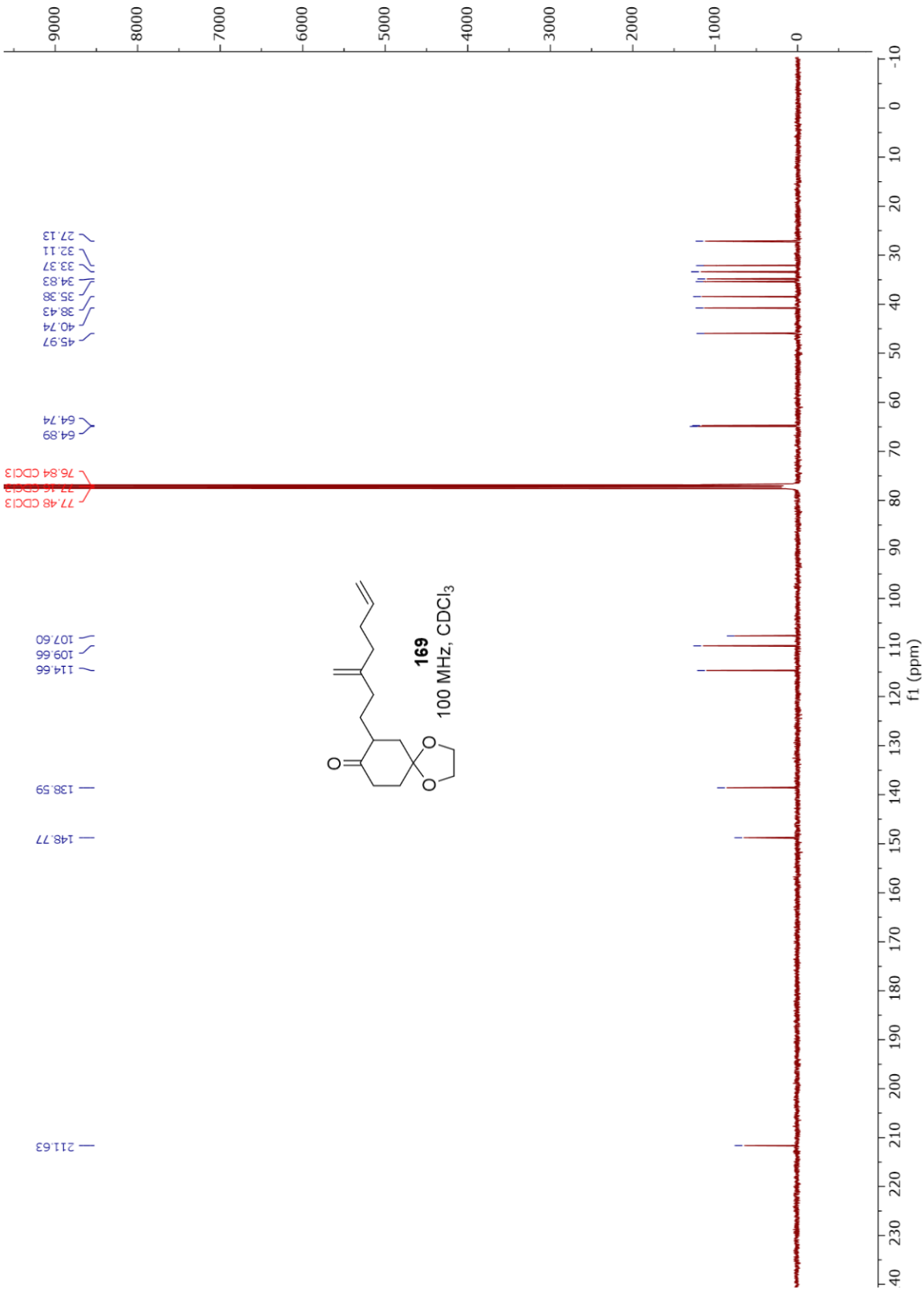
169
100 MHz, CDCl3
f1 (ppm)
211.63
148.77
138.59
114.66
109.66
107.60
77.48 CDCl3
76.84 CDCl3
64.89
64.74
45.97
40.74
38.43
35.38
34.83
33.37
32.11
27.13

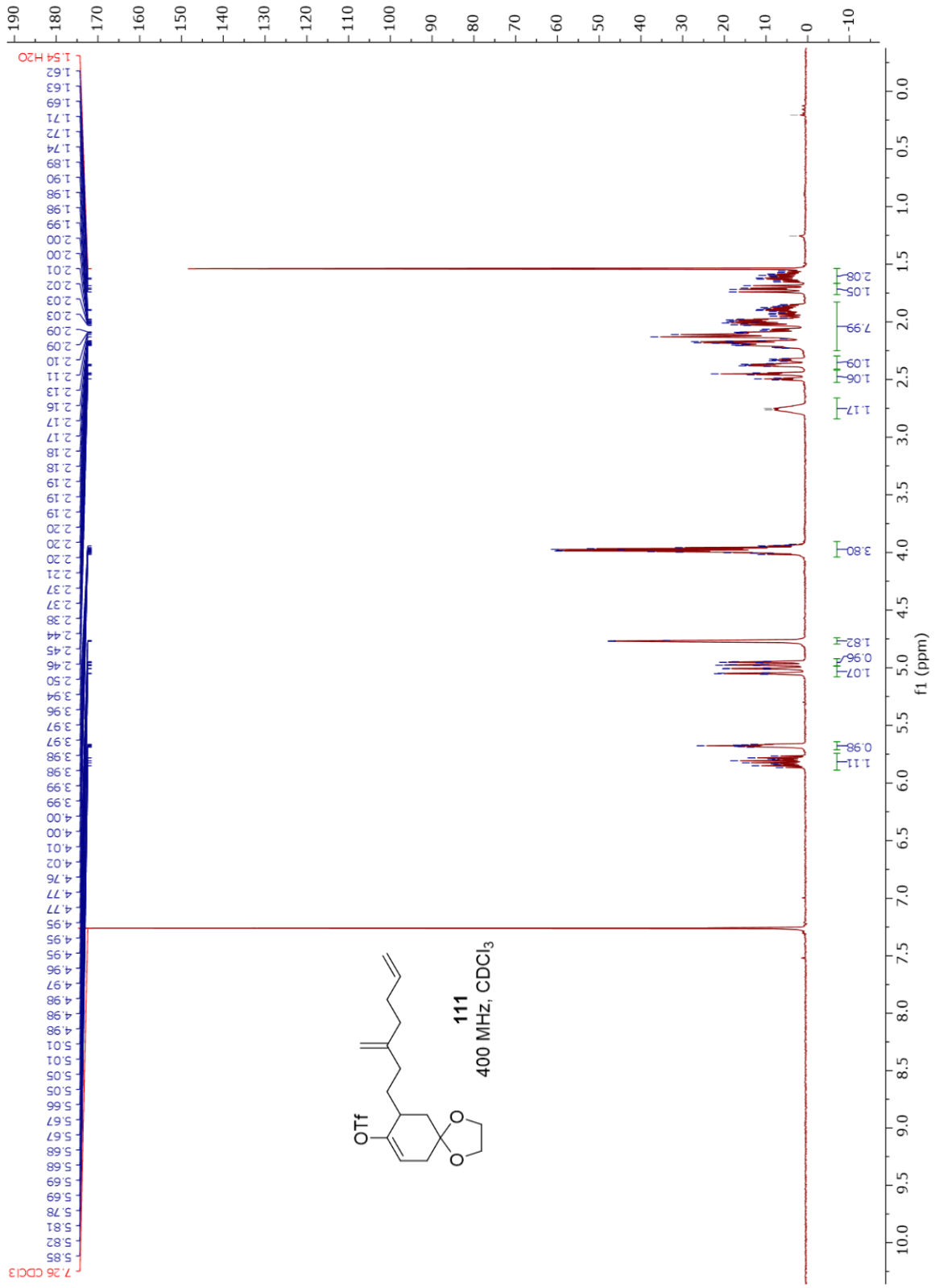
111
400 MHz, CDCl3
OTf
f1 (ppm)

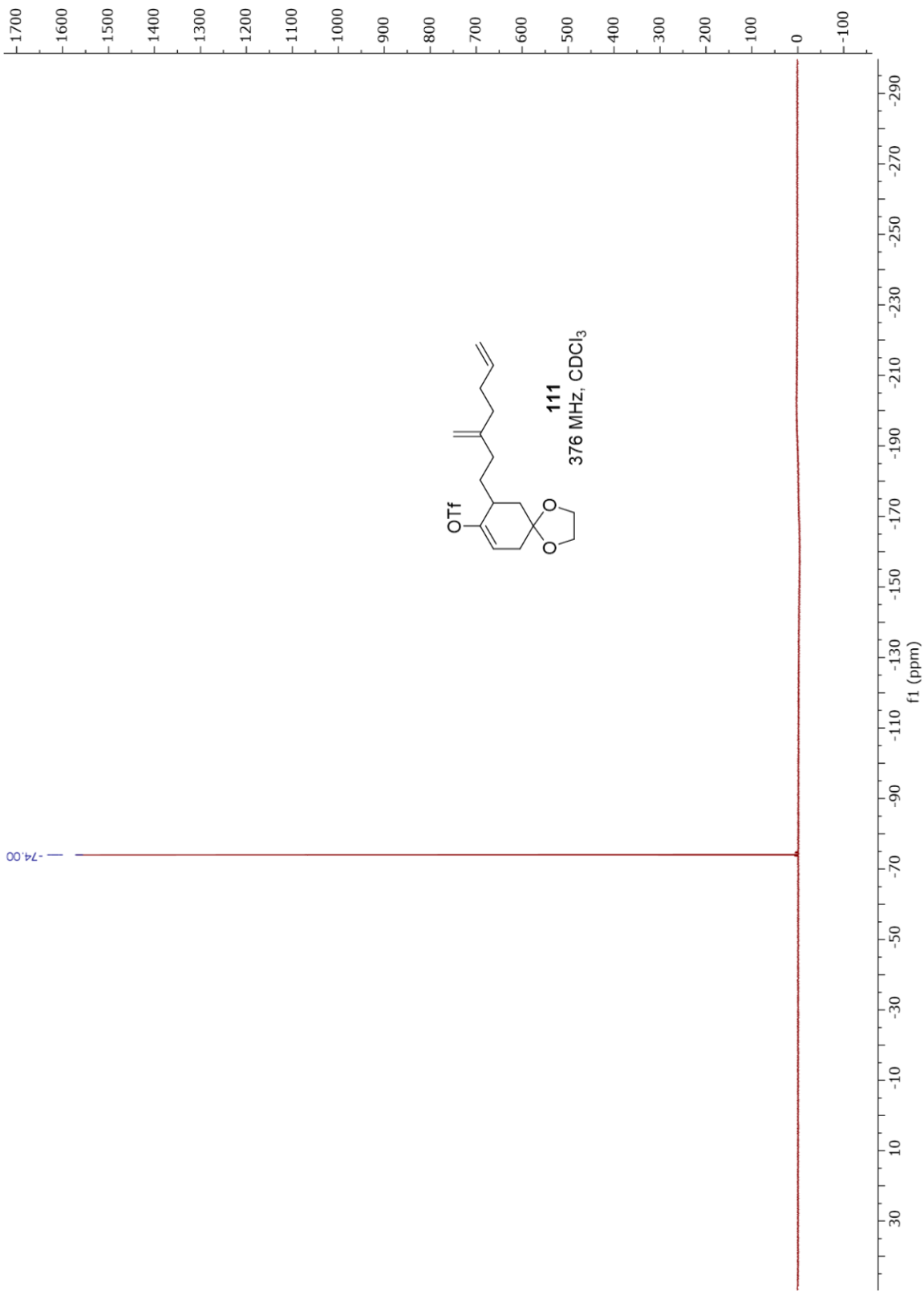
111
376 MHz, CDCl3
OTf
O
O
-74.00
f1 (ppm)

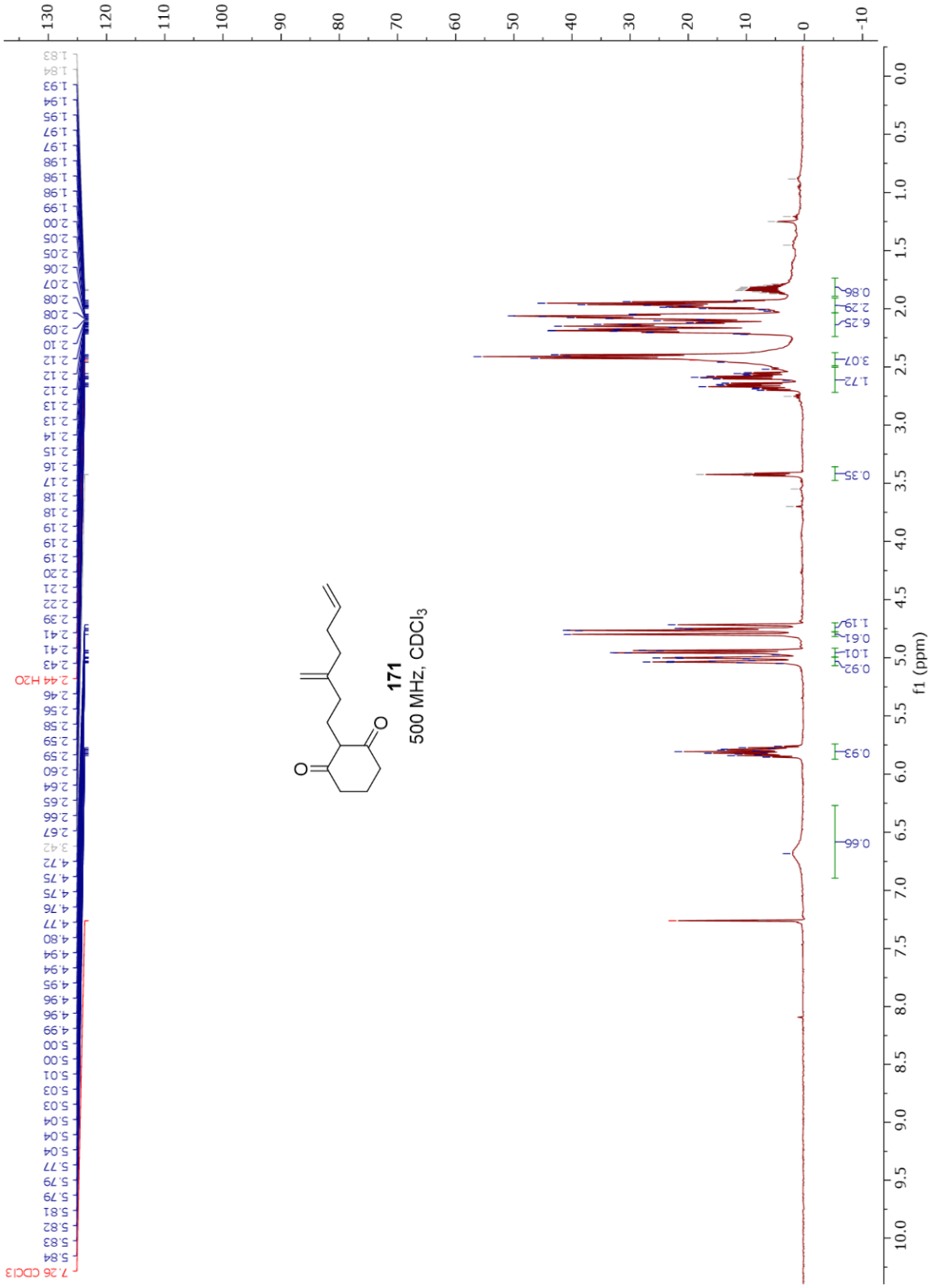
171
500 MHz, CDCl3
f1 (ppm)
7.26 CDCl3
2.44 H2O

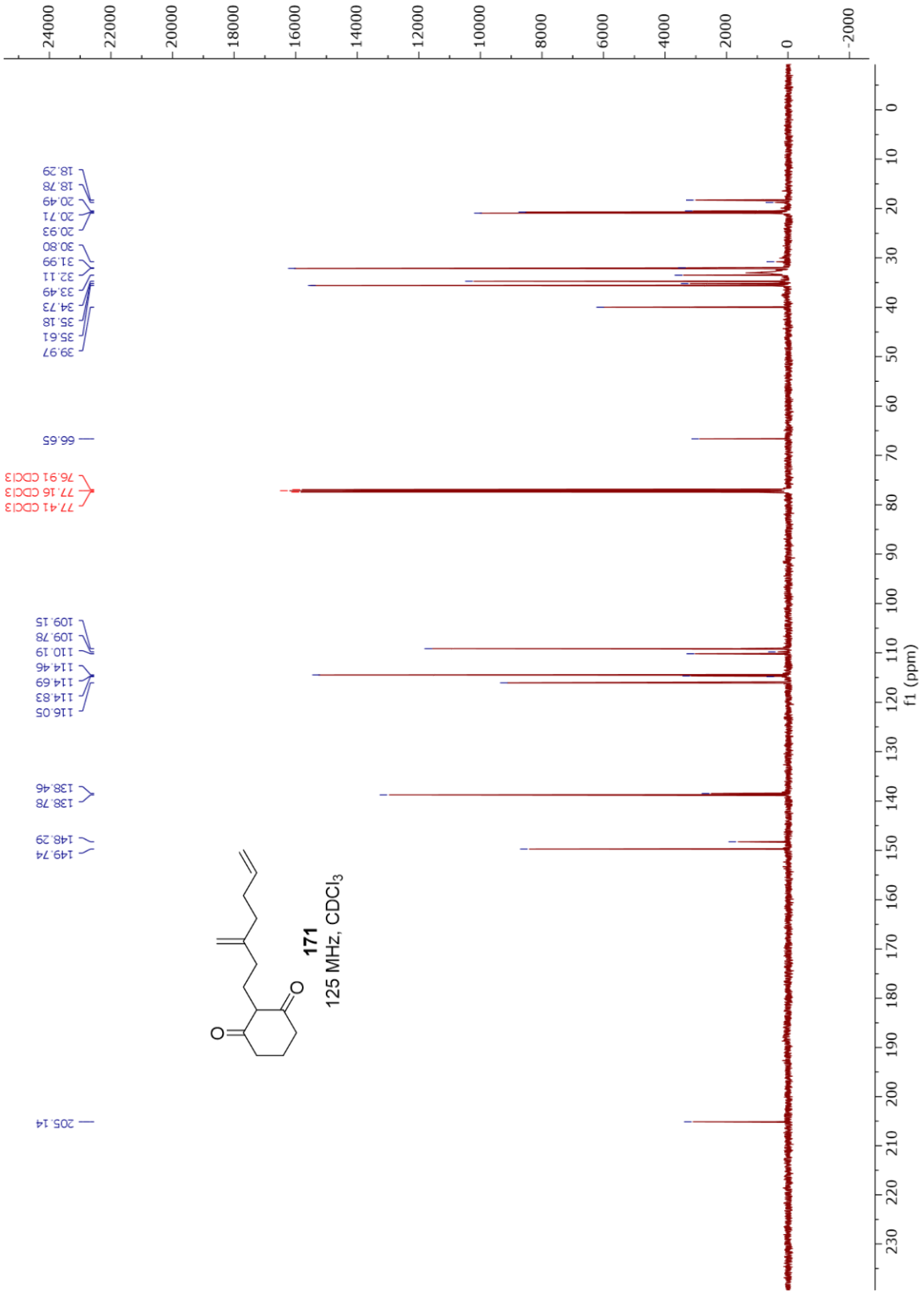
171
125 MHz, CDCl3
f1 (ppm)
205.14
149.74
148.29
138.78
138.46
116.05
114.83
114.69
114.46
110.19
109.78
109.15
77.41 CDCl3
77.16 CDCl3
76.91 CDCl3
66.65
39.97
35.61
35.18
34.73
33.49
32.11
31.99
30.80
20.93
20.71
20.49
18.78
18.29

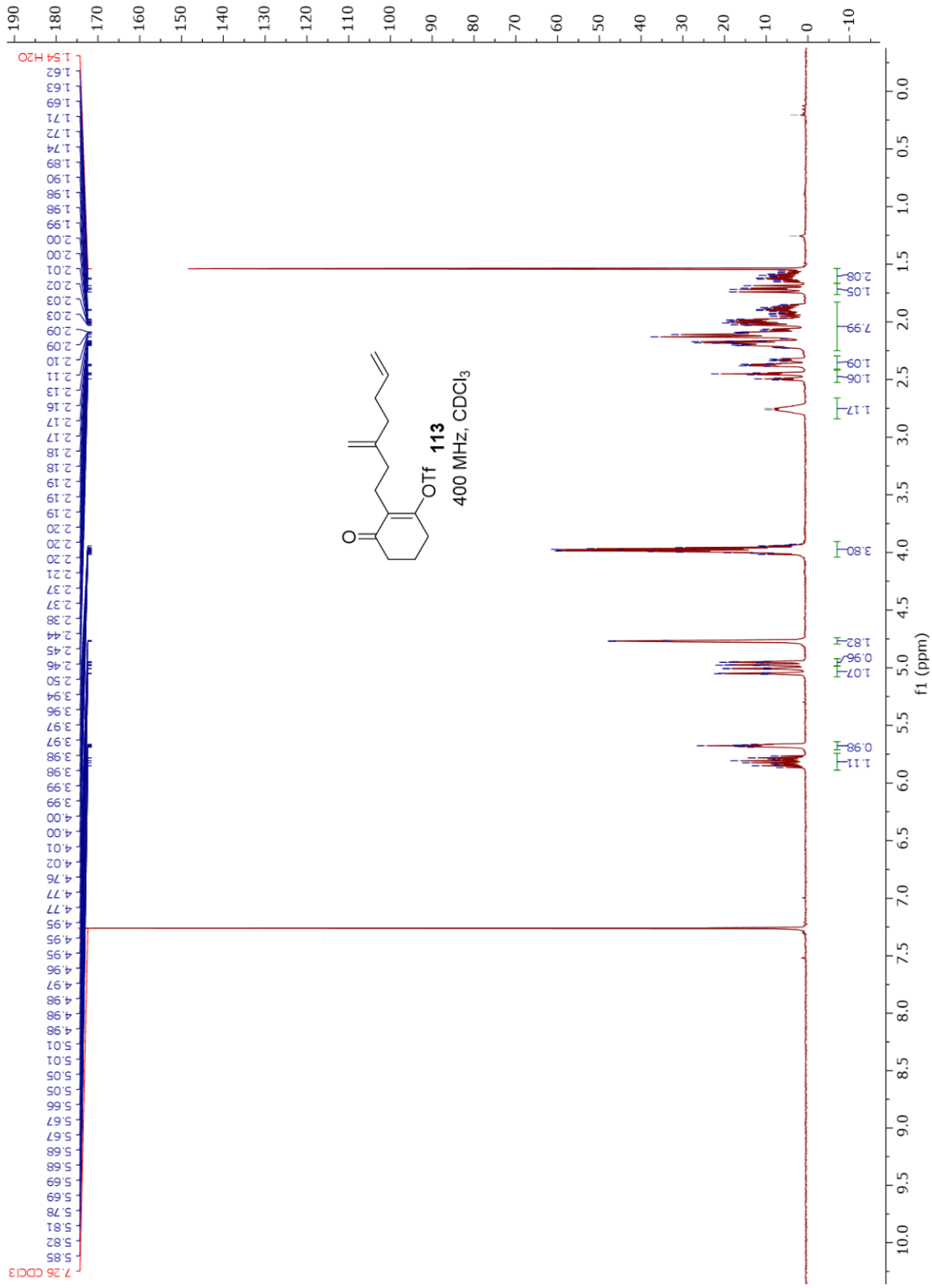
OTf
113
400 MHz, CDCl3
f1 (ppm)

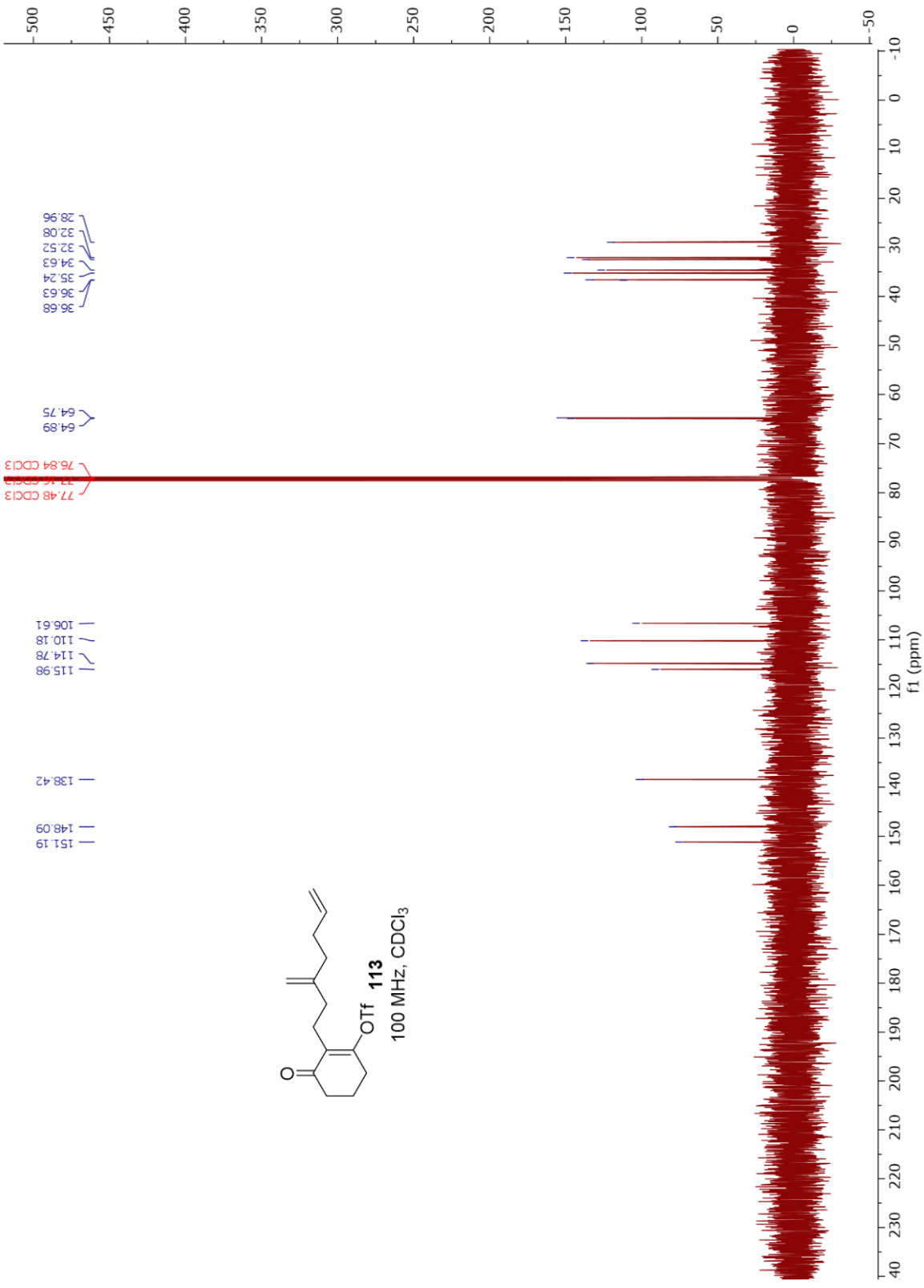
113
100 MHz, CDCl3
OTf
O
151.19
148.09
138.42
115.98
114.78
110.18
106.61
77.48 CDCl3
76.84 CDCl3
64.89
64.75
36.68
36.63
35.24
34.63
32.52
32.08
28.96
f1 (ppm)

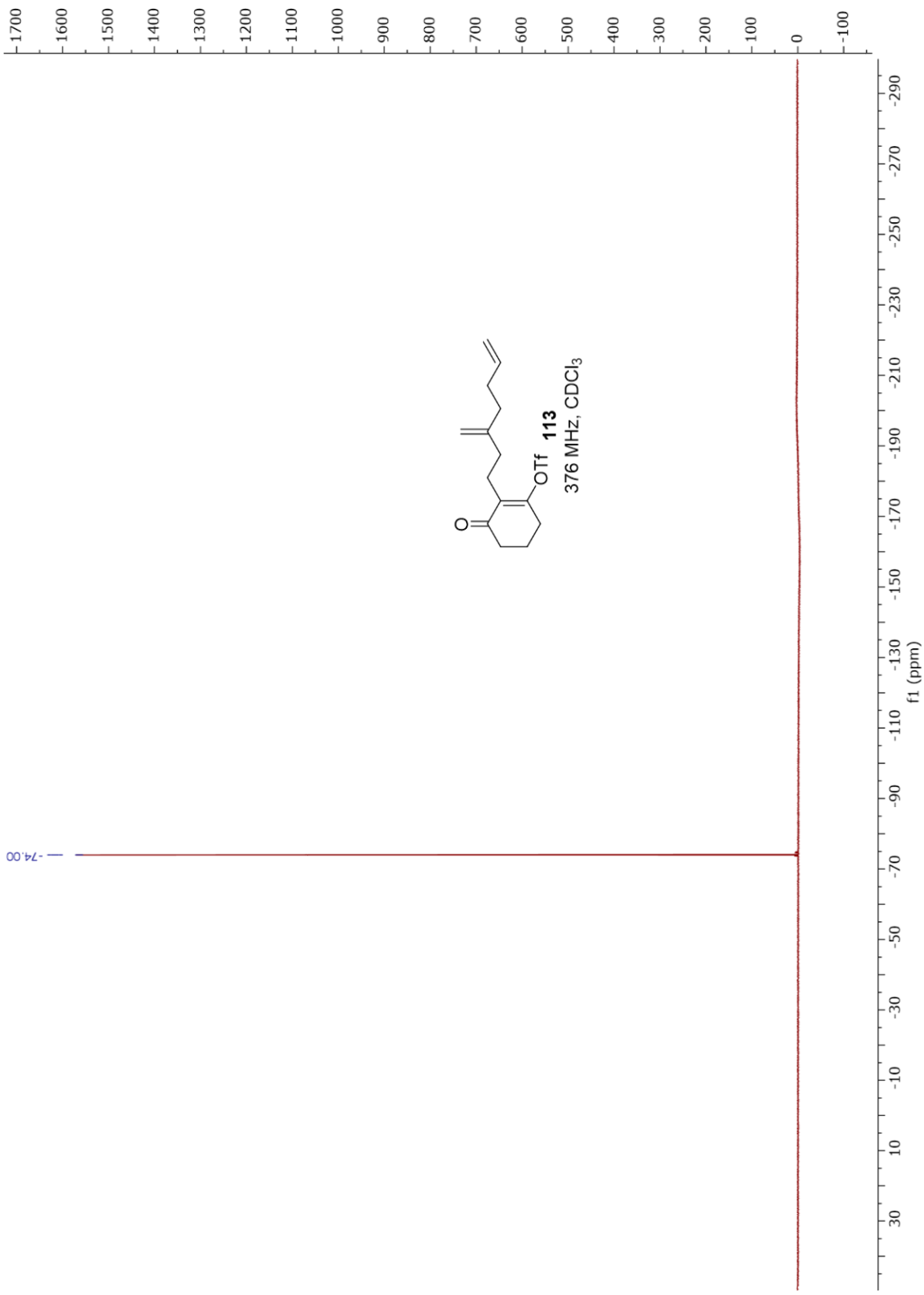
-74.00
f1 (ppm)
OTf
113
376 MHz, CDCl3
O

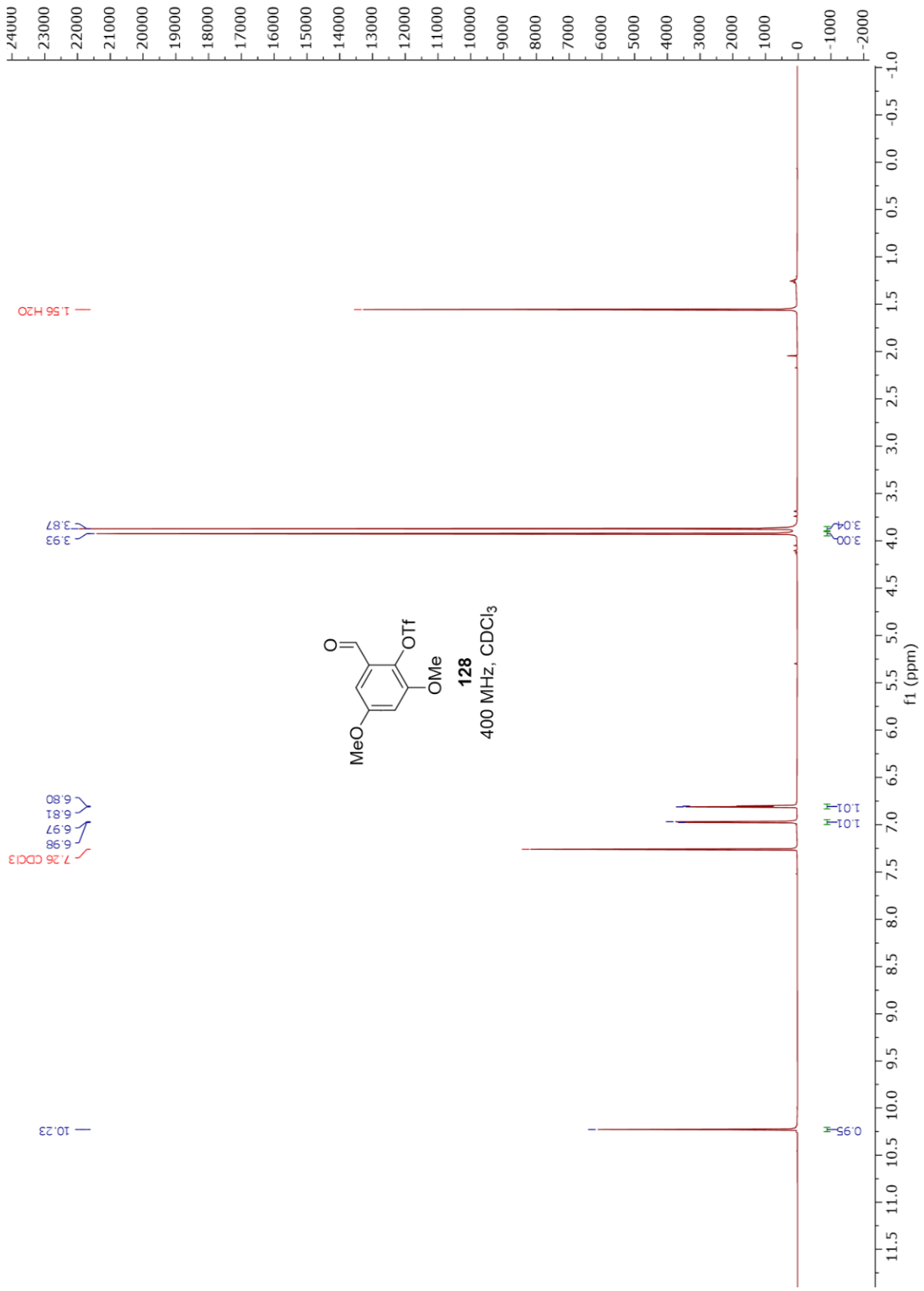
10.23
7.26 CDCl3
6.98
6.97
6.81
6.80
3.93
3.87
1.56 H2O
0.95
1.01
1.01
3.00
3.04
O
OTf
OMe
MeO
128
400 MHz, CDCl3
f1 (ppm)

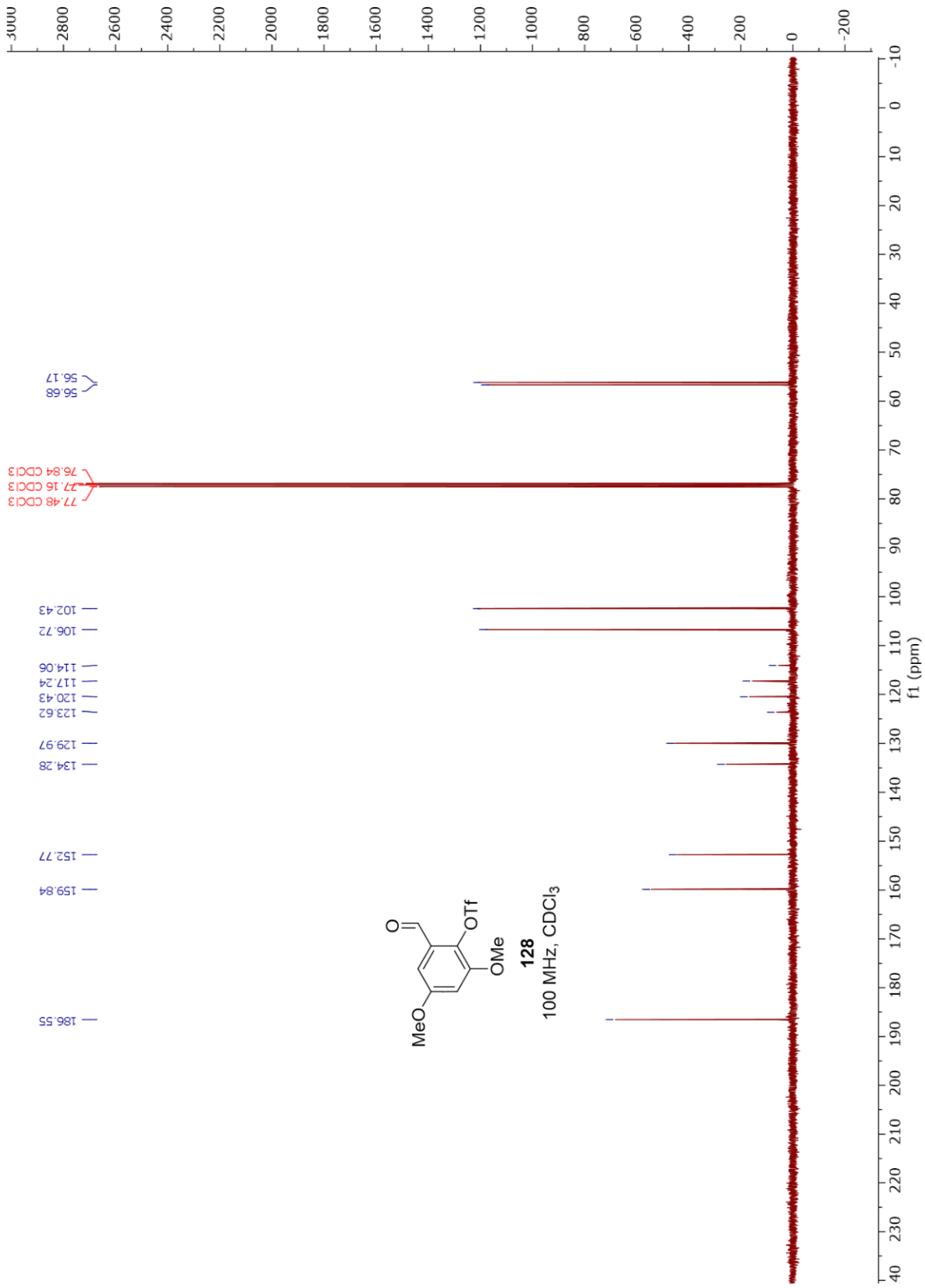
186.55
159.84
152.77
134.28
129.97
123.62
120.43
117.24
114.06
106.72
102.43
77.48 CDCl3
77.16 CDCl3
76.84 CDCl3
56.68
56.17
MeO
OMe
OTf
O
128
100 MHz, CDCl3
f1 (ppm)

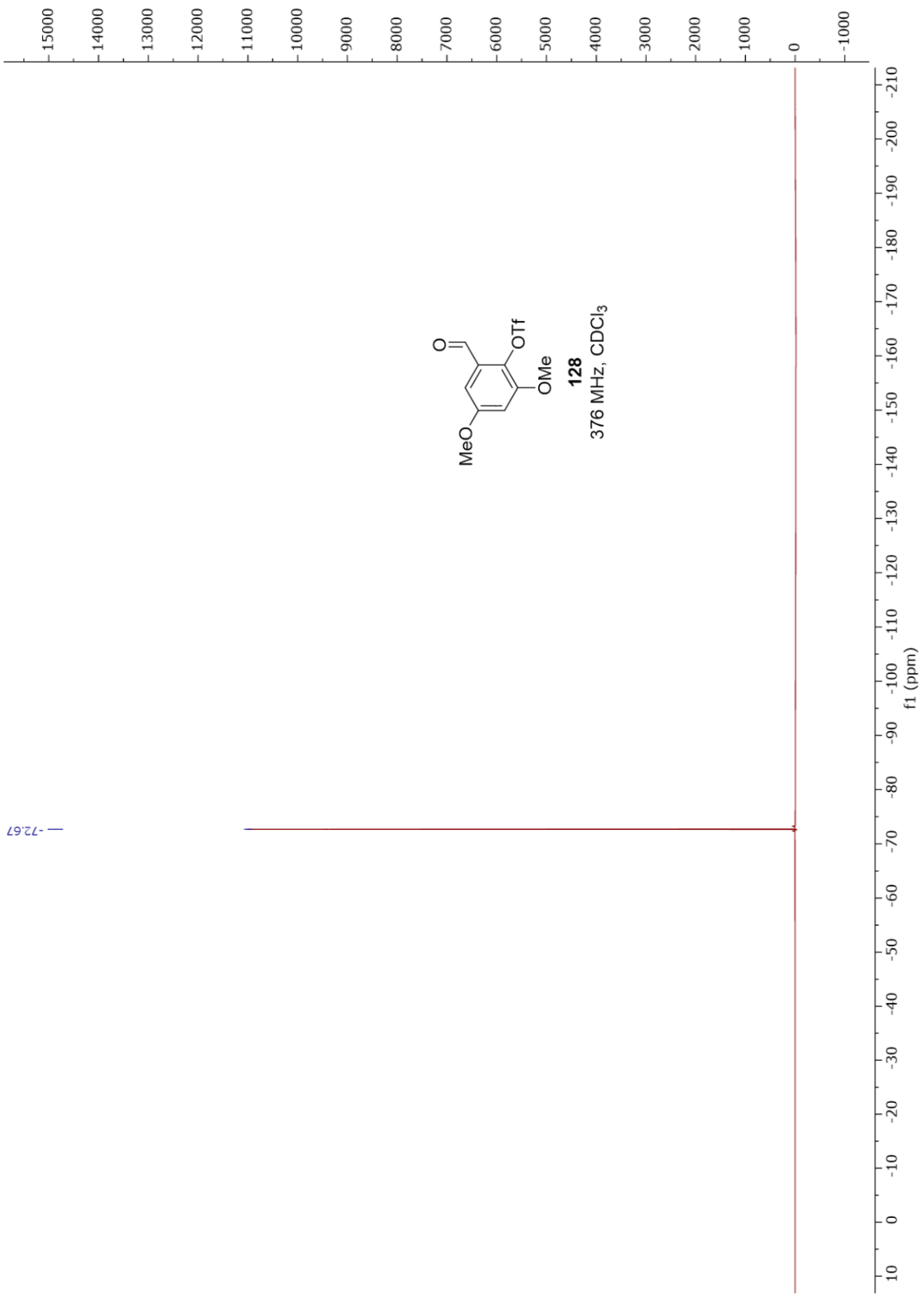
-72.67
f1 (ppm)
MeO
OMe
OTf
O
128
376 MHz, CDCl3

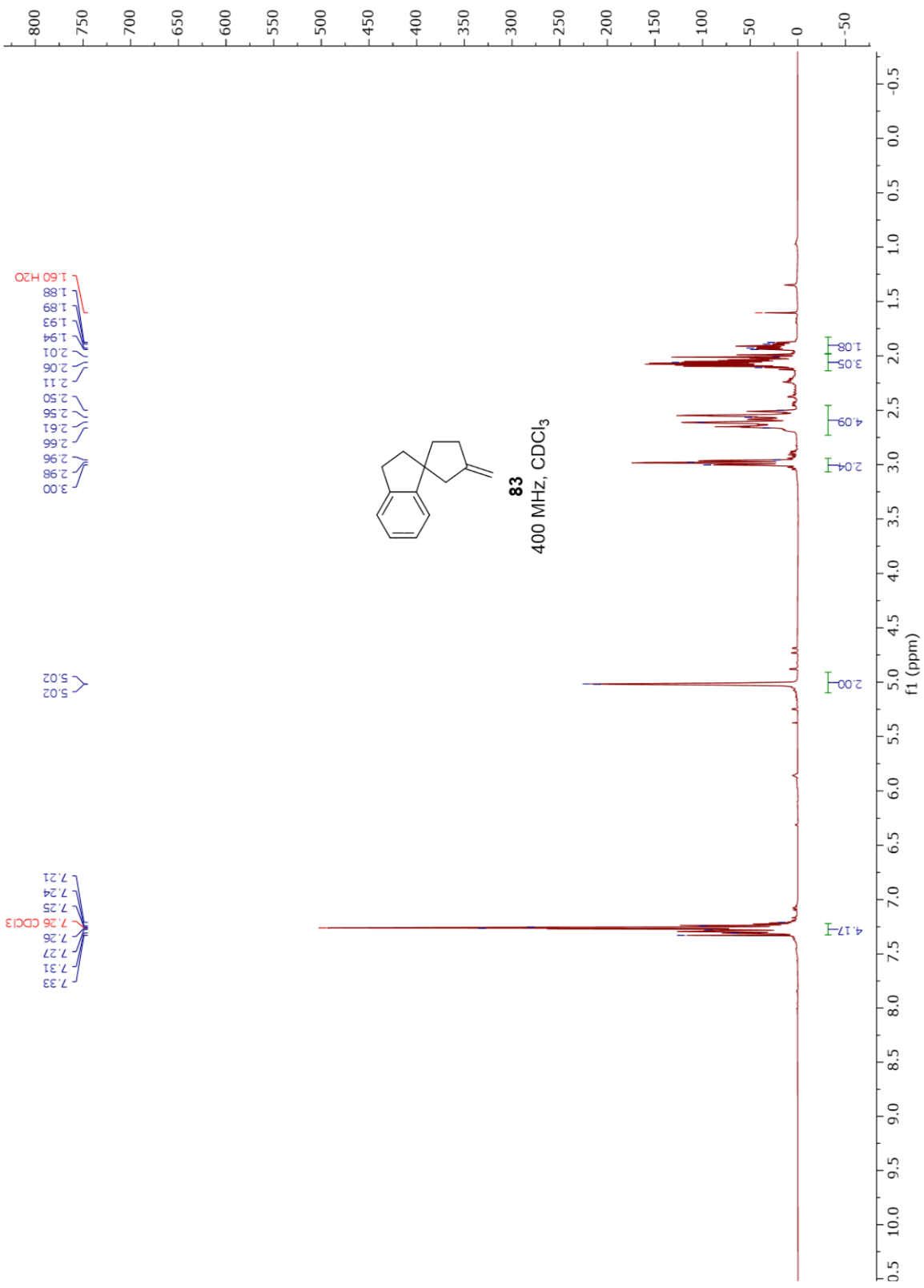
83
400 MHz, $CDCl_3$
f1 (ppm)
7.33
7.31
7.27
7.26
7.26 CDCl3
7.25
7.24
7.21
5.02
5.02
3.00
2.98
2.96
2.66
2.61
2.56
2.50
2.11
2.06
2.01
1.94
1.93
1.89
1.88
1.60 H2O
4.17
2.00
2.04
4.09
3.05
1.08

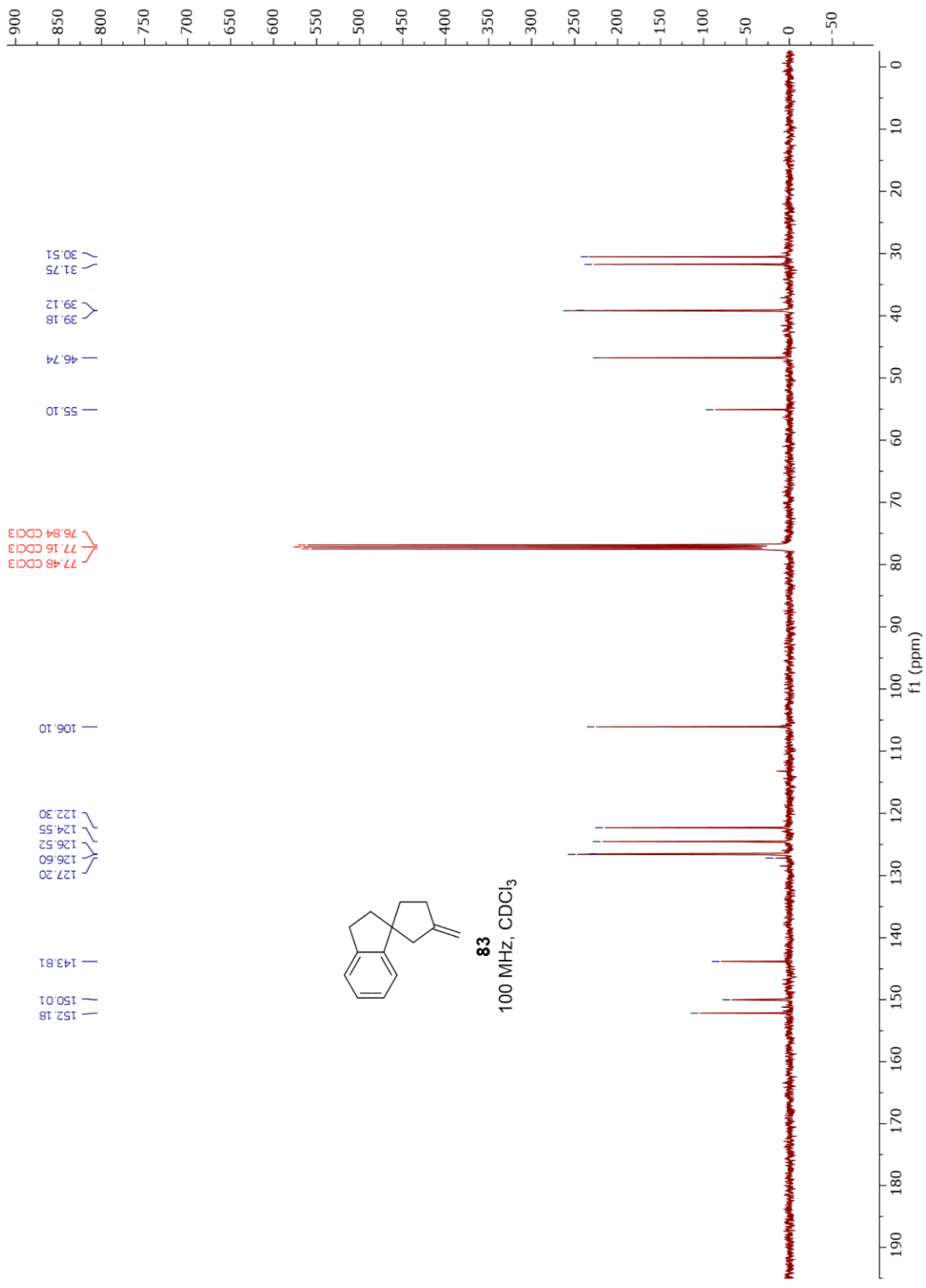
77.48 CDCl3
77.16 CDCl3
76.84 CDCl3
152.18
150.01
143.81
127.20
126.60
126.52
124.55
122.30
106.10
55.10
46.74
39.18
39.12
31.75
30.51
83
100 MHz, CDCl3
f1 (ppm)

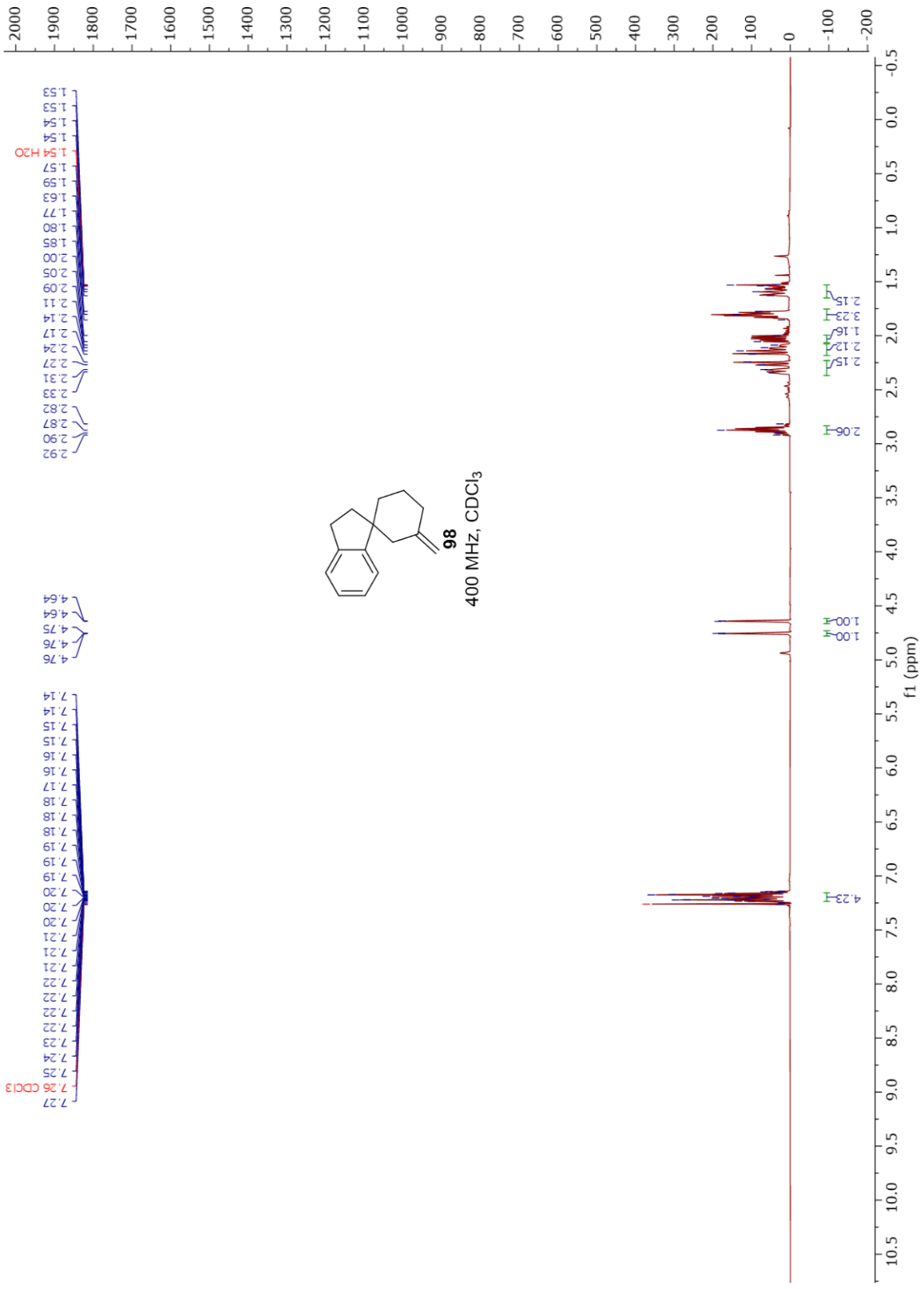
98
400 MHz, CDCl3
f1 (ppm)
7.27
7.26 CDCl3
1.54 H2O

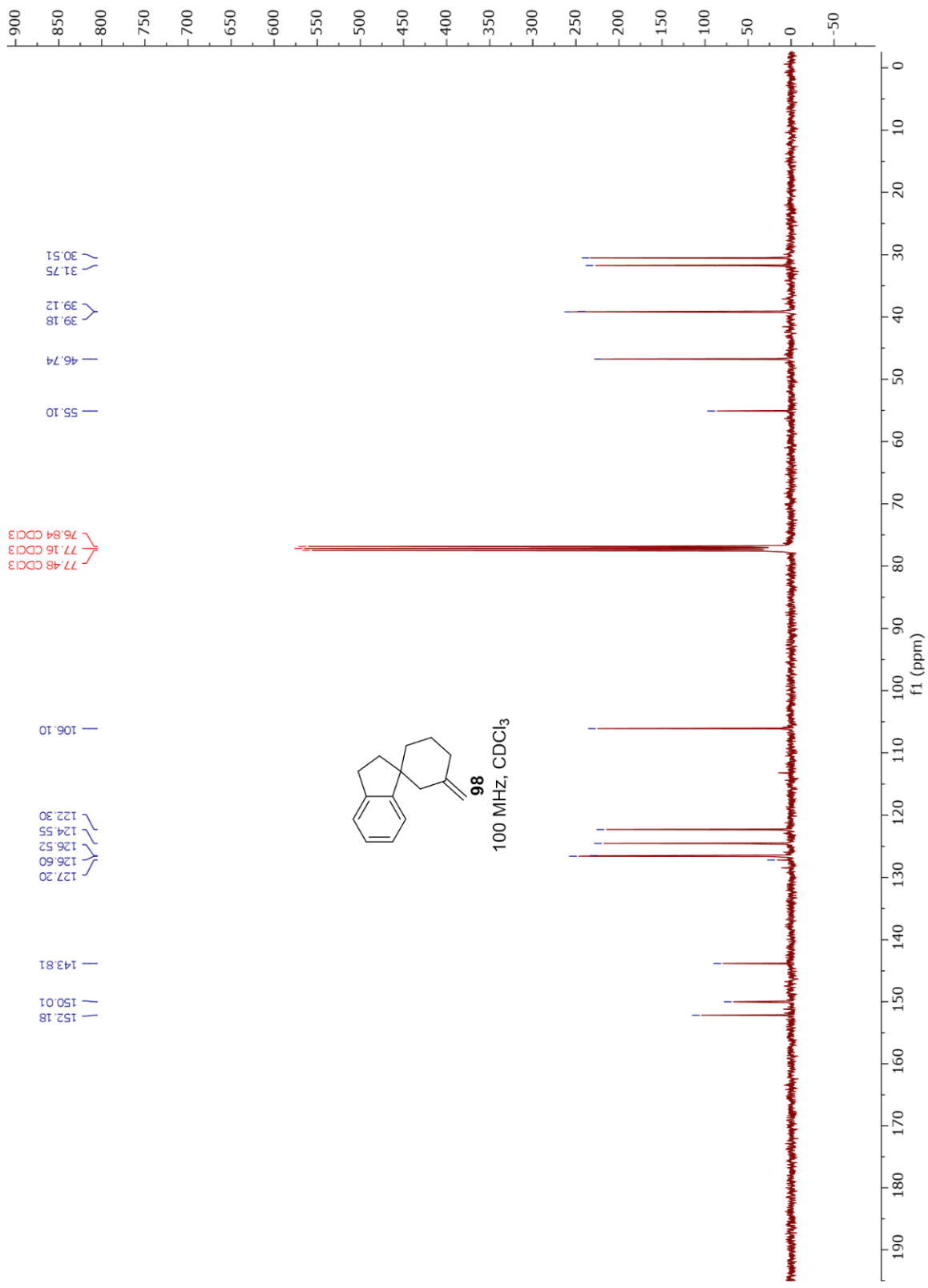
98
100 MHz, CDCl3
f1 (ppm)
152.18
150.01
143.81
127.20
126.60
126.52
124.55
122.30
106.10
77.48 CDCl3
77.16 CDCl3
76.84 CDCl3
55.10
46.74
39.18
39.12
31.75
30.51

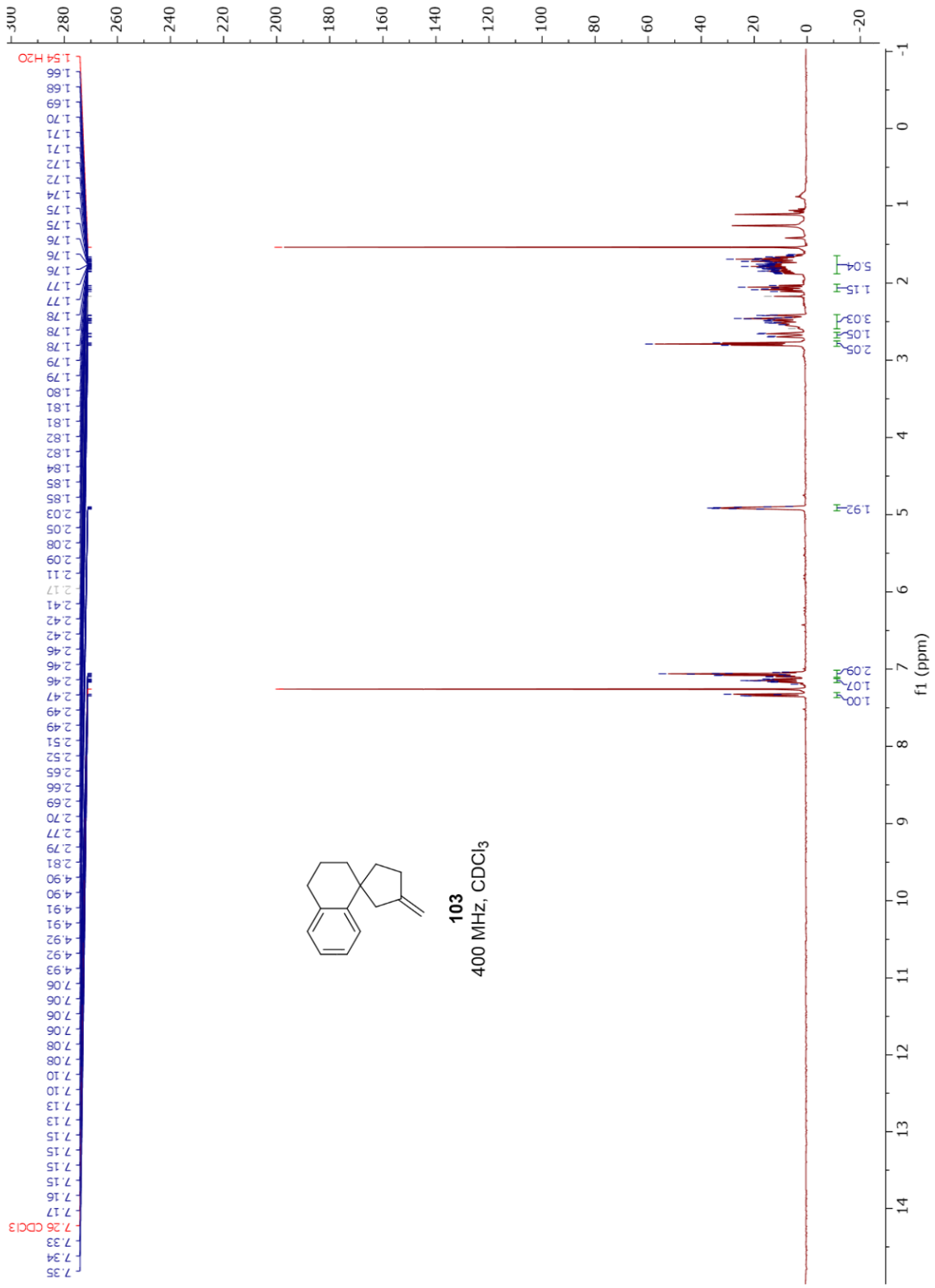
103
400 MHz, CDCl3
f1 (ppm)
1.54 H2O
7.26 CDCl3
5.04
1.15
3.03
1.05
2.05
1.92
1.00
1.07
2.09

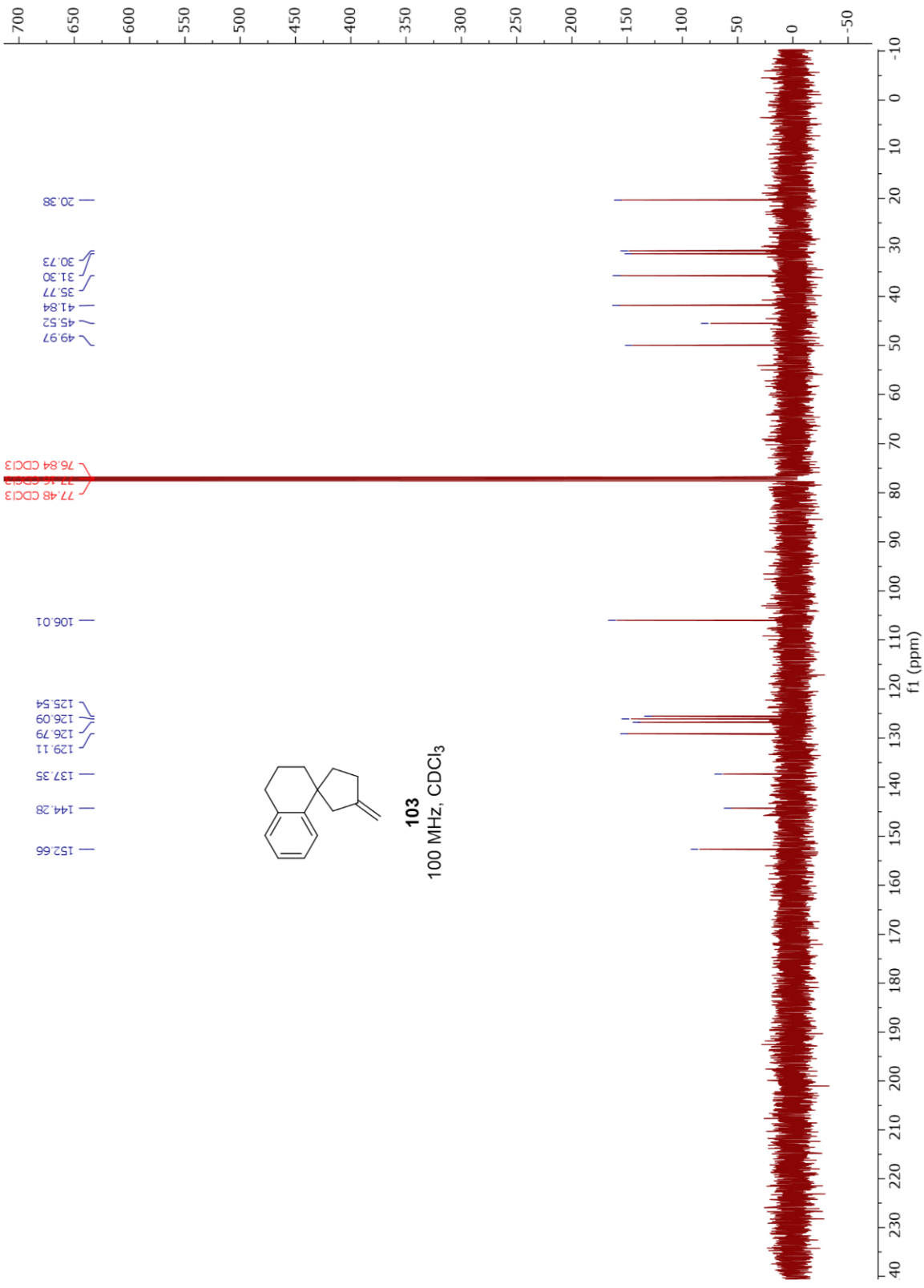
103
100 MHz, CDCl3
f1 (ppm)
20.38
30.73
31.30
35.77
41.84
45.52
49.97
76.84 CDCl3
77.48 CDCl3
106.01
125.54
126.09
126.79
129.11
137.35
144.28
152.66

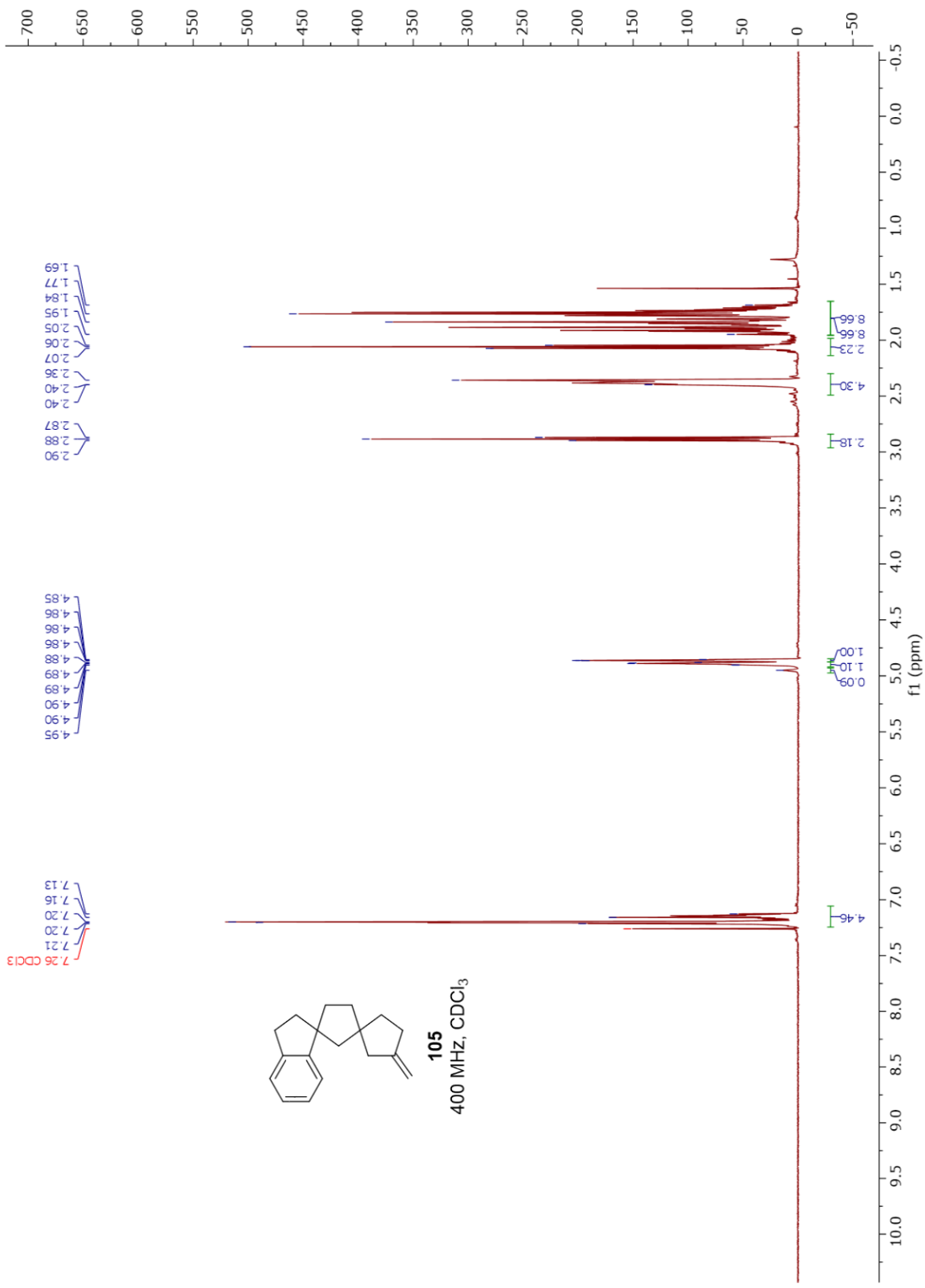
105
400 MHz, CDCl3
f1 (ppm)

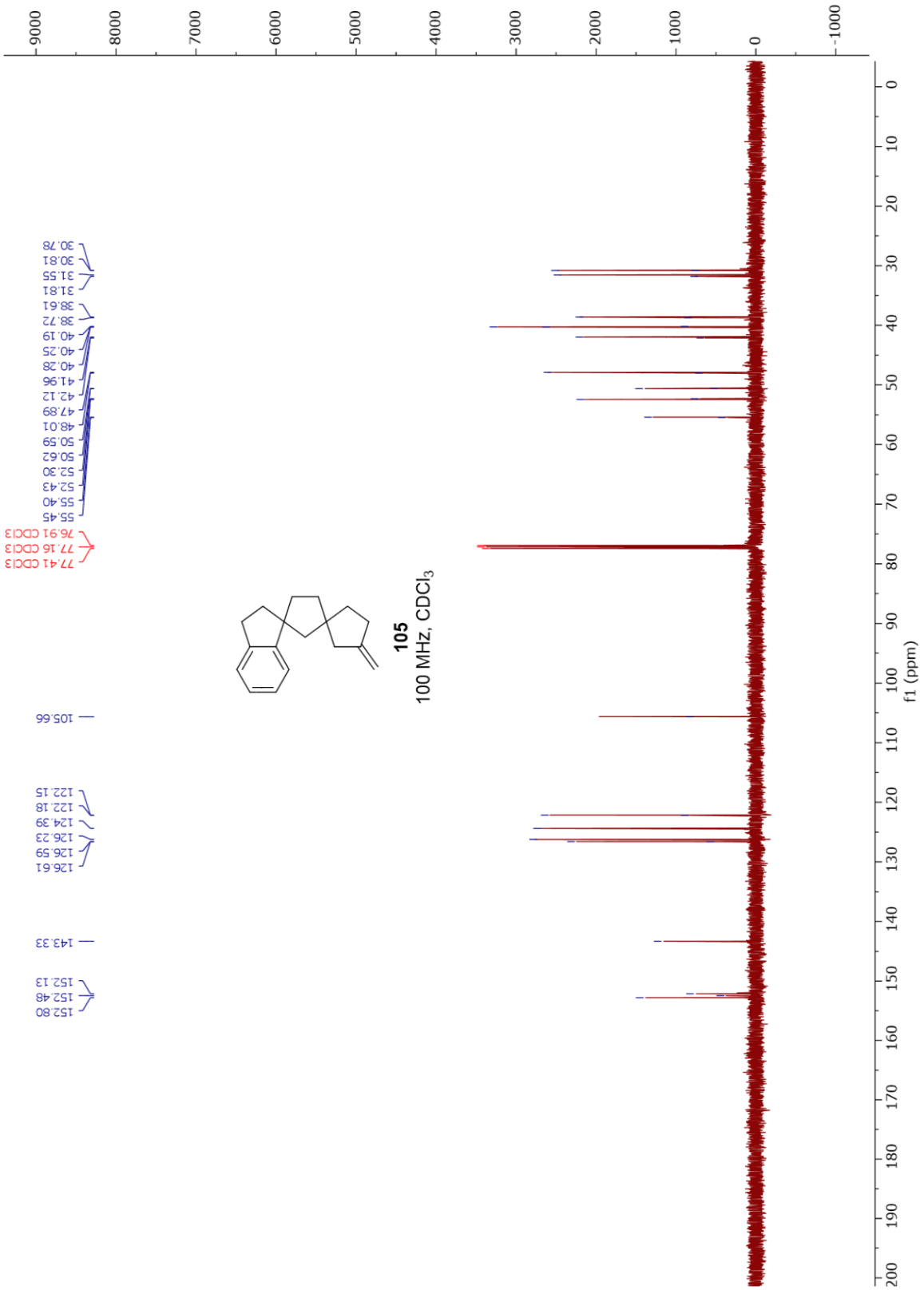
105
100 MHz, CDCl3
f1 (ppm)
77.41 CDCl3
77.16 CDCl3
76.91 CDCl3
105.66
143.33
152.80
152.48
152.13

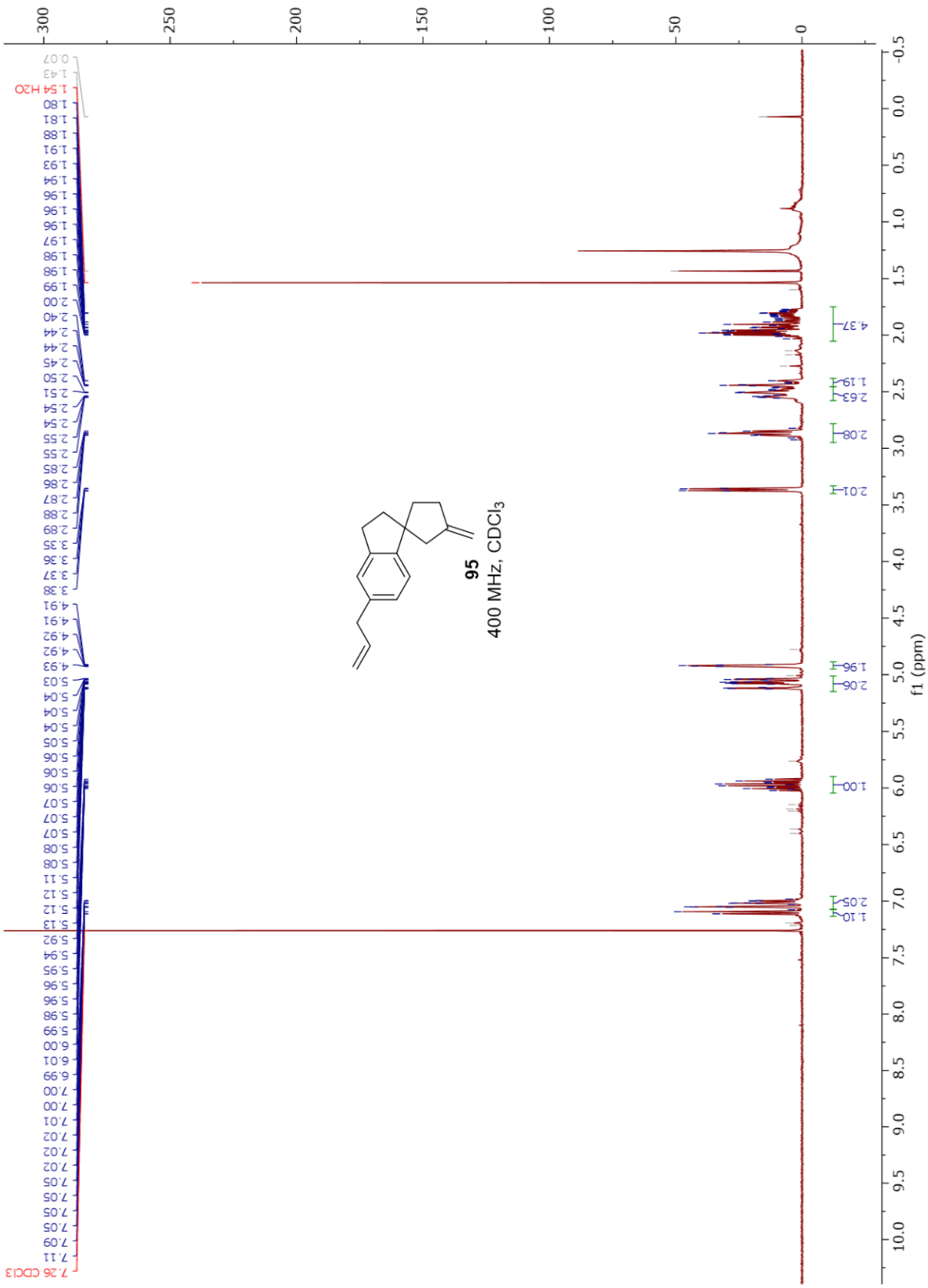
95
400 MHz, CDCl3
f1 (ppm)

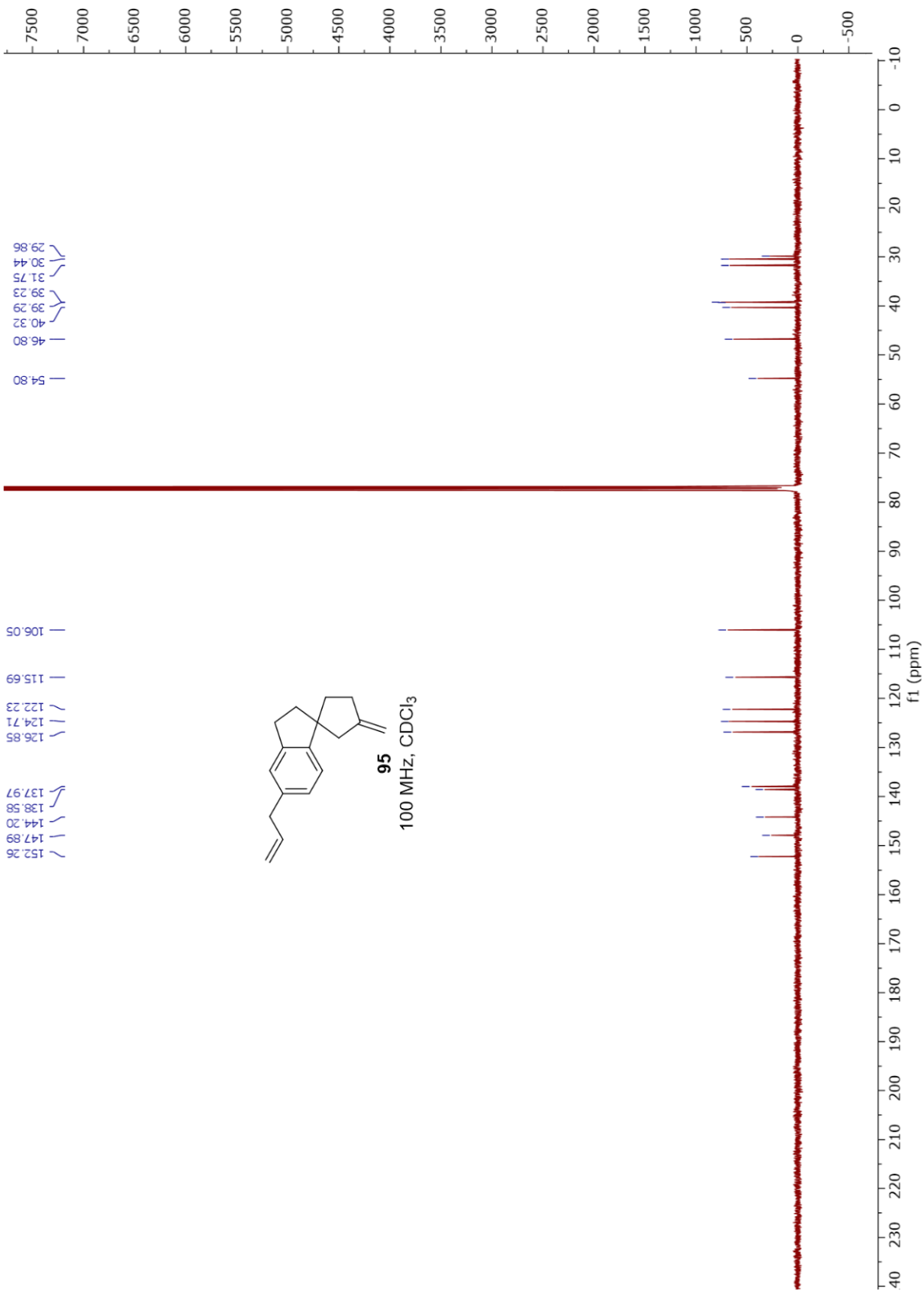
29.86
30.44
31.75
39.23
39.29
40.32
46.80
54.80
106.05
115.69
122.23
124.71
126.85
137.97
138.58
144.20
147.89
152.26
95
100 MHz, CDCl3
f1 (ppm)

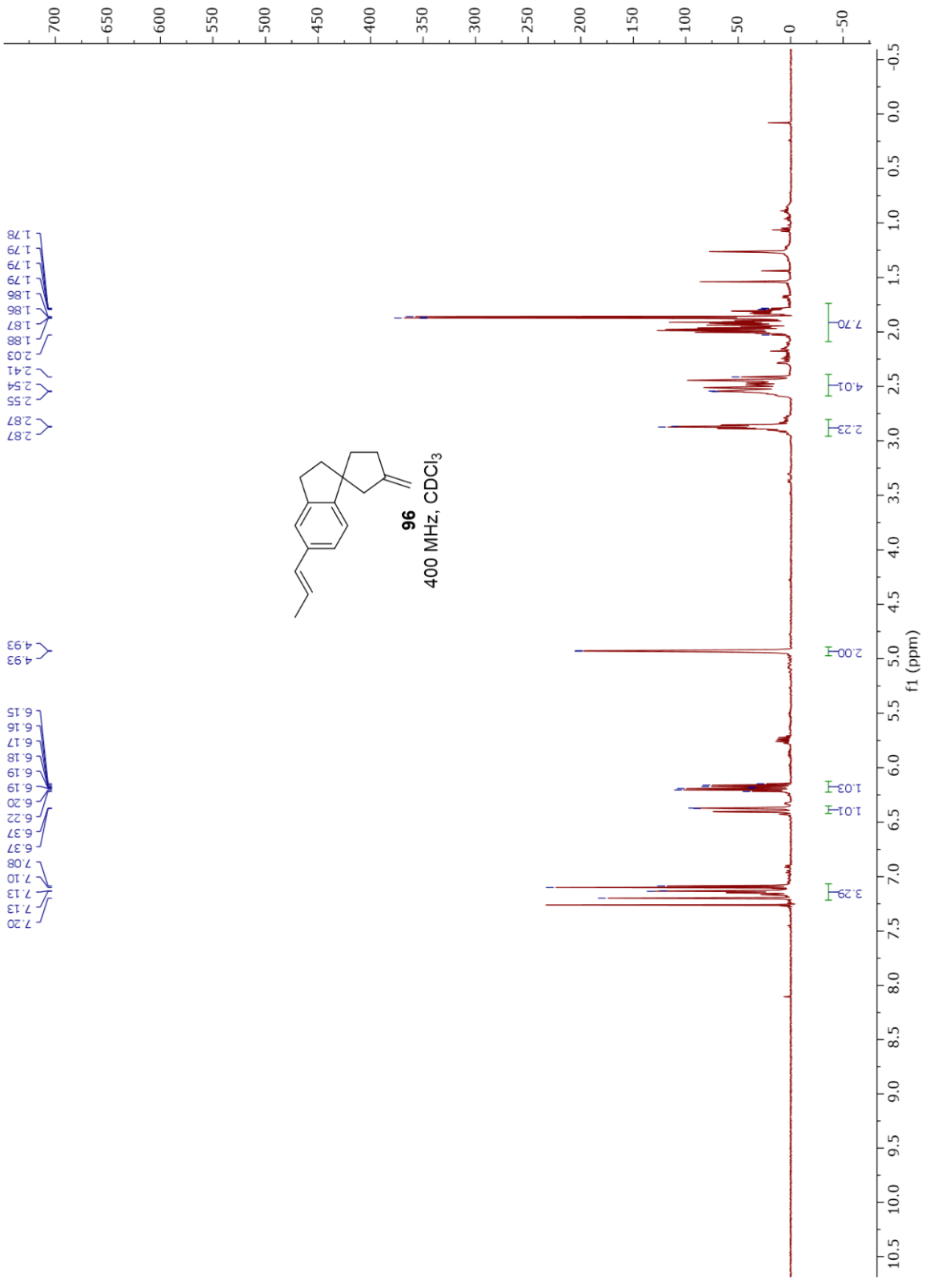
96
400 MHz, CDCl3
f1 (ppm)

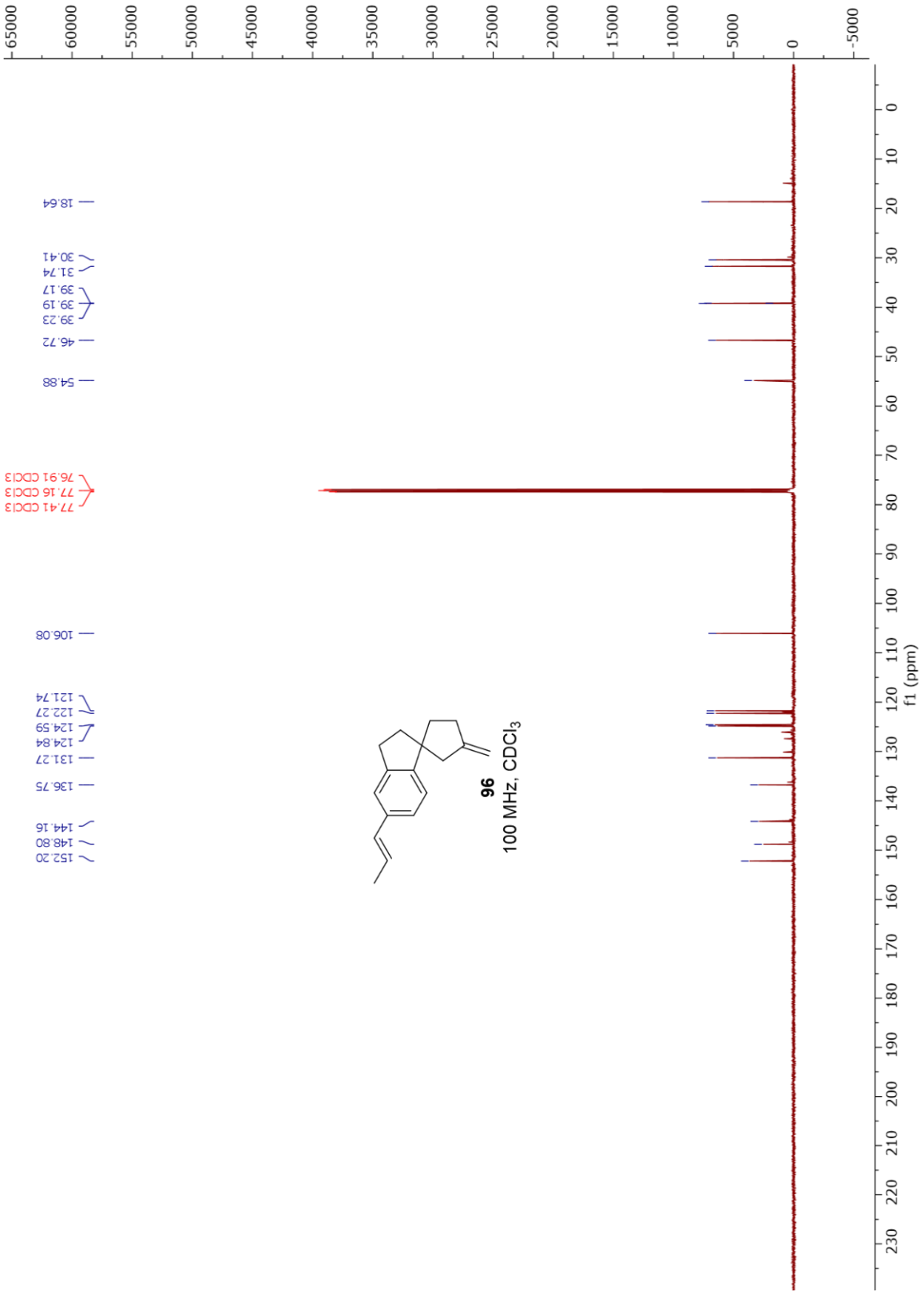
18.64
30.41
31.74
39.17
39.19
39.23
46.72
54.88
76.91 CDCl3
77.16 CDCl3
77.41 CDCl3
106.08
121.74
122.27
124.59
124.84
131.27
136.75
144.16
148.80
152.20
96
100 MHz, CDCl3
f1 (ppm)

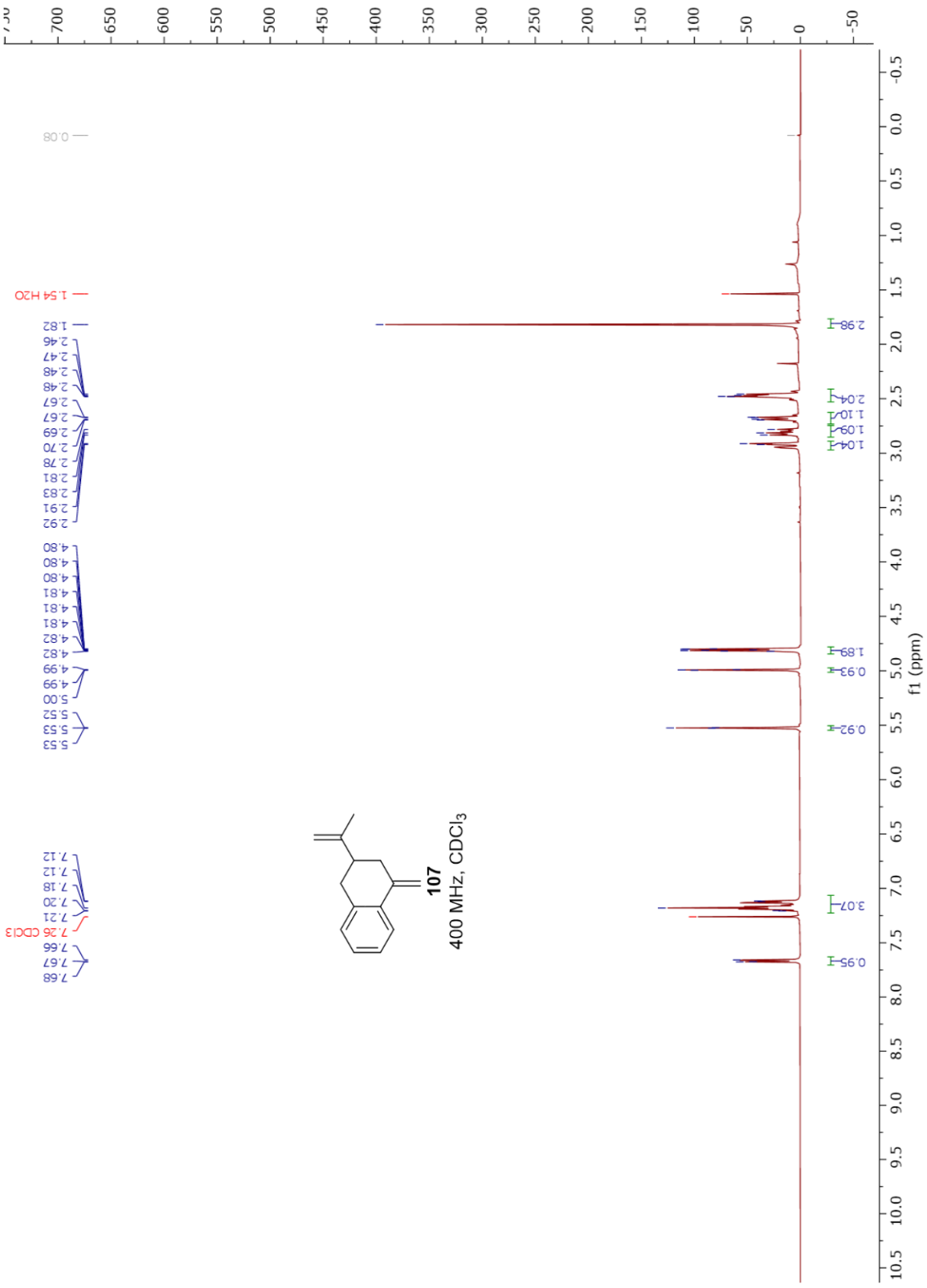
107
400 MHz, CDCl3
f1 (ppm)

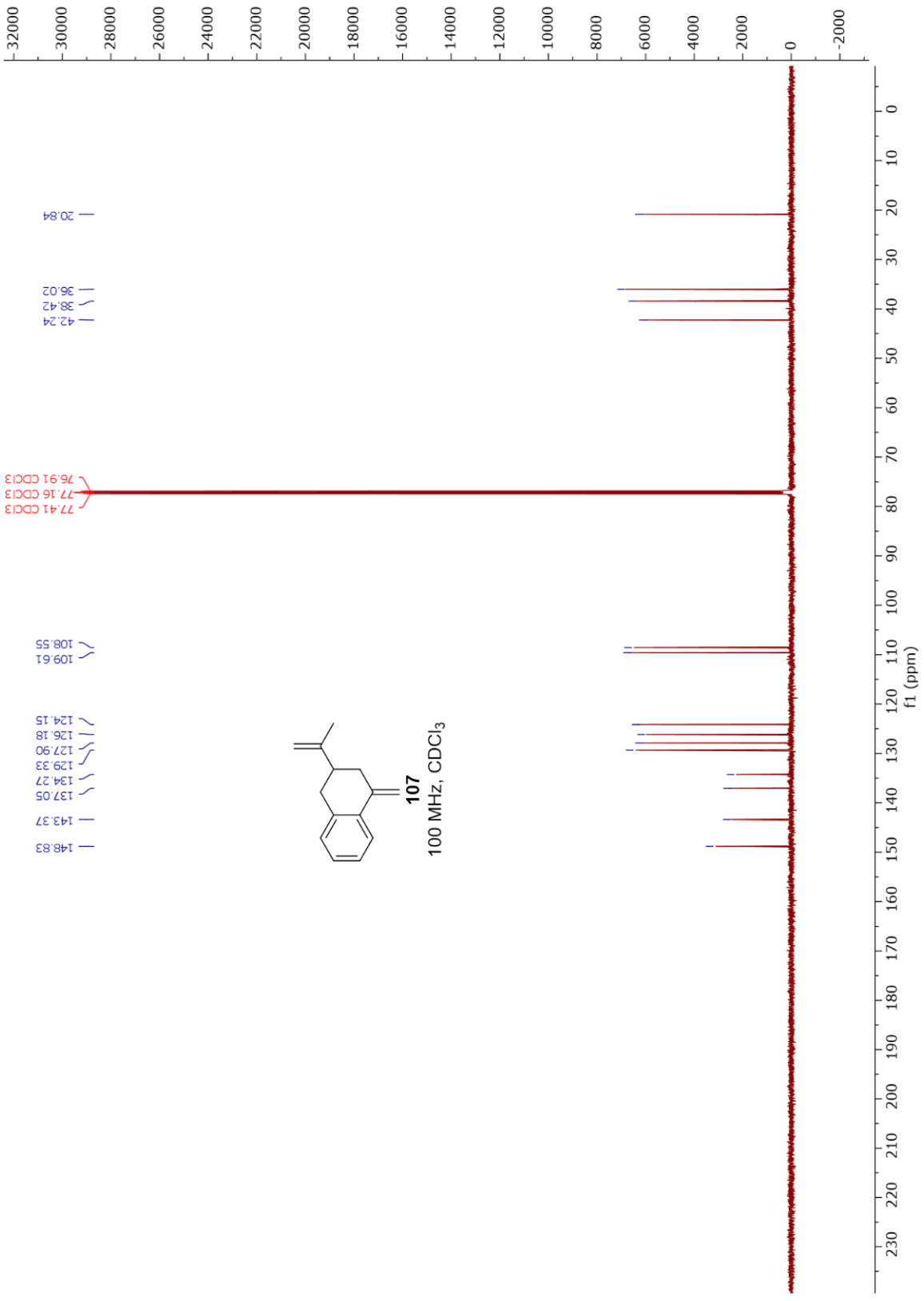
20.84
36.02
38.42
42.24
76.91 CDCl3
77.16 CDCl3
77.41 CDCl3
108.55
109.61
124.15
126.18
127.90
129.33
134.27
137.05
143.37
148.83
107
100 MHz, CDCl3
f1 (ppm)

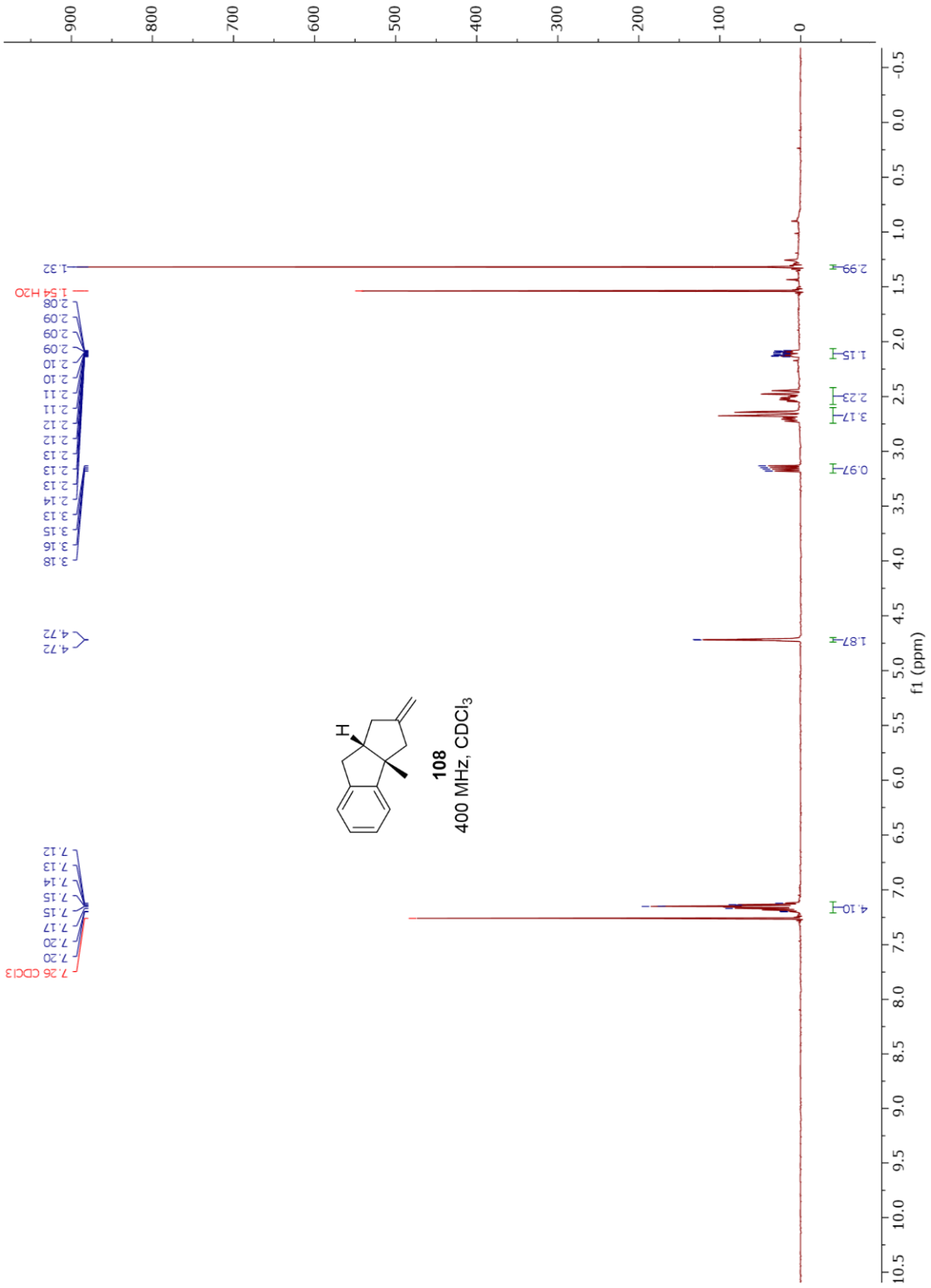
108
400 MHz, CDCl3
f1 (ppm)

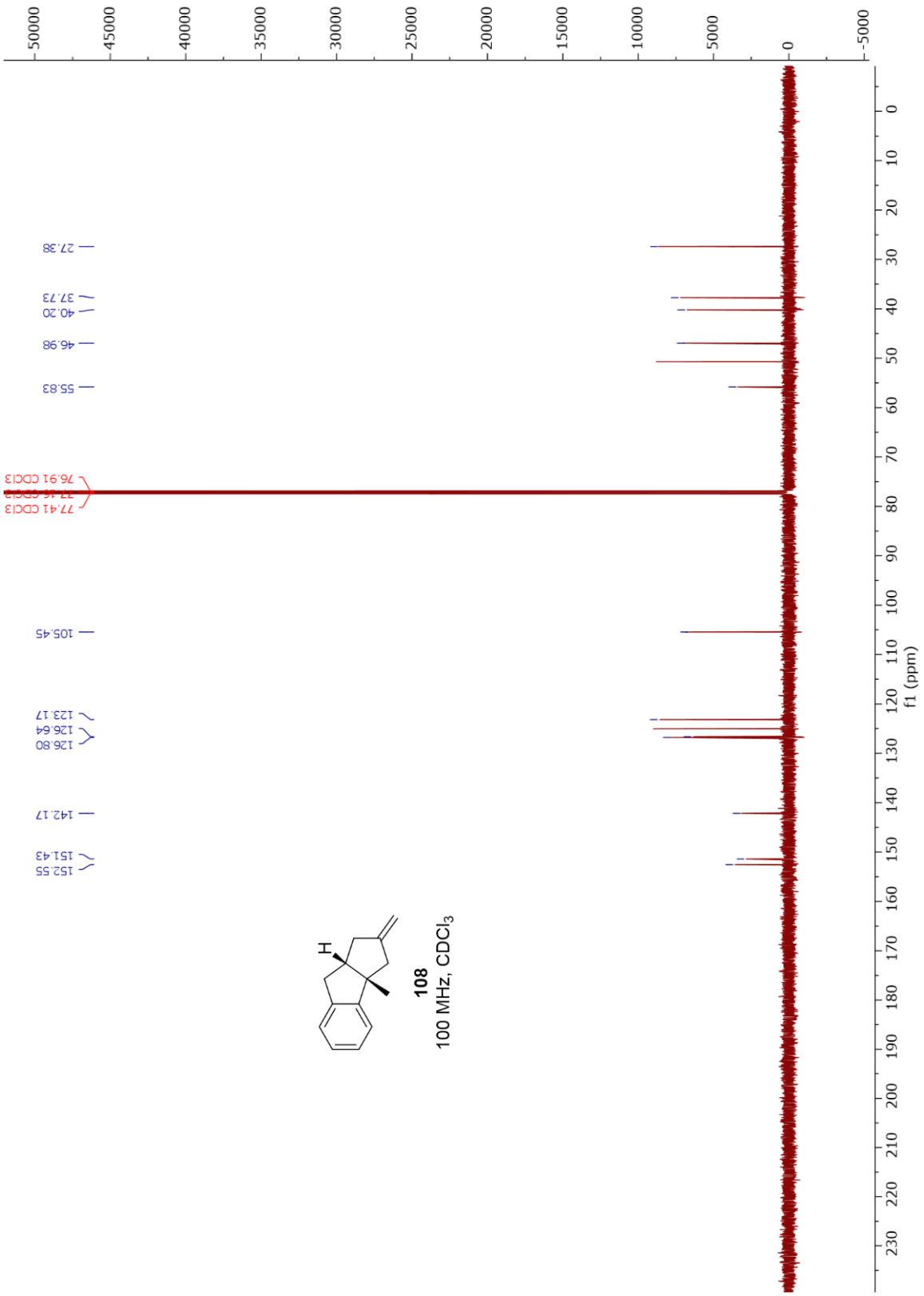
152.55
151.43
142.17
126.80
126.64
123.17
105.45
77.41 CDCl3
77.16 CDCl3
76.91 CDCl3
55.83
46.98
40.20
37.73
27.38
f1 (ppm)
108
100 MHz, CDCl3

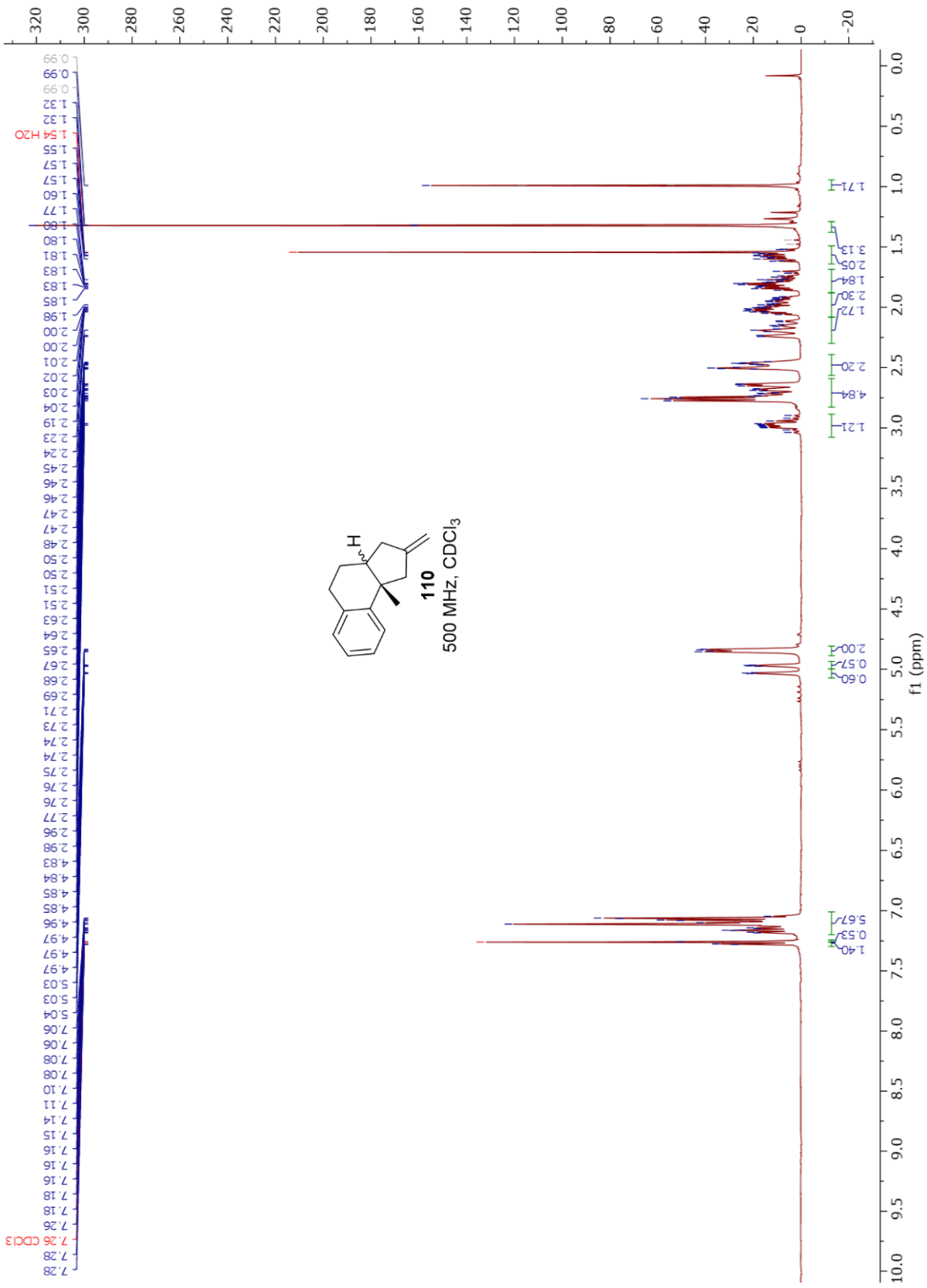
110
500 MHz, CDCl3
f1 (ppm)

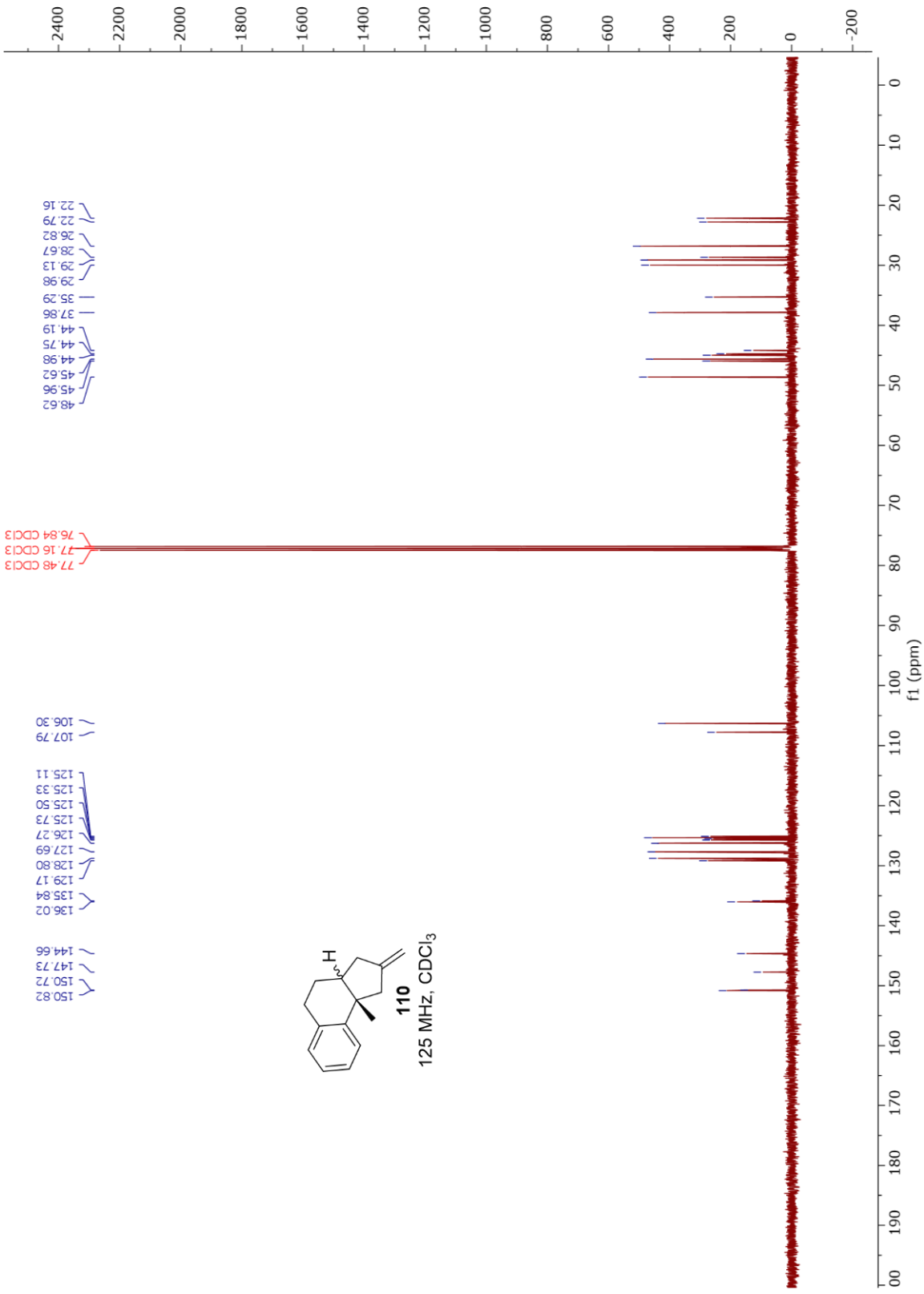
H
110
125 MHz, CDCl3
f1 (ppm)
77.48 CDCl3
77.16 CDCl3
76.84 CDCl3

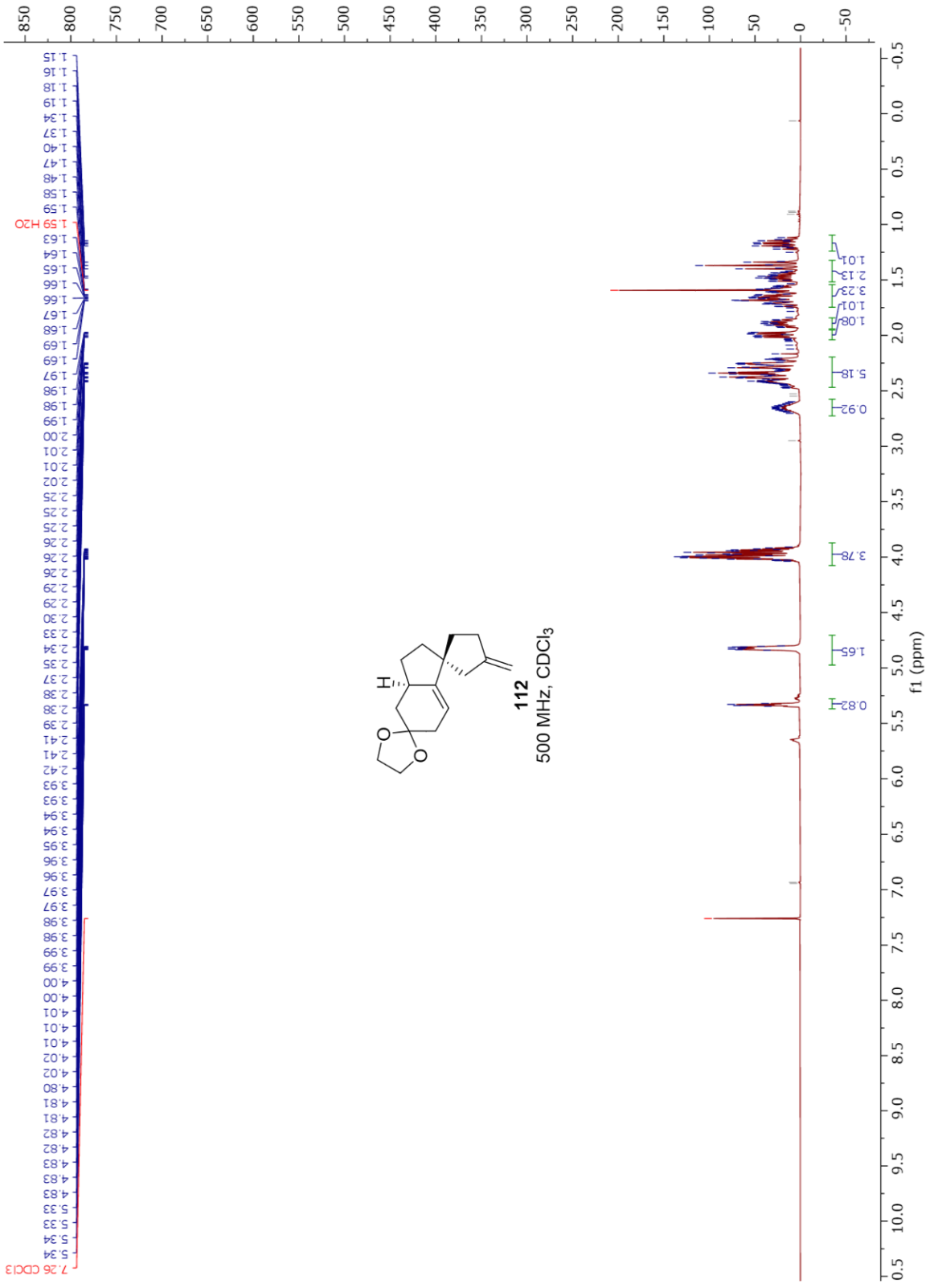
112
500 MHz, CDCl3
H
O
O
H2O
CDCl3
f1 (ppm)
1.01
2.13
3.23
1.01
1.08
5.18
0.92
3.78
1.65
0.82

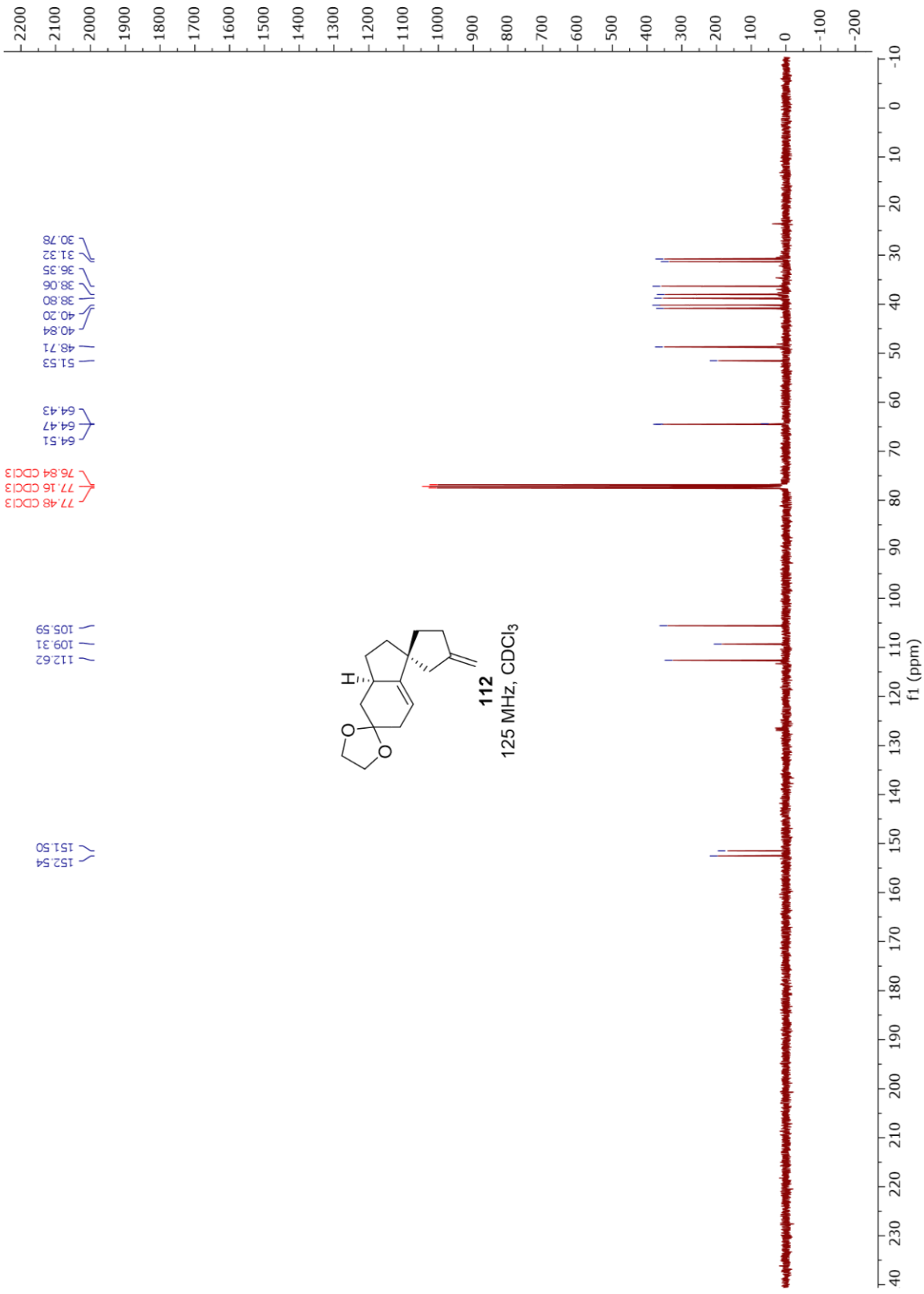
152.54
151.50
112.62
109.31
105.59
77.48 CDCl3
77.16 CDCl3
76.84 CDCl3
64.51
64.47
64.43
51.53
48.71
40.84
40.20
38.80
38.06
36.35
31.32
30.78
H
O
O
112
125 MHz, CDCl3
f1 (ppm)

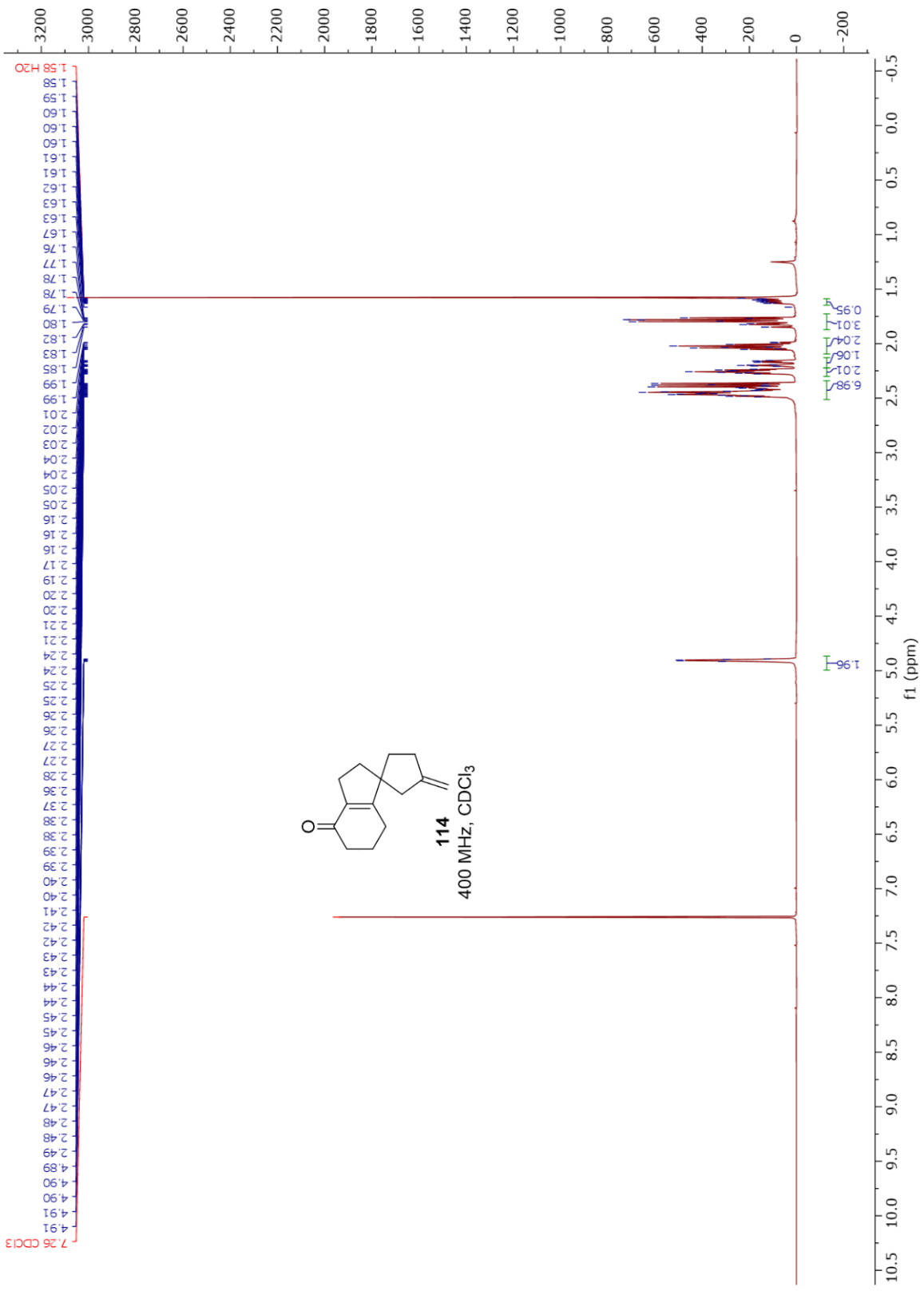
114
400 MHz, CDCl3
f1 (ppm)

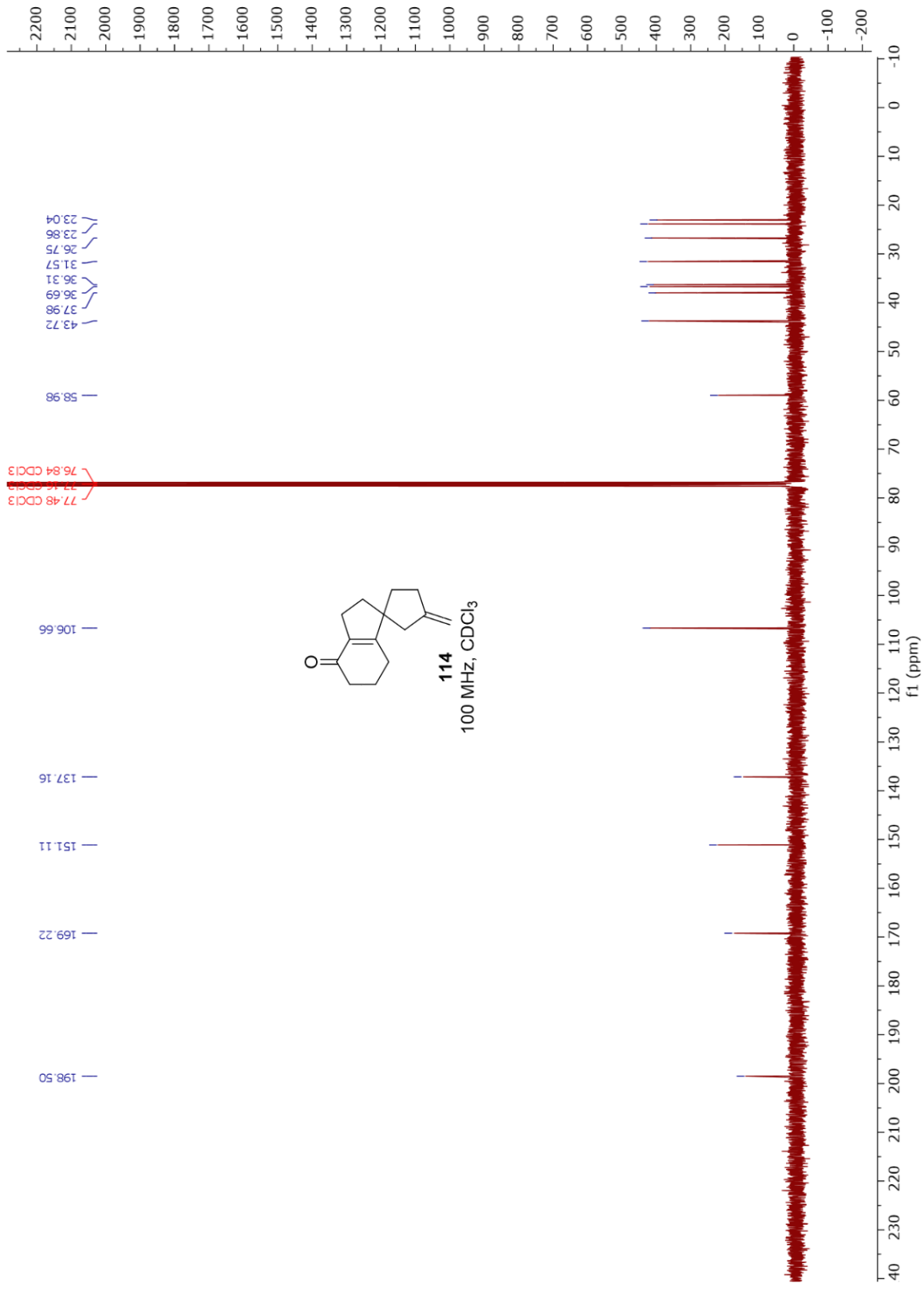
198.50
169.22
151.11
137.16
106.66
77.48 CDCl3
76.84 CDCl3
58.98
43.72
37.98
36.69
36.31
31.57
26.75
23.86
23.04
O
114
100 MHz, CDCl3
f1 (ppm)

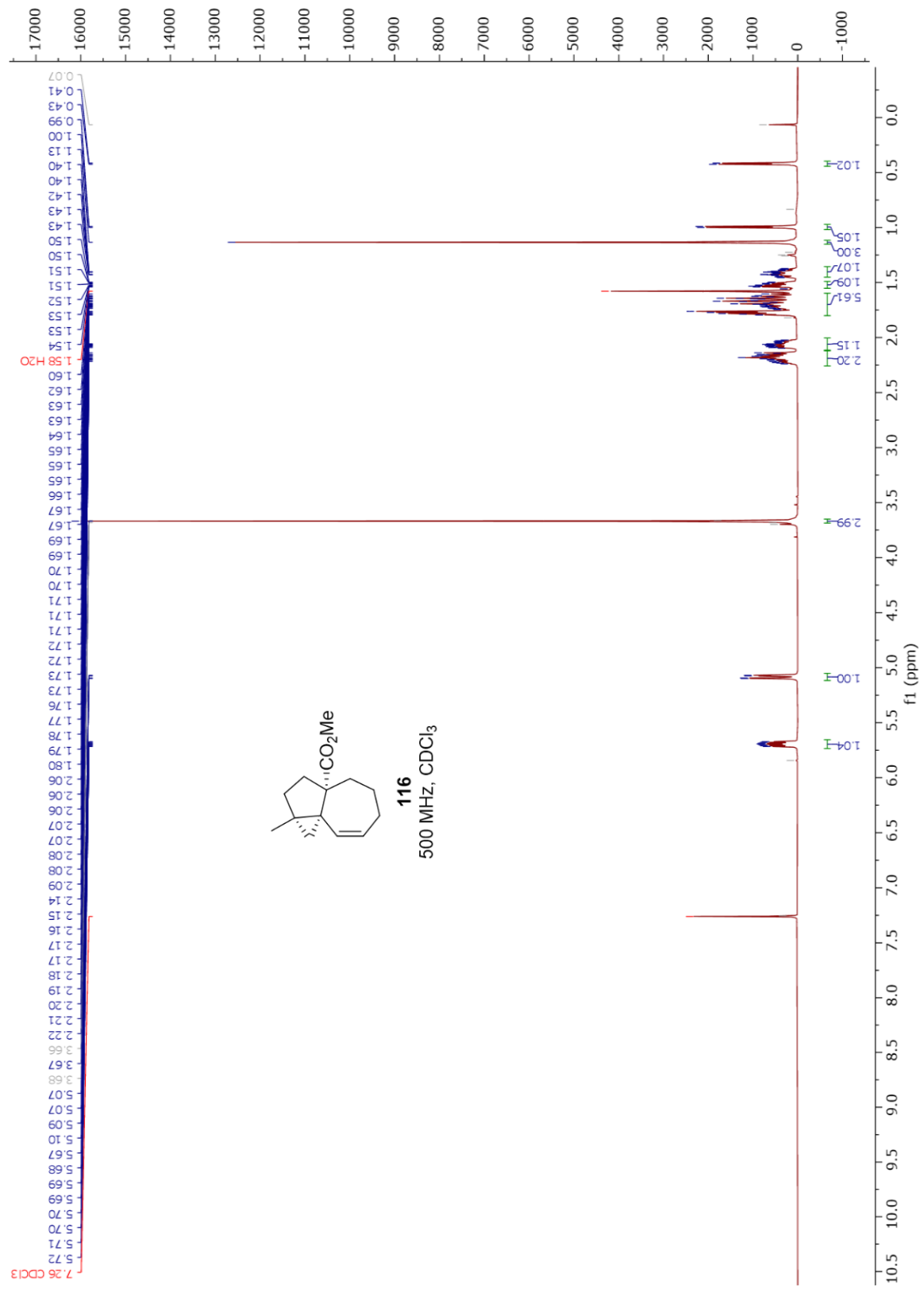
CO2Me
116
500 MHz, CDCl3
f1 (ppm)

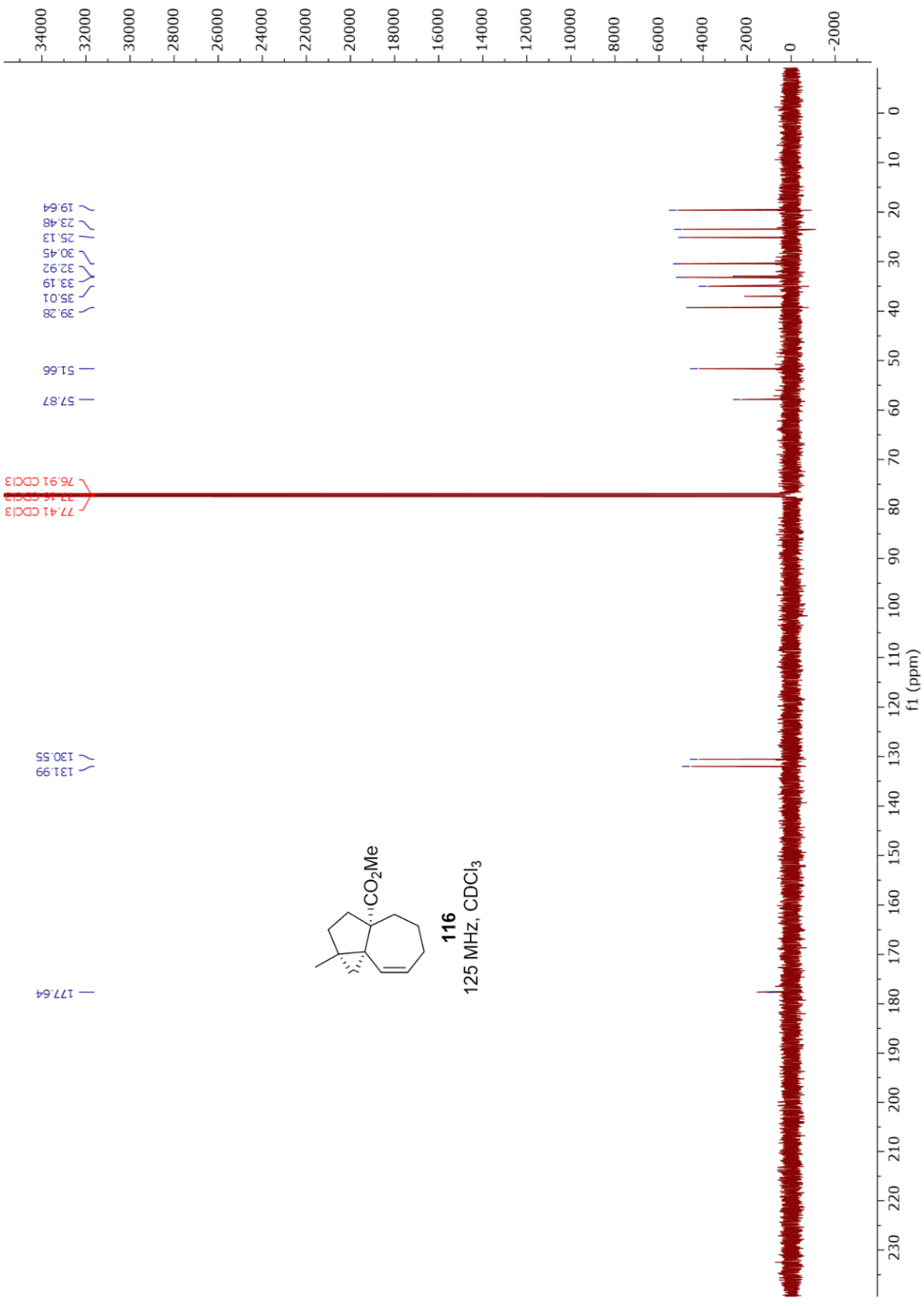
CO2Me
116
125 MHz, CDCl3
f1 (ppm)
177.64
131.99
130.55
77.41 CDCl3
76.91 CDCl3
57.87
51.66
39.28
35.01
33.19
32.92
30.45
25.13
23.48
19.64

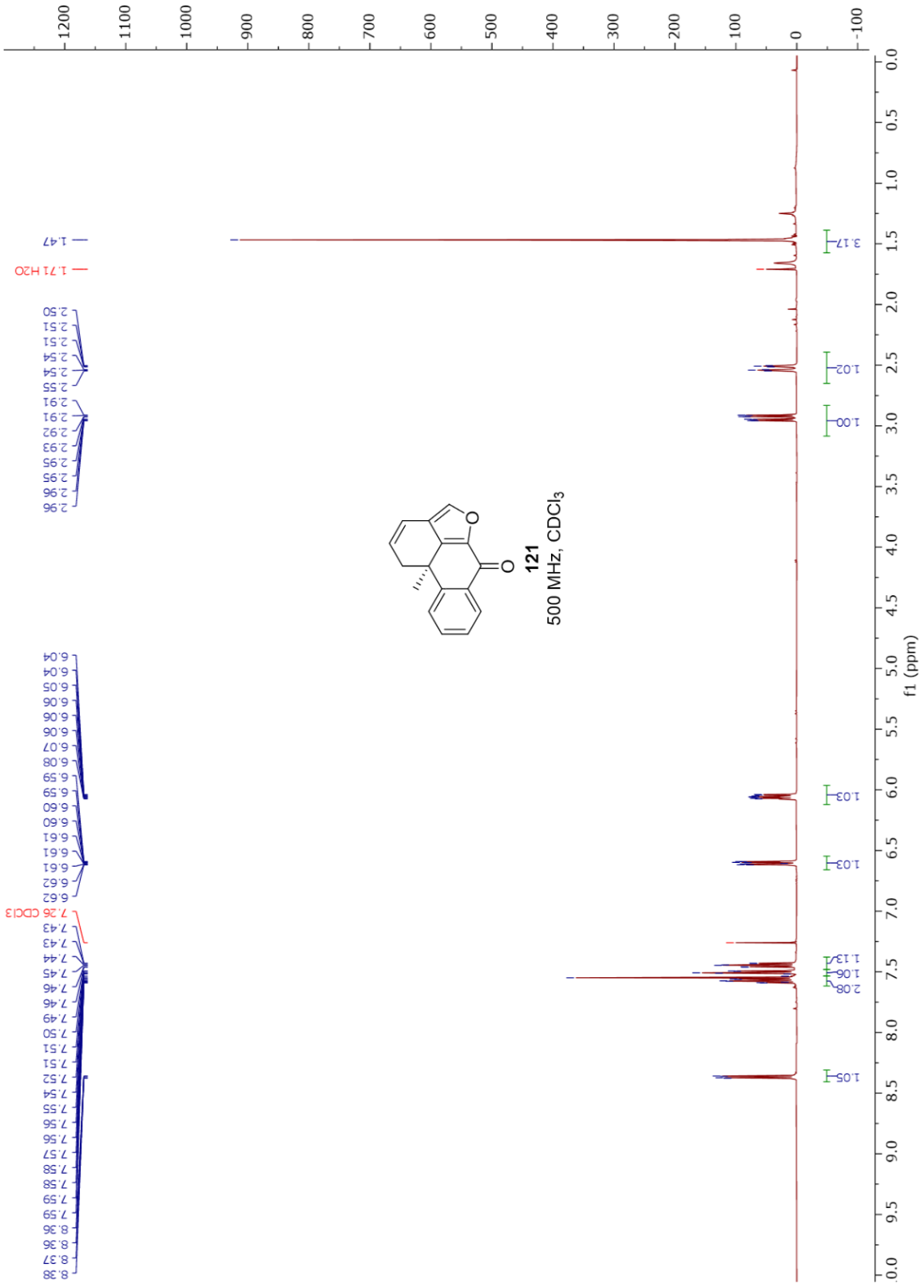
121
500 MHz, CDCl3
f1 (ppm)

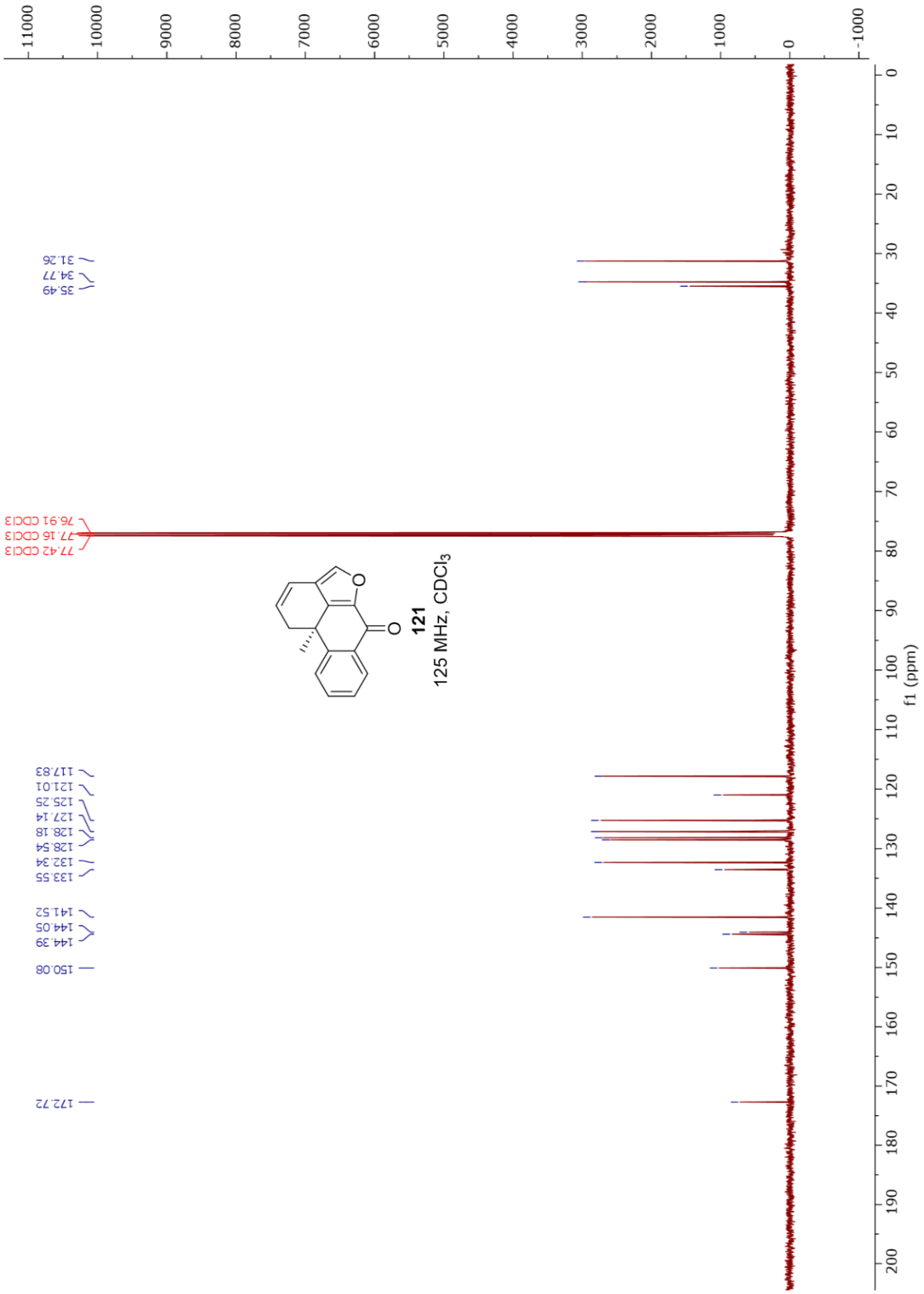
121
125 MHz, CDCl3
f1 (ppm)
77.42 CDCl3
77.16 CDCl3
76.91 CDCl3
35.49
34.77
31.26
133.55
132.34
128.54
128.18
127.14
125.25
121.01
117.83
144.39
144.05
141.52
150.08
172.72

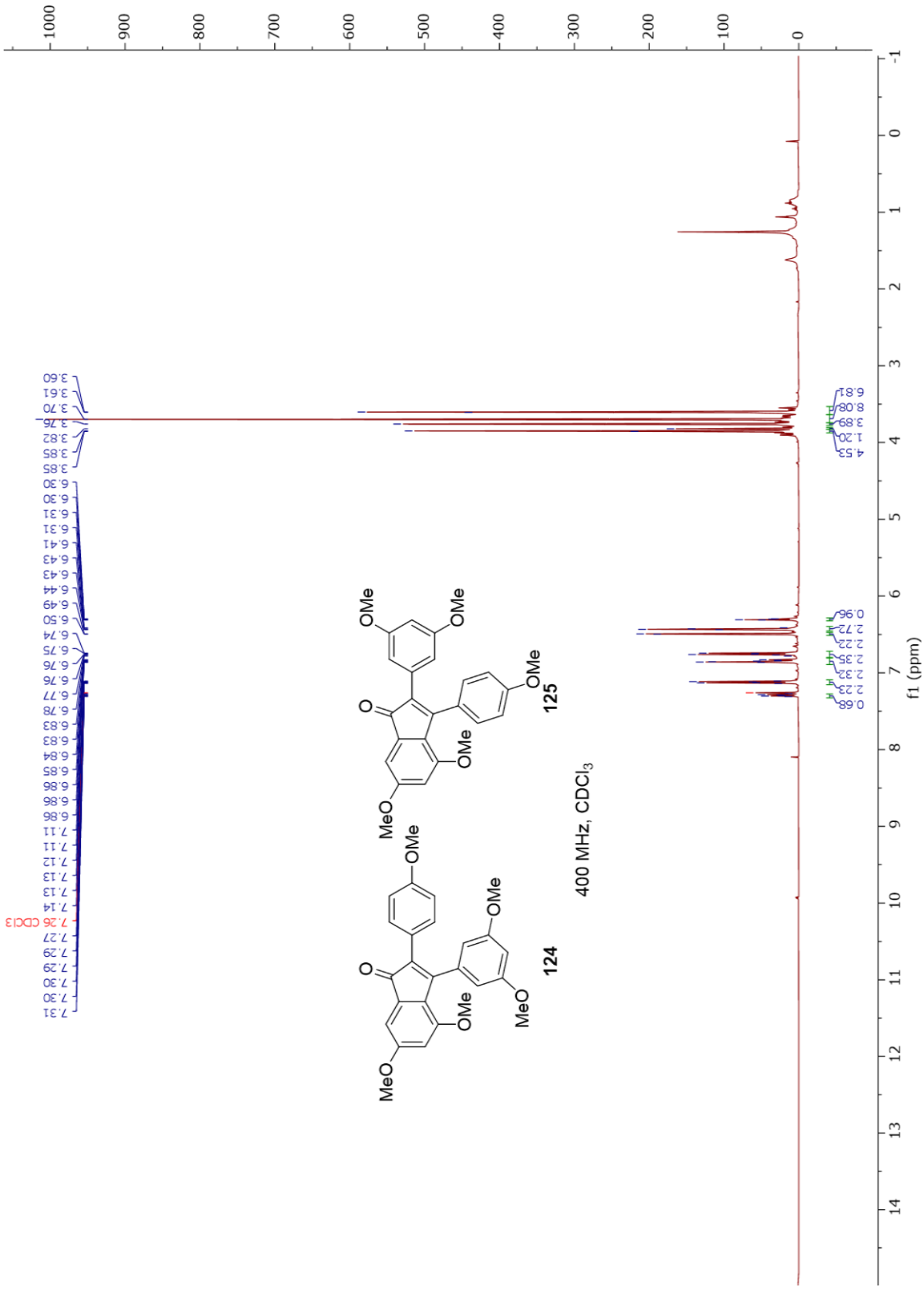
400 MHz, CDCl3
124
125
f1 (ppm)

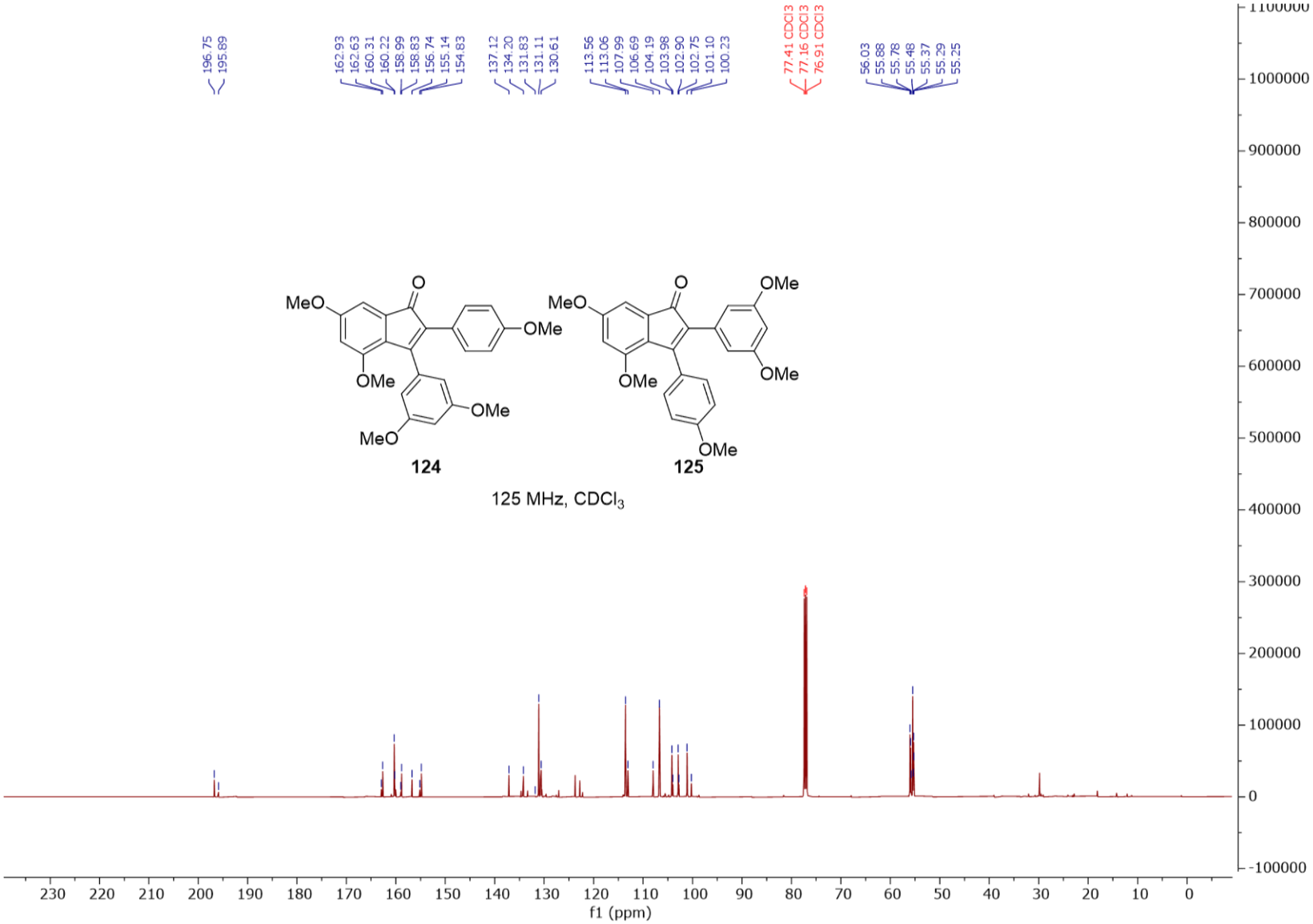
196.75
195.89
162.93
162.63
160.31
160.22
158.99
158.83
156.74
155.14
154.83
137.12
134.20
131.83
131.11
130.61
113.56
113.06
107.99
106.69
104.19
103.98
102.90
102.75
101.10
100.23
77.41 CDCl3
77.16 CDCl3
76.91 CDCl3
56.03
55.88
55.78
55.48
55.37
55.29
55.25
MeO
OMe
OMe
MeO
OMe
124
125
125 MHz, CDCl3
f1 (ppm)

Chapter 3

Intermolecular Nickel Heck Cascades

3.1 Intermolecular Heck Cascades

While a considerable amount of attention has been given to Heck cascades, much of that interest has been focused on intramolecular cascades.[1] This is likely because intramolecular cascades are less challenging to control as the geometric constraints of a molecule can facilitate highly predictable cascades. In contrast, intermolecular Heck cascades will inherently have access to multiple reaction pathways, which can render the design process quite challenging. As such, there are limited examples of such cascades. However, based on the success of the Larock annulation with our Ni-Heck conditions in the previous chapter, we were curious to see how Ni might behave in this context. One example that caught our eye was an intriguing variant first reported by the de Meijere group, which was later improved upon by the Zhou group as shown in

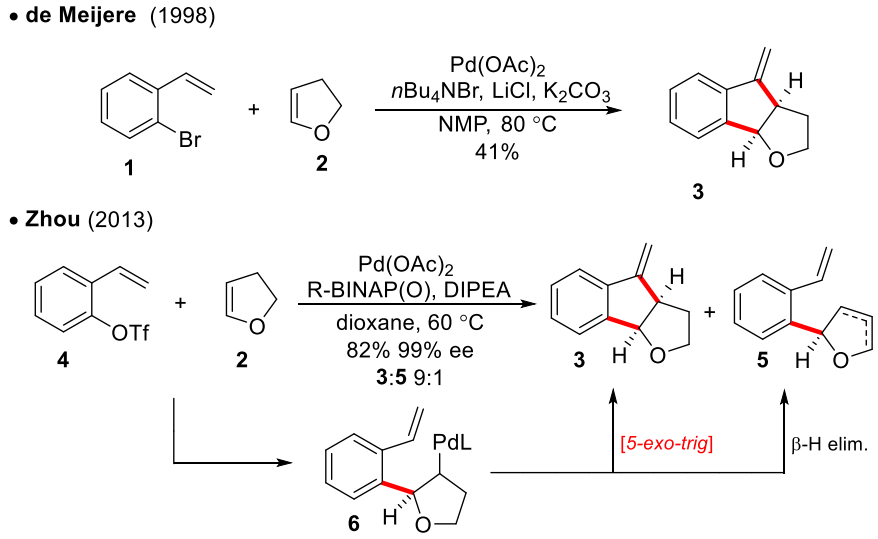

Scheme 3.1 Intermolecular Heck cascades by the de Meijere and Zhou groups.

Scheme 3.1.[2,3] In the initial report, the de Meijere group described the coupling of *o*-bromostyrene **1** and 2,3-dihydrofuran (DHF) **2** to give indene **3**. While the reaction is quite impressive, the report is limited to a handful of olefins coupling partners and generally proceeds in low to moderate yield. The Zhou group later investigated this cascade more deeply and in the

course of their studies they found that through the use of aryl triflate **4** and monophosphine oxide bidentate ligands, the reaction could be accomplished in not only high yield, but also excellent *ee*. In both cases, the reaction proceeds first by an intermolecular migratory insertion of the aryl Pd species into the olefin partner to arrive at the intermediate **6**. From there, the alkyl Pd species undergoes an intramolecular cyclization in a [5-*exo*-trig] fashion and following β-hydride elimination the observed indene product **3** is obtained. However, as the Pd in **6** possesses syn β-H a β-hydride elimination can occur, which can provide a mix of different alkene isomers **5**. In fact, this is the reason that the de Meijere example is run under ligand free conditions as the presence of a phosphine ligand was found to promote the β-hydride elimination event. The Zhou case also suffered from the formation of uncyclized products **5** in every example they reported. As Ni undergoes β-hydride elimination less readily than its congener, we felt that this cascade would be an excellent opportunity to see how both our conditions and Ni react to this challenging cascade reaction.

3.2 Discovery of the [6-Endo-Trig] Selectivity

To begin our studies on the intermolecular Heck cascade, aryl triflate **4** and *n*-butyl vinyl ether **7** were subjected to our standard base mediated Heck conditions at 60 ˚C. Pleasingly, we isolated the expected indene **8** arising from the [5-*exo*-trig] pathway in a 40% yield as well as 11% of an unidentified side product **9**. While the yield was modest, it was still comparable to that observed by the de Meijere group.[2] Enticed by the result, we then attempted the cascade with **4**. The overall yield was a modest 34%, but now the indene **3** was isolated in a 4.5:1 ratio favoring the product **10**, which appeared to be structurally related to **9**. Intrigued, we decided to attempt the reaction with yet another olefin, 1-octene **11**, and no indene **12** was observed at all. In fact,

the reaction gave product **13** in a 58% as the major product, with some minor formation of separable isomers. After subjecting **13** to a battery of NMR experiments, it was assigned as the

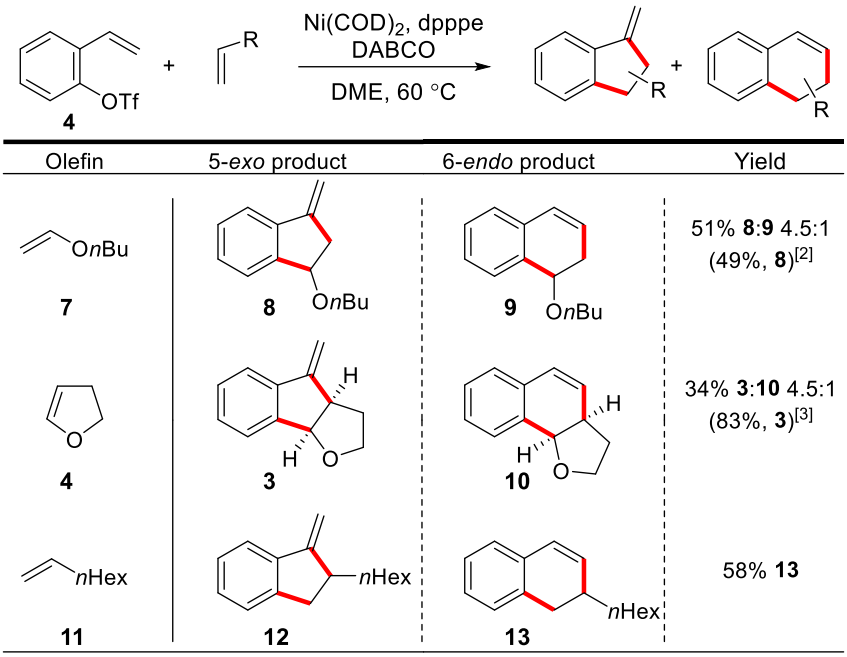

Table 3.1 Initial discovery of the 6-*endo* selectivity: Olefin (4.0 equiv.), $Ni(COD)_2$ (10 mol%), dpppe (12 mol%), DABCO (3.0 equiv.), DME (0.15 M), 60 °C, 5-20 hr.

dihydronaphthalene, which could arise from a [6-*endo*-trig] selective cyclization. **10** and **9** were subsequently assigned as the corresponding dihydronaphthalene products. These results were particularly exciting as this was our first example where Ni provides divergent reactivity to Pd in a Heck cascade. As such, we then subjected a variety of different olefins to the reaction to see how general the selectivity appeared to be. Use of styrene **14** or diphenylacetylene **17** only yielded the indene products **15** and **18** respectively. Given **11**'s apparent strong selectivity for dihydronaphthalene formation, we attempted the reaction with cyclopentene **29**, but neither [5-*exo*-trig] or [6-*endo*-trig] products were observed. Instead a complex mixture of unidentified products was found. As such, we attempted the reaction with norbornene **20** anticipating that the additional strain could render the olefin more reactive. Indeed, the reaction did proceed more smoothly, but indene **21** was favored over dihydronaphthalene **22** in a 15:1 ratio. N-Boc

dihydropyrrole **23** proved a very challenging substrate with only trace indene product **24** being observed in the reaction. The reaction was complicated by the need for a large excess of **23**,

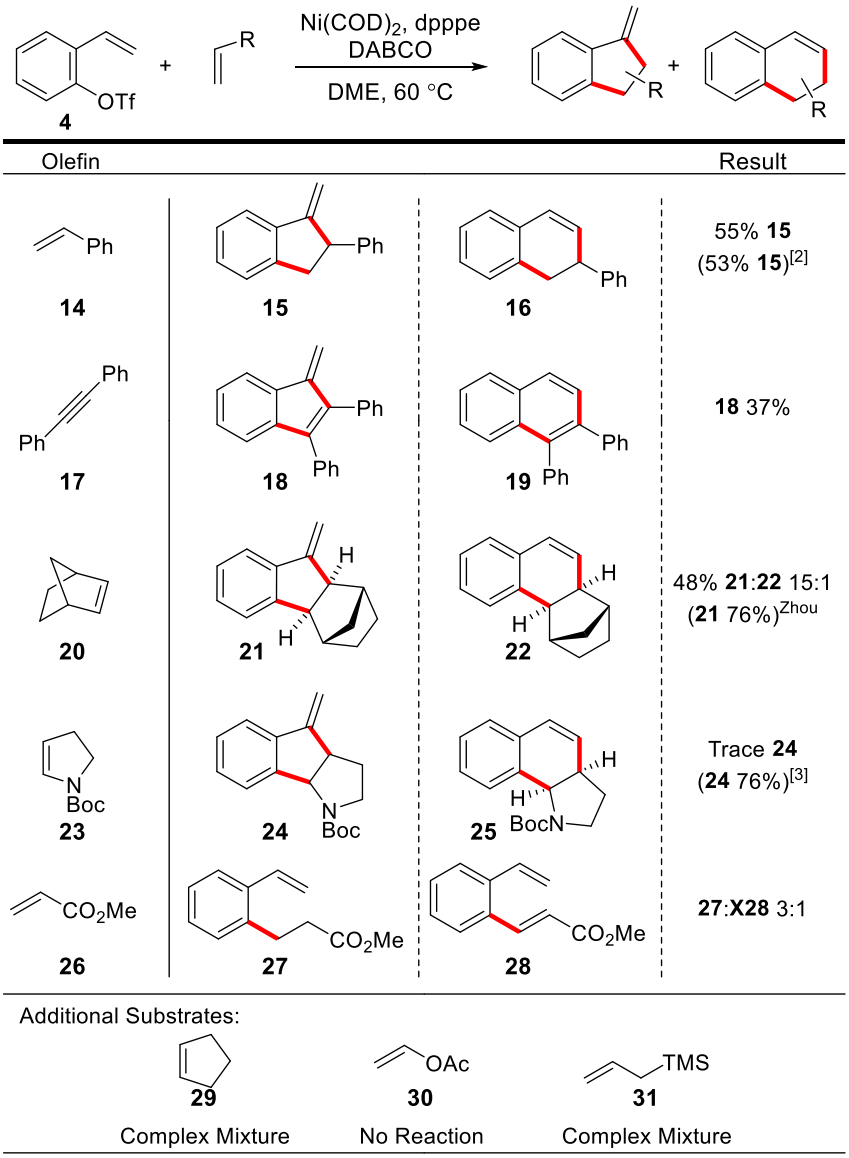

Table 3.2 Initial screening of olefin partners: Olefin (4.0 equiv.), $Ni(COD)_2$ (10 mol%), dpppe (12 mol%), DABCO (3.0 equiv.), DME (0.15 M), 60 °C, 20 hr.

which made the separation of any products challenging. While methyl acrylate **26** gave only uncyclized products, it was interesting to note that the reduced ester **27** was formed in a 3:1 ratio with the traditional Heck product **28**, which is indicative of Ni's recalcitrant β-hydride

elimination.[4,5] The reaction was also attempted with vinyl acetate **30** and allyl TMS **31**, but both proved to be ineffective similar to what the Skrydstrup group reported.[6]

3.3 Optimization for Dihydronaphthalene Formation

While our first results were promising, further screening of the olefin coupling partner indicated the cascade is quite sensitive to any perturbation in the coupling partners. As such, we decided to try to optimize the reactions with **2** and **7** for dihydronaphthalene formation to develop a better understanding of the factors controlling the cascade. As **2** has proceeded with formation of both the indene and dihydronaphthalene, but favoring the latter, we decided to begin our optimizations with it. Our first step was to screen a variety of phosphine ligands to see if any general trends similar to those observed in the intramolecular cascades could be surmised. Looking at Table 3.3, some dependence on bite angle is apparent, with dppb giving **10** as the sole product of the reaction in a 29% yield. Decreasing the linker length in the ligand gave lower yields, but quite intriguingly, increasing the linker length leads to the formation of **3** as well as its

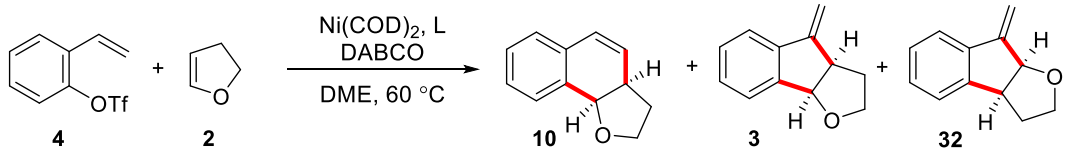

4 **2** **10** **3** **32**

L	**4** Conversion[a]	**10** Yield[a]	**3** Yield[a]	**32** Yield[a]
dppe	100%	22%	0%	0%
dppp	100%	25%	0%	0%
dppb	100%	29%	0%	0%
dpppe	100%	21%	4%	5%
dpphex	72%	15%	4%	4%
R-BINAP	72%	12%	0%	0%
R-BINAP(O)	56%	2%	0%	0%
DPEPhos	45%	0%	0%	0%
Xantphos	43%	0%	0%	0%

Table 3.3 Ligand screening for intermolecular cascade with DHF: [a]Determined by ^{1}H NMR using methyl 3,5-dinitrobenzoate as an internal standard; **2** (4.0 equiv.), $Ni(COD)_2$ (10 mol%), L (12 mol%), DABCO (3.0 equiv.), DME (0.3 M), 60 °C, 20 hr.

regioisomer **32**. The formation of **32** is rather interesting as the reaction is proceeding via the cationic pathway, which is reported to be highly selective for α-selective additions into electron

rich olefins.[7,8] Other ligands fared less well with only *R*-BINAP giving any appreciable product formation, while the corresponding mono phosphine oxide *R*-BINAP(O), which had been key to the Zhou group's report, gave poor conversion and trace **10**.[3] Further, it is intriguing that DPEPhos performs so poorly, even though it was almost interchangeable with dpppe in the intermolecular cascades.

With an optimal ligand chosen, we turned to investigating the effect of the conditions of the reaction. As the reaction proceeds via an intermolecular step, we were curious to see what effect varying the concentration would have upon the reaction. Somewhat surprisingly, there was only a very mild effect observed even when varying the concentration from 0.05 M to 0.5 M as shown in Table 3.4. In fact, the only major difference that was observed was that the reaction

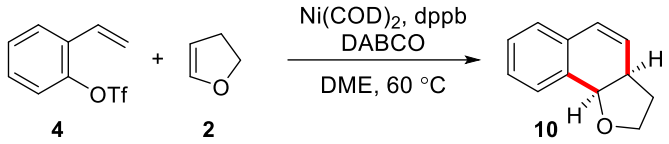

4 **2** **10**

[M]	t (hr)	**10** Yield[a]
0.05	20	24%
0.1	3	23%
0.15	3	24%
0.2	3	24%
0.3	3	25%
0.5	3	31%

Table 3.4 Concentration screening for intermolecular cascade with DHF: [a]Determined by ^{1}H NMR using methyl 3,5-dinitrobenzoate as an internal standard; **2** (4.0 equiv.), $Ni(COD)_2$ (10 mol%), dppb (12 mol%), DABCO (3.0 equiv.), DME (0.3 M), 60 °C.

became considerably slower when run at dilute concentrations. The reaction proved much more sensitive to variation of the **2** equivalents with the yield increasing up to 54% when 40 equivalents were used, as shown in Table 3.5. This would seem to suggest that a competing pathway proceeds more quickly than our desired intermolecular migratory insertion, but this will be discussed in more detail later in this chapter. Neither loading of Ni or ligand appeared to have much effect on the reaction. However, running the reaction at 23 ˚C saw a marked improvement in the yield

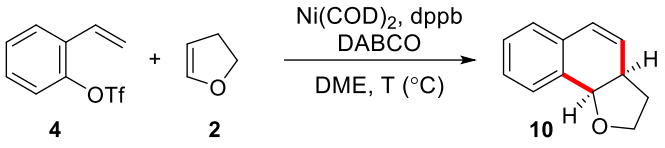

4 **2** **10**

2 equiv.	Ni mol%	dppb mol%	T (°C)	**10** Yield[a]
2	10	12	60	16%
4	10	12	60	24%
10	10	12	60	38%
20	10	12	60	46%
40	10	12	60	54%
4	2.5	12	60	25%
4	5	12	60	25%
4	20	12	60	22%
4	10	20	60	20%
4	10	12	23	45%

Table 3.5 Further condition screening for intermolecular cascade with DHF: [a]Determined by ^{1}H NMR using methyl 3,5-dinitrobenzoate as an internal standard; **2** (4.0 equiv.), $Ni(COD)_2$ (10 mol%), dppb (12 mol%), DABCO (3.0 equiv.), DME (0.3 M), 60 °C.

giving **10** in 45% yield and with a much cleaner reaction profile. Given that **4** is potentially temperature sensitive, it is possible that the low yield is due to decomposition of the styrene starting material. However, running the reaction without the Ni catalyst, no conversion was observed even after heating for 20 hr, which suggests thermal decomposition is not operative under these conditions.

With these results in hand, our attention turned to **7** to see how general these observations may be. Indeed, during the ligand screening, the dppe-dpphex family of ligands performed similarly with dppp and dppb giving the best yields while dpppe and dpphex promoted the [5-*exo*-trig] pathway. However, in this case we also observed a significant amount of uncyclized product **33**, which was not observed with **2**. The formation of the uncyclized product seemed to be the defining issue for **7** as even with the best ligand, *R*-BINAP, the uncyclized product was still formed in a 16% yield. This proclivity for β-hydride elimination could be due to C-C bond rotation moving the Ni such that it is no longer close to the styrene, thus giving more time for interaction with the highly activate benzylic position. Next, we attempted the cascade with **7** at high concentration and

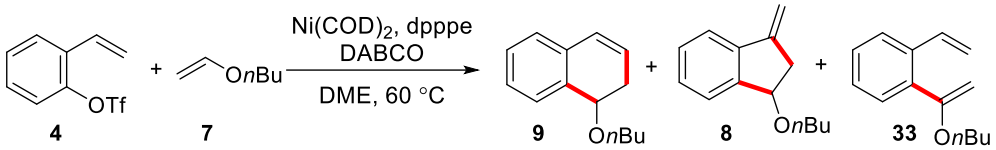

L	**9** Yield[a]	**8** Yield[a]	**33** Yield[a]
dppe	6%	0%	39%
dppp	19%	0%	30%
dppb	18%	0%	59%
dpppe	11%	40%	25%
dpphex	4%	19%	1%
R-BINAP	36%	0%	16%
R-BINAP(O)	0%	0%	0%
DPEPhos	0%	0%	0%
Xantphos	0%	0%	0%

Table 3.6 Ligand screening for intermolecular cascade with *n*-butyl vinyl ether: [a]Determined by ^{1}H NMR using methyl 3,5-dinitrobenzoate as an internal standard; **7** (4.0 equiv.), $Ni(COD)_2$ (10 mol%), L (12 mol%), DABCO (3.0 equiv.), DME (0.3 M), 60 °C.

23 ˚C and pleasingly, **9** was formed in a 54% yield. Intriguingly, the yield of **33** also increased and we now observed the formation of a small amount of **8**. Further attempts to increase the yield by increasing the equivalents of **7** proved ineffective with essentially no variation in yield even

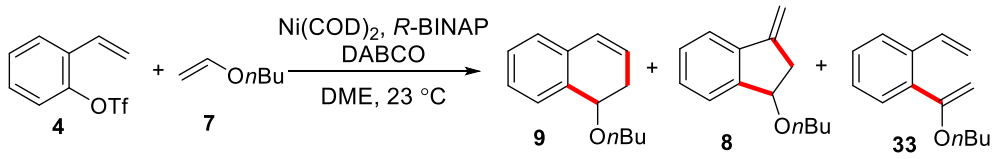

7 equiv.	**9** Yield[a]	**8** Yield[a]	**33** Yield[a]
10	54%	6%	25%
20	53%	6%	27%
40	51%	7%	33%

Table 3.7 Equivalents screening for intermolecular cascade with *n*Butyl vinyl ether: [a]Determined by ^{1}H NMR using methyl 3,5-dinitrobenzoate as an internal standard; $Ni(COD)_2$ (10 mol%), *R*-BINAP (12 mol%), DABCO (3.0 equiv.), DME (0.5 M), 23 °C.

when 40 equivalents were used. While some slightly similar trends are observed for both **2** and **7**, it appears that each olefin is likely to require screening to identify an optimal ligand as well as further screening to address any issues unique to that partner.

3.4 Current Scope of Base-Mediated Intermolecular Heck Cascade

From here, we decided to conduct a brief survey of the scope of the reaction with our current conditions. The previously successful olefins, **2**, **7**, and **11** performed well, all now giving

either high or exclusive selectivity for the [6-*endo*-trig] dihydronaphthalene products. Additionally, we found that further increasing the concentration of the reaction gave a slight

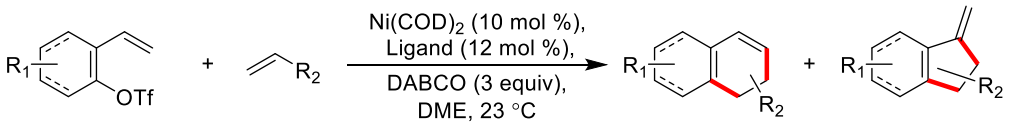

Entry	OTf	Partner	Ligand	6-*Endo* Product	5-*Exo* Product	Yield
1	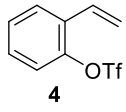 **4**	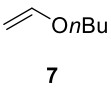 **7**	BINAP	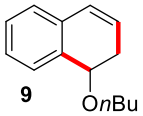 **9**	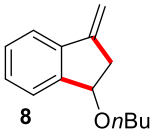 **8**	**9** 60%, **8** 5% (**8** 49%)[2]
2[a]	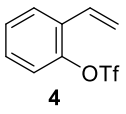 **4**	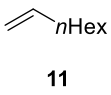 **11**	dpppe	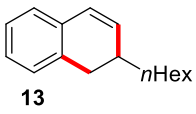 **13**	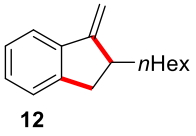 **12**	**13** 58%
3	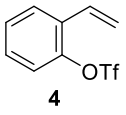 **4**	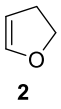 **2**	dppb	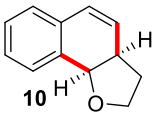 **10**	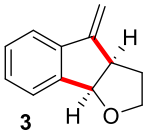 **3**	**10** 61% (**3** 83%)[3]
4	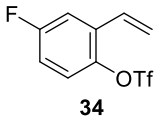 **34**	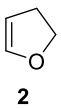 **2**	dppb	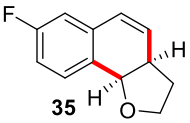 **35**	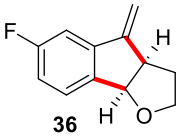 **36**	**35** 52% (**36** 80%)[3]
5	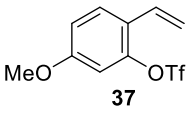 **37**	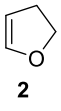 **2**	dppb	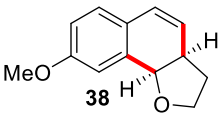 **38**	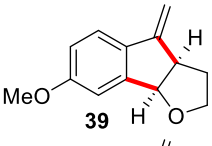 **39**	**38** 59% (**39** 67%)[3]
7	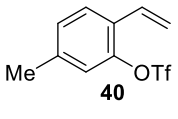 **40**	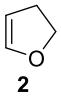 **2**	dppb	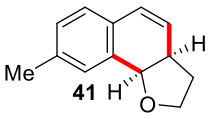 **41**	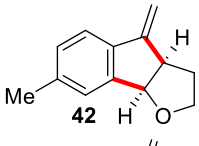 **42**	**41** 62%
8	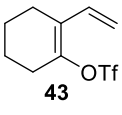 **43**	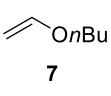 **7**	dpppe	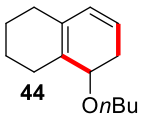 **44**	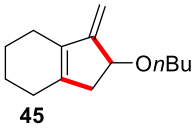 **45**	**45** 27%
9	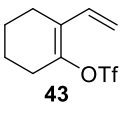 **43**	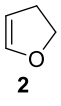 **2**	dpppe	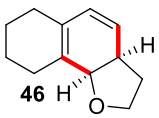 **46**	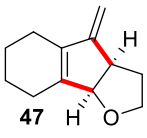 **47**	**48** 23%

Table 3.8 6-*endo* selective intermolecular cascade under base promoted conditions: [a] Reaction performed at 60 °C; Olefin (10 equiv.), $Ni(COD)_2$ (10 mol%), L (12 mol%), DME (1 M), 23 °C, 4 - 12 hr.

increase in the yield with **9** and **10** now being obtained in 60% and 61% yield respectively. The reaction also proved to be tolerant of variation in the aryl coupling partner, with F, Me, and OMe substituents all giving dihydronaphthalene products in good yield. We also investigated the use of vinyl triflate **43**, but only [5-*exo*-trig] products **45** and **47** were observed even after extensive screening of alternative phosphine ligands. While not the desired [6-*endo*-trig] product, **45** is notable for the apparent β-selectivity of the initial Heck reaction, which is unusual for cationic Heck reactions.[7,8]

3.5 Outlook of the Base-Mediated Intermolecular Heck Cascade

While we had achieved considerable improvements in the conditions for both yield and selectivity, our feeling at this point was that the base mediated conditions were non optimal for this particular application. For one, a major goal of this project was to render the reaction enantioselective and our attempts with **7** and *R*-BINAP only yielded a 19% *ee*. This, coupled with the challenges we observed with enantioselectivity in the previous chapter, led us to wonder if a different reaction manifold may prove more effective. The most obvious alternative is the reducing metal approach.[9–11] These would allow us to not only use chiral phosphine ligands,[12,13] but also nitrogen based ligands such as the bisoxazoline (BOX) ligand family, which has been widely used and highly effective in Ni catalysis.[10] In the hopes of achieving an effective, general, and ultimately enantioselective intermolecular Heck cascade, we turned our attention to this new approach.

3.6 Racemic Reducing Metal Condition Optimization

As a starting point for our study, we decided to utilize Garg's conditions, and then briefly screened a number of reaction conditions, examining the halide coupling partner, Ni precatalyst,

use of a nitrogen ligand, and reductant.[9] From this initial assessment, the literature conditions with $NiCl_2(PnBu_3)_2$ and aryl bromide **1** proved best giving the desired dihydronaphthalene **10** in a 49% yield with no indene **3** product observed. In fact, no **3** was observed in any of the conditions showing selectivity was maintained even after switching to the neutral Heck mechanism.

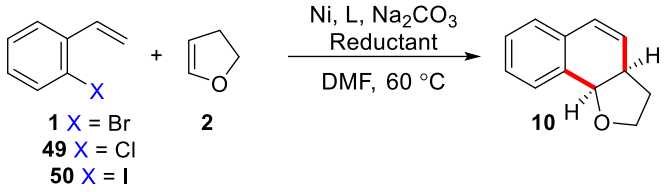

1 X = Br
49 X = Cl
50 X = I

2

10

X	Ni source	L	Reductant	Yield[a]
Br	$NiCl_2(PnBu)_2$	-	Mn	49%
Br	$NiCl_2(PnBu)_2$	-	Zn	0%
Br	$NiCl_2$(DME)	1,10-phen	Mn	9%
Br	$NiCl_2$(DME)	1,10-phen	Zn	1%
Cl	$NiCl_2(PnBu)_2$	-	Mn	0%[b]
Cl	$NiCl_2$(DME)	1,10-phen	Mn	23%
I	$NiCl_2(PnBu)_2$	-	Mn	29%
I	$NiCl_2$(DME)	1,10-phen	Mn	22%

Table 3.9 Initial screening for racemic reducing metal conditions:[a]Isolated yields, [b]No reaction; **2** (10 equiv.), Ni (10 mol%), L (12 mol%), Reductant (3.0 equiv.), Na_2CO_3 (3.0 equiv.), DMF (0.3 M), 60 °C, 20 hr.

Next, we screened a veritable cornucopia of solvents. In line with literature reports, highly polar amide-based solvents proved to be the most effective, but DMF remained the optimal solvent. It should be noted that this reaction is very sensitive to the presence of water. Generally,

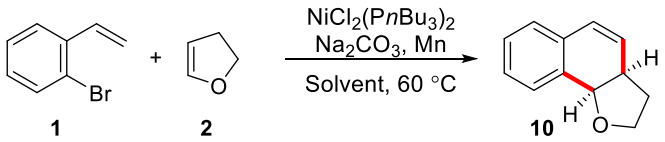

1

2

10

Solvent	Yield[a]	Solvent	Yield	Solvent	Yield
DMF	49%	DMSO	0%[b]	MeCN	0%[b]
DMA	42%	MeOH	0%[b]	ethyl acetate	0%[b]
NMP	43%	DME	0%[b]	toluene	0%[b]
DMPU	19%	dioxane	0%[b]	-	0%

Table 3.10 Solvent screen for racemic conditions:[a]Isolated yield, [b]No reaction; **2** (10 equiv.), $NiCl_2(PnBu_3)_2$ (10 mol%), Mn (3.0 equiv.), Na_2CO_3 (3.0 equiv.), Solvent (0.3 M), 60 °C, 20 hr.

our optimal results were achieved with solvents that contained <5 ppm H_2O as measured by Karl Fischer titration. Reactions run in degassed DMF with ~30 ppm H_2O, comparable to commercial anhydrous grade solvent, suffered a 10-20% decrease in yield. This sensitivity also extended to the reagents, and most of the olefin coupling partners were distilled prior to use to limit the water content of the reaction.

Following the solvent screen, we examined a collection of ligands. Intriguingly, while the commercial precatalyst $NiCl_2(PnBu_3)_2$ gives a 49% yield, use of $NiCl_2$(DME) and $PnBu_3$ only gave a 7% yield and had to be run at 100 ˚C for any conversion to be observed. As both the solutions of $NiCl_2(PnBu_3)_2$ and the $NiCl_2$(DME) and $PnBu_3$ mixture were visually indistinguishable, it would appear that the free ligand is able to form at the very least a similar complex, so it is unclear what exactly led to this issue. We suspected our commercial sample of $PnBu_3$ may have decomposed in some fashion, but when $NiCl_2(PnBu_3)_2$ was prepared freshly using the same bottle of $PnBu_3$ slightly superior yields to the commercial precatalyst were observed.

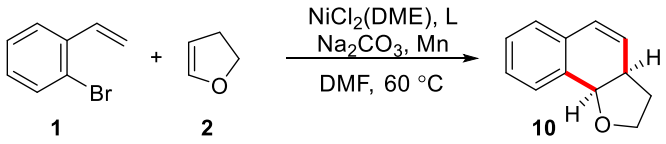

1 **2** **10**

L	**10** Yield[a]	L	**10** Yield[a]	L	**10** Yield[a]
$PnBu_3$	7%[b]	dppe	2%[b]	BINAP	7%
PPh_3	40%	dppp	3%[c]	DPEPhos	36%
PCy_3	29%[c]	dppb	10%[c]	Xantphos	9%[c]
P(2-furyl)$_3$	21%[c]	dpppe	9%[c]	DPPF	17%
$P(OPh)_3$	15%[c]	dpphex	10%[c]	bipy	4%

Table 3.11 Ligand screen for racemic conditions:[a]Determined by ^{1}H NMR using methyl 3,5-dinitrobenzoate as an internal standard, [b]Run at 100 °C, [c]Run at 80 °C; **2** (10 equiv.), $NiCl_2$(DME) (10 mol%), monodentate ligand (20 mol%) or bidentate ligand (12 mol %), Mn (3.0 equiv.), Na_2CO_3 (3.0 equiv.), DMF (0.3 M), 60 °C, 20 hr.

Besides $PnBu_3$, monodentate ligands generally outperformed bidentate ligands, though DPEPhos did provide the second-best yield of the ligands investigated. While yields were low in many cases and many reactions required 80 ˚C or even 100 ˚C for conversion to occur, it is worth noting that

no [5-*exo*-trig] product was observed in any case. Furthermore, the consistently exclusive α-selectivity in the initial Heck coupling is notable when our earlier cationic conditions had issues on more than one occasion.

Both for optimization purposes and in an effort to address the observed peculiar behavior of our $NiCl_2(DME)$/*n*PBu_3 system, we turned to screening various Ni sources for the reaction. As P*n*Bu_3 fared poorly as the free ligand, PPh_3 was chosen as the standard ligand in cases where the precatalyst lacks phosphine ligands. It should be noted that, while in the previous chapter the number of potential Ni sources was limited to Ni^0 species, using the reducing metal conditions now allows for the use of essentially any Ni^{II} salt. We were also curious to see if any of the Ni

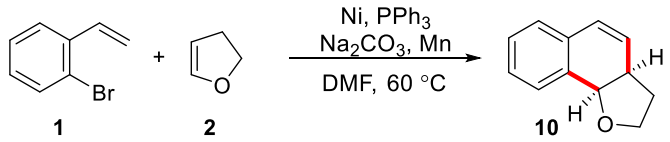

1 **2** **10**

Ni	**10** Yield[a]	Ni	**10** Yield[a]	Ni	**10** Yield[a]
$NiCl_2$(dppp)	9%	$NiBr_2$	0%[c]	$Ni(OAc)_2•4H_2O$	0%[b]
$NiCl_2(PPh_3)_2$	32%	$NiCl_2$	26%	$Ni(acac)_2$	0%[b]
$NiBr_2(PPh_3)_2$	30%	$NiCl_2•6H_2O$	29%	$Ni(PPh_3)_4$	23%
(*R*-BINAP)Ni(*o*-tolyl)Cl	18%	NiI_2	0%[c]	$Ni(COD)_2$	35%
$NiBr_2$(DME)	34%	NiF_2	0%[c]	$Ni(stb^F)_3$	30%

Table 3.12 Ni source screen for racemic conditions:[a]Determined by ^{1}H NMR using methyl 3,5-dinitrobenzoate as an internal standard, [b]Run at 100 °C, [c]Run at 80 °C; **2** (10 equiv.), Ni (10 mol%), PPh_3 (20 mol%), Mn (3.0 equiv.), Na_2CO_3 (3.0 equiv.), DMF (0.3 M), 60 °C, 20 hr.

sources with phosphine ligands already bound would see a similar increase in yield as seen with $NiCl_2(P$*n*$Bu_3)_2$ compared to $NiCl_2$(DME) and P*n*Bu_3. While $NiCl_2$(dppp) and the Jamison precatalyst (*R*-BINAP)Ni(*o*-tolyl)Cl did outperform their corresponding free ligand, the effect was not as pronounced as with P*n*Bu_3. Furthermore, PPh_3 and $NiCl_2$(DME) gave a higher yield than either $NiCl_2(PPh_3)_2$ or $NiBr_2(PPh_3)_2$ indicating that the effect is ligand specific rather than general and would need to be identified empirically. It is interesting to note that NiX_2(DME) salts performed much better than the corresponding NiX_2, perhaps due to differential solubility

properties. Somewhat remarkably, $NiCl_2$•$6H_2O$ was modestly competent in the reaction, which was surprising given the previously observed sensitivity of the reaction to H_2O content. Ni^0 sources also performed well giving product in only slightly lower yield compared to the best Ni^{II} salts.

For the next screening, we examined the effect of Ni loading, concentration, temperature, and **2** equivalents. The reaction was relatively insensitive to the Ni loading with 5 mol% only giving a 5% lower yield than our standard conditions and 20 mol% showing an almost identical yield. Similar to the base-mediated conditions, the reaction was also insensitive to concentration with the only variation being an 8% drop in yield at 0.05 M. Temperature proved to be more crucial, as unlike our previous conditions, the reaction with **2** requiring elevated temperatures with

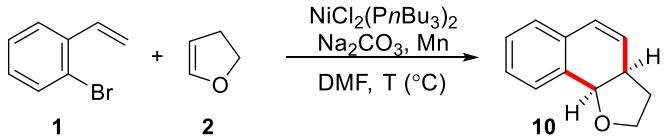

1 **2** **10**

Ni mol%	[M]	T (°C)	**2** equiv.	**10** Yield[a]
2.5	0.3	60	10	0%
5.0	0.3	60	10	34%
10	0.3	60	10	39%
20	0.3	60	10	40%
10	0.05	60	10	32%
10	0.1	60	10	40%
10	0.5	60	10	41%
10	0.3	50	10	13%
10	0.3	70	10	43%
10	0.3	60	2	33%
10	0.3	60	5	39%
10	0.3	60	20	47%
10	0.3	60	40	41%

Table 3.13 Further condition screening for racemic conditions:[a]Determined by ^1H NMR using methyl 3,5-dinitrobenzoate as an internal standard; **2**, $NiCl_2(PnBu_3)_2$ (10 mol%), Mn (3.0 equiv.), Na_2CO_3 (3.0 equiv.), DMF, T (°C), 20 hr.

the reaction proceeding with low conversion at 50 ˚C. However, increasing the temperature to 70 ˚C gave minimal improvement in the yield yet gave a slightly messier reaction profile. Intriguingly, the equivalents of **2** did not show as strong of an effect as observed previously with

the use of 2 equivalents only leading to a 7% decrease in yield. Additionally, while 20 equivalents of **2** did improve the yield, 40 equivalents gave an essentially identical yield to the standard conditions.

From here, we then turned to examine the effect of the base upon the reaction. The choice of base had proved crucial for the success of our base-mediated conditions, but with the reducing metal conditions the reaction proceeded smoothly in the absence of any base with only a 9% drop in yield. In this case, the Mn presumably quenches the HBr byproduct through the formation of H_2 and $MnBr_2$. Furthermore, most bases appeared to have at best no effect on the yield or more commonly a deleterious one. Only Li_2CO_3 and Proton Sponge outperformed Na_2CO_3 though Li_2CO_3 required the reaction not be run at 80 ˚C for the reaction to proceed to completion.

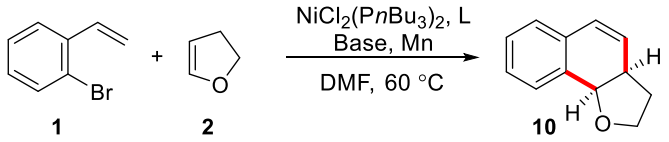

1 **2** **10**

Base	**10** Yield[a]	Base	**10** Yield[a]	Base	**10** Yield[a]
-	38%	K_3PO_4	0%[b]	Et_3N	42%
Na_2CO_3	47%	K_2HPO_4	39%	Cy_2NMe	35%
Li_2CO_3	57%[b]	DBU	2%[c]	PMP	41%
K_2CO_3	0%	pyridine	27%[b]	Bu_3N	30%
Cs_2CO_3	0%	DABCO	19%	urotropine	23%[b]
$NaHCO_3$	34%[b]	DIPEA	40%[b]	Proton Sponge	49%

Table 3.14 Base screen for racemic conditions:[a]Determined by GC using dodecane as an internal standard, [b]Run at 80 °C; **2** (10 equiv.), $NiCl_2(PnBu_3)_2$ (10 mol%), Mn (3.0 equiv.), Base (3.0 equiv.), DMF (0.3 M), 60 °C, 20 hr.

While Li_2CO_3 had provided a superior yield, we conducted the additive screening with Na_2CO_3 for the sake of consistency. In addition, if a successful additive could be identified, we planned to examine any potential interactive effects between our reaction components. Pleasingly, several additives proved beneficial, particularly those with a bromide anion such as LiBr, NaBr, and KBr which gave **10** in 59%, 70%, and 69% yield respectively. Metal halide additives are

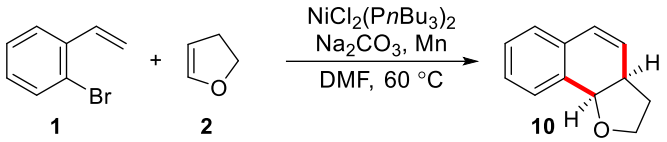

1 2 **10**

Additive	**10** Yield[a]	Additive	**10** Yield[a]	Additive	**10** Yield[a]	Additive	**10** Yield[a]
Bu_4NCl	42%	LiCl	29%	NaI	59%	$MgCl_2$	2%
Bu_4NBr	50%	LiBr	59%	KCl	43%	TESOTf	14%
Bu_4NI	56%	LiI	53%	KBr	69%	LiOTf	0%
Bu_4NOAc	2%	NaCl	47%	KI	52%	$LiPF_6$	34%
CsF	1%	NaBr	70%	$MnCl_2$	25%	TEMPO	3%

Table 3.15 Additive screen for racemic conditions:[a]Determined by GC using dodecane as an internal standard; **2** (10 equiv.), $NiCl_2(PnBu_3)_2$ (10 mol%), Mn (3.0 equiv.), Na_2CO_3 (3.0 equiv.), Additive (3.0 equiv.), DMF (0.3 M), 60 °C, 20 hr.

reported to have similar beneficial effects throughout the Ni literature and they are generally thought to work through promotion of Ni^{II} to Ni^0 reduction.[14–17] For additives that had negative effects, it is intriguing to note that the addition of triflate anions from either TESOTf or LiOTf seriously hinder the reaction with poor conversion with the former and no reaction observed with the latter even at 80 ˚C. $LiPF_6$ also decreased the yield considerably, but the reaction proceeded with almost complete conversion. It appears that non-coordinating anions inhibit the reaction, though the exact mechanism is unknown. One hypothesis would be that triflate anions prevent Ni^{II} reduction by the reducing metal as has been reported by the Weix group.[17] Alternatively, the highly hydroscopic salts could just be a source of adventitious water, but given that both the triflate additives suffered from poor conversion rather than just poor yield, as is usually the case with "wet" reactions, this seems unlikely. As in the previous chapter, TEMPO inhibited the reaction, but did not shut it down completely, since it did proceed with 30% conversion.

Finally, we investigated the effect of different base and additive combinations. In the absence of base, the presence of bromide anion still promoted the reaction, but to a lesser degree with NaBr giving the highest yield by a small margin. Of the three best performing bases from our base screen in Table 3.16, the combination of Na_2CO_3/NaBr proved the best, though all three bases are essentially interchangeable. Then, the equivalents of NaBr were varied and it was found

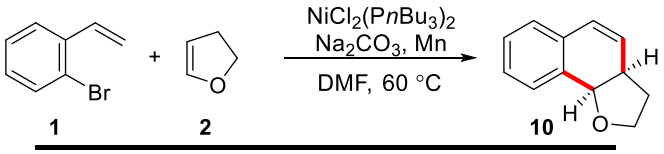

1 **2** **10**

Base	Additive (equiv.)	**10** Yield[a]
-	LiBr (2)	47%
-	NaBr (2)	60%
-	KBr (2)	56%
Na_2CO_3	NaBr (2)	70%[b]
Li_2CO_3	NaBr (2)	68%
Proton Sponge	NaBr (2)	68%
Na_2CO_3	NaBr (0.5)	55%
Na_2CO_3	NaBr (1)	59%
Na_2CO_3	NaBr (3)	62%

Table 3.16 Effect of base and additive combinations:[a]Determined by GC using dodecane as an internal standard; **10** (10 equiv.), $NiCl_2(PnBu_3)_2$ (10 mol%), Mn (3.0 equiv.), Base (3.0 equiv.), Additive, DMF (0.3 M), 60 °C, 20 hr.

that 2 equivalents are optimal, as either increasing or decreasing equivalents led to a marked drop in yield.

3.7 Initial Screening of Chiral Ligands

Now that effective racemic conditions had been determined, our focus turned toward rendering the reaction enantioselective. As phosphine ligands had performed the best in the racemic conditions, we initially focused on that class of ligands, but they provided consistently low to modest *ee* values. After screening our collection of chiral phosphine ligands, a selection of which is shown in Table 3.17, with little success, we resorted to nitrogen-based ligands. Pleasingly, we began to see promising *ee* values with BOX-type ligand **56** and the related semicorrin **57**, which gave the products in 64% and 78% *ee* respectively, albeit in poor yield. In order to take advantage of this promising *ee*, it appeared that our standard conditions would need to be reoptimized in order to account for the new ligand class.

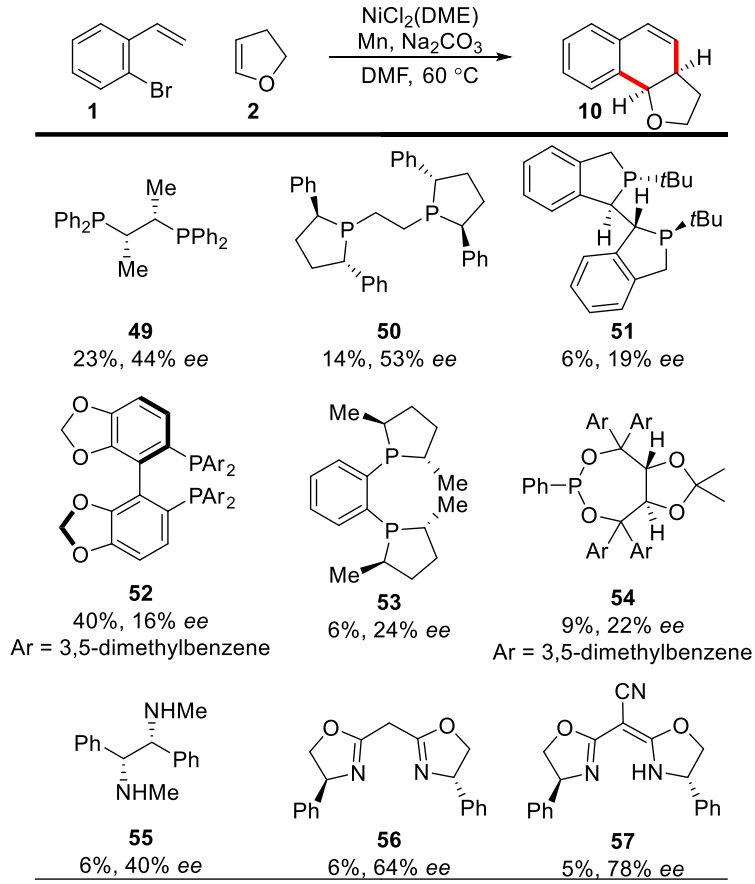

Table 3.17 Initial chiral ligand screening: **2** (10 equiv.), $NiCl_2$(DME) (10 mol%), Ligand (12 mol%), Na_2CO_3 (3.0 equiv.), Mn (2.0 equiv.), DMF (0.3 M), 60 °C, 20 hr.

3.8 Optimization of Enantioselective Conditions

Our first step was to identify an effective solvent and reductant for the reaction. While we screened a wide variety of solvents, once again only highly polar, aprotic solvents gave any product at all, but unlike the racemic conditions, DMSO rather than amide-based solvents proved the best. As with the racemic conditions, the reaction was very sensitive to water content and required solvent that was highly anhydrous with the best results observed with <5 ppm H_2O. For the reductant, we screened Mn, Zn, and the organic reductant tetrakis(dimethylamino)ethylene (TDAE) in the hopes of having a homogeneous reaction mixture.[18] However, only Mn or Zn provided any product and it appeared that in our hands the TDAE was unable to effect the Ni^{II} to Ni^0 reduction, as no reaction was observed at any temperature. Further, Zn was generally as

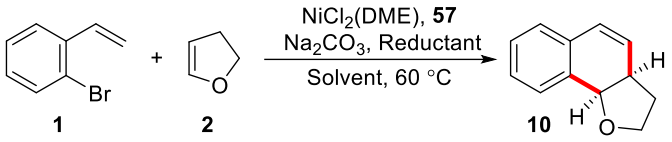

Solvent	Reductant	Yield[a]	*ee*
DMF	Mn	5%	78%
DMF	Zn	9%	-
DMA	Mn	11%	-
DMA	Zn	6%	-
NMP	Mn	5%	-
NMP	Zn	11%	-
DMPU	Mn	10%	-
DMPU	Zn	16%	-
DMSO	Mn	25%	86%
DMSO	Zn	27%	78%

Table 3.18 Solvent and reductant screen for enantioselective condtiions: [a]Determined by GC using dodecane as an internal standard , [b]No reaction; **2** (10 equiv.), $NiCl_2$(DME) (10 mol%), **57** (12 mol%), Reductant (3.0 equiv.), Na_2CO_3 (3.0 equiv.), Solvent (0.3 M), 60 °C, 20 hr.

effective at promoting the reaction as Mn, contrary to the racemic conditions. Still, Mn provided essentially identical yields and, more importantly, an 8% increase in *ee* in the reaction with DMSO.

With solvent and reductant chosen, we then explored the effect of the Ni source. Several different sources performed well in the reaction, giving yields similar to or slightly better than $NiCl_2$(DME). However, for the effective sources the variance in yield was mostly negligible, but several of them, namely $NiBr_2$, $NiBr_2$(DME), $Ni(OAc)_2$•$4H_2O$, and $Ni(COD)_2$, gave a slight decrease in *ee*. $Ni(^{F}stb)_3$ provided a modest boost in yield while maintaining a good level of *ee*.[19] As $Ni(^{F}stb)$ is not commercially available and the overall benefit was low, for the purposes of

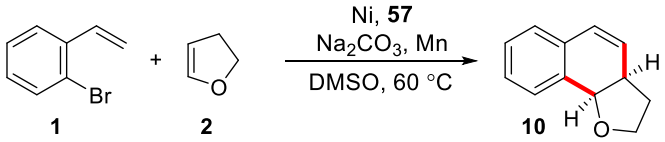

Ni	**10** Yield[a]	*ee*	Ni	**10** Yield[a]	*ee*
$NiCl_2$	0%[b]	-	$Ni(OAc)_2$•$4H_2O$	26%	81%
$NiBr_2$	26%	81%	$Ni(ClO_4)_2$•$4H_2O$	4%[b]	-
$NiBr_2$(DME)	28%	83%	$N(PPh_3)_4$	13%[b]	-
NiI_2	0%[b]	-	$Ni(COD)_2$	29%	83%
$Ni(OAc)_2$	22%	-	$Ni(stb^{F})_3$	32%	86%

Table 3.19 Ni source screen for enantioselective conditions:[a]Determined by GC using dodecane as an internal standard, [b]Run at 80 °C; **2** (10 equiv.), Ni (10 mol%), **57** (12 mol%), Mn (3.0 equiv.), Na_2CO_3 (3.0 equiv.), DMSO (0.3 M), 60 °C, 20 hr.

screening we continued to use the readily available $NiCl_2$(DME).

From here, we then screened a variety of inorganic and amine bases in the reaction, though we did not expect to see significant positive effects. Indeed, most bases had little influence on the reaction and in the absence of any base, the yield was only 6% lower than our previous best results.

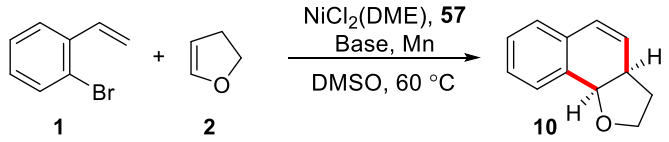

Base	**10** Yield[a]	*ee*	Base	**10** Yield[a]	*ee*
-	25%	-	DABCO	47%	87%
Na_2CO_3	31%	86%	DIPEA	25%	-
Li_2CO_3	31%	87%	Et_3N	29%	84%
K_2CO_3	27%[b]	-	Proton Sponge	30%	-
NaOAc	29%	84%	Cy_2NMe	36%	-
K_2HPO_4	32%	87%	PMP	36%	-

Table 3.20 Base screen for enantioselective conditions:[a]Determined by GC using dodecane as an internal standard, [b]Run at 80 °C; **2** (10 equiv.), $NiCl_2$(DME) (10 mol%), **57** (12 mol %), Mn (3.0 equiv.), Base (3.0 equiv.), DMSO (0.3 M), 60 °C, 20 hr.

However, DABCO provided a substantial increase in yield giving **10** in 47% yield and 87% *ee*. It is unclear as to what role DABCO is playing here. It could be simply acting as a base and promoting the reductive elimination as in our base-mediated conditions, but an alternate role is possible as well.

Additive	**10** Yield[a]	*ee*	Additive	**10** Yield[a]	*ee*
LiCl	29%	-	KCl	36%	-
LiBr	31%	-	KBr	38%	89%
LiI	22%	-	KI	23%	-
NaCl	33%	-	nBu_4NBr	36%	-
NaBr	34%	-	LiOTf	22%	-
NaI	28%	-	$LiPF_6$	26%	-

Table 3.21 Additive screen for enantioselective conditions:[a]Determined by GC using dodecane as an internal standard, [b]Run at 80 °C; **2** (10 equiv.), $NiCl_2$(DME) (10 mol%), **57** (12 mol %), Mn (3.0 equiv.), Base (3.0 equiv.), DMSO (0.3 M), 60 °C, 20 hr.

While the *ee* of the reaction was consistently good, we were curious if any other ligand classes or substitution patterns could improve the yield while at least maintaining the degree of enantioselectivity. For the BOX ligands, the Ph moiety proved optimal as *t*Bu, Bn, and *i*Pr all failed to give product in appreciable yield. Interestingly though, indabox type ligands such as **67** also performed poorly, which may indicate that some rotational freedom is desirable. Further, the tetraphenyl BOX **68** performed poorly, but the corresponding semicorrin **69** gave **10** in 52% yield and 85% *ee*. It should be noted that while the nitrile of the semicorrin ligand had an apparently

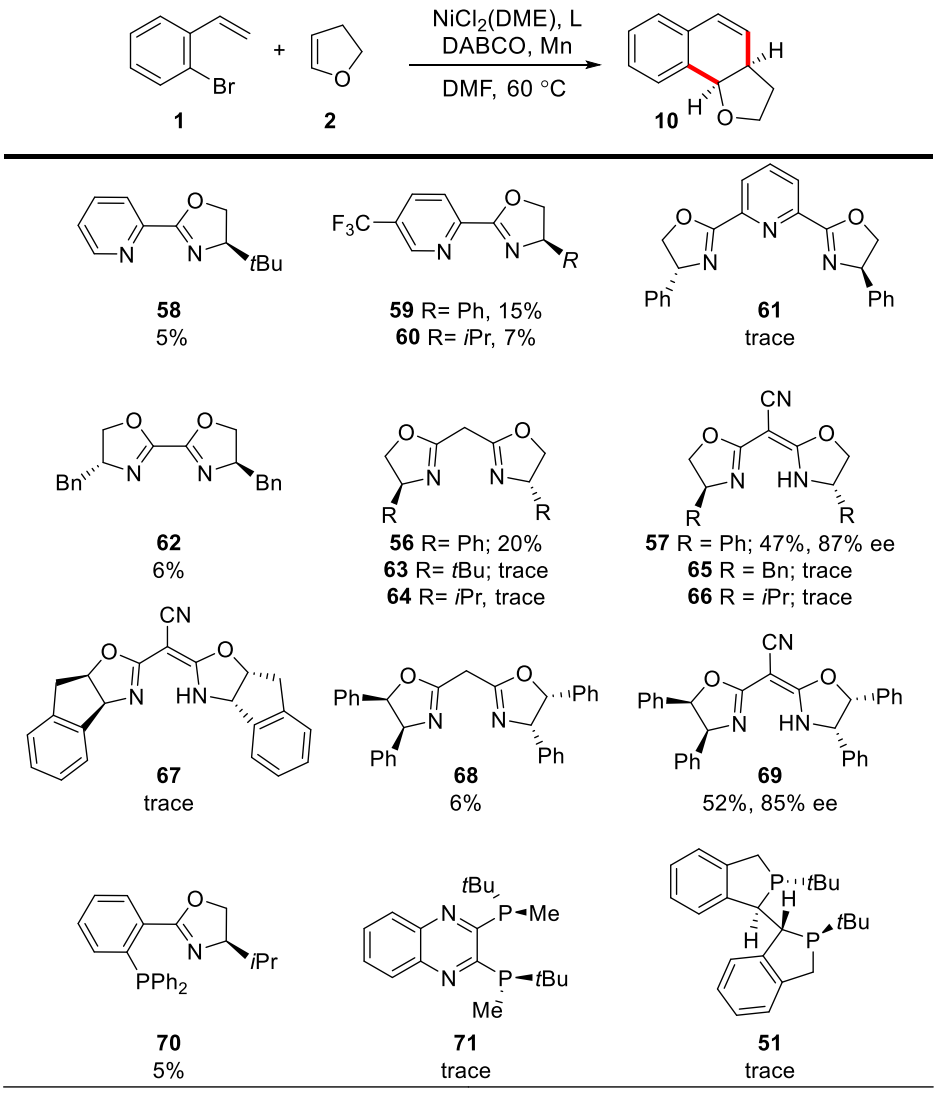

Table 3.22 Continued screening of chiral ligands:

positive effect, any type of alkyl substituent at that position completely inhibited the reaction with only trace product being observed. Additionally, phosphine ligands continued to perform poorly, even QuinoxP* **71** and Duanphos **51**, both of which recently reported to be effective for enantioselective intermolecular Ni-Heck reactions.[20]

To conclude our screening, we finished with screening our best Ni sources with our best ligands. A selection of these results is shown in Table 3.23. While most of the combinations we attempted gave similar results with yields between 45-50%, Ni(^{F}stb)$_3$ and tetraphenyl semicorrin **69** enjoyed a cooperative effect that gave our best yield so far at 60% with 85% *ee*.

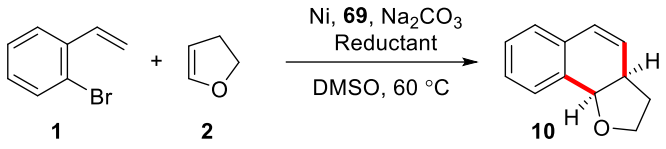

Ni	Yield[a]	*ee*
$NiCl_2$(DME)	47%	-
$Ni(COD)_2$	49%	-
Ni(^{F}stb)$_3$	60%	85%

Table 3.23 Cooperative effects between ligand and Ni source: [a]Determined by GC using dodecane as an internal standard; **2** (10 equiv.), Ni (10 mol%), **69** (12 mol%), Mn (3.0 equiv.), DABCO (3.0 equiv.), DMSO (0.3 M), 60 °C, 20 hr.

3.9 Attempts to Inhibit Homopolymerization

Likely the most troublesome side reaction that was identified over the course of the project was homopolymerization of the styrene **1**. What first brought the issue to our attention was that in most of the reactions for both base- and reducing metal-mediated conditions a significant amount of a sticky residue was formed. Further, the ^{1}H NMR spectra of the residue, as well as the crude reaction mixture showed signals very similar to polystyrene with broad peaks around 7 and 2 ppm. As such, our first thought was that the decomposition pathway may be due to thermal instability. However, once again, running the reaction in the absence of Ni proceeded with no consumption of starting materials. We then suspected the process may be radical in nature,

potentially initiated by homolytic cleavage of a Ni-C bond at some point in the cycle. Running the reaction in the presence of radical inhibitors such as BHT or *t*Bu-catechol (TBC) only resulted in slightly lower yield of **10** with no effect on the formation of the residue. Based on these results, it was suspected that the polymerization was arising from a competitive migratory insertion wherein the Ar-Ni species undergoes an intermolecular Heck reaction with another molecule of **1** rather than **2**. The polymerization also appeared to be selective for styrenes, as no broad signals were apparent in the 3-4 ppm range, indicating that **2** was not incorporated into the structure. This explains why large equivalents of **2** were required for the desired olefin to outcompete the undesired migratory insertion of **1**. Ultimately, we found that adding a solution of **1** and **2** portion wise (20 mol% once an hour over 5 hours) led to a significant decrease in polymerization and a

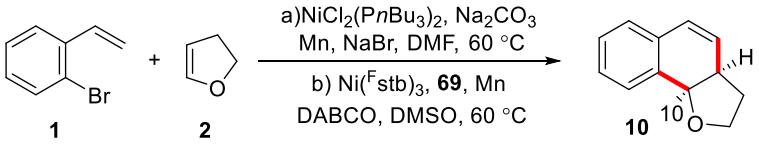

1 **2** **10**

Conditions	Dosing	Yield[a]	*ee*
a	N	55%	-
a	Y	66%	-
b	N	60%	85%
b	Y	81%	87%

Table 3.24 Inhibition of homopolymerization by portionwise addition of starting materials : [a]Isolated yield; **2** (10 equiv.), $NiCl_2(PnBu_3)_2$ (10 mol%), Mn (3.0 equiv.), Na_2CO_3 (3.0 equiv.), DMF (0.3 M), 60 °C, Addition of 20 mol% of **1**/hour over 5 hours, 20 hr; b) **2** (10 equiv.), $Ni(stb^F)_3$ (10 mol%), **69** (12 mol%), Mn (3.0 equiv.), DABCO (3.0 equiv.), DMSO (0.3 M), 60 ° C, Addition of 20 mol% of **1**/hour over 5 hours, 20 h.

substantial increase (10-20%) in yield for both the racemic and enantioselective reducing metal conditions as shown in Table 3.24. It was found that adding a solution of both **1** and **2** was superior to simply adding a stock solution of **1** to the reaction. Further, the addition could be done using a syringe pump with identical results, but operationally, the portionwise procedure proved simpler. We hypothesize that the slow addition of **1** works by decreasing the effective concentration of **1**

in the reaction mixture, thus minimizing the amount of homopolymerization, while maintaining the relative concentration of **1** and **2** thus allowing the desired cascade to predominate.

The observant reader will note that yields for the racemic conditions are actually lower than what we reported earlier with our optimized conditions. This is due to an unexplained 15-20% drop in the yield for every reaction we ran under both the racemic and enantioselective reducing metal conditions. This phenomenon began during our optimization studies of the enantioselective conditions. Despite preparing or ordering new reagents and solvent, regenerating the glovebox catalyst, replacing the glovebox catalyst, changing the glovebox atmosphere from the house N_2 to high purity Ar cylinders, or even setting up and running the reaction in other gloveboxes, we were unable to either identify or ameliorate the cause of this sudden declining yield. However, it must be noted that outside of this unexplained event, the yields of the reactions are quite reproducible with yield variance between runs usually within 0-3%.

3.10 Racemic Reducing Metal Conditions: Aryl Substrate Scope

With both racemic and enantioselective conditions optimized, we started to investigate the scope of the reaction. To begin, we looked at how the reaction would scale up. It should be noted that all of the following reactions are reported with their isolated yield and were run for 36 hr rather than 20 hr as in the screening, because we had noticed a small (3-5%) increase in yield with the

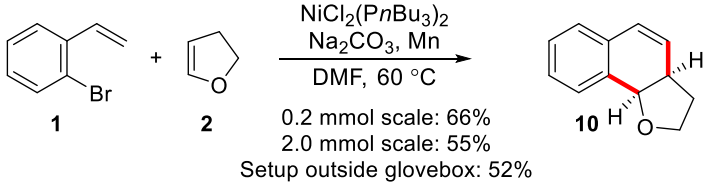

Scheme 3.2 Optimized racemic conditions with standard substrate: **2** (10 equiv.), $NiCl_2(PnBu_3)_2$ (10 mol%), Na_2CO_3 (3.0 equiv.), Mn (3.0 equiv.), DMF (0.3 M), 60 °C, Portonwise addition of **1** and **2** over 5 hours, 36 hr.

additional 16 hr of reaction time. Pleasingly, the reaction scaled well, giving **10** in a 55% yield at a 2.0 mmol scale. Further, the reaction was able to be setup entirely outside of the glovebox using only standard Schlenk techniques to give **10** in a 52% yield. This is particularly notable as one of the great hindrances of Ni^0 catalysis is that it often requires a glovebox to avoid catalyst death.

We next wanted to explore the scope of aryl coupling partners. Pleasingly, a variety of substitutions were tolerated in the reaction including fluoro, methyl, methyl and benzyl ethers, silyl protecting groups, and anilines. Extended π-systems such as naphthalenes were also competent in the reaction. Trifluoromethyl groups and methyl esters were tolerated to a lesser

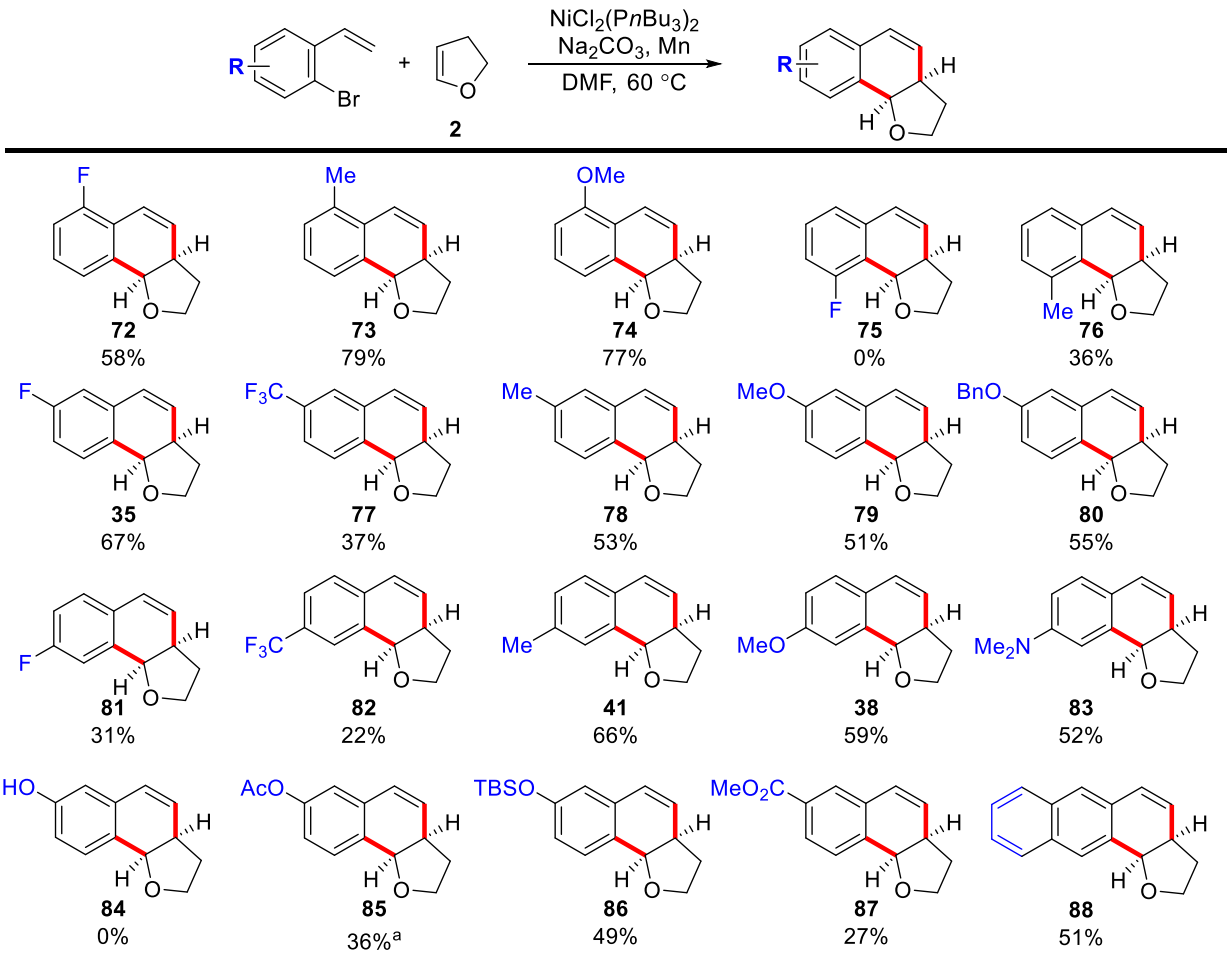

Table 3.25 Substrate scope of aryl partner: [a]Isolated as a mixture with uncyclized product; **2** (10 equiv.), $NiCl_2(PnBu_3)_2$ (10 mol%), Na_2CO_3 (3.0 equiv.), Mn (3.0 equiv.), DMF (0.3 M), 60 °C, 36 hr.

degree, though product was still isolated. A free phenol however was not tolerated at all with the reaction suffering from poor conversion and the formation of a complex mixture of products in which none of the desired **84** could be observed. Additionally, the acetate product **85** was the one instance where uncyclized products, akin to **3**,[3] were observed, though a small amount of the desired product was still isolated. Polysubstituted aryl partners were also effective in the reaction allowing access to some quite interesting structures as shown in Table 3.26. However, 3,5-dimethoxystyrene derivative **91** did not perform well and was in fact isolated as a 2:1 mixture with its uncyclized product. We attributed this difficulty to the additional steric bulk of the methoxy-group *ortho* to the bromide similar to what was observed with *o*-F or *o*-Me groups.

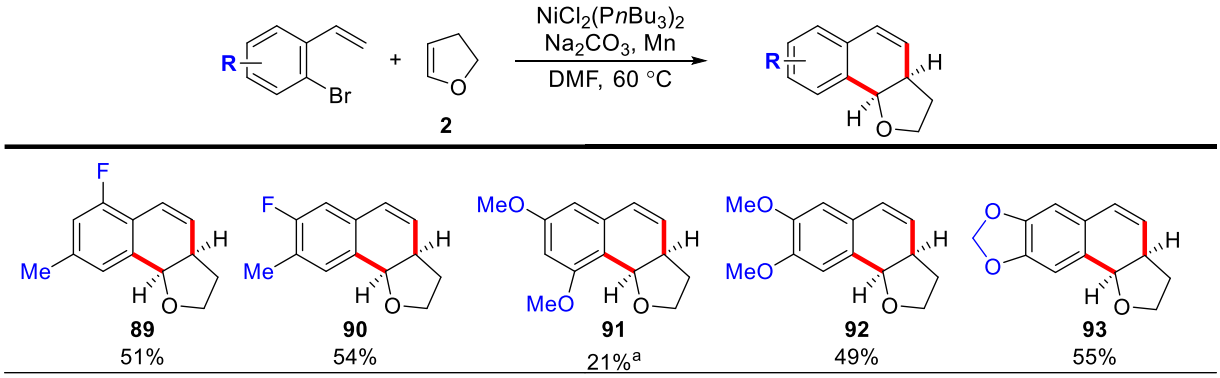

Table 3.26 Substrate scope of aryl partner: [a]Isolated as a 2:1 mixture with uncyclized product; **XX** (10 equiv.), $NiCl_2(PnBu_3)_2$ (10 mol%), Na_2CO_3 (3.0 equiv.), Mn (3.0 equiv.), DMF (0.3 M), 60 °C, 36 hr.

We also decided to attempt the cascade with allyl substrate **94**, similar to an example from the Zhou report.[3] However, whereas the Zhou example uses norbornene **20** in order to preclude the possibility of β-hydride elimination, we opted to attempt the reaction with **2** to test the bounds of our system. The reaction profile was complex, but dihydronaphthalene **96** was isolated in a 16% yield.

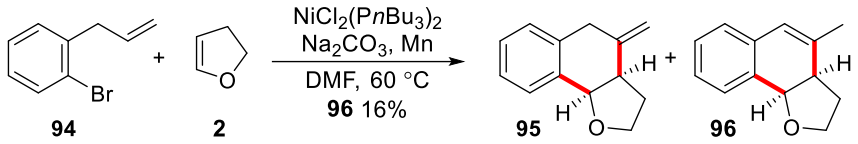

Scheme 3.3 Cascade with allyl coupling bromide: **2** (10 equiv.), $NiCl_2(PnBu_3)_2$ (10 mol%), Na_2CO_3 (3.0 equiv.), Mn (3.0 equiv.), NaBr (2.0 equiv.), DMF (0.3 M), 60 °C, 20 hr, **96** 16%.

Presumably, olefin **95** is formed first and then undergoes isomerization to **96**. While the yield is indeed quite poor, this result is still notable for successfully achieving the [6-*exo*-trig] cyclization in a system where competing β-hydride elimination is possible.

3.11 Racemic Reducing Metal Conditions: Olefin Partner Scope

After establishing the scope of the aryl coupling partner, we then began to explore the scope of potential olefin coupling partners. Based on our previous experience, we suspected that the conditions were likely not to be general, as each olefin may require a varying set of conditions based on its different electronic or steric characteristics. Pleasingly, 1-octene **11** was a competent coupling partner giving **13** in a 40% yield. Interestingly, we found that the NaBr additive had essentially no effect with **13** being formed in 42% yield in the absence of NaBr. Cycloalkenes such as cyclopentene **26** and cycloheptene **99** proved to be competent under these conditions giving dihydronaphthalenes **98** and **101** in 47% and 34% yield, respectively, though undesired indene **100** was observed with **99**. The success of **26** is notable given its failure to react under the base-mediated conditions. Norbornene **20** also was an effective olefin coupling partner, though the selectivity still favored the indene **21** over dihydronaphthalene **22**, albeit in an improved 2.4:1 ratio. Additionally, the NaBr additive provided a slight shift in the selectivity between **21** and **22**. Unfortunately, **23** remained a challenging substrate with neither the indene **24** or dihydronaphthalene **25** being observed. This lack of reactivity could potentially be due the bulk of the Boc group, which could be preventing olefin coordination or migratory insertion. Styrene

14 behaved similarly to what was previously observed, with only the [5-*exo*-trig] product **15** being formed. It should be noted that *n*-butyl vinyl ether **7** also proved ineffective in these conditions giving neither **8** or **9**.

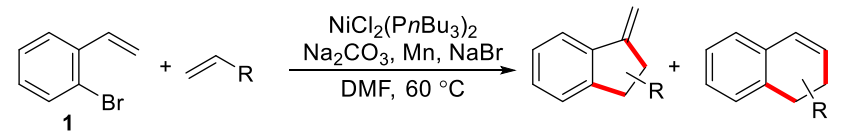

Olefin	5-*exo* Product	6-*endo* Product	Result
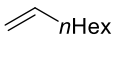 **11**	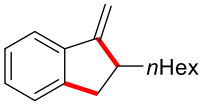 **12**	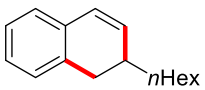 **13**	**13** 40%, 42%[a]
 **26**	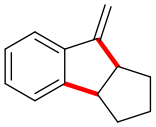 **97**	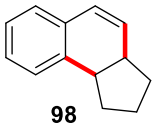 **98**	**98** 42%, 47%[a]
 **99**	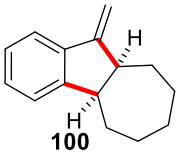 **100**	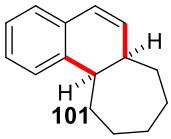 **101**	**101** 34%[a], **100** 2%[a]
 **20**	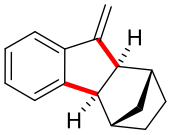 **21**	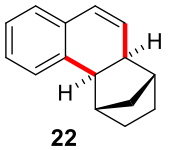 **22**	**21** 33%, **22** 14% **21** 41%[a],:**22** 13%[a]
 **23**	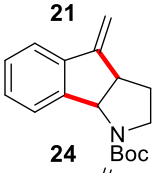 **24**	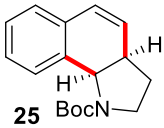 **25**	0%
 **14**	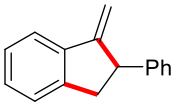 **15**	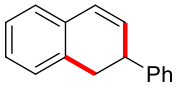 **16**	**15** 40%[a]

Table 3.27 Initial screening of olefin partners:[a]Run without NaBr [b]2 equiv of olefin used; Olefin (10 equiv.), $NiCl_2(PnBu_3)_2$ (10 mol%), Na_2CO_3 (3.0 equiv.), NaBr (2.0 equiv.), Mn (3.0 equiv.), DMF (0.3 M), 60 °C, 36 hr.

Beyond variation with different olefins, we were curious to see how substituted DHF rings would fare in the reaction. Using 5-Ph-DHF **102**, tetracycle **103** was formed in a modest 28% yield, but pleasingly as a single diastereomer. The more challenging disubstituted DHF **104** gave

dihydronaphthalene **105** in a poor 22% yield and as a 1.5:1 mixture of diastereomers. Finally, we attempted the reaction with aryl bromide **106** and 5-Me-DHF **107**, which pleasingly gave anisole **108** in a 53% yield and in a 12:1 dr.

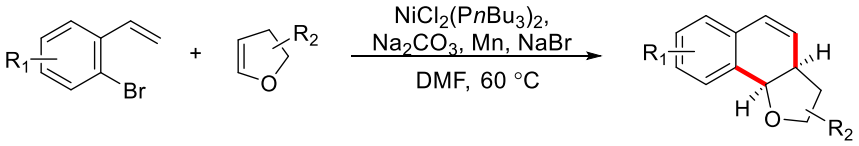

Aryl-Br	Olefin	Product	Yield
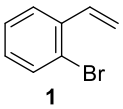 **1**	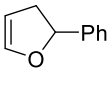 **102**	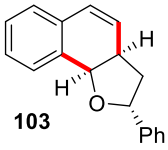 **103**	28% single diasteromer
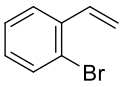 **1**	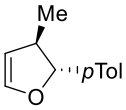 **104**	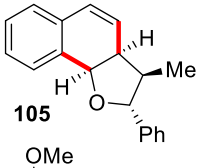 **105**	22% 1.5:1 dr
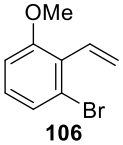 **106**	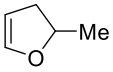 **107**	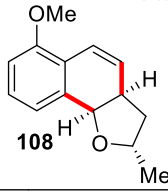 **108**	53% 12:1 dr

Table 3.28 Racemic cascade with functionalized DHF substrates::Olefin (10 equiv.), $NiCl_2(PnBu_3)_2$ (10 mol%), Na_2CO_3 (3.0 equiv.), NaBr (2.0 equiv.), Mn (3.0 equiv.), DMF (0.3 M), 60 °C, 36 hr.

3.12 Enantioselective Reducing Metal Conditions: Aryl Substrate Scope

Next, we explored the scope of the enantioselective conditions in the same fashion as previously. With our optimized conditions, **10** was isolated an 81% yield in an 87% *ee* on a 0.2 mmol scale and, pleasingly, the reaction scaled well, giving a 73% yield on a 2 mmol scale with

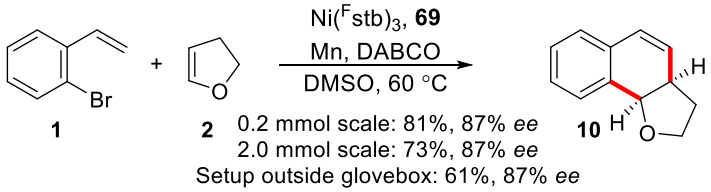

Scheme 3.4 Optimized enantioselective conditions with standard substrate: **2** (10 equiv.), $Ni(^{F}stb)_3$ (10 mol%), DABCO (3.0 equiv.), Mn (3.0 equiv.), DMSO (0.3 M), 60 °C, portonwise addition of **1** and **2** over 5 hours, 36 hr.

the *ee* being maintained. The reaction was also readily set up using Schlenk conditions outside of the glovebox giving **10** in a 61% yield and 87% *ee*.

From here, we moved on to screening the aryl coupling partner. The enantioselective conditions proved to be quite tolerant of a variety of functionalities providing dihydronaphthalene products in good yield and *ee* in most cases examined. Overall, the yields are generally higher than those seen in the racemic case and in the case of dihydronaphthalene **75** a modest yield was

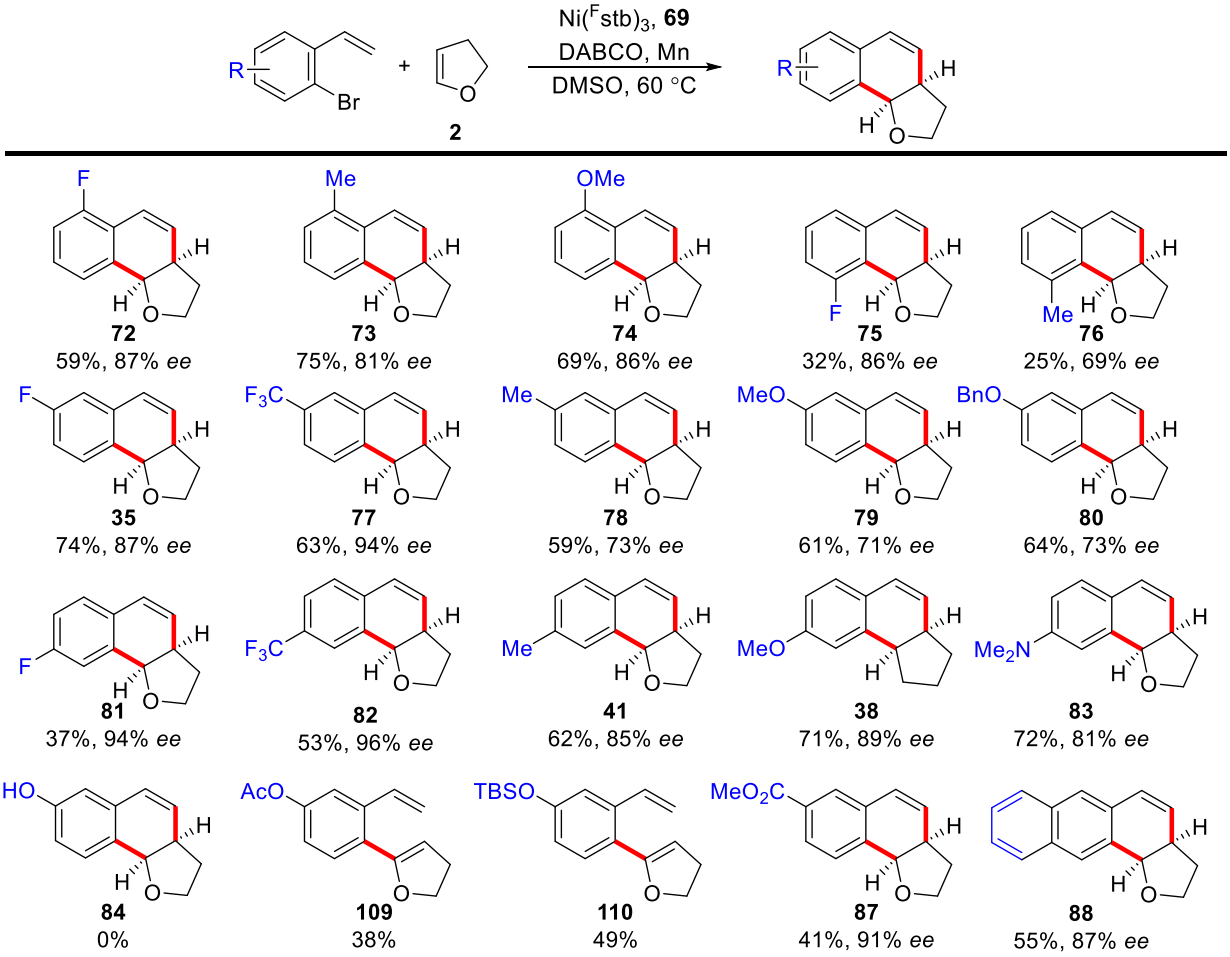

Table 3.29 Substrate scope of aryl partner: [a]Isolated as a mixture with uncyclized product; **2** (10 equiv.), $Ni(^{F}stb)_3$ (10 mol%), DABCO (3.0 equiv.), Mn (3.0 equiv.), DMSO (0.3 M), 60 °C, 36 hr.

observed, but still higher than the 0% previously obtained. However, in two cases, acetate **109** and silyl ether **110**, no desired product was observed and instead only the isomerized uncyclized

products were formed. It is currently unclear as to why these two substrates were unable to complete the cyclization The selective formation of that particulate alkene isomer is interesting as in the de Meijere and Zhou reports, the uncyclized isomers tended to favor the two other possible alkene isomers.[2,3] Still it was gratifying to see that the [6-*endo*-trig] selectivity remained high and that enantioselectivity was conserved across the board with the lowest examples still remaining above 70% *ee*. Gratifyingly, some substituents, namely CF_3 or CO_2Me, gave excellent *ee* with the highest reaching 96%. The polysubstituted arenes also performed well giving good yield and *ee* except in the case of **91**, which once again was isolated as a 2:1 mixture with an uncyclized isomer.

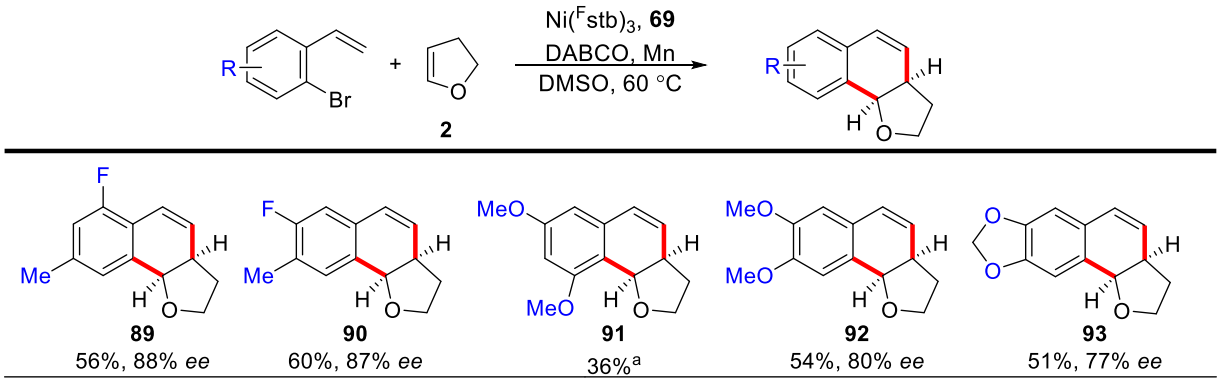

Table 3.30 Substrate scope of aryl partner: [a]Isolated as a 2:1 mixture with uncyclized product; 2 (10 equiv.), $Ni(^{F}stb)_3$ (10 mol%), DABCO (3.0 equiv.), Mn (3.0 equiv.), DMSO (0.3 M), 60 °C, 36 hr.

We also wanted to investigate the use of heteroaryl coupling partners but currently only thiophene **111** has successfully undergone the reaction. Corresponding vinyl pyridine coupling partners proved too unstable and generally polymerized even before the reaction could be run.

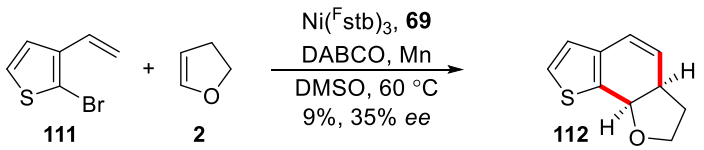

Scheme 3.5 Cascade with heteroaryl bromide: $Ni(^{F}stb)_3$ (10 mol%), **2** (12 mol%), DABCO (3.0 equiv.), Mn (3.0 equiv.), DMSO (0.3 M), 60 °C, 36 hr, 9%, 35% *ee*.

Further, 3-bromo-2-vinylfuran also suffered a similar fate. As such, while the yield and *ee* for **112** are poor it provides an important proof of concept for the use of heteroaryl partners, which could open the door to a variety of intriguing polyheterocyclic frameworks. A key part for any future work would be to identify and effectively utilize heterocyclic coupling partners.

3.13 Enantioselective Reducing Metal Conditions: Olefin Partner Scope

Now we began to investigate the scope of the olefin coupling partner. Intriguingly, *n*-butyl vinyl ether **7** underwent the reaction quite smoothly and gave **9** in a 53% yield, in contrast to its failure in the racemic conditions. However, the *ee* was lacking at only 15%. At first glance, this is not particularly surprising, as acyclic systems are not often used in intermolecular asymmetric Heck reactions due to their lack of rigidity giving rise to a number of conformers, complicating any attempts to induce enantioselectivity.[3,20,21] However, the rigid and cyclic **26** also failed to give acceptable selectivity with **98** being formed with only 54% *ee*. Once again, it appears that the sensitivity of the cascade to variation in the olefin partner is limiting the generality of our conditions. It seemed likely that each olefin would require at the very least a ligand screen in order to identify an appropriate ligand similar to what the Zhou group reported in their variant of this reaction.[3] However, it was decided that this would be the focus of future work in this area and thus our current studies with the enantioselective conditions would focus on DHF-based coupling partners. Nevertheless, we did attempt the reaction with a few more olefins with some intriguing results. 2-methyl-DHF **113** did undergo the reaction but gave the indene **114** and dihydronaphthalene **115** in a 1:1 mixture. This example is notable for the formation of an all-carbon quaternary center in an intermolecular fashion, which is a non-trivial feat, but may also account for the increased selectivity for the undesired indene product **114**. Additionally, attempts with 3,4-DHF **116** gave exclusively [6-*endo*-trig] products, but the desired **117** was isolated as a

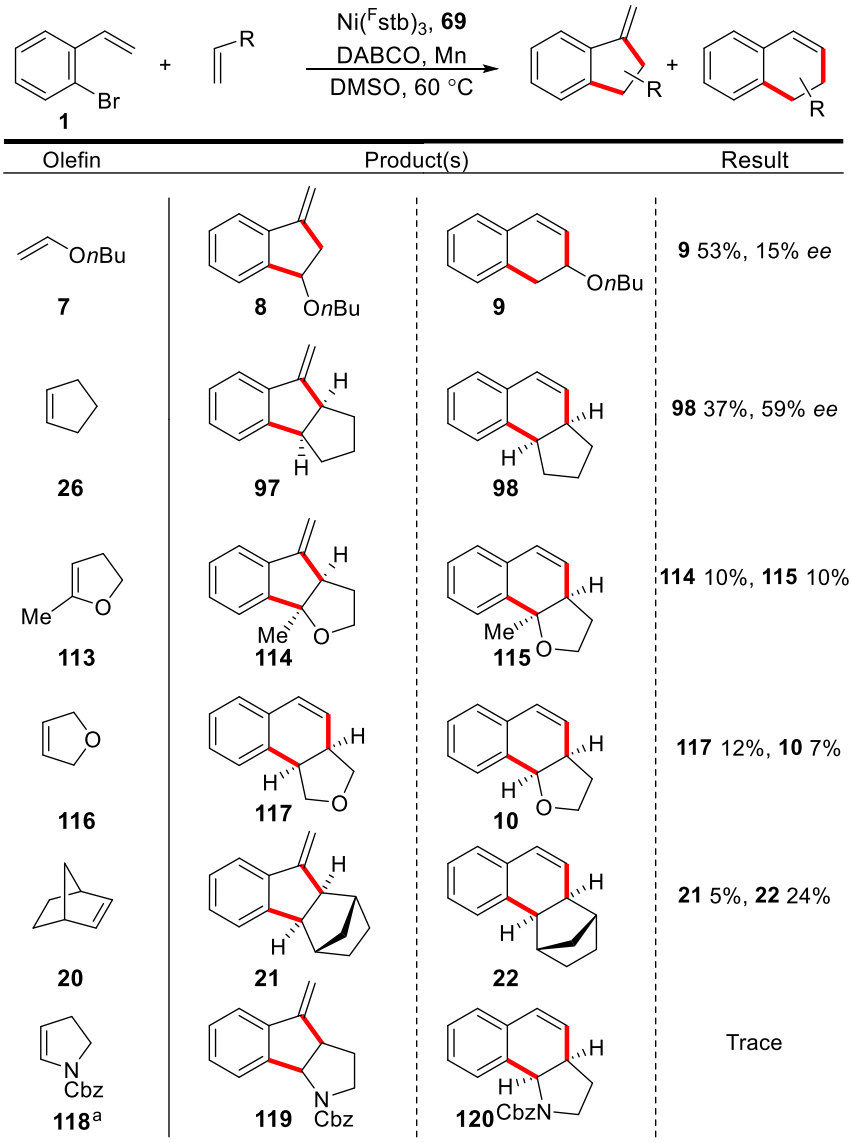

Table 3.31 Initial screening of olefin partners:[a]2 equiv of olefin used; Olefin (10 equiv.), Ni(^{F}stb)$_3$ (10 mol%), **69** (12 mol%), Mn (3.0 equiv.), DMSO (0.3 M), 60 °C, 36 hr.

1.8:1 mixture with **10**, which arises from the isomerization of **116** to the more reactive **2**. Norbornene **20** suffered from poorer yields than observed under either of our other conditions, but as compared to previous attempts, the dihydronaphthalene **22** was now the major product in a 5:1 ratio to indene **21**. We then attempted the reaction with Cbz-protected dihydropyrrole **118** in the hopes that it may be more reactive than **23**, but once again only a trace amount of potential products

were detected in the crude reaction mixture. It is clear that substantial work remains to be done in order to more fully develop the scope for the olefin partners in the reaction.

We were very intrigued to see how the reaction would fare with the substituted DHF substrates. As these olefins were all prepared as racemates it was unclear if the *ee* would be maintained as it would require our system to conduct a potentially challenging kinetic resolution of the enantiomeric olefins. Thus, we were very pleased when the reaction with **102** gave **103** in a 52% yield as a single diastereomer and 82% *ee*. The enantioenriched product proved to be crystalline and allowed us to confirm the relative stereochemistry, but the absolute stereochemistry remains unknown. The good *ee* of this reaction is particularly exciting as it opens the possibility for a broader scope of functionalized products. Once again, the more challenging **104** gave a poor yield and the product was unable to be isolated in a pure fashion. However, the *ee* of the sample indicated an *ee* likely to be in the good to excellent range and in addition the dr of the reaction was

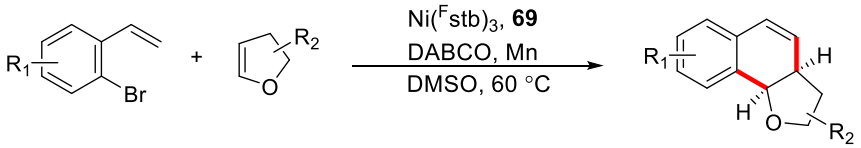

Aryl-Br	Olefin	Product	Yield
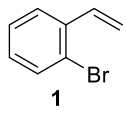 **1**	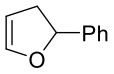 **102**	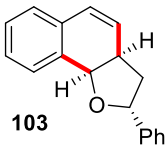 **103**	52%, 82% *ee* single diastereomer confirmed by X-Ray
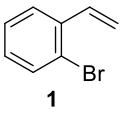 **1**	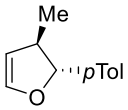 **104**	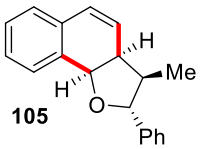 **105**	29%, >90% *ee* 10:1 dr
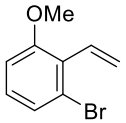 **106**	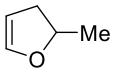 **107**	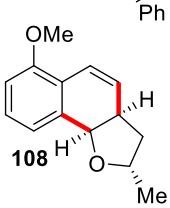 **108**	60%, 87% *ee* 12:1 dr

Table 3.32 Enantioselective cascade with functionalized DHF substrates::Olefin (10 equiv.), Ni(^{F}stb)$_3$ (10 mol%), **69** (12 mol%), DABCO (3.0 equiv.), Mn (3.0 equiv.), DMSO (0.3 M), 60 °C, 36 hr.

significantly improved over that observed in the racemic case. Finally, **107** also turned out to be an effective coupling partner giving **108** in a 60% yield and a good 87% *ee* and 12:1 dr.

3.14 Enantioselective Reducing Metal Conditions: Alternate Aryl Partners

During the course of our studies, the Zhou group reported an asymmetric intermolecular Heck reaction using Ni catalysis.[13] This report was notable to us both for its uncomfortably close subject material and for the use of sulfonates under reducing metal conditions. To the best of our

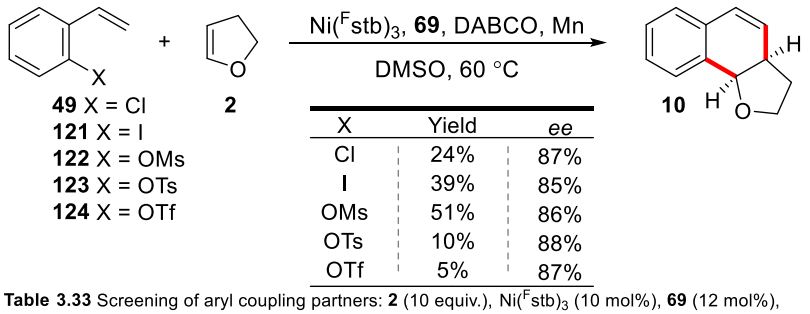

X	Yield	*ee*
Cl	24%	87%
I	39%	85%
OMs	51%	86%
OTs	10%	88%
OTf	5%	87%

Table 3.33 Screening of aryl coupling partners: **2** (10 equiv.), $Ni(^{F}stb)_3$ (10 mol%), **69** (12 mol%), DABCO (3.0 equiv.), Mn (3.0 equiv.), DMSO (0.3 M), 60 °C, 20 hr.

knowledge, this was the first example of a sulfonate reacting efficiently under reducing metal conditions in the context of a classical Heck reaction. Other examples we had found suffered from poor yields when sulfonates were used.[9] As such, we decided to see how aryl sulfonates and other groups may fare in our conditions. The chloride and iodide substrates gave modest yields at best while the tosylate and triflate were almost completely incompetent in the reaction. However, the mesylate performed quite well in the reaction giving **10** with exclusive [6-*endo*-trig] selectivity and in a 51% yield and notably an 86% *ee*, which is essentially identical to that observed with **1**. In fact, it was striking to note that, no matter the aryl partner used, the *ee* was remarkably consistent with all examples within an acceptable margin of error. The success of the mesylate is particularly intriguing as it now allows for the use of phenol starting materials, greatly increasing the potential scope of the reaction. It should also be noted that we attempted our cascade under the

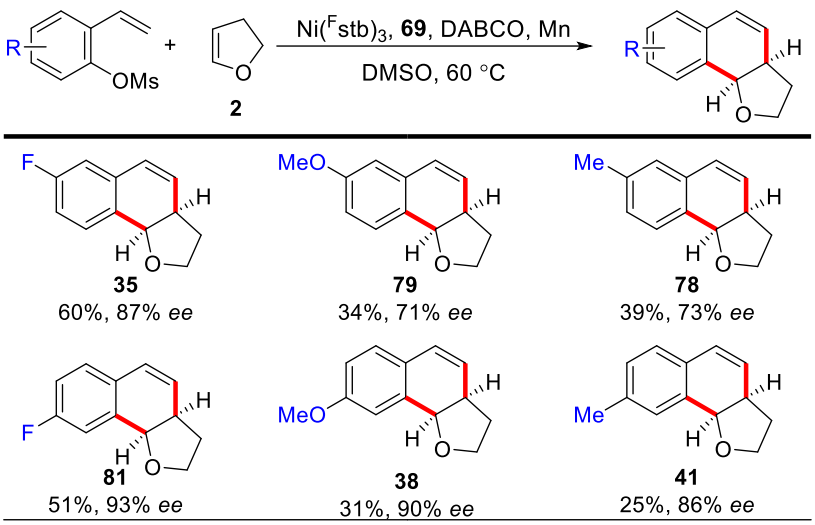

Table 3.34 Scope of aryl mesylate partners: **2** (10 equiv.), $Ni(^{F}stb)_3$ (10 mol%), **69** (12 mol%), DABCO (3.0 equiv.), Mn (3.0 equiv.), DMSO (0.3 M), 60 °C, 20 hr.

Zhou groups conditions for intermolecular Ni Heck reactions with all three sulfonate substrates and no **10** formation was observed in any of them.[20]

We conducted a brief screen of the aryl mesylates to see how it would compare to the corresponding bromides. Pleasingly, the *ee* values were consistent to what was observed with bromides though interestingly, the mesylate apparently favors electron-deficient substrates, with **35** and **81** far outperforming the corresponding methoxy or methyl substrates.

3.15 General Trends in the Intermolecular Ni-Heck Cascade

With a plethora of results in hand, we were curious if there were general trends which we could discern from our data. The most obvious pattern was that electron-rich aryl bromides tend to have higher yields, but lower *ee*'s when compared to their electron-poor counterparts as shown in Table 3.35. In the case of *ee*, we hypothesize that this trend arises from the substituents either enhancing (EDGs) or depressing (EWGs) the proclivity for migratory insertion of the Ar-Ni species into the olefin coupling partner. EDGs lead to a more electron rich and thus nucleophilic complex that is able to undergo migratory insertion more readily, thus leading to a lower ΔΔG

between the two possible enantiomers and lower *ee*. Conversely, EWG could inhibit the migratory insertion thus leading to a higher ΔΔG and higher *ee*. The best evidence for this proposal is the

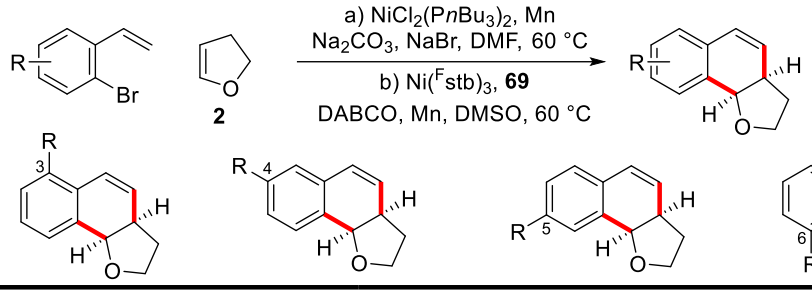

	3	4	5	6
R = F	A. 58% B. 59%, 87% *ee*	A. 67% B. 74%, 87% *ee*	A. 31% B. 37%, 94% *ee*	A. 0% B. 32%, 86% *ee*
R = Me	A. 79% B. 75%, 81% *ee*	A. 53% B. 59%, 73% *ee*	A. 66% B. 62%, 85% *ee*	A. 36% B. 25%, 69% *ee*
R = OMe	A. 77% B. 69%, 86% *ee*	A. 51% B. 61%, 71% *ee*	A. 59% B. 71%, 89% *ee*	— —

Table 3.35 Effects of substitution around the aryl coupling partner: a) $NiCl_2(PnBu_3)_2$ (10 mol%), Mn (3.0 equiv.), Na_2CO_3 (3.0 equiv.), NaBr (2.0 equiv.), DMF (0.3 M), 60 °C, 36 hr; b) Ni(^{F}stb) (10 mol%), **69** (12 mol%), Mn (3.0 equiv.), DABCO (3.0 equiv.), DMSO (0.3 M), 60 °C, 36 hr.

sharp decline in *ee* when EDGs are at the 4- or 6-positions and thus able to donate to the Ni center most effectively via resonance effects. However, this does explain why the highest *ee*'s are observed with EWG at the 5-position rather than the 4-position. The results of the disubstituted substrates would seem to suggest that the substituent effects are averaged out thus allowing very electron-rich substrates **92** and **93** to still be formed with good *ee*.

When considering the trends for the yield, we suspect the roles of the two groups are reversed, as now the EWG can serve to activate the styrene moiety by making it more electrophilic, thus promoting the competitive polymerization pathway. The best evidence for this is a sharp drop in yield when an EWG is present at the 5-position and in fact when substrates with resonance EWG such as esters or nitriles were placed at this position the material would polymerize during purification or even when stored at –35 ˚C in the glovebox. However, this proposition would seem to suggest that an EWG at the 3-position would lead to at least a similar drop in yield due to the

proximity, and while **72** does have a decreased yield compared to **35** the effect is markedly lower than that observed with **81**.

3.16 Total Syntheses of Furomollugin and Norcardione B

With effective conditions now developed and explored, we set out to investigate the robustness and applicability of our method to synthetic challenges by applying it to the synthesis of natural product scaffolds. The formation of a dihydronaphthalene core lends itself to the synthesis of naphthalene-based natural products and gratifyingly, two appropriate targets were identified. The first was furomollugin **127**, a naphthohydroquinone which exhibits anti-hepatitis B activity.[22,23] Starting from our standard substrate **10**, the styrene was oxidized using a Fe^{II} mediated Wacker-type oxidation to yield ketone **125**.[24] Carbonylation with methyl chloroformate yields enol **126** in a 51% yield over two steps. Subsequent oxidation with DDQ yielded **127** in 4 steps from commercial materials and a 25% overall yield using our racemic conditions. The second target was nocardione B **129**, which is a Cdc25B tyrosine phosphatase inhibitor, giving it

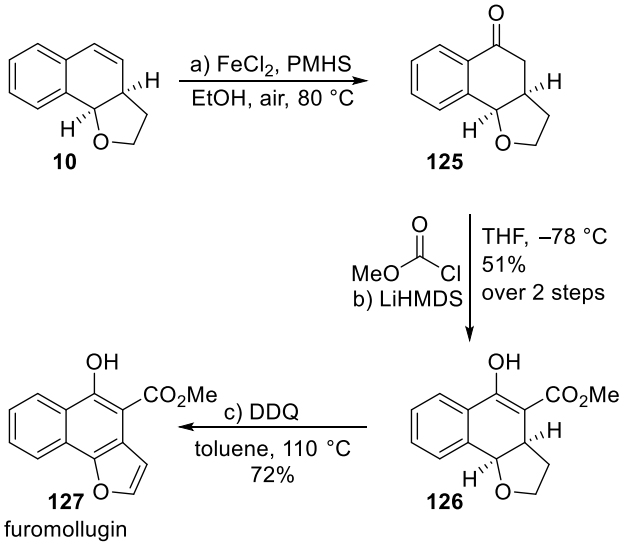

Scheme 3.6 Total synthesis of furomollugin: $FeCl_2$ (10 mol%), PMHS (3.0 equiv.), EtOH (0.25 M), 80 °C, 1 hr; b) LiHMDS (2.0 equiv.), methyl chloroformate (2.0 equiv.), THF (0.25 M), –78 °C → 23 °C , 12 hr, 51% over 2 steps; c) DDQ (5.0 equiv.), toluene (0.15 M), 110 °C, 12 hr, 72%.

antifungal activity.[25] For this synthesis, we took advantage of the kinetic resolution of racemic **107** under our enantioselective conditions to access **108** in 87% *ee*. The styrene moiety was then dihydroxylated with OsO_4 to give diol **128** in 89% yield and a 13:1 dr. The subsequent Swern oxidation had initially been envisioned to yield the dione, but it further oxidized the product to the desired target **129** in an excellent 93% yield, but with some slight erosion of *ee* to 76%. This completed the synthesis of **129** in 5 steps from commercial materials a one-step improvement from the previous best reported synthesis.[26]

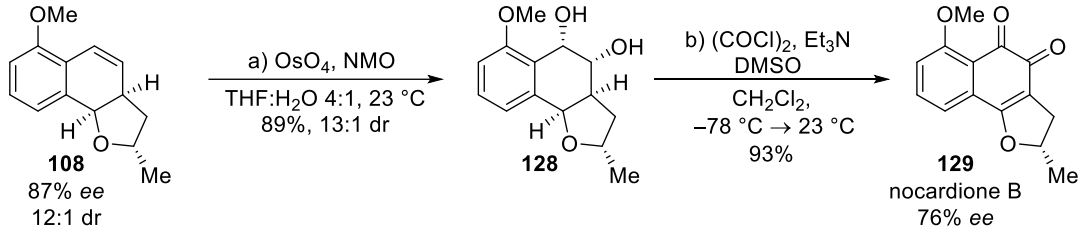

Scheme 3.7 Total synthesis of nocardione B: a) OsO_4 (5 mol%), NMO (4.0 equiv.), THF:H_2O (4:1, 0.1 M), 23 °C, 12 hr, 89%, 13:1 dr; b) $(COCl)_2$ (6.0 equiv.), Et_3N (20.0 equiv.), DMSO (12.8 equiv.), CH_2Cl_2 (0.1 M), –78 °C → 23 °C, 4 hr, 93%.

Section 3.17 Origin of the [6-endo-trig] Selectivity

At this point, the main question that remained was the source of the [6-*endo*-trig] selectivity. One of the first proposals was that the reaction was not actually proceeding via a

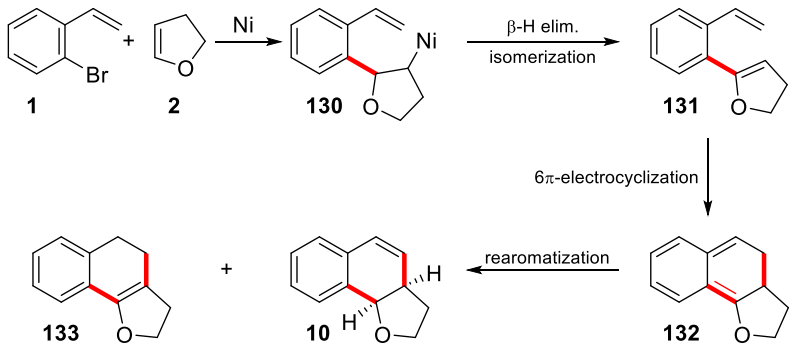

Scheme 3.8 Proposed electrocyclization as source of [6-*endo*-trig] cyclization.

metal mediated cyclization, but rather a 6π-electrocyclization as shown in Scheme 3.8. However, this was quickly discounted as the tetraene **123** formed in the electrocyclization would undergo

rearomatization, which should generate either **10** or its olefin isomer **133**. As **133** was never observed, it seemed unlikely that this was the reaction pathway, especially considering many of the reactions with the base-mediated conditions could be run at 23 ˚C, which is too low a temperature for a thermally promoted electrocyclization.

We then sought to understand if the selectivity for the [6-*endo*-trig] product was caused by properties inherent to the canonical reactivity of Ni species, as that was the major difference between our initial results and the Zhou group's report.[3] As discussed in the previous chapter, computational studies have suggested that Pd possesses a significant energy barrier difference leading the [5-*exo*-trig] pathway to be favored over [6-*endo*-trig] by ~4 kcal/mol.[27] However, while this holds for the majority of Heck literature, there are a handful of examples wherein [6-*endo*-trig] selectivity is competitive or even selected for in the Pd Heck reaction.[8,28–30] As such, it is then reasonable to assume that Ni, which is reported to have no such bias toward the [5-*exo*-

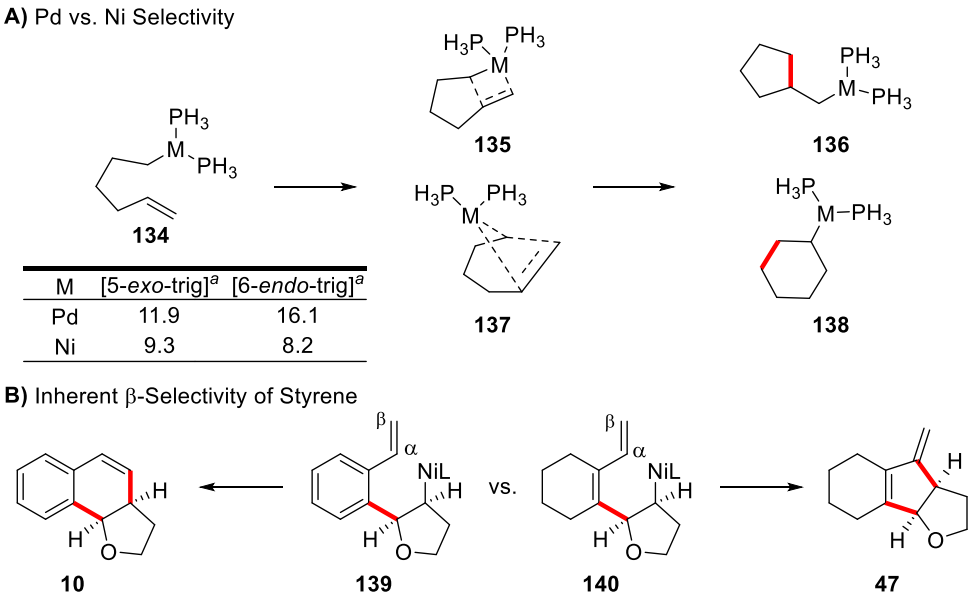

M	[5-*exo*-trig][a]	[6-*endo*-trig][a]
Pd	11.9	16.1
Ni	9.3	8.2

Scheme 3.9 A) Energy barrier differences for intramolecular cyclization Pd and Ni **B)** Styrene's β-selectivity as a possible source of the [6-*endo*-trig] selectivity: [a]Values in kcal/mol.

trig] pathway and, in fact, even a small bias towards the [6-*endo*-trig], would be able to access the dihydronaphthalene products under appropriate conditions. Further, we suspect that the substrate itself is a significant contributor to the selectivity. Styrenes are well known to be β-selective in the Heck reaction, with a myriad of examples in the literature on the conversion of aryl halides and styrenes into stilbenes.[8,21] Thus, we suspect that the inherent β-selectivity of the styrene moiety is promoting the [6-*endo*-trig] pathway and Ni's proclivity for undergoing either pathway allows for dihydronaphthalene formation to dominate. Some evidence for this proposal is that the vinyl triflate **43** never gave any identifiable [6-*endo*-trig] product and instead only [5-*exo*-trig] products were isolated even with a variety of different phosphine ligands. As the 1,3-diene moiety is not as β-selective as a styrene, the [6-*endo*-trig] cyclization is now no longer favored.

In order to more thoroughly investigate this hypothesis, we have begun a collaboration with the Anderson group at the University of Chicago where their expertise on DFT calculations for transition metal complexes is being applied to our system. The study is still ongoing, but very preliminary results suggest that similar to an earlier computational study reported by Goméz-Bengoa group,[27] both pathways are within 1 kcal/mol of one another, with a slight preference for the [6-*endo*-trig] pathway. This is intriguing, as we had originally expected a more significant energy difference when the styrene was the coupling partner. Further calculations and refinements are ongoing, and a full report and analysis will be included in the published work.

3.18 Conclusion

In this chapter, we have described a novel variant of an intermolecular Heck cascade wherein Ni exhibits distinct and complementary reactivity to the literature reports with Pd. This cascade allows for the synthesis of dihydronaphthalenes in contrast to the indene products observed with Pd. We described our initial attempts to apply our base-mediated conditions with

some success to a small assortment of aryl triflate and olefin coupling partners. Then, we developed both racemic and enantioselective conditions for aryl bromides and mesylates using reducing metal conditions. Both conditions were tolerant of a wide variety of aryl partners and to a lesser degree several olefin partners were also competent in the reaction. Further, the enantioselective conditions were consistently able to give good to excellent enantioselectivity for reaction with DHF-type olefins and even conduct kinetic resolutions of racemic substituted DHF rings. The racemic conditions were applied to access the natural product Furomollugin while the enantioselective conditions enabled the synthesis of nocardione B. Computational studies are currently ongoing to better understand the rationale for the observed high selectivity for the [6-*endo*-trig] pathway.

3.19 References

[1] B. Ju, W. Kong, *Asian J. Org. Chem.* **2020**, *9*, 1154–1161.

[2] S. Bräse, J. Rümper, K. Voigt, S. Albecq, G. Thurau, R. Villard, B. Waegell, A. de Meijere, *European J. Org. Chem.* **1998**, *1998*, 671–678.

[3] J. Hu, H. Hirao, Y. Li, J. S. Zhou, *Angew. Chem. Int. Ed* **2013**, *52*, 8676–8680.

[4] G. P. Boldrini, D. Savoia, E. Tagliavini, C. Trombini, A. U. Ronchi, *J. Organomet. Chem.* **1986**, *301*, C62–C64.

[5] S. Iyer, C. Ramesh, A. Ramani, *Tetrahedron Lett.* **1997**, *38*, 8533–8536.

[6] T. M. Gøgsig, J. Kleimark, S. O. Nilsson Lill, S. Korsager, A. T. Lindhardt, P.-O. Norrby, T. Skrydstrup, *J. Am. Chem. Soc.* **2012**, *134*, 443–452.

[7] J. Ruan, J. Xiao, *Acc. Chem. Res.* **2011**, *44*, 614–626.

[8] I. P. Beletskaya, A. V. Cheprakov, *Chem. Rev.* **2000**, *100*, 3009–3066.

[9] J.-N. Desrosiers, L. Hie, S. Biswas, O. V. Zatolochnaya, S. Rodriguez, H. Lee, N. Grinberg, N. Haddad, N. K. Yee, N. K. Garg, C. H. Senanayake, *Angew. Chem. Int. Ed* **2016**, *55*, 11921–11924.

[10] X. Qin, M. W. Y. Lee, J. S. Zhou, *Angew. Chem. Int. Ed* **2017**, *56*, 12723–12726.

[11] S. Bhakta, T. Ghosh, *Adv. Synth. Catal.* **2020**, *362*, 5257–5274.

[12] J.-N. Desrosiers, J. Wen, S. Tcyrulnikov, S. Biswas, B. Qu, L. Hie, D. Kurouski, L. Wu, N. Grinberg, N. Haddad, C. A. Busacca, N. K. Yee, J. J. Song, N. K. Garg, X. Zhang, M. C. Kozlowski, C. H. Senanayake, *Org. Lett.* **2017**, *19*, 3338–3341.

[13] J. S. Zhou, X. Huang, S. Teng, Y. R. Chi, *Chem. Commun.* **2021**, *57*, 3933–3936.

[14] Y. Fujiwara, J. A. Dixon, F. O'Hara, E. D. Funder, D. D. Dixon, R. A. Rodriguez, R. D. Baxter, B.

Herlé, N. Sach, M. R. Collins, Y. Ishihara, P. S. Baran, *Nature* **2012**, *492*, 95–99.

[15] S. Ni, N. M. Padial, C. Kingston, J. C. Vantourout, D. C. Schmitt, J. T. Edwards, M. M. Kruszyk, R. R. Merchant, P. K. Mykhailiuk, B. B. Sanchez, S. Yang, M. A. Perry, G. M. Gallego, J. J. Mousseau, M. R. Collins, R. J. Cherney, P. S. Lebed, J. S. Chen, T. Qin, P. S. Baran, *J. Am. Chem. Soc.* **2019**, *141*, 6726–6739.

[16] X. Wang, G. Ma, Y. Peng, C. E. Pitsch, B. J. Moll, T. D. Ly, X. Wang, H. Gong, *J. Am. Chem. Soc.* **2018**, *140*, 14490–14497.

[17] L. Huang, L. K. G. Ackerman, K. Kang, A. M. Parsons, D. J. Weix, *J. Am. Chem. Soc.* **2019**, *141*, 10978–10983.

[18] A. García-Domínguez, Z. Li, C. Nevado, *J. Am. Chem. Soc.* **2017**, *139*, 6835–6838.

[19] L. Nattmann, R. Saeb, N. Nöthling, J. Cornella, *Nat. Catal.* **2020**, *3*, 6–13.

[20] X. Huang, S. Teng, Y. R. Chi, W. Xu, M. Pu, Y. D. Wu, J. S. Zhou, *Angew. Chem. Int. Ed* **2021**, *60*, 2828–2832.

[21] M. Oestreich, *The Mizoroki-Heck Reaction*, John Wiley And Sons, **2009**.

[22] L.-K. Ho, M.-J. Don, H.-C. Chen, S.-F. Yeh, J.-M. Chen, *J. Nat. Prod.* **1996**, *59*, 330–333.

[23] L. Xia, Y. R. Lee, *Org. Biomol. Chem.* **2013**, *11*, 6097–6107.

[24] B. Liu, F. Jin, T. Wang, X. Yuan, W. Han, *Angew. Chemie Int. Ed.* **2017**, *56*, 12712–12717.

[25] T. Otani, Y. Sugimoto, Y. Aoyagi, Y. Igarashi, T. Furumai, N. Saito, Y. Yamada, T. Asao, T. Oki, *J. Antibiot. (Tokyo).* **2000**, *53*, 337–344.

[26] Y. Tanada, K. Mori, *Eur. J. Chem.* **2001**, *2001*, 4313–4319.

[27] B. Fiser, J. M. Cuerva, E. Gómez-Bengoa, *Organometallics* **2018**, *37*, 390–395.

[28] H.-J. Ha, Y.-G. Ahn, J.-S. Woo, *Bull. Korean Chem. Soc* **1998**, *19*, 818–819.

[29] J. W. Dankwardt, L. A. Flippin, *J. Org. Chem.* **1995**, *60*, 2312–2313.

[30] S. Lemaire-Audoire, M. Savignac, C. Dupuis, J. P. Genêt, *Tetrahedron Lett.* **1996**, *37*, 2003–2006.

3.20 Experimental Section

General Information All reactions outside of the glovebox were carried out under a nitrogen atmosphere with dry solvents under anhydrous conditions using standard Schlenk technique, unless otherwise noted. All glove box reactions were carried out under a nitrogen atmosphere with dry solvents degassed by freeze-pump-thaw and stored in sealed Schlenk flasks over 4 Å molecular sieves. Dry tetrahydrofuran (THF), toluene, diethyl ether (Et_2O) dichloromethane (CH_2Cl_2), and acetonitrile (CH_3CN) were obtained by passing commercially available pre-dried, oxygen-free formulations through activated alumina columns. Dry dimethoxyethane (DME) and 1,4-dioxane were prepared by distillation from Na/Benzophenone. Dry Dry DMF and DMSO were prepared by distillation from CaH_2 and then storing over activated 4 Å molecular sieves until KF titration showed <5 ppm H_2O (usually 1-3 days). Reagents were purchased at the highest commercial quality and used without further purification, unless otherwise stated. 1,4-diazabicyclo[2.2.2]octane (DABCO) was purified via sublimation. $Ni(COD)_2$ and 1,5-bis(diphenylphosphine)pentane (dpppe) were purchased from Strem. $NiCl_2(P\textit{n}Bu_3)$ was purchased from Sigma Aldrich. Yields refer to chromatographically and spectroscopically (^1H and ^{13}C NMR) homogeneous materials, unless otherwise stated. Reactions were magnetically stirred and monitored by thin-layer chromatography (TLC) carried out on 0.25 mm E. Merck silica gel plates (60F-254) using UV light as visualizing agent, and an ethanolic solution of phosphomolybdic acid and cerium sulfate or a solution of $KMnO_4$ in aq. $NaHCO_3$ and heat as developing agents. SiliCycle silica gel (60, academic grade, particle size 0.040–0.063 mm) was used for flash column chromatography. Preparative thin-layer chromatography separations were carried out on 0.50 mm E. Merck silica gel plates (60F-254). NMR spectra were recorded on Bruker 500 MHz or 400 MHz instruments and calibrated using residual undeuterated solvent as an internal reference. The following abbreviations were used to explain the multiplicities: s = singlet, d = doublet, t = triplet, q = quartet, br = broad,

app = apparent. IR spectra were recorded on a Perkin-Elmer 1000 series FT-IR spectrometer. High-resolution mass spectra (HRMS) were recorded on Agilent 6244 Tof-MS using ESI (Electrospray Ionization). All *ee* measurements were determined by HPLC on Daicel Chiralcel or Chiralpak columns.

Base Mediated Intermolecular Ni Heck Cascades

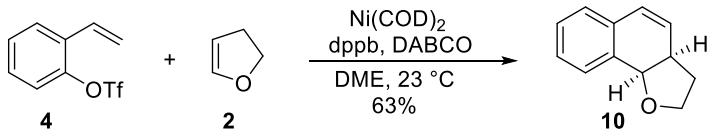

4 **2** **10**

Dihydronapthlene 10. To a dry vial in a glove box was added dppb (26.0 mg, 0.060 mmol, 0.12 equiv.), DABCO (0.168 g, 1.50 mmol, 3.0 equiv.), and $Ni(COD)_2$ (13.4 mg, 0.050 mmol, 0.10 equiv.), followed by DME (0.3 mL), and the resultant mixture was stirred at 23 °C for 15 min. Then, a solution of triflate **4** (0.126 g, 0.500 mmol, 1.0 equiv.) and DHF (0.38 mL, 5.00 mmol, 10 equiv.) in DME (0.2 mL) was added and the flask was sealed and stirred at 23 °C for 4 h. Upon completion, the reaction was diluted with Et_2O (5 mL) and then filtered through a silica plug, eluting with Et_2O. The filtrate was concentrated, and the residue was purified via flash column chromatography (silica gel, hexanes:Et_2O, 49:1) to give dihydronapthlene **10** (54.0 mg, 63% yield) as a colorless oil. **10**: R_f = 0.19 (silica gel, hexanes:Et_2O, 49:1); IR (film) ν_{max} 3057, 3023, 2967, 2940, 2871 cm^{-1}; ^1H NMR (400 MHz, $CDCl_3$) δ 7.43–7.36 (m, 1 H), 7.33–7.20 (m, 2 H), 7.12 (dd, *J* = 7.1, 1.7 Hz, 1 H), 6.45 (dd, *J* = 9.7, 2.2 Hz, 1 H), 5.78 (dd, *J* = 9.7, 3.1 Hz, 1 H), 4.86 (d, *J* = 7.1 Hz, 1 H), 3.86 (td, *J* = 8.1, 5.1 Hz, 1 H), 3.75 (q, *J* = 7.6 Hz, 1 H), 3.22–3.11 (m, 1 H), 2.43 (dq, *J* = 12.2, 8.0 Hz, 1 H), 2.02 (dddd, *J* = 12.2, 7.2, 5.1, 3.9 Hz, 1 H); ^{13}C NMR (101 MHz, $CDCl_3$) δ 132.46, 132.25, 129.90, 129.58, 128.82, 127.76, 127.04, 126.35, 77.14, 66.08, 38.65, 33.66; HRMS (ESI) calcd for $C_{12}H_{12}$ $[(M+H)–H_2O]^+$ 155.0855, found 155.0855.

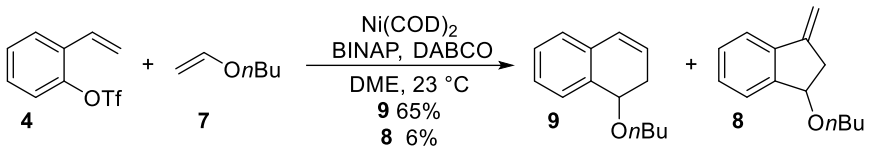

Dihydronapthalene 9. To a dry vial in a glove box was added *rac*-BINAP (37.4 mg, 0.060 mmol, 0.12 equiv.), DABCO (0.168 g, 1.50 mmol, 3.0 equiv.), and $Ni(COD)_2$ (13.4 mg, 0.05 mmol, 0.10 equiv.), followed by DME (0.3 mL), and the mixture was stirred at 23 °C for 15 min. Then, a solution of triflate **4** (0.126 g, 0.500 mmol, 1.0 equiv.) and *n*-butyl vinyl ether (0.640 mL, 5.00 mmol, 10 equiv.) in DME (0.2 mL) was added and the flask was sealed and stirred at 23 °C for 4 h. Upon completion, the reaction contents were diluted with Et_2O (5 mL), and then filtered through a silica plug, eluting with Et_2O. The filtrate was concentrated, and the residue was purified via flash column chromatography (silica gel, hexanes:Et_2O, 49:1) to give dihydronapthalene **9** (65.0 mg, 65% yield) as a colorless oil. **9**: R_f = 0.23 (silica gel, hexanes:Et_2O, 49:1); IR (film) ν_{max} 3063, 3035, 2957, 2932, 2871, 1652 cm^{-1}; ^1H NMR (400 MHz, $CDCl_3$) δ 7.37–7.30 (m, 1 H), 7.30–7.16 (m, 3 H), 7.10 (dd, *J* = 7.2, 1.5 Hz, 1 H), 6.51 (dt, *J* = 9.6, 2.0 Hz, 1 H), 6.00 (dt, *J* = 9.6, 4.2 Hz, 1 H), 4.41 (t, *J* = 5.9 Hz, 1 H), 3.53–3.43 (m, 2 H), 3.38 (dt, *J* = 9.2, 6.7 Hz, 1 H), 2.66–2.48 (m, 2 H), 1.58–1.46 (m, 2 H), 1.45–1.17 (m, 4 H), 0.88 (t, *J* = 7.4 Hz, 3 H); ^{13}C NMR (101 MHz, $CDCl_3$) δ 134.42, 133.77, 128.24, 127.67, 127.30, 126.95, 126.58, 126.11, 74.61, 68.22, 66.01, 32.13, 30.12, 19.51, 15.43, 14.04; HRMS (ESI) calcd for $C_{14}H_{19}O$ $[M+H]^+$ 203.1430, found 203.1426.

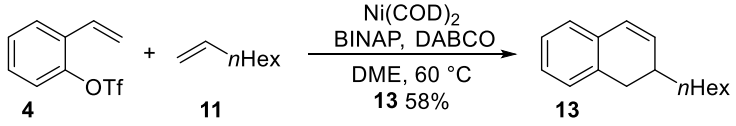

Synthesis of Dihydronapthlene 13

To a dry vial in a glove box was added dpppe (26.4 mg, 0.060 mmol, 0.12 equiv.), DABCO (0.168 g, 1.50 mmol, 3.0 equiv.), and $Ni(COD)_2$ (13.4 mg, 0.050 mmol, 0.10 equiv.),

followed by DME (0.3 mL), and the mixture was stirred at 23 °C for 15 min. Then, a solution of triflate **4** (0.126 g, 0.500 mmol, 1.0 equiv.) and 1-octene **11** (0.784 mL, 5.00 mmol, 10 equiv.) in DME (0.2 mL) was added and the flask was sealed and stirred at 23 °C for 4 h. Upon completion, the reaction contents diluted with Et_2O (5 mL), and then filtered through a silica plug, eluting with Et_2O. The filtrate was concentrated, and the residue was purified via flash column chromatography (silica gel, hexanes) to give dihydronapthlene **13** as a colorless oil (62.1 mg, 58% yield) **13**: R_f = 0.41 (silica gel, hexanes); IR (film) ν_{max} 3056, 3027, 3017, 2955, 2924, 2853 cm^{-1}; ^1H NMR (500 MHz, $CDCl_3$) δ 7.39 (m, 1 H), 7.31–7.20 (m, 2 H), 7.12 (dd, *J* = 7.2, 1.6 Hz, 1 H), 6.45 (dd, *J* = 9.7, 2.2 Hz, 1 H), 5.78 (ddd, *J* = 9.7, 3.2, 0.8 Hz, 1 H), 4.86 (d, *J* = 7.1 Hz, 1 H), 3.86 (td, *J* = 8.1, 5.1 Hz, 1 H), 3.79–3.71 (m, 1 H), 3.16 (s, 1 H), 2.43 (dtd, *J* = 12.2, 8.2, 7.4 Hz, 1 H), 2.02 (dddd, *J* = 12.3, 7.3, 5.1, 3.9 Hz, 1 H); ^{13}C NMR (126 MHz, $CDCl_3$) δ 135.28, 134.14, 127.86, 127.50, 126.94, 126.88, 126.44, 125.78, 34.59, 34.08, 34.04, 31.94, 29.54, 27.07, 22.75, 14.20; HRMS (ESI) calcd for $C_{16}H_{23}$ $[M+H]^+$ 215.1790, found 215.1794.

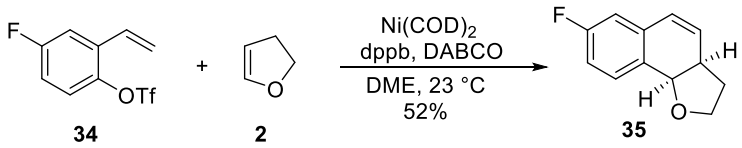

Dihydronapthlene 35. Following the same procedure as **10**, triflate **34** (135 mg, 0.50 mmol, 1 equiv.) and **2** (0.38 mL, 5.00 mmol, 10 equiv.) were converted to dihydronapthlene **35**. The reaction was worked up as usual and then purified via flash column chromatography (silica gel, hexanes:EtOAc 19:1) to give **35** (49.4 mg, 52%) as a light yellow oil. **35**: R_f = 0. (silica gel, hexanes); IR (film) ν_{max} 3054, 2986, 2685, 2305, 1610, 1579 cm^{-1}; ^1H NMR (400 MHz, $CDCl_3$) δ 7.35 (dd, *J* = 8.3, 5.7 Hz, 1H), 6.92 (td, *J* = 8.5, 2.6 Hz, 1H), 6.82 (dd, *J* = 9.3, 2.7 Hz, 1H), 6.40 (dd, *J* = 9.7, 2.3 Hz, 1H), 5.84 (dd, *J* = 9.7, 3.1 Hz, 1H), 4.82 (d, *J* = 7.1 Hz, 1H), 3.84 (td, *J* = 8.1, 5.1 Hz, 1H), 3.73 (q, *J* = 7.6 Hz, 1H), 3.21 – 3.11 (m, 1H), 2.44 (dq, *J* =

12.2, 8.0 Hz, 1H), 2.02 (dddd, *J* = 12.2, 7.2, 5.1, 3.8 Hz, 1H); ^{13}C NMR (101 MHz, $CDCl_3$) δ 163.10 (d, *J* = 245.8 Hz), 134.33 (d, *J* = 8.1 Hz), 131.43, 131.22 (d, *J* = 8.6 Hz), 128.28 (d, *J* = 3.1 Hz), 125.62 (d, *J* = 2.1 Hz), 114.16 (d, *J* = 21.5 Hz), 113.60 (d, *J* = 21.9 Hz), 76.44, 65.96, 38.79, 33.53.; ^{19}F NMR (376 MHz, $CDCl_3$) δ -113.99; HRMS (ESI) calcd for $C_{12}H_{10}F$ [(M+H)–H_2O]$^+$ 173.0761, found 173.0759.

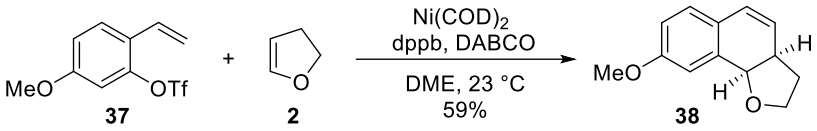

Dihydronapthlene 38. Following the same procedure as **10**, triflate **37** (141 mg, 0.50 mmol, 1 equiv.) and **2** (0.38 mL, 5.00 mmol, 10 equiv.) were converted to dihydronapthlene **38**. The reaction was worked up as usual and then purified via flash column chromatography (silica gel, hexanes:EtOAc 19:1→9:1) to give **38** (60.1 mg, 59%) as a colorless oil. **38**: R_f = 0.47 (silica gel, hexanes:EtOAc 4:1); IR (film) ν_{max} 3053, 2967, 2875, 2305, 1608, 1571 cm^{-1}; ^{1}H NMR (400 MHz, $CDCl_3$) δ 7.04 (d, *J* = 8.3 Hz, 1H), 6.97 (d, *J* = 2.7 Hz, 1H), 6.81 (dd, *J* = 8.3, 2.7 Hz, 1H), 6.39 (dd, *J* = 9.7, 2.1 Hz, 1H), 5.66 (dd, *J* = 9.7, 3.3 Hz, 1H), 4.86 (d, *J* = 7.3 Hz, 1H), 3.90 – 3.83 (m, 1H), 3.82 (s, 3H), 3.76 (q, *J* = 7.5 Hz, 1H), 3.17 – 3.06 (m, 1H), 2.40 (dtd, *J* = 12.1, 8.1, 7.2 Hz, 1H), 2.04 – 1.92 (m, 1H); ^{13}C NMR (101 MHz, $CDCl_3$) δ 159.28, 134.17, 128.13, 127.12, 125.71, 125.38, 114.63, 114.33, 66.17, 55.51, 38.46, 33.77; HRMS (ESI) calcd for $C_{13}H_{13}O$ [(M+H)–H_2O]$^+$ 185.0961, found 185.0960.

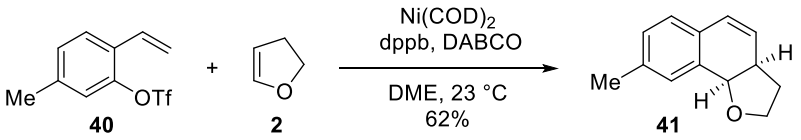

Dihydronapthlene 41. Following the same procedure as **10**, triflate **40** (133 mg, 0.50 mmol, 1 equiv.) and **2** (0.38 mL, 5.00 mmol, 10 equiv.) were converted to dihydronapthlene **41**. The reaction was worked up as usual and then purified via flash column chromatography

(silica gel, hexanes:EtOAc 19:1) to give **41** (57.7 mg, 62%) as a colorless oil. **41**: R_f = 0.21 (silica gel, hexanes:EtOAc 19:1); IR (film) ν_{max} 3024, 2965, 2918, 2868, 1612 cm^{-1}; ^1H NMR (400 MHz, $CDCl_3$) δ 7.24 – 7.19 (m, 1H), 7.12 – 7.05 (m, 1H), 7.01 (d, *J* = 7.7 Hz, 1H), 6.42 (dd, *J* = 9.7, 2.2 Hz, 1H), 5.72 (dd, *J* = 9.7, 3.2 Hz, 1H), 4.83 (d, *J* = 7.2 Hz, 1H), 3.85 (td, *J* = 8.1, 5.2 Hz, 1H), 3.75 (q, *J* = 7.5 Hz, 1H), 3.14 (td, *J* = 7.2, 3.5 Hz, 1H), 2.42 (dq, *J* = 12.1, 8.0 Hz, 1H), 2.35 (s, 3H), 2.00 (dddd, *J* = 12.3, 7.2, 5.2, 4.1 Hz, 1H); ^{13}C NMR (101 MHz, $CDCl_3$) δ 137.60, 132.38, 130.28, 129.55, 129.37, 128.78, 126.96, 126.12, 66.02, 38.63, 33.80, 21.39; No molecular ion was detected.

General Procedures for Reducing Metal Mediated Intermolecular Ni Heck Cascades

General procedure A: Racemic reducing metal conditions for condition screening

In a N_2-filled glove box, Ni-precatalyst (0.02 mmol, 10 mol%) or [Ni source (0.02 mmol, 10 mol%) and ligand (0.024 mmol, 12 mol%)], base (0.6 mmol, 3.0 equiv.), reducing metal (0.6 mmol, 3.0 equiv.), additive (0.4 mmol, 2.0 equiv.) and dry solvent (0.4 mL) were charged into a dry 2-dram vial. After stirring (using rod-shaped stir bar; stirring rate 500-650 rpm) at room temperature for 15 min, *o*-bromostyrene (36.6 mg, 0.2 mmol, 1.0 equiv.) in dry solvent (0.27 mL) and 2,3-dihydrofuran (0.15 mL, 2.0 mmol, 10 equiv.) were added. The vial was then sealed with a Teflon cap and stirred at room temperature for 1 h. The reaction mixture was then stirred in a pre-heated heating block maintained at 60 °C for 18 h. The reaction vial was cooled to room temperature outside the glove box and diluted with Et_2O (2 mL) before being filtered through a short plug of silica gel with Et_2O washings into a vial pre-charged with dodecane (~10 mg) as an internal standard. The filtrate was diluted finally to a volume of ~10 mL and subjected to GC to determine the conversion, yield, and by-product (5-*exo*-trig product, if any).

General procedure B: Racemic reducing metal conditions for product isolation

In a N_2-filled glove box, $NiCl_2(PnBu_3)_2$ (10.7 mg, 0.02 mmol, 10 mol%), Na_2CO_3 (63.6 mg, 0.6 mmol, 3.0 equiv.), Mn (33 mg, 0.6 mmol, 3.0 equiv.), NaBr (41.1 mg, 0.4 mmol, 2.0 equiv.) and dry DMF (0.4 mL) were charged into a dry 2-dram vial. After stirring (using rod-shaped stir bar; stirring rate 500-650 rpm) at room temperature for 15 min, aryl bromide (0.2 mmol, 1.0 equiv.) in dry DMF (0.27 mL) and olefin (2.0 mmol, 10 equiv.) were added. The vial was then sealed with a Teflon cap and stirred at room temperature for 1 h. The reaction mixture was then stirred in a pre-heated heating block maintained at 60 °C for 18 h. The reaction vial was cooled to room temperature outside the glove box and diluted with Et_2O (2 mL) before being filtered through a short plug of silica gel with Et_2O washings. The filtrate was diluted with Et_2O (25 mL), washed with water (3 × 5 mL), brine (5 mL), dried over Na_2SO_4 and concentrated under reduced pressure. The crude product was purified by flash column chromatography on silica gel using EtOAc/hexanes as eluent.

General procedure C: Enantioselective reducing metal conditions for condition screening

In a N_2-filled glove box, Ni-source (0.02 mmol, 10 mol%), ligand (0.03 mmol, 15 mol%), base (0.6 mmol, 3.0 equiv.), reducing metal (0.6 mmol, 3.0 equiv.), additive (0.4 mmol, 2.0 equiv.) and dry solvent (0.4 mL) were charged into a dry 2-dram vial. After stirring (using rod-shaped stir bar; stirring rate 500-650 rpm) at room temperature for 15 min, *o*-bromostyrene (36.6 mg, 0.2 mmol, 1.0 equiv.) in dry solvent (0.27 mL) and 2,3-dihydrofuran **2** (0.15 mL, 2.0 mmol, 10 equiv.) were added. The vial was then sealed with a Teflon cap and stirred at room temperature for 1 h. The reaction mixture was then stirred in a pre-heated heating block maintained at 60 °C for 18 h. The reaction vial was cooled to room temperature outside the glove box and diluted with Et_2O (2 mL) before being filtered through a short plug of silica gel with Et_2O washings into a vial pre-charged with dodecane (~10 mg) as an internal standard. The filtrate was diluted

finally to a volume of ~10 mL and subjected to GC to determine the conversion, yield and by-product (5-*exo*-trig product, if any). The rest of the solution was concentrated under reduced pressure and part of the residue was purified by preparative TLC on silica gel. The product was dissolved in *i*PrOH/hexanes (1/9) and subjected to chiral HPLC analysis (*i*PrOH/hexanes) to determine the enantiomeric excess (ee) of the product. To facilitate the determination of ee, racemic products were obtained either from the racemic method mentioned above or by using racemic ligand of same class.

General procedure D: Enantioselective reducing metal conditions for product isolation

In a N_2-filled glove box, $Ni(^{F}stb)_3$ (20.1 mg, 0.02 mmol, 10 mol%), ligand **69** (14.5 mg, 0.03 mmol, 15 mol%), DABCO (67.3 mg, 0.6 mmol, 3.0 equiv.), Mn (33 mg, 0.6 mmol, 3.0 equiv.) and dry DMSO (0.4 mL) were charged into a dry 2-dram vial. After stirring (using rod-shaped stir bar; stirring rate 500-650 rpm) at room temperature for 15 min, aryl bromide or mesylate (0.2 mmol, 1.0 equiv.) in dry DMSO (0.27 mL) and cyclic olefin (2.0 mmol, 10 equiv.) were added. The vial was then sealed with a Teflon cap and stirred at room temperature for 1 h. The reaction mixture was then stirred in a pre-heated heating block maintained at 60 °C for 18 h. The reaction vial was cooled to room temperature outside the glove box and diluted with Et_2O (2 mL) before being filtered through a short plug of silica gel with Et_2O washings. The filtrate was diluted with Et_2O (25 mL), washed with water (3 × 5 mL), brine (5 mL), dried over Na_2SO_4 and concentrated under reduced pressure. The crude product was purified by flash column chromatography on silica gel using EtOAc/hexanes as eluent. The product was dissolved in *i*PrOH/hexanes (1/9) and subjected to chiral HPLC analysis (*i*PrOH/hexanes) to determine the enantiomeric excess (ee) of the product. To facilitate the determination of ee, racemic products were obtained either from the racemic method mentioned above or by using racemic ligand of same class.

Data for Reducing Metal Mediated Intermolecular Ni Heck Cascade Products

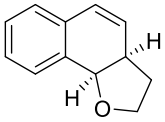

Dihydronaphthalene 10 General Procedure B: 66%; General Procedure D w/Br: 81% and 87% *ee*; Spectral data was same as above.

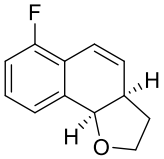

Dihydronaphthalene 72 General Procedure B: 58%; General Procedure D w/Br: 59% and 87% *ee*; ^{1}H NMR (400 MHz, $CDCl_3$) δ 7.25 – 7.14 (m, 2H), 7.05 – 6.94 (m, 1H), 6.73 (dd, *J* = 9.9, 2.2 Hz, 1H), 5.86 (dd, *J* = 9.9, 3.2 Hz, 1H), 4.85 (d, *J* = 7.1 Hz, 1H), 3.86 (td, *J* = 8.1, 5.1 Hz, 1H), 3.74 (q, *J* = 7.6 Hz, 1H), 3.21 – 3.10 (m, 1H), 2.44 (dq, *J* = 12.2, 8.0 Hz, 1H), 2.08 – 1.97 (m, 1H); ^{13}C NMR (101 MHz, $CDCl_3$) δ 158.67 (d, *J* = 248.9 Hz), 134.60 (d, *J* = 3.5 Hz), 130.56 (d, *J* = 2.0 Hz), 128.48 (d, *J* = 8.4 Hz), 125.07 (d, *J* = 3.1 Hz), 120.15 (d, *J* = 14.2 Hz), 118.01 (d, *J* = 5.4 Hz), 115.47 (d, *J* = 21.6 Hz), 76.40 (d, *J* = 2.9 Hz), 66.15, 38.50, 33.54; ^{19}F NMR (376 MHz, $CDCl_3$) δ -123.48.

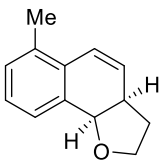

Dihydronaphthalene 73 General Procedure B: 79%; General Procedure D w/Br: 75% and 81% *ee*; ^{1}H NMR (400 MHz, $CDCl_3$) δ 7.41 – 7.34 (m, 1H), 7.32 – 7.24 (m, 1H), 6.83 (dd, *J* =

10.0, 2.4 Hz, 1H), 5.93 (dd, *J* = 10.0, 3.0 Hz, 1H), 4.93 (d, *J* = 7.0 Hz, 1H), 4.00 (td, *J* = 8.2, 4.7 Hz, 1H), 3.88 (q, *J* = 7.6 Hz, 1H), 3.32 – 3.22 (m, 1H), 2.57 (dq, *J* = 12.2, 8.2 Hz, 1H), 2.50 (s, 3H), 2.19 (dddd, *J* = 12.1, 7.2, 4.7, 3.4 Hz, 1H); ^{13}C NMR (101 MHz, $CDCl_3$) δ 133.98, 132.34, 130.76, 130.21, 130.05, 127.63, 127.36, 122.95, 77.74, 66.13, 38.32, 33.55, 19.11.

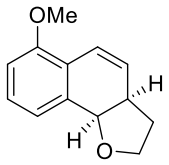

Dihydronaphthalene 74 General Procedure B: 77%; General Procedure D w/Br: 69% and 86% *ee*; ^{1}H NMR (400 MHz, $CDCl_3$) δ 7.21 (t, *J* = 7.9 Hz, 1H), 7.02 (dd, *J* = 7.5, 1.0 Hz, 1H), 6.88 (dd, *J* = 10.0, 2.3 Hz, 1H), 6.84 (dd, *J* = 8.2, 1.1 Hz, 1H), 5.76 (dd, *J* = 10.0, 3.1 Hz, 1H), 4.83 (d, *J* = 7.1 Hz, 1H), 3.91 – 3.81 (m, 1H), 3.84 (s, 3H), 3.73 (q, *J* = 7.6 Hz, 1H), 3.18 – 3.08 (m, 1H), 2.42 (dq, *J* = 12.1, 8.0 Hz, 1H), 2.02 (dddd, *J* = 12.1, 7.2, 4.9, 3.9 Hz, 1H); ^{13}C NMR (101 MHz, $CDCl_3$) δ 155.15, 133.68, 128.84, 128.27, 121.92, 121.21, 119.81, 111.03, 77.19, 66.15, 55.83, 38.33, 33.69.

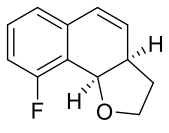

Dihydronaphthalene 75 General Procedure B: 0%; General Procedure D w/Br: 69% and 86% *ee*; ^{1}H NMR (400 MHz, $CDCl_3$) δ 7.35 – 7.10 (m, 1H), 7.08 – 6.86 (m, 2H), 6.47 (dt, *J* = 9.7, 2.3 Hz, 1H), 5.79 (ddd, *J* = 9.7, 2.8, 0.9 Hz, 1H), 5.12 (d, *J* = 7.2 Hz, 1H), 3.88 (tdd, *J* = 8.1, 4.6, 0.7 Hz, 1H), 3.73 (tdd, *J* = 8.0, 6.9, 0.7 Hz, 1H), 3.25 – 3.15 (m, 1H), 2.48 (dq, *J* = 12.2, 8.2 Hz, 1H), 2.06 (dddd, *J* = 11.9, 7.2, 4.6, 2.9 Hz, 1H); ^{13}C NMR (101 MHz, $CDCl_3$) δ 163.03, 160.56, 134.45, 131.26, 130.15, 130.06, 125.67, 122.82, 119.18, 114.93, 69.83, 65.97, 38.20, 33.61; ^{19}F NMR (376 MHz, $CDCl_3$) δ -121.25.

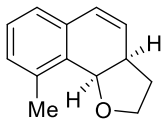

Dihydronaphthalene 76 General Procedure B: 36%; General Procedure D w/Br: 25% and 69% *ee*; ^{1}H NMR (400 MHz, $CDCl_3$) δ 7.18 (t, *J* = 7.5 Hz, 1H), 7.09 (d, *J* = 7.5 Hz, 1H), 6.97 (dd, *J* = 7.5, 1.3 Hz, 1H), 6.43 (dd, *J* = 9.6, 2.5 Hz, 1H), 5.70 (ddd, *J* = 9.7, 2.7, 0.9 Hz, 1H), 4.96 (d, *J* = 7.2 Hz, 1H), 3.83 (td, *J* = 8.1, 4.7 Hz, 1H), 3.73 (tdd, *J* = 7.9, 6.9, 0.6 Hz, 1H), 3.25 – 3.14 (m, 1H), 2.53 – 2.40 (m, 1H), 2.45 (s, 3H), 2.06 (dddd, *J* = 11.9, 7.2, 4.7, 2.8 Hz, 1H); ^{13}C NMR (101 MHz, $CDCl_3$) δ 138.06, 132.37, 130.16, 129.95, 129.58, 128.53, 126.80, 125.32, 73.51, 65.67, 38.61, 33.74, 18.61.

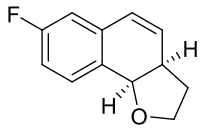

Dihydronaphthalene 35 General Procedure B: 67%; General Procedure D w/Br: 74% and 87% *ee*, General Procedure D w/OMs: 60% and 87% *ee*; ^{1}H NMR (400 MHz, $CDCl_3$) δ 7.35 (dd, *J* = 8.3, 5.7 Hz, 1H), 6.92 (td, *J* = 8.5, 2.6 Hz, 1H), 6.82 (dd, *J* = 9.3, 2.6 Hz, 1H), 6.40 (dd, *J* = 9.7, 2.2 Hz, 1H), 5.84 (dd, *J* = 9.7, 3.1 Hz, 1H), 4.82 (d, *J* = 7.1 Hz, 1H), 3.84 (td, *J* = 8.1, 5.1 Hz, 1H), 3.73 (q, *J* = 7.7 Hz, 1H), 3.21 – 3.11 (m, 1H), 2.44 (dtd, *J* = 12.2, 8.3, 7.4 Hz, 1H), 2.02 (dddd, *J* = 12.3, 7.2, 5.2, 3.9 Hz, 1H); ^{13}C NMR (101 MHz, $CDCl_3$) δ 164.32, 161.88, 134.29, 131.43, 131.26, 128.26, 125.61, 114.05, 113.49, 76.44, 65.96, 38.79, 33.53; ^{19}F NMR (376 MHz, $CDCl_3$) δ -114.00.

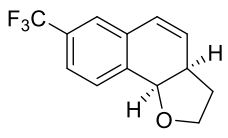

Dihydronaphthalene 77 General Procedure B: 37%; General Procedure D w/Br: 63% and 94% *ee*; ^{1}H NMR (400 MHz, $CDCl_3$) δ 7.55 – 7.45 (m, 2H), 7.35 (d, *J* = 1.7 Hz, 1H), 6.47 (dd,

J = 9.7, 2.1 Hz, 1H), 5.91 (dd, *J* = 9.7, 3.4 Hz, 1H), 4.92 (d, *J* = 7.4 Hz, 1H), 3.87 (td, *J* = 8.0, 5.4 Hz, 1H), 3.74 (q, *J* = 7.5 Hz, 1H), 3.23 – 3.12 (m, 1H), 2.44 (dtd, *J* = 12.2, 8.1, 7.2 Hz, 1H), 2.00 (ddt, *J* = 12.2, 7.3, 5.0 Hz, 1H); ^{13}C NMR (101 MHz, $CDCl_3$) δ 136.16, 132.69, 131.28, 131.05 – 130.12 (m), 129.64, 125.23, 124.21 (q, *J* = 3.9 Hz), 123.43 (q, *J* = 3.8 Hz), 66.07, 38.51, 33.40; ^{19}F NMR (376 MHz, $CDCl_3$) δ -62.78.

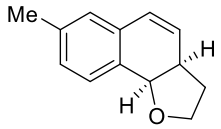

Dihydronaphthalene 78 General Procedure B: 53%; General Procedure D w/Br: 59% and 73% *ee*, General Procedure D w/OMs: 39% and 73% *ee*; ^{1}H NMR (400 MHz, $CDCl_3$) δ 7.28 (d, *J* = 7.6 Hz, 1H), 7.06 (d, *J* = 7.6 Hz, 1H), 6.94 (s, 1H), 6.41 (dd, *J* = 9.7, 2.3 Hz, 1H), 5.76 (ddd, *J* = 9.7, 3.2, 0.8 Hz, 1H), 4.83 (d, *J* = 7.1 Hz, 1H), 3.84 (td, *J* = 8.1, 5.0 Hz, 1H), 3.79 – 3.66 (m, 1H), 3.20 – 3.09 (m, 1H), 2.42 (dq, *J* = 12.1, 8.1 Hz, 1H), 2.33 (s, 3H), 2.01 (dddd, *J* = 12.2, 7.2, 5.1, 3.8 Hz, 1H); ^{13}C NMR (101 MHz, $CDCl_3$) δ 138.51, 132.12, 129.93, 129.62, 129.48, 128.38, 127.76, 126.43, 77.00, 65.99, 38.75, 33.72, 21.32.

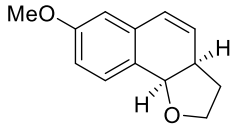

Dihydronaphthalene 79 General Procedure B: 51%; General Procedure D w/Br: 61% and 71% *ee*, General Procedure D w/OMs: 34% and 71% ee; ^{1}H NMR (400 MHz, $CDCl_3$) δ 7.31 (d, *J* = 8.3 Hz, 1H), 6.78 (dd, *J* = 8.3, 2.6 Hz, 1H), 6.67 (d, *J* = 2.7 Hz, 1H), 6.41 (dd, *J* = 9.6, 2.3 Hz, 1H), 5.78 (ddd, *J* = 9.7, 3.0, 0.8 Hz, 1H), 4.80 (d, *J* = 6.9 Hz, 1H), 3.88 – 3.77 (m, 1H), 3.81 (s, 3H), 3.79 – 3.68 (m, 1H), 3.20 – 3.09 (m, 1H), 2.43 (dq, *J* = 12.1, 8.1 Hz, 1H), 2.01 (dddd, *J* = 12.2, 7.2, 5.0, 3.6 Hz, 1H); ^{13}C NMR (101 MHz, $CDCl_3$) δ 160.07, 133.55, 130.80, 130.76, 126.38, 124.88, 112.87, 112.59, 76.79, 65.88, 55.47, 38.83, 33.66.

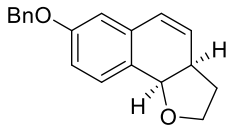

Dihydronaphthalene 80 General Procedure B: 51%; General Procedure D w/Br: 61% and 71% *ee*; ^{1}H NMR (400 MHz, $CDCl_3$) δ 7.47 – 7.29 (m, 6H), 6.85 (dd, *J* = 8.2, 2.6 Hz, 1H), 6.76 (d, *J* = 2.6 Hz, 1H), 6.40 (dd, *J* = 9.7, 2.3 Hz, 1H), 5.78 (dd, *J* = 9.7, 3.0 Hz, 1H), 5.08 (s, 2H), 4.81 (d, *J* = 6.9 Hz, 1H), 3.84 (td, *J* = 8.1, 5.0 Hz, 1H), 3.74 (q, *J* = 7.6 Hz, 1H), 3.20 – 3.10 (m, 1H), 2.43 (dq, *J* = 12.2, 8.1 Hz, 1H), 2.02 (dddd, *J* = 12.2, 7.2, 5.0, 3.6 Hz, 1H); ^{13}C NMR (101 MHz, $CDCl_3$) δ 159.28, 137.14, 133.59, 130.82, 130.76, 128.70, 128.05, 127.52, 126.36, 125.15, 113.78, 113.60, 76.78, 70.16, 65.89, 38.82, 33.65.

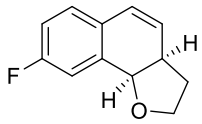

Dihydronaphthalene 81 General Procedure B: 51%; General Procedure D w/Br: 61% and 71% *ee*; General Procedure D w/ OMs: 51% and 93%; ^{1}H NMR (400 MHz, $CDCl_3$) δ 7.12 (dd, *J* = 9.0, 2.7 Hz, 1H), 7.07 (dd, *J* = 8.3, 5.6 Hz, 1H), 6.95 (td, *J* = 8.5, 2.7 Hz, 1H), 6.40 (dd, *J* = 9.7, 2.1 Hz, 1H), 5.77 (dd, *J* = 9.7, 3.4 Hz, 1H), 4.86 (d, *J* = 7.4 Hz, 1H), 3.85 (td, *J* = 8.0, 5.5 Hz, 1H), 3.74 (q, *J* = 7.5 Hz, 1H), 3.17 – 3.06 (m, 1H), 2.41 (dtd, *J* = 12.2, 8.1, 7.1 Hz, 1H), 2.03 – 1.91 (m, 1H); ^{13}C NMR (101 MHz, $CDCl_3$) δ 163.41, 160.95, 135.02 (d, *J* = 7.1 Hz), 128.84 (d, *J* = 2.7 Hz), 128.44 (d, *J* = 3.0 Hz), 128.37 (d, *J* = 7.9 Hz), 125.27 (d, *J* = 1.2 Hz), 116.33 (d, *J* = 21.9 Hz), 115.31 (d, *J* = 21.5 Hz), 76.80, 66.17, 38.29, 33.60; ^{19}F NMR (376 MHz, $CDCl_3$) δ -113.98.

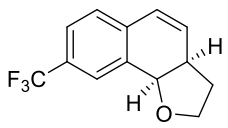

Dihydronaphthalene 82 General Procedure B: 22%; General Procedure D w/Br: 53% and 96% *ee*; ^{1}H NMR (400 MHz, $CDCl_3$) δ 7.68 – 7.63 (m, 2H), 7.53 (d, *J* = 7.9 Hz, 2H), 7.20 (d, *J* = 7.9 Hz, 2H), 6.48 (dd, *J* = 9.7, 2.1 Hz, 2H), 5.94 (dd, *J* = 9.7, 3.4 Hz, 2H), 4.90 (d, *J* = 7.3 Hz, 2H), 3.87 (td, *J* = 8.0, 5.4 Hz, 2H), 3.74 (q, *J* = 7.5 Hz, 2H), 3.24 – 3.13 (m, 2H), 2.45 (dq, *J* = 12.2, 8.0 Hz, 2H), 2.01 (ddt, *J* = 12.3, 7.3, 5.1 Hz, 2H); ^{13}C NMR (101 MHz, $CDCl_3$) δ 135.47 (d, *J* = 1.5 Hz), 133.27, 132.46, 129.56 (q, *J* = 32.5 Hz), 127.10, 126.41 (q, *J* = 3.8 Hz), 125.65 (q, *J* = 4.0 Hz), 125.36, 122.88; ^{19}F NMR (376 MHz, $CDCl_3$) δ -62.46.

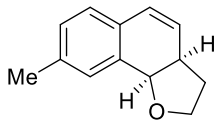

Dihydronaphthalene 41 General Procedure B: 51%; General Procedure D w/Br: 61% and 71% *ee*; General Procedure D w/ OMs: 51% and 93%; ^{1}H NMR (400 MHz, $CDCl_3$) δ 7.24 – 7.19 (m, 1H), 7.09 (dd, *J* = 7.7, 1.8 Hz, 1H), 7.01 (d, *J* = 7.6 Hz, 1H), 6.42 (dd, *J* = 9.7, 2.2 Hz, 1H), 5.72 (dd, *J* = 9.7, 3.2 Hz, 1H), 4.83 (d, *J* = 7.2 Hz, 1H), 3.85 (td, *J* = 8.0, 5.2 Hz, 1H), 3.75 (q, *J* = 7.5 Hz, 1H), 3.19 – 3.10 (m, 1H), 2.42 (dq, *J* = 12.1, 8.0 Hz, 1H), 2.34 (s, 3H), 2.00 (dddd, *J* = 12.3, 7.2, 5.2, 4.0 Hz, 1H); ^{13}C NMR (101 MHz, $CDCl_3$) δ 137.60, 132.36, 130.27, 129.54, 129.37, 128.78, 126.95, 126.11, 77.26, 66.02, 38.63, 33.80, 21.39.

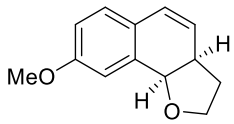

Dihydronaphthalene 38 General Procedure B: 66%; General Procedure D w/Br: 62% and 85% *ee*; General Procedure D w/ OMs: 31% and 90%; ^{1}H NMR (400 MHz, $CDCl_3$) δ 7.04 (d, *J* = 8.3 Hz, 1H), 6.97 (d, *J* = 2.7 Hz, 1H), 6.81 (dd, *J* = 8.3, 2.7 Hz, 1H), 6.39 (dd, *J* = 9.7, 2.1 Hz, 1H), 5.66 (dd, *J* = 9.7, 3.3 Hz, 1H), 4.86 (d, *J* = 7.3 Hz, 1H), 3.86 (td, *J* = 8.0, 5.3 Hz, 1H), 3.82 (s, 3H), 3.76 (q, *J* = 7.5 Hz, 1H), 3.17 – 3.06 (m, 1H), 2.40 (dtd, *J* = 12.1, 8.1, 7.2 Hz, 1H), 2.04 – 1.92 (m, 1H); ^{13}C NMR (101 MHz, $CDCl_3$) δ 159.28, 134.17, 128.13, 127.11, 125.71, 125.37, 114.63, 114.32, 66.17, 55.51, 38.47, 33.77.

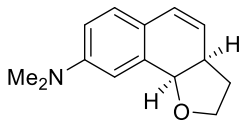

Dihydronaphthalene 83 General Procedure B: 52%; General Procedure D w/Br: 72% and 81% *ee*; ^{1}H NMR (400 MHz, $CDCl_3$) δ 7.00 (d, *J* = 8.4 Hz, 1H), 6.81 (d, *J* = 2.7 Hz, 1H), 6.63 (dd, *J* = 8.4, 2.7 Hz, 1H), 6.37 (dd, *J* = 9.6, 2.1 Hz, 1H), 5.55 (dd, *J* = 9.6, 3.2 Hz, 1H), 4.85 (d, *J* = 7.1 Hz, 1H), 3.91 – 3.73 (m, 2H), 3.17 – 3.06 (m, 1H), 2.97 (s, 7H), 2.39 (dq, *J* = 12.1, 7.9 Hz, 1H), 2.04 – 1.93 (m, 1H); ^{13}C NMR (101 MHz, $CDCl_3$) δ 150.38, 133.58, 127.91, 126.05, 125.15, 121.48, 113.59, 112.43, 78.16, 77.36, 66.22, 40.76, 38.67, 33.93.

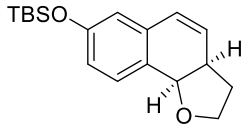

Dihydronaphthalene 86 General Procedure B: 49%; ^{1}H NMR (400 MHz, $CDCl_3$) δ 7.24 (d, *J* = 8.1 Hz, 1H), 6.70 (dd, *J* = 8.1, 2.5 Hz, 1H), 6.60 (d, *J* = 2.5 Hz, 1H), 6.37 (dd, *J* = 9.7, 2.3 Hz, 1H), 5.79 – 5.71 (m, 1H), 4.77 (d, *J* = 6.9 Hz, 1H), 3.82 (td, *J* = 8.1, 5.1 Hz, 1H), 3.74 (q, *J* = 7.6 Hz, 1H), 3.19 – 3.08 (m, 1H), 2.42 (dq, *J* = 12.2, 8.1 Hz, 1H), 2.01 (dddd, *J* = 12.2, 7.2, 5.1, 3.6 Hz, 1H), 0.98 (s, 9H), 0.19 (s, 6H); ^{13}C NMR (101 MHz, $CDCl_3$) δ 156.15, 133.55, 130.78, 130.44, 126.33, 125.36, 119.10, 118.67, 65.84, 38.80, 33.64, 25.84, 18.35, -4.25.

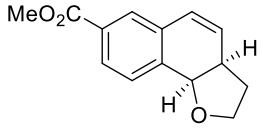

Dihydronaphthalene 87 General Procedure B: 27%; General Procedure D w/Br: 41% and 91% *ee*; ^{1}H NMR (400 MHz, $CDCl_3$) δ 7.90 (dd, *J* = 7.8, 1.8 Hz, 1H), 7.78 (d, *J* = 1.7 Hz, 1H), 7.50 – 7.43 (m, 1H), 6.48 (dd, *J* = 9.7, 2.1 Hz, 1H), 5.87 (dd, *J* = 9.7, 3.4 Hz, 1H), 4.91 (d, *J* = 7.4 Hz, 1H), 3.91 (s, 3H), 3.86 (td, *J* = 8.0, 5.5 Hz, 1H), 3.79 – 3.69 (m, 1H), 3.22 – 3.11 (m, 1H), 2.43 (dtd, *J* = 12.2, 8.1, 7.1 Hz, 1H), 2.05 – 1.93 (m, 1H); ^{13}C NMR (101 MHz, $CDCl_3$) δ

166.89, 137.31, 132.29, 130.51, 130.30, 129.34, 128.73, 127.83, 125.61, 76.44, 66.06, 52.13, 38.51, 33.48.

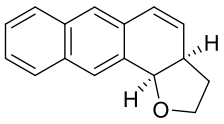

Dihydronaphthalene 88 General Procedure B: 51%; General Procedure D w/Br: 55% and 87% *ee*; ^{1}H NMR (400 MHz, $CDCl_3$) δ 7.86 (s, 1H), 7.84 – 7.73 (m, 2H), 7.55 (s, 1H), 7.49 – 7.37 (m, 2H), 6.65 (dd, *J* = 9.7, 2.1 Hz, 1H), 5.86 (dd, *J* = 9.7, 3.2 Hz, 1H), 5.05 (d, *J* = 6.5 Hz, 1H), 3.94 (td, *J* = 8.2, 4.9 Hz, 1H), 3.83 (q, *J* = 7.7 Hz, 1H), 3.26 – 3.15 (m, 1H), 2.45 (dq, *J* = 12.2, 8.0 Hz, 1H), 2.04 (dddd, *J* = 12.2, 7.3, 4.9, 3.9 Hz, 1H); ^{13}C NMR (101 MHz, $CDCl_3$) δ 133.92, 133.24, 131.24, 130.40, 130.25, 128.85, 127.99, 127.79, 126.93, 126.42, 125.88, 125.54, 77.55, 66.54, 38.97, 33.63.

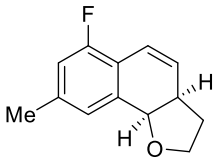

Dihydronaphthalene 89 General Procedure B: 51%; General Procedure D w/Br: 56% and 88% *ee*; ^{1}H NMR (400 MHz, $CDCl_3$) δ 7.01 (d, *J* = 1.5 Hz, 1H), 6.85 – 6.78 (m, 1H), 6.68 (dd, *J* = 9.9, 2.3 Hz, 1H), 5.79 (dd, *J* = 9.8, 3.2 Hz, 1H), 4.81 (d, *J* = 7.2 Hz, 1H), 3.85 (td, *J* = 8.0, 5.2 Hz, 1H), 3.74 (q, *J* = 7.5 Hz, 1H), 3.19 – 3.08 (m, 1H), 2.42 (dq, *J* = 12.2, 8.0 Hz, 1H), 2.33 (s, 3H), 2.06 – 1.93 (m, 1H); ^{13}C NMR (101 MHz, $CDCl_3$) δ 159.69, 157.22, 138.99 (d, *J* = 8.1 Hz), 134.11 (d, *J* = 4.2 Hz), 129.34, 129.21 (d, *J* = 2.2 Hz), 125.67 (d, *J* = 2.9 Hz), 117.83 (d, *J* = 5.1 Hz), 117.17 (d, *J* = 14.5 Hz), 115.82 (d, *J* = 21.4 Hz), 76.42 (d, *J* = 3.1 Hz), 65.98, 38.38, 33.53, 21.23 (d, *J* = 1.6 Hz), ^{19}F NMR (376 MHz, $CDCl_3$) δ -124.48.

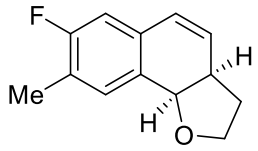

Dihydronaphthalene 90 General Procedure B: 54%; General Procedure D w/Br: 60% and 87% *ee*; ^{1}H NMR (400 MHz, $CDCl_3$) δ 7.20 (d, *J* = 7.7 Hz, 1H), 6.77 (d, *J* = 10.0 Hz, 1H), 6.36 (dd, *J* = 9.7, 2.2 Hz, 1H), 5.77 (dd, *J* = 9.7, 3.2 Hz, 1H), 4.79 (d, *J* = 7.1 Hz, 1H), 3.83 (td, *J* = 8.1, 5.2 Hz, 1H), 3.73 (q, *J* = 7.6 Hz, 1H), 3.19 – 3.09 (m, 1H), 2.49 – 2.34 (m, 1H), 2.26 (d, *J* = 2.0 Hz, 3H), 2.00 (dddd, *J* = 12.3, 7.2, 5.2, 3.9 Hz, 1H); ^{13}C NMR (101 MHz, $CDCl_3$) δ 132.70 (d, *J* = 5.7 Hz), 131.78 (d, *J* = 8.2 Hz), 130.25, 127.90 (d, *J* = 3.6 Hz), 125.41 (d, *J* = 2.2 Hz), 123.89 (d, *J* = 17.7 Hz), 76.53, 65.92, 38.70, 33.68, 14.49 (d, *J* = 3.5 Hz); ^{19}F NMR (376 MHz, $CDCl_3$) δ -118.54.

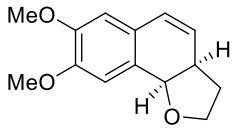

Dihydronaphthalene 92 General Procedure B: 49%; General Procedure D w/Br: 54% and 80% *ee*; ^{1}H NMR (400 MHz, $CDCl_3$) δ 6.95 (s, 1H), 6.65 (s, 1H), 6.35 (dd, *J* = 9.6, 2.2 Hz, 1H), 5.69 (dd, *J* = 9.6, 3.2 Hz, 1H), 4.83 (d, *J* = 7.3 Hz, 1H), 3.90 (s, 3H), 3.88 (s, 3H), 3.83 (td, *J* = 8.0, 5.4 Hz, 1H), 3.78 – 3.69 (m, 1H), 3.19 – 3.08 (m, 1H), 2.42 (dtd, *J* = 12.2, 8.2, 7.2 Hz, 1H), 1.99 (dddd, *J* = 12.4, 7.2, 5.4, 4.2 Hz, 1H), ^{13}C NMR (101 MHz, $CDCl_3$) δ 149.10, 148.47, 128.08, 125.67, 125.39, 125.08, 112.62, 110.32, 77.22, 65.87, 56.16, 38.48, 33.86.

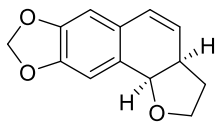

Dihydronaphthalene 93 General Procedure B: 55%; General Procedure D w/Br: 51% and 77% *ee*; ^{1}H NMR (400 MHz, $CDCl_3$) δ 6.89 (s, 1H), 6.61 (s, 1H), 6.31 (dd, *J* = 9.7, 2.2 Hz, 1H), 5.93 (dd, *J* = 10.0, 1.4 Hz, 2H), 5.68 (dd, *J* = 9.7, 3.2 Hz, 1H), 4.77 (d, *J* = 7.2 Hz, 1H),

3.82 (td, *J* = 8.0, 5.2 Hz, 1H), 3.72 (q, *J* = 7.5 Hz, 1H), 3.11 (ddq, *J* = 10.2, 7.0, 3.5 Hz, 1H), 2.40 (dq, *J* = 12.1, 8.0 Hz, 1H), 2.05 – 1.93 (m, 1H); ^{13}C NMR (101 MHz, $CDCl_3$) δ 147.76, 146.86, 128.12, 126.81, 126.60, 125.94, 110.03, 107.47, 101.15, 77.40, 65.86, 38.42, 33.73.

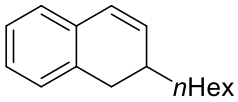

Dihydronaphthalene 13 General Procedure B: 40%; General Procedure B w/o NaBr: 42%; Spectral data was the same as above

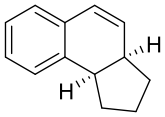

Dihydronaphthalene 98 General Procedure B: 40%; General Procedure B w/o NaBr: 47% General Procedure D w/Br: 37% and 59% *ee*; ^{1}H NMR (400 MHz, $CDCl_3$) δ 7.15 – 7.11 (m, 3H), 7.08 – 6.99 (m, 1H), 6.31 (dd, *J* = 9.7, 2.4 Hz, 1H), 5.68 (dd, *J* = 9.7, 2.9 Hz, 1H), 3.14 – 2.95 (m, 2H), 2.17 – 1.96 (m, 2H), 1.78 – 1.65 (m, 1H), 1.69 – 1.53 (m, 3H); ^{13}C NMR (101 MHz, $CDCl_3$) δ 138.76, 132.62, 131.84, 128.03, 127.08, 126.70, 126.28, 125.47, 42.09, 38.80, 35.54, 33.96, 23.70.

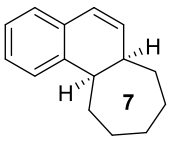

Dihydronaphthalene 101 General Procedure B w/o NaBr: 36%; ^{1}H NMR (400 MHz, $CDCl_3$) δ 7.25 – 7.08 (m, 3H), 7.06 – 6.96 (m, 1H), 6.40 (dd, *J* = 9.6, 2.4 Hz, 1H), 5.72 (dt, *J* = 9.6, 1.9

Hz, 1H), 2.96 – 2.82 (m, 2H), 2.08 – 1.72 (m, 6H), 1.72 – 1.35 (m, 4H); ^{13}C NMR (101 MHz, $CDCl_3$) δ 141.22, 133.39, 133.02, 127.46, 127.34, 126.38, 126.29, 125.89, 44.11, 38.04, 31.68, 30.93, 29.52, 27.67, 24.76.

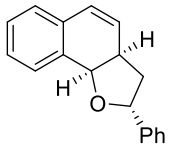

Dihydronaphthalene 103 General Procedure B: 28%; General Procedure D w/Br: 52% and 82% *ee*; ^{1}H NMR (400 MHz, $CDCl_3$) δ 7.41 – 7.36 (m, 1H), 7.36 – 7.13 (m, 6H), 7.07 (dd, *J* = 7.1, 1.7 Hz, 1H), 6.46 (dd, *J* = 9.7, 2.2 Hz, 1H), 5.78 (dd, *J* = 9.7, 3.1 Hz, 1H), 5.18 (d, *J* = 6.7 Hz, 1H), 4.86 (dd, *J* = 9.1, 6.3 Hz, 1H), 3.29 – 3.19 (m, 1H), 2.45 – 2.23 (m, 2H); ^{13}C NMR (101 MHz, $CDCl_3$) δ 143.43, 132.70, 132.34, 129.64, 129.48, 128.89, 128.49, 127.89, 127.39, 127.37, 127.05, 125.90, 79.96, 77.88, 42.47, 39.75.

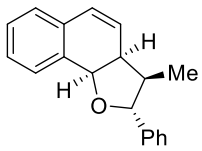

Dihydronaphthalene 105 General Procedure B: 28%, 1.5:1 dr; General Procedure D w/Br: 29%, 10:1 and 82% *ee*; ^{1}H NMR (400 MHz, $CDCl_3$) δ 7.49 – 7.40 (m, 1H), 7.40 – 6.96 (m, 8H), 6.63 (dd, *J* = 9.9, 2.5 Hz, 1H), 5.99 (dd, *J* = 9.9, 2.9 Hz, 1H), 5.29 (d, *J* = 6.4 Hz, 1H), 4.27 (d, *J* = 9.8 Hz, 1H), 3.26 – 3.17 (m, 1H), 2.69 – 2.54 (m, 1H), 2.34 (s, 3H), 2.32 – 2.25 (m, 1H), 1.14 (d, *J* = 6.9 Hz, 3H); ^{13}C NMR (101 MHz, $CDCl_3$) δ 139.19, 137.37, 133.03, 132.87, 129.84, 129.23, 129.02, 128.61, 127.95, 127.24, 126.54, 125.13, 87.02, 77.97, 47.57, 44.09, 21.41, 12.80.

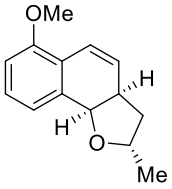

Dihydronaphthalene 108 General Procedure B: 53%, 12:1; General Procedure D w/Br: 60%, 12:1 and 87% *ee*; ^{1}H NMR (400 MHz, $CDCl_3$) δ 7.19 (dd, *J* = 8.2, 7.5 Hz, 1H), 7.01 (d, *J* = 7.1 Hz, 0H), 6.89 (dd, *J* = 10.0, 2.3 Hz, 1H), 6.83 (dd, *J* = 8.3, 1.1 Hz, 1H), 5.75 (dd, *J* = 10.0, 3.1 Hz, 1H), 5.00 (d, *J* = 6.7 Hz, 1H), 4.10 – 3.95 (m, 1H), 3.83 (s, 3H), 3.18 (ddt, *J* = 9.7, 7.4, 2.6 Hz, 1H), 2.17 (ddd, *J* = 12.1, 5.6, 2.5 Hz, 1H), 1.98 (ddd, *J* = 12.1, 9.3, 7.6 Hz, 1H), 1.28 (d, *J* = 6.1 Hz, 3H); ^{13}C NMR (101 MHz, $CDCl_3$) δ 155.13, 134.11, 128.95, 128.32, 121.89, 121.26, 120.39, 111.04, 76.78, 74.56, 55.83, 41.42, 39.39, 21.48.

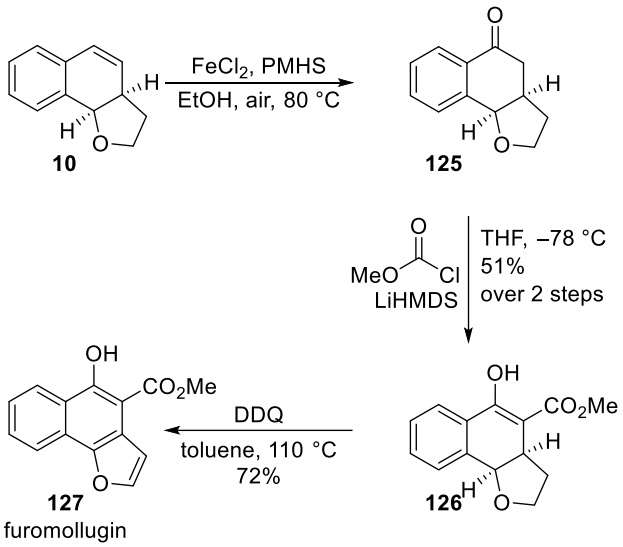

Ketoester 126 A flask was charged with $FeCl_2$ (13 mg, 0.1 mmol, 0.1 equiv) followed by olefin **10** (172 mg, 1.0 mmol, 1.0 equiv) in EtOH (4.0 mL), and PMHS (0.7 mL, 3.0 mmol, 3.0 equiv). The reaction mixture was stirred under air balloon atmosphere at 80 °C for 8 h. After the mixture was cooled to room temperature, KF (500 mg, 3.0 mmol, 3.0 equiv) was added and the mixture was stirred for 1 h, filtered through Celite and then washed with ethyl acetate (3 x

10 mL). The solvent was evaporated under reduced pressure to give the crude product. The residue was used for the next steps without further characterization.

To a stirred solution of the above crude ketone **125** (130 mg, 0.69 mmol, 1.0 equiv) in THF (4.0 mL) was added LiHMDS solution (1 M in THF; 1.4 mL, 1.4 mmol, 2.0 equiv) at -78 °C. The resulting mixture was stirred at -20 °C for 1 h and then methyl cyanoformate (0.11 mL, 1.4 mmol, 2.0 equiv) was added at -78 °C and stirred at 23 °C for 12 h. The reaction mixture was quenched with saturated aqueous NH_4Cl (2 mL) followed by H_2O (1 mL) and extracted with Et_2O (30 mL). The organic extracts were washed with brine (2 mL), dried (Na_2SO_4) and concentrated in vacuo. Flash column chromatographic purification (silica gel, EtOAc /hexanes 1:19) of the crude mixture furnished ester **126** (126 mg, 0.51 mmol, 51% yield over 2 steps) as a colorless foam. **126** $R_f = 0.5$ (silica gel, 15% EtOAc in hexanes); ^{1}H NMR (400 MHz, $CDCl_3$) δ 12.53 (s, 1H), 7.85 (dd, *J* = 7.8, 1.4 Hz, 1H), 7.56 (dt, *J* = 7.7, 1.3 Hz, 1H), 7.46 (td, *J* = 7.5, 1.4 Hz, 1H), 7.41 – 7.31 (m, 1H), 5.21 (d, *J* = 8.8 Hz, 1H), 3.93 – 3.83 (m, 1H), 3.86 (s, 3H), 3.79 (td, *J* = 8.5, 3.7 Hz, 1H), 3.35 (dt, *J* = 9.8, 8.3 Hz, 1H), 2.45 – 2.31 (m, 1H), 1.75 – 1.60 (m, 1H); ^{13}C NMR (101 MHz, $CDCl_3$) δ 173.35, 163.34, 138.29, 131.62, 127.97, 127.68, 127.42, 124.46, 97.30, 75.78, 66.38, 51.97, 36.33, 33.57.

Furomollugin 127 To a solution of ester **126** (110 mg, 0.44 mmol, 1.0 equiv) in toluene (3 mL) was added 2,3-dichloro-5,6-dicyano-l,4-benzoquinone (500 mg, 2.2 mmol, 5.0 equiv) and the reaction mixture was heated at 110 °C for 12 h. The reaction mixture was cooled to room temperature and filtered through Celite with Et_2O washings. The filtrate was diluted with Et_2O (30 mL), washed with saturated aqueous solution of $NaHCO_3$ (4 mL), water (3 × 4 mL), brine (2 mL), dried over Na_2SO_4 and concentrated under reduced pressure. The crude product was purified by flash column chromatography (silica gel, EtOAc /hexanes 1:19) of furomollugin **127** (78 mg, 0.32 mmol, 72% yield) as a light-yellow solid. **127** $R_f = 0.6$ (silica gel, 15% EtOAc in hexanes); ^{1}H NMR (400 MHz, $CDCl_3$) δ 12.26 (s, 1H), 8.46 (dt, *J* = 8.4, 1.0 Hz, 1H), 8.19

(dt, *J* = 8.2, 0.9 Hz, 1H), 7.75 – 7.66 (m, 2H), 7.52 (ddd, *J* = 8.3, 6.9, 1.2 Hz, 1H), 7.18 (d, *J* = 2.0 Hz, 1H), 4.08 (s, 3H); ^{13}C NMR (101 MHz, $CDCl_3$) δ 172.22, 159.54, 144.63, 144.51, 130.30, 125.32, 125.19, 125.14, 123.19, 120.02, 119.93, 109.52, 99.48, 52.47.

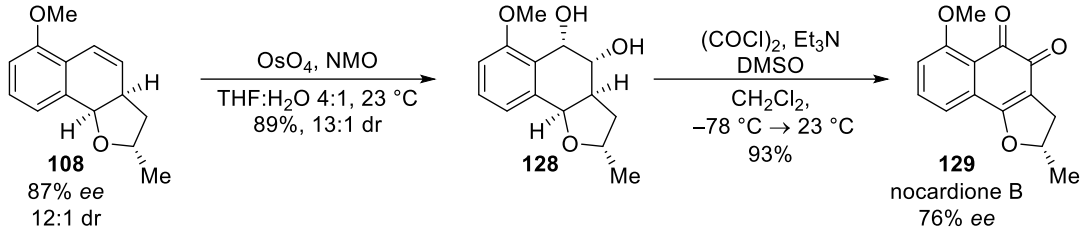

Diol 128 To a stirred solution of the olefin **108** (106 mg, 0.49 mmol, 1.0 equiv) in 4:1 THF:H_2O (5 mL) were added *N*-methylmorpholine *N*-oxide (230 mg, 1.9 mmol, 4.0 equiv) and OsO_4 (4% in H_2O, 0.16 mL, 0.024 mmol, 0.05 equiv) at 0 °C. The reaction mixture was then stirred at 23 °C for 12 h. Subsequently, the reaction mixture was quenched with saturated aqueous solution of $Na_2S_2O_3$ (2 mL), stirred for 5 min and extracted with EtOAc (2 × 30 mL). The combined organic layers were washed with brine (5 mL), dried over anhydrous Na_2SO_4, and concentrated under reduced pressure. Flash column chromatographic purification (silica gel, EtOAc /hexanes 4:1) of the crude mixture furnished diol **128** (109 mg, 0.44 mmol, 89% yield, 13:1 *dr*) as a white solid. **128** R_f = 0.3 (silica gel, 80% EtOAc in hexanes); ^{1}H NMR (400 MHz, $CDCl_3$) δ 7.32 (t, *J* = 8.0 Hz, 1H), 7.08 (d, *J* = 7.7 Hz, 1H), 6.83 (dd, *J* = 8.3, 1.0 Hz, 1H), 5.10 (t, *J* = 3.4 Hz, 1H), 5.03 (d, *J* = 5.6 Hz, 1H), 4.24 (dp, *J* = 8.7, 6.1 Hz, 1H), 3.86 (s, 3H), 3.73 (ddd, *J* = 10.7, 8.7, 3.7 Hz, 1H), 2.69 (dddd, *J* = 10.7, 7.2, 5.5, 1.6 Hz, 1H), 2.64 (d, *J* = 3.3 Hz, 1H), 2.52 (d, *J* = 8.7 Hz, 1H), 2.42 (ddd, *J* = 12.8, 6.3, 1.6 Hz, 1H), 1.80 (ddd, *J* = 12.9, 8.7, 7.3 Hz, 1H), 1.31 (d, *J* = 6.1 Hz, 3H); ^{13}C NMR (101 MHz, $CDCl_3$) δ 157.49, 136.05, 129.94, 124.81, 122.25, 109.86, 77.52, 73.92, 69.64, 64.45, 55.78, 41.23, 36.80, 21.95.

Nocardione B 129 To a stirred solution of $(COCl)_2$ (0.18 mL, 2.2 mmol, 6.0 equiv) in DCM (2.0 mL) was added DMSO (0.33 mL, 4.6 mmol, 12.8 equiv) at -78 °C. The reaction mixture was continued to stir at -78 °C for 30 min, a solution of **128** (90 mg, 0.36 mmol, 1.0 equiv) in

DCM (2.0 mL) was added dropwise over 5 min. The resulting mixture was continued to stir at -78 °C for 2h, Et_3N (1.0 mL, 7.2 mmol, 20.0 equiv) was then added dropwise to the solution. The reaction mixture was continued to stir at -78 °C for 1 h and then allowed to warm slowly to room temperature and stirred for 4 h. Saturated aqueous NH_4Cl solution (2.0 mL) was added, and the mixture was extracted with EtOAc (2 × 30 mL). The combined extracts were washed with brine, dried over Na_2SO_4, and concentrated in vacuo. The residue was purified by flash column chromatographic purification (silica gel, EtOAc /hexanes 4:1) to furnish nocardione B **129** (82 mg, 0.33 mmol, 93% yield) as an orange solid. **129** R_f = 0.3 (silica gel, 80% EtOAc in hexanes); ^{1}H NMR (400 MHz, $CDCl_3$) δ 7.57 (dd, *J* = 8.6, 7.5 Hz, 1H), 7.26 (dd, *J* = 7.5, 1.0 Hz, 1H), 7.15 (dd, *J* = 8.7, 1.0 Hz, 1H), 5.27 – 5.14 (m, 1H), 3.97 (s, 3H), 3.24 (dd, *J* = 15.3, 9.8 Hz, 1H), 2.70 (dd, *J* = 15.3, 7.3 Hz, 1H), 1.55 (d, *J* = 6.3 Hz, 3H); ^{13}C NMR (101 MHz, $CDCl_3$) δ 180.40, 175.72, 169.28, 161.94, 135.90, 129.74, 118.21, 117.38, 116.80, 114.68, 84.21, 56.51, 33.73, 22.12.

3.21 X-Ray Crystallographic Data

General information: The diffraction data were measured at 100 K on a Bruker D8 VENTURE diffractometer equipped with a microfocus Mo-target X-ray tube (λ = 0.71073 Å) and PHOTON 100 CMOS detector. Data were collected using ω scans to survey a hemisphere of reciprocal space. Data reduction and integration were performed with the Bruker APEX4 software package (Bruker AXS, version 2021.4-0, 2021). Data were scaled and corrected for absorption effects using the multi-scan procedure as implemented in SADABS (Bruker AXS, version 2014/5, Krause, Herbst-Irmer, Sheldrick & Stalke, *J. Appl. Cryst.* **2015**, *48*, 3-10). The structure was solved by SHELXT (Version 2018/2: Sheldrick, G. M. *Acta Crystallogr*. **2015**, ***A71***, 3-8) and refined by a full-matrix least-squares procedure using OLEX2 (O. V. Dolomanov, L. J. Bourhis, R. J. Gildea, J. A. K. Howard and H. Puschmann. J. Appl.

Crystallogr. **2009**, *42*, 339-341) (XL refinement program version 2018/3, Sheldrick, G. M. Acta Crystallogr. **2015**, *C71*, 3-8). Crystallographic data and details of the data collection and structure refinement are listed in Table 1.

Specific details for structure refinement: All atoms were refined with anisotropic thermal parameters. All hydrogen atoms were included in idealized positions for structure factor calculations. All structures are drawn with thermal ellipsoids at 50% probability.

Figure 3.1 ORTEP representation of **103**

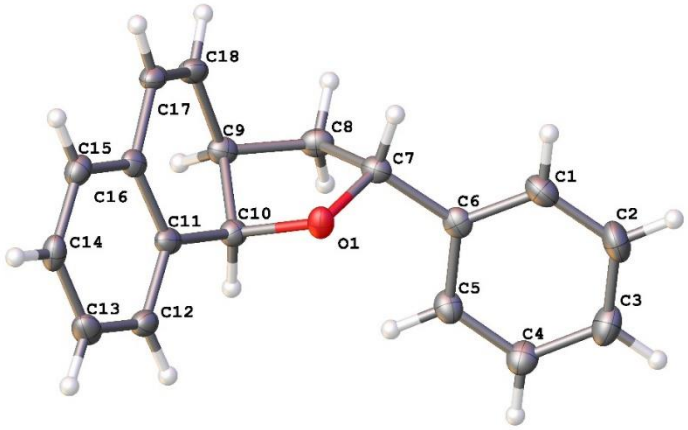

Crystal data and structure refinement for 1088_JK_Snyder1.

Identification code	1088_JK_Snyder1
Empirical formula	$C_{18}H_{16}O$
Formula weight	248.31
Temperature/K	100(2)
Crystal system	trigonal
Space group	$P3_1$
a/Å	18.7624(9)
b/Å	18.7624(9)
c/Å	9.7976(6)
α/°	90
β/°	90
γ/°	120
Volume/Å^3	2986.9(3)
Z	9
ρ_{calc}g/cm^3	1.242

Figure 3.1 cont.	
μ/mm^{-1}	0.075
F(000)	1188.0
Crystal size/mm^3	0.43 × 0.171 × 0.07
Radiation	MoKα (λ = 0.71073)
2Θ range for data collection/°	4.342 to 56.544
Index ranges	$-25 \leq h \leq 25$, $-25 \leq k \leq 24$, $-13 \leq l \leq 11$
Reflections collected	52229
Independent reflections	9378 [R_{int} = 0.0597, R_{sigma} = 0.0511]
Data/restraints/parameters	9378/1/514
Goodness-of-fit on F^2	1.049
Final R indexes [I>=2σ (I)]	R_1 = 0.0469, wR_2 = 0.0895
Final R indexes [all data]	R_1 = 0.0678, wR_2 = 0.0962
Largest diff. peak/hole / e $Å^{-3}$	0.26/-0.22

$R_{int} = \Sigma \mid F_o^2 - \langle F_o^2 \rangle \mid / \Sigma \mid F_o^2 \mid$

$R1 = \Sigma \mid \mid F_o \mid - \mid F_c \mid \mid / \Sigma \mid F_o \mid$

$wR2 = [\Sigma [w (F_o^2 - F_c^2)^2] / \Sigma [w (F_o^2)^2]]^{1/2}$

Goodness-of-fit = $[\Sigma [w (F_o^2 - F_c^2)^2] / (n-p)]^{1/2}$

n: number of independent reflections; p: number of refined parameters

3.22 NMR Spectra

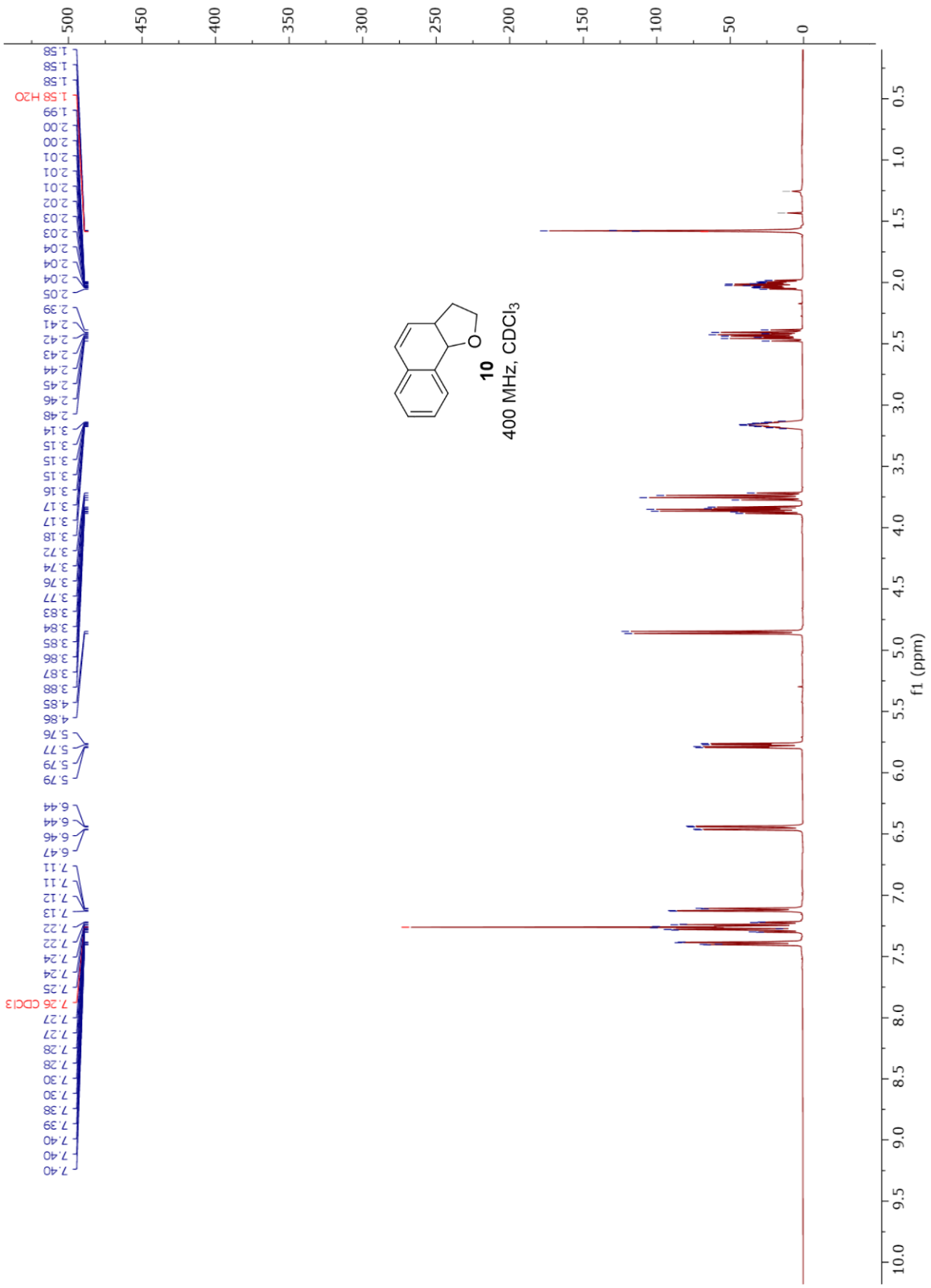

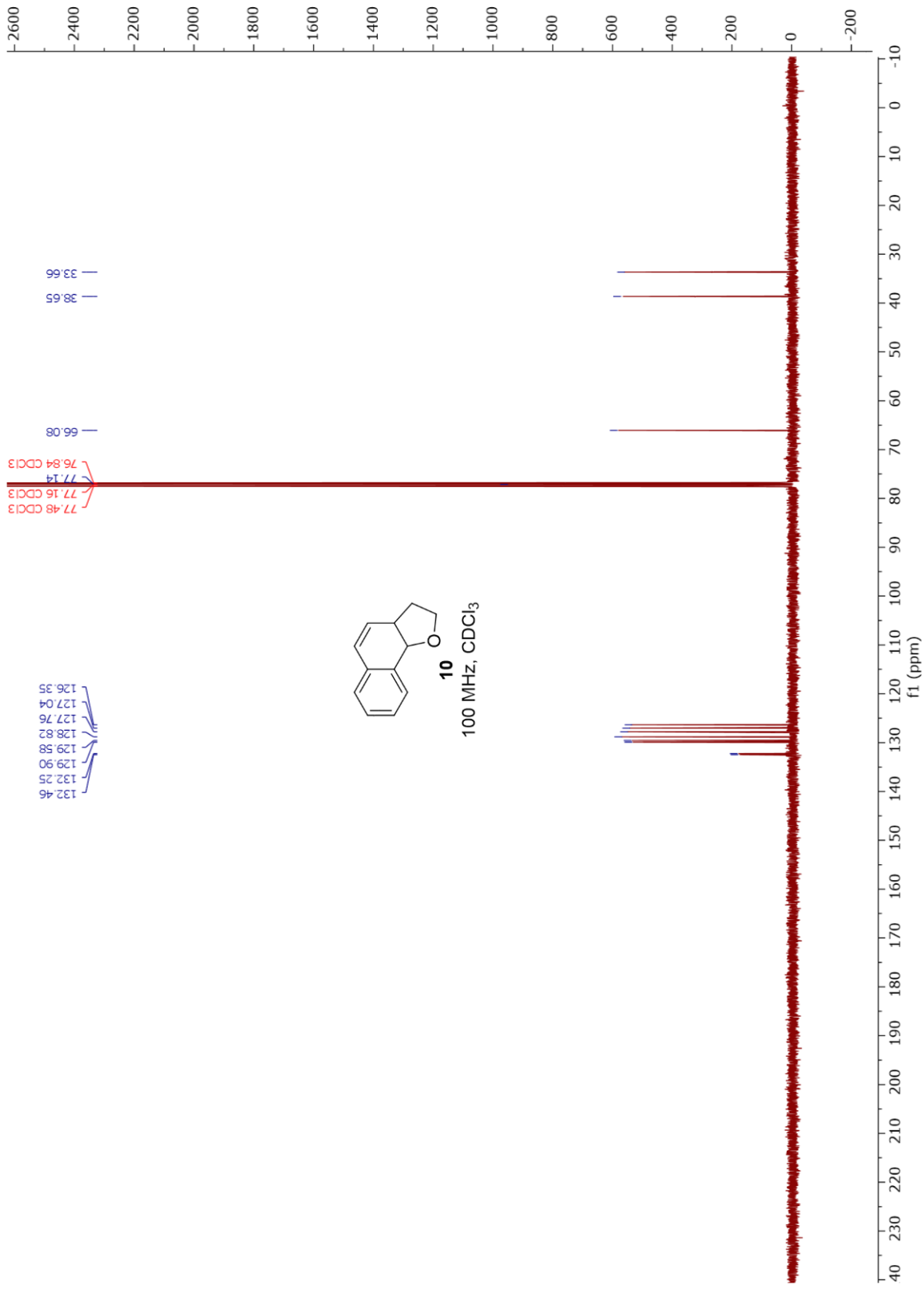
10
100 MHz, CDCl3
f1 (ppm)
33.66
38.65
66.08
76.84 CDCl3
77.14
77.16 CDCl3
77.48 CDCl3
126.35
127.04
127.76
128.82
129.58
129.90
132.25
132.46

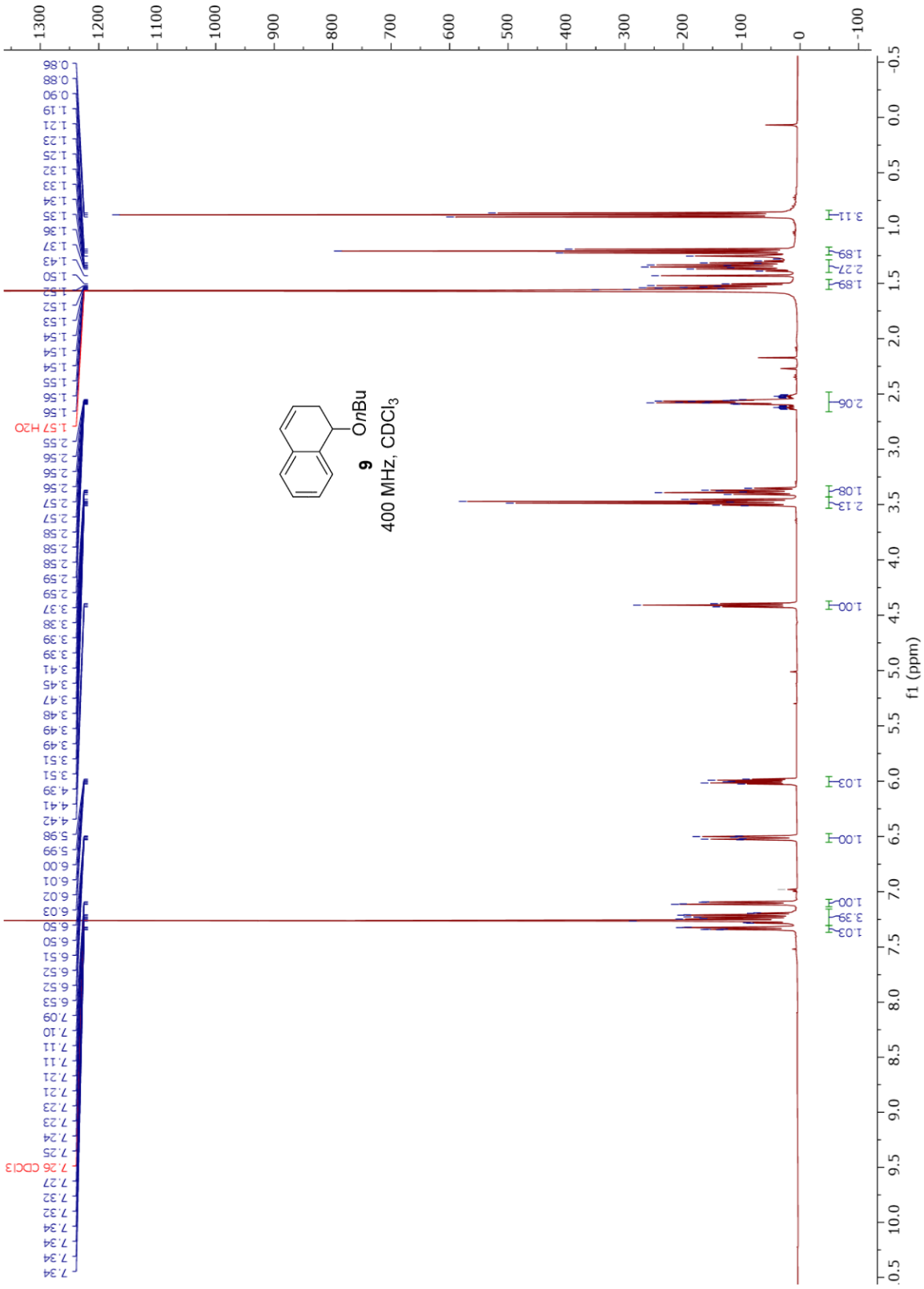
OnBu
9
400 MHz, CDCl3
f1 (ppm)

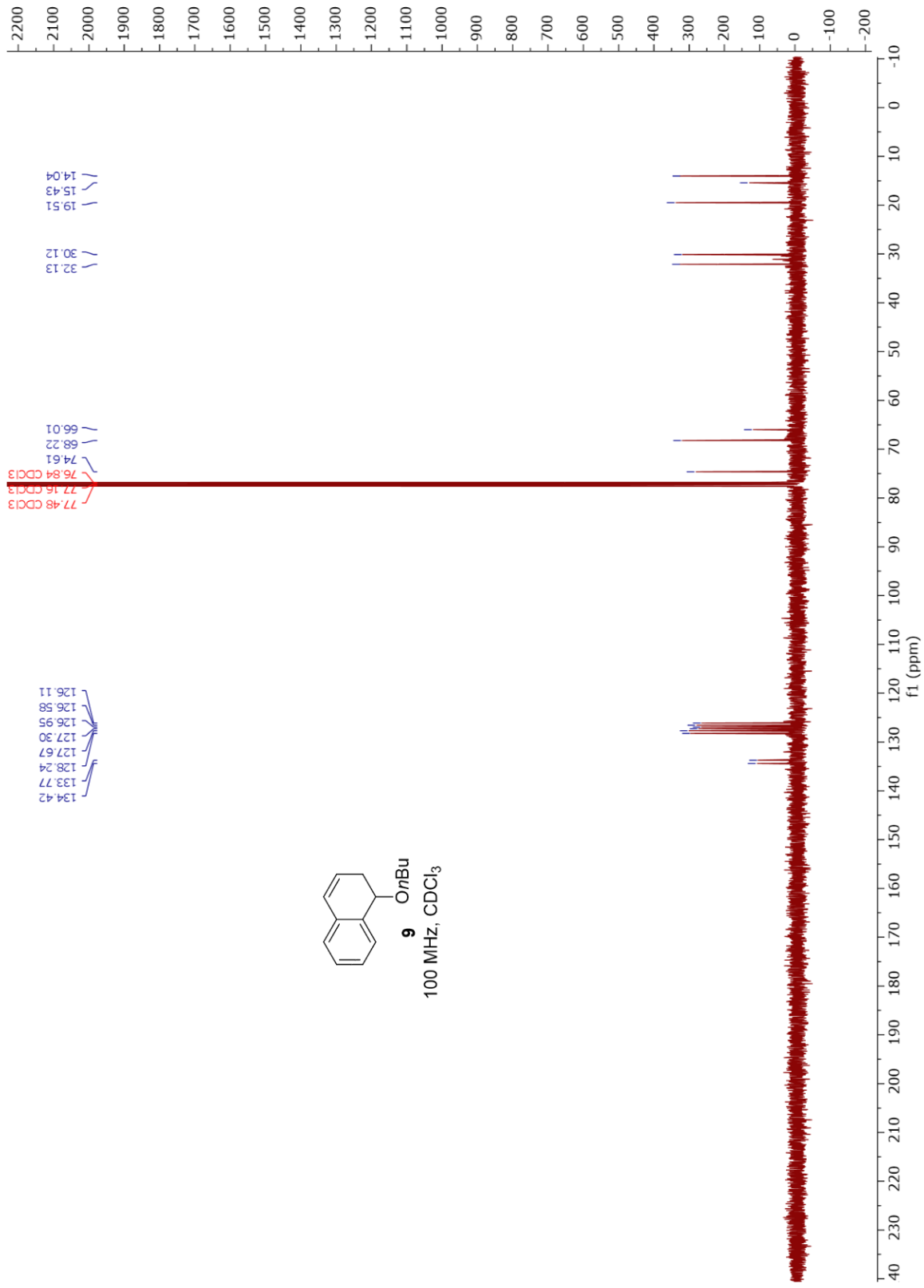
14.04
15.43
19.51
30.12
32.13
66.01
68.22
74.61
76.84 CDCl3
77.16 CDCl3
77.48 CDCl3
126.11
126.58
126.95
127.30
127.67
128.24
133.77
134.42
OnBu
9
100 MHz, CDCl3
f1 (ppm)

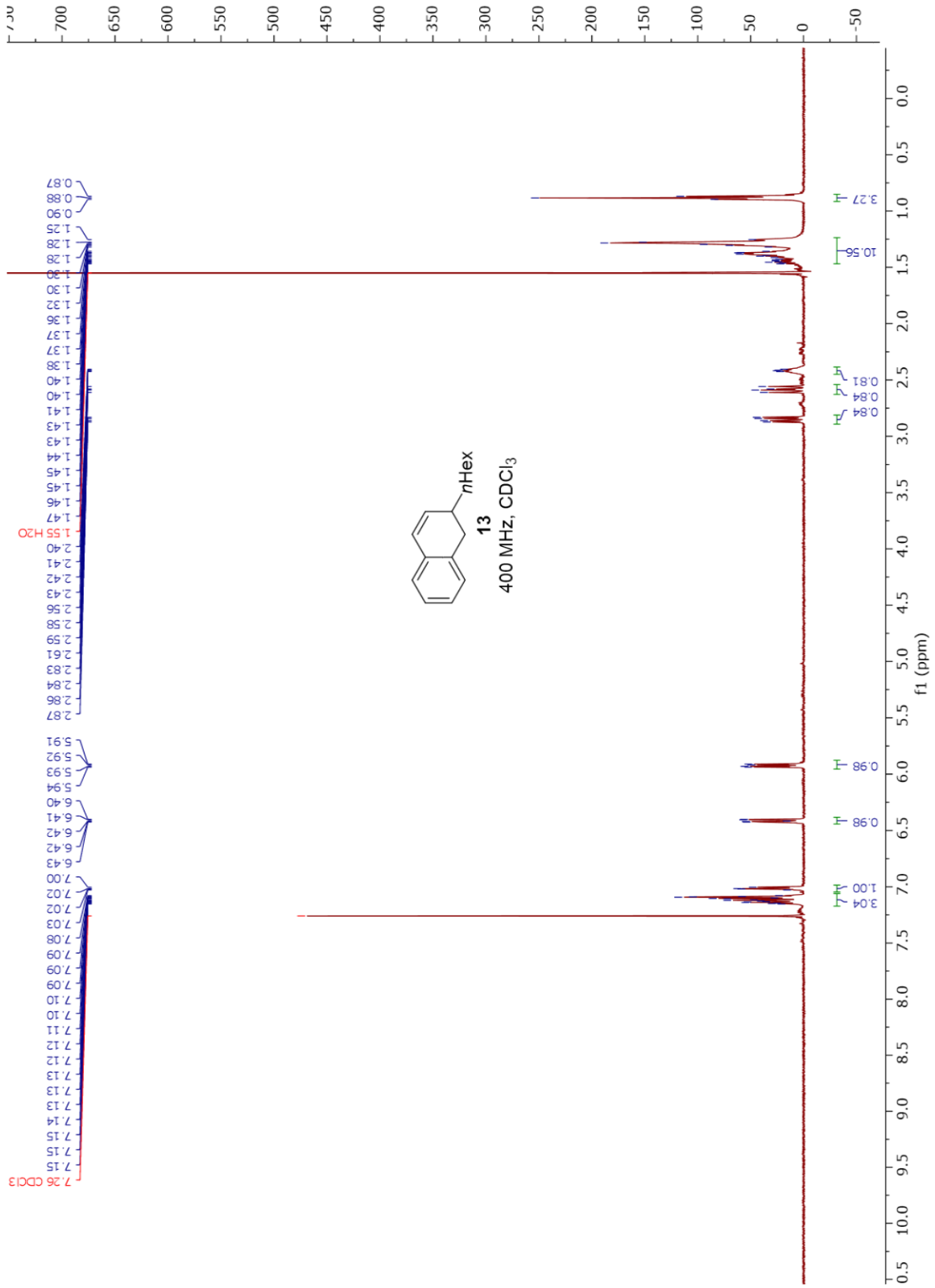
nHex
13
400 MHz, CDCl3
f1 (ppm)

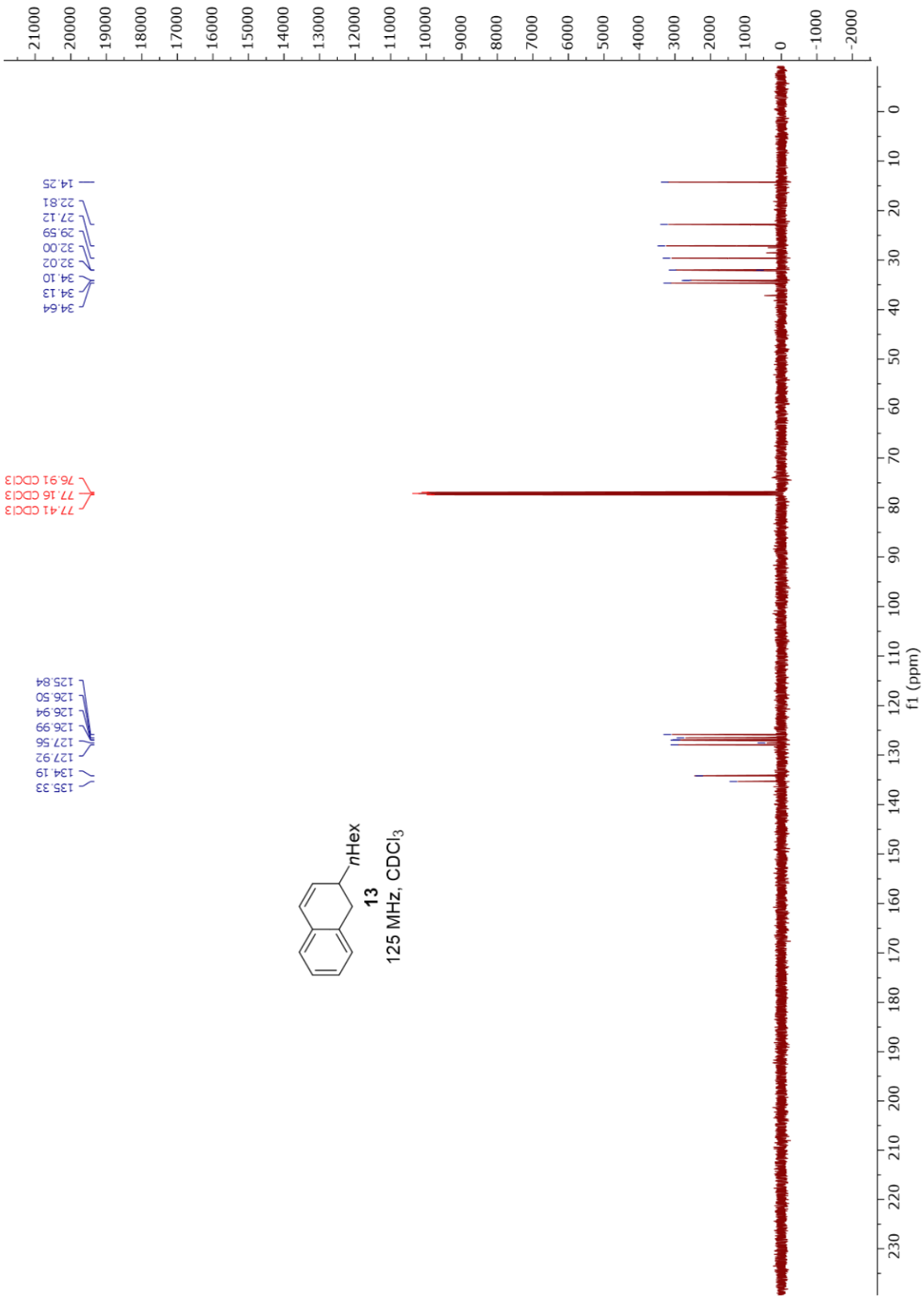
nHex
13
125 MHz, CDCl3
f1 (ppm)

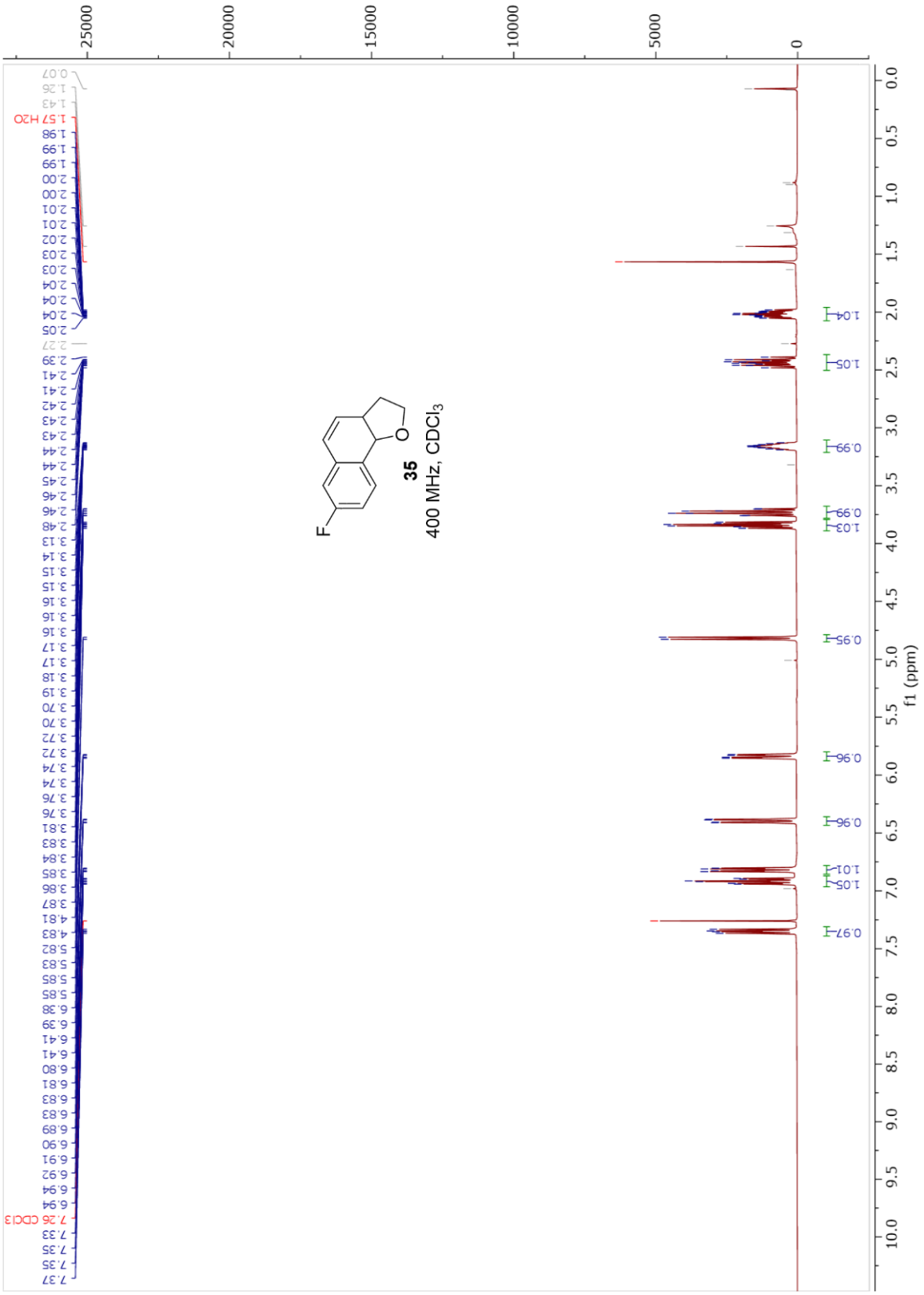
35
400 MHz, CDCl3
F
O
f1 (ppm)
1.57 H2O
7.26 CDCl3

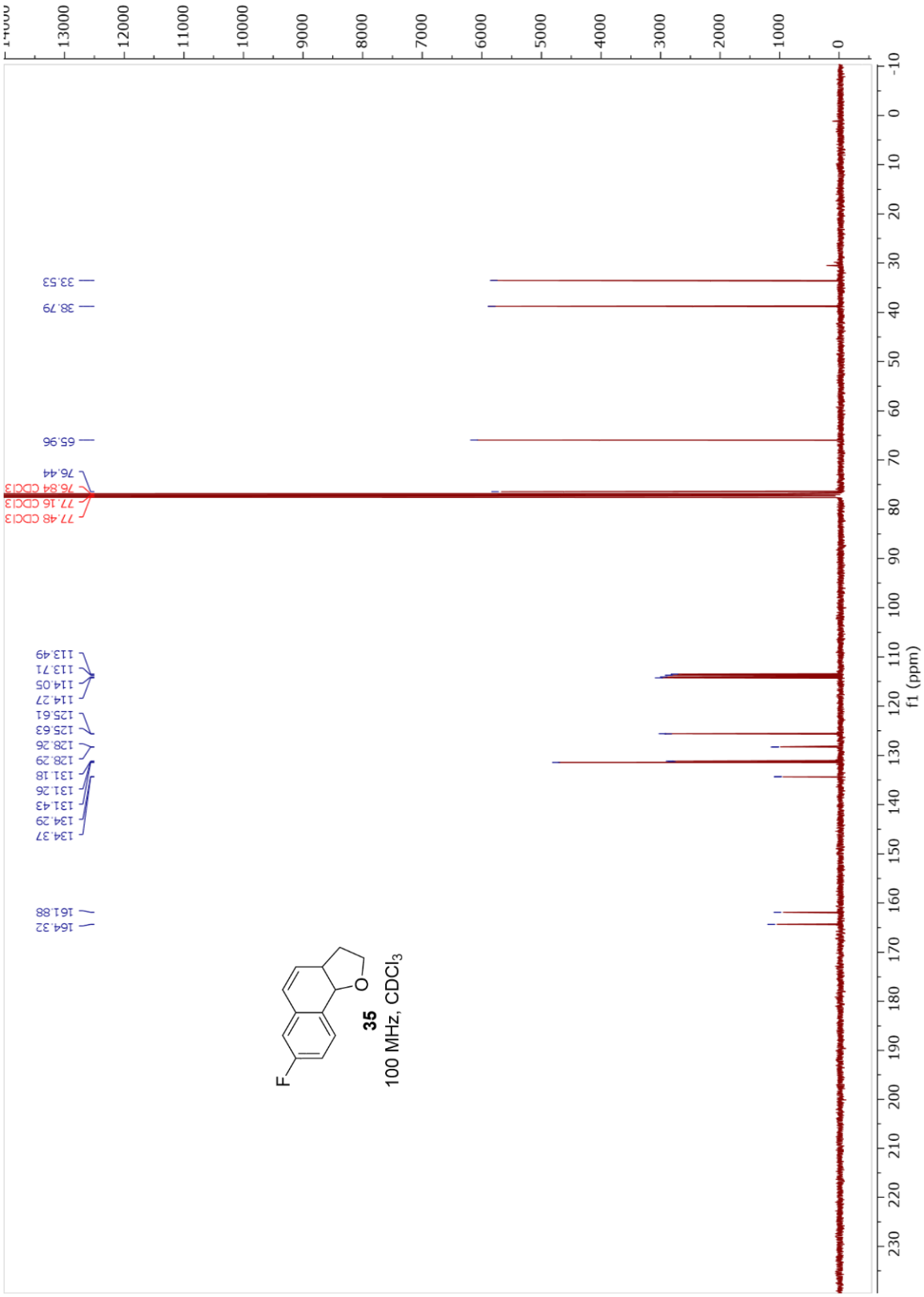
33.53
38.79
65.96
76.44
76.84 CDCl3
77.16 CDCl3
77.48 CDCl3
113.49
113.71
114.05
114.27
125.61
125.63
128.26
128.29
131.18
131.26
131.43
134.29
134.37
161.88
164.32
F
O
35
100 MHz, CDCl3
f1 (ppm)

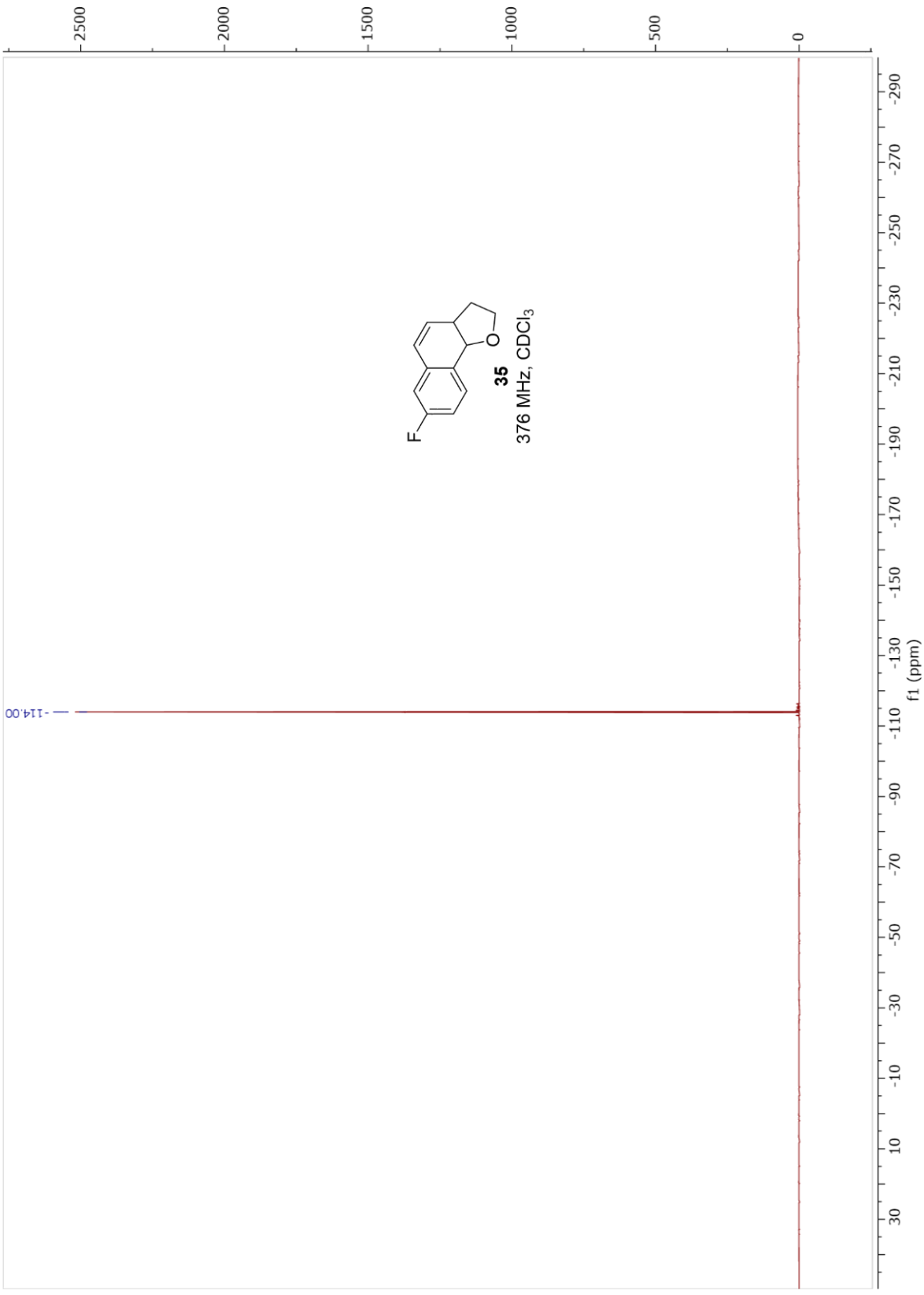
2500
2000
1500
1000
500
0
-114.00
30
10
-10
-30
-50
-70
-90
-110
-130
-150
-170
-190
-210
-230
-250
-270
-290
f1 (ppm)
F
O
35
376 MHz, CDCl3

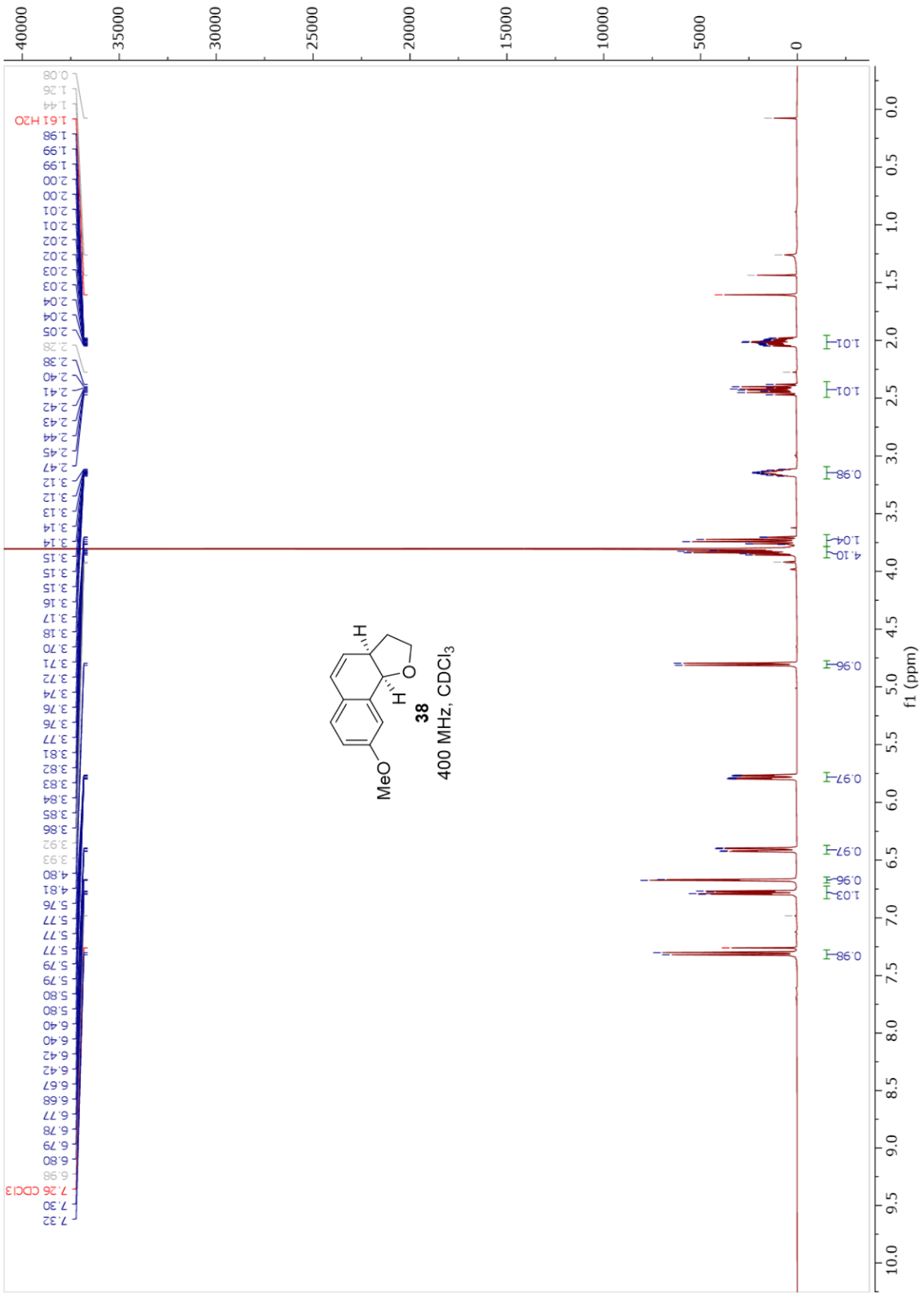
MeO
H
O
H
38
400 MHz, CDCl3
f1 (ppm)

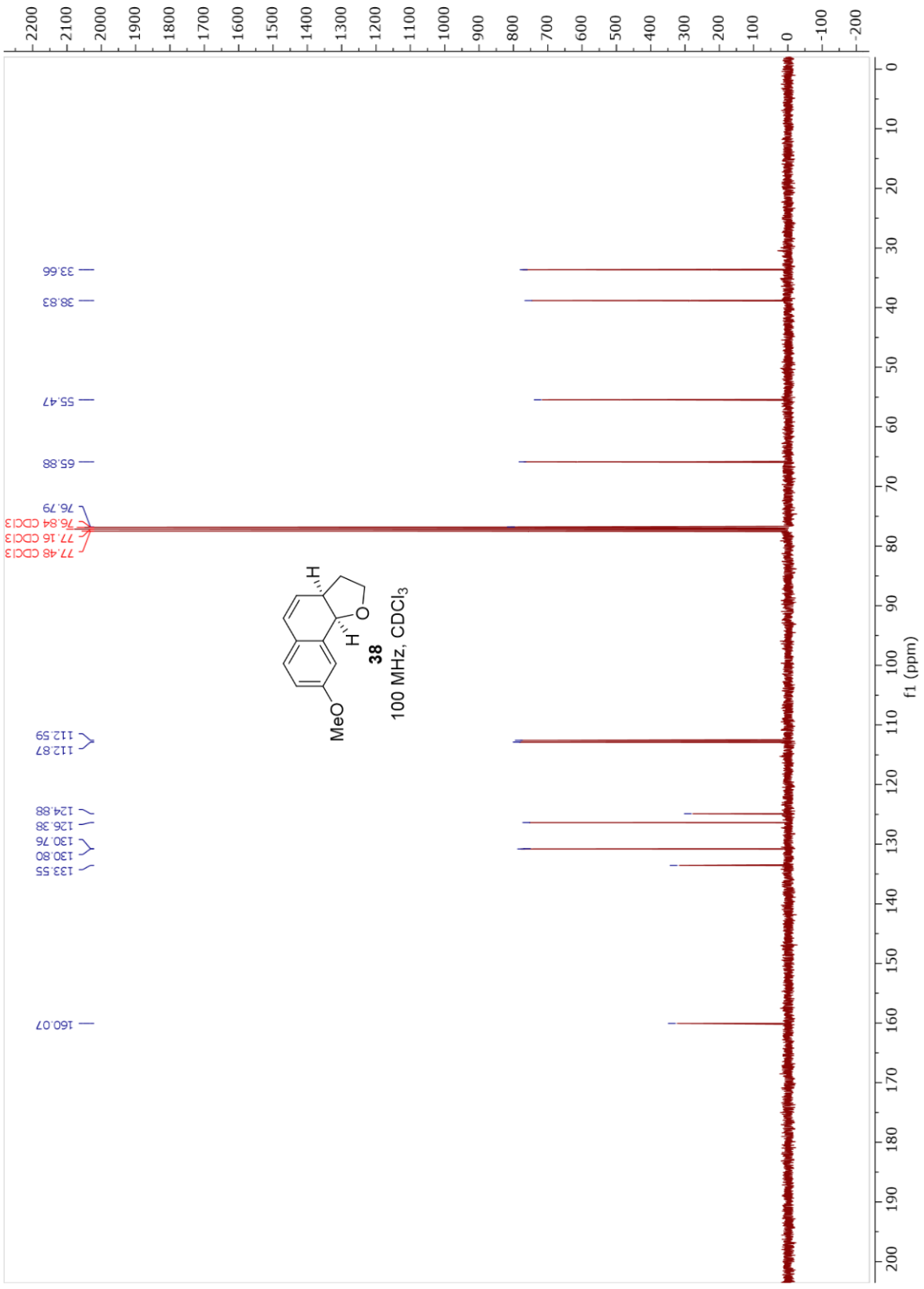
38
100 MHz, CDCl3
MeO
H
H
O
33.66
38.83
55.47
65.88
76.79
76.84 CDCl3
77.16 CDCl3
77.48 CDCl3
112.87
112.59
124.88
126.38
130.76
130.80
133.55
160.07
f1 (ppm)

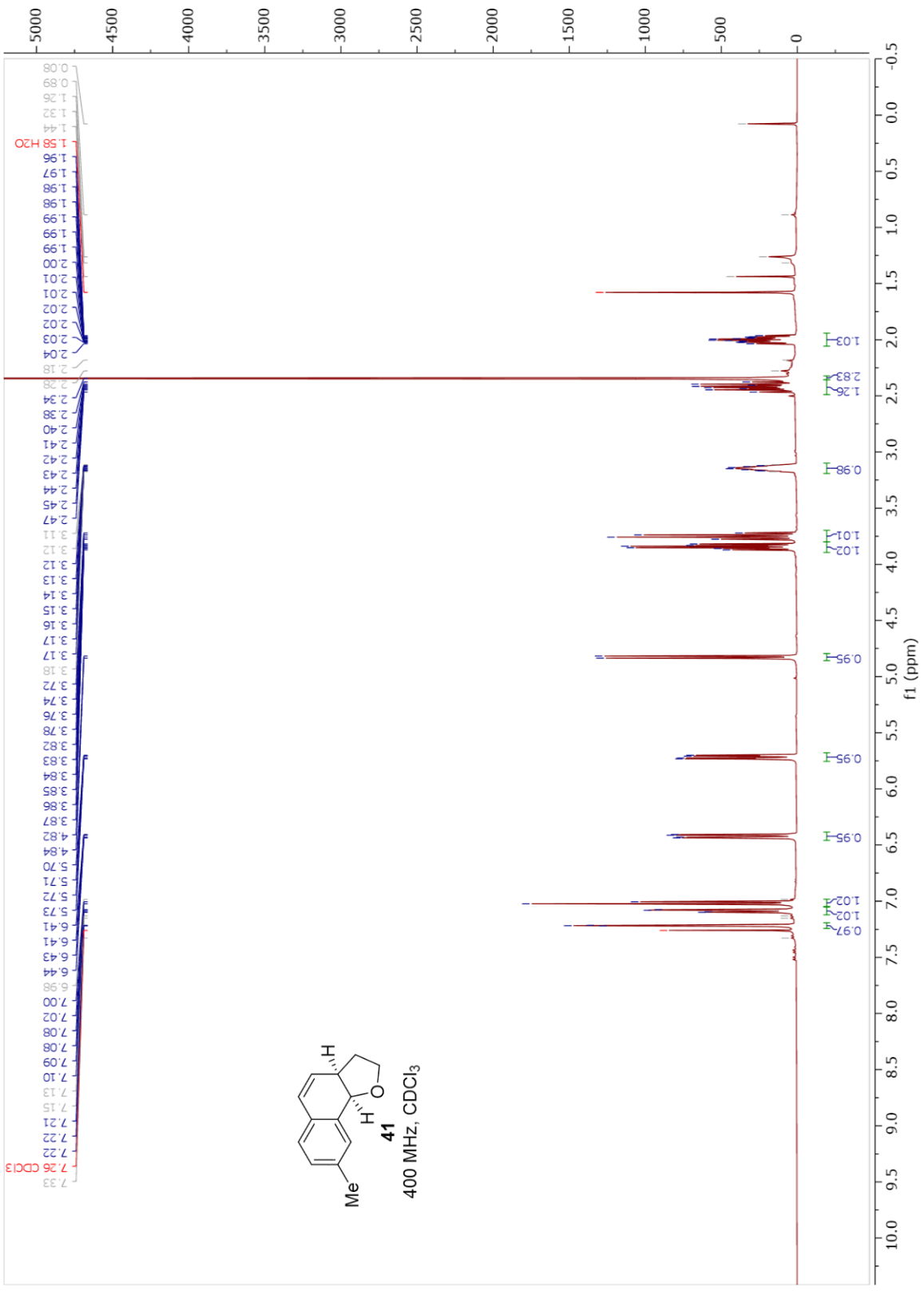
41
400 MHz, CDCl3
Me
H
O
H
f1 (ppm)
7.26 CDCl3
1.58 H2O

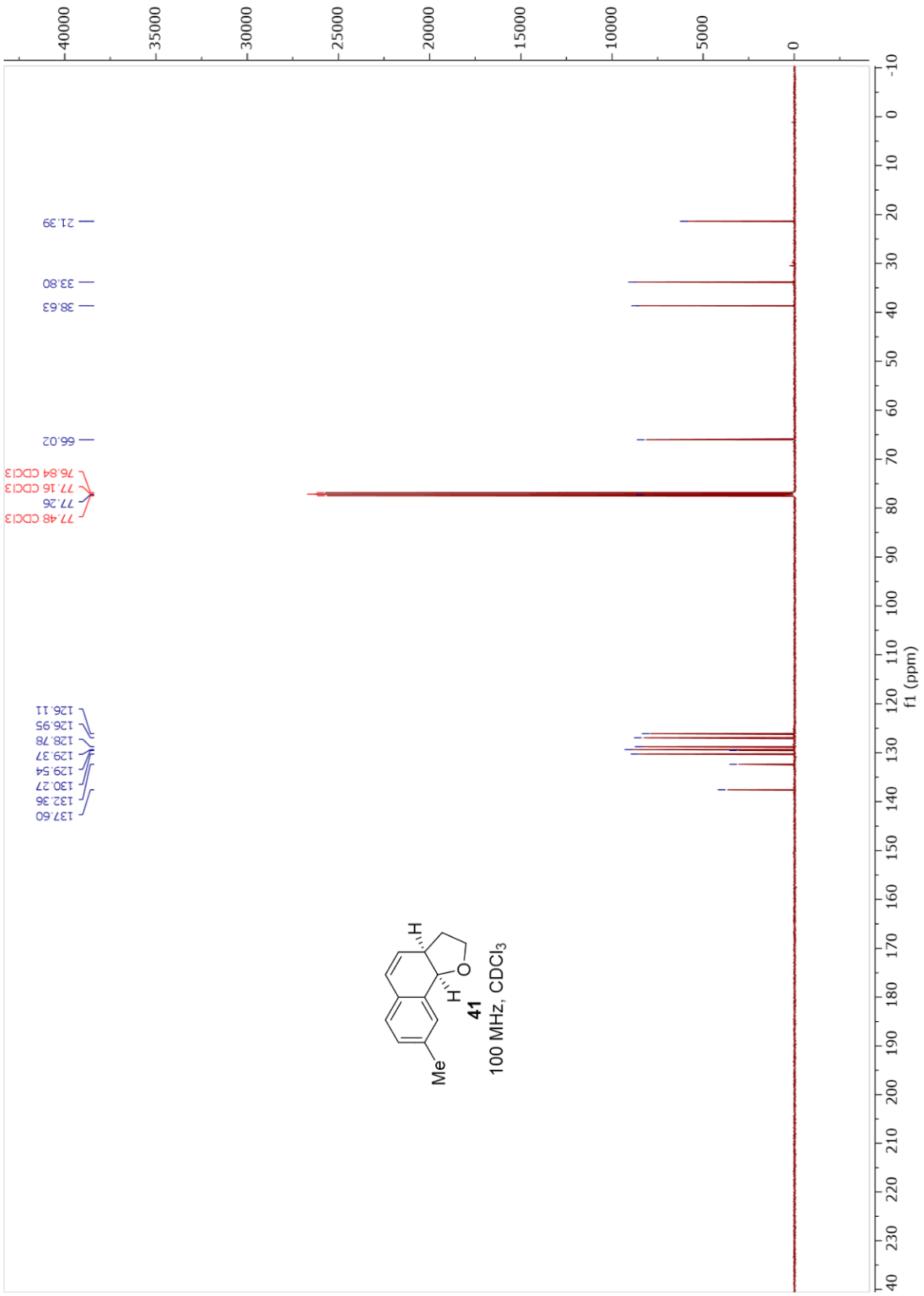
21.39
33.80
38.63
66.02
76.84 CDCl3
77.16 CDCl3
77.26
77.48 CDCl3
126.11
126.95
128.78
129.37
129.54
130.27
132.36
137.60
f1 (ppm)
Me
H
O
H
41
100 MHz, CDCl3

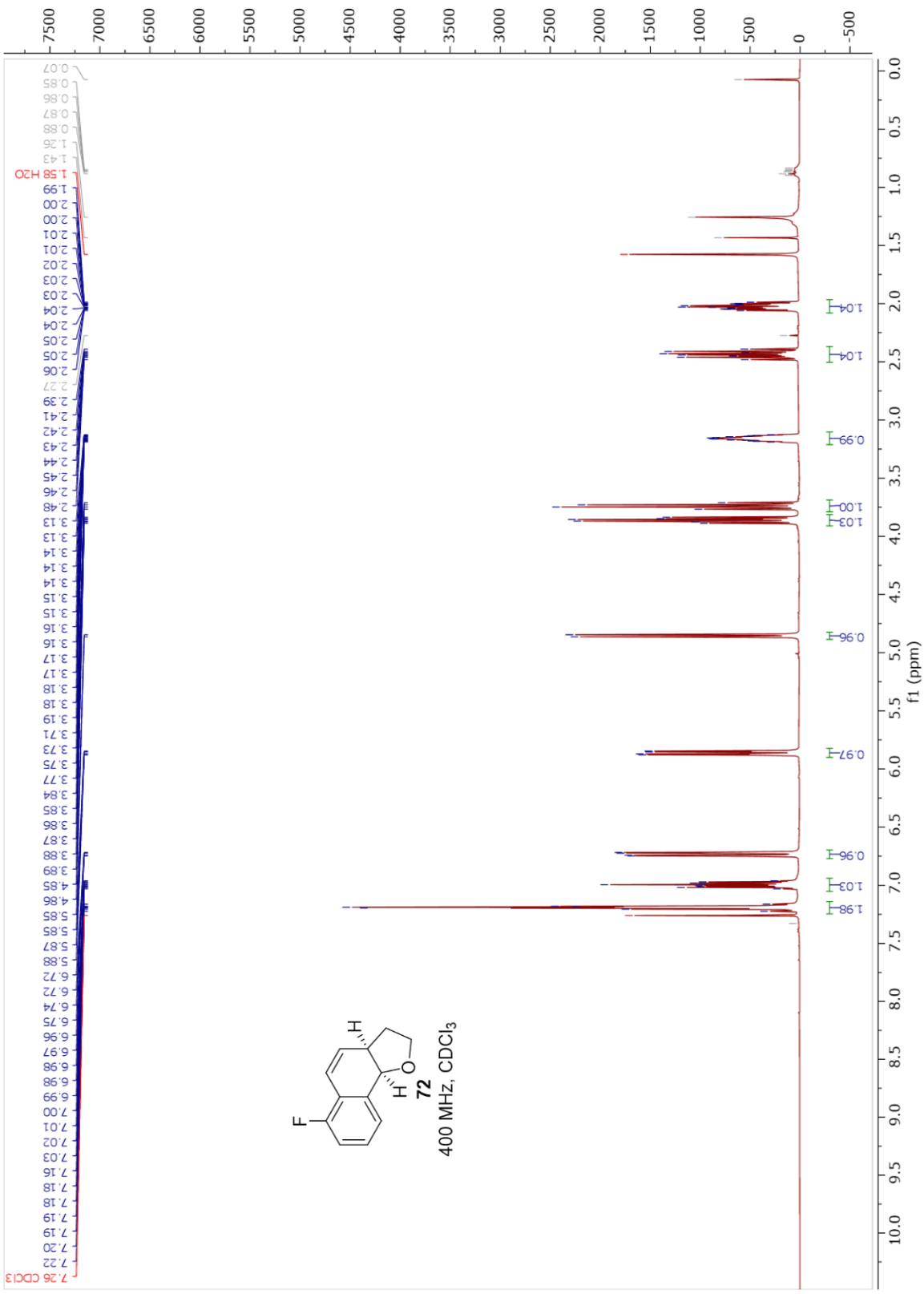
72
400 MHz, CDCl3
f1 (ppm)

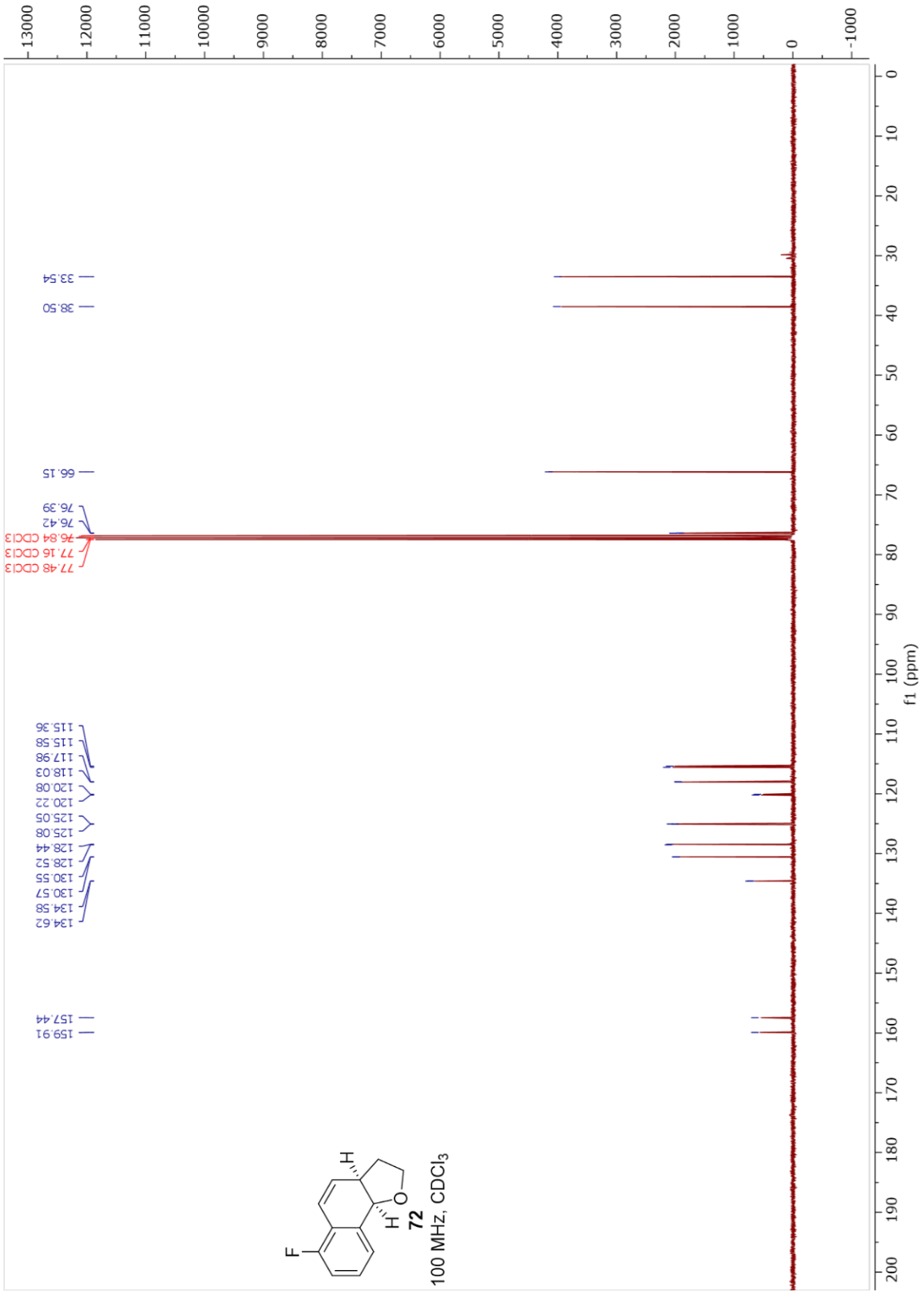
33.54
38.50
66.15
76.39
76.42
76.84 CDCl3
77.16 CDCl3
77.48 CDCl3
115.36
115.58
117.98
118.03
120.08
120.22
125.05
125.08
128.44
128.52
130.55
130.57
134.58
134.62
157.44
159.91
f1 (ppm)
72
100 MHz, CDCl3

-123.48
F
H
O
H
72
376 MHz, CDCl3
f1 (ppm)

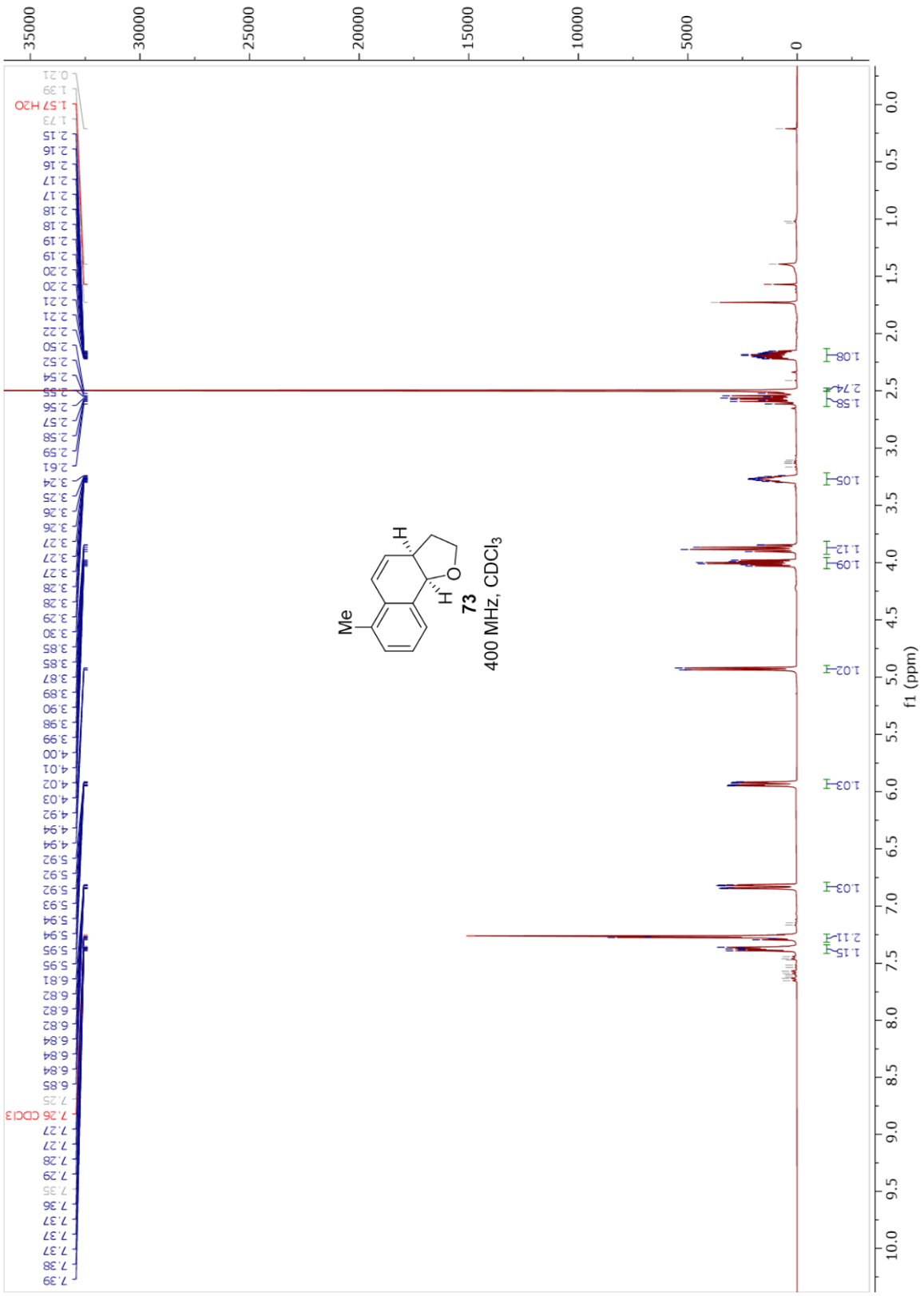
Me
H
O
H
73
400 MHz, CDCl3
f1 (ppm)

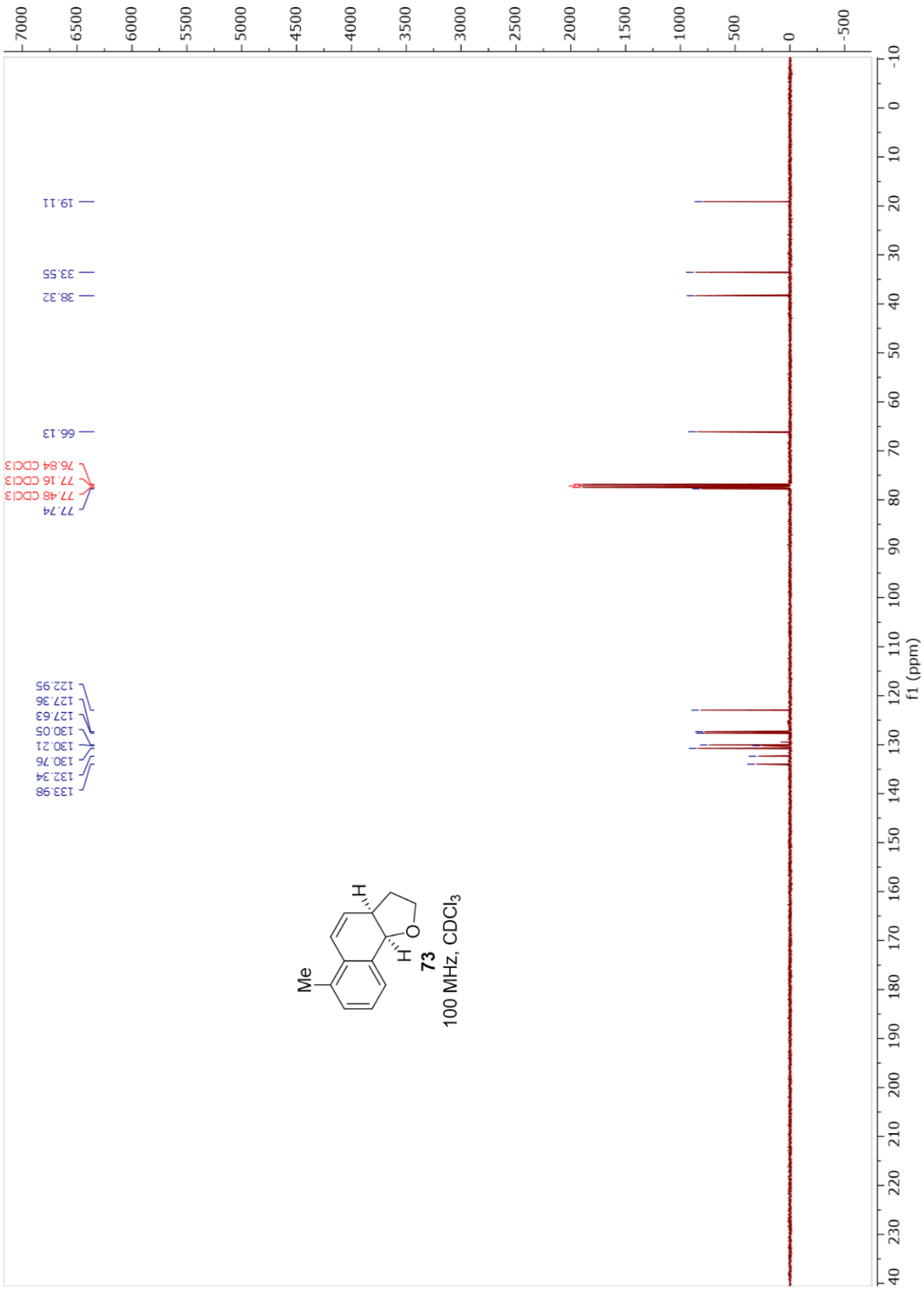
19.11
33.55
38.32
66.13
76.84 CDCl3
77.16 CDCl3
77.48 CDCl3
77.74
122.95
127.36
127.63
130.05
130.21
130.76
132.34
133.98
Me
H
O
H
73
100 MHz, CDCl3
f1 (ppm)

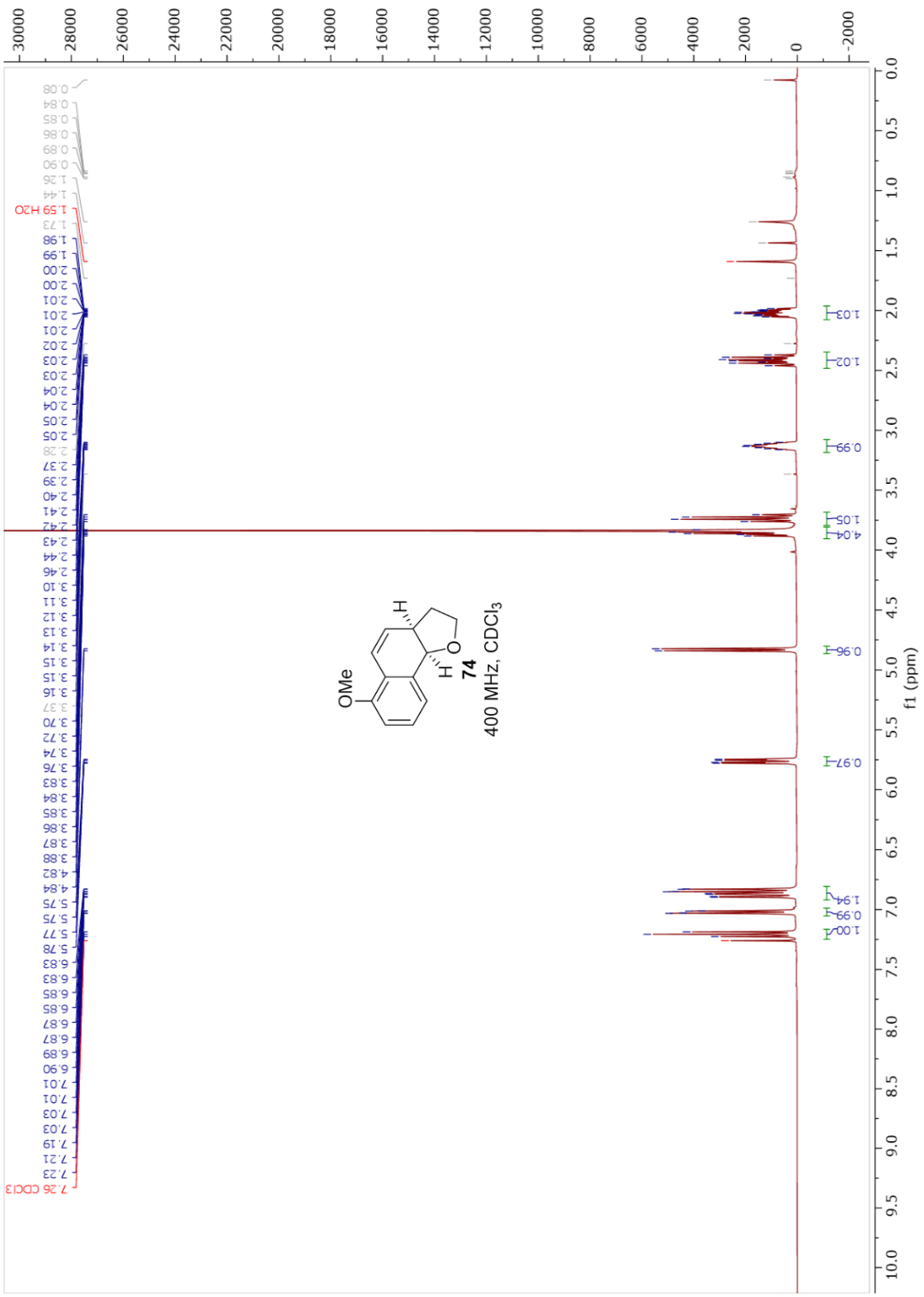
OMe
H
O
H
74
400 MHz, CDCl3
f1 (ppm)

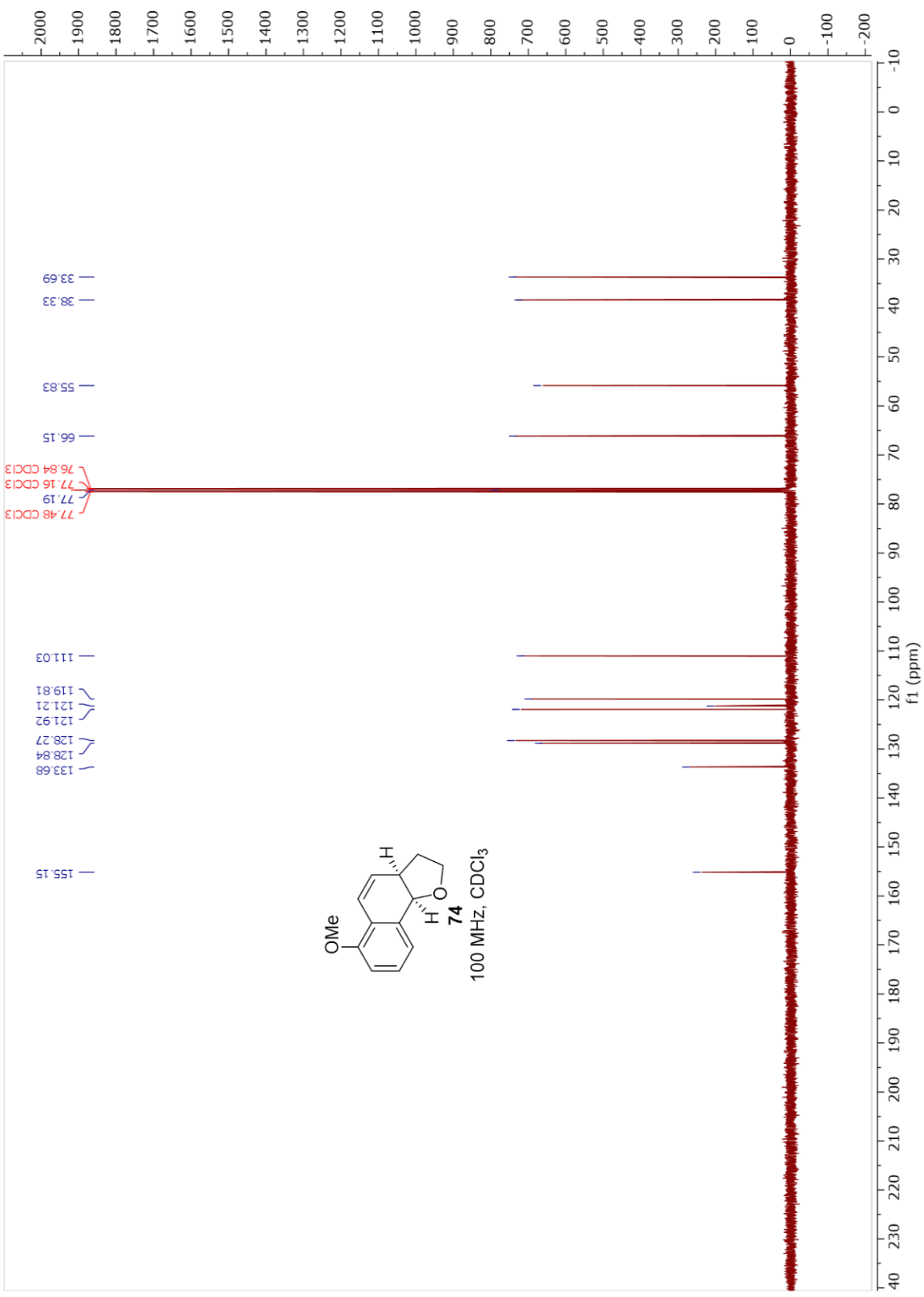
155.15
133.68
128.84
128.27
121.92
121.21
119.81
111.03
77.48 CDCl3
77.19
77.16 CDCl3
76.84 CDCl3
66.15
55.83
38.33
33.69
OMe
H
O
H
74
100 MHz, CDCl3
f1 (ppm)

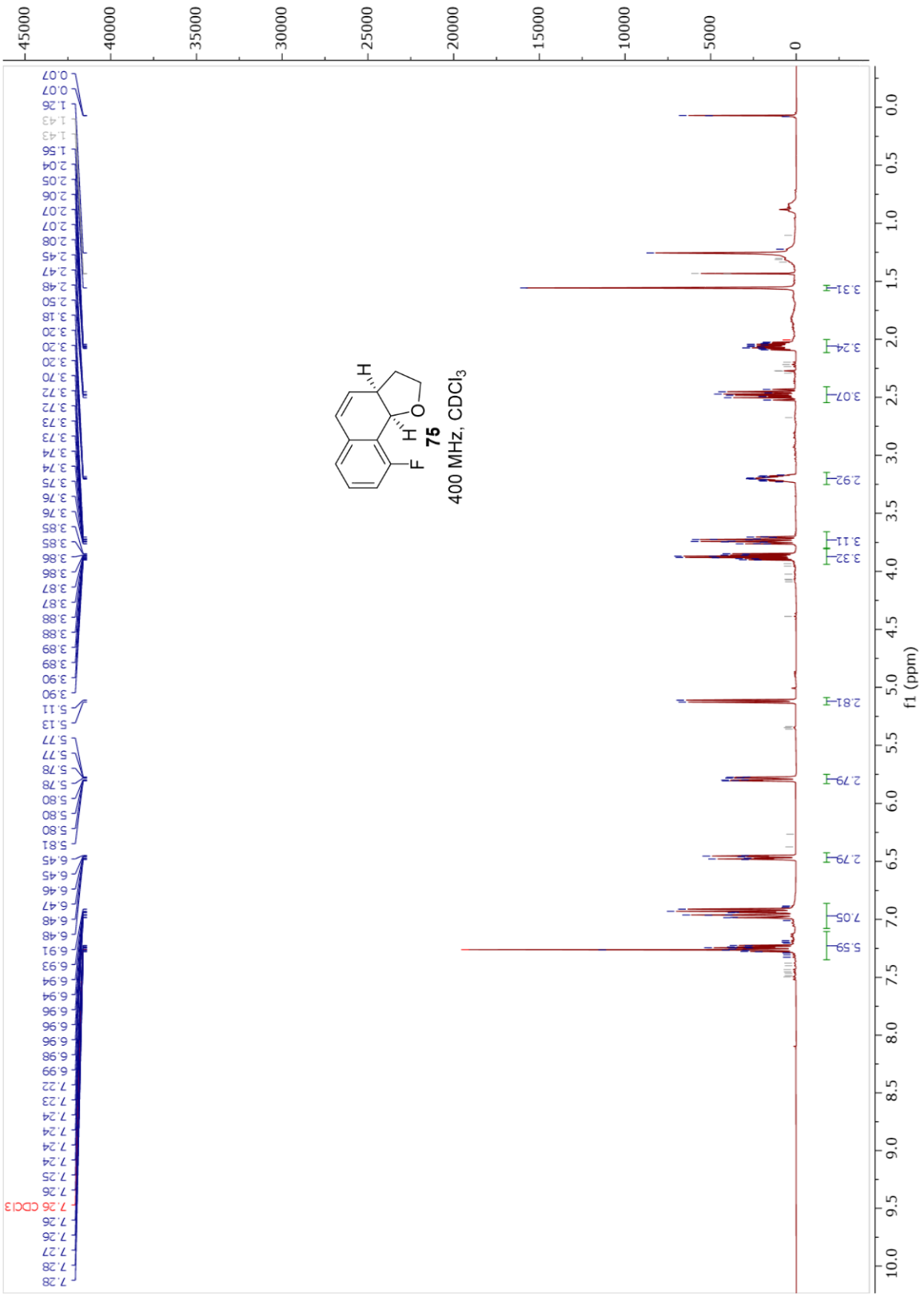
75
400 MHz, CDCl3
f1 (ppm)

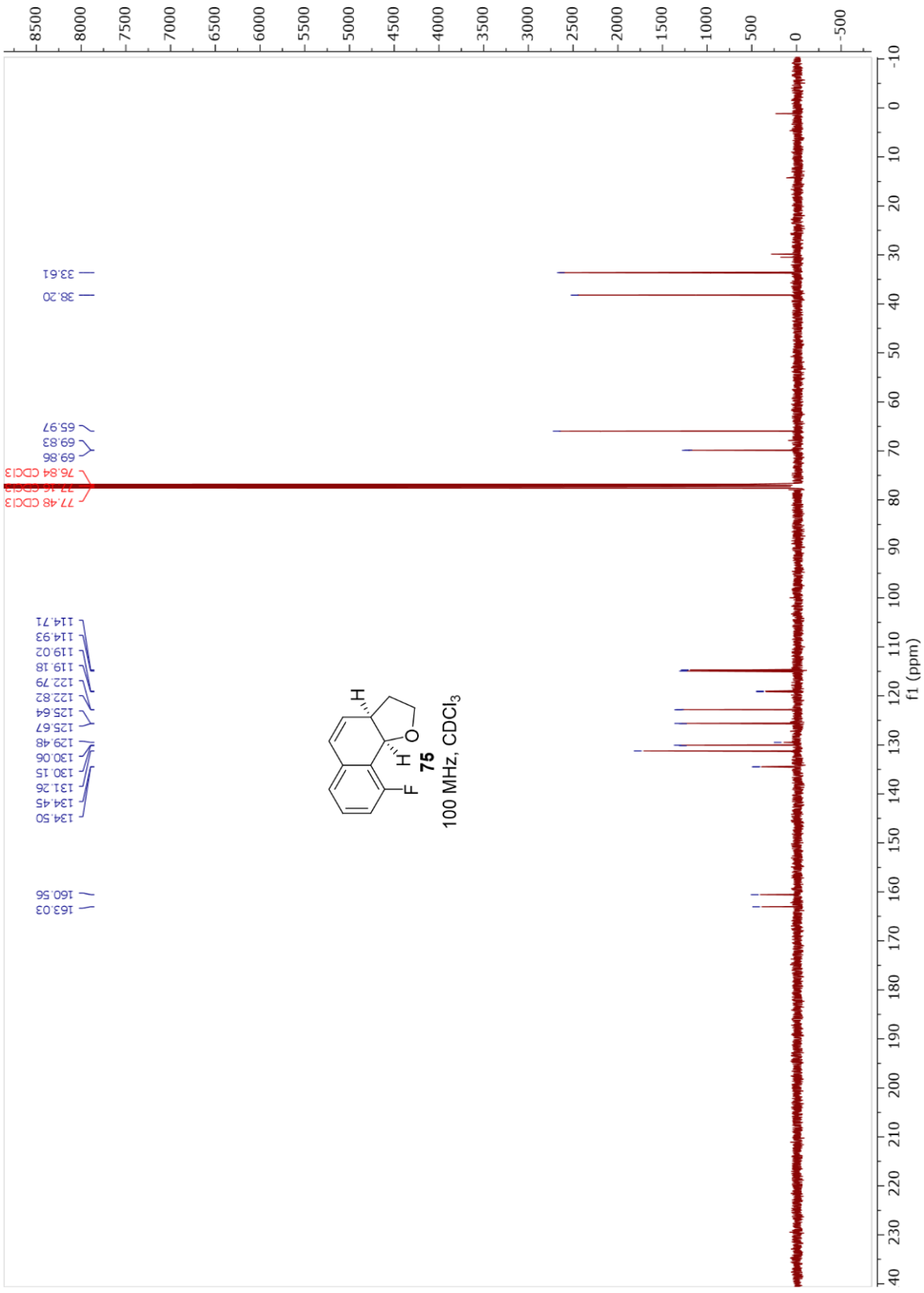
33.61
38.20
65.97
69.83
69.86
76.84 CDCl3
77.16 CDCl3
77.48 CDCl3
114.71
114.93
119.02
119.18
122.79
122.82
125.64
125.67
129.48
130.06
130.15
131.26
134.45
134.50
160.56
163.03
H
O
H
F
75
100 MHz, CDCl3
f1 (ppm)

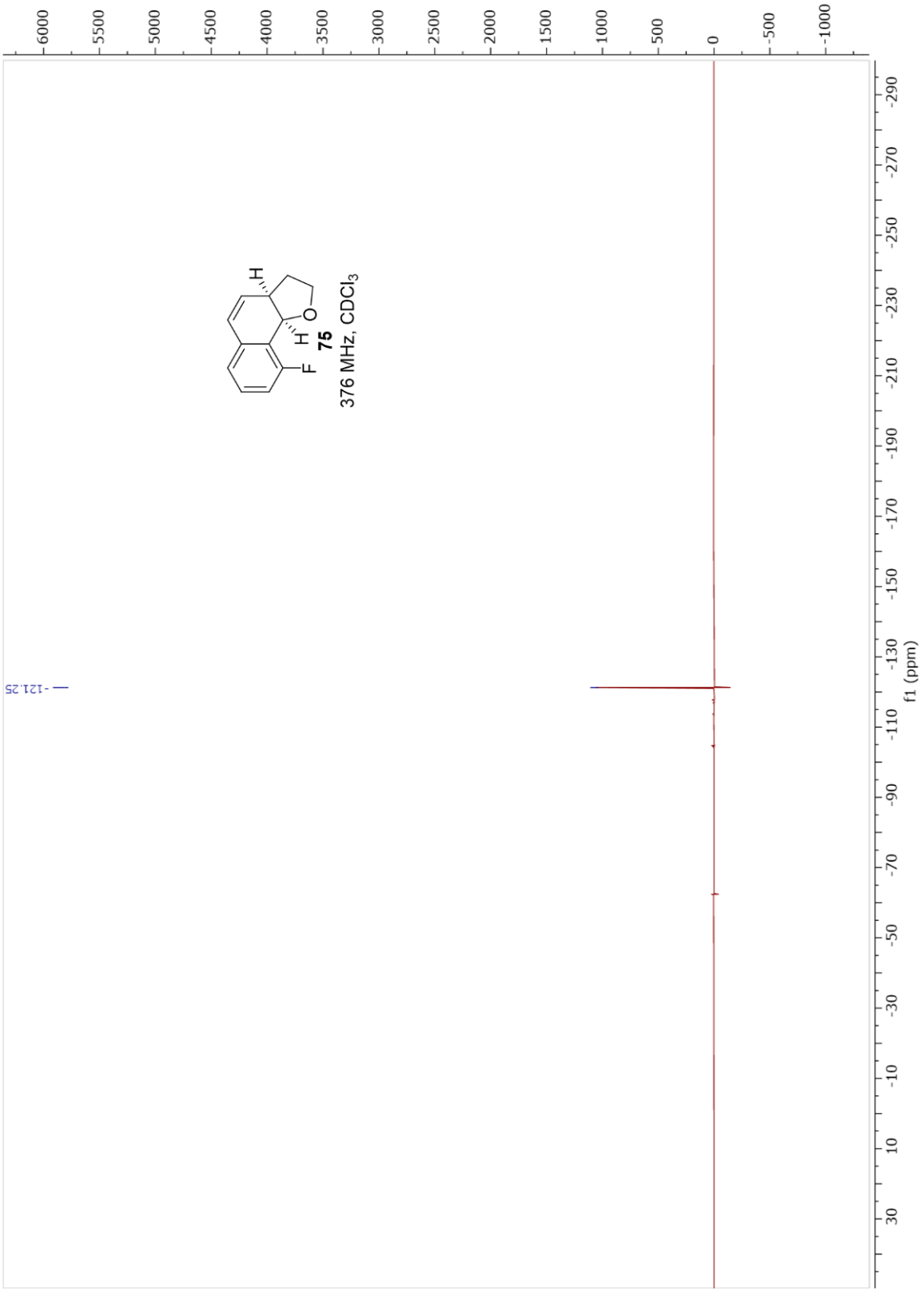
6000
5500
5000
4500
4000
3500
3000
2500
2000
1500
1000
500
0
-500
-1000
-121.25
30
10
-10
-30
-50
-70
-90
-110
-130
-150
-170
-190
-210
-230
-250
-270
-290
f1 (ppm)
H
O
H
F
75
376 MHz, CDCl3

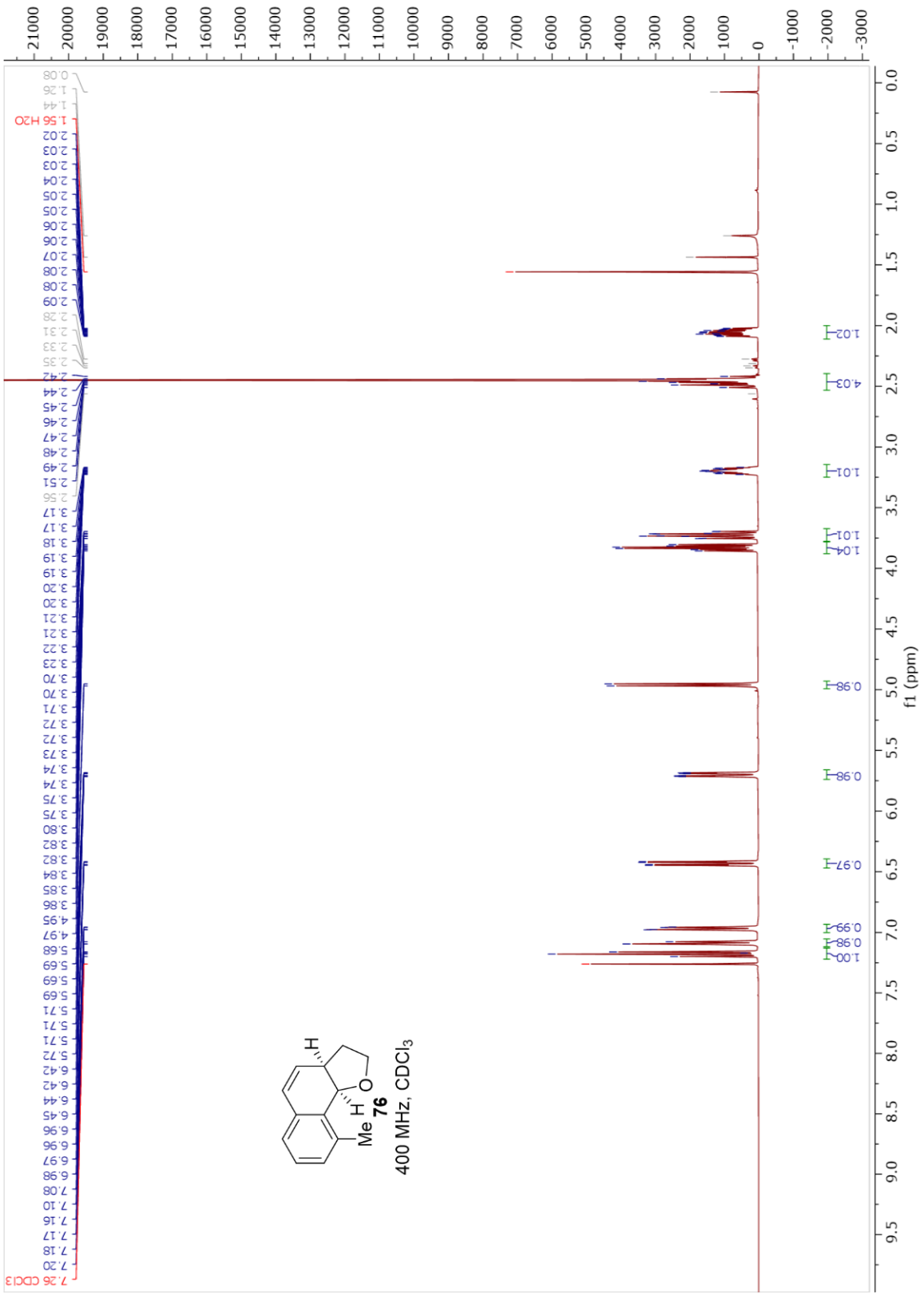
H
O
H
Me
76
400 MHz, CDCl3
f1 (ppm)

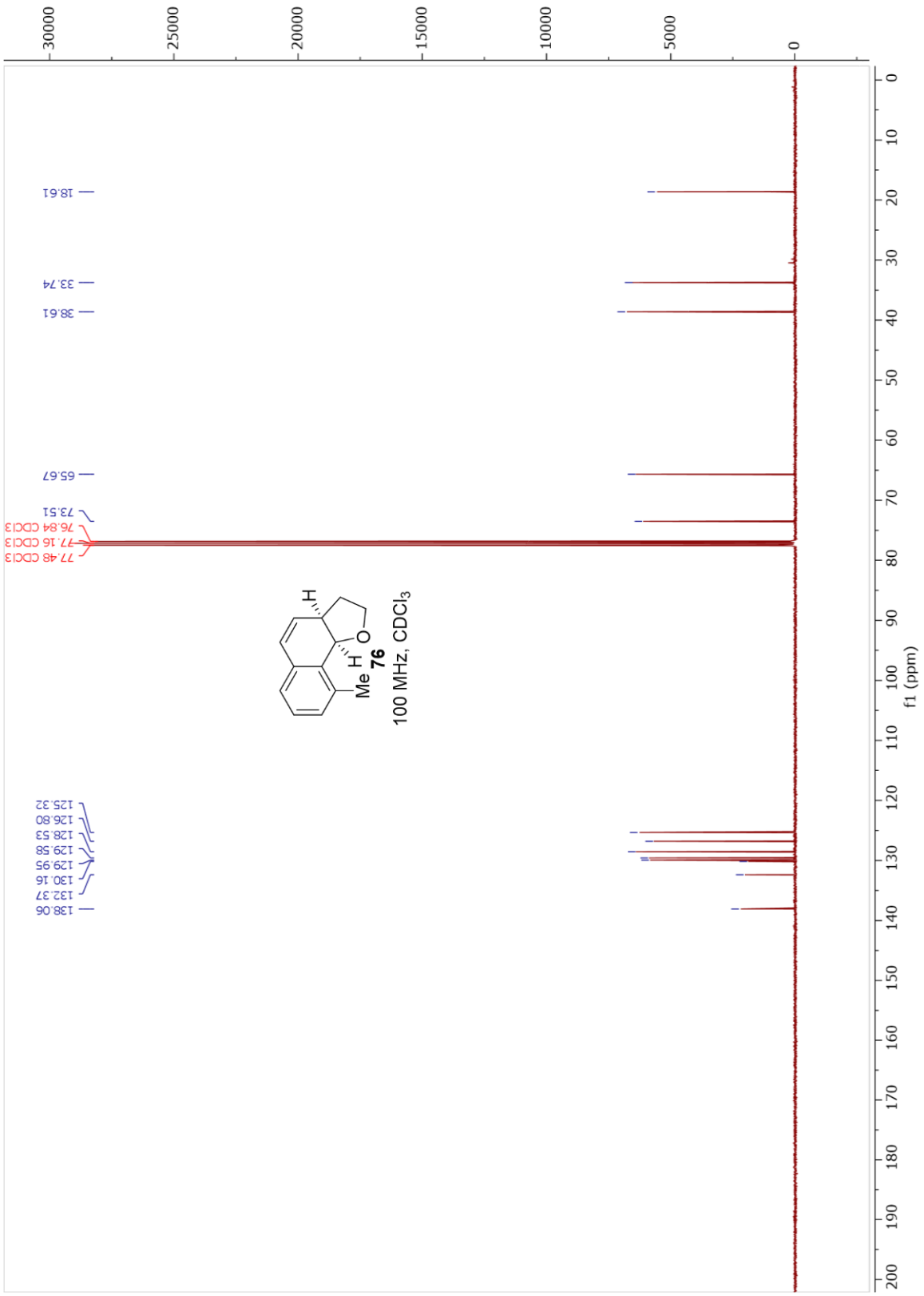
18.61
33.74
38.61
65.67
73.51
76.84 CDCl3
77.16 CDCl3
77.48 CDCl3
125.32
126.80
128.53
129.58
129.95
130.16
132.37
138.06
Me
H
O
H
76
100 MHz, CDCl3
f1 (ppm)

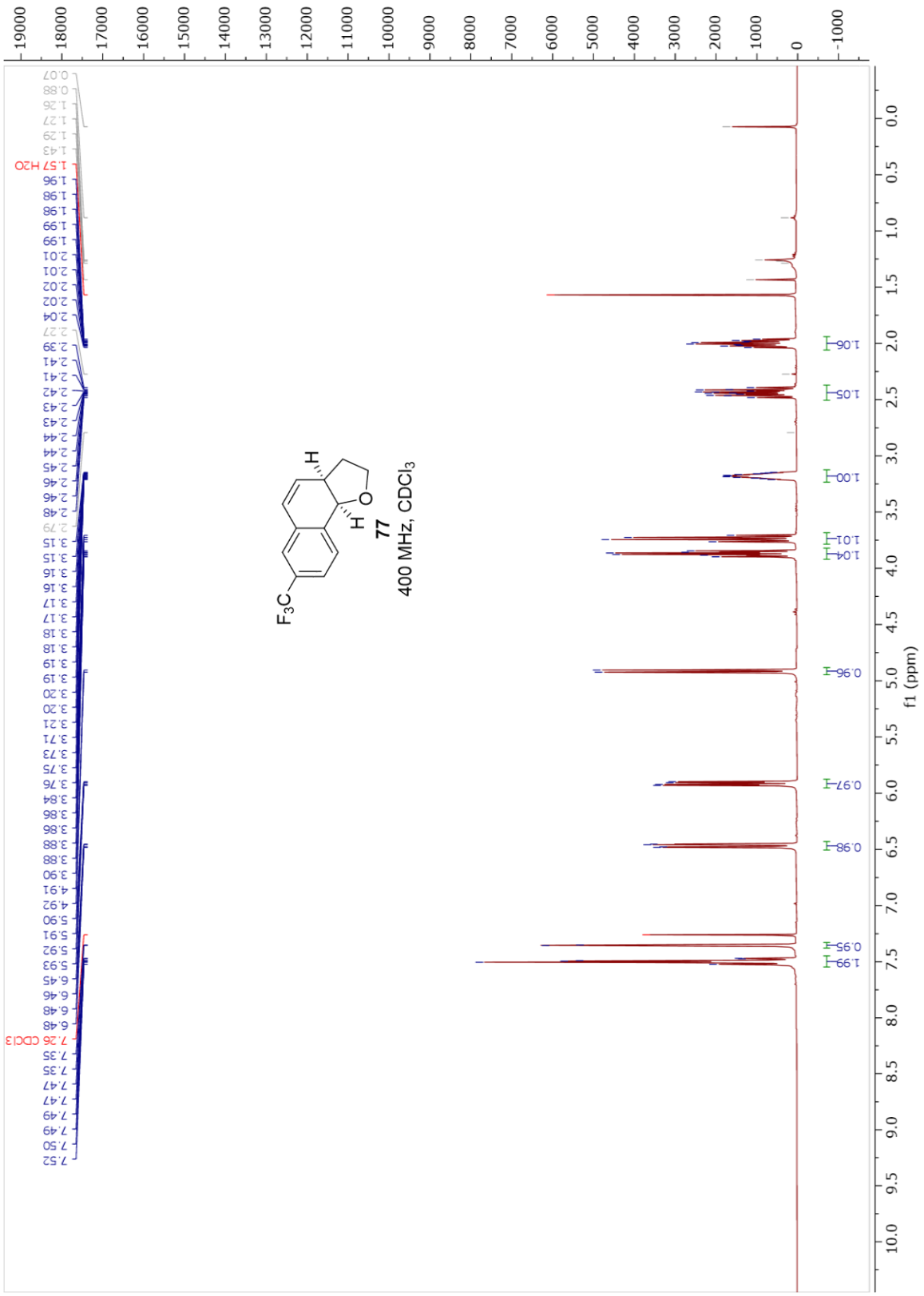
77
400 MHz, CDCl3
F3C
H
O
H
f1 (ppm)
1.99
0.95
0.98
0.97
0.96
1.04
1.01
1.00
1.05
1.06
1.57 H2O
7.26 CDCl3

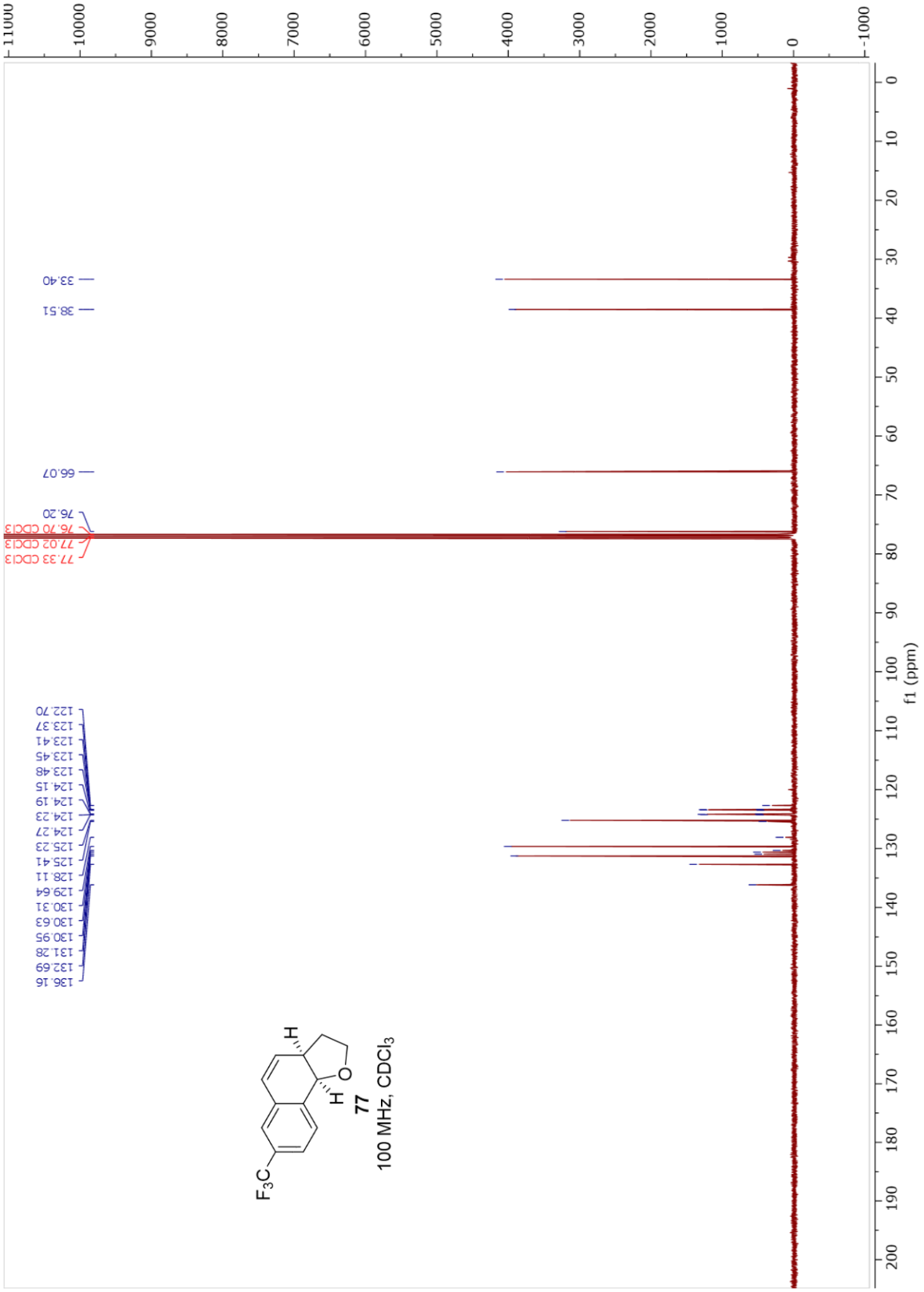
77
100 MHz, CDCl3
F3C
H
O
H
33.40
38.51
66.07
76.20
77.02 CDCl3
76.70 CDCl3
77.33 CDCl3
122.70
123.37
123.41
123.45
123.48
124.15
124.19
124.23
124.27
125.23
125.41
128.11
129.64
130.31
130.63
130.95
131.28
132.69
136.16
f1 (ppm)

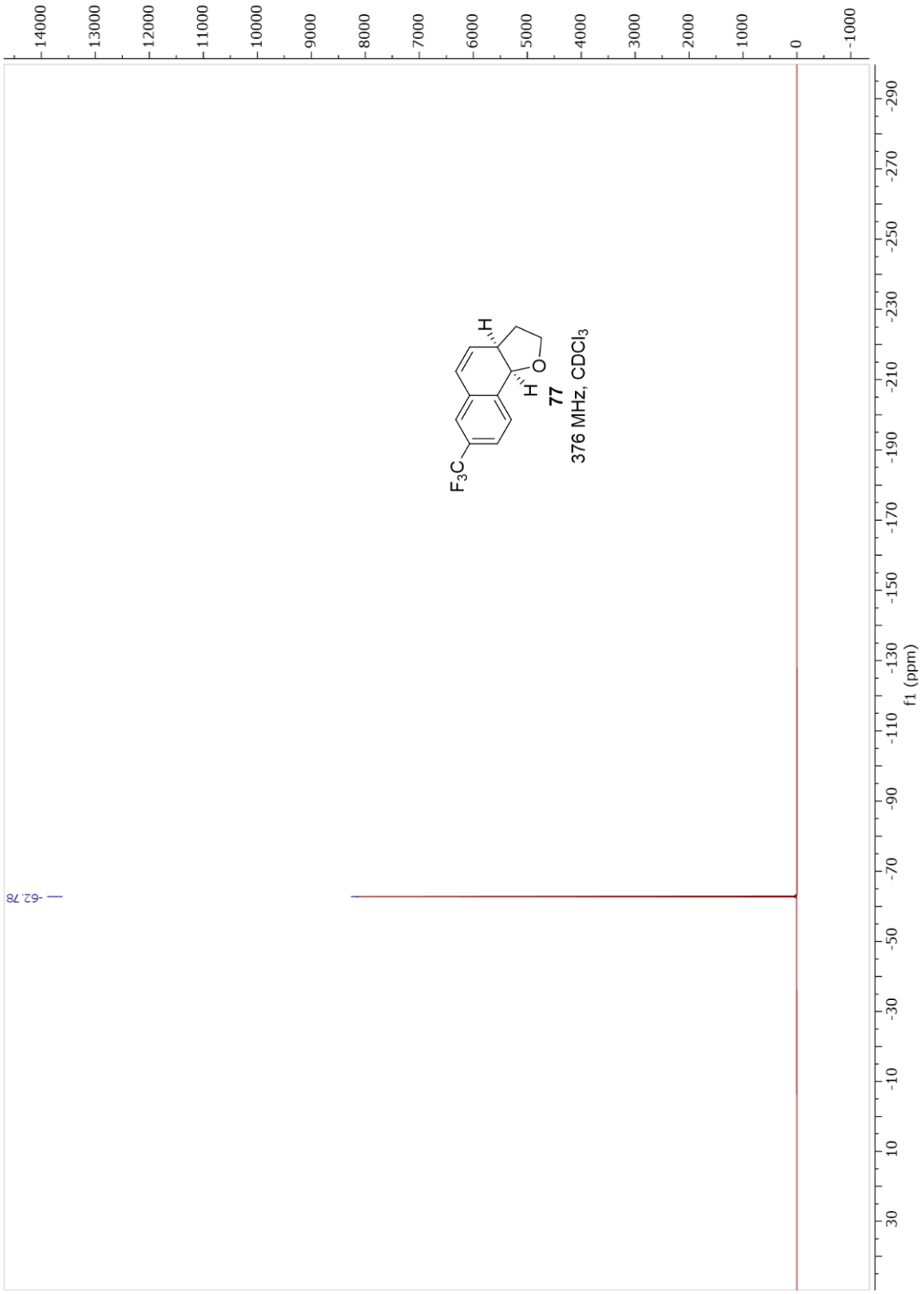
14000
13000
12000
11000
10000
9000
8000
7000
6000
5000
4000
3000
2000
1000
0
-1000
30
10
-10
-30
-50
-70
-90
-110
-130
-150
-170
-190
-210
-230
-250
-270
-290
f1 (ppm)
-62.78
F3C
H
O
H
77
376 MHz, CDCl3

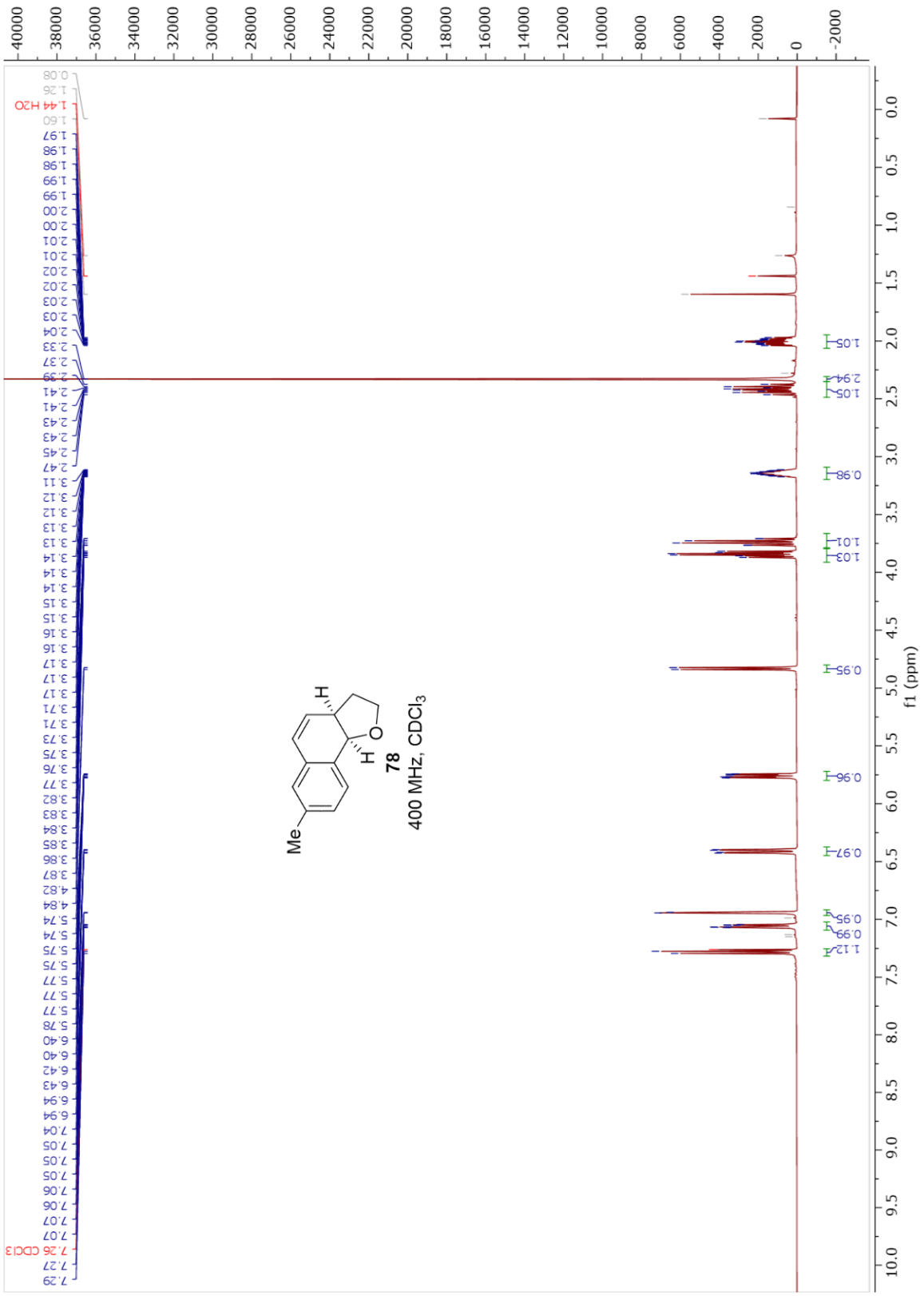
78
400 MHz, CDCl3
Me
O
H
H
f1 (ppm)
7.26 CDCl3
1.44 H2O

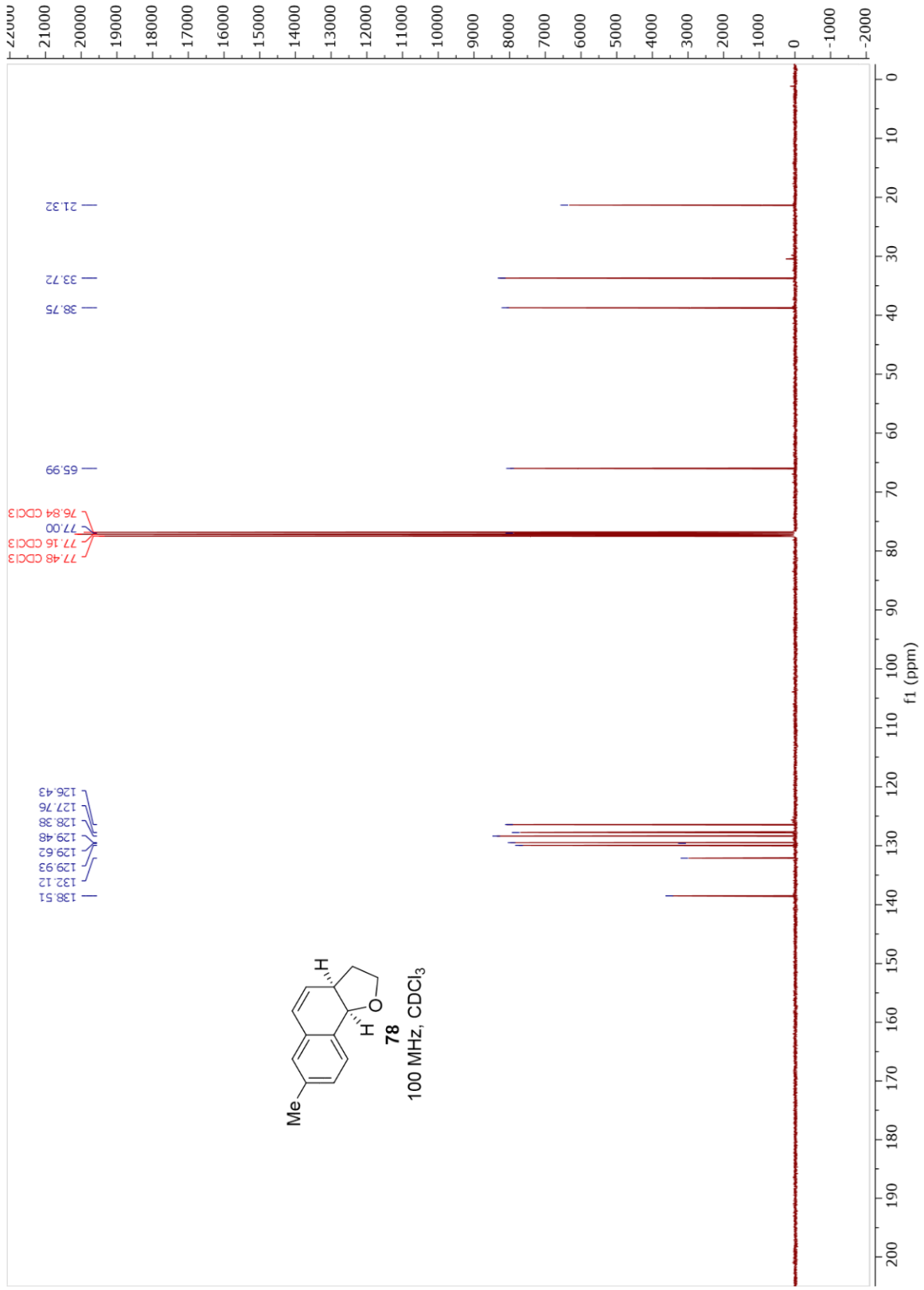
21.32
33.72
38.75
65.99
76.84 CDCl3
77.00
77.16 CDCl3
77.48 CDCl3
126.43
127.76
128.38
129.48
129.62
129.93
132.12
138.51
f1 (ppm)
Me
H
O
H
78
100 MHz, CDCl3

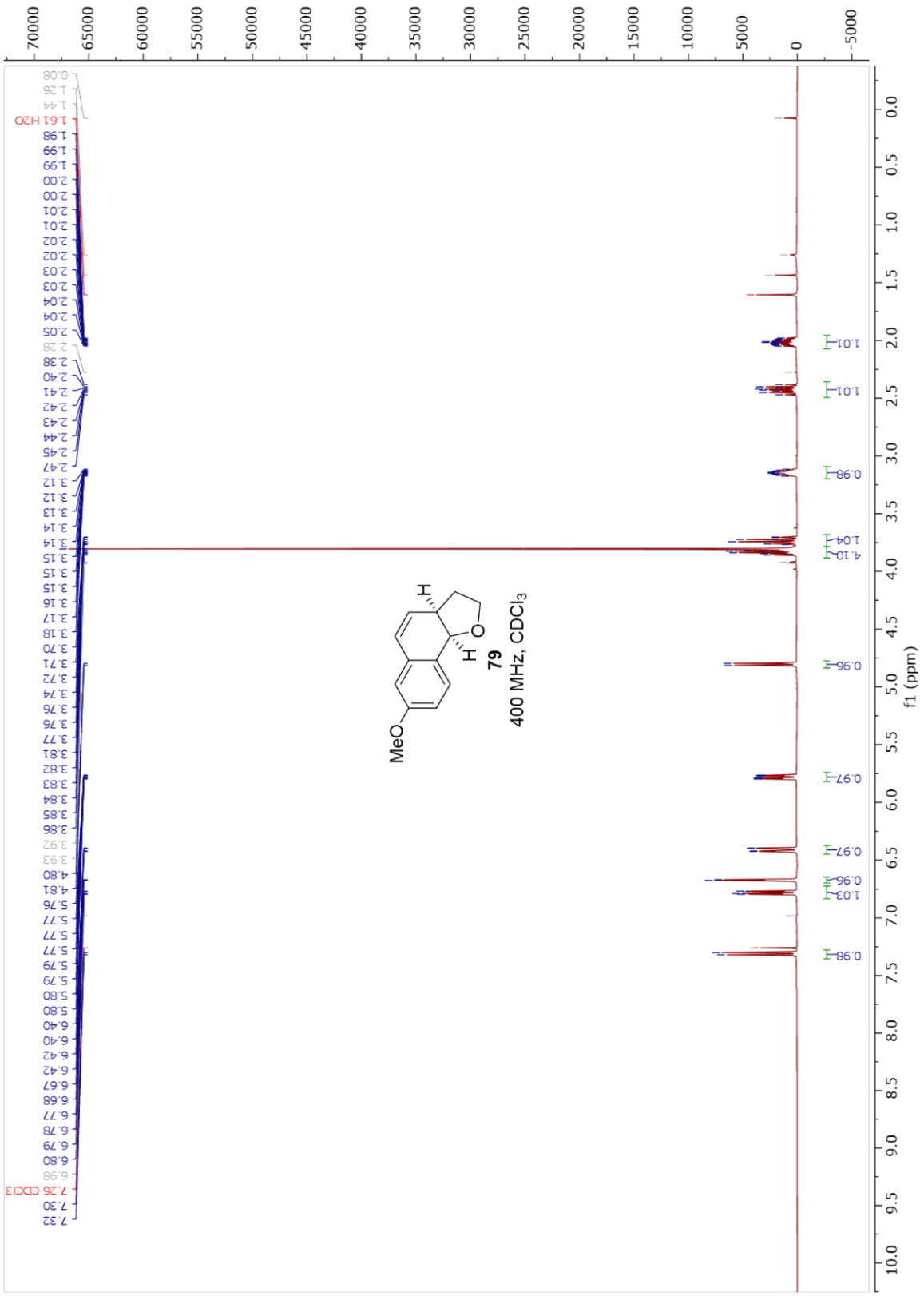
MeO
H
O
H
79
400 MHz, CDCl3
f1 (ppm)

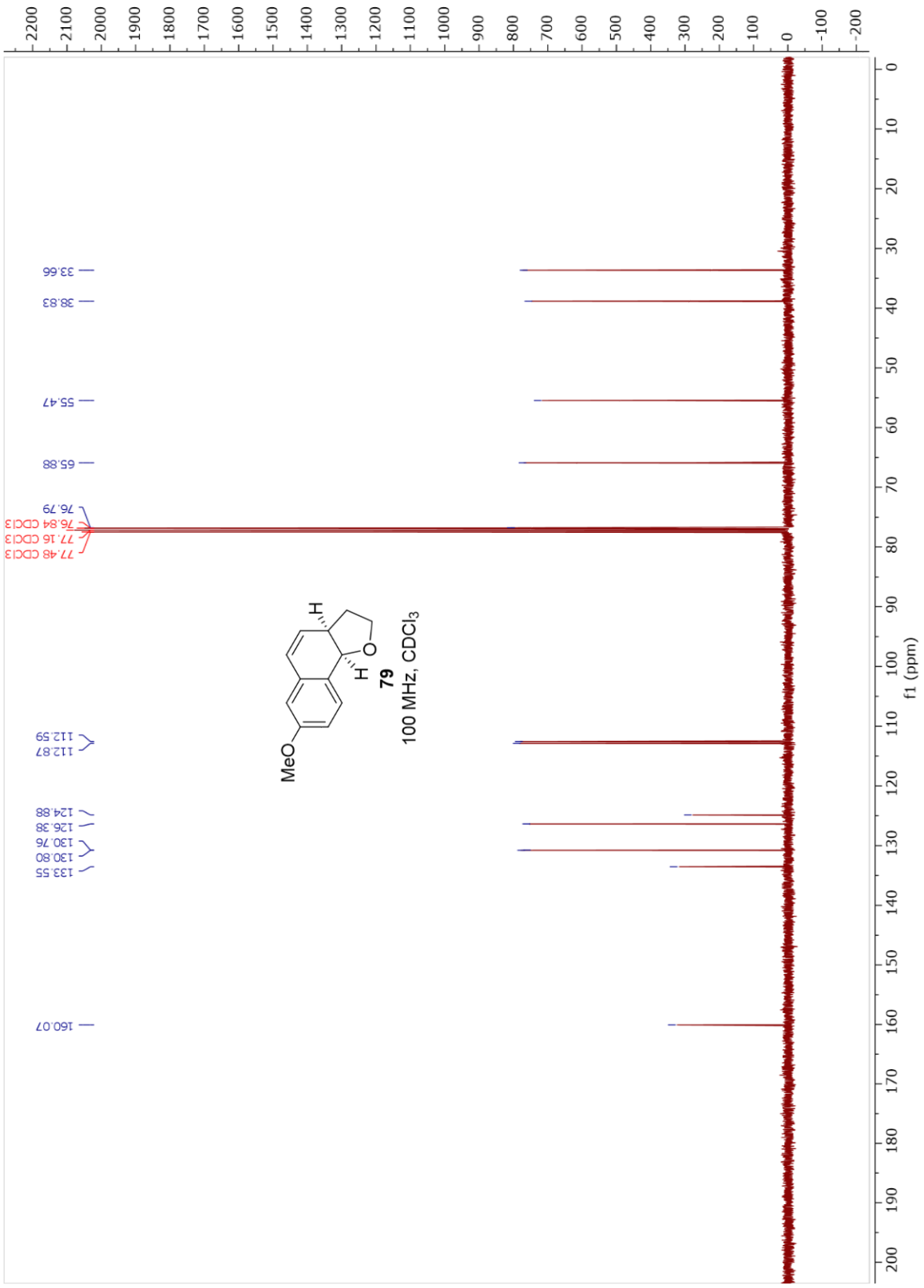
160.07
133.55
130.80
130.76
126.38
124.88
112.87
112.59
77.48 CDCl3
77.16 CDCl3
76.84 CDCl3
76.79
65.88
55.47
38.83
33.66
MeO
H
O
H
79
100 MHz, CDCl3
f1 (ppm)

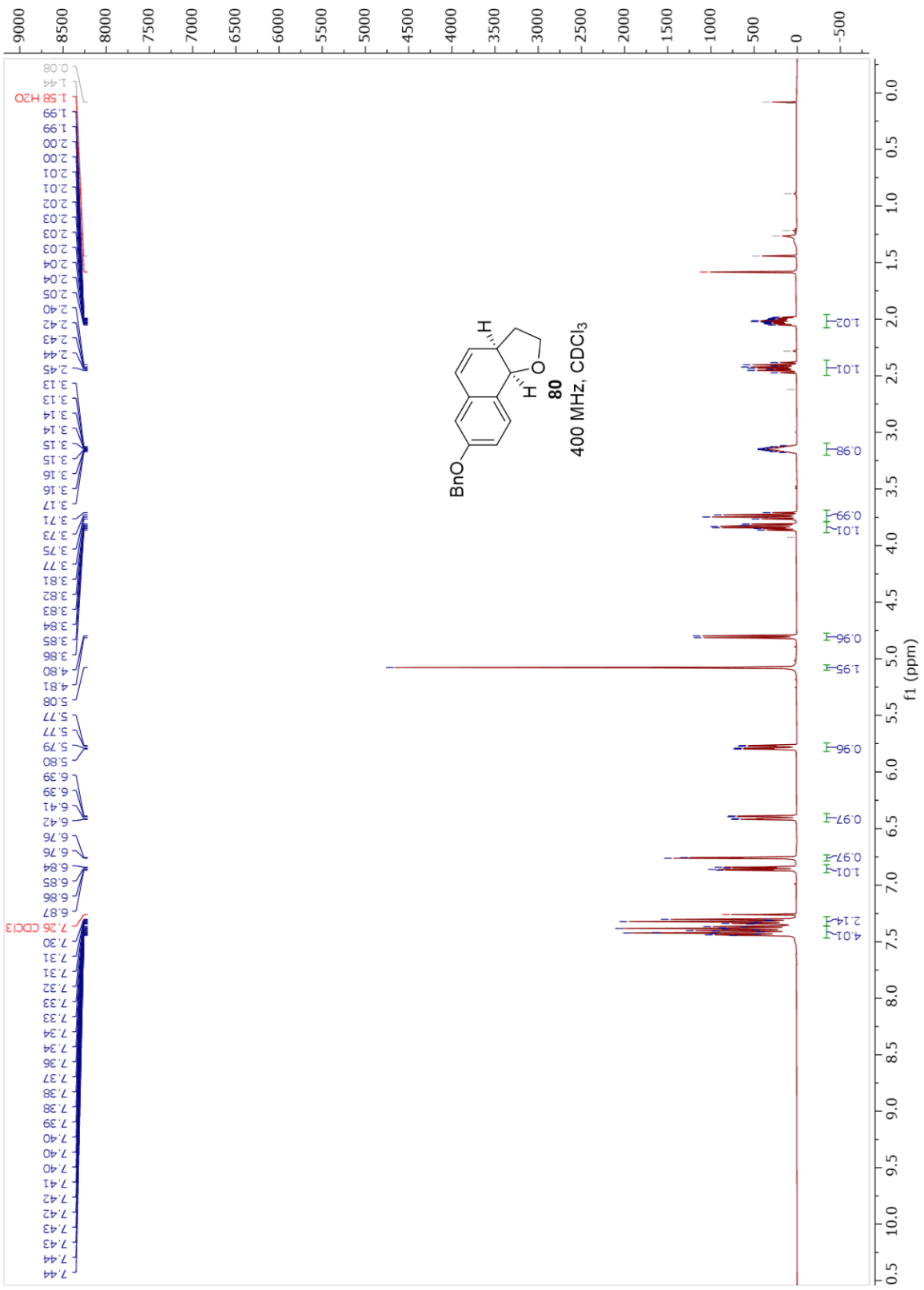
BnO
H
O
H
80
400 MHz, CDCl3
f1 (ppm)

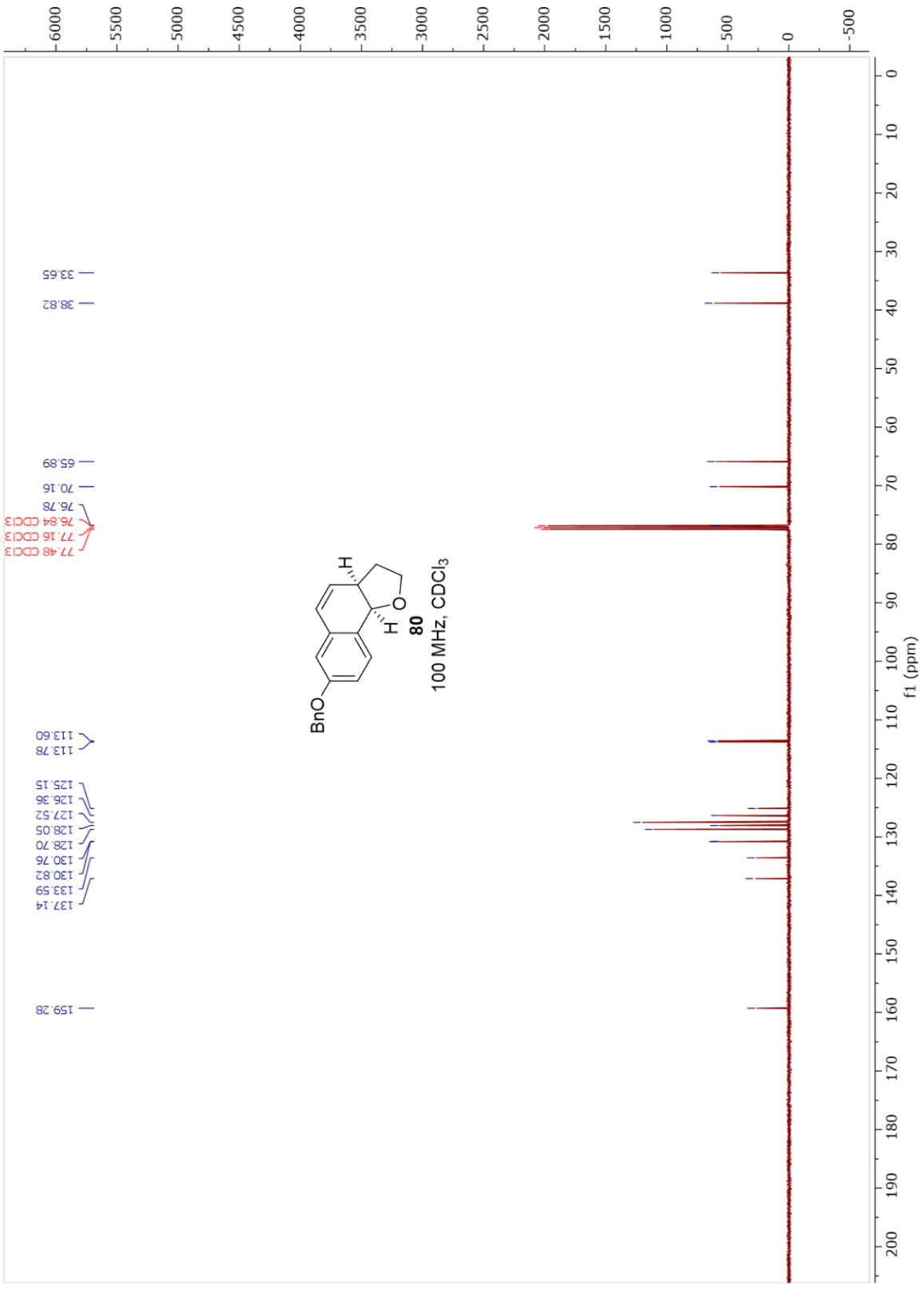
33.65
38.82
65.89
70.16
76.78
76.84 CDCl3
77.16 CDCl3
77.48 CDCl3
113.60
113.78
125.15
126.36
127.52
128.05
128.70
130.76
130.82
133.59
137.14
159.28
BnO
H
O
H
80
100 MHz, CDCl3
f1 (ppm)

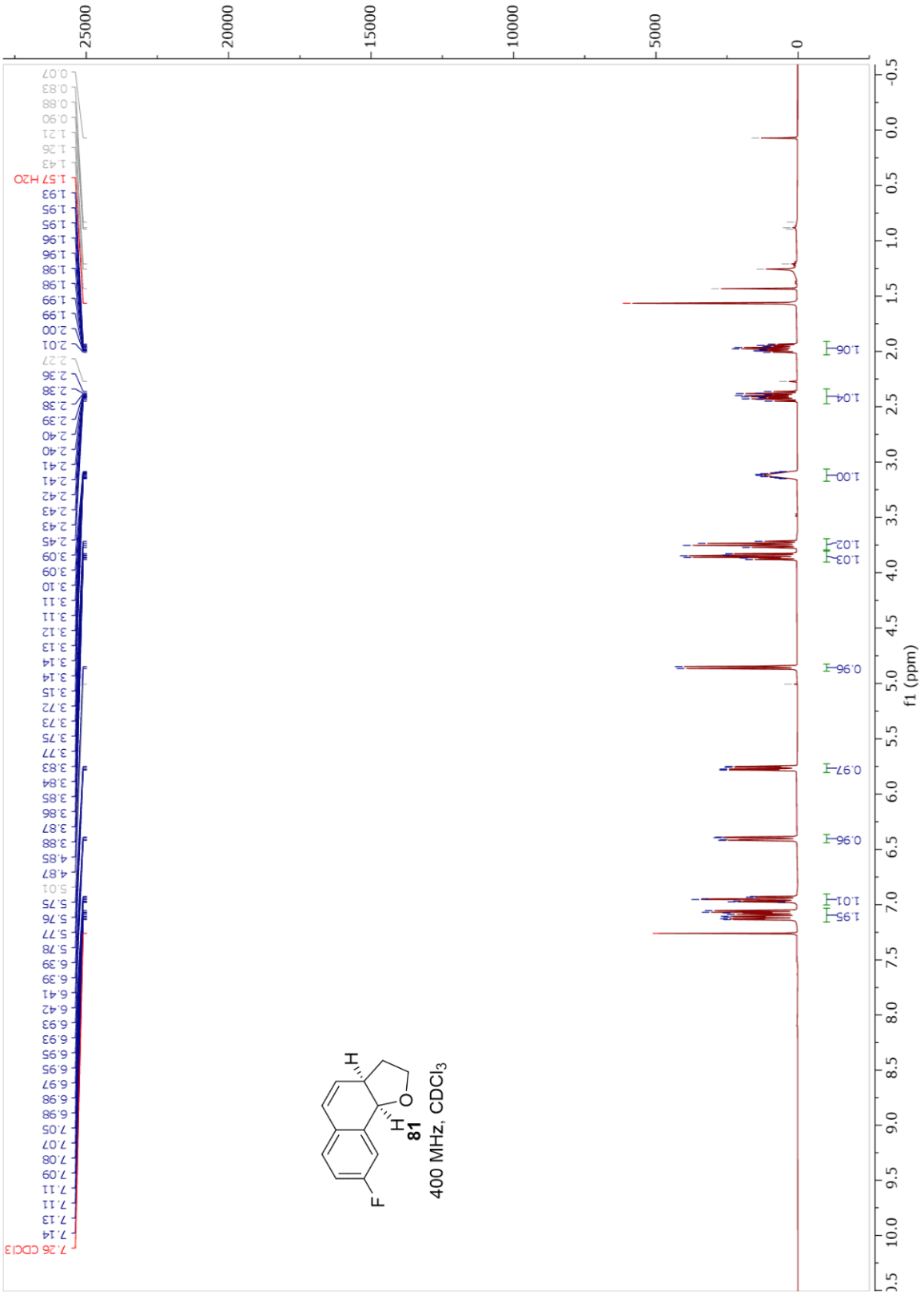
81
400 MHz, CDCl3
f1 (ppm)

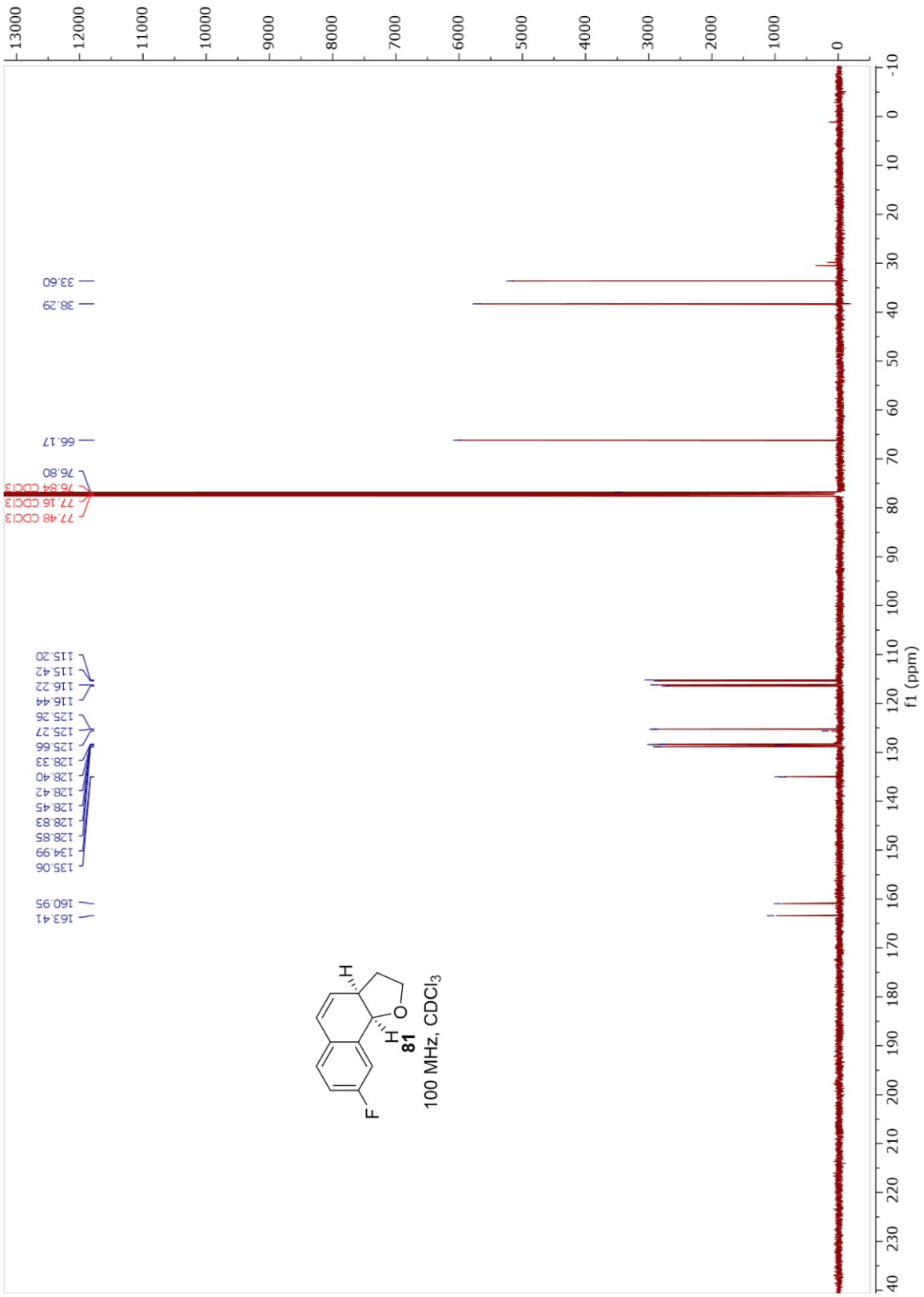
33.60
38.29
66.17
76.80
76.84 CDCl3
77.16 CDCl3
77.48 CDCl3
115.20
115.42
116.22
116.44
125.26
125.27
125.66
128.33
128.40
128.42
128.45
128.83
128.85
134.99
135.06
160.95
163.41
H
O
H
F
81
100 MHz, CDCl3
f1 (ppm)

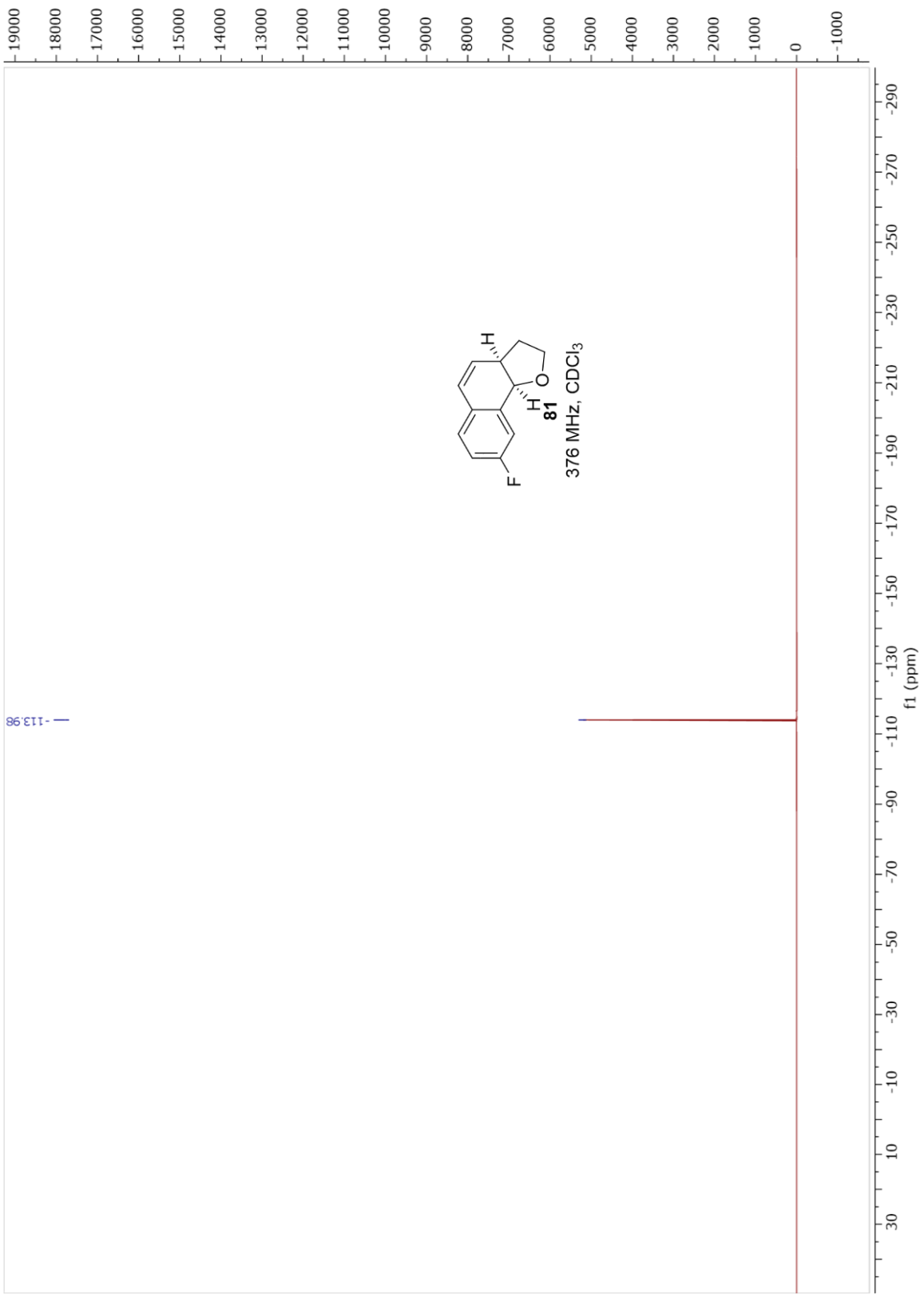
-113.98
f1 (ppm)
81
376 MHz, CDCl3

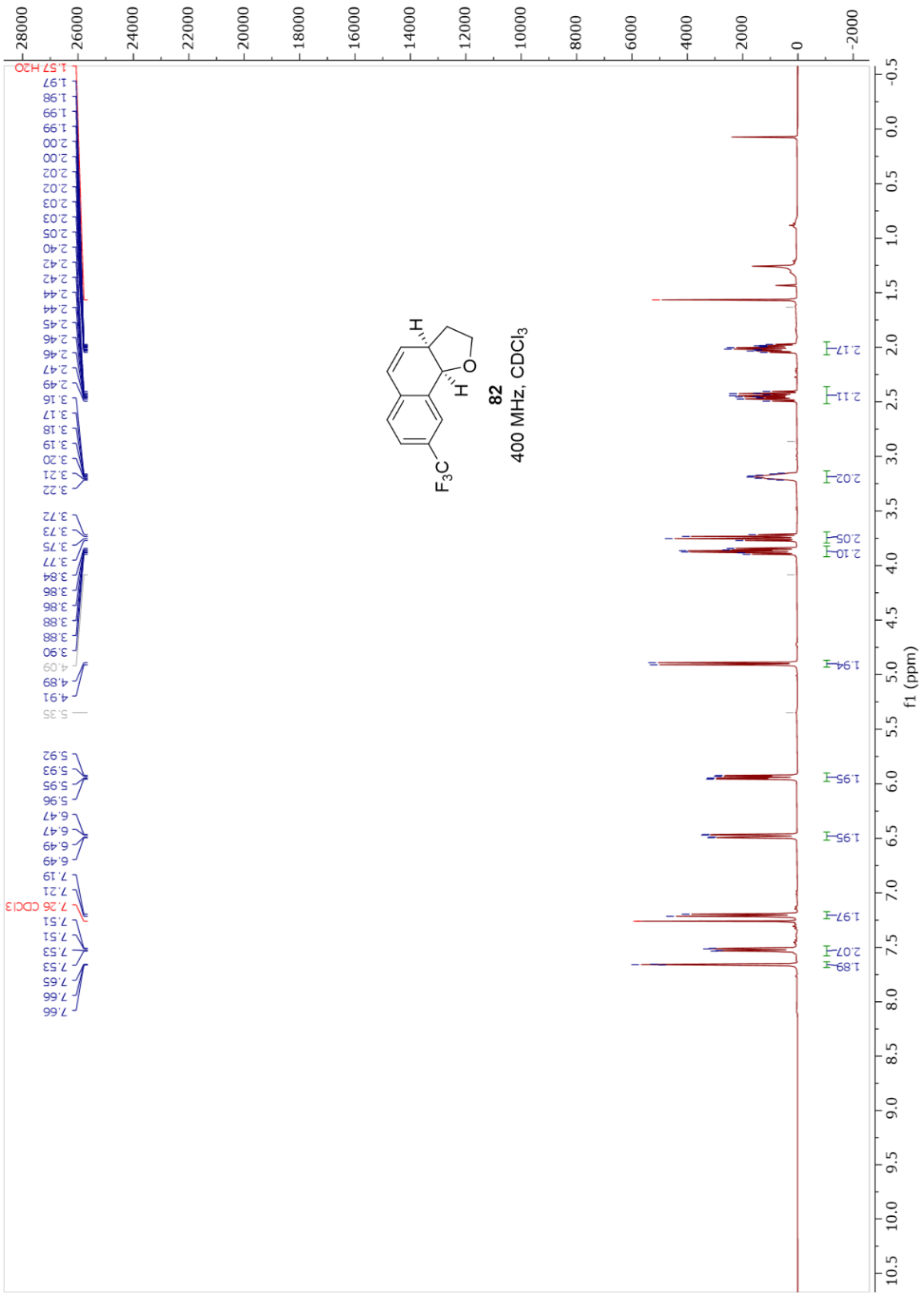
82
400 MHz, CDCl3
F3C
H
O
H
f1 (ppm)

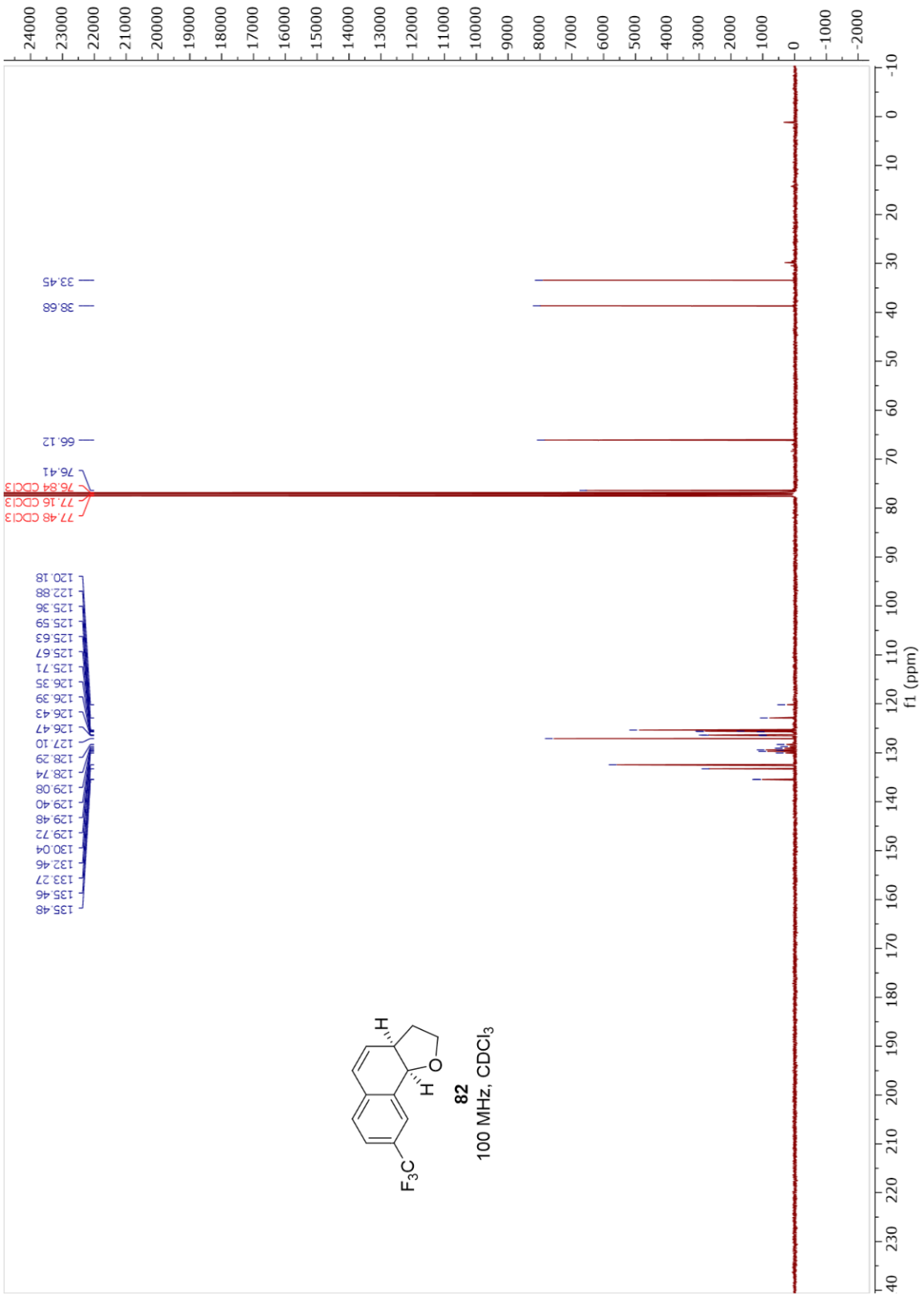
82
100 MHz, CDCl3
F3C
H
O
H
33.45
38.68
66.12
76.41
76.84 CDCl3
77.16 CDCl3
77.48 CDCl3
120.18
122.88
125.36
125.59
125.63
125.67
125.71
126.35
126.39
126.43
126.47
127.10
128.29
128.74
129.08
129.40
129.48
129.72
130.04
132.46
133.27
135.46
135.48
f1 (ppm)

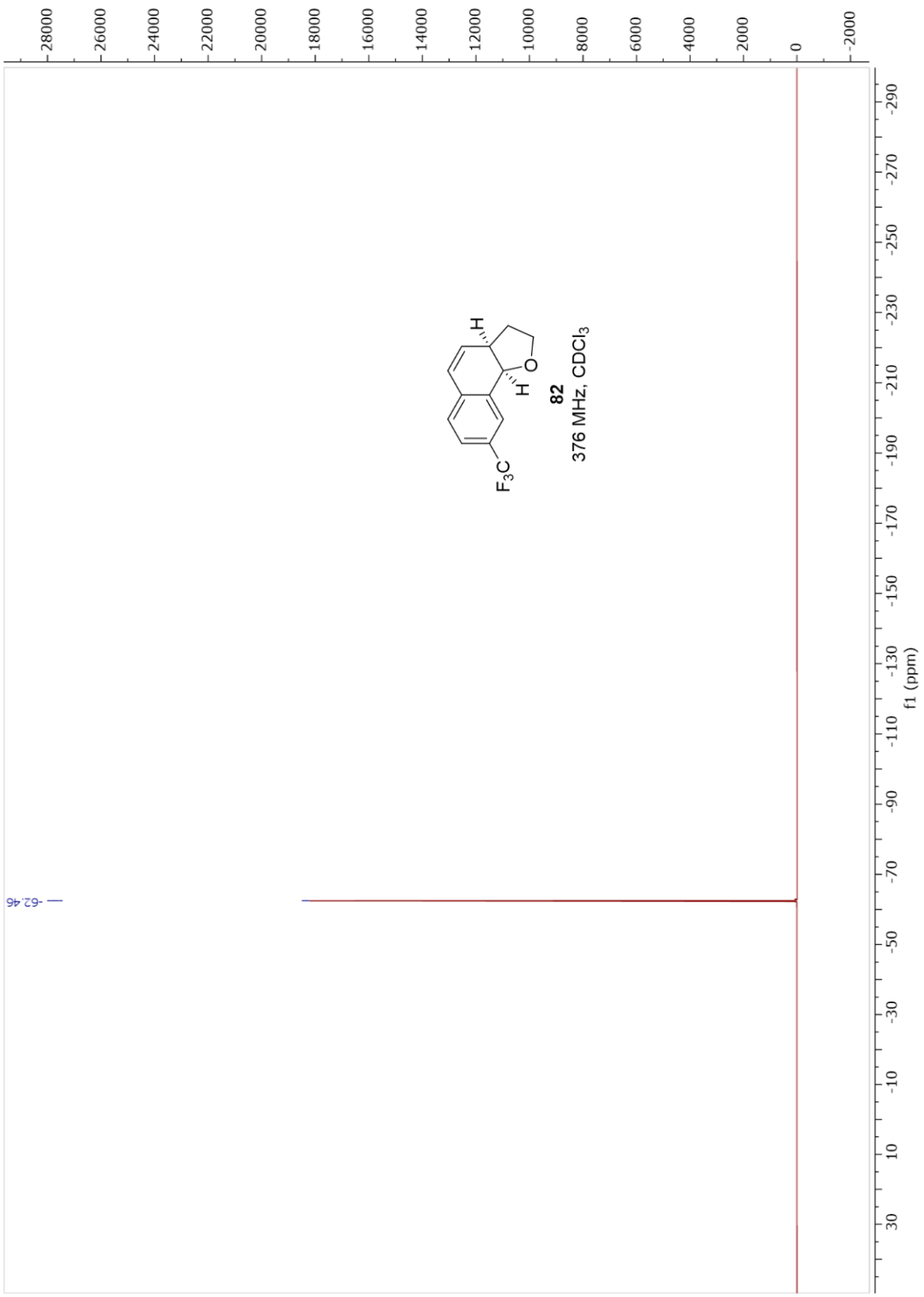
82
376 MHz, CDCl3
F3C
H
H
O
-62.46
f1 (ppm)

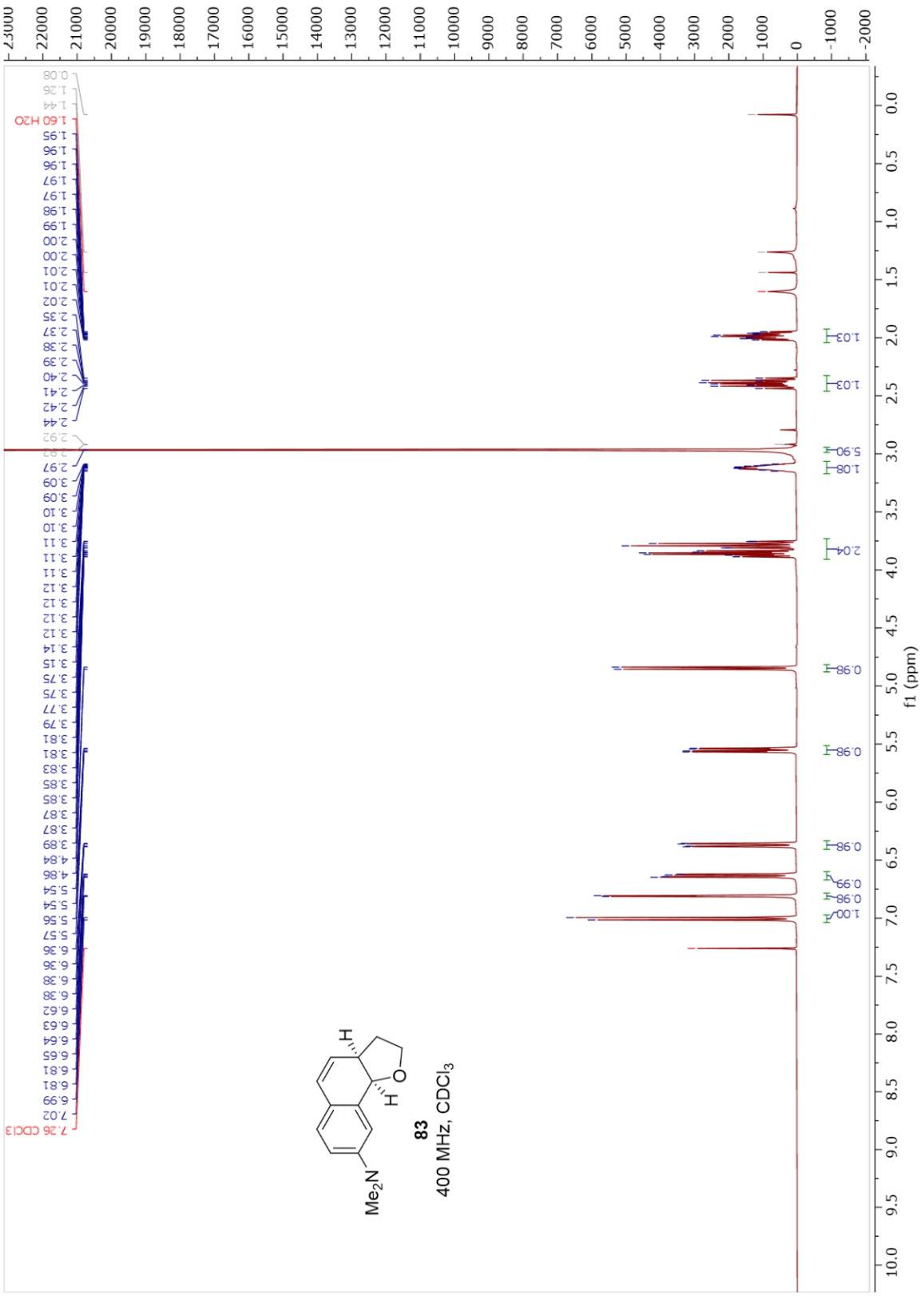
Me2N
83
400 MHz, CDCl3
f1 (ppm)

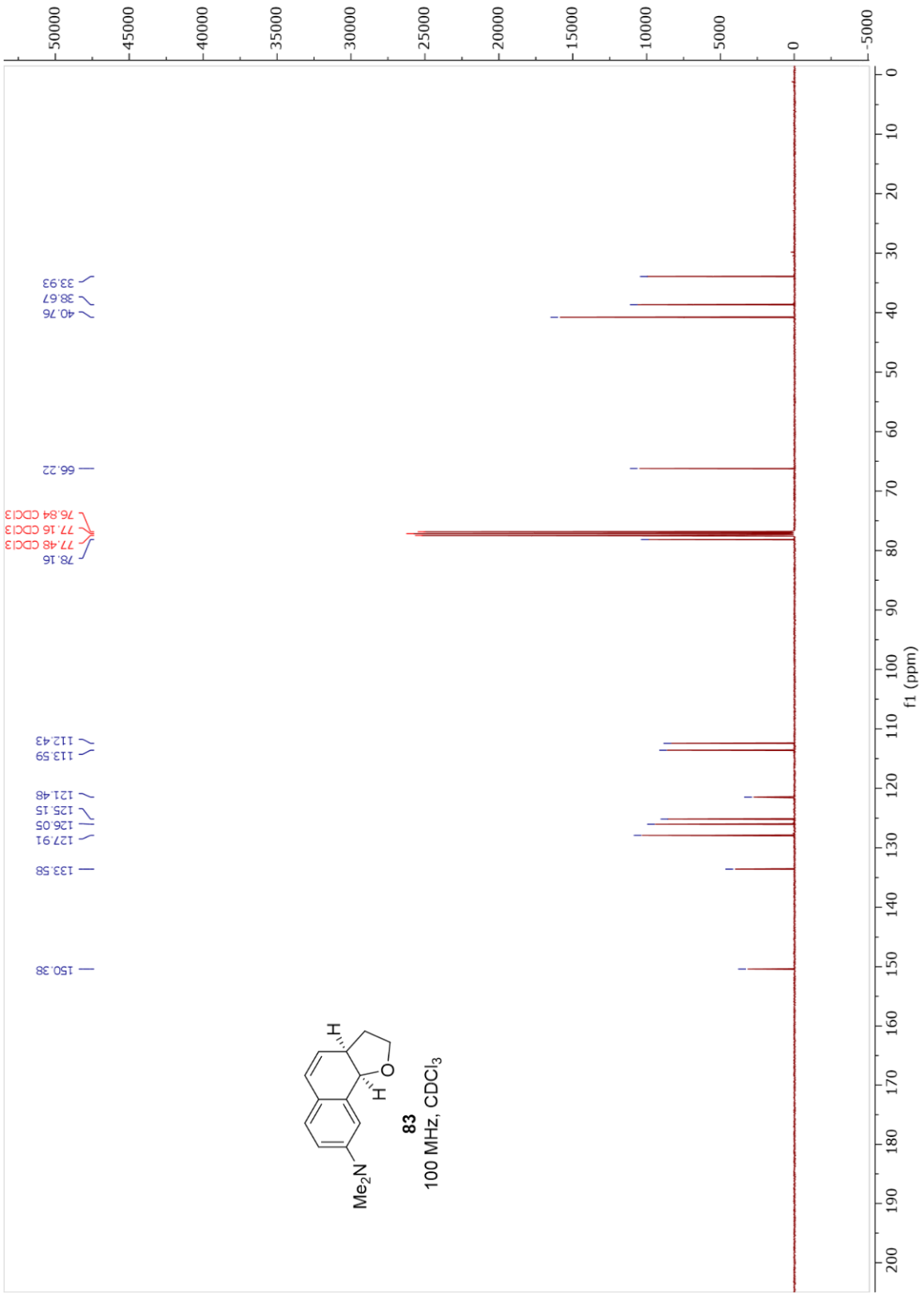
33.93
38.67
40.76
66.22
76.84 CDCl3
77.16 CDCl3
77.48 CDCl3
78.16
112.43
113.59
121.48
125.15
126.05
127.91
133.58
150.38
50000
45000
40000
35000
30000
25000
20000
15000
10000
5000
0
-5000
0
10
20
30
40
50
60
70
80
90
100
110
120
130
140
150
160
170
180
190
200
f1 (ppm)
H
O
H
Me2N
83
100 MHz, CDCl3

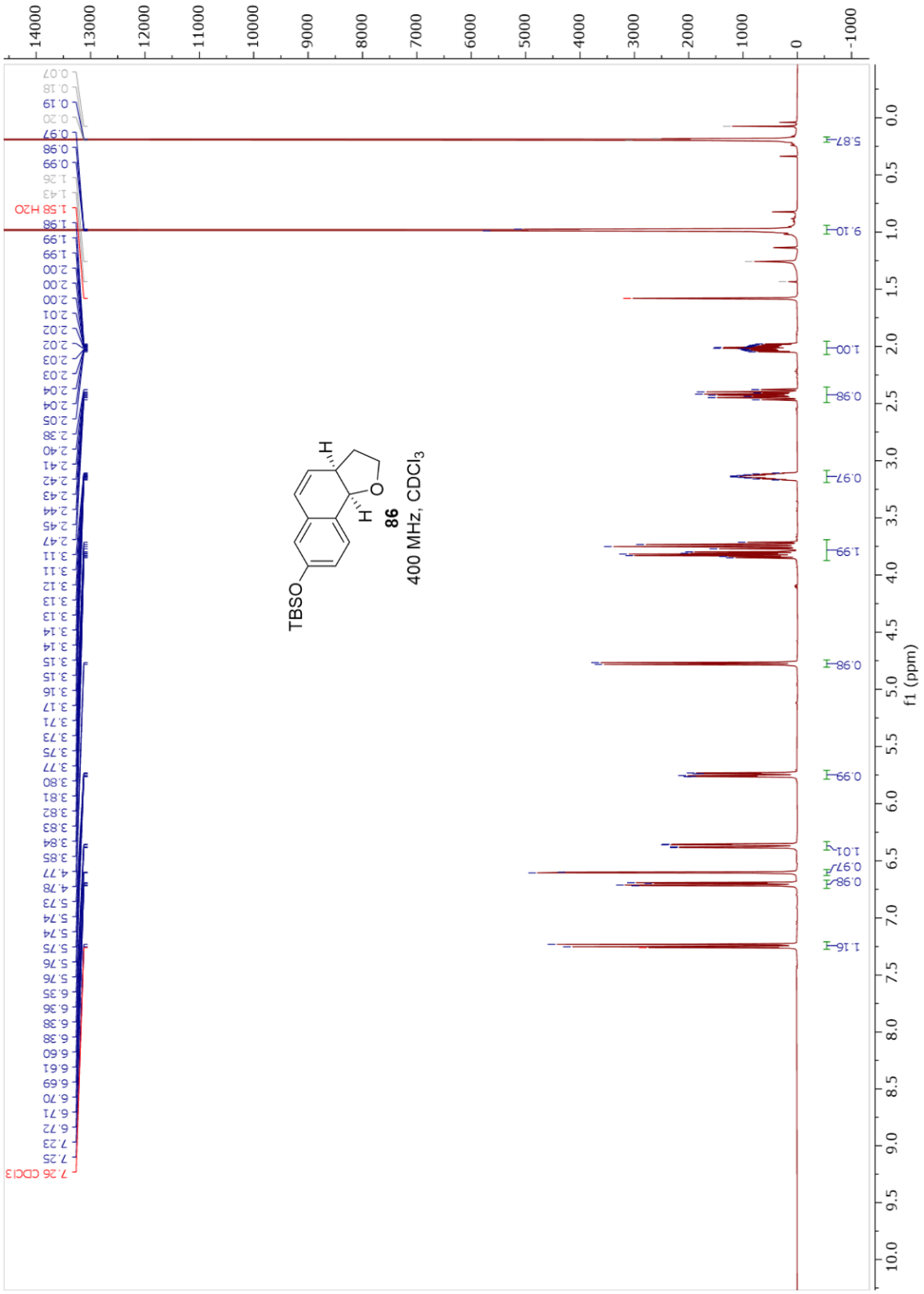
TBSO
H
H
O
86
400 MHz, CDCl3
f1 (ppm)

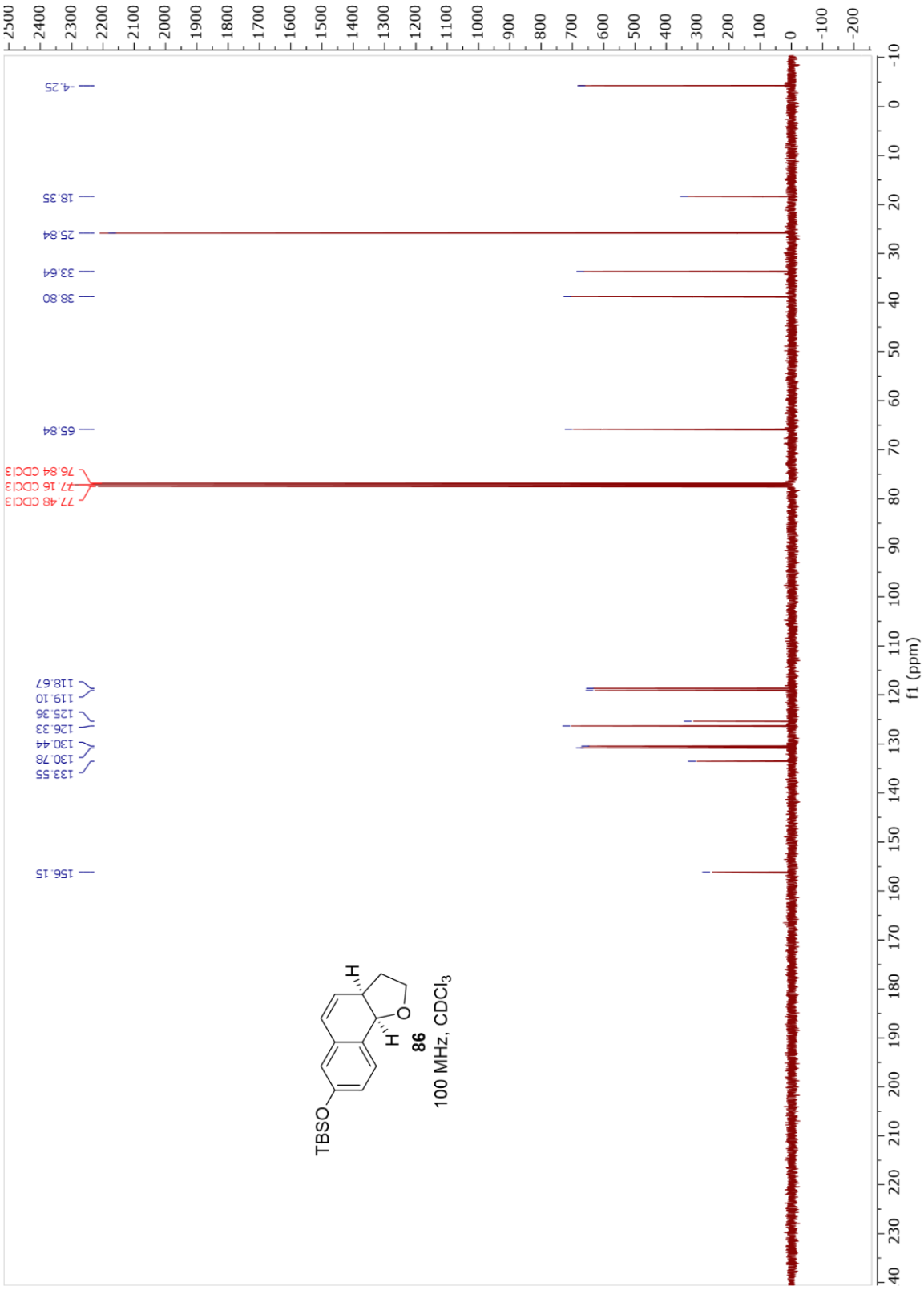
-4.25
18.35
25.84
33.64
38.80
65.84
76.84 CDCl3
77.16 CDCl3
77.48 CDCl3
118.67
119.10
125.36
126.33
130.44
130.78
133.55
156.15
TBSO
H
O
H
86
100 MHz, CDCl3
f1 (ppm)

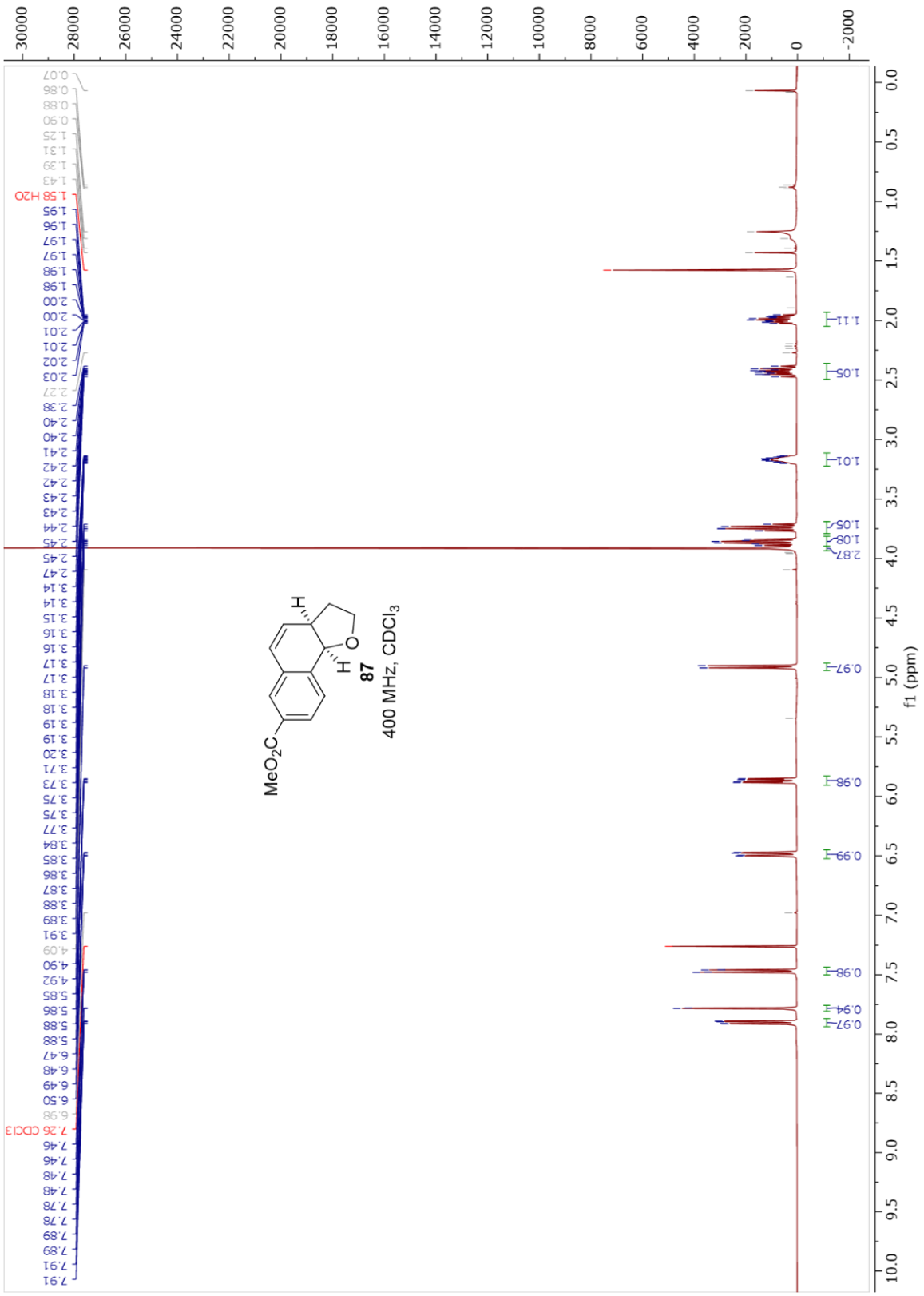
MeO2C
H
O
H
87
400 MHz, CDCl3
f1 (ppm)

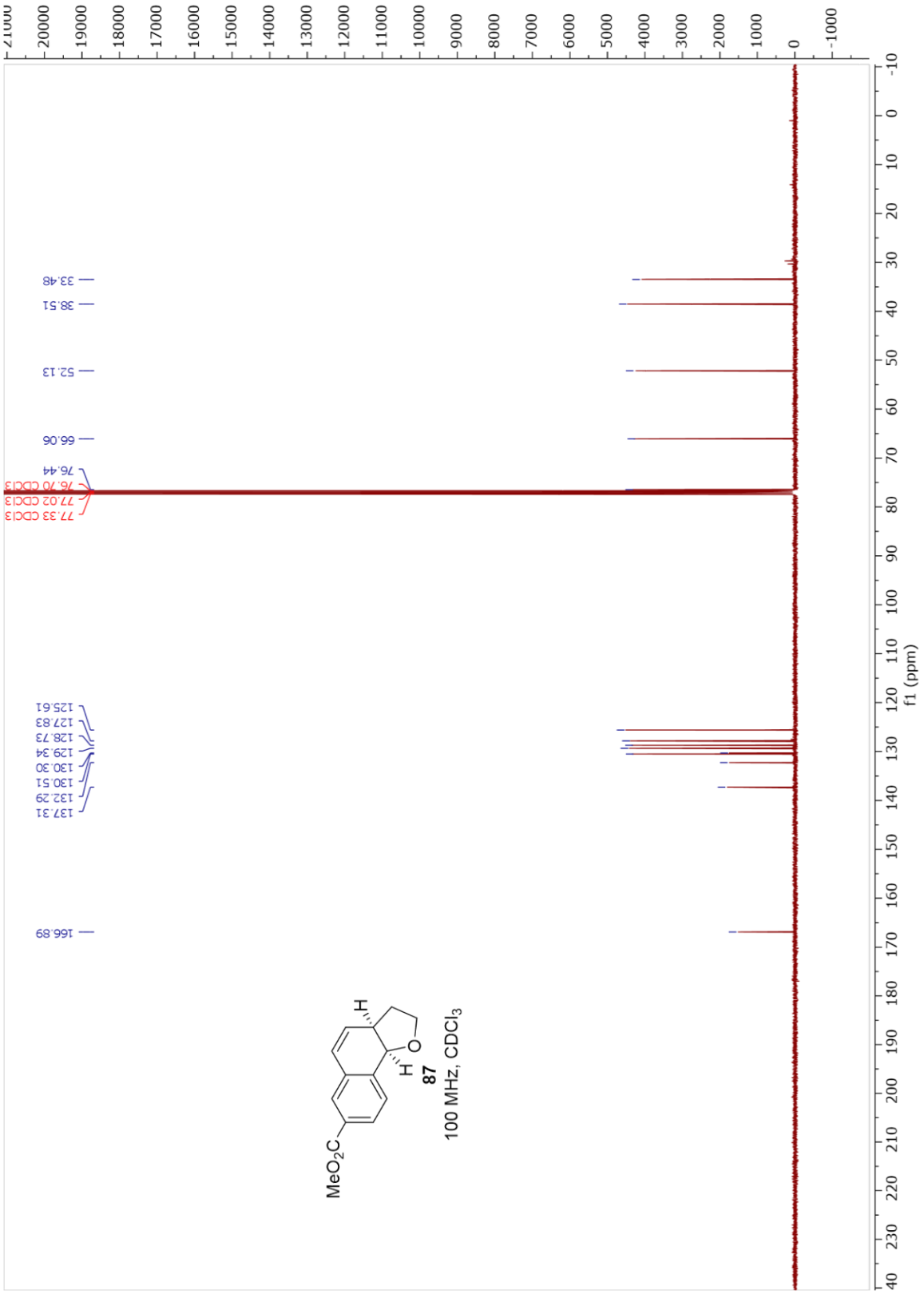
166.89
137.31
132.29
130.51
130.30
129.34
128.73
127.83
125.61
77.33 CDCl3
77.02 CDCl3
76.70 CDCl3
76.44
66.06
52.13
38.51
33.48
f1 (ppm)
MeO2C
H
O
H
87
100 MHz, CDCl3

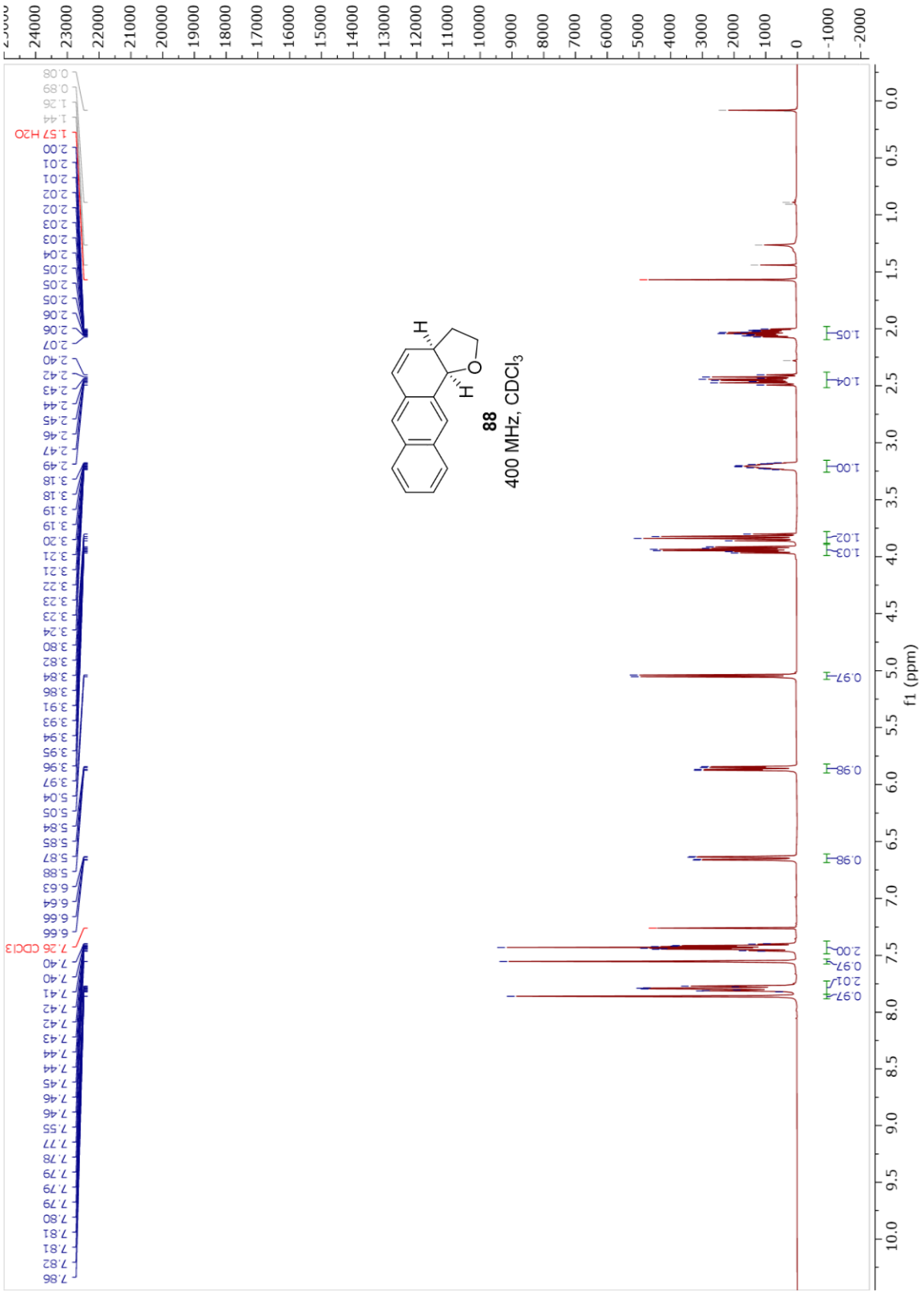
88
400 MHz, CDCl3
f1 (ppm)

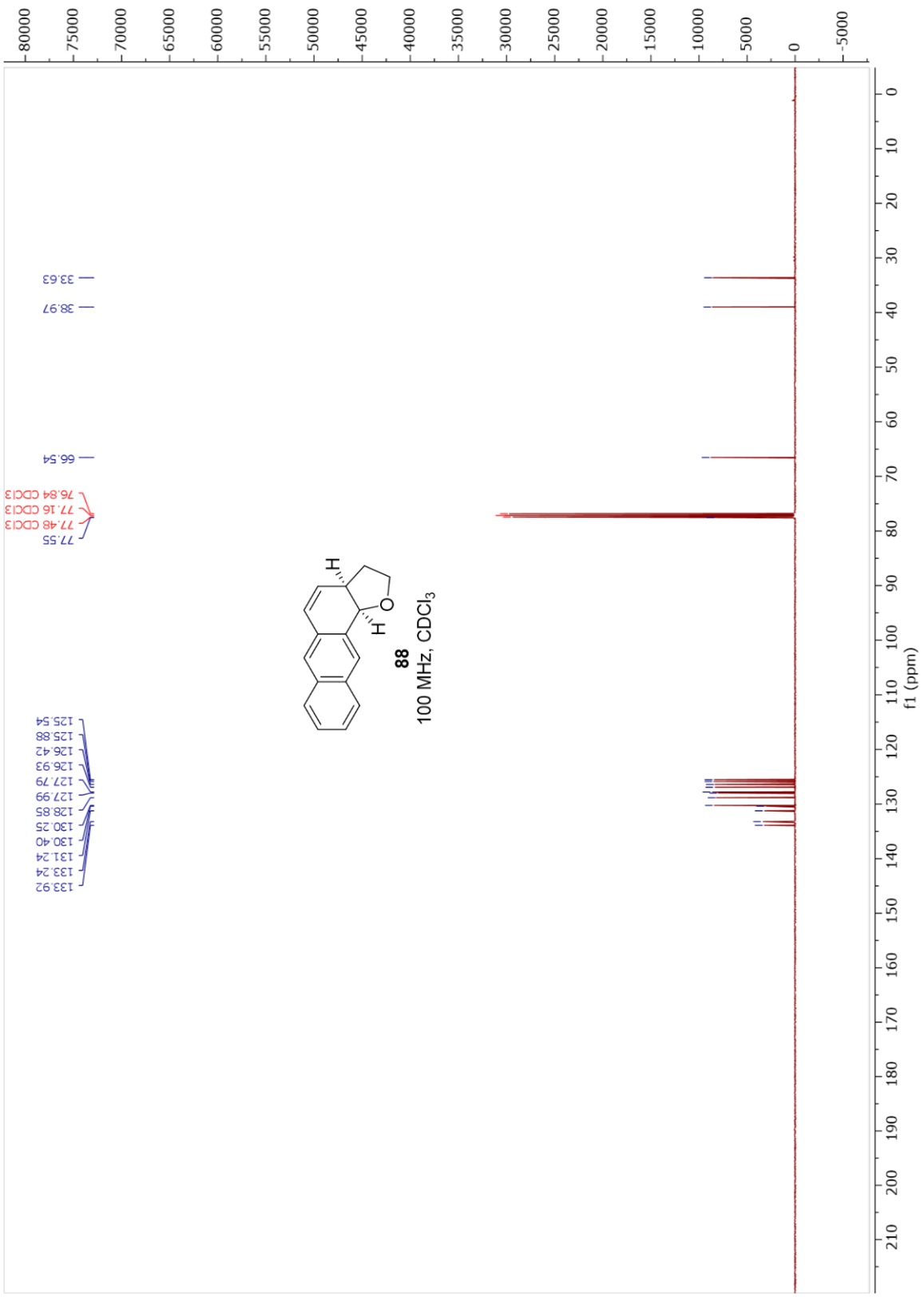
33.63
38.97
66.54
76.84 CDCl3
77.16 CDCl3
77.48 CDCl3
77.55
125.54
125.88
126.42
126.93
127.79
127.99
128.85
130.25
130.40
131.24
133.24
133.92
H
O
H
88
100 MHz, CDCl3
f1 (ppm)

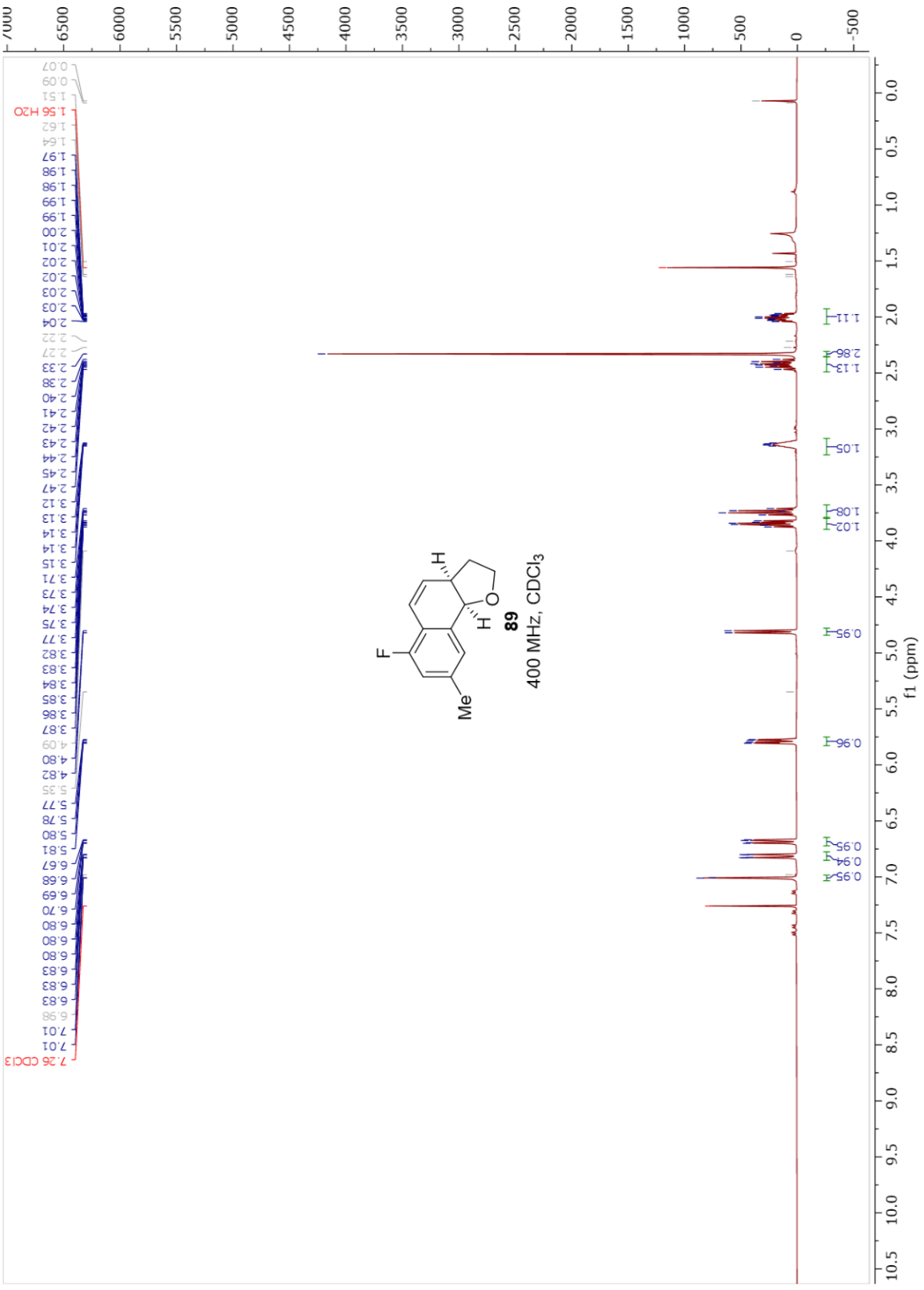
F
Me
H
O
H
89
400 MHz, CDCl3
f1 (ppm)

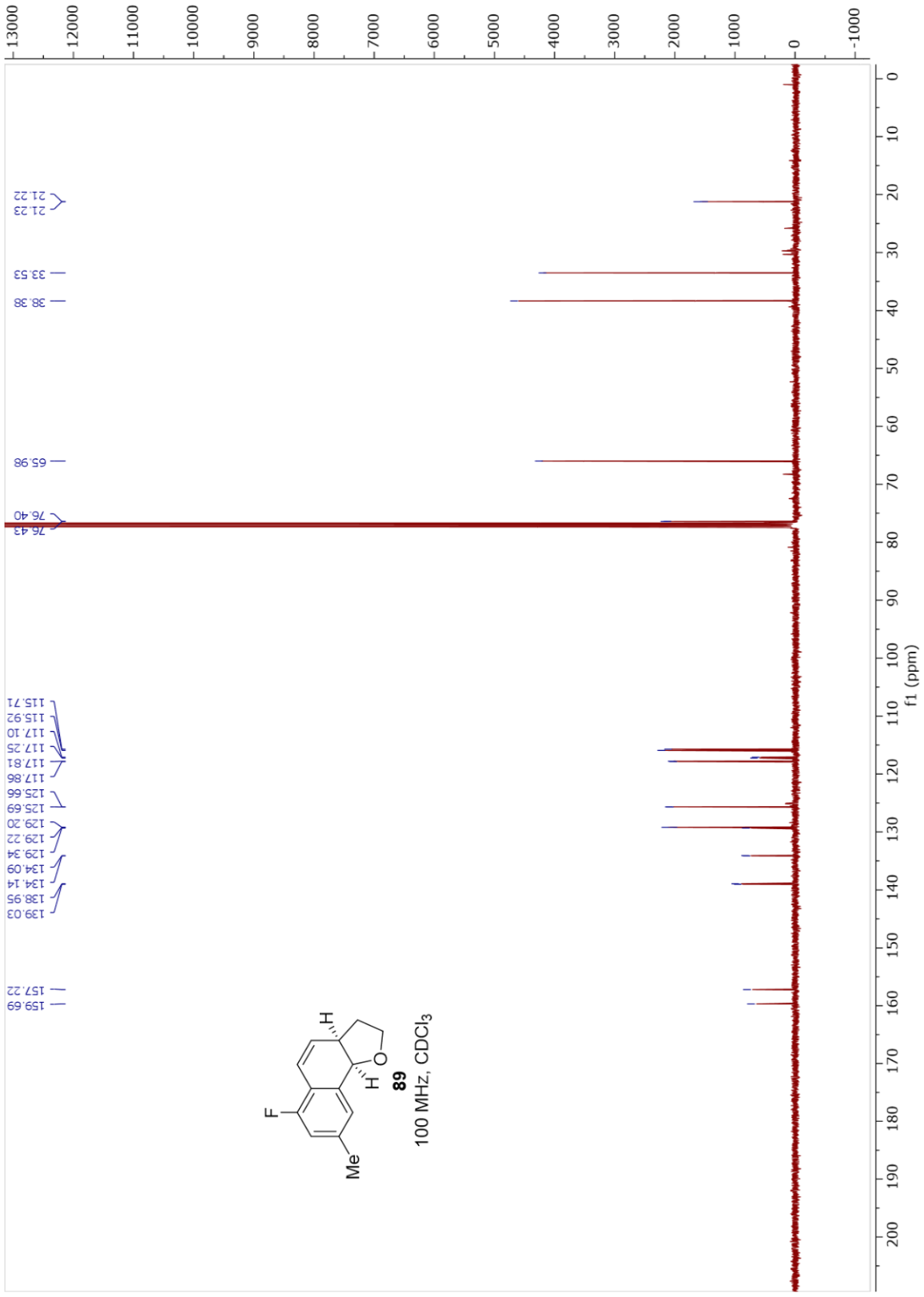
21.22
21.23
33.53
38.38
65.98
76.40
76.43
115.71
115.92
117.10
117.25
117.81
117.86
125.66
125.69
129.20
129.22
129.34
134.09
134.14
138.95
139.03
157.22
159.69
F
Me
H
O
H
89
100 MHz, CDCl3
f1 (ppm)

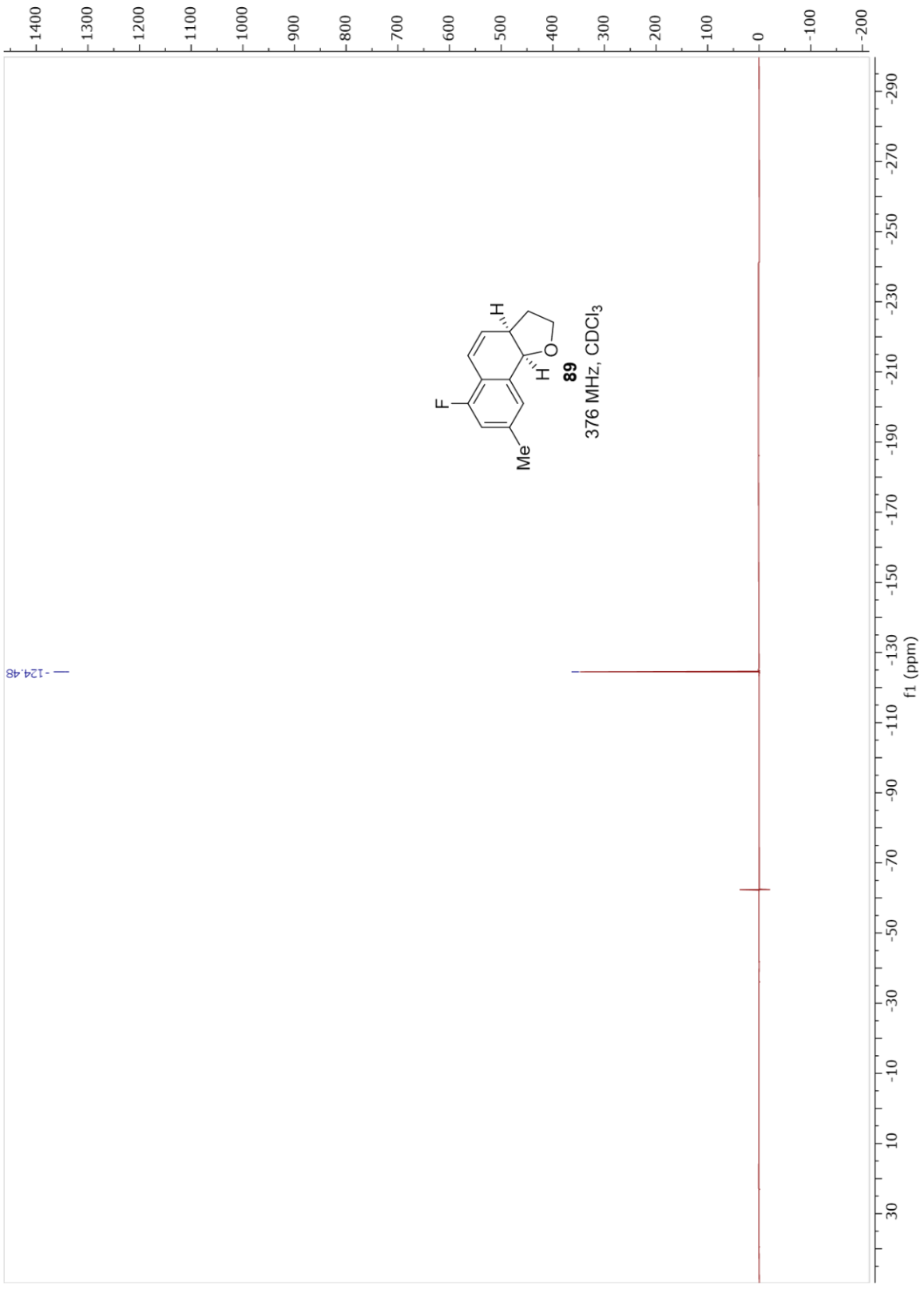
-124.48
F
Me
H
O
H
89
376 MHz, CDCl3
f1 (ppm)

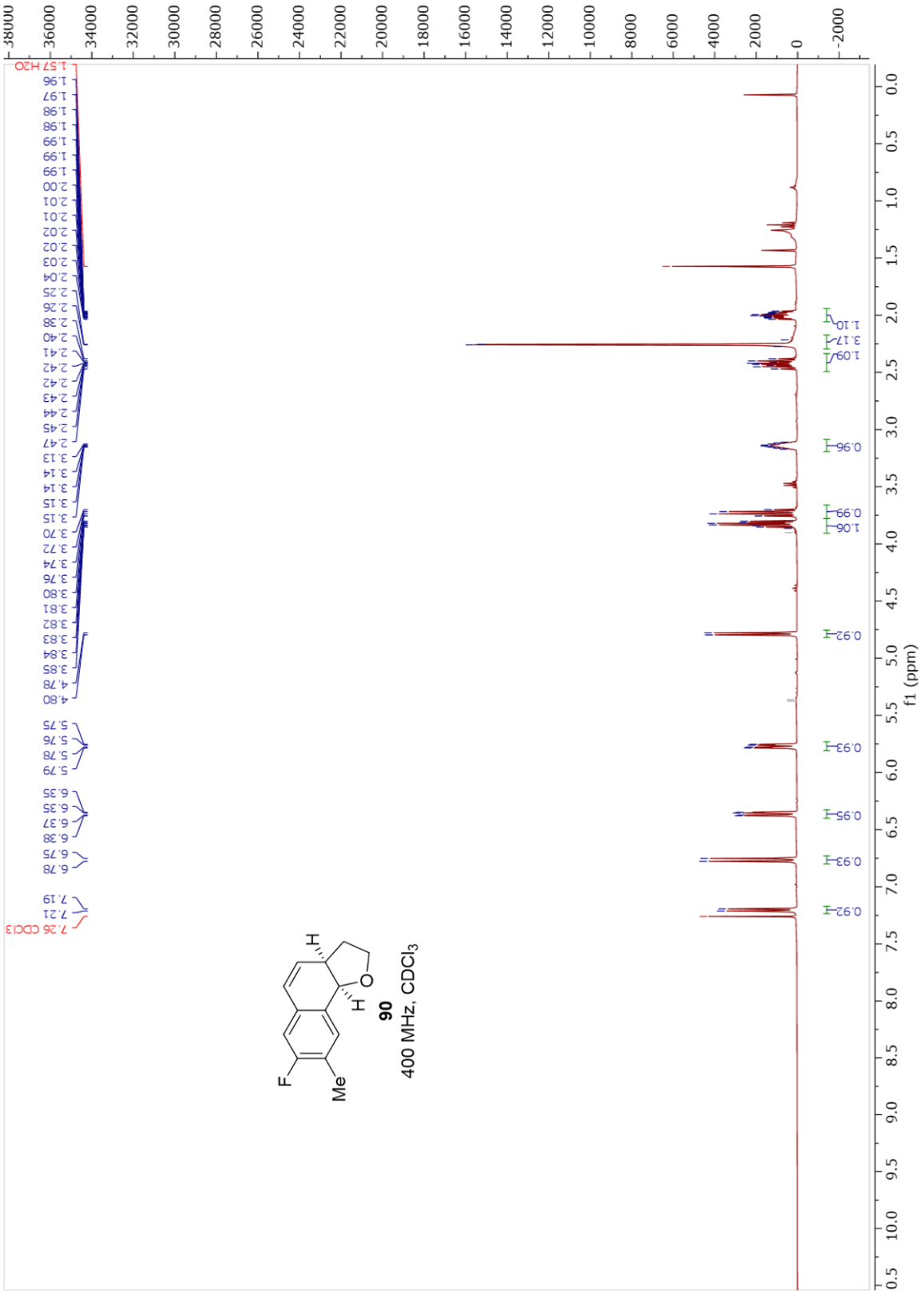
F
Me
H
O
H
90
400 MHz, CDCl3
f1 (ppm)

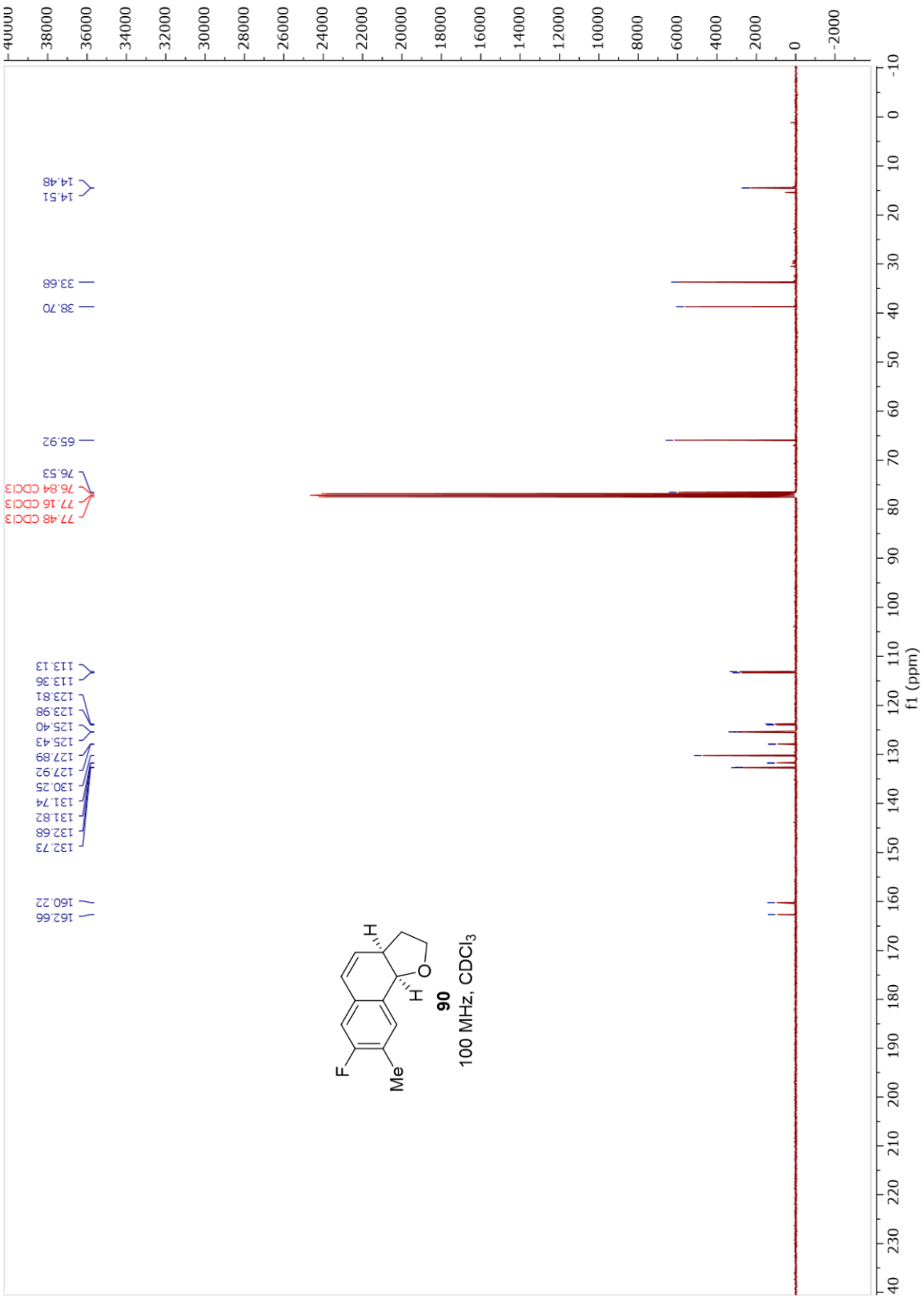
14.48
14.51
33.68
38.70
65.92
76.53
76.84 CDCl3
77.16 CDCl3
77.48 CDCl3
113.13
113.36
123.81
123.98
125.40
125.43
127.89
127.92
130.25
131.74
131.82
132.68
132.73
160.22
162.66
F
Me
O
H
H
90
100 MHz, CDCl3
f1 (ppm)

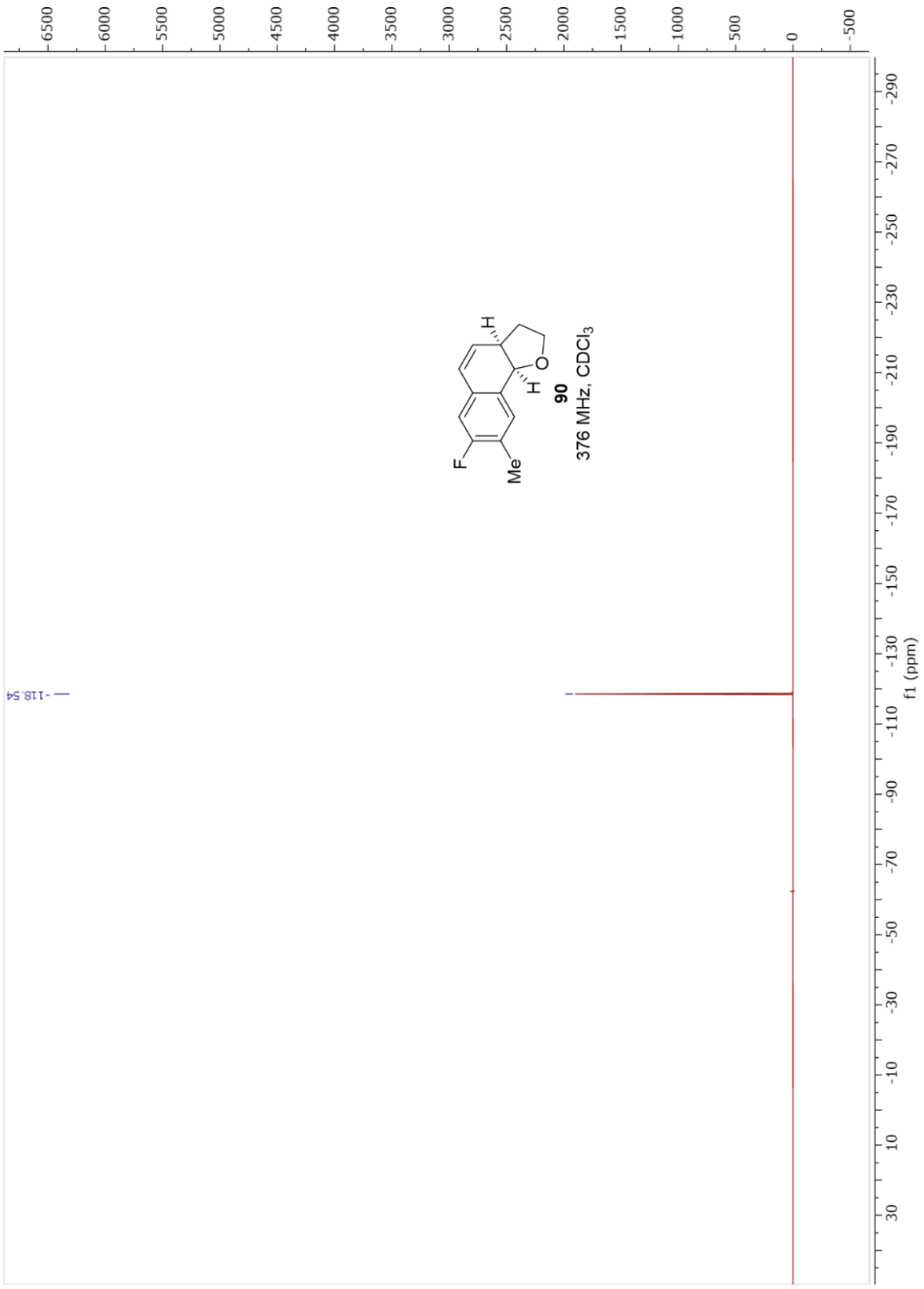
-118.54
f1 (ppm)
90
376 MHz, CDCl3
F
Me
H
O
H

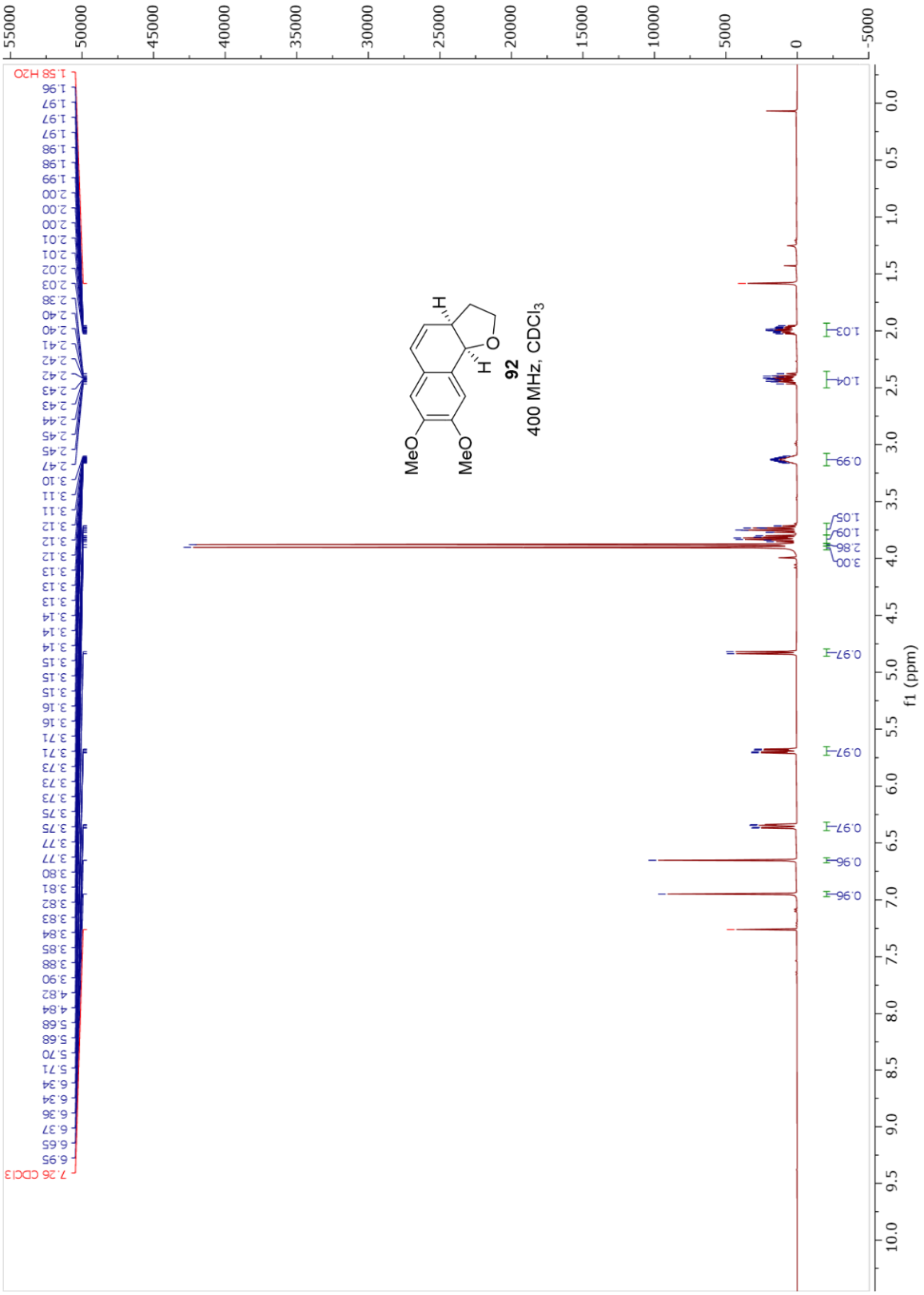
MeO
MeO
H
H
O
92
400 MHz, CDCl3
f1 (ppm)

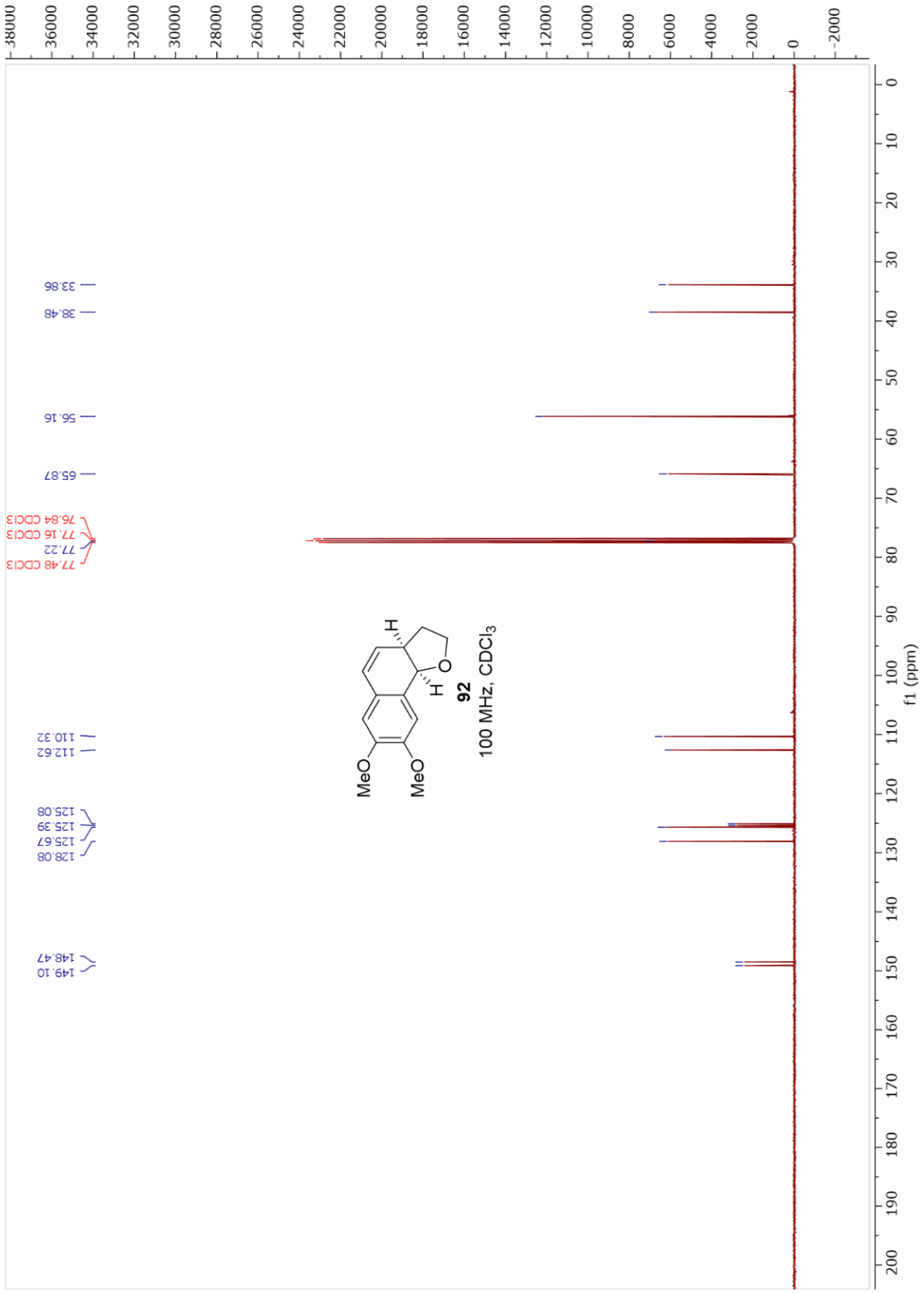
33.86
38.48
56.16
65.87
76.84 CDCl3
77.16 CDCl3
77.22
77.48 CDCl3
110.32
112.62
125.08
125.39
125.67
128.08
148.47
149.10
MeO
MeO
H
O
H
92
100 MHz, CDCl3
f1 (ppm)

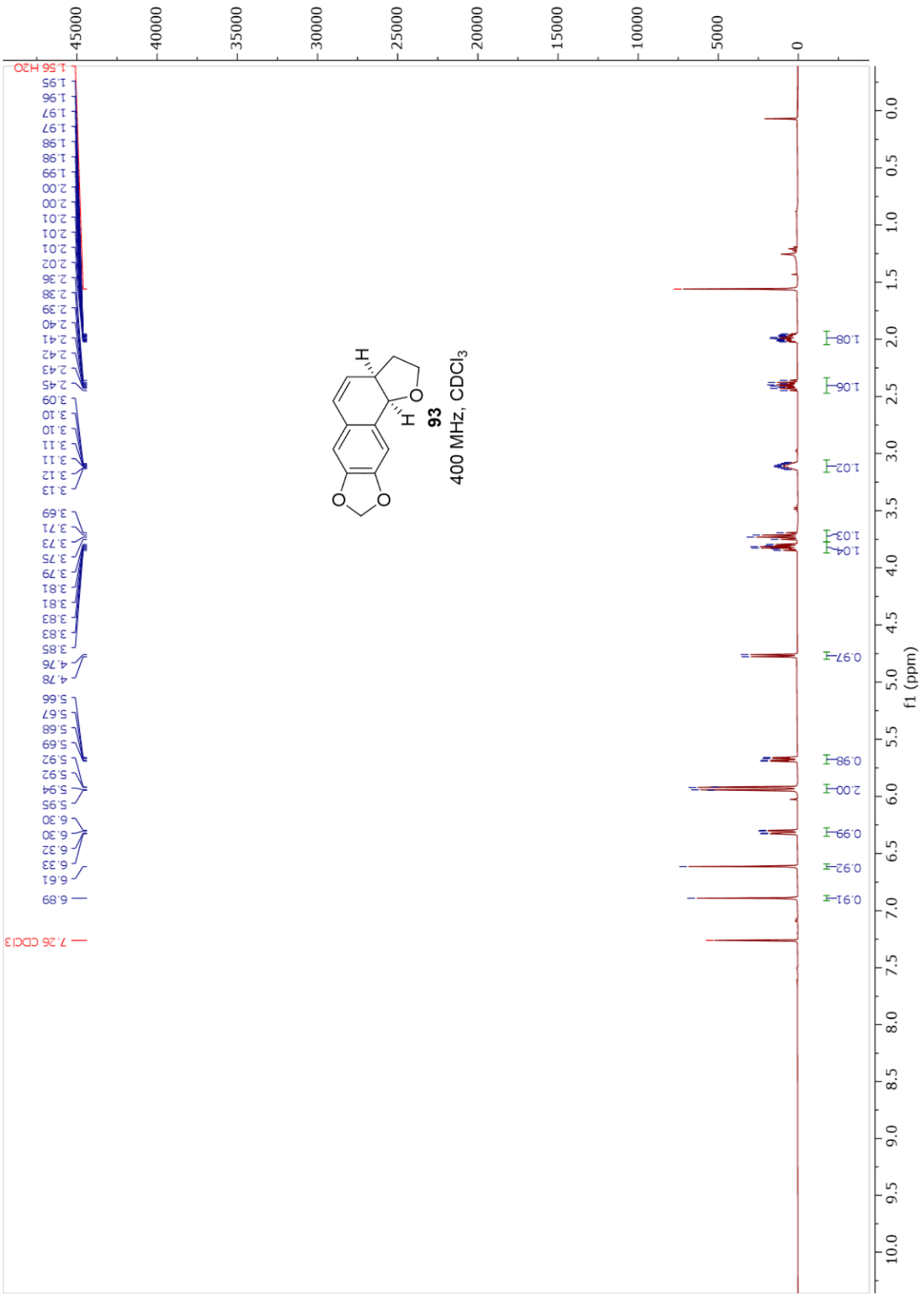
93
400 MHz, CDCl3
f1 (ppm)

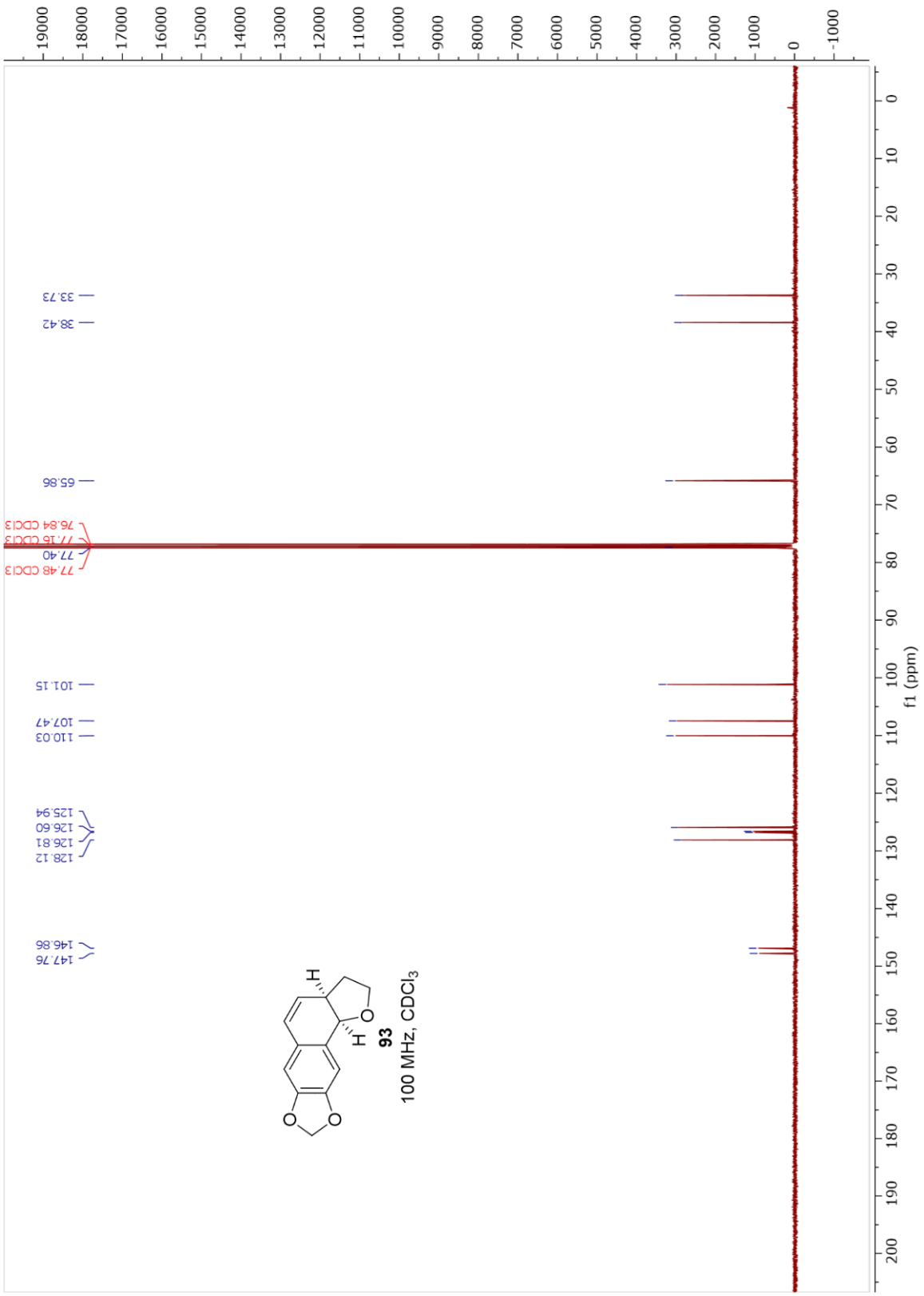
93
100 MHz, CDCl3
f1 (ppm)
33.73
38.42
65.86
76.84 CDCl3
77.16 CDCl3
77.40
77.48 CDCl3
101.15
107.47
110.03
125.94
126.60
126.81
128.12
146.86
147.76

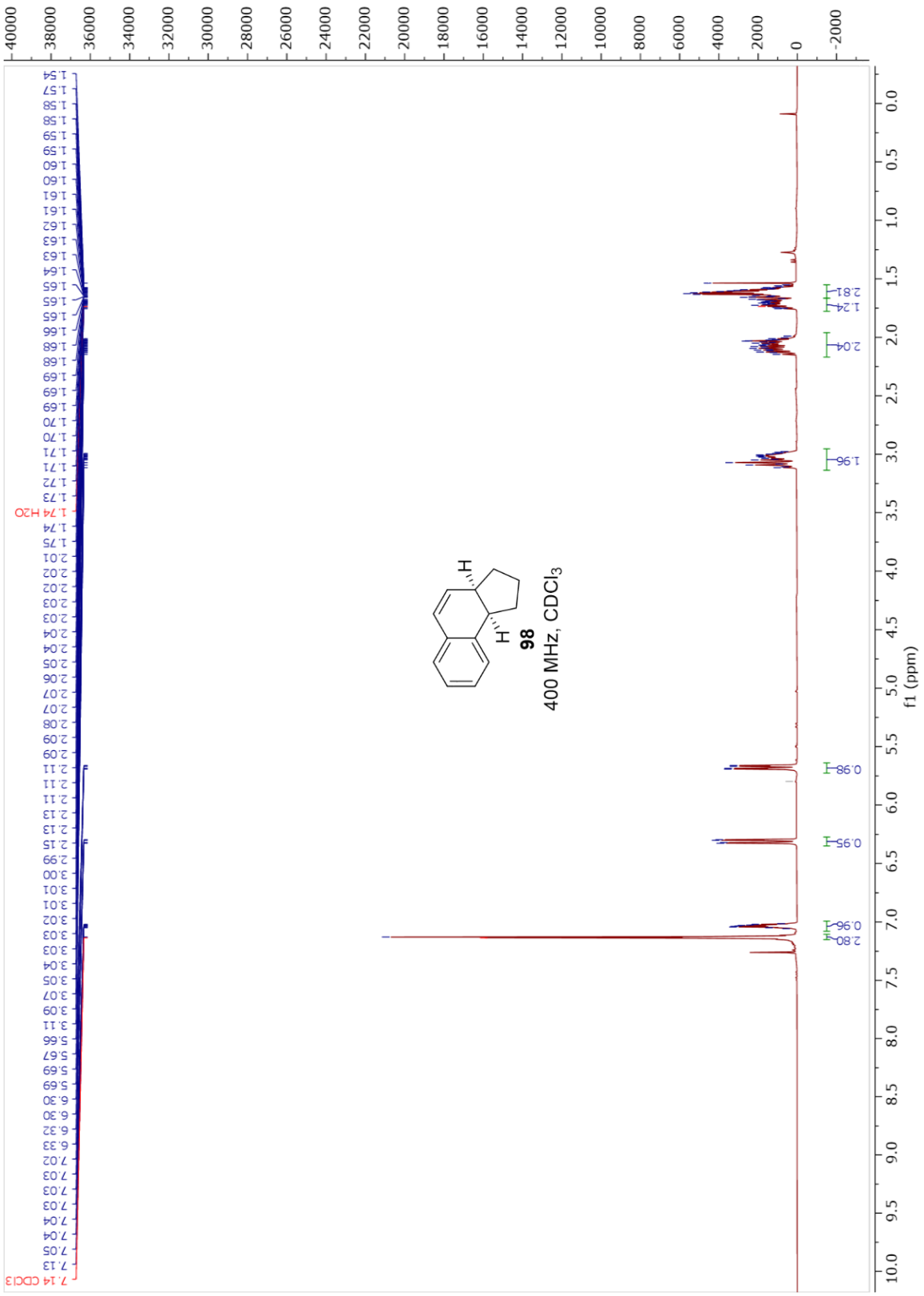
98
400 MHz, CDCl3
f1 (ppm)
7.14 CDCl3
1.74 H2O
2.80
0.96
0.95
0.98
1.96
2.04
1.24
2.81

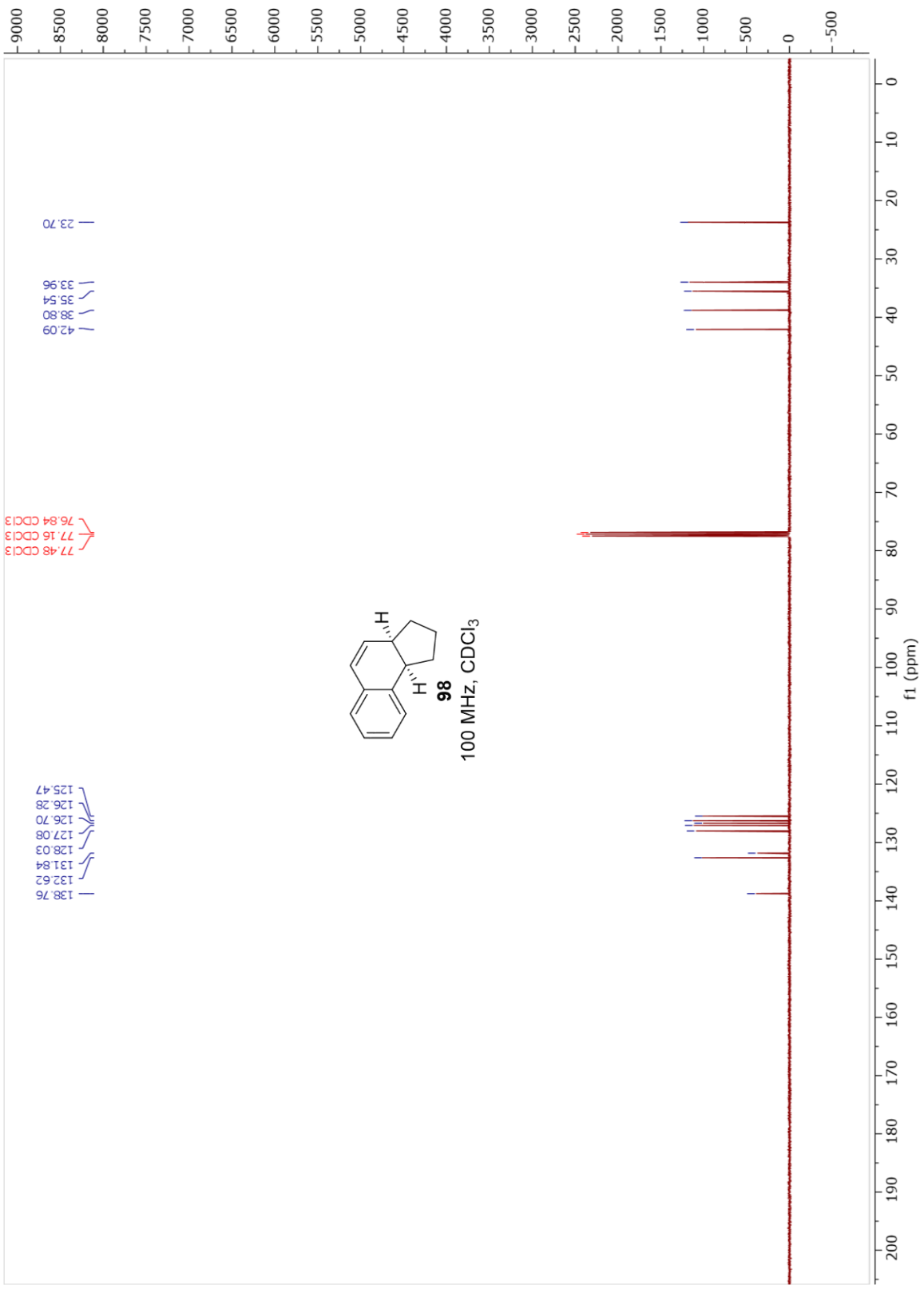
23.70
33.96
35.54
38.80
42.09
76.84 CDCl3
77.16 CDCl3
77.48 CDCl3
125.47
126.28
126.70
127.08
128.03
131.84
132.62
138.76
H
H
98
100 MHz, CDCl3
f1 (ppm)

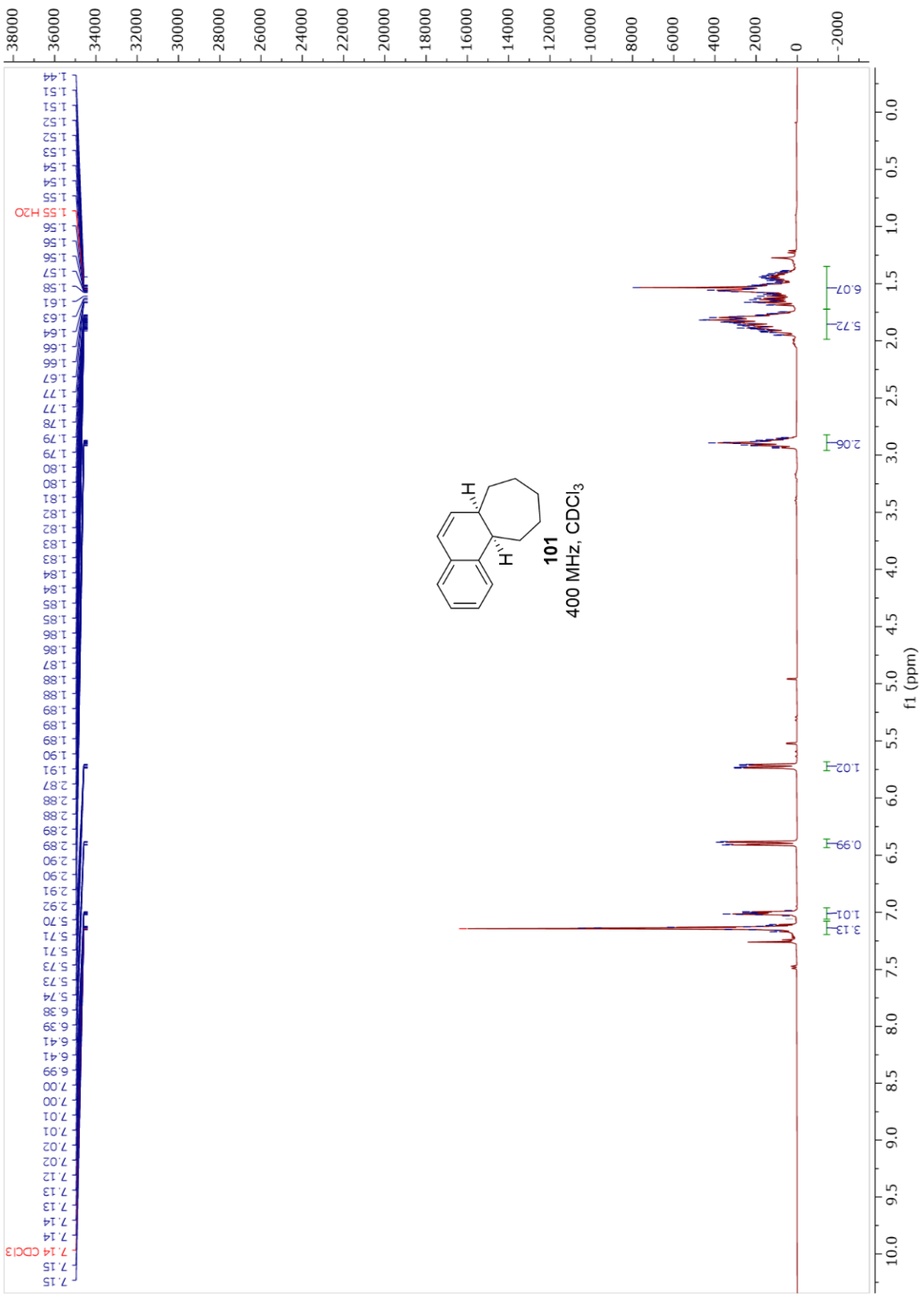
101
400 MHz, CDCl3
f1 (ppm)
6.07
5.72
2.06
1.02
0.99
1.01
3.13
1.55 H2O
7.14 CDCl3

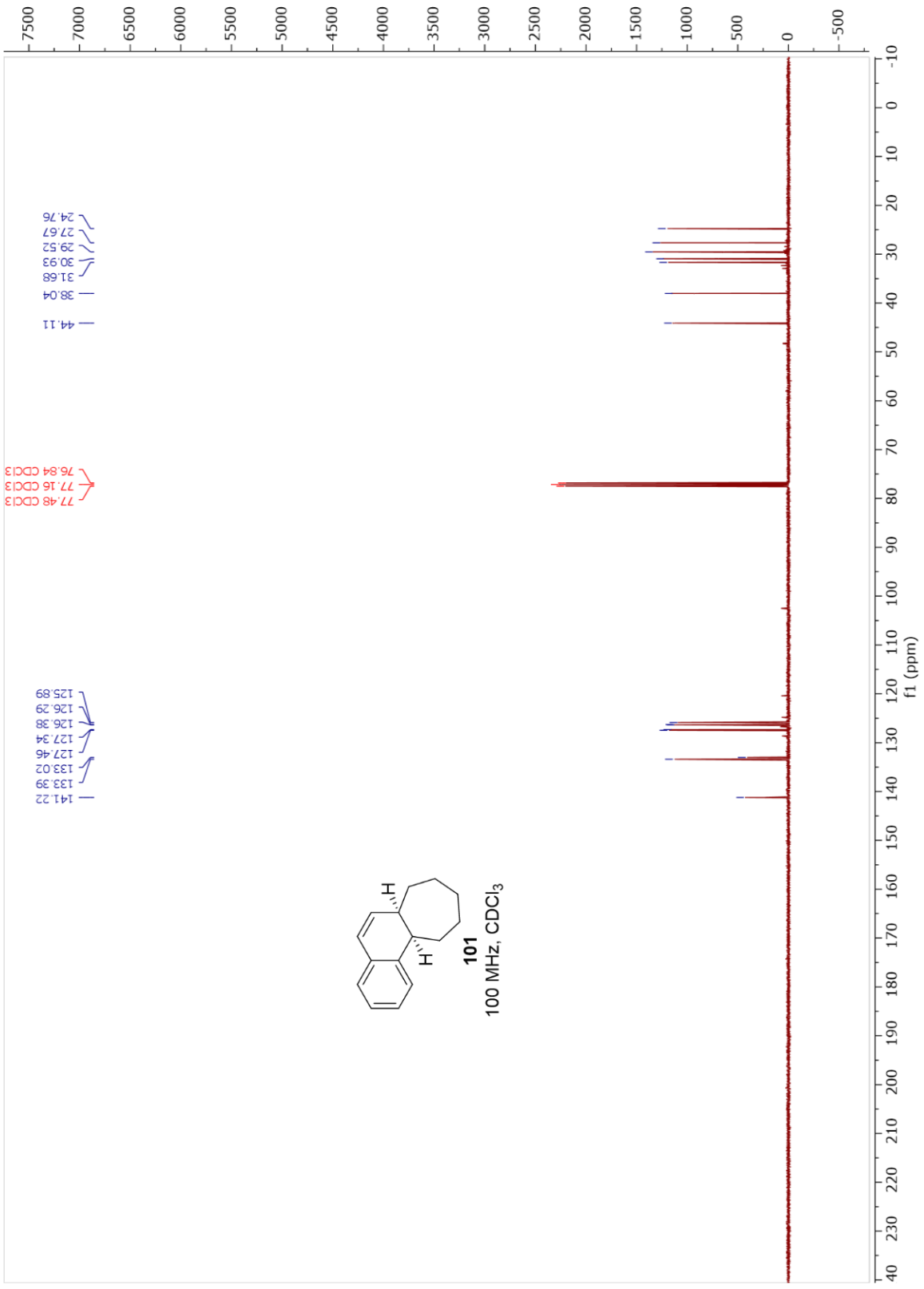
101
100 MHz, CDCl3
H
H
141.22
133.39
133.02
127.46
127.34
126.38
126.29
125.89
77.48 CDCl3
77.16 CDCl3
76.84 CDCl3
44.11
38.04
31.68
30.93
29.52
27.67
24.76
f1 (ppm)

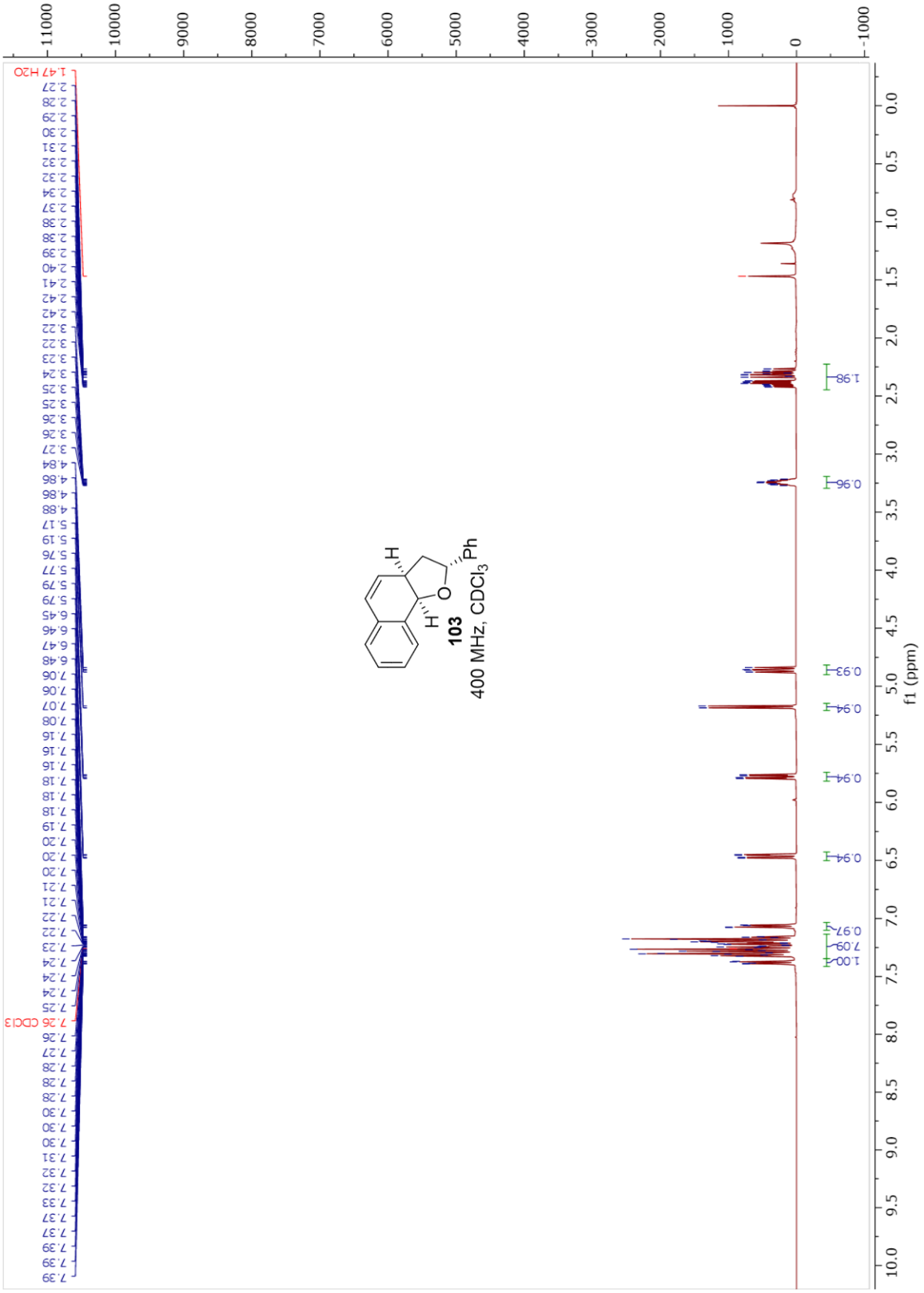
H
H
O
Ph
103
400 MHz, CDCl3
f1 (ppm)
1.98
0.96
0.93
0.94
0.94
0.94
0.97
7.09
1.00
1.47 H2O
7.26 CDCl3

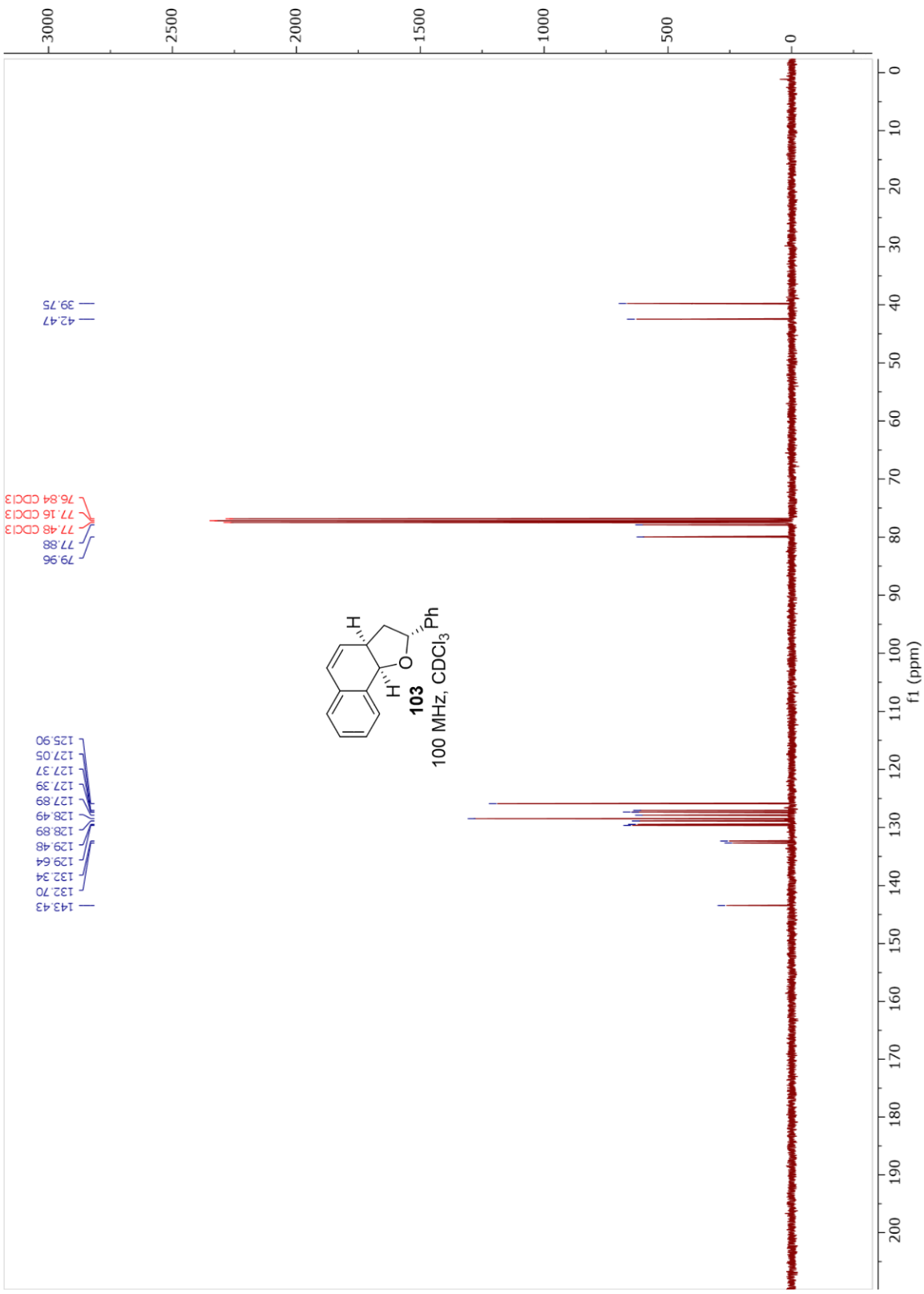
103
100 MHz, CDCl3
f1 (ppm)
143.43
132.70
132.34
129.64
129.48
128.89
128.49
127.89
127.39
127.37
127.05
125.90
79.96
77.88
77.48 CDCl3
77.16 CDCl3
76.84 CDCl3
42.47
39.75

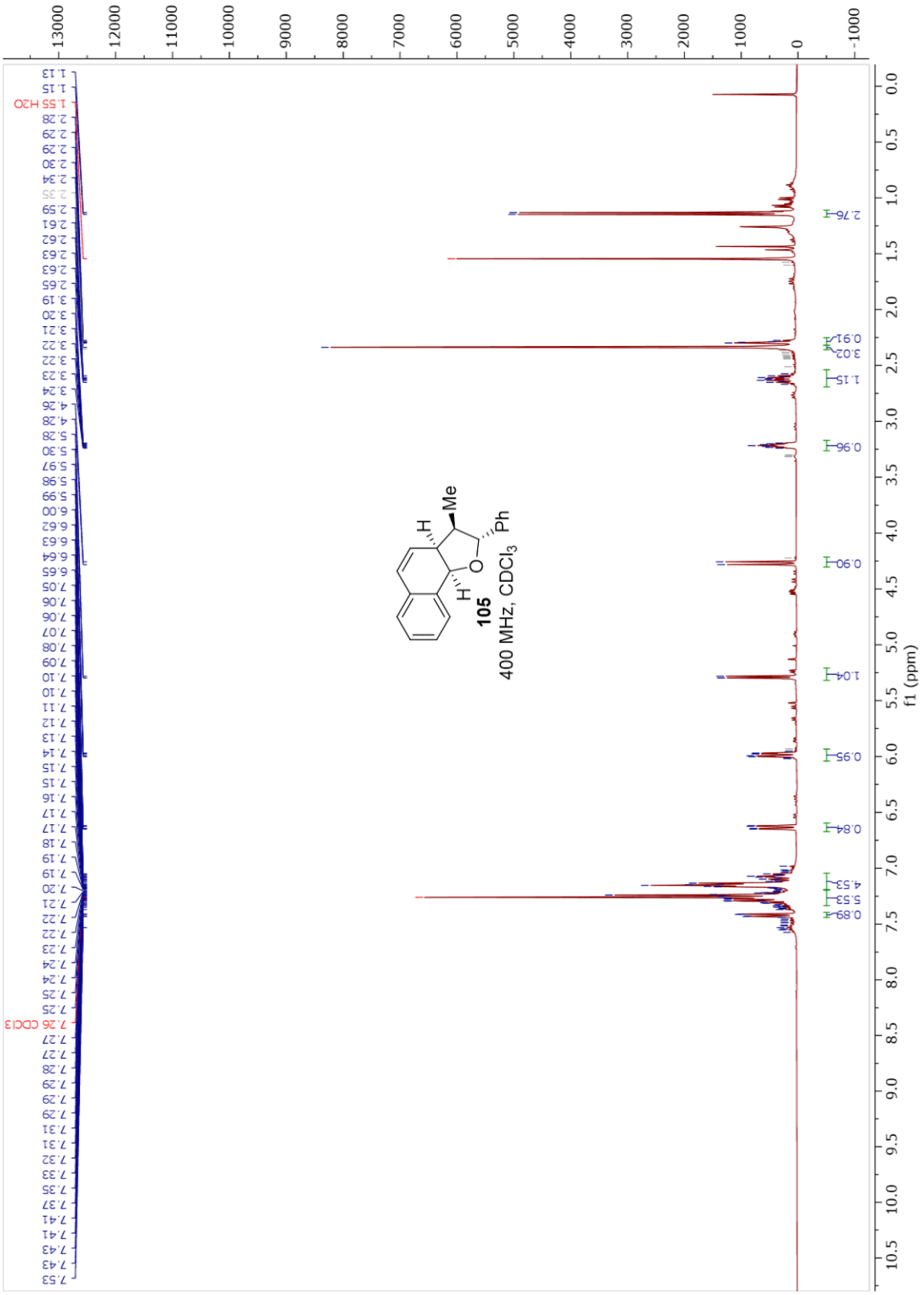
Me
H
Ph
O
H
105
400 MHz, CDCl3
f1 (ppm)
H2O
CDCl3

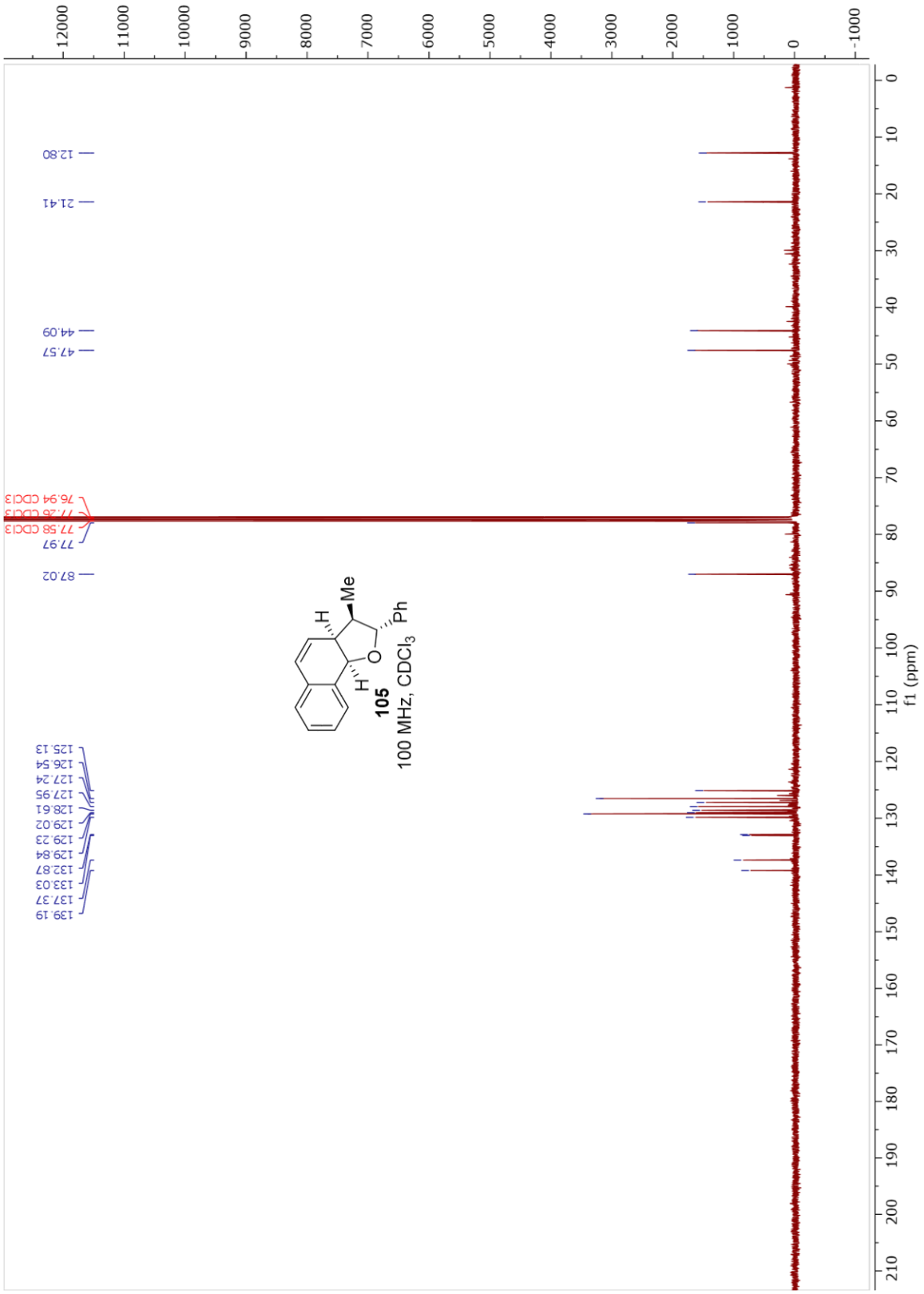
12.80
21.41
44.09
47.57
76.94 CDCl3
77.26 CDCl3
77.58 CDCl3
77.97
87.02
125.13
126.54
127.24
127.95
128.61
129.02
129.23
129.84
132.87
133.03
137.37
139.19
Me
H
H
O
Ph
105
100 MHz, CDCl3
f1 (ppm)

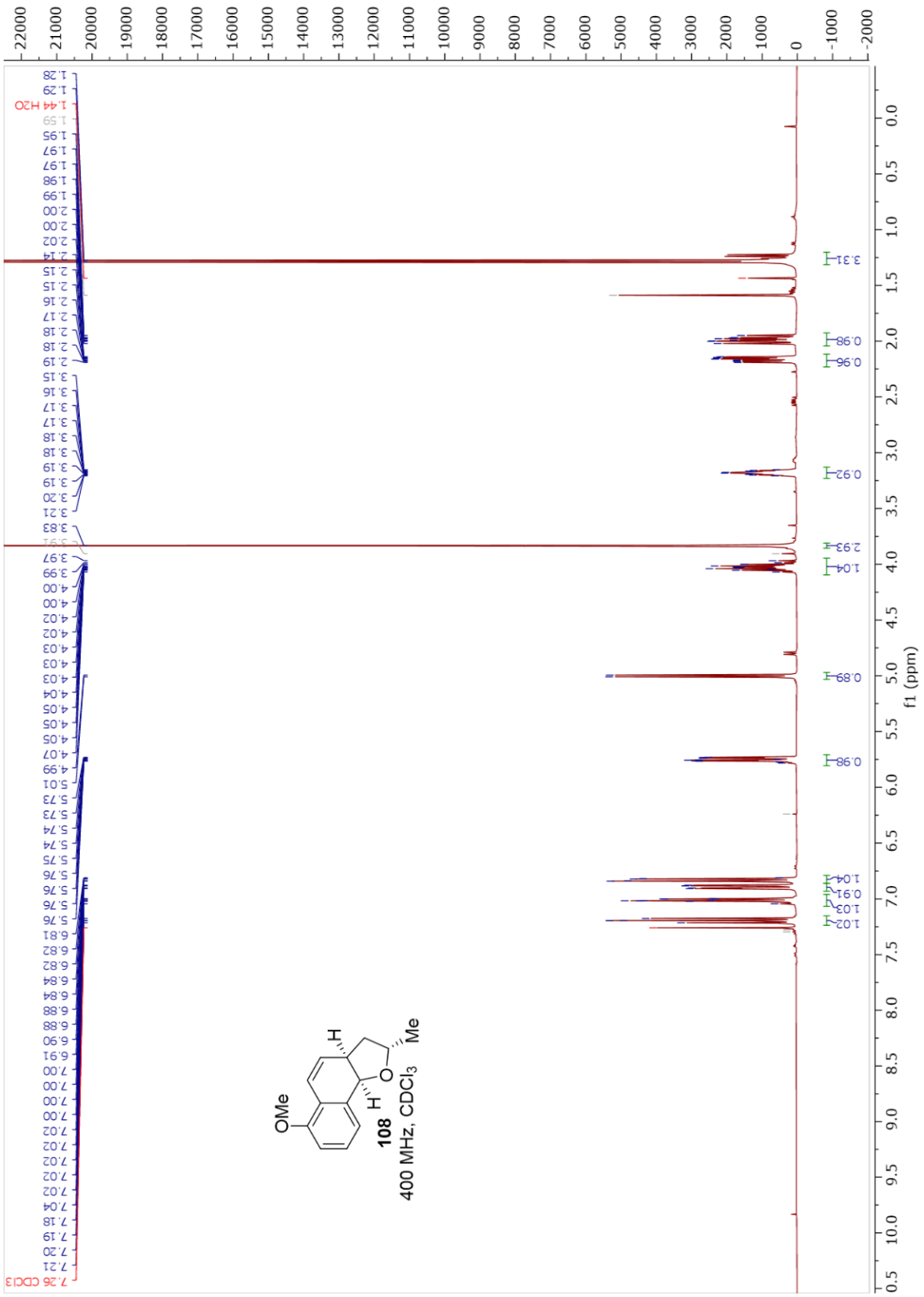
OMe
H
H
O
Me
108
400 MHz, CDCl3
f1 (ppm)

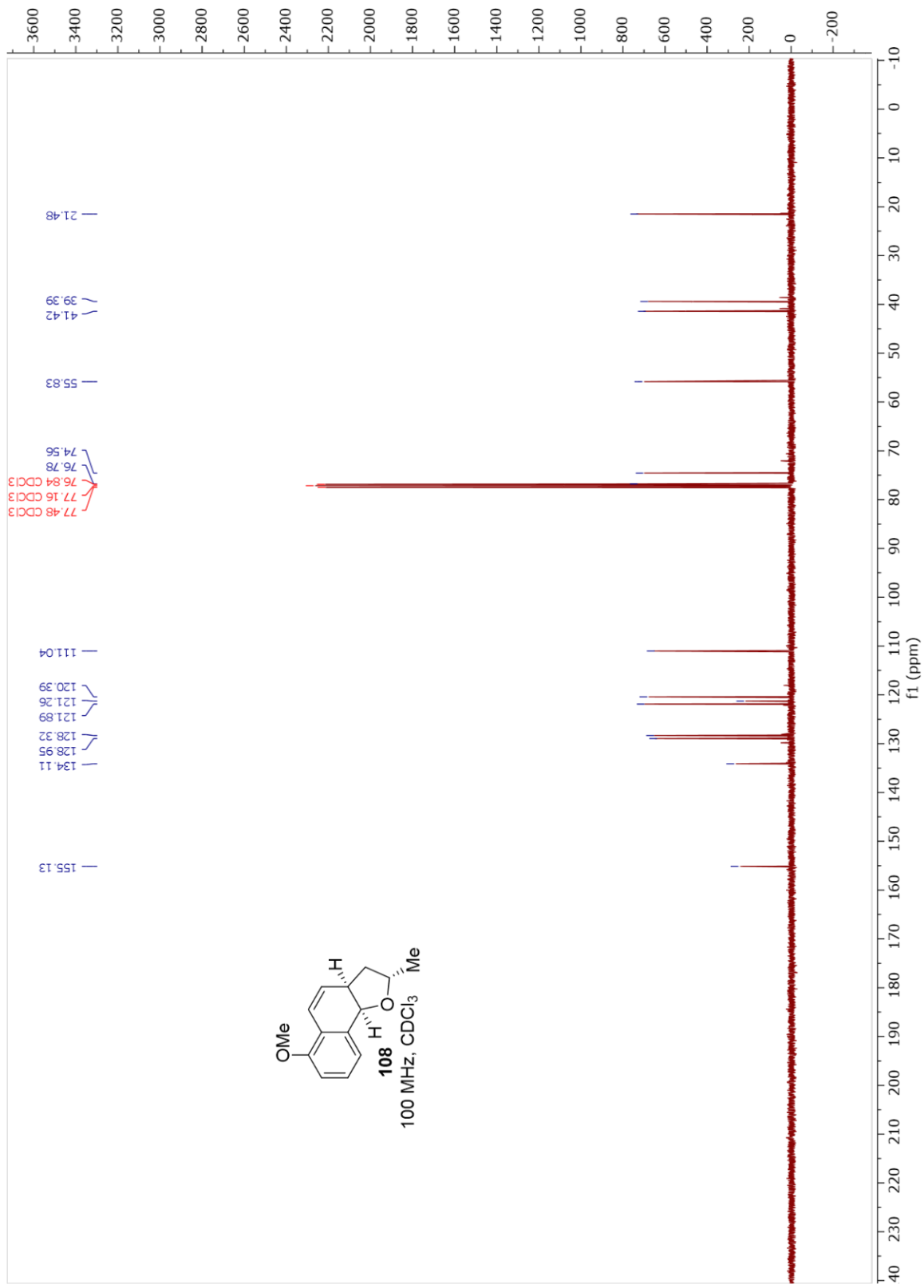
155.13
134.11
128.95
128.32
121.89
121.26
120.39
111.04
77.48 CDCl3
77.16 CDCl3
76.84 CDCl3
76.78
74.56
55.83
41.42
39.39
21.48
f1 (ppm)
OMe
H
H
O
Me
108
100 MHz, CDCl3

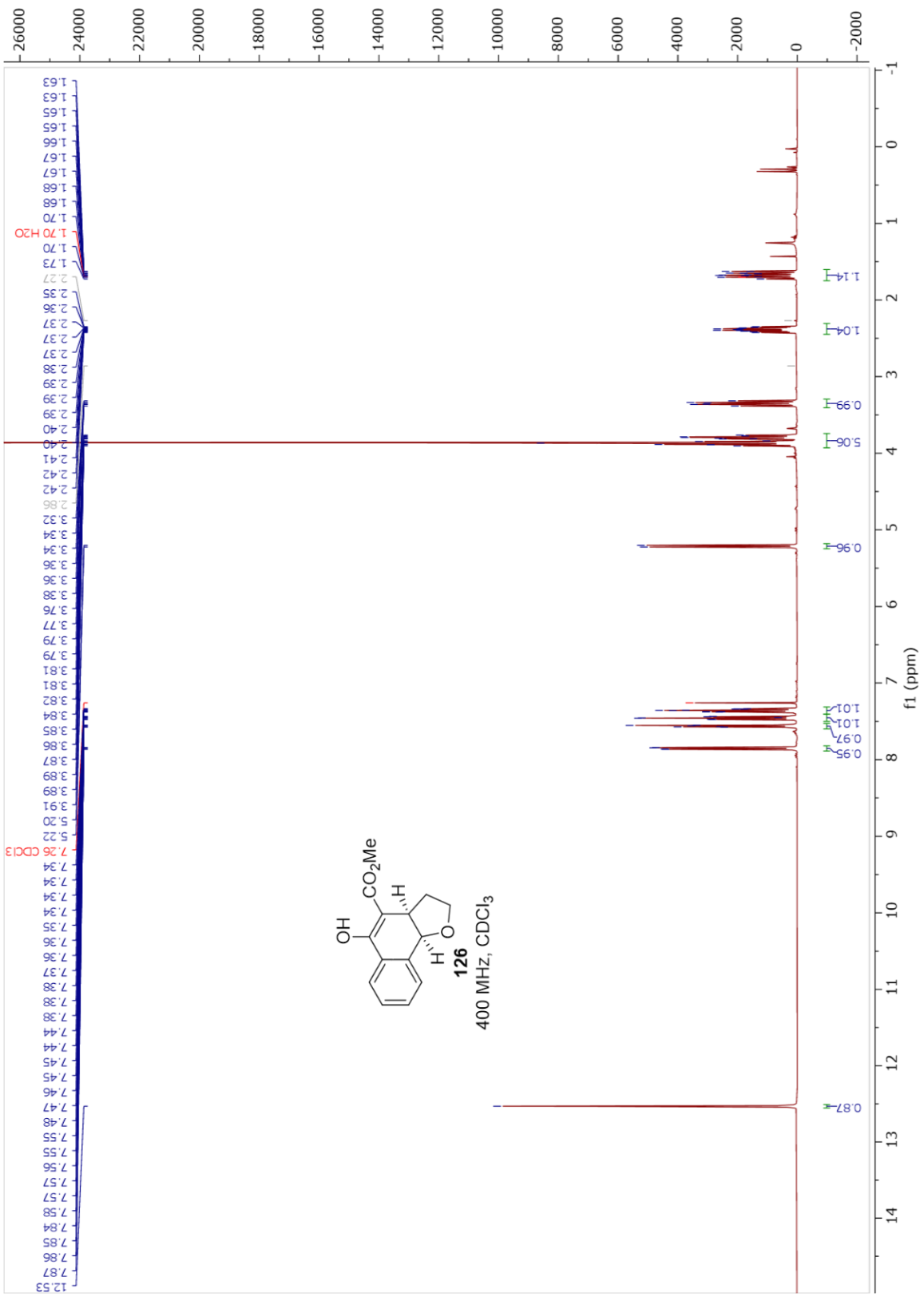
OH
CO2Me
H
O
H
126
400 MHz, CDCl3
f1 (ppm)

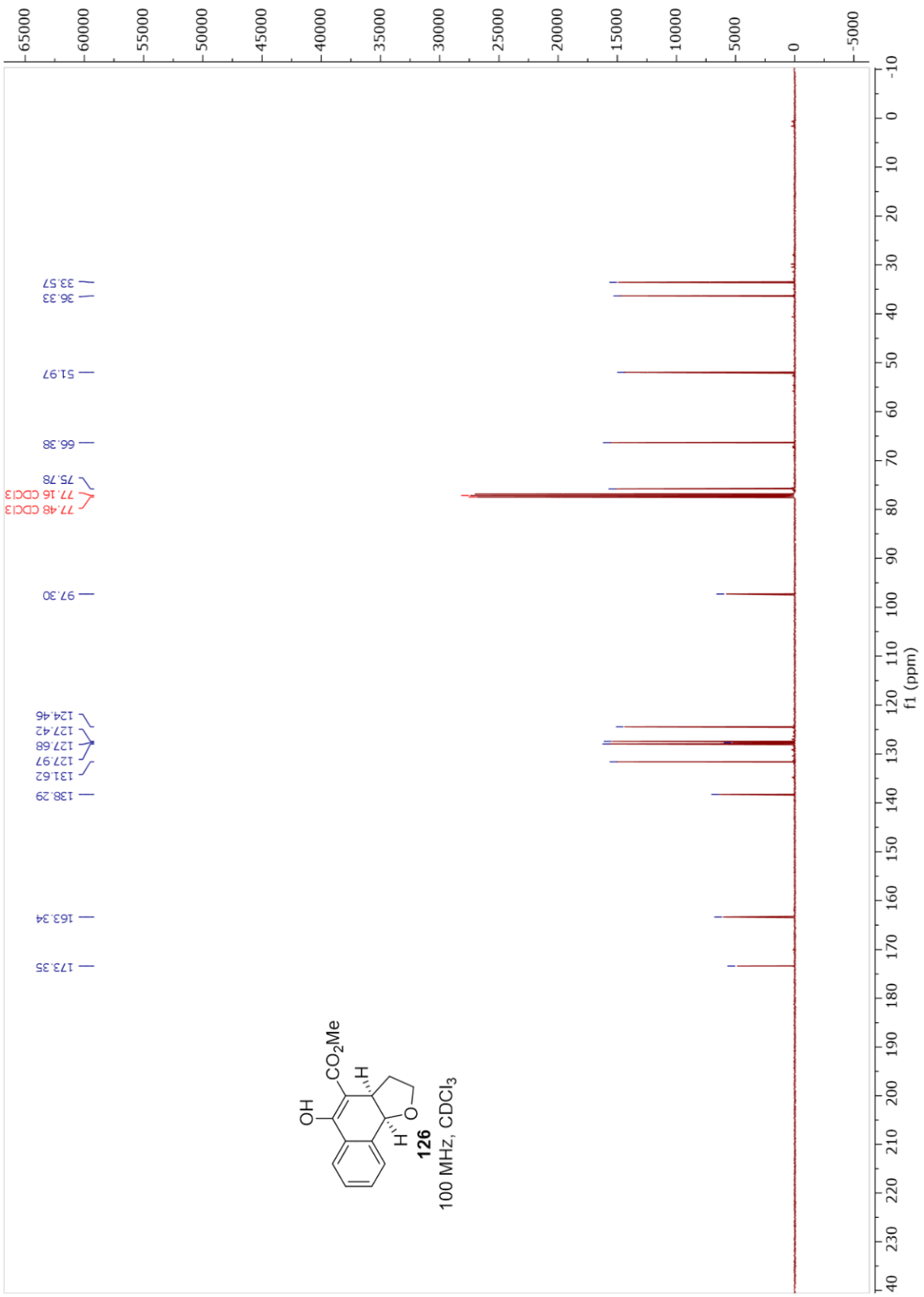
173.35
163.34
138.29
131.62
127.97
127.68
127.42
124.46
97.30
77.48 CDCl3
77.16 CDCl3
75.78
66.38
51.97
36.33
33.57
f1 (ppm)
126
100 MHz, CDCl3

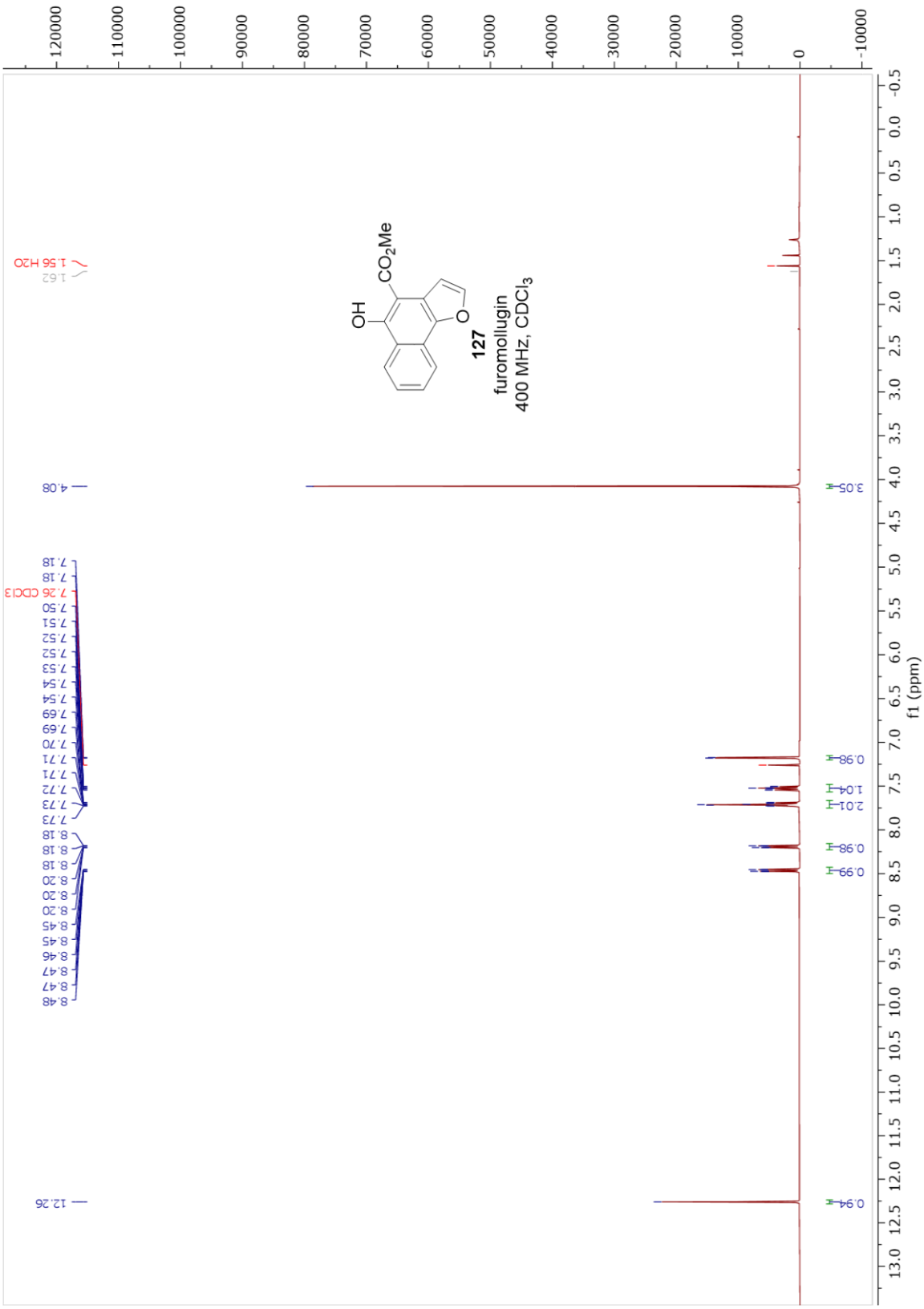
OH
CO2Me
O
127
furomollugin
400 MHz, CDCl3
f1 (ppm)

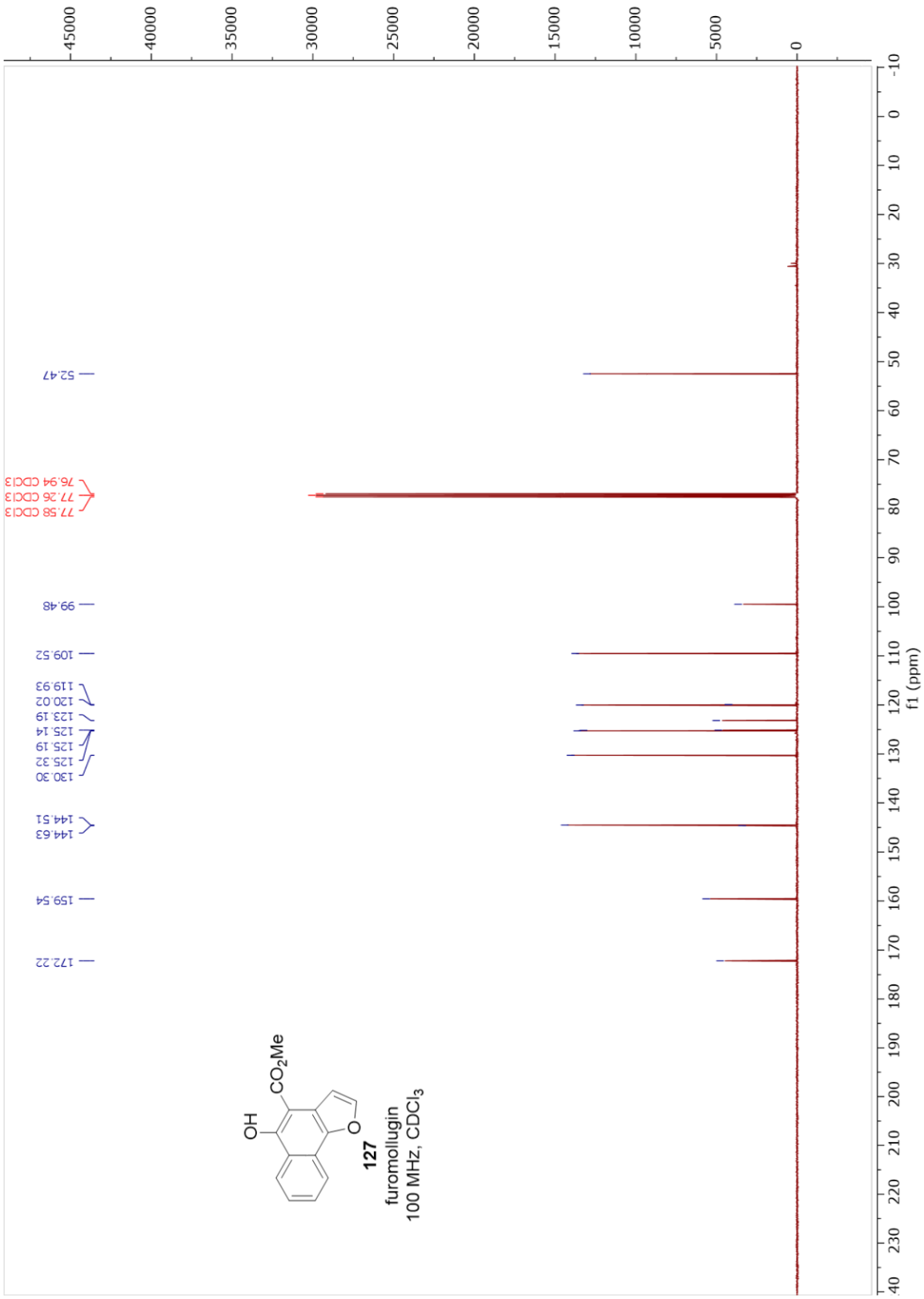
45000
40000
35000
30000
25000
20000
15000
10000
5000
0
-10
0
10
20
30
40
50
60
70
80
90
100
110
120
130
140
150
160
170
180
190
200
210
220
230
240
f1 (ppm)
52.47
76.94 CDCl3
77.26 CDCl3
77.58 CDCl3
99.48
109.52
119.93
120.02
123.19
125.14
125.19
125.32
130.30
144.51
144.63
159.54
172.22
OH
CO2Me
O
127
furomollugin
100 MHz, CDCl3

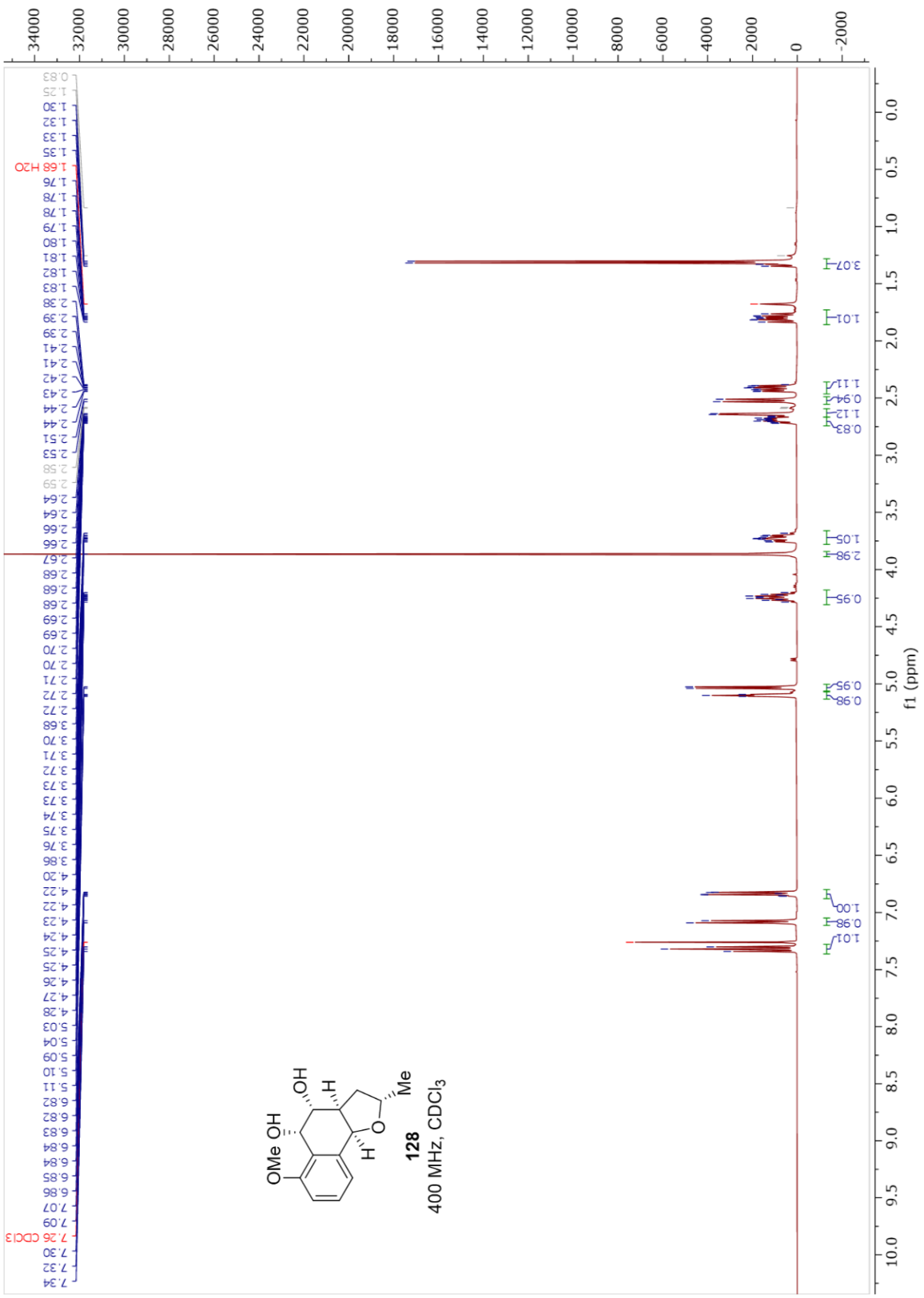
OMe OH
OH
H
H
O
Me
128
400 MHz, CDCl3
f1 (ppm)

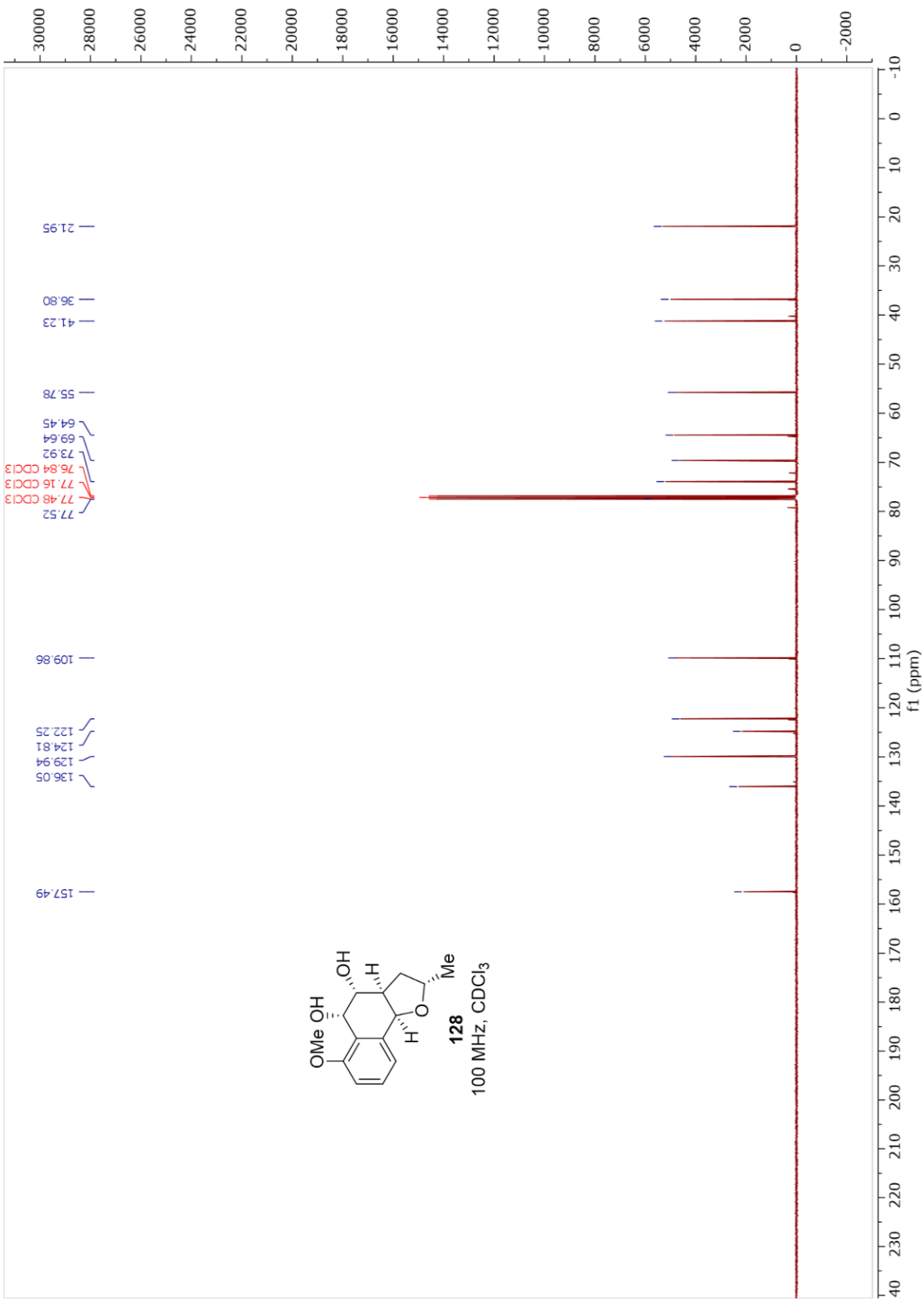
21.95
36.80
41.23
55.78
64.45
69.64
73.92
76.84 CDCl3
77.16 CDCl3
77.48 CDCl3
77.52
109.86
122.25
124.81
129.94
136.05
157.49
OMe OH
OH
H
H
O
Me
128
100 MHz, CDCl3
f1 (ppm)

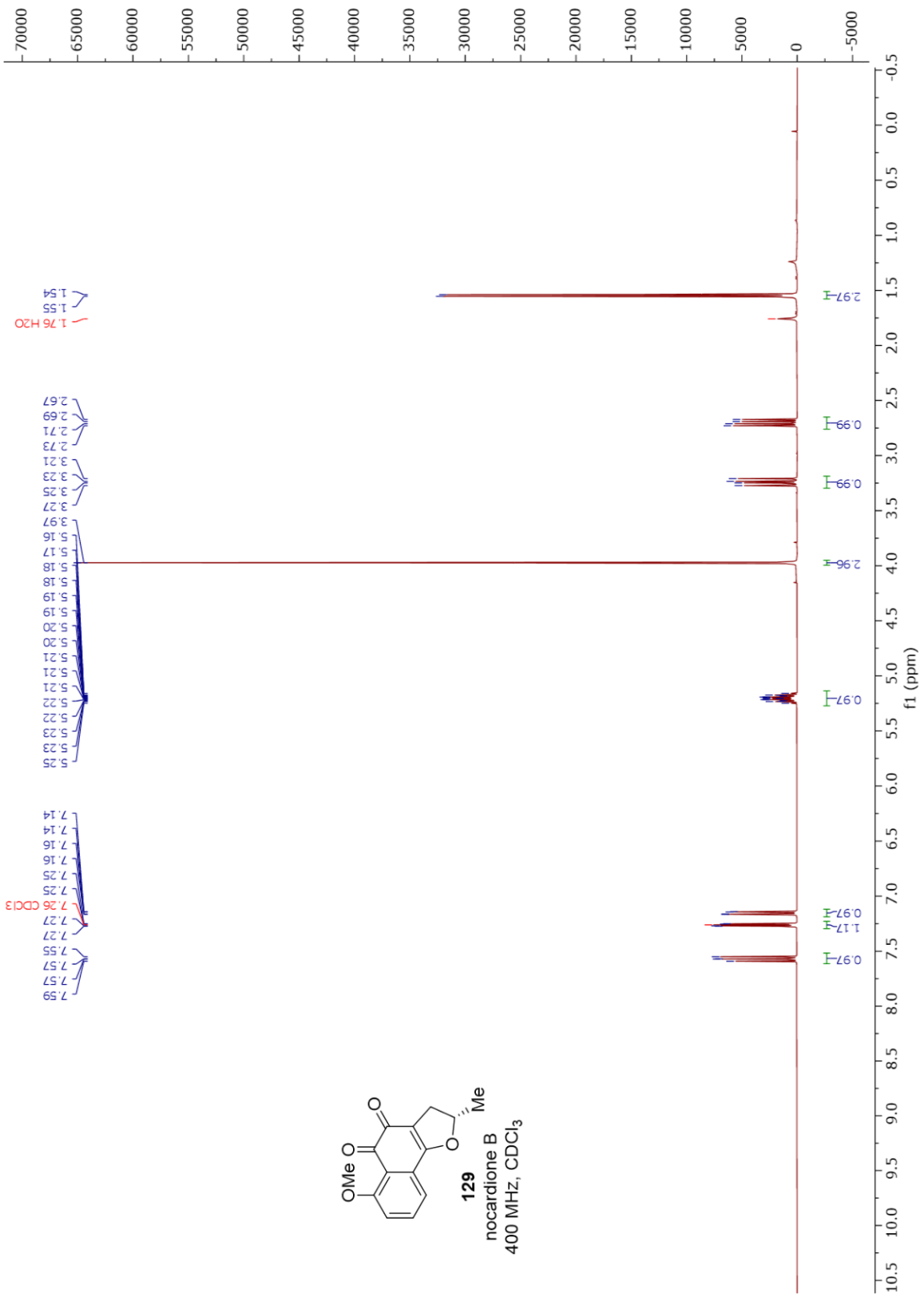
OMe O
Me
O
O
129
nocardione B
400 MHz, CDCl3
f1 (ppm)

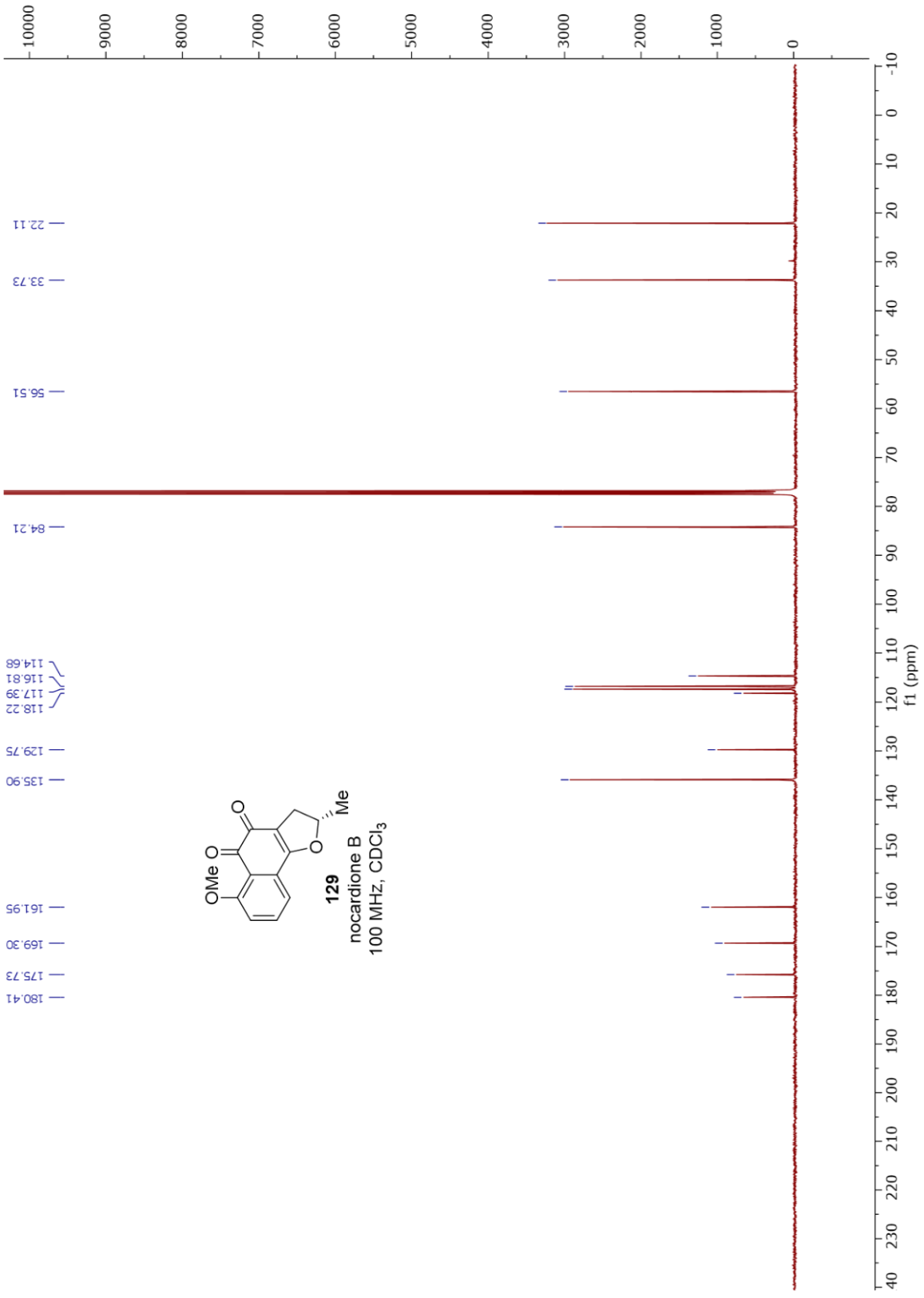
22.11
33.73
56.51
84.21
114.68
116.81
117.39
118.22
129.75
135.90
161.95
169.30
175.73
180.41
OMe O
O
O
Me
129
nocardione B
100 MHz, CDCl3
f1 (ppm)

Chapter 4

Further Studies Toward Retigeranic Acid A

4.1 A New Approach

While our Ni-Heck chemistry has led to some very exciting areas of research, unfortunately it did not prove to be a salve for the troubles of our synthesis of retigeranic acid A **1**. In order to push forward, a new approach would need to be designed. As altering the metal had not proved sufficient, our next thought was to modify the nature of the cascade intermediate. Specifically, we

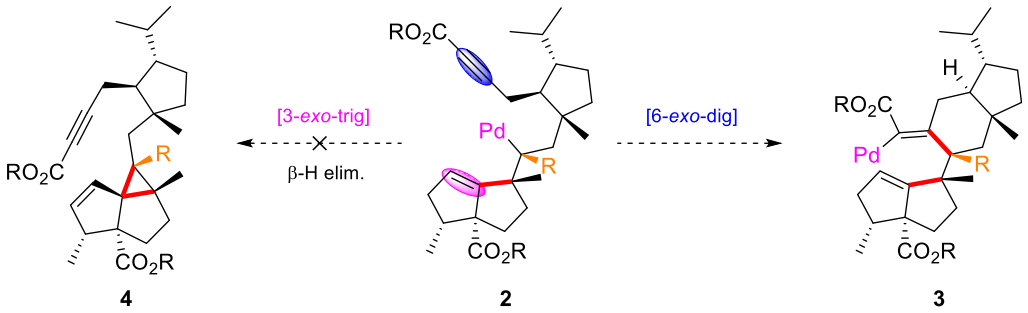

Scheme 4.1 Proposed Pd-enolate Heck Cascade and potential chemoselectivity.

were curious as to whether there was a substrate modification, as shown in Scheme 4.1, that would allow the Pd to selectively react with the ynoate (highlighted in blue) over the unactivated olefin (highlighted in purple). One such alteration would be the incorporation of a carbonyl group, shown as the R highlighted in orange, such that the alkyl-Pd species would instead be a Pd-enolate. However, it was not immediately evident whether or not this alteration would have the desired effect as the literature seemed unclear as to whether the desired [6-*exo*-dig] Michael addition or the [3-*exo*-trig] migratory insertion would prevail.

The Tsuji group has investigated the reactivity of Pd-enolates as part of their broader studies on decarboxylative allylation reactions.[1,2] Starting from aldehyde **5**, they found that the allyl-Pd enolate **6** generated from decarboxylation, could undergo an intramolecular aldol reaction to give β-ketoalcohol **8** in excellent yield. Further, they found that the allyl-Pd enolate **10** proceeded via a Michael addition on to the pendant enone to give bicycles **11** and **12.** These

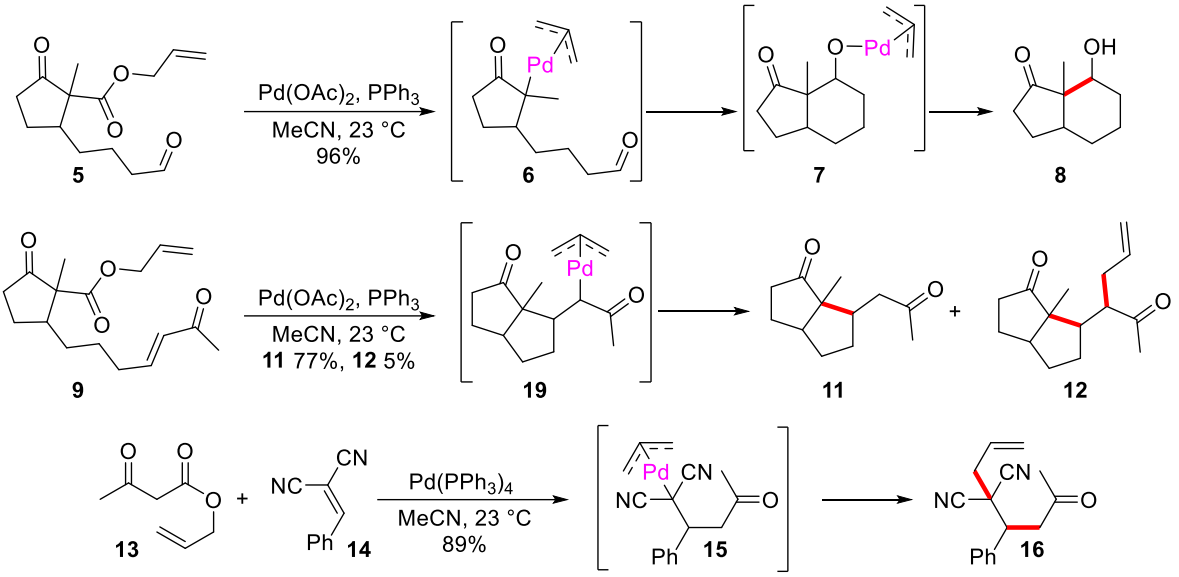

Scheme 4.2 Representative examples of Pd-enolate Aldol and Michael reactions from the Tsuji group.

reactions are impressive given that no direct allylation product was observed in either case. In fact,only around 5% of allylated product **12**, which arises from allylation of the Pd-enolate generated after the Michael addition, was isolated. The reaction could even be conducted in an intramolecular fashion using allyl acetoacetate **13** and the highly reactive benzylidenemalononitrile **14** to give the allylated **16**, the softer malonitrile anion apparently favoring allylation. While this reaction mode was originally described more than 30 years ago, it has not been studied in any extensive fashion with most examples being of the intermolecular variant.[3–6] Regardless, the initial Tsuji studies indicate that at least on a fundamental level our proposed Michael addition is feasible, though this would be the first example with an ynoate.

How the Pd-enolate would interact with the unactivated olefin was less straight forward. Numerous examples of sp^2-sp^3 couplings of Pd-enolates are known,[7,8] but most precedents proceed via reductive elimination of an sp^2 intermediate as opposed to the migratory insertion pathway proposed in our system. A representative example is shown in Scheme 4.3.[9] More akin to our system is the intramolecular coupling of silyl enol ethers with olefins.[10–13] The exact

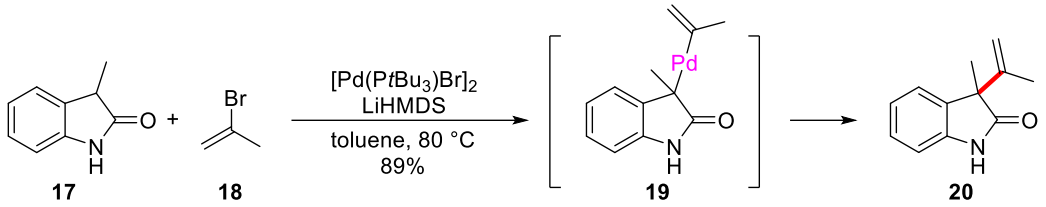

Scheme 4.3 Representative example of vinylation of Pd enolates.

mechanism of these reactions is not entirely established, but two major proposals exist. In the first, the Pd^{II} species binds to the olefin, as illustrated in Scheme 4.4, and acts as a Lewis acid in order to sufficiently activate it for the silyl enol ether to attack in a fashion akin to the Wacker oxidation. This reaction is quite powerful and allows for the formation of bicyclo structures like **23** and **24**.[10,14] Trans-annular cyclizations reported from the Fuchs groups show how subtle variations in substrate design can lead to significant changes in product formation.[12] In their example, the geometry of the cyclic alkene determined where the alkyl Pd intermediate, formed after the transannular attack of the silyl enol ether, can undergo β-hydride elimination due to the presence or lack of syn β-H. Further, this approach can even be coupled with the Heck reaction as shown in an example form the Coudanne group.[13] Here, following the oxidative addition into the

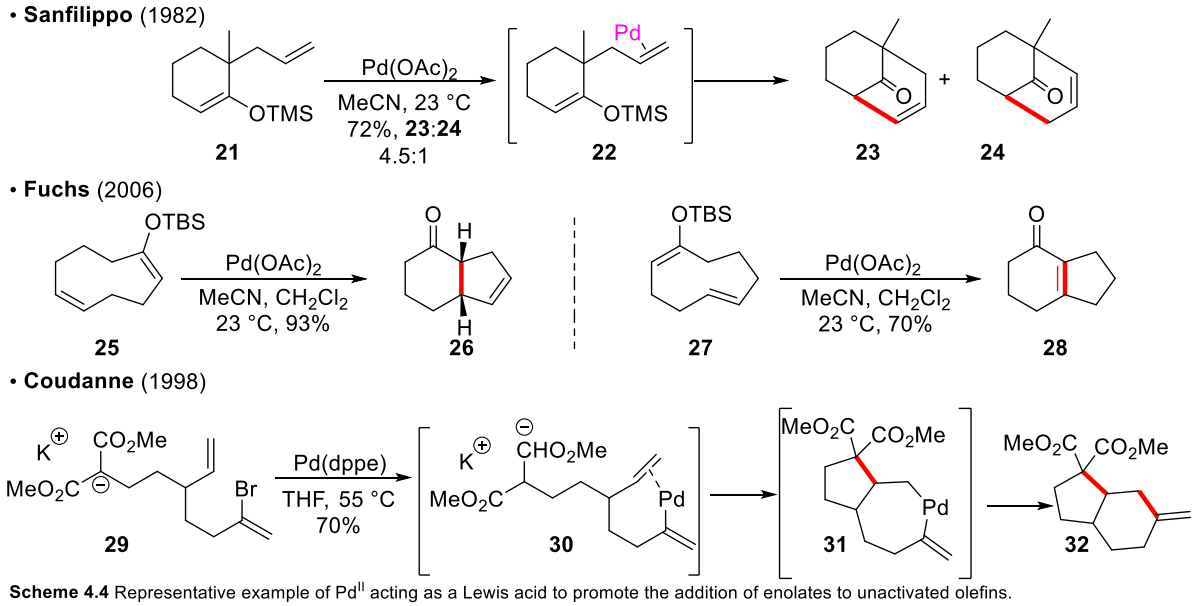

Scheme 4.4 Representative example of Pd^{II} acting as a Lewis acid to promote the addition of enolates to unactivated olefins.

vinyl bromide **29**, the resultant Pd^{II} species activates the olefin for intramolecular attack by the malonate to yield **31**. Subsequent reductive elimination gives the observed hydrindane product **32**. In the second proposal for the mechanism of silyl enol ethers reacting with unactivated olefins, the Pd^{II} undergoes transmetalation with the silyl group, usually TMS, and the resultant σ-Pd or π-allyl Pd species then undergoes a migratory insertion onto the unactivated olefin. The overall picture is further complicated by a series of recent reports from the Newhouse group wherein they describe a Ni-mediated vicinal difunctionalization.[15–17] The reaction is reported to proceed via

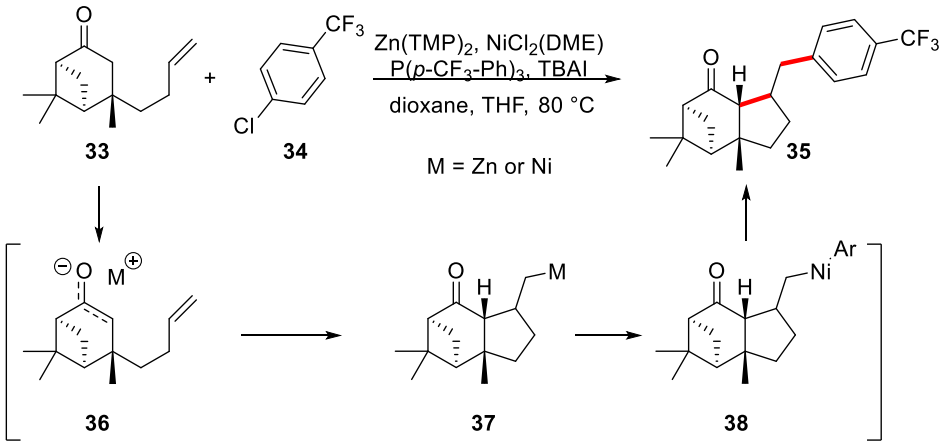

Scheme 4.5 Newhouse's Ni mediated vivcinal difunctionalization of unactivated olefins.

formation of Ni enolate **36**, which then undergoes migratory insertion and reductive elimination from intermediate **38** to yield the difunctionalized product **35**. While this appears relatively straight forward, the exact mechanism of the reaction is complicated by the fact that the cyclization product can be observed in the absence of the Ni catalyst.[16] As such, it is not entirely clear if the Ni-enolate is actually undergoing the migratory insertion or rather transmetalation of an alkyl-Zn **37**. With all of these examples in mind, we decided to push forward in the hopes we would be able to bias our substrate to effectively promote our desired [6-*exo*-dig] cyclization. Further, if the [3-*exo*-trig] pathways are still operative, possible elaboration of the resulting vinyl cyclopropane product is discussed later in this chapter.

4.2 Retrosynthesis of Enoate Substrate

At the start of the next chapter of our studies, we opted to begin with the enoate cascade substrate **39** as we envisioned that it would be easily accessible with previously established chemistry. Establishing the tetrasubstituted enoate moiety promised to be particularly challenging given the difficulty of synthesizing such highly substituted olefins especially in a stereoselective fashion.[18] Although, in theory, the *E*/*Z* ratio of the olefin was irrelevant (as the formation of the Pd-enolate would ablate any stereochemical information at that position), for the sake of simplifying data interpretation and in case the olefin isomers possessed different reactivity, we

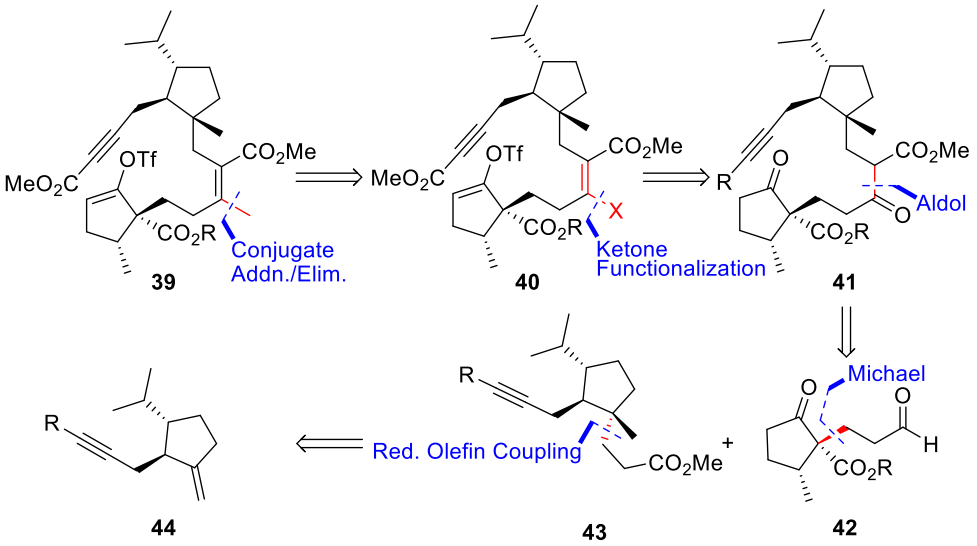

Scheme 4.6 Retrosynthesis of enoate cascade presuor.

hoped to access the *E* isomer in a stereoselective fashion. However, our previous olefination approach would be unlikely to provide satisfactory results given the low selectivity observed in the formation of a trisubstituted olefin. As such, we instead hypothesized that the methyl moiety could be introduced via a conjugate addition/elimination reaction into β-substituted enoate **40**, which in turn could be accessed from ketoester **41**. The northern and southern fragments could be coupled via an aldol reaction starting from ester **43** and aldehyde **42**. We previously synthesized

43 in in our earlier studies using a reductive olefin coupling with methyl acrylate and cyclopentene **44**. Similarly, **42** could be accessed from *R*-pulegone using adapted literature procedures.[19]

4.3 Synthesis of Enoate Cascade Precursor

Starting from cyclopentene **43**, which was accessed in an enantiopure fashion in Chapter 1 of this text, we subjected it to Baran's reductive olefin coupling. Pleasingly, the reaction proceeded smoothly and gave the ester **45** in 62% yield. The diastereoselectivity of the reaction was high, similar to that observed with vinyl sulphones. However, some very minor signals that

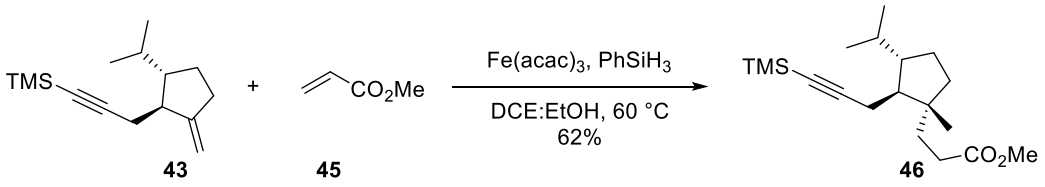

Scheme 4.7 Reductive olefin coupling with methyl acrylate: Methyl acrylate **45** (3.0 equiv.), $Fe(acac)_3$ (20 mol%), $PhSiH_3$ (1.5 equiv.), DCE (0.13 M), EtOH (1 M), 60 °C, 1 hr, 62%.

could belong to the epimer were observed in the ^1H NMR spectra, but none of them were sufficiently resolved to conclusively identify the impurity. It should be noted that the best results were achieved with freshly distilled methyl acrylate **45**, with commercial grade giving **46** in only a 42% yield.

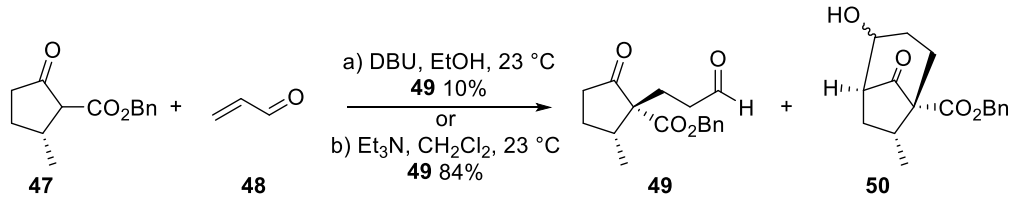

Scheme 4.8 Michael addition to access aldol precuror: a) DBU (25 mol%), acrolein (1.5 equiv.), EtOH (0.1 M), 23 °C, 15 min, 10%; b) Et_3N (1,5 equiv.) acrolein (1.5 equiv.), CH_2Cl_2 (0.1 M), 23 °C, 16 hr, 84%.

Next, using ketoester **47,** we attempted a Michael addition into acrolein **48** using DBU catalyzed conditions. Unfortunately, DBU proved too potent a base as the aldehyde **49** underwent subsequent intramolecular aldol reaction to give bridged product **50**. Switching to a weaker amine

base such as Et_3N prevented the undesired aldol reaction giving **49** in 84%, though the reaction was significantly slower.

With the aldol precursors in hand, we next turned to the coupling of **49** and **46**. Using LDA to generate the ester enolate proved ineffective giving no aldol product **51** at all. Instead, **49** underwent a retro-Michael pathway giving ketoester **47**. As the issue appeared to be the basicity of the enolate of **46**, we attempted to utilize a $CeCl_3$ additive, which had enabled our earlier Julia-Kocienski reaction.[20] $CeCl_3$ was effective in preventing the retro-Michael pathway, but the

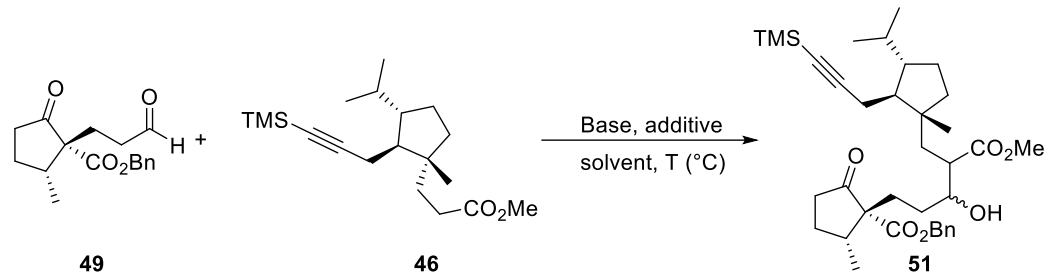

49 **46** **51**

49 equiv.	**46** equiv.	Base (equiv.)	Additive (equiv.)	Solvent	T	t (hr)	Yield
1.1	1.0	LDA (1.1)	-	THF	–78 → 23 °C	14	0%
1.0	1.5	LiHMDS (1.5)	$CeCl_3$ (2.0)	THF	–78 → 23 °C	12	11%
1.3	1.0	DIPEA (2.0)	nBu_2BOTf (1.3)	CH_2Cl_2	–78 → 0 °C	2	40%

Table 4.1 Initial attempts with intermolecular aldol reaction.

reaction suffered from poor conversion and **51** was formed in only 11% yield. We next attempted the reaction using boron enolate chemistry.[21] The initial attempt proceeded with moderate conversion giving **51** in a 40% yield as an ultimately inconsequential mix of diastereomers. Subsequent oxidation with DMP gave ketoester **52** in a 30% yield over 2 steps as a 1:1 mix of epimers as shown in Table 4.10. Suspecting the low yield was due to insufficient formation of the boron enolate, ester **46** was used in excess, but this only improved the overall yield by 5%. Conducting the enolate formation at 0 ˚C rather than –78 ˚C and extending the reaction time of the aldol increased the yield dramatically to 72%. Longer reaction times, however, proved unnecessary as a 79% yield was achieved in only 2 hours suggesting the issue hindering conversion

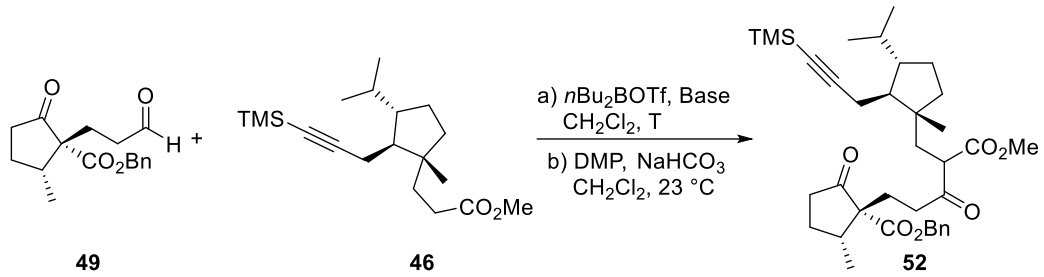

49 **46** **52**

49 equiv.	**46** equiv.	Base (equiv.)	nBu$_2$BOTf equiv.	T	t (hr)	Yield[a]
1.2	1.0	DIPEA (2.0)	1.3	–78 → 0 °C	2	30%
1.0	1.5	DIPEA (1.6)	1.5	–78 → 0 °C	2	35%
1.0	1.5	DIPEA (1.6)	1.5	–78 → 23 °C	12	72%[b]
1.0	1.5	DIPEA (1.6)	1.4	–78 → 0 °C	2	79%[b]
1.0	1.5	DIPEA (1.6)	1.4	–65 → 0 °C	2	52%[b]
1.0	1.5	Et_3N (1.9)	1.4	–65 → 0 °C	2	20%[b]
1.0	1.5	DIPEA (1.9)	1.4	–78 → 0 °C	2	69%[c]

Table 4.2 Optimization of ketoester formation. [a]Over 2 steps [b]deprotonation at 0 °C [c]Run on 2.5 mmol scale; b) DMP (2.5 equiv.), $NaHCO_3$ (5 equiv.), CH_2Cl_2 (0.1M), 23 °C, 4-12 hr.

was indeed enolate formation. Starting the aldol reaction at –65 ˚C rather than –78 ˚C or using Et_3N in place of DIPEA both proved deleterious.

With the ketoester **52** in hand, we next turned to the enoate formation. Our first approach was to convert the ketoester into a vinyl triflate and then utilize an organocuprate to introduce the

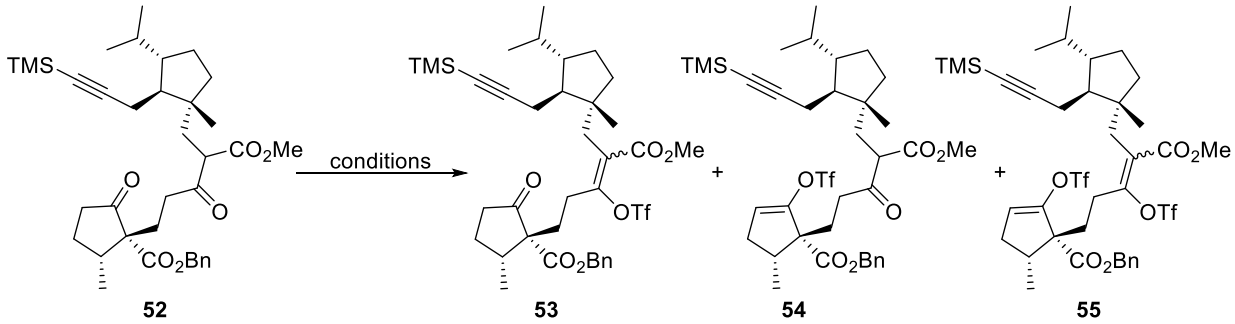

52 **53** **54** **55**

Base (equiv.)	Tf source (equiv.)	Solvent	T	Results
KHMDS (3.1)	Comins' (3.0)	THF	–78 → 23 °C	trace **54**
KHMDS (2.4)	Comins' (2.3)	THF	–78 → 23 °C	trace **54**
KHMDS (1.2)	Comins' (1.2)	THF	–78 → 23 °C	NR
KHMDS (2.5)	Tf_2O (2.5)	THF	–78 °C	complex mixture
KHMDS (1.2)	Tf_2O (1.2)	THF	–78 °C	complex mixture
LiOH (7.5)	Tf_2O (2.5)	hexanes	5 °C	NR
NaH (1.5)	Tf_2O (1.4)	CH_2Cl_2	0 → 23 °C	NR
NaH (2.5), DIPEA (7.5)	Tf_2O (2.5)	CH_2Cl_2	0 → 23 °C	NR
DIPEA (7.5), DMAP (0.2)	Tf_2O (2.5)	CH_2Cl_2	0 °C	NR

Table 4.3 Attempted ketoester triflation.

desired methyl group. Ideally, we could form bis-triflate **55** in a single step, but the reaction proved quite challenging. Using KHMDS and different triflation reagents, we were able to observe the formation of mono-triflate **54**, but functionalization of the ketoester moiety was never observed. This absence could be explained by the likely instability of the β-triflate enoate. However, the corresponding triflates from the model system ethyl acetoacetate were stable enough to isolate and purify via column chromatography. Attempts to form the mono triflate **53** by using lower equivalents of KHMDS or using weaker bases, such as DIPEA or LiOH, were similarly ineffective.

As such, we tried to see what functionality, if any, we could introduce with the ketoester. The vinyl acetate **56** was made in 90% and with a 10:1 *Z*/*E* ratio.[22] Formation of the vinyl phosphonate **57** was more challenging, but provided sufficient material to proceed.[23] The vinyl

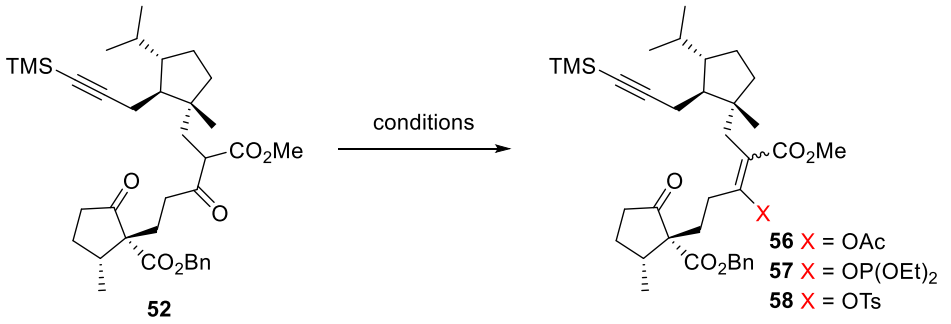

52

X	X source (equiv.)	Base (equiv.)	Additive (equiv.)	Solvent	Yield	*Z*/*E*
OAc	Ac_2O (0.25 M)	Et_3N (8.0)	DMAP (0.5)	-	90%	10:1
$OP(OEt)_2$	$PO(OEt)_2Cl$ (2.0)	NaH (2.0)	-	THF	33%	6:1
OTs	TsCl (1.5)	NaH (1.5)	TMEDA (1.5)	toluene	0%	-
OTs	Ts_2O (4.0)	Et_3N (8)	DMAP (4.0)	CH_2Cl_2	12%	1:15
OTs	TsCl (4.0)	Et_3N (8.0)	DMAP (4.0), LiCl (5.0)	CH_2Cl_2	68%	2:1
OTs	TsCl (4.0)	Et_3N (4.0)	NMI (4.0), LiCl (4.0)	CH_2Cl_2	90%	10:1

Table 4.4 Ketoester functionalization.

tosylate **58** proved far more challenging, but was ultimately accessible in 90% yield in a 10:1 *Z*/*E* ratio.[24] The superior efficacy of N-methyl imidazole (NMI) as an activator for stereoselective vinyl tosylate formation has been noted before; however, we additionally found a strong dependence on the presence of water in the reaction. While the literature reports the reaction being

run under anhydrous conditions,[24] we found that the *Z*/*E* selectivity suffered with the absence of water. For example, flame drying the LiCl at the start of the reaction led to a *Z*/*E* ratio of 1:1.

We next turned our attention to the introduction of the methyl group. Conjugate addition using stochiometric amounts of organocuprates with **56** were ineffective with no reaction occurring even upon warming the reaction. Similarly, attempts to use a $CrCl_2$ mediated sp^3-sp^2 cross coupling were ineffective,[22] although the reaction did proceed to full conversion as the MeMgBr attacked the cyclopentenone, but left the vinyl acetate intact. Despite reports of its higher reactivity relative to the acetate, vinyl phosphonate **58** proved unreactive to organocuprate addition.

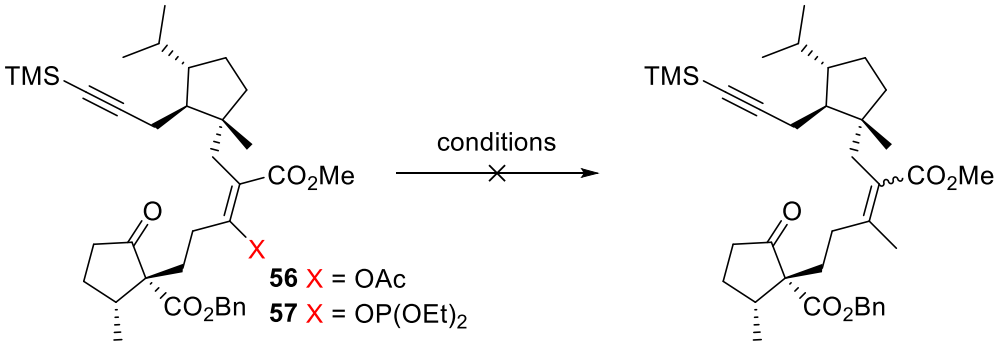

X	Me source (equiv.)	Additive (equiv.)	Solvent
OAc	MeMgBr (3.0)	CuCN (3.0)	THF
OAc	MeLi (3.0)	CuI (1.5)	THF
OAc	MeMgBr (1.5)	$CrCl_2$ (0.2)	THF
$OP(OEt)_2$	MeLi (4.0)	CuI (2.0)	THF

Table 4.5 Attempted conjugate addition.

As the conjugate addition approach proved ineffective, the next option was a Pd-mediated Negishi cross coupling.[24] The first attempt with in situ prepared MeZnCl proceeded with low conversion, but did provide the desired enoate **59** in 11% yield. Raising the reaction temperature did provide better conversion, but now gave **59** and ketone **61** in a 1:1 mixture. **61** likely arises from a Tsuji-Trost type mechanism, but it is interesting to note that no benzylated product was

observed. The limited literature on this cousin of the allylic allylation reaction seems to suggest that benzylation is only favored over protonation in cases where the resultant benzyl species is stabilized by either electron donating groups[25] or extended π-systems[26]. While, either **59** or **60**

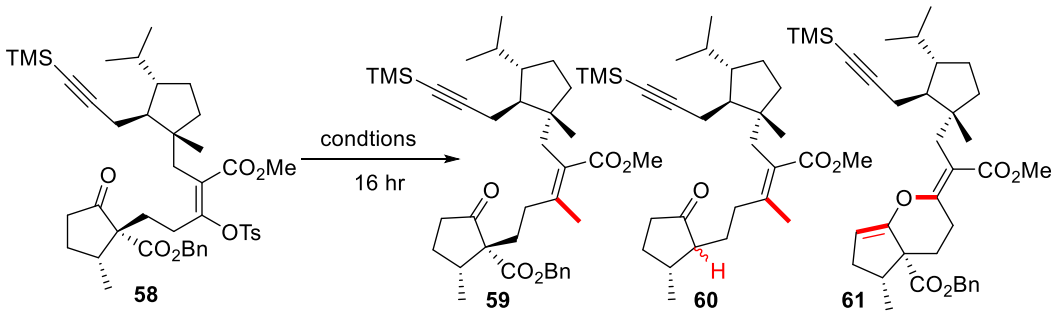

Me Source (equiv.)	Additive (equiv.)	Pd (mol%)	Ligand (mol%)	T(°C)	Solvent	**59**	**60**	**61**
MeMgBr (4)	$ZnCl_2$ (4)	$Pd(OAc)_2$ (10)	SPhos (20)	23	THF	11%	0%	0%
MeMgBr (4)	$ZnCl_2$ (4)	$Pd(OAc)_2$ (10)	SPhos (20)	60	THF	25%	25%	0%
MeMgBr (4)	$ZnCl_2$ (4)	$Pd(OAc)_2$ (10)	RuPhos (20)	60	THF	14%	14%	0%
$ZnMe_2$ (4)	-	$Pd_2(dba)_3$ (5)	SPhos (20)	60	THF	19%	0%	12%
$ZnMe_2$ (4)	-	$Pd_2(dba)_3$ (5)	SPhos (20)	80	DMF	8%	0%	30%
Me_4Sn (2)	LiCl (3)	$Pd(OAc)_2$ (10)	SPhos (20)	110	DMF	0%	50%	0%
Me_4Sn (2)	LiCl (3)	$Pd(OAc)_2$ (10)	CPhos (20)	110	DMF	0%	58%	0%

Table 4.6 Cross coupling approach to enoate synthesis.

are acceptable substrates for the route, we wanted to selectively form one or the other for the sake of material preparation. Changing the ligand to RuPhos gave **59** and **60** in a 1:1 ratio and in an overall lower yield. Using $ZnMe_2$ suppressed the formation of **60**, but now the tentatively identified vinylogous vinyl carbonate **61** was formed in a 12% yield. **61** potentially arises by deprotonation of the cyclopentanone with subsequent conjugate addition of the oxygen. Increasing the temperature led to **61** now being the major product of the reaction. As once again, basicity appears to be the issue, we turned to an alternative non-basic Me source, Me_4Sn. Pleasingly, the Stille reaction proceeded smoothly giving **60** in 50% yield with none of **59** being detected in the reaction. By using CPhos, **60** was able to be accessed in a 58% yield, 10:1 *Z*/*E* ratio, and a 10:1 ratio favoring the desired trans-cyclopentanone. From here, we were able to use the same triflation, deprotection, and carbonylation procedure used in our earlier studies. The only significant

difference was the substitution of LiHMDS for *n*BuLi, as it gave significantly cleaner reactions—though the yields were still moderate.

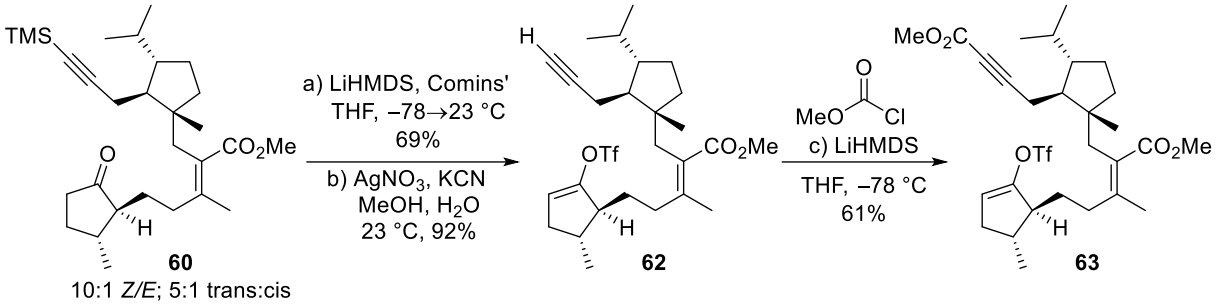

Scheme 4.9 Enoate cascade precursors. a) LiHMDS (2.0 equiv.), Comins' reagent (2.0 equiv.), THF (0.1 M), –78→ 23 °C, 12 hr, 69%; b) $AgNO_3$ (2.7 quiv.), KCN (10.0 equiv.), MeOH (22 M), H_2O (0.25 M), 23 °C, 30 min, 100%; c) LiHMDS (3.0 equiv.), methyl chloroformate (2.0 equiv.), THF (0.1 M), – 78 °C, 4 hr, 61% brsm.

With our cascade precursors in hand, we decided to utilize the TMS-alkyne **64** first in the reaction. It was not expected to successfully undergo the requisite [6-*exo*-dig] cyclization, but the previous TMS-alkyne substrate gave significantly cleaner reaction profiles compared to the ynoate

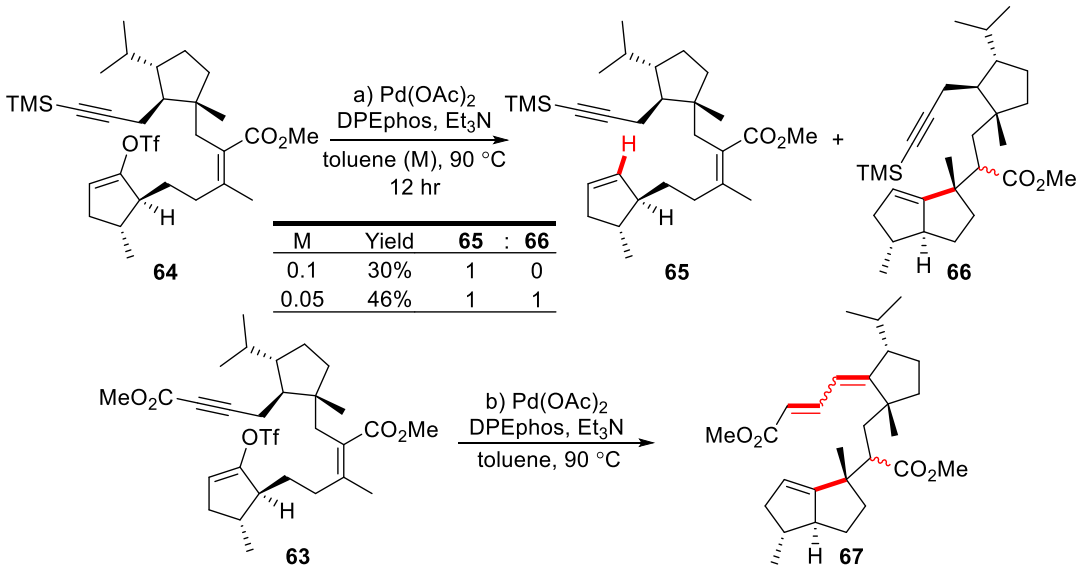

Scheme 4.10 Cascade attempts with enoate substrates:a) $Pd(OAc)_2$ (20 mol%), DPEPhos (40 mol%), Et_3N (3 equiv.), toluene, 90 ° C, 12 hr; b) $Pd(OAc)_2$ (20 mol%), DPEPhos (40 mol%), Et_3N (3 equiv.), toluene (0.05 M), 90 °C, 12 hr.

so we hoped to probe how operative the [3-*exo*-trig] or β-hydride elimination pathways were. With our previous conditions, only hydride reduction product **65** was isolated in a 30% yield. This product potentially arises due to the challenging migratory insertion in to the tetrasubstituted

enoate, which leads to the vinyl-Pd species formed following oxidative addition being long lived. The Pd can then bind a molecule of Et_3N and generate a Pd-H species through β-hydride elimination. Reductive elimination regenerates the Pd^0 and yields **65**. As this pathway requires an intermolecular step, we wondered if reducing the concentration could help to inhibit the reduction process. When running the reaction at 0.05 M, we now isolated monocyclization product **66** in a 23% yield as a 1:1 mixture, while **65** was still formed, but in a reduced yield. We were pleased to note that the formation of products from either the [3-*exo*-trig] or β-hydride elimination pathways were not observed. The cascade was attempted again with our standard base mediated Ni-Heck conditions, but even with the less hindered triflate only trace conversion was observed. With this result, we then attempted the cascade with ynoate **63**. As expected, the reaction profile was substantially more complex, and the only product we were tentatively able to identify was the monocyclized dienoate **67**, which was identified by the characteristic patterning of the α,β, and γ olefin signals in the ^1H NMR. We had previously observed this isomerization in our earlier studies, but it was at this point that we were able to determine the likely structure of the compound. As this isomerization is believed to be phosphine catalyzed and promoted by amine bases[27], our next step was to screen alternative bases that may prevent the isomerization from occurring. When using K_2CO_3, to our surprise the reaction was relatively clean but did not go to full conversion. The major product was tentatively identified as the arene **68**, which could arise via a [2+2+2] cyclotrimerization reaction.[28] The assignment was made on the basis of the absence of alkyne signals in the ^{13}C spectra and the presence of 9 signals above 100 ppm, only one of which gave any signal in the DEPT. This suggests that the alkyne has been reduced to the tetrasubstituted olefin. Further, the presence of the acetate group, presumably coming from the $Pd(OAc)_2$, was discerned from the new singlet at 2.12 ppm that integrates to 3H, the upfield shift of the only vinyl

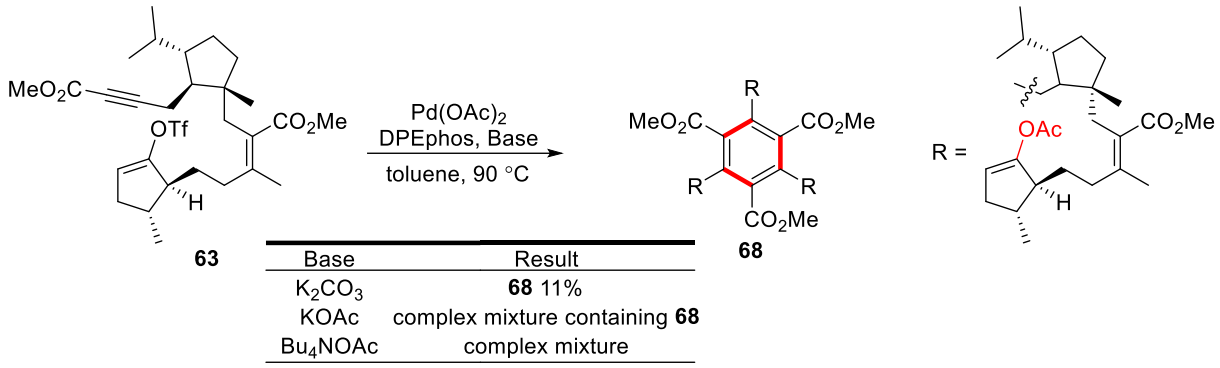

Base	Result
K_2CO_3	**68** 11%
KOAc	complex mixture containing **68**
Bu_4NOAc	complex mixture

Scheme 4.11 Screening of alternate bases to avoid ynoate isomerization: $Pd(OAc)_2$ (20 mol%), DPEPhos (40 mol%), Base (5 equiv.), toluene (0.05 M), 90 °C, 12 hr.

signal to 5.52 ppm, and the addition of a new signals in the ester and alkyl region of the ^{13}C spectra. The assignment is supported by COSY, DEPT, and HMBC experiments. The use of KOAc or Bu_4NOAc also proved ineffective with both giving complex mixtures from which no identifiable products were isolable.

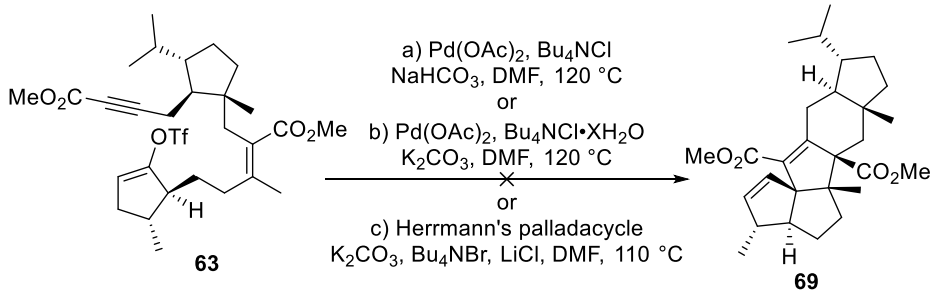

Scheme 4.12 Enoate cascade attempts with ligand free conditions: a) $Pd(OAc)_2$ (5 mol%), Bu_4NCl (1 equiv.), $NaHCO_3$ (2.5 equiv.), DMF (0.05 M), 120 °C, 12 hr; b) $Pd(OAc)_2$ (5 mol%), $Bu_4NCl•H_2O$ (1 equiv.), K_2CO_3 (4 equiv.), DMF (0.05 M), 120 °C, 12 hr; c) Herrmann's palladacycle (5 mol%), K_2CO_3 (2.5 equiv.), Bu_4NBr (0.5 equiv.), LiCl (0.5 equiv.), DMF (0.05 M), 110 °C, 12 hr.

At this point, it appeared that tetrasubstituted enoate was simply too hindered to effectively undergo the desired [5-*exo*-trig] cyclization. We wondered if decreasing the size of the Pd species by using ligand-free Jeffery conditions[29] or smaller under-ligated species such as the $PdP(oTol_3)$ that arises from Herrmann's Palladacycle.[30] Unfortunately, all of our attempts only yielded complex mixtures from which no identifiable products were isolated. As such, we turned our attention next to the enone substrate **70**.

4.4 Retrosynthesis of Enone Substrate

While the enoate substrate had proved to be too challenging for our proposed cascade, it is important to note that we never observed the formation of either [3-*exo*-trig] or β-hydride elimination products, which suggested that utilizing a less hindered and hopefully more reactive enone **70** may ameliorate our issues. In order to access **70**, we decided to form the enone moiety by means of an intermolecular Nozaki–Hiyama–Kishi (NHK) coupling of aldehyde **71** and vinyl

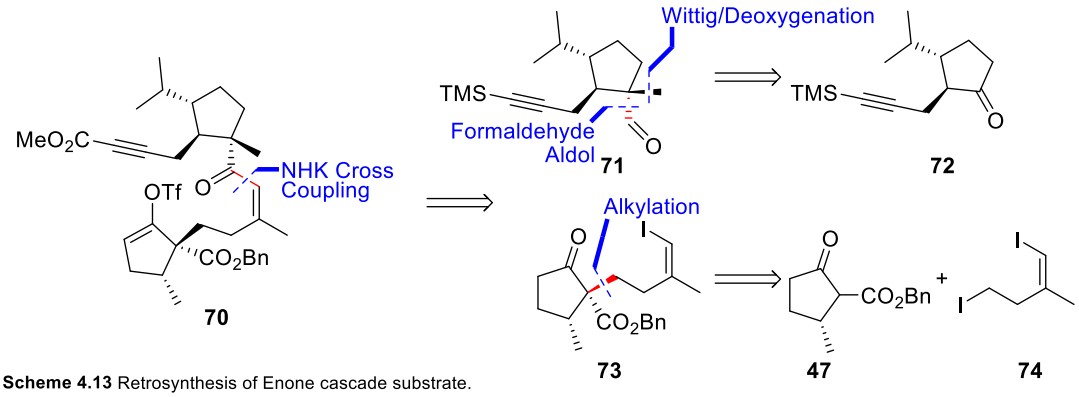

Scheme 4.13 Retrosynthesis of Enone cascade substrate.

iodide **73**. **71** could potentially be accessed from ketone **72** via a Wittig homologation to give a cyclopentaldehyde, aldol reaction with formaldehyde, and then deoxygenation via a Caglioti reaction.[31] **73** could be accessed via alkylation of *R*-pulegone derived ketoester **47** with diiodide **74**, which has been synthesized in a stereoselective fashion previously.[32]

4.5 Caglioti Approach to NHK Precursor

To begin, ketone **72** underwent a Wittig homologation to cleanly give vinyl ether, that was then hydrolyzed under acidic conditions to yield aldehyde **75** in a >20:1 ratio favoring the shown isomer. We did attempt to directly install the requisite methyl group by reacting **75** with MeI in the presence of KO*t*Bu, but, as with our previous experience, the hindrance of the pendant alkyne forces the electrophile to establish a 1,2-anti relationship leading to the formation of the undesired

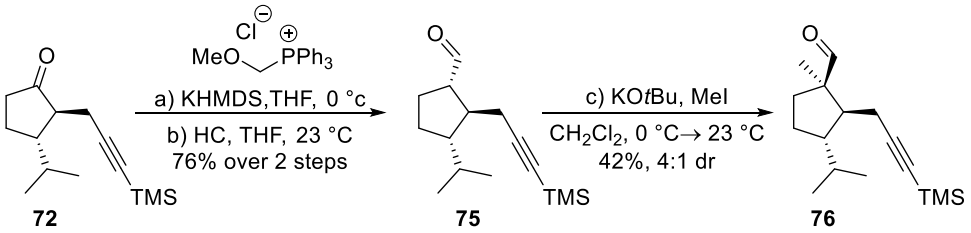

Scheme 4.14 Wittig homologation to access aldehyde: a) KHMDS(2.0 equiv.), PPh_3CH_2OMeCl (2.2 equiv.), THF (0.1 M), 0 °C, 1 hr; b) 6M HCl (600 equiv.), THF (0.04 M), 23 °C, 4 hr, 76% over 2 steps; c) KO*t*Bu (1.3 equiv.), MeI (3.0 equiv.), CH_2Cl_2 (0.2 M),.0 °C→23 °C, 10 hr, 42% 4:1 dr.

diastereomer **76** in a 42% yield and a 4:1 dr. As such, the aldehyde moiety must be installed after the methyl group in order to access the desired diastereomer **71**. Thus, our next approach was to utilize hydroxymethylation[33] of **75** followed by deoxygenation of the aldehyde to form the desired

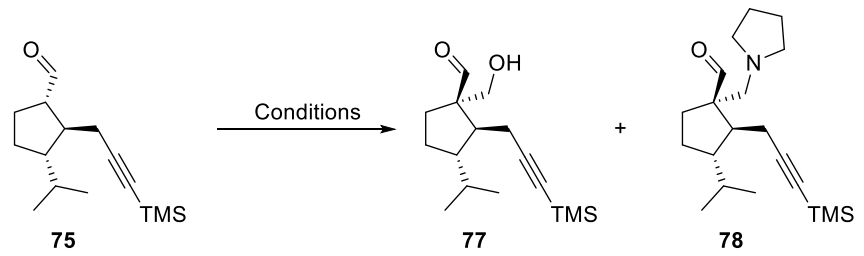

Conditions	Result
pyrrolidine, $(CH_2O)_n$, AcOH, DMSO, 23 °C	**78** 42%
DL-proline, formalin, DMSO, 23 °C	No reaction
DL-proline, formalin, DMSO, 100 °C	No reaction
79, KH_2PO_4, K_2HPO_4, toluene, 100 °C	No reaction
80, KH_2PO_4, K_2HPO_4, toluene, 100 °C	No reaction

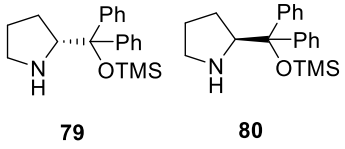

Table 4.7 Attempted amine catalyzed aldol reactions.

methyl group. We began this approach using a secondary amine promoted aldol reaction with paraformaldehyde. However, using either catalytic or stoichiometric amounts of pyrrolidine led to the exclusive formation of the Mannich product **78**. Attempts to use other pyrrolidine-based catalysts such as proline or Jørgenson-type catalysts **79** or **80** simply gave no conversion, even under forcing reactions. Switching to base-promoted aldol conditions from the Li group proved to be effective giving complete conversion to a 4:1 mixture of β-hydroxy aldehyde **77** and its formaldehyde adduct **81**.[34] Separation of **77** and **81** was challenging, but fortunately proved

unnecessary as the formation of the tosyl hydrazone **82** proceeded cleanly with the mixture giving the precursor for the reduction.

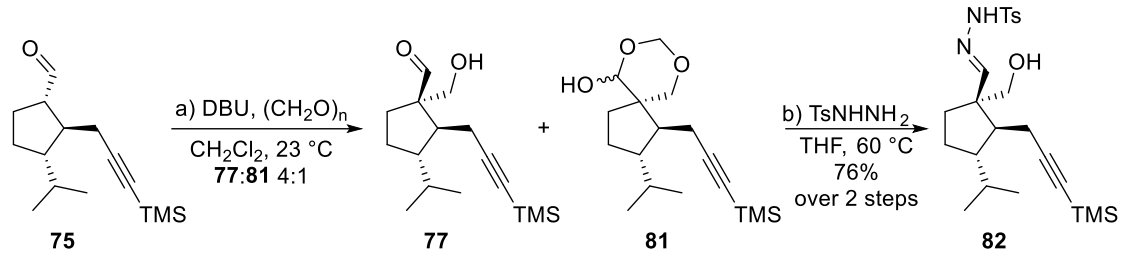

Scheme 4.15 Synthesis of precursor for the Cagligotti reaction: a) DBU (12 equiv.), $(CH_2O)_n$ (3 equiv.); CH_2Cl_2 (0.1 M), 23 °C, 3 hr, 110%, **77**:**81** 4:1; b) $TsNHNH_2$ (1.5 equiv.), THF (0.25 M), 60 °C, 4 hr, 70% over 2 steps.

The Caglioti reaction is a modification of the Wolff-Kishner reduction and is closely related to the Shapiro and Bamford-Stevens reactions, which also utilize tosyl hydrazone degradation.[31] The two main features of the Caglioti are the use of a preformed tosyl hydrazone and a hydride source such as $NaBH_4$, $LiAlH_4$, or even catechol borane. The reaction is noted for

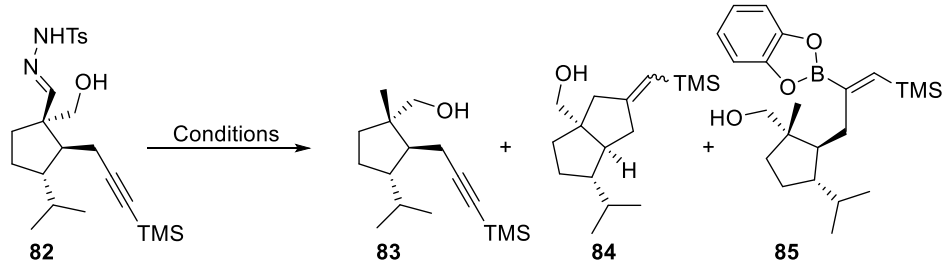

Conditions	Results
$NaBH_4$ (10 equiv.), MeOH, 65 °C	**84**
$NaBH_4$ (10 equiv.), MeOH, 23 °C	**84**
$NaBH_3CN$ (10 eq equiv.), AcOH, MeOH, 65 °C	**84**
Catechol borane (2 equiv.), Bu_4NOAc, $CHCl_3$, 23 °C	**85**
DIBAL-H (5 equiv.), DCM, 0 °C	**83**:**84** 1:3
$LiAlH_4$ (7.5 equiv.), THF, 65 °C	**83**:**84** 1:2
$LiAlH_4$ (5 equiv.), THF, 23 °C	**83**:**84** 3:1

Table 4.8 Attempted deoxygenation via the Caglioti reaction.

its mild conditions and broad functional group tolerance especially in comparison to the Wolff-Kishner and its derivatives. We began our efforts with $NaBH_4$ in refluxing MeOH, which gave clean conversion to two non-polar products. Unexpectedly, we found that the product turned out

to be bicycle **84** as a 1:1 *E*/*Z* mixture. **84** is presumably formed by hydrazone decomposition generating a primary carbanion or carbene species that can then cyclize on to the pendant alkyne. Similar cyclizations have been reported during alkyl lithium induced fragmentation of aziridinyl

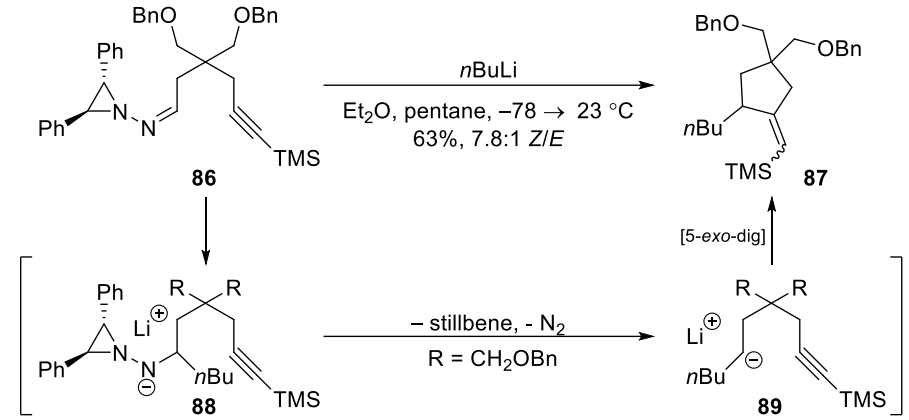

Scheme 4.16 Anionic cyclization triggered by hydrazone decomposition.

hydrazone **86**.[35] Attempts to use more mild conditions with $NaBH_4$, $NaBH_3CN$, or catechol borane proved ineffective, with only the formation of **84** or **85** being observed. Aluminum hydrides proved more promising with DIBAL-H finally giving a small amount of the desired **83**. The best result was observed with $LiAlH_4$ at ambient temperatures where **83** was favored 3:1 over **84**, but the reaction profile was complex and overall mass recovery of the reaction was quite low.

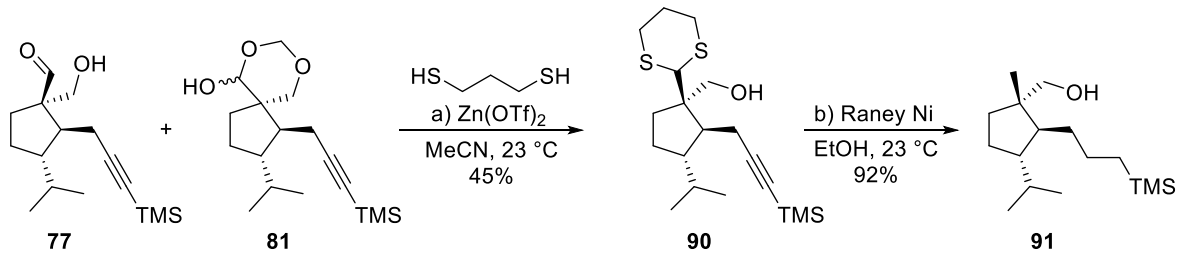

Scheme 4.17 Dithiane reduction mediated by Raney Ni: a) 1,3-propanedithiol (3 equiv.), $Zn(OTf)_2$ (20 mol%), MeCN (0.1 M), 23 °C, 4 hr, 45%; b) Raney Ni, EtOH (0.1 M), 23 °C, 92%.

As an alternative, we decided to attempt a desulfurization using Raney Ni. Based on literature precedent,[36] we hoped that we would be able to selectively reduce dithiane **90**, but despite several attempts, the reaction always proceeded with concomitant reduction of the alkyne

to give alcohol **91**. As such, it appeared that the deoxygenation approach would be untenable without significant alterations to the substrate.

4.6 HAT Approach

Our next approach to find a way to harness the HAT chemistry used in our previous routes to introduce the aldehyde moiety. In order for this approach to be successful, a suitable C_1-radical acceptor would need to be identified. Serendipitously, in an unrelated literature search we came across a report from the Hart group wherein they disclosed that *O*-benzylformaldoxime can serve as a C_1-radical acceptor to introduce methyl amine moiety.[37] This led us to a report from the Carriera group on a related reaction using sulfonyl oxime ethers with Co-mediated HAT conditions which yielded formal anti-Markovnikov hydroformylation products.[38] We attempted the reaction using the Co conditions with **43** and oxime **92**, but no reaction was observed. As Baran's Fe-mediated conditions had previously proved effective with **43**, we opted to see if they would perform more satisfactorily. Pleasingly, using 5 equivalents of **92** the desired oxime ether **93**

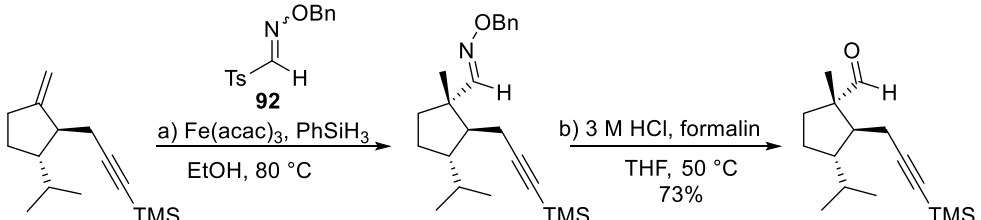

92 equiv.	**92** *E*/*Z*	Yield
5.0	13:1	44%
3.0	13:1	41%
3.0	1:66	0%
1.5	13:1	73%

Table 4.9 HAT enabled formal Markovnikov hydroformylation: $Fe(acac)_3$ (20 mol%), $PhSiH_3$ (1.5 equiv.), EtOH (0.125 M), 80 °C, 1 hr; b) 3 M HCl (20 mol%), formalin (0.25 M), THF (0.1 M), 50 °C, 48 hr, 73%.

was isolated in a 44% yield as a single diastereomer. While the reaction performed similarly with 3 equivalents of **92**, it was found that further decreasing to 1.5 equivalents improved the yield to 73%. It is important to note that only the *E* isomer of **92** was effective, as when the reaction was

attempted with the *Z* isomer no reaction was observed and unreacted **43** was isolated. We suspect that the less hindered *Z*-**92** is able to react directly with the Fe-H species preventing the desired HAT with **43** from occurring. Subsequent acidic hydrolysis of **93** in the presence of formalin yielded the desired aldehyde **71**. This example once again highlights both the power and versatility of HAT chemistry to quickly construct complex structures.

4.7 Vinyl Iodide NHK Precursor

With **71** in hand, we turned our focus to accessing vinyl iodide **73** from ketoester **47** and diiodide **74**. Both the *E* and *Z* isomers of the required diiodide are accessible essentially as single isomers using Negishi's Zr-mediated carboalumination chemistry.[32] Both procedures were very effective; however, we did find it necessary to use neat $AlMe_3$, as the reaction was incredibly sluggish when using $AlMe_3$ as a solution in hexanes.

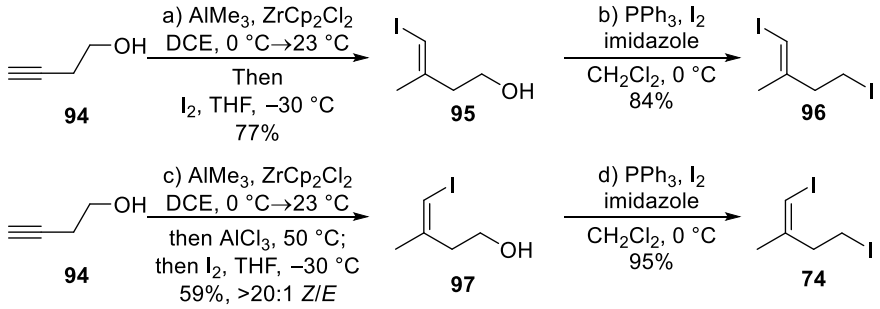

Scheme 4.18 Stereoselective synthesis of vinyl iodides: a) $ZrCp_2Cl_2$ (0.25 equiv.), $AlMe_3$ (2.5 equiv.), DCE (0.1 M), 0 °C → 23 °C, 24 hr; I_2 (2.0 equiv.), THF (0.5 M), –30 °C, 2 hr; 77%; b) PPh_3 (1,4 equiv.), I_2 (1.4 equiv.), imidazole (2.0 equiv.), CH_2Cl_2 (0.1 M), 0 °C; 4 hr, 84%; c) $ZrCp_2Cl_2$ (0.25 equiv.), $AlMe_3$ (2.5 equiv.), DCE (0.1 M), 0 °C → 23 °C, 24 hr; $AlCl_3$ (2.0 equiv.), 50 °C, 24 hr; I_2 (2.0 equiv.), THF (0.5 M), –30 °C, 2 hr; 59% >20:1 *Z*/*E*; d) PPh_3 (1,4 equiv.), I_2 (1.4 equiv.), imidazole (2.0 equiv.), CH_2Cl_2 (0.1 M), 0 °C; 4 hr, 95%.

In contrast to the ease of the preparation of **74** and **96**, ketoester **73** promised to be slightly more challenging given that the intermolecular formation of a quaternary center is often non-trivial. As expected, conditions from the Grigg group[39] and KO*t*Bu proved lackluster, with yields averaging 40%. A major side reaction was the elimination of the iodide to yield the diene **99**, which

consumes both base and **96**, stalling the reaction. We attempted to avoid this issue by preforming the enolate by stirring **47** and KO*t*Bu before the addition of **96**, but this yielded no improvement.

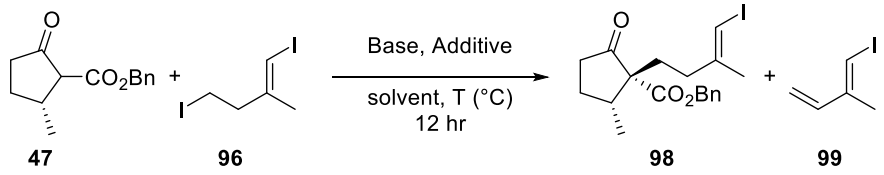

96 equiv.	Base (equiv.)	Additive (equiv.)	Solvent	T (°C)	Yields
1.4	KO*t*Bu (1.1)	-	*t*BuOH (1 M)	95	39%
2.0	Cs_2CO_3 (2.0)	HMPA (1.2)	dioxane (0.2 M)	80	18%
1.0	NaH (1.2)	-	DMF (1 M)	50	19%
1.2	K_2CO_3, (5.0)	-	DMF (0.28 M)	75	11%
1.4	KHMDS (1.1)	-	THF (1 M)	60	25%
1.4	KHMDS (1.2)	HMPA (5.0)	THF (2 M)	60	27%

Table 4.10 Alkylation approach to access NHK precursor.

Attempts to use excess ketoester or large excess of the iodide were similarly ineffective. We screened alternative conditions to see if weaker or irreversible bases would avoid this issue, but unfortunately all cases gave even lower yields of **98** and higher yields of O-alkyation and other side products, greatly complicating purification. The *Z* isomer **74** performed similarly, giving vinyl iodide **73** in a 40% yield.

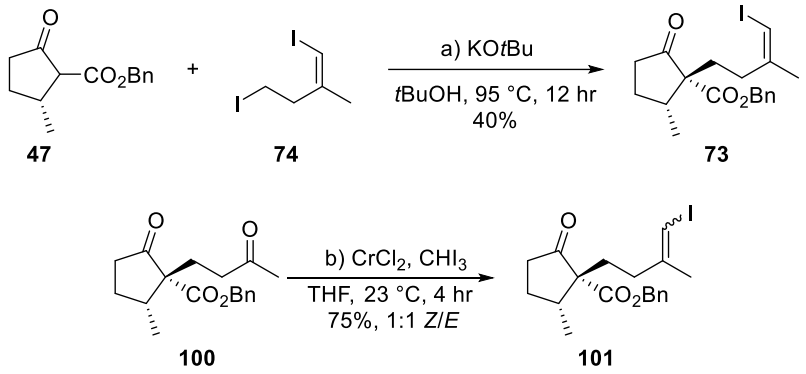

Scheme 4.19 Synthesis of *Z*-vinyl iodide NHK Precursor and Takai olefination approach: a) **74** (1.4 equiv.), KO*t*Bu (1.1 equiv.), *t*BuOH (1 M), 95 °C, 12 hr, 40%; b) $CrCl_2$ (8 equiv.), CHI_3 (2 equiv.), THF (0.1 M), 23 °C, 4 hr, 75% 1:1 *Z*/*E*.

An alternative approach to the vinyl iodide moiety is the Takai olefination of diketone **100**, which was accessed in Chapter 1 of this text.[40,41] This reaction was quick, clean, and relatively

high yielding giving the vinyl iodide **101** as a 1:1 *Z*/*E* mixture. While the reaction was much cleaner than the alkylation, the olefination requires 8 equivalents of $CrCl_2$, which limits the scalability of the reaction. A procedure that is catalytic in Cr was attempted, but only a 25% yield was observed.[42] Further, formation of the corresponding vinyl bromide with a $TiCl_4/CHBr_3$ system proved completely ineffective.[43]

4.8 NHK Cross Coupling

Now that the two pieces were in hand, we began our study of the NHK cross coupling.[44,45] As our aldehyde is neopentylic, it was suspected that the coupling would be quite challenging, and so for our initial screening the less sterically demanding **98** was used. DMSO proved to be the optimal solvent for the reaction giving the desired **102** in a 55% yield. Only recovered starting material or deiodination product **104** was observed in THF or DMF. DMP oxidation then cleanly yielded

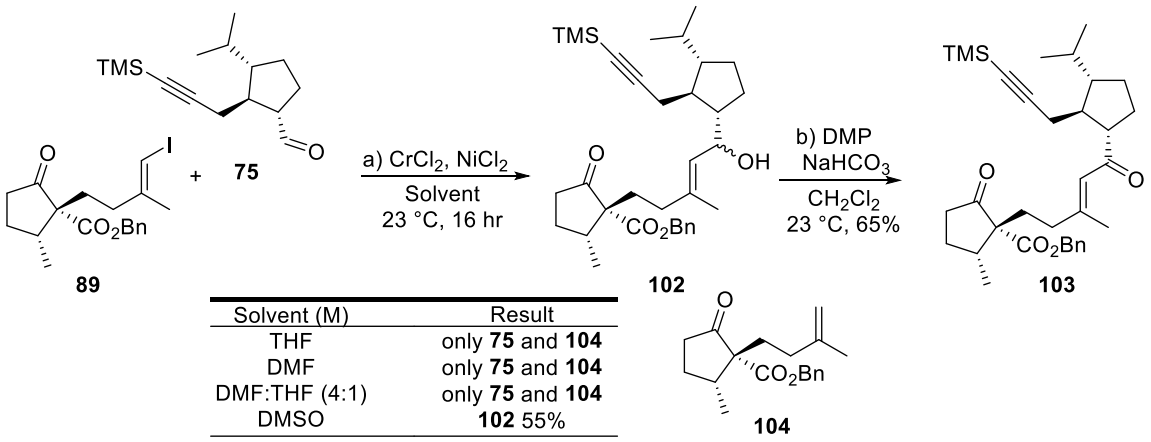

Solvent (M)	Result
THF	only **75** and **104**
DMF	only **75** and **104**
DMF:THF (4:1)	only **75** and **104**
DMSO	**102** 55%

Table 4.11 Initial NHK screening and enone formation: a) **89** (1.5 equiv.), $CrCl_2$ (8 equiv.), $NiCl_2$ (0.1 equiv.), Solvent (0.067 M), 23 °C, 16 hr; b) DMP (1.5 equiv.), $NaHCO_3$ (4 equiv.), CH_2Cl_2, 23 °C, 65%.

enone **103**. With this result in hand, we subjected aldehyde **71** to NHK conditions. As expected, the reaction proved challenging with allylic alcohol **105** being formed in only a 28% yield, but with considerable amounts of **104** observed. Heating the reaction may help the reaction overcome the issue posed by the hindrance, but this experiment has not been run as yet. Oxidation with DMP

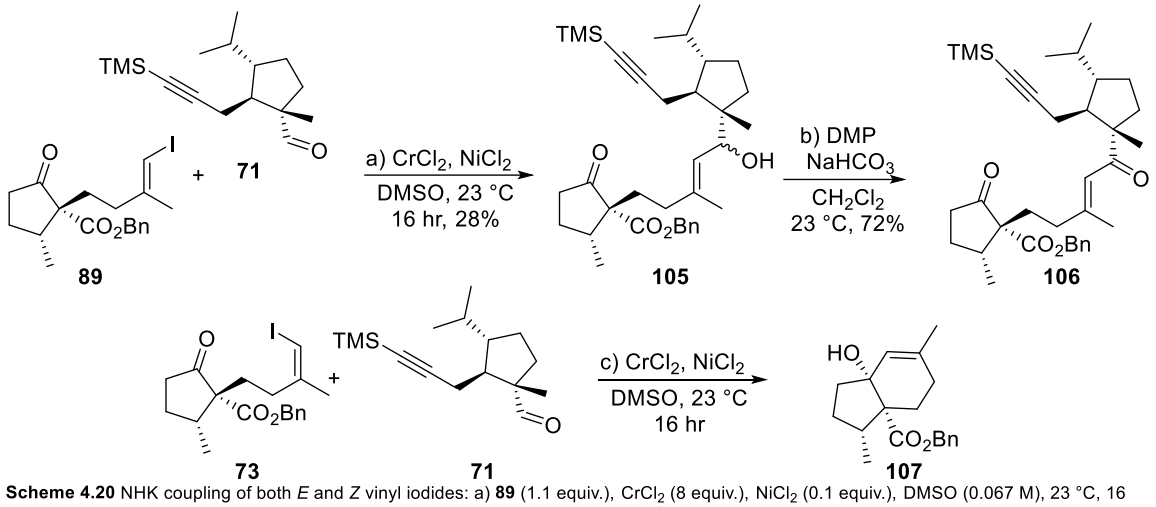

Scheme 4.20 NHK coupling of both *E* and *Z* vinyl iodides: a) **89** (1.1 equiv.), $CrCl_2$ (8 equiv.), $NiCl_2$ (0.1 equiv.), DMSO (0.067 M), 23 °C, 16 hr, 49%; b) DMP (4 equiv.), $NaHCO_3$ (4 equiv.), CH_2Cl_2 (0.1 M), 23 °C, 72%; c) **73** (1.1 equiv.), $CrCl_2$ (8 equiv.), $NiCl_2$ (0.1 equiv.), DMSO (0.067 M), 23 °C, 16 hr.

gave enone **106** in a 72% yield. We next attempted the reaction with the desired *Z* isomer, but, to our surprise, the main product of the reaction was bicycle **107** arising from an intramolecular attack of either a vinyl-Ni or Cr species onto the ketone.[46] As the NHK reaction is run at low concentration to avoid dimerization reactions, this intramolecular pathway seemed quite challenging to overcome. Since the NHK reaction is generally quite tolerant of functionality, we hoped that by reducing the ketone and removing the electrophilic site, the reaction could proceed. The vinyl iodide **101** from the Takai olefination was reduced with $NaBH_4$ in a 71% yield as a mixture of diastereomers. The following NHK coupling yielded product, but it appeared to only arise from one olefin isomer. Indeed, upon DMP oxidation, **106** identical to that observed with

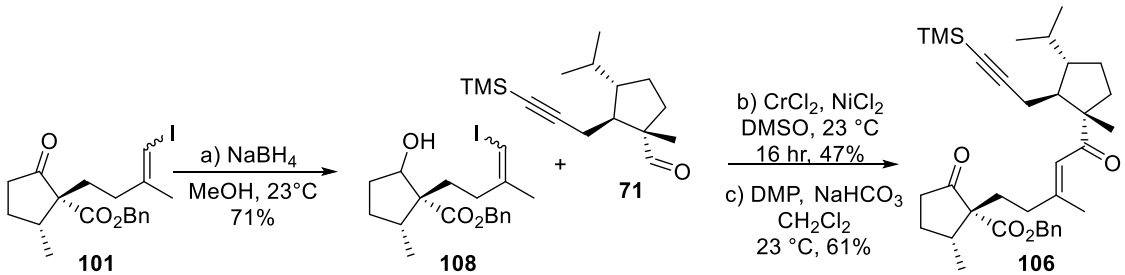

Scheme 4.21 NHK coupling of reduced vinyl iodide:a) $NaBH_4$ (1.2 equiv.), MeOH (0.1 M), 23 °C, 71%; b) **108** (1.5 equiv.), $CrCl_2$ (8 equiv.), $NiCl_2$ (0.1 equiv.), DMSO (0.067 M), 23 °C, 16 hr, 47%; c) DMP (5.0 equiv.), $NaHCO_3$ (10 equiv.), CH_2Cl_2 (0.1 M), 23 °C, 14 hr, 61%.

the coupling of **89** and **71**. As such, it is possible that the alcohol moiety quenched the *Z*-vinyl-Ni or Cr species or simply that the *Z* isomer is too hindered to effectively participate in the coupling. Next steps that have yet to be conducted are silyl protection of **108** and running the reaction at elevated temperatures.

4.9 Enone Cascade Attempt

While we were unable to access the *Z* isomer of the enone, we pushed forward to the cascade, as ultimately the stereochemical information at that position should be ablated following Pd-enolate formation. Therefore, we used our standard conditions to access triflate **109** and we then subject the silyl alkyne to Heck cascade conditions. The reaction profile was quite clean

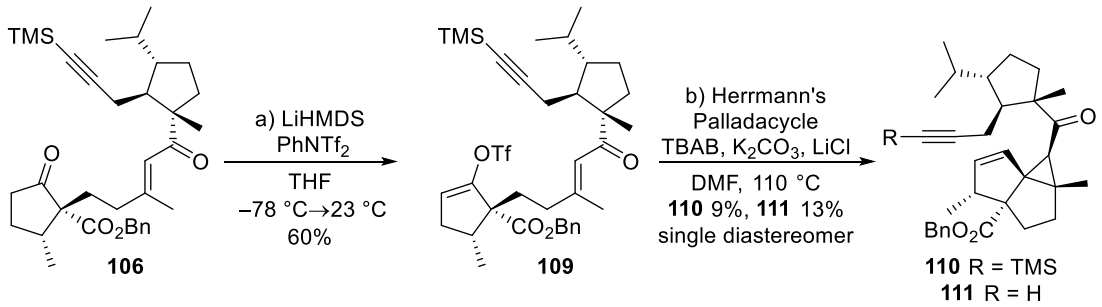

Scheme 4.22 Synthesis of enone precursor and Heck cascade: a) LiHMDS (1.1 equiv.), $PhNTf_2$ (1.5 equiv.), THF (0.1 M), –78 °C→23 °C, 12 hr, 60%; b) Herrmann's Palladacycle (5 mol%), K_2CO_3 (2.5 equiv.), TBAB (0.5 equiv.), LiCl (0.5 equiv.), DMF (0.05 M), 110 °C, **110** 9%, **111** 13%.

proceeding with full conversion of **109**, but mass recovery was low. To our surprise, the sole products of the reaction were the vinyl cyclopropane **110** and its desilylated form **111** in a combined 22% yield. Even more surprising was the fact that both compounds were formed as single diastereomers, which would suggest that [3-*exo*-trig] cyclization occurs faster than Pd-enolate formation can occur. If the cyclization had occurred through a Pd-enolate, then at least some formation of the epimer would be expected. However, the reaction is quite low yielding, so we cannot be entirely certain that the cyclization of the Pd-enolate is not simply highly

diastereoselective. If our supposition is correct, it would indicate that the Pd-enolate approach is unlikely to succeed in this application and our strategy will have to adapt.

4.10 Using the Vinyl Cyclopropane or: How I Learned to Stop Worrying and Love the [3-exo-trig] Pathway

The apparent unavoidability of the [3-*exo*-trig] pathway led us to wonder how such a product could be used to our advantage. Vinyl cyclopropanes are well known to be highly reactive species that can readily undergo C-C bond cleavage under a variety of conditions due to the high strain energy inherent to the 3-membered ring. [47–49] As a result of their reactivity, vinyl cyclopropanes have found extensive use in the synthesis of natural products. In fact, the Hudlicky synthesis of **1** relies on a rearrangement of a vinyl cyclopropane to form the angular triquinane and

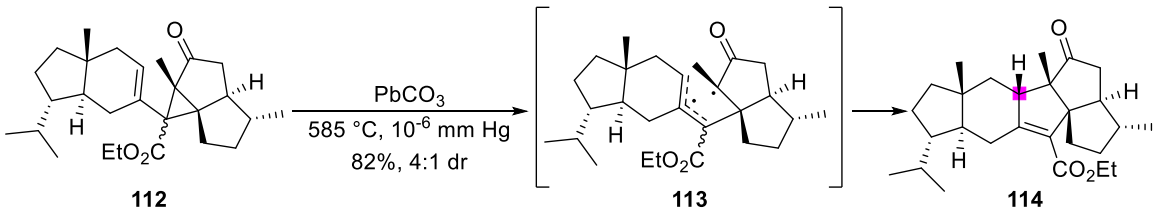

112 **113** **114**

Scheme 4.23 Vinylcyclopropane rearrangement from Hudlicky's synthesis of **1**.

complete the overall carbon framework of the target.[50] Our structure however, would have to proceed via a formal [3+2] cycloaddition to yield the desired product. One way to initiate such a reaction would be to utilize a radical initiated radical cascade.[51–53] A closely related example from the Feldman group is shown in Scheme 4.35.[52] Initially, the thiyl radical adds into the olefin and the radical adjacent to the cyclopropane undergoes retro-[3-*exo*-trig] cyclization to yield radical **119**. Subsequent [5-*exo*-trig] cyclization affords the tertiary radical **120** that can then proceed via a SN2' type pathway to yield the linear triquinane **116** and its diastereomer **117**. The

bridged compound **118** was also observed and arises from the α-ester radical **121** undergoing a [6-*endo*-trig] cyclization.

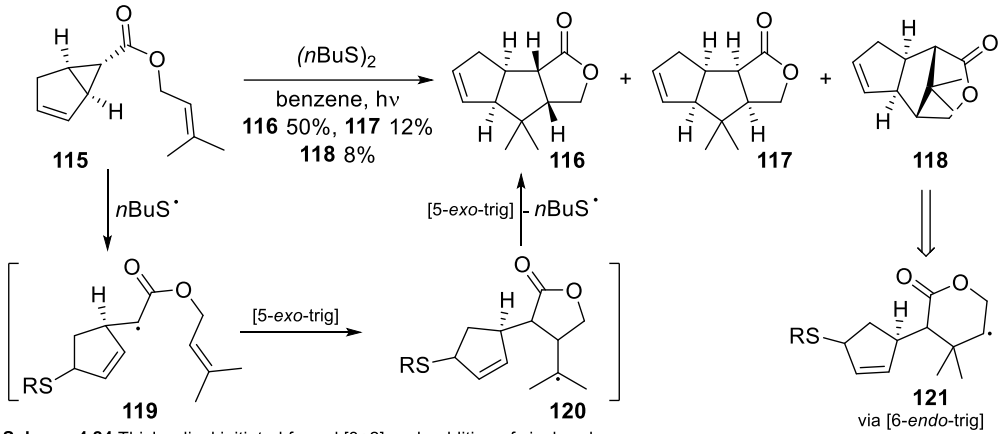

Scheme 4.24 Thiyl radical initiated formal [3+2] cycloaddition of vinyl cyclopropane.

Another approach would be Rh^{I} mediated C-C activation.[47,48,54] While there are numerous examples of related transformations,[48,49] our case would be a particularly challenging one simply due to the steric demands of such a highly substituted ring system. However, one promising

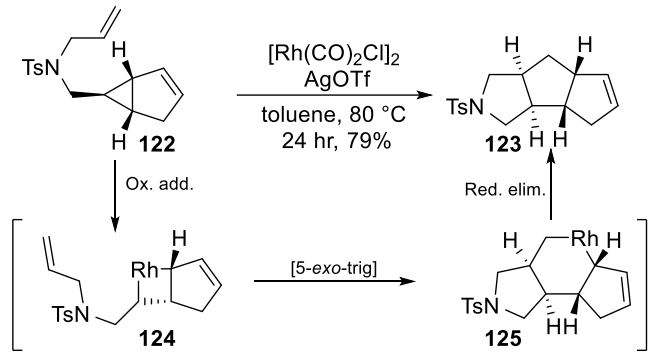

Scheme 4.25 Rh catalyzed [3+2] cycloaddition of vinyl cyclopropane.

example from the Yu group is shown in Scheme 4.36.[55] Here, a cationic Rh species inserts into the cyclopropane to give rhodacycle **124**, which then undergoes a [5-*exo*- trig] cyclization. The resultant rhodacycle **125** can complete the reaction by reductive elimination to form the final C-C bond giving the linear triquinane product **123**.

4.11 Synthesis of Model Vinylcyclopropane Substrate

As preparation of sufficient quantities of the requisite vinyl cyclopropane **126** to probe these approaches would be challenging in the time remaining, we opted to instead utilize the model

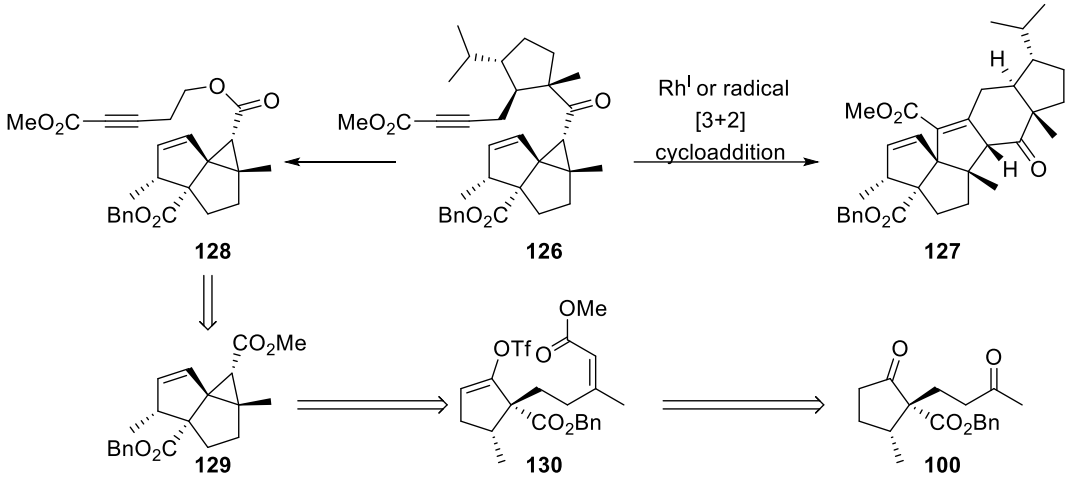

Scheme 4.26 Proposed usage of the vinyl cyclopropane and retrosynthesis of simplified model system.

system **128**, which could be accessed through hydrolysis and esterification of tricycle **129**. In turn, **129** could be accessed via a Heck cascade from triflate **130**, which should be accessible through olefination and triflation of previously synthesized diketone **100**.

To begin, we attempted the olefination of **100** using either Wittig or Horner-Wadsworth-Emmons conditions. Unlike with our earlier Julia-Kocienski where little to no reactive was observed, these reactions were quite promiscuous—generating a wide variety of unidentified side products to the point that it was unclear if any desired product **131** had been formed at all.

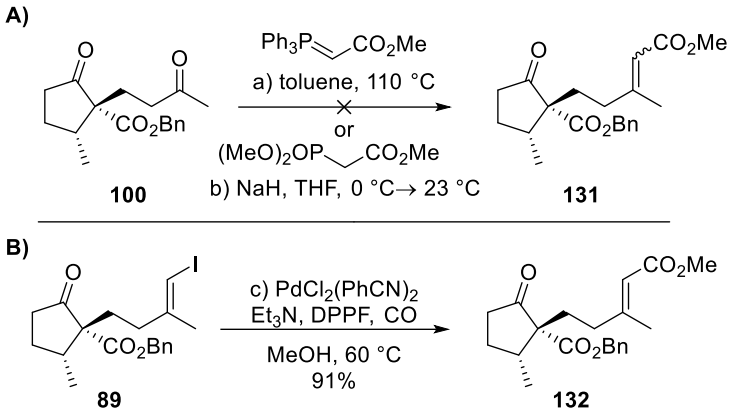

Scheme 4.27 Synthesis of enoate via **A)** olefination or **B)** carbonylation: a)Ph_3PCHCO_2Me (1.2 equiv.), toluene (0.5 M), 110 °C; b) trimethylphosphonoacetate (1.1 equiv.), NaH (1.2 equiv.), THF (0.4 M), 0 °C→ 23 °C; c) $PdCl_2(PhCN)_2$ (10 mol%), DPPF (30 mol%), Et_3N (2 equiv.), MeOH (0.1 M), 60 °C, 1 hr, 91%; d) $PdCl_2(PhCN)_2$ (10 mol%), DPPF (30 mol%), Et_3N (2 equiv.), MeOH (0.1 M), 60 °C, 1 hr, 83%.

Therefore, we took a different tack and decided to attempt the carbonylation of **100**. Pleasingly, using conditions from the Trost group,[56] the carbonylation proceeded smooth giving enoate **132** as a single isomer in a 91% yield. The following triflation step required some brief

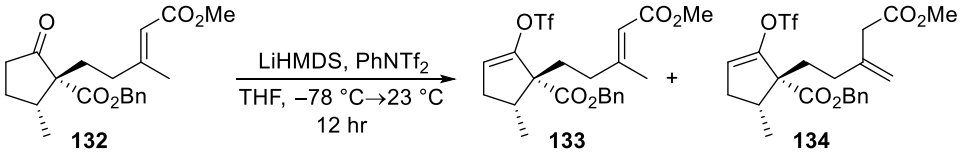

LiHMDS equiv.	$PhNTf_2$ equiv.	**133** Yield	*E*/*Z*	**134** Yield
2	2.0	31%	1:1	63%
1.1	1.1	60%	1:1	9%
1.0	1.0	45%	>20:1	0%
1.0	1.5	84%	>20:1	0%

Table 4.12 Vinyl triflate formation: LiHMDS, $PhNTf_2$ reagent, THF (0.1 M), –78 °C → 23 °C, 12 hr.

optimization as previously unobserved reactivity complicated the reaction. With the initial conditions, triflate **133** was isolated as the minor product in a 1:1 *Z*/*E* ratio. Further, the major product was found to be the 1,1-disbustitued olefin **134**. We suspected that the enoate was undergoing γ-deprotonation, and the subsequent allyl anion was causing isomerization of the olefin. Protonation of the allylic anion at the α-position of the ester then led to the formation of **134**. With some minor screening, we found that using exactly one equivalent of LiHMDS and an excess of $PhNTf_2$ allowed for the clean formation of **133** as a single isomer. Pleasingly, the Heck

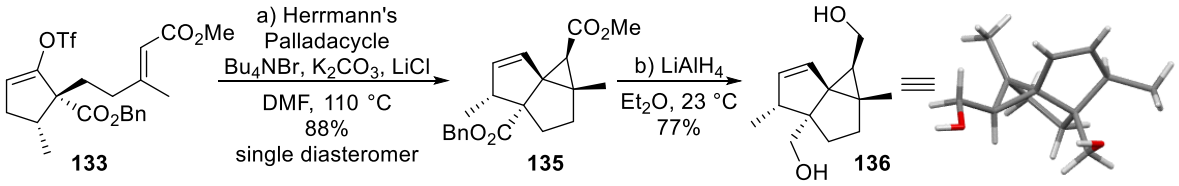

Scheme 4.28 Heck cascade of model system and structure confirmation: a) Herrmann's Palladacycle (5 mol%), K_2CO_3 (2.5 equiv.), Bu_4NBr (0.5 equiv.), LiCl (0.5 equiv.), DMF (0.1 M), 100 °C, 12 hr, 88%; b) $LiAlH_4$ (5.5 equiv.), Et_2O (0.05 M), 0 °C → 23 °C, 6 hr, 77%.

cascade proceeded very cleanly giving the product **135** in an 88% yield and as a single diastereomer. In order to confirm the structure, **135** was subjected to $LiAlH_4$ reduction to yield diol **136**, which we initially intended to further derivatize. However, **136** proved to be highly crystalline and a suitable crystal for X-ray analysis was readily available. As shown in Scheme 4.28, the reaction appears to have proceeded stereospecifically, with the hydroxy methyl and methyl groups on the cyclopropane retaining the cis configuration from the enoate. This provides further evidence that the [3-*exo*-trig] pathway is indeed outcompeting the Pd-enolate formation.

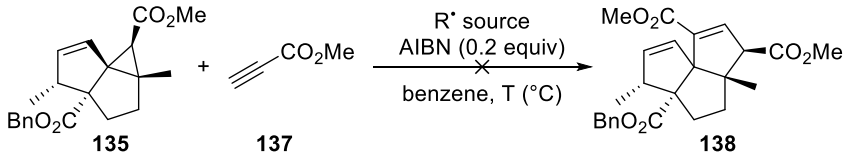

R• source	R• equiv.	[M]	T (°C)
$(n\text{BuS})_2$	0.2	0.05 M	70
$(n\text{BuS})_2$	0.2	0.1 M	100
Ph_2S_2	0.2	0.1 M	100
$(n\text{Bu}_3\text{Sn})_2$	0.2	0.1 M	80

Table 4.13 Attempted radical induced [3+2] cycloaddition with methyl propiolate: **137** (10 equiv.), R• (20 mol%), AIBN (20 mol%), benzene, 12 hr.

With **135** in hand, we decided to attempt the an intermolecular radical induced [3+2] cycloaddition.[51–53] Unfortunately, despite several attempts with different R• sources, the only reaction observed was oligomerization of methyl propiolate **137**. Even attempting the reaction with a more potent radical acceptor such as methyl acrylate **45** only led to recovered starting material, without any epimerization of the methyl ester. This apparent lack of reactivity could arise from the inability of the thiyl or stannyl radical to add into this vinyl cyclopropane, but this

seemed unlikely given the success of even more hindered systems.[53] Another, possible explanation is that the addition of the radical to the cyclopropane does in fact occur, but that the reverse reaction of radical mediated cyclopropane formation and subsequent loss of R• occurs at a faster rate than the intermolecular trapping with **137** or **45**. The lack of epimerization at the ester position would seem to count against this possibility, until one remembers that the Heck cascade proceeds with a similar retention of configuration. Further, for the epimerization in the radical case to occur, the ester must undergo a C-C bond rotation before ring closing again. Based on molecular models, we suspect that the bicyclic framework of the ring opened radical species, which forces the radical to remain in close proximity to newly formed olefin, promotes the cyclopropanation reaction to the exclusion of other pathways. This gets at the larger issue of both the radical and Heck cascade approaches in that both the desired cascade and the [3-*exo*-trig] pathway form a C-C bond at the same carbon and proceed through essentially identical termination pathways. Such a cascade can only succeed if the desired pathway can occur faster than the [3-*exo*-trig] cyclization, which is not the case for our cascade. In order to avoid the same issues that have plagued this cascade from the start, we decided to turn our attention toward the Rh^{I} mediated [3+2].

4.12 Rh [3+2] Cycloaddition Attempts

Given the challenges of the Heck and the radical cascades, the Rh^{I} strategy was particularly appealing, in that it side steps the issue described in the previous section. The reason is easy to see when comparing the intermediates of the Heck, radical, and Rh approaches. Whereas intermediates

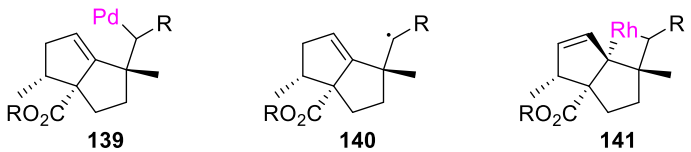

Figure 4.1 Comparision of the intermediates of the Heck, radical and Rh, approaches.

139 and **140** have competing pathways that proceed via the same elementary step, the rhodacylce **141** can either undergo the required migratory insertion or reductive elimination to reform the cyclopropane ring, which simply returns starting material that can reenter the catalytic cycle. Now, this is not to say that other pathways are not possible, simply that this approach allows us to effectively avoid the issues of previous strategies.

To begin our studies, we first attempted an intermolecular [3+2] with methyl butynoate **142**.[54,57] Using Wilkinson's catalyst and AgOTf, which acts as a halide scavenger to form the more reactive cationic Rh complex, we observed no reaction at all. We suspected that this was due to the challenging sterics of the required C-C bond activation. As such, we opted for the phosphine ligand free and hopefully less bulky $[Rh(CO)_2Cl]_2$ as the precatalyst. In contrast to the radical [3+2] conditions, **135** was indeed fully consumed under the Rh conditions, however, the mixture of unidentified products had failed to incorporate the ynoate **142** into the structure as evidenced by the presences of only one methyl ester signal in the ^1H NMR.

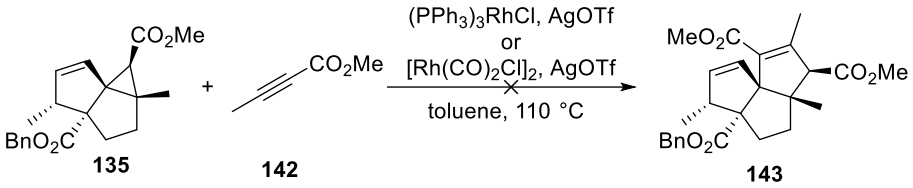

Scheme 4.29 Attempted intermolecular Rh catalyzed [3+2]: methyl butynoate **142** (2 equiv.), Wilkinson's catalyst (10 mol%) or $[Rh(CO)_2Cl]_2$ (5 mol%), AgOTf (10 mol%), toluene (0.1 M), 110 °C.

As the intermolecular migratory insertion appeared to be challenging, we hoped that by linking the ynoate, the migratory insertion could be effectively promoted. In order to access requisite substrate, **135** was subjected to basic hydrolysis, selectively hydrolyzing the methyl ester to give carboxylic acid **144** in quantitative yield. Using EDC coupling, the alkyne **145** was accessed from **146** and butynol **94**. Finally, the free alkyne was carbonylated using our standard conditions to give ynoate **146** in a 63% yield.

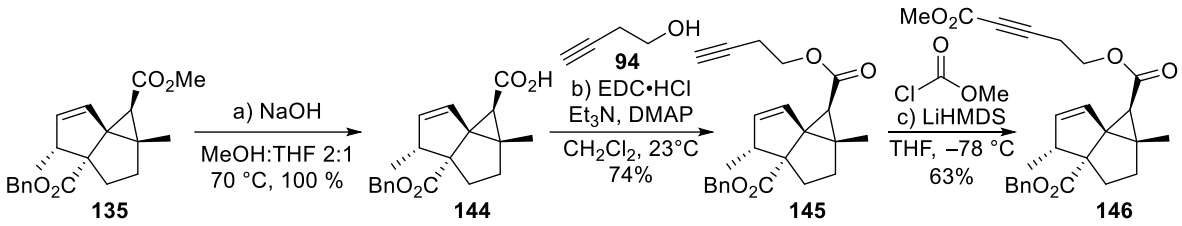

Scheme 4.30 Synthesis of intramolecular [3+2] model system: a) NaOH (8 equiv., 2 M), MeOH:THF (0.02 M, 2:1), 70 °C, 16 hr, 100%; b) 3-butynol **94** (1.5 equiv.), EDC•HCl (1.5 equiv.), Et_3N (2.0 equiv.), DMAP (1.0 equiv.), CH_2Cl_2 (0.1 M), 23 °C, 4 hr, 74%; c) LiHMDS (1.2 equiv.), methyl chloroformate (1.3 equiv.), THF (0.4 M), –78 °C, 10 hr, 63%.

With our intramolecular substrate in hand, we first attempted the reaction with the free alkyne **145**. Similar to the intermolecular case, we observed no reaction when Wilkinson's catalyst was used. However, even in the presence of $[Rh(CO)_2Cl]_2$ only a small amount of conversion was observed. Running the reaction in DME gave a similar result and only in dioxane was full conversion observed, albeit to a complex mixture. One component of the mixture was suspected to be the diene **149**, which would arise as a result of C-C activation of the other, more hindered

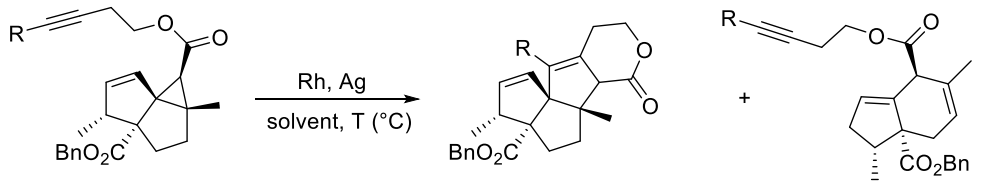

R	Rh (mol%)	Ag (Mol%)	Solvent [M]	T (°C)	t (hr)	Result
H	$(PPh_3)_3RhCl$ (10)	AgOTf (10)	toluene (0.05 M)	110	20	No reaction
H	$[Rh(CO)_2Cl]_2$ (5)	AgOTf (10)	toluene (0.05 M)	100	20	No reaction
H	$[Rh(CO)_2Cl]_2$ (5)	AgOTf (10)	DME (0.05 M)	100	20	No reaction
H	$[Rh(CO)_2Cl]_2$ (5)	AgOTf (10)	dioxane (0.05 M)	100	10	Complex, **149** observed
CO_2Me	$[Rh(CO)_2Cl]_2$ (5)	AgOTf (10)	dioxane (0.05 M)	100	10	Complex, **150** observed
CO_2Me	$[Rh(CO)_2Cl]_2$ (5)	$AgSbF_6$ (10)	dioxane (0.05 M)	100	20	No reaction
CO_2Me	$[Rh(CO)_2Cl]_2$ (5)	AgOTf (10)	dioxane (0.05 M)	110	4	Complex, **150** observed
CO_2Me	$[Rh(CO)_2Cl]_2$ (5)	$AgSbF_6$ (10)	DCE (0.05 M)	75	20	No Reaction

Table 4.14 Screening of conditions for Rh [3+2] for cis VCP.

bond of the cyclopropane that is still activated by the vinyl group. With at least some tentative evidence of C-C bond activation, we turned to the ynoate. Subjection of ynoate **146** to the reaction conditions in dioxane gave a similar result with a complex mixture containing suspected diene **150**. Raising the reaction temperature to 110 ˚C significantly shortened the reaction time, but the

overall outcome was the same. Finally, using $AgSbF_6$ as an activator was ineffective as previous attempts had shown.

As we tried to understand how to best move forward with the reaction, we wondered if the issue was arising from the use of the *cis*-vinyl cyclopropane **146**, where the *cis* refers to the vinyl group and the π-system that takes place in the cycloaddition. It has been reported by the Yu

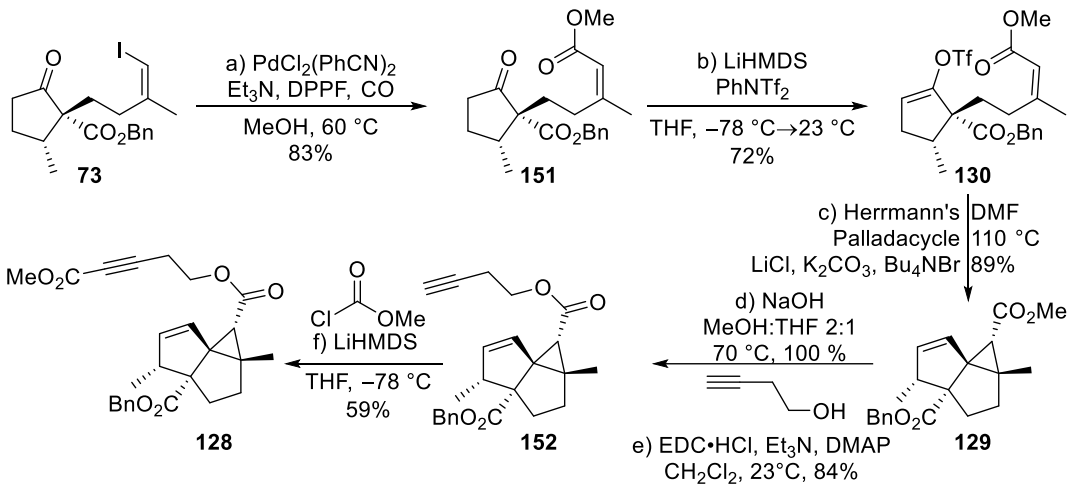

Scheme 4.31 Synthesis of trans VCP for Rh [3+2] cycloaddition: a) $PdCl_2(PhCN)_2$ (10 mol%), DPPF (30 mol%), Et_3N (3 equiv.), CO, MeOH (0.05 M), 60 °C, 1 hr, 83%; b) LiHMDS (1.0 equiv.), $PhNTf_2$ (1.5 equiv.), THF (0.1 M), –78 °C→ 23 °C, 12 hr, 72%; c) Herrmann's palladacycle (5 mol%), K_2CO_3 (2.5 equiv.), LiCl (0.5 equiv.), Bu_4NBr (0.5 equiv.), DMF (0.1 M), 110 °C, 12 hr, 89%; d) NaOH (8 equiv., 2 M), MeOH:THF (0.02 M, 2:1), 70 °C, 16 hr, 100%; e) 3-butynol (1.5 equiv.), EDC•HCl (1.5 equiv.), Et_3N (2.0 equiv.), DMAP (1.0 equiv.), CH_2Cl_2 (0.1 M), 23 °C, 4 hr, 84%; c) LiHMDS (1.2 equiv.), methyl chloroformate (1.3 equiv.), THF (0.4 M), –78 °C, 5 hr, 59%.

group that *cis*-vinyl cyclopropanes prefer to react in a [5+2] manner, which our bicyclic framework precludes from occurring, while the *trans*-vinyl cyclopropanes react solely through a [3+2] pathway.[55] In the hopes this would explain the reticence of the reaction, we synthesized the corresponding *trans*-vinyl cyclopropane starting from **73**. An identical sequence to that used with **73** yielded the ynoate **128**. One item of interest from this route is the fact that the Heck cascade exclusively gave the epimer of **129**, giving further credence to our proposal that the reaction is proceeding through an alkyl-Pd species rather than the enolate.

With the *trans*-vinyl cyclopropane in hand, **128** was subjected to the previous reaction conditions at 110 ˚C and unfortunately yielded similarly complex mixtures to that observed with **146**. We attempted running the reaction at a lower dilution to see if there were any intermolecular pathways that could be further suppressed. Pleasingly, running the reaction at 0.025 M gave an

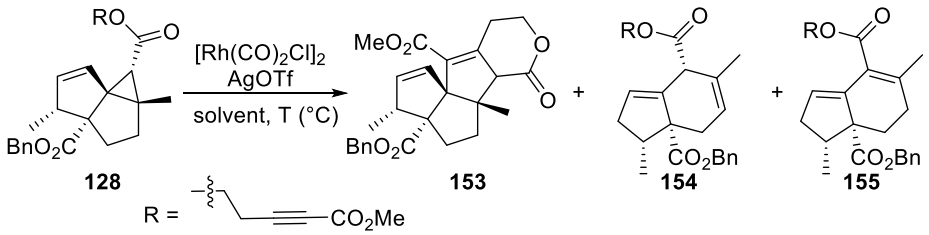

Solvent [M]	T (°C)	t (hr)	Result
dioxane (0.05 M)	110	12	**154** & **155** observed
dioxane (0.025 M)	110	12	**154** 12%, **155** 8%
dioxane (0.01 M)	110	24	Low conversion
dioxane:DME (9:1, 0.025 M)	110	12	**154** & **155** observed
dioxane (0.025 M)	150	2	complex

Table 4.15 Screening of conditions for Rh [3+2] for trans VCP: $[Rh(CO)_2Cl]_2$ (10 mol%), AgOTf (24 mol%), solvent, T (°C).

overall cleaner reaction from which clean samples of dienes **154** and **155** could finally be isolated allowing us to more conclusively proved that C-C activation is occurring, albeit an undesired one. Decreasing the concentration to 0.01 M greatly decreased conversion with significant amounts of starting material observed after 24 hr. However, the reaction was much cleaner with the starting material, **154**, and **155** comprising the majority of the crude mixture. Mixed solvent systems or very forcing conditions proved ineffective in promoting the reaction as well.

4.13 Future Directions

There are still opportunities to explore in the hopes of completing our total synthesis. While our attempts with the Rh [3+2] had yet to show activation of the desired doubly activated C-C bond, it is important to note that it has been observed with a singly activated C-C bond. What this could suggest is that the additional carbonyl is inhibiting the desired reactivity. As such, future

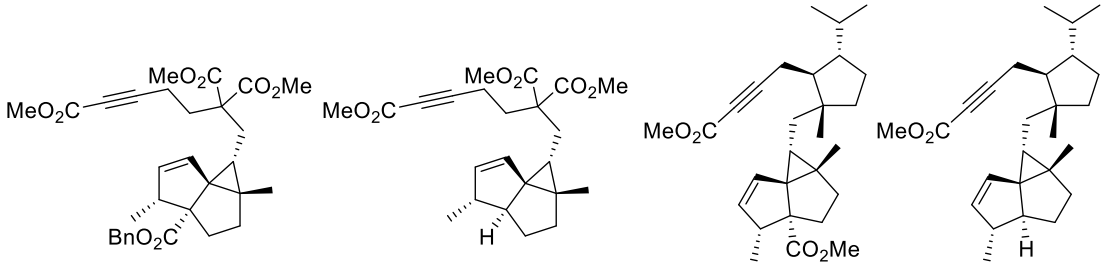

Figure 4.2 Possible future substrates for the Rh [3+2].

work could focus on *trans*-vinyl cyclopropanes **156** or **157** with alkyl linkers to the ynoate moiety. Further, given that the benzyl ester has proven problematic with Pd in the synthesis of ynoate **63**, it is not unreasonable to think it may exhibit similar issues with Rh. Particularly given the fact that in most of Rh reactions conducted mixtures of highly polar side products, potentially arising from debenzylation to give a carboxylic acid, were observed. Thus, future substrates such as **157**, **158**, and **159** which either have a methyl ester or no ester at all could hopefully prevent such issues.

4.14 Conclusion

In this section, we reported on our most recent attempts towards the completion of the synthesis of retigeranic acid A **1**. To that end, we have developed a Pd-enolate strategy to probe the potential selectivity of Pd-enolates for Michael additions over migratory insertion into unactivated olefins. We designed and executed a synthesis of enoate **63** that featured a Boron-mediated aldol reaction, stereoselective vinyl tosylate formation, and a concurrent Stille coupling/decarboxylation reaction. The enoate substrate proved too hindered for the cascade, but from it we identified the deleterious effects of the combination of amine bases and phosphine ligands, as well as the need for dilute reaction conditions. Next, we accessed the enone substrate **109** via an HAT coupling with an unusual C_1 radical acceptor and a challenging NHK cross coupling. The clean formation of the vinyl cyclopropane product **110** and **111** showed that in our case the [3-*exo*-trig] pathway occurs rapidly enough that it is unlikely that another pathway,

especially one as challenging as our [6-*exo*-dig] pathway, could predominate. From there, we attempted to finish the synthesis via the vinyl cyclopropane given how readily it is formed. Radical induced [3+2] cycloaddition proved ineffective potentially due to the same issues faced by the Heck cascade. Finally, the Rh^{I} [3+2] cycloaddition comprises our most recent and promising attempts to successfully conclude the synthesis. While desired C-C bond activation has not been identified, a remarkable C-C activation between two all carbon quaternary centers has been observed. Future work will focus on this approach.

4.15 References

[1] J. Nokami, H. Watanabe, T. Mandai, M. Kawada, J. Tsuji, *Tetrahedron Lett.* **1989**, *30*, 4829–4832.

[2] J. Tsuji, *Proc. Japan Acad. Ser. B* **2004**, *80*, 349–358.

[3] M. Schmitt, A. J. Grenning, J. A. Tunge, *Tetrahedron Lett.* **2012**, *53*, 4494–4497.

[4] J. A. Tunge, E. C. Burger, *European J. Org. Chem.* **2005**, *2005*, 1715–1726.

[5] J. G. Shim, H. Nakamura, Y. Yamamoto, *J. Org. Chem.* **1998**, *63*, 8470–8474.

[6] N. T. Patil, Z. Huo, Y. Yamamoto, *J. Org. Chem.* **2006**, *71*, 6991–6995.

[7] J. Magano, J. R. Dunetz, *Chem. Rev.* **2011**, *111*, 2177–2250.

[8] F. Dénès, A. Pérez-Luna, F. Chemla, *Chem. Rev.* **2010**, *110*, 2366–2447.

[9] J. Huang, E. Bunel, M. M. Faul, *Org. Lett.* **2007**, *9*, 4343–4346.

[10] A. S. Kende, B. Roth, P. J. Sanfilippo, *J. Am. Chem. Soc.* **1982**, *104*, 1784–1785.

[11] I. Yoshihiko, A. Hirokazu, H. Toshikazu, M. Akira, S. Takeo, *J. Am. Chem. Soc.* **2002**, *101*, 494–496.

[12] A. S. Kende, C. E. M. Nelson, S. Fuchs, *Tetrahedron Lett.* **2005**, *46*, 8149–8152.

[13] I. Coudanne, J. Castro, G. Balme, *Synlett* **1998**, *1998*, 995–997.

[14] M. Toyota, M. Ihara, *Synlett* **2002**, *2002*, 1211–1222.

[15] D. Huang, S. M. Szewczyk, P. Zhang, T. R. Newhouse, *J. Am. Chem. Soc.* **2019**, *141*, 5669–5674.

[16] D. Olivieri, D. Huang, A. K. Bodnar, S. Yu, T. R. Newhouse, *Tetrahedron* **2020**, *76*, 131417.

[17] D. Huang, T. R. Newhouse, *Acc. Chem. Res.* **2021**, *54*, 1118–1130.

[18] A. B. Flynn, W. W. Ogilvie, *Chem. Rev.* **2007**, *107*, 4698–4745.

[19] J. W. Lane, K. L. Spencer, S. R. Shakya, N. C. Kallan, P. J. Stengel, T. Remarchuk, *Org. Process Res. Dev.* **2014**, *18*, 1641–1651.

[20] H. Fuwa, K. Ishigai, K. Hashizume, M. Sasaki, *J. Am. Chem. Soc.* **2012**, *134*, 11984–11987.

[21] T. Inoue, J. F. Liu, D. C. Buske, A. Abiko, *J. Org. Chem.* **2002**, *67*, 5250–5256.

[22] J. Li, Q. Ren, X. Cheng, K. Karaghiosoff, P. Knochel, *J. Am. Chem. Soc.* **2019**, *141*, 18127–18135.

[23] F.-W. Sum, L. Weiler, *Can. J. Chem.* **1979**, *57*, 1431–1441.

[24] Y. Ashida, K. Nakata, D. Yoshitake, Y. Sato, Y. Miyazaki, Y. Tanabe, *Asian J. Org. Chem.* **2020**, *9*, 604–615.

[25] R. R. P. Torregrosa, S. N. Mendis, A. Davies, J. A. Tunge, *Synthesis (Stuttg).* **2018**, *50*, 3205–3216.

[26] R. R. P. Torregrosa, Y. Ariyarathna, K. Chattopadhyay, J. A. Tunge, *J. Am. Chem. Soc.* **2010**, *132*, 9280–9282.

[27] S. D. Rychnovsky, J. Kim, *J. Org. Chem.* **2002**, *59*, 2659–2660.

[28] G. Domínguez, J. Pérez-Castells, *Chem. Soc. Rev.* **2011**, *40*, 3430–3444.

[29] I. P. Beletskaya, A. V. Cheprakov, *Chem. Rev.* **2000**, *100*, 3009–3066.

[30] W. A. Herrmann, C. Brossmer, C. P. Reisinger, T. H. Riermeier, K. Öfele, M. Beller, *Chem. – A Eur. J.* **1997**, *3*, 1357–1364.

[31] Z. Wang, *Compr. Org. Name React. Reagents* **2010**, 589–594.

[32] G. Wang, E. I. Negishi, *European J. Org. Chem.* **2009**, *2009*, 1679–1682.

[33] N. Mase, F. Tanaka, C. F. Barbas, *Org. Lett.* **2003**, *5*, 4369–4372.

[34] X. Zhang, B. N. Kakde, R. Guo, S. Yadav, Y. Gu, A. Li, *Angew. Chemie* **2019**, *131*, 6114–6119.

[35] J. Il Hwang, Y. T. Hong, S. Kim, *Adv. Synth. Catal.* **2005**, *347*, 1513–1516.

[36] A. L. Hurski, M. V. Barysevich, T. S. Dalidovich, M. V. Iskryk, N. U. Kolasava, V. N. Zhabinskii, V. A. Khripach, *Chem. – A Eur. J.* **2016**, *22*, 14171–14174.

[37] D. J. Hart, F. L. Seely, *J. Am. Chem. Soc.* **1988**, *110*, 1631–1633.

[38] B. Gaspar, E. M. Carreira, *J. Am. Chem. Soc.* **2009**, *131*, 13214–13215.

[39] R. Grigg, U. Sakee, V. Sridharan, S. Sukirthalingam, R. Thangavelauthum, *Tetrahedron* **2006**, *62*, 9523–9532.

[40] Z. Wang, *Compr. Org. Name React. Reagents* **2010**, 2748–2752.

[41] K. Takai, S. Toshikawa, A. Inoue, R. Kokumai, *J. Am. Chem. Soc.* **2003**, *125*, 12990–12991.

[42] K. Takai, T. Ichiguchi, S. Hikasa, *Synlett* **1999**, *1999*, 1268–1270.

[43] Y. R. Bhorge, S. H. Chang, C. T. Chang, T. H. Yan, *Tetrahedron* **2012**, *68*, 4846–4851.

[44] K. Takai, *Org. React.* **2004**, 253–612.

[45] A. Gil, F. Albericio, M. Álvarez, *Chem. Rev.* **2017**, *117*, 8420–8446.

[46] P. Shukla, C. H. Cheng, *Org. Lett.* **2006**, *8*, 2867–2869.

[47] M. Meazza, H. Guo, R. Rios, *Org. Biomol. Chem.* **2017**, *15*, 2479–2490.

[48] P. H. Chen, B. A. Billett, T. Tsukamoto, G. Dong, *ACS Catal.* **2017**, *7*, 1340–1360.

[49] J. Wang, S. A. Blaszczyk, X. Li, W. Tang, *Chem. Rev.* **2020**, *121*, 110–139.

[50] T. Hudlicky, L. Radesca-Kwart, L. Li, T. Bryant, *Tetrahedron Lett.* **1988**, *29*, 3283–3286.

[51] M. E. Jung, H. L. Rayle, *J. Org. Chem.* **1997**, *62*, 4601–4609.

[52] K. S. Feldman, R. E. Ruckle, A. L. Romanelli, *Tetrahedron Lett.* **1989**, *30*, 5845–5848.

[53] C. C. Huval, K. M. Church, D. A. Singleton, *Synlett* **1994**, *1994*, 273–274.

[54] P. A. Wender, H. Rieck, M. Fuji, *J. Am. Chem. Soc.* **1998**, *120*, 10976–10977.

[55] L. Jiao, S. Ye, Z. X. Yu, *J. Am. Chem. Soc.* **2008**, *130*, 7178–7179.

[56] B. M. Trost, H. Yang, C. S. Brindle, G. Dong, *Chem. – A Eur. J.* **2011**, *17*, 9777–9788.

[57] P. Binger, P. Wedemann, S. I. Kozhushkov, A. de Meijere, *European J. Org. Chem.* **1998**, *1998*, 113–119.

4.16 Experimental Section

General Information All reactions were carried out under an argon atmosphere with dry solvents under anhydrous conditions, unless otherwise noted. Dry tetrahydrofuran (THF), toluene, diethyl ether (Et_2O) dichloromethane (CH_2Cl_2), and acetonitrile (CH_3CN) were obtained by passing commercially available pre-dried, oxygen-free formulations through activated alumina columns. Yields refer to chromatographically and spectroscopically (^1H and ^{13}C NMR) homogeneous materials, unless otherwise stated. Reagents were purchased at the highest commercial quality and used without further purification, unless otherwise stated. Reactions were magnetically stirred and monitored by thin-layer chromatography (TLC) carried out on 0.25 mm E. Merck silica gel plates (60F-254) using UV light as visualizing agent, and an ethanolic solution of phosphomolybdic acid and cerium sulfate or a solution of $KMnO_4$ in aq. $NaHCO_3$ and heat as developing agents. SiliCycle silica gel (60, academic grade, particle size 0.040–0.063 mm) was used for flash column chromatography. Preparative thin-layer chromatography separations were carried out on 0.50 mm E. Merck silica gel plates (60F-254). NMR spectra were recorded on Bruker 500 MHz instruments and calibrated using residual undeuterated solvent as an internal reference. The following abbreviations were used to explain the multiplicities: s = singlet, d = doublet, t = triplet, q = quartet, br = broad, app = apparent.

Synthesis of Enoate Cascade Substrates

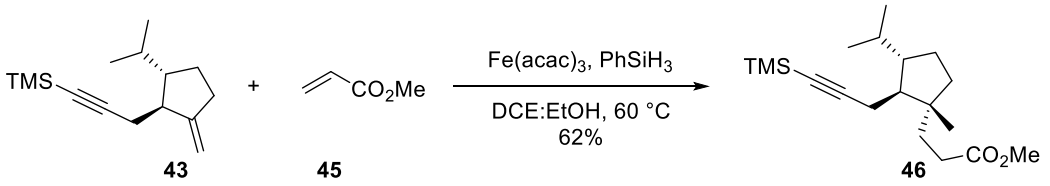

Ester 46 To a flask was added DCE (39 mL), EtOH (5 mL), $Fe(acac)_3$ (353 mg g, 1.0 mmol, 20 mol%), cyclopentene **43** (1.17 g, 5 mmol, 1.0 equiv.), and methyl acrylate **45** (1.35 mL, 15 mmol, 3.0 equiv.) to give a red suspension. Then $PhSiH_3$ (0.92 mL, 7.5 mmol, 1.5 equiv.) was added and the mixture was immediately placed in a preheated oil bath at 60 ˚C and the reaction was stirred at that temperature until complete consumption of starting material was indicated by TLC (silica gel,

hexanes). Then the reaction was cooled to 23 ˚C and diluted with brine (40 mL) and extracted with Et_2O (3 x 40 mL). The combined organic layers were washed with brine (40 mL), dried with $MgSO_4$, and concentrated. The resultant residue was purified first by a short silica plug (hexanes:Et_2O 19:1) to remove inorganic salts followed by gravity column chromatography (silica gel, toluene) to give ester **46** as a colorless oil (998 mg, 62%). **46**: R_f = 0.22 (silica gel, hexanes:Et_2O 19:1); ^1H NMR (400 MHz, $CDCl_3$) δ 3.66 (s, 3H), 2.38 – 2.24 (m, 2H), 2.19 (d, *J* = 6.7 Hz, 2H), 1.98 – 1.79 (m, 2H), 1.71 – 1.43 (m, 5H), 1.39 – 1.28 (m, 3H), 0.90 (d, *J* = 6.9 Hz, 3H), 0.86 (s, 3H), 0.81 (d, *J* = 6.7 Hz, 3H), 0.13 (s, 9H).

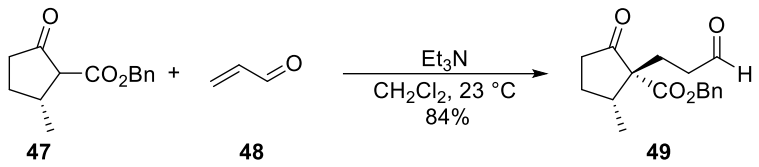

47 **48** **49**

Aldehyde 49 Starting from a literature procedure,[1] ketoester **47** (2.40 g, 11.3 mmol, 1.0 equiv.) was added to a dry flask under N_2 followed by CH_2Cl_2 (110 mL), Et_3N (2.40 mL, 17.0 mmol, 1.5 equiv.), and acrolein (1.14 mL, 17.0 mmol, 1.5 equiv.) and the colorless solution was stirred until full consumption of the starting material was indicated by TLC (silica gel, hexanes:EtOAc 4:1), usually 10-16 hr. The resultant reaction was then concentrated and the residue was purified by flash column chromatography (silica gel, hexanes:EtOAc 4:1) to give **49** as a colorless oil (1.21 g, 84%). **49** R_f = 0.23 (silica gel, hexanes:EtOAc 4:1); ^1H NMR (400 MHz, $CDCl_3$) δ 9.74 (t, *J* = 1.2 Hz, 1H), 7.41 – 7.27 (m, 5H), 5.19 (d, *J* = 12.2 Hz, 1H), 5.08 (d, *J* = 12.2 Hz, 1H), 2.92 – 2.78 (m, 1H), 2.59 – 2.42 (m, 2H), 2.29 – 2.09 (m, 3H), 2.03 (dddd, *J* = 12.6, 8.5, 6.5, 1.6 Hz, 1H), 1.93 (ddd, *J* = 14.5, 10.2, 5.3 Hz, 1H), 1.72 (dtd, *J* = 12.7, 11.3, 8.6 Hz, 1H), 0.98 (d, *J* = 6.8 Hz, 3H).

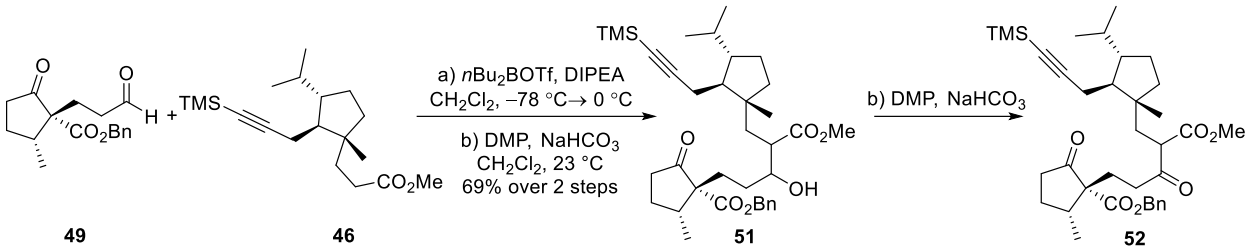

Ketoester 52 To a dry flask was added **46** (1.10 g, 3.41 mmol, 1.5 equiv.) as a solution in CH_2Cl_2 (13.7 mL) and the colorless solution was cooled to 0 ˚C. DIPEA (0.76 mL ,4.35 mmol, 1.9 equiv.) was added immediately followed by Bu_2BOTf (3.21 mL, 1.0 M CH_2Cl_2, 1.4 equiv.) and the reaction was stirred at the same temperature for 2 hr. The mixture was then cooled to –78 ˚C and **49** (660 mg, 2.29 mmol, 1.0 equiv.) was added as a solution in CH_2Cl_2 (9.3 mL) then stirred at the same temperature for 1 hr. Then the reaction was warmed to 0 ˚C and stirred for 1 hr. The reaction was then cooled to –78 ˚C and quenched with a buffered H_2O_2 solution (30 mL: 2.76 mL of pH 7 phosphate buffer + 1.32 mL 30% $H_2O_{2\,(aq)}$ + 25 mL MeOH) and the mixture was warmed to 0 ˚C then stirred for 4 hr. The reaction was concentrated to ¼ volume and diluted with DI H_2O (15 mL) and EtOAc (15 mL) and the layers were separated. The aqueous layer was extracted with EtOAc (3 x 15 mL) and the combined organic layers were dried with $MgSO_4$ and concentrated. The resultant residue was purified by flash column chromatography (silica gel, hexanes:EtOAc 19:1 to 3:1) to give alcohol **51** as a colorless oil (1.10 g, 79%). **51** R_f = 0.28 (silica gel, hexanes:EtOAc 3:1).

To a flask was added **51** (1.10 g, 1.81 mmol, 1.0 equiv.) was added as a solution in CH_2Cl_2 (18 mL) followed by $NaHCO_3$ (760 mg, 9.05 mmol, 5 equiv.) and DMP (1.92 g, 4.53 mmol, 2.5 equiv.) and the white suspension was stirred at 23 ˚C until full consumption of the starting material was indicated by TLC (silica gel, hexanes:EtOAc 3:1). The reaction was then filtered through a celite plug with CH_2Cl_2 and concentrated. The resultant residue was purified by flash column

chromatography (silica gel, hexanes:EtOAc 9:1) to give ketoester **52** as a colorless oil (961 g, 88%, 69% over 2 steps). **52** R_f = 0.56 (silica gel, hexanes:EtOAc 4:1). ^{1}H NMR (400 MHz, $CDCl_3$) δ 7.41 – 7.27 (m, 5H), 5.18 (d, *J* = 12.3 Hz, 1H), 5.12 – 5.04 (m, 1H), 4.05 (t, *J* = 6.7 Hz, 1H), 3.69 (p, *J* = 1.3 Hz, 3H), 3.57 – 3.46 (m, 1H), 3.07 – 2.88 (m, 1H), 2.70 – 2.44 (m, 2H), 2.33 – 1.64 (m, 11H), 1.42 – 1.13 (m, 3H), 1.01 – 0.92 (m, 3H), 0.90 (dd, *J* = 8.9, 6.4 Hz, 3H), 0.84 – 0.64 (m, 6H), 0.13 (d, *J* = 3.1 Hz, 9H).

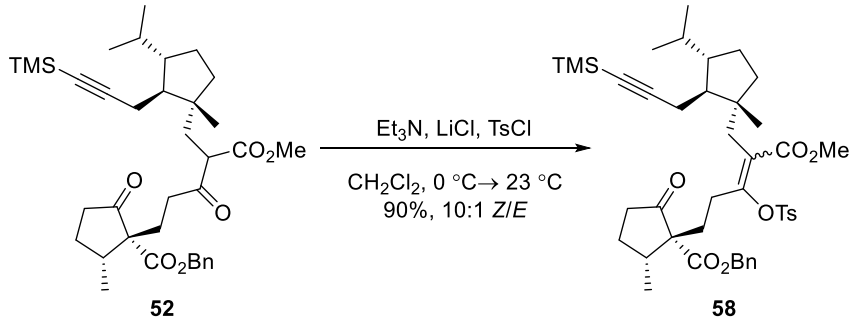

Vinyl Tosylate 58 Starting from a literature procedure,[2] to a flask was added LiCl (88 mg, 2.10 mmol, 3 equiv.), **52** (255 mg, 0.42 mmol, 1.0 equiv.), and CH_2Cl_2 (4.2 mL) followed by Et_3N (0.23 mL, 1.67 mmol, 4.0 equiv.) and NMI (0.13 mL, 1.67 mmol, 4.0 equiv.) and the colorless suspension was stirred at 23 ˚C for 10 min. The now yellow suspension was then cooled to 0 ˚C and TsCl (317 mg, 1.67 mmol, 4.0 equiv.) was added. The reaction was allowed to warm to 23 ˚C and stir overnight. The reaction was quenched with DI H_2O (8 mL) and the layers were separated and the aqueous layer was extracted with EtOAc (2 x 10 mL). the combined organic layers were dried with $MgSO_4$ and then concentrated. The resultant residue was purified by flash column chromatography (silica gel, hexanes:EtOAc 9:1 to 17:3) to give **58** as a colorless oil (288 mg, 90%). *Z*-**58** R_f = 0.24 (silica gel, 17:3); ^{1}H NMR (400 MHz, $CDCl_3$) δ 7.84 – 7.78 (m, 2H), 7.38 – 7.26 (m, 7H), 5.15 (d, *J* = 12.2 Hz, 1H), 5.06 (d, *J* = 12.3 Hz, 1H), 3.59 (s, 3H), 2.74 – 2.62 (m, 1H), 2.62 – 2.44 (m, 3H), 2.44 (s, 3H), 2.42 – 2.24 (m, 3H), 2.24 – 1.81 (m, 8H), 1.79 – 1.63 (m,

2H), 1.57 – 1.39 (m, 2H), 1.37 – 1.18 (m, 4H), 0.89 (t, *J* = 7.2 Hz, 6H), 0.82 – 0.74 (m, 6H), 0.13 (d, *J* = 6.2 Hz, 9H).

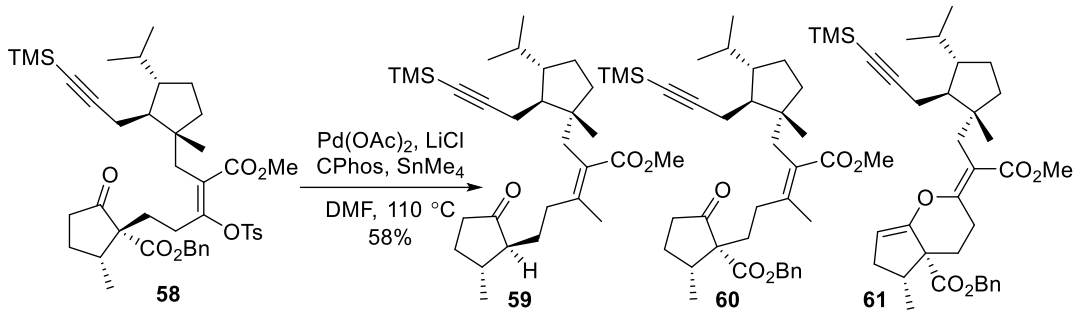

Enoate 59 To a vial was added LiCl (21 mg, 0.496 mmol, 3.0 equiv.) then the vial was flame dried under vacuum, flushed with N_2, and allowed to cool to 23 ˚C. $Pd(OAc)_2$ (3.7 mg, 0.165 mmol, 10 mol%), **58** (126 mg, 0.165 mmol, 1.0 equiv.) as a solution in DMF (1.7 mL), and $SnMe_4$ (0.05 mL, 0.33 mmol, 2 equiv) were added sequentially and the vial was sealed and heated to 110 ˚C overnight. The reaction was then cooled to 23 ˚C and quenched with saturated NH_4Cl (5 mL) the diluted with Et_2O (5 mL). The layers were separated, and the aqueous layer was extracted with Et_2O (3 x 5 mL). The combined organic layers were washed with H_2O (2 x 5 mL), dried with Na_2SO_4, then concentrated. The resultant residue was purified by flash column chromatography (silica gel, hexanes:EtOAc 93:7) to give **59** as a colorless oil (53 mg, 68%). **59** R_f = 0.55 (silica gel, hexanes:EtOAc 17:3); ^{1}H NMR (400 MHz, $CDCl_3$) δ 3.71 (s, 3H), 2.58 (d, *J* = 14.2 Hz, 1H), 2.40 – 2.24 (m, 4H), 2.21 – 1.97 (m, 5H), 1.86 (s, 3H), 1.66 – 1.59 (m, 3H), 1.55 – 1.21 (m, 7H), 1.16 (d, *J* = 6.3 Hz, 3H), 0.88 (d, *J* = 6.8 Hz, 4H), 0.79 (d, *J* = 6.7 Hz, 3H), 0.77 (s, 3H), 0.09 (s, 9H); ^{13}C NMR (101 MHz, $CDCl_3$) δ 220.44, 171.70, 143.95, 126.95, 107.90, 85.02, 56.33, 51.26, 49.50, 48.42, 46.24, 39.39, 37.99, 37.29, 36.82, 32.43, 30.93, 29.52, 29.48, 25.32, 22.70, 22.38, 20.44, 20.13, 19.54, 16.37.

60 R_f = 0.51 (silica gel, hexanes:EtOAc 17:3); ^{1}H NMR (500 MHz, $CDCl_3$) δ 7.39 – 7.29 (m, 5H), 5.19 (d, *J* = 12.3 Hz, 1H), 5.07 (d, *J* = 12.3 Hz, 1H), 3.71 (s, 3H), 2.58 – 2.48 (m, 2H), 2.44 – 2.29 (m, 3H), 2.29 – 2.15 (m, 2H), 2.12 – 2.01 (m, 3H), 1.97 – 1.86 (m, 2H), 1.84 (s, 3H), 1.81 – 1.68 (m, 3H), 1.54 – 1.13 (m, 8H), 1.03 – 0.94 (m, 3H), 0.88 (d, *J* = 6.8 Hz, 3H), 0.79 (d, *J* = 6.7 Hz, 3H), 0.76 (s, 3H), 0.16 – 0.08 (m, 9H); ^{13}C NMR (126 MHz, $CDCl_3$) δ 216.02, 171.69, 170.23, 143.76, 135.44, 128.76, 128.57, 128.48, 127.43, 108.15, 85.13, 66.95, 62.65, 51.42, 49.68, 48.44, 40.63, 39.36, 38.77, 37.41, 29.88, 29.82, 29.61, 28.30, 22.81, 22.56, 20.70, 20.58, 20.30, 16.42, 15.85.

61 R_f = 0.54 (silica gel, hexanes:EtOAc 17:3); ^{1}H NMR (400 MHz, $CDCl_3$) δ 7.39 – 7.28 (m, 5H), 5.24 (d, *J* = 12.5 Hz, 1H), 5.21 – 5.16 (m, 1H), 5.09 (d, *J* = 12.5 Hz, 1H), 3.74 (s, 3H), 2.69 – 2.53 (m, 3H), 2.36 – 2.01 (m, 8H), 1.95 – 1.79 (m, 1H), 1.73 – 1.57 (m, 1H), 1.53 – 1.38 (m, 3H), 1.37 – 1.17 (m, 7H), 0.89 (dd, *J* = 10.7, 6.7 Hz, 6H), 0.82 – 0.76 (m, 6H), 0.16 – 0.05 (m, 9H).; ^{13}C NMR (101 MHz, $CDCl_3$) δ 172.31, 170.03, 154.36, 153.21, 135.93, 128.65, 128.29, 128.26, 110.29, 107.73, 106.26, 85.41, 66.88, 55.67, 51.67, 49.93, 49.22, 46.57, 45.62, 39.32, 37.82, 34.82, 31.09, 29.95, 29.85, 29.73, 23.41, 23.09, 22.38, 20.78, 19.43, 17.04, 14.80.

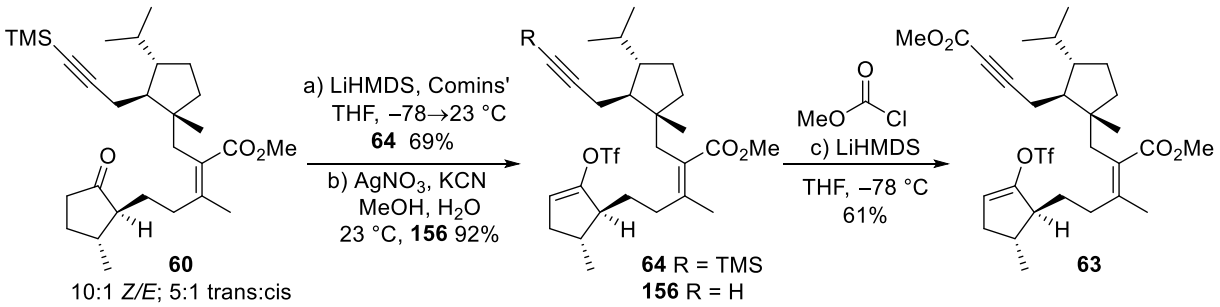

Synthesis of triflate 63

Triflate 64 To a dry flask was added **60** (608 mg, 1.29 mmol, 1.0 equiv.) as a solution in benzene (4 mL) and **60** was then dried azeotropically with benzene (3 x 2 mL) then THF (7.8 mL) was

added to give a colorless solution. The solution was cooled to –78 ˚C and LiHMDS (2.6 mL, 1.0 M THF, 2.0 equiv.) then the light-yellow reaction was stirred at the same temperature for 1 hr. Comins' reagent (1.01 g, 2.58 mmol, 2.0 equiv.) was added as a solution in THF (4.1 mL) and the reaction was allowed to warm to 23 ˚C overnight. The reaction was quenched with saturated $NaHCO_3$ (10 mL) and was diluted with DI H_2O (10 mL) and Et_2O (10 mL). The layers were separated and the aqueous layer was extracted with Et_2O (3 x 10 mL). The combined organic layers were washed with DI H_2O (3 x 10 mL), dried with MgSO4, and concentrated. The resultant residue was then purified by flash column chromatography (silica gel, hexanes:Et_2O 97:3) to give **64** as a colorless oil (537 mg, 69%). **64** R_f = 0.71 (silica gel, hexanes:EtOAc 40:3); ^{1}H NMR (400 MHz, $CDCl_3$) δ 5.63 – 5.57 (m, 1H), 3.72 (s, 3H), 2.66 – 2.51 (m, 2H), 2.42 – 2.23 (m, 4H), 2.21 – 2.05 (m, 4H), 2.05 – 1.92 (m, 2H), 1.85 (s, 3H), 1.78 – 1.63 (m, 2H), 1.55 – 1.41 (m, 3H), 1.38 – 1.21 (m, 4H), 1.14 (d, *J* = 6.9 Hz, 3H), 0.89 (d, *J* = 6.9 Hz, 4H), 0.79 (d, *J* = 6.7 Hz, 4H), 0.76 (s, 3H), 0.12 (s, 10H); ^{19}F NMR (376 MHz, $CDCl_3$) δ -73.56.

Alkyne 156 To a flask was added vinyl triflate **64** (537 mg, 0.89 mmol, 1.0 equiv.) as a solution in MeOH (0.89 mL) to give a colorless solution that was sonicated at 23 ˚C. $AgNO_3$ (285 mg, 2.4 mmol, 2.7 equiv.) was added as a solution in MeOH:H_2O (4.8 mL, 3:1) and the reaction became a grey-brown suspension that sonicated for 20 min. Then KCN (578 mg, 8.9 mmol, 10.0 equiv.) was added as a solution in H_2O (0.89 mL) and a gummy grey solid formed. The reaction was sonicated for 20 min or until full consumption of starting material was indicated by TLC (silica gel, hexanes:Et_2O 19:1). The reaction was then diluted with DI H_2O (8 mL) and hexanes (10 mL), and the layers were separated. The aqueous layer was extracted with hexanes (3 x 10 mL) and the combined organic layers were dried with $MgSO_4$, filtered, and concentrated. The resultant residue was then purified via flash column chromatography (silica gel, hexanes:Et_2O 19:1) to give alkyne

156 as a colorless oil (435 mg, 100%). **156**: R_f = 0.22 (silica gel, hexanes:Et_2O 19:1); ^1H NMR (400 MHz, $CDCl_3$) δ 5.63 – 5.55 (m, 1H), 3.72 (s, 3H), 2.76 (d, *J* = 14.1 Hz, 1H), 2.60 (ddt, *J* = 16.4, 8.3, 2.8 Hz, 1H), 2.44 – 2.05 (m, 8H), 2.03 – 1.95 (m, 1H), 1.94 (t, *J* = 2.7 Hz, 1H), 1.85 (d, *J* = 4.4 Hz, 3H), 1.76 – 1.40 (m, 6H), 1.38 – 1.23 (m, 4H), 1.13 (d, *J* = 6.9 Hz, 3H), 0.89 (d, *J* = 6.8 Hz, 3H), 0.80 (t, *J* = 3.4 Hz, 6H).; ^{19}F NMR (376 MHz, $CDCl_3$) δ -73.55.

Ynoate 63 To a dry flask was added alkyne **156** (435 mg, 0.82 mmol, 1.0 equiv.). which was dried azeotropically (3 x 4 mL benzene) then dissolved in THF (8.2 mL) and the colorless solution was cooled to –78 ˚C. Then, LiHMDS (1.64 mL, 1.0 M THF, 2.0 equiv.) was added to give a yellow solution that was stirred at the same temperature for 1 hr. Next, methyl chloroformate (0.13 mL, 1.64 mmol, 2 equiv.) was added and the reaction was stirred at the same temperature for 2 hr. The reaction was then quenched with saturated $NaHCO_3$ (5 mL), diluted with Et_2O (5 mL), and the layers were separated. The aqueous layer was extracted with Et_2O (3 x 5 mL), washed with brine, dried with $MgSO_4$, filtered and concentrated. The resultant residue was purified via flash column chromatography (silica gel, hexanes:Et_2O 9:1) to give ynoate **63** as a colorless oil (295 mg, 61%). **63**: R_f = 0.18 (silica gel, hexanes:Et_2O 9:1); ^1H NMR (500 MHz, $CDCl_3$) δ 5.62 – 5.57 (m, 1H), 3.74 (s, 3H), 3.73 (s, 3H), 2.59 (ddq, *J* = 16.4, 5.9, 2.8 Hz, 2H), 2.43 – 2.32 (m, 3H), 2.30 – 2.07 (m, 4H), 2.01 – 1.92 (m, 1H), 1.85 (s, 3H), 1.89 – 1.78 (m, 1H), 1.75 – 1.65 (m, 2H), 1.63 – 1.45 (m, 2H), 1.43 (s, 1H), 1.40 – 1.26 (m, 4H), 1.13 (d, *J* = 6.9 Hz, 3H), 0.90 (d, *J* = 6.8 Hz, 3H), 0.85 – 0.74 (m, 6H); ^{19}F NMR (470 MHz, $CDCl_3$) δ -73.53.

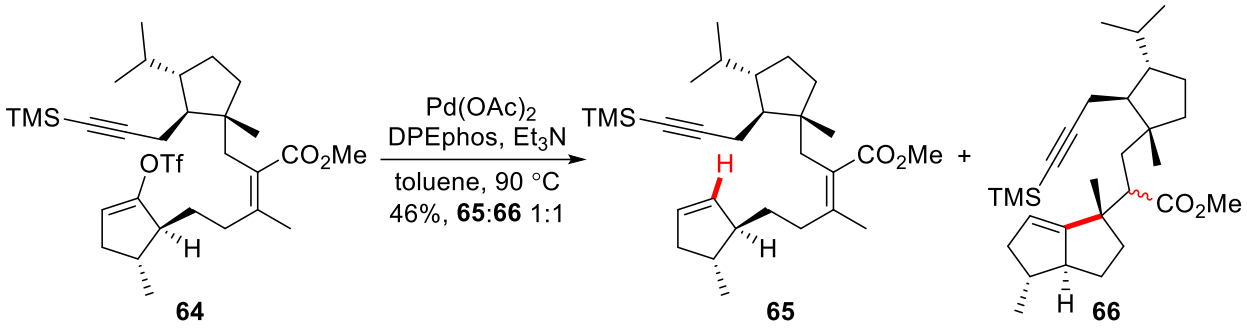

Cascade reaction of vinyl triflate 64 To a dry vial under Ar was added $Pd(OAc)_2$ (0.6 mg, 0.0025 mmol, 20 mol%), DPEPhos (2.7 mg, 0.005 mmol, 40 mol%), Et_3N (6 µL, 0.0375 mmol, 3.0 equiv.) and toluene (0.1 mL) to give a reddish-brown suspension that was sparged for 15 min with Ar. Then vinyl triflate **64** (7.6 mg, 0.0125 mmol, 1.0 equiv.) was added as a solution in degassed toluene (0.16 mL) and the mixture was sparged for a further 5 min, sealed with a Teflon lined cap, and heated to 90 ˚C for 12 hr. The reaction was then cooled to 23 ˚C, diluted with Et_2O (2 mL), filtered through a celite plug, and concentrated. The resultant residue was purified via preparatory TLC (silica gel, hexanes:Et_2O 19:1) to give ester **66** (1.3 mg, 23%) as a colorless oil and enoate **65** (1.3 mg, 23%) as a colorless oil. **66**: R_f = 0.63 (silica gel, hexanes:Et_2O 9:1); ^{1}H NMR (400 MHz, $CDCl_3$) δ 6.07 – 6.02 (m, 1H), 3.73 (s, 2H), 3.73 (s, 1H), 2.91 (d, *J* = 10.2 Hz, 1H), 2.84 (s, 1H), 2.61 (d, *J* = 14.2 Hz, 1H), 2.46 – 2.20 (m, 8H), 2.17 (s, 2H), 2.16 – 2.05 (m, 1H), 2.04 – 1.92 (m, 4H), 1.92 – 1.86 (m, 4H), 1.70 (dt, *J* = 9.6, 4.8 Hz, 1H), 1.34 – 1.27 (m, 5H), 0.91 – 0.87 (m, 5H), 0.79 (dd, *J* = 6.7, 1.0 Hz, 4H), 0.77 (d, *J* = 2.0 Hz, 3H), 0.11 (s, 9H).

65: R_f = R_f = 0.58 (silica gel, hexanes:Et_2O 9:1); ^{1}H NMR (400 MHz, $CDCl_3$) δ 6.34 (dd, *J* = 5.7, 1.4 Hz, 1H), 5.84 (dd, *J* = 5.6, 2.6 Hz, 1H), 3.70 (s, 3H), 2.57 – 2.45 (m, 2H), 2.39 – 2.22 (m, 3H), 2.14 – 1.98 (m, 4H), 1.84 (s, 3H), 1.77 – 1.72 (m, 1H), 1.31 (dd, *J* = 8.2, 3.9 Hz, 3H), 1.28 (s, 2H), 1.24 – 1.17 (m, 2H), 1.05 (d, *J* = 7.0 Hz, 5H), 0.89 (d, *J* = 6.8 Hz, 6H), 0.79 (d, *J* = 6.7 Hz, 3H), 0.73 (s, 3H), 0.13 (s, 14H).

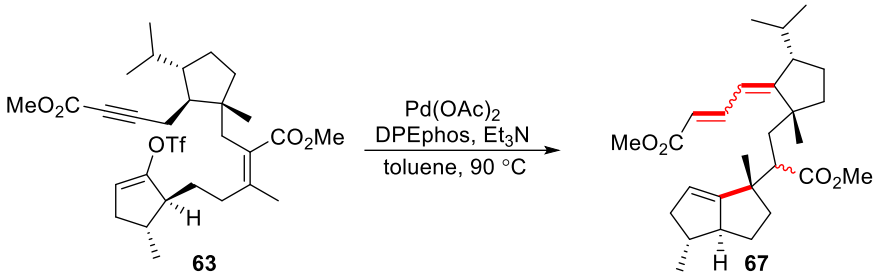

Cascade reaction of ynoate 63 To a dry vial under Ar was added $Pd(OAc)_2$ (0.8 mg, 0.0039 mmol, 20 mol%), DPEPhos (4.0 mg, 0.0076 mmol, 40 mol%), Et_3N (8 μL, 0.0375 mmol, 3.0 equiv.) and toluene (0.15 mL) to give a reddish-brown suspension that was sparged for 15 min with Ar. Then vinyl triflate **63** (11.2 mg, 0.019 mmol, 1.0 equiv.) was added as a solution in degassed toluene (0.23 mL) and the mixture was sparged for a further 5 min, sealed with a Teflon lined cap, and heated to 90 ˚C for 12 hr. The reaction was then cooled to 23 ˚C, diluted with Et_2O (2 mL), filtered through a celite plug, and concentrated. The resultant residue was purified via preparatory TLC (silica gel, hexanes:Et_2O 17:3) to give ester **67** as a colorless oil in a mixture with unidentified compounds. **67**: R_f = 0.33 (silica gel, hexanes:Et_2O 17:3); ^1H NMR (400 MHz, $CDCl_3$) δ 7.49 (dd, *J* = 15.2, 11.6 Hz, 1H), 6.08 – 6.00 (m, 1H), 5.76 (d, *J* = 15.1 Hz, 1H), 3.74 (d, *J* = 1.2 Hz, 3H), 3.73 – 3.67 (m, 3H), 2.91 – 2.82 (m, 1H), 2.76 (s, 1H), 2.64 – 2.12 (m, 7H), 1.99 – 1.95 (m, 1H), 1.95 – 1.59 (m, 11H), 1.35 – 1.30 (m, 3H), 0.99 (d, *J* = 6.2 Hz, 3H), 0.96 – 0.81 (m, 9H).

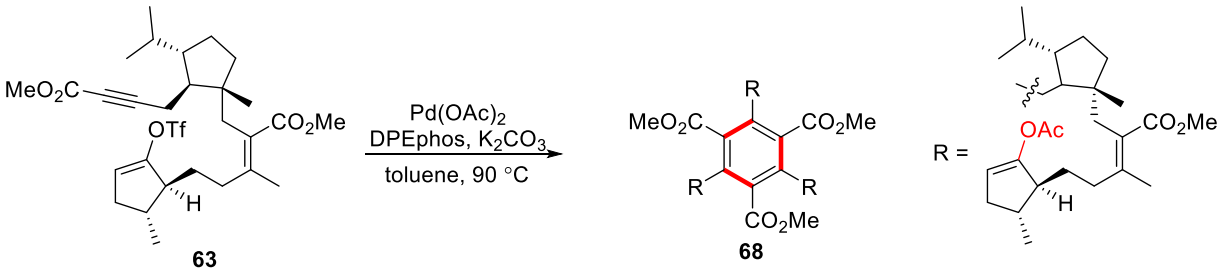

Cascade reaction of ynoate 63 with K_2CO_3 To a dry vial under Ar was added $Pd(OAc)_2$ (1.2 mg, 0.0025 mmol, 20 mol%), DPEPhos (3.4 mg, 0.0051 mmol, 40 mol%), K_2CO_3 (17.6 mg, 0.127 mmol, 5.0 equiv.) and toluene (0.2 mL) to give a reddish-brown suspension that was sparged for 15 min with Ar. Then vinyl triflate **63** (15 mg, 0.0254 mmol, 1.0 equiv.) was added as a solution in degassed toluene (0.31 mL) and the mixture was sparged for a further 5 min, sealed with a Teflon lined cap, and heated to 90 ˚C for 12 hr. The reaction was then cooled to 23 ˚C, diluted with Et_2O (2 mL), filtered through a celite plug, and concentrated. The resultant residue was purified via preparatory TLC (silica gel, hexanes:Et_2O 17:3) to give arene **68** (1.4 mg, 11%) as a colorless oil. **68**: R_f = 0.56 (silica gel, hexanes:Et_2O 17:3); ^{1}H NMR (500 MHz, $CDCl_3$) δ 5.54 (s, 1H), 3.76 (s, 3H), 3.71 (s, 3H), 3.06 (dd, *J* = 15.1, 11.2 Hz, 1H), 2.82 (d, *J* = 14.7 Hz, 1H), 2.61 – 2.54 (m, 1H), 2.54 – 2.43 (m, 3H), 2.27 (d, *J* = 14.7 Hz, 1H), 2.12 (s, 3H), 1.86 (d, *J* = 15.2 Hz, 3H), 1.80 (s, 3H), 1.75 – 1.58 (m, 5H), 1.34 – 1.24 (m, 4H), 1.03 (d, *J* = 6.5 Hz, 3H), 0.86 (d, *J* = 6.8 Hz, 4H), 0.79 – 0.74 (m, 6H); ^{13}C NMR (126 MHz, $CDCl_3$) δ 172.10, 168.15, 167.63, 157.83, 144.21, 140.01, 131.46, 127.68, 122.75, 53.24, 52.27, 51.35, 48.13, 47.83, 45.67, 40.70, 40.58, 39.49, 38.83, 32.69, 32.18, 31.41, 28.69, 22.63, 22.34, 20.96, 20.86, 20.80, 18.64, 16.43.

Synthesis of Enone Substrate

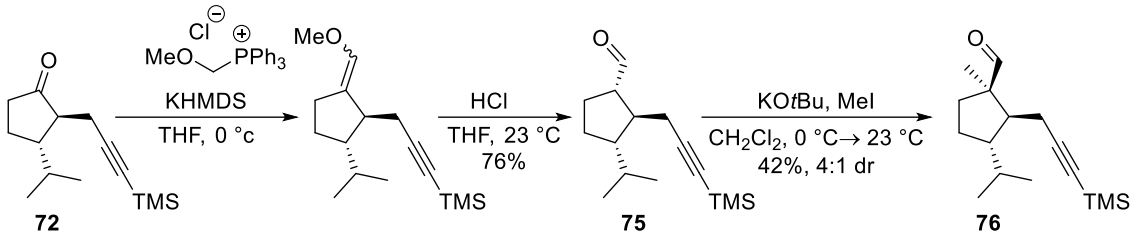

Aldehyde 75 To a dry flask under N_2 is added methoxymethyl triphenylphosphonium chloride (3.20 g, 9.37 mmol, 2.2 equiv.) and THF (15 mL) and the white suspension was cooled to 0 ˚C. KHMDS (16.9 mL, 0.5 M toluene, 2.0 equiv.) was added and the dark-red/orange suspension was stirred for 30 min at the same temperature. Then ketone **72** (1.0 g, 4.24 mmol, 1.0 equiv.) was added as a solution in THF (4 mL + 2 mL wash) and the orange suspension was stirred until the full consumption of starting material was indicated by TLC (silica gel, hexanes:Et_2O 9:1), usually 1-2 hr. The reaction was quenched with NH_4Cl (10 mL) then diluted with DI H_2O (10 mL) and Et_2O (10 mL). The layers were separated and the aqueous layer was extracted with Et_2O (3 x 10 mL). The combined organic layers were concentrated then dissolved in THF (100 mL) and 6M HCl (42 mL) was added. The colorless solution was allowed to stir at 23 ˚C until full consumption of starting material was indicated by TLC (silica gel, hexanes:Et_2O 19:1), usually from 1-4 hr. The now yellow solution was concentrated to ~1/3 volume and was then extracted with Et_2O (3 x 20 mL). The combined organic layers were dried with $MgSO_4$ then concentrated. The resultant residue was purified by flash column chromatography (silica gel, hexanes:acetone 99:1 to 99:2) to give **75** (804 mg, 76%, >20:1 dr) as a light yellow oil that was stored at –20 ˚C. **75** R_f = 0.41 (hexanes:Et_2O 19:1); ^{1}H NMR (400 MHz, $CDCl_3$) δ 9.69 (d, *J* = 2.0 Hz, 1H), 2.74 – 2.64 (m, 1H), 2.44 (dd, *J* = 16.9, 4.7 Hz, 1H), 2.26 (dd, *J* = 16.9, 7.4 Hz, 1H), 2.16 (qd, *J* = 7.4, 4.7 Hz, 1H), 1.97

– 1.80 (m, 1H), 1.80 – 1.52 (m, 4H), 1.40 – 1.23 (m, 1H), 0.94 (d, *J* = 6.7 Hz, 3H), 0.84 (d, *J* = 6.7 Hz, 3H), 0.14 (s, 9H).

Aldehyde 76 To a dry flask under N_2 was added **75** (50 mg, 0.2 mmol, 1.0 equiv.) as a solution in CH_2Cl_2 (1.0 mL) and the light-yellow solution was cooled to 0 ˚C. Then KO*t*Bu (29 mg, 0.26 mmol, 1.3 equiv.) and MeI (0.04 mL, 0.6 mmol, 3.0 equiv.) were added sequentially and the reaction was stirred for 30 min at 0 ˚C. The reaction was then warmed to 23 ˚C and allowed to stir overnight. The reaction was then quenched with NH_4Cl (4 mL) and diluted with CH_2Cl_2 (4 mL). The layers were separated, and the aqueous layer was extracted with CH_2Cl_2 (3 x 4 mL). The combined organic layer was dried with Na_2SO_4 then concentrated. The resultant residue was purified by flash column chromatography (silica gel, hexanes:EtOAc 199:1 to 197:3) to give **76** (22 mg, 42%, 4:1 dr) as a colorless oil that quickly became yellow upon exposure to air. **76** R_f = 0.28 (silica gel, hexanes:acetone 49:1); ^{1}H NMR (400 MHz, $CDCl_3$) δ 9.79 (s, 1H), 2.37 – 2.31 (m, 2H), 2.22 – 1.97 (m, 1H), 1.85 – 1.67 (m, 5H), 1.53 – 1.30 (m, 4H), 1.24 (s, 3H), 1.11 (s, 1H), 0.94 (d, *J* = 6.5 Hz, 3H), 0.84 (d, *J* = 6.5 Hz, 3H), 0.14 (s, 9H).

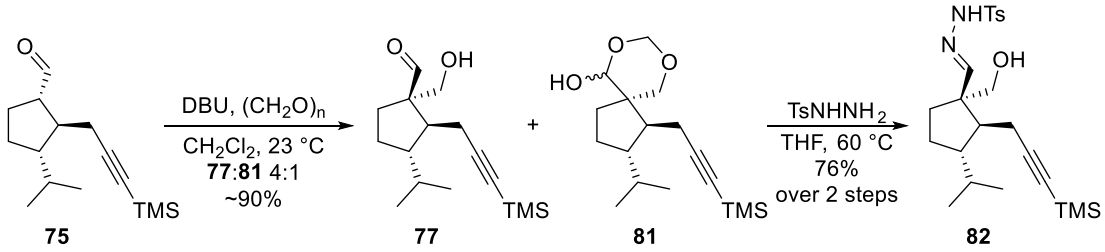

Aldehyde 77 and hemiacetal 81 To a dry flask under N_2 was added **75** (100 mg, 0.4 mmol, 1.0 equiv.) as a solution in CH_2Cl_2 (4 mL) followed by $(CH_2O)_n$ (36 mg, 1.2 mmol, 3.0 equiv.) and distilled DBU (0.18 mL, 1.2 mmol, 3.0 equiv). The reaction was stirred at 23 ˚C until full consumption of starting material was indicated by TLC (silica gel, hexanes:EtOAc 17:3). The reaction was then concentrated and the resultant residue was purified via flash column

chromatography (silica gel, hexanes:acetone 9:1) to **77** and **81** (101 mg, 90%, **77**:**81** 4:1) as a colorless oil. **77** R_f = 0.28 (hexane:EtOAc 17:3); ^{1}H NMR (500 MHz, $CDCl_3$) δ 9.86 (s, 1H), 5.32 (d, *J* = 5.1 Hz, 1H), 5.05 (d, *J* = 6.1 Hz, 1H), 4.68 (d, *J* = 6.2 Hz, 1H), 3.82 (dd, *J* = 11.4, 6.2 Hz, 1H), 3.76 (d, *J* = 10.9 Hz, 1H), 3.57 (dd, *J* = 11.3, 7.0 Hz, 2H), 2.86 (d, *J* = 5.1 Hz, 1H), 2.49 – 2.30 (m, 6H), 1.98 – 1.89 (m, 2H), 1.87 – 1.79 (m, 4H), 1.77 – 1.60 (m, 7H), 1.37 – 1.34 (m, 1H), 1.27 – 1.16 (m, 2H), 0.96 (d, *J* = 6.8 Hz, 3H), 0.94 (d, *J* = 6.9 Hz, 4H), 0.84 (d, *J* = 6.7 Hz, 4H), 0.79 (d, *J* = 6.6 Hz, 3H), 0.16 (s, 7H), 0.15 (d, *J* = 1.5 Hz, 12H).

Tosyl hydrazone 82 To dry vial was added **77** and **81** (101 mg, 0.36 mmol, 1.0 equiv.) as a solution in THF (1.43 mL) followed by tosyl hydrazine (99.7 mg, 0.536 mmol, 1.5 equiv.) to give a colorless solution. The vial was sealed and heated to reflux until full consumption of starting material was indicated by TLC (silica gel, hexanes:EtOAc 7:3), usually 4-10 hr. The reaction was then concentrated and purified by flash column chromatography (silica gel, hexanes:EtOAc 17:3 to 7:3) to give **82** (136 mg, 85%, 76% over 2 steps) as a white solid. **82** R_f = 0.31 (hexanes:EtOAc 7:3); ^{1}H NMR (500 MHz, $CDCl_3$) δ 7.79 (d, *J* = 8.3 Hz, 2H), 7.65 (s, 1H), 7.36 – 7.30 (m, 2H), 7.30 (s, 1H), 3.55 (d, *J* = 11.4 Hz, 1H), 3.48 (d, *J* = 11.4 Hz, 1H), 2.42 (s, 3H), 2.09 – 2.01 (m, 1H), 1.90 (dd, *J* = 17.5, 4.3 Hz, 1H), 1.69 – 1.55 (m, 6H), 1.36 – 1.29 (m, 1H), 0.89 (d, *J* = 6.6 Hz, 3H), 0.79 (d, *J* = 6.5 Hz, 3H), 0.14 (s, 10H).

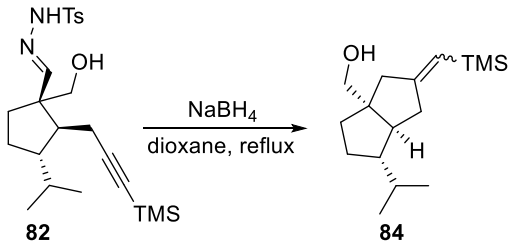

Bicycle 84 To a flask was added **82** (22.4 mg, 0.05 mmol, 1.0 equiv.) as a solution in dioxane (1 mL) followed by $NaBH_4$ (18.5 mg, 0.5 mmol, 10 equiv.). The flaks was fitted with a reflux

condenser and then heated to reflux until full consumption of starting material was indicated by TLC (silica gel, hexanes:EtOAc 7:3), usually ~2 hr. The reaction was then quenched with DI H_2O (3 mL) and diluted with Et_2O (3 mL) and the layers were separated. The aqueous layer was extracted with Et_2O (3 x 5 mL) then the combined organic layers were dried with Na_2SO_4 and concentrated. The resultant residue was purified by flash column chromatography (silica gel, hexanes:EtOAc 9:1) to give **84** (9.7 mg, 73 %, 1:1 *Z*/*E*) as a colorless oil. **84** R_f = 0.82 (silica gel, hexanes:EtOAc 7:3); ^{1}H NMR (400 MHz, $CDCl_3$) δ 5.33 – 5.25 (m, 2H), 3.51 – 3.34 (m, 4H), 2.61 (dd, *J* = 15.5, 9.5 Hz, 1H), 2.49 – 2.38 (m, 2H), 2.36 – 2.28 (m, 1H), 2.21 – 2.03 (m, 4H), 1.82 – 1.65 (m, 6H), 1.46 (dq, *J* = 13.5, 6.7 Hz, 2H), 1.40 – 1.11 (m, 10H), 0.93 (d, *J* = 8.2 Hz, 7H), 0.87 (d, *J* = 6.7 Hz, 7H), 0.08 (s, 18H).

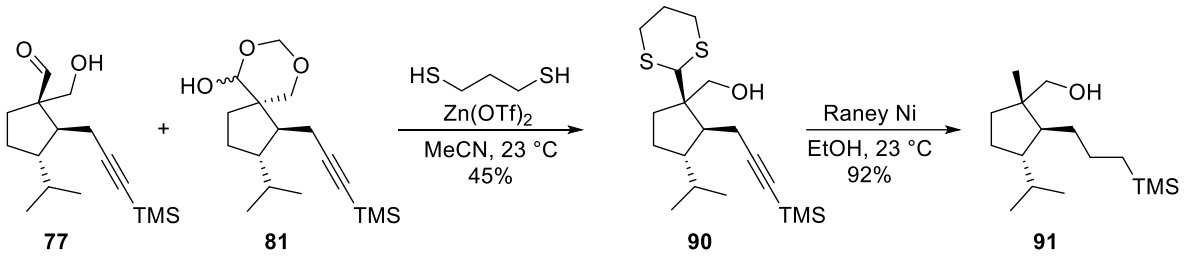

Dithiane 90 To a dry flask under N_2 was added **77** and **81** (28 mg, 0.1 mmol, 1.0 equiv.) as a solution in MeCN (1.0 mL), $Zn(OTf)_2$ (7.3 mg, 0.02 mmol, 20 mol%) and 1,3-propanedithiol (0.03 mL, 0.3 mmol, 3.0 equiv.). The solution was then stirred at 23 ˚C overnight. The reaction was then concentrated and the resultant residue was purified by flash column chromatography (silica gel, hexane:EtOAc 195:5 to 9:1) to give **90** (16.7 mg, 45%) as a colorless oil. **90** R_f = 0.42 (silica gel, 17:3); ^{1}H NMR (400 MHz, $CDCl_3$) δ 4.65 (s, 1H), 3.64 (dd, *J* = 12.2, 4.4 Hz, 1H), 3.51 (dd, *J* = 12.2, 9.6 Hz, 1H), 3.02 – 2.80 (m, 4H), 2.74 (dd, *J* = 17.2, 5.6 Hz, 1H), 2.53 (dd, *J* = 17.2, 5.7 Hz, 1H), 2.35 (dd, *J* = 9.7, 4.5 Hz, 1H), 2.16 – 2.06 (m, 1H), 1.99 – 1.72 (m, 4H), 1.66 – 1.50 (m, 2H), 1.38 – 1.21 (m, 1H), 0.92 (d, *J* = 6.7 Hz, 3H), 0.84 (d, *J* = 6.6 Hz, 3H), 0.17 (s, 9H).

Alcohol 91 To a dry flask under N_2 was added Ranel Ni (~0.1 mL, suspension in water), which was then washed with EtOH (2 x 1 mL). EtOH (0.5 mL) was added to the flask followed by **90** (16.7 mg, 0.045 mmol, 1.0 equiv.) as a solution in EtOH (0.5 mL) and the suspension was stirred until the full consumption of starting material was indicated by TLC (silica gel, hexanes:EtOAc 17:3). The reaction was then decanted, and the Raney Ni was washed with EtOH (3 x 1 mL) and the combined organic layers were filtered through celite and concentrated. The resultant residue was purified by flash column chromatography (silica gel, hexane:EtOAc 9:1) to give **91** (11.2 mg, 92%) as a colorless oil. **91** R_f = 0.40 (silica gel, hexanes:EtOAc 17:3); ^{1}H NMR (400 MHz, $CDCl_3$) δ 3.43 (dd, *J* = 10.7, 6.0 Hz, 1H), 3.37 (dd, *J* = 10.7, 5.3 Hz, 1H), 1.71 (ddq, *J* = 10.5, 6.8, 3.5 Hz, 1H), 1.64 – 1.40 (m, 1H), 1.40 – 1.20 (m, 3H), 0.90 (d, *J* = 6.9 Hz, 3H), 0.86 (s, 3H), 0.80 (d, *J* = 6.7 Hz, 3H), 0.53 – 0.43 (m, 2H), -0.03 (s, 9H).

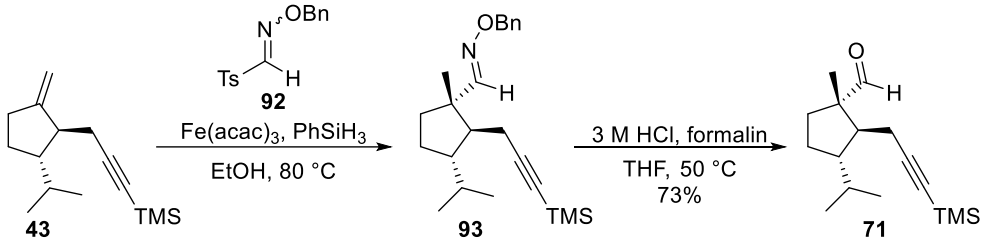

Oxime 93 To a flask was added olefin **43** (50 mg, 0.21 mmol, 1.0 equiv.) as a solution in EtOH (1.7 mL) followed by oxime **92** (88.2 mg, 0.32 mmol, 1.5 equiv.), $Fe(acac)_3$ (15 mg, 0.064 mmol, 30 mol%), and $PhSiH_3$ (40 μL, 0.32 mmol, 1.5 equiv.) then the red suspension was placed in a preheated oil bath at 80 ˚C until full consumption of starting material was indicated by TLC (silica gel, hexanes), usually 1 hr. Then the reaction was cooled to 23 ˚C and diluted with brine (4 mL) and extracted with Et_2O (3 x 5 mL). The combined organic layers were washed with brine (5 mL), dried with $MgSO_4$, and concentrated. The resultant residue was purified first by a short silica plug (hexanes:EtOAc 9:1) to remove inorganic salts followed by flash column chromatography (silica

gel, hexanes:Et_2O 49:1) to give **93** (57 mg, 73%, 1:1. 5 *Z*:*E*) as a colorless oil. 93: R_f = 0.39 (silica gel, hexanes:Et_2O 19:1); ^1H NMR (400 MHz, $CDCl_3$) δ 7.43 (s, 1H), 7.40 – 7.27 (m, 5H), 5.04 (s, 1H), 4.91 (dd, *J* = 4.4, 2.3 Hz, 1H), 2.39 – 2.13 (m, 4H), 1.95 – 1.58 (m, 6H), 1.53 – 1.28 (m, 3H), 1.28 – 1.17 (m, 1H), 1.06 (s, 3H), 0.96 – 0.78 (m, 6H), 0.14 (s, 9H).

Aldehyde 71 To a flask was added **93** (57 mg, 0.16 mmol, 1.0 equiv.) as a solution in THF (2 mL) followed by formalin (0.8 mL) and 3 M HCl (2 mL). The solution was then heated to 50 ˚C for 12 hr. The reaction was the concentrated and extracted with Et_2O (3 x 5 mL). The combined organic layers were dried with $MgSO_4$ and concentrated. The resultant residue was purified by flash column chromatography (silica gel, hexanes:Et_2O 49:1) to give **71** (33 mg, 80%) as a colorless oil. **71**: R_f = 0.37 (silica gel, hexanes:Et_2O 19:1); ^1H NMR (400 MHz, $CDCl_3$) δ 9.49 (s, 1H), 2.38 – 2.27 (m, 1H), 2.22 – 2.02 (m, 2H), 1.87 – 1.65 (m, 4H), 1.52 – 1.21 (m, 3H), 1.11 (s, 3H), 0.93 (d, *J* = 6.7 Hz, 3H), 0.86 (d, *J* = 6.7 Hz, 3H), 0.13 (s, 9H).

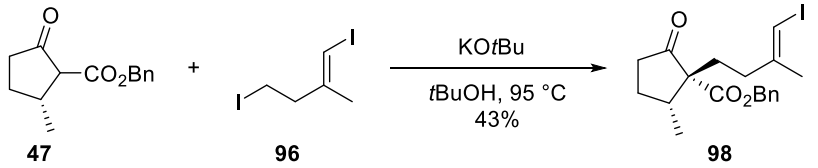

47 96 98

Vinyl Iodide 98 To a flask was added ketoester **47** (4.12 g, 17.8 mmol, 1.0 equiv), *t*BuOH (18 mL), and KO*t*Bu to give a solid yellow mass that was heated to 95 ˚C for 10 min to give a orange suspension. The flask was removed from the oil bath, then diiodide **96**[3] (6.85 g, 21.3 mmol, 1.2 equiv.) was added to give a white suspension that was was once again heated to 95 ˚C for 12 hr. The reaction was then cooled to 23 ˚C diluted with DI H_2O (40 mL), and then extracted with Et_2O (3 x 50 mL). The combined organic fractions were dried with $MgSO_4$ and concentrated. The resultant residue was purified by gravity column chromatography (silica gel, CH_2Cl_2) to give **98** (3.32 g, 43%). **98** R_f = 0.76 (silica gel, hexanes:EtOAc 9:1); ^1H NMR (400 MHz, $CDCl_3$) δ 7.41 –

7.26 (m, 5H), 5.93 – 5.88 (m, 1H), 5.18 (d, *J* = 12.3 Hz, 1H), 5.07 (d, *J* = 12.3 Hz, 1H), 2.58 – 2.47 (m, 1H), 2.47 – 2.34 (m, 1H), 2.28 – 1.95 (m, 4H), 1.82 (s, 3H), 1.87 – 1.64 (m, 2H), 0.99 (d, *J* = 6.8 Hz, 3H).

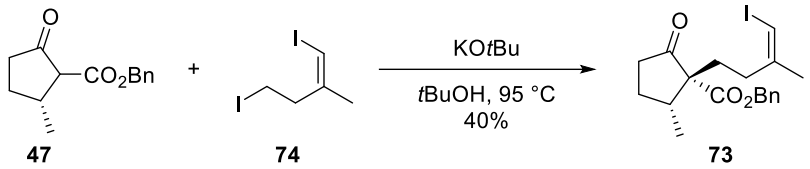

Vinyl Iodide 173 Using the same procedure as **98**, ketoester **47** (721 mg, 3.11 mmol, 1.0 equiv) and diiodide **74**[3] (1.10 g, 3.46 mmol, 1.1 equiv.) was converted into vinyl iodide **73**. The reaction was worked as usual and the resultant residue was purified by gravity column chromatography (silica gel, CH_2Cl_2) to give **73** (529 mg, 40%) as a light-yellow oil. **73** R_f = 0.79 (silica gel, hexanes:EtOAc 9:1); ^{1}H NMR (400 MHz, $CDCl_3$) δ 7.38 – 7.29 (m, 5H), 5.85 – 5.79 (m, 1H), 5.18 (d, *J* = 12.3 Hz, 1H), 5.09 (d, *J* = 12.3 Hz, 1H), 2.59 – 2.48 (m, 1H), 2.48 – 2.34 (m, 2H), 2.30 – 2.13 (m, 1H), 2.13 – 1.58 (m, 8H), 1.02 (d, *J* = 7.0 Hz, 3H); ^{13}C NMR (101 MHz, $CDCl_3$) δ 216.12, 170.48, 147.22, 135.46, 128.75, 128.55, 128.45, 74.75, 66.93, 62.75, 53.57, 39.83, 38.96, 33.75, 31.09, 28.72, 28.32, 23.32, 15.94.

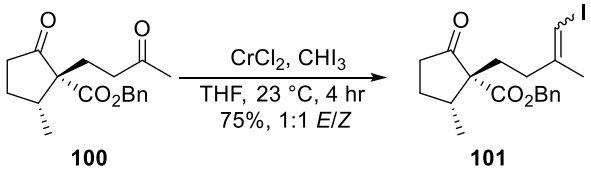

Vinyl iodide 101 To a dry flask in the glovebox was added anhydrous $CrCl_2$ (4.92 g, 40 mmol, 8.0 equiv.) then the flask was sealed and removed from the glovebox. Degassed THF (20 mL) was added to give a green/white suspension. Diketone **100** (1.51 g, 5 mmol, 1.0 equiv.) was added as a solution in degassed THF (15 mL) followed by CHI_3 (3.98 g, 10 mmol, 2.0 equiv.) as a solution

in degassed THF (15 mL). The dark red suspension was stirred at 23 ˚C until full consumption of the starting material was indicated by TLC (silica gel, CH_2Cl_2), usually 4-5 hr. The reaction was then poured into 1M HCl (100 mL) and then extracted with Et_2O (3 x 50 mL). The combined organic layer was then dried with $MgSO_4$ and concentrated. The resultant residue was purified by flash column chromatography to give **101** (1.6 g, 75%).

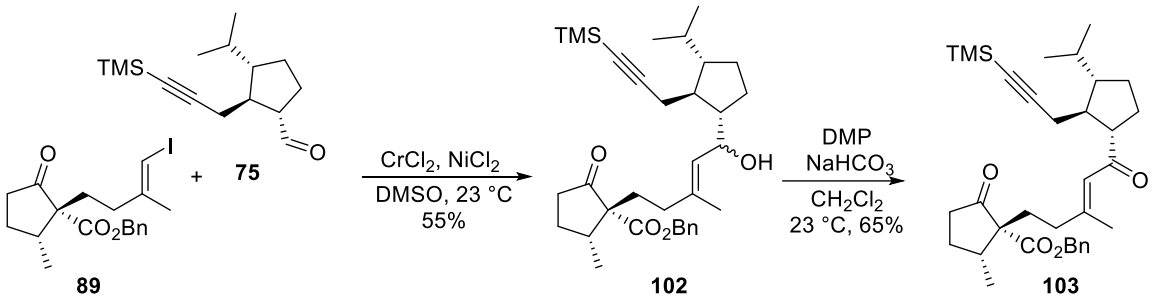

Allylic alcohol 102 To a dry vial in the glovebox was added $CrCl_2$ (85.4 mg, 0.7 mmol, 7.0 equiv.), $NiCl_2$ (1.3 mg, 0.01 mmol, 10 mol%), and DMSO (1.0 mL) to give a dark blue suspension that was stirred for 10 min at 23 ˚C. Then aldehyde **75** (25 mg, 0.1 mmol, 1.0 equiv.) was added as a solution in DMSO (0.25 mL) followed by vinyl iodide **89** (63.9 mg, 0.15 mmol, 1.5 equiv.) as a solution in DMSO (0.25 mL) and the reaction was stirred at the same temperature for 20 hr. The reaction was then removed from the glovebox, diluted with DI H_2O (4 mL) and EtOAc (4 mL), and was stirred for 15 min. The layers were separated, and the aqueous layer was extracted with EtOAc (3 x 5 mL) and the combined organic layers were washed with DI H_2O (3 x 5 mL), dried with $MgSO_4$, and concentrated. The resultant residue was purified by flash column chromatography (silica gel, hexanes:acetone 9:1) to give **102** (31 mg, 55%) as a colorless oil. **102** R_f = 0.18 (silica gel, hexanes:acetone 9:1); ^{1}H NMR (400 MHz, $CDCl_3$) δ 7.40 – 7.27 (m, 5H), 5.26 – 5.12 (m, 2H), 5.07 (d, *J* = 12.3 Hz, 1H), 2.58 – 2.34 (m, 2H), 2.33 – 2.09 (m, 3H), 2.08 –

1.92 (m, 1H), 1.92 – 1.66 (m, 5H), 1.69 – 1.21 (m, 5H), 1.00 (d, *J* = 6.9 Hz, 3H), 0.84 (d, *J* = 6.7 Hz, 3H), 0.15 (s, 8H).

Enone 103 To a vial was added **102** (31 mg, 0.055 mmol, 1.0 equiv.) as a solution in CH_2Cl_2 (0.6 mL) followed by DMP (35 mg, 0.083 mmol, 1.5 equiv.) and $NaHCO_3$ (19 mg, 0.22 mmol, 4.0 equiv.) to give a white suspension that was stirred at 23 ˚C overnight. The reaction was then concentrated and the resultant residue was purified by flash column chromatography (silica gel, hexanes:EtOAc 19:1 to 9:1) to give enone **103** (19.7 mg, 65%) as a colorless oil. **103** R_f = 0.38 (silica gel, hexanes:acetone 9:1); ^{1}H NMR (400 MHz, $CDCl_3$) δ 7.40 – 7.27 (m, 5H), 6.13 – 6.06 (m, 1H), 5.18 (d, *J* = 12.3 Hz, 1H), 5.08 (d, *J* = 12.2 Hz, 1H), 2.82 (dt, *J* = 9.0, 6.5 Hz, 1H), 2.60 – 2.48 (m, 1H), 2.41 – 2.13 (m, 5H), 2.11 (d, *J* = 1.2 Hz, 3H), 2.09 – 1.93 (m, 3H), 1.89 – 1.54 (m, 4H), 1.47 – 1.34 (m, 1H), 1.00 (d, *J* = 6.8 Hz, 3H), 0.92 (d, *J* = 6.7 Hz, 3H), 0.84 (d, *J* = 6.7 Hz, 3H), 0.13 (s, 9H).

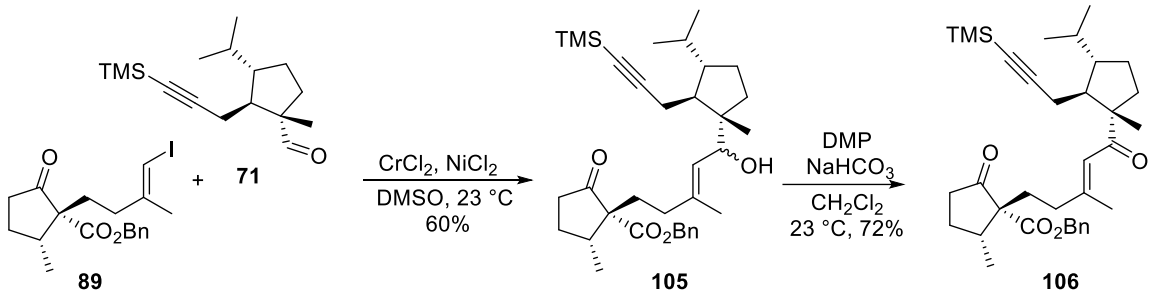

Allylic Alcohol 105 Using the same procedure as **102**, vinyl iodide **89** (31 mg, 0.073 mmol, 1.1 equiv.) and aldehyde **71** (17.5 mg, 0.060 mmol, 1.0 equiv), were converted into **105**. The reaction was worked up as usual and the resultant residue was purified by flash column chromatography (silica gel, hexanes:acetone 9:1) to give **105** (20.4 mg, 60%) as a colorless oil that contained an unidentified impurity that was inseparable by column chromatography. **105** R_f = 0.21 (silica gel, hexanes:acetone 9:1).

Enone 106 Using the same procedure **103**, allylic alcohol **105** (21 mg, 0.037 mmol, 1.0 equiv.) was converted to enone **106**. The reaction was worked up as usual and the resultant residue was purified by flash column chromatography (silica gel, hexanes:acetone 19:1) to give **106** (15 mg, 72%, 37% over 2 steps) as a colorless oil. **106** R_f = 0.40 (silica gel, hexanes:acetone 9:1); ^{1}H NMR (400 MHz, $CDCl_3$) δ 7.40 – 7.24 (m, 5H), 6.26 – 6.21 (m, 1H), 5.19 (d, *J* = 12.3 Hz, 1H), 5.08 (d, *J* = 12.2 Hz, 1H), 2.60 – 2.48 (m, 1H), 2.41 – 2.13 (m, 4H), 2.07 (d, *J* = 1.2 Hz, 2H), 2.06 – 1.94 (m, 2H), 1.94 – 1.60 (m, 4H), 1.46 (dt, *J* = 12.5, 7.1 Hz, 1H), 1.39 – 1.22 (m, 1H), 1.15 (s, 3H), 1.00 (d, *J* = 6.8 Hz, 3H), 0.92 (d, *J* = 6.7 Hz, 3H), 0.83 (d, *J* = 6.7 Hz, 3H), 0.11 (s, 9H).

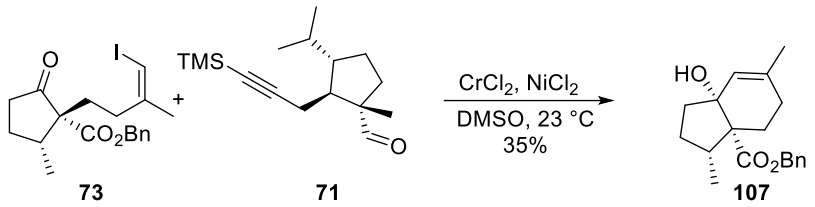

73 **71** **107**

Alcohol 107 Vinyl iodide **73** (31.3 mg, 0.074 mmol, 1.5 equiv) and aldehyde **71** (13 mg, 0.049 mmol, 1.5 equiv.) were reacted using the same procedure as **102**. The resultant residue was purified by flash column chromatography (silica gel, hexanes:acetone 19:1) to give bicycle **107** (5.1 mg, 35%) as a colorless oil. **107** R_f = 0.34 (silica gel, hexanes:acetone 9:1); ^{1}H NMR (500 MHz, $CDCl_3$) δ 7.41 – 7.29 (m, 5H), 5.42 – 5.38 (m, 1H), 5.20 (d, *J* = 12.3 Hz, 1H), 5.13 (d, *J* = 12.4 Hz, 1H), 3.69 (s, 1H), 2.15 – 1.99 (m, 3H), 1.97 – 1.76 (m, 4H), 1.64 (s, 3H), 1.66 – 1.56 (m, 2H), 0.99 (d, *J* = 7.1 Hz, 3H).

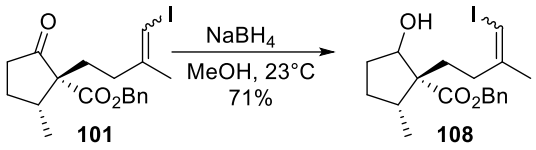

Alcohol 108 To a colorless solution of **101** (36 mg, 0.85, 1.0 equiv.) in MeOH (1 mL) at 0 ˚C was added $NaBH_4$ (4.6 mg, 0.12 mmol, 1.4 equiv.) and the reaction was stirred for 20 min. The reaction was then concentrated and then saturated NH_4Cl (2 mL) and CH_2Cl_2 (2 mL) were added. The layers were separated, and the aqueous layer was extracted with CH_2Cl_2 (3 x 3 mL). The combined organic layers were dried with $MgSO_4$ and concentrated. The resultant residue was purified by flash column chromatography (silica gel, hexanes:EtOAc 9:1) to give **108** (30.6 mg, 71%, 1:1 dr) as a colorless oil. **108** R_f = 0.72 (silica gel, hexanes:acetone 4:1); ^{1}H NMR (400 MHz, $CDCl_3$) δ 7.44 – 7.28 (m, 10H), 5.81 – 5.73 (m, 2H), 5.30 – 5.15 (m, 3H), 5.10 (d, *J* = 12.1 Hz, 1H), 4.26 – 4.00 (m, 2H), 3.20 (d, *J* = 8.4 Hz, 1H), 3.11 (d, *J* = 9.3 Hz, 1H), 2.56 – 2.40 (m, 2H), 2.22 – 1.95 (m, 5H), 1.99 – 1.79 (m, 3H), 1.78 (d, *J* = 1.5 Hz, 3H), 1.74 (d, *J* = 1.1 Hz, 3H), 1.60 – 1.42 (m, 1H), 1.42 – 1.22 (m, 2H), 0.98 (d, *J* = 6.9 Hz, 3H), 0.95 (d, *J* = 6.7 Hz, 3H).

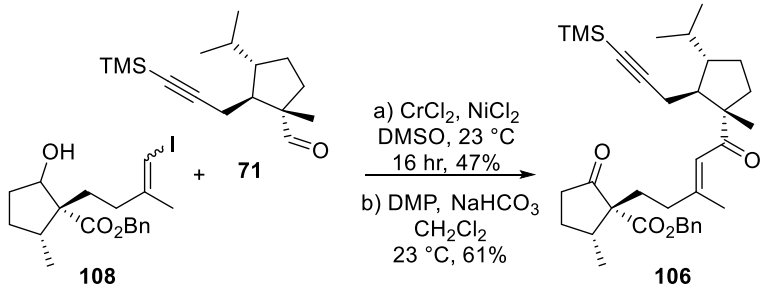

Enone 106 Using the same procedure as **102**, vinyl iodide **108** (30.6 mg, 0.071 mmol, 1.5 equiv.) and aldehyde **71** (9.0 mg, 0.034 mmol, 1.0 equiv.), were converted into the NHK product. The reaction was worked up as usual and the resultant residue was purified by flash column

chromatography (silica gel, hexanes:EtOAc 9:1 to 4:1) to give the NHK product (9 mg, 47%) as a colorless oil. R_f = 0.23 (silica gel, hexanes:acetone 4:1).

Using the same procedure as **103**, the above NHK product (9.0 mg, 0.016 mmol, 1.0 equiv.) was converted to enone **106**. The reaction was worked up as usual and the resultant residue was purified by flash column chromatography (silica gel, hexanes:acetone 19:1) to give **106** (5.5 mg, 61%, 29% over 2 steps) as a colorless oil. Spectral data matched that for **106** prepared from vinyl iodide **89**.

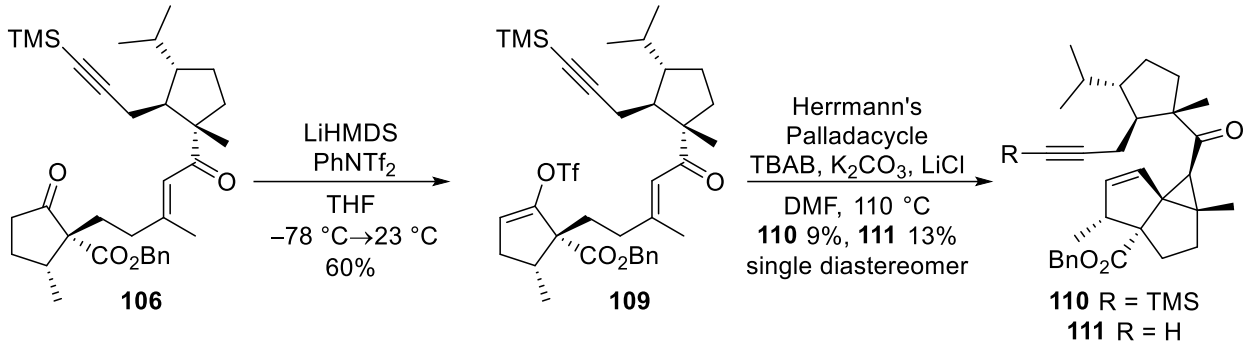

Triflate 109 To a dry flask was added **106** (24 mg, 0.043 mmol, 1.0 equiv.) which was then dried azeotropically with benzene (3 x 1 mL) then THF (0.3 mL) was added to give a colorless solution. The solution was cooled to –78 ˚C and LiHMDS (0.05 mL, 1.0 M THF, 1.1 equiv.) then the light-yellow reaction was stirred at the same temperature for 1 hr. $PhNTf_2$ (23 mg, 0.0645 mmol, 1.5 equiv.) was added as a solution in THF (0.13 mL) and the reaction was allowed to warm to 23 ˚C overnight. The reaction was quenched with saturated $NaHCO_3$ (2 mL) and was diluted with DI H_2O (2 mL) and Et_2O (5 mL). The layers were separated, and the aqueous layer was extracted with Et_2O (3 x 5 mL). The combined organic layers were washed with DI H_2O (3 x 5 mL), dried with MgSO4, and concentrated. The resultant residue was then purified by flash column

chromatography (silica gel, hexanes:EtOAc 19:1 to 9:1) to give **109** (18 mg, 60%). as a colorless oil. **109** R_f = 0.22 (silica gel, hexanes:EtOAc 9:1); ^{1}H NMR (400 MHz, $CDCl_3$) δ 7.35 (d, *J* = 2.6 Hz, 5H), 6.28 – 6.23 (m, 1H), 5.86 (t, *J* = 2.6 Hz, 1H), 5.23 (d, *J* = 12.1 Hz, 1H), 5.10 (d, *J* = 12.2 Hz, 1H), 2.54 (ddd, *J* = 15.5, 8.0, 2.9 Hz, 1H), 2.49 – 2.17 (m, 5H), 2.17 – 2.01 (m, 2H), 2.08 (d, *J* = 1.2 Hz, 3H), 2.01 – 1.90 (m, 2H), 1.93 – 1.61 (m, 3H), 1.54 – 1.23 (m, 3H), 1.15 (s, 3H), 0.96 (d, *J* = 7.0 Hz, 3H), 0.93 (d, *J* = 6.8 Hz, 3H), 0.83 (d, *J* = 6.7 Hz, 3H), 0.11 (s, 9H); ^{19}F NMR (376 MHz, $CDCl_3$) δ -73.92.

Cascade reaction of 109 A dry vial was brought into the glovebox then Herrmann's palladacycle (1.2 mg, 0.0013 mmol, 5.0 mol%.), LiCl (0.6 mg, 0.013 mmol, 0.5 equiv.), Bu_4NBr (2 mg, 0.013 mmol, 0.5 equiv.), K_2CO_3 (9 mg, 0.065 mmol, 2.5 equiv.), and DMF (0.2 mL) were added to the vial and the yellow suspension was stirred at 23 ˚C for 15 min. Triflate **109** (18 mg, 0.0259 mmol, 1.0 equiv.) was added as a solution in DMF (0.22 mL) then the vial was sealed and heated to 110 ˚C for 10 hr. The reaction was then diluted with DI H_2O (2 mL) and then was extracted with Et_2O (3 x 4 mL). The combined organic layers were washed with DI H_2O (3 x 2 mL), dried with $MgSO_4$, and concentrated. The resultant residue was then purified by preparatory thin layer chromatography (silica gel, hexanes:EtOAc 19:1) to give vinyl cyclopropane **110** (1.2 mg, 9%) as a colorless oil and alkyne **111** (1.6 mg, 13%) as a colorless oil. **110** R_f = 0.78 (silica gel, hexanes:EtOAc 9:1); ^{1}H NMR (400 MHz, $CDCl_3$) δ 7.35 – 7.27 (m, 6H), 6.27 (dd, *J* = 6.0, 2.9 Hz, 1H), 5.57 (dd, *J* = 5.9, 1.7 Hz, 1H), 5.13 (d, *J* = 12.7 Hz, 1H), 5.05 (d, *J* = 12.8 Hz, 1H), 2.17 (s, 4H), 2.81 – 2.80 (m, 4H), 2.15 – 2.01 (m, 4H), 2.10 – 1.77 (m, 1H), 1.43 (s, 3H), 1.08 (s, 3H), 1.04 – 0.97 (m, 6H), 0.92 (d, *J* = 6.8 Hz, 3H), 0.79 (d, *J* = 6.7 Hz, 3H), 0.12 (s, 9H).

111 R_f = 0.75 (silica gel, hexanes:EtOAc 9:1); ^{1}H NMR (500 MHz, $CDCl_3$) δ 7.34 – 7.23 (m, 5H), 6.26 (dd, *J* = 6.1, 3.0 Hz, 1H), 5.57 (d, *J* = 6.2 Hz, 1H), 5.15 (d, *J* = 12.7 Hz, 1H), 5.02 (d, *J* = 13.1

Hz, 1H), 2.88 – 2.84 (m, 1H), 2.27 (s, 1H), 2.19 – 2.14 (m, 2H), 2.08 – 2.00 (m, 1H), 1.88 (d, *J* = 2.8 Hz, 1H), 1.64 (s, 1H), 1.43 (d, *J* = 0.8 Hz, 3H), 1.09 (d, *J* = 5.3 Hz, 3H), 1.00 (d, *J* = 7.3 Hz, 3H), 0.92 (d, *J* = 6.8 Hz, 3H), 0.80 (d, *J* = 6.7 Hz, 3H).

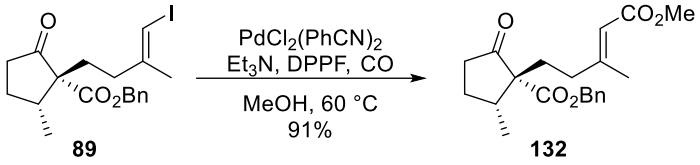

89 132

Enoate 132 To a dry flask was added $PdCl_2(PhCN)_2$ (298 mg, 0.78 mmol, 10 mol%), DPPF (1.29 g, 2.37 mmol, 30 mol%), Et_3N (2.2 mL, 15.6 mmol, 2.0 equiv.), and degassesd MeOH (60 mL) to give a brown suspension. Vinyl iodide **100** (3.32 g, 7.79 mmol, 1.0 equiv.) was added as a solution in degassed MeOH (18 mL) and then CO was bubbled through the reaction for 20 min. The mixture was then heated to 60 ˚C until full consumption of starting material was indicated by TLC (silica gel, hexane:EtOAc 9:1). The reaction was then cooled to 23 ˚C, filtered through celite, and concentrated. The resultant residue was purified by flash column chromatography (silica gel, hexanes:EtOAc 9:1 to 17:3) to give **132** (2.53 g, 91%). **132** R_f = 0.24 (silica gel, hexanes:EtOAc 17:3); ^{1}H NMR (500 MHz, $CDCl_3$) δ 7.39 – 7.27 (m, 5H), 5.69 – 5.65 (m, 1H), 5.18 (d, *J* = 11.9 Hz, 1H), 5.07 (d, *J* = 12.2 Hz, 1H), 3.67 (d, *J* = 1.5 Hz, 3H), 2.58 – 2.49 (m, 1H), 2.36 (td, *J* = 13.4, 4.5 Hz, 1H), 2.28 – 2.17 (m, 2H), 2.14 (d, *J* = 1.6 Hz, 3H), 2.08 – 1.93 (m, 3H), 1.85 – 1.67 (m, 2H), 0.99 (dd, *J* = 7.0, 1.5 Hz, 3H); ^{13}C NMR (101 MHz, $CDCl_3$) δ 215.97, 170.23, 167.28, 159.69, 135.38, 128.78, 128.61, 128.47, 115.60, 66.98, 62.57, 50.98, 40.72, 38.79, 35.38, 30.24, 28.28, 19.02, 15.82.

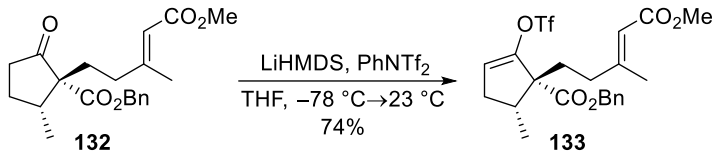

Triflate 133 To a dry flask was added **132** (2.51 g, 7.02 mmol, 1.0 equiv.) as a solution in benzene (8 mL) then **132** was dried azeotropically with benzene (3 x 5 mL) then THF (40 mL) was added to give a colorless solution. The solution was cooled to –78 ˚C and LiHMDS (7.0 mL, 1.0 M THF, 1.0 equiv.) then the light-yellow reaction was stirred at the same temperature for 1 hr. $PhNTf_2$ (3.76 g, 10.53 mmol, 1.5 equiv.) was added as a solution in THF (30 mL) and the reaction was allowed to warm to 23 ˚C overnight. The reaction was quenched with saturated $NaHCO_3$ (50 mL) and was diluted with DI H_2O (50 mL) and Et_2O (60 mL). The layers were separated, and the aqueous layer was extracted with Et_2O (3 x 50 mL). The combined organic layers were washed with DI H_2O (3 x 30 mL), dried with $MgSO_4$, and concentrated. The resultant residue was then purified by flash column chromatography (silica gel, hexanes:EtOAc 23:2 to 4:1) to give **133** (2.55 g, 74%). as a colorless oil. **133** R_f = 0.35 (silica gel, hexanes:EtOAc 9:1); ^{1}H NMR (400 MHz, $CDCl_3$) δ 7.41 – 7.28 (m, 5H), 5.85 (t, *J* = 2.6 Hz, 1H), 5.71 – 5.65 (m, 1H), 5.23 (d, *J* = 12.1 Hz, 1H), 5.10 (d, *J* = 12.2 Hz, 1H), 3.68 (s, 3H), 2.53 (ddd, *J* = 15.6, 8.0, 3.0 Hz, 1H), 2.41 (h, *J* = 7.2 Hz, 1H), 2.31 – 2.19 (m, 1H), 2.15 (d, *J* = 1.3 Hz, 3H), 2.14 – 2.02 (m, 2H), 2.02 – 1.86 (m, 2H), 0.95 (d, *J* = 7.0 Hz, 3H); ^{13}C NMR (101 MHz, $CDCl_3$) δ 171.06, 167.19, 159.04, 148.27, 135.39, 128.72, 128.70, 128.59, 118.40, 115.91, 67.25, 60.74, 51.01, 40.36, 35.58, 35.16, 31.71, 18.92, 16.22.; ^{19}F NMR (376 MHz, $CDCl_3$) δ -73.93.

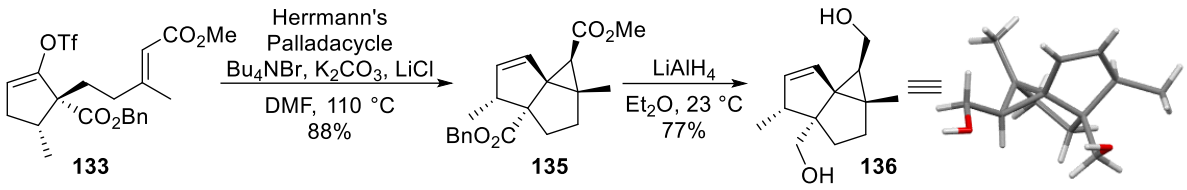

Vinyl cyclopropane 135 A dry Schlenk flask was brought into the glovebox then Herrmann's palladacycle (121 mg, 0.13 mmol, 2.5 mol%), LiCl (109 mg, 2.6 mmol, 0.5 equiv.), Bu_4NBr (400 mg, 2.6 mmol, 0.5 equiv.), K_2CO_3 (1.80 g, 13 mmol, 2.5 equiv.), and DMF (30 mL) were added to the vial and the yellow suspension was stirred at 23 ˚C for 15 min. Triflate **133** (2.55 g, 5.20 mmol, 1.0 equiv.) was added as a solution in DMF (22 mL) then the flask was sealed removed from the glovebox and heated to 110 ˚C for 14 hr. The reaction was then diluted with DI H_2O (40 mL) and then was extracted with Et_2O (3 x 40 mL). The combined organic layers were washed with DI H_2O (3 x 20 mL), dried with $MgSO_4$, and concentrated. The resultant residue was then purified by flash column chromatography (silica gel, hexanes:EtOAc 19:1) to give vinyl cyclopropane **135** (1.45 g, 88%) as a colorless oil. **135** R_f = 0.42 (silica gel, hexanes:EtOAc 9:1); ^{1}H NMR (400 MHz, $CDCl_3$) δ 7.37 – 7.24 (m, 5H), 6.11 (dd, *J* = 6.0, 2.9 Hz, 1H), 5.60 (dd, *J* = 6.0, 1.8 Hz, 1H), 5.18 (d, *J* = 12.7 Hz, 1H), 5.02 (d, *J* = 12.6 Hz, 1H), 3.62 (s, 3H), 2.88 (qdd, *J* = 7.4, 2.9, 1.8 Hz, 1H), 2.17 (s, 2H), 2.10 – 1.86 (m, 4H), 1.64 (s, 0H), 1.20 (s, 3H), 1.03 (d, *J* = 7.4 Hz, 3H); ^{13}C NMR (101 MHz, $CDCl_3$) δ 174.40, 171.16, 136.36, 135.34, 128.51, 127.99, 127.98, 127.03, 69.96, 65.92, 56.49, 51.43, 48.49, 38.18, 37.42, 33.70, 30.71, 15.58, 13.67.

Diol 136 To a dry flask under N_2 was added **135** (68 mg, 0.2 mmol, 1.0 equiv.) as a solution in Et_2O (4 mL) and the colorless solution was cooled to 0 ˚C. $LiAlH_4$ (19 mg, 0.5 mmol, 2.5 equiv.) was added and the reaction was warmed to 23 ˚C. After 3 hr, $LiAlH_4$ (19 mg, 0.5 mmol, 2.5 equiv.) was added to push the reaction to completion. Upon full consumption of starting material as indicated by TLC (silica gel, hexanes:EtOAc 9:1) the reaction was quenched with a saturated

solution of Rochelle's salt (5 mL) and diluted with EtOAc (5 mL) and the mixture was stirred until the phases separated. The layers were then separated and the aqueous layer was extracted with EtOAc (3 x 5 mL). The combined organic layers were dried with $MgSO_4$ then concentrated. The resultant residue was purified by flash column chromatography (silica gel, hexanes:acetone 7:3) to give **136** (32.3 mg, 77%) as a white crystalline solid. X-Ray quality crystals were obtained by recrystallization by slow evaporation from CH_2Cl_2/hexanes. **136** R_f = 0.26 (silica gel, hexanes:acetone 7:3); ^{1}H NMR (500 MHz, $CDCl_3$) δ 5.73 (dd, *J* = 6.0, 1.8 Hz, 1H), 5.60 (dd, *J* = 5.9, 3.1 Hz, 1H), 3.85 (dd, *J* = 11.3, 6.7 Hz, 1H), 3.74 – 3.68 (m, 1H), 3.66 (d, *J* = 11.4 Hz, 1H), 3.46 (d, *J* = 11.3 Hz, 1H), 2.73 (qdd, *J* = 7.5, 3.1, 1.8 Hz, 1H), 2.16 (s, 2H), 2.00 – 1.81 (m, 2H), 1.59 (ddd, *J* = 13.9, 9.0, 2.5 Hz, 1H), 1.40 (dd, *J* = 8.5, 6.7 Hz, 1H), 1.28 – 1.24 (m, 1H), 1.15 (d, *J* = 7.5 Hz, 3H), 1.04 (s, 3H).

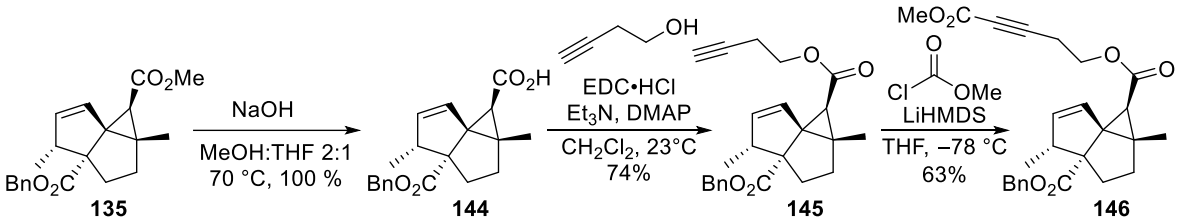

Carboxylic acid 144 To a flask was added **135** (1.02 g, 3.0 mmol, 1.0 equiv.), MeOH:H_2O (150 mL, 2:1), and 3 M NaOH (8 mL, 24 mmol, 8.0 equiv.) and the colorless solution was heated to 70 ˚C until full consumption of the starting material was indicated by TLC (silica gel, hexanes:EtOAc 9:1), usually 12-24 hr. The now yellow reaction was brought to pH 1 with 3 M HCl to give a white suspension that was then extracted with EtOAc (3 x 100 mL). The combined organic layers were dried with Na_2SO_4 and concentrated. The resultant residue was purified by flash column chromatography (silica gel, hexanes:acetone 3:1) to give **144** (1.01 g, 100%) as a light-yellow oil. **144** R_f = 0.33 (silica gel, hexanes:EtOAc 7:3); ^{1}H NMR (400 MHz, $CDCl_3$) δ 7.34 – 7.21 (m, 5H),

6.05 (dd, *J* = 6.0, 2.9 Hz, 1H), 5.56 (dd, *J* = 6.0, 1.8 Hz, 1H), 5.12 (d, *J* = 12.6 Hz, 1H), 5.01 (d, *J* = 12.6 Hz, 1H), 3.60 (s, 0H), 2.89 – 2.79 (m, 1H), 2.06 – 1.80 (m, 4H), 1.19 (d, *J* = 3.2 Hz, 3H), 0.97 (d, *J* = 7.4 Hz, 3H).

Alkyne 145 To a dry flask was added **144** (168 mg, 0.515 mmol, 1.0 equiv.), CH_2Cl_2 (5.2 mL), DMAP (58 mg, 0.515 mmol, 1.0 equiv.), 3-butynol (0.06 mL, 0.775 mmol, 1.5 equiv.), Et_3N (0.14 mL, 1.3 mmol, 2.0 equiv,), and EDC•HCl (148 mg, 0.773 mmol, 1.5 equiv.). The solution was allowed to stir at 23 ˚C until full consumption of starting material was indicated by TLC (silica gel, hexanes:acetone 3:1). Then the reaction was quenched with saturated $NaHCO_3$ (5 mL) and the layers were separated. The aqueous layer was extracted with EtOAc (3 x 5 mL) then the combined organic layers were washed with DI H_2O (3 x 5 mL), dried with $MgSO_4$, and concentrated. The resultant residue was purified by flash column chromatography (silica gel, hexanes:Et_2O 9:1) to give **145** (139 mg, 74%) as a light yellow oil. **145** R_f = 0.28 (silica gel, hexanes:Et_2O 9:1); ^{1}H NMR (400 MHz, $CDCl_3$) δ 7.34 – 7.21 (m, 5H), 6.04 (dd, *J* = 6.0, 2.9 Hz, 1H), 5.56 (dd, *J* = 6.0, 1.8 Hz, 1H), 5.11 (d, *J* = 12.6 Hz, 1H), 5.00 (d, *J* = 12.6 Hz, 1H), 2.88 – 2.67 (m, 1H), 2.06 – 1.81 (m, 4H), 1.19 (d, *J* = 3.2 Hz, 3H), 0.96 (d, *J* = 7.4 Hz, 3H).

Ynoate 146 To a dry flask was added alkyne **145** (100 mg, 0264 mmol, 1.0 equiv.). which was dried azeotropically (3 x 2 mL benzene) then dissolved in THF (0.66 mL) and the colorless solution was cooled to –78 ˚C. Then, LiHMDS (0.32 mL, 1.0 M THF, 1.2 equiv.) was added to give a yellow solution that was stirred at the same temperature for 1 hr. Next, methyl chloroformate (0.06 mL, 0.792 mmol, 3.0 equiv.) was added and the reaction was stirred at the same temperature for 2 hr then the reaction was allowed to warm to 23 ˚C overnight. The reaction was then quenched with saturated NH_4Cl (5 mL), diluted with Et_2O (5 mL), and the layers were separated. The aqueous layer was extracted with Et_2O (3 x 5 mL), dried with $MgSO_4$, filtered and concentrated.

The resultant residue was purified via flash column chromatography (silica gel, hexanes:EtOAc 9:1 to 17:3) to give ynoate **146** as a colorless oil (73 mg, 63%). **146**: R_f = 0.37 (silica gel, hexanes:Et_2O 17:3); ^1H NMR (400 MHz, $CDCl_3$) δ 7.38 – 7.27 (m, 5H), 6.10 (dd, *J* = 6.0, 2.9 Hz, 1H), 5.62 (dd, *J* = 6.0, 1.8 Hz, 1H), 5.16 (d, *J* = 12.7 Hz, 1H), 5.04 (d, *J* = 12.7 Hz, 1H), 4.21 (dt, *J* = 10.8, 6.8 Hz, 1H), 4.11 (dt, *J* = 10.8, 6.7 Hz, 1H), 3.75 (s, 3H), 2.94 – 2.84 (m, 1H), 2.58 (td, *J* = 6.7, 1.8 Hz, 2H), 2.10 – 1.85 (m, 4H), 1.72 (s, 1H), 1.21 (s, 3H), 1.03 (d, *J* = 7.4 Hz, 3H); ^{13}C NMR (101 MHz, $CDCl_3$) δ 174.22, 170.20, 136.22, 135.40, 128.39, 127.91, 127.83, 126.73, 85.06, 69.85, 65.84, 60.71, 56.57, 52.70, 48.35, 38.39, 37.27, 33.46, 30.48, 19.26, 15.45, 13.51.

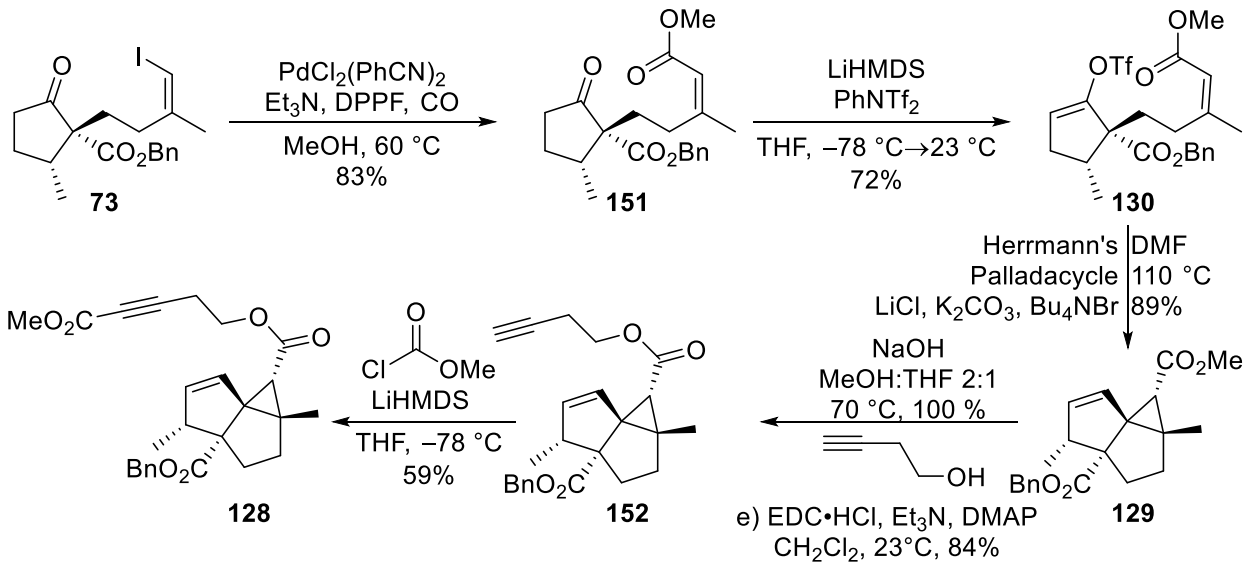

Enoate 151 Using the same procedure as **132**, vinyl iodide **73** (1.8 g, 4.22 mmol, 1.0 equiv.) was converted to enoate **151**. The reaction was worked up as usual and the resultant residue was purified by flash column chromatography (silica gel, hexanes:EtOAc 9:1 to 17:3) to give **151** (1.26 g, 83%) as a colorless oil. **151** R_f = 0.28 (silica gel, hexanes:EtOAc 17:3); ^1H NMR (400 MHz, $CDCl_3$) δ 7.36 – 7.22 (m, 5H), 5.64 – 5.58 (m, 1H), 5.12 (d, *J* = 12.3 Hz, 1H), 5.04 (d, *J* = 12.3 Hz, 1H), 3.62 (s, 3H), 2.91 (td, *J* = 11.2, 5.6 Hz, 1H), 2.54 – 2.38 (m, 2H), 2.24 – 2.08 (m, 2H), 2.07 – 1.95 (m, 1H), 1.99 – 1.87 (m, 2H), 1.86 (d, *J* = 1.4 Hz, 3H), 1.80 – 1.64 (m, 1H), 1.00 (d, *J*

= 6.8 Hz, 3H); ^{13}C NMR (101 MHz, $CDCl_3$) δ 216.31, 170.67, 166.72, 160.35, 135.52, 128.73, 128.50, 128.41, 116.09, 66.86, 63.08, 50.98, 39.36, 39.03, 29.83, 28.41, 28.25, 25.18, 15.97.

Triflate 130 Using the same procedure as **133**, enoate **151** (1.26 g, 3.52 mmol, 1.0 equiv.) was converted to triflate **130**. The reaction was worked up as usual and the resultant residue was purified by flash column chromatography (silica gel, hexanes:EtOAc 49:1 to 4:1) to give **130** (1.24 g, 72%) as a colorless oil. **130** R_f = 0.28 (silica gel, hexanes:EtOAc 4:1); ^{1}H NMR (500 MHz, $CDCl_3$) δ 7.39 – 7.28 (m, 5H), 5.84 (t, *J* = 2.7 Hz, 1H), 5.67 (d, *J* = 1.5 Hz, 1H), 5.22 (d, *J* = 12.2 Hz, 1H), 5.10 (d, *J* = 12.2 Hz, 1H), 3.66 (s, 3H), 3.01 (td, *J* = 12.0, 4.7 Hz, 1H), 2.68 (h, *J* = 7.3 Hz, 1H), 2.56 (ddd, *J* = 15.7, 8.1, 3.0 Hz, 1H), 2.24 (td, *J* = 12.0, 4.6 Hz, 1H), 2.11 (ddd, *J* = 15.7, 7.7, 2.3 Hz, 1H), 1.99 – 1.90 (m, 1H), 1.89 (d, *J* = 1.4 Hz, 3H), 0.98 (d, *J* = 7.0 Hz, 2H); ^{13}C NMR (101 MHz, $CDCl_3$) δ 171.54, 166.65, 159.81, 148.18, 135.55, 128.68, 128.50, 118.42, 116.33, 67.14, 60.94, 50.99, 39.32, 35.35, 30.91, 28.23, 25.21, 16.36.; ^{19}F NMR (376 MHz, $CDCl_3$) δ -73.92.

Vinyl cyclopropane 129 Using the same procedure as **135**, triflate **130** (1.24 g, 2.54 mmol, 1.0 equiv.) was converted to **129**. The reaction was worked up as usual and the resultant residue was purified by flash column chromatography (silica gel, hexanes:EtOAc 19:1 to 9:1) to give **129** (767 mg, 89%) as a colorless oil. **129** R_f = 0.39 (silica gel, hexanes:EtOAc 9:1); ^{1}H NMR (400 MHz, $CDCl_3$) δ 7.39 – 7.27 (m, 5H), 5.59 (dd, *J* = 5.9, 1.8 Hz, 1H), 5.46 (dd, *J* = 5.9, 2.8 Hz, 1H), 5.08 (d, *J* = 12.7 Hz, 1H), 4.98 (d, *J* = 12.8 Hz, 1H), 3.50 (s, 3H), 3.00 (dtdd, *J* = 9.3, 7.5, 4.8, 2.7 Hz, 1H), 2.69 – 2.56 (m, 1H), 2.36 – 2.23 (m, 1H), 2.09 – 1.95 (m, 2H), 1.17 (s, 3H), 1.00 (d, *J* = 7.5 Hz, 3H).

Carboxylic acid 160 Using the same procedure as **144**, vinyl cyclopropane **129** (727 mg, 2.14 mmol, 1.0 equiv.) was converted to **160**. The reaction was worked up as usual and the resultant

residue was purified by flash column chromatography (silica gel, hexanes:acetone 4:1) to give **160** (700 mg, 100%) as a colorless oil. **160** R_f = 0.28 (silica gel, hexanes:acetone 4:1); ^{1}H NMR (500 MHz, $CDCl_3$) δ 7.36 – 7.23 (m, 5H), 5.60 (dd, *J* = 5.9, 1.8 Hz, 1H), 5.46 (dd, *J* = 5.9, 2.9 Hz, 1H), 5.02 (d, *J* = 12.6 Hz, 1H), 4.96 (d, *J* = 12.6 Hz, 1H), 3.03 – 2.95 (m, 1H), 2.63 – 2.54 (m, 1H), 2.36 – 2.27 (m, 1H), 2.04 – 1.94 (m, 3H), 1.19 (s, 3H), 0.99 (d, *J* = 7.5 Hz, 3H).

Alkyne 152 Using the same procedure as **145**, carboxylic acid **16-** (700 mg, 2.15 mmol, 1.0 equiv.) was converted to **152**. The reaction was worked up as usual and the resultant residue was purified by flash column chromatography (silica gel, hexanes:acetone 19:1) to give **152** (657 mg, 84%) as a colorless oil. **152** R_f = 0.33 (silica gel, hexanes:Et_2O 9:1); ^{1}H NMR (500 MHz, $CDCl_3$) δ 7.36 – 7.25 (m, 5H), 5.57 (dd, *J* = 5.9, 1.8 Hz, 1H), 5.44 (dd, *J* = 5.9, 2.9 Hz, 1H), 5.05 (d, *J* = 12.8 Hz, 1H), 4.96 (d, *J* = 12.8 Hz, 1H), 4.04 – 3.89 (m, 2H), 3.02 – 2.94 (m, 1H), 2.67 – 2.57 (m, 1H), 2.38 (td, *J* = 7.0, 2.7 Hz, 2H), 2.34 – 2.24 (m, 1H), 2.06 – 1.95 (m, 2H), 1.93 (t, *J* = 2.7 Hz, 1H), 1.16 (s, 3H), 0.98 (d, *J* = 7.5 Hz, 3H); ^{13}C NMR (101 MHz, $CDCl_3$) δ 174.44, 170.94, 136.55, 136.08, 129.41, 128.46, 128.10, 127.89, 80.38, 69.89, 68.09, 65.68, 61.99, 58.82, 52.46, 39.43, 36.07, 35.36, 33.79, 31.08, 21.48, 19.01, 15.61.

Ynoate 128 Using the same procedure as **146**, alkyne **152** (650 mg, 1.72 mmol, 1.0 equiv.) was converted to **128**. The reaction was worked up as usual and the resultant residue was purified by flash column chromatography (silica gel, hexanes:EtOAc 9:1 to 17:3) to give **128** (442 mg, 59%) as a colorless oil. **128** R_f = 0.15 (silica gel, hexanes:Et_2O 9:1); ^{1}H NMR (500 MHz, $CDCl_3$) δ 7.36 – 7.27 (m, 5H), 5.62 – 5.57 (m, 1H), 5.46 (dd, *J* = 6.1, 2.8 Hz, 1H), 5.05 (d, *J* = 12.7 Hz, 1H), 4.98 (d, *J* = 12.8 Hz, 1H), 4.06 – 3.97 (m, 1H), 3.93 (dt, *J* = 10.8, 6.8 Hz, 1H), 3.76 (s, 3H), 3.00 (d, *J* = 7.8 Hz, 1H), 2.68 – 2.58 (m, 1H), 2.53 (t, *J* = 6.9 Hz, 2H), 2.35 – 2.25 (m, 1H), 2.09 – 1.97 (m, 3H), 1.32 – 1.19 (m, 1H), 1.18 (s, 3H), 1.00 (d, *J* = 7.5 Hz, 3H).

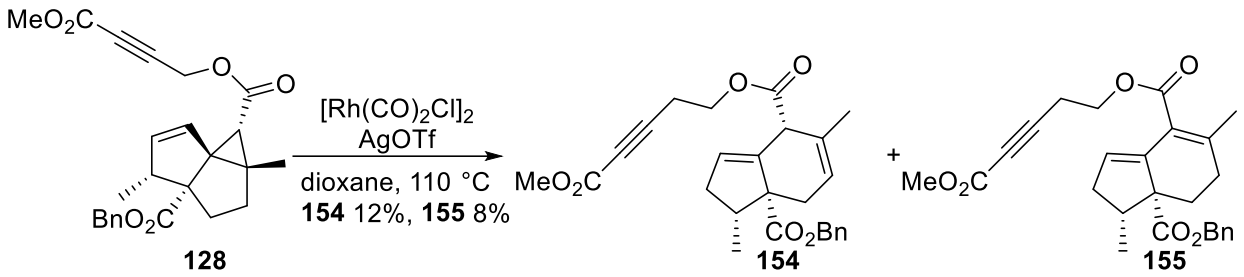

Rh [3+2] of trans-VCP 128 To a dry vial in the glovebox was added $[Rh(CO)_2Cl]_2$ (2.2 mg, 0.0057 mmol, 10 mol%), AgOTf (3.5 mg, 0.014 mmol, 24 mol%), and dioxane (0.74 mL) to give a white suspension that was stirred for 15 min at 23 ˚C. Vinyl cyclopropane **128** (25 mg, 0.057 mmol, 1.0 equiv.) was added as a solution in dioxane (1.6 mL) then the vial was sealed and the now yellow suspension was heated to 110 ˚C for 14 hr. The reaction was then cooled and filtered through a silica plug and concentrated. The resultant residue was purified by preparative thin layer chromatography (silica gel, hexanes:EtOAc 9:1) to give diene **154** (3.1 mg, 12%) and enoate **155** (2.0 mg, 8%). **154** R_f = 0.25 (silica gel, hexanes:EtOAc 17:3); ^{1}H NMR (400 MHz, $CDCl_3$) δ 7.39 – 7.26 (m, 5H), 6.04 – 5.99 (m, 1H), 5.71 (dq, *J* = 5.6, 1.7 Hz, 1H), 5.15 (d, *J* = 12.8 Hz, 1H), 4.90 (d, *J* = 12.8 Hz, 1H), 3.89 (dt, *J* = 10.7, 6.7 Hz, 1H), 3.87 – 3.78 (m, 1H), 3.77 (s, 3H), 3.77 – 3.69 (m, 1H), 3.25 (dd, *J* = 17.0, 5.8 Hz, 1H), 2.56 – 2.44 (m, 1H), 2.43 (t, *J* = 6.7 Hz, 2H), 2.32 – 2.15 (m, 2H), 1.83 (dq, *J* = 17.1, 2.6 Hz, 1H), 1.68 (dt, *J* = 2.6, 1.2 Hz, 3H), 0.98 (d, *J* = 6.7 Hz, 2H); ^{13}C NMR (101 MHz, $CDCl_3$) δ 173.27, 170.70, 154.00, 137.85, 136.27, 131.22, 128.82, 128.61, 128.07, 127.91, 124.96, 85.24, 74.04, 66.50, 61.22, 57.19, 52.80, 48.11, 47.70, 39.83, 35.42, 29.85, 21.90, 19.07, 15.04.

155 R_f = 0.22 (silica gel, hexanes:EtOAc 17:3); ^{1}H NMR (400 MHz, $CDCl_3$) δ 7.37 – 7.26 (m, 5H), 5.91 (s, 1H), 5.16 (d, *J* = 12.7 Hz, 1H), 5.08 (d, *J* = 12.6 Hz, 1H), 4.40 – 4.33 (m, 2H), 3.75 (s, 3H), 2.75 (t, *J* = 6.6 Hz, 2H), 2.49 (dt, *J* = 12.3, 6.0 Hz, 2H), 2.33 (s, 1H), 2.29 – 2.19 (m, 1H), 2.17 (s, 3H), 2.16 – 2.08 (m, 0H), 1.85 (s, 3H), 1.44 – 1.30 (m, 1H), 0.95 (d, *J* = 6.9 Hz, 3H).

4.17 X-Ray Cyrstalographic Data

General information: The diffraction data were measured at 100 K on a Bruker D8 VENTURE diffractometer equipped with a microfocus Mo-target X-ray tube (λ = 0.71073 Å) and PHOTON 100 CMOS detector. Data were collected using ω scans to survey a hemisphere of reciprocal space. Data reduction and integration were performed with the Bruker APEX4 software package (Bruker AXS, version 2021.4-0, 2021). Data were scaled and corrected for absorption effects using the multi-scan procedure as implemented in SADABS (Bruker AXS, version 2014/5, Krause, Herbst-Irmer, Sheldrick & Stalke, *J. Appl. Cryst.* **2015**, *48*, 3-10). The structure was solved by SHELXT (Version 2018/2: Sheldrick, G. M. *Acta Crystallogr*. **2015**, ***A71***, 3-8) and refined by a full-matrix least-squares procedure using OLEX2 (O. V. Dolomanov, L. J. Bourhis, R. J. Gildea, J. A. K. Howard and H. Puschmann. J. Appl. Crystallogr. **2009**, *42*, 339-341) (XL refinement program version 2018/3, Sheldrick, G. M. Acta Crystallogr. **2015**, *C71*, 3-8). Crystallographic data and details of the data collection and structure refinement are listed in Table 1.

Specific details for structure refinement: All atoms were refined with anisotropic thermal parameters. All hydrogen atoms were included in idealized positions for structure factor calculations. All structures are drawn with thermal ellipsoids at 50% probability.

Figure 4.3 ORTEP representation of **136**

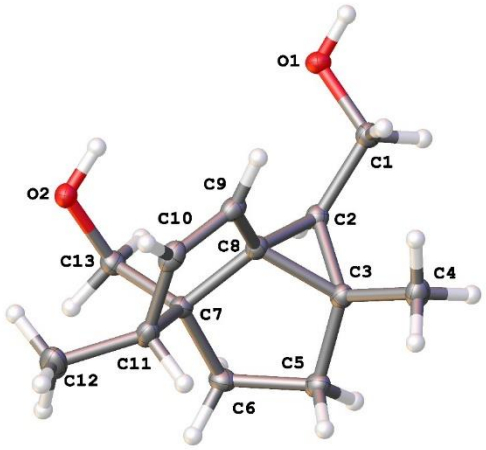

Crystal data and structure refinement for 1044_jkm_1.

Identification code	1044_jkm_1
Empirical formula	$C_{13}H_{20}O_2$
Formula weight	208.29
Temperature/K	100(2)
Crystal system	monoclinic
Space group	$P2_1$
a/Å	9.1811(7)
b/Å	12.2200(10)
c/Å	10.5461(8)
α/°	90
β/°	99.339(2)
γ/°	90
Volume/Å^3	1167.52(16)
Z	4
ρ_{calc}g/cm^3	1.185
μ/mm^{-1}	0.078
F(000)	456.0
Crystal size/mm^3	0.194 × 0.164 × 0.089
Radiation	MoKα (λ = 0.71073)
2Θ range for data collection/°	5.142 to 52.932
Index ranges	$-11 \leq h \leq 11$, $-15 \leq k \leq 15$, $-13 \leq l \leq 13$
Reflections collected	20706
Independent reflections	4802 [R_{int} = 0.0379, R_{sigma} = 0.0372]
Data/restraints/parameters	4802/1/291
Goodness-of-fit on F^2	1.050

Figure 4.3 cont.

Final R indexes [I>=2σ (I)]	R_1 = 0.0348, wR_2 = 0.0672
Final R indexes [all data]	R_1 = 0.0453, wR_2 = 0.0708
Largest diff. peak/hole / e Å^{-3}	0.19/-0.16

$R_{int} = \Sigma \mid F_o^2 - \langle F_o^2 \rangle \mid / \Sigma \mid F_o^2 \mid$

$R1 = \Sigma \mid \mid F_o \mid - \mid F_c \mid \mid / \Sigma \mid F_o \mid$

$wR2 = [\Sigma [w (F_o^2 - F_c^2)^2] / \Sigma [w (F_o^2)^2]]^{1/2}$

Goodness-of-fit = $[\Sigma [w (F_o^2 - F_c^2)^2] / (n-p)^{1/2}$

n: number of independent reflections; p: number of refined parameters

4.18 NMR Spectra

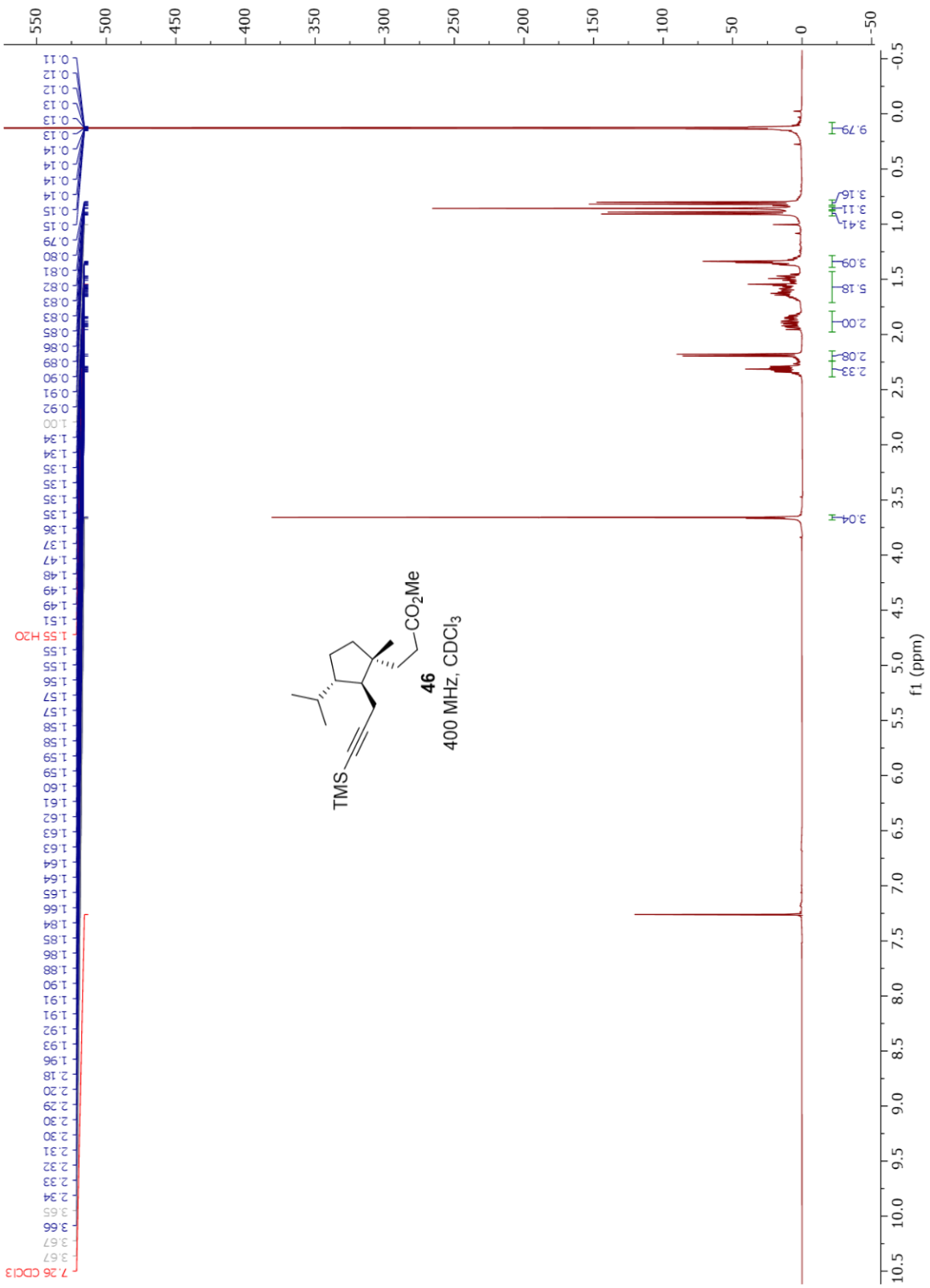

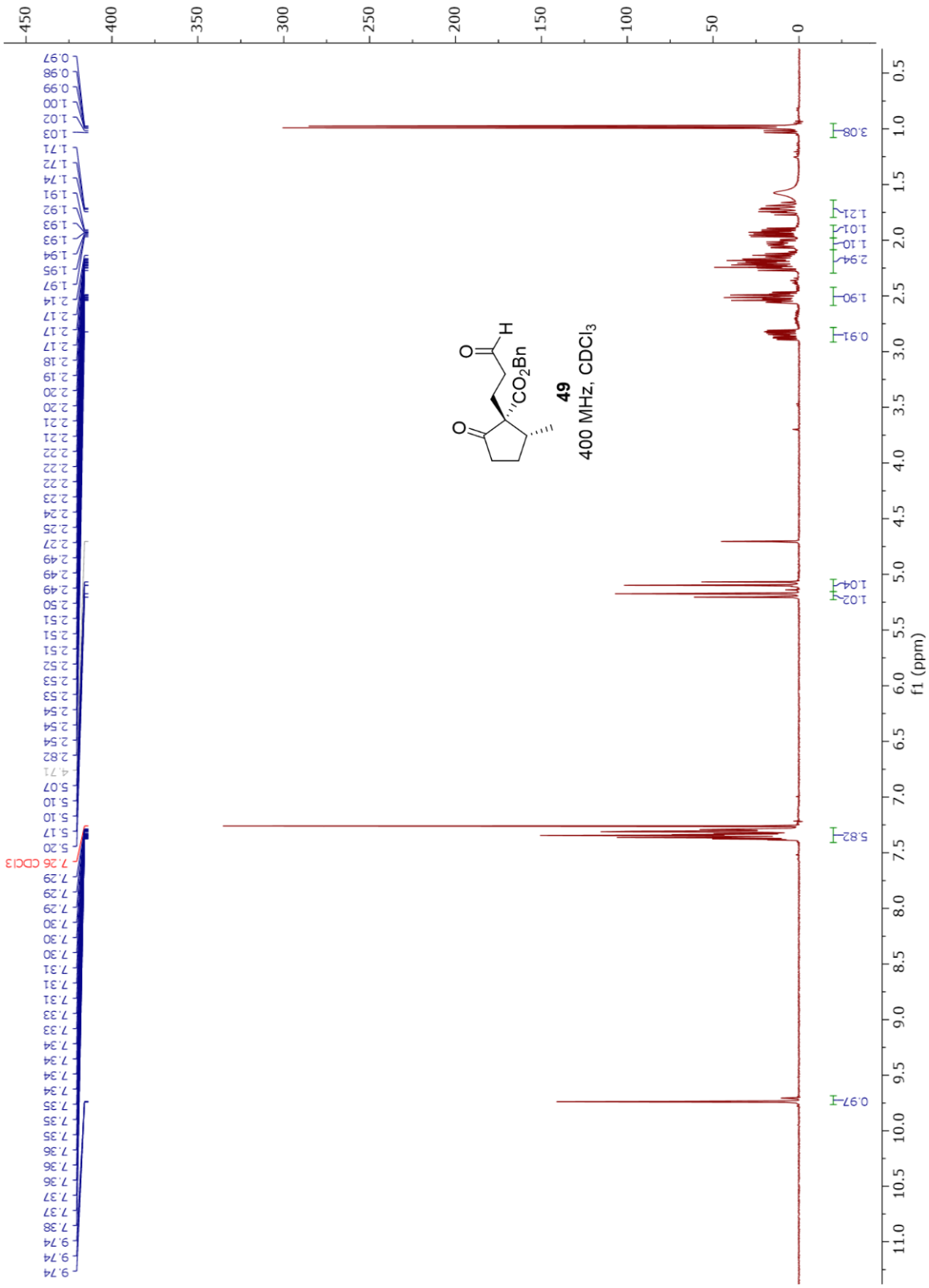
49
400 MHz, CDCl3
CO2Bn
H
O
O
7.26 CDCl3
3.08
1.21
1.01
1.10
2.94
1.90
0.91
1.02
1.04
5.82
0.97
f1 (ppm)

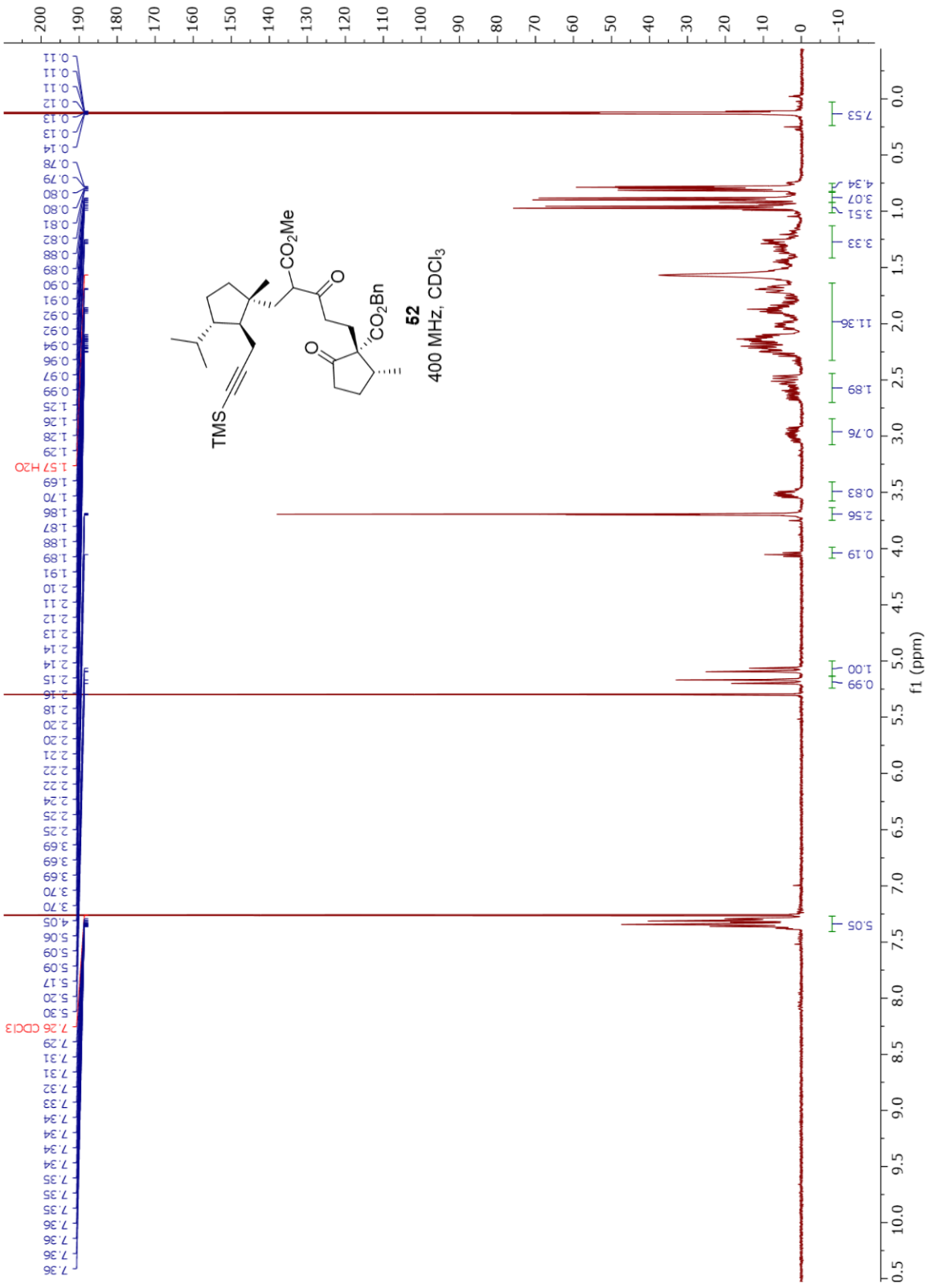
CO2Me
CO2Bn
TMS
O
O
O
52
400 MHz, CDCl3
f1 (ppm)

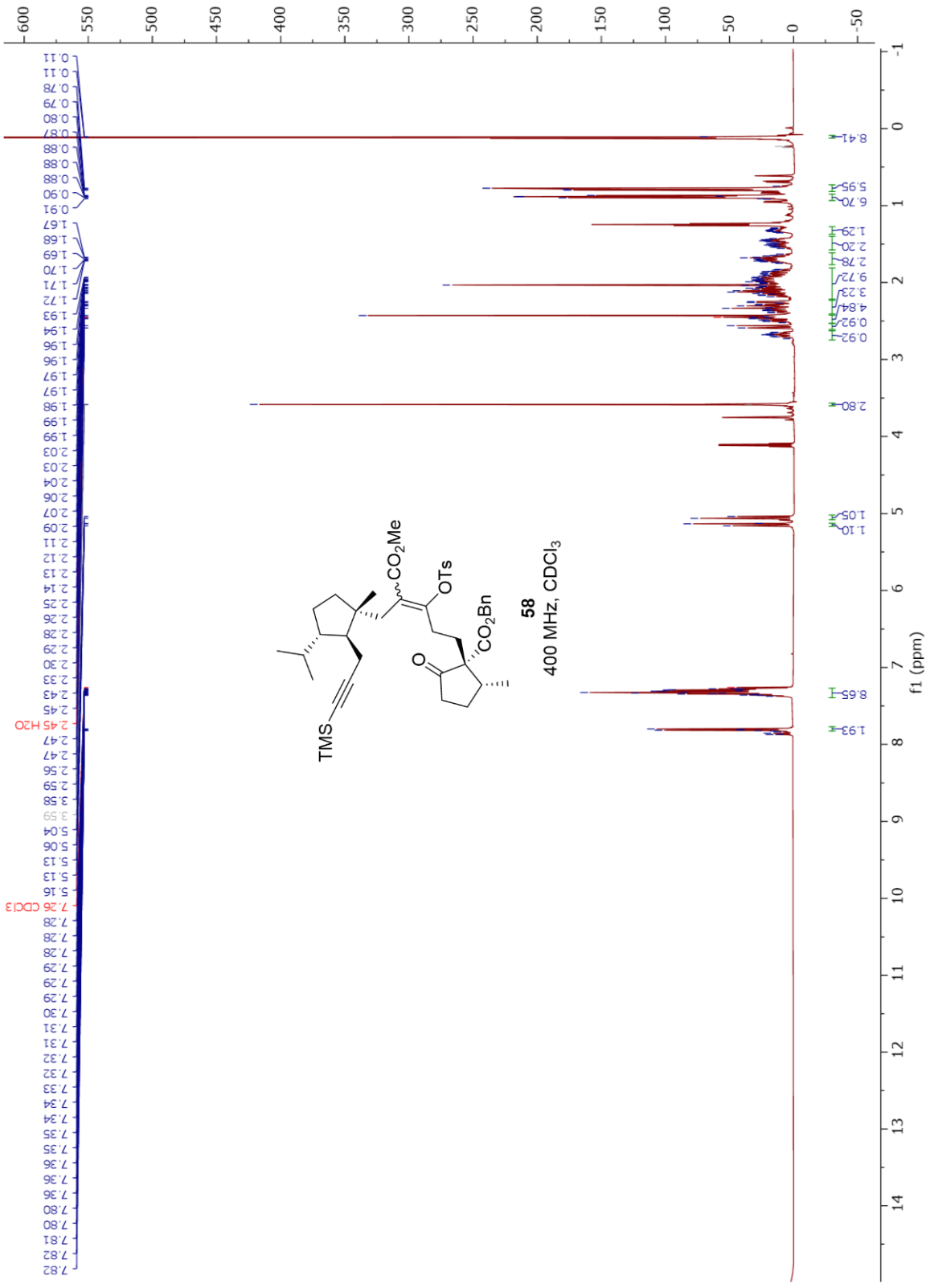
58
400 MHz, CDCl3
CO2Me
OTs
CO2Bn
TMS
O
f1 (ppm)

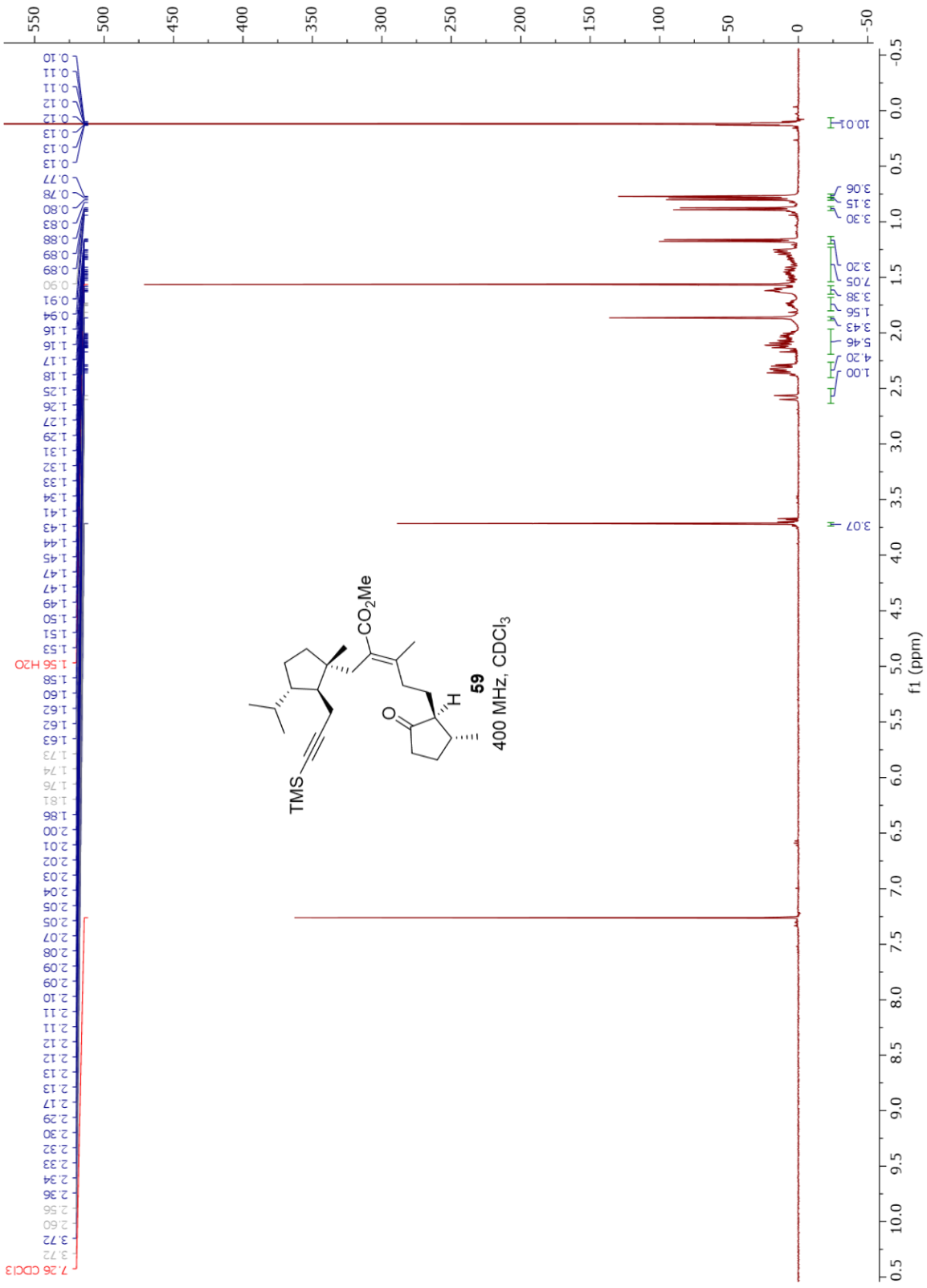
TMS
CO2Me
O
H
59
400 MHz, CDCl3
f1 (ppm)

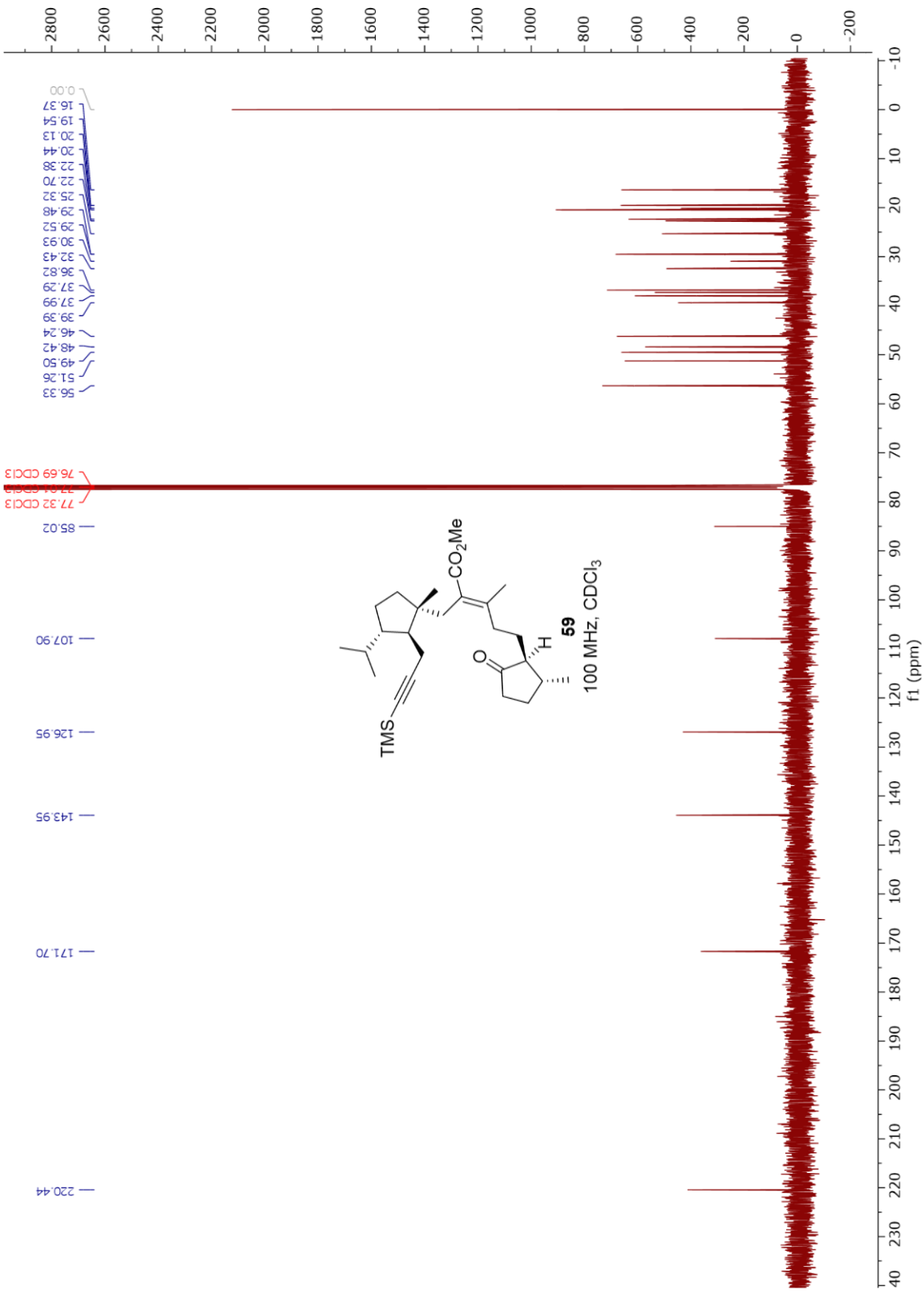
59
100 MHz, CDCl3
CO2Me
TMS
H
O
f1 (ppm)
0.00
16.37
19.54
20.13
20.44
22.38
22.70
25.32
29.48
29.52
30.93
32.43
36.82
37.29
37.99
39.39
46.24
48.42
49.50
51.26
56.33
76.69 CDCl3
77.04 CDCl3
77.32 CDCl3
85.02
107.90
126.95
143.95
171.70
220.44

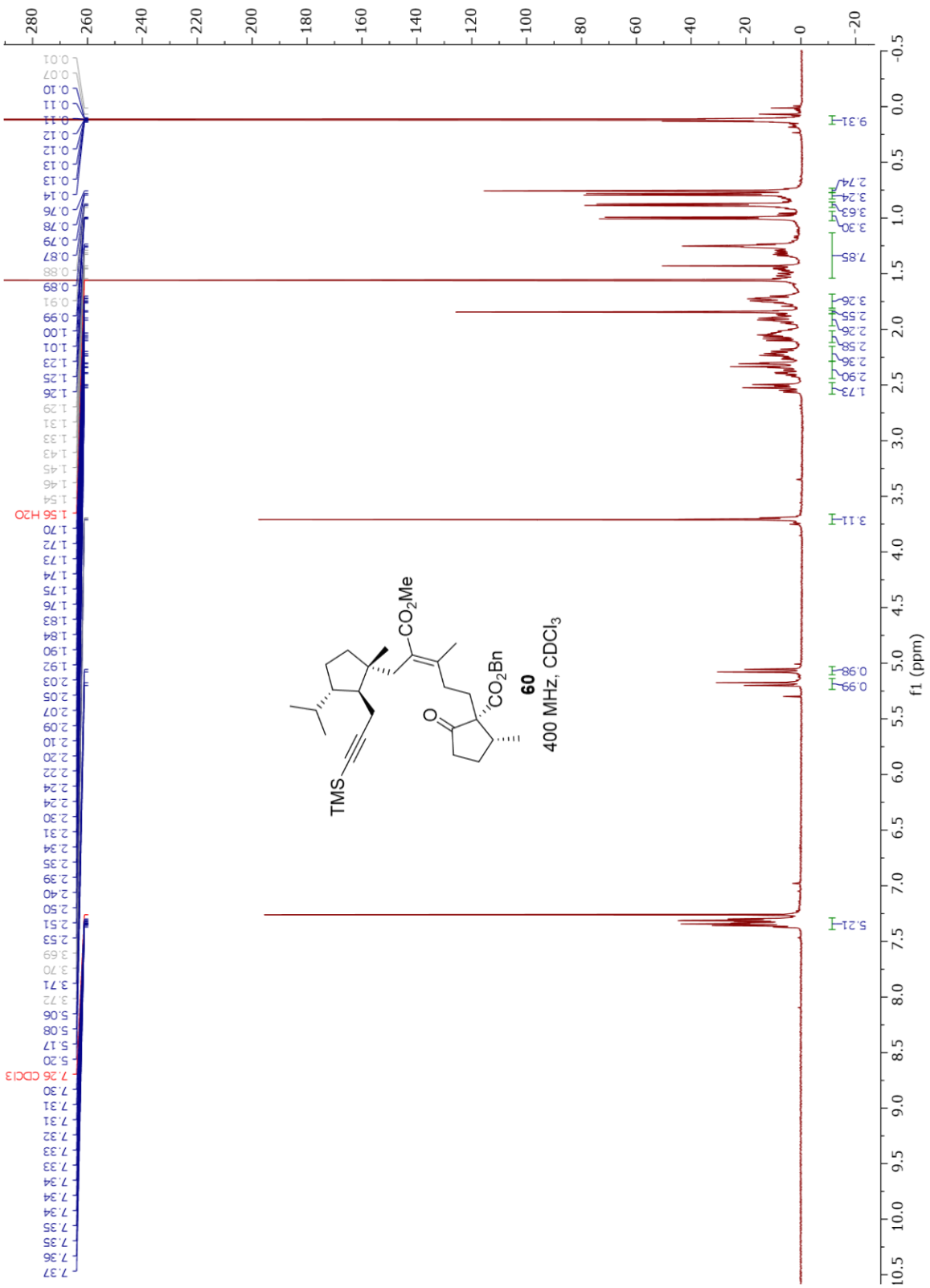
TMS
CO2Me
CO2Bn
O
60
400 MHz, CDCl3
f1 (ppm)

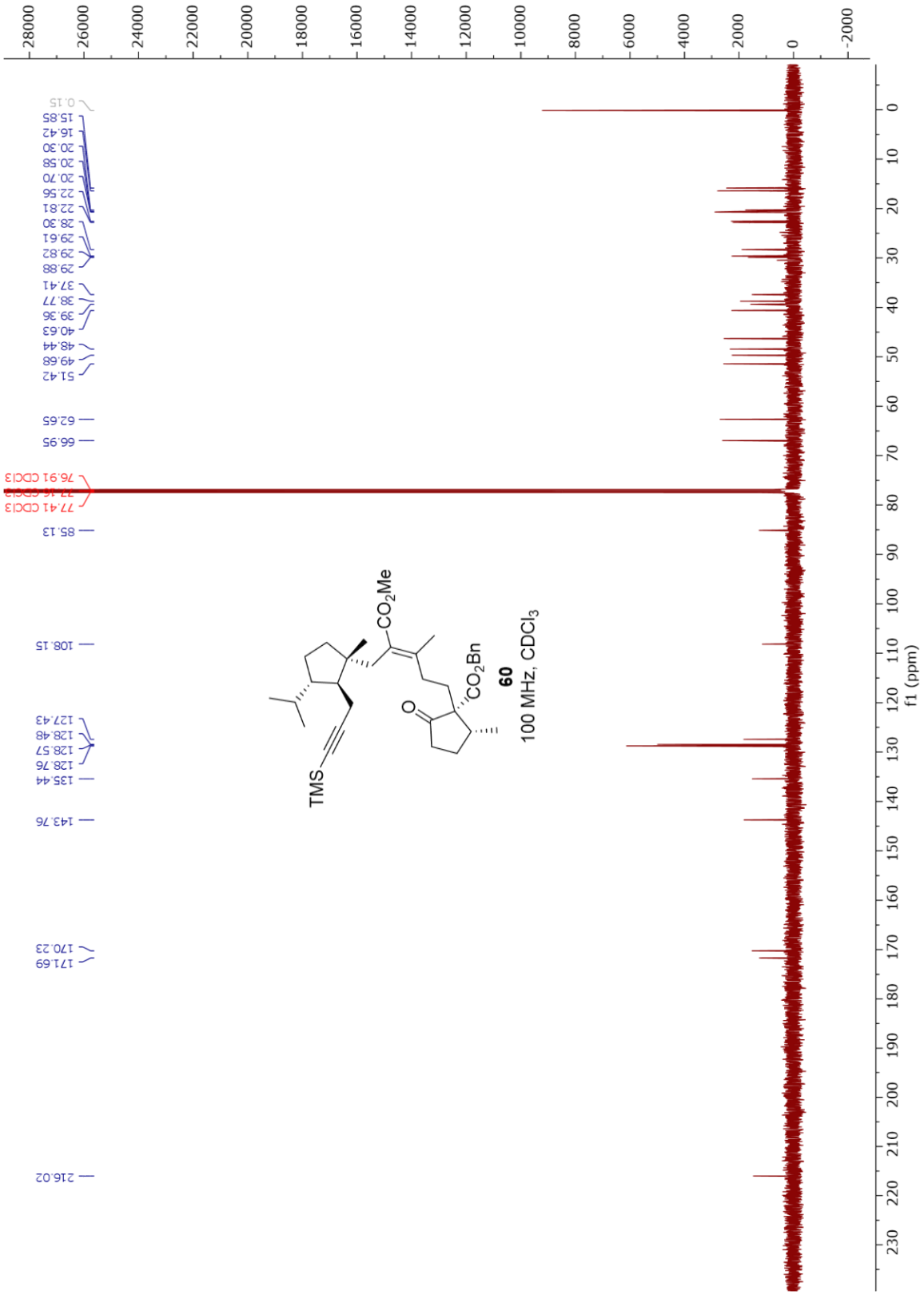
TMS
CO2Me
CO2Bn
O
60
100 MHz, CDCl3
f1 (ppm)

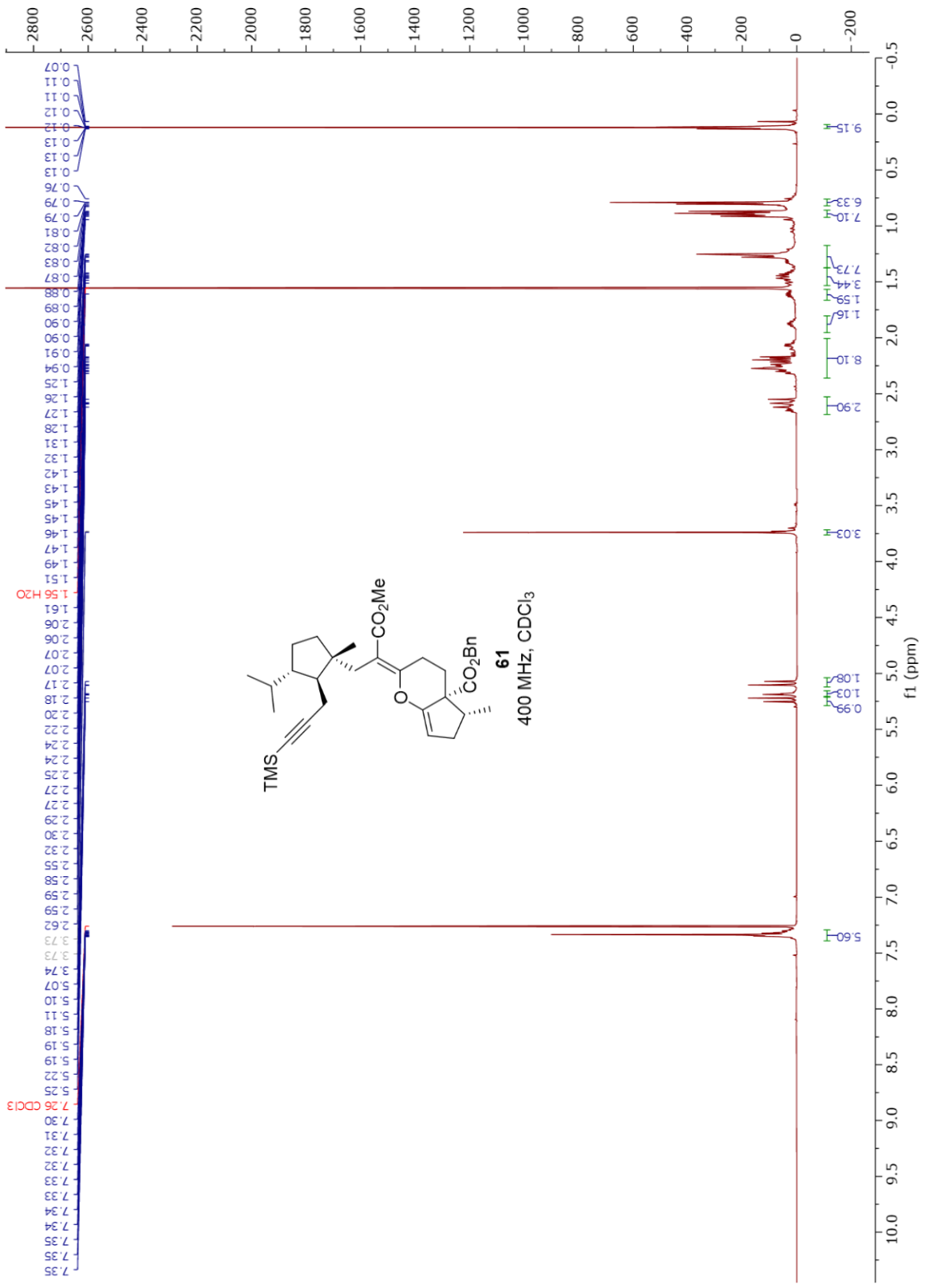
TMS
CO2Me
CO2Bn
O
61
400 MHz, CDCl3
f1 (ppm)

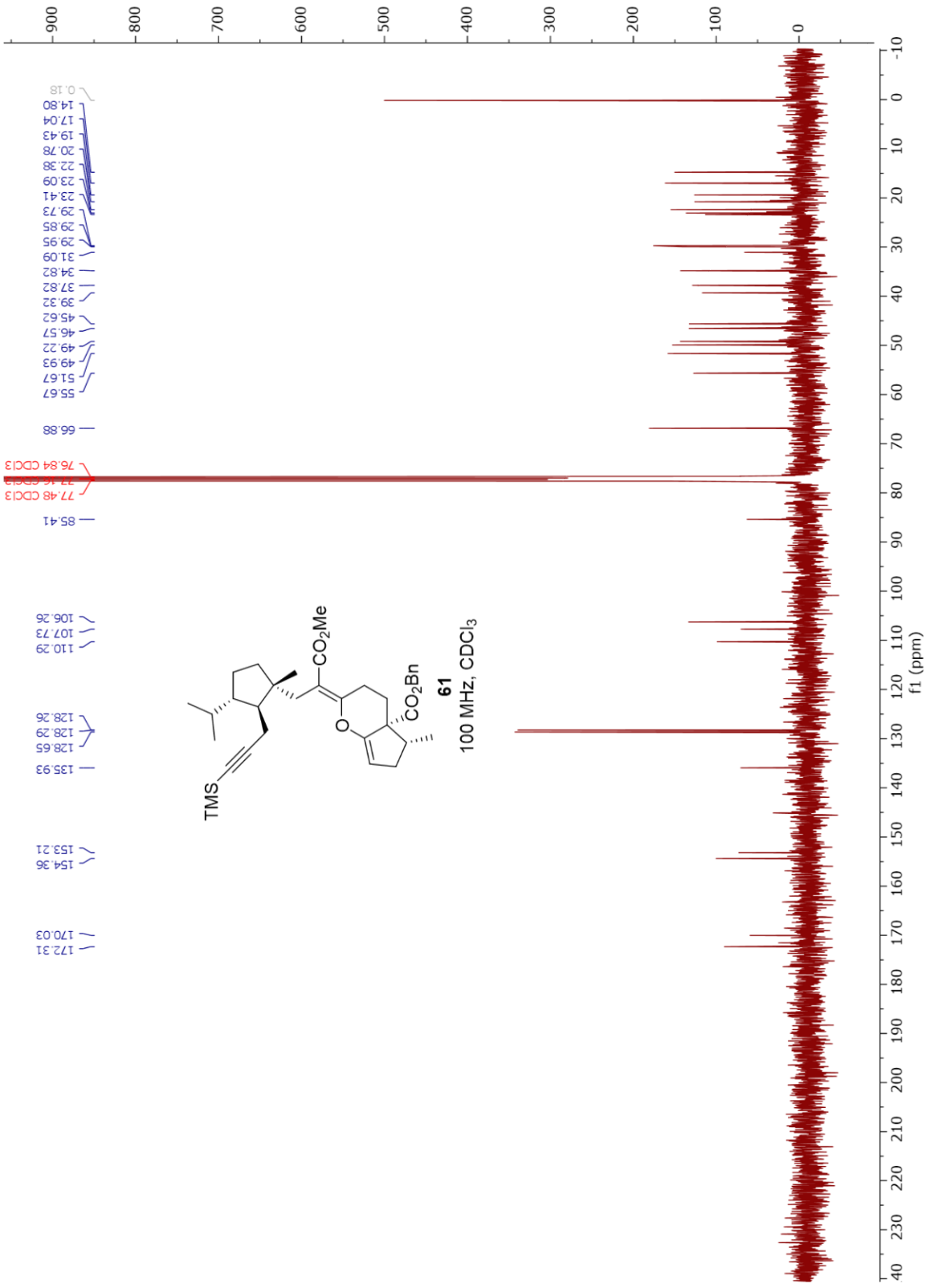
61
100 MHz, CDCl3
CO2Me
CO2Bn
TMS
f1 (ppm)

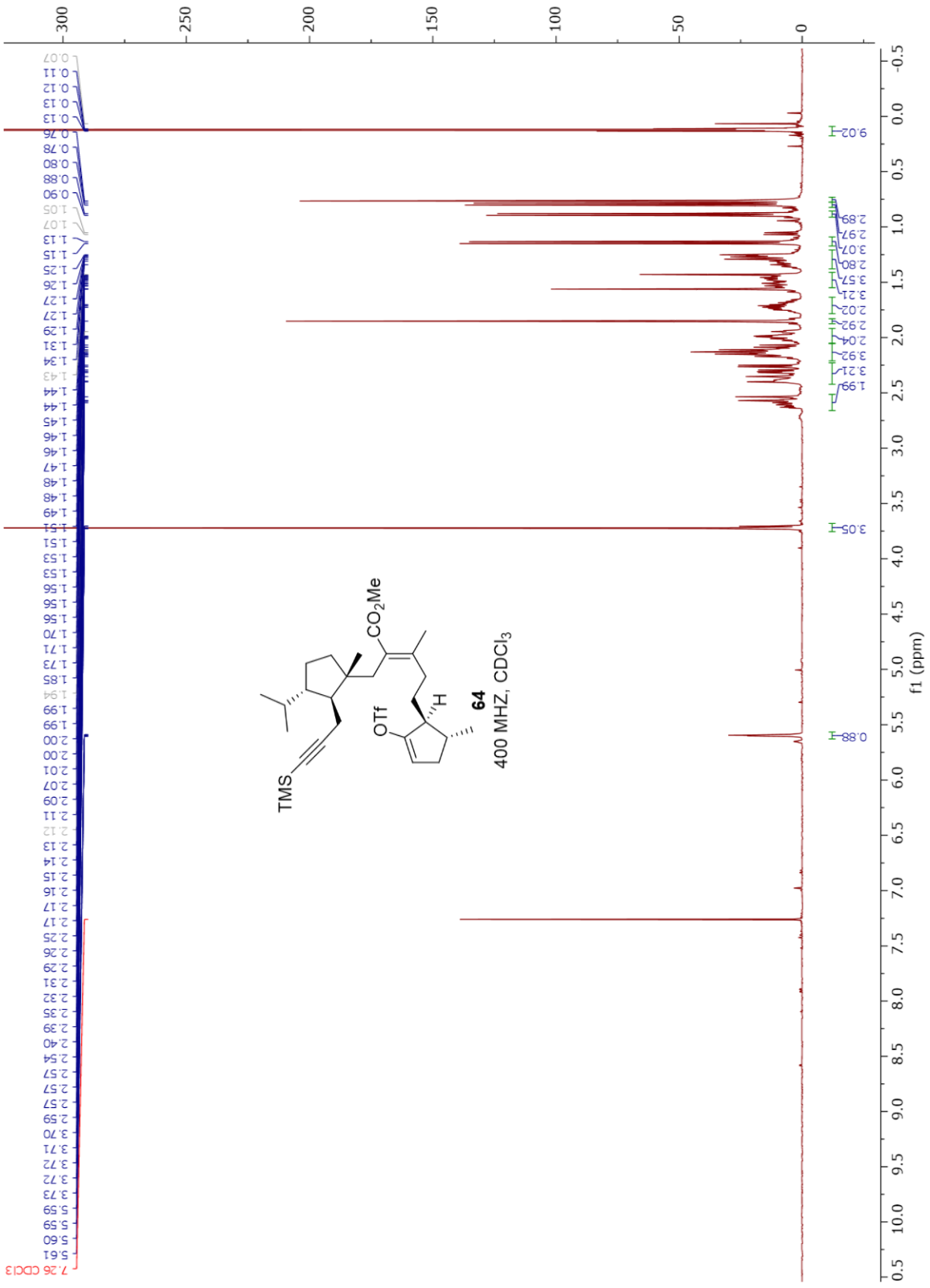
CO2Me
TMS
OTf
H
64
400 MHZ, CDCl3
f1 (ppm)

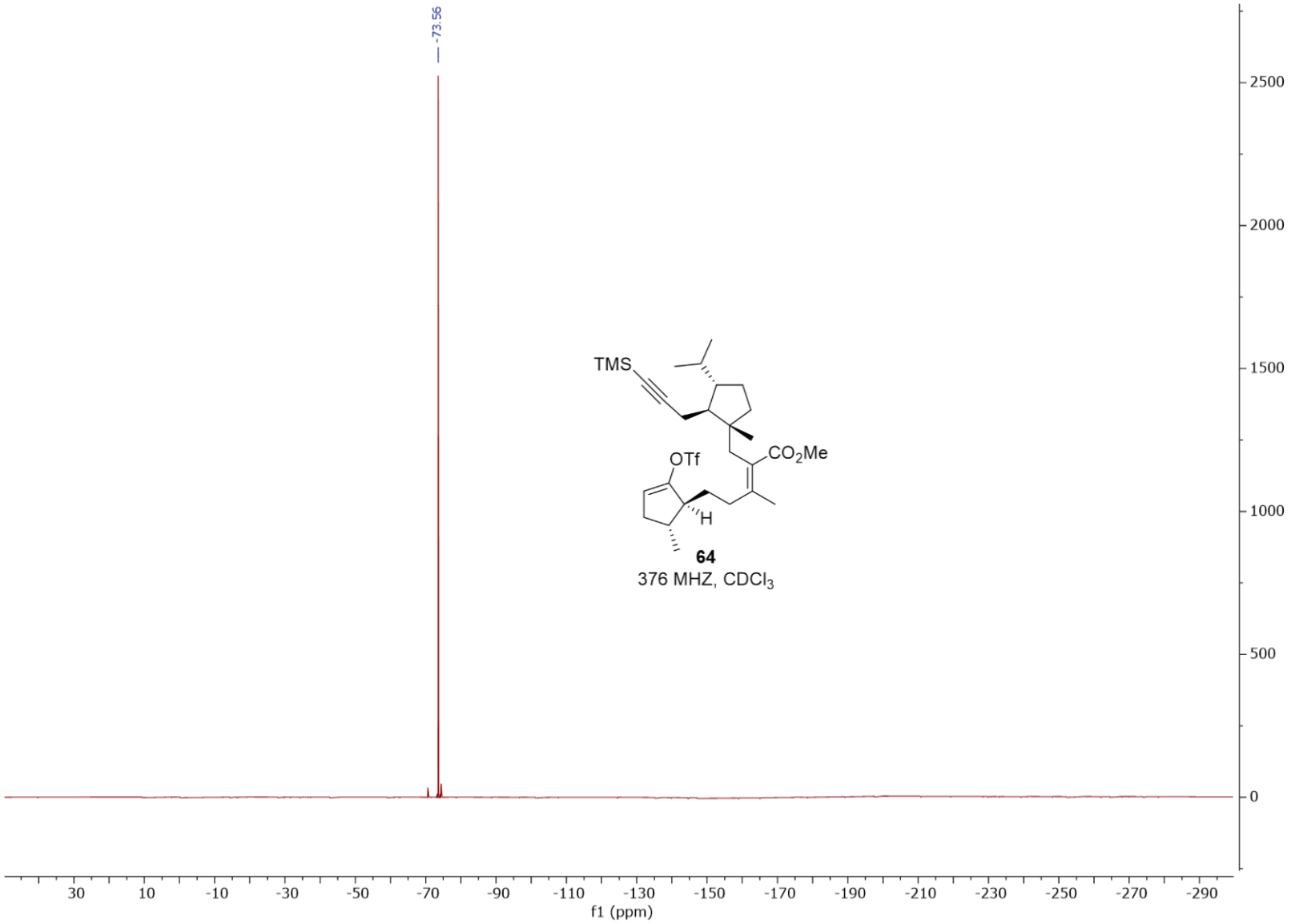

64

376 MHZ, $CDCl_3$

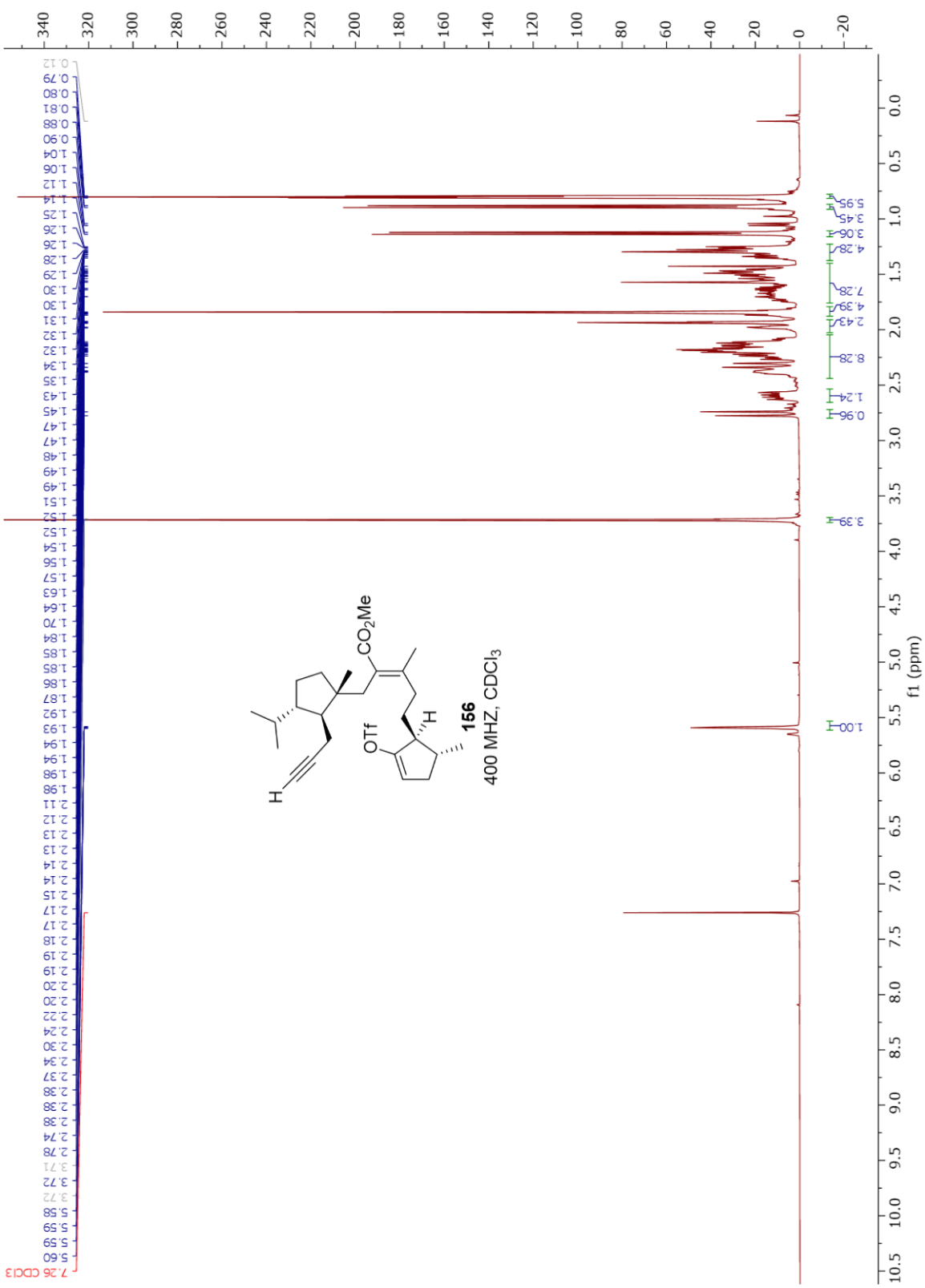
CO2Me
OTf
H
H
156
400 MHZ, CDCl3
f1 (ppm)

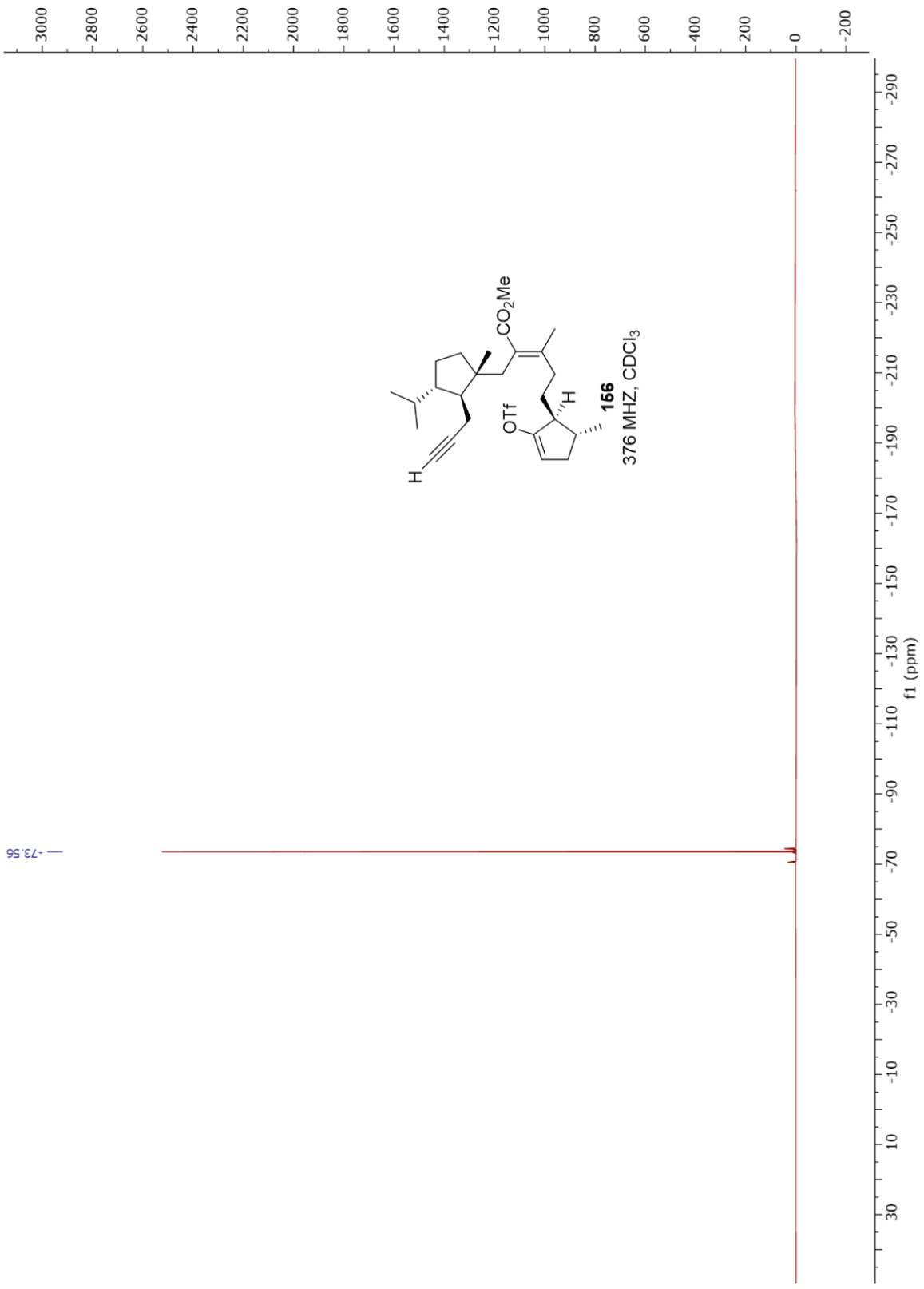
CO2Me
OTf
H
H
156
376 MHZ, CDCl3
-73.56
f1 (ppm)

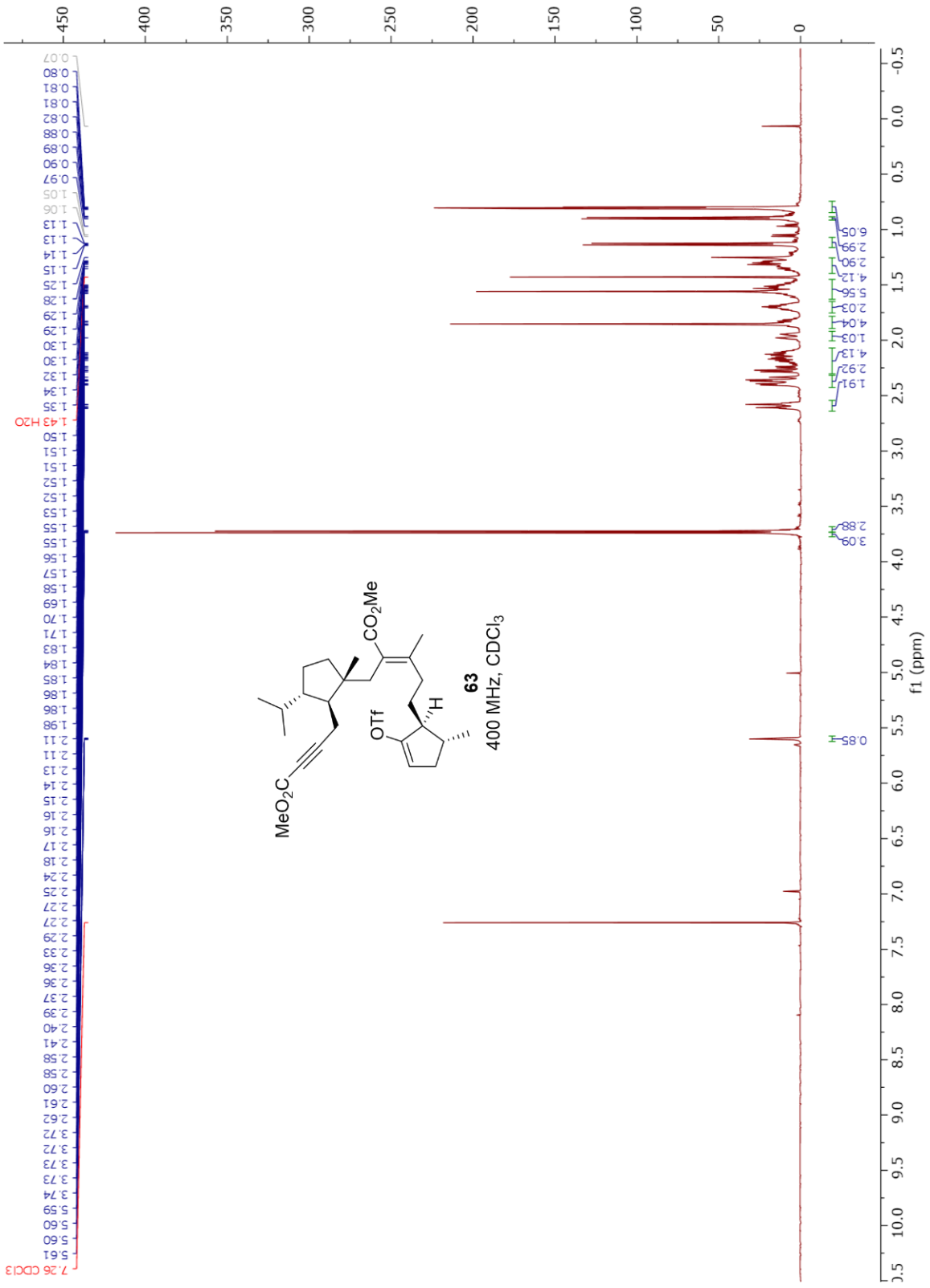
63
400 MHz, CDCl3
f1 (ppm)

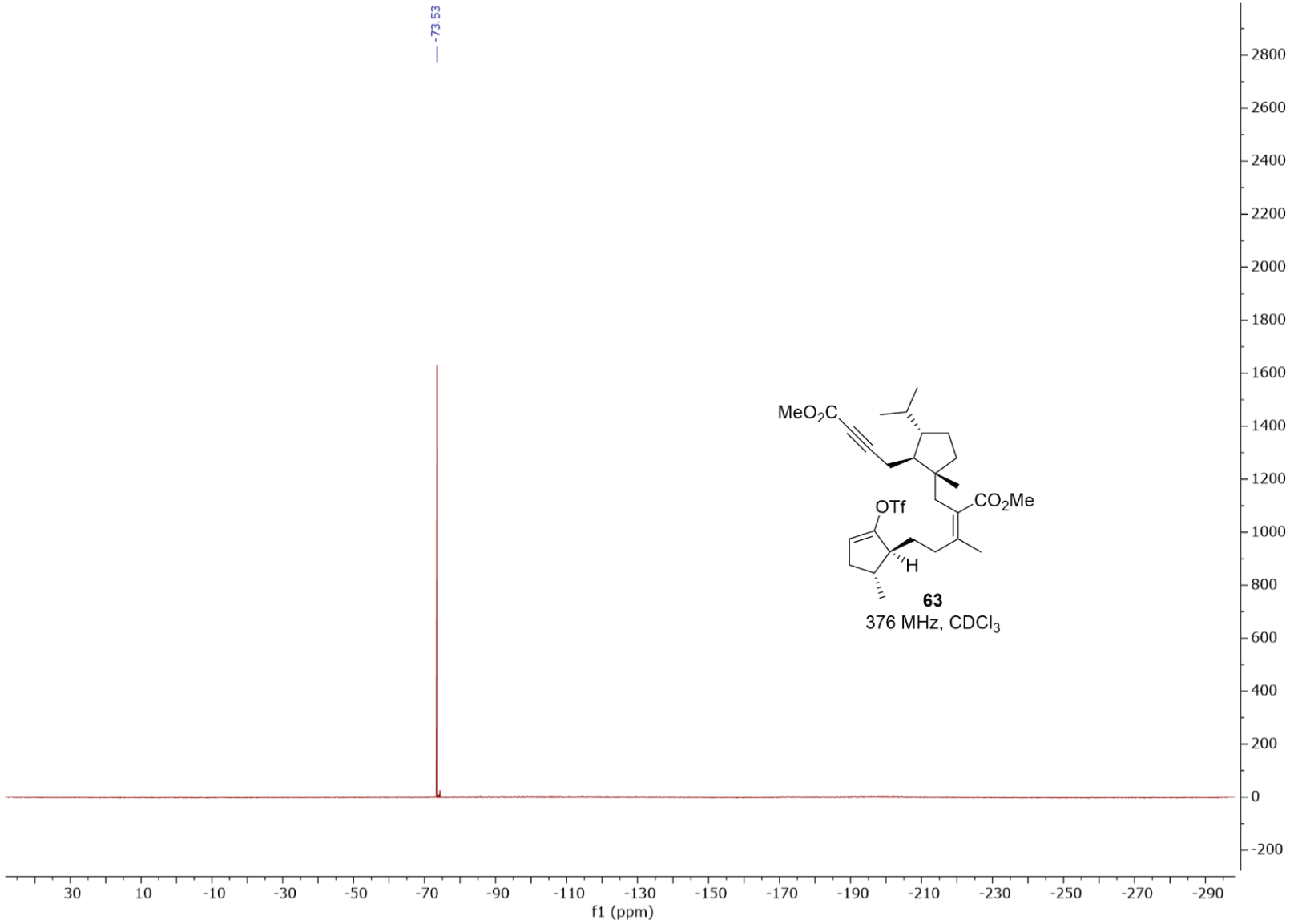
-73.53
MeO2C
CO2Me
OTf
H
63
376 MHz, CDCl3
2800
2600
2400
2200
2000
1800
1600
1400
1200
1000
800
600
400
200
0
-200
30
10
-10
-30
-50
-70
-90
-110
-130
-150
-170
-190
-210
-230
-250
-270
-290
f1 (ppm)

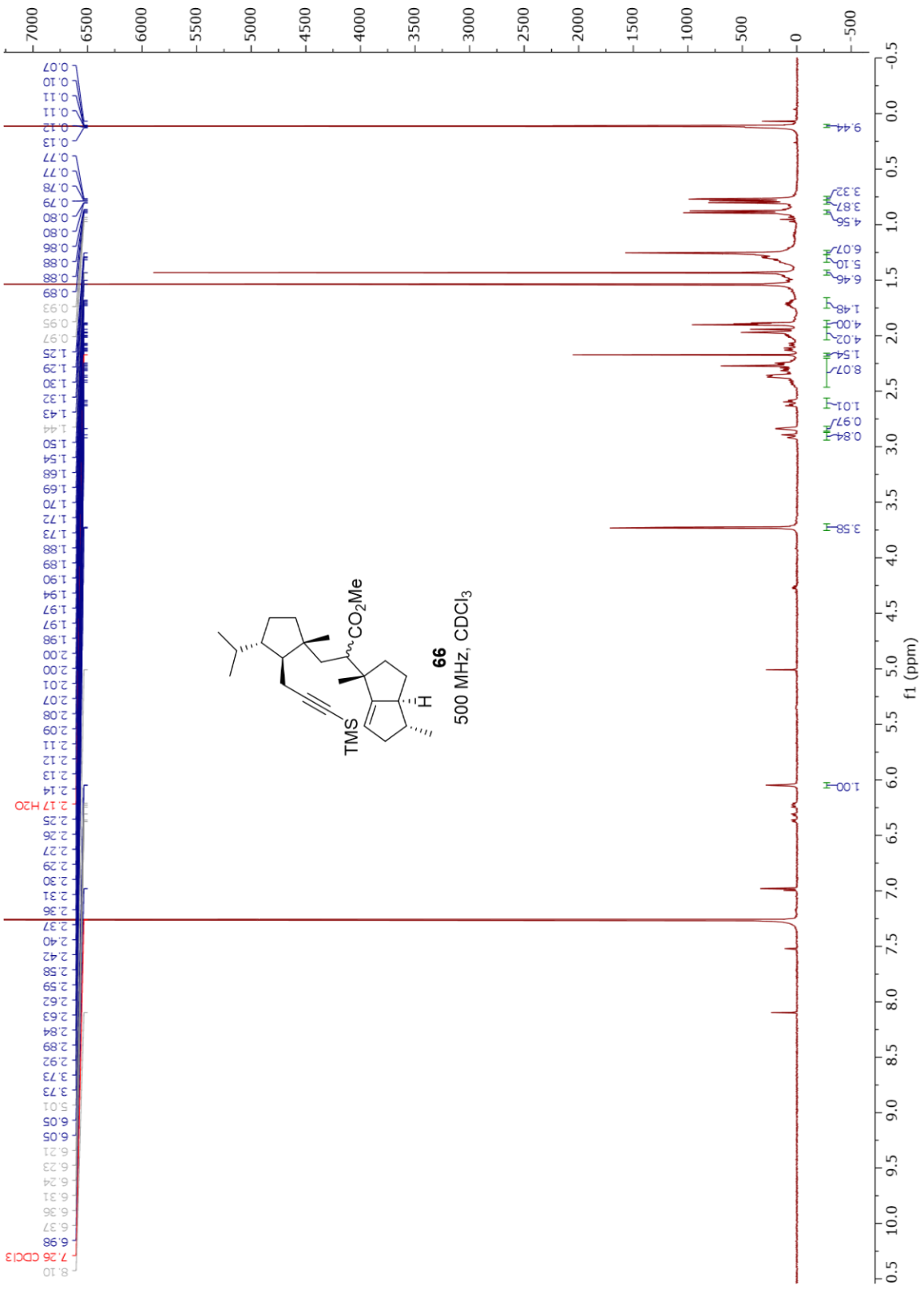
CO2Me
TMS
H
66
500 MHz, CDCl3
f1 (ppm)

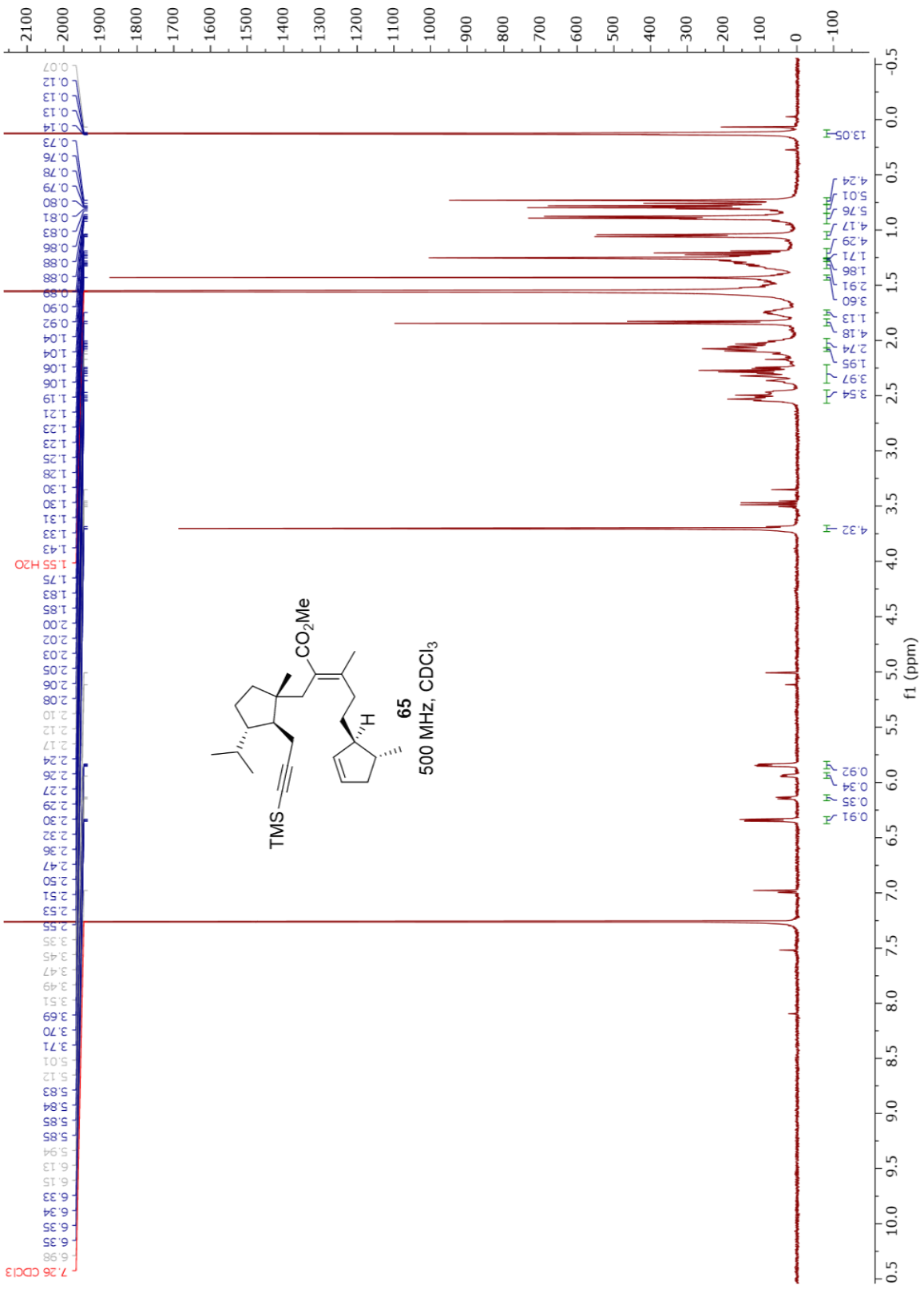
CO2Me
TMS
H
65
500 MHz, CDCl3
f1 (ppm)

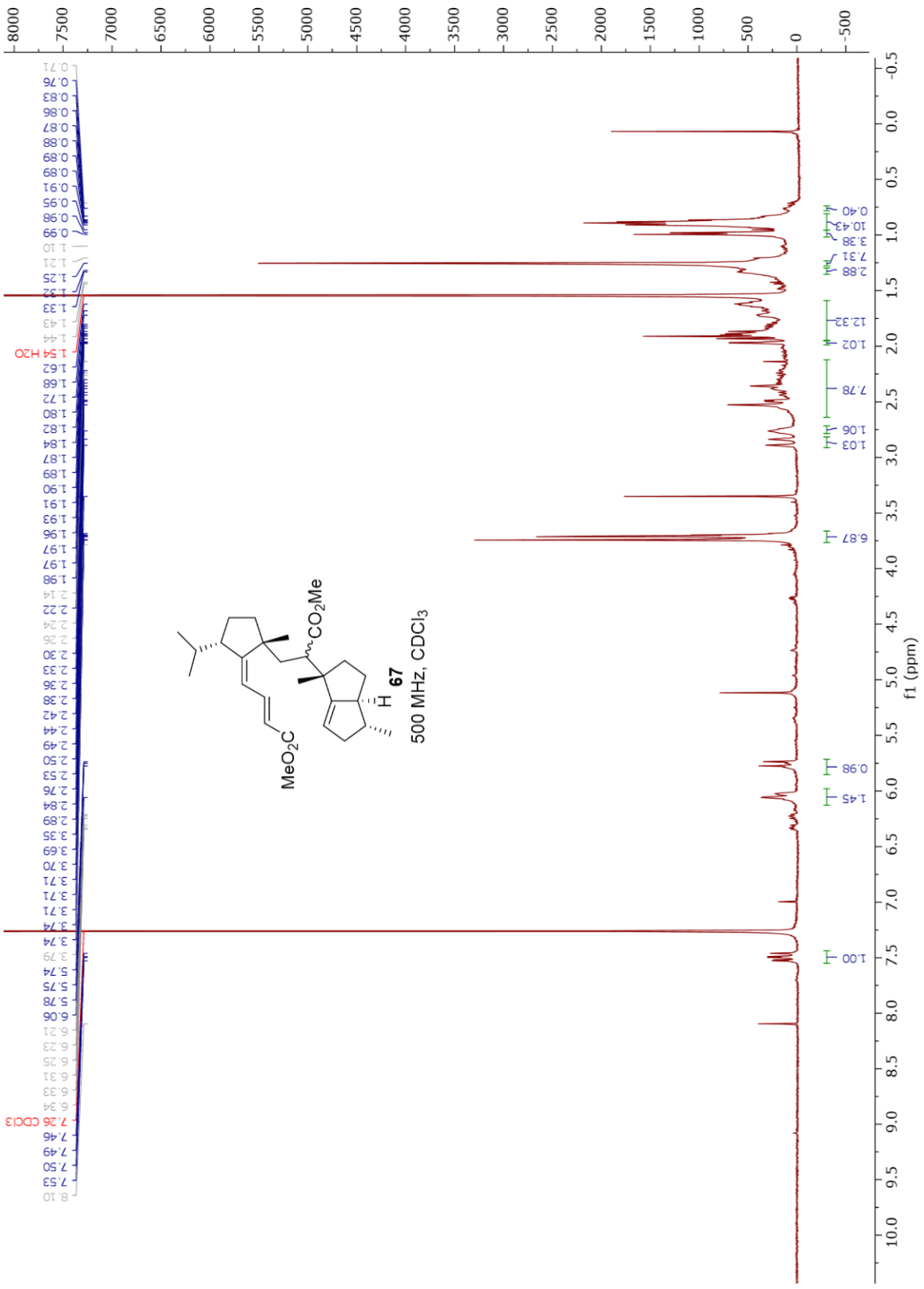
MeO2C
CO2Me
67
500 MHz, CDCl3
f1 (ppm)

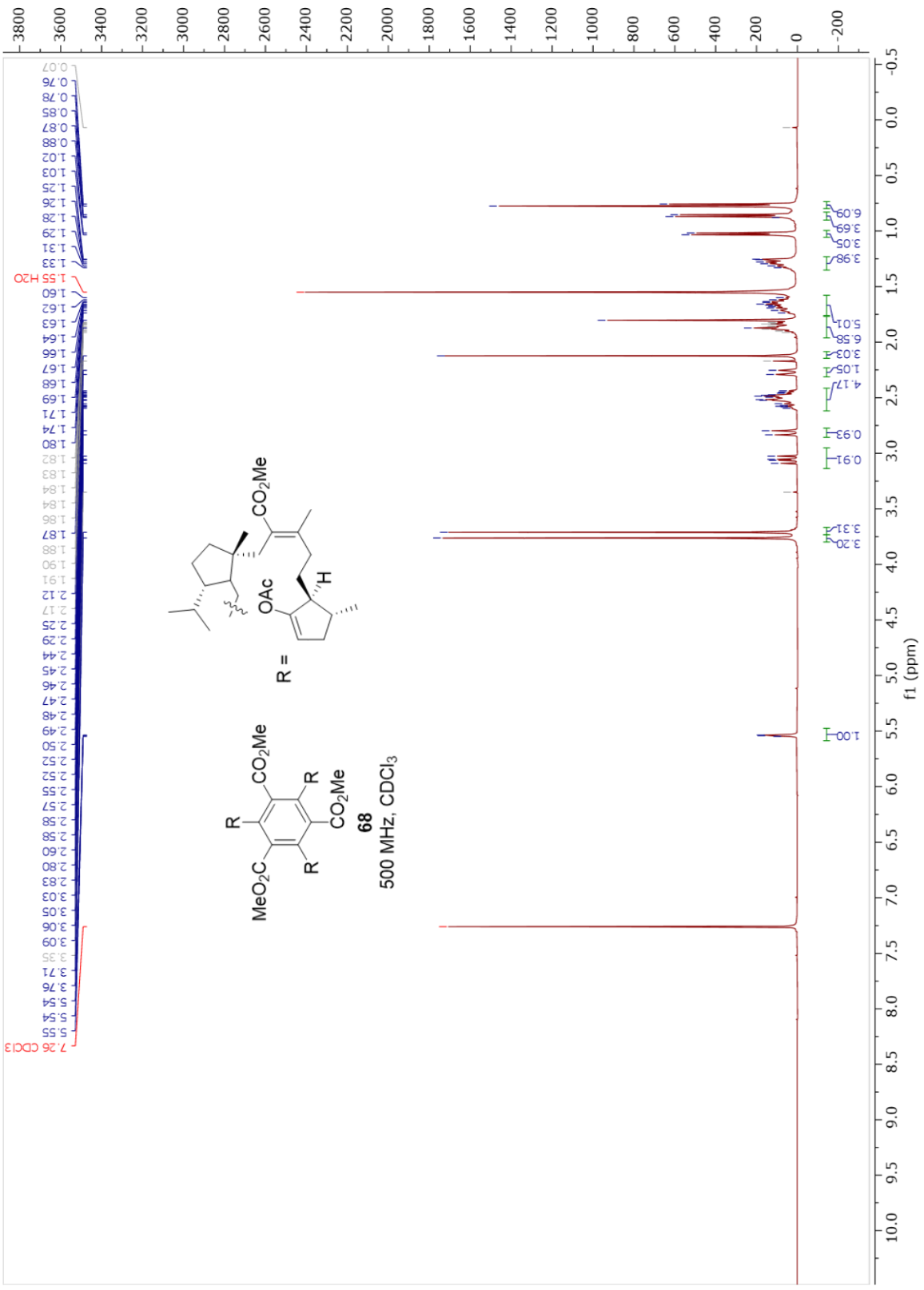
68
500 MHz, CDCl3
R =
OAc
H
CO2Me
MeO2C
f1 (ppm)

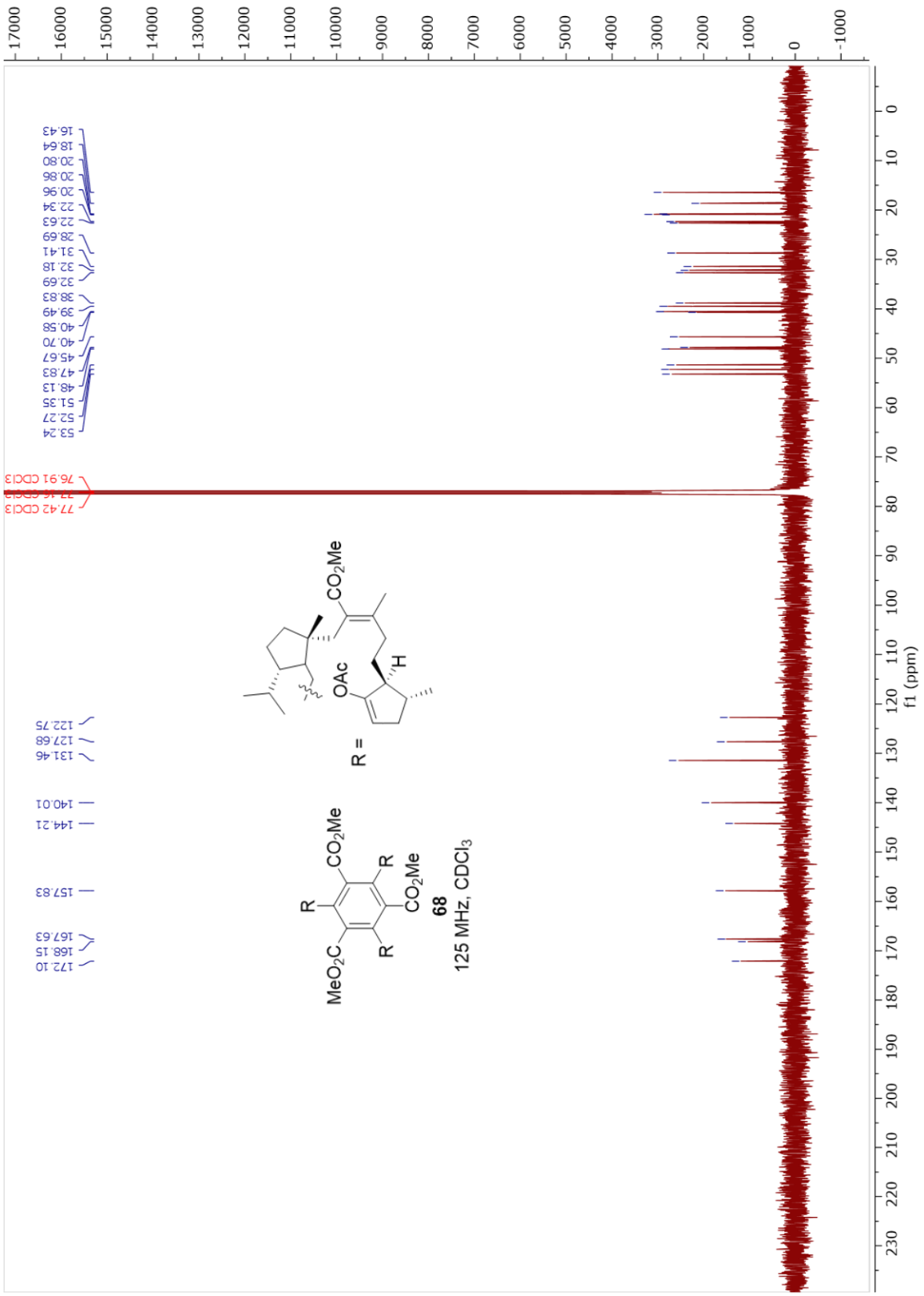
16.43
18.64
20.80
20.86
20.96
22.34
22.63
28.69
31.41
32.18
32.69
38.83
39.49
40.58
40.70
45.67
47.83
48.13
51.35
52.27
53.24
76.91 CDCl3
77.16 CDCl3
77.42 CDCl3
122.75
127.68
131.46
140.01
144.21
157.83
167.63
168.15
172.10
CO2Me
OAc
H
R =
MeO2C
CO2Me
R
R
R
CO2Me
68
125 MHz, CDCl3
f1 (ppm)

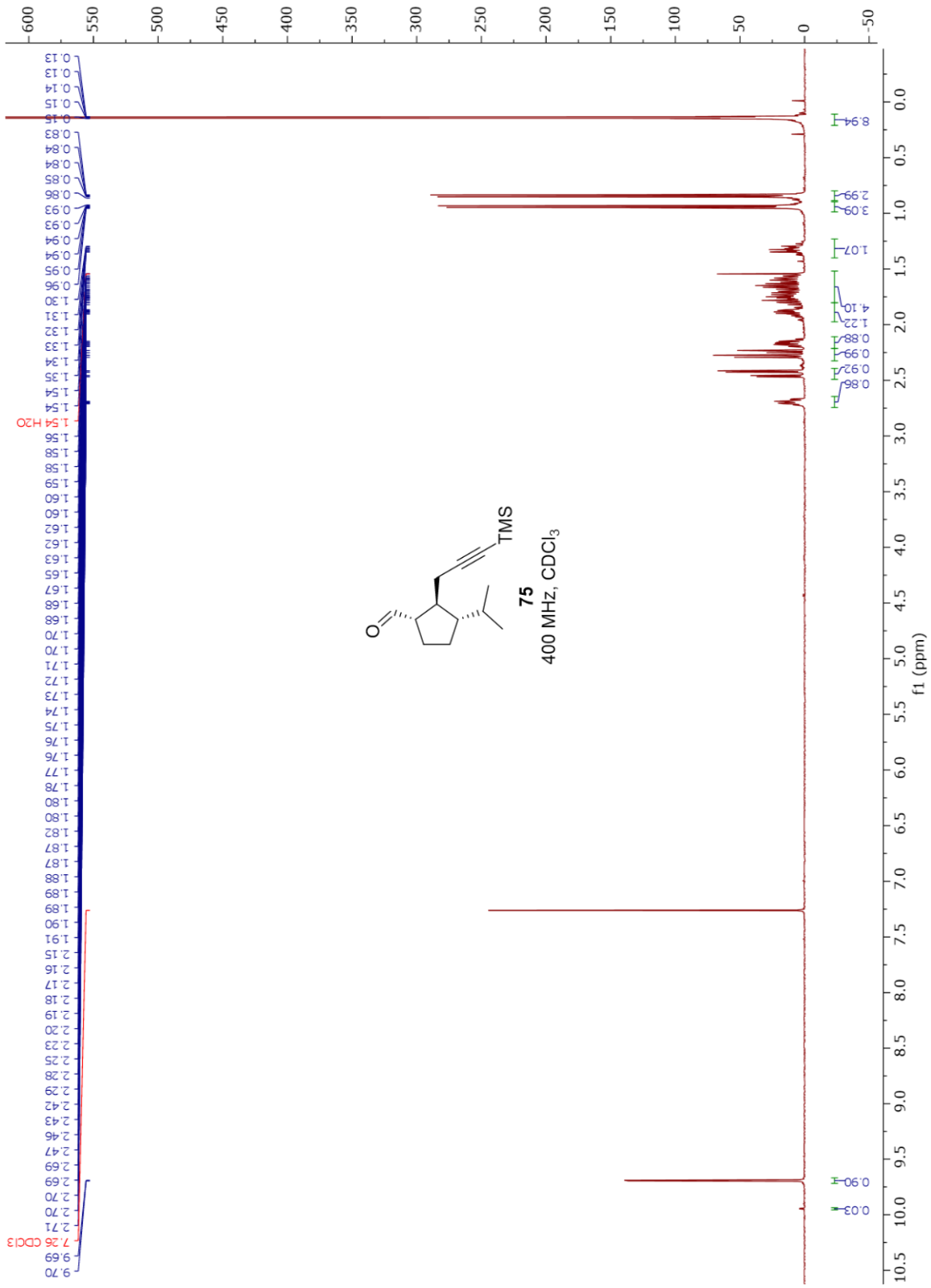
TMS
O
75
400 MHz, CDCl3
f1 (ppm)
7.26 CDCl3
1.54 H2O

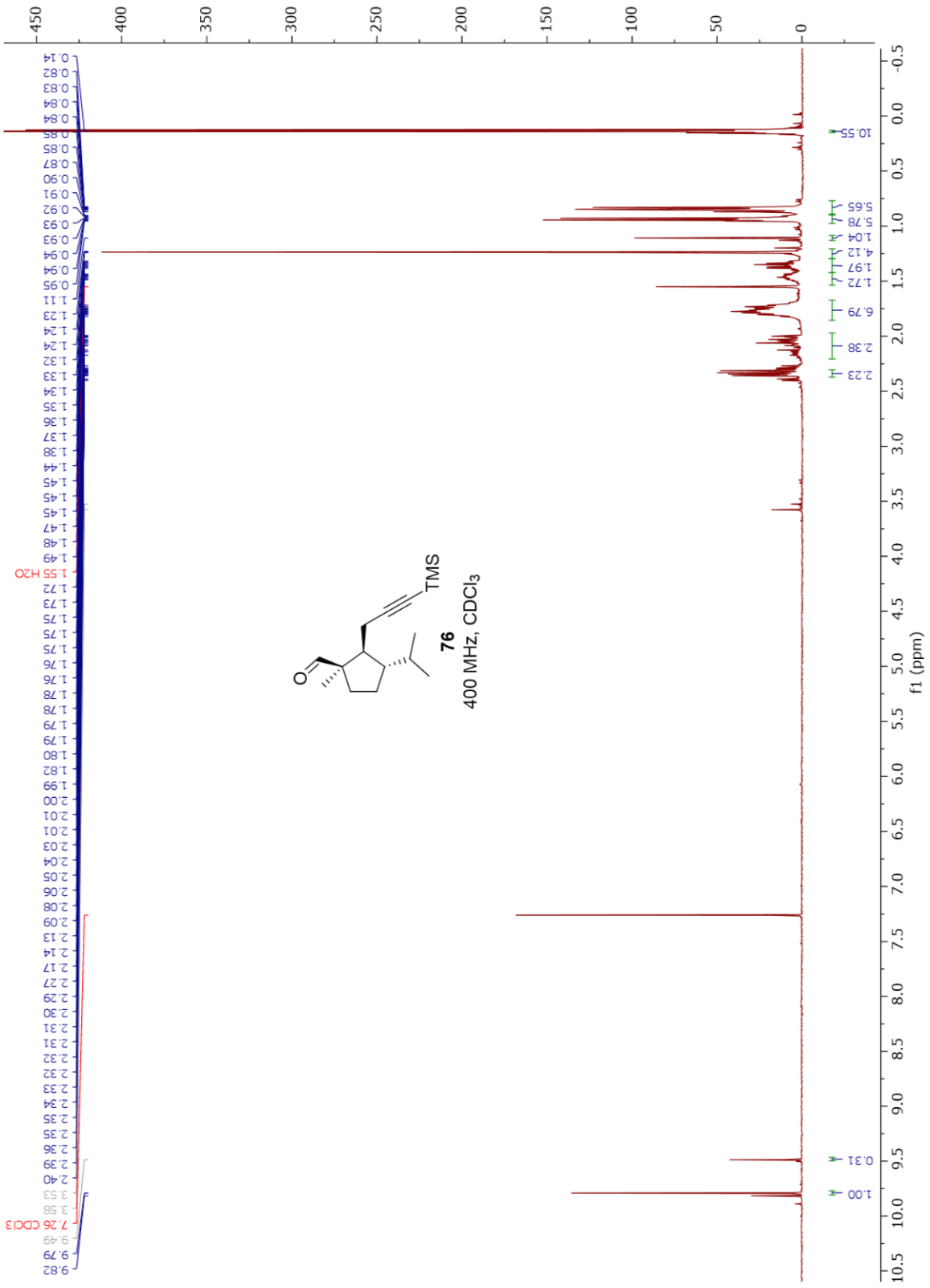
TMS
O
76
400 MHz, CDCl3
f1 (ppm)

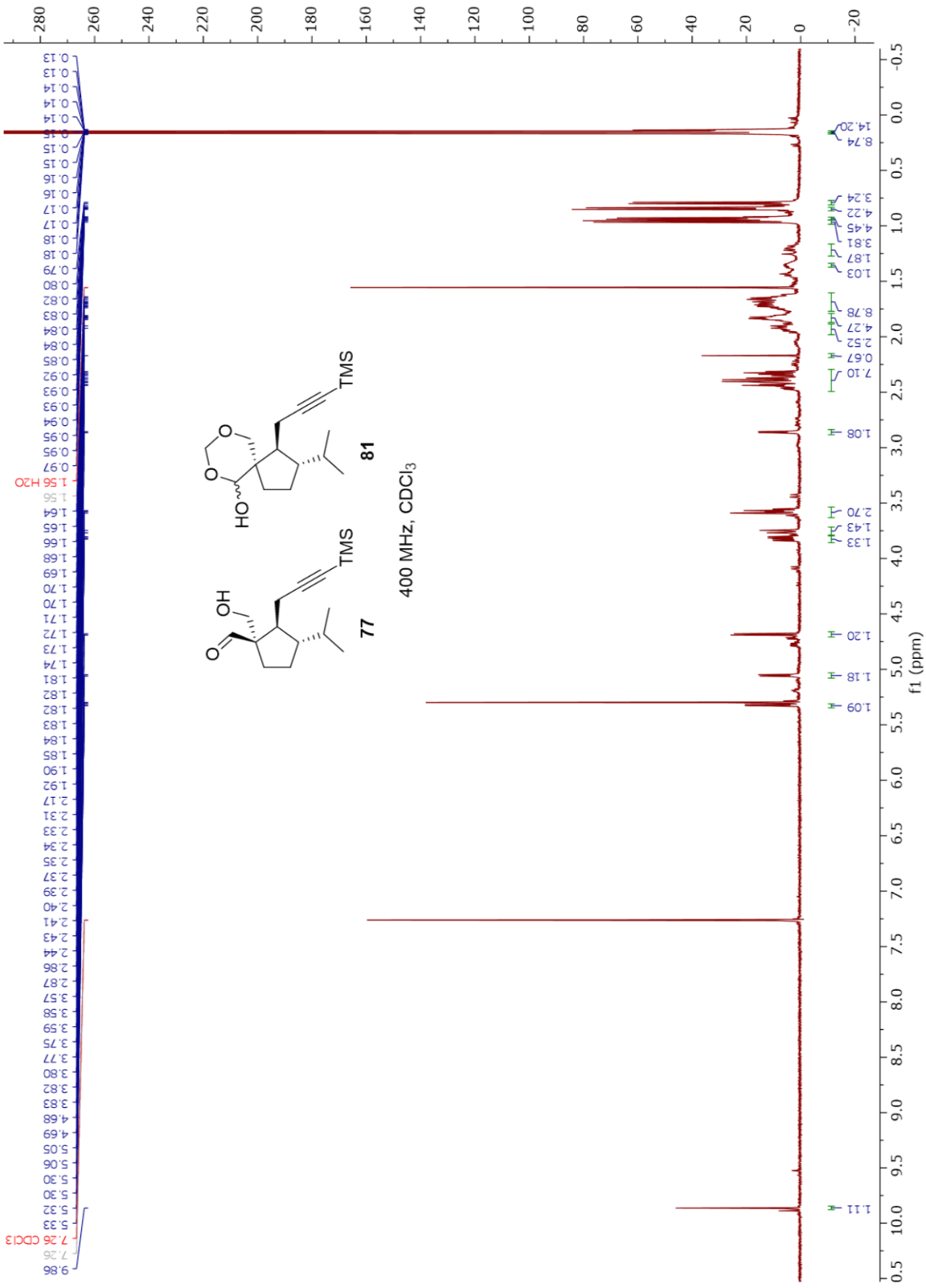
TMS
81
HO
O
O
TMS
77
OH
O
400 MHz, CDCl3
f1 (ppm)

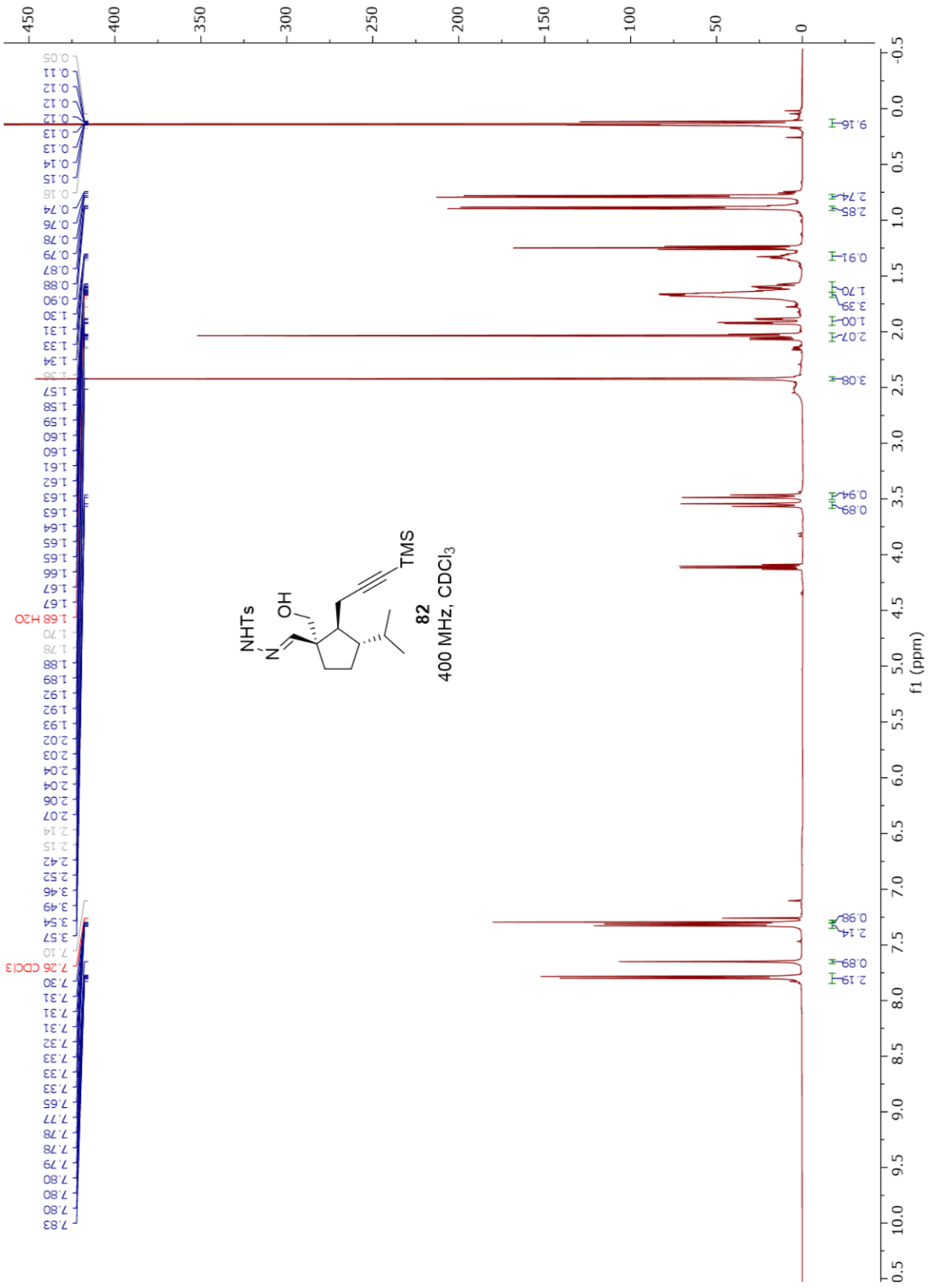
NHTs
OH
TMS
82
400 MHz, CDCl3
f1 (ppm)
7.26 CDCl3
1.68 H2O

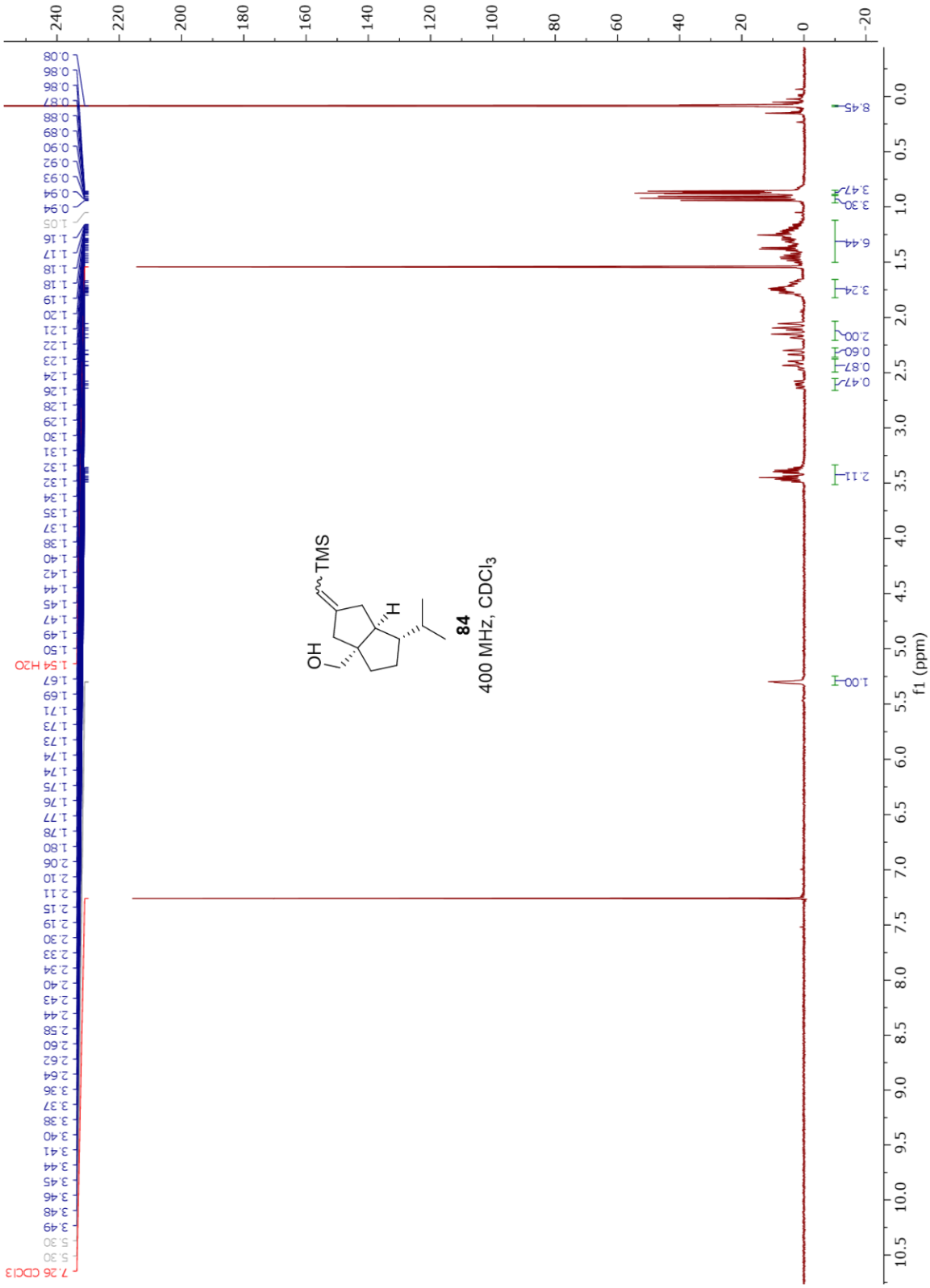
TMS
OH
H
84
400 MHz, CDCl3
f1 (ppm)
7.26 CDCl3
1.54 H2O
8.45
3.47
3.30
6.44
3.24
2.00
0.60
0.87
0.47
2.11
1.00

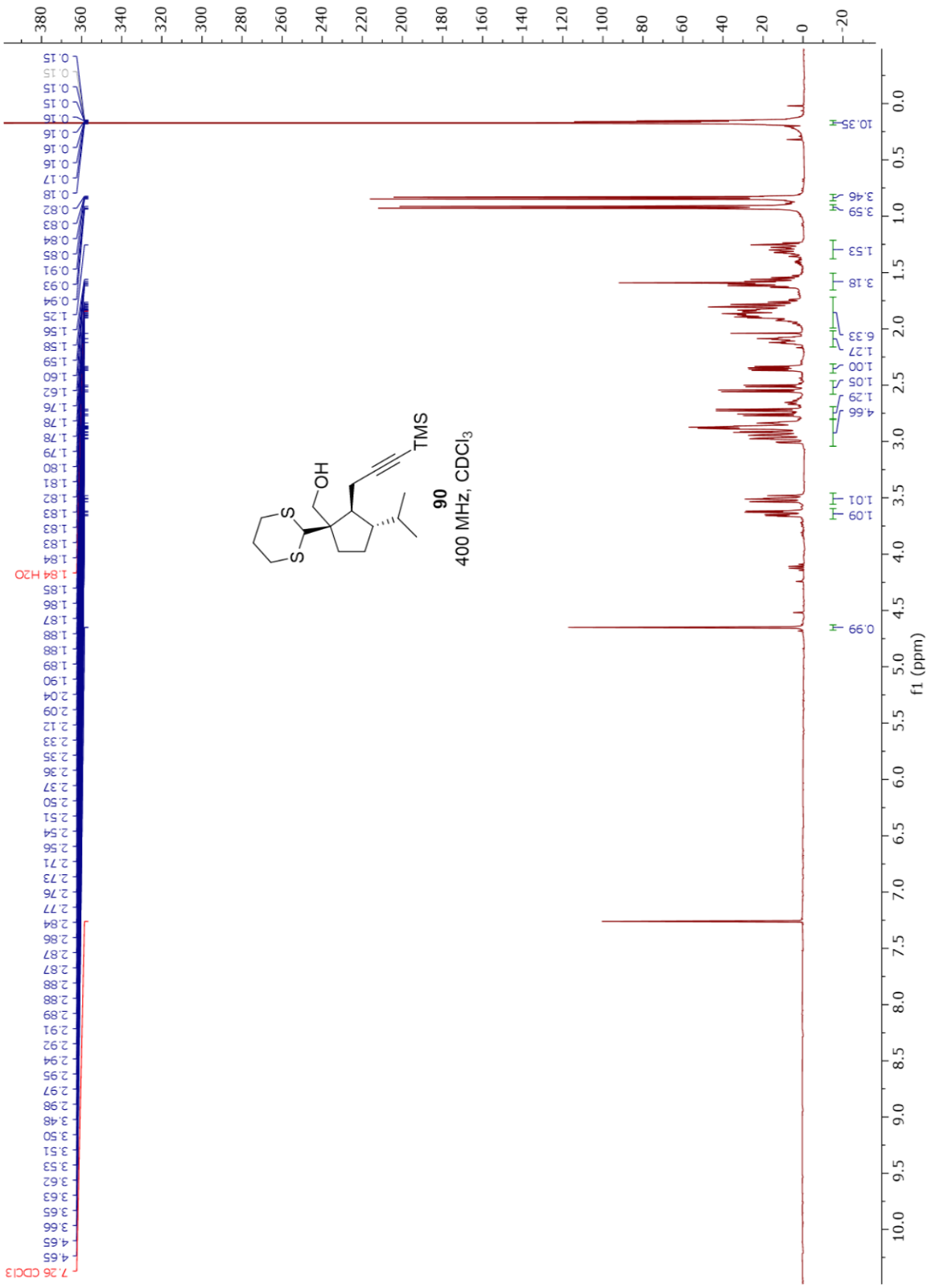
TMS
OH
S
S
90
400 MHz, CDCl3
f1 (ppm)

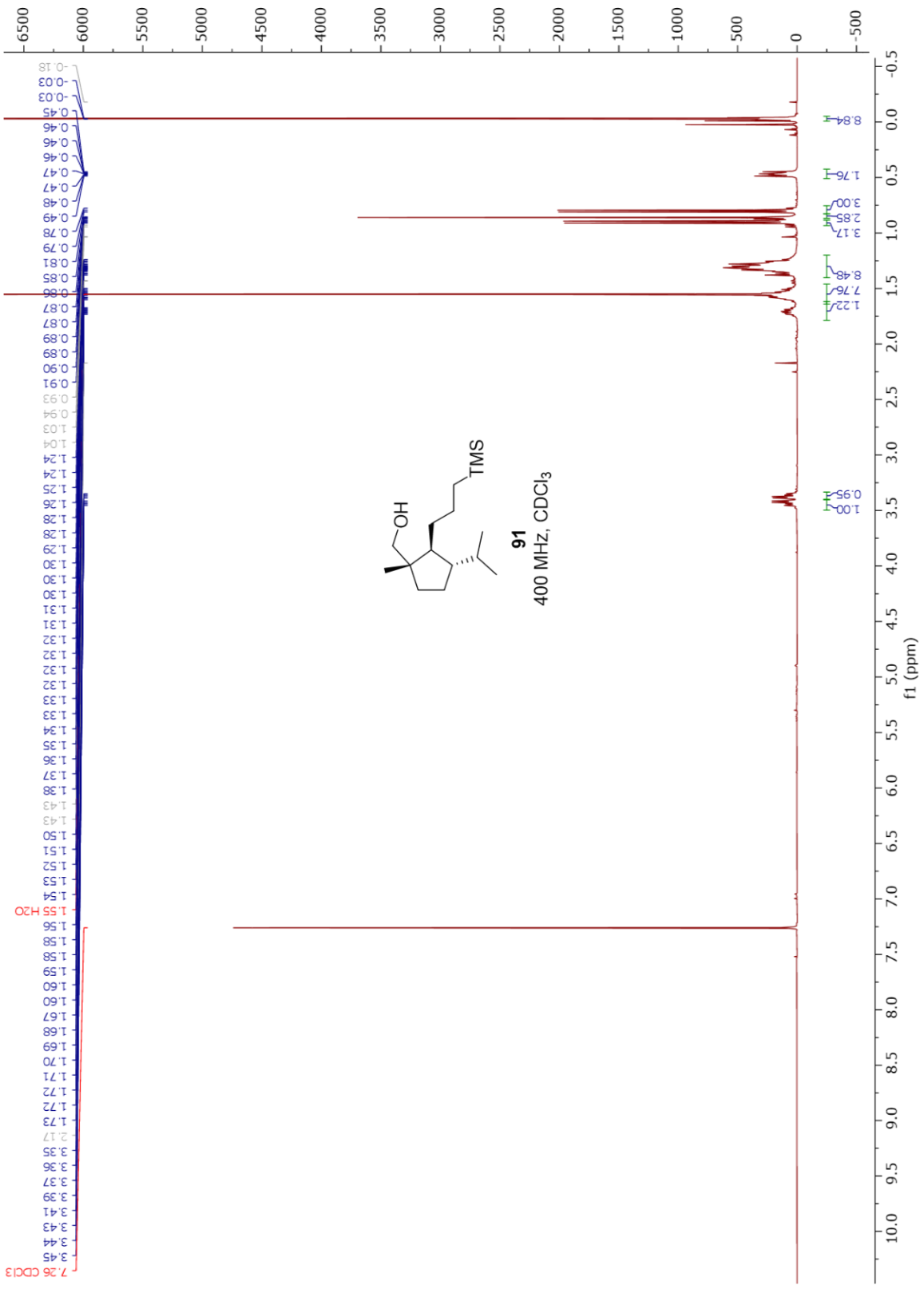
TMS
OH
91
400 MHz, CDCl3
f1 (ppm)

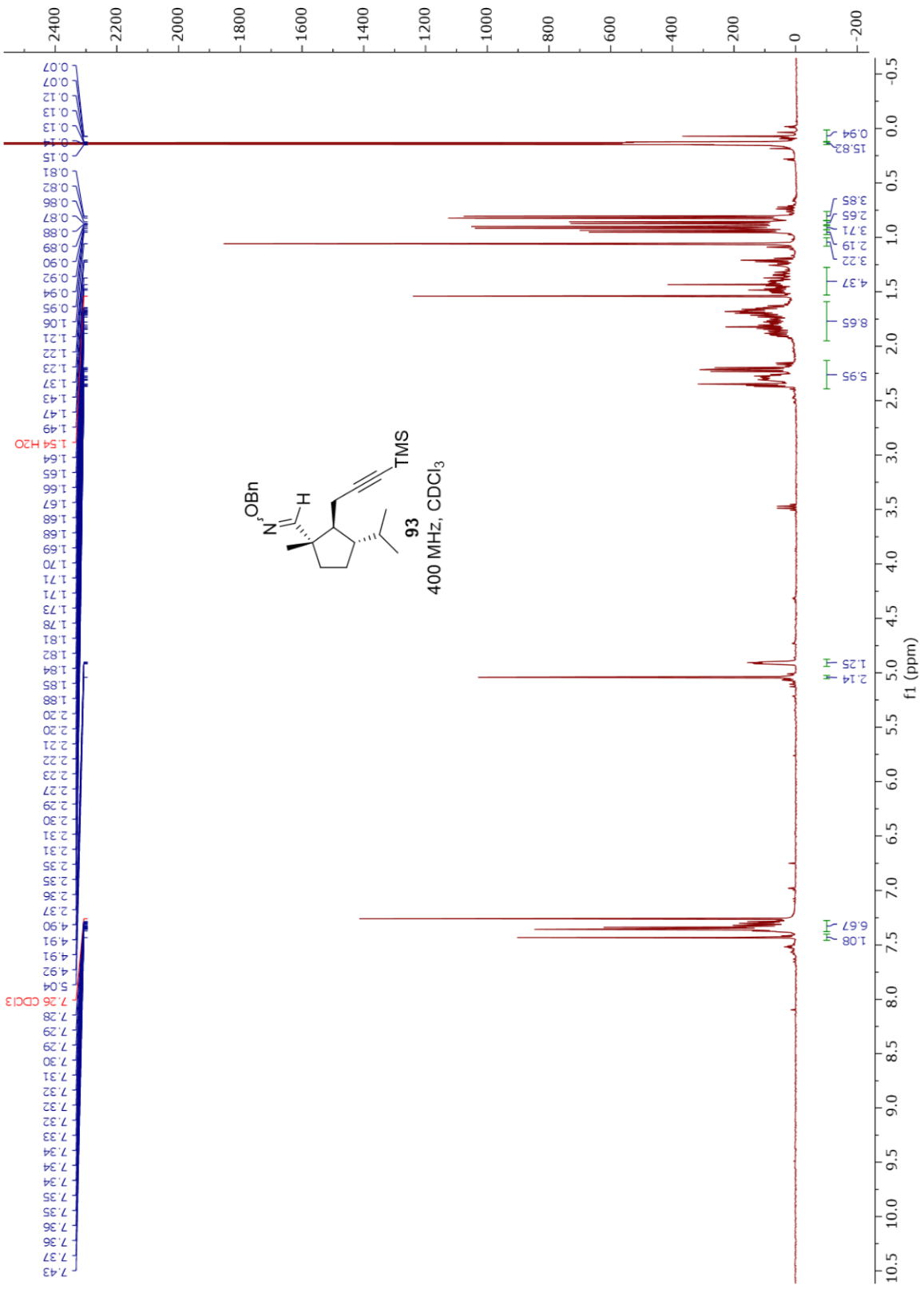
OBn
N
H
TMS
93
400 MHz, CDCl3
f1 (ppm)

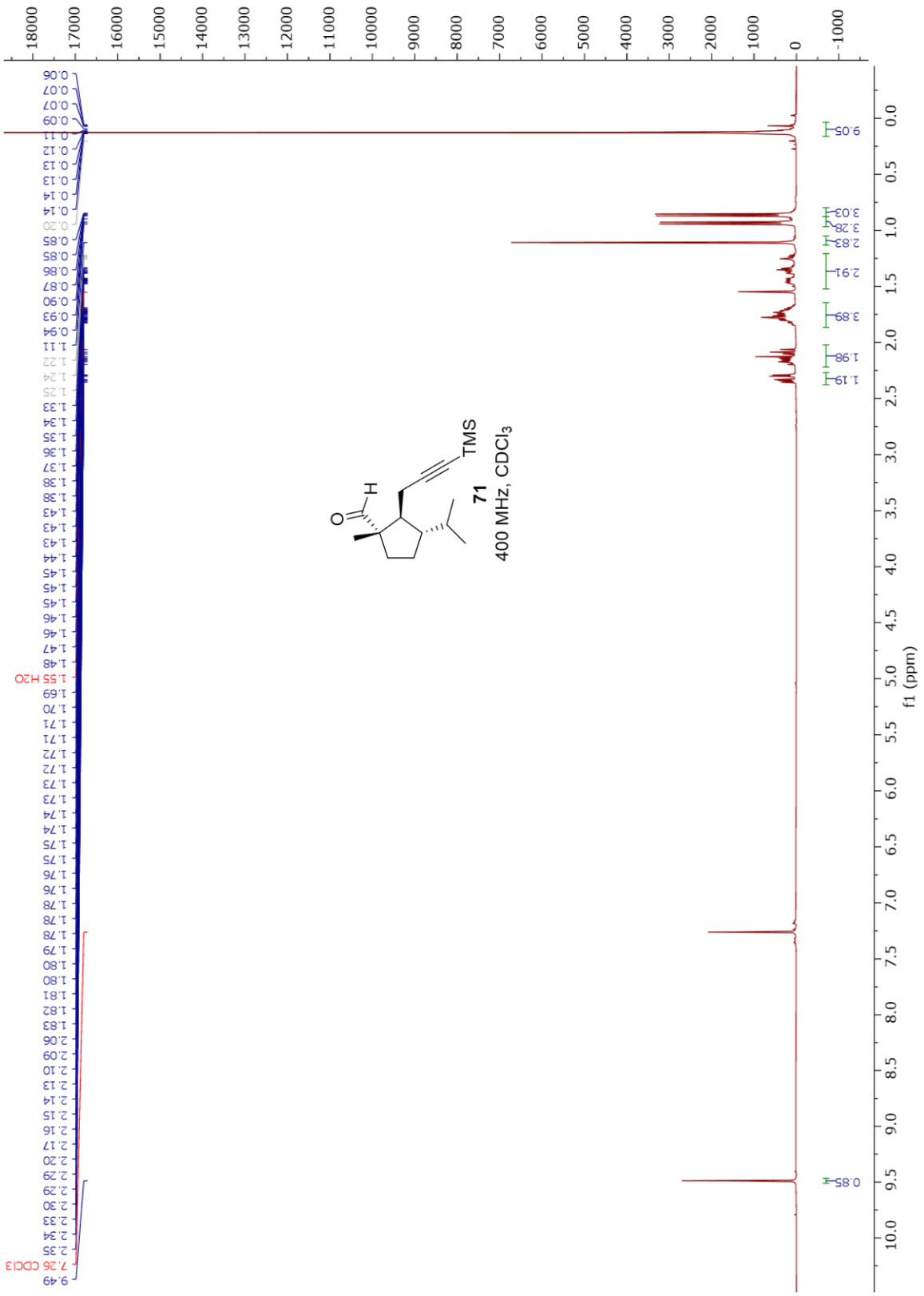
TMS
O
H
71
400 MHz, CDCl3
f1 (ppm)
7.26 CDCl3
1.55 H2O

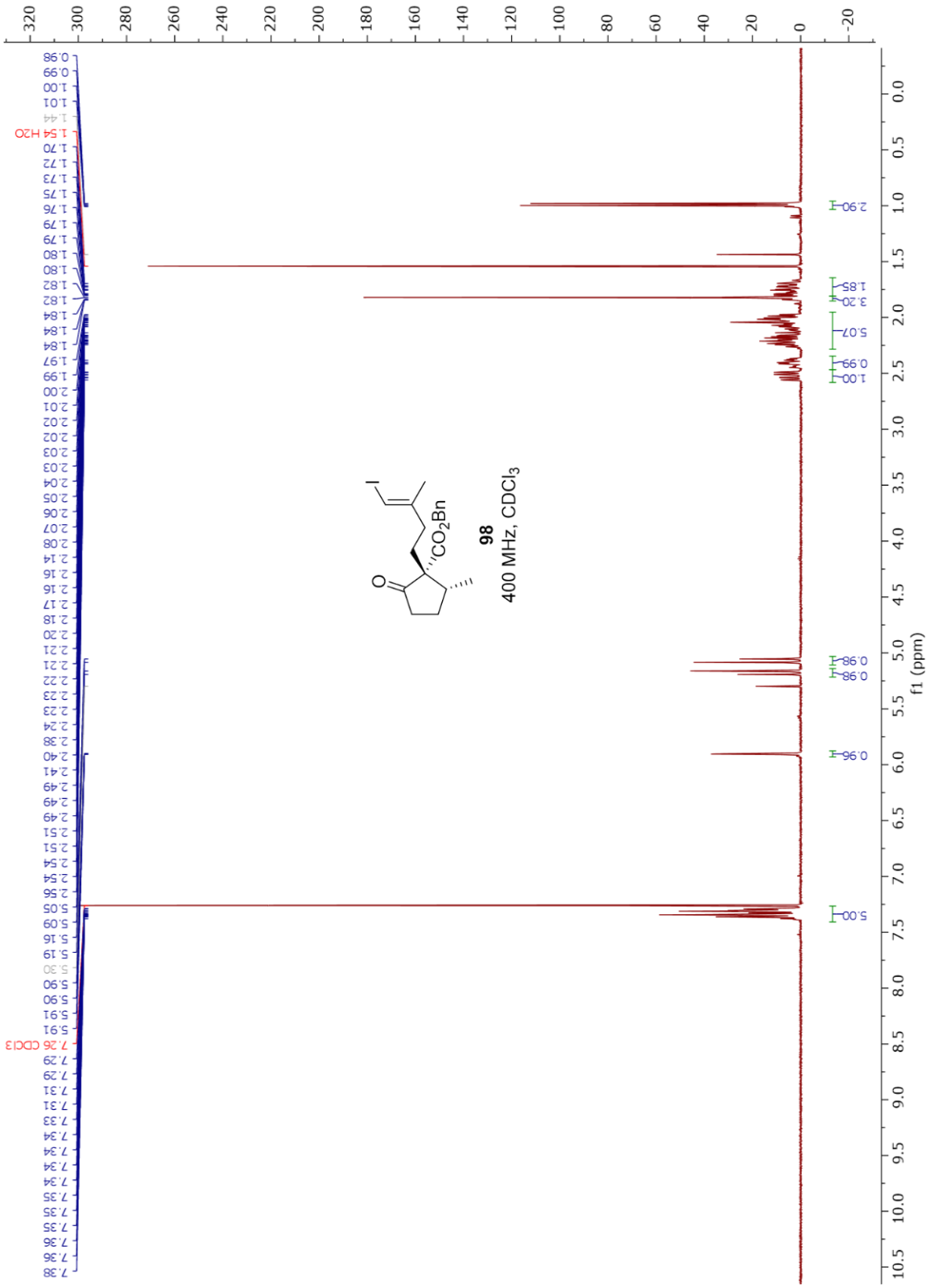
98
400 MHz, CDCl3
CO2Bn
I
O
f1 (ppm)
7.26 CDCl3
1.54 H2O
5.00
2.90
1.85
3.20
5.07
1.00
0.99
0.98
0.98
0.96

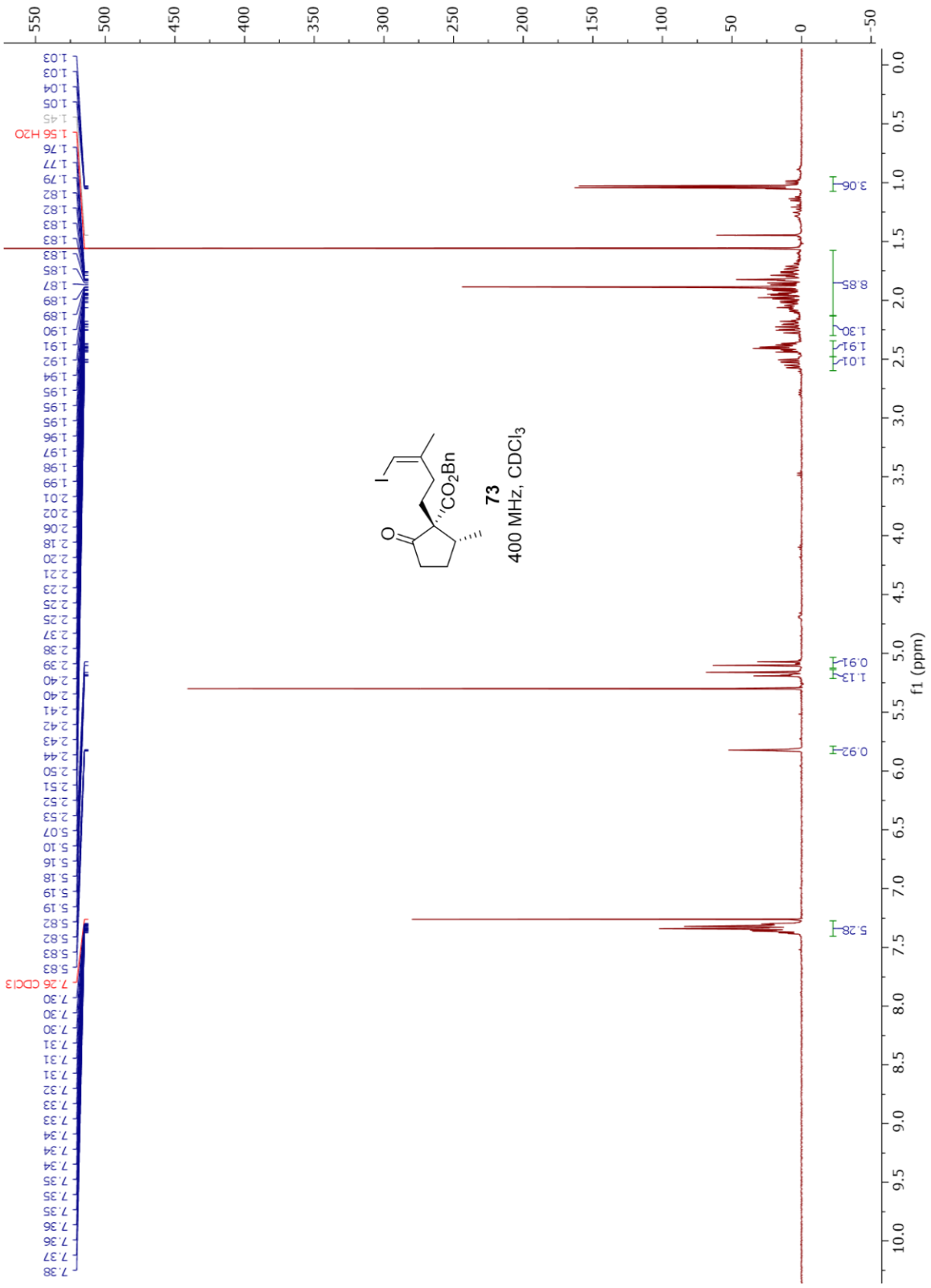
I
CO2Bn
O
73
400 MHz, CDCl3
f1 (ppm)

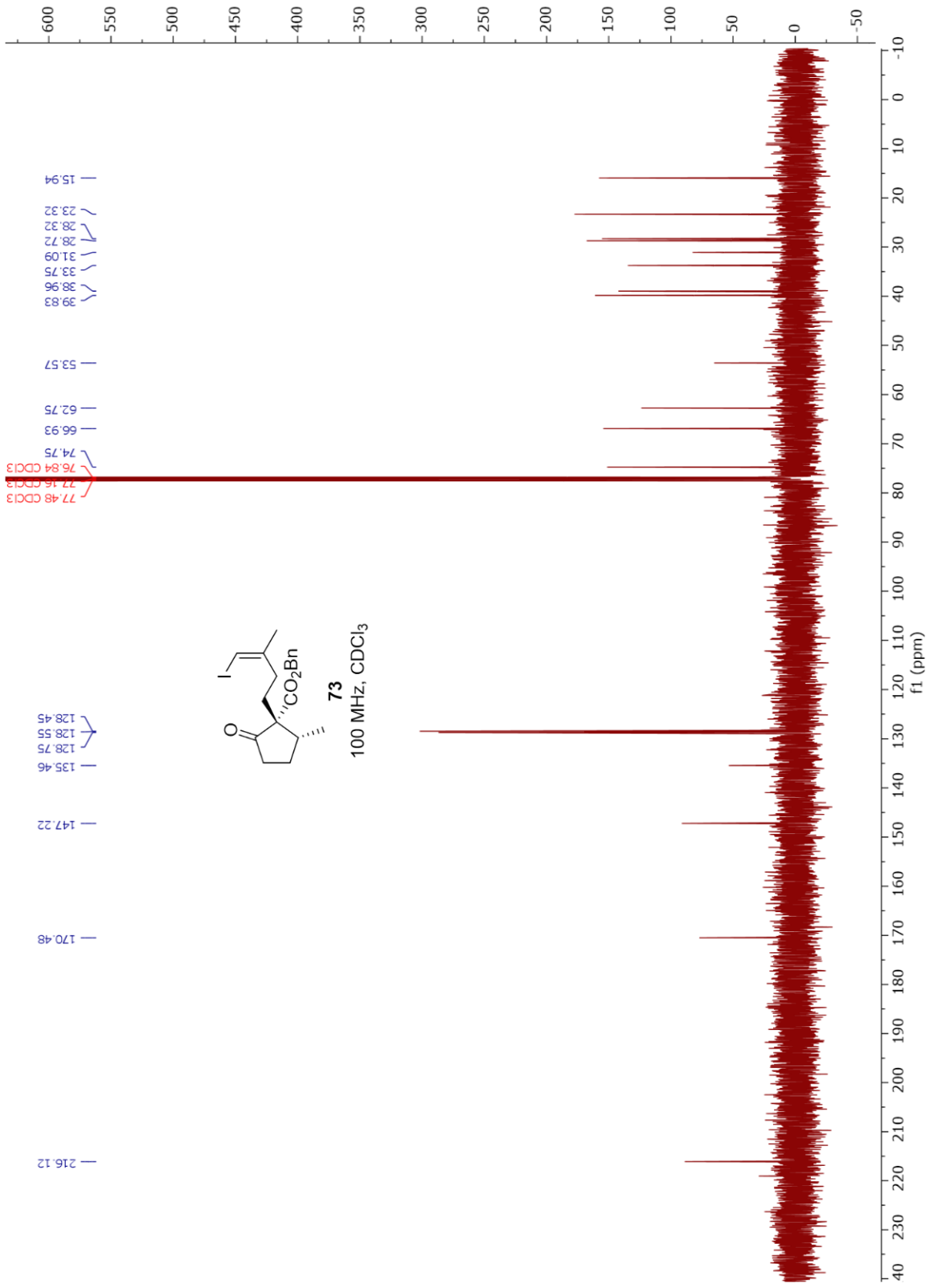
73
100 MHz, CDCl3
CO2Bn
O
I
15.94
23.32
28.32
28.72
31.09
33.75
38.96
39.83
53.57
62.75
66.93
74.75
76.84 CDCl3
77.16 CDCl3
77.48 CDCl3
128.45
128.55
128.75
135.46
147.22
170.48
216.12
f1 (ppm)

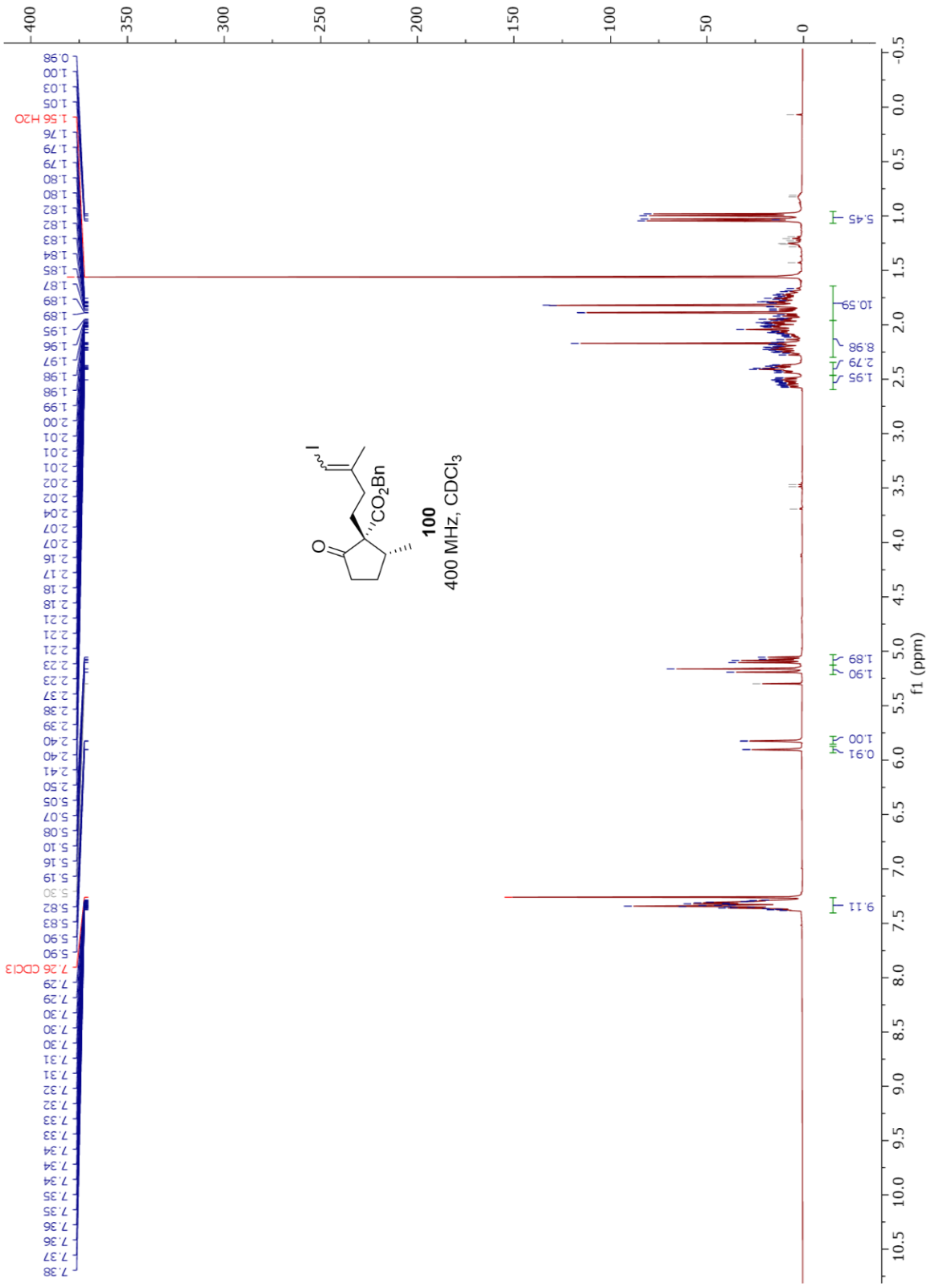
CO2Bn
O
I
100
400 MHz, CDCl3
f1 (ppm)

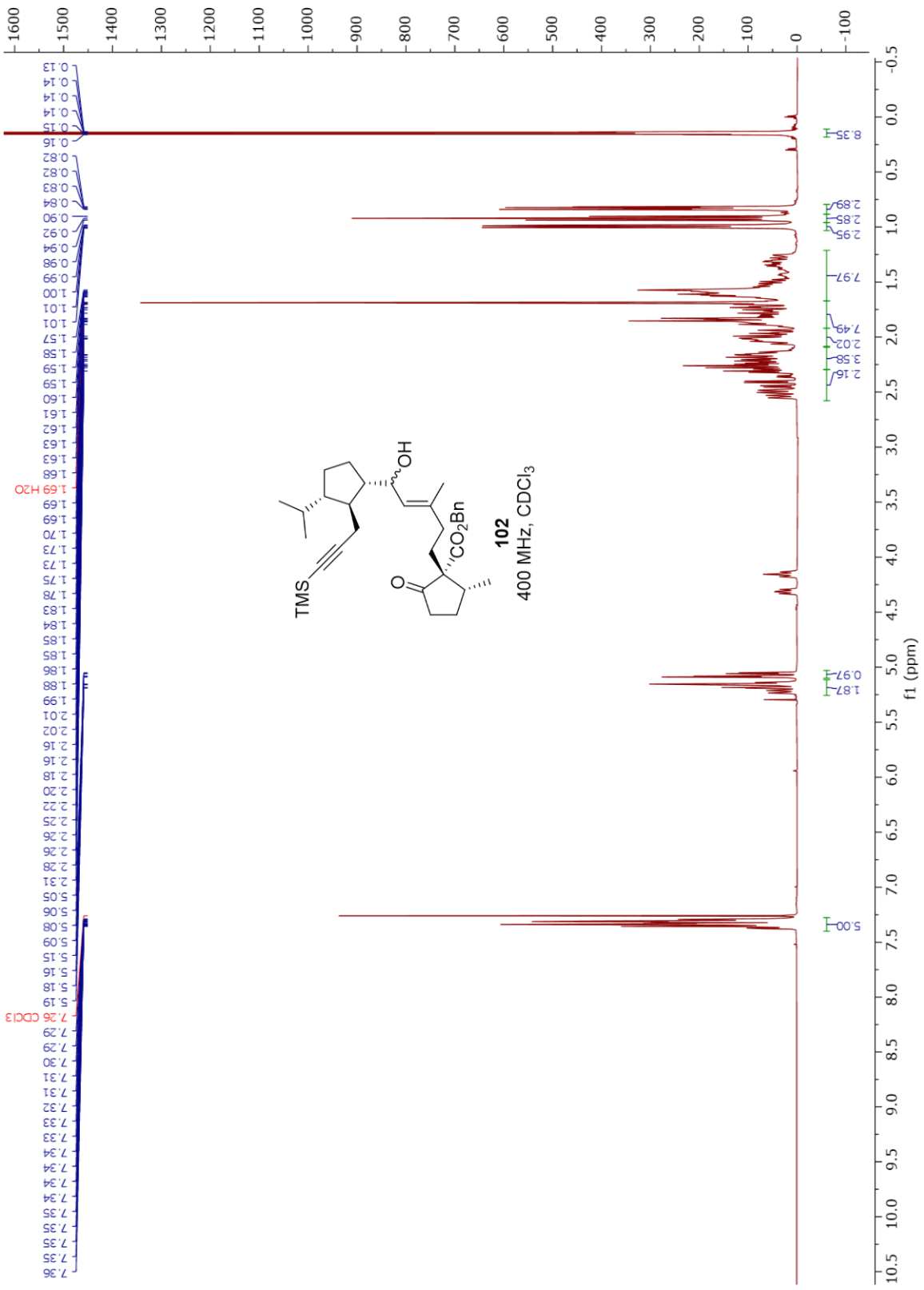
TMS
OH
CO2Bn
O
102
400 MHz, CDCl3
f1 (ppm)

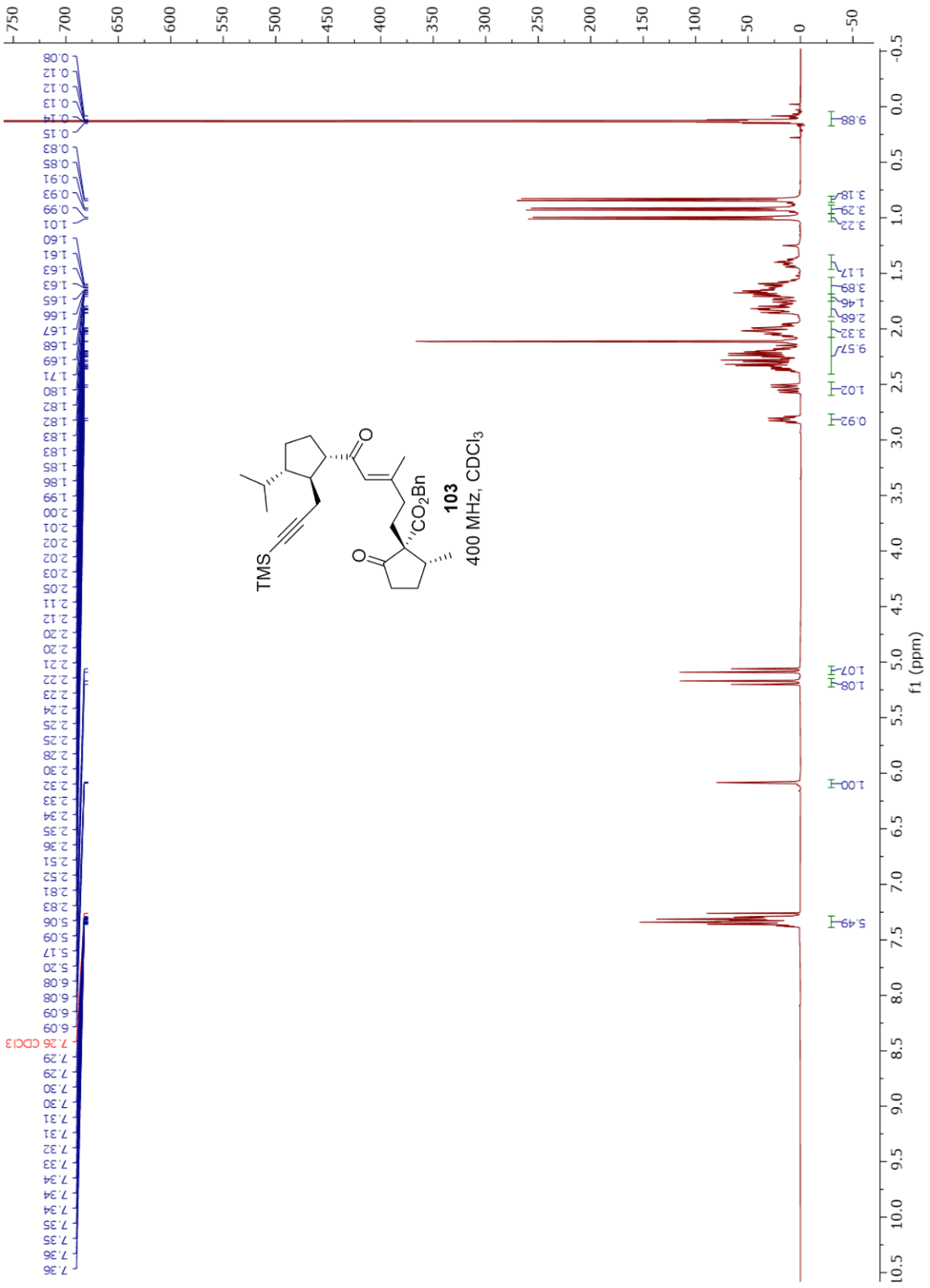
TMS
CO2Bn
O
O
103
400 MHz, CDCl3
f1 (ppm)
7.26 CDCl3
9.88
3.18
3.29
3.22
1.17
3.89
1.46
2.68
3.32
9.57
1.02
0.92
1.08
1.07
1.00
5.49

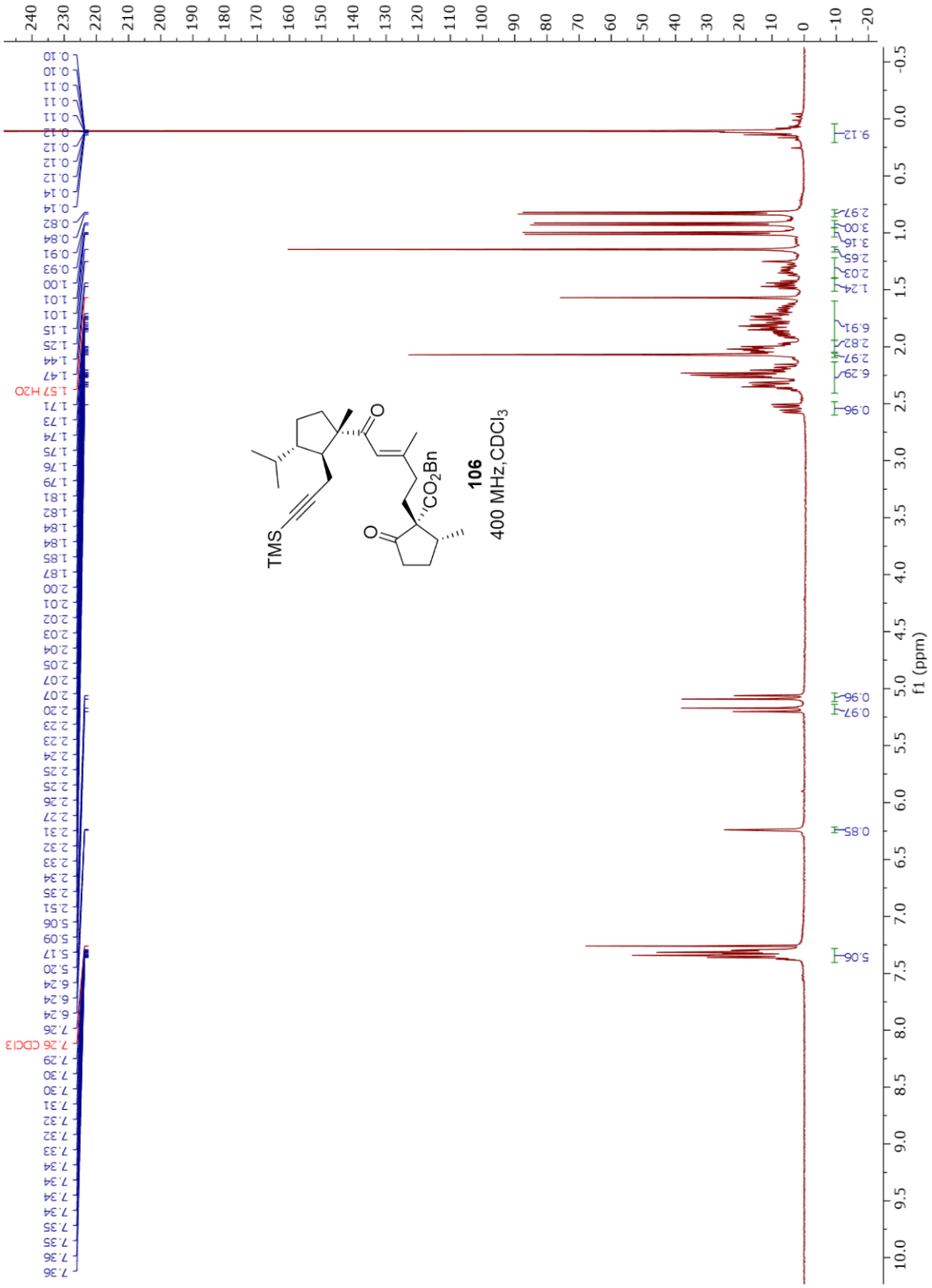
TMS
CO2Bn
O
O
106
400 MHz,CDCl3
f1 (ppm)
H2O
CDCl3

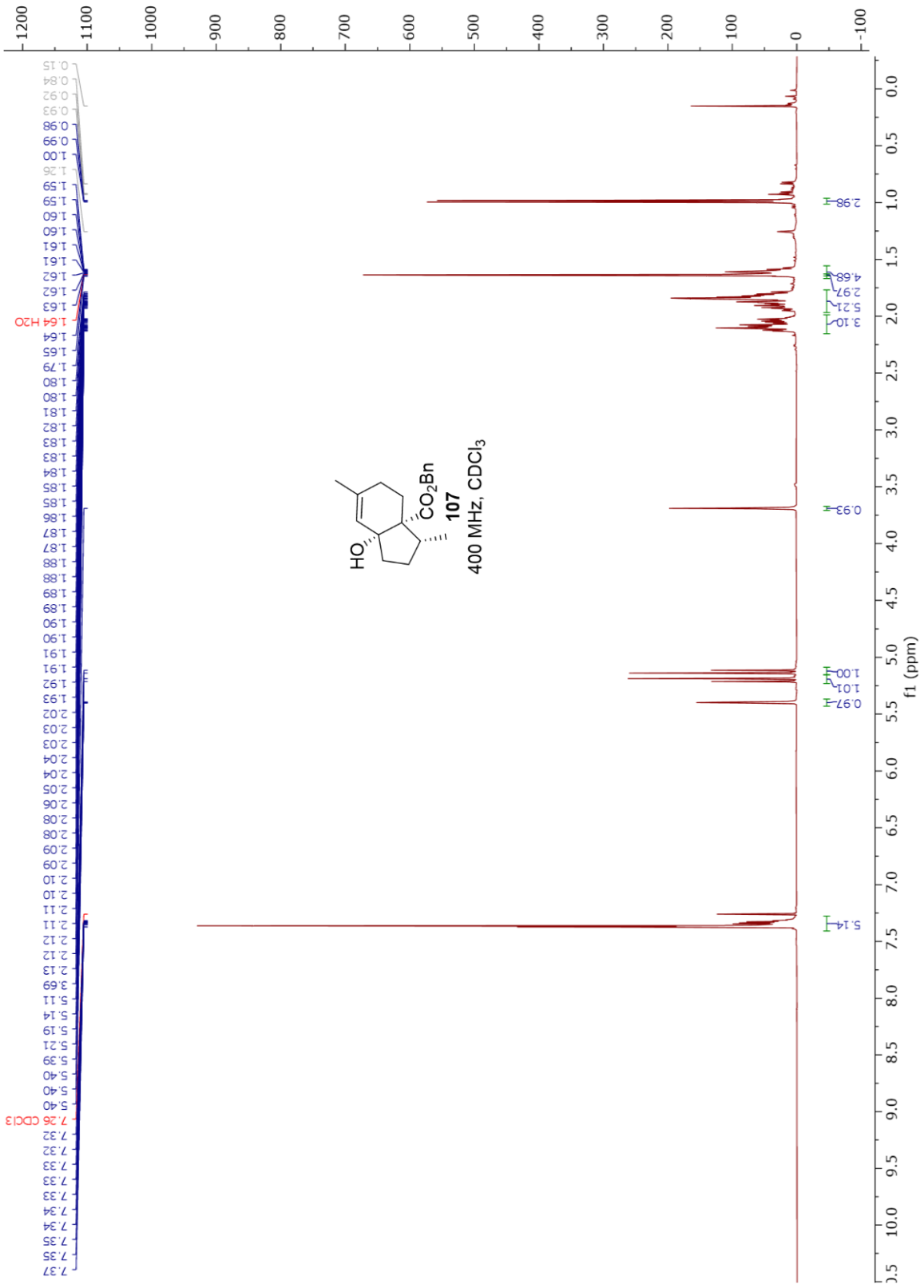
HO
CO2Bn
107
400 MHz, CDCl3
f1 (ppm)

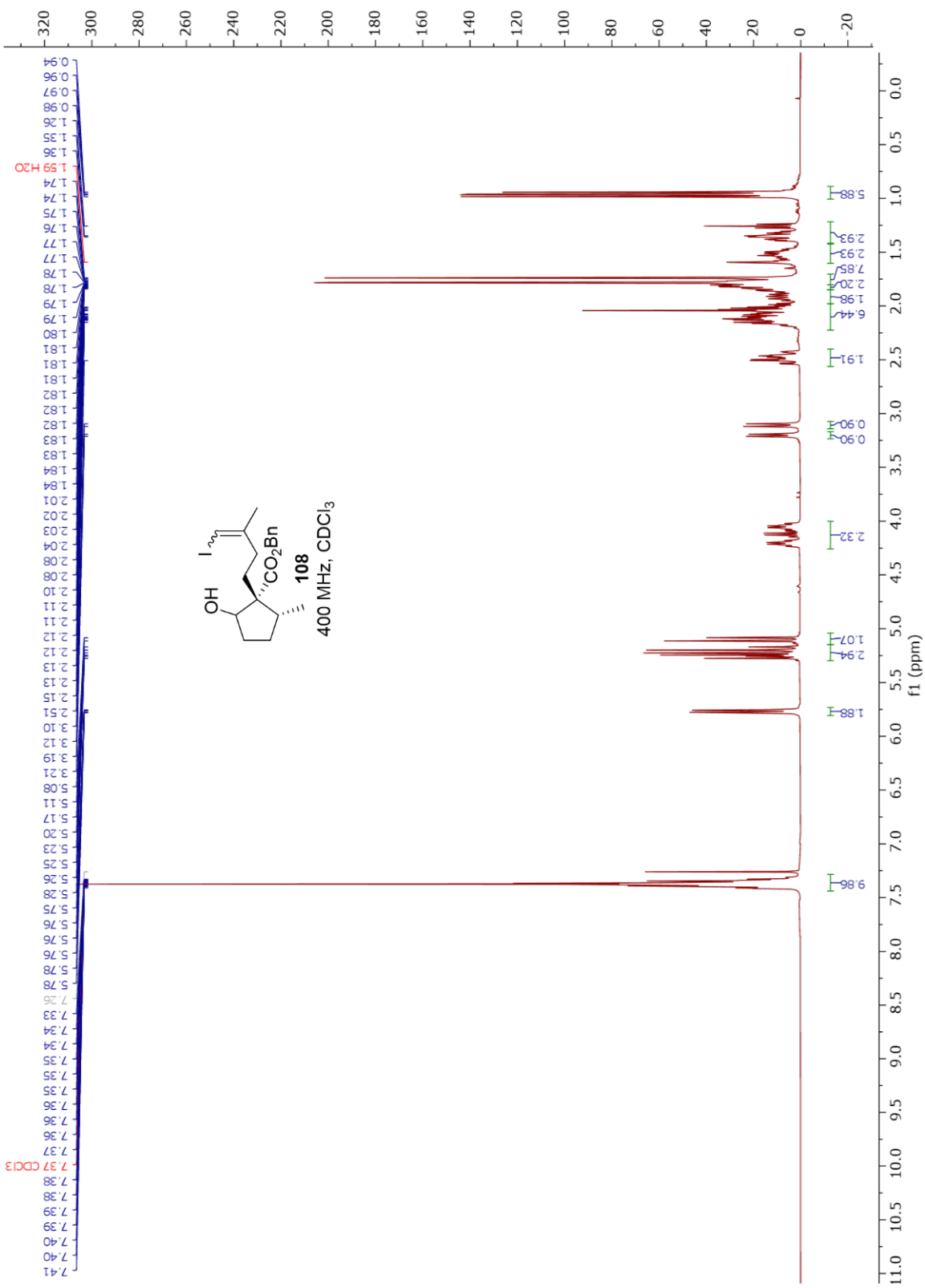
OH
I
CO2Bn
108
400 MHz, CDCl3
f1 (ppm)

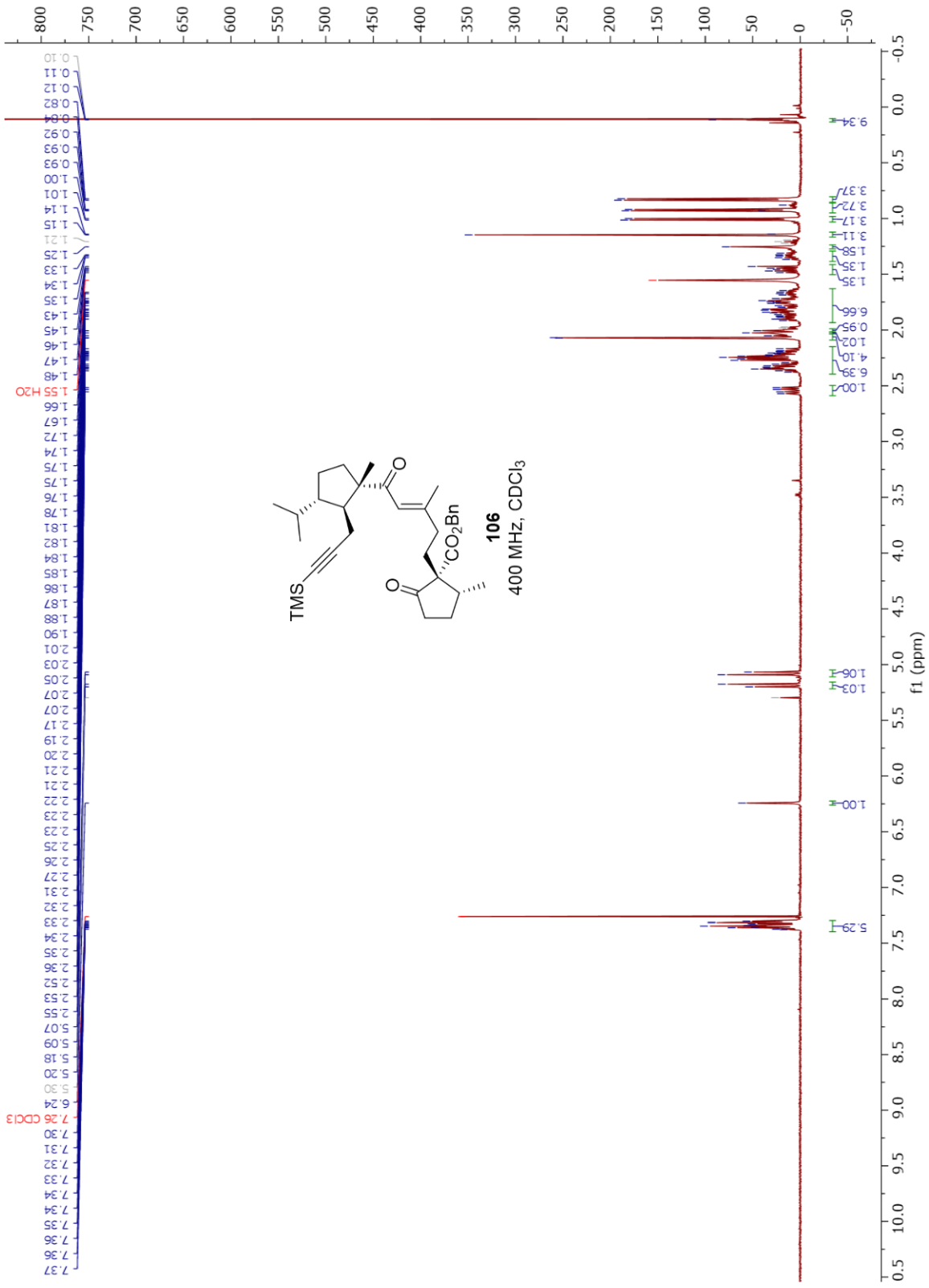
TMS
CO2Bn
106
400 MHz, CDCl3
f1 (ppm)
1.55 H2O
7.26 CDCl3

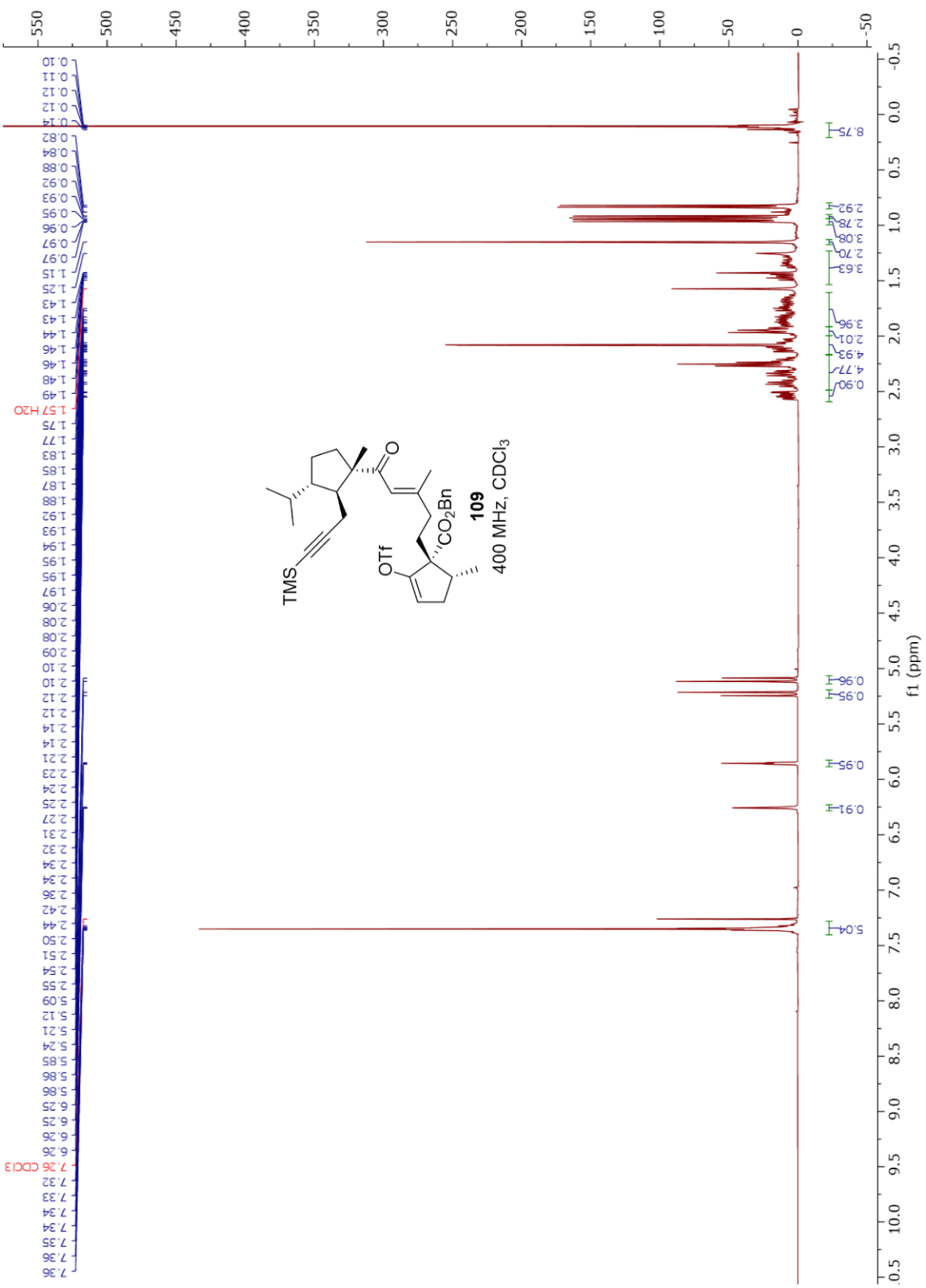
TMS
OTf
CO2Bn
O
109
400 MHz, CDCl3
f1 (ppm)

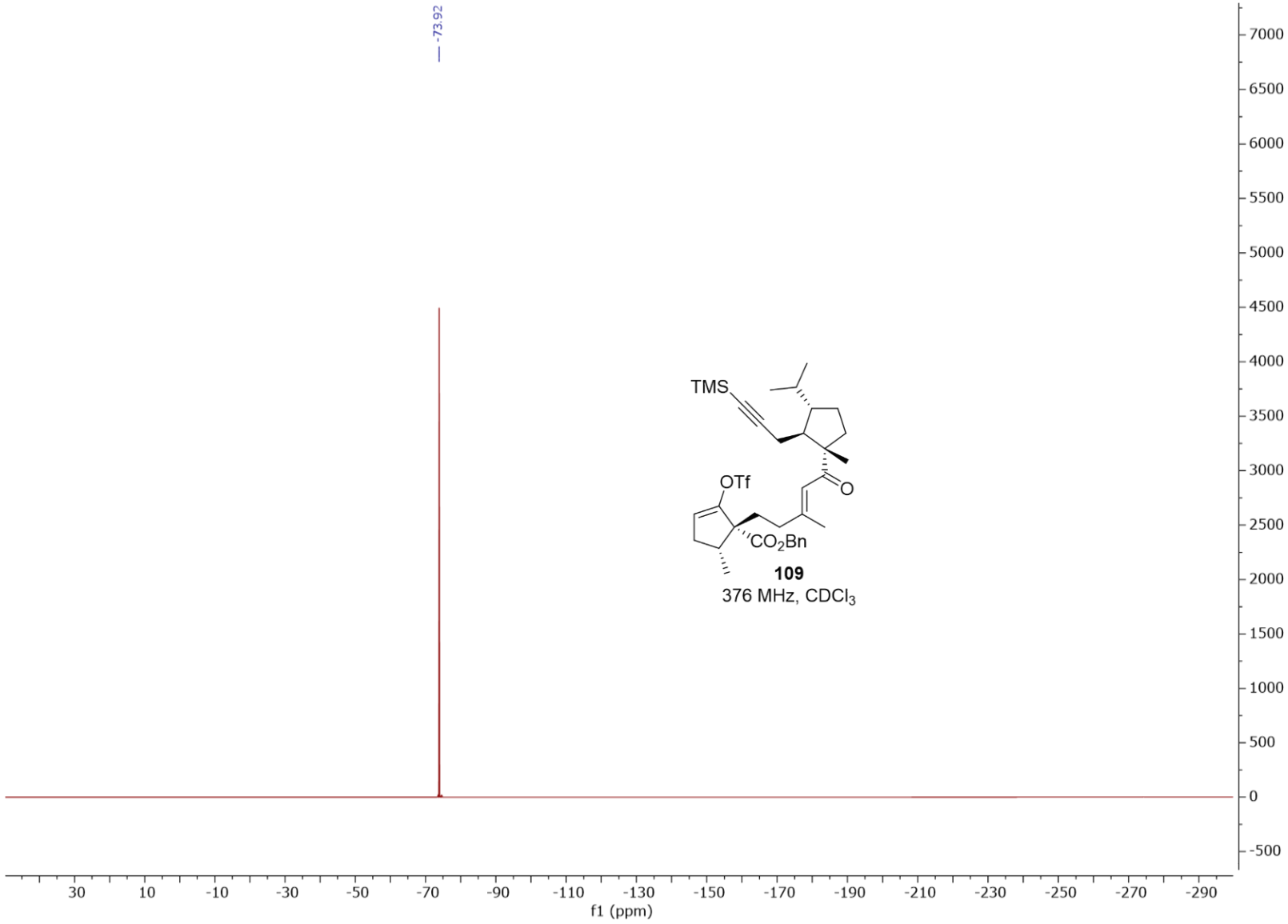
-73.92
TMS
OTf
O
CO2Bn
109
376 MHz, CDCl3
7000
6500
6000
5500
5000
4500
4000
3500
3000
2500
2000
1500
1000
500
0
-500
30
10
-10
-30
-50
-70
-90
-110
-130
-150
-170
-190
-210
-230
-250
-270
-290
f1 (ppm)

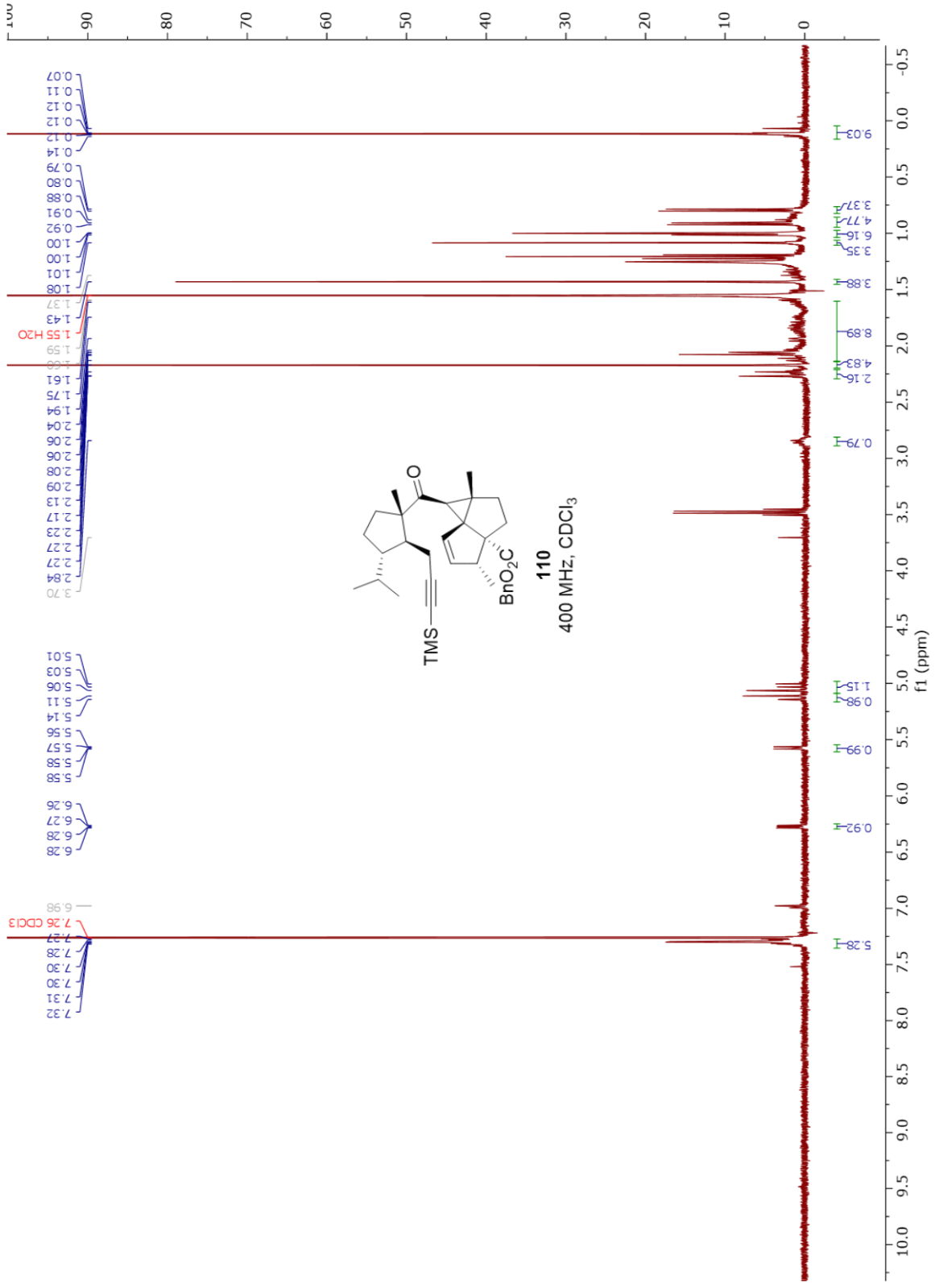
TMS
BnO2C
110
400 MHz, CDCl3
f1 (ppm)

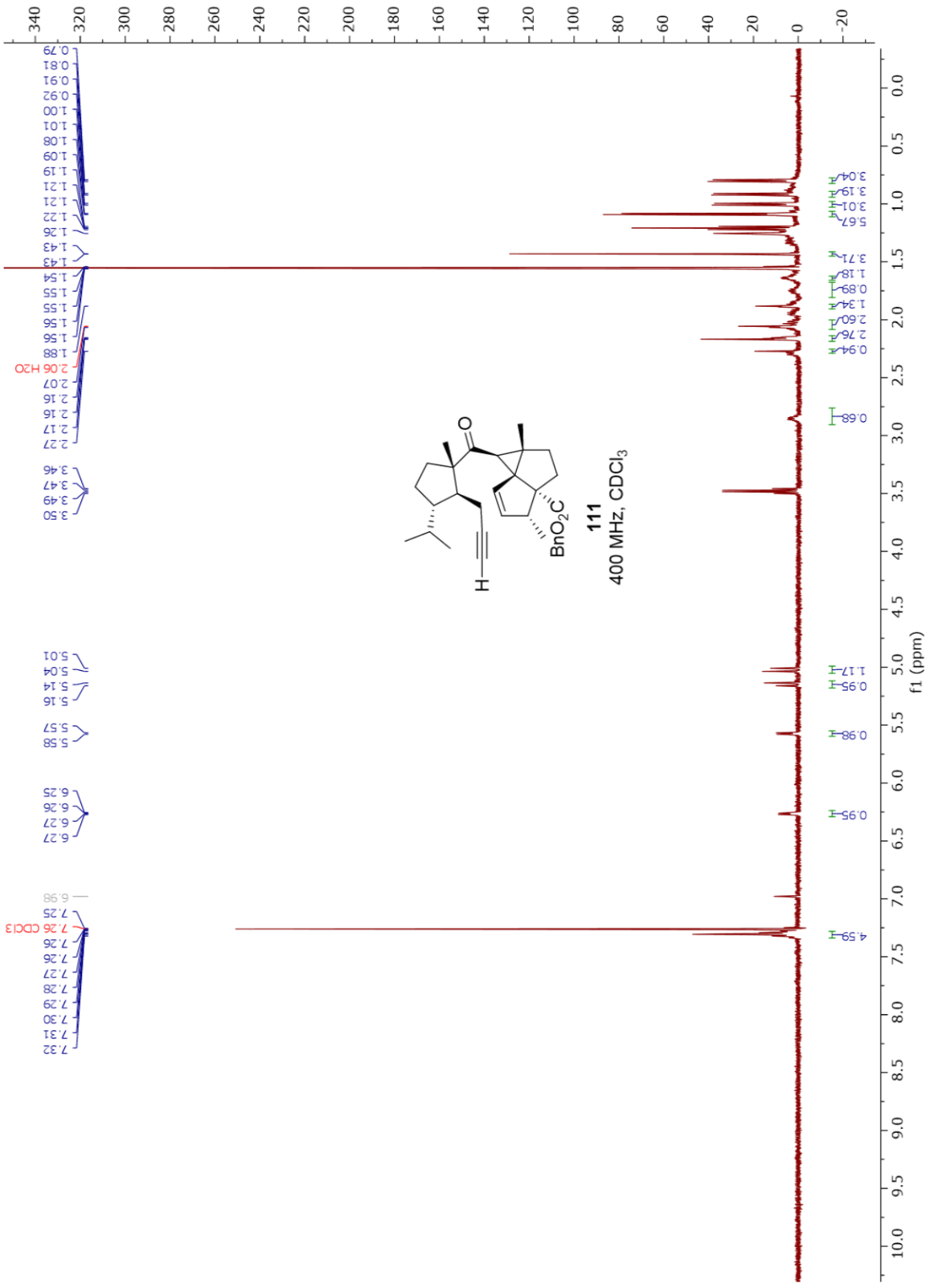
111
400 MHz, CDCl3
BnO2C
H
O
CDCl3
H2O
f1 (ppm)

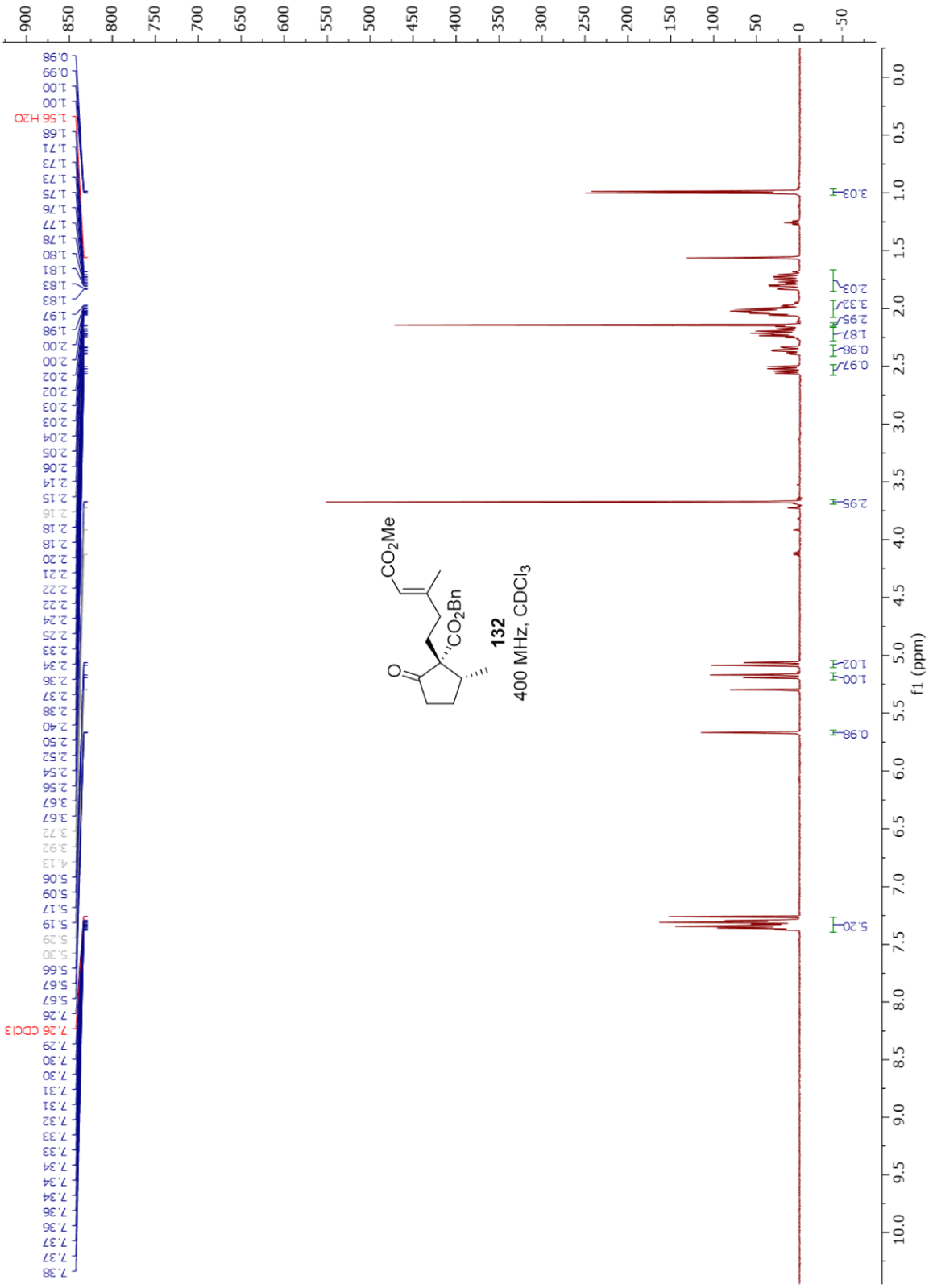
CO2Me
CO2Bn
O
132
400 MHz, CDCl3
f1 (ppm)

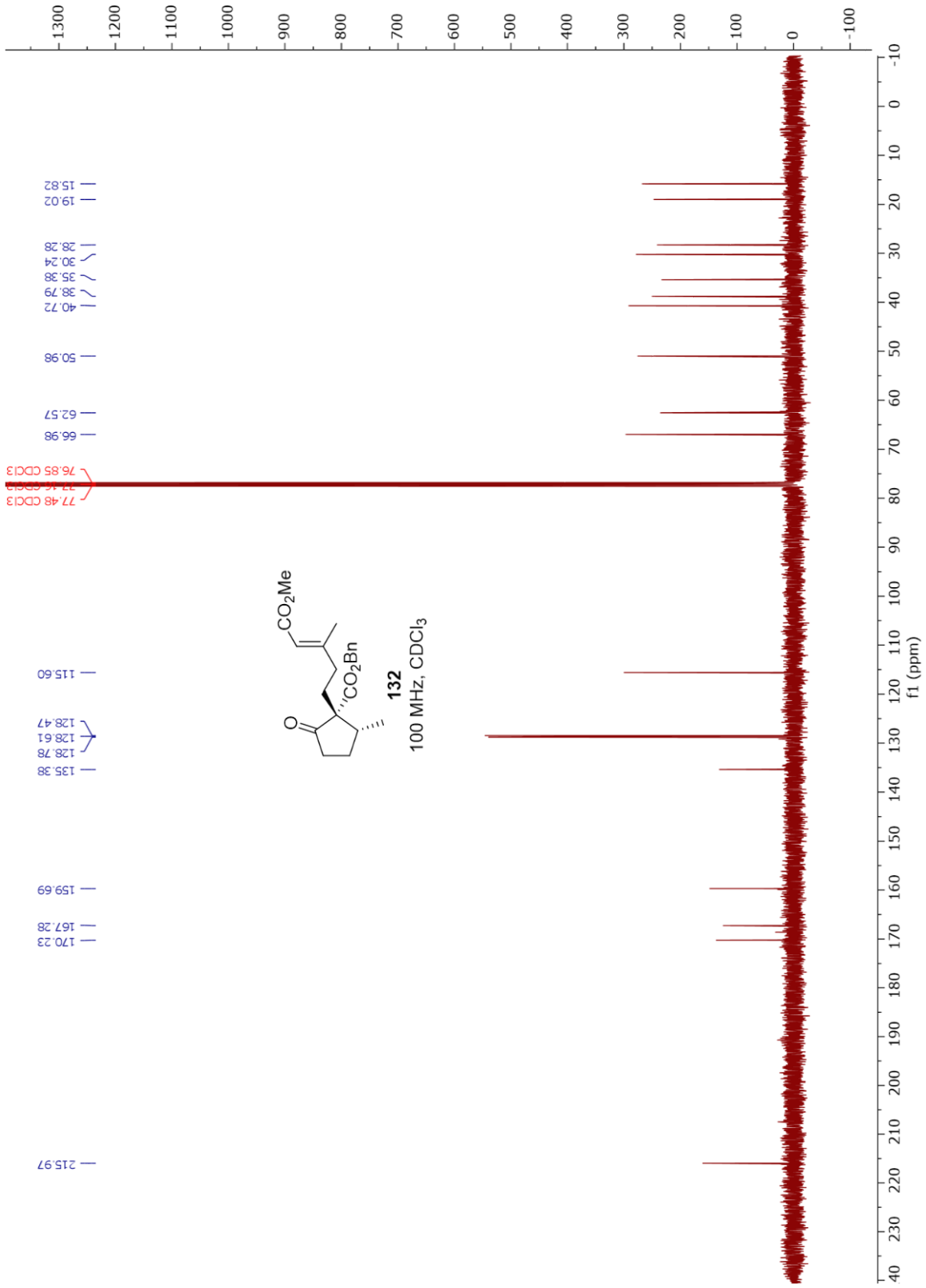
15.82
19.02
28.28
30.24
35.38
38.79
40.72
50.98
62.57
66.98
76.85 CDCl3
77.48 CDCl3
115.60
128.47
128.61
128.78
135.38
159.69
167.28
170.23
215.97
CO2Me
CO2Bn
O
132
100 MHz, CDCl3
f1 (ppm)

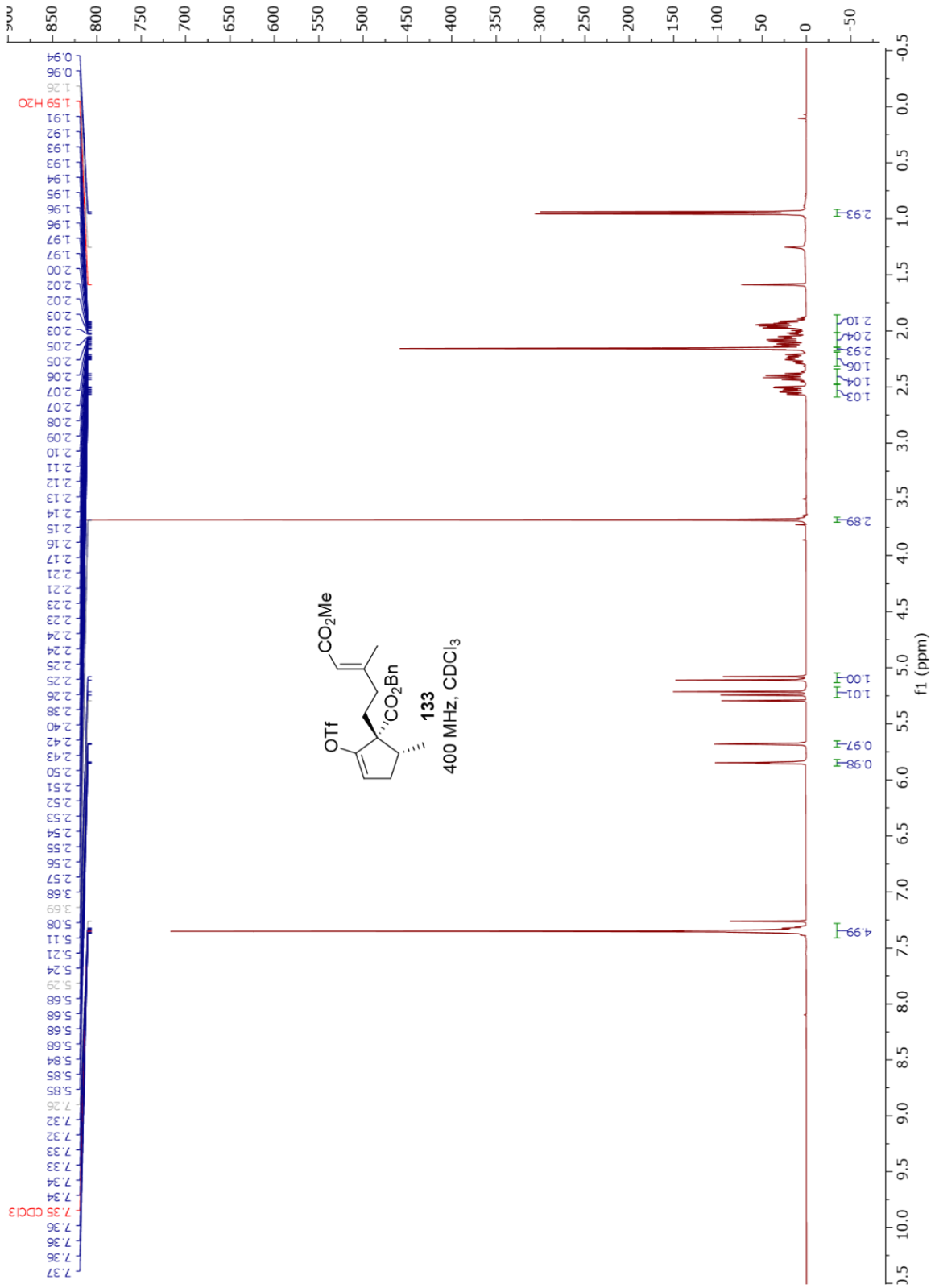
CO2Me
OTf
CO2Bn
133
400 MHz, CDCl3
f1 (ppm)

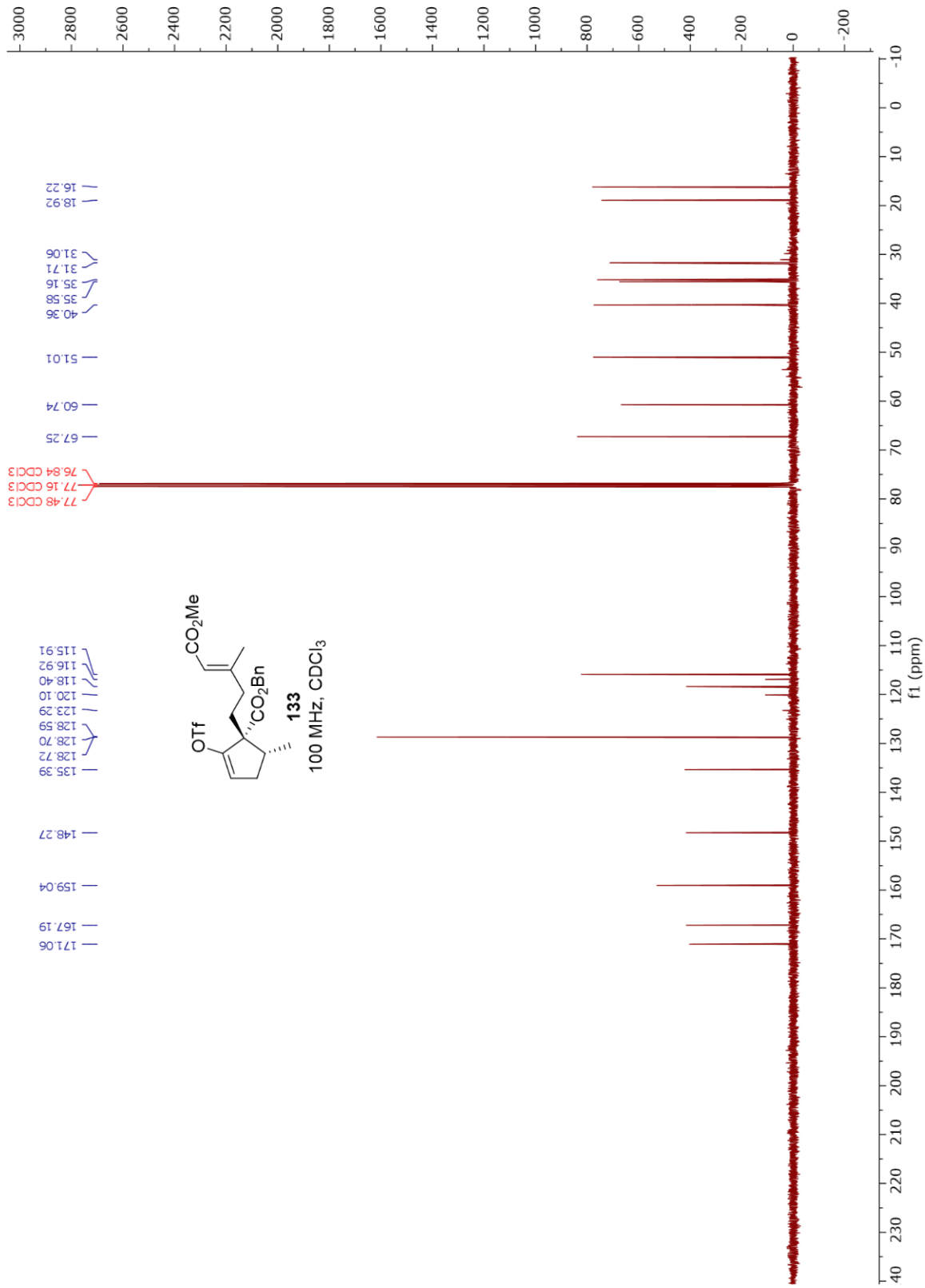
133
100 MHz, CDCl3
OTf
CO2Bn
CO2Me
16.22
18.92
31.06
31.71
35.16
35.58
40.36
51.01
60.74
67.25
76.84 CDCl3
77.16 CDCl3
77.48 CDCl3
115.91
116.92
118.40
120.10
123.29
128.59
128.70
128.72
135.39
148.27
159.04
167.19
171.06
f1 (ppm)

CO2Me
OTf
CO2Bn
133
376 MHz, CDCl3
-73.93
f1 (ppm)

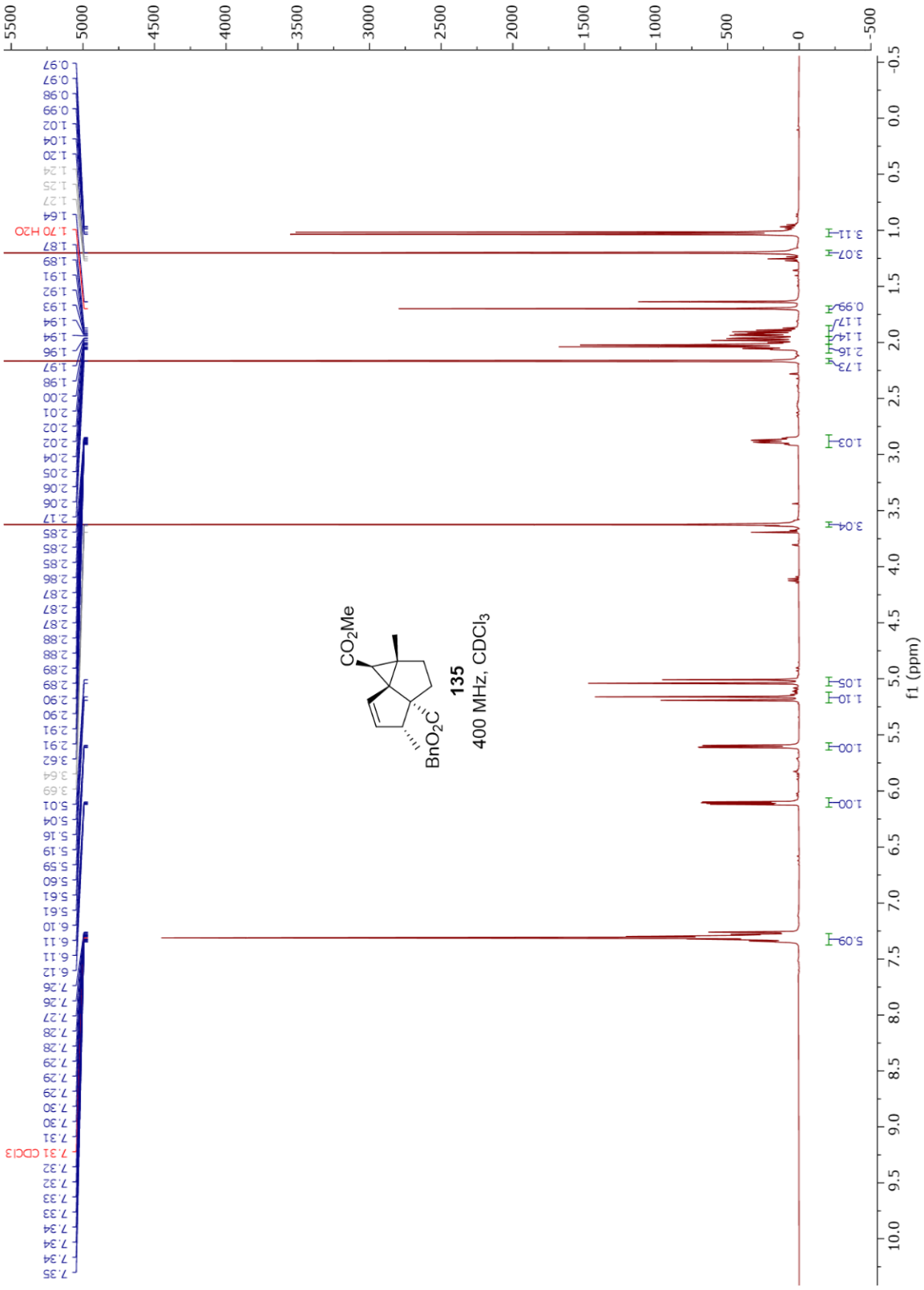
CO2Me
BnO2C
135
400 MHz, CDCl3
f1 (ppm)

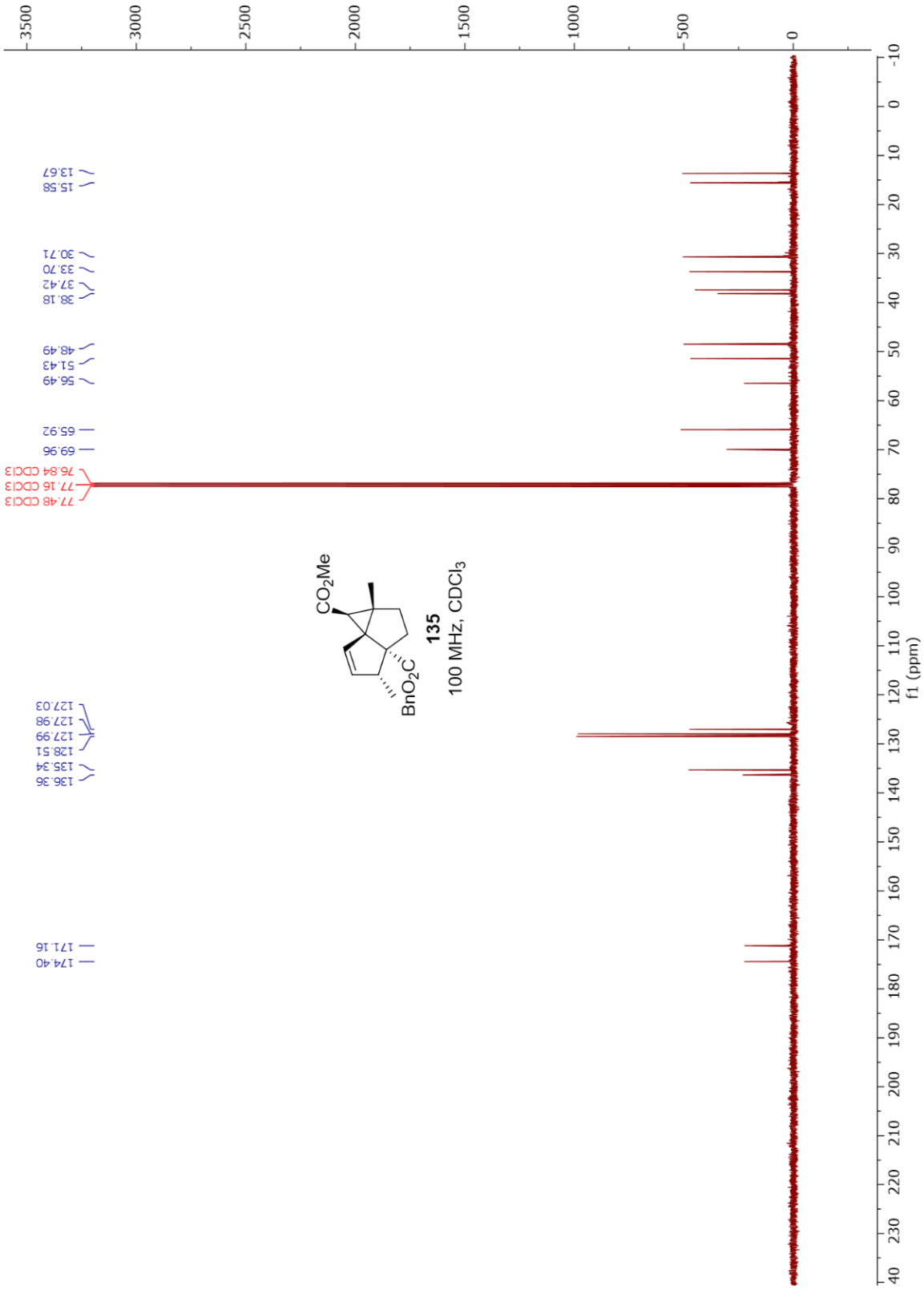
CO2Me
BnO2C
135
100 MHz, CDCl3
f1 (ppm)
13.67
15.58
30.71
33.70
37.42
38.18
48.49
51.43
56.49
65.92
69.96
76.84 CDCl3
77.16 CDCl3
77.48 CDCl3
127.03
127.98
127.99
128.51
135.34
136.36
171.16
174.40

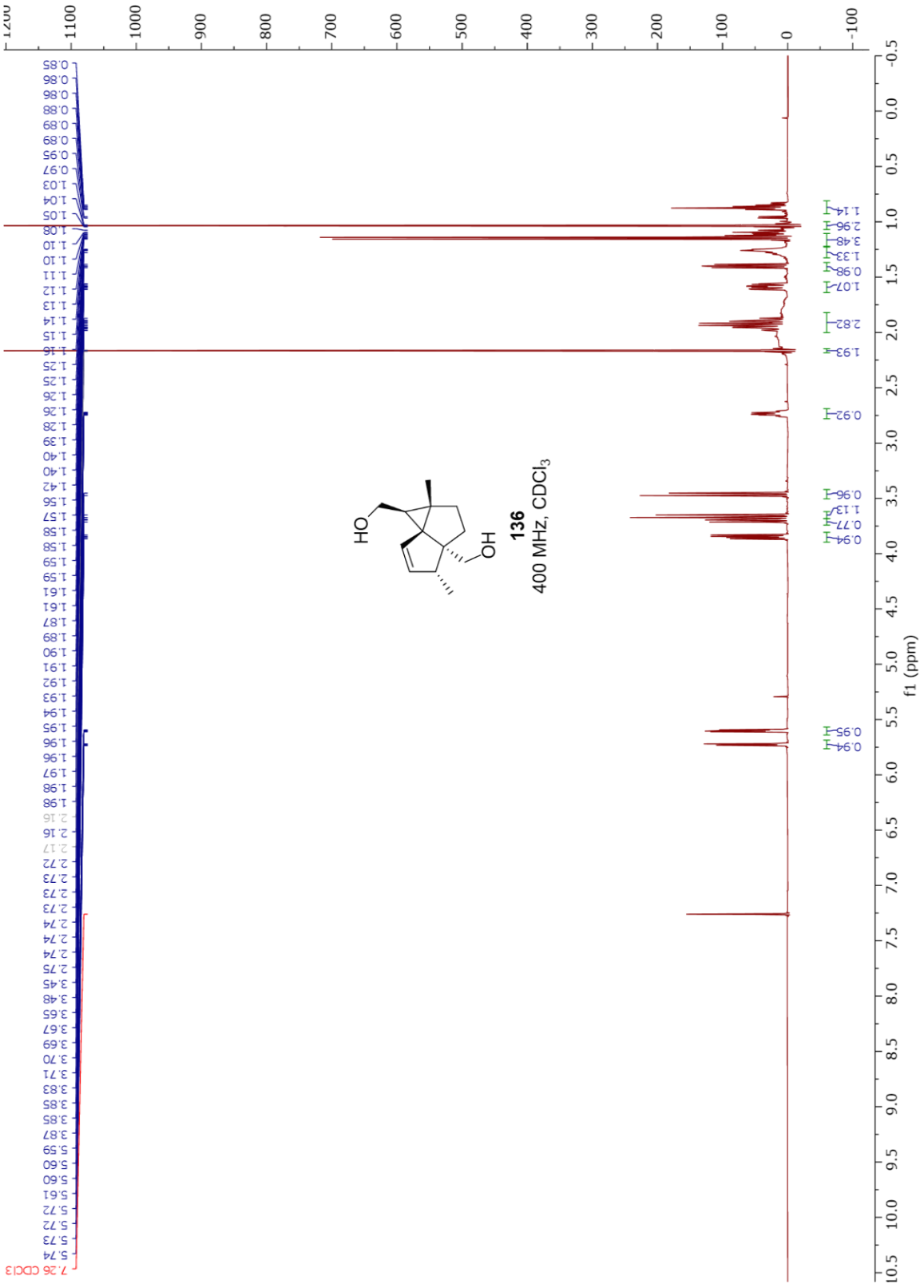
HO
OH
136
400 MHz, CDCl3
f1 (ppm)

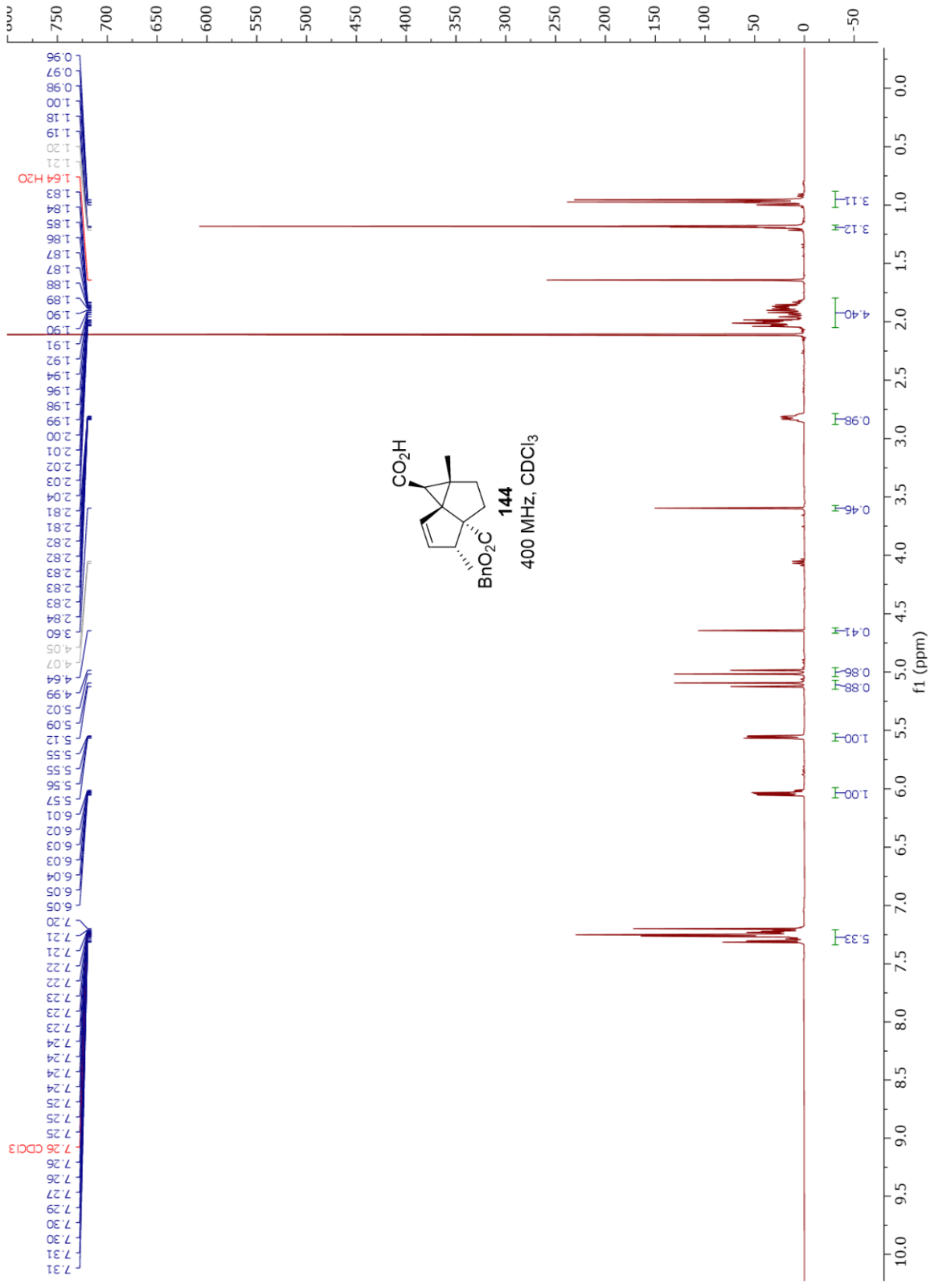
CO2H
BnO2C
144
400 MHz, CDCl3
f1 (ppm)

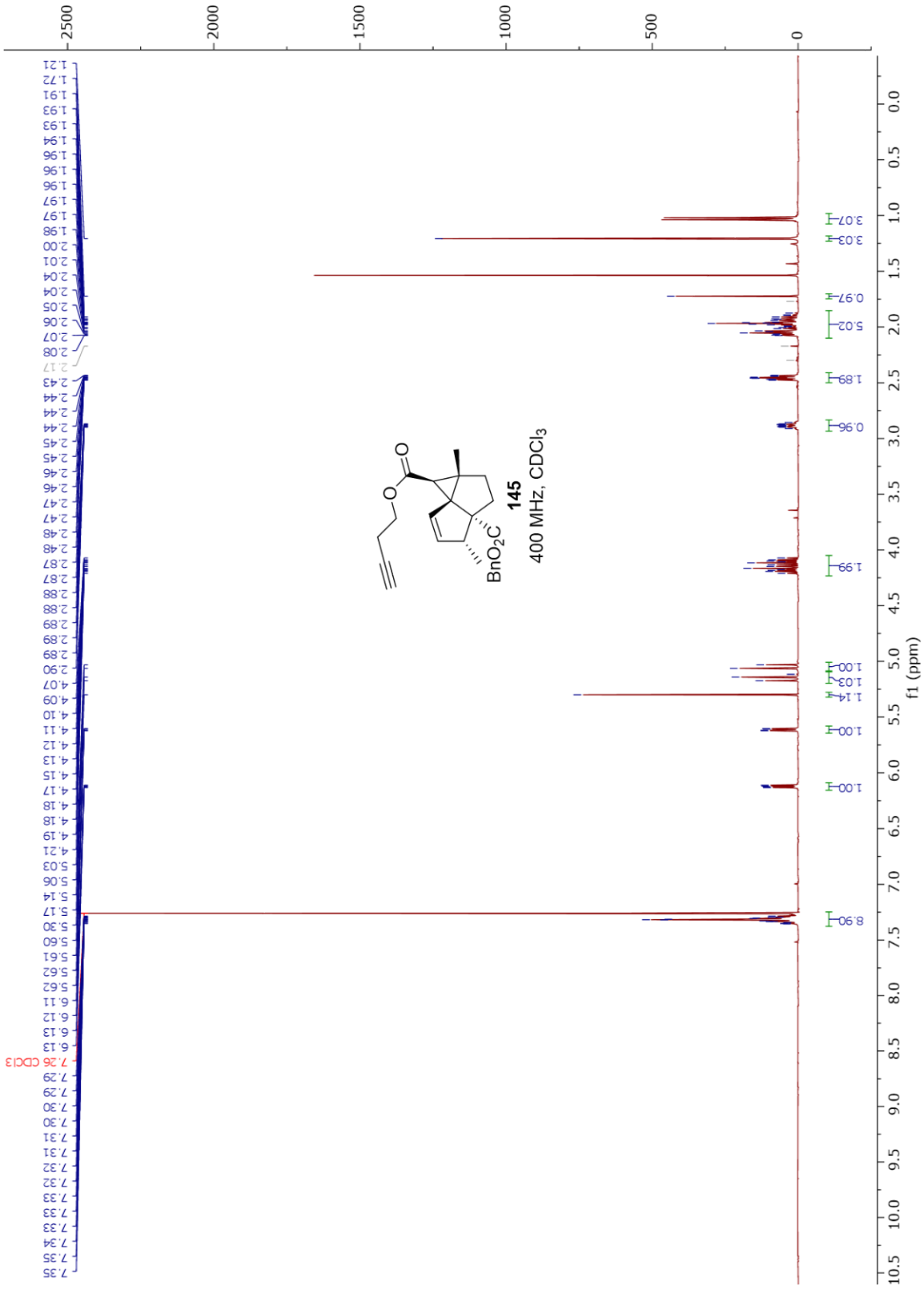
145
400 MHz, CDCl3
BnO2C
f1 (ppm)
7.26 CDCl3

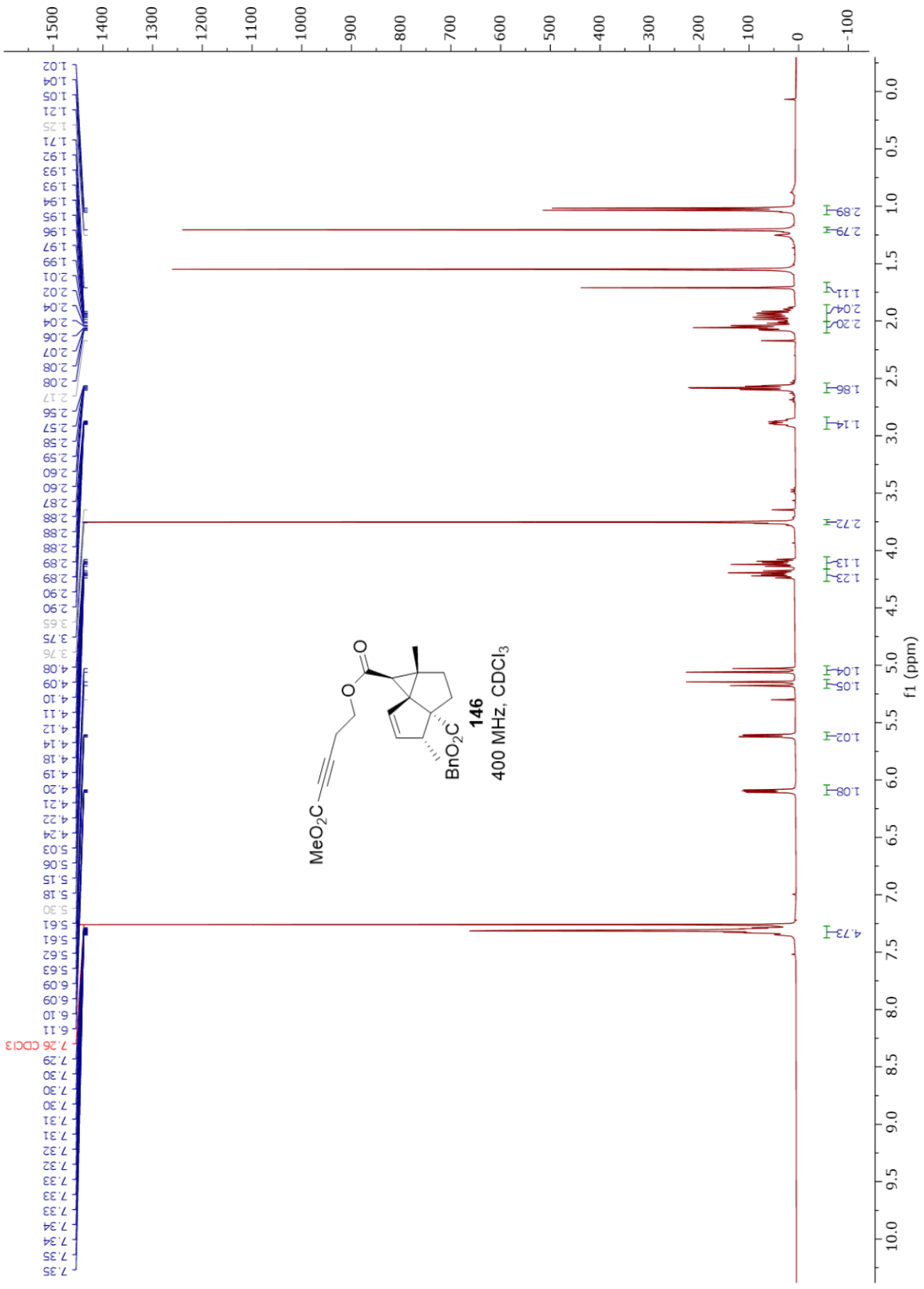
MeO2C
O
O
BnO2C
146
400 MHz, CDCl3
f1 (ppm)
7.26 CDCl3

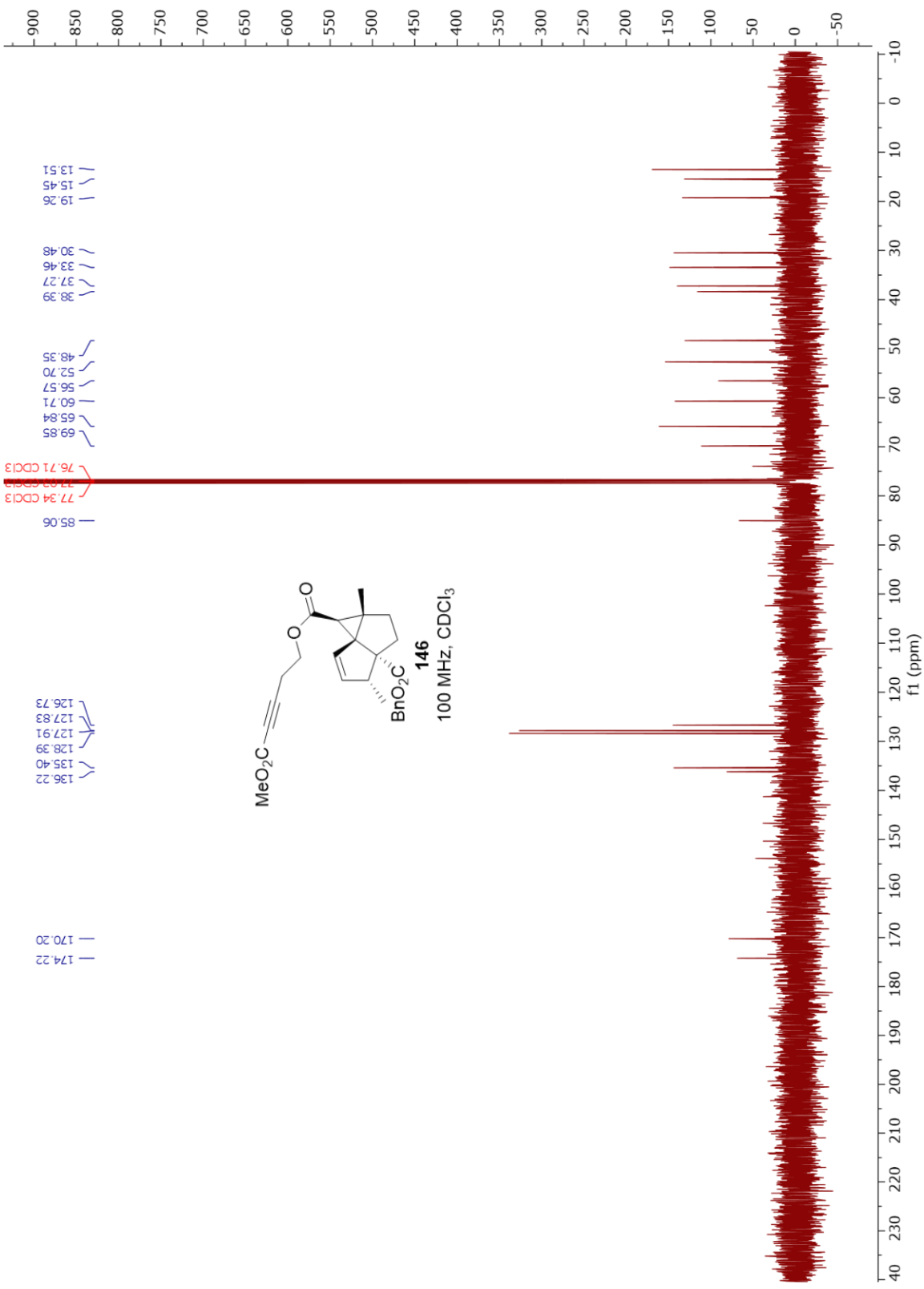
MeO2C
BnO2C
146
100 MHz, CDCl3
f1 (ppm)
13.51
15.45
19.26
30.48
33.46
37.27
38.39
48.35
52.70
56.57
60.71
65.84
69.85
76.71 CDCl3
77.03 CDCl3
77.34 CDCl3
85.06
126.73
127.83
127.91
128.39
135.40
136.22
170.20
174.22

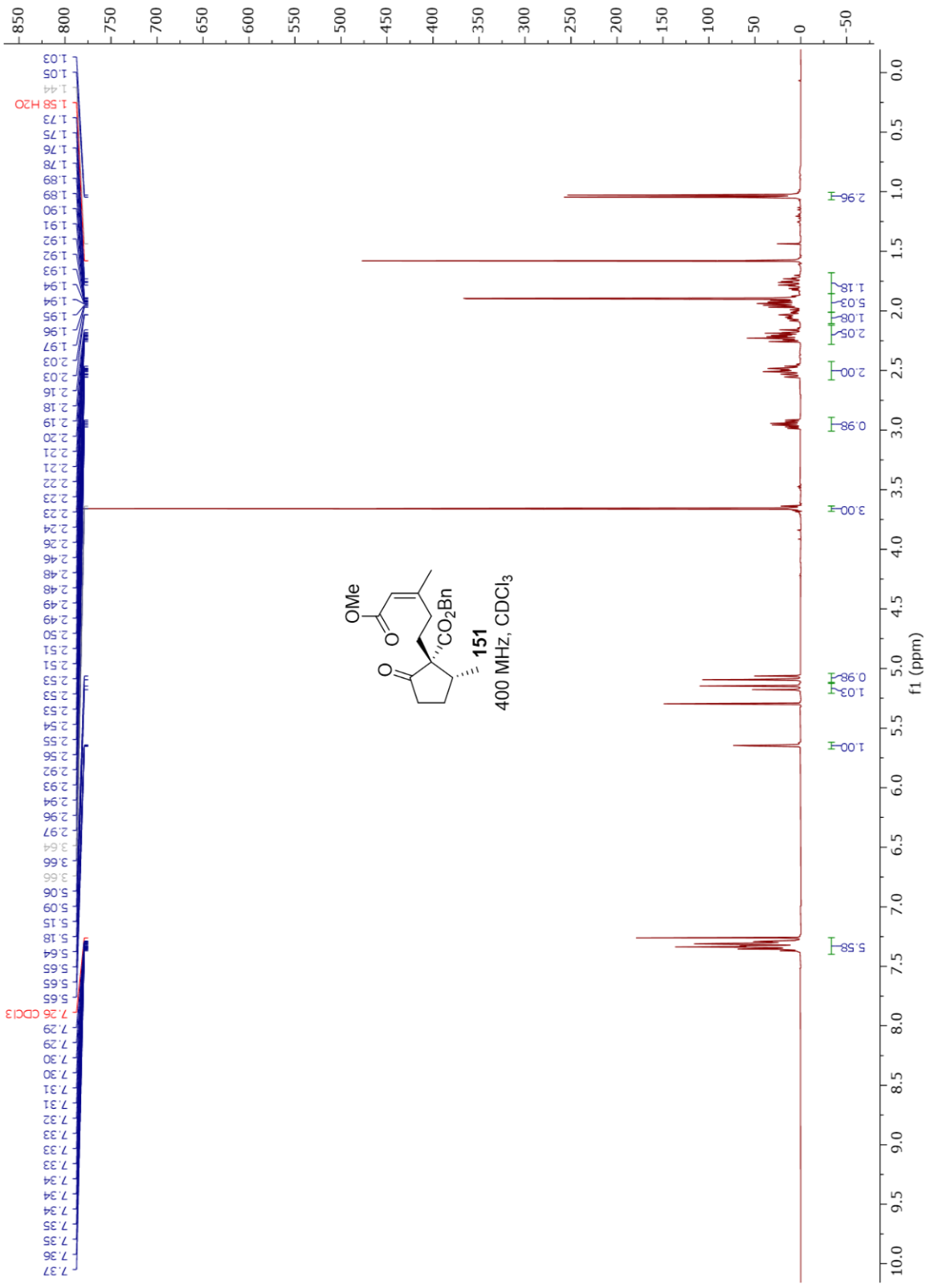
OMe
O
O
CO2Bn
151
400 MHz, CDCl3
f1 (ppm)

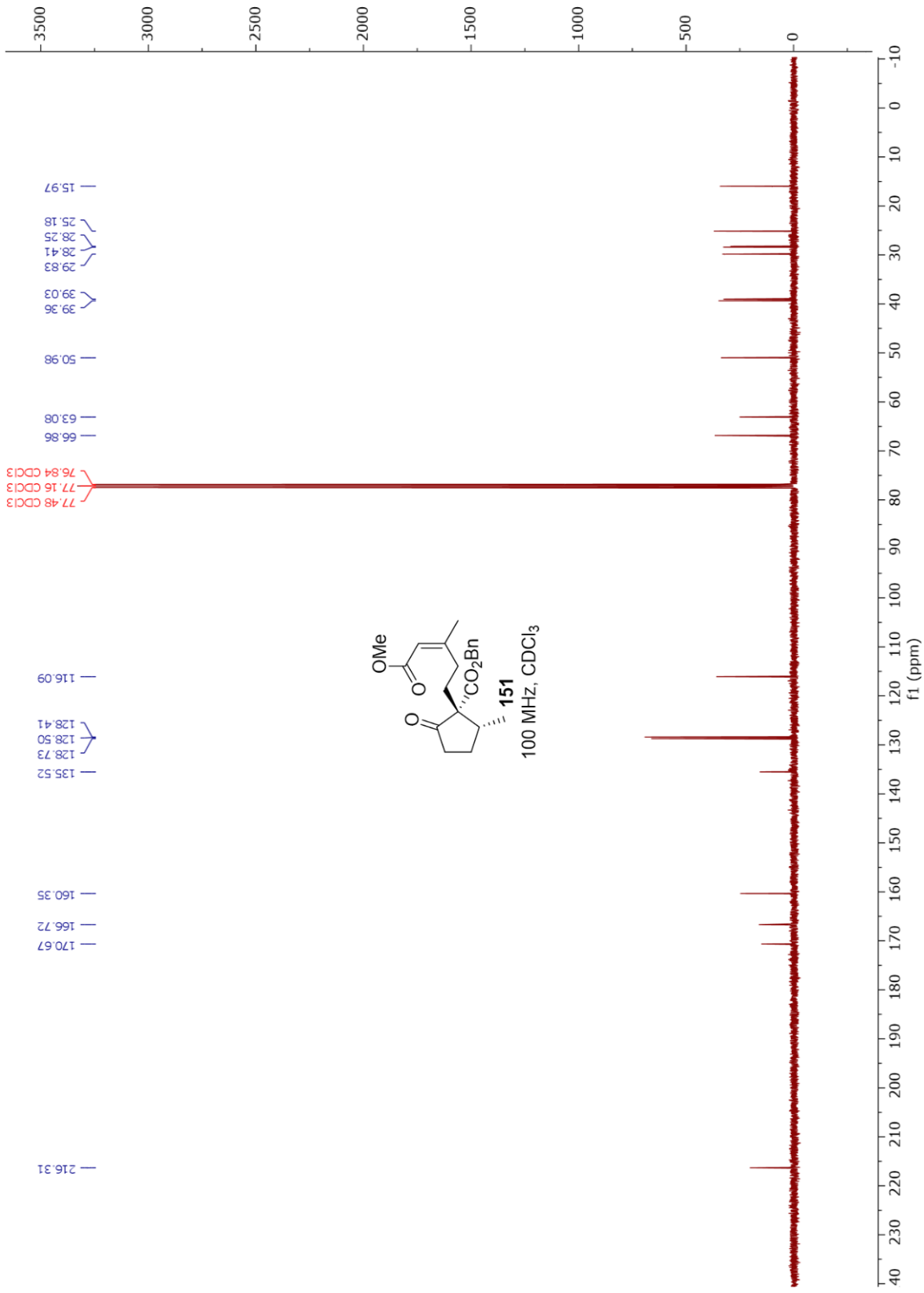
15.97
25.18
28.25
28.41
29.83
39.03
39.36
50.98
63.08
66.86
76.84 CDCl3
77.16 CDCl3
77.48 CDCl3
116.09
128.41
128.50
128.73
135.52
160.35
166.72
170.67
216.31
OMe
O
O
CO2Bn
151
100 MHz, CDCl3
f1 (ppm)

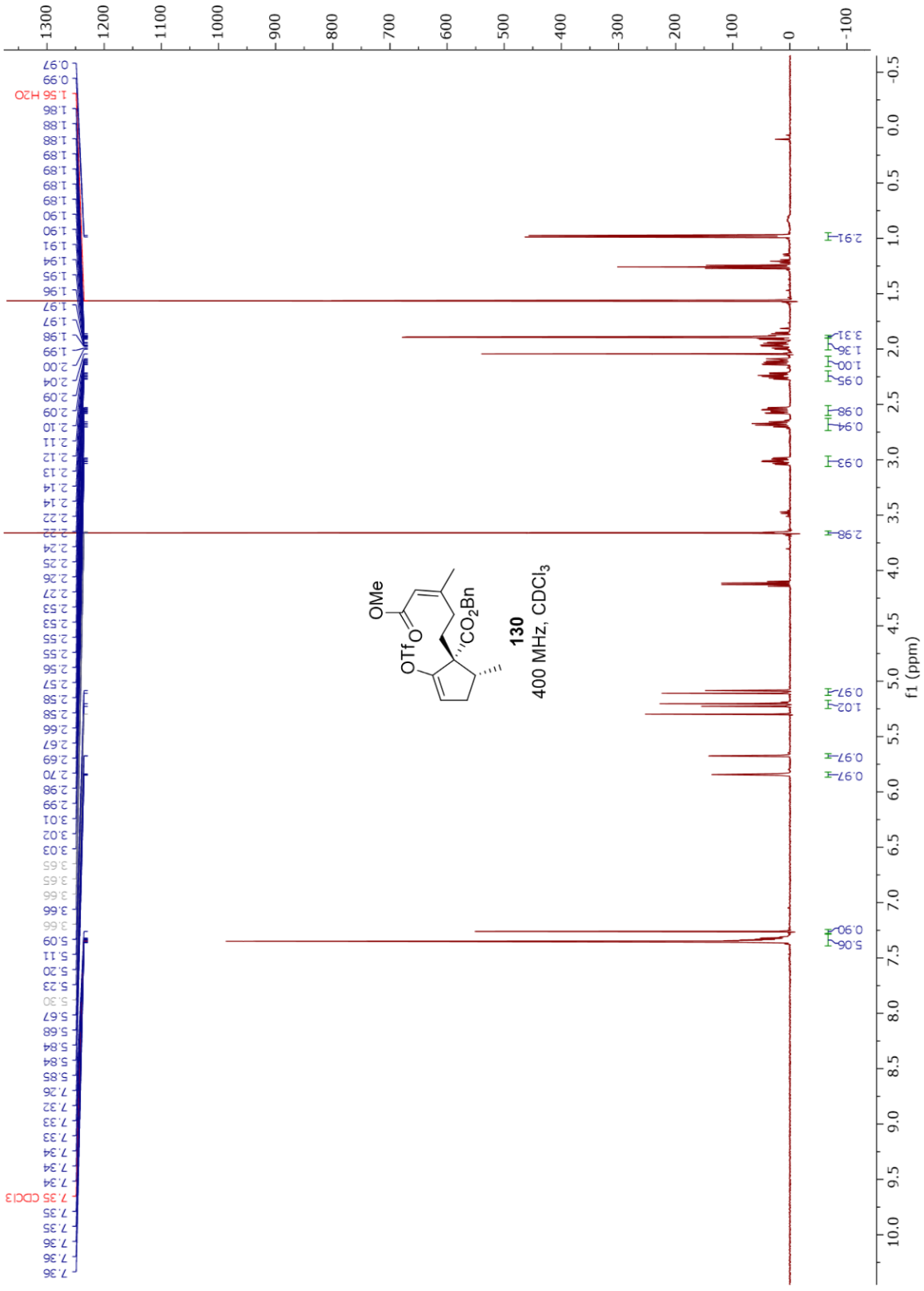
OMe
OTf
O
CO2Bn
130
400 MHz, CDCl3
f1 (ppm)

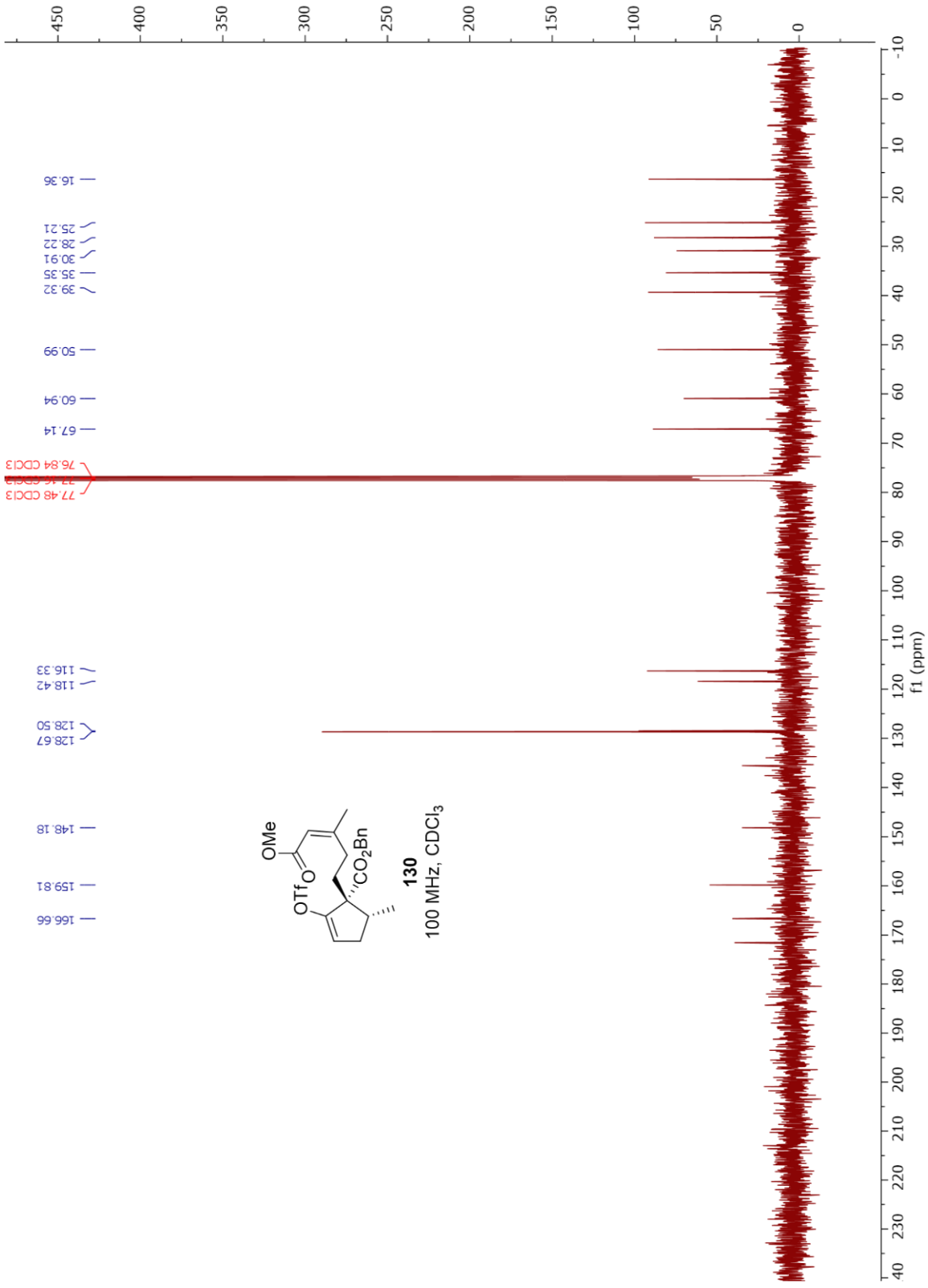
16.36
25.21
28.22
30.91
35.35
39.32
50.99
60.94
67.14
76.84 CDCl3
77.48 CDCl3
116.33
118.42
128.50
128.67
148.18
159.81
166.66
OMe
OTf
O
CO2Bn
130
100 MHz, CDCl3
f1 (ppm)

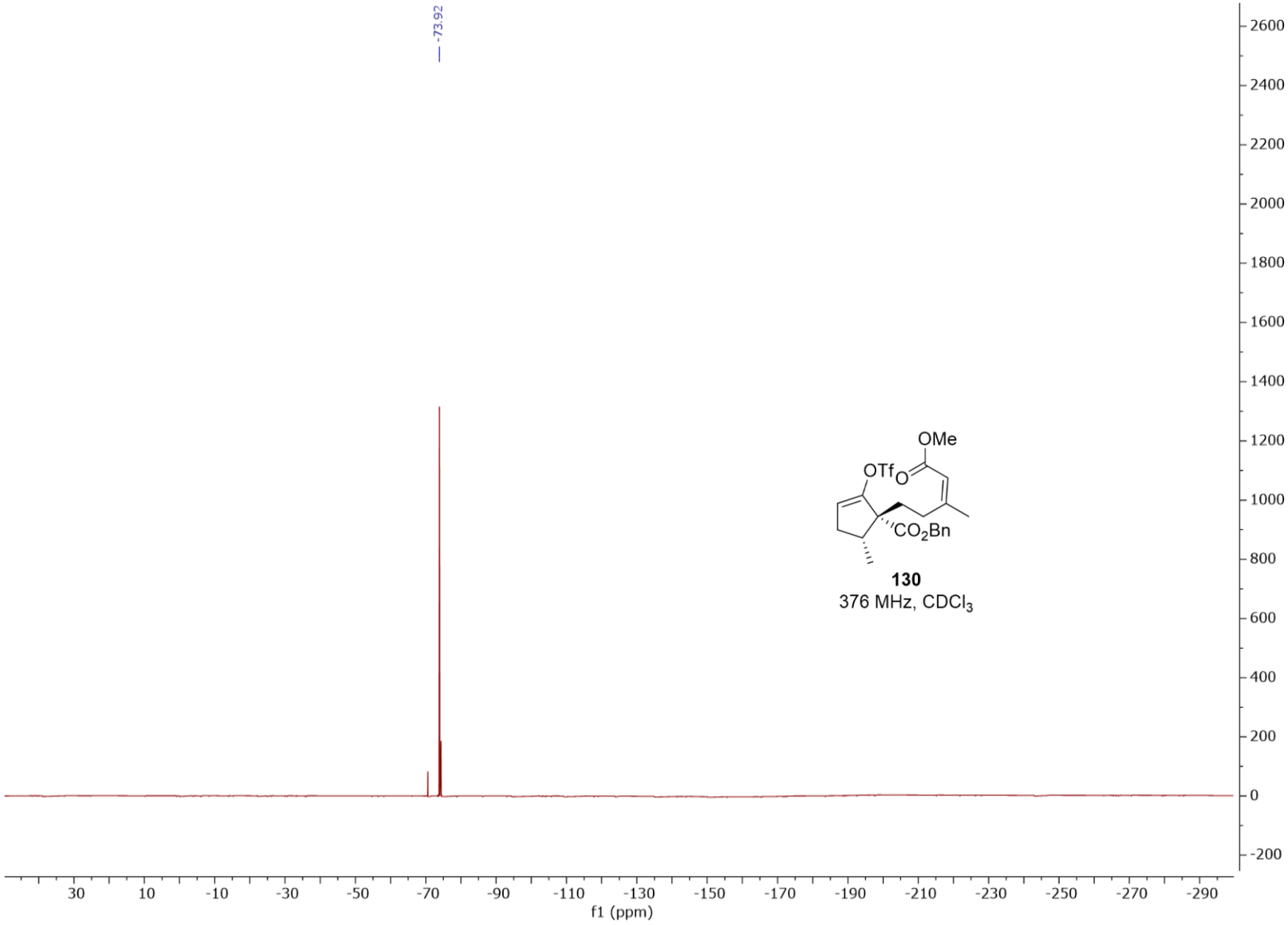
-73.92
OMe
OTf
O
CO2Bn
130
376 MHz, CDCl3
2600
2400
2200
2000
1800
1600
1400
1200
1000
800
600
400
200
0
-200
30
10
-10
-30
-50
-70
-90
-110
-130
-150
-170
-190
-210
-230
-250
-270
-290
f1 (ppm)

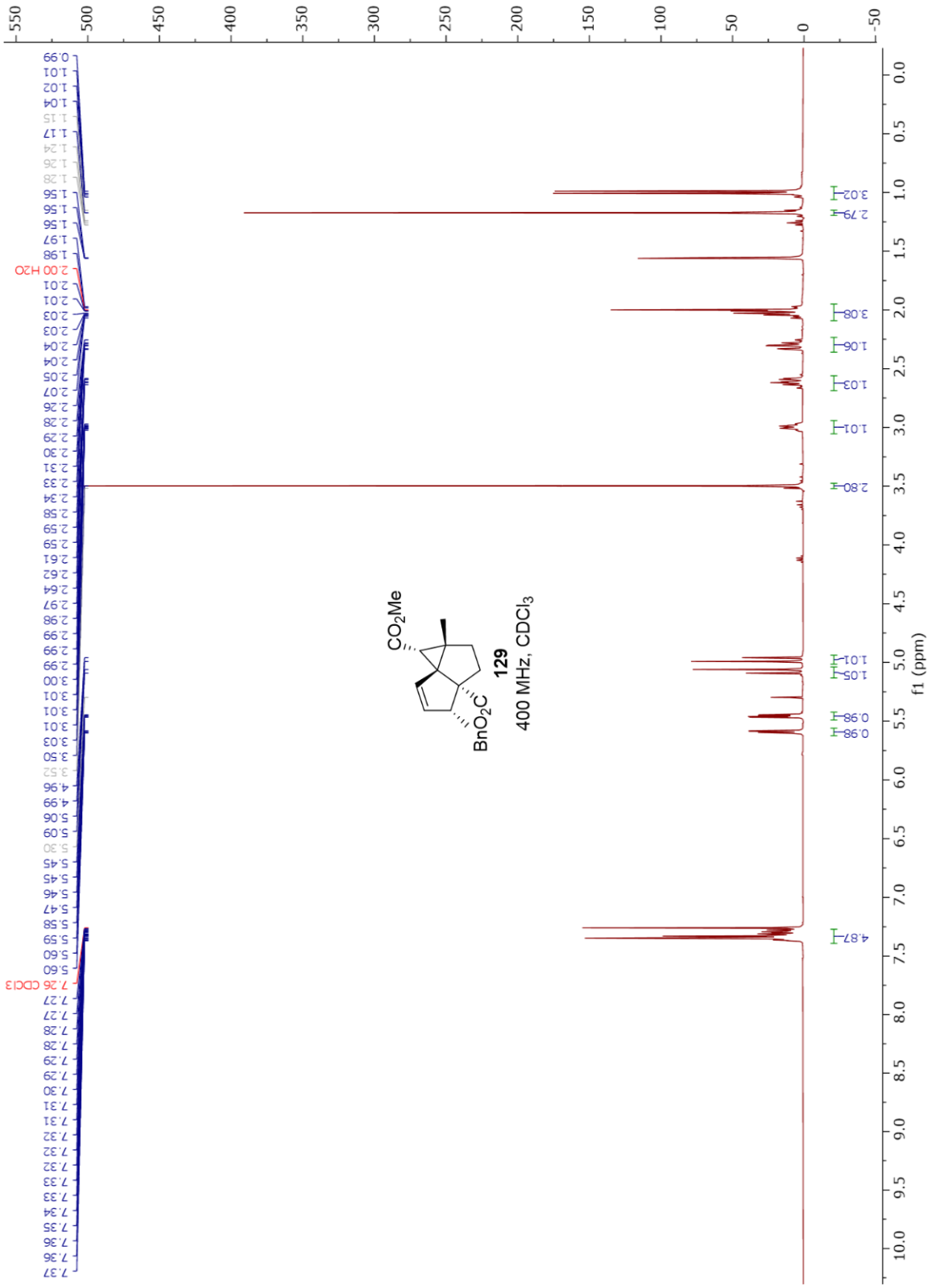
CO2Me
BnO2C
129
400 MHz, CDCl3
f1 (ppm)
7.26 CDCl3
2.00 H2O
4.87
0.98
0.98
1.05
1.01
2.80
1.01
1.03
1.06
3.08
2.79
3.02

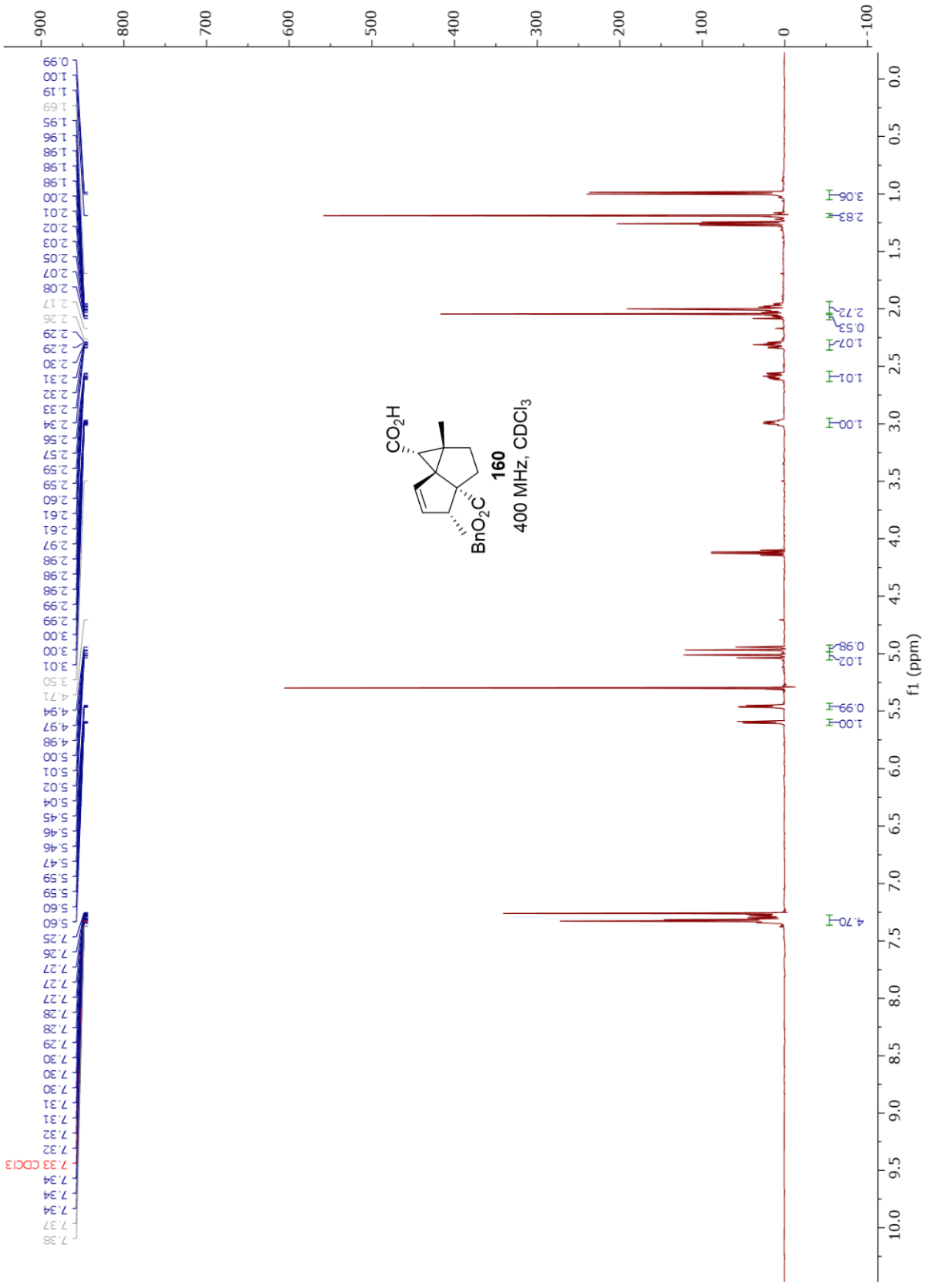
CO2H
BnO2C
160
400 MHz, CDCl3
f1 (ppm)
7.33 CDCl3

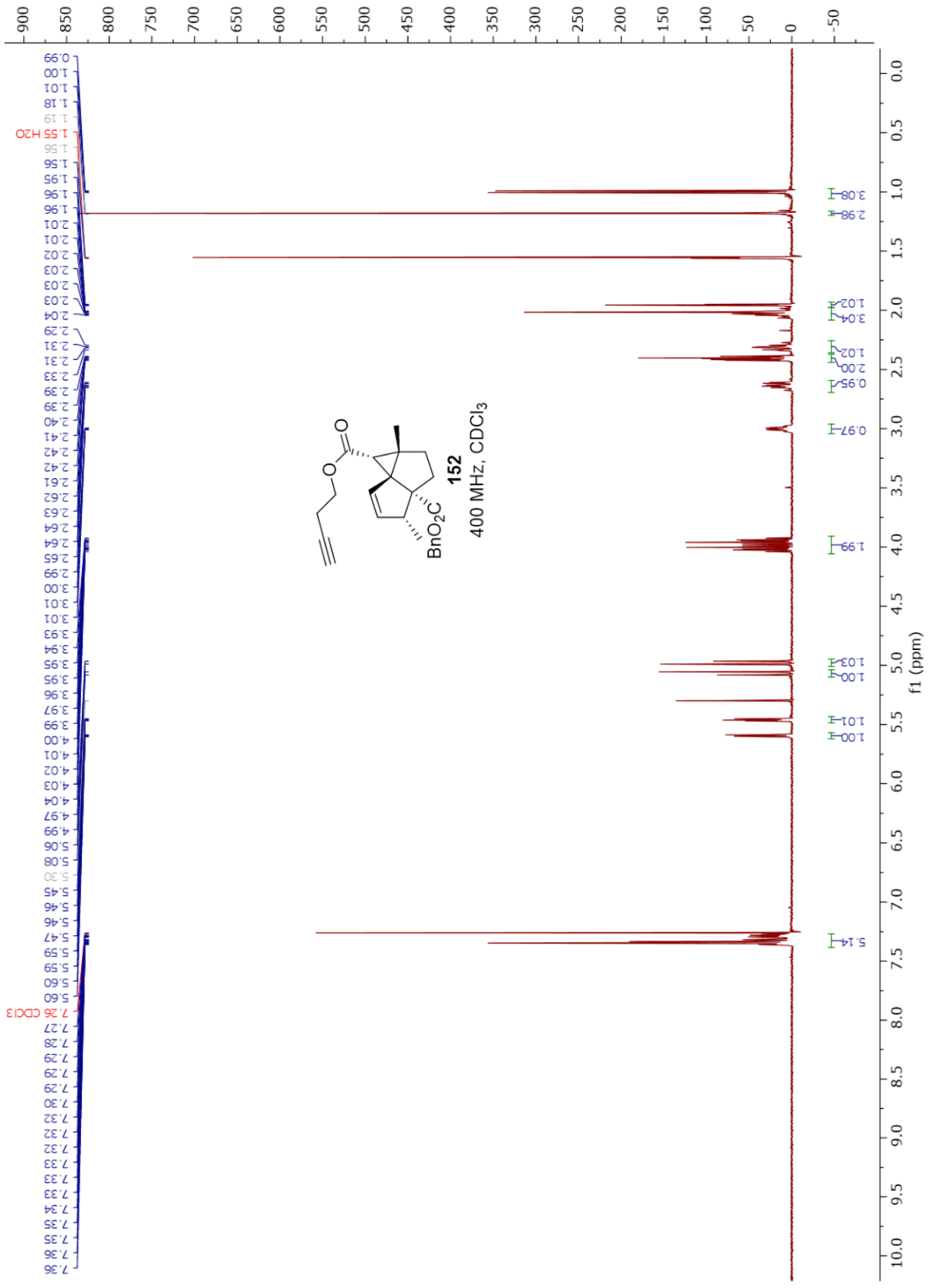
152
400 MHz, CDCl3
BnO2C
f1 (ppm)

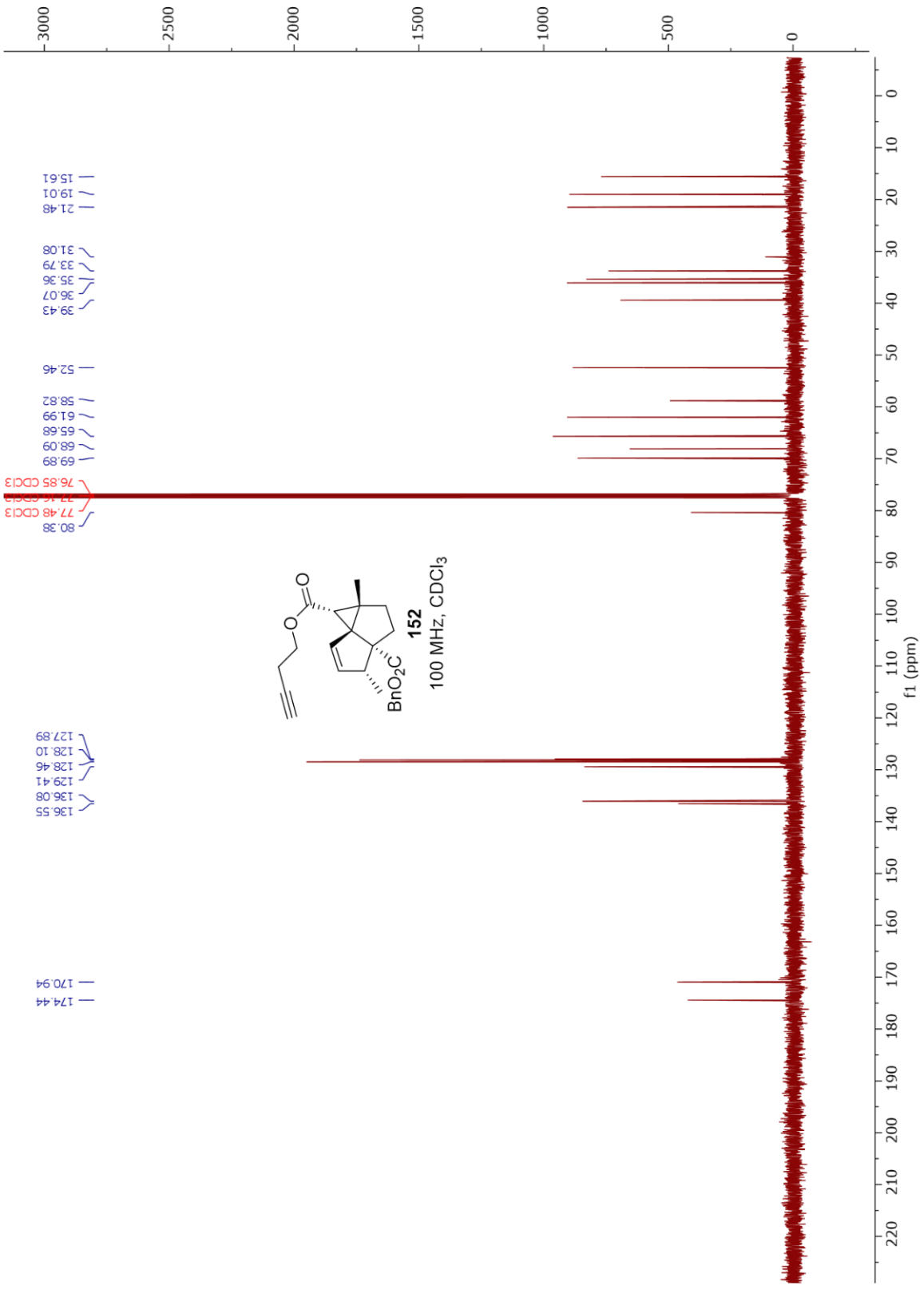
15.61
19.01
21.48
31.08
33.79
35.36
36.07
39.43
52.46
58.82
61.99
65.68
68.09
69.89
76.85 CDCl3
77.16 CDCl3
77.48 CDCl3
80.38
127.89
128.10
128.46
129.41
136.08
136.55
170.94
174.44
152
100 MHz, CDCl3
BnO2C
f1 (ppm)

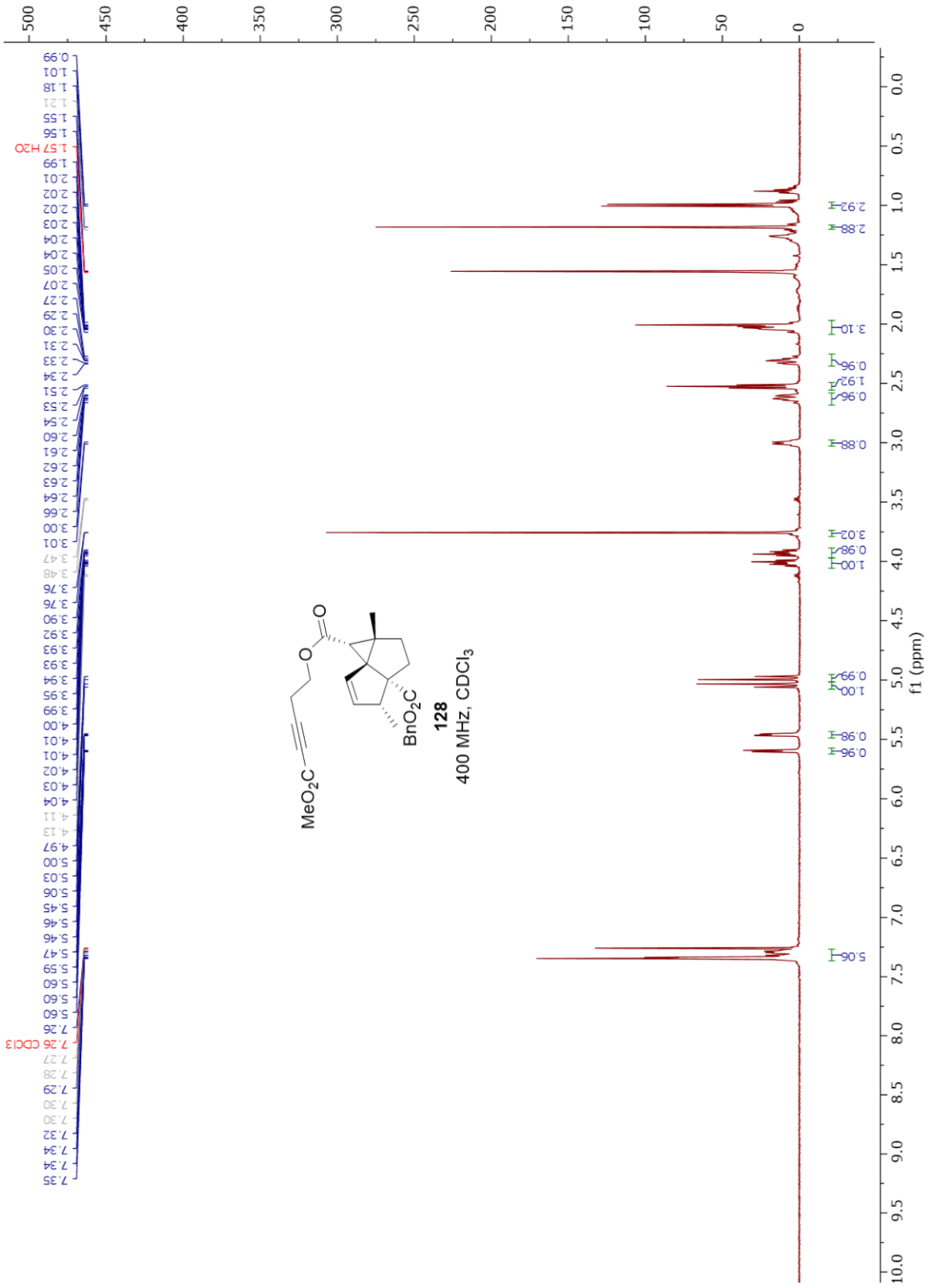
MeO2C
BnO2C
128
400 MHz, CDCl3
f1 (ppm)

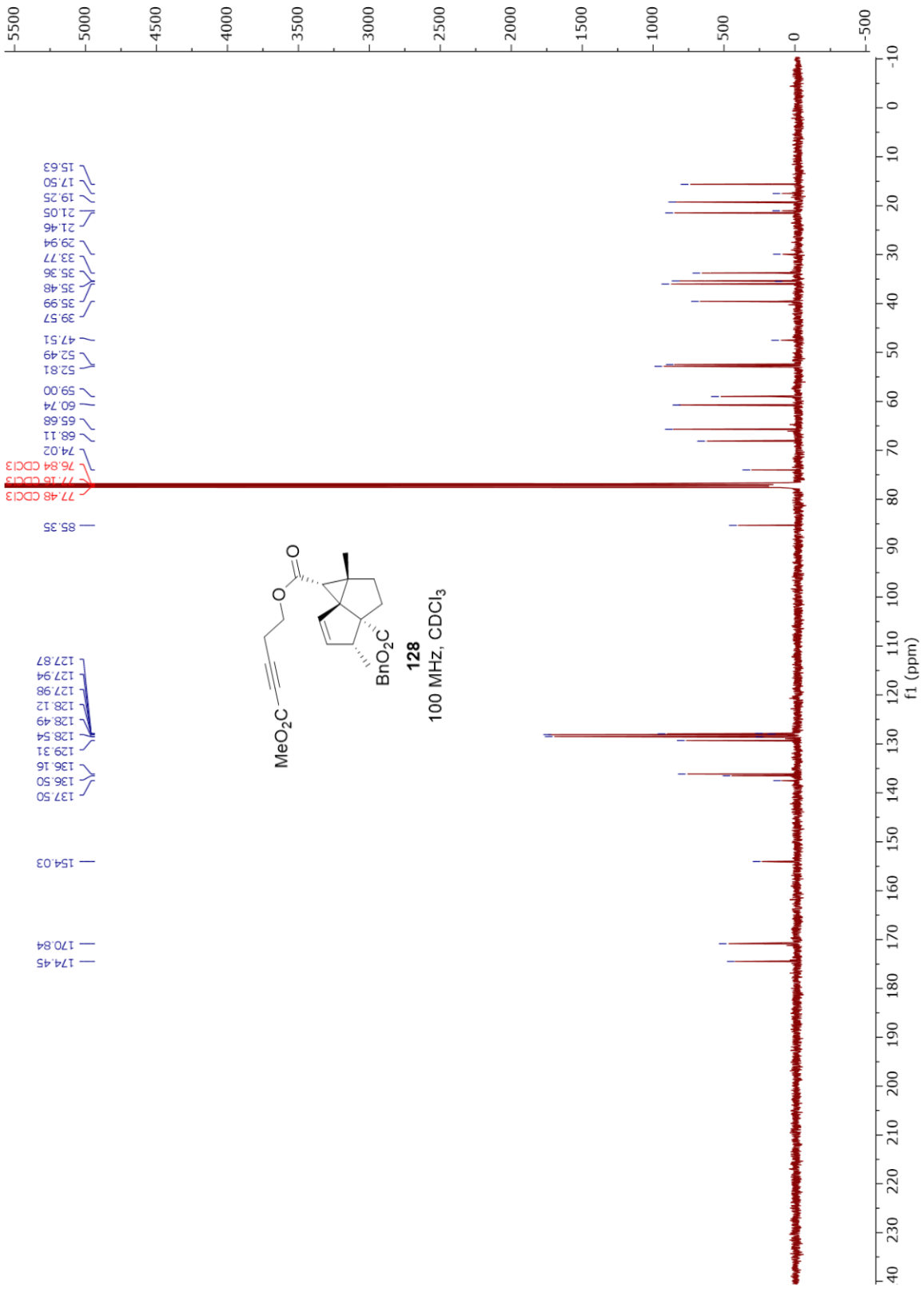
MeO2C
BnO2C
128
100 MHz, CDCl3
f1 (ppm)
77.48 CDCl3
76.84 CDCl3
174.45
170.84
154.03
137.50
136.50
136.16
129.31
128.54
128.49
128.12
127.98
127.94
127.87
85.35
74.02
68.11
65.68
60.74
59.00
52.81
52.49
47.51
39.57
35.99
35.48
35.36
33.77
29.94
21.46
21.05
19.25
17.50
15.63

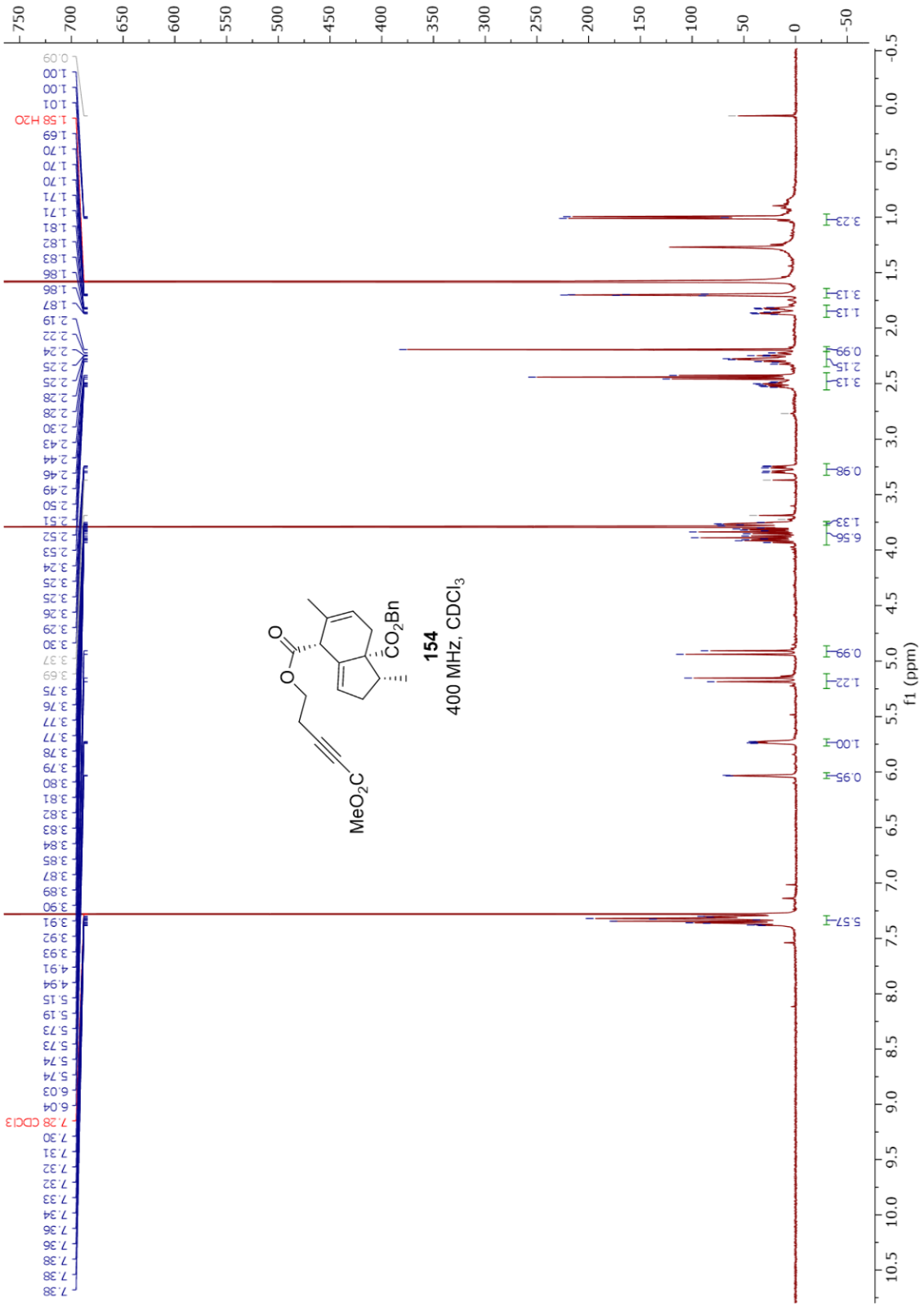
154
400 MHz, CDCl3
CO2Bn
MeO2C
f1 (ppm)

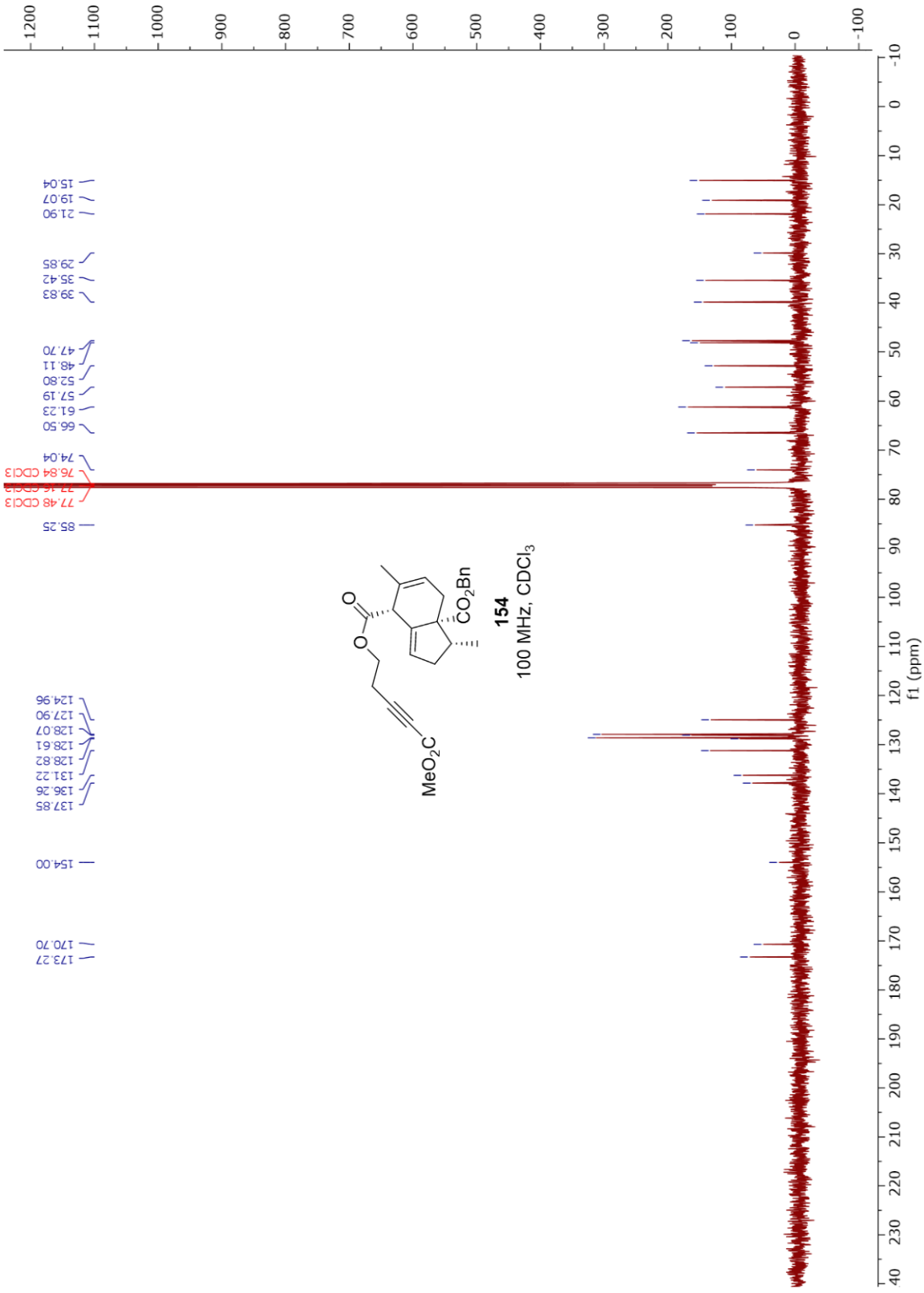
154
100 MHz, CDCl3
CO2Bn
MeO2C
O
O
15.04
19.07
21.90
29.85
35.42
39.83
47.70
48.11
52.80
57.19
61.23
66.50
74.04
76.84 CDCl3
77.16 CDCl3
77.48 CDCl3
85.25
124.96
127.90
128.07
128.61
128.82
131.22
136.26
137.85
154.00
170.70
173.27
f1 (ppm)

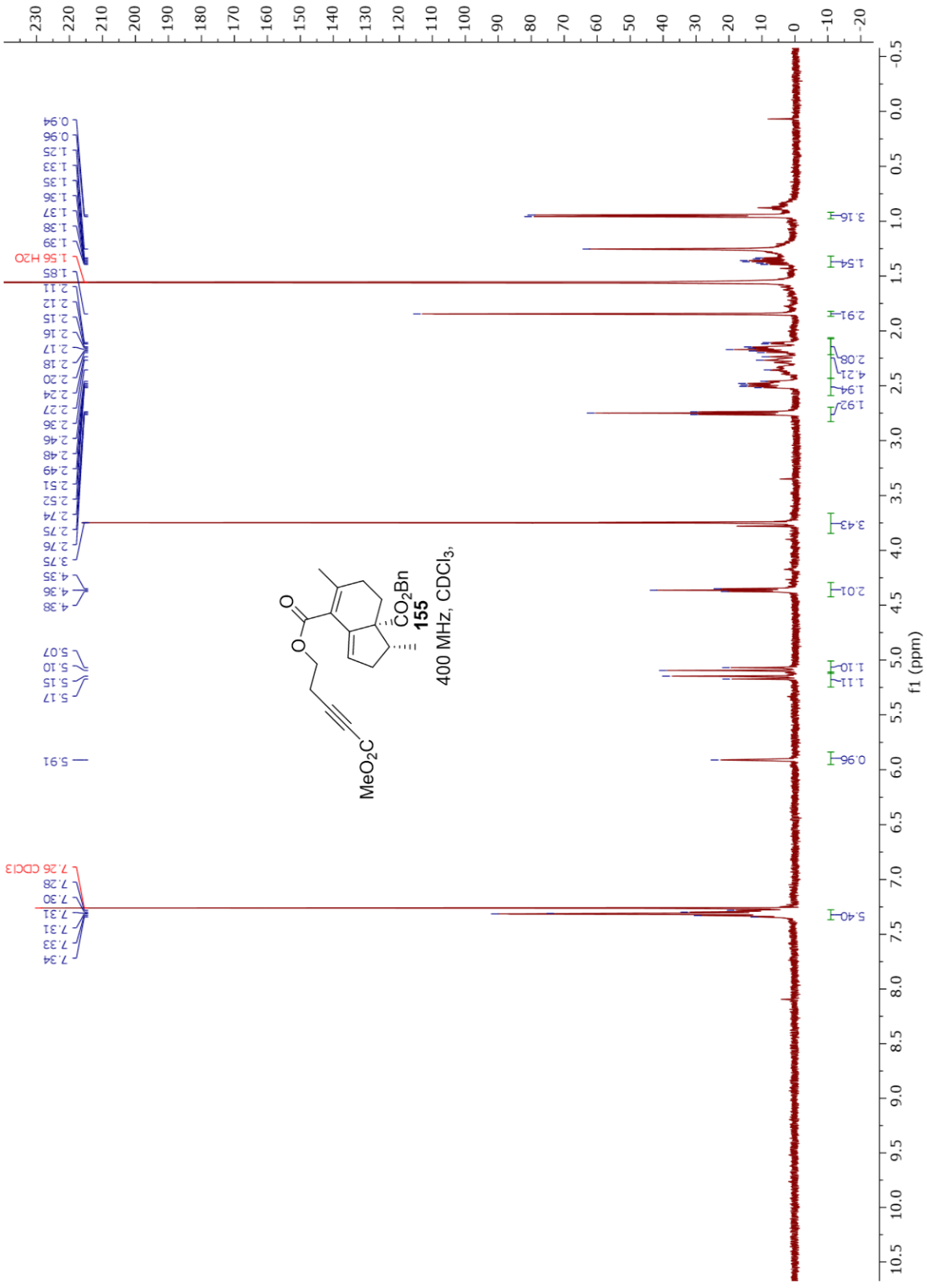
CO2Bn
155
400 MHz, CDCl3,
MeO2C
f1 (ppm)